INVERTEBRATE NEUROBIOLOGY: SENSORY SYSTEMS, INFORMATION INTEGRATION, LOCOMOTOR- AND BEHAVIORAL OUTPUT

EDITED BY: Sylvia Anton and Philippe Lucas
PUBLISHED IN: Frontiers in Physiology

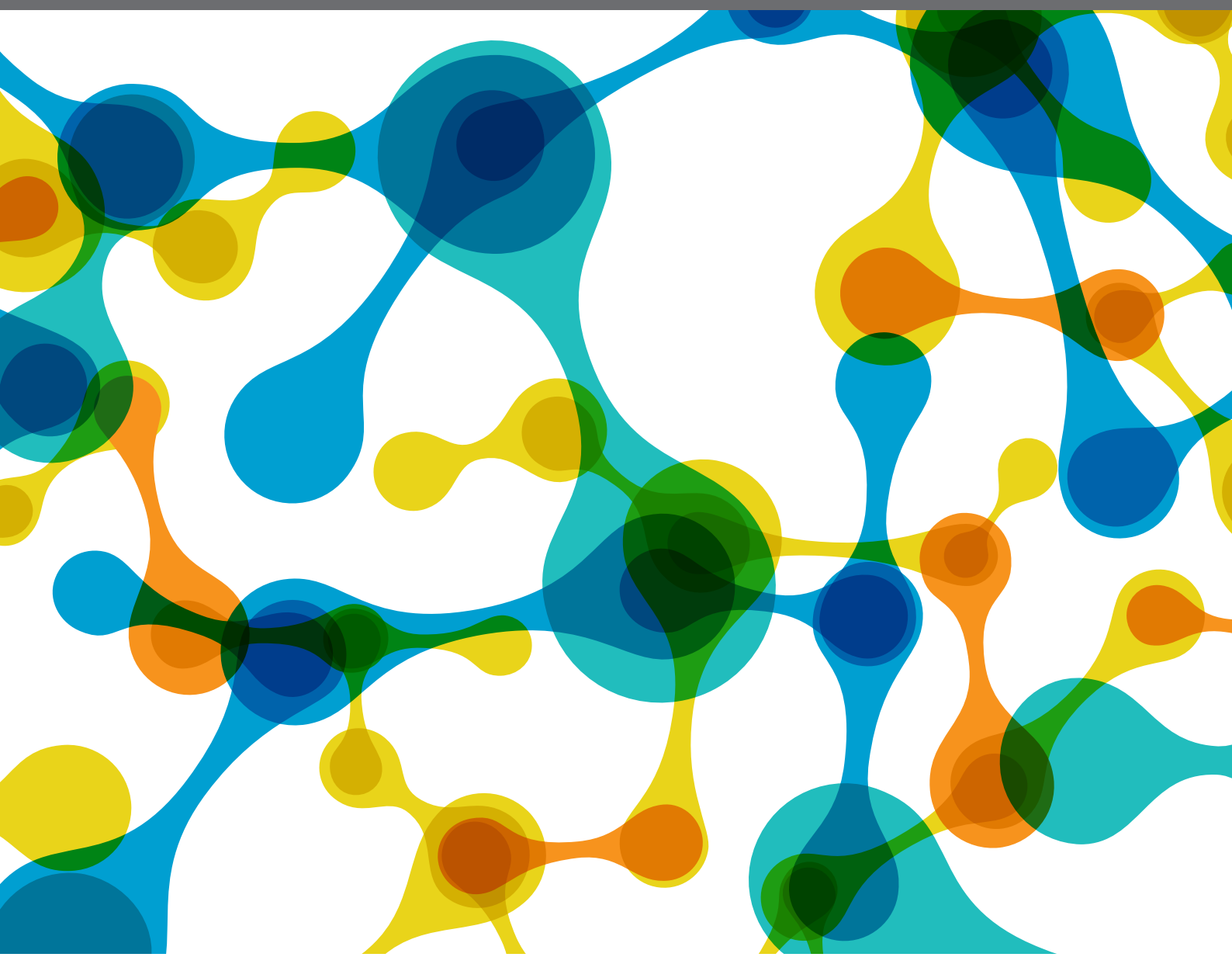

frontiers Research Topics

frontiers

ISSN 1664-8714
ISBN 978-2-88974-079-6
DOI 10.3389/978-2-88974-079-6

About Frontiers

Frontiers is more than just an open-access publisher of scholarly articles: it is a pioneering approach to the world of academia, radically improving the way scholarly research is managed. The grand vision of Frontiers is a world where all people have an equal opportunity to seek, share and generate knowledge. Frontiers provides immediate and permanent online open access to all its publications, but this alone is not enough to realize our grand goals.

Frontiers Journal Series

The Frontiers Journal Series is a multi-tier and interdisciplinary set of open-access, online journals, promising a paradigm shift from the current review, selection and dissemination processes in academic publishing. All Frontiers journals are driven by researchers for researchers; therefore, they constitute a service to the scholarly community. At the same time, the Frontiers Journal Series operates on a revolutionary invention, the tiered publishing system, initially addressing specific communities of scholars, and gradually climbing up to broader public understanding, thus serving the interests of the lay society, too.

Dedication to Quality

Each Frontiers article is a landmark of the highest quality, thanks to genuinely collaborative interactions between authors and review editors, who include some of the world's best academicians. Research must be certified by peers before entering a stream of knowledge that may eventually reach the public - and shape society; therefore, Frontiers only applies the most rigorous and unbiased reviews.
Frontiers revolutionizes research publishing by freely delivering the most outstanding research, evaluated with no bias from both the academic and social point of view. By applying the most advanced information technologies, Frontiers is catapulting scholarly publishing into a new generation.

What are Frontiers Research Topics?

Frontiers Research Topics are very popular trademarks of the Frontiers Journals Series: they are collections of at least ten articles, all centered on a particular subject. With their unique mix of varied contributions from Original Research to Review Articles, Frontiers Research Topics unify the most influential researchers, the latest key findings and historical advances in a hot research area! Find out more on how to host your own Frontiers Research Topic or contribute to one as an author by contacting the Frontiers Editorial Office: frontiersin.org/about/contact

INVERTEBRATE NEUROBIOLOGY: SENSORY SYSTEMS, INFORMATION INTEGRATION, LOCOMOTOR- AND BEHAVIORAL OUTPUT

Topic Editors:
Sylvia Anton, Institut National de la Recherche Agronomique (INRA), France
Philippe Lucas, Institut National de recherche pour l'agriculture, l'alimentation et l'environnement (INRAE), France

Citation: Anton, S., Lucas, P., eds. (2022). Invertebrate Neurobiology: Sensory Systems, Information Integration, Locomotor- and Behavioral Output. Lausanne: Frontiers Media SA. doi: 10.3389/978-2-88974-079-6

Table of Contents

frontiers in Physiology

EDITORIAL
published: 26 November 2021
doi: 10.3389/fphys.2021.807521

Editorial: Invertebrate Neurobiology: Sensory Systems, Information Integration, Locomotor- and Behavioral Output

Philippe Lucas[1] *and Sylvia Anton*[2]*

[1] INRAE, Sorbonne Université, INRAE, CNRS, UPEC, IRD, Université de Paris, Institute of Ecology and Environmental Sciences of Paris, Paris, France, [2] INRAE/Agrocampus Ouest/Université Rennes 1, Institute of Genetics, Environment and Plant Protection, Agrocampus Ouest, Angers, France

Keywords: invertebrate, neurophysiology, neuroanatomy, locomotion, sensory cues

Editorial on the Research Topic

Invertebrate Neurobiology: Sensory Systems, Information Integration, Locomotor- and Behavioral Output

OPEN ACCESS

Edited and reviewed by:
Graziano Fiorito, Zoological Station Anton Dohrn, Italy

***Correspondence:**
Sylvia Anton
sylvia.anton@inrae.fr

Specialty section:
This article was submitted to Invertebrate Physiology, a section of the journal Frontiers in Physiology

Received: *02 November 2021*
Accepted: *09 November 2021*
Published: *26 November 2021*

Citation:
Lucas P and Anton S (2021) Editorial: Invertebrate Neurobiology: Sensory Systems, Information Integration, Locomotor- and Behavioral Output. Front. Physiol. 12:807521. doi: 10.3389/fphys.2021.807521

Invertebrates are a very diverse group of animals, which have developed sophisticated sensory systems, brain functions and motor systems to respond with adaptive behavior to signals emanating from various environments of biotic and abiotic origin. Strong sensory and cognitive capacities are found in invertebrates with small brains, which can therefore serve as model organisms to understand nervous system function also in organisms with bigger brains (Chittka and Niven, 2009). As a follow-up of a conference on the neurobiology of invertebrates in Versailles/France in May 2018, we collected articles in the present Research Topic in Frontiers in Invertebrate Physiology on various aspects of invertebrate neurobiology in different taxa, reaching from molecular over cellular studies up to sensory, brain and motor function and its plasticity, as well as behavioral output. We also include recent methodological developments, improving the feasibility of studies in these fields. The Research Topic comprises 17 original Research articles and 5 Reviews.

A first group of articles treats various aspects of insect olfaction. Identification, expression and functional analyses of antennal olfactory genes are presented in the rice grasshopper, two moth species, and a migratory locust. In the rice grasshopper, *Oxya chinensis*, different olfactory genes coding for odorant-binding proteins, chemosensory proteins, sensory neuron membrane proteins, as well as odorant and ionotropic receptors have been identified. For some of these genes, sex-biased expression was found (Cui et al.). An odorant receptor (OR) for repellents in the Asian cornborer *Ostrinia furnacalis,* and a plant odor-specific OR in the oriental armyworm *Mythimna separata* were functionally characterized using heterologous expression in *Xenopus* oocytes (Yu et al.; Zhang et al.). In the locust *Schistocerca gregaria*, Jiang et al. mapped the presence of a large number of ORs on the antennal sensillum types and found primarily a single OR expressed in each sensillum. However, some OR-specific cell clusters

in certain sensilla were formed during development, as shown by comparing the expression of ORs between different nymph stages. Two reviews concern the characteristics of odorant stimuli, crucial for electrophysiological and behavioral experiments, taking the ecology of insects into consideration. A first review article treats the characterization of dynamic odorant stimuli (Pannunzi and Nowotny), summarizing the critical questions to define odor concentrations in space and their dynamics, as well as the spatio-temporal structure of odor stimuli in a natural environment from an experimental and theoretical point of view. Conchou et al. review what is known on insect odorscapes, i.e., the complex odor distribution in a natural environment, how insects deal with it and how odorscapes might be manipulated for sustainable pest control. Two electrophysiological studies investigate odor responses at different levels of the olfactory pathway. Coding of slowly fluctuating olfactory cues is described in so-called ON-OFF olfactory receptor neurons in the cockroach *Periplaneta americana* (Hellwig et al.) and modulation of odor responses within the lateral horn, a superior olfactory brain center was shown to enhance bilateral contrast of odor inputs in the fruitfly *Drosophila melanogaster* (Mohamed et al.). Another innovative study describes the peripheral and central olfactory system and odor-guided behavior in head lice *Pediculus humanis capitis*, highly specialized insects which have hardly been studied before (Ortega Insaurralde et al.).

A second series of articles deals with plasticity of chemosensory systems and methodological considerations to study this. Hostachy, Couzi, Hanafi-Portier, et al. describe experimental parameters to be taken into account when testing proboscis extension responses to sugar solutions in the moth *Agrotis ipsilon*. The same authors subsequently test the influence of pre-exposure with conspecific and heterospecific sex pheromones on gustatory habituation and find effects after different delays depending on the pheromone used, thus suggesting that different central pathways are implicated in the different observed effects (Hostachy, Couzi, Portemer et al.). Nouvian and Galizia describe a newly developed device for aversive learning in freely moving honey bees: an automated Y-maze, suitable to test olfactory or visual cues. A study in the fruitfly *Drosophila melanogaster* demonstrates elegantly that thermogenetically generated stochastic activity patterns of olfactory projection neurons can replace conditioned stimuli within mushroom body neurons (Warth Pérez Arias et al.). In the cockroach *Periplaneta americana*, both classical and operant learning paradigms using olfactory cues and a sucrose reward revealed inter-individual learning differences, comparable to what has been found earlier in honey bees and humans (Arican et al.). Extending on the topic of individuality in insects, Sánchez-Alcañiz and Molla Albaladejo review the genetic bases of behavioral individuality in *Drosophila melanogaster,* which occurs in olfactory-guided behavior and olfactory learning, but also in various other contexts.

A different sensory modality is investigated in another paper. Meiser et al. studied modulation of the sensitivity of touch cells in the leech. They found a non-synaptic mechanism switching the response behavior of these sensory neurons from rapidly to slowly adapting spiking.

Four other papers deal with locomotor control and its modulation in different invertebrates. Emanuel et al. review what is known on the role of different regions in the central nervous system in controlling posture and locomotion in insects. Two original articles deal with the role of serotonin (5-HT) on influencing motoneurons and behavioral output. In crayfish, a single 5-HT neuron was shown to differentially modulate motoneurons (simultaneous excitatory and inhibitory effects in different leg motoneurons) in the abdominal ganglia (Bacqué-Cazenave et al.). In the pond snail *Lymnaea stagnalis*, serotonin seems to influence accelerated locomotion, which subsequently improves cognitive abilities (decision-making under uncertainty) (Aonuma et al.). Another review article presents the current knowledge on a specific group of clock neurons in *Drosophila melanogaster*, DN1p neurons, and specifically their role in the circadian regulation of motor control. Lamaze and Stanewsky specifically discuss that these neurons might be responsible for two locomotion peaks per day in constant darkness.

Another paper deals with a nicotinic acetylcholine receptor subunit in cockroaches. These receptors are important for synaptic transmission in the brain and represent targets for neonicotinoid insecticides. Here a new receptor subunit was characterized and its expression in the brain described (Cartereau et al.).

Finally, a research paper demonstrates how wing scale pigmentation in the Bogong moth, *Agrotis infusa*, leads to visual camouflage within its natural environment (Stavenga et al.).

Taken together, this Research Topic expands our view on recent advances in various domains within invertebrate neurobiology by assembling original articles using multidisciplinary approaches and reviews on major themes of interest.

AUTHOR CONTRIBUTIONS

Both authors listed have made a substantial, direct, and intellectual contribution to the work and approved it for publication.

ACKNOWLEDGMENTS

We thank the following funders for support of the conference on the neurobiology of invertebrates in Versailles/France in May 2018: Frontiers, INRA Department of Plant Health and Environment, INRA Research Center Versailles.

REFERENCES

Chittka, L., and Niven, J. (2009). Are bigger brains better? *Curr. Biol.* 19, R995–R1008. doi: 10.1016/j.cub.2009.08.023

Conflict of Interest: The authors declare that the research was conducted in the absence of any commercial or financial relationships that could be construed as a potential conflict of interest.

Publisher's Note: All claims expressed in this article are solely those of the authors and do not necessarily represent those of their affiliated organizations, or those of the publisher, the editors and the reviewers. Any product that may be evaluated in this article, or claim that may be made by its manufacturer, is not guaranteed or endorsed by the publisher.

frontiers in Physiology

ORIGINAL RESEARCH
published: 09 April 2019
doi: 10.3389/fphys.2019.00367

Functional Analysis of MsepOR13 in the Oriental Armyworm *Mythimna separata* (Walker)

Kunpeng Zhang[1,2†], Yilu Feng[3†], Lixiao Du[3], Shanshan Gao[2], Hang Yan[2], Kun Li[2], Nana Liu[2], Junxiang Wu[1] and Guirong Wang[3*]*

[1] State Key Laboratory of Crop Stress, Northwest A&F University, Yangling, China, [2] College of Biology and Food Engineering, Anyang Institute of Technology, Anyang, China, [3] State Key Laboratory for Biology of Plant Diseases and Insect Pests, Institute of Plant Protection, Chinese Academy of Agricultural Sciences, Beijing, China

Olfaction in insects has a critical role in recognizing the host, finding food, and choosing mating partners, as well as avoiding predators. Odorant receptors (ORs), which are housed in the dendritic membrane of sensory neurons and extended into the lymph of sensilla on insect antennae, are participating in the detection of volatile compounds in insects. In the present study, we identified an OR gene, named *MsepOR13*, in the oriental armyworm *Mythimna separata* (Walker). Quantitative real-time polymerase chain reaction revealed that *MsepOR13* was expressed mainly in the antennae of male and female moths. In *in vitro* heterologous expression experiments, MsepOR13 was widely tuned to 32 of the 67 different compounds tested. Furthermore, MsepOR13 responded to eugenol at a low concentration of 10^{-9} M, with an EC50 value of 3.91×10^{-6} M. The high sensitivity suggests an important role for the OR13 gene in the moth olfactory system.

Keywords: ***Mythimna separata*, odorant receptor, eugenol, *Xenopus* oocytes, odorant tuning**

OPEN ACCESS

Edited by:
Sylvia Anton,
Institut National de la Recherche Agronomique (INRA), France

Reviewed by:
Nicolas Montagné,
Sorbonne Universités, France
Liang Sun,
Tea Research Institute (CAAS), China

***Correspondence:**
Junxiang Wu
junxw@nwsuaf.edu.cn
Guirong Wang
grwang@ippcaas.cn

† These authors have contributed equally to this work

Specialty section:
This article was submitted to Invertebrate Physiology, a section of the journal Frontiers in Physiology

Received: *12 December 2018*
Accepted: *18 March 2019*
Published: *09 April 2019*

Citation:
Zhang K, Feng Y, Du L, Gao S, Yan H, Li K, Liu N, Wu J and Wang G (2019) Functional Analysis of MsepOR13 in the Oriental Armyworm Mythimna separata (Walker). Front. Physiol. 10:367. doi: 10.3389/fphys.2019.00367

INTRODUCTION

Chemoreception of odorants in the environment is critically important for the survival of insects. During evolution, insects have evolved a powerful sense of olfaction to locate hosts and mating partners, identify oviposition sites, discriminate toxic food, and escape predators (Schneider, 1969; Bruce et al., 2005; Bruyne and Baker, 2008; Hansson and Stensmyr, 2011; Gadenne et al., 2016), as they are surrounded by various chemical compounds emitted from conspecifics, predators, and host plants (Bentley and Day, 1989; Schneider, 1992; Hansson and Stensmyr, 2011). These odorants are diffused to the surface on olfactory appendages, which mainly consisting of antennae and maxillary palps (Steinbrecht, 1997), and enter the lymph through pores of the sensilla, which are hair-like structures. Odorant molecules interact with odorant-binding proteins (OBPs) in the sensilla lymph and are transferred toward the dendrites of olfactory sensory neurons (OSNs), where odorant receptors (ORs) are expressed. Activation of ORs leads to chemical information being transduced to electrical signals, which are conveyed to the antennal lobe and finally decoded by the insect brain (Vogt, 2003; Leal, 2013).

Owing to the availability of the *Drosophila melanogaster* genome sequence, the first insect OR was identified in *D. melanogaster* based on the homology of OR sequences in vertebrates and nematodes and the restricted expression of these genes in olfactory tissues (Clyne et al., 1999;

Vosshall et al., 1999). Compared with G-protein coupled receptors (GPCRs), insect ORs have the opposite membrane topology, with their N-terminus inside and their C-terminus outside the cell; this is an inverse membrane topology to that found in vertebrate ORs (Buck and Axel, 1991; Benton et al., 2006; Fleischer et al., 2017; Butterwick et al., 2018). It is now generally accepted that insect ORs transduce chemical signals by forming heteromeric complexes with an OR co-receptor (Orco) that operate as non-selective cation channels (Koji et al., 2008; Wicher et al., 2008).

In recent decades, with progress in sequencing technology and bioinformatics tools, numerous ORs have been reported in many species from various insect orders, including Lepidoptera, Diptera, Hymenoptera, Coleoptera, Hemiptera, Orthoptera, and Phthiraptera. The number of OR genes varies considerably among insect species. For example, there are 65 ORs in *Helicoverpa armigera* (Liu et al., 2012; Zhang et al., 2015a) and 62 ORs in *Mythimna separata* (Du et al., 2018), based on antennal transcriptomic analysis, whereas 163 ORs have been obtained from the genome of *Apis mellifera* (Robertson and Wanner, 2006) and 256 ORs have been identified in the genome of *Tribolium castaneum* (Engsontia et al., 2008). The variation in number of ORs between insects is assumed to correlate with evolutionary adaption to certain ecological and physiological demands (Fleischer et al., 2017).

Although increasing numbers of OR genes have been identified during recent decades, the functional characterization of the encoded proteins lags significantly behind. Heterologous *in vitro* expression systems, such as cultured cell lines and *Xenopus* oocytes, and *in vivo* expression systems, such as the "empty neuron system" of *Drosophila*, have been successfully established for functional analysis of insect ORs (Dobritsa et al., 2003; Gonzalez et al., 2016; Wang et al., 2016). These systems have been applied for functional characterization of both pheromone and non-pheromone receptors in several species, including *D. melanogaster* (Hallem et al., 2004; Kreher et al., 2005; Hallem et al., 2006), *Anopheles gambiae* (Lu et al., 2007; Carey et al., 2010; Wang et al., 2010), *B. mori* (Sakurai et al., 2004, 2011; Nakagawa et al., 2005; Grosse-Wilde et al., 2011), *Heliothis virescens* (Ewald et al., 2010; Wang et al., 2011), *Ostrinia nubilalis* (Wanner et al., 2010; Yuji et al., 2011; Leary et al., 2012), *O. furnacalis* (Miura et al., 2010; Liu W. et al., 2018), *Spodoptera littoralis* (de Fouchier et al., 2017), *Cydia pomonella* (Bengtsson et al., 2014; Gonzalez et al., 2015; Cattaneo et al., 2017), *H. armigera* (Liu Y. et al., 2013; Cao et al., 2016; Chang et al., 2016; Di et al., 2017), *H. assulta* (Chang et al., 2016; Cui et al., 2018), *Plutella xylostella* (Sun et al., 2013; Liu Y. et al., 2018), *S. exigua* (Liu C. et al., 2013; Liu et al., 2014), and *S. litura* (Zhang et al., 2015b).

The oriental armyworm *M. separata* (Walker) (Lepidoptera: Noctuidae) is an economically important and common lepidopteran pest, which is widely distributed in eastern Asia and Australia, and attacks many crop plants including maize, sorghum, and rice. *M. separata* migrates long distances, resulting in widespread incidence, which can lead to complete crop loss (Sharma and Davies, 1983; Jiang et al., 2011). In recent years, *M. separata* has been observed in many regions of China and poses a severe threat to corn production. In order to control this pest, high doses of insecticides are often applied; however, this has some negative effects, including environmental pollution, insect resistance, and harm to non-target organisms (Lv et al., 2014; Duan et al., 2017). Outbreaks of *M. separata* represent a great challenge in crop protection worldwide (Liu et al., 2017).

Compared with the use of chemical pesticides, olfactory-baited trapping is an effective and environmentally friendly method to manage *M. separata*. The sex pheromone of *M. separata* has been used in this way (Wei, 1985; Zhu et al., 1987), but the effect was unsatisfactory for unknown reasons. *Pterocarya stenoptera* and *Salix babylonica* are also used to attract *M. separata* in the field (Lihuang et al., 2017), although the mechanism of attraction is unknown. In previous work, we identified the ORs in *M. separata* using transcriptomic analysis (Du et al., 2018), but no study on their function has been reported except for MsepOR1, responding to the major sex pheromone compound Z11-16:Ac (Mitsuno et al., 2010). In the present study, we cloned an OR, named *MsepOR13*, in *M. separata* and analyzed the expression patterns in different tissues of both sexes by quantitative real-time polymerase chain reaction (qRT-PCR). Functional analysis was completed using *in vitro* expression in a *Xenopus* oocyte system with two-electrode, voltage-clamp physiological recordings.

MATERIALS AND METHODS

Insect Rearing

The *M. separata* colony, maintained at the laboratory of Henan Agricultural University, Zhengzhou, China, was reared on an artificial diet at 28 ± 1°C, 70% ± 5% relative humidity, and a 14 h:10 h light:dark (L:D) photoperiod. Adult male and female moths were fed with 10% sugar solution.

RNA Extraction and cDNA Synthesis

Male and female antennae, proboscises, labial palps, and legs (a mixture of female and male) of virgin male or female individuals were collected 3 days after eclosion, immediately frozen in liquid nitrogen, and stored at −70°C until RNA extraction. Total RNA of 20 adult male or female moths was isolated using TRIzol reagent (Invitrogen, Carlsbad, CA, United States) following the manufacturer's instructions. Total RNA was dissolved in RNase-free water and gel electrophoresis was performed to assess its integrity. RNA concentration and purity were determined on a Nanodrop ND-2000 spectrophotometer (NanoDrop products, Wilmington, DE, United States).

First, total RNA was treated with DNase I (Fermentas, Glen Burnie, MD, United States) for 30 min at 37°C to remove residual gDNA. Then, 1 μg total RNA was used to synthesize single-stranded cDNA as per the First Strand cDNA Synthesis Kit (Fermentas) manufacturer's instructions. The cDNA of antennal samples was used as a template to clone the *MsepOR13* gene. The cDNA samples isolated from different female and male tissue types were used as templates for RT-qPCR.

Cloning of *MsepOR13* Gene From *M. separata*

The sequence of *MsepOR13* was identified in *M. separata* by transcriptomic analysis (Du et al., 2018). Specific primers were designed by Primer 5.0 (PREMIER Biosoft International, Palo Alto, CA, United States) to clone the full-length sequence of MsepOR13 (**Table 1**). Antennal cDNA from female and male moths was used to amplify the full-length sequence of *MsepOR13* using primeSTAR HS (Premix) (TaKaRa, Dalian, China). PCR reactions of 50 μL contained 25 μL 2×primeSTAR HS (Premix), 1.5 μL sense and anti-sense primers (10 μM), 2 μL cDNA, and 20 μL double-distilled H_2O. Reactions were carried out under the following conditions: 95°C for 3 min; 35 cycles of 95°C for 30 s, 57°C for 30 s, and 72°C for 1 min; and 72°C for 10 min; before being held at 16°C. PCR products were analyzed on a 1.5% agarose gel and the sequence was sub-cloned to the vector pEASY-Blunt (TransGene, Beijing, China). The sequencing was completed in Sangon Biotech, Shanghai, China.

Sequence Analysis

The amino acid sequence of MsepOR13 was determined using the ExPASy-Translate tool[1]. The sequence was aligned with ORs from *Peridroma saucia* (PsauOR, GenBank: AVF19631.1), *Athetis lepigone* (AlepOR19, GenBank: AOE48024.1), and *Athetis dissimilis* (AdisOR31, GenBank: ALM26220.1) using DNAMAN version 8 (Lynnon LLC, San Ramon, CA, United States).

Tissue Expression Profile of *MsepOR13*

Quantitative polymerase chain reaction was performed to determine the expression of *MsepOR13*. Male and female antennae, proboscises, labial palps, and legs (a mixture of female and male) were collected from 3-day-old *M. separata* adults after eclosion. RNA extraction and cDNA synthesis were performed following the protocol described above. *MsepRPS3* was chosen as the reference gene. The primers are listed in **Table 1**. GoTaq qPCR Master Mix (Promega, Madison, WI, United States) was used for qPCR, and the reactions were carried out on an Applied Biosystems 7500 Fast Real-Time PCR System (ABI, Carlsbad, CA, United States). The reactions (20 μL) consisted of 10 μL GoTaq qPCR Master Mix, 0.8 μL gene primer (10 μM), 1 μL cDNA, and 7.4 μL RNase-free water. The reactions were carried out under the following conditions: 95°C for 2 min; 40 cycles of 95°C for 15 s, and 60°C for 50 s. Each qPCR reaction was performed in triplicate with three independent biological samples to check reproducibility. The melting curves were inspected to check the specificity of the primers, and the amplification efficiencies were calculated by the standard curve method. The efficiency of the primers for *MsepOR13* and *MsepRPS3* were 97 and 105%, respectively. *MsepOR13* relative expression levels were analyzed using the relative $2^{-\Delta\Delta CT}$ quantitation method, where $\Delta C_T = C_T$ (*MsepOR13*) – C_T (*MsepRPS3*), $\Delta\Delta C_T = \Delta C_T$ (different samples) – ΔC_T (legs (female and male mixture)). Statistical comparison of expression of *MsepOR13* was assessed using one-way nested analysis of variance (ANOVA), followed by least-significant difference (LSD) tests.

[1]http://web.expasy.org/translate/

TABLE 1 | Primers' sequence in this study.

Primers	Sequences 5′–3′	Purpose
MsepOR13-F	ATGGCGGATATTCCAACGG	Gene cloning
MsepOR13-R	TTAACGATTCAAAAATGTAA ACAAGGT	
MsepOrco-F	ATGATGACCAAAGTGAAGGC	
MsepOrco-R	TTACTTGAGTTGCACCAACAC	
MsepOR13-qF	GGAAGCAGCGTGTCAATGTT	qPCR
MsepOR13-qR	AGGTCTCGGGAAGTTCTCCA	
MsepRPS3-qF	AATGAGTTCTTGACCAGGGAG	
MsepRPS3-qR	GTGTCCTCGTCGCCATAAT	
MsepOR13-A	TCAgggcccGCCACCATGGCG GATATTCCAACGG	cRNA synthesizing
MsepOR13-S	TCAgcggccgcCTTAACGAT TCAAAAATGTAAACAAGGT	
MsepOrco-A	TCAgggcccGCCACCATGAT GACCAAAGTGAAGGC	
MsepOrco-S	TCAgcggccgcTTACTTGAG TTGCACCAACAC	

MsepOR13 Expression in *Xenopus* Oocytes and Electrophysiological Recordings

The full-length *MsepOR13* was first cloned into a pEASY-Blunt vector and then ligated into a pT7Ts expression vector using primers containing *Apa I* (GGGCCC) and *Not I* (GCGGCCGC) sites. The expression vector was linearized using *Sma I* (CCCGGG) (Fermentas, Glen Burnie, MD, United States) and the cRNA was synthesized using an mMESSAGE mMACHINE T7 kit (Ambion, Austin, TX, United States). Mature healthy *Xenopus* oocytes (stages V–VII) were incubated with 2 mg/mL collagenase I in pH 7.6 washing buffer consisting of 96 mM NaCl, 2 mM KCl, 5 mM $MgCl_2$, and 5 mM HEPES at room temperature for about 1 h until almost of them were separated a signal one. Then, 27.6 ng MsepOR13 cRNA and 27.6 ng MsepOrco cRNA were microinjected together into oocytes, and the oocytes were cultured in 1× Ringer's buffer (washing buffer supplemented with 0.8 mM $CaCl_2$, 5% dialyzed horse serum, 50 mg/mL tetracycline, 100 mg/mL streptomycin, and 550 mg/mL sodium pyruvate) for 4–7 days. The whole-cell currents of injected oocytes were recorded with an OC-725C oocyte clamp at a holding potential of −80 mV (Warner Instruments, Hamden, CT, United States), following previously described experimental procedures (Cui et al., 2018; Liu W. et al., 2018; Liu Y. et al., 2018). Oocytes were exposed to different compounds at 10^{-4} M for 15 s each, in a random order, with intervals between exposures that allowed the current to return to baseline. Dose–response curves were acquired from 10^{-9} to 10^{-4} M in ascending order of concentration. All data acquisition and analysis were carried out with Digidata 1440A and Pclamp10.0 (Axon Instruments, Inc., Union City, CA, United States), and dose–response data were analyzed using GraphPad Prism 5. Statistical comparison

TABLE 2 | Test odorants in functional analysis of MsepOR13 in *M. separate.*

Class	Odorant	CAS no.	Purity (%)	Class	Odorant	CAS no.	Purity (%)	Class	Odorant	CAS no.	Purity (%)
Terpenoid	β-Citronellol	106-22-9	95	Terpenoid	Cedrol	77-53-2	99	Aromatic	Ethyl benzoate	93-89-0	99
	Geraniol	106-24-1	98		β-Ionone	79-77-6	96		Butyl salicylate	2052-14-4	99
	(1S)-(−)-Verbenone	1196-01-6	93		Eucalyptol	13877-91-3	99		Methyl eugenol	93-15-2	98
	(S)-*cis*-Verbenol	18881-04-4	95		(R)-(−)-Piperitone	4573-50-6	94		δ-Decanolactone	705-86-2	98
	3,7-Dimethyl-3-octanol	78-69-3	98	Aromatic	Methyl benzoate	93-58-3	98	Alcohol	*cis*-3-Hexen-1-ol	928-96-1	98
	(1R)-(−)-Myrtenol	19894-97-4	95		4-Ethylbenzaldehyde	4748-78-1	99		*cis*-2-Hexen-1-ol	928-94-9	95
	(−)-*trans*-Pinocarveol	547-61-5	96		3-Vinylbenzaldehyde	19955-99-8	97		1-Heptanol	111-70-6	98
	(−)-Linalool	126-91-0	95		Benzaldehyde	100-52-7	99		1-Hexanol	111-27-3	98
	Linalool	78-70-6	97		4-Ethylacetophenone	937-30-4	97		*trans*-3-Hexen-1-ol	928-97-2	97
	Myrcene	123-35-3	95		Cinnamaldehyde	104-55-2	95		4-Hydroxy-4-methyl-2-pentanone	123-42-2	99
	(R)-(+)-Limonene	5989-27-5	97		Benzyl acetate	140-11-4	99		1-Octanol	111-87-5	98
	α-Pinene	80-56-8	98		Methyl salicylate	68917-75-9	99		*trans*-2-Hexen-1-ol	928-95-0	95
	(−)-β-Pinene	18172-67-3	99		2,6-Di-tert-butylphenol	128-39-2	99		1-Octen-3-ol	3391-86-4	98
	Camphene	79-92-5	95		Acetophenone	98-86-2	99	Ester	*cis*-3-Hexenyl acetate	3681-71-8	98
	(S)-(−)-Limonene	5989-54-8	95		Salicylaldehyde	90-02-8	98		*trans*-2-Hexenyl acetate	2497-18-9	98
	α-Terpinene	99-86-5	95		Methyl 2-methoxybenzoate	606-45-1	97		Geranyl acetate	105-87-3	97
	(−)-*trans*-Caryophyllene	87-44-5	98		Benzyl alcohol	100-51-6	99	Aldehyde	*trans*-2-Hexen-1-al	6728-26-3	95
	(−)-Caryophyllene oxide	1139-30-6	95		2-Phenylethanol	60-12-8	99		Heptanal	111-71-7	95
	Farnesene	502-61-4	98		4-Methoxybenzyl alcohol	105-13-5	98	Ketone	(±)-Camphor	76-22-2	98
	(1R)-(−)-Myrtenal	18486-69-6	97		Methyl phenylacetate	101-41-7	98		2-Pentadecanone	2345-28-0	95
	(±)-Citronellal	106-23-0	95		Eugenol	97-53-0	99		*cis*-Jasmone	488-10-8	94
	Ocimene	13877-91-3	90		Phenyl acetaldehyde	122-78-1	95				
	Nerolidol	40716-66-3	98		Methyl 4-hydroxybenzoate	99-76-3	99				

```
atggcggatattccaacggactattccacgttcgaaggatttagacctcactttaatgcg
 M  A  D  I  P  T  D  Y  S  T  F  E  G  F  R  P  H  F  N  A
ttggccagggtcggctatttcaaaatagtattgaagcctttgtctccaacgaagcgatct
 L  A  R  V  G  Y  F  K  I  V  L  K  P  L  S  P  T  K  R  S
ttacataacgcataccgttttatatgttcggcttttattttaacttacaatttgcaacac
 L  H  N  A  Y  R  F  I  C  S  A  F  I  L  T  Y  N  L  Q  H
gtcatacgggttattaaggtccgacacagtatcaatctgatagtggacacgctgttcata
 V  I  R  V  I  K  V  R  H  S  I  N  L  I  V  D  T  L  F  I
ctgctcaccacgctgaacacgctgggaaagcaagcagccttcaacctgaggacccatcgc
 L  L  T  T  L  N  T  L  G  K  Q  A  A  F  N  L  R  T  H  R
attgataatctcatcaccatcatcaacggacctatcttcgcagctagcaaagaataccac
 I  D  N  L  I  T  I  I  N  G  P  I  F  A  A  S  K  E  Y  H
gtggaagtgttaaaacaaaacgcgttgatgatgtcgcgtctcctggctttgtaccacggg
 V  E  V  L  K  Q  N  A  L  M  M  S  R  L  L  A  L  Y  H  G
gctatcttcagctgcgcttccatgtggaccatcttcccgatcgtcaacagacttctcggc
 A  I  F  S  C  A  S  M  W  T  I  F  P  I  V  N  R  L  L  G
acggaagtacagtttactggatactttccttttgaaactaccagtacgatggcattctcg
 T  E  V  Q  F  T  G  Y  F  P  F  E  T  T  S  T  M  A  F  S
ctggcattggcctacatgactattctgataactattcaagcttacggcaatgtaacaatg
 L  A  L  A  Y  M  T  I  L  I  T  I  Q  A  Y  G  N  V  T  M
gattgtacgattgtagcgttctacgcgcaagccaagatacaaatacagatgcttcgatac
 D  C  T  I  V  A  F  Y  A  Q  A  K  I  Q  I  Q  M  L  R  Y
aatctcgaacacctcctggagtgtgatgaaactaaaaggaaaagcattcagttaactaag
 N  L  E  H  L  L  E  C  D  E  T  K  R  K  S  I  Q  L  T  K
aggcccattcaatacacgtttatatcgatgaagaccaggagaaaaggggagatacaggac
 R  P  I  Q  Y  T  F  Y  I  D  E  D  Q  E  K  G  E  I  Q  D
agactcaagaaatgtgtgctgcattataatcaaatcttacggtttgccaaagaagtagaa
 R  L  K  K  C  V  L  H  Y  N  Q  I  L  R  F  A  K  E  V  E
tcgatatttggagaagcaatggtcatccaattctttgtgatggcctgggtaatatgtatg
 S  I  F  G  E  A  M  V  I  Q  F  F  V  M  A  W  V  I  C  M
acaatgtacaaaattgttgggttaagcatagtttcagcggagttcgtgtccatggccatg
 T  M  Y  K  I  V  G  L  S  I  V  S  A  E  F  V  S  M  A  M
tatttgggttgtatgctcgcccagctgtttatttactgctatttcgggacacaactcaaa
 Y  L  G  C  M  L  A  Q  L  F  I  Y  C  Y  F  G  T  Q  L  K
gttgagagcgagtcggtgaatcaatcgatatattgctccgactggctgcgcctgtccccg
 V  E  S  E  S  V  N  Q  S  I  Y  C  S  D  W  L  R  L  S  P
aggttccggagacaactcctcgtgatgatgcagtgctgtgagcgcccgctcacgcctcgg
 R  F  R  R  Q  L  L  V  M  M  Q  C  C  E  R  P  L  T  P  R
accgcatacgtcatccctatgtctttggacacctatataagcgtgctgagggcatcgtac
 T  A  Y  V  I  P  M  S  L  D  T  Y  I  S  V  L  R  A  S  Y
accttgtttacatttttgaatcgttaa
 T  L  F  T  F  L  N  R  -
```

FIGURE 1 | Nucleotide and amino acid sequences of the *MsepOR13* gene in *Mythimna separata*.

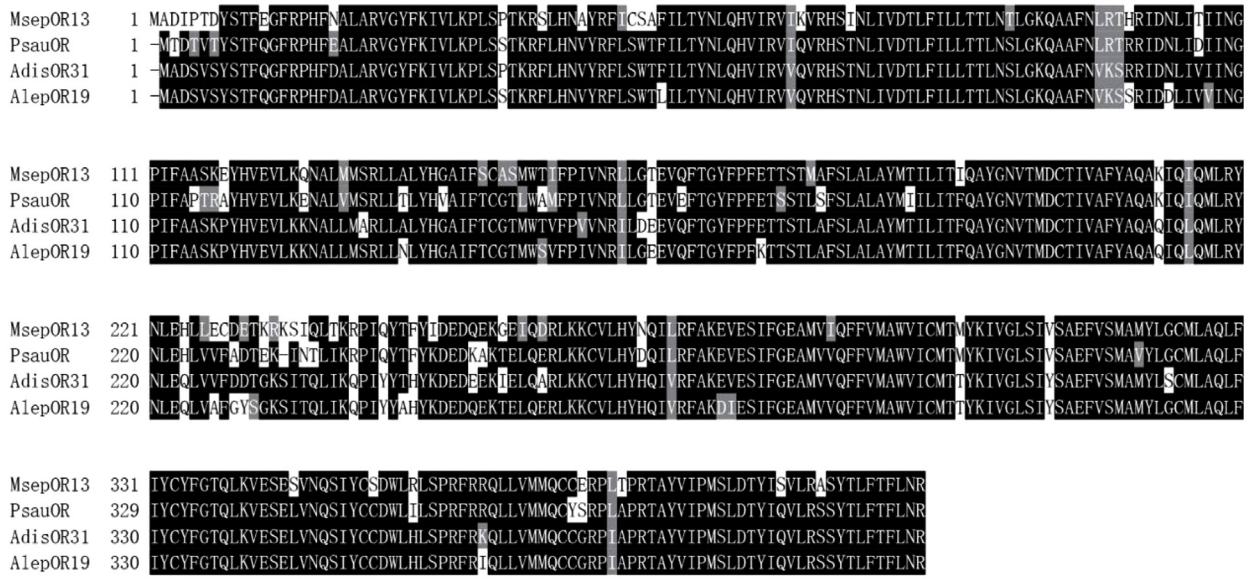

FIGURE 2 | Alignment of the amino acid sequences of MsepOR13 to those of its homologs in other species. Amino acids identical in all sequences are marked with black shading. Numbers to the right refer to the position of the last residue in a line in each odorant receptor (OR) sequence. The horizontal lines indicate the position of predicted transmembrane domains.

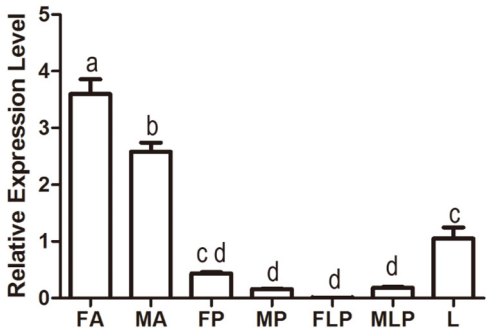

FIGURE 3 | Tissue- and sex-specific expression of *MsepOR13* in *M. separata*. FA, female antennae; MA, male antennae; FP, female proboscis; MP, male proboscis; FLP, female labial palp; MLP, male labial palp; L, legs (both sexes mixed). Error bars represent the standard error; those labeled with different letters are significantly different ($p < 0.05$, ANOVA, LSD).

of responses to different odors of MsepOR13 was assessed using ANOVA, followed by LSD tests.

Odorant Panel

Sixty-seven plant volatile compounds purchased from Sigma-Aldrich were used in this experiment (**Table 2**) and were classified into six groups: terpenoid, aromatic, alcohol, ester, aldehyde, and ketone. All compounds were dissolved in dimethyl sulfoxide (DMSO) at a concentration of 1 M as stock solutions. Before the experiments, the stock solutions were diluted in 1× Ringer's buffer to working concentrations, and 1× Ringer's buffer containing 0.1% DMSO was used as a negative control.

RESULTS

Gene Cloning and Sequence Analysis of MsepOR13

Based on the transcriptome of *M. separata* (Du et al., 2018), we obtained the full-length sequence of *MsepOR13*. It contained 1227 bp, encoding 408 amino acids (**Figure 1**) Three amino acid sequences from *P. saucia* (PsauOR, GenBank Accession No. AVF19631.1), *A. lepigone* (AlepOR19, GenBank Accession No. AOE48024.1), and *A. dissimilis* (AdisOR31, GenBank Accession No. ALM26220.1) were aligned with MsepOR13 (**Figure 2**) and found to have 84, 81, and 83% identity, respectively.

Tissue Expression Profiles of *MsepOR13*

Quantitative polymerase chain reaction was carried out to evaluate the expression profile of *MsepOR13* in different tissues of both sexes in *M. separata*. The results showed that *MsepOR13* was mainly expressed in antennae compared with other tissues and exhibited much higher relative expression level in female antennae than male antennae (**Figure 3**). *MsepOR13* was less expressed in proboscis and labial palp in both sexes and there was no significant difference in the expression levels of *MespOR13* between leg (mixture of female and male moths) and female proboscis.

Functional Characterization of MsepOR13 in the *Xenopus* Oocyte Expression System

The *Xenopus* oocyte expression system was used to identify candidate ligands for MespOR13. The cRNA of *MsepOR13* and

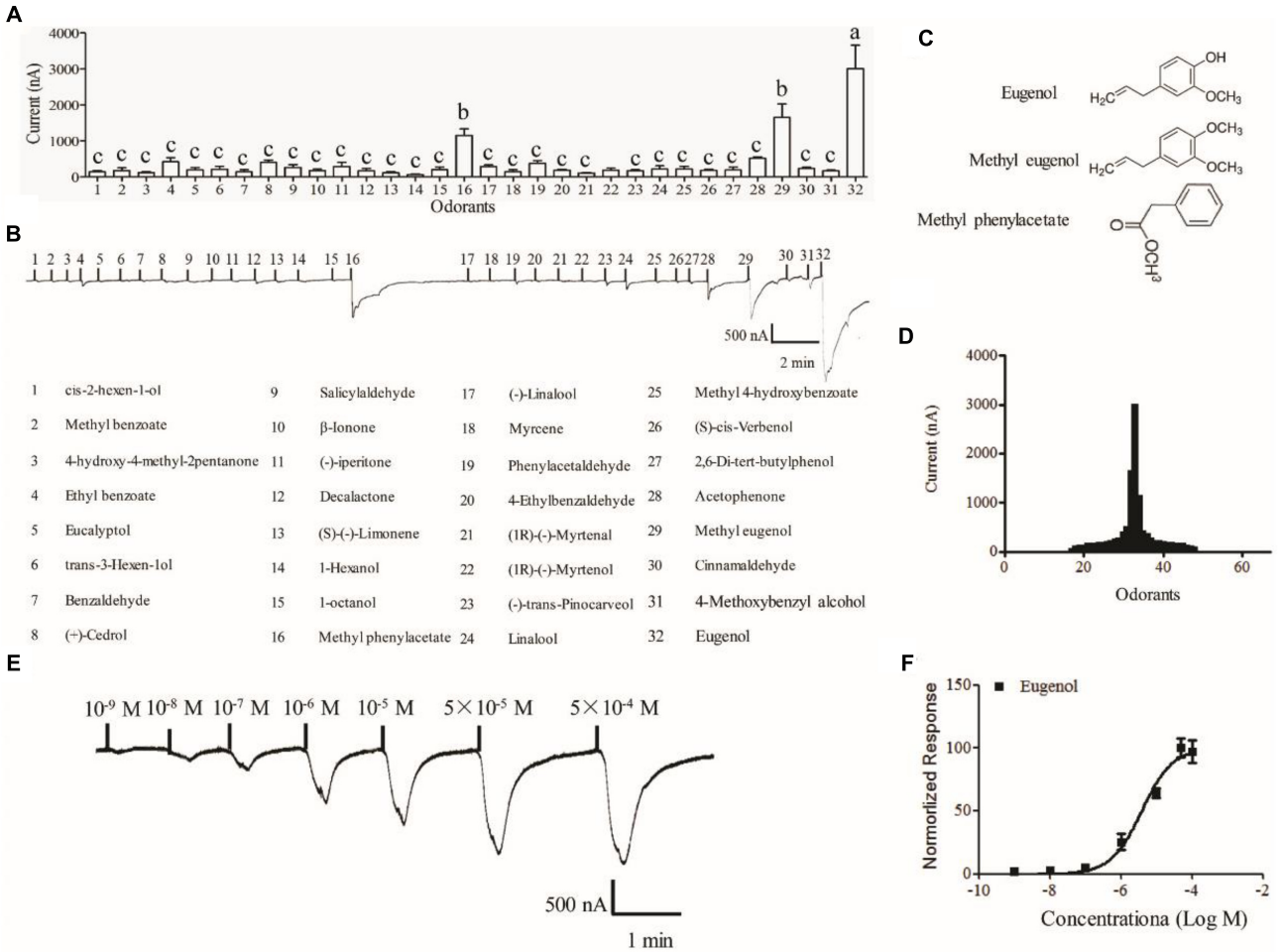

FIGURE 4 | Functional response of *Xenopus oocytes*, with co-expressed MsepOR13/Orco, to volatile compounds. **(A)** Response profile of MsepOR13/Orco *Xenopus oocytes*. Error bars indicate standard error of the mean and bars labeled with different letters are significantly different ($p < 0.001$, ANOVA, LSD, $N = 3$–8); **(B)** responses of MsepOR13/Orco *Xenopus* oocytes to odorants in 10^{-4} M solution; **(C)** structure of the main ligands of MsepOR13. **(D)** Tuning curve for the MsepOR13 for an odorant panel comprising 67 odorants, arranged along the x-axis according to the strength of the response they elicit. The odorants that elicited the strongest responses were placed near the center of the distribution, while those that elicit the weakest responses were placed near the edges. **(E)** MsepOR13/Orco *Xenopus* oocytes stimulated with a range of eugenol concentrations. **(F)** Dose–response curve of MsepOR13/Orco *Xenopus* oocytes with eugenol. Responses were normalized by defining the maximal response as 100. The response value is given as mean ± standard error ($N = 6$).

MespOrco were co-injected into *Xenopus* oocytes, and responses to 67 compounds were recorded using a two-electrode voltage clamp. MsepOR13 was tuned to 32 odorants from all six classes and was most sensitive to eugenol, with responses of about 3011 nA (**Figures 4A,B,D**). In addition, methyl eugenol and methyl phenylacetate elicited the second strongest responses, of about 1655 and 1150 nA, respectively (**Figures 4A,D**). Interestingly, these three main legends shared similar structure, a benzene ring (**Figure 4C**). The other 29 odorants elicited the same response level. Acetophenone elicited a relatively higher response (523.3 nA) and 1-hexanol elicited the lowest response with an amplitude of 60 nA (**Figures 4A,D**). In the dose–response study, *Xenopus* oocyte co-expressing MsepOR13/MsepORco responded to 10^{-9} M of eugenol and the peak amplitude occurred at the concentration of 10^{-5} M (**Figure 4E**). The EC50 value of eugenol was 3.91×10^{-6} M (**Figure 4F**).

DISCUSSION

Detection of chemical odors in the environment is essential for the survival of insects. Accordingly, insects have evolved remarkable sensitive and discriminatory olfactory systems for locating hosts and food sources, identifying mating partners and oviposition sites, or escaping predators (Schneider, 1969; Hansson and Stensmyr, 2011; Gadenne et al., 2016). Previous studies have shown that ORs play an important part in the recognition of odorants and the process of chemo-electrical transduction (Leal, 2013; Wicher, 2014; Bohbot and Pitts, 2015). In this study, we cloned an OR gene, *MsepOR13*, in *M. separata*. The sequence contained 1227 bp, encoding 408 amino acids. As showed in the qPCR experiment, MsepOR13 exhibited female antennae-biased expression, which suggested that it might play a vital role in regulating female-specific behaviors, such as

oviposition sites selection (Liu et al., 2015). Meanwhile, we found *MsepOR13* was also expressed in legs indicating that legs might assist insects to choose suitable oviposition sites. Previous studies found that female butterflies perceive oviposition stimulant by their foreleg tarsus and further determine the suitable feeding plant for larvae in *Papilio polytes* (Nakayama et al., 2003). Furtherly, 4 ORs were also identified by the legs transcriptome analysis in *Ectropis obliqua* (Ma et al., 2016), indicating that ORs expressed in legs was a ubiquitous phenomenon. During the past decade, the sex pheromone receptors have been well-deorphanized in many Lepidoptera species. However, the identification of ligands for the non-pheromone receptor ORs has significantly lagged behind, except for a few species such as *D. melanogaster* (Hallem et al., 2004; Kreher et al., 2005; Hallem et al., 2006), *A. gambiae* (Lu et al., 2007; Carey et al., 2010; Wang et al., 2010), and *S. littoralis* (Montagné et al., 2012; de Fouchier et al., 2017). In this study, MsepOR13 responded to 32 odorants and only three ligands elicited relative large response; this phenomenon was also found in studies of *S. littoralis* (de Fouchier et al., 2017) and *H. armigera* (Di et al., 2017). Narrowly tuned receptors are thought to be important in the detection of odors of high biological salience. In *D. melanogaster*, several ORs selectively responded to odors that are necessary and sufficient for vital behaviors such as avoiding toxic microbes and choosing oviposition sites (Stensmyr et al., 2012; Dweck et al., 2013, 2015; Ronderos et al., 2014). In mosquitoes, receptors that selectively respond to human emanations play a crucial part in host recognition and blood feeding (Hughes et al., 2010; Mcbride et al., 2014). Sex pheromone perception in moths also involves such specific pathways (Miura et al., 2010; Liu Y. et al., 2018). The homolog of MsepOR13 in *S. littoralis*, SlitOR31 shared 80% amino acid identity with MsepOR13. But SlitOR31 was narrowly tuned to eugenol, which is different from the function of MsepOR13. The difference of their function might relate with the different environment and the selective pressures they face.

In *M. separata*, the three main ligands containing a benzene ring were structurally similar; a similar phenomenon has been found in functional studies of ORs in *A. gambiae* (Wang et al., 2010), *S. littoralis* (de Fouchier et al., 2017), and *H. armigera* (Di et al., 2017). Among all the ligands, eugenol activated the strongest response in MsepOR13/Orco *Xenopus* oocytes, and could response at a 10^{-9} M concentration, with an EC50 value of 3.91×10^{-6} M. Actually, MspeOR13 responding to eugenol showed the similar sensitivity with the reported pheromone receptors to sex pheromones (Liu C. et al., 2013; Chang et al., 2016; Liu W. et al., 2018; Liu Y. et al., 2018), suggesting that eugenol might be important to *M. separata*. It has been reported that eugenol can repel the *H. armigera* moth (Xu, 2004), and also repel *Populus yunnanensis* oviposition (Ma et al., 2016). In *Tribilium castaneum*, eugenol has apparently repellent activity toward adults and toxic effects on both larvae and adults (Han and Huang, 2009). However, in *Mamestra brassicae*, eugenol was found to attract larvae and moths (Yan, 2015). The functions of eugenol with respect to *M. separata* require further study, especially behavioral experiments, in order to develop environmentally friendly approaches to control this economically significant insect. Based on the high sensitivity of MsepOR13 to eugenol, we predict that MsepOR13 may have an important role in the reception of eugenol in *M. separata*; thus, its function could be further explored using the CRISPR-Cas9 system.

AUTHOR CONTRIBUTIONS

KZ and YF designed the experiments. HY, KL, and NL carried out the experiments. LD and SG analyzed the experimental results. JW and GW wrote the manuscript.

FUNDING

This work was supported by the National Public Welfare Industry (Agriculture) Scientific Research of China (201403031), the National Key Research and Development Program of China (2017YFD0201807), and the Project of Agricultural Science and Technology Innovation.

REFERENCES

Bengtsson, J. M., Gonzalez, F., Cattaneo, A. M., Montagné, N., Walker, W. B., Bengtsson, M., et al. (2014). A predicted sex pheromone receptor of codling moth *Cydia pomonella* detects the plant volatile pear ester. *Front. Ecol. Evol.* 2:33. doi: 10.3389/fevo.2014.00033

Bentley, M. D., and Day, J. F. (1989). Chemical ecology and behavioral aspects of mosquito oviposition. *Annu. Rev. Entomol.* 34, 401–421. doi: 10.1146/annurev.en.34.010189.002153

Benton, R., Sachse, S., Michnick, S., and Vosshall, L. (2006). Atypical membrane topology and heteromeric function of *Drosophila* odorant receptors in vivo. *PLoS. Biol.* 4:e20. doi: 10.1371/journal.pbio.0040020

Bohbot, J. D., and Pitts, R. J. (2015). The narrowing olfactory landscape of insect odorant receptors. *Front. Ecol. Evol.* 3:39. doi: 10.3389/fevo.2015.00039

Bruce, T. J., Wadhams, L. J., and Woodcock, C. M. (2005). Insect host location: a volatile situation. *Trends Plant Sci.* 10, 269–274. doi: 10.1016/j.tplants.2005.04.003

Bruyne, M. D., and Baker, T. C. (2008). Odor detection in insects: volatile codes. *J. Chem. Ecol.* 34, 882–897. doi: 10.1007/s10886-008-9485-4

Buck, L., and Axel, R. (1991). A novel multigene family may encode odorant receptors: a molecular basis for odor recognition. *Cell* 65, 175–187. doi: 10.1016/0092-8674(91)90418-X

Butterwick, J. A., Del Mármol, J., Kim, K. H., Kahlson, M. A., Rogow, J. A., Walz, T., et al. (2018). Cryo-EM structure of the insect olfactory receptor Orco. *Nature* 560, 447–452. doi: 10.1038/s41586-018-0420-8

Cao, S., Liu, Y., Guo, M., and Wang, G. (2016). A conserved odorant receptor tuned to floral volatiles in three *Heliothinae* species. *PLoS One* 11:e0155029. doi: 10.1371/journal.pone.0155029

Carey, A. F., Guirong, W., Chih-Ying, S., Zwiebel, L. J., and Carlson, J. R. (2010). Odorant reception in the malaria mosquito *Anopheles gambiae*. *Nature* 464, 66–71. doi: 10.1093/nar/gkt484

Cattaneo, A. M., Gonzalez, F., Bengtsson, J. M., Corey, E. A., Jacquinjoly, E., Montagné, N., et al. (2017). Candidate pheromone receptors of codling moth *Cydia pomonella* respond to pheromones and kairomones. *Sci. Rep.* 7:41105. doi: 10.1038/srep41105

Chang, H., Guo, M., Bing, W., Yang, L., Dong, S., and Wang, G. (2016). Sensillar expression and responses of olfactory receptors reveal different peripheral coding in two *Helicoverpa* species using the same pheromone components. *Sci. Rep.* 6:18742. doi: 10.1038/srep18742

Clyne, P. J., Warr, C. G., Freeman, M. R., Lessing, D., Kim, J., and Carlson, J. R. (1999). A novel family of divergent seven-transmembrane proteins : candidate odorant receptors in *Drosophila*. *Neuron* 22, 327–338. doi: 10.1016/S0896-6273(00)81093-4

Cui, W. C., Bing, W., Guo, M. B., Liu, Y., Jacquin-Joly, E., Yan, S. C., et al. (2018). A receptor-neuron correlate for the detection of attractive plant volatiles in *Helicoverpa assulta* (*Lepidoptera: Noctuidae*). *Insect Biochem. Mol. Biol.*

de Fouchier, A., Montagnã©, N., Steiner, C., Binyameen, M., Schlyter, F., Chertemps, T., et al. (2017). Functional evolution of *Lepidoptera* olfactory receptors revealed by deorphanization of a moth repertoire. *Nat. Commun.* 8:15709. doi: 10.1038/ncomms15709

Di, C., Ning, C., Huang, L. Q., and Wang, C. Z. (2017). Design of larval chemical attractants based on odorant response spectra of odorant receptors in the cotton bollworm. *Insect Biochem. Mol. Biol.* 84, 48–62. doi: 10.1016/j.ibmb.2017.03.007

Dobritsa, A. A., van der Goes van Naters, W., Warr, C. G., Steinbrecht, R. A., and Carlson, J. R. (2003). Integrating the molecular and cellular basis of odor coding in the *Drosophila* antenna. *Neuron* 37, 827–841. doi: 10.1016/S0896-6273(03)00094-1

Du, L., Zhao, X., Liang, X., Gao, X., Liu, Y., and Wang, G. (2018). Identification of candidate chemosensory genes in *Mythimna separata* by transcriptomic analysis. *BMC Genomics* 19:518. doi: 10.1186/s12864-018-4898-0

Duan, Y., Gong, Z., Wu, R., Miao, J., Jiang, Y., Li, T., et al. (2017). Transcriptome analysis of molecular mechanisms responsible for light-stress response in *Mythimna separata* (Walker). *Sci. Rep.* 7:45188. doi: 10.1038/srep45188

Dweck, H. M., Ebrahim, S. M., Farhan, A., Hansson, B., and Stensmyr, M. (2015). Olfactory proxy detection of dietary antioxidants in *Drosophila*. *Curr. Biol.* 25, 455–466. doi: 10.1016/j.cub.2014.11.062

Dweck, H. M., Ebrahim, S. M., Kromann, S., Bown, D., Hillbur, Y., Sachse, S., et al. (2013). Olfactory preference for egg laying on citrus substrates in *Drosophila*. *Curr. Biol.* 23, 2472–2480. doi: 10.1016/j.cub.2013.10.047

Engsontia, P., Sanderson, A. P., Cobb, M., Walden, K. K., Robertson, H. M., and Brown, S. (2008). The red flour beetle's large nose: an expanded odorant receptor gene family in *Tribolium castaneum*. *Insect Biochem. Mol. Biol.* 38, 387–397. doi: 10.1016/j.ibmb.2007.10.005

Ewald, G. W., Thomas, G., Elisabeth, B., Heinz, B., and Jürgen, K. (2010). Candidate pheromone receptors provide the basis for the response of distinct antennal neurons to pheromonal compounds. *Eur. J. Neurosci.* 25, 2364–2373. doi: 10.1111/j.1460-9568.2007.05512.x

Fleischer, J., Pregitzer, P., Breer, H., and Krieger, J. (2017). Access to the odor world: olfactory receptors and their role for signal transduction in insects. *Cell Mol. Life. Sci.* 75, 485–508. doi: 10.1007/s00018-017-2627-5

Gadenne, C., Barrozo, R. B., and Anton, S. (2016). Plasticity in insect olfaction: to smell or not to smell? *Annu. Rev. Entomol.* 61, 317–333. doi: 10.1146/annurev-ento-010715-023523

Gonzalez, F., Bengtsson, J. M., Walker, W. B., Sousa, M. F. R., Cattaneo, A. M., Montagné, N., et al. (2015). A conserved odorant receptor detects the same 1-Indanone analogs in a tortricid and a noctuid moth. *Front. Ecol. Evol.* 3:131. doi: 10.3389/fevo.2015.00131

Gonzalez, F., Witzgall, P., and Walker, W. B. (2016). Protocol for heterologous expression of insect odourant receptors in *Drosophila*. *Front. Ecol. Evol.* 4:24. doi: 10.3389/fevo.2016.00024

Grosse-Wilde, E., Kuebler, L. S., Bucks, S., Vogel, H., Wicher, D., and Hansson, B. S. (2011). Antennal transcriptome of *Manduca sexta*. *Proc. Natl. Acad. Sci. U.S.A.* 108, 7449–7454. doi: 10.1073/pnas.1017963108

Hallem, E., Dahanukar, A., and Carlson, J. (2006). Insect odor and taste receptors. *Annu. Rev. Entomol.* 51, 113–135. doi: 10.1016/j.inoche.2009.11.022

Hallem, E. A., Ho, M. G., and Carlson, J. R. (2004). The molecular basis of odor coding in the *Drosophila* antenna. *Cell* 117, 965–979. doi: 10.1016/j.cell.2004.05.012

Han, Q., and Huang, S. (2009). The bioactivity of eugenol against the red flour beetle *Tribolium castaneum*. *J. Chongqing Normal Univ*. 26, 16–19. doi: 10.3969/J.ISSN.1672-6693.2009.03.005

Hansson, B., and Stensmyr, M. (2011). Evolution of insect olfaction. *Neuron* 72, 698–711. doi: 10.1016/j.neuron.2011.11.003

Hughes, D. T., Pelletier, J., Luetje, C. W., and Leal, W. S. (2010). Odorant Receptor from the southern house mosquito narrowly tuned to the oviposition attractant skatole. *J. Chem. Ecol.* 36, 797–800. doi: 10.1007/s10886-010-9828-9

Jiang, X., Luo, L., Zhang, L., Sappington, T. W., and Hu, Y. (2011). Regulation of migration in *Mythimna separata* (Walker) in China: a review integrating environmental, physiological, hormonal, genetic, and molecular factors. *Environ. Entomol.* 40, 516–533. doi: 10.1603/EN10199

Koji, S., Maurizio, P., Takao, N., Tatsuro, N., Vosshall, L. B., and Kazushige, T. (2008). Insect olfactory receptors are heteromeric ligand-gated ion channels. *Nature* 452, 1002–1006. doi: 10.1038/nature06850

Kreher, S. A., Jae Young, K., and Carlson, J. R. (2005). The molecular basis of odor coding in the *Drosophila* larva. *Neuron* 46, 445–456. doi: 10.1016/j.neuron.2005.04.007

Leal, W. S. (2013). Odorant reception in insects: roles of receptors, binding proteins, and degrading enzymes. *Annu. Rev. Entomol.* 58, 373–391. doi: 10.1146/annurev-ento-120811-153635

Leary, G. P., Allen, J. E., Bunger, P. L., Luginbill, J. B., Linn, C. E., Macallister, I. E., et al. (2012). Single mutation to a sex pheromone receptor provides adaptive specificity between closely related moth species. *Proc. Natl. Acad. Sci. U.S.A.* 109, 14081–14086. doi: 10.1073/pnas.1204661109

Lihuang, K., Zhang, Z., Kim, K., Huang, Q., and Lei, C. (2017). Antennal and behavioral responses of *Mythimna separata* (Walker) to three plant volatiles. *Environ. Sci. Pollut. Res. Int.* 24, 24953–24964. doi: 10.1007/s11356-017-0140-x

Liu, C., Liu, Y., Guo, M., Cao, D., Dong, S., and Wang, G. (2014). Narrow tuning of an odorant receptor to plant volatiles in *Spodoptera exigua* (Hübner). *Insect Mol. Biol.* 23, 487–496. doi: 10.1111/imb.12096

Liu, C., Liu, Y., Walker, W. B., Dong, S., and Wang, G. (2013). Identification and functional characterization of sex pheromone receptors in beet armyworm *Spodoptera exigua* (Hübner). *Insect Biochem. Mol. Biol.* 43, 747–754. doi: 10.1016/j.ibmb.2013.05.009

Liu, W., Jiang, X. C. W., Cao, S., Yang, B., and Wang, G. R. (2018). Functional studies of sex pheromone receptors in asian corn borer *Ostrinia furnacalis*. *Front. Physiol.* 9:591. doi: 10.3389/fphys.2018.00591

Liu, Y., Gu, S., Zhang, Y., Guo, Y., and Wang, G. (2012). Candidate olfaction genes identified within the *Helicoverpa armigera* antennal transcriptome. *PLoS One* 7:e48260. doi: 10.1371/journal.pone.0048260

Liu, Y., Liu, C., Lin, K., and Wang, G. (2013). Functional specificity of sex pheromone receptors in the cotton bollworm *Helicoverpa armigera*. *PLoS One* 8:e62094. doi: 10.1371/journal.pone.0062094

Liu, Y., Liu, Y., Jiang, X., and Wang, G. (2018). Cloning and functional characterization of three new pheromone receptors from the diamondback moth, *Plutella xylostella*. *J. Insect. Physiol.* 107, 14–22. doi: 10.1016/j.jinsphys.2018.02.005

Liu, Y., Sun, L., Cao, D., Walker, W., Zhang, Y., and Wang, G. (2015). Identification of candidate olfactory genes in *Leptinotarsa decemlineata* by antennal transcriptome analysis. *Front. Ecol. Evol.* 3:60. doi: 10.3389/fevo.2015.00060

Liu, Z., Wang, X., Lei, C., and Zhu, F. (2017). Sensory genes identification with head transcriptome of the migratory armyworm, *Mythimna separata*. *Sci. Rep.* 7:46033. doi: 10.1038/srep46033

Lu, T., Qiu, Y. T., Wang, G., Kwon, J. Y., Rutzler, M., Kwon, H. W., et al. (2007). Odor coding in the maxillary palp of the malaria vector mosquito *Anopheles gambiae*. *Curr. Biol.* 17, 1533–1544. doi: 10.1016/j.cub.2007.07.062

Lv, M., Wu, W., and Liu, H. (2014). Effects of fraxinellone on the midgut enzyme activities of the 5th instar larvae of oriental armyworm, *Mythimna separata* walker. *Toxins* 6, 2708–2718. doi: 10.3390/toxins6092708

Ma, Y., Zhang, X., Xu, Y., and Xiao, C. (2016). Effect of volatiles from *Populus yunnanensis* on oviposition preference of patato tuber moth, *Phthorimaea operculell*. *Plant Prot.* 42, 99–103. doi: 10.3969/j.issn.0529-1542.2016.02.017

Mcbride, C. S., Felix, B., Omondi, A. B., Spitzer, S. A., Joel, L., Rosemary, S., et al. (2014). Evolution of mosquito preference for humans linked to an odorant receptor. *Nature* 515, 222–227. doi: 10.1038/nature13964

Mitsuno, H., Sakurai, T. M., Yasuda, T., Kugimiya, S., Ozawa, R., Toyohara, H., et al. (2010). Identification of receptors of main sex-pheromone components of three *Lepidopteran* species. *Eur. J. Neurosci.* 28, 893–902. doi: 10.1111/j.1460-9568.2008.06429.x

Miura, N., Nakagawa, T., Touhara, K., and Ishikawa, Y. (2010). Broadly and narrowly tuned odorant receptors are involved in female sex pheromone reception in *Ostrinia moths*. *Insect Biochem. Mol. Biol.* 40, 64–73. doi: 10.1016/j.ibmb.2009.12.011

Montagné, N., Chertemps, T., Brigaud, I., François, A., François, M. C., de Fouchier, A., et al. (2012). Functional characterization of a sex pheromone receptor in the pest moth *Spodoptera littoralis* by heterologous expression in *Drosophila*. *Eur. J. Neurosci.* 36, 2588–2596. doi: 10.1111/j.1460-9568.2012.08183.x

Nakagawa, T., Sakurai, T., Nishioka, T., and Touhara, K. (2005). Insect sex-pheromone signals mediated by specific combinations of olfactory receptors. *Science* 307, 1638–1642. doi: 10.1126/science.1106267

Nakayama, T., Honda, K., Ômura, H., and Hayashi, N. (2003). Oviposition stimulants for the tropical swallowtail butterfly, Papilio polytes, feeding on a rutaceous plant, *Toddalia asiatica*. *J. Chem. Ecol.* 29, 1621–1634. doi: 10.1023/a:1024274814402

Robertson, H. M., and Wanner, K. W. (2006). The chemoreceptor superfamily in the honey bee, *Apis mellifera*: expansion of the odorant, but not gustatory, receptor family. *Genome. Res.* 16, 1395–1403. doi: 10.1101/gr.5057506

Ronderos, D. S., Chun-Chieh, L., Potter, C. J., and Smith, D. P. (2014). Farnesol-detecting olfactory neurons in *Drosophila*. *J. Neurosci.* 34, 3959–3968. doi: 10.1523/jneurosci.4582-13.2014

Sakurai, T., Mitsuno, H., Haupt, S. S., Uchino, K., Yokohari, F., Nishioka, T., et al. (2011). A single sex pheromone receptor determines chemical response specificity of sexual behavior in the silkmoth *Bombyx mori*. *PLoS Genetics* 7:e1002115. doi: 10.1371/journal.pgen.1002115

Sakurai, T., Nakagawa, T. H., Mori, H., Endo, Y., Tanoue, S., Yasukochi, Y., et al. (2004). Identification and functional characterization of a sex pheromone receptor in the silkmoth *Bombyx mori*. *Proc. Natl. Acad. Sci. U.S.A.* 101, 16653–16658. doi: 10.1073/pnas.0407596101

Schneider, D. (1969). Insect olfaction: deciphering system for chemical messages. *Science* 163, 1031–1037. doi: 10.1126/science.163.3871.1031

Schneider, D. (1992). 100 years of pheromone research - an essay on *Lepidoptera*. *Naturwissenschaften* 79, 241–250. doi: 10.1007/BF01175388

Sharma, H. C., and Davies, J. C. (1983). *The Oriental Armyworm, Mythimna Separata (Walker). Distribution, Biology and Control: a Literature Review. Miscellaneous Reports – Centre for Overseas Pest Research (UK)*. London: Overseas Development Administration.

Steinbrecht, R. A. (1997). Pore structures in insect olfactory sensilla: a review of data and concepts. *Int. J. Insect Morphol. Embryol.* 26, 229–245. doi: 10.1016/s0020-7322(97)00024-x

Stensmyr, M., Dweck, H. M., Farhan, A., Ibba, I., Strutz, A., Mukunda, L., et al. (2012). A conserved dedicated olfactory circuit for detecting harmful microbes in *Drosophila*. *Cell* 151, 1345–1357. doi: 10.1016/j.cell.2012.09.046

Sun, M., Liu, Y., Walker, W. B., Liu, C., Lin, K., Gu, S., et al. (2013). Identification and characterization of pheromone receptors and interplay between receptors and pheromone binding proteins in the diamondback moth. *Plutella xyllostella*. *PLoS One* 8:e62098. doi: 10.1371/journal.pone.0062098

Vogt, R. G. (2003). Biochemical diversity of odor detection: OBPs, ODEs and SNMPs. *Insect Pheromone Biochem. Mol. Biol.* 2003, 391–445. doi: 10.1016/B978-012107151-6/50016-5

Vosshall, L. B., Amrein, H., Morozov, P. S., Rzhetsky, A., and Axel, R. (1999). A spatial map of olfactory receptor expression in the Drosophila antenna. *Cell* 96, 725–736. doi: 10.1016/S0092-8674(00)80582-6

Wang, B., Liu, Y., He, K., and Wang, G. (2016). Comparison of research methods for functional characterization of insect olfactory receptors. *Sci. Rep.* 6:32806. doi: 10.1038/srep32806

Wang, G., Vásquez, G. M., Schal, C., Zwiebel, L. J., and Gould, F. (2011). Functional characterization of pheromone receptors in the tobacco budworm *Heliothis virescens*. *Insect Mol. Biol.* 20, 125–133. doi: 10.1111/j.1365-2583.2010.01045.x

Wang, G. R., Carey, A. F., Carlson, J. R., and Zwiebel, L. J. (2010). Molecular basis of odor coding in the malaria vector mosquito *Anopheles gambiae*. *Proc. Natl. Acad. Sci. U.S.A.* 107, 4418–4423. doi: 10.1073/pnas.0913392107

Wanner, K. W., Nichols, A. S., Allen, J. E., Bunger, P. L., Garczynski, S. F., Linn, C. E., et al. (2010). Sex pheromone receptor specificity in the European corn borer moth, *Ostrinia nubilalis*. *PLoS One* 5:e8685. doi: 10.1371/journal.pone.0008685

Wei, Z. H. (1985). Preliminary report on the sex pheromone of the armyworm *Mythimna separata*. *Acta Entomol. Sin.* 28, 348–350. doi: 10.16380/j.kcxb.1985.03.018

Wicher, D. (2014). Olfactory signaling in insects. *Prog. Mol. Biol. Transl. Sci.* 130, 37–54. doi: 10.1016/bs.pmbts.2014.11.002

Wicher, D., Schäfer, R., Bauernfeind, R., Stensmyr, M. C., Heller, R., Heinemann, S. H., et al. (2008). *Drosophila* odorant receptors are both ligand-gated and cyclic-nucleotide-activated cation channels. *Nature* 452, 1007–1011. doi: 10.1038/nature06861

Xu, Y. (2004). *The Test Of Components which trap Helicoverpa armigera and the design of contstitute*. Master's thesis, Henan Agricultural University, Henan.

Yan, H. (2015). *Aritificial Breeding and control Technology of Mamestra Brassicae*. Master's thesis, Henan Agricultural University, Henan.

Yuji, Y., Nami, M., Ryo, N., Ken, S., and Yukio, I. (2011). Sex-linked pheromone receptor genes of the European corn borer, *Ostrinia nubilalis*, are in tandem arrays. *PLoS One* 6:e18843. doi: 10.1371/journal.pone.0018843

Zhang, J., Wang, B., Dong, S., Cao, D., Dong, J., Walker, W. B., et al. (2015a). Antennal transcriptome analysis and comparison of chemosensory gene families in two closely related noctuidae moths, *Helicoverpa armigera* and *H. assulta*. *PLoS One* 10:e0117054. doi: 10.1371/journal.pone.0117054

Zhang, J., Yan, S., Liu, Y., Jacquinjoly, E., Dong, S., and Wang, G. (2015b). Identification and functional characterization of sex pheromone receptors in the common cutworm (*Spodoptera litura*). *Chem. Sens.* 40, 7–16. doi: 10.1093/chemse/bju052

Zhu, P., Kong, F., and Yu, Y. (1987). Sex pheromone of oriental armyworm *Mythimna separata* Walker. *J. Chem. Ecol.* 13, 977–981. doi: 10.1007/BF01020531

Conflict of Interest Statement: The authors declare that the research was conducted in the absence of any commercial or financial relationships that could be construed as a potential conflict of interest.

frontiers in Physiology

ORIGINAL RESEARCH
published: 18 April 2019
doi: 10.3389/fphys.2019.00434

The Sensory Machinery of the Head Louse *Pediculus humanus capitis*: From the Antennae to the Brain

*Isabel Ortega Insaurralde[1], Sebastián Minoli[2], Ariel Ceferino Toloza[1], María Inés Picollo[1] and Romina B. Barrozo[2]**

[1]Centro de Investigaciones de Plagas e Insecticidas (CIPEIN), CONICET- CITEDEF, Buenos Aires, Argentina, [2]Laboratorio Fisiología de Insectos, Departamento Biodiversidad y Biología Experimental (DBBE), Facultad Ciencias Exactas y Naturales, Instituto Biodiversidad y Biología Experimental y Aplicada (IBBEA, CONICET-UBA), Universidad de Buenos Aires, Buenos Aires, Argentina

Insect antennae are sophisticated sensory organs, usually covered with sensory structures responsible for the detection of relevant signals of different modalities coming from the environment. Despite the relevance of the head louse *Pediculus humanus capitis* as a human parasite, the role of its antennal sensory system in the highly dependent relation established with their hosts has been barely studied. In this work, we present a functional description of the antennae of these hematophagous insects by applying different approaches, including scanning electron microscopy (SEM), anterograde antennal fluorescent backfills, and behavioral experiments with intact or differentially antennectomized lice. Results constitute a first approach to identify and describe the head louse antennal sensilla and to determine the role of the antenna in host recognition. SEM images allowed us to identify a total of 35–40 sensilla belonging to seven different morphological types that according to their external architecture are candidates to bear mechano-, thermo-, hygro-, or chemo-receptor functions. The anterograde backfills revealed a direct neural pathway to the ipsilateral antennal lobe, which includes 8–10 glomerular-like diffuse structures. In the two-choice behavioral experiments, intact lice chose scalp chemicals and warm surfaces (i.e., 32°C) and avoided wet substrates. Behavioral preferences disappeared after ablation of the different flagellomeres of their antenna, allowing us to discuss about the location and function of the different identified sensilla. This is the first study that integrates morphological and behavioral aspects of the sensory machinery of head lice involved in host perception.

Keywords: head louse, *Pediculus humanus capitis*, host perception, behavior, antennal lobe, sensilla

OPEN ACCESS

Edited by:
Philippe Lucas, Institut National de la Recherche Agronomique (INRA), France

Reviewed by:
Jérôme Casas, Université de Tours, France
Bente Gunnveig Berg, Norwegian University of Science and Technology, Norway

***Correspondence:**
Romina B. Barrozo
rbarrozo@bg.fcen.uba.ar

Specialty section:
This article was submitted to Invertebrate Physiology, a section of the journal Frontiers in Physiology

Received: *21 December 2018*
Accepted: *29 March 2019*
Published: *18 April 2019*

Citation:
Ortega Insaurralde I, Minoli S, Toloza AC, Picollo MI and Barrozo RB (2019) The Sensory Machinery of the Head Louse Pediculus humanus capitis: From the Antennae to the Brain. Front. Physiol. 10:434. doi: 10.3389/fphys.2019.00434

INTRODUCTION

Lice are members of the order Phthiraptera, which contains nearly 5,000 species of wingless insects. They are obligate ectoparasites, living exclusively on their warm-blooded hosts. Due to the massive infestations found in children's heads of all around the world, the head louse *Pediculus humanus capitis* gains its sanitary and epidemiological relevance. This fact was reflected in the increasing number of studies found in the literature including toxicological, evolutionary,

and genetic aspects of the biology of these hematophagous insects (Kirkness et al., 2010; Toloza et al., 2010, 2018; Olds et al., 2012; Veracx and Raoult, 2012; Bressa et al., 2015; Tovar-Corona et al., 2015; Boyd et al., 2017). However, much less information is available about how these insects exploit sensory cues released by their hosts to make appropriate feeding decisions.

Besides the eyes, the antennae of insects are the main peripheral sensory organs involved in the detection of external cues relevant to their lives, such as host odors, sexual pheromones, or refuge signals, among other. Along their surfaces, a variable number of sensilla adapted to assess different modalities of stimuli are present. Irrespectively of their form and function, all sensilla are cuticular structures that encapsulate and protect neurons, which in response to the detection of specific stimuli trigger electrical signals that travel to primary relay centers in the brain (i.e., the antennal lobes, antennal mechano-sensory and motor centers, tritocerebrum, and the gnathal ganglion), where the processing of the incoming information begins. Then, further integration at higher brain centers will allow in return a stereotyped motor behavior. As a general rule, the architecture of the sensory machinery of a given species is strongly tuned to maximize the communication with their environment, for what the functional study of their sensory structures gives the opportunity to speculate about the natural habits and preferences of the individuals.

A pioneer work of Wigglesworth (1941) showed that the body louse, *Pediculus humanus humanus,* is responsive to host odors, temperature, humidity, light, and contact cues. Later morphological studies of their antenna evinced the presence of chemo-, mechano-, and thermo-hygroreceptors (Keilin and Nuttall, 1930; Miller, 1969; Slifer and Sekhon, 1980; Steinbrecht, 1994). Recently, the first functional evidences about the role of odorant receptor (OR) genes of body and head lice were reported (Pelletier et al., 2015). Although no ORs tuned to host-related isolated compounds were found, it was shown that PhumOR2 responds to a narrow set of repellent compounds (Pelletier et al., 2015). Additionally, Crespo and Vickers (2012) found that the antennae of the chewing slender pigeon louse, *Columbicola columbae*, hold few sensilla and that the antennal sensory neurons project to aglomerular antennal lobes in the brain, suggesting a simplification of their sensory machinery.

This work aimed to gain an insight into the sensory biology of the head louse *P. humanus capitis* as a first approach to understand the sensory modalities detected by the antenna related to host perception. We investigated the external morphology of its antennae. Then, we performed anterograde antennal stainings to identify and follow neural projections up to central brain structures. Finally, we studied the effect of removing different segments of the antennae on the behavior of head lice confronted to different host stimuli (i.e., scalp chemicals, humidity, and heat).

MATERIALS AND METHODS

Insects

Head lice *P. humanus capitis* were used throughout this study. Insects were collected by dry combing the hair of children that regularly attend to elementary schools in Buenos Aires, Argentine. Once collected, head lice were transported to the laboratory according to the protocol developed by Picollo et al. (1998), which was approved by an *ad hoc* committee belonging to the Centro de Investigaciones de Plagas e Insecticidas (CONICET-CITEDEF), Buenos Aires, Argentina. Only females were selected at the laboratory for the bioassays due to their abundance and big size. Insects were individually examined under a stereomicroscope and discarded if damaged. Then, they were transferred to an environmental chamber at 18 ± 0.5°C, 70–80 ± 1% relative humidity (RH) in the dark until the experiments. The period between collection and the start of the experiments was no longer than 2 h.

Morphology of the Antenna: Scanning Electron Microscopy

Intact females were immersed in 70% ethanol for 24 h at 22 ± 1°C. Specimens were then mounted on aluminum stubs with double-sided sticky tape and coated with gold-palladium. The antennae were then examined under a scanning electron microscope (Carl Zeiss NTS SUPRA 40, Centro de Microscopía Avanzada, Facultad de Ciencias Exactas y Naturales, Universidad de Buenos Aires). Length and diameter of different sensory structures of the antenna from 10 individuals were measured using the software Image J (National Institutes of Health, USA, https://imagej.nih.gov/ij/).

Neural Projections: Anterograde Antennal Backfills

Live females were ventrally glued to a double-sided taped slide leaving their antennae free. Both antennae were then cutoff between the pedicel and the first flagellomere by using dissection micro-scissors under a stereoscopic microscope, and their opened tips were immediately inserted inside the glass capillaries filled with 1% neurobiotin (Neurobiotin Tracer®, Vector Laboratories, Burlingame, USA) in 0.25 M KCl. Then, live insects were maintained inside the closed Petri dishes with a wet cotton (to assure the maintenance of a humid ambient) during 6 h to allow the neuronal tracer to diffuse through the antennal nerves. After this time, the brains were dissected in Millonig's buffer and fixed in 4% paraformaldehyde overnight at 4°C. Then, brains were rinsed in Millonig's buffer and dehydrated and rehydrated through an ethanol series and propylene oxide (Barrozo et al., 2009). Samples were then incubated in Oregon Green-avidin (Oregon green® 488 conjugate A6374, Molecular probes, OR, USA) with 0.2% Triton X and 1% BSA overnight at 4°C.

All preparations were cleared and mounted in Vectashield medium (Vectashield Mounting Medium®, Vector laboratories, USA), and afterward, whole mounts were optically sectioned with a laser scanning confocal microscope (Olympus FV300/BX61). Following confocal scanning of the brains, 3D reconstructions of stacks of three brains were carried out by using Reconstruct © (v1.1.0.0 by John C. Fiala).

Antennal Excisions and Behavioral Assays

On the basis of the morphological studies carried out in section "Morphology of the Antenna: Scanning Electron Microscopy,"

it was possible to distinguish three flagellomeres forming the flagellum, where most of the sensilla were found. In order to study the role of the sensilla present in the different flagellomeres in the response to host-related stimuli, excisions at different levels were carried out. In all cases, the surgery was performed 2 h before the behavioral experiments with a pair of micro-scissors on immobilized lice under a stereoscopic microscope. Individuals were randomly assigned to one of four treatments: (1) *INT*: intact animals with both complete antennae, (2) *F3-*: animals without the third flagellomeres of both antennae, (3) *F2F3-*: animals without the second and third flagellomeres of both antennae, and (4) *1ANT*: animals with one intact antenna and the other without the second and third flagellomeres. Because ablation of flagellomeres/s could affect lice behavior, *1ANT* served as a surgery control group.

The responses of lice to three host-related stimuli (i.e., scalp chemicals, humidity, and heat) were examined in two-choice walking experiments performed in an experimental room under controlled light intensity (20 ± 1 lux), constant temperature (22 ± 1°C), and ambient relative humidity (50 ± 1%). A circular arena (5.5 cm diameter) covered with a filter paper as substrate was divided into two equal zones. A particular stimulus was added at one zone of the arena, while the opposite was maintained as the corresponding control side (see below for details). In each assay, a louse was released at the center of the arena, and its spatial behavior was recorded during 5 min with the aid of a video camera (KIR-J639CE20, Sony, China) connected to a digital video recorder (DVR5104HE, Dahua Technology Co. ltd, Hangzhou, China). A minimum of 15 replicates were carried out for each experimental series. The position of the stimulus was switched between left and right zones in a pseudorandom manner in order to avoid the effect of potential unwanted spatial heterogeneities. Insects were used only once and then discarded.

Three independent experimental series were performed in which the behavioral responses of intact and antennectomized head lice to chemical, hygric, and thermal stimuli were tested. The methodology applied to present the stimuli to the lice is described later.

Set Up of the Chemical Stimuli

Human head samples (i.e., volatile and non-volatile molecules) were obtained following the protocol described by Ortega Insaurralde et al. (2016). This study showed that although head lice are arrested around human scalp samples, they did not show differences between the human samples of different volunteers nor with the aging of the scalp sample (i.e., 60 h-old samples are as much attractive as 0 h-old samples) (Ortega Insaurralde et al., 2016). Thus, a piece of filter paper (1 cm × 1 cm) was rubbed during 30 s against the scalp of one 30-year-old female volunteer who had not bathed or used perfumed products in the 24 h previous to the extraction. Immediately after rubbing, the filter paper was located at one side of the circular arena, while a clean filter paper was placed at the opposite side. All filter papers were handled with gloves and clean forceps to avoid skin contamination. The base of the whole circular arena was homogeneously heated at 32 ± 2°C to mimic natural host conditions. Intact (*INT*) or differentially antennectomized lice (*F3-*, *F2F3-* or *1ANT*) were individually released at the center of the arena and their behavior recorded in video.

Set Up of the Hygric Stimulus

To generate a hygric heterogeneity in the experimental arena, the filter paper used as a substrate of half of the circular arena was maintained dry, while the opposite half was homogeneously loaded with 100 µl of tap water using a micropipette. The base of the whole circular arena was maintained at room temperature (22 ± 1°C). Immediately after (in order to minimize water evaporation), intact (*INT*) or differentially antennectomized lice (*F3-*, *F2F3-* or *1ANT*) were individually released at the center of the arena and their behavior registered in video.

Set Up of the Thermal Stimulus

A thermal heterogeneity was generated by heating the floor of half of the arena with a thermostatized metallic plate, while the other half was maintained at ambient temperature. Once the thermal equilibrium was achieved, the heated side was stabilized at 32 ± 2°C and the other side at 22 ± 2°C (ambient temperature). Temperature at the floor of both zones was measured before and after each assay with a contact thermocouple (Lutron electronic, PTM-806, Taiwan) to verify the thermal stability. Intact (*INT*) or antennectomized lice (*F3-*, *F2-F3-* or *1ANT*) were individually released at the center of the arena and their behavior registered in video.

Data Analyses and Statistical Comparisons

Behavioral outputs were quantified offline from the video films by using the software The Observer (Noldus®). The preference of head lice to stay at each side of the arena was quantified as the time spent in each zone for each individual. The percentage of time at the stimulus side was calculated as a measure of its preference. Each bar in the figures represents the mean time spent at the stimulus side and the standard errors for each group of insects.

The total walking time was registered for each individual. The percentage of the experimental time walking was calculated as a measure of the activation elicited by the stimulus. Each bar in the figures represents the mean active time and the standard errors for each group of insects.

Statistical differences among groups (i.e., *INT*, *F3-*, *F2-F3-*, and *1ANT*) for both variables (i.e., preference and activity) were assessed by means of one-way ANOVAs followed by Tukey's HSD comparisons, after checking assumptions of homoscedasticity and normality of data. Analyses were carried out by using the statistical package R (v.3.3.1) (R Development Core Team, 2016).

RESULTS

External Morphology of Antenna and Sensilla

SEM inspection allowed us to describe the external morphology of the antenna of the head louse through the characterization

of the sensilla. From the base to the tip, the antenna was composed by the scapus, the pedicellum, and the composed flagellum, with a total length of 295.15 ± 15.12 μm (**Figure 1A**). The average length for the scapus was 53.32 ± 6.15 μm; for the pedicellum, 78.20 ± 5.54 μm; and for the flagellum, 150.18 ± 9.07 μm. The flagellum was subdivided into three sub-segments or flagellomeres, from proximal to distal named F1, F2, and F3, each one with a mean length of 50.3 ± 5.1, 41.74 ± 3.14, and 58.16 ± 4.13 μm, respectively.

Seven types of sensory structures were identified along the antenna of the head louse (**Figures 1B–I**): bristles, tuft organs, pore organs, single pore, and three morphs of sensilla basiconica: finger-like basiconica, sharp-end basiconica, and round-end basiconica.

Bristles were found in all segments of the antennae (**Figures 1A,B**). They showed a well-developed socket at the base and became constricted at the distal end. No pores were observed along their surface. The scapus, the pedicellum, and the F1 only presented bristles. Three bristles were identified on the scapus, and 5–7 on the pedicellum, all of them being similar in length: 16.46 ± 1.02 μm. Longer bristles were found at the flagellum than at the scapus and pedicellum. F1 and F2 bore from five to six bristles each of 25.56 ± 2.24 and 26.98 ± 1.67 μm of mean length, respectively. F3 only exhibited three bristles of 22.39 ± 2.69 μm of mean length.

Two tuft organs were identified, one located at the dorso-lateral side of F2 and the other at the dorso-lateral side of F3 (**Figures 1B,C**). Each tuft organ consisted of a deep and circular pit (3.54 ± 0.21 μm diameter) from which six pegs emerged and each with a mean length of 3.31 ± 0.18 μm.

Two pore organs centered in an oval and shallow depression (29.30 ± 2.40 μm diameter) were present on the distal dorso-lateral side of F3 (**Figures 1B,D**). Each pore organ exhibited a sun-like shape, bearing a central plate (0.32 ± 0.02 μm diameter) surrounded by 49 ± 1 grooves of a mean length of 0.73 ± 0.04 μm.

A single pore (**Figures 1B,E**) of 0.49 ± 0.03 μm diameter was located at the dorso-medial side of F3 and next to the tuft and pore organs.

The distal end of F3 exhibited different types of sensilla basiconica (**Figure 1F**). Among them, 10 sensilla of three

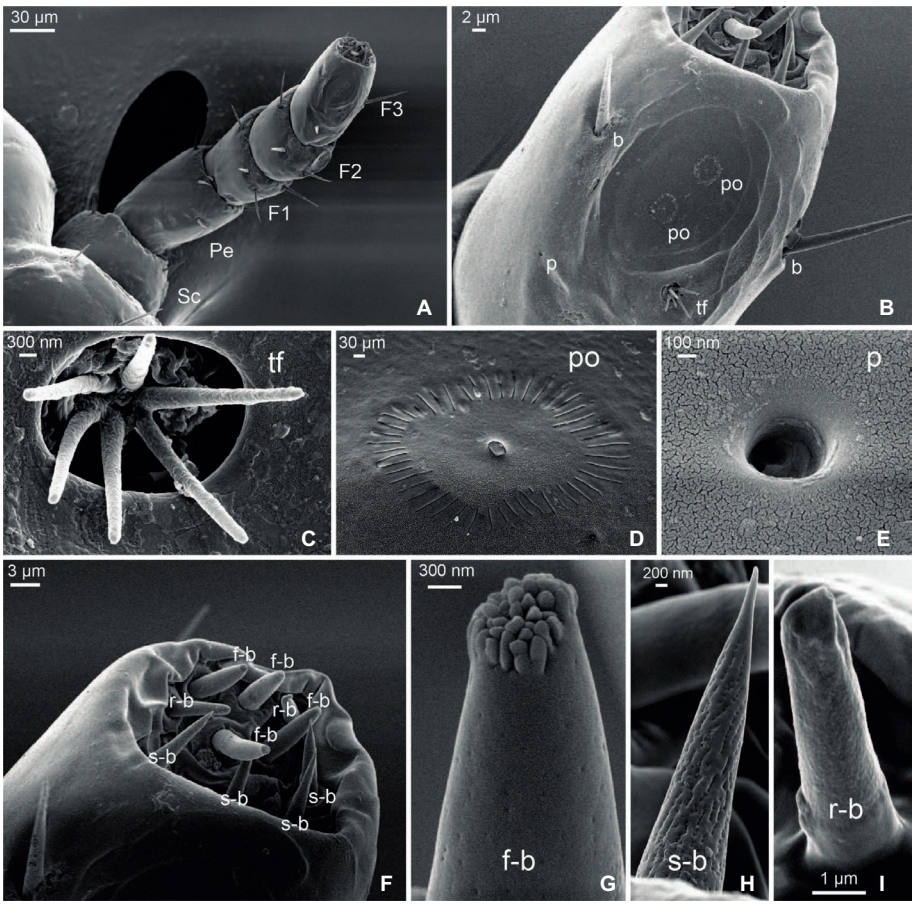

FIGURE 1 | Scanning electron micrographs of the antenna of head lice. **(A)** General view of the whole antenna constituted by scapus (Sc), pedicellum (Pe), and a composed flagellum with three flagellomeres (F1, F2, and F3). **(B)** Detail of F3 showing one tuft organ (tf), two pore organs (po), two bristles (b), and one single pore (p). **(C)** Detail of a tuft organ. **(D)** Detail of a pore organ. **(E)** Detail of a single pore. **(F)** Magnification of the distal end of F3 showing three types of basiconica sensilla: finger-like (f-b), sharp-end (s-b), and round-end (r-b). **(G)** Detail of a finger-like basiconica sensillum. **(H)** Detail of a sharp-end basiconica sensillum. **(I)** Detail of a round-end basiconica sensillum.

morphological types were identified: four finger-like, four sharp-end, and two rounded-end ones. The finger-like basiconica (8.13 ± 0.95 μm long) were characterized by the presence of numerous short pegs at their tip and by the presence of pores all along their surface (**Figure 1G**). The sharp-end basiconica (9.25 ± 0.03 μm) also exhibited multiple pores uniformly distributed along the cuticle, although these sensilla had a fine and pointed end (**Figure 1H**). Finally, the rounded-end basiconica (6.56 ± 0.16 μm long) presented a unique pore at the tip (**Figure 1I**).

Neural Projections of Antennal Sensilla

The confocal scanning of brains allowed us to calculate the dimensions of the head louse brain (excluding the optic lobes): 246.25 ± 11.19 μm wide, 185 ± 2 μm height. Coming from the antennae, an ipsilateral neural track (i.e., the antennal nerve: AN) reached the brain antero-ventrally and innervated a rounded-shape neuropil, likely the antennal lobe (AL) (**Figures 2A,B**). Each AL was situated ventrally and close to the esophageal connectives when observed from an anterior view (**Figures 2A,B**). The ALs measured 54.17 ± 2.46 μm wide and 38.16 ± 1.74 μm height. Inside ALs, diffuse glomerular arrangements were recognized (**Figures 2A,B**). 3D reconstructions (**Figures 2C,D**) revealed about 8–10 glomerular-like structures. Three different individuals were used for 3D reconstructions of the AL. All analyzed samples about the same glomerular structures, in number and positions, were identified. In a single neurobiotin preparation, we found a neural projection to the medial ipsilateral protocerebrum (**Figure 2A**).

Behavioral Responses to Host Cues

Antennal Flagellomeres Involved in the Response to Human Scalp Chemicals

Insects both with intact antennae (*INT*) and with only one intact antenna (*1ANT*) remained significantly more time than the antennectomized groups *F3-* and *F2F3-* at the scalp chemical side of the arena (**Figure 3A**, one-way ANOVA, $F = 15.76$, $df = 3$, $p = 1.74e\text{-}07$, Tukey's HSD comparisons: *INT* vs. *F3-*, $p < 0.001$; *INT* vs. *F2F3-*, $p < 0.01$; *1ANT* vs. *F3-*, $p < 0.001$; and *1ANT* vs. *F2F3-*, $p = 0.02$). These results suggest that the absence of the flagellomere F3 is enough to cause the loss of preference in these insects.

Besides, scalp chemicals are known to exert an arresting effect on head lice (Ortega Insaurralde et al., 2016). Our results show that *INT* lice exhibited a significant lower activity level than all the other groups (**Figure 3B**, one-way ANOVA, $F = 16.7$, $df = 3$, $p < 0.001$, Tukey's HSD comparisons: *INT* vs. *1ANT*, $p = 0.0055$; *INT* vs. *F3-*, $p < 0.001$; and *INT* vs. *F2F3-*, $p < 0.01$), suggesting that all the chemosensory machineries are needed to evoke an arrestment around scalp compounds (i.e., volatiles and non-volatiles).

Altogether, these results evince that when the antennae of lice were symmetrically cutoff (i.e., *F3-* and *F2F3-*) both the

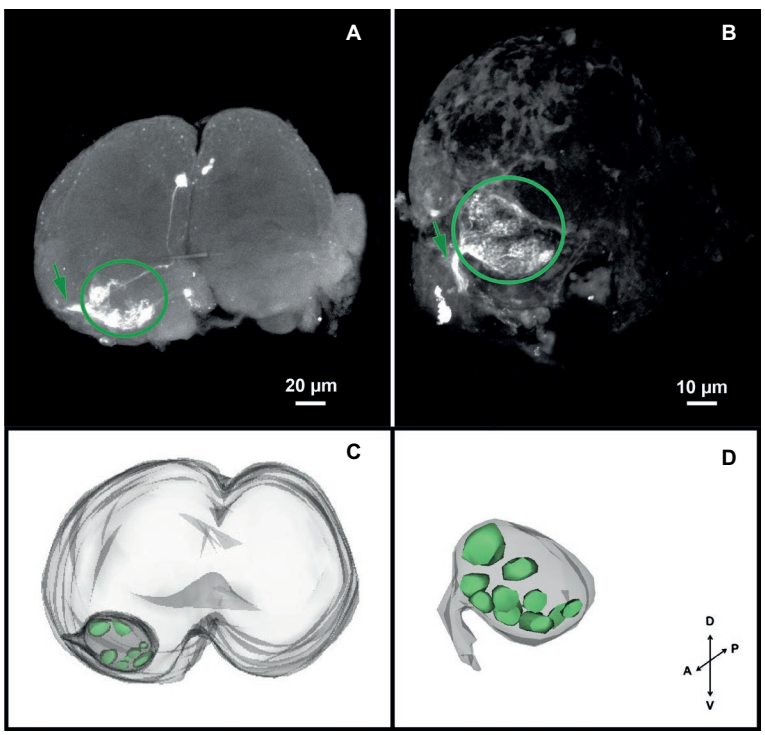

FIGURE 2 | Antennal projections to the brain and antennal lobe organization of head lice. **(A,B)** Anterior views of the brain, showing neurobiotin antennal backfills. An antennal nerve (arrow) reaches the brain antero-ventrally and innervates the ipsilateral antennal lobe (circle), where diffuse globular structures were identified. **(C,D)** 3D reconstruction of the AL where 8–10 glomerular-like structures were evinced. Orientation bars: *D*, dorsal; *V*, ventral; *P*, posterior; *A*, anterior.

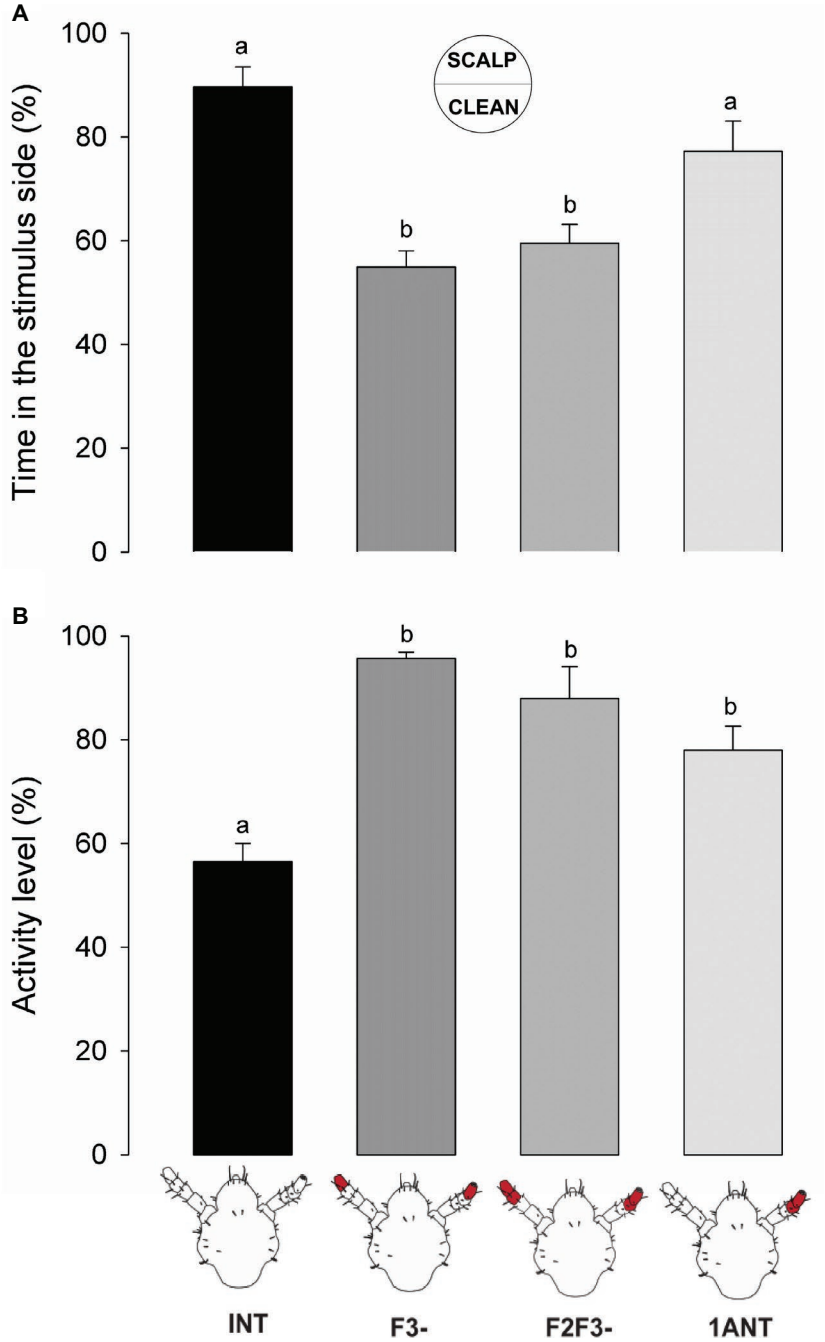

FIGURE 3 | Behavioral responses of intact and antennectomized head lice to scalp chemicals. **(A)** Preference of intact and antennectomized lice in a two-choice arena, measured as the percentage of time spent at the scalp chemical side. Intact insects (*INT)* and those with only one antenna ablated (*1ANT)* spent significantly more time at the scalp chemicals side of the arena than those with F3 (*F3-*) or F2 and F3 (*F2F3-*) ablated. **(B)** Activity levels of intact and antennectomized head lice, measured as the percentage of the experimental time they remained active over the arena. *INT* lice were significantly less active than all antennectomized ones (*F3-*, *F2F3-*, and *1ANT*). Each column represents the mean of 15 insects. Different letters indicate significant differences (one-way ANOVA, $p < 0.05$).

preference and the arrestment for the stimulus side disappeared. Intermediate results were observed in *1ANT*, where lice displayed a similar preference for the scalp chemicals as *INT* animals, but they were not arrested by such chemicals. Besides, sensory structures present in the F3 seem to be necessary and enough to perceive host chemical stimuli.

Antennal Flagellomeres Involved in Response to Humid Substrates

Lice with intact antennae (*INT*) remained significantly less time at the wet side of the arena than the symmetrically antennectomized insects (*F3-* and *F2-F3-*) (**Figure 4A**, one-way ANOVA, $F = 5.047$, $df = 3$, $p = 0.00364$, Tukey's HSD

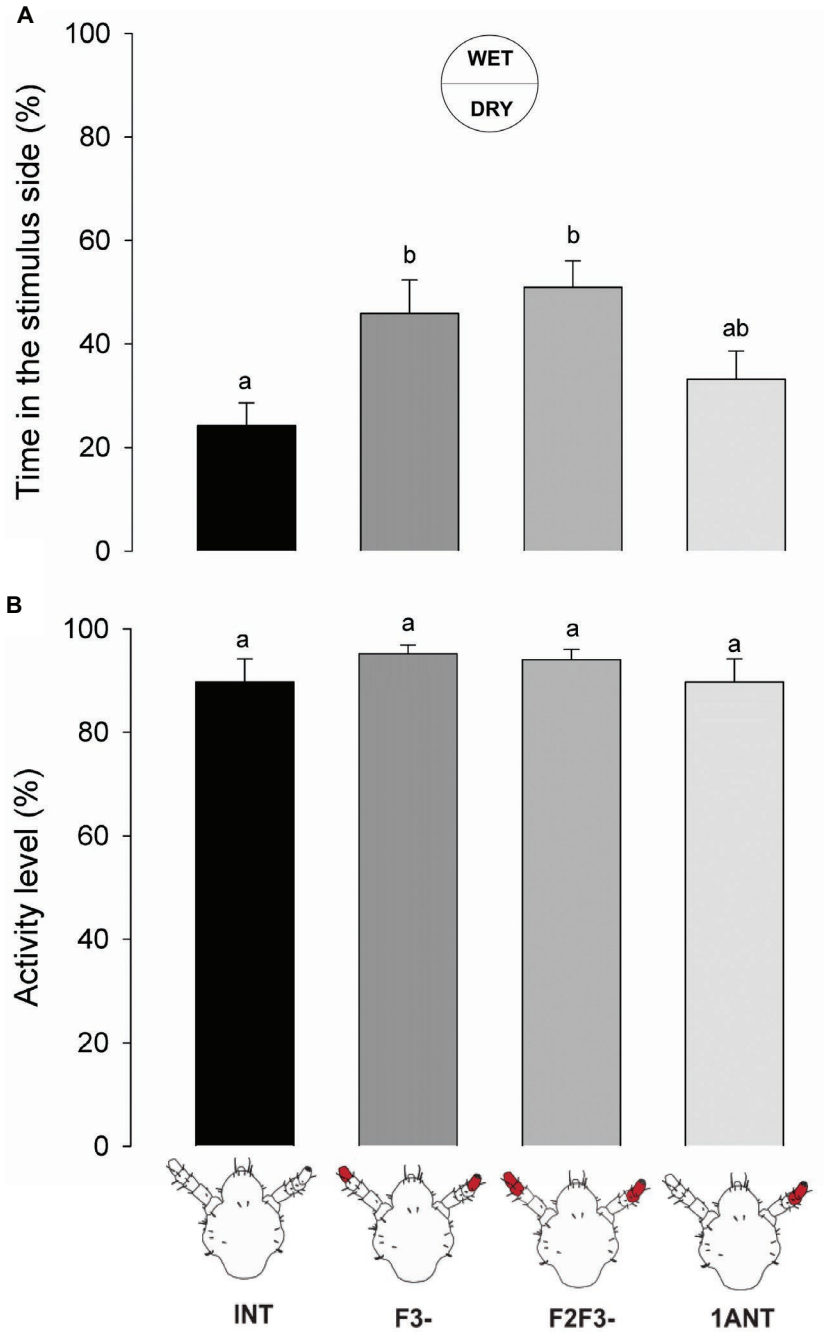

FIGURE 4 | Behavioral responses of intact and antennectomized head lice to a humid substrate. **(A)** Hygric preference of intact and antennectomized lice in a two-choice arena, measured as the percentage of the time spent at the wet side. *INT* lice spent less time at the humid side of the arena than the symmetrically antennectomized ones (*F3-* and *F2F3-*). Lice with *1ANT* displayed intermediate hygric avoidance. **(B)** Activity levels of intact and antennectomized head lice, measured as the percentage of the experimental time they remained active over the arena. All groups displayed similar activity levels. Each column represents the mean of 15 insects. Different letters indicate significant differences (one-way ANOVA, $p < 0.05$).

comparisons: *INT* vs. *F3-*, $p = 0.032$; and *INT* vs. *F2F3-*, $p = 0.005$). Insects with only one antenna (*1ANT*) showed an intermediate hygric avoidance behavior, although they showed no significant difference with the other experimental groups (Tukey's HSD comparison, *1ANT* vs. *INT*, $p = 0.644$; *1ANT* vs. *F3-*, $p = 0.356$; and *1ANT* vs. *F2F3-*, $p = 0.104$).

On the other hand, the activity levels of lice from different experimental groups did not differ significantly (**Figure 4B**, one-way ANOVA, $F = 1.451$, $df = 3$, $p = 0.238$), suggesting that humidity generates a spatial aversion but not a kinetic modulation. Additionally, it confirms that ablation of antennal segments had no effects on the normal locomotion of lice.

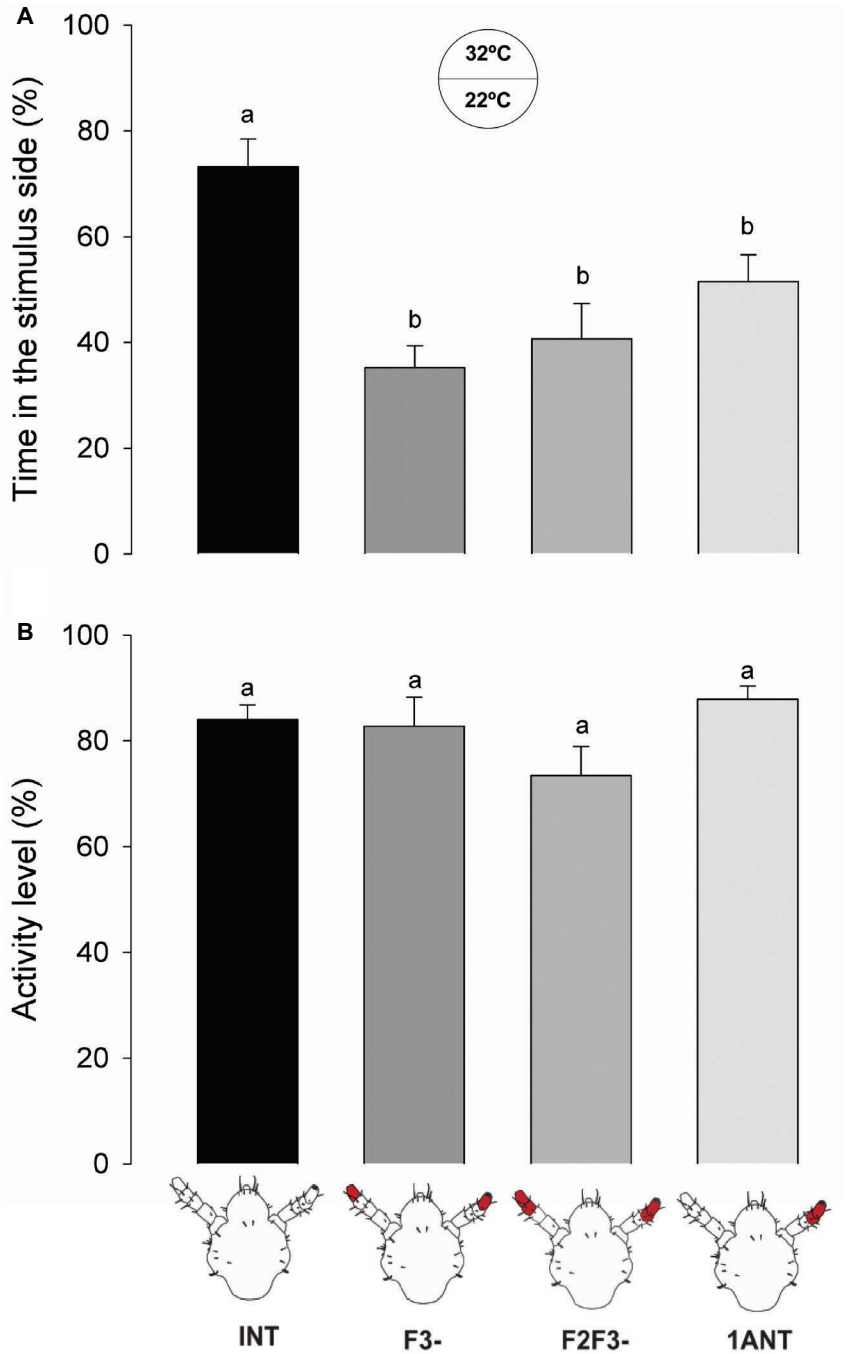

FIGURE 5 | Behavioral responses of intact and antennectomized head lice to a warm substrate. **(A)** Thermal preference of intact and antennectomized lice in a two-choice arena, measured as the percentage of the time spent at the heated (32°C) side. *INT* lice spent significantly more time in the warmer side of the arena than all antennectomized ones (*F3-*, *F2F3-*, and *1ANT*). **(B)** Activity levels of intact and antennectomized head lice, measured as the percentage of the experimental time they remained active over the arena. All groups displayed similar activity levels. Each column represents the mean of 15 insects. Different letters indicate significant differences (one-way ANOVA, $p < 0.05$).

Similar to the previous series, ablation of F3 and/or F2 and F3 caused a significant loss of the aversive response to the wet zone of the arena suggesting that F3 probably contains the sensory structures involved in humidity detection.

Antennal Flagellomeres Involved in Response to Heat

The warmer zone of the arena was preferred for head lice with intact antennae (*INT*) in relation to all the antennectomized

insects (i.e., *F3-*, *F2-F3-*, and *1ANT*; **Figure 5A**, one-way ANOVA, $F = 9.819$, $df = 3$, $p < 0.001$, Tukey's HSD comparisons: *INT* vs. *1ANT*, $p = 0.029$; *INT* vs. *F3-*, $p < 0.001$; and *INT* vs. *F2F3-*, $p < 0.001$). The absence of F3 in lice was enough to cause the observed loss of preference for the warmer side of the arena.

No significant differences between the activity levels of the different groups of insects were observed (one-way ANOVA, $F = 2.384$, $df = 3$, $p = 0.075$, **Figure 5B**), suggesting that surgery did not affect the normal locomotion of insects.

These results suggest that thermo-receptors present in the F3 might be responsible for the thermal preference of head lice and that both antennae are necessary.

DISCUSSION

This work constitutes the first approach in the functional study of the role of the antennae of head lice in the detection and perception of environmental and/or host-related stimuli. As it happens with most animals that develop parasitic lifestyles, a relatively simple and closely host-tuned sensory system was found in *P. humanus capitis*. However, although its high epidemiological relevance as a human parasite, no morphological or functional studies of its sensory system were available in the literature before this work.

Morphology of the Antennae

According to our description based on the SEM photographs, the overall sensory scheme of the human head louse antenna is represented by 35–40 sensilla belonging to seven different morphological types. In comparison to other blood-sucking insects (Barrozo et al., 2017), lice present a relatively low number of sensory structures on their antennae. Chapman (1982) proposed that insects living in environments where relevant stimuli doses are particularly high (like it happens in head lice walking over the human scalp) would probably have a relative low number of sensilla. This particular sensory condition may provide low sensibility, but in turn, it would offer a simplified process of integration in the central system. Another hypothesis that could explain the narrow sensorial machinery would be that a low number of sensilla could be an adaptation to prevent dehydration (Kristoffersen et al., 2008), and since human lice in general are prone to die quickly off-host due to water unbalance (Nuttall, 1919; Wigglesworth, 1941; Buxton, 1946), this could be the case.

Head louse antennae and sensilla showed to be similar to those of other Phthiraptera members described before (Miller, 1969; Ubelaker et al., 1973; Slifer and Sekhon, 1980; Baker and Chandrapatya, 1992). Along all the suborders of Phthiraptera (i.e., Anoplura, Ischnocera, Amblycera, and Rhynchophthirina), the morphology of the antennae is quite similar and conserved, characterizing the concentration of sensilla in the distal end (Baker and Chandrapatya, 1992; Soler Cruz and Martín Mateo, 1998). The head lice (*P. humanus capitis*) and body lice (*P. humanus humanus*), being closely related species, present quite comparable sensory structures. For example, Steinbrecht (1994) found tuft organs in the body lice, concluding after an exhaustive study that these structures represent thermo/hygroreceptors. Similarly, we identified tuft organs in the F2 and F3 of the head lice antennae. Steinbrecht (1994) also identified pore organs in the body lice and suggested that they could be bimodal olfactory-thermoreceptors. Here, two pore organs in the F3 of head lice were found. Besides, in other members of Phthiraptera such as livestock lice *Damalinia forficula, D. lipeuroides,* and *D. reduncae* (Soler Cruz and Martín Mateo, 1998), a single pore sensillum was observed; same structure was found and described here for the first time in the head lice. This sensillum type is similar to coeloconica sensilla identified in the other blood-sucking insects such as the kissing bugs *Triatoma infestans* (Bernard, 1974) and *Rhodnius prolixus* (Catalá and Schofield, 1994) or the bed bug *Cimex lectularius* (Steinbrecht and Muller, 1976). McIver and Siemicki (1985) assumed that these coeloconica sensilla might function as thermo-hygroreceptors in kissing bugs.

On the other hand, the pegs of the apex of the antennae of body lice were previously postulated as chemoreceptors (Wigglesworth, 1941; Slifer and Sekhon, 1980). In our work, we showed for the first time the fine structure of three morphs of these apical pegs, named basiconica. Based on their external morphology, the finger-like and the sharp-end basiconica seemed to be olfactory sensilla, as the cuticle presents uniformly distributed pores. The protrusions observed at the tip of the finger-like basiconica could increase the exposed surface to detect odors from the environment. Conversely, the round-end basiconica presented no pores along its surface but a single pore at the tip, suggesting a gustatory role or contact chemoreception.

Overall in the head louse antennae and purely based on sensilla morphology and similarities with sensory structures of other insects, we hypothesize about their function: bristles as mechanoreceptors, tuft organs as thermo-hygroreceptors, pore organs as chemo- and thermo-receptors, the single pore as thermo/hygroreceptors, finger-like and sharp-end basiconica as olfactory chemoreceptors, and rounded-end basiconica as contact chemoreceptors. Future functional studies like single sensillum electrophysiological recordings will further complement and confirm our hypothesis.

Antennal Projections to the Brain

Sensory afferents originating from each antenna entered through antennal nerves and innervated ipsilaterally the lateral and anteroventral region of the head louse brain. Such antennal arborizations ended in the first olfactory integration neuropil: the antennal lobe (AL), without bypassing this neuropil. Even if the glomerular organization of the ALs was quite diffuse, we could identify around 8–10 glomerular structures. These results contrast with the aglomerular ALs previously reported for a closely related species, the pigeon lice *C. columbae* (Phthiraptera: Ischnocera) (Crespo and Vickers, 2012). On the opposite side, head lice showed a rather simple AL compared

to other insects, such as dipterans with around 50–70 glomeruli (Laissue et al., 1999; Fishilevich and Vosshall, 2005; Ignell et al., 2005; Riabinina et al., 2016; Lin et al., 2018, etc.), bees with 160–200 (Arnold et al., 1985; Galizia et al., 1999; Roselino et al., 2015, etc.), 60–80 for moths (Masante-Roca et al., 2005; Couton et al., 2009; Zhao et al., 2016, etc.), or even some ants bearing up to 400 glomeruli (Zube and Rössler, 2008; Stieb et al., 2011, etc.). The relatively low number of glomeruli of head lice is probably the result of their life style: they are strict specialist organisms that live their entire lives on the head of human beings, which offer food, refuge, and place to lay eggs. Thus, relevant odors must be only those released by their hosts. Besides and supporting these data, the analysis of the genome of lice evinced a rather small repertoire of chemosensory-related genes (Kirkness et al., 2010). On the contrary, other blood feeders have a broader array of potential hosts than head lice. This fact likely implies more complex sensory systems tuned to perceive a major diversity of host cues. For example, it was shown for kissing bugs and mosquitoes that they use carbon dioxide and a diversity of host-emitted odors as signaling cues to find a vertebrate host (Guerenstein and Lazzari, 2009; Takken and Verhulst, 2013). About 22 glomeruli were identified in the ALs of the kissing bug *Rhodnius prolixus* (Barrozo et al., 2009) and about 50–60 in the mosquitoes *Aedes aegypti* and *Anopheles gambiae* (Ignell et al., 2005; Ghaninia et al., 2007). Taking into consideration the multiple studies on insects of different orders, the less developed ALs are most likely to be a convergent adaptation to a similar lifestyle and specific ecological and ethological requirements rather than an intrinsic feature of a given taxon (Kollman et al., 2016). The possession of few or non-defined AL glomeruli would not be direct indicators of absence or poor sensitivity to host-related cues. In different insects, conspicuous olfactory responsiveness to relevant odors was found even if they present a rather simple or aglomerular antennal lobes, e.g., head lice (this work), the pigeon louse *C. columbae* (Crespo and Vickers, 2012), but also the dragonfly *Libellula depressa* (Paleaoptera) (Rebora et al., 2013) and the psyllid *Trioza apicalis* (Homoptera) (Kristoffersen et al., 2008).

Role of the Antenna in Host Detection

In a pioneer work, Wigglesworth (1941) showed through behavioral assays in a two-choice arena that the body louse *P. humanus humanus* is repelled by certain odors and avoids humid regions. However, the avoidance behavior stopped once the antennae were covered with cellulose paint. Later, Mumcuoglu et al. (1986) and Peock and Maunder (1993) observed that the aggregation behavior to feces of body lice and the repellency to piperonal disappeared after partial antennectomy. In the head louse *P. humanus capitis*, Ortega Insaurralde et al. (2016) observed an arrestant effect of human scalp chemicals in a two-choice arena. In the same species, Galassi et al. (2018) showed an oriented response to host odors in a T-tube olfactometer with intact antennae. In the present work, we show that the removal of the distal end flagellomere (i.e., *F3*-) of both antennae abolished this preference, suggesting that sensilla present in this segment are probably involved in host perception. F3 bears multiporous sensilla, several basiconica (i.e., finger-like and sharp-end sensilla), and pore organs, all of them being potential olfactory structures. However, we cannot discard that uniporous round-end basiconica sensilla (i.e., with potential contact chemoreceptive function) might be involved in the detection of non-volatile components present in human scalp samples. Therefore, one or both chemosensory modalities, olfaction and gustation, could guide louse behavior in our set-up. Although insects with only one intact antenna preferred the side of the arena added with scalp samples, arrestment or decrease in the activity levels only occurred when the two antennae were intact. Possibly a reduced antennal input, due to the excision of F2 and F3 of one antenna, would not be enough to trigger significant insects' arrestment.

Head lice with intact antennae showed aversiveness to humid or wet surfaces. However, the removal of F3 significantly diluted this behavior. Water balance is a matter of importance among insects, and in fact, some terrestrial insects are prone to conserve and "grab" water from the environment under different adaptation (Hadley, 1994). However, when head lice are over a host, they feed several times a day with large intakes of water involved in every blood meal. Consequently, if a head louse has parasitized a host, water would not be a limiting resource. But, in general, excessive humidity in the environment facilitates fungi proliferation, sometimes with deleterious effects for insects, so that different species developed distinct limits of tolerance for humid environments, according to their physiology and habitat adaptations (Guarneri et al., 2002; Rowley and Hanson, 2007). Our results showed that the sensilla involved in moistness detection in head lice are located in F3. Previous works proposed the tuft organs as responsible for humidity sensing in the body lice (Steinbrecht, 1994).

Finally, only head lice with both intact antennae chose to spend more time in the warmer zone of the arena. Heat is among the most relevant stimuli used by hematophagous insects to find their warm-blooded hosts (Lazzari, 2009). At the same time, ambient temperature is known to depict the spatial and geographical distribution of most animals in earth. However, up to now, no information was available about the thermal preference of the head louse. It seems that the response to thermal stimulus depends exclusively on the bilateral input of both antennae, since the preference for the thermal stimulus disappeared in insects with only one antenna *(1ANT)*. This response also faded when F3 and both F2 and F3 were ablated. The candidate sensilla to evaluate the thermal information can be the tuft organs, the pore organs, and the single pore sensillum, all three present in the F3.

Overall, our work provides new information about the sensory physiology of head lice including the structures involved in stimuli detection and processing as well as the behavior displayed in response to host-associated stimuli. Future studies should be focused on the verification of the function of each antennal sensillum type by means of electrophysiological recordings, by anterograde labeling of single sensilla, and by the study of sensory structures present in other parts of their body, such as legs and mouthparts.

AUTHOR CONTRIBUTIONS

IO and RB carried out the experiments. RB, SM, AT, and MP designed the experiments and provided the financial support. IO, RB, and SM wrote the manuscript. RB, SM, AT, and MP critically revised the manuscript.

FUNDING

RB, SM, AT, and MP are members of the Scientific and Technical Researcher Career of the National Scientific and Technical Research Council (CONICET). IO is a fellowship holder of the CONICET. The financial support for this research was provided by ANPCyT (Agencia Nacional de Promoción Científica y Tecnológica, grant code Préstamo BID PICT 2013-0353 to MP and AT; grant code 2013-1253 to RB and SM).

ACKNOWLEDGMENTS

We are indebted to the children who donate their insects for this study and school authorities that allowed us to do that. We specially thank Agustín Alvarez Costa and Ramiro Méndez for helping with the figures. We thank Martin Berón de Astrada for his advice related to the antennal backfills and the reviewers for their useful comments and suggestions.

REFERENCES

Arnold, G., Masson, C., and Budharugsa, S. (1985). Comparative study of the antennai lobes and their afferent pathway in the worker bee and the drone (*Apis Mellifera*). *Cell Tissue Res.* 242, 593–605.

Baker, G. T., and Chandrapatya, A. (1992). Sensilla on the mouthparts and antennae of the elephant louse, *Haematomyzus elephantis* piaget (Phthiraptera: Haematomyzidae). *J. Morphol.* 214, 333–340. doi: 10.1002/jmor.1052140308

Barrozo, R. B., Couton, L., Lazzari, C. R., Insausti, T. C., Minoli, S., Fresquet, N., et al. (2009). Antennal pathways in the central nervous system of a blood-sucking bug, *Rhodnius prolixus*. *Arthropod Struct. Dev.* 38, 101–110. doi: 10.1016/j.asd.2008.08.004

Barrozo, R. B., Reisenman, C. E., Guerenstein, P., Lazzari, C. R., and Lorenzo, M. (2017). An inside look at the sensory biology of triatomines. *J. Insect Physiol.* 97, 3–19. doi: 10.1016/j.jinsphys.2016.11.003

Bernard, J. (1974). Étude électrophysiologique de récepteurs impliqués dans l'orientation vers l'hôte et dans l'acte hématophage chez un Hémiptère: *Triatoma infestans*. Ph.D. Thesis. France: University of Rennes.

Boyd, B. M., Allen, J. M., Nguyen, N., Vachaspati, P., Quicksall, Z. S., Tandy Warnow, T., et al. (2017). Primates, lice and bacteria: speciation and genome evolution in the symbionts of hominid lice. *Mol. Biol. Evol.* 34, 1743–1757. doi: 10.1093/molbev/msx117

Bressa, M. J., Papeschi, A. G., and Toloza, A. C. (2015). Cytogenetic features of human head and body lice (Phthiraptera: Pediculidae). *J. Med. Entomol.* 52, 918–924. doi: 10.1093/jme/tjv089

Buxton, P. A. (1946). *The louse: An account of the lice which infest man, their medical importance and control*. (London, United Kingdom: Edward Arnold & Co).

Catalá, S., and Schofield, C. (1994). Antennal sensilla of *Rhodnius*. *J. Morphol.* 219, 193–203. doi: 10.1002/jmor.1052190208

Chapman, R. F. (1982). Chemoreception: The significance of receptor numbers. *Adv. Insect Physiol.* 247–356. doi: 10.1016/s0065-2806(08)60155-1

Couton, L., Minoli, S., Kiêu, K., Anton, S., and Rospars, J. P. (2009). Constancy and variability of identified glomeruli in antennal lobes: computational approach in *Spodoptera littoralis*. *Cell Tissue Res.* 337, 491–511. doi: 10.1007/s00441-009-0831-9

Crespo, J. G., and Vickers, N. J. (2012). Antennal lobe organization in the slender pigeon louse, *Columbicola columbae* (Phthiraptera: Ischnocera). *Arthropod Struct. Dev.* 41, 227–230. doi: 10.1016/j.asd.2012.02.008

Fishilevich, E., and Vosshall, L. (2005). Genetic and functional subdivision of the *Drosophila* antennal lobe. *Curr. Biol.* 15, 1548–1553. doi: 10.1016/j.cub.2005.07.066

Galassi, F. G., Fronza, G., Toloza, A. C., Picollo, M. I., and Gonzalez Audino, P. (2018). Response of *Pediculus humanus capitis* (Phthiraptera: Pediculidae) to volatiles of whole and individual components of the human scalp. *J. Med. Entomol.* 55, 527–533. doi: 10.1093/jme/tjx243

Galizia, C. G., McIlwrath, S. L., and Menzel, R. (1999). A digital three-dimensional atlas of the honeybee antennal lobe based on optical sections acquired by confocal microscopy. *Cell Tissue Res.* 295, 383–394. doi: 10.1007/s004410051245

Ghaninia, M., Hansson, B., and Ignell, R. (2007). The antennal lobe of African malaria mosquito *Anopheles gambiae* - innervation and three-dimensional reconstruction. *Arthropod Struct. Dev.* 36, 23–39. doi: 10.1016/j.asd.2006.06.004

Guarneri, A. A., Lazzari, C., Diotaiuti, L., and Lorenzo, M. (2002). The effect of relative humidity on the behaviour and development of *Triatoma brasiliensis*. *Physiol. Entomol.* 27, 142–147. doi: 10.1046/j.1365-3032.2002.00279.x

Guerenstein, P. G., and Lazzari, C. R. (2009). Host-seeking: how triatomines acquire and make use of information to find blood. *Acta Trop.* 110, 148–158. doi: 10.1016/j.actatropica.2008.09.019

Hadley, N. F. (1994). *Water relations of terrestrial arthropods*. (San Diego: Academic Press).

Ignell, R., Dekker, T., Ghaninia, M., and Hansson, B. S. (2005). Neuronal architecture of the mosquito deuterocerebrum. *J. Comp. Neurol.* 493, 207–240. doi: 10.1002/cne.20800

Keilin, D., and Nuttall, G. H. F. (1930). Iconographic studies of *Pediculus humanus*. *Parasitology* 22, 1–10. doi: 10.1017/S0031182000010921

Kirkness, E. F., Haas, B. J., Sun, W., Braig, H. R., Perotti, M. A., Clark, J. M., et al. (2010). Genome sequences of the human body louse and its primary endosymbiont provide insights into the permanent parasitic lifestyle. *Proc. Natl. Acad. Sci. USA* 107, 12168–12173. doi: 10.1073/pnas.1003379107

Kollman, M., Schmidt, R., Heuer, C. M., and Schachtner, J. (2016). Variations on a theme: antennal lobe architecture across Coleoptera. *PLoS One* 11:e0166253. doi: 10.1371/journal.pone.0166253

Kristoffersen, L., Hansson, B. S., Anderbrant, O., and Larsson, M. C. (2008). Aglomerular hemipteran antennal lobes- basic neuroanatomy of a small nose. *Chem. Senses* 33, 771–778. doi: 10.1093/chemse/bjn044

Laissue, P. P., Reiter, C., Hiesinger, P. R., Halter, S., Fischbach, K. F., and Stocker, R. F. (1999). Three-dimensional reconstruction of the antennal lobe in *Drosophila melanogaster*. *J. Comp. Neurol.* 405, 543–552. doi: 10.1002/(SICI)1096-9861(19990322)405:4<543::AID-CNE7>3.0.CO;2-A

Lazzari, C. R. (2009). *Orientation towards hosts in haematophagous insects: An integrative perspective*. 1st Edn. (Amsterdam: Elsevier Ltd).

Lin, T., Li, C., Liu, J., Smith, B. H., Lei, H., and Zeng, X. (2018). Glomerular organization in the antennal lobe of the oriental fruit fly *Bactrocera dorsalis*. *Front. Neuroanat.* 12, 1–19. doi: 10.3389/fnana.2018.00071

Masante-Roca, I., Gadenne, C., and Anton, S. (2005). Three-dimensional antennal lobe atlas of male and female moths, *Lobesia botrana* (Lepidoptera: Tortricidae) and glomerular representation of plant volatiles in females. *J. Exp. Biol.* 208, 1147–1159. doi: 10.1242/jeb.01508

McIver, S. B., and Siemicki, R. (1985). Fine structure of antennal putative thermo-hygro sensilla of adult *Rhodnius prolixus* Stal (Hemiptera: Reduviidae). *J. Morphol.* 183, 15–23. doi: 10.1002/jmor.1051830103

Miller, J. F. (1969). Antennal tuft organs of *Pediculus humanus* Linn. and *Pthirus pubis* (Linn.) (Anoplura: Pediculidae). *J. New York Entomol. Soc.* 77, 85–89.

Mumcuoglu, Y., Galun, R., and Ikan, R. (1986). The aggregation response of human body louse (Pediculus Humanus) (Insecta:Anoplura) to its excretory products. *Int. J. Trop. Insect Sci.* 7:629. doi: 10.1017/S1742758400011565

Nuttall, G. H. F. (1919). The biology of *Pediculus humanus*. *Parasitology* 11, 201–220. doi: 10.1017/S0031182000004194

Olds, B. P., Coates, B. S., Steele, B. D., Sun, W., Agunbiade, T. A., Yoon, K. S., et al. (2012). Comparison of the transcriptional profiles of head and body lice. *Insect Mol. Biol.* 21, 257–268. doi: 10.1111/j.1365-2583.2012.01132.x

Ortega Insaurralde, I., Toloza, A. C., Gonzalez Audino, P., and Picollo, M. I. (2016). Arrestant effect of human scalp components in *Pediculus humanus capitis* (Anoplura: Pediculidae) behavior. *J. Med. Entomol.* 54, 258–263. doi: 10.1093/jme/tjw192

Pelletier, J., Xu, P., Yoon, K. S., Clark, J. M., and Leal, W. S. (2015). Odorant receptor-based discovery of natural repellents of human lice. *Insect Biochem. Mol. Biol.* 66, 103–109. doi: 10.1016/j.ibmb.2015.10.009

Peock, S., and Maunder, J. W. (1993). Arena tests with piperonal, a new louse repellent. *J. R. Soc. Health* 113, 292–294.

Picollo, M. I., Vassena, C. V., Casadio, A. A., Massimo, J., and Zerba, E. N. (1998). Laboratory studies of susceptibility and resistance to insecticides in *Pediculus capitis* (Anoplura, Pediculidae). *J. Med. Entomol.* 35, 814–817. doi: 10.1093/jmedent/35.5.814

R Development Core Team (2016). *R: A language and environment for statistical computing*. Vienna: R Foundation for Statistical Computing.

Rebora, M., Dell Otto, A., Rybak, J., Piersanti, S., Gaino, E., and Hansson, B. (2013). The antennal lobe of *Libellula depressa* (Odonata, Libellulidae). *Zoology* 116, 205–214. doi: 10.1016/j.zool.2013.04.001

Riabinina, O., Task, D., Marr, E., Lin, C.-C. C., Alford, R., O'Brochta, D. A., et al. (2016). Organization of olfactory centres in the malaria mosquito Anopheles gambiae. *Nat. Commun.* 7:13010. doi: 10.1038/ncomms13010

Roselino, A. C., Hrncir, M., da Cruz Landim, C., Giurfa, M., and Sandoz, J. C. (2015). Sexual dimorphism and phenotypic plasticity in the antennal lobe of a stingless bee, *Melipona scutellaris*. *J. Comp. Neurol.* 523, 1461–1473. doi: 10.1002/cne.23744

Rowley, M., and Hanson, F. (2007). Humidity detection and hygropreference behavior in larvae of the tobacco hornworm, *Manduca sexta*. *J. Insect Sci.* 7, 1536–2442. doi: 10.1673/031.007.3901

Slifer, E., and Sekhon, S. S. (1980). Sense organs on the antennal flagellum of the human louse, *Pediculus humanus* (Anoplura). *J. Morphol.* 164, 161–166. doi: 10.1002/jmor.1051640205

Soler Cruz, M. D., and Martín Mateo, M. P. (1998). Sensory equipment of the antennal flagellum of several species of *Damalinia* (Phthiraptera: Trichodectidae). *Micron* 29, 431–438. doi: 10.1016/S0968-4328(98)00026-2

Steinbrecht, R. A. (1994). The tuft organs of the human body louse *Pediculus humanus corporis* – Cryofixation study of a thermo-hygrosensitive sensillum. *Tissue Cell* 26, 259–275. doi: 10.1016/0040-8166(94)90101-5

Steinbrecht, R. A., and Muller, B. (1976). Fine structure of the antennal receptors of the bed bug, *Cimex lectularius* L. *Tissue Cell* 8, 615–636. doi: 10.1016/0040-8166(76)90035-5

Stieb, S. M., Kelber, C., Wehner, R., and Rössler, W. (2011). Antennal-lobe organization in desert ants of the genus *Cataglyphis*. *Brain Behav. Evol.* 77, 136–146. doi: 10.1159/000326211

Takken, W., and Verhulst, N. O. (2013). Host preferences of blood-feeding mosquitoes. *Annu. Rev. Entomol.* 58, 433–453. doi: 10.1146/annurev-ento-120811-153618

Toloza, A. C., Laguna, M. F., Ortega Insaurralde, I., Vassena, C., and Risau-Gusman, S. (2018). Insights about head lice transmission from field data and mathematical modeling. *J. Med. Entomol.* 55, 929–937. doi: 10.1093/jme/tjy026

Toloza, A. C., Zyglado, J., Biurrum, F., Rotman, A., and Picollo, M. I. (2010). Bioactivity of argentinean essential oils against permethrin-resistant head lice, *Pediculus humanus capitis*. *J. Insect Sci.* 10:185. doi: 10.1673/031.010.14145

Tovar-Corona, J. M., Castillo-Morales, A., Chen, L., Olds, B. P., Clark, J. M., Reynolds, S. E., et al. (2015). Alternative splice in alternative lice. *Mol. Biol. Evol.* 32, 2749–2759. doi: 10.1093/molbev/msv151

Ubelaker, J. E., Payne, E., Allison, V. F., and Moore, D. V. (1973). Scanning electron microscopy of the human pubic louse, *Phthirus pubis* (Linnaeus, 1758). *J. Parasitol.* 59, 913–919. doi: 10.2307/3278434

Veracx, A., and Raoult, D. (2012). Biology and genetics of human head and body lice. *Trends Parasitol.* 28, 563–571. doi: 10.1016/j.pt.2012.09.003

Wigglesworth, V. (1941). The sensory physiology of the human louse *Pediculus humanus corporis* De Geer (Anoplura). *Parasitology* 32, 67–109.

Zhao, X. C., Chen, Q. Y., Guo, P., Xie, G. Y., Tang, Q. B., Guo, X. R., et al. (2016). Glomerular identification in the antennal lobe of the male moth *Helicoverpa armigera*. *J. Comp. Neurol.* 524, 2993–3013. doi: 10.1002/cne.24003

Zube, C., and Rössler, W. (2008). Caste- and sex-specific adaptations within the olfactory pathway in the brain of the ant *Camponotus floridanus*. *Arthropod Struct. Dev.* 37, 469–479. doi: 10.1016/j.asd.2008.05.004

Conflict of Interest Statement: The authors declare that the research was conducted in the absence of any commercial or financial relationships that could be construed as a potential conflict of interest.

frontiers in Physiology

ORIGINAL RESEARCH
published: 04 June 2019
doi: 10.3389/fphys.2019.00678

Aversive Training of Honey Bees in an Automated Y-Maze

Morgane Nouvian[1]* *and C. Giovanni Galizia*[1,2]

[1] Department of Biology, University of Konstanz, Konstanz, Germany, [2] Centre for the Advanced Study of Collective Behaviour, University of Konstanz, Konstanz, Germany

Honeybees have remarkable learning abilities given their small brains, and have thus been established as a powerful model organism for the study of learning and memory. Most of our current knowledge is based on appetitive paradigms, in which a previously neutral stimulus (e.g., a visual, olfactory, or tactile stimulus) is paired with a reward. Here, we present a novel apparatus, the yAPIS, for aversive training of walking honey bees. This system consists in three arms of equal length and at 120° from each other. Within each arm, colored lights (λ = 375, 465 or 520 nm) or odors (here limonene or linalool) can be delivered to provide conditioned stimuli (CS). A metal grid placed on the floor and roof delivers the punishment in the form of mild electric shocks (unconditioned stimulus, US). Our training protocol followed a fully classical procedure, in which the bee was exposed sequentially to a CS paired with shocks (CS+) and to another CS not punished (CS−). Learning performance was measured during a second phase, which took advantage of the Y-shape of the apparatus and of real-time tracking to present the bee with a choice situation, e.g., between the CS+ and the CS−. Bees reliably chose the CS− over the CS+ after only a few training trials with either colors or odors, and retained this memory for at least a day, except for the shorter wavelength (λ = 375 nm) that produced mixed results. This behavior was largely the result of the bees avoiding the CS+, as no evidence was found for attraction to the CS−. Interestingly, trained bees initially placed in the CS+ spontaneously escaped to a CS− arm if given the opportunity, even though they could never do so during the training. Finally, honey bees trained with compound stimuli (color + odor) later avoided either components of the CS+. Thus, the yAPIS is a fast, versatile and high-throughput way to train honey bees in aversive paradigms. It also opens the door for controlled laboratory experiments investigating bimodal integration and learning, a field that remains in its infancy.

Keywords: honey bees, aversive learning, automation, Y-maze, bimodal

OPEN ACCESS

Edited by:
Philippe Lucas,
Institut National de la Recherche Agronomique (INRA), France

Reviewed by:
Matthieu Dacher,
Sorbonne Universités, France
Martin Fritz Strube-Bloss,
University of Wuerzburg, Germany

***Correspondence:**
Morgane Nouvian
morgane.nouvian@uni-konstanz.de

Specialty section:
This article was submitted to Invertebrate Physiology, a section of the journal Frontiers in Physiology

Received: *04 March 2019*
Accepted: *13 May 2019*
Published: *04 June 2019*

Citation:
Nouvian M and Galizia CG (2019) Aversive Training of Honey Bees in an Automated Y-Maze. Front. Physiol. 10:678. doi: 10.3389/fphys.2019.00678

INTRODUCTION

Karl von Frisch performed the earliest conditioning experiments on honey bees, simultaneously demonstrating that they can see colors and that they can learn color-reward associations (von Frisch, 1914). Since then, numerous studies have used learning paradigms to gain insights into how honey bees perceive and understand the world (Menzel, 2001; Srinivasan, 2010; Sandoz, 2011; Avargues-Weber and Giurfa, 2014). The vast majority of this work focused on appetitive

learning, in which one stimulus (the conditioned stimulus, CS) is paired with a reward – usually a droplet of sugary water (the unconditioned stimulus, US). In outdoor settings, the presence of a reward can lure honey bees to willingly participate in the experiment. They will then shuttle back and forth from the hive to the experimental set-up, thus inscribing the learning process in the naturalistic context of foraging. Typically, at the experimental station the bees are given the choice between two alternatives, only one of which being rewarded, that they can examine at leisure before making a choice. This approach has been extensively used to probe the limits of honey bee cognition, especially in visual tasks (Giurfa et al., 2001; Hempel de Ibarra et al., 2014; Howard et al., 2018) but not exclusively (Srinivasan et al., 1998; Ravi et al., 2016). Among the major drawbacks of using free-flying bees, however, is the difficulty to gain insights into the underlying neural circuits, either through pharmacology or electrophysiology. Such a mechanistic understanding necessitates well-controlled lab-based experiments. The most famous procedure that fits this criterion is the conditioning of the proboscis extension response (PER), which has been instrumental in establishing the honey bee as a model system for learning and memory. Harnessed bees are presented repeatedly with the CS while their antennae is stimulated with a droplet of sugar, thus releasing a reflexive extension of the proboscis to lick the sugar. After a few trials the CS itself triggers extension of the proboscis, thus indicating Pavlovian conditioning (Giurfa and Sandoz, 2012). While olfactory PER produces high learning rates and a robust memory, adapting this protocol to visual tasks has proven challenging (Avargues-Weber and Mota, 2016).

Comparatively, aversive paradigms are still few and rarely used, although recent efforts have been made to close this gap. These includes conditioning of the sting extension reflex, in which the bees are harnessed and the CS (an odor) is paired with either electric shocks or heat (Vergoz et al., 2007; Tedjakumala and Giurfa, 2013; Junca et al., 2014). More recently, place avoidance assays have been developed (Agarwal et al., 2011; Dinges et al., 2013; Kirkerud et al., 2017). In these assays the walking bee receives shocks when she enters the half of the arena marked by a specific color, and thus learns to escape to the other side, marked by a different color. Nonetheless, a major issue of these assays was that the bee always started within one of the stimuli, and was thus never in the position of evaluating both alternatives before making a choice. In addition, how the bee was learning (whether it was operant, classical or a mix of both) was never clear. Here, we present a new apparatus, the Y-APIS, that solve these issues. The shape of the arena was modified from a linear chamber to a Y-maze, and each arm was fitted with colored lights and an odor delivery system. Real-time tracking inside the apparatus allowed for any stimulus (CS or US) to be delivered relative to the position of the bee, so that the bee could be offered a real choice between two alternatives. The Y-maze (or T-maze) is a simple but powerful tool for the study of animal behavior, and it has been used to assess decision-making and sensory perception in a wide range of species, from slime molds (Reid et al., 2012) to rodents (Flexner et al., 1963), birds (Bonadonna and Sanz-Aguilar, 2012) and fish (Cognato et al., 2012), passing by insects (Giurfa et al., 2001).

To validate our approach we trained honey bees in a simple differential conditioning, in which the CS+ was paired with shocks but not the CS−. We show that honey bees successfully solved the task after only a few training trials both in the visual and in the olfactory modality, with an exception when the CS+ was within the UV range. Further experiments revealed that they did so by avoiding the CS+ rather than by increased attraction to the CS− (i.e., there was no safety learning). As a final proof of concept, we trained honey bees to a bimodal task, in which a color and an odor were paired with the shocks simultaneously. Both sensory modalities were equally efficient in triggering the avoidance response, thus suggesting that the Y-APIS could be a powerful tool for future investigations focusing on sensory integration and learning across modalities.

MATERIALS AND METHODS

Honey Bees

During summer, the bees were caught from outdoor colonies as they flew away and are thus most likely foragers. The bee colonies (*Apis mellifera*) were housed on the roof of the University of Konstanz, Germany. During winter, honey bees were taken from caged colonies kept indoor under a 12/12 h light-dark cycle (including UV lights) and provided with pollen, liquid bee food (APIFONDA®) and water to forage on. They were caught when flying in the meshed cage, outside of the hive. All bees were introduced in the apparatus immediately after being caught. **Table 1** recapitulates the bees participating in the different experiments. Bees from experiments 1 and 2 were pooled to analyze the general behavior of bees inside the apparatus. To allow more direct comparisons, data from a single bee sometimes contribute to more than one figure: **Figures 6B**, **8B** are subsets of the dataset fully presented in **Figure 7**, and **Figure 5B** is a subset of the data fully presented in **Figure 8A**.

Training Apparatus: Y-APIS

Honey bees were trained individually in an automated Y-maze custom-build at the University of Konstanz (**Figures 1A,B**). This apparatus was a modification of a previous linear chamber (Kirkerud et al., 2013, 2017). It is made of three arms (inner dimensions: 14 cm long, 2 cm wide and 0.55 cm high), at 120° from each other. Individual bees were inserted via one of the upper doors and allowed to walk freely in all three arms. The position of the bee in each arm was monitored using an array of 26 infrared photocells. The US consisted of a train (2 Hz) of mild electric shocks (10 V for 200 ms) delivered by the electric grid placed on the floor and ceiling of each arm. The CS consisted in odors delivered into the air stream at the distal end of each arm, or light delivered along the entire length of an arm.

Odors

A constant clean air flow (300 mL/min) ran from the distal end of each arm to the central area, where it was evacuated by active vacuuming and a passive slit (**Figures 1A,B**). Smaller air flows

TABLE 1 | Overview of experiments.

Experiment	CS	Season	Sample size	Figures
Calibration	Colors	Winter	3 groups × 18 bees	1E
1	Odors	Winter	4 Nt × 2 symmetrical trainings × 20 bees	3B, 4, 5A
1	Colors	Winter	3 color pairs × 4 Nt × 2 symmetrical trainings × 20 bees	3B, 4, 6A
2	Odors	Summer	(2 symmetrical trainings + 1 control) × 48 bees	3B,C, 4A–D, 5B, 8A
2	Colors	Summer	3 color pairs × (2 symmetrical trainings + 1 control) × 48 bees	3B,C, 4A–D, 6B, 7, 8B
3	Odors	Summer	(2 symmetrical trainings + 2 controls) × 48 bees	9A
3	Colors	Summer	(2 symmetrical trainings + 2 controls) × 48 bees	9B
3	Bimodal	Summer	(2 symmetrical trainings + 2 controls) × 48 bees	9C

(100 mL/min) joined the main one just before its entry into each arm. By default, each flow ran through a clean vial, and for odor delivery its path was switched to a similar vial containing 0.5 mL of the pure odorant, using solenoid valves (Bürkert 6724, FFKM/PEEK). The odorants were R-(+)-limonene and linalool (Sigma-Aldrich, >94% – CAS:5989-27-5 and >97% – CAS: 78-70-6, respectively). Honey bees can learn and discriminate these odors (Kirkerud et al., 2013). Using a photo-ionization device (PID, Aurora Scientific Inc., 200A) we confirmed that the odor was well defined spatially and temporally (**Figure 1C**).

Colors

Bees have trichromatic vision, ranging from the human green to UV. Monochromatic LEDs were situated underneath the transparent floor of the apparatus in alternating rows (**Figure 1B**). Throughout this study, we refer to them in human color space, i.e., green (λ = 520 nm, 3.5 mW LED, Kingbright KP-1608VGC-A), blue (λ = 465 nm, 27 mW LED, Kingbright KP-1608VBC-D) and ultra-violet (UV; λ = 375 nm, 9.9 mW LED, Nichia NSSU100DT). Green (520 nm) is mainly perceived by the long-wavelength receptor alone (in human trichromatic vision, activating L only yields red). Blue (465 nm) is perceived by the bees' long- and middle-wavelength photoreceptor (in humans, L and M activation yields yellow). The UV stimulus is perceived by both middle- and short-wavelength photoreceptors (in humans, activating M and S photoreceptors yields a bright blue). Honey bees have very good color discrimination within these regions of the visual spectrum, and should thus be able to easily identify these different stimuli (Avargues-Weber and Giurfa, 2014).

In preliminary experiments, we found that forager bees were strongly phototactic, and the phototactic strength depended on the wavelength. Therefore, we calibrated light intensities to equalize their preference in a two-choice test (**Figure 1E**). This corresponded to 64, 44, and 24% of the maximum intensity for 520, 465 and 375 nm, respectively. The exact spectra and their intensity with these settings, as seen from inside the apparatus, are presented in **Figure 1D**.

Training Procedures

Acquisition trials (**Figure 2**) followed a classical differential conditioning protocol. After 1 min of adaptation to the apparatus in the dark, we exposed the bees to a variable number of training trials. Each trial consisted of 10 s exposure to the CS (light or odor throughout the apparatus) followed by 30 s of inter-trial interval (dark/no odor), then 10 s to the other CS also followed by 30 s rest. For trained animals, the US shocks were paired with the CS+ during the full 10 s of exposure. For control animals, the shocks were given also for 10 s but in the middle of the inter-trial interval (from 10 to 20 s after the end of a CS). The bees reacted to the shocks as previously described, by accelerating and hissing (Kirkerud et al., 2013; Wehmann et al., 2015). Sequences were pseudo-randomized (**Figure 2**). After the training phase, all bees had 4 min to rest in the dark before the start of the testing phase. Up to four yAPIS were used in parallel, and within each experimental group the bees were distributed equally on these systems. This also allowed for associated groups (e.g., blue shocked vs. green, green shocked vs. blue and the corresponding unpaired control group) to be tested in parallel whenever possible.

Memory Testing

Each test lasted for 20 s, followed by 30 s of rest. Thanks to the real time tracking of the bee available in our apparatus, the stimuli could be presented relative to the bee position. Two stimuli configurations were used, depending on the experiment (**Figure 2**). In the "spontaneous" configuration, two CSs were presented relative to the bee position, such that the bee always started in the dark and faced the choice between the two stimuli. In the case of colors, the bee was naturally willing to make a choice due to positive phototaxis. In the case of odors, these two choice arms were made attractive by a dim blue illumination (2.5% of maximum intensity). In the "forced" choice, two arms contained the CS+, including where the bee started. The remaining arm always contained the CS−. An advantage of this configuration was that odors could be tested in the dark, without the need for an additional light to induce phototaxis. The right/left positions of each CS relative to the bee were alternated between tests. Whenever the protocol included different tests, their order was balanced across animals. In order to test 24 h memory, trained bees were taken out of the apparatus and held individually overnight in a dark and moist chamber, with *ad libitum* solid food (APIFONDA®). This protocol ensured that 98% of the bees survived.

Data Collection

The yAPIS system collected all data onto a log file. Measurements consisted in the position of the bee along the arm, the arm the bee

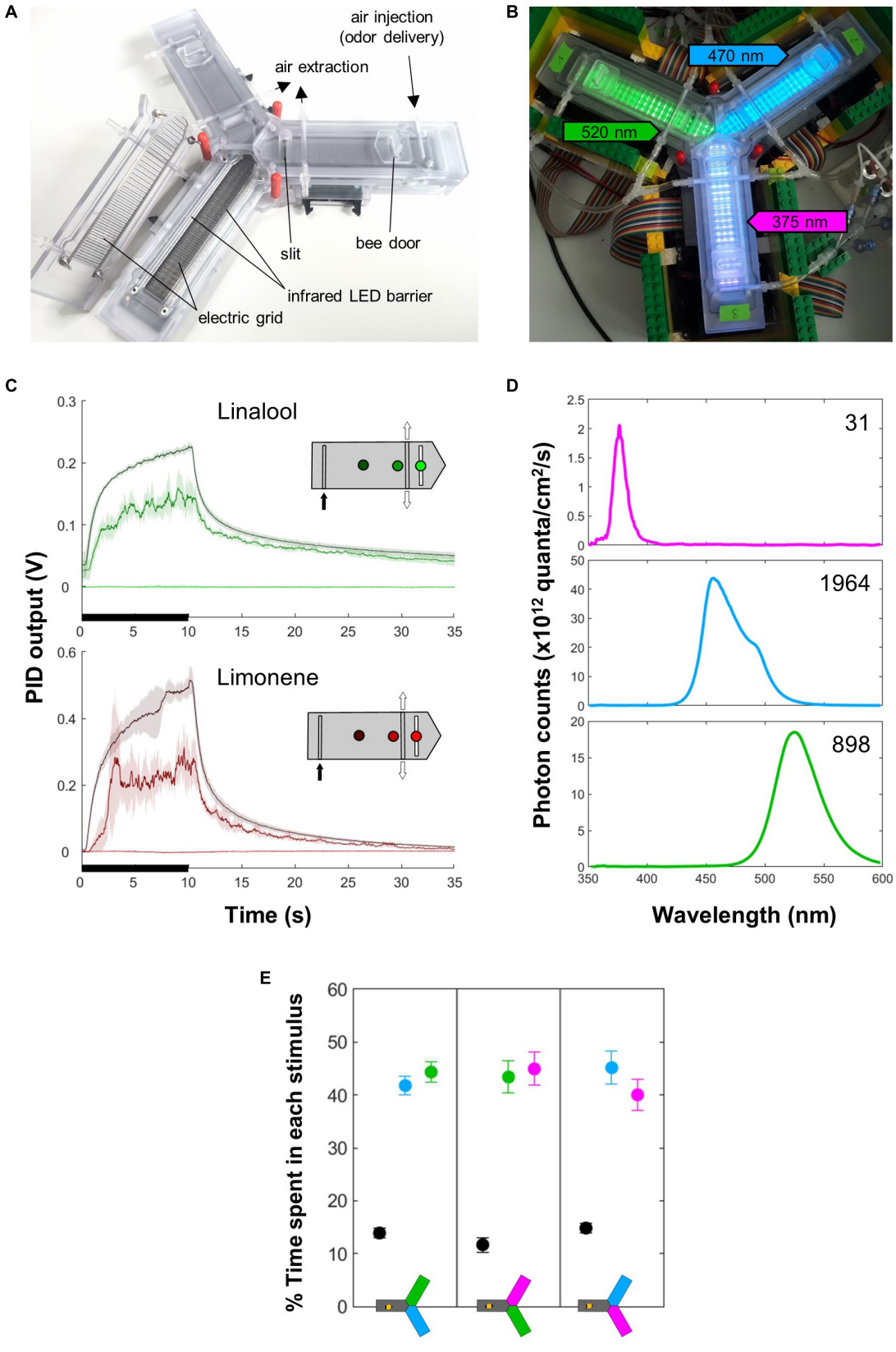

FIGURE 1 | Continued

FIGURE 1 | Apparatus. **(A)** The apparatus. Each arm is equipped with an entry door, an infrared LED barrier that records the position of the bee, and two electric grids (on the floor and ceiling) that serve for delivery of mild electric shocks (US). A constant air flow (in which odors can be injected) runs from the distal part of the system and is evacuated centrally through an active vacuum and a passive slit. The LEDs used as CS are situated below the floor. **(B)** The apparatus in place, with the different lights on: green (520 nm) in arm 1, blue (470 nm) in arm 2, UV (375 nm) in arm 3 (the intensities do not match what was used for experiments). **(C)** PID measurements show that odor delivery (black bars) is well defined spatially and temporally. Each curve corresponds to a position within the arm, as indicated on the inset. Mean ± SD of five consecutive measurements spaced by 30 s. The insets indicate the different points where the measures were taken inside the arm. The odor was injected at the distal end (black arrow) and evacuated centrally by the vacuum (white arrows). **(D)** Light spectrum of the different LEDs, measured inside the apparatus at the intensities used during the experiments. The number is the upper right corner indicates the total photon count ($\times 10^{12}$). **(E)** The light intensities were chosen so that naïve bees did not exhibit preferences between any two lights in a choice test. All lights elicited strong positive phototaxis. n = 18 bees × 3 groups.

was in, each electric shock, the current flow during the shock, the odor delivery events and the lights on/off events.

Data Analysis

The data was analyzed using a custom script written in Python 3.7, and statistical tests were implemented in Matlab R2018b. We defined a criterion for unhealthy or exhausted bees: bees that moved slower than 6 mm/s during the test phase were excluded, and new bees were measured instead. Learning scores are based on the percentage of time spent in each light environment. Direct comparisons of the two lights in a "spontaneous" choice test were performed using Wilcoxon signed rank tests. Mann–Whitney U-tests were performed to observe the change in distributions between the control group and a trained group. In all statistical tables, the uncorrected p-value from the test are reported as "p," and false discovery rate corrected p-values as "FDR" (Verhoeven et al., 2005). In **Figure 8**, we pooled the two symmetrical training groups and compared them to a single control group by attributing the roles of CS+ and CS− to the correct stimuli. Analyses using ANOVA tests were followed by a *post hoc* Tukey's honest significant difference (HSD) test when required. The outliers were defined as values that are more than 1.5 times the interquartile range away from 25th and 75th percentiles.

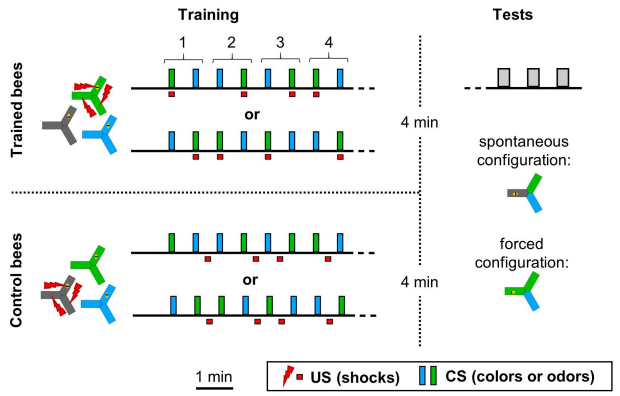

FIGURE 2 | Experimental design. During the training phase the CS and/or US were presented throughout the entire apparatus for 10 s. Honeybees were trained with one of two training sequences, such that half of the bees were trained with sequence 1 and the other half with sequence 2. Control bees were subjected to the same CS sequences, but with the shocks unpaired from both CS. In this example, the bees had four training trials with each CS. Performance could be tested with two CS configurations, depending on the experiment. In the "spontaneous" choice, the CS were placed so that the bee started in the dark arm and was confronted with a choice between the two other arms. In the case of colors, the bee was naturally willing to make a choice due to positive phototaxis. In the case of odors, these two choice arms were made attractive by a dim blue illumination. In the "forced" choice, two arms contained the CS+, including the one where the bee started. The last arm always contained the CS–. In this configuration, the odor choice was tested in the dark. No shocks were ever given during the tests, which lasted 20 s.

RESULTS

Honey Bee Behavior Inside the yAPIS System

Bees placed inside the apparatus moved constantly within, as exemplified in **Figure 3A**. They explored all three arms of the apparatus, with a very slight preference for Arm 3 [**Figure 3B**; ANOVA, $F(2,3645) = 46.87$, $p < 0.001$]. Even though the apparatus were shielded from the light inside a black fabric box, Arm 3 always faced away from the wall where it may have received more residual light than the other two arms. Looking more closely at the spatial distribution of the bees inside the apparatus revealed that they spent more time at the far end of the arms and in the central area (**Figure 3C**, positions 25 and 1, respectively). Furthermore, they seemed to react to the presence of the vacuum at position 9, often turning back at this point (also visible on **Figure 3A**).

The bees' walking speed was 30 mm/s on average, but depended on the season: summer bees were a little bit faster than artificially reared bees (**Figure 4A**; ANOVA, $F(1,3356) = 223.41$, $p < 0.001$). As a result only 5% of bees were below the exclusion criteria of 6 mm/s in summer while 14% of bees were excluded in winter. In addition, the bees' speed depended strongly on the phase considered [ANOVA, $F(2,3356) = 807.95$, $p < 0.001$; *post hoc* multiple comparisons (Tukey's HSD): all $p < 0.001$]. Bees were fastest during the training phase, most likely as a response to the electric shocks – as already demonstrated in Kirkerud et al. (2017). Their average speed during the STM test was slower, however, the number of training trials received (and hence the duration of the training) only had a small impact on the bees' speed during this second phase [**Figure 4B**; ANOVA, $F(3,636) = 4.6$, $p = 0.0034$, *post hoc* multiple comparisons (Tukey's HSD): 1 vs. 4, $p = 0.0055$, 2 vs. 4, $p = 0.0094$]. Thus the decrease in speed between training and STM most likely resulted from the bees settling down after the shocks rather than exhaustion. Finally, bees were slowest during the LTM test, likely as a result of being contained for 24 h (even though our procedure had a very good survival rate –

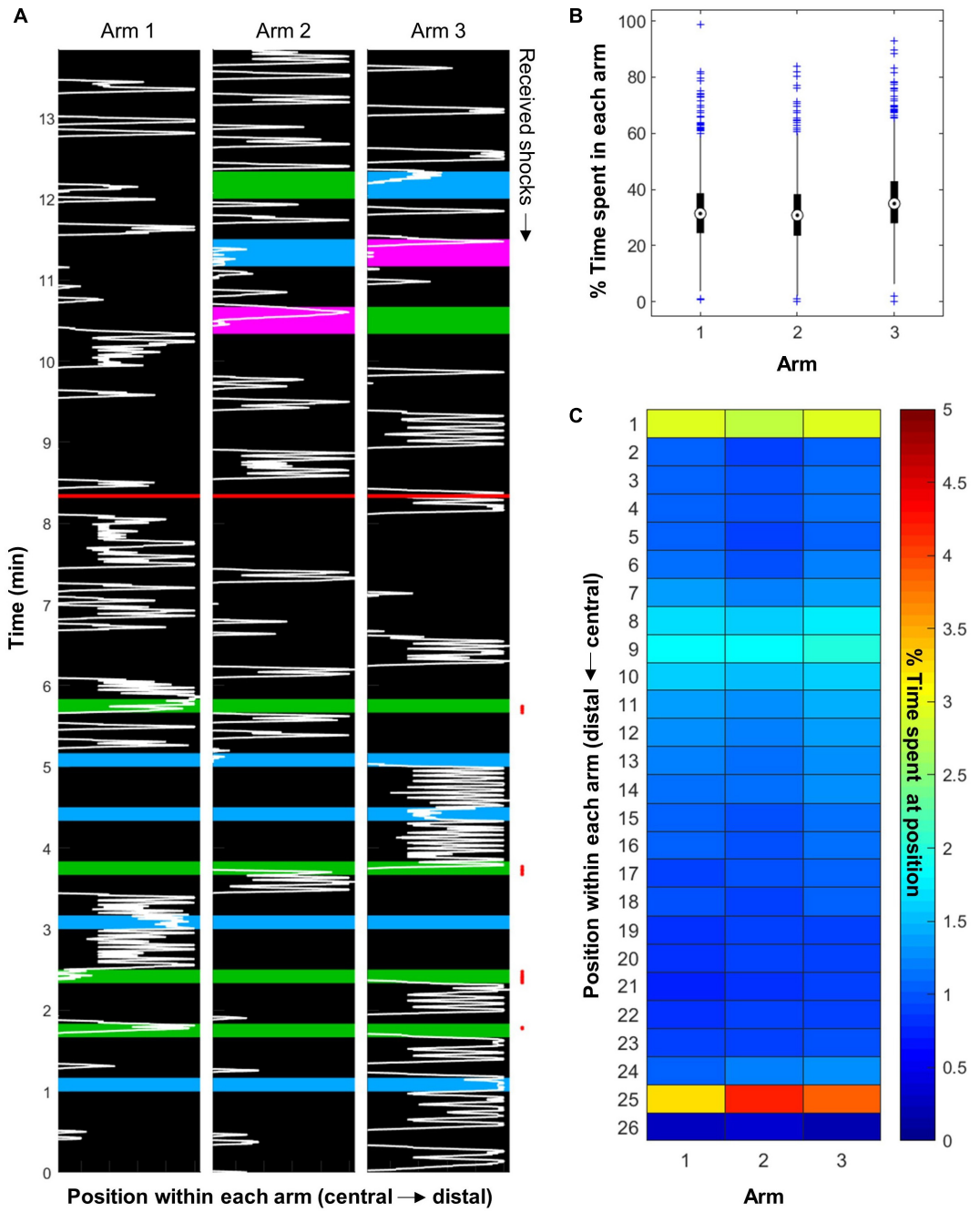

FIGURE 3 | Honeybees explored the whole apparatus. **(A)** Representative example of bee movement inside the apparatus (bee trained with four training trials in the blue vs. green paradigm, with green shocked, and tested with all three color pairs). The background color represents the light inside each arm. The red line separates the training phase from the STM test. The red points on the right mark the received electric shocks. **(B)** The bees explored the whole apparatus, and had a slight preference for Arm 3 (n = 1216 bees). **(C)** Bees spent more time at the far end of each arm and in the central area. They also seemed to react to the presence of the vacuum, which is on top of position 9 (n = 576 bees).

98%). It could also be that they were habituated to the arena the second time.

Electric shocks delivery was quantified by measuring the current flow. A bee only received the shock when she contacted adjacent wires of the grid thus closing the circuit, which happened for 34.4 ± 13.81% of the delivered shocks (**Figure 4C**). Since the full US is a train of 20 shocks at 2 Hz, the bees received on average seven shocks within the 10 s of US delivery. The mean intensity of the shocks received by each bee was 1.38 ± 0.67 μA (**Figure 4D**). The upper outliers in these figures correspond to

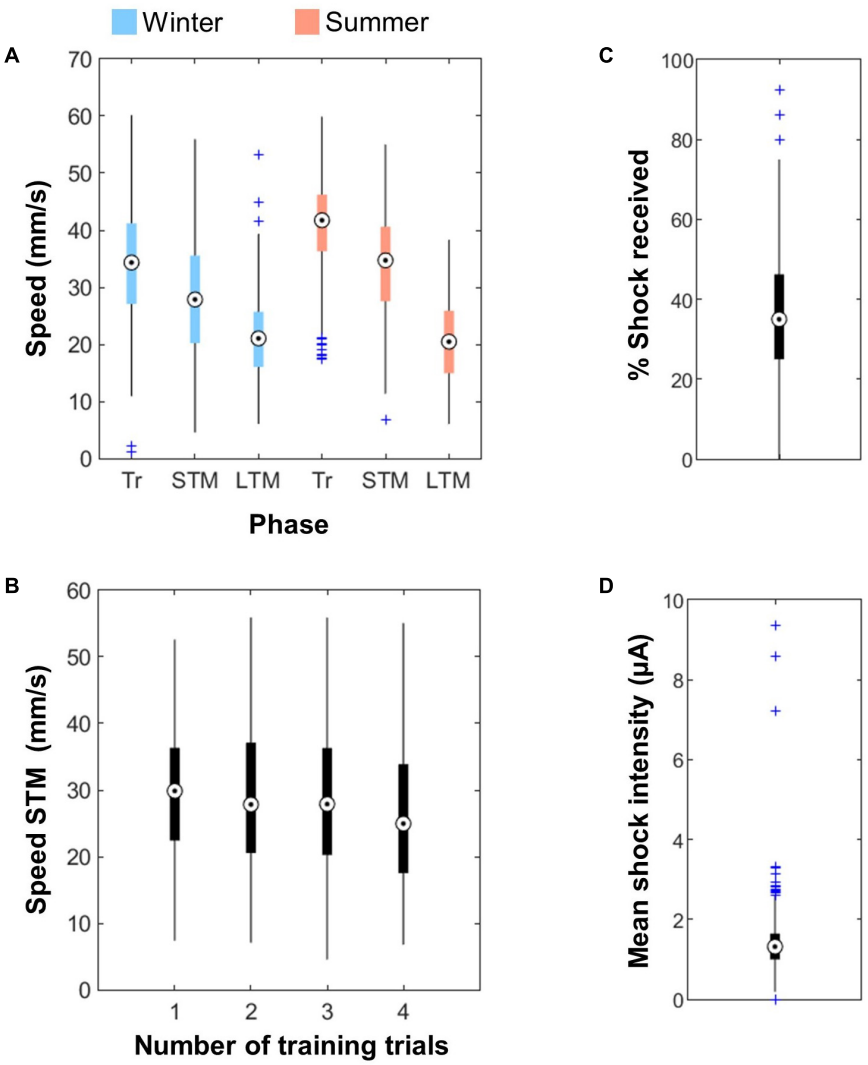

FIGURE 4 | Walking speed and shocks. **(A)** Walking speed of the bees during the training phase (Tr), the STM test and the LTM test. Summer bees (n = 576 for Tr + STM, 288 for LTM) were slightly faster than bees reared under artificial conditions during winter (n = 640). The bees' speed also depended on the phase considered. **(B)** The walking speed of the bees during the STM test was slightly reduced after 4 training trials (n = 640). **(C)** Around 35% of the shocks delivered were actually received by the bees (n = 1216 bees). **(D)** Intensity of the shocks received by the bees (mean for each individual bee, n = 1216).

bees that defecated inside the apparatus (which was rare and only happened in winter), thereby creating short-circuits.

Bees Learn to Associate Odors to Punishment

We used the yAPIS to train bees to differentiate two odors as CSs (**Figure 5**, **Table 2**, and **Supplementary Figure S1**). Half of the bees were trained with limonene as CS+ and linalool as CS−, while for the other half CS+ and CS− were reversed, balancing any potential bias in preference. Bees were kept in the dark during the whole training. During testing, the arm where the bee was positioned was identified, and the two odorants were delivered into the other two arms, along with a blue background illumination. Positive phototaxis induced the bees to move toward these arms, and then to make a choice between the two odorants. Each bee went through two testing sessions: one 4 min after the end of the training (short-term memory, STM), and another 24 h later (long-term memory, LTM). An avoidance of the CS+ arm against the CS− arm was observed after two or more training trials when the bees were tested shortly after the training (STM, **Figure 5A**). A day later, a specific memory trace was only observed in bees that received four training trials with each CS. Strikingly, bees spent more time in the dark arm during this LTM test, but the reason why (e.g., decrease of the phototactic response, avoidance of both odorants?) could not be evaluated in this dataset, and will be addressed below. These experiments were performed during winter, using a honey bee colony kept in a standardized day/light rhythm, with access to pollen and food, but not to a natural free-space environment.

When we repeated the 4-trial STM experiment in summer (**Figure 5B**), we found similar results. This suggests that artificial rearing did not affect olfactory learning.

Some Color Pairs Are Easier to Learn Than Others

We trained 12 groups of 40 bees, corresponding to four numbers of training trials (Nt, from 1 to 4 for each CS) across the three color pairs available in the yAPIS (blue vs. green, blue vs. UV, and green vs. UV). In each group, half of the bees were trained to one color of the pair whereas the other half was trained to the other color, so that any pre-existing preference was balanced by pooling the data. Independently of the number of training trials, bees spent overall more time in the CS− (∼50%) than in the CS+ (∼30%) during the STM test (**Supplementary Figure S2**). This learning was highly significant (**Table 3**, "All pairs"). After 24 h, the learning effect disappeared in bees that received only one training trial, indicating that only short-term learning had occurred, but was maintained in all the other groups (**Table 3**). However, we noted that performance differed widely between color pairs.

Therefore, we analyzed the data separating the different color groups, pooling symmetric training in order to compensate for unequal color preference (**Figure 6** and **Table 3**). The unpooled data can be found in **Supplementary Figures S3** (STM) and **S4** (LTM). Here, we found that training blue vs. green produced significant STM already after 1 trial, and significant LTM after two training trials (**Figure 6Ai**). Training either blue or green against UV, however, did not elicit clear learning, except in few cases possibly due to random fluctuations (**Figures 6Aii, Aiii**; e.g., Nt = 3 STM for the blue–UV pair). Similarly, the LTM test was only significant for Nt = 3 and 4 for green vs. UV. These experiments were conducted during winter, with bees reared inside a warm cage under an artificial "sky" (including UV lights). Possibly, the difference in performance could be due to these rearing conditions. Therefore, we compared their performances to those of summer bees, by repeating the four-trial STM protocol. Summer bees performed better in all groups, and solved the task with all color pairs (**Figure 6B**). As for caged bees, the strongest learning scores were found for the blue vs. green condition.

TABLE 2 | Summary of statistical results for the olfactory conditioning (**Figure 5**), Wilcoxon signed-rank tests.

Odor pair	Nt	*n*	STM		LTM	
			z	*p*	*z*	*p*
Linalool vs. limonene	1	40	−0.1954	0.8451	−0.1697	0.8652
	2	40	−2.2747	**0.0229***	−1.3125	0.1894
	3	40	−2.6514	**0.008****	−1.1629	0.2449
	4	40	−3.0109	**0.0026****	−2.2603	**0.0238***

*$p < 0.05$, **$p < 0.01$, ***$p < 0.001$.

Given that this analysis showed that the color pair used influenced the learning score, we analyzed whether within one pair the two colors were learned equally well or not. We trained another nine groups of 48 summer bees, including three unpaired control groups (**Table 1**). To get a finer understanding, we also tested the behavior of these bees when faced with all three color pairs (**Figure 7** and **Table 4**). In this figure and the following, the data from trained bees (T) is compared to the data from the control groups (C). For each group of bees, the percentages of time spent in the environments available during a given test (e.g., dark, blue, and green) are plotted and stacked into a single bar. Since we included all environments, the resulting stack always totalize 100% (the whole test duration). In the blue/green pair, bees learned to avoid blue when punished, and to avoid green when punished. In the blue/UV pair, blue as CS+ decreased bee visits, but UV did so only marginally. In the green/UV situation, learning effects were marginal (i.e., significance disappeared with FDR correction). Thus, we concluded from this experiment that honey bees can readily attach an aversive memory to the blue and green wavelengths, but not to UV. Possibly, the phototactic attraction elicited by a light within the UV range is more resilient to aversive classical conditioning.

Differential Conditioning Produces Aversive but Not Safety Learning

In aversive differential conditioning, avoiding the CS+ or seeking the CS− are entangled behaviors, but distinct learning events. In order to characterize more precisely the association(s) formed by the honey bees during our training protocol, we extended the test phase: in addition to testing the CS+ against the CS− as before, we also tested either one separately against a novel stimulus (i.e.,

TABLE 3 | Summary of statistical results for the visual conditioning (**Figure 6**), Wilcoxon signed-rank tests.

Color pair	Nt	*n*	STM		LTM	
			z	*p*	*z*	*p*
All pairs	1	120	−3.4199	**0.0006*****	−0.9064	0.3647
	2	120	−5.0756	**<0.0001*****	−2.128	**0.0333***
	3	120	−5.9321	**<0.0001*****	−3.4446	**0.0006*****
	4	120	−3.5752	**0.0003*****	−2.5827	**0.0098****
Blue vs. green	1	40	−2.1101	**0.0349***	−0.2512	0.8017
	2	40	−4.5028	**<0.0001*****	−2.1246	**0.0336***
	3	40	−3.9383	**<0.0001*****	−2.5161	**0.0119***
	4	40	−4.661	**<0.0001*****	−2.5259	**0.0115***
Blue vs. UV	1	40	−2.2313	**0.0257***	−0.7317	0.4644
	2	40	−1.3676	0.1714	−0.6838	0.4941
	3	40	−4.8006	**<0.0001*****	−1.1963	0.2316
	4	40	−0.7675	0.4428	0.3847	0.7005
Green vs. UV	1	40	−1.4651	0.1429	−0.6183	0.5364
	2	40	−2.7555	**0.0059****	−1.0319	0.3021
	3	40	−1.0215	0.307	−2.0653	**0.0389***
	4	40	−0.6977	0.4853	−2.1951	**0.0282***

*$p < 0.05$, **$p < 0.01$, ***$p < 0.001$.

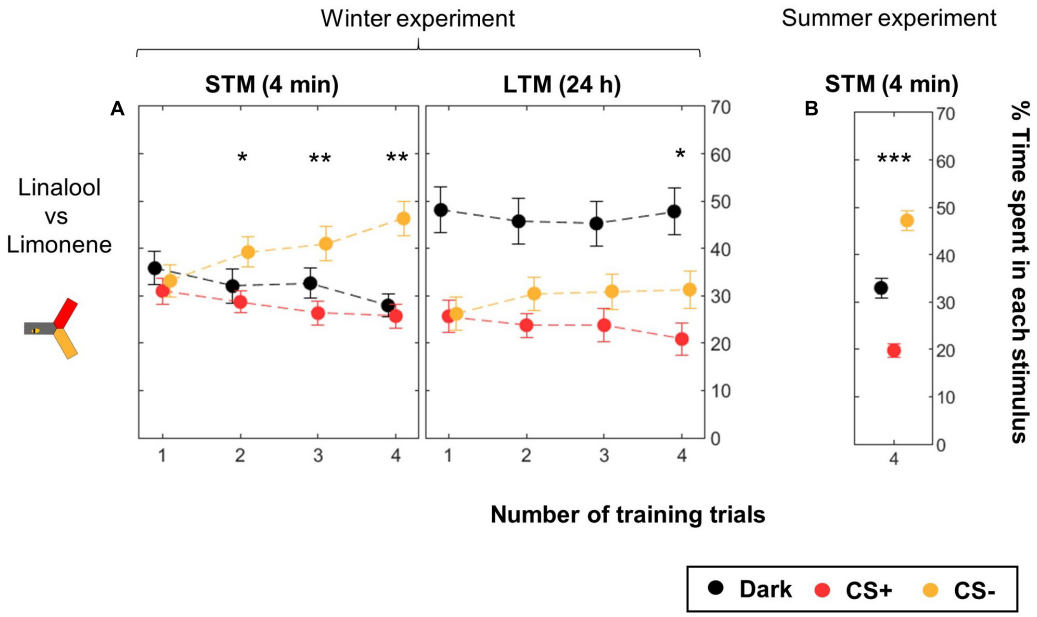

FIGURE 5 | Differential conditioning of odors. During training, shocks were paired with the CS+ (red) but not with the CS− (yellow). Twenty bees were trained to one odor, and 20 bees to the other odor. The same bees were tested twice, 4 min after the end of the training and again 24 h later. Data is represented as mean ± SEM. Wilcoxon signed rank tests comparing CS+ to CS−, $*p < 0.05$, $**p < 0.01$, $***p < 0.001$. **(A)** Winter experiment, $n = 160$ bees (four numbers of CS presentation × 40 bees). **(B)** Summer experiment, $n = 96$ bees.

CS+ vs. New or CS− vs. New). In the case of odors, we kept the background lights in two of the arms but only presented one of the odors at a time (i.e., CS+ vs. None or CS− vs. None). With this experimental design, a pre-existing bias for or against a stimulus would influence the results. Therefore, we statistically tested the trained bees against an independent group of control bees. Bees in the control group experienced both the CSs and the shocks but not in close temporal association (unpaired control, see **Figure 2**). We used four training trials for each CS.

Bees trained for the odorants linalool vs. limonene avoided the CS+ whenever present, but did not change their behavior toward the CS− (**Figure 8A** and **Table 5**). This indicates that the CS+ odor had become aversive, but the CS− odor had not changed valence. As in the previous data set, during the LTM test bees spent a larger amount of time in the dark. They did so significantly more than the control bees and only when the CS+ was present. Hence, rather than a general decrease in phototactic behavior or a loss of specificity of the memory, the data indicate that the aversive memory was strengthened while being consolidated during the 24 h between the tests, resulting in stronger aversion of the CS+ that kept the bee away from both choice arms.

For the visual paradigm, we focused on the blue/green pair for conditioning as it produced the most reliable performance (see **Figure 6**), and hence UV was the novel stimulus. Nonetheless, the short-term outcome was the same with all the color pairs (as can be seen by looking in details at **Figure 7**). When tested to choose between the CS+ and the CS− shortly after conditioning, trained bees spent less time than control bees in the CS+, going instead into the arm containing the CS− (**Figure 8B** and **Table 5**). This avoidance of the CS+ was also evident when it was presented against the novel stimulus, whereas the behavior toward the CS− did not change, indicating that no association had been formed with the CS−. Similar results were obtained when the bees were tested again 24 h later, indicating that the aversive memory formed was stable for this length of time. Overall, we conclude that in our apparatus, aversive differential conditioning relied exclusively on the bees learning to avoid the shocked CS, and not on safety learning of the CS that was never shocked.

Trained Bees Spontaneously Escape From the CS+ When Provided With an Alternative

In the experiments presented above, a choice behavior was induced by presenting two stimuli in two alternative arms, while the bee was in the third, dark arm. These tests took advantage of the positive phototactic behavior exhibited by honey bees inside the yAPIS. If the CS+ induced learned aversion, we figured that a bee should also try to escape from it. We tested this by delivering the CS+ in two arms, including the one occupied by the bee at the start of the test. The third arm always contained the CS−. As before, no shocks were given during the tests, and during the training the US (and the associated CS+) were always delivered in all arms at the same time. Thus, escape behavior was not a useful strategy during the training trials. Nonetheless, we found that trained bees encountering this new test configuration successfully escaped the CS+ arm and stayed in the CS− arm instead, thus spending a higher percentage of their time there

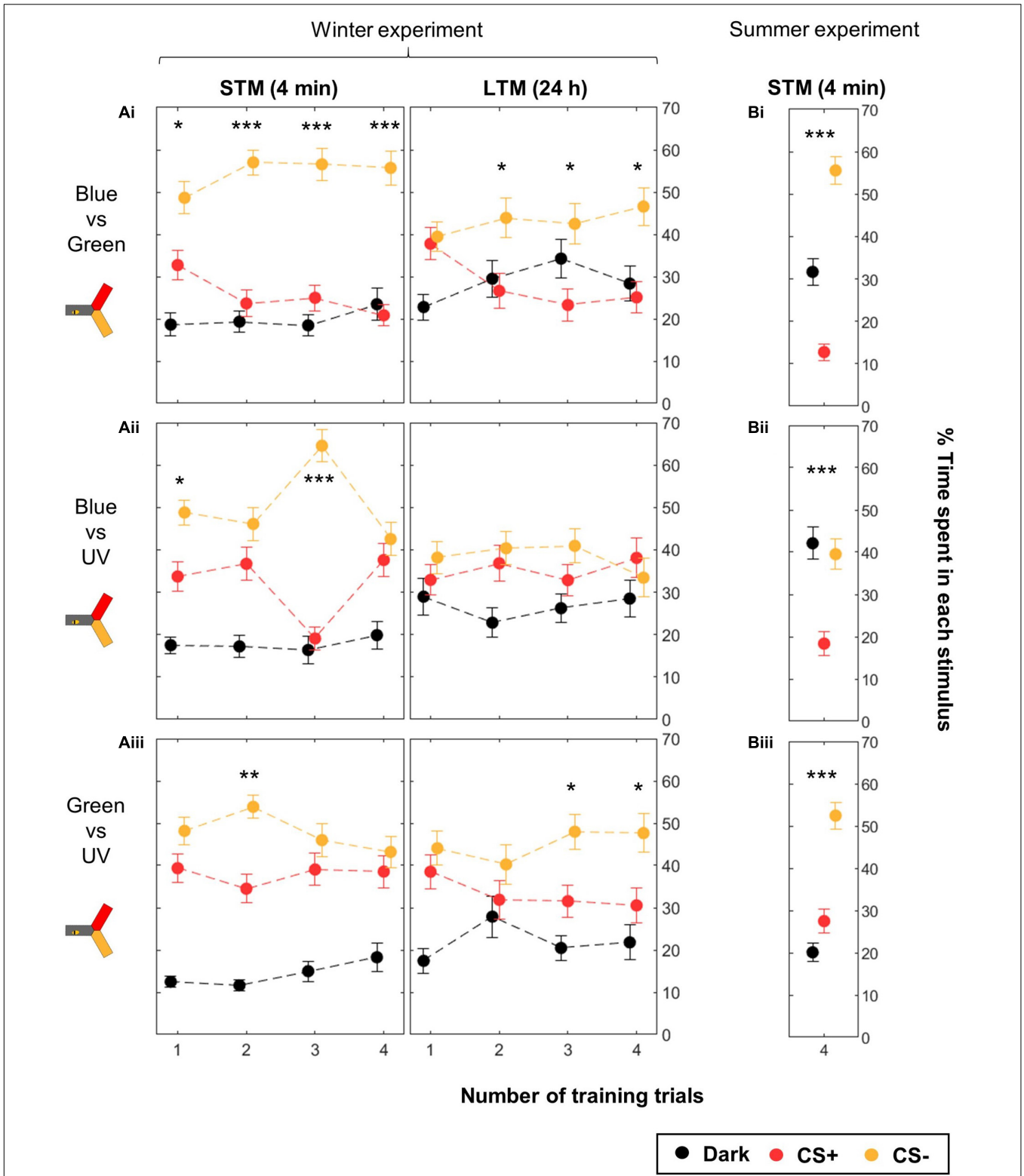

FIGURE 6 | Differential conditioning of colors: learning performance depends on the color pair. During training, shocks were paired with the CS+ (red) but not with the CS– (yellow). For each color pair and each number of CS presentations, half of the bees were trained to one color, and the other half to the other color. During winter **(A)** the same bees were tested twice, 4 min after the end of the training and again 24 h later. Data is represented as mean ± SEM. Wilcoxon signed rank tests comparing CS+ to CS–, $*p < 0.05$, $**p < 0.01$, $***p < 0.001$. **(A)** Winter experiment, $n = 480$ bees (3 color pairs × 4 numbers of training trials × 40 bees). **(B)** Summer experiment, $n = 144$ bees (3 color pairs × 48 bees).

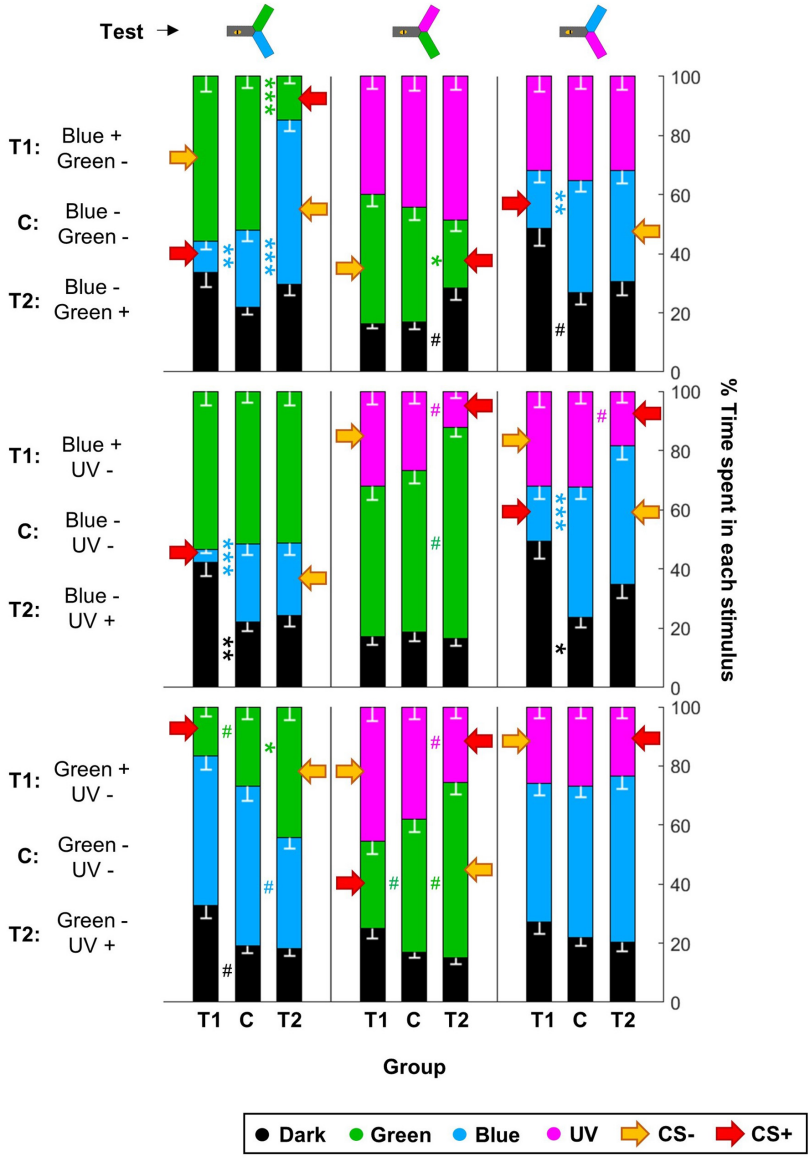

FIGURE 7 | UV is resistant to aversive training. During training, shocks were paired with the CS+ but not the CS– for trained animals (T1 and T2), while control bees (C) received shocks unpaired from both CS. Each bee participated in all three tests after training. Red arrows highlight the CS+. For each group of bees, the percentages of time spent in the environments available during a given test (e.g., dark, blue, and green) are plotted and stacked into a single bar. Since we included all environments, the resulting stack always totalize 100% (the whole test duration). Data is represented as mean – SEM; n = 48 bees × 9 groups. Mann–Whitney U-tests comparing C to T1 or T2, corrected with FDR, *$p < 0.05$, **$p < 0.01$, ***$p < 0.001$, #0.05 > $p >$ corrected threshold.

than the control bees (**Figures 9A,B** and **Table 6**). This was true whether the CSs were colors or odors, thus indicating that honey bees spontaneously tried to escape when presented with the CS+. Interestingly, this protocol provided a way of measuring odor learning without the need for creating phototactic attraction with background illumination.

Honey Bees Learn Both Components in a Bimodal Stimulus

Finally, we investigated if the yAPIS could be a good instrument for the study of bimodal learning. We trained honey bees in a simple bimodal task, where the CS was a combination of an odorant and a color stimulus. We used blue + limonene and green + linalool as CSs. As before, the experiments were balanced: half of the bees were trained to associate the shocks with blue+limonene, whereas for the other half the shocks were paired with green + linalool. The performance of the bees was then evaluated by giving a choice between the same bimodal stimuli, or by testing the colors alone or the odors alone (**Figure 9C** and **Table 6**). Trained bees spent significantly less time than control bees in the arms that contained the complete CS+

TABLE 4 | Summary of statistical results for the second visual conditioning (**Figure 7**), Wilcoxon signed-rank tests, "*p* FDR" indicates the *p*-value corrected with FDR.

Group	Test	Color	$n_t = n_c$	STM		
				z	*p*	*p* FDR
BG (T1)	B vs. G	D	48	−0.6414	0.5212	0.5864
		B	48	3.6829	**0.0002*****	**0.0012****
		G	48	−1.0168	0.3092	0.6957
	G vs. U	D	48	−0.5019	0.6157	0.6157
		G	48	−0.814	0.4157	0.6236
		U	48	0.8134	0.416	0.5349
	B vs. U	D	48	−2.11	**0.0349***	**0.1047**
		B	48	3.7668	**0.0002*****	**0.0012****
		U	48	0.8507	0.3949	0.7108
GB (T2)	B vs. G	D	48	−1.3007	0.1934	0.3481
		B	48	−4.9576	**<0.0001*****	**<0.001*****
		G	48	6.1851	**<0.0001*****	**<0.001*****
	G vs. U	D	48	−2.0592	**0.0395***	**0.0889**
		G	48	2.7116	**0.0067****	**0.0201***
		U	48	−0.613	0.5399	0.6942
	B vs. U	D	48	−0.3922	0.6949	0.7818
		B	48	0.1544	0.8773	0.8773
		U	48	0.7888	0.4302	0.6453
BU (T1)	B vs. G	D	48	−3.0354	**0.0024****	**0.0072****
		B	48	4.5918	**<0.0001*****	**<0.001*****
		G	48	−0.6789	0.4972	0.7458
	G vs. U	D	48	0.0916	0.9270	0.9270
		G	48	0.6343	0.5259	0.6761
		U	48	−0.8512	0.3946	0.7103
	B vs. U	D	48	−2.4309	**0.0151***	**0.0340***
		B	48	4.3551	**<0.0001*****	**<0.001*****
		U	48	0.2358	0.8136	0.9152
UB (T2)	B vs. G	D	48	0.2455	0.8061	0.9068
		B	48	0.3117	0.7552	0.9710
		G	48	−0.1504	0.8805	0.8805
	G vs. U	D	48	0.3261	0.7444	1.1165
		G	48	−2.5832	**0.0098****	**0.0882**
		U	48	2.3388	**0.0193***	**0.0869**
	B vs. U	D	48	−1.6384	0.1013	0.2280
		B	48	−0.5800	0.5619	1.0115
		U	48	2.2046	**0.0275***	**0.0825**
GU (T1)	B vs. G	D	48	−2.2059	**0.0274***	**0.1233**
		B	48	0.5396	0.5895	0.6632
		G	48	1.9856	**0.0471***	**0.1413**
	G vs. U	D	48	−1.6121	0.1069	0.2406
		G	48	2.6163	**0.0089****	**0.0801**
		U	48	−1.3811	0.1673	0.3011
	B vs. U	D	48	−0.7987	0.4244	0.6367
		B	48	0.6486	0.5166	0.6642
		U	48	0.0941	0.9250	0.9250
UG (T2)	B vs. G	D	48	0.4140	0.6789	0.7637
		B	48	2.4044	**0.0162***	**0.0729**
		G	48	−2.9378	**0.0033****	**0.0297***
	G vs. U	D	48	0.9599	0.3371	0.5056
		G	48	−2.3196	**0.0204***	**0.0612**
		U	48	1.9675	**0.0491***	**0.1105**
	B vs. U	D	48	0.3041	0.7611	0.7611
		B	48	−1.0113	0.3119	0.5613
		U	48	0.5485	0.5833	0.7500

(Continued)

TABLE 4 | Continued

$^*p < 0.05$, $^{**}p < 0.01$, $^{***}p < 0.001$.

or a component of the CS+. We conclude that the bees had associated both the color and the odor with the shocks, so that each stimulus was sufficient to trigger an aversive response on its own. Thus, the yAPIS provides a robust, lab-based method to further probe how bimodal compounds are integrated and learned.

DISCUSSION

Animals have to make choices between different environments to escape dangers in many situations, and learn about which environments are dangerous based on previous experience. Choice behaviors can be exploited to study the mechanisms of sensory coding, learning and memory, and decision making (Guerrieri et al., 2005; Hadar and Menzel, 2010; Devaud et al., 2015; Klappenbach et al., 2017). Recent technological developments allow for increasingly automated systems (e.g., Yang et al., 2011; Itskov et al., 2014; Alisch et al., 2018), affording for large-scale screening and standardized conditions.

In this study, we present a new tool for the study of aversive learning with potential to include bimodal forms of training. Walking honey bees are both trained and tested in an automated Y-maze that we named yAPIS, presented here. This system is based on our previous, linear APIS system, where bees could choose between two halves of a linear space environment, that they explored at the beginning (Kirkerud et al., 2013; Wehmann et al., 2015). In the three-arm system presented here, however, bees make repeated left-right choices at a central decision point. We used the yAPIS to perform aversive learning experiments. During the training phase, the apparatus was controlled as a single unit presenting the chosen CS throughout, paired with electric shocks (the US) if appropriate. This arrangement ensured that the association was entirely classical, with no operant components: the animal's own behavior had no influence on its exposure to the stimuli. Learning was then tested by measuring the place preference of the bee when offered a choice between two alternative stimuli. Using this methodology, we successfully trained bees in olfactory, visual, and bimodal tasks. Learning was already evident after one or two training trials, and four training trials led to a consistent long-term memory after 24 h.

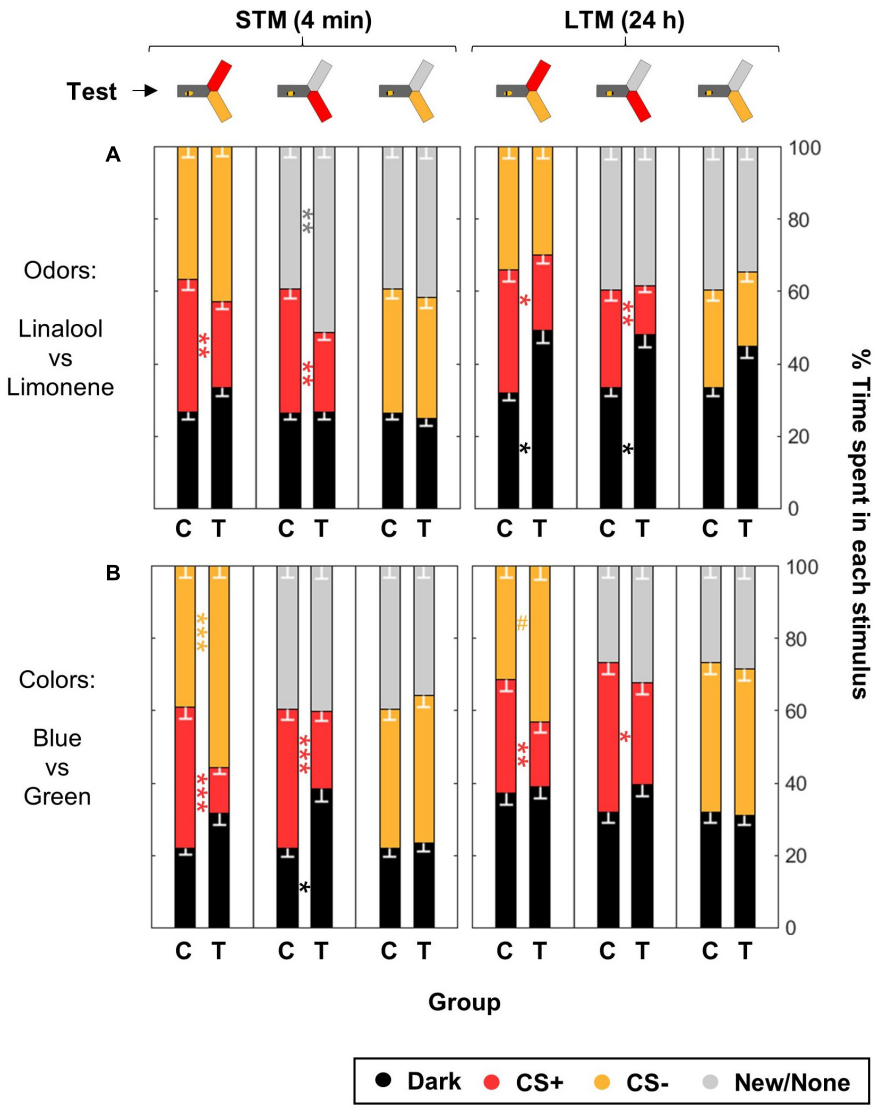

FIGURE 8 | Differential conditioning produces aversive learning of the CS+ but not safety learning of the CS–. During training, shocks were paired with the CS+ but not the CS– for trained animals (T), while control bees (C) received shocks unpaired from both CS. After training, the bees were confronted to three tests: CS+ vs. CS–, CS+ vs. New/None and CS– vs. New/None. Each bee participated in all tests. For each group of bees, the percentages of time spent in the environments available during a given test (e.g., dark, CS+, and CS–) are plotted and stacked into a single bar. Since we included all environments, the resulting stack always totalize 100% (the whole test duration). Data is represented as mean – SEM. n = 96 trained bees and 48 control bees for each sensory modality. Mann–Whitney U-tests comparing C to T, corrected with FDR, $*p < 0.05$, $**p < 0.01$, $***p < 0.001$, #0.05 > $p >$ corrected threshold. **(A)** In the case of odors, bees were trained with Linalool and Limonene, and each odor was tested against a blank control (because of the dim blue illumination used to make the choice arms attractive during odor tests, the choice was thus blue vs. blue + odor). **(B)** In the case of colors, bees were trained with blue and green, and the novel color was UV.

UV Cannot Be Easily Conditioned in an Aversive Paradigm

We found that not all colors can be learned equally well. Bees did not learn consistently to avoid UV light that was associated with shocks. Bees artificially reared indoor during the winter months performed very erratically when trained with this light. The performance of outdoor summer bees was better, but remained weaker when UV was the CS+ compared to when the shocks were associated with the blue or green lights. The UV light, in absolute terms, was dimmer than the blue or green lights (**Figure 1D**), thus one concern could be that the bees were not able to perceive this light. However, several observations argue against this explanation. First, in honeybees the short-wavelength receptor is known to be more sensitive than the other two photoreceptors by an order of magnitude (von Helversen, 1972; Lunau and Maier, 1995), thus the photon counts cannot be directly interpreted. Furthermore, our behavioral experiments found that the UV light elicited the same attraction (measured as the time spent in each light) as the blue or green lights in two-choice tests (**Figure 1E**). Taken

TABLE 5 | Summary of statistical results for the experiments testing for safety learning (**Figure 8**), Wilcoxon signed-rank tests, "*p* FDR" indicates the *p*-value corrected with FDR.

Group	Test	Color	$n_t = 2n_c$	STM			LTM		
				z	*p*	*p* FDR	*z*	*p*	*p* FDR
Odors	CS+ vs. CS−	D	96	−1.9390	0.0525	0.0945	−2.8685	**0.0041****	**0.0123***
		CS+	96	3.2759	**0.0011****	**0.0099****	2.9959	**0.0027****	**0.01215***
		CS−	96	−1.7128	0.0867	0.1301	1.0460	0.2956	0.3801
	CS+ vs. None	D	96	0.5221	0.6016	0.7735	−2.7182	**0.0066****	**0.01485***
		CS+	96	3.1998	**0.0014****	**0.0063****	3.2526	**0.0011****	**0.0099****
		None	96	−3.1236	**0.0018****	**0.0054****	0.2229	0.8236	0.8236
	CS− vs. None	D	96	0.8403	0.4008	0.9018	−1.8974	0.0578	0.1040
		CS−	96	0.3463	0.7291	0.7291	1.8407	0.0657	0.0986
		None	96	−0.5172	0.6050	0.6806	1.0172	0.3090	0.3476
Colors	CS+ vs. CS−	D	96	−1.3807	0.1674	0.3013	−0.4691	0.639	0.9585
		CS+	96	6.5451	**<0.0001*****	**<0.001*****	3.6267	**0.0003*****	**0.0027****
		CS−	96	−3.7234	**0.0002*****	**0.0006*****	−2.1341	**0.0328***	**0.0984**
	CS+ vs. New	D	96	−2.7046	**0.0068****	**0.0153***	−1.9422	0.0521	0.1172
		CS+	96	4.6076	**<0.0001*****	**<0.001*****	3.0392	**0.0024****	**0.0108***
		New	96	0.0485	0.9613	0.9613	−1.0516	0.293	0.5274
	CS− vs. New	D	96	−0.4702	0.6382	0.8205	−0.0234	0.9813	0.9813
		CS−	96	−0.4163	0.6772	0.7619	0.18	0.8571	1.1020
		New	96	0.912	0.3618	0.5427	−0.0788	0.9372	1.0544

*$p < 0.05$, **$p < 0.01$, ***$p < 0.001$.

together, these observations suggest that our bees were able to see the UV light.

Our learning results are broadly symmetrical to those obtained after appetitive learning: bees trained to associate a colored light with a reward in free-flying experiments do so better and faster within a certain range in the UV, peaking around 420 nm (Menzel, 1967). Naïve bees on their first foraging flight exhibit a preference for the same range of wavelengths, although this innate bias is quickly overridden by appetitive learning (Giurfa et al., 1995). Thus, honey bees seem to be primed to associate a positive valence to UV light, which may explain the low success of our protocol when UV was paired with shocks. Nonetheless this finding is rather surprising given that honey bees are known for the plasticity of their response. In the olfactory system, innate valences of odors, including pheromones, can easily be reversed through training: alarm pheromones can be associated to a reward (Sandoz et al., 2001; Nouvian et al., 2015), while attractive Nasanov compounds can be associated to a punishment (Roussel et al., 2012).

Bees Do Not Show Safety Learning

During differential conditioning, honey bees are not only exposed to the shocked CS+, but also to a safe CS−. Thus, they could potentially learn which stimulus is associated with the shocks (aversive learning) but also which stimulus signal the absence of shocks (safety learning) (Schleyer et al., 2018). We investigated whether these two forms of learning co-occurred in our protocol by testing the behavior of the bees toward the CS+ and the CS− independently from each other. We found strong evidence for the existence of an aversive memory, but none for one related to the CS−. In a previous work, some indications were found that honey bees exhibited relief learning (Kirkerud et al., 2017). Relief learning is slightly different from safety learning in that the CS− signals the end of the punishment rather than its absence (Gerber et al., 2014). Relief learning is linked to the timing of a stimulus, and proposed neural models for the cellular mechanisms include spike-timing dependent plasticity and bidirectional modulation of the coincidence detection machinery (Gerber et al., 2014). On the other hand, safety learning implies much longer time-scales and the mechanisms supporting this form of learning remain elusive. In vertebrates, the neural substrates supporting these two forms of learning are known to rely on different brain structures (Mohammadi et al., 2014).

Multi-Sensory Integration During Aversive Training

Honey bees make use of both visual and olfactory information when foraging (Reinhard et al., 2004; Leonard and Masek, 2014), but also when they perform other important tasks such as defending the nest (Nouvian et al., 2016). However, our understanding of multimodal integration remains poor. Early studies postulated that both components of an olfactory-visual compound were learned independently from each other (Couvillon and Bitterman, 1989; Couvillon et al., 1997), a notion that is also supported in our results (**Figure 9**). Later works, however, found synergistic effects in appetitive training (Gerber and Smith, 1998; Mota et al., 2011). Namely, PER responses to odors were potentiated or refined by a color context. It is important to note that this seemingly asymmetrical role for odors and colors may be the produce of the protocol, since bees always respond more reliably to odors than to colors when harnessed (Avargues-Weber and Mota, 2016), and

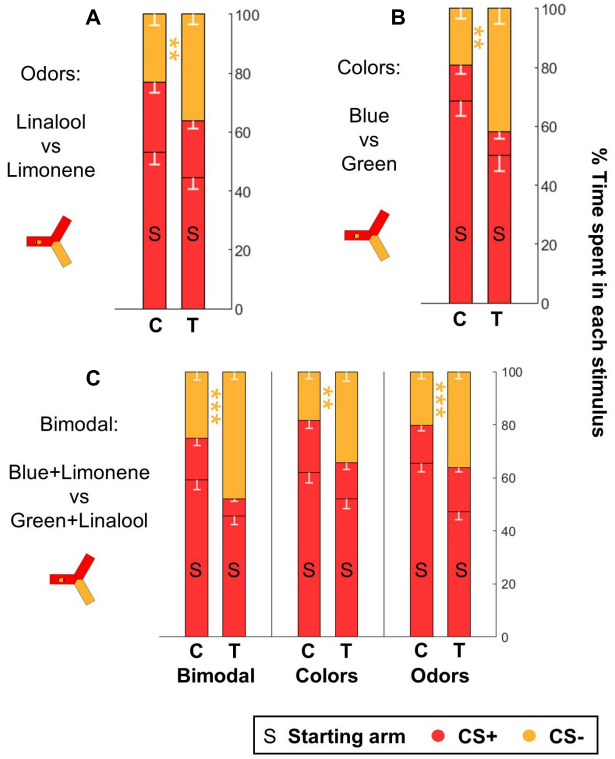

FIGURE 9 | Honeybees learn both color and odor information when trained with bimodal stimuli. After classical training, honeybees spontaneously escaped from the CS+ when they were provided with the CS– as alternative, both after odor **(A)** and after color **(B)** learning (n = 48 trained bees and 48 control bees for each sensory modality). **(C)** Honeybees trained in a bimodal task (n = 96 trained bees and 96 control bees) performed well both when presented with the same compound stimuli (color+odor), with only the colors or with only the odors. Each bee participated in all three tests after training. Data is represented as mean – SEM. Mann–Whitney U-tests comparing C to T, corrected with FDR, $^{**}p < 0.01$, $^{***}p < 0.001$.

TABLE 6 | Summary of statistical results for the experiments with forced choice tests (**Figure 9**), Wilcoxon signed-rank tests, "p FDR" indicates the p-value corrected with FDR.

Group	Test	$n_t = n_c$	STM		
			z	p	p FDR
Odors	/	48	2.9014	**0.0037****	/
Colors	/	48	3.2001	**0.0014****	/
Bimodal	Bimodal	96	4.8234	**<0.0001*****	**<0.001*****
	Only colors	96	3.0999	**0.0019****	**0.0019****
	Only odors	96	4.4974	**<0.0001*****	**<0.001*****

$^{*}p < 0.05$, $^{**}p < 0.01$, $^{***}p < 0.001$.

tend to generalize between the compound stimulus and the odor (Mansur et al., 2018). In our set-up, the behavioral read-out of learning (spatial avoidance of the CS+) was triggered equally well by both colors and odors. Thus, the yAPIS offers the opportunity for more balanced experiments, in which the extent to which visual and olfactory traces interact (or are independent) could be assessed in an aversive context. For example, we could see how trained honeybees would react to ambiguous or contradictory compounds. The mushroom bodies are thought to be responsible for the formation of both appetitive and aversive memory, and studies in *Drosophila* indicate that these two circuits are mostly independent, and act by shifting the balance of common output neurons (Klappenbach et al., 2017; Cognigni et al., 2018). It would be interesting to verify if multi-sensory stimuli are similarly compartmentalized such that the different elements are only integrated at a late stage in the circuitry.

DATA AVAILABILITY

The raw data supporting the conclusions of this manuscript will be made available by the authors, without undue reservation, to any qualified researcher.

ETHICS STATEMENT

This study was carried out in accordance with the recommendations of the "3Rs" principles as stated in the Directive 2010/63/EU governing animal use within the European Union. The use of (non-transgenic) honey bees for research purposes has been reported to the "Regierungspräsidium" as required.

AUTHOR CONTRIBUTIONS

MN and CGG conceived the study. MN designed, performed and analyzed the experiments, and wrote the original draft. MN and CGG edited the manuscript.

FUNDING

MN was supported by a postdoctoral fellowship from the Fyssen Foundation, and received some funding for equipment from the Zukunftskolleg (University of Konstanz). CGG is supported by the DFG Centre of Excellence 2117 "Centre for the Advanced Study of Collective Behaviour" (ID: 422037984).

ACKNOWLEDGMENTS

We would like to thank the workshop at the University of Konstanz for their technical help, as well as Gabriel Michau who wrote the Python script used for analyzing the data. We would also like to thank two dedicated student assistants, Feng Liu and Caroline Grüschel, who helped to perform the experiments.

SUPPLEMENTARY MATERIAL

The Supplementary Material for this article can be found online at: https://www.frontiersin.org/articles/10.3389/fphys.2019.00678/full#supplementary-material

REFERENCES

Agarwal, M., Giannoni Guzman, M., Morales-Matos, C., Del Valle Diaz, R. A., Abramson, C. I., and Giray, T. (2011). Dopamine and octopamine influence avoidance learning of honey bees in a place preference assay. *PLoS One* 6:e25371. doi: 10.1371/journal.pone.0025371

Alisch, T., Crall, J. D., Kao, A. B., Zucker, D., and De Bivort, B. L. (2018). MAPLE (modular automated platform for large-scale experiments), a robot for integrated organism-handling and phenotyping. *Elife* 7:e37166. doi: 10.7554/eLife.37166

Avargues-Weber, A., and Giurfa, M. (2014). Cognitive components of color vision in honey bees: how conditioning variables modulate color learning and discrimination. *J. Comp. Physiol. A* 200, 449–461. doi: 10.1007/s00359-014-0909-z

Avargues-Weber, A., and Mota, T. (2016). Advances and limitations of visual conditioning protocols in harnessed bees. *J. Physiol.* 110, 107–118. doi: 10.1016/j.jphysparis.2016.12.006

Bonadonna, F., and Sanz-Aguilar, A. (2012). Kin recognition and inbreeding avoidance in wild birds: the first evidence for individual kin-related odor recognition. *Anim. Behav.* 84, 509–513. doi: 10.1016/j.anbehav.2012.06.014

Cognato, G. P., Bortolotto, J. W., Blazina, A. R., Christoff, R. R., Lara, D. R., Vianna, M. R., et al. (2012). Y-Maze memory task in zebrafish (*Danio rerio*): the role of glutamatergic and cholinergic systems on the acquisition and consolidation periods. *Neurobiol. Learn. Mem.* 98, 321–328. doi: 10.1016/j.nlm.2012.09.008

Cognigni, P., Felsenberg, J., and Waddell, S. (2018). Do the right thing: neural network mechanisms of memory formation, expression and update in *Drosophila*. *Curr. Opin. Neurobiol.* 49, 51–58. doi: 10.1016/j.conb.2017.12.002

Couvillon, P. A., Arakaki, L., and Bitterman, M. E. (1997). Intramodal blocking in honeybees. *Anim. Learn. Behav.* 25, 277–282. doi: 10.3758/bf03199085

Couvillon, P. A., and Bitterman, M. E. (1989). Reciprocal overshadowing in the discrimination of color-odor compounds by honeybees: further tests of a continuity model. *Anim. Learn. Behav.* 17, 213–222. doi: 10.3758/bf03207637

Devaud, J. M., Papouin, T., Carcaud, J., Sandoz, J. C., Grunewald, B., and Giurfa, M. (2015). Neural substrate for higher-order learning in an insect: mushroom bodies are necessary for configural discriminations. *Proc. Natl. Acad. Sci. U.S.A.* 112, E5854–E5862. doi: 10.1073/pnas.1508422112

Dinges, C. W., Avalos, A., Abramson, C. I., Craig, D. P., Austin, Z. M., Varnon, C. A., et al. (2013). Aversive conditioning in honey bees (Apis mellifera anatolica): a comparison of drones and workers. *J. Exp. Biol.* 216, 4124–4134. doi: 10.1242/jeb.090100

Flexner, J. B., Flexner, L. B., and Stellar, E. (1963). Memory in mice as affected by intracerebral Puromycin. *Science* 141, 55–59.

Gerber, B., and Smith, B. H. (1998). Visual modulation of olfactory learning in honeybees. *J. Exp. Biol.* 201, 2213–2217.

Gerber, B., Yarali, A., Diegelmann, S., Wotjak, C. T., Pauli, P., and Fendt, M. (2014). Pain-relief learning in flies, rats, and man: basic research and applied perspectives. *Learn. Mem.* 21, 232–252. doi: 10.1101/lm.032995.113

Giurfa, M., Núñez, J., Chittka, L., and Menzel, R. (1995). Color preferences of flower-naive honeybees. *J. Comp. Physiol. A* 177, 247–259.

Giurfa, M., and Sandoz, J. C. (2012). Invertebrate learning and memory: fifty years of olfactory conditioning of the proboscis extension response in honeybees. *Learn. Mem.* 19, 54–66. doi: 10.1101/lm.024711.111

Giurfa, M., Shaowu, Z., Jenett, A., Menzel, R., and Srinivasan, M. V. (2001). The concepts of "sameness" and "difference" in an insect. *Nature* 410, 930–933. doi: 10.1038/35073582

Guerrieri, F., Schubert, M., Sandoz, J. C., and Giurfa, M. (2005). Perceptual and neural olfactory similarity in honeybees. *PLoS Biology* 3:e60. doi: 10.1371/journal.pbio.0030060

Hadar, R., and Menzel, R. (2010). Memory formation in reversal learning of the honeybee. *Front. Behav. Neurosci.* 4:186. doi: 10.3389/fnbeh.2010.00186

Hempel de Ibarra, N., Vorobyev, M., and Menzel, R. (2014). Mechanisms, functions and ecology of color vision in the honeybee. *J. Comp. Physiol. A* 200, 411–433. doi: 10.1007/s00359-014-0915-1

Howard, S. R., Avargues-Weber, A., Garcia, J. E., Greentree, A. D., and Dyer, A. G. (2018). Numerical ordering of zero in honey bees. *Science* 360, 1124–1126. doi: 10.1126/science.aar4975

Itskov, P. M., Moreira, J. M., Vinnik, E., Lopes, G., Safarik, S., Dickinson, M. H., et al. (2014). Automated monitoring and quantitative analysis of feeding behaviour in *Drosophila*. *Nat. Commun.* 5:4560. doi: 10.1038/ncomms5560

Junca, P., Carcaud, J., Moulin, S., Garnery, L., and Sandoz, J. C. (2014). Genotypic influence on aversive conditioning in honeybees, using a novel thermal reinforcement procedure. *PLoS One* 9:e97333. doi: 10.1371/journal.pone.0097333

Kirkerud, N. H., Schlegel, U., and Giovanni Galizia, C. (2017). Aversive learning of colored lights in walking honeybees. *Front. Behav. Neurosci.* 11:94. doi: 10.3389/fnbeh.2017.00094

Kirkerud, N. H., Wehmann, H. N., Galizia, C. G., and Gustav, D. (2013). APIS - a novel approach for conditioning honey bees. *Front. Behav. Neurosci.* 7:29. doi: 10.3389/fnbeh.2013.00029

Klappenbach, M., Nally, A., and Locatelli, F. F. (2017). Parallel memory traces are built after an experience containing aversive and appetitive components in the crab Neohelice. *Proc. Natl. Acad. Sci. U.S.A.* 114, E4666–E4675. doi: 10.1073/pnas.1701927114

Leonard, A. S., and Masek, P. (2014). Multisensory integration of colors and scents: insights from bees and flowers. *J. Comp. Physiol. A* 200, 463–474. doi: 10.1007/s00359-014-0904-4

Lunau, K., and Maier, E. J. (1995). Innate color preferences of flower visitors. *J. Comp. Physiol. A* 177, 1–19. doi: 10.1007/s00114-013-1060-3

Mansur, B. E., Rodrigues, J. R. V., and Mota, T. (2018). Bimodal patterning discrimination in harnessed honey bees. *Front. Psychol.* 9:1529. doi: 10.3389/fpsyg.2018.01529

Menzel, R. (1967). Investigations into the honey bee's learning of spectral colors. *Zeitschrift fur vergleichende Physiologie* 56, 22–62.

Menzel, R. (2001). Searching for the memory trace in a mini-brain, the honeybee. *Learn. Mem.* 8, 53–62. doi: 10.1101/lm.38801

Mohammadi, M., Bergado-Acosta, J. R., and Fendt, M. (2014). Relief learning is distinguished from safety learning by the requirement of the nucleus accumbens. *Behav. Brain Res.* 272, 40–45. doi: 10.1016/j.bbr.2014.06.053

Mota, T., Giurfa, M., and Sandoz, J. C. (2011). Color modulates olfactory learning in honeybees by an occasion-setting mechanism. *Learn. Mem.* 18, 144–155. doi: 10.1101/lm.2073511

Nouvian, M., Hotier, L., Claudianos, C., Giurfa, M., and Reinhard, J. (2015). Appetitive floral odors prevent aggression in honeybees. *Nat. Commun.* 6:10247. doi: 10.1038/ncomms10247

Nouvian, M., Reinhard, J., and Giurfa, M. (2016). The defensive response of the honeybee *Apis mellifera*. *J. Exp. Biol.* 219, 3505–3517.

Ravi, S., Garcia, J. E., Wang, C., and Dyer, A. G. (2016). The answer is blowing in the wind: free-flying honeybees can integrate visual and mechano-sensory inputs for making complex foraging decisions. *J. Exp. Biol.* 219, 3465–3472. doi: 10.1242/jeb.142679

Reid, C. R., Latty, T., Dussutour, A., and Beekman, M. (2012). Slime mold uses an externalized spatial "memory" to navigate in complex environments. *Proc. Natl. Acad. Sci., U.S.A.* 109, 17490–17494. doi: 10.1073/pnas.1215037109

Reinhard, J., Srinivasan, M. V., Guez, D., and Zhang, S. W. (2004). Floral scents induce recall of navigational and visual memories in honeybees. *J. Exp. Biol.* 207, 4371–4381. doi: 10.1242/jeb.01306

Roussel, E., Padie, S., and Giurfa, M. (2012). Aversive learning overcomes appetitive innate responding in honeybees. *Anim. Cogn.* 15, 135–141. doi: 10.1007/s10071-011-0426-1

Sandoz, J. C. (2011). Behavioral and neurophysiological study of olfactory perception and learning in honeybees. *Front. Syst. Neurosci.* 5:98. doi: 10.3389/fnsys.2011.00098

Sandoz, J. C., Pham-Delegue, M. H., Renou, M., and Wadhams, L. J. (2001). Asymmetrical generalisation between pheromonal and floral odors in appetitive olfactory conditioning of the honey bee (Apis mellifera L.). *J. Comp. Physiol. A* 187, 559–568. doi: 10.1007/s003590100228

Schleyer, M., Fendt, M., Schuller, S., and Gerber, B. (2018). Associative Learning of Stimuli Paired and Unpaired With Reinforcement: evaluating evidence from maggots, flies, bees, and rats. *Front. Psychol.* 9:1494. doi: 10.3389/fpsyg.2018.01494

Srinivasan, M. V. (2010). Honey bees as a model for vision, perception, and cognition. *Ann. Rev. Entomol.* 55, 267–284. doi: 10.1146/annurev.ento.010908.164537

Srinivasan, M. V., Zhang, S. W., and Zhu, H. (1998). Honeybees link sights to smells. *Nature* 396, 637–638. doi: 10.1038/25272

Tedjakumala, S. R., and Giurfa, M. (2013). Rules and mechanisms of punishment learning in honey bees: the aversive conditioning of the sting extension response. *J. Exp. Biol.* 216, 2985–2997. doi: 10.1242/jeb.086629

Vergoz, V., Roussel, E., Sandoz, J. C., and Giurfa, M. (2007). Aversive learning in honeybees revealed by the olfactory conditioning of the sting extension reflex. *PLoS One* 2:e288. doi: 10.1371/journal.pone.0000288

Verhoeven, K. J. F., Simonsen, K. L., and Mcintyre, L. M. (2005). Implementing false discovery rate control: increasing your power. *Oikos* 108, 643–647. doi: 10.1111/j.0030-1299.2005.13727.x

von Frisch, K. (1914). *Der Farbensinn und Formensinn der Biene, Zoologische Jahrbücher. Abteilung für allgemeine Zoologie und Physiologie der Tiere*. Champaign, IL: University of Illinois Urbana-Champaign.

von Helversen, O. (1972). Zur spektralen Unterschiedsempfindlichkeit der Honigbiene. *J. Comp. Physiol. A* 80, 439–472. doi: 10.1007/bf00696438

Wehmann, H. N., Gustav, D., Kirkerud, N. H., and Galizia, C. G. (2015). The sound and the fury–bees hiss when expecting danger. *PLoS One* 10:e0118708. doi: 10.1371/journal.pone.0118708

Yang, M., Silverman, J. L., and Crawley, J. N. (2011). Automated three-chambered social approach task for mice. *Curr. Prot. Neurosci.* 56, 8.26.1–8.26.16. doi: 10.1002/0471142301.ns0826s56

Conflict of Interest Statement: The authors declare that the research was conducted in the absence of any commercial or financial relationships that could be construed as a potential conflict of interest.

frontiers in Physiology

BRIEF RESEARCH REPORT
published: 09 July 2019
doi: 10.3389/fphys.2019.00851

Third-Order Neurons in the Lateral Horn Enhance Bilateral Contrast of Odor Inputs Through Contralateral Inhibition in *Drosophila*

*Ahmed A. M. Mohamed, Bill S. Hansson and Silke Sachse**

Department of Evolutionary Neuroethology, Max Planck Institute for Chemical Ecology, Jena, Germany

The survival and reproduction of *Drosophila melanogaster* depends heavily on its ability to determine the location of an odor source and either to move toward or away from it. Despite the very small spatial separation between the two antennae and the redundancy in sensory neuron projection to both sides of the brain, *Drosophila* can resolve the concentration gradient by comparing the signal strength between the two antennae. When an odor stimulates the antennae asymmetrically, ipsilateral projection neurons from the first olfactory center are more strongly excited compared to the contralateral ones. However, it remains elusive how higher-order neurons process such asymmetric or lateralized odor inputs. Here, we monitored and analyzed for the first time the activity patterns of a small cluster of third-order neurons (so-called ventrolateral protocerebrum neurons) to asymmetric olfactory stimulation using two-photon calcium imaging. Our data demonstrate that lateralized odors evoke distinct activation of these neurons in the left and right brain hemisphere as a result of contralateral inhibition. Moreover, using laser transection experiments we show that this contralateral inhibition is mediated by presynaptic neurons most likely located in the lateral horn. Finally, we propose that this inhibitory interaction between higher-order neurons facilitates odor lateralization and plays a crucial role in olfactory navigation behavior of *Drosophila*, a theory that needs to be experimentally addressed in future studies.

Keywords: olfaction, calcium imaging, *Drosophila*, odor processing, contralateral inhibition

OPEN ACCESS

Edited by:
Sylvia Anton,
Institut National de la Recherche Agronomique (INRA), France

Reviewed by:
Hong Lei,
Arizona State University, United States
Paul Szyszka,
University of Otago, New Zealand

***Correspondence:**
Silke Sachse
ssachse@ice.mpg.de

Specialty section:
This article was submitted to Invertebrate Physiology, a section of the journal Frontiers in Physiology

Received: *20 March 2019*
Accepted: *20 June 2019*
Published: *09 July 2019*

Citation:
Mohamed AAM, Hansson BS and Sachse S (2019) Third-Order Neurons in the Lateral Horn Enhance Bilateral Contrast of Odor Inputs Through Contralateral Inhibition in Drosophila. Front. Physiol. 10:851. doi: 10.3389/fphys.2019.00851

INTRODUCTION

Chemotaxis is important for the survival of many animals since chemicals that are emitted by the environment can be exploited as cues for potentially positive (e.g., food, mate, or oviposition site) or negative (toxicity, competitors, predators, or parasitoids) interactions. Especially insects rely heavily on their sense of smell to ensure survival and reproduction and have, in most cases, a highly developed and sophisticated olfactory system. To navigate toward (or away from) an odor source, walking and flying insects usually use multiple strategies. Besides anemotaxis, one of the most used strategies is to detect an odor gradient across the two antennae by comparing their signal strength, and to turn toward or away from the stronger olfactory signal, a phenomenon termed "osmotropotaxis" (Martin, 1965; Hangartner, 1967; Kennedy and Moorhouse, 1969). Confusing this strategy, by spatially reversing the antennae (i.e., by crossing and fixing them), impairs chemotaxis as shown in bees, ants, and locusts (Martin, 1965; Hangartner, 1967; Kennedy and Moorhouse, 1969). The vinegar fly *Drosophila melanogaster* also uses the same strategy to navigate

toward or away from an odor source (Borst and Heisenberg, 1982; Duistermars et al., 2009; Gaudry et al., 2013). At the neuronal level, the peripheral olfactory system (i.e., the antennae) of vinegar flies responds differently to lateralized odors (i.e., a bilaterally asymmetric odor stimulation) compared to symmetric odor application (Louis et al., 2008; Duistermars et al., 2009). However, little is known about where the information from both antennae becomes integrated and how higher brain centers process asymmetric odor stimulation to ensure reliable navigation toward odors.

The olfactory circuitry of *Drosophila* has been fairly well characterized, making it a premier model system for studying odor processing strategies. Sixty-two odorant receptors (ORs) are expressed in the dendrites of olfactory receptor neurons (ORNs) (Clyne et al., 1999; Vosshall et al., 1999). The ORNs are housed in hair-like structures called sensilla on the peripheral olfactory appendages (i.e., the antennae and maxillary palps) and express usually one (sometimes two) OR type each. The axons of all ORNs expressing a given OR type converge onto the same glomerulus in the antennal lobe (AL, the analogous to the vertebrate olfactory bulb) (Vosshall et al., 2000; Couto et al., 2005). ORNs synapse onto second-order neurons, so-called projection neurons (PNs, analog to mitral/tufted cells in vertebrates). The axonal terminals of PNs relay the olfactory information from the AL to two higher-order neuropils, which are the mushroom bodies (MBs) (analogs to the piriform cortex in mammals), representing a center of learning and memory, and the lateral horn (LH) (analogous to the mammalian amygdala) that mediates predominantly behaviorally innate responses (Dubnau et al., 2001; Heimbeck et al., 2001; Heisenberg, 2003; Strutz et al., 2014). Third-order neurons, such as MB and LH output neurons (MBONs, LHONs) convey the information to next level protocerebral regions, as, e.g., the ventrolateral protocerebrum (VLP) whose functions remain, so far, largely elusive.

In *Drosophila*, unlike most insects, the majority of ORNs projects from the antennae bilaterally to both brain hemispheres (Stocker et al., 1990; Couto et al., 2005). This bilateral redundancy in morphology may imply that odor inputs are symmetrically directed to both hemispheres. However, the input from the left and right antennae is coded distinctively since ORNs release an asymmetric amount of neurotransmitters in the ipsi- and contralateral AL (Gaudry et al., 2013). As a consequence, the ipsilateral PNs are 30–50% more strongly activated by asymmetric bilateral odor input than the sister neurons in the contralateral AL (Gaudry et al., 2013). In addition, odor lateralization has also been demonstrated at the synaptic level in the AL. Neuronal tracing from serial electron microscopy sections showed that PNs of a given glomerulus share a higher number of synapses with the ipsilateral ORNs than with the contralateral ones (Tobin et al., 2017). Hence, odor input from the ipsi- and contralateral antenna seems to be coded in different ways at the AL level.

In order to study how lateralized odors are processed by higher-order neurons, we investigated the neuronal responses of a specific cluster of LHONs, so-called VLP neurons (hereafter VLPn), to asymmetric and symmetric odor stimulations using two-photon functional imaging. We found that odor-evoked responses of VLPn were suppressed when an odor was presented to the contralateral side. Hence, the detection of an odor gradient is accomplished in a way that asymmetric odor stimulation suppresses the responses in contralateral VLPn. Notably, the observed contralateral suppression is not induced by VLPn in the contralateral hemisphere, but, most likely, mediated by presynaptic neurons located in the LH. Our data demonstrate for the first time that higher-order neurons respond distinctively to a lateralized odor stimulus through contralateral inhibition and therefore enhance the contrast of odor concentration gradient between both brain hemispheres.

RESULTS AND DISCUSSION

Contralateral Stimuli Suppress Odor Responses in VLP Neurons

Ventrolateral protocerebrum neurons have their postsynaptic dendrites in the LH and send their axonal terminals to the VLP, where they synapse onto further higher-order neurons (**Figures 1A,B**). Previous studies have shown that these third-order neurons receive input from olfactory PNs in the LH and respond to a variety of different odors (Liang et al., 2013; Strutz et al., 2014). Furthermore, VLPn exhibit a stereotypic innervation pattern in both neuropils and are involved in innate odor-guided behavior (details will be described in Mohamed et al., in preparation). To investigate how these third-order neurons respond to lateralized odors, we measured their responses to symmetric and asymmetric odor stimulations. In order to provide an unilateral odor input, we surgically ablated one antenna and monitored odor-evoked calcium signals at the two-photon microscope of VLPn of the ipsi- as well as contralateral brain hemisphere to the intact antenna before and after antennal removal (**Figures 1C,D**). To selectively measure VLPn, we expressed GCaMP6f under control of the enhancer-trap line *NP5194-Gal4* (Jefferis et al., 2007), which labels a subpopulation of these third-order neurons (cell count = 4.8125 ± 0.1875 neurons). Surprisingly, we observed an asymmetry of the odor-evoked signals between the ipsi- and contralateral side to the odor before and after antennal removal. On the one hand, the calcium signals to the odor acetophenone were significantly increased in VLPn on the ipsilateral side to the intact antenna after removing the contralateral antenna compared to bilateral stimulation (i.e., with intact antennae) (**Figure 1E**). On the other hand, the odor-evoked responses were strongly reduced in contralateral VLPn to the intact antenna. Hence, our results suggest that VLPn receive a contralateral inhibition in response to asymmetric stimulation with the odor acetophenone. To test whether this contralateral suppression was odor-independent, we used the food odor isoamyl acetate (Schubert et al., 2014) and the male-specific sex pheromone *cis*-vaccenyl acetate (Kurtovic et al., 2007) as additional olfactory stimuli. As expected, VLPn on the ipsilateral side to the odor showed a similar contralateral inhibition to asymmetric stimulation with these two odors. This inhibition is characterized by a significantly increased ipsilateral response to the odor after removing the contralateral antenna (**Figures 1F,G**). Since Duistermars et al. (2009) has reported that sensory signals

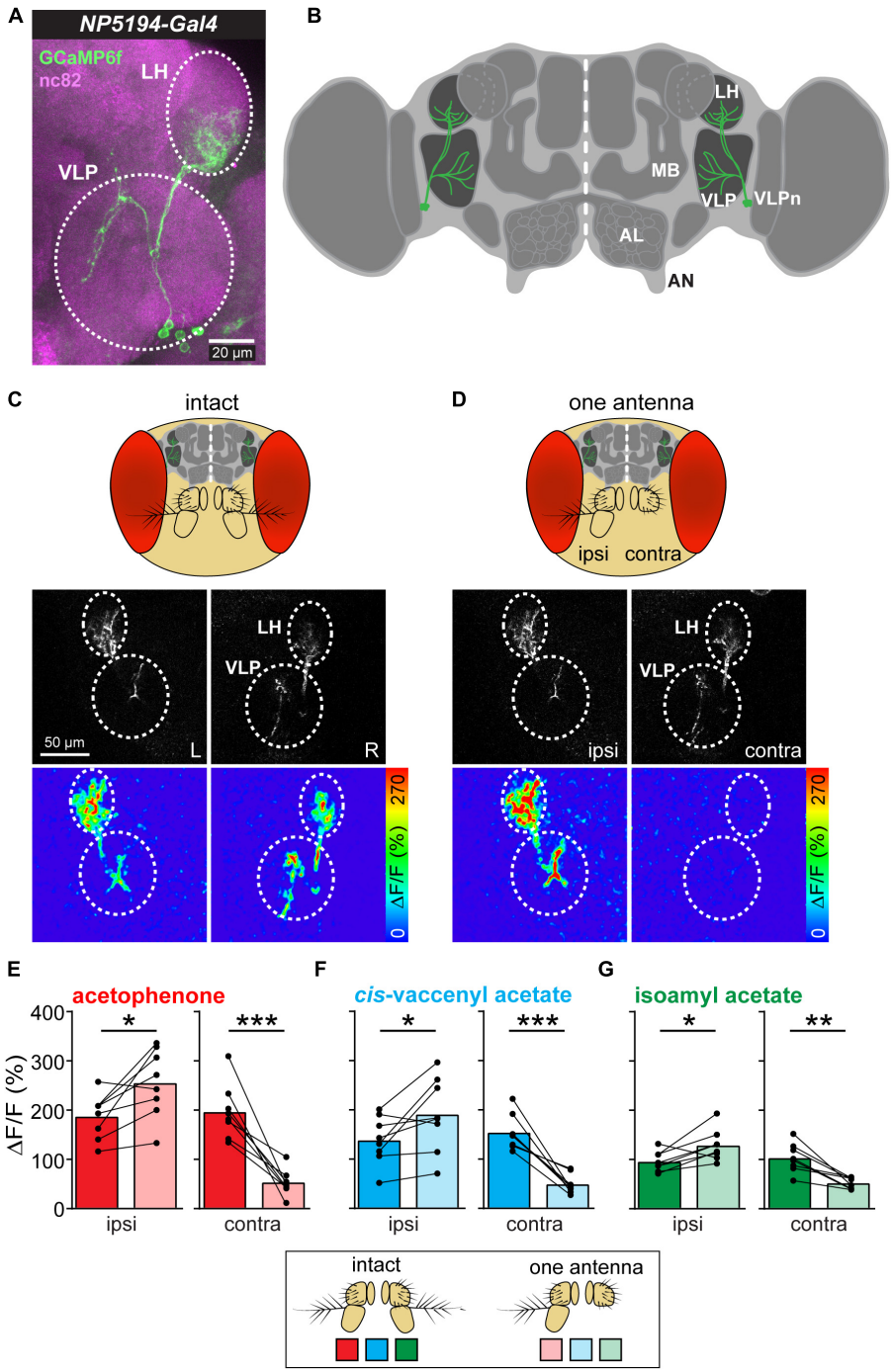

FIGURE 1 | Asymmetric odor stimulation induces contralateral suppression. **(A)** Confocal z-projections of VLPn labeled by *NP5194-Gal4* in an adult female brain. Labeling of GFP (green) and the neuropil marker nc82 (magenta) are shown. Dashed circles represent the lateral horn (LH) and ventrolateral protocerebrum (VLP). Scale bar = 20 µm. **(B)** Schematic illustration of the *Drosophila* brain showing the innervation pattern of the VLPn in the LH and the VLP. Mushroom body (MB), antennal lobe (AL), and antennal nerve (AN) are shown for orientation. **(C,D)** *Upper panel*: Schematic head of *Drosophila* with intact antennae **(C)** and after removal of the third antennal segment of one antenna **(D)**. *Middle panel*: Gray-scale image represents the VLPn structure expressing GCaMP6f. Dashed circles indicate the LH and the VLP in the left (L) and right (R) brain hemispheres. Scale bar = 50 µm. *Lower panel*: false-color coded images showing odor-evoked responses from a representative animal before **(C)** and after **(D)** antennal removal. Dashed circles represent the LH and VLP. **(E–G)** Calcium signals obtained with two-photon imaging from flies bearing *UAS-GCaMP6f* under control of *NP5194-Gal4* from the ipsi- and contralateral sides (to the intact antenna) before and after antennal removal to stimulation with acetophenone **(E)**, *cis*-vaccenyl acetate **(F)**, and isoamyl acetate **(G)**. Dots and lines represent individual flies, bars represent the mean ($n = 8$; $^{*}p < 0.05$; $^{**}p < 0.01$; $^{***}p < 0.001$, paired *t*-test).

from the left antenna contribute disproportionately more to odor tracking than signals from the right side, we sought to analyze whether the observed contralateral inhibition is different between both brain hemispheres. However, we could not find any significant difference between the odor-evoked calcium responses of the right and left sides (data not shown) indicating that the contralateral inhibition is not side-specific.

As mentioned above, lateralized odors are coded at the PN level in a way that ipsilateral PNs are more strongly activated by an asymmetric odor stimulus than their contralateral sister PNs (Gaudry et al., 2013). This asymmetry in PN responses can be attributed to two main mechanisms: First, the release of neurotransmitter at the ORN-to-PN synapse in the AL is asymmetric (Gaudry et al., 2013), and second, PNs have significantly more synapses with ipsilateral than with contralateral ORNs (Tobin et al., 2017). The last finding is similar to the mechanosensory system of leeches, where individual mechanoreceptor neurons exhibit a higher number of synapses with the ipsilateral postsynaptic neurons than with the contralateral sister cells (Lockery and Kristan, 1990) enabling the animal to detect the stimulus orientation. Also the mammalian olfactory system processes the input from both nostrils separately. In the periphery, odor responses within the olfactory epithelium as well as odor-evoked intrinsic signals at the glomerular layer in the olfactory bulb of rats reveal strong olfactory lateralization (Parthasarathy and Bhalla, 2013).

Our results provide evidence that odor inputs are distinctively encoded in the two hemispheres at the level of third-order olfactory neurons of *Drosophila*. Notably, we observed that an asymmetric odor stimulation does not only activate the ipsilateral VLPn to the intact antenna significantly more strongly than their contralateral sister neurons, but also leads to a contralateral suppression (i.e., the ipsilateral VLPn were more strongly activated by a lateralized odor stimulus than a symmetric stimulus). This finding is reminiscent of the visual system, where higher-order neurons exhibit a contralateral inhibition when stimulated with an asymmetric visual stimulus (Shiozaki and Kazama, 2017; Sun et al., 2017). However, in contrast to our results, visual neurons show a strong inhibition to a contralateral stimulus, while VLPn reveal no, or only a very weak, response to contralateral odor stimulation. This finding can be explained by the fact that the contralateral PNs to the odor input still become strongly activated due to the bilateral projections of their cognate ORNs (Gaudry et al., 2013). This PN activation would in turn result in an excitation of the contralateral VLPn and therefore, due to the contralateral inhibition, compensate the PN input.

Taken together, our results show that olfactory input from both antennae leads to a contralateral inhibition in a subset of olfactory third-order neurons which seems to be odor-independent.

Contralateral Inhibition Occurs Presynaptic to VLPn

We next wondered how this contralateral inhibition in VLPn is induced. We envisioned two different circuit models that could account for it. In the first model, we propose that the contralateral inhibition is taking place at the VLP level and is mediated by inhibitory neurons connecting the ipsi- and contralateral VLP neuropils. This model is supported by the fact that VLPn possess presynaptic densities in the VLP, but hardly in the LH (Mohamed et al., in preparation) (**Figure 2A**). We termed this model "VLP inhibition." In the second model, termed "LH inhibition," we hypothesize that the inhibitory neurons are located in the LH resulting in a contralateral inhibition of the excitatory PN input to VLPn (**Figure 2B**). Notably, such neurons that connect the LH of both hemispheres have been previously reported (referred to as PV12a1) and express GABA as a neurotransmitter (Dolan et al., 2018). In order to test these two hypotheses, we silenced the VLPn in one brain hemisphere by laser transection, while keeping the other side intact and monitoring the odor-evoked responses before and after VLPn manipulation (**Figures 2C,D**). If the "VLP inhibition" model were correct, transecting VLPn of one side would increase the activation of the contralateral neurons to the transection, as the transected side would fail to activate the inhibitory neurons and therefore contralateral suppression to odor input would not occur. Alternatively, if the "LH inhibition" model were true, transecting VLPn on one side would not affect the activation of the contralateral VLPn, since the contralateral suppression would have occurred prior to the VLP neuropil. When we compared the VLPn responses to odor stimulation with acetophenone, isoamyl acetate, and *cis*-vaccenyl acetate before and after transection on either side, the calcium responses remained constant on the contralateral side, while the response was almost abolished on the transected side (**Figures 2E–H**). Since we did not observe any response increase after transection in the contralateral VLPn, our results support the "LH inhibition" model. Hence, we conclude that the contralateral suppression occurs at the presynaptic site of VLPn, namely at the level of the PN-to-VLPn synapse within the LH. A similar mechanism of information sharing between the two brain hemispheres has recently been reported for the mouse olfactory system, where particular neurons interconnect mirror-symmetric mitral/tufted cells of the two olfactory bulbs (Grobman et al., 2018).

CONCLUSION AND FUTURE PERSPECTIVE

In this perspective article, we aimed to investigate the neuronal response of higher-order neurons, VLPn, to a lateralized olfactory stimulus. We demonstrate that activation of these neurons induces contralateral inhibition. This inhibition occurs most likely presynaptically to the VLPn in the LH. In addition, this contralateral suppression may contribute to flies' navigation behavior following the concentration gradient across the two antennae. However, navigation toward (or away from) an odor involves the integration of multimodal sensory information (Baker and Hansson, 2016). Chemotaxis uses, besides olfactory information, visual and mechanosensory cues. Interestingly, the VLP neuropil receives inputs from neurons of all three sensory modalities (Lai et al., 2012; Zhu, 2013; Zhou et al., 2015), and thus represents a putative brain region for multimodal integration. For

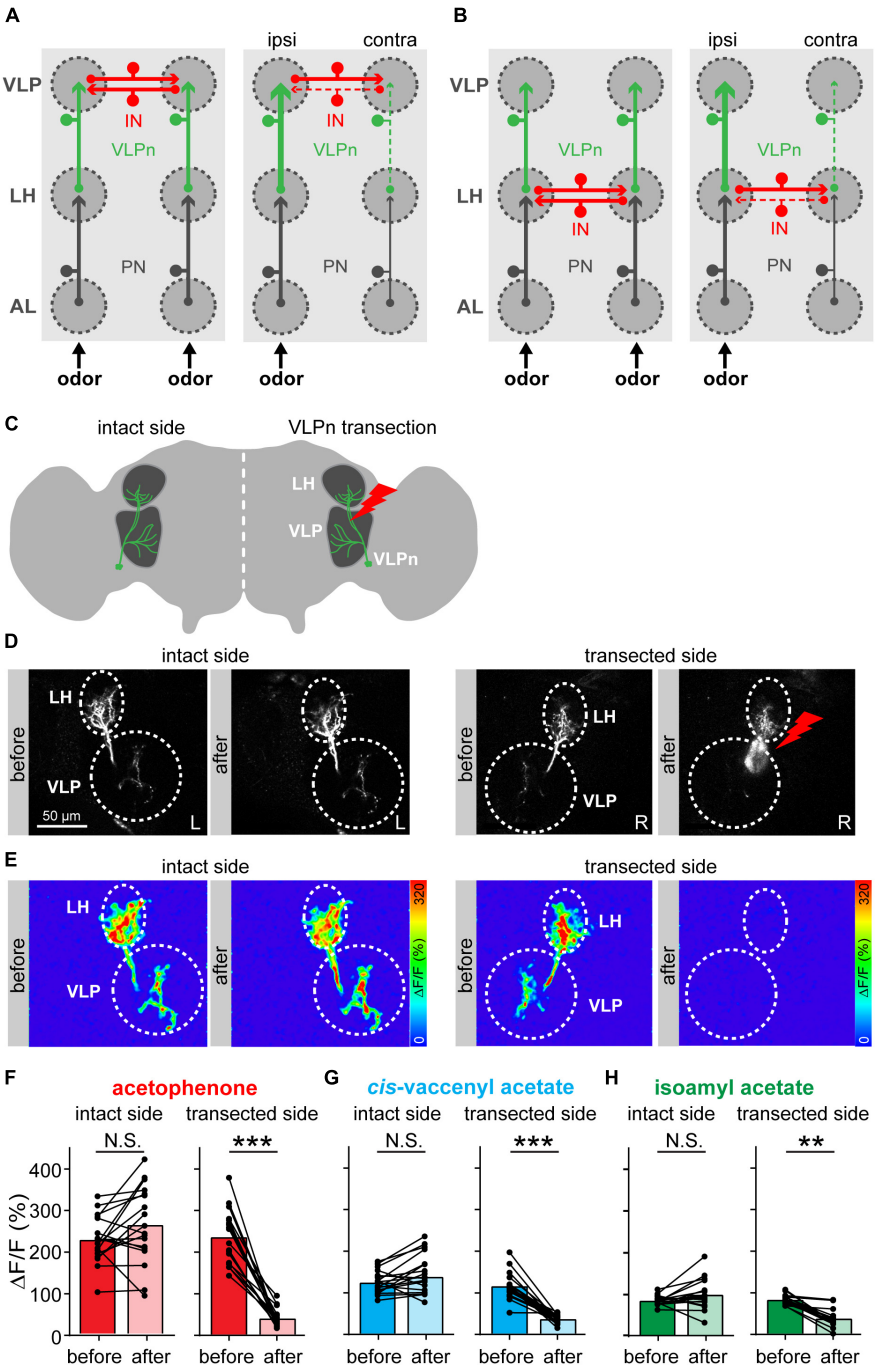

FIGURE 2 | Contralateral inhibition takes place presynaptically to VLPn. **(A,B)** Two proposed models for the contralateral suppression in VLPn. In both models, projection neurons (PNs, black) activate downstream the VLPn (green). Presynaptic input is represented by an arrow, postsynapses are indicated by a small circle. In the VLP inhibition model **(A)**, inhibitory neurons (INs, red) connect the VLPn of both sides at their postsynaptic sites (i.e., within the VLP neuropil). In this case, activation of VLPn on one side would be required to induce inhibition in the contralateral VLPn. In the LH inhibition model **(B)**, the IN (red) connects the VLPn of both sides at their presynaptic sites (i.e., in the LH). Here, activation of VLPn would not be required to cause contralateral inhibition. In both models **(A,B)**, the strength of activation is represented by the line size; solid lines represent active neurons and dashed lines represent not activated and/or inhibited neurons. **(C)** Schematic drawing of the laser transection experiment. VLPn were transected only on one brain side, while leaving VLPn on the contralateral side intact. This allowed us to abolish any odor-evoked responses of VLPn in the transected side. **(D)** Gray-scale images of VLPn expressing GCaMP6f under control of *NP5194-Gal4* before and after laser transection in the intact and transected side. Scale bar = 50 µm. **(E)** Examples of false-color coded images of odor-induced Ca^{2+} signals corresponding to each gray-scale image shown in **D** from a representative fly. **(F–H)** Paired comparisons of the calcium signals before and after the transection of VLPn across different flies. Odor-evoked Ca^{2+} signals were recorded and analyzed for both sides (i.e., intact and transected side). Ca^{2+} signals were abolished in VLPn in the transected side after transection. The intact brain hemisphere shows a slight, but not significant, increase prior to the transection. Dots and lines represent individual flies, bars represent the mean (n = 18; $^{*}p < 0.05$; $^{**}p < 0.01$; $^{***}p < 0.001$, paired t-test).

a future perspective, it would be highly interesting to investigate the role of VLPn for integrating visual and mechanosensory information along with the olfactory input. Moreover, it will be intriguing to manipulate the activity of VLPn of only one side of the brain, using a genetic approach (Wu et al., 2016), and to observe the behavioral consequences regarding navigation along odor plumes.

MATERIALS AND METHODS

Flies Stocks

Flies were reared on standard cornmeal molasses medium under 12 h/12 h light/dark cycle at 25°C. Four to six days old adult females were used for calcium imaging experiments, and 5–10 days old flies were used for the immunostaining. The following stocks were used: *NP5194-Gal4* (gift from Greg Jefferis), *20XUAS-IVS-GCaMP6f* (VK00005) [Bloomington Drosophila Stock Center (BDSC) 52869], and *UAS-mCD8-GFP* (BDSC 5137).

Immunostaining and Confocal Microscopy

Immunostaining was performed as previously described (Vosshall et al., 2000). In brief, brains were dissected in phosphate-buffered saline (PBS) (Ca^{2+}, Mg^{2+} free) in room temperature, and then fixed in 4% paraformaldehyde (PFA) in PBS for 30 min at 25°C. Afterward, the brains were washed three to four times for 1.5–2 h in total in PBS-T (PBS + 0.3% Triton X-100) and blocked for 1 h in PBS-T + 4% normal goat serum (NGS) at room temperature. Brains were then transferred into primary antibody diluted in PBS-T + 4% NGS and incubated for 48 h at 4°C. Then, brains were washed three to four times in PBS-T at 25°C before incubation in secondary antibody for 24 h at 4°C. After secondary antibodies, brains were mounted in VectaShield (Vector Labs) after three to four times for washing with PBS-T. Stained brains were acquired with Zeiss LSM 880 with a 40× water immersion objective lens. The following primary antibodies were applied: chicken anti-GFP (1:500, Life Technologies) and mouse anti-nc82 [1:30; Developmental Studies Hybridoma Bank (DSHB)]; secondary antibodies are Alexa Fluor 488 goat anti-chicken (1:300, Life Technologies) and Alexa Fluor 633 goat anti-mouse (1:300, Life Technologies).

Two-Photon Calcium Imaging

In vivo preparation of the flies for calcium imaging was previously described in Strutz et al. (2012). In short, flies were briefly anesthetized on ice and fixed with the neck onto a custom-made Plexiglas mounting block with copper plate (Athene Grids, Plano) and a needle before the head to stabilize the proboscis. Head was glued to the stage using Protemp II (3 M ESPE). We added Ringer's solution [NaCl: 130 mM, KCl: 5 mM, $MgCl_2$: 2 mM, $CaCl_2$: 2 mM, sucrose: 36 mM, and HEPES–NaOH (pH 7.3): 5 mM] (Estes et al., 1996) to the head. A small window was cut in the fly's head to expose the underneath brain. Care was taken while removing all fat, trachea, and air sacs to reduce light scattering.

Ventrolateral protocerebrum neurons were imaged using two-photon laser scanning microscope (2PCLSM, Zeiss LSM 710 meta NLO) equipped with an infrared Chameleon Ultra^{TM} diode-pumped laser (Coherent, Santa Clara, CA, United States) and a 40× water immersion objective lens (W Plan-Apochromat 40×/1.0 DIC M27). The microscope and the laser were placed on a smart table UT2 (New Corporation, Irvine, CA, United States). The fluorophore of GCaMP was excited with 925 nm. Fluorescence was collected with an internal GaAsP detector. For each individual measurement, a series of 40 frames acquired at a resolution of 256 × 256 pixels was taken with a frequency of 4 Hz. Odors were applied during frames 8–14 (i.e., after 2 s from the start of recording for 2 s); 1.5–2 min of clean air was applied between odors, in order to flush any residues of odors and to let the neurons go back to its resting phase. Odor source was lateralized by removing one antenna just before imaging. The identity of the intact antenna was pseudo-randomized between preparations.

Odor Delivery System

Pure compounds were diluted in mineral oil and were freshly prepared after approximately 1 week. Fifty milliliters of glass bottles with custom-made lid insert (POM; HL Kunststofftechnik, Landsberg, Germany) were equipped with push-in adapter (jenpneumatik & Schlauchtechnik GmbH, Jena, Germany) for the tubing system. Odors were delivered via Teflon-tubes (jenpneumatik & Schlauchtechnik GmbH, Jena, Germany) and were changed for each odor to avoid contamination. For controlling the odor delivery, we used the LabVIEW software (National Instruments) which was connected to the ZEN software (Zeiss) to trigger both image acquisition as well as odor delivery. A continuous airstream, whose flow of 1 L min^{-1} was monitored by a flowmeter. A peek tube guided the airflow to the fly's antennae. Behind the chamber with the fly was an air extraction system (flow rate 5 L min^{-1}) to prevent contamination of the room air.

Functional Imaging Data Analysis

Functional imaging data were analyzed using ImageJ[1]. All recordings were corrected for movement using a plugin in ImageJ. A region of interest was assigned on the LH of each animal and the change in fluorescence was measured. The raw fluorescence signals were converted to $\Delta F/F_0$, where F_0 is the averaged baseline fluorescence values of 2 s before the odor onset (i.e., 0–7 frames). For the average $\Delta F/F_0$, average of frames 11–18 was calculated for each trail and averaged among trails. The VLPn could be reliably identified from the fluorescence baseline of GCaMP6f.

Laser Transection

Transections of the VLPn tract were performed in one brain hemisphere. Using the baseline fluorescence of GCaMP at 925 nm, we selected a transection area (∼30 μm in a single focal plane) on the tract few micrometers before its entry site into the LH. The transection area was continuously illuminated

[1]https://fiji.sc/

with 760 nm for 1 min. To confirm a complete lesion of the VLPn tract, a fast z-stack with 925 nm was generated. Successful transection resulted in a small cavitation bubble (Vogel and Venugopalan, 2003). After transection was complete, we left the animal for 5 min for neuronal recovery before continuing with calcium imaging.

DATA AVAILABILITY

All datasets generated for this study are included in the manuscript and/or the supplementary files.

AUTHOR CONTRIBUTIONS

AAMM and SS conceived and designed the study. AAMM performed all the experiments. AAMM and SS analyzed the data and interpreted the results. BSH provided intellectual and financial support. AAMM, BSH, and SS wrote the manuscript.

FUNDING

The Max Planck Society and the Marie Curie FP7 Programme through FLiACT (AAMM) supported this work.

ACKNOWLEDGMENTS

We would like to thank Silke Trautheim for her excellent support for fly rearing and Veit Grabe for sharing the schematics of the *Drosophila* head and brain. We also acknowledge the Bloomington *Drosophila* Stock Center (NIH P40OD018537) and Greg Jefferis for reagents. We thank the members of the Sachse and Hansson labs for discussions and comments on the study.

REFERENCES

Baker, T. C., and Hansson, B. S. (2016). "Moth sex pheromone olfaction flux and flexibility in the coordinated confluences of visual and olfactory pathways," in *Pheromone Communication in Moths: Evolution, Behavior, and application*, ed. J. D. Allison (California: University of California press), 139–171.

Borst, A., and Heisenberg, M. (1982). Osmotropotaxis in *Drosophila* melanogaster. *J. Comp. Physiol.* 147, 479–484. doi: 10.1007/bf00612013

Clyne, P. J., Warr, C. G., Freeman, M. R., Lessing, D., Kim, J. H., and Carlson, J. R. (1999). A novel family of divergent seven-transmembrane proteins: candidate odorant receptors in *Drosophila*. *Neuron* 22, 327–338. doi: 10.1016/s0896-6273(00)81093-4

Couto, A., Alenius, M., and Dickson, B. J. (2005). Molecular, anatomical, and functional organization of the *Drosophila* olfactory system. *Curr. Biol.* 15, 1535–1547. doi: 10.1016/j.cub.2005.07.034

Dolan, M.-J., Frechter, S., Bates, A. S., Dan, C., Huoviala, P., Roberts, R. J. V., et al. (2018). Neurogenetic dissection of the *Drosophila* innate olfactory processing center. *bioRxiv*

Dubnau, J., Grady, L., Kitamoto, T., and Tully, T. (2001). Disruption of neurotransmission in *Drosophila* mushroom body blocks retrieval but not acquisition of memory. *Nature* 411, 476–480. doi: 10.1038/35078077

Duistermars, B. J., Chow, D. M., and Frye, M. A. (2009). Flies require bilateral sensory input to track odor gradients in flight. *Curr. Biol.* 19, 1301–1307. doi: 10.1016/j.cub.2009.06.022

Estes, P. S., Roos, J., van der Bliek, A., Kelly, R. B., Krishnan, K. S., and Ramaswami, M. (1996). Traffic of dynamin within individual < strong > < em > *Drosophila* < /em > < /strong > synaptic boutons relative to compartment-specific markers. *J. Neurosci.* 16, 5443–5456. doi: 10.1523/jneurosci.16-17-05443.1996

Gaudry, Q., Hong, E. J., Kain, J., de Bivort, B. L., and Wilson, R. I. (2013). Asymmetric neurotransmitter release enables rapid odour lateralization in *Drosophila*. *Nature* 493, 424–428. doi: 10.1038/nature11747

Grobman, M., Dalal, T., Lavian, H., Shmuel, R., Belelovsky, K., Xu, F., et al. (2018). A mirror-symmetric excitatory link coordinates odor maps across olfactory bulbs and enables odor perceptual unity. *Neuron* 99, 800.e–813.e. doi: 10.1016/j.neuron.2018.07.012

Hangartner, W. (1967). Spezifität und Inaktivierung des Spurpheromons von Lasius fuliginosus Latr. und Orientierung der Arbeiterinnen im Duftfeld. *Zeitschrift für vergleichende Physiologie* 57, 103–136. doi: 10.1007/bf00303068

Heimbeck, G., Bugnon, V., Gendre, N., Keller, A., and Stocker, R. F. (2001). A central neural circuit for experience-independent olfactory and courtship behavior in *Drosophila* melanogaster. *Proc. Natl. Acad. Sci. U.S.A.* 98, 15336–15341. doi: 10.1073/pnas.011314898

Heisenberg, M. (2003). Mushroom body memoir: from maps to models. *Nat. Rev. Neurosci.* 4, 266–275. doi: 10.1038/nrn1074

Jefferis, G. S., Potter, C. J., Chan, A. M., Marin, E. C., Rohlfing, T., Maurer, C. R. Jr., et al. (2007). Comprehensive maps of *Drosophila* higher olfactory centers: spatially segregated fruit and pheromone representation. *Cell* 128, 1187–1203. doi: 10.1016/j.cell.2007.01.040

Kennedy, J. S., and Moorhouse, J. E. (1969). Laboratory observations on locust responses to wind-borne grass odour. *Entomol. Experiment. et Appl.* 12, 487–503. doi: 10.1111/j.1570-7458.1969.tb02547.x

Kurtovic, A., Widmer, A., and Dickson, B. J. (2007). A single class of olfactory neurons mediates behavioural responses to a *Drosophila* sex pheromone. *Nature* 446, 542–546. doi: 10.1038/nature05672

Lai, J. S., Lo, S. J., Dickson, B. J., and Chiang, A. S. (2012). Auditory circuit in the *Drosophila* brain. *Proc. Natl. Acad. Sci. U.S.A.* 109, 2607–2612. doi: 10.1073/pnas.1117307109

Liang, L., Li, Y., Potter, C. J., Yizhar, O., Deisseroth, K., Tsien, R. W., et al. (2013). GABAergic projection neurons route selective olfactory inputs to specific higher-order neurons. *Neuron* 79, 917–931. doi: 10.1016/j.neuron.2013.06.014

Lockery, S., and Kristan, W. (1990). Distributed processing of sensory information in the leech. II. Identification of interneurons contributing to the local bending reflex. *J. Neurosci.* 10, 1816–1829. doi: 10.1523/jneurosci.10-06-01816.1990

Louis, M., Huber, T., Benton, R., Sakmar, T. P., and Vosshall, L. B. (2008). Bilateral olfactory sensory input enhances chemotaxis behavior. *Nat. Neurosci.* 11, 187–199. doi: 10.1038/nn2031

Martin, H. (1965). Osmotropotaxis in the Honey-Bee. *Nature* 208:59. doi: 10.1038/208059a0

Parthasarathy, K., and Bhalla, U. S. (2013). Laterality and symmetry in rat olfactory behavior and in physiology of olfactory input. *J. Neurosci.* 33, 5750–5760. doi: 10.1523/JNEUROSCI.1781-12.2013

Schubert, M., Hansson, B., and Sachse, S. (2014). The banana code—natural blend processing in the olfactory circuitry of *Drosophila* melanogaster. *Front. Physiol.* 5:59. doi: 10.3389/fphys.2014.00059

Shiozaki, H. M., and Kazama, H. (2017). Parallel encoding of recent visual experience and self-motion during navigation in *Drosophila*. *Nat. Neurosci.* 20:1395. doi: 10.1038/nn.4628

Stocker, R. F., Lienhard, M. C., Borst, A., and Fischbach, K. F. (1990). Neuronal architecture of the antennal lobe in *Drosophila*-melanogaster. *Cell Tissue Res.* 262, 9–34. doi: 10.1007/bf00327741

Strutz, A., Soelter, J., Baschwitz, A., Farhan, A., Grabe, V., Rybak, J., et al. (2014). Decoding odor quality and intensity in the *Drosophila* brain. *eLife* 3:e04147. doi: 10.7554/eLife.04147

Strutz, A., Völler, T., Riemensperger, T., Fiala, A., and Sachse, S. (2012). "Calcium imaging of neural activity in the olfactory system of *Drosophila*," in *Genetically Encoded Functional Indicators*, ed. J.-R. Martin (Totowa, NJ: Humana Press), 43–70. doi: 10.1007/978-1-62703-014-4_3

Sun, Y., Nern, A., Franconville, R., Dana, H., Schreiter, E. R., Looger, L. L., et al. (2017). Neural signatures of dynamic stimulus selection in *Drosophila*. *Nat. Neurosci.* 20:1104. doi: 10.1038/nn.4581

Tobin, W. F., Wilson, R. I., and Lee, W.-C. A. (2017). Wiring variations that enable and constrain neural computation in a sensory microcircuit. *eLife* 6:e24838.

Vogel, A., and Venugopalan, V. (2003). Mechanisms of pulsed laser ablation of biological tissues. *Chem. Rev.* 103, 577–644. doi: 10.1021/cr010379n

Vosshall, L. B., Amrein, H., Morozov, P. S., Rzhetsky, A., and Axel, R. (1999). A spatial map of olfactory receptor expression in the *Drosophila* antenna. *Cell* 96, 725–736. doi: 10.1016/s0092-8674(00)80582-6

Vosshall, L. B., Wong, A. M., and Axel, R. (2000). An olfactory sensory map in the fly brain. *Cell* 102, 147–159. doi: 10.1016/s0092-8674(00)00021-0

Wu, M., Nern, A., Williamson, W. R., Morimoto, M. M., Reiser, M. B., Card, G. M., et al. (2016). Visual projection neurons in the *Drosophila* lobula link feature detection to distinct behavioral programs. *eLife* 5:e21022. doi: 10.7554/eLife.21022

Zhou, C., Franconville, R., Vaughan, A. G., Robinett, C. C., Jayaraman, V., and Baker, B. S. (2015). Central neural circuitry mediating courtship song perception in male *Drosophila*. *eLife* 4:e08477. doi: 10.7554/eLife.08477

Zhu, Y. (2013). The *Drosophila* visual system: from neural circuits to behavior. *Cell Adhes. Migr.* 7, 333–344. doi: 10.4161/cam.25521

Conflict of Interest Statement: The authors declare that the research was conducted in the absence of any commercial or financial relationships that could be construed as a potential conflict of interest.

frontiers in Physiology

REVIEW
published: 02 August 2019
doi: 10.3389/fphys.2019.00972

Insect Odorscapes: From Plant Volatiles to Natural Olfactory Scenes

*Lucie Conchou[1], Philippe Lucas[1], Camille Meslin[1], Magali Proffit[2], Michael Staudt[2] and Michel Renou[1]**

[1]INRA, Sorbonne Université, INRA, CNRS, UPEC, IRD, University P7, Institute of Ecology and Environmental Sciences of Paris, Paris, France, [2]CEFE, CNRS, EPHE, IRD, Université de Montpellier, Université Paul-Valéry Montpellier, Montpellier, France

Olfaction is an essential sensory modality for insects and their olfactory environment is mostly made up of plant-emitted volatiles. The terrestrial vegetation produces an amazing diversity of volatile compounds, which are then transported, mixed, and degraded in the atmosphere. Each insect species expresses a set of olfactory receptors that bind part of the volatile compounds present in its habitat. Insect odorscapes are thus defined as species-specific olfactory spaces, dependent on the local habitat, and dynamic in time. Manipulations of pest-insect odorscapes are a promising approach to answer the strong demand for pesticide-free plant-protection strategies. Moreover, understanding their olfactory environment becomes a major concern in the context of global change and environmental stresses to insect populations. A considerable amount of information is available on the identity of volatiles mediating biotic interactions that involve insects. However, in the large body of research devoted to understanding how insects use olfaction to locate resources, an integrative vision of the olfactory environment has rarely been reached. This article aims to better apprehend the nature of the insect odorscape and its importance to insect behavioral ecology by reviewing the literature specific to different disciplines from plant ecophysiology to insect neuroethology. First, we discuss the determinants of odorscape composition, from the production of volatiles by plants (section "Plant Metabolism and Volatile Emissions") to their filtering during detection by the olfactory system of insects (section "Insect Olfaction: How Volatile Plant Compounds Are Encoded and Integrated by the Olfactory System"). We then summarize the physical and chemical processes by which volatile chemicals distribute in space (section "Transportation of Volatile Plant Compounds and Spatial Aspects of the Odorscape") and time (section "Temporal Aspects: The Dynamics of the Odorscape") in the atmosphere. The following sections consider the ecological importance of background odors in odorscapes and how insects adapt to their olfactory environment. Habitat provides an odor background and a sensory context that modulate the responses of insects to pheromones and other olfactory signals (section "Ecological Importance of Odorscapes"). In addition, insects do not respond inflexibly to single elements in their odorscape but integrate several components of their environment (section "Plasticity and Adaptation to Complex and Variable Odorscapes"). We finally discuss existing methods of odorscape manipulation for sustainable pest insect control and potential future developments in the context of agroecology (section "Odorscapes in Plant Protection and Agroecology").

Keywords: insect olfaction, plant volatiles, odorscape, volatilome, olfactome, plant-insect interaction, landscape, sensory ecology

OPEN ACCESS

Edited by:
Carolina E. Reisenman, University of California, Berkeley, United States

Reviewed by:
Markus Knaden, Max-Planck-Gesellschaft (MPG), Germany
Shannon Bryn Olsson, National Centre for Biological Sciences, India

****Correspondence:***
Michel Renou
michel.renou@inra.fr

Specialty section:
This article was submitted to Invertebrate Physiology, a section of the journal Frontiers in Physiology

Received: *15 April 2019*
Accepted: *11 July 2019*
Published: *02 August 2019*

Citation:
Conchou L, Lucas P, Meslin C, Proffit M, Staudt M and Renou M (2019) Insect Odorscapes: From Plant Volatiles to Natural Olfactory Scenes. Front. Physiol. 10:972. doi: 10.3389/fphys.2019.00972

INTRODUCTION

Olfaction is a very important sensory modality for insects and volatile organic compounds (VOCs) serve as chemical cues to recognize and locate vital resources such as food, mate, or enemies. Insects live in a very complex chemical world from which they must extract this relevant information. Considerable progresses in sensitivity and selectivity of analytical methods have allowed to identify minute amounts of the semiochemicals that mediate a wide variety of insect-insect or insect-plant interactions. Yet, we do not possess a global envision of the chemical environment insects live in.

It has long been acknowledged that animals experience their own species-specific sensory world. As early as 1934, Jakob von Uexküll defined the Umwelt (von Uexküll, 1934) as the subjectively perceived surroundings about which information is available to an organism through its senses. In neuroethological terms, the Umwelt corresponds to the range of stimuli the insect's receptor set can detect and translate into a neural code which is further interpreted in the brain to finally trigger the appropriate physiological or behavioral response. This notion of a sensory world proper to a species appears particularly appropriate for olfaction since individual olfactory receptors (ORs) detect only a small fraction of existing volatile chemicals and considerable variation has been documented in the number and tuning of ORs expressed by different insect species. Accordingly, the odorscape can be defined as the ensemble of the VOCs that constitute a sensory space proper to a particular insect species.

The VOCs constituting the insect odorscape may serve different ecological functions independently of their chemical nature. Volatile signals are chemicals that are produced by a living organism with the function of exchanging information with other living organisms. For instance, a plant attracts pollinators by advertising for the presence of a reward, e.g., nectar, when its flowers are receptive; a molested aphid emits an alarm pheromone inducing escape in congeners; or a female moth at sexual maturity signals herself to conspecific males by releasing a volatile sex pheromone. On the other hand, cues carry information about the availability of a resource to the receiver, although they are not emitted for a communication purpose and can be released by a lifeless source. Receivers must extract signals and cues from a background composed of many other VOCs, which might alter their perception. For instance, the ability of *Manduca sexta* moths to locate their host plant is significantly decreased in a background of benzaldehyde or geraniol compared to host plant odor alone (Riffell et al., 2014).

Plant and insect species live in close intimacy with each other. The standing biodiversity of both taxa is to a large extent the result of their ancient co-evolution (Labandeira, 2007; Labandeira et al., 2007). Insects depend on plants as food sources either directly for phytophagous and pollinator species or indirectly for parasitoids and predators. This explains the importance of volatile compounds of plant origin (volatile plant compounds or VPCs) for insect ecology. Almost all kinds of plant tissues (leaves, flowers, fruits, roots, etc.) and types of vegetation (trees, grasses, shrubs, etc.) release VPCs albeit with different profiles and in different amounts. Moreover, plants make up most of the biomass of most terrestrial ecosystems, making them the major source of biogenic volatiles and therefore of insect odorscapes. Overall, the terrestrial vegetation produces and releases an amazing variety of volatiles including isoprenoids, benzenoids, oxygenated low-molecular weight VOCs, sulfur-containing compounds, fatty acid-derived volatiles, etc. These VPCs can be emitted either constitutively or in response to a variety of abiotic and biotic stimuli or stresses. They are involved in a wide variety of ecological functions. They can for instance protect plants against abiotic stress and mediate plant-plant and various plant-animal interactions (Unsicker et al., 2009; Loreto and Schnitzler, 2010). Moreover, due to their high abundance and reactivity, VPCs drive air chemical processes that affect air quality and climate at regional and global scales, affecting plant growth in return (Penuelas and Staudt, 2010).

Finally, it is expected that the atmospheric content in VPCs varies locally according to the composition of the plant communities specifically associated to natural habitats or agricultural landscapes, resulting in the perception by insects of distinct "odorscapes." The concept of a sensory-scape has been first used for physical sensory modalities. The term soundscape was noted by Michael Southworth in his 1969 article titled "The Sonic Environment of Cities" (Southworth, 1969) and developed in more detail 8 years later by Canadian composer and naturalist R. Murray Schafer in his seminal work, "Tuning of the World" (Schafer, 1977). Some years after Bernie Krause contributed by his recordings to the emergence of soundscape ecology (Pijanowski et al., 2011). Indeed the term "scape" adds a notion of spatiality, or spatial determination to a sensory word. Concerning olfaction, the term odor-landscapes has been used to describe the spatiotemporal distribution of chemical concentrations resulting from their propagation in fluid media (Atema, 1996; Moore and Crimaldi, 2004). The concept of landscape also involves a notion of movement by the receptor organism and the stimuli detected by an insect are changing as it moves in its milieu. Due to variations in the emission rates, the physical transportation, and interception on surfaces and chemical degradation, the distribution of VPCs in the insect environment is heterogeneous in space and varies in time, which in addition to chemical complexity makes describing the fine structure of odorscapes particularly challenging. This review aims to better apprehend the olfactory environment of the insect in its chemical (sections "Plant Metabolism and Volatile Emissions" and "Insect Olfaction: How Volatile Plant Compounds Are Encoded and Integrated by the Olfactory System"), spatial (section "Transportation of Volatile Plant Compounds and Spatial Aspects of the Odorscape"), temporal (section "Temporal Aspects: The Dynamics of the Odorscape"), ecological, and cognitive (sections "Ecological Importance of Odorscapes" and "Plasticity and Adaptation to Complex and Variable Odorscapes") dimensions. We also discuss how a better knowledge of insect odorscapes may benefit sustainable crop protection (section "Odorscapes in Plant Protection and Agroecology").

PLANT METABOLISM AND VOLATILE EMISSIONS

Plants produce a bewildering variety of VOCs comprising a great diversity of chemical structures. Volatility is measured by vapor pressure and is limited by the molecular weight (around 300 g) and also depends on the polarity of the chemical structure. A large majority of VPCs stem from four different metabolic pathways: the mevalonic acid (MVA) and methylerythritol phosphate (MEP) pathways for isoprenoids, the lipoxygenase (LOX) pathway for fatty acid derivatives, the shikimic acid pathway for benzenoids and phenylpropanoids, and the amino acid derivatives pathway (Baldwin, 2010). In addition, diverse metabolic paths produce various alkenes and low-molecular weight oxygenated compounds like ethylene, acetaldehyde, acetone, or methanol (Jardine et al., 2017) that may play a role in insect-plant interactions. Some VPCs are ubiquitously emitted from a wide range of plant species while others are released only from specific plant taxa. Hence, the composition of volatile emissions typically differs between plant species. Secondary metabolites in general have been extensively used in plant classification (chemotaxonomy) and modern algorithms for data analyses confirm the close relationship between the volatile metabolome and plant taxonomy (Vivaldo et al., 2017).

However, VPC emissions are also highly variable within a plant species. Since all VPC metabolic pathways do not respond in the same way or with the same intensity to biotic and abiotic factors, the amounts and the composition of volatiles released from a given plant species can strongly vary with environmental conditions, including plant-plant interactions, above or below ground (Delory et al., 2016). Some plant volatile emissions are stimulated by the attack of an herbivorous insect and serve as chemical weapons to protect plants against these attacks (Unsicker et al., 2009; Dicke, 2016; Rowen and Kaplan, 2016) either directly, or by attracting their natural enemies. For instance, species of the *Allium* genus such as the leek (*Allium porrum*) produce alk(en)yl-cysteine sulfoxides that are precursors of volatile thiosulfinates and disulfides (Dugravot et al., 2005). The production of these sulfur-containing VPCs increases sharply after attack by the leek moth, *Acrolepiopsis assectella*, a specialist feeder. Attacked leek plants are not avoided by the moth but females of *Diadromus pulchellus* an endoparasitoid wasp of young moth chrysalids, are more strongly attracted to damaged leek. In addition, the frass of *A. assectella* larvae contains dimethyl disulfide, dipropyl disulfide, and methyl-propyl disulfide that attract the wasps (Dugravot and Thibout, 2006). In poplars (*Populus nigra*) attacked by *Lymantria dispar* caterpillars, a clear increase of nitrogenous and aromatic compounds has been observed in the volatile emissions (McCormick et al., 2014). Even plant-associated microorganisms such as epiphytic bacteria on flowers and leaves can significantly affect the VPC composition released by a plant organ (Helletsburger et al., 2017).

Within a plant, the composition of the emissions can largely differ among organs and may vary with the circadian rhythm, the plant's age and phenological state (maturity, senescence, etc.) (Hare, 2010). For example, a recent field study on VOC emissions from maritime pine revealed that pinene emissions from branches have a distinctly different enantiomeric signature (optical isomers) than pinene emissions from the stems of the same trees (Staudt et al., 2019). Such a minute diversification in VPC production may have important ecological implications, since many insects such as bark beetles possess stereo-selective ORs that distinguish between optical VPC isomers (Andersson, 2012).

INSECT OLFACTION: HOW VOLATILE PLANT COMPOUNDS ARE ENCODED AND INTEGRATED BY THE OLFACTORY SYSTEM

A VPC only becomes an odor if it gets detected by a biological sensor, here the olfactory system of an insect. Thus, to the volatilome of plants corresponds the olfactome of insects, the spectrum of all the volatile compounds that are detected by a species (**Figure 1**). In this section, we briefly examine how volatile compounds are detected by the insect olfactory system. Insect olfaction is a complex sensory process that runs from the specific detection by binding onto ORs expressed in olfactory receptor neurons (ORNs) to neural code, blend perception (integration in brain), and behavior.

The stimulus quality is first encoded in the pool of odorant-binding proteins (OBPs) and ORs expressed in the olfactory organs of a given insect species. While OBPs are generally thought to play an important role in the solubilization and transport of the odorants (Pelosi et al., 2017), here we will only focus on the ORs, as they are the molecular actors that trigger the olfactory signaling cascade. ORs are hosted by ORNs enclosed inside the olfactory sensilla on the antennae and palps of insects. Typically, ORs have a seven-transmembrane topology and form heterodimers with a co-receptor named Orco (Butterwick et al., 2018). While Orco is fully conserved across species, sharing up to 94% sequence identity with orthologs from different species (Butterwick et al., 2018; Soffan et al., 2018), the sequence identity of the other ORs can vary greatly within and between species (Hansson and Stensmyr, 2011). Additionally, the size of the OR repertoire, i.e., the content of OR sequences in a genome, differs from one species to another, reflecting their ecology and lifestyle as well as the evolutionary history of the species. Extreme examples of OR repertoire sizes can be found among parasitic and social insects. The human body louse (*Pediculus humanus*), an obligate parasite with a very specific ecological niche with a relatively constant environment, has only 10 ORs (Kirkness et al., 2010). On the contrary, some ants, that have a complex social organization in which olfaction plays an important role and that are exposed to various environment, express up to 350 ORs (Zhou et al., 2012). However, in addition to the size of the OR repertoire, the chemical tuning of each individual OR is fundamental to evaluate the olfactory capacity of an insect species. Indeed, the capacity of each OR to detect

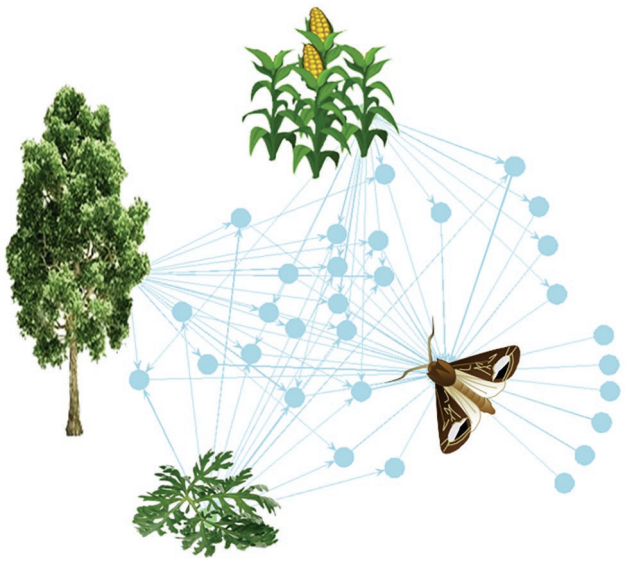

FIGURE 1 | The plant-VPC-insect network. The complex odorscape of a moth (*Agrotis ipsilon*) shown as a communication network between plants, VPCs, and insect spaces. The network graph is based on the chemical analyses of plant VPCs and recordings of EAG responses from the literature (Greiner et al., 2002; Jerkovic et al., 2003; Degen et al., 2004; McCormick et al., 2014). It has been drawn using the R package "network" (R Core Team, 2013). The plant species release VPCs (blue spots) that are detected by the olfactory system of the moth. The information contained in VPCs circulates from the plants to the insect (blue arrows). Each plant emits a variety of VPCs and one VPC can be produced by different plant species. For simplification, the VPCs not detected by the moth have been omitted. The olfactory system of the moth detects VPCs released by its host plant, maize, as well as by companion plants, such as a weed (*Artemisia vulgaris*) and trees surrounding the fields (*Populus nigra*). Most of the VPCs are shared between two or three plants. This simplified network does not take into account the intensity of the emissions, which can largely differ among VPCs released by a same plant, and moreover varies according to the biomass of individual plants and of the whole plant communities.

volatiles varies in terms of specificity and sensitivity. Specialist ORs have a very narrow binding spectrum. It is usually the case for the ORs that bind pheromone compounds. Other ORs are more broadly tuned. In addition, the spectrum width increases with odorant concentration, the ORs being more narrowly tuned at low concentrations (de Fouchier et al., 2017). Combinatorial coding, where each odorant activates a different set of ORs, allows the discrimination of a greater number of odorants than the number of OR types, increasing the olfactory capacity of an individual insect. Finally, different subsets of ORs are expressed depending on sex or life stage, in order to accommodate the ecological needs of individuals (Poivet et al., 2013). The size of the repertoire, the diversity, the tuning, and the timing of expression of ORs make the description of the olfactome a complex task. Owing to the generalization of DNA and protein sequencing methods, an increasing amount of OR sequences is now available. The deorphanization of receptors is the limiting step, requiring heavy and sophisticated techniques. The development of high-throughput methods should play a crucial role in the upcoming years in this essential step to get a sense of the true olfactome of each species. Furthermore, the notion of OR repertoire should be treated in all its complexity. Indeed, while the sequence information is important, it is not sufficient. Major shifts in the olfactory system can be achieved through a change in the expression of ORs, or even a change in the neuronal projection to the brain (Dekker et al., 2006; Kopp et al., 2008; Tait et al., 2016).

The firing response of insect ORNs is proportional to the aerial concentration of odorants and has a much wider dynamic range than that of their vertebrate counterparts (Rospars et al., 2014). This intensity coding informs insects on the absolute levels of odorants in the atmosphere and allows detection of changes in aerial concentrations. However, because of turbulences in natural conditions, the odor plume does not form a continuous gradient pointing to its source (Celani et al., 2014), making odor navigation at large distances a challenging task. This point will be discussed more in section "The Odorscape as a Source of Spatial Information: Habitats, Trails, and Landmarks".

All ecologically relevant sources release odor blends rather than individual odorants. Perception of blends of VPCs plays a pivotal role in the recognition of the host plant and avoidance of non-host plants (Bruce and Pickett, 2011; Cha et al., 2011). Blend recognition involves the sensory integration of the information carried by ORNs at different levels in the insect brain, the antennal lobe and the protocerebron (Silbering and Galizia, 2007; Galizia and Rössler, 2010; Galizia, 2014). Not only does the nature of each component matter, but also its proportion in the blend. Detailed investigations on blend perception, for instance in bees, have shown that in some cases the insect still perceives the individual components (elemental processing), but most often a distinct entity is perceived (configural processing) (Deisig et al., 2006). In addition, interactions between the components of a blend can lead to a reduced perception of the blend, compared to that of its individual components, a process termed "mixture suppression" (Ache et al., 1988). Thus, olfaction is a highly integrative sensory process which makes the prediction of insect responses in complex odorscapes difficult. Furthermore, multi-modal integration, for instance between vision and olfaction, can increase responses to odorants (Strube-Bloss and Rossler, 2018).

Eventually, the odor perception may trigger a conspicuous change in insect behavior. Male moths, for instance, are sexually aroused and attracted by the female-emitted pheromone. They take flight and navigate the pheromone plume upwind toward the source performing chemically triggered anemotaxy (Cardé and Willis, 2008). This behavior is innate. However, because of the integration in the insect brain of the complex olfactory input from a pool of ORNs, the detection of an odorant does not preclude of the type of behavior that follows. The males of several noctuid moth species also possess ORNs specifically tuned to some of the components of the pheromones produced by females of sympatric species. Activation of these ORNs inhibits their attraction to their own pheromone (Berg and Mustaparta, 1995; Berg et al., 2014). For plant volatiles, it has long been acknowledged that phytophagous insect species

sharing large parts of their olfactome nevertheless show different preferences in their behavioral responses to host plant volatiles (Bruce et al., 2005). In other words, the full knowledge of the olfactome will not suffice to predict the behavior.

Insects can also be innately repelled by specific odorants. Geosmin, an earthly smelling substance of bacterial origin, deters oviposition by *Drosophila melanogaster* females, preventing them from laying their eggs on fruits colonized by harmful molds (Stensmyr et al., 2012). Based on such attraction or avoidance behaviors, the concept of valence is commonly applied to insects. Valence value is considered as positive when the insect is attracted, negative when it is repelled. This does not postulate a hedonic value, which could be questionable in arthropods. It seems essential to determine whether odor valence conserves the same value among species, is stable during an individual life, and is treated in specific neuronal circuits according to its value. Since it has long been acknowledged that the same odorant may attract some, while repelling other insect species, it is easy to confirm that valence pertains to the species. Isothyocyanates for instance, repel generalist herbivores but attract *Brassicaceae* specialists (Hopkins et al., 2009). Several bark beetle species avoid hexanol isomers and monoterpenes associated with deciduous non-host trees, while the same molecules are attractive to insects feeding on deciduous trees and their parasitoids (Zhang et al., 1999; Byers et al., 2004). Carbon dioxide (CO_2) is a salient odorant for many insects (Guerenstein and Hildebrand, 2008). CO_2 attracts hematophagous insects seeking for a host (Stange, 1996). The tobacco hawk moth *M. sexta* is attracted to elevated CO_2 levels emitted from fresh opening flowers of *Datura wrightii* (Solanaceae) that likely contain large amounts of nectar (Thom et al., 2004). By contrast, CO_2 elicits innate avoidance in *Drosophila* (Suh et al., 2004) but this behavior is context dependent, testifying that valence may change during the life of an individual. Indeed, *Drosophila* prefers feeding on rotting fruits that emit CO_2 as a by-product of fermentation by microorganisms and yeasts. Two compounds, 2,3-butanedione and 1-hexanol, present in *Drosophila* food sources, but more abundant during fruit ripening, strongly inhibit the response of CO_2-sensitive ORNs by direct interaction with the CO_2 receptor, suppressing the avoidance of CO_2 by flies (Turner and Ray, 2009). The valence of an odorant often changes with its concentration. *D. melanogaster* for instance shows an innate and robust attraction to vinegar but higher concentrations of vinegar are less attractive (Semmelhack and Wang, 2009). Experimental evidence establishing the localization of valence treatment in the insect olfactory system is scarce. For instance, no valence-specific activation of ORNs was found in *Drosophila* flies, but the categorization of odors as pleasant or unpleasant seems to be established at the antennal lobe level (Knaden et al., 2012) and might be maintained from the antennal lobe to the lateral horn (Min et al., 2013).

To conclude this brief overview of the insect olfactory system, the behavioral activity of a given odorant is not only odorant dependent but also receptor, species and context dependent. This level of complexity calls for integrative approaches from gene to behavior in order to understand what insects smell.

TRANSPORTATION OF VOLATILE PLANT COMPOUNDS AND SPATIAL ASPECTS OF THE ODORSCAPE

Because insect behavior depends on how volatile compounds are distributed in space and time, insect chemical ecology has very early paid attention to the processes that determine odorant fate in the atmosphere (Riffell et al., 2008). The dispersion of the odorant molecules in the atmosphere depends on the characteristics of the sources, the importance of the compartments where they can be sequestrated (sinks), and the physical laws describing fluid movements. Biological sources of volatile compounds are considerably variable in their emission capacity. As the cuticle area above the pheromone gland of a female moth is in the range of tens of square micrometers, a single female may be approximated as a point source. On the contrary, the billions of yellow flowers from a blooming field of rape constitute a huge source of floral volatiles covering hundreds of square meters. VPC exchanges have been analyzed only in a few agricultural ecosystems. In a maize field, fluxes at ecosystem scale show large differences between families of VPCs, 8 ± 5 μg m^{-2} h^{-1} for isoprene and 4 ± 6 μg m^{-2} h^{-1} for monoterpenes but 231 ± 19 μg m^{-2} h^{-1} for methanol (Bachy et al., 2016). Once released in the air, the pheromone and the crop plant volatile molecules are carried by air flows according to identical physical processes but generate plumes with different shapes and dimensions. The pheromone forms a meandering plume, roughly cone shaped, with its main dimension in the wind axis. Such a narrow plume builds a chemical trail that insects can follow upwind. The physical structure of the plume has been analyzed and modeled, revealing a statistical distribution of pheromone molecules into intermittent filaments (Celani et al., 2014). The emissions of an individual plant, or plant organ, behave probably much like a pheromone, enabling the insect to fly back up the source. By comparison, the dispersion of VPCs at field scale has not been so finely investigated but one can expect that it builds up local odorant ambiances that resolve into broad downwind odor cones. Thus, odorscapes can be seen in space as trails and scenes, similar to the paths and sceneries of a physical landscape, although less stable. In such odorscapes, insects can stay on a spot and be durably exposed to local high concentrations, move to a more suitable habitat, or navigate an odor plume.

Most of the physics beyond the distribution of odors is known from environmental fluid mechanics. Volatile organic compounds spread away from their source through molecular diffusion and through transportation by wind and other air flows. Diffusion is the net movement of molecules from a region of high concentration to a region of low concentration as a result of their random motion. It is slow and acts significantly only at very small distances (below 1 m). Its contribution to the distribution of VPCs at field scale is therefore much smaller than that of air transport. By contrast, diffusion might be the major driver of VPC movements in the soil.

Wind is of course the strongest factor of horizontal dispersion of odors in natural landscapes but in fact, three types of air movement co-occur: advection, convection, and turbulence,

resulting in transport and dilution of VPCs not only horizontally, but also vertically. Advection is the bulk transport of a substance by a flow: the wind carries away the VPCs horizontally, quickly, and on long distances. Convection is the vertical transport by thermals, finite parcels of fluid consisting in the same fluid as its surroundings but at a different temperature. Differences in air temperature or moisture can lead the atmosphere to stratify in layers of different densities, which limits vertical transport of VPCs. Differences in air density may be stable, which for example explains smog episodes over cities. Finally, turbulences may arise from three main mechanisms. When the wind encounters physical obstacles like bushes or trees, local vortices or turbulences are generated. Shear turbulence is created by a flow scrubbing against a rough surface like the ground. Surface roughness depends on the vegetation cover and hence shear turbulence is different over bare soils, grasslands, crop fields, and forests. Convective turbulence is created by rising/sinking thermals. All turbulent flows cause stirring of odor pockets with the formation of eddies of different diameters and speeds. Eddies are then transported horizontally by advection. Turbulences cause intermittency in odorant signals, with pockets of odorized air separated by clean air, and favor mixing between ambient air and air carrying the signal. Introduction of ambient air into the plume dilutes odorants and mixes odorants from different sources or with airborne oxidants. For instance, Riffell et al. (2014) showed that the ratio of volatiles in the plume emanating from flowers of *Datura wrightii* changed with distance, as the background volatiles from neighboring vegetation, including creosote bush plants, became intermixed with *D. wrightii* volatiles. The average VPC concentration decreases as the square of the distance from the source but local conditions can alter this rule. At landscape scale, local topography can favor the build-up of high levels of VPCs through valley or basin effects.

Although an odor emanating from a discrete source is typically represented as a scent cone produced by a moving fluid entering a quiescent body of the same fluid, the actual shape of an odor is dictated by air movements and must be seen as a plume (Murlis et al., 1992). Turbulences and random changes in the wind direction will cause this plume to meander, resulting in a "chemical trail." Insects such as moths can fly over several hundreds of meters navigating upwind through such pheromone plumes (Shorey, 1976; Cardé and Charlton, 1984; Elkinton et al., 1987). An insect flying through a diversified landscape will experience areas differently odorized, both with respect to the nature of the volatile compounds and their mixing rates. Furthermore, vertical stratifications in the distribution of VPCs have been observed in many ecosystems. For example, in a neotropical forest, sesquiterpenes were most abundant in the air near the ground, whereas monoterpenes prevailed at higher canopy levels (Jardine et al., 2011, 2015). Finally, while we have gained a better knowledge of odor distribution at the field scale, the micro-distribution of VPCs at the scale of an insect's body size (millimeters to centimeters) remains to be investigated. One should expect a large heterogeneity in accordance with the diversity of microhabitats created by the plant cover.

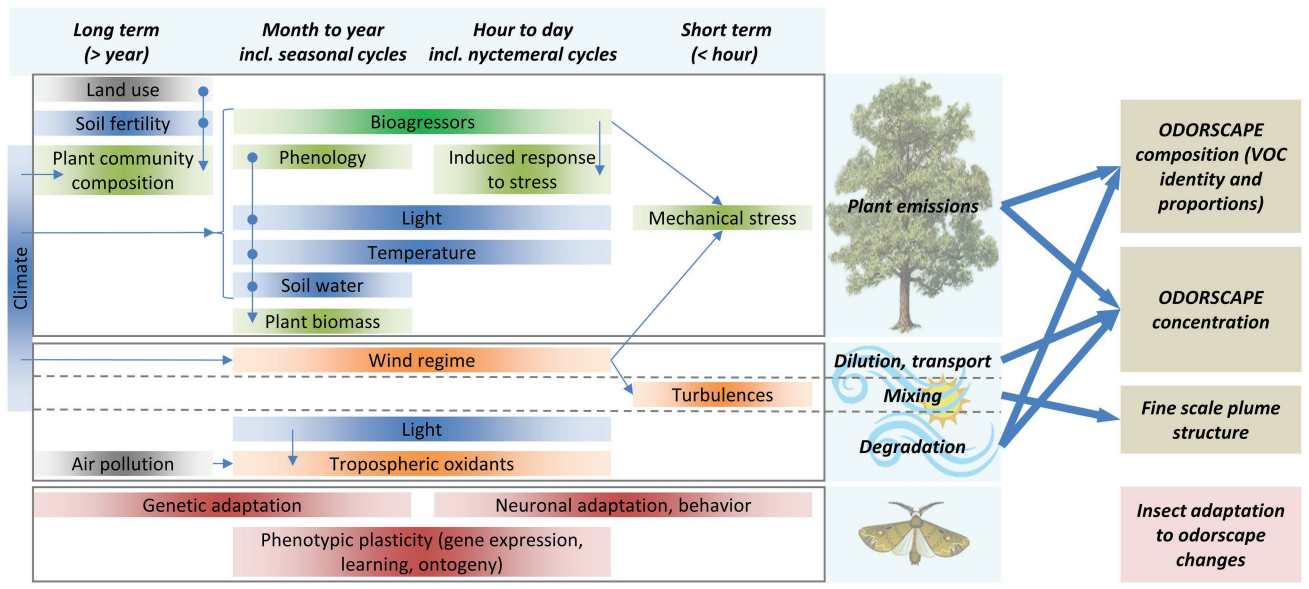

FIGURE 2 | Odorscapes are highly variable at a diversity of time scales. The left part of this chart depicts the factors that determine volatile emissions by plants (top), atmospheric processes (middle), and the processes by which insects can adapt to changes in their olfactory environment (bottom), classified horizontally by the time scale at which they act or vary. Thin arrows depict indirect impacts, through influence on another factor. Box color: dark blue = climate and soil factors, green = plant physiology and ecology, orange = atmospheric physico-chemistry, brown = insect adaptation processes, gray = anthropic factors. Although this is not represented for readability issues, extremes of most climate and soil factors do cause stress responses in plants. VOC sources other than plants (especially anthropogenic VOC) are ignored. On the right side, thick arrows depict how plant emissions and atmospheric processes determine the characteristics of the odorscape.

TEMPORAL ASPECTS: THE DYNAMICS OF THE ODORSCAPE

Because of the variations in emissions, sinks, and atmospheric transport of VPCs, the odorscape composition changes considerably at seasonal, daily, hourly, and even minute to second time scales (**Figure 2**). A survey of VOCs in the atmosphere of rural and urban districts in Great Britain has shown that the maximum concentration of some VOCs may reach values 100 times higher than average, even above rural areas (Cape, 2003). Measures of fluxes over crop fields, forests, and other plant communities have all shown variations at all time scales listed above (Bachy et al., 2016; Schallhart et al., 2016).

Temporal Variations in Emission

Emissions of VPCs can occur by sudden and short bursts. Plants respond to herbivory by rapidly modifying their emissions after attacks (Maffei et al., 2007). Wounding triggers bursts of so-called green leaf volatiles formed from the enzymatic breakdown of membrane lipids through the lipoxygenase pathway (LOX). The emission response is almost instantaneous and lasts only a few hours (see e.g., Staudt et al., 2010). Likewise, in plants that store VPCs in their tissues (e.g., essential oil in aromatic plants or oleoresin in conifers) or VPC precursors (e.g., glucosinolates in *Brassicaceae* or cyanogenic glucosides in *Rosaceae*), mechanic stress and injuries including herbivore attacks induce immediate emission bursts. However, the induction of many other stress-related VPCs is associated with gene activation and the resulting metabolic adjustments, which proceed over hours and days (Arimura et al., 2008).

Temperature positively drives both physical and physiological processes, leading to marked daily emission changes. In addition, the emissions of many VPCs are light dependent, because their biosynthesis is tightly linked to photosynthetic processes that deliver primary carbon substrates and biochemical energy. Foliar isoprene emissions, for example, cease at night. During the day, they can fluctuate rapidly, in response to changes in cloud cover and shading by the canopy (Singsaas and Sharkey, 1998). Light influence on stomatal conductance constrains emissions of polar water-soluble VPCs such as methanol, which can be further modified by diurnal changes in transpiration and water transport (Rissanen et al., 2018). On the other hand, emissions of apolar hydrophobic VPCs are independent of stomatal conductance, even though these VPCs diffuse principally through stomata (Niinemets et al., 2002). In addition to exogenous factors, an endogenous clock also controls dial emission variations. Photo-positive and less frequently photo-negative endogenous circadian rhythms have been reported for constitutive and stress-induced VPC emissions (Zeng et al., 2017).

Environmental factors exert various longer term effects on VPC emissions, independently of the aforementioned short-term modulations. Weather conditions and particularly the prevailing temperature regimes continuously up- and down-regulate the VPC-producing metabolism in plants (Fischbach et al., 2002; Staudt et al., 2003). Seasonal drought events can positively and negatively modulate VPC emissions, depending on the stress intensity (Staudt et al., 2008). Phenology is also a major driver since VPCs are mostly emitted from leaves and flowers that are absent or physiologically inactive during specific periods (Filella et al., 2013). The main periods of low emissions correspond to the cold season in temperate and subpolar climates, and to the dry season in arid subtropical climates. During these seasons, a large majority of insects, which depend directly or indirectly on plants as food sources, are inactive.

At decennial time scale, human activity and climatic change have profoundly modified natural odorscapes in the past and will continue to alter VPC emissions in the future at local, regional, and global scales (Lathière et al., 2010). Interestingly, these long-term changes in quantity and composition of VPC emissions can feedback on climate evolution since their reaction products in the atmosphere influence ozone concentrations and other parameters that will alter the balance between insolation absorbed by the Earth and the energy radiated back to space (e.g., Harper and Unger, 2018). Rising temperature and atmospheric CO_2 concentration will directly affect VPC biosynthesis in addition to changing plant growth rates, phenology, and the length of the vegetation periods (Penuelas and Staudt, 2010; Staudt et al., 2017). Furthermore, the frequency and intensity of heat spells and drought stress will increase in some regions, potentially increasing the proportions of stress-induced VPCs in the atmosphere. Land use itself can deeply alter the odorscape, not only by changing profoundly the type and size of VPC sources (Hantson et al., 2017), but also by affecting the microclimate and the strength of VPC sinks.

Atmospheric Degradation of Volatile Plant Compounds

Physical, chemical, and biological sinks limit the mixing ratios of VPCs in the air. Soils, for instance, can act as sinks for VPCs through mechanisms of dissolution and adsorption onto organic, mineral, and aqueous surfaces, and through degradation by aerobic and anaerobic microorganisms (Insam and Seewald, 2010). VPCs can also be deposited on or taken up by plants and eventually metabolized (e.g., Karl et al., 2010). However, the main VPC sink remains their atmospheric chemical degradation through reaction with atmospheric oxidants (**Figure 3**). The main oxidants are the hydroxyl radical (OH), ozone (O_3), and the nitrate radical (NO_3). O_3 and the OH radical are secondary pollutants predominantly photochemically formed, essentially under sunlit conditions (Atkinson and Arey, 2003). In the troposphere, O_3 is produced from the photolysis of NO_2 to NO and a triplet O, the latter reacting with O_2 to form O_3. The OH radical – often referred to as the "detergent" of the troposphere – is formed from the photolysis of O_3 to O_2 and singlet O, which further reacts with a water molecule yielding two OH radicals. The nitrate radical is produced from the reaction of O_3 with NO_2 leading to O_2 and NO_3. The NO_3 radical is considered an important oxidant only at night, because it photolyzes rapidly during the day. The reactivity of VPCs to these oxidants and their resulting atmospheric lifetimes are highly variable. For example, the O_3 reactivity of benzyl alcohol, linalool, and β-caryophyllene differs by more than three orders of magnitude (Atkinson and Arey, 2003). The sesquiterpene β-caryophyllene is so reactive that under most

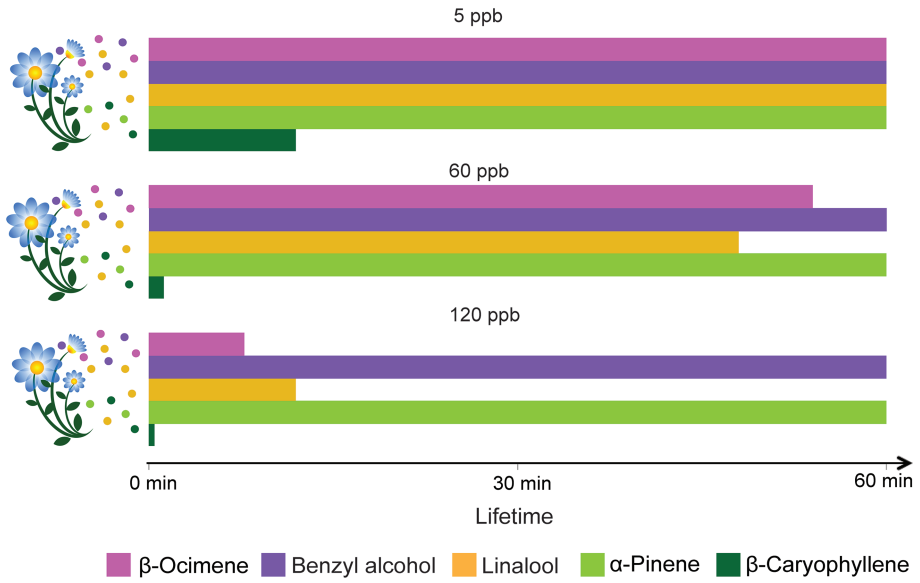

FIGURE 3 | Effect of ozone concentration on odor plume composition over time. Lifetimes in the atmosphere, measured up to 60 min, of volatiles emitted commonly by flowers (β-ocimene, benzyl alcohol, and linalool) and by leaves (linalool, α-pinene and β-caryophyllene) are presented under the influences of the O_3 levels indicated above the histograms. The degree of O_3 reactivity is based on the structural properties of the VPCs (Atkinson and Arey, 2003).

conditions, it will last only a few minutes (**Figure 3**). The products of VPC reaction with atmospheric oxidants (mostly addition at double bonds) will first yield transitory unstable intermediates (radicals and ozonides) that rapidly react further to produce more stable oxygenated derivatives such as ketones, aldehydes, and organic nitrates. These secondarily formed oxygenated VPCs are generally less reactive than the primary ones (Atkinson and Arey, 2003). The number of hypothetical products formed from VPC-oxidant reactions increases exponentially with the number of carbon atoms present in the VPC molecules (Goldstein and Galbally, 2007). As a result, the initial bouquet of emitted VPCs becomes gradually mixed with a characteristic blend of its numerous degradation products during its aerial transport. The extent to which such secondary VPCs affect insect behaviors is not yet well understood, even though impairment of insect orientation has been reported. For instance, primary pollutants in diesel exhaust (Girling et al., 2013) can differentially degrade floral VPCs and affect the foraging efficiency of honeybees. Similarly, laboratory experiments with herbivorous insects, bumble bees, and parasitoids indicated that realistic O_3 concentrations impair insect attraction to their host plants (Fuentes et al., 2013, 2016; Farré-Armengol et al., 2016). A modeling framework was used to simulate the modification of floral scent plumes by dispersion and chemical degradation and its impact on foraging pollinators (Fuentes et al., 2016). Even moderate levels of air pollutants (e.g., 60 ppb O_3) can substantially degrade floral volatiles, increase the foraging time of insects, and reduce their ability to locate host plants. The study also highlights that plant-pollinator interactions could be sensitive to changes in floral scent composition, especially if insects are unable to adapt to the modified odorscape.

The atmospheric concentration of oxidants varies temporally and spatially. In particular, OH and NO_3 radical concentrations show pronounced diurnal variations, though in opposite trends. In addition, the intensity of turbulent transport is usually different during day and night. At night, the tropospheric boundary layer is low (10–100 m) with little turbulence whereas it is high (>1,000 m) and strongly turbulent during the day. As a result, the air volume into which VPCs released from the ground are mixed is much greater by day. VPC concentrations can therefore be higher and more stable at night even though emissions are generally lower (e.g., Staudt et al., 2019). Atmospheric chemical degradation and turbulence conditions also change seasonally. During the cold season, VPC breakdown by airborne radicals and oxidants is relatively lower, the atmospheric nighttime stratification is stronger and often extends over morning hours, during which mist often settles and allows VPCs to accumulate in the boundary layer. Therefore, and considering that most VPC emissions are absent during the cold season, an olfactory signal might be more salient during winter. So far, it is unknown whether winter atmospheric conditions facilitate pheromone communication by the very few species of so-called winter moths that mate during winter. Finally, the chemical and radiative properties of the earth's atmosphere fluctuate over longer time scales. For example, air pollution events and concentrations of associated key oxidants such as tropospheric O_3 have been steadily increasing during the Anthropocene (Ainsworth, 2017).

ECOLOGICAL IMPORTANCE OF ODORSCAPES

Resource-indicating odor cues only represent a fraction of the odorants a searching insect will encounter. For instance, a floral

odor that signals a valuable food source to pollinators is always mixed with the volatiles released by the vegetative parts of the plants. This blend is itself intertwined with volatiles emanating from the rest of the local plant community. Considerable efforts have been and still are devoted to understanding how and why insects respond to specific odor cues. On the contrary, the way insects deal with global odorscapes is rarely explicitly addressed. Background odors have often been considered as a sensory noise impairing the detection of resource-indicating cues. However, the literature contains enough examples illustrating the variety of modes by which the olfactory environment modulates insect behavior. Behavioral responses often depend on the integration of several stimuli interacting with each other either synergistically or antagonistically. The odorscape can provide a sensory context and/or convey spatial information helping insects to locate resources. The following sections will review some of these important ecological functions of the odorscapes.

The Odorscape as a Background to the Signal: Olfactory Noise

Plant odors although varying in composition among species comprise many ubiquitous volatiles. For instance, limonene, β-ocimene, β-myrcene, and linalool are recorded in the floral scents of over 70% of plant families (Knudsen et al., 2006). Similarly, green leaf volatiles are very frequently emitted by angiosperm leaves (Hatanaka, 1993). There is therefore a high probability for any source in an ecosystem to emit odors that overlap in composition with those emitted by the plant(s) dominating the local landscape. In addition, many insect ORs respond to more than one odorant and their binding specificity decreases with increasing odorant concentration (Andersson et al., 2015). Therefore, interferences between odors *in natura* are likely, either because they share part of their constituents or because their respective volatiles activate overlapping sets of ORs. Riffell et al. (2014) have investigated the impact of a background of creosote bush odor (*Larrea tridentata*, a landscape-dominating plant) on the perception of and behavioral response to *Datura wrightii* odors (a resource-plant) by the sphingid moth *M. sexta*. They show that a background of either benzaldehyde (a compound shared by *D. wrightii* and creosote bush) or geraniol (released only by creosote bush but binding to different *M. sexta* ORs) impairs the capacity of *M. sexta* to detect and track a *D. wrightii* odor plume. Both volatiles alter the neural representation of *D. wrightii* odors by antennal lobe neurons and impair the moth's ability to track the time structure of the stimulus. Physiologically, this impairment could result either from sensory adaptation to the background, or from an inability to discriminate signal and background odor pockets from one another (see section "The Odorscape as a Source of Spatial Information: Habitats, Trails, and Landmarks"). Background interference, if acting through sensory adaptation, would make cues or signals appear less intense, increase the minimum detectable signal concentration (Martelli et al., 2013), and therefore reduce the maximum distance from which an insect is able to track an odor plume, depending on the relative concentrations of signal and background.

Background odorants and VPCs in particular can also interfere with the chemical signals produced by insects. When tested in an arena smeared with perfume *Iridomyrmex purpureus* ants antennated both nestmate and non-nestmate individuals more frequently, compared to a control arena (Conversano et al., 2014). Insect sex pheromone signals must be less prone to background interferences than other signals because they are often composed of specific chemicals, that are detected by particularly finely tuned and highly sensitive ORs. However, in several moth species, high concentrations of some VPCs directly activate pheromone-sensitive ORNs and/or reduce their response to the sex pheromone, probably because of competition for the OR-binding site (Den Otter et al., 1978; Party et al., 2009; Hatano et al., 2015; Rouyar et al., 2015), with consequences on behavior. For instance in *Agrotis ipsilon* males, addition of a heptanal background increased the latency of flight responses to the pheromone source in a wind tunnel (Rouyar et al., 2015). In *Spodoptera littoralis* males, the sudden transition from an odor-free background to a linalool background resulted in a temporary disorientation of the insect (Party et al., 2013). In the same species, a continuous linalool background, although reducing response intensity, improved the temporal resolution of responses to pulsed pheromone stimuli by pheromone-ORNs (Rouyar et al., 2011). Coding of stimulus time structure is essential for navigation (see section "The Odorscape as a Source of Complementary Information to Insects Searching for a Mate"). Testing whether VPC backgrounds improve or impair navigation efficiency will require a detailed analysis of wind tunnel flight trajectories. Whether and under which circumstances the high VPC concentrations required in order to observe interferences with sex pheromone detection can be reached *in natura* is still an open question (Badeke et al., 2016).

The Odorscape as a Background to the Signal: Olfactory Context

Many VOCs are emitted by a diversity of organisms in a variety of situations, and may only make sense to a given insect when encountered in a specific context. Background odors, besides their potential for interference with signal detection, may provide such a context. Indeed, many cases where the addition of contextual/background odors enhances the attractiveness or repulsiveness of a resource cue have been documented (Schröder and Hilker, 2008). A striking example of such a context dependence is that of the Scots pine, which produces a volatile bouquet that attracts egg parasitoids in response to oviposition by *Diprion pini*, a herbivorous sawfly. Compared to constitutive pine emissions, the VPC bouquet released by oviposited pine twigs only differs by significantly higher emissions of (E)-β-farnesene. However, females of the egg parasitoid *Closterocerus* (syn.: *Chrysonotomya*) *ruforum* do not respond to the sesquiterpene when presented alone, while they are attracted when (E)-β-farnesene is offered in combination with the volatile emissions of egg-free pine twigs (Mumm and Hilker, 2005). The ratio of (E)-β-farnesene to the other pine twig terpenoid volatiles (context) is key to the attraction of the parasitoid (Beyaert et al., 2010).

Recent experiments suggest that a realistic odor context may enhance the capacity of male moths to discriminate among conspecific and heterospecific mates, which is essential to maintain reproductive isolation among closely related species. When presented with calling females in a clean air background in a no-choice situation, male *S. littoralis* were attracted toward females of the sibling species *S. litura* almost as much as to conspecific females (Saveer et al., 2014). However, while the addition of host plant (cotton) odor did not affect their attraction toward conspecific signals (either synthetic full pheromone blend or calling female), it significantly reduced attraction toward heterospecific signals (either main pheromone component alone or *S. litura* calling female) (Borrero-Echeverry et al., 2018).

The Odorscape as a Source of Complementary Information to Insects Searching for a Mate

The olfactory environment is also itself a source of information. This has been particularly studied in the context of mate selection, where odors from the surrounding plant community inform mate-searching insects on the quality of resources available around a potential mate. For instance, many publications report that volatiles emitted by host plants (i.e., plant species the insect and/or its offspring can feed on) enhance moth attraction to sex pheromones and increase their reproductive behavior (Yang et al., 2004). Looking at field trapping data, it is not always clear whether increased catches to traps lured with a combination of pheromone and host plant odor result from a true synergy or a mere addition of food-searching and mate-searching individuals. Flight attraction of *Cydia pomonella* males to blends of female sex pheromone and the host plant volatile pear ester represents a case of synergy between host plant VPCs and pheromone documented at neurophysiological and behavioral levels (Trona et al., 2013). In a wind tunnel, pear ester by itself elicited virtually no contact to source, while its addition to the sex pheromone almost doubled the proportion of moths contacting the source compared to pheromone alone. Pheromonal and host plant information are already integrated in the moth antennal lobe since the cumulus region, which receives inputs from pheromone-ORNs, was more strongly activated by the blend than by the sex pheromone alone, while pear ester alone did not activate it at all. Similarly, aggregation pheromone and plant volatiles do act synergistically on the walking locomotion of several palm tree weevil species that gather on host trees to feed and mate (Rochat et al., 2000; Said et al., 2005). In males of the polyphagous moth *S. littoralis*, mate choice is linked to host plant choice: when offered a choice between two identical sex pheromone sources placed on two different host plant species, the males went for the source located on the most preferred host plant (Thöming et al., 2013; Proffit et al., 2015).

Conversely, odors of non-host plants (i.e., low quality or unsuitable for feeding) can antagonize pheromone signals. The volatile emissions from non-host gymnosperms or toxic angiosperms reduce *S. littoralis* male attraction toward the sex pheromone (Binyameen et al., 2013) while angiosperm odors antagonize attraction of conifer-associated bark beetles toward both their aggregation pheromone and host-tree odors (Zhang et al., 1999; Zhang and Schlyter, 2004). These effects of VPCs could explain why forests with higher tree species diversity suffer lower herbivory impact (Jactel and Brockerhoff, 2007) and more generally contribute to "associational resistance," an ecological syndrome where a good-quality host plant located near non-host or low-quality host plants is less likely to be impacted by herbivores (Jactel et al., 2011; Zakir et al., 2013). Insects can also discriminate against particularly well-defended plant individuals of their host species and modulate their response to pheromones accordingly. In *S. littoralis*, male attraction toward the sex pheromone is reduced by herbivore-induced plant volatiles, which signal high levels of anti-herbivore defenses (Hatano et al., 2015). In *Ips typographus*, attraction to the aggregation pheromone is antagonized by 1,8-cineole, a host-tree compound, whose emission rate correlates with tree resistance to *I. typographus* attacks (Andersson et al., 2010; Schiebe et al., 2012). Pheromone-ORNs and 1,8-cineole-responsive ORNs are located inside the same sensillum type in *I. typographus* antennae. A cross talk between those two ORN types was observed, such that activation of 1,8-cineole ORNs inhibits the firing of pheromone-ORNs.

The Odorscape as a Source of Spatial Information: Habitats, Trails, and Landmarks

A resource is usually closely associated to a specific environment or habitat. Furthermore, cues emanating from the habitat are usually more salient than resource-emitted signals, such that VPCs from the habitat may allow the insect to locate broad areas within which the probability to find resources of interest is high. How insects use habitat information in their foraging behavior has long been a matter of debate. They may forage sequentially, first for habitat cues at long range, then for resource cues at shorter range. Alternatively, resource-foraging behavior may be modified or triggered in the presence of habitat cues. A detailed review of the literature pertaining to the use of habitat cues by insect can be found in Webster and Carde (2017).

Once within a suitable habitat, insects must navigate to locate a resource. For animals larger than a millimeter, searches take place in a turbulent environment, which adds considerable difficulties for odor source location. Indeed, as mentioned before, turbulences prevent the formation of stable odor gradients. Instead, plumes are patchy distributions of odor filaments (whiffs) interspersed with pockets of clean air (blanks; see **Figure 4**) (Murlis et al., 1992; Cardé and Willis, 2008; Riffell et al., 2008). Moreover, active olfactory sampling behaviors and self-generated airflows such as wing flapping, antennal flicking, and body movements modify the structure of the plume and increase the speed of encounters with odor whiffs by the antennae (Sane and Jacobson, 2006; Houot et al., 2014; Huston et al., 2015). Whiff intensity as well as whiff and blank duration are distributed according to power laws with the shortest whiffs lasting just a few milliseconds (Celani et al., 2014).

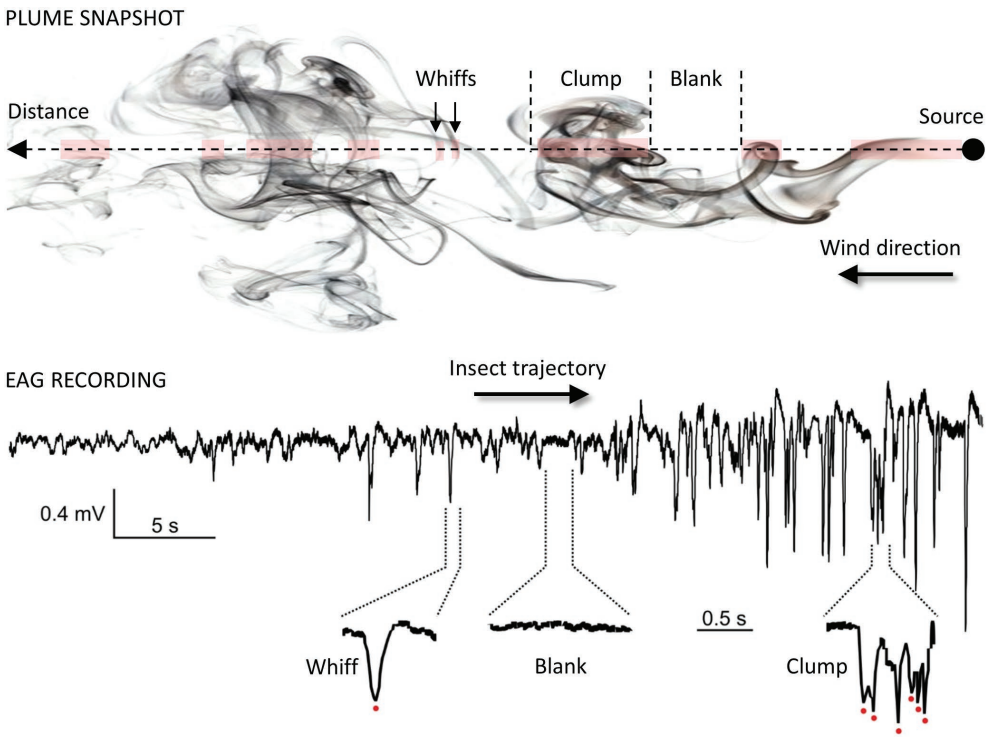

FIGURE 4 | Temporal structure of the odor plume. *Plume snapshot* (upper part): the wind transports odorants away from the source along its main direction. The mean odorant concentration in the odor plume decreases with the square of the distance but local vertices mix together odorized and clean air, making the local odor concentration vary considerably around the average. As a result, odor plumes are highly intermittent signals, consisting of series of whiffs, clumps and blanks (odor/no-odor events). Foraging insects cannot rely on a chemical gradient but use the fast temporal dynamic of the plume to locate distant mates and host plants (Budick and Dickinson, 2006; Cardé and Willis, 2008). *EAG recording* (lower part): the complex structure of odor plumes can be visualized with the EAG technique (Vickers et al., 2001; Riffell et al., 2008; Nagel and Wilson, 2011) since the insect antenna responds gradually and dynamically to odor stimuli. Here, the EAG was recorded from an *Agrotis ipsilon* antenna attached to a walking red palm weevil (*Rhynchophorus ferrugineus*). The weevil was attracted to an odor source containing 10 µg of its aggregation pheromone (4-methyl-5-nonanol, ferrugineol) mixed with 10 µg of the main component of the *A. ipsilon* pheromone, (Z)7-dodecenyl acetate (Z7-12:Ac). Z7-12:Ac is thus used as a tracer of ferrugineol. The distance between the starting point of the insect and the odor source it reached was 1.75 m. Portions of the EAG recording corresponding to a whiff, a blank, and a clump of whiffs are enlarged and show single detection events (red dots).

While the time-averaged odor concentration decreases with the square of the distance to the source, instantaneous concentrations at a point vary rapidly over several orders of magnitude. Consequently, the time needed to obtain a reliable concentration average is much longer than the time insects actually take to make navigational decisions and the plume does not provide any directional information. Insects must respond to instantaneous odor concentration changes when locating an odor source and speed and precision of their olfactory system are crucial to accurately encode the temporal information about sensory cues. First, *Drosophila* ORNs have a very short response latency (down to 3 ms) and high precision (standard deviation below 1 ms) (Egea-Weiss et al., 2018). The latency of behavioral responses ranges from 70–85 ms after ORN response onset in *Drosophila* (Bhandawat et al., 2007; Gaudry et al., 2013) to 150–200 ms in moths (Baker and Haynes, 1987; Mafra-Neto and Cardé, 1996). Second, insects can exhibit a locomotion response to very brief odor exposures, e.g., single encounters of sex pheromone lasting 20 ms in the almond moth *Cadra cautella* (Mafra-Neto and Cardé, 1996). Third, odor space coding is linked to odor time coding. The noctuid moth *Helicoverpa zea* and the honey bee discriminate odor sources separated from each other by only a few millimeters. This remarkable capacity of spatial resolution has been postulated to rely on slight temporal differences in the arrival of odorants based on the high degree of temporal resolution of the insect olfactory system (Baker et al., 1998; Szyszka et al., 2012). Interestingly, although the recognition of odor blends requires more neuronal resources compared to single odorants, modeling studies and physiological observations indicate that multi-component odor mixtures elicit more reliable and faster olfactory coding than single odorants (Chan et al., 2018).

Navigational strategies of moths tracking a pheromone plume have been extensively investigated and there are a number of excellent reviews on the subject (e.g., Vickers, 2000, 2006; Cardé and Willis, 2008). Moths and *Drosophila* flies combine two sensory inputs to track odor plumes: the encounters of attractive odorants and the detection of the wind direction which is assessed mechanically (Bell and Wilson, 2016; Suver et al., 2019) and possibly also visually (Frye et al., 2003). For all insects tracking an odor plume, the wind direction constitutes the primary directional cue that guides them toward the source.

Cockroaches, moths, and *Drosophila* appear to exploit the intermittence of odor plumes during odor-guided behavior: they surge upwind when they detect a whiff and switch to a crosswind casting behavior (moths and *Drosophila*) or to turns (cockroach) when encountering a blank (Mafra-Neto and Cardé, 1994; Willis and Avondet, 2005; Budick and Dickinson, 2006).

Contrary to their use of odor plumes as olfactory trails, we have little evidence that insects use spatial information from local odor sources as topographic-olfactory information. Evanescence of odors that can be quickly swept away by wind and changes in wind direction can make olfactory cues poorly reliable as landmarks. However, a species of desert ants, *Cataglyphis fortis*, uses olfactory cues when foraging for dead arthropods in the Tunisian salt pans (Buehlmann et al., 2015). Both the unpredictable food distribution and the high surface temperatures might account for the fact that this ant species does not use pheromone trails. *C. fortis* not only locates sparsely distributed food, or pinpoints its inconspicuous nest entrance by following odor plumes, but it also uses environmental odors as olfactory landmarks when following habitual routes.

PLASTICITY AND ADAPTATION TO COMPLEX AND VARIABLE ODORSCAPES

As described in the previous sections, odorscapes are both very complex and variable over time. Flexibility and integration capacities allow insects to adjust their behavior accordingly. To deal with the complexity of their olfactory environment, insects may not use all available chemical information but select the relevant cues. Besides, although many of their behaviors are innate, insects also show a remarkable plasticity through learning or physiological changes, allowing them to adjust to changes in their physiological needs or their environment. Exposure to specific VPC environments may have long-term effects on insect physiology as well as on evolutionary adaptation.

Selective Attention and Salience Among Components of the Odorscape

With hundreds of VPCs constantly changing in concentration, odorscapes contain probably more information than the insect brain can efficiently process at any given time. Furthermore, insects cannot focus their olfaction on a specific area, like it is possible to focus vision in a direction for instance. Thus, the insect brain would be overloaded by the amount of information coming from the olfactory environment unless special adaptation such as selective attention reduces the stimulus set available to them to a subset of salient and relevant information. A growing body of literature provides behavioral and neurophysiological evidence of attention-like processes in insects for acoustic or visual stimuli (Wang et al., 2008; Nityananda, 2016). Experimental evidence for such "odor salience filters" is still scarce, probably due to the general consensus that ORs work as efficient filters performing low-level extraction of scene features according to the molecular structure of its constituents. In bees, the acquisition of a Pavlovian association between the unconditional stimulus (US), a sugar, and an odor used as conditional stimulus (CS) is delayed if the experimental bee was previously exposed to the CS without US (Fernandez et al., 2012), a process termed latent inhibition. Furthermore, not all VPCs that insects detect in the odorscape have the same importance, or salience, for them. Bumblebee performances in an associative learning protocol are linked to the salience of individual VPCs, estimated from the amplitude of electroantennogram responses (Katzenberger et al., 2013). Conditioning in *Apis mellifera* also revealed that the conditioned proboscis extension response to an odorant depends on the salience of the odorant used for conditioning, more salient (Smith, 1991) or more concentrated odorants (Wright and Smith, 2004) permitting stronger acquisitions.

Behavioral Plasticity of Responses to Volatile Plant Compounds

Volatiles may have an intrinsic behavioral significance (valence), independently of their salience. Some signals such as pheromones have a hard-wired valence and elicit stereotypic behavioral responses. Responses to other components of the odorscape may be plastic. In polyphagous pollinators and herbivores, responses to floral or vegetative plant odors depend on learning and/or past experiences. Learning to associate plant chemical traits to the presence or absence of a reward is remarkably common and highly adaptive in generalist pollinators such as bees or moths (review in Jones and Agrawal, 2017). Indeed, the identity of the plant species providing the best nectar/pollen resource may change rapidly over the course of the flowering season, and a flower's nectar content decreases when it gets older (Raguso and Weiss, 2015). Being able to learn new associations and to forget when a particular resource gets exhausted is therefore essential. In herbivores, ovipositing females need to lay their eggs on plant species that are suitable for their offspring's development. While oligophagous species are able to achieve this efficiently *via* innate preferences (Gripenberg et al., 2010), polyphagous species rely more on plasticity based on their past experiences and prefer plant species they have successfully fed or mated on (Anderson and Anton, 2014; Carrasco et al., 2015).

Long-Term Effects of Odorscapes on Insect Olfactory Behaviors

The physiological status of the receiver insect, like mating or starving, may also change the valence of an odor. *Agrotis ipsilon* immature males do not respond to the sex pheromone although they are able to detect it (Gadenne et al., 2001). The same is true for recently mated mature males. Furthermore, while the attractivity of floral odor and pheromone to unmated males adds up, presence of the sex pheromone inhibits the attraction of mated males to floral odors (Barrozo et al., 2010).

While the perception of VPCs in the odorscape can trigger fast behavioral responses, long or repeated pre-exposures to odorants may lead to long-term physiological changes through processes that may or may not involve sensory detection.

In the moth *S. littoralis*, a brief pre-exposure to gustatory stimuli can change the behavioral and physiological responses to olfactory stimuli after 24 h and vice versa (Minoli et al., 2012). This long-term modulation of moth behavior correlates with modifications within the olfactory system, including up-regulation of a gene involved in olfaction (Guerrieri et al., 2012). Besides sensory effects, the physiological effects of prolonged exposures to VPCs should also be considered. Many isoprenoids have toxic effects when ingested by an insect or at high aerial concentrations. Lethality or effects on development have been well documented because of the potential use of essential oils as natural biocides, or to exploit the plant resistance to herbivory. However, non-lethal effects remain insufficiently documented. For instance, thymol, the main phenolic VPC from *Thymus vulgaris*, is used to fight the bee parasite *Varroa destructor,* but has also important effects on the bee cognitive behavior (Bergougnoux et al., 2012). The consequences of the exposure of insect populations to sub-lethal concentrations of such potentially neurotoxic volatiles would deserve further investigations.

Evolutionary Adaptations in the Odorscape

The environments insects live in are very diverse and subject to long-term changes, including in their olfactory aspects (**Figure 1**). Insects have developed an olfactory system with remarkable sensitivity, specificity, and dynamics. How the evolution of this system contributes to insects' adaptation to their lifestyle and environment is currently a hot research topic. The insect chemosensory gene families show high diversification rates, which can support fast adaptation of odorant detection capacities (Andersson et al., 2015). Antennal morphology is also very diverse and subject to selection pressures (Elgar et al., 2018). Olfactory system adaptation must be driven not only by the identity of the target signals to be detected but also by the characteristics of the olfactory environment these signals must be detected against. This remark certainly holds for OR tuning, although exploring this question will have to wait for more deorphanization data to be made available. Hansson and Stensmyr (2011) suggest that antennal morphology may reflect constraints imposed by the physical environment rather than adaptations to detect specific types of odorants. Antenna size correlates with increased sensitivity (detection surface and number of sensilla), and the sexual dimorphism in moth is a classic example where male's larger/more elaborate antennae are an adaptation to the very low amounts of pheromone released by the females. However, attempts to correlate antennal size with pheromone volatility across species have given contradictory results (Elgar et al., 2018). Higher sensitivity may also be an advantage in environments where picking the signal is very difficult. One such example may be found in the highly specific, olfaction-driven fig tree/Agaonid pollinator mutualism. Western African populations of *Ficus sur* are pollinated by two sister species of Agaonid fig wasps (Kerdelhue et al., 1999). Although roughly sympatric, these two species differ both in their habitat preferences and their antennal morphology. *Ceratosolen silvestrianus*, mostly found in open habitats where population density of *F. sur* is high, has straight antennae. On the contrary, *C. flabellatus*, more abundant in forests where their host tree is at low density, have ramified antennae bearing more sensilla. In this case, the difficulty to pick up the signal may pertain either to the scarcity of the resource or to the physical structure of the forest habitat, which may impair the formation/persistence of navigable plumes.

Reciprocally, it is highly possible that insect community composition, especially the sensory abilities of the species composing that community as well as the identity of co-occurring plant species, influences the evolution of VPC emissions by plants and as a consequence the odorscape. For instance, the influence of pollinator- or herbivore-mediated selection on the emission of VPCs by plants has already been shown in the context of pairwise plant-species interactions (Becerra et al., 2009; Schiestl and Johnson, 2013). In addition, divergent seasonal patterns of scent emission by flowers have been revealed in a Mediterranean plant-community in relation to pollinator seasonal abundance and local plant abundance (Filella et al., 2013). More specifically, this study shows that VPC emission is higher in plant species that bloom early in the flowering period when pollinators are rare relative to flowers than in species blooming later in the season when there is a surplus of pollinators relative to flowers. The authors hypothesize that inter-specific competition for pollinator attraction might explain this variation. So far, due to the limited number of studies exploring the association between VPCs and plant-insect community structure, we have limited evidence of the effect of insect association on odorscape composition. Interestingly, a very recent study conducted at the community level pointed out an association between VPC chemical classes emitted by flowers and pollinator groups (Kantsa et al., 2019). In another study, behavioral responses of pollinator species to floral odors were found to explain a large part of the plant-pollinator network structure (Junker et al., 2010). This recent use of network-based methods to explore the importance of chemical signals in the structuring of plant-insect community will probably open the path to new discoveries on the evolution of plant-insect chemical communication.

ODORSCAPES IN PLANT PROTECTION AND AGROECOLOGY

Manipulating the odorscapes of herbivorous pest species has already important practical implications in plant protection as an alternative to pesticides. Mating disruption methods use a synthetic sex pheromone to disturb the chemical communication between sexes. Dispensing the synthetic pheromone in the field results in the confusion of male moths which follow false trails and cannot localize females any more (Cardé and Minks, 1995). This interrupts normal mating behavior, thereby affecting chances of reproduction of pest insects. Large cultivated areas are generally treated by mating disruption to prevent introgression of mated females (Witzgall et al., 2010). Mating disruption is currently successfully used against numerous moth species in various types of crop plants, either in fields (cotton, maize), orchards (apple trees), vineyards, or even forests. Interestingly, this diversity of treated crop plants indicates that it is feasible to modify the odorscape in very different plant covers.

Modifying the odorscape implies to be able to release biologically active concentrations of odorants in the field at economically relevant costs. The success of mating disruption has promoted research for efficient dispenser technology, because the synthetic pheromone is often costly to produce. This development led, in less than 50 years, from the first hand-applied meso-dispensers to biodegradable, mechanically sprayable micro-formulations. A striking example of this development has been reviewed for the European grapevine moth, *Lobesia botrana* (Hummel, 2017). Active dispensers releasing the pheromone as puffs of aerosol at night when moths are active have been experimented, for instance against *Cydia pomonella* (McGhee et al., 2016). The decrease in moth populations obtained with these dispensers demonstrates the feasibility of a very precise control of the odorscape by adjusting the emission rates and the temporal release pattern of odorants. Still, the diffusion technology remains a bottleneck limiting the development of semiochemical uses in plant protection.

Modifying the odorscape by introducing other plant species that naturally release different VPCs can also reduce the damage caused by pest insects. Non-host plants inter-cropped with host plants decreased the oviposition of Anthomyiid flies on the hosts (Finch et al., 2003). To explain this phenomenon, it was proposed that females landed indifferently on the foliage of one or the other plant species, relying upon unspecific visual stimuli rather than on olfactory cues, but flew away from non-host plants without laying eggs because of the unsuitability of contact chemostimuli. After several errors, they finally flew away from the mixed field, this behavior resulting in a statistical reduction of the number of successful ovipositions on hosts. However, the role of non-host volatiles in oviposition deterrence has been confirmed later. For instance, methyl salicylate released by birch trees has been identified as the main factor in the reduction of mating and number of processionary moth nests on pine trees surrounded by birch trees (Jactel et al., 2011). This phenomenon is exploited in push and pull strategies, in which a pest insect is repelled from a protected crop by a repellent plant while it is attracted by plants of lesser economic value to field edges where it can be destroyed (Cook et al., 2007; Khan et al., 2010).

CONCLUSIONS

The chemical complexity of plant volatilomes and insect olfactomes has been intensively investigated. A considerable amount of information is available regarding the identity of the volatiles mediating biotic interactions that involve insects. But we need now to grasp the complexity of the dense information networks mediated by semiochemicals. A recent analysis of a pollination network at the landscape level shows that the composition and intensity of volatile floral emissions, among other floral traits, correlate to the level of specialization of each plant species, as well as to visitation rates by the different pollinator guilds (Kantsa et al., 2018). It is striking to note that the level of complexity in their ecological role is highly variable among volatile compounds. Some semiochemicals, like most of the pheromones, are involved in specialized and confidential communication. On the other hand, single components, like β-ocimene for instance, play central roles in many biotic interactions, including pollination, and are produced and detected by diverse organisms (Farré-Armengol et al., 2017). This multifunctionality and the interweaving of olfactory interactions are serious obstacles to decipher odorscape ecological functions at multitrophic levels. It also makes it difficult to assess the impact of biotic factors (the rise of an invasive species for instance), or abiotic factors (like global warming or pollution) on olfactory communication at ecosystem scale. Using network analysis approaches in order to study how the information flows within ecosystems should overcome the apparent intricacy of odorscapes.

The ecological relevance of the concept of odorscape is stressed by the growing body of evidence indicating that the olfactory environment and other contextual information do influence the way insects respond to specific signals. Indeed, insect odorscapes are essentially multidimensional, including not only chemical identities, but also physical and temporal parameters, plus sensory, perceptual, and cognitive features. Adapting their responses to the context becomes particularly important to insects when the signal itself is ambiguous. This partly explains why insects may reliably respond to ubiquitous plant volatiles in complex olfactory scenes mixing VPCs from host and non-host plants (Meiners, 2015). Context dependence is also particularly important to consider when developing infochemicals to be applied in plant protection. For instance, genetically modified wheat constitutively producing the aphid alarm pheromone (E)-β-farnesene, although attractive to parasitoids in the lab, failed to improve aphid biocontrol in the field. This was probably because constitutive emission by the plants broke down the spatio-temporal correlation between (E)-β-farnesene and aphid presence (Bruce et al., 2015). Studying single odor signals is useful in gaining knowledge about the ecological function of these signals. But in the end, we need to consider the signals within their context in order to fully understand how infochemical networks function at the ecosystem level.

Since odorscapes are key elements of ecosystem functioning, it becomes essential to evaluate the impact of atmospheric pollution and climate change on their evolution. The study of the effect of anthropogenic volatile pollutants is just emerging and their impact on plant-to-plant and plant-to-insect communication is barely understood (Jürgens and Bischoff, 2017). There are indications that air pollution affects interactions between plants and insects beneficial to agriculture with potential consequences on plant productivity (Girling et al., 2013; Farré-Armengol et al., 2016). We need to better investigate the biological effects of atmospheric VPC reaction products on insect and plant communication (Simpraga et al., 2016). It is well established that plants modify their volatile emissions in response to biotic or abiotic stresses. Since plant metabolism responses are relatively fast compared to occurrence of visible damage, monitoring of induced VPCs could provide early alerts and allow for fast and timely implementation of remediation solutions. More studies are urgently needed, first to describe present odorscapes in a diversity of ecosystems, then to follow their evolution and evaluate how it affects the ecosystem functioning. Monitoring the odorscape composition could also serve as a reliable indicator of ecosystem quality and of

biodiversity levels, a major concern in times of diminution of insect populations (Dirzo et al., 2014).

Global change is expected to have a profound impact on ecosystems, including VPC emissions and transport (**Figure 1**). Current knowledge on the impact of CO_2 and temperature on plant physiology suggests a global increase in VPC emission rates as a result of climate change (Holopainen et al., 2018). How will insects respond to the resulting alterations in odorscape concentration, composition, and structure? As discussed in section "Evolutionary Adaptations in the Odorscape", insects have developed a remarkably adaptable olfactory system, as shown by the rapid evolution of OR genes and the diversity of antennal shapes. While it is clear that OR tuning adapts to the characteristics of the signal to be detected, studies showing how the insect olfactory system adapts to specific olfactory environments, be it *via* OR tuning or antennal morphology, are needed. A combination of molecular and neuroethological methods, applied to proper models and with a sound ecological background, will allow to gain a deeper understanding of the mechanisms involved in the insect adaptation to changing environments.

Achieving this goal will require a proper description of olfactory landscapes, which depends on our capacity to isolate and identify the diverse volatile organic compounds that occur often in very small concentrations. Improvements in analytical techniques have made VPCs some of the best studied plant metabolites. Detection limits in the low ng/L range (< 1 ppbv) allow the quantification of VPCs released by single plants and are close to the detection ability of living organisms (Bicchi and Maffei, 2012). The most universal detector, the flame ionization detector is stable, linear, and offers minimum detectable amounts in the order of 0.1 ng. To bring detection limits further down, sample enrichment by dynamic head space collections on porous polymer sorbents is often used to the detriment of the temporal resolution. Yet, in natural conditions, transport of the odorant molecules by air profoundly reshapes the stimulus both spatially and temporally. The aerial concentration of VPCs undergoes considerable variation over time. It is essential to monitor this variation in order to properly describe natural odorscapes. Proton transfer reaction-mass spectrometry allows real-time trace gas monitoring at the pptv level. However, it cannot discriminate different compounds within one nominal mass, a serious limit to the apprehension of odorscape complexity. Fortunately, increasingly miniaturized set-ups combining fast trapping with fast online GC analysis and sensitivity in the ppbv range have facilitated remote field analyses. While these technical advances have created opportunities for detailed views on the time courses of VPC emissions, describing the fine temporal and spatial structure of odorscapes remains a complicated task and we still have very little insight into how it might vary across habitat types. One more argument to the necessity of studying the physics of the odorscape is the fact that notable differences between the atmospheric conditions prevailing between diurnal and nocturnal environments might have contributed to the success of olfactory communication in nocturnal insects. For instance, the lower wind, turbulence, and oxidant levels that prevail at night might facilitate the persistence of chemical trails over longer distances, and lower background VPC emissions might lead to lower olfactory noise, potentially making olfaction more reliable at night, and the cost-benefit balance for maintaining large olfactory organs more favorable (Elgar et al., 2018).

Finally, progresses in odorscape characterization will open the path to many more agronomic applications. Mating disruption, a method based on the manipulation of one critical component of moth odorscape at field scale, has offered a successful substitute to pesticides in the control of major lepidopteran pest species. At close range, repellent molecules are used to deterring hematophagous or parasite insects. Essential oil fumigations are used to eliminate pests of stored goods, but the concentrations in treated premises reach values 10^6 times stronger than their concentrations in a natural odorscape. The huge diversity of components of essential oils provides a big reservoir of potential semiochemicals to control insects (Mossa, 2016). However, the diffusion in the field of adapted aerial concentrations of costly bioactive odorants, with different volatilities, is still a serious limitation to odorscape manipulation. New formulation technologies, which include VOCs in sprayable and biodegradable nanocapsules, will resolve many technical problems posed by field application. Besides these purely technical solutions, one might prefer natural release, for instance by plant varieties selected for their specific VPC emissions. This option will also offer the advantage of more natural solutions in agroecology.

AUTHOR CONTRIBUTIONS

All authors contributed to analyze the literature and write the manuscript. MR coordinated the project.

FUNDING

This work was supported by a grant from ANR project ODORSCAPE (ANR15-CE02-010-01).

REFERENCES

Ache, B. W., Gleeson, R. A., and Thompson, H. A. (1988). Mechanisms for mixture suppression in olfactory receptors of the spiny lobster. *Chem. Senses* 13, 425–434. doi: 10.1093/chemse/13.3.425

Ainsworth, E. A. (2017). Understanding and improving global crop response to ozone pollution. *Plant J.* 90, 886–897. doi: 10.1111/tpj.13298

Anderson, P., and Anton, S. (2014). Experience-based modulation of behavioural responses to plant volatiles and other sensory cues in insect herbivores. *Plant Cell Environ.* 37, 1826–1835. doi: 10.1111/pce.12342

Andersson, M. N. (2012). Mechanisms of odor coding in coniferous bark beetles: from neuron to behavior and application. *Psyche*. 2012:149572. doi: 10.1155/2012/149572

Andersson, M. N., Larsson, M. C., Blaženec, M., Jakuš, R., Zhang, Q. H., and Schlyter, F. (2010). Peripheral modulation of pheromone response by inhibitory host compound in a beetle. *J. Exp. Biol.* 213, 3332–3339. doi: 10.1242/jeb.044396

Andersson, M. N., Löfstedt, C., and Newcomb, R. D. (2015). Insect olfaction and the evolution of receptor tuning. *Front. Ecol. Evol.* 3:53. doi: 10.3389/fevo.2015.00053

Arimura, G.-I., Kopke, S., Kunert, M., Volpe, V., David, A., Brand, P., et al. (2008). Effects of feeding *Spodoptera littoralis* on lima bean leaves: IV. Diurnal and nocturnal damage differentially initiate plant volatile emission. *Plant Physiol.* 146, 965–973. doi: 10.1104/pp.107.111088

Atema, J. (1996). Eddy chemotaxis and odor landscapes: exploration of nature with animal sensors. *Biol. Bull.* 191, 129–138. doi: 10.2307/1543074

Atkinson, R., and Arey, J. (2003). Gas-phase tropospheric chemistry of biogenic volatile organic compounds: a review. *Atmos. Environ.* 37, 197–219. doi: 10.1016/S1352-2310(03)00391-1

Bachy, A., Aubinet, M., Schoon, N., Amelynck, C., Bodson, B., Moureaux, C., et al. (2016). Are BVOC exchanges in agricultural ecosystems overestimated? Insights from fluxes measured in a maize field over a whole growing season. *Atmos. Chem. Phys.* 16, 5343–5356. doi: 10.5194/acp-16-5343-2016

Badeke, E., Haverkamp, A., Hansson, B. S., and Sachse, S. (2016). A challenge for a male noctuid moth? Discerning the female sex pheromone against the background of plant volatiles. *Front. Physiol.* 7:143. doi: 10.3389/fphys.2016.00143

Baker, T. C., Fadamiro, H. Y., and Cosse, A. A. (1998). Moth uses fine tuning for odour resolution. *Nature* 393:530. doi: 10.1038/31131

Baker, T. C., and Haynes, K. F. (1987). Manoeuvres used by flying male oriental fruit moths to relocate a sex pheromone plume in an experimentally shifted wind-field. *Physiol. Entomol.* 12, 263–279. doi: 10.1111/j.1365-3032.1987.tb00751.x

Baldwin, I. T. (2010). Plant volatiles. *Curr. Biol.* 20, R392–R397. doi: 10.1016/j.cub.2010.02.052

Barrozo, R., Gadenne, C., and Anton, S. (2010). Switching attraction to inhibition: mating-induced reversed role of sex pheromone in an insect. *J. Exp. Biol.* 213, 2933–2939. doi: 10.1242/jeb.043430

Becerra, J. X., Noge, K., and Venable, D. L. (2009). Macroevolutionary chemical escalation in an ancient plant-herbivore arms race. *Proc. Natl. Acad. Sci. USA* 106, 18062–18066. doi: 10.1073/pnas.0904456106

Bell, J. S., and Wilson, R. I. (2016). Behavior reveals selective summation and max pooling among olfactory processing channels. *Neuron* 91, 425–438. doi: 10.1016/j.neuron.2016.06.011

Berg, B. G., and Mustaparta, H. (1995). The significance of major pheromone components and interspecific signals as expressed by receptor neurons in the oriental tobacco budworm moth, *Helicoverpa assulta*. *J. Comp. Physiol. A* 177, 683–694. doi: 10.1007/BF00187627

Berg, B. G., Zhao, X. C., and Wang, G. (2014). Processing of pheromone information in related species of Heliothine moths. *Insects* 5, 742–761. doi: 10.3390/insects5040742

Bergougnoux, M., Treilhou, M., and Armengaud, C. (2012). Exposure to thymol decreased phototactic behaviour in the honeybee (*Apis mellifera*) in laboratory conditions. *Apidologie* 44, 82–89. doi: 10.1007/s13592-012-0158-5

Beyaert, I., Wäschke, N., Scholz, A., Varama, M., Reinecke, A., and Hilker, M. (2010). Relevance of resource-indicating key volatiles and habitat odour for insect orientation. *Anim. Behav.* 79, 1077–1086. doi: 10.1016/j.anbehav.2010.02.001

Bhandawat, V., Olsen, S. R., Gouwens, N. W., Schlief, M. L., and Wilson, R. I. (2007). Sensory processing in the *Drosophila* antennal lobe increases reliability and separability of ensemble odor representations. *Nat. Neurosci.* 10, 1474–1482. doi: 10.1038/nn1976

Bicchi, C., and Maffei, M. (2012). "The plant Volatilome: methods of analysis" in *High-throughput phenotyping in plants: Methods and protocols, vol 91. Methods in molecular biology*. ed. J. Normanly (Berlin: Springer Science+Business Media), 289–310.

Binyameen, M., Hussain, A., Yousefi, F., Birgersson, G., and Schlyter, F. (2013). Modulation of reproductive behaviors by non-host volatiles in the polyphagous Egyptian cotton leafworm, *Spodoptera littoralis*. *J. Chem. Ecol.* 39, 1273–1283. doi: 10.1007/s10886-013-0354-4

Borrero-Echeverry, F., Bengtsson, B., Nakamuta, K., and Peter Witzgall, P. (2018). Plant odor and sex pheromone are integral elements of specific mate recognition in an insect herbivore. *Evolution* 72, 2225–2233. doi: 10.1111/evo.13571

Bruce, T. J. A., Aradottir, G. I., Smart, L. E., Martin, J. L., Caulfield, J. C., Doherty, A., et al. (2015). The first crop plant genetically engineered to release an insect pheromone for defence. *Sci. Rep.* 5:11183. doi: 10.1038/srep11183

Bruce, T. J. A., and Pickett, J. A. (2011). Perception of plant volatile blends by herbivorous insects - finding the right mix. *Phytochemistry* 72, 1605–1611. doi: 10.1016/j.phytochem.2011.04.011

Bruce, T. J., Wadhams, L. J., and Woodcock, C. M. (2005). Insect host location: a volatile situation. *Trends Plant Sci.* 10, 269–274. doi: 10.1016/j.tplants.2005.04.003

Budick, S. A., and Dickinson, M. H. (2006). Free-flight responses of *Drosophila melanogaster* to attractive odors. *J. Exp. Biol.* 209, 3001–3017. doi: 10.1242/jeb.02305

Buehlmann, C., Graham, P., Hansson, B. S., and Knaden, M. (2015). Desert ants use olfactory scenes for navigation. *Anim. Behav.* 106, 99–105. doi: 10.1016/j.anbehav.2015.04.029

Butterwick, J. A., Del Marmol, J., Kim, K. H., Kahlson, M. A., Rogow, J. A., Walz, T., et al. (2018). Cryo-EM structure of the insect olfactory receptor Orco. *Nature* 560, 447–452. doi: 10.1038/s41586-018-0420-8

Byers, J. A., Zhang, Q.-H., and Birgersson, G. (2004). Avoidance of nonhost plants by a bark beetle, *Pityogenes bidentatus*, in a forest of odors. *Naturwiss* 91, 215–219. doi: 10.1007/s00114-004-0520-1

Cape, J. N. (2003). Effects of airborne volatile organic compounds on plants. *Environ. Pollut.* 122, 145–157. doi: 10.1016/S0269-7491(02)00273-7

Cardé, R. T., and Charlton, R. E. (1984). "Olfactory sexual communication in Lepidoptera: strategy, sensitivity and selectivity" in *Insect communication*. ed. T. Lewis (London: Academic Press), 241–265.

Cardé, R. T., and Minks, A. K. (1995). Control of moth pests by mating disruption: successes and constraints. *Annu. Rev. Entomol.* 40, 559–585. doi: 10.1146/annurev.en.40.010195.003015

Cardé, R. T., and Willis, M. A. (2008). Navigational strategies used by insects to find distant, wind-borne sources of odor. *J. Chem. Ecol.* 34, 854–866. doi: 10.1007/s10886-008-9484-5

Carrasco, D., Larsson, M. C., and Anderson, P. (2015). Insect host plant selection in complex environments. *Curr. Opin. Insect Sci.* 8, 1–7. doi: 10.1016/j.cois.2015.01.014

Celani, A., Villermaux, E., and Vergassola, M. (2014). Odor landscapes in turbulent environments. *Phys. Rev.* 4:041015. doi: 10.1103/PhysRevX.4.041015

Cha, D. H., Linn, C. E., Teal, P. E., Zhang, A., Roelofs, W. L., and Loeb, G. M. (2011). Eavesdropping on plant volatiles by a specialist moth: significance of ratio and concentration. *PloS One* 6:e17033. doi: 10.1371/journal.pone.0017033

Chan, H., Hersperger, F., Marachlian, E., Smith, B. H., Locatelli, F., Szyszka, P., et al. (2018). Odorant mixtures elicit less variable and faster responses than pure odorants. *PLoS Comput. Biol.* 14:e1006536. doi: 10.1371/journal.pcbi.1006536

Conversano, T. E. J., van Wilgenburg, E., and Elga, M. A. (2014). Background odour may impair detection of chemical signals for social recognition. *Austral Entomol.* 53, 432–435. doi: 10.1111/aen.12087

Cook, S. M., Khan, Z. R., and Pickett, J. A. (2007). The use of push-pull strategies in integrated pest management. *Annu. Rev. Entomol.* 52, 375–400. doi: 10.1146/annurev.ento.52.110405.091407

de Fouchier, A., Walker, W. B., Montagné, N., Steiner, C., Binyameen, M., Schlyter, F., et al. (2017). Functional evolution of Lepidoptera olfactory receptors revealed by deorphanization of a moth repertoire. *Nat. Commun.* 8, 15709–15709. doi: 10.1038/ncomms15709

Degen, T., Dillmann, C., Marion Poll, F., and Turlings, T. C. J. (2004). High genetic variability of herbivore-induced volatile emission within a broad range of maize inbred lines. *Plant Physiol.* 135, 1928–1938. doi: 10.1104/pp.104.039891

Deisig, N., Giurfa, M., Lachnit, H., and Sandoz, J. C. (2006). Neural representation of olfactory mixtures in the honeybee antennal lobe. *Eur. J. Neurosci.* 24, 1161–1174. doi: 10.1111/j.1460-9568.2006.04959.x

Dekker, T., Ibba, I., Siju, K. P., Stensmyr, M. C., and Hansson, B. S. (2006). Olfactory shifts parallel superspecialism for toxic fruit in *Drosophila melanogaster* sibling, *D. sechellia*. *Curr. Biol.* 16, 101–109. doi: 10.1016/j.cub.2005.11.075

Delory, B. M., Delaplace, P., Fauconnier, M.-L., and du Jardin, P. (2016). Root-emitted volatile organic compounds: can they mediate belowground plant-plant interactions? *Plant Soil* 402, 1–26. doi: 10.1007/s11104-016-2823-3

Den Otter, C. J., Schuil, H. A., and Sander-van Oosten, A. (1978). "Reception of host-plant odours and female sex pheromone in *Adoxophyes orana* (Lepidoptera: Tortricidae): electrophysiology and morphology" in *Proceedings of the 4th international symposium - insect and host plant - 4-9 June*. eds. R. F. Chapman and E. A. Bernays (Fulmer Grange, Slough, England: Entomologia Experimentalis et Applicata), 570–578.

Dicke, M. (2016). Plant phenotypic plasticity in the phytobiome: a volatile issue. *Curr. Opin. Plant Biol.* 32, 17–23. doi: 10.1016/j.pbi.2016.05.004

Dirzo, R., Young, H. S., Galetti, M., Ceballos, G., Isaac, N. J. B., and Collen, B. (2014). Defaunation in the Anthropocene. *Science* 345, 401–406. doi: 10.1126/science.1251817

Dugravot, S., Mondy, N., Mandon, N., and Thibout, E. (2005). Increased sulfur precursors and volatiles production by the leek *Allium porrum* in response to specialist insect attack. *J. Chem. Ecol.* 31, 1299–1314. doi: 10.1007/s10886-005-5287-0

Dugravot, S., and Thibout, E. (2006). Consequences for a specialist insect and its parasitoid of the response of *Allium porrum* to conspecific herbivore attack. *Physiol. Entomol.* 31, 73–79. doi: 10.1111/j.1365-3032.2005.00489.x

Egea-Weiss, A., Renner, A., Kleineidam, C. J., and Szyszka, P. (2018). High precision of spike timing across olfactory receptor neurons allows rapid odor coding in *Drosophila*. *iScience* 4, 76–63. doi: 10.1016/j.isci.2018.05.009

Elgar, M. A., Zhang, D., Wang, Q., Wittwer, B., Pham, H. T., Johnson, T. L., et al. (2018). Insect antennal morphology: the evolution of diverse solutions to odorant perception. *Yale J. Biol. Med.* 91, 457–469.

Elkinton, J. S., Schal, C., Ono, T., and Carde, R. T. (1987). Pheromone puff trajectory and upwind flight of male gypsy moths in a forest. *Physiol. Entomol.* 12, 399–406. doi: 10.1111/j.1365-3032.1987.tb00766.x

Farré-Armengol, G., Filella, I., Llusià, J., and Peñuelas, J. (2017). β-Ocimene, a key floral and foliar volatile involved in multiple interactions between plants and other organisms. *Molecules* 22:1148. doi: 10.3390/molecules22071148

Farré-Armengol, G., Penuelas, J., Li, T., Yli-Pirila, P., Filella, I., Llusia, J., et al. (2016). Ozone degrades floral scent and reduces pollinator attraction to flowers. *New Phytol.* 209, 152–160. doi: 10.1111/nph.13620

Fernandez, V. M., Giurfa, M., Devaud, J.-M., and Farina, W. F. (2012). Latent inhibition in an insect: the role of aminergic signaling. *Learn. Mem.* 19, 593–597. doi: 10.1101/lm.028167.112

Filella, I., Primante, C., Llusia, J., Martín González, A. M., Seco, R., Farré-Armengol, G., et al. (2013). Floral advertisement scent in a changing plant-pollinators market. *Sci. Rep.* 3:3434. doi: 10.1038/srep03434

Finch, S., Billiard, H., and Collier, R. H. (2003). Companion planting - do aromatic plants disrupt host-plant finding by the cabbage root fly and the onion fly more effectively than non-aromatic plants? *Entomol. Exp. Appl.* 109, 183–195. doi: 10.1046/j.0013-8703.2003.00102.x

Fischbach, R. J., Staudt, M., Zimmer, I., Rambal, S., and Schnitzler, J. P. (2002). Seasonal pattern of monoterpene synthase activities in leaves of the evergreen tree *Quercus ilex*. *Physiol. Plant.* 114, 354–360. doi: 10.1034/j.1399-3054.2002.1140304.x

Frye, M. A., Tarsitano, M., and Dickinson, M. H. (2003). Odor localization requires visual feedback during free flight in *Drosophila melanogaster*. *J. Exp. Biol.* 206, 843–855. doi: 10.1242/jeb.00175

Fuentes, J. D., Chamecki, M., Roulston, T. H., Chen, B., and Pratt, K. R. (2016). Air pollutants degrade floral scents and increase insect foraging times. *Atmos. Environ.* 214, 361–374. doi: 10.1016/j.atmosenv.2016.07.002

Fuentes, J. D., Roulston, T. H., and Zenker, J. (2013). Ozone impedes the ability of a herbivore to find its host. *Environ. Res. Lett.* 8:014048. doi: 10.1088/1748-9326/8/1/014048

Gadenne, C., Dufour, M. C., and Anton, S. (2001). Transient post-mating inhibition of behavioural and central nervous responses to sex pheromone in an insect. *Proc. R. Soc. London, Ser. B* 268, 1631–1635. doi: 10.1098/rspb.2001.1710

Galizia, C. G. (2014). Olfactory coding in the insect brain: data and conjectures. *Eur. J. Neurosci.* 39, 1784–1795. doi: 10.1111/ejn.12558

Galizia, C., and Rössler, W. (2010). Parallel olfactory systems in insects: anatomy and function. *Annu. Rev. Entomol.* 55, 399–420. doi: 10.1146/annurev-ento-112408-085442

Gaudry, Q., Hong, E. J., Kain, J., de Bivort, B. L., and Wilson, R. I. (2013). Asymmetric neurotransmitter release enables rapid odour lateralization in *Drosophila*. *Nature* 439, 424–428. doi: 10.1038/nature11747

Girling, R. D., Lusebrink, I., Farthing, E., Newman, T. A., and Poppy, G. M. (2013). Diesel exhaust rapidly degrades floral odours used by honeybees. *Sci. Rep.* 3, 1–5. doi: 10.1038/srep02779

Goldstein, A. H., and Galbally, I. E. (2007). Known and unexplored organic constituents in the earth's atmosphere. *Environ. Sci. Technol.* 41, 1514–1521. doi: 10.1021/es072476p

Greiner, B., Gadenne, C., and Anton, S. (2002). Central processing of plant volatiles in *Agrotis ipsilon* males is age-independent in contrast to sex pheromone processing. *Chem. Senses* 27, 45–48. doi: 10.1093/chemse/27.1.45

Gripenberg, S., Mayhew, P. J., Parnell, M., and Roslin, T. (2010). A meta-analysis of preference-performance relationships in phytophagous insects. *Ecol. Lett.* 13, 383–393. doi: 10.1111/j.1461-0248.2009.01433.x

Guerenstein, P. G., and Hildebrand, J. G. (2008). Roles and effects of environmental carbon dioxide in insect life. *Annu. Rev. Entomol.* 53, 161–178. doi: 10.1146/annurev.ento.53.103106.093402

Guerrieri, F., Gemeno, C., Monsempes, C., Anton, S., Jacquin-Joly, E., Lucas, P., et al. (2012). Experience-dependent modulation of antennal sensitivity and input to antennal lobes in male moths (*Spodoptera littoralis*) pre-exposed to sex pheromone. *J. Exp. Biol.* 215, 2334–2341. doi: 10.1242/jeb.060988

Hansson, B. S., and Stensmyr, M. C. (2011). Evolution of insect olfaction. *Neuron* 72, 698–711. doi: 10.1016/j.neuron.2011.11.003

Hantson, S., Knorr, W., Schurgers, G., Pugh, T. A. M., and Arneth, A. (2017). Global isoprene and monoterpene emissions under changing climate, vegetation, CO_2 and land use. *Atmos. Environ.* 155, 35–45. doi: 10.1016/j.atmosenv.2017.02.010

Hare, J. D. (2010). Ontogeny and season constrain the production of herbivore-inducible plant volatiles in the field. *J. Chem. Ecol.* 36, 1363–1374. doi: 10.1007/s10886-010-9878-z

Harper, K. L., and Unger, N. (2018). Global climate forcing driven by altered BVOC fluxes from 1990 to 2010 land cover change in maritime Southeast Asia. *Atmos. Chem. Phys.* 18, 16931–16952. doi: 10.5194/acp-18-16931-2018

Hatanaka, A. (1993). The biogeneration of green odour by green leaves. *Phytochemistry* 34, 1201–1218. doi: 10.1016/0031-9422(91)80003-J

Hatano, E. A., Saveer, A., Borrero-Echeverry, F., Strauch, M., Zakir, A., Bengtsson, M., et al. (2015). A herbivore-induced plant volatile interferes with host plant and mate location in moths through suppression of olfactory signaling pathways. *BMC Biol.* 13:75. doi: 10.1186/s12915-015-0188-3

Helletsburger, C., Dötterl, S., Ruprecht, U., and Junker, R. R. (2017). Epiphytic bacteria alter floral scent emission. *J. Chem. Ecol.* 43, 1073–1077. doi: 10.1007/s10886-017-0898-9

Holopainen, J. K., Virjamo, V., Ghimire, R. P., Blande, J. D., Julkunen-Tiitto, R., and Kivimäenpää, M. (2018). Climate change effects on secondary compounds of forest trees in the Northern hemisphere. *Front. Plant Sci.* 9:1445. doi: 10.3389/fpls.2018.01445

Hopkins, R. J., van Dam, N. M., and van Loon, J. J. A. (2009). Role of glucosinolates in insect-plant relationships and multitrophic interactions. *Annu. Rev. Entomol.* 54, 57–83. doi: 10.1146/annurev.ento.54.110807.090623

Houot, B., Burkland, R., Tripathy, S., and Daly, K. C. (2014). Antennal lobe representations are optimized when olfactory stimuli are periodically structured to simulate natural wing beat effects. *Front. Cell. Neurosci.* 8:159. doi: 10.3389/fncel.2014.00159

Hummel, H. E. (2017). A brief review on *Lobesia botrana* mating disruption by mechanically distributing and releasing sex pheromones from biodegradable mesofiber dispensers. *Biochem. Mol. Biol. J.* 3, 1–6. doi: 10.21767/2471-8084.100032

Huston, S. J., Stopfer, M., Cassenaer, S., Aldworth, Z. N., and Laurent, G. (2015). Neural encoding of odors during active sampling and in turbulent plumes. *Neuron* 88, 403–418. doi: 10.1016/j.neuron.2015.09.007

Insam, H., and Seewald, M. S. A. (2010). Volatile organic compounds (VOCs) in soils. *Biol. Fertil. Soils* 46, 199–213. doi: 10.1007/s00374-010-0442-3

Jactel, H., Birgersson, G., Andersson, S., and Schlyter, F. (2011). Non-host volatiles mediate associational resistance to the pine processionary moth. *Oecologia* 166, 703–711. doi: 10.1007/s00442-011-1918-z

Jactel, H., and Brockerhoff, E. G. (2007). Tree diversity reduces herbivory by forest insects. *Ecol. Lett.* 10, 835–848. doi: 10.1111/j.1461-0248.2007.01073.x

Jardine, K. J., Fernandes de Souza, F. V., Oikawa, P., Higuchi, N., Bill, M., Porras, R., et al. (2017). Integration of C1 and C2 metabolism in trees. *Int. J. Mol. Sci.* 18:E2045. doi: 10.3390/ijms18102045

Jardine, A. B., Jardine, K. J., Fuentes, J. D., Martin, S. T., Martins, G., Durgante, F., et al. (2015). Highly reactive light-dependent monoterpenes in the Amazon. *Geophys. Res. Lett.* 42, 1576–1583. doi: 10.1002/2014GL062573

Jardine, K., Yañez Serrano, A., Arneth, A., Abrell, A., Jardine, A., van Haren, J., et al. (2011). Within canopy sesquiterpene ozonolysis in Amazonia. *J. Geophys. Res.* 116:D19301. doi: 10.1029/2011JD016243

Jerkovic, I., Mastelic, J., Milos, M., Juteau, F., Masotti, V., and Viano, J. (2003). Chemical variability of *Artemisia vulgaris* L. essential oils originated from the Mediterranean area of France and Croatia. *Flavour Fragr. J.* 18, 436–440. doi: 10.1002/ffj.1246

Jones, P. L., and Agrawal, A. A. (2017). Learning in insect pollinators and herbivores. *Annu. Rev. Entomol.* 62, 53–71. doi: 10.1146/annurev-ento-031616-034903

Junker, R. R., Hocherl, N., and Bluthgen, N. J. (2010). Responses to olfactory signals reflect network structure of flower-visitor interactions. *J. Anim. Ecol.* 79, 8180–8823. doi: 10.1111/j.1365-2656.2010.01698.x

Jürgens, A., and Bischoff, M. (2017). Changing odour landscapes: the effect of anthropogenic volatile pollutants on plant–pollinator olfactory communication. *Funct. Ecol.* 56–64, 56–64. doi: 10.1111/1365-2435.12774

Kantsa, A., Raguso, R. A., Dyer, A. G., Olesen, J. M., Tscheulin, T., and Petanidou, T. (2018). Disentangling the role of floral sensory stimuli in pollination networks. *Nat. Commun.* 9:1041. doi: 10.1038/s41467-018-03448-w

Kantsa, A., Raguso, R. A., Lekkas, T., Kalantzi, O. I., and Petanidou, T. (2019). Floral volatiles and visitors: a meta-network of associations in a natural community. *J. Ecol.* 1–13. doi: 10.1111/1365-2745.13197

Karl, T., Harley, P., Emmons, L., Thornton, B., Guenther, A., Basu, C., et al. (2010). Efficient atmospheric cleansing of oxidized organic trace gases by vegetation. *Science* 330, 816–819. doi: 10.1126/science.1192534

Katzenberger, T. D., Lunau, K., and Junker, R. R. (2013). Salience of multimodal flower cues manipulates initial responses and facilitates learning performance of bumblebees. *Behav. Ecol. Sociobiol.* 67, 1587–1599. doi: 10.1007/s00265-013-1570-1

Kerdelhue, C., Le Clainche, I., and Rasplus, J.-Y. (1999). Molecular phylogeny of the *Ceratosolen* species pollinating *Ficus* of the subgenus *Sycomorus* sensu stricto: biogeographical history and origins of the species-specificity sreakdown sases. *Mol. Phylogenet. Evol.* 11, 401–414.

Khan, Z. R., Midega, C. A. O., Bruce, T. J. A., Hooper, A. M., and Pickett, J. A. (2010). Exploiting phytochemicals for developing a 'push-pull' crop protection strategy for cereal farmers in Africa. *J. Exp. Bot.* 61, 4185–4196. doi: 10.1093/jxb/erq229

Kirkness, E. F., Haas, B. J., Sun, W., Braig, H. R., Perotti, M. A., Clark, J. M., et al. (2010). Genome sequences of the human body louse and its primary endosymbiont provide insights into the permanent parasitic lifestyle. *Proc. Natl. Acad. Sci. USA* 107, 12168–12173. doi: 10.1073/pnas.1003379107

Knaden, M., Strutz, A., Ahsan, J., Sachse, S., and Hansson, B. S. (2012). Spatial representation of odorant valence in an insect brain. *Cell Rep.* 1, 392–399. doi: 10.1016/j.celrep.2012.03.002

Knudsen, G. K., Eriksson, R., Gershenzon, J., and Stahl, B. (2006). Diversity and distribution of floral scent. *Bot. Rev.* 72, 1–120. doi: 10.1663/0006-8101(2006)72[1:DADOFS]2.0.CO;2

Kopp, A., Barmina, O., Hamilton, A. M., Higgins, L., McIntyre, L. M., and Jones, C. D. (2008). Evolution of gene expression in the *Drosophila* olfactory system. *Mol. Biol. Evol.* 25, 1081–1092. doi: 10.1093/molbev/msn055

Labandeira, C. C. (2007). The origin of herbivory on land: initial patterns of plant tissue consumption by arthropods. *Insect Sci.* 14, 259–275. doi: 10.1111/j.1744-7917.2007.00152.x

Labandeira, C. C., Kvaček, J., and Mostovski, M. B. (2007). Pollination drops, pollen, and insect pollination of Mesozoic gymnosperms. *Taxon* 56, 663–695. doi: 10.2307/25065852

Lathière, J., Hewitt, C. N., and Beerling, D. J. (2010). Sensitivity of isoprene emissions from the terrestrial biosphere to 20th century changes in atmospheric CO_2 concentration, climate, and land use. *Glob. Biogeochem. Cycles* 24:GB1004. doi: 10.1029/2009GB003548

Loreto, F., and Schnitzler, J.-P. (2010). Abiotic stresses and induced BVOCs. *Trends Plant Sci.* 15, 154–166. doi: 10.1016/j.tplants.2009.12.006

Maffei, M. E., Mithöfer, A., and Boland, W. (2007). Insects feeding on plants: rapid signals and responses preceding the induction of phytochemical release. *Phytochemistry* 68, 2946–2959. doi: 10.1016/j.phytochem.2007.07.016

Mafra-Neto, A., and Cardé, R. T. (1994). Fine-scale structure of pheromone plumes modulates upwind orientation of flying moths. *Nature* 369, 142–144. doi: 10.1038/369142a0

Mafra-Neto, A., and Cardé, R. T. (1996). Dissection of the pheromone-modulated flight of moths using single-pulse response as a template. *Experientia* 52, 373–379. doi: 10.1007/BF01919543

Martelli, C., Carlson, J. R., and Emonet, T. (2013). Intensity invariant dynamics and odor-specific latencies in olfactory receptor neuron response. *J. Neurosci. Methods* 33, 6285–6297. doi: 10.1523/JNEUROSCI.0426-12.2013

McCormick, A. C., Irmisch, S., Reinecke, A., Boecklerr, G. A., Veit, D., Reichelt, M., et al. (2014). Herbivore-induced volatile emission in black poplar: regulation and role in attracting herbivore ennemies. *Plant Cell Environ.* 37, 1909–1923. doi: 10.1111/pce.12287

McGhee, P. S., Miller, J. R., Thomson, D. R., and Gut, L. J. (2016). Optimizing aerosol dispensers for mating disruption of codling moth, *Cydia pomonella* L. *J. Chem. Ecol.* 42, 612–616. doi: 10.1007/s10886-016-0724-9

Meiners, T. (2015). Chemical ecology and evolution of plant–insect interactions: a multitrophic perspective. *Curr. Opin. Insect Sci.* 8, 22–28. doi: 10.1016/j.cois.2015.02.003

Min, S., Ai, M., Shin, S. A., and Suh, G. S. B. (2013). Dedicated olfactory neurons mediating attraction behavior to ammonia and amines in *Drosophila*. *Proc. Natl. Acad. Sci. USA* 110, E1321–E1329. doi: 10.1073/pnas.1215680110

Minoli, S., Kauer, I., Colson, V., Party, V., Renou, M., Anderson, P., et al. (2012). Brief exposure to sensory cues elicits stimulus-nonspecific general sensitization in an insect. *PLoS One* 7:e34141. doi: 10.1371/journal.pone.0034141

Moore, P. A., and Crimaldi, J. (2004). Odor landscapes and animal behavior: tracking odor plumes in different physical words. *J. Mar. Syst.* 49, 55–64. doi: 10.1016/j.jmarsys.2003.05.005

Mossa, A.-T. H. (2016). Green pesticides: essential oils as biopesticides in insect-pest management. *J. Environ. Sci. Technol.* 9, 354–378. doi: 10.3923/jest.2016.354.378

Mumm, R., and Hilker, M. (2005). The significance of background odour for an egg parasitoid to detect plants with host eggs. *Chem. Senses* 30, 337–343. doi: 10.1093/chemse/bji028

Murlis, J., Elkinton, J. S., and Cardé, R. T. (1992). Odor plumes and how insects use them. *Annu. Rev. Entomol.* 37, 305–332.

Nagel, K. I., and Wilson, R. I. (2011). Biophysical mechanisms underlying olfactory receptor neuron dynamics. *Nat. Neurosci.* 14, 208–216. doi: 10.1038/nn.2725

Niinemets, Ü., Reichstein, M., Staudt, M., Seufert, G., and Tenhunen, J. D. (2002). Stomatal constraints may effect emissions of oxygenated monoterpenes from the foliage of *Pinus pinea*. *Plant Physiol.* 130, 1371–1385. doi: 10.1104/pp.009670

Nityananda, V. (2016). Attention-like processes in insects. *Proc. Biol. Sci.* 283:20161986. doi: 10.1098/rspb.2016.1986

Party, V., Hanot, C., Büsser, D. S., Rochat, D., and Renou, M. (2013). Changes in odor background affect the locomotory response to pheromone in moths. *PLoS One* 8:e52897. doi: 10.1371/journal.pone.0052897

Party, V., Hanot, C., Said, I., Rochat, D., and Renou, M. (2009). Plant terpenes affect intensity and temporal parameters of pheromone detection in a moth. *Chem. Senses* 34, 763–774. doi: 10.1093/chemse/bjp060

Pelosi, P., Iovinella, I., Zhu, J., Wang, G., and Dani, F. R. (2017). Beyond chemoreception: diverse tasks of soluble olfactory proteins in insects. *Biol. Rev.* 93, 184–200. doi: 10.1111/brv.12339

Penuelas, J., and Staudt, M. (2010). BVOCs and global change. *Trends Plant Sci.* 15, 133–144. doi: 10.1016/j.tplants.2009.12.005

Pijanowski, B. C., Villanueva-Rivera, L. J., Dumyahn, S. L., Farina, A., Krause, B. L., Napoletano, B. M., et al. (2011). Soundscape ecology: the science of sound in the landscape. *Bioscience* 61, 203–216. doi: 10.1525/bio.2011.61.3.6

Poivet, E., Gallot, A., Montagne, N., Glaser, N., Legeai, F., and Jacquin-Joly, E. (2013). A comparison of the olfactory gene repertoires of adults and larvae in the noctuid moth *Spodoptera littoralis*. *PLoS One* 8:e60263. doi: 10.1371/journal.pone.0060263

Proffit, M., Khallaf, M. A., Carrasco, D., Larsson, M. C., and Anderson, P. (2015). 'Do you remember the first time?' Host plant preference in a moth is modulated by experiences during larval feeding and adult mating. *Ecol. Lett.* 18, 365–374. doi: 10.1111/ele.12419

R Core Team (ed.) (2013). *R: A language and environment for statistical computing foundation for statistical computing*. Vienna, Austria. Available at: http://www.R-project.org/

Raguso, R., and Weiss, M. R. (2015). Concerted changes in floral colour and scent, and the importance of spatio-temporal variation in floral volatiles. *J. Indian I. Sci.* 95, 69–92.

Riffell, J. A., Abrell, L., and Hildebrand, J. G. (2008). Physical processes and real-time chemical measurement of the insect olfactory environment. *J. Chem. Ecol.* 34, 837–853. doi: 10.1007/s10886-008-9490-7

Riffell, J. A., Shlizerman, E., Sanders, E., Abrell, L., Medina, B., Hinterwirth, A. J., et al. (2014). Sensory biology. Flower discrimination by pollinators in a dynamic chemical environment. *Science* 344, 1515–1518. doi: 10.1126/science.1251041

Rissanen, K., Hölttä, T., and Bäck, J. (2018). Transpiration directly regulates the emissions of water-soluble short-chained OVOCs. *Plant Cell Environ.* 41, 2288–2298. doi: 10.1111/pce.13318

Rochat, D., Nagnan-le Meillour, P., Esteban-Duran, J. R., Malosse, C., Perthuis, B., Morin, J. P., et al. (2000). Identification of pheromone synergists in the American weevil, *Rhynchophorus palmarum*, and attraction of related *Dynamis borassi* (Coleoptera, Curculionidae). *J. Chem. Ecol.* 26, 155–187. doi: 10.1023/A:1005497613214

Rospars, J. P., Gremiaux, A., Jarriault, D., Chaffiol, A., Monsempes, C., Deisig, N., et al. (2014). Heterogeneity and convergence of olfactory first-order neurons account for the high speed and sensitivity of second-order neurons. *PLoS Comput. Biol.* 10:e1003975. doi: 10.1371/journal.pcbi.1003975

Rouyar, A., Deisig, N., Dupuy, F., Limousin, D., Wycke, M.-A., Renou, M., et al. (2015). Unexpected plant odor responses in a moth pheromone system. *Front. Physiol.* 6:148. doi: 10.3389/fphys.2015.00148

Rouyar, A., Party, V., Prešern, J., Blejec, A., and Renou, M. (2011). A general odorant background affects the coding of pheromone stimulus intermittency in specialist olfactory receptor neurones. *PLoS One* 6:e26443. doi: 10.1371/journal.pone.0026443

Rowen, E., and Kaplan, I. (2016). Eco-evolutionary factors drive induced plant volatiles: a meta-analysis. *New Phytol.* 210, 284–294. doi: 10.1111/nph.13804

Said, I., Renou, M., Morin, J.-P., Ferreira, J. M. S., and Rochat, D. (2005). Interactions between acetoin, a plant volatile, and pheromone in *Rhynchophorus palmarum*: Behavioral and olfactory neuron responses. *J. Chem. Ecol.* 31, 1789–1805. doi: 10.1007/s10886-005-5927-4

Sane, S. P., and Jacobson, N. P. (2006). Induced airflow in flying insects II. Measurement of induced flow. *J. Exp. Biol.* 209, 43–56. doi: 10.1242/jeb.01958

Saveer, A. M., Becher, P. G., Birgersson, G., Hansson, B. S., Witzgall, P. W., and Bengtsson, M. (2014). Mate recognition and reproductive isolation in the sibling species *Spodoptera littoralis* and *Spodoptera litura*. *Front. Ecol. Evol.* 2:18. doi: 10.3389/fevo.2014.00018

Schafer, M. S. (1977). *The tuning of the world*. New-York: Knopf.

Schallhart, S., Rantala, P., Nemitz, E., Taipale, D., Tillmann, R., Mentel, T. F., et al. (2016). Characterization of total ecosystem-scale biogenic VOC exchange at a Mediterranean oak–hornbeam forest. *Atmos. Chem. Phys.* 16, 7171–7194. doi: 10.5194/acp-16-7171-2016

Schiebe, C., Hammerbacher, A., Birgersson, G., Witzell, J., Brodelius, P. E., Gershenzon, J., et al. (2012). Inducibility of chemical defenses in Norway spruce bark is correlated with unsuccessful mass attacks by the spruce bark beetle. *Oecologia* 170, 183–198. doi: 10.1007/s00442-012-2298-8

Schiestl, F. P., and Johnson, S. D. (2013). Pollinator-mediated evolution of floral signals. *Trends Ecol. Evol.* 28, 307–315. doi: 10.1016/j.tree.2013.01.019

Schröder, R., and Hilker, M. (2008). The relevance of background odor in resource location by insects: a behavioral approach. *Bioscience* 58, 308–316. doi: 10.1641/B580406

Semmelhack, J. L., and Wang, J. W. (2009). Select *Drosophila* glomeruli mediate innate olfactory attraction and aversion. *Nature* 459, 218–223. doi: 10.1038/nature07983

Shorey, H. H. (1976). *Animal communication by pheromones*. London: Academic Press.

Silbering, A. F., and Galizia, C. G. (2007). Processing of odor mixtures in the *Drosophila* antennal lobe reveals both global inhibition and glomerulus-specific interactions. *J. Neurosci.* 27, 11966–11977. doi: 10.1523/JNEUROSCI.3099-07.2007

Simpraga, M., Takabayashi, J., and Holopainen, J. K. (2016). Language of plants: where is the word? *J. Integr. Plant Biol.* 58, 343–349. doi: 10.1111/jipb.12447

Singsaas, E. L., and Sharkey, T. D. (1998). The regulation of isoprene emission responses to rapid leaf temperature fluctuations. *Plant Cell Environ.* 21, 1181–1188. doi: 10.1046/j.1365-3040.1998.00380.x

Smith, B. H. (1991). The olfactory memory of the honeybee *Apis mellifera*. I odorant modulation of short- and intermediate-term memory after single-trial conditioning. *J. Exp. Biol.* 161, 367–382.

Soffan, S., Subandiyah, S., Makino, H., Watanabe, T., and Horiike, T. (2018). Evolutionary analysis of the highly conserved insect odorant coreceptor (Orco) revealed a positive selection mode, implying functional flexibility. *J. Insect Sci.* 18, 1–8. doi: 10.1093/jisesa/iey120

Southworth, M. (1969). The sonic environment of cities. *Environ. Behav.* 1, 49–70. doi: 10.1177/001391656900100104

Stange, G. (1996). "Sensory and behavioural responses of terrestrial invertebrates to biogenic carbon dioxide gradients" in *Advances in bioclimatology*. Vol. 4, ed. G. Stanhill (Berlin: Springer), 223–253.

Staudt, M., Byron, J., Piquemal, K., and Williams, J. (2019). Compartment specific chiral pinene emissions identified in a maritime pine forest. *Sci. Total Environ.* 654, 1158–1166. doi: 10.1016/j.scitotenv.2018.11.146

Staudt, M., Ennajah, A., Mouillot, F., and Joffre, R. (2008). Do volatile organic compound emissions of Tunisian cork oak populations originating from contrasting climatic conditions differ in their responses to summer drought? *Can. J. For. Res.* 38, 2965–2975. doi: 10.1139/X08-134

Staudt, M., Jackson, B., El-aouni, H., Buatois, B., Lacroze, J. P., Poessel, J. L., et al. (2010). Volatile organic compound emissions induced by the aphid *Myzus persicae* differ among resistant and susceptible peach cultivars and a wild relative. *Tree Physiol.* 30, 1320–1334. doi: 10.1093/treephys/tpq072

Staudt, M., Joffre, R., and Rambal, S. (2003). How growth conditions affect the capacity of *Quercus ilex* leaves to emit monoterpenes. *New Phytol.* 158, 61–73. doi: 10.1046/j.1469-8137.2003.t01-1-00722.x

Staudt, M., Morin, X., and Chuine, I. (2017). Contrasting direct and indirect effects of warming and drought on isoprenoid emissions from Mediterranean oaks. *Reg. Environ. Chang.* 17, 2121–2133. doi: 10.1007/s10113-016-1056-6

Stensmyr, M. C., Dweck, H. K., Farhan, A., Ibba, I., Strutz, A., Mukunda, L., et al. (2012). A conserved dedicated olfactory circuit for detecting harmful microbes in *Drosophila*. *Cell* 151, 1345–1357. doi: 10.1016/j.cell.2012.09.046

Strube-Bloss, M. F., and Rossler, W. (2018). Multimodal integration and stimulus categorization in putative mushroom body output neurons of the honeybee. *R. Soc. Open Sci.* 5:171785. doi: 10.1098/rsos.171785

Suh, G. S. B., Wong, A. M., Hergarden, A. C., Wang, J. W., Simon, A. F., Benzer, S., et al. (2004). A single population of olfactory sensory neurons mediates an innate avoidance behaviour in *Drosophila*. *Nature* 431, 854–859. doi: 10.1038/nature02980

Suver, M. P., Matheson, A. M. M., Sarkar, S., Damiata, M., Schoppik, D., and Nagel, K. I. (2019). Encoding of wind direction by central neurons in *Drosophila*. *Neuron* 102, 828–842. doi: 10.1016/j.neuron.2019.03.012

Szyszka, P., Stierle, J. S., Biergans, S., and Galizia, C. G. (2012). The speed of smell: odor-object segregation within milliseconds. *PLoS One* 7:e36096. doi: 10.1371/journal.pone.0036096

Tait, C., Batra, S., Ramaswamy, S. S., Feder, J. L., and Olsson, S. B. (2016). Sensory specificity and speciation: a potential neuronal pathway for host fruit odour discrimination in *Rhagoletis pomonella*. *Proc. Biol. Sci.* 283:20162101. doi: 10.1098/rspb.2016.2101

Thom, C., Guerenstein, P. G., Mechaber, W. L., and Hildebrand, J. G. (2004). Floral CO_2 reveals flower profitability to moths. *J. Chem. Ecol.* 30, 1285–1288. doi: 10.1023/B:JOEC.0000030298.77377.7d

Thöming, G., Larsson, M. C., Hansson, B. S., and Anderson, P. (2013). Comparison of plant preference hierarchies of male and female moths and the impact of larval rearing hosts. *Ecol. Lett.* 94, 1744–1752. doi: 10.1890/12-0907.1

Trona, F., Anfora, G., Balkenius, A., Bengtsson, M., Tasin, M., Knight, A., et al. (2013). Neural coding merges sex and habitat chemosensory signals in an insect herbivore. *Proc. Biol. Sci.* 280:20130267. doi: 10.1098/rspb.2013.0267

Turner, S. L., and Ray, A. (2009). Modification of CO_2 avoidance behaviour in *Drosophila* by inhibitory odorants. *Nature* 461, 277–281. doi: 10.1038/nature08295

Unsicker, S. B., Kunert, G., and Gershenzon, J. (2009). Protective perfurmes: the role of vegetative volatiles in plant defense against herbivores. *Curr. Opin. Plant Biol.* 12, 479–485. doi: 10.1016/j.pbi.2009.04.001

Vickers, N. J. (2000). Mechanisms of animal navigation in odor plumes. *Biol. Bull.* 198, 203–212. doi: 10.2307/1542524

Vickers, N. J. (2006). Winging it: moth flight behavior and responses of olfactory neurons are shaped by pheromone plume dynamics. *Chem. Senses* 31, 155–166. doi: 10.1093/chemse/bjj011

Vickers, N. J., Christensen, T. A., Baker, T. C., and Hildebrand, J. G. (2001). Odour-plume dynamics influence the brain's olfactory code. *Nature* 410, 466–470. doi: 10.1038/35068559

Vivaldo, G., Masi, E., Taiti, C., Caldarelli, G., and Mancuso, S. (2017). The network of plant volatile organic compounds. *Sci. Rep.* 7:11050. doi: 10.1038/s41598-017-10975-x

von Uexküll, J. (1934). *Umwelt und Innerwelt der Tiere (Milieu animal et milieu humain)*. Paris: Rivages-Payot; reedited 2010.

Wang, X., Peng, Y., Guo, J., Ye, Y., Zhang, K., Yu, F., et al. (2008). Mushroom bodies modulate salience-based selective fixation behavior in *Drosophila*. *Eur. J. Neurosci.* 27, 1441–1451. doi: 10.1111/j.1460-9568.2008.06114.x

Webster, B., and Carde, R. T. (2017). Use of habitat odour by host-seeking insects. *Biol. Rev. Camb. Philos. Soc.* 92, 1241–1249. doi: 10.1111/brv.12281

Willis, M. A., and Avondet, J. L. (2005). Odor-modulated orientation in walking male cockroaches *Periplaneta americana*, and the effects of odor plumes of different structure. *J. Exp. Biol.* 208, 721–735. doi: 10.1242/jeb.01418

Witzgall, P., Kirsch, P., and Cork, A. (2010). Sex pheromones and their impact on pest management. *J. Chem. Ecol.* 36, 80–100. doi: 10.1007/s10886-009-9737-y

Wright, G. A., and Smith, B. (2004). Different thresholds for detection and discrimination of odors in the honey bee (*Apis mellifera*). *Chem. Senses* 29, 127–135. doi: 10.1093/chemse/bjh016

Yang, Z. H., Bengtsson, M., and Witzgall, P. (2004). Host plant volatiles synergize response to sex pheromone in codling moth, *Cydia pomonella*. *J. Chem. Ecol.* 30, 619–629. doi: 10.1023/B:JOEC.0000018633.94002.af

Zakir, A., Bengtsson, M., Sadek, M. M., Hansson, B. S., Witzgall, P., and Anderson, P. (2013). Specific response to herbivore-induced de novo synthesized plant volatiles provides reliable information for host plant selection in a moth. *J. Exp. Biol.* 216, 3257–3263. doi: 10.1242/jeb.083188

Zeng, L., Wang, X., Kang, M., Dong, F., and Yang, Z. (2017). Regulation of the rhythmic emission of plant volatiles by the circadian clock. *Int. J. Mol. Sci.* 18:2408. doi: 10.3390/ijms18112408

Zhang, Q.-H., and Schlyter, F. (2004). Olfactory recognition and behavioural avoidance of angiosperm nonhost volatiles by conifer-inhabiting bark beetles. *Agric. For. Entomol.* 6, 1–19. doi: 10.1111/j.1461-9555.2004.00202.x

Zhang, Q. H., Schlyter, F., and Anderson, P. (1999). Green leaf volatiles interrupt pheromone response of spruce bark beetle, *Ips typographus*. *J. Chem. Ecol.* 25, 2847–2861. doi: 10.1023/A:1020816011131

Zhou, X., Slone, J. D., Rokas, A., Berger, S. L., Liebig, J., Ray, A., et al. (2012). Phylogenetic and transcriptomic analysis of chemosensory receptors in a pair of divergent ant species reveals sex-specific signatures of odor coding. *PLoS Genet.* 8:e1002930. doi: 10.1371/journal.pgen.1002930

Conflict of Interest Statement: The authors declare that the research was conducted in the absence of any commercial or financial relationships that could be construed as a potential conflict of interest.

frontiers in Physiology

ORIGINAL RESEARCH
published: 07 August 2019
doi: 10.3389/fphys.2019.00943

Encoding of Slowly Fluctuating Concentration Changes by Cockroach Olfactory Receptor Neurons Is Invariant to Air Flow Velocity

*Maria Hellwig†, Alexander Martzok‡ and Harald Tichy**

Department of Neurobiology, Faculty of Life Sciences, University of Vienna, Vienna, Austria

The ON and OFF olfactory receptor neurons (ORNs) on the cockroach antenna display a high sensitivity for the rate at which odorant concentration changes. That rate of change acts as a gain control signal that improves the sensitivity of both ORNs for fluctuating concentration changes. By means of extracellular recording techniques, we find in both types of ORNs an increased gain for the rate of concentration change when the duration of the oscillation period increases. During long-period oscillations with slow concentration changes, the high gain for the rate of concentration change improves the ORNs ability to detect low rates of concentration changes when the fluctuations are weak. To be useful in plume tracking, gain control must be invariant to the air flow velocity. We describe that raising the level of the flow rate has no effect on the ON-ORN responses to concentration changes down to rates of 2%/s, but exerts a slight increase on the OFF-ORN response during these extremely low rates. At 4%/s, however, the OFF-ORN response is also unaffected by the flow rate level. The asymmetry corresponds with a generally higher sensitivity of the OFF-ORN to concentration changes. Nevertheless, the gain of both ORNs for the concentration rate change is robust against the air flow velocity. This makes possible an instantaneous analysis of the rate of concentration change for both directions of change by one or the other ORN. Therefore, the ON and OFF ORNs are optimized to encode concentration increments and decrements in a turbulent odorant plume.

Keywords: olfactory receptor neurons, ON and OFF responses, rate of concentration change, gain control, air flow velocity

OPEN ACCESS

Edited by:
Sylvia Anton,
Institut National de la Recherche Agronomique (INRA), France

Reviewed by:
Monika Stengl,
University of Kassel, Germany
Peter Kloppenburg,
University of Cologne, Germany

****Correspondence:***
Harald Tichy
harald.tichy@univie.ac.at
orcid.org/0000-0003-1582-513
†orcid.org/0000-0002-1800-2229
‡orcid.org/0000-0002-6926-2995

Specialty section:
This article was submitted to Invertebrate Physiology, a section of the journal Frontiers in Physiology

Received: *03 May 2019*
Accepted: *09 July 2019*
Published: *07 August 2019*

Citation:
Hellwig M, Martzok A and Tichy H (2019) Encoding of Slowly Fluctuating Concentration Changes by Cockroach Olfactory Receptor Neurons Is Invariant to Air Flow Velocity. Front. Physiol. 10:943. doi: 10.3389/fphys.2019.00943

INTRODUCTION

The primary objective of this study was to determine what effect the rate of the air flow carrying the odorant across a cockroach's antenna has upon the activity of olfactory receptor neurons (ORNs). The work leading up to this study began with the identification of pairs of ORNs in a structurally identifiable sensillum type which respond antagonistically to the same change in odorant concentration. In this way, concentration increments and decrements are encoded by excitatory signals. During slow and continuous concentration changes, both types of ORNs not

only signal the moment-to-moment succession of odorant concentrations but also the rate at which concentration changes (Burgstaller and Tichy, 2011, 2012; Tichy and Hellwig, 2018). Furthermore, the rate of concentration change modulates the gain of responses for fluctuations in the odorant concentration. When odor concentration changes slowly, both ORN types improve the gain for the rate of change at the expense of the gain for the instantaneous concentration. This suggests that the ORNs are optimized to detect minute changes in odorant concentration, even if they persist in one direction.

The instantaneous odorant concentration and its rate of change are two independent variables because each can be changed without producing a change in the other. Concentration has been very often manipulated in insect olfactory research, but the rate of concentration change has received less attention. In most studies, odorants were applied as transient concentration pulses. The rate of concentration change at the onset of the odorant pulse was not measured and its possible effect on the response magnitude was not determined. Stimulus-response functions were based on the mean pulse concentration and the mean discharge of the pulse period. According to this concept, the effect of changes in the velocity of odorant pulses was studied in two types of ORNs on the antennae of *Drosophila* (Zhou and Wilson, 2012). Pulse velocity was changed by varying the amount of volume of the odorant-loaded air that was delivered during the pulse period. If pulse concentration was kept constant, the ORNs responses were invariant to changes in the pulse flow rate. Unfortunately, the phasic component of the response as a possible candidate for encoding the rate of concentration change was neglected. The ORNs were regarded as "transducers of concentration," responding to given concentration pulses independently of the pulse velocity (Zhou and Wilson, 2012).

In contrast, the ON and OFF ORNs of the cockroach may be transducers of the "rate of concentration change," with an additional dependence on the instantaneous concentration at which the change occurs. The observation of potentially different transduction mechanisms is based, however, on different methods of delivering the odorant. While concentration pulses rapidly immerse the whole sensillum into the stimulus concentration, slow concentration changes gradually increase the concentration at the sensillum surface. For example, it requires 10 s to increase the concentration from 0 to 50% at a rate of 5%/s, but 25 s at a rate of 2%/s. Therefore, when increasing the concentration on the sensillum surface at a rate of 5%/s, an instantaneous concentration of 25% is reached 5 s after the onset of the concentration increase, and after 12.5 s at a rate of 2%/s. Furthermore, the higher the flow rate, the greater is the volume of odorant-loaded air that passes over the antenna. Thus, the same gradual concentration increase delivered at a higher flow rate involves a greater quantity of molecules arriving per unit time on the sensillum surface.

In natural foraging environments, wind speed and the direction of wind flow are the most important factors affecting odorant concentration. We can expect that animals tracking a turbulent odorant plume discriminate flow velocity invariant concentration changes. Flying insects use wind information and visual feedback to efficiently track an odor plume, but walking lobsters and crabs perform true chemotaxis, whereby the temporal analysis of odorant pulse features guides orientation along plumes. In behavioral studies, lobsters use a spatial gradient in pulse size and shape to locate the odorant source (Moore and Atema, 1991). The spatial distribution of the pulse onset slopes and the correlated pulse amplitudes provide the strongest gradient pointing to the source. In such an "odor landscape," the peak height of pulses and the onset slope of these peaks increase with decreasing distance to the odor source (Moore and Atema, 1991; Zettler and Atema, 1999). Electrophysiological recordings provide evidence for the existence of "pulse slope detectors" on chemoreceptors of the lateral antennules of the American lobster (Zettler and Atema, 1999). In the cockroach, the ON and OFF ORNs on the antennae meet the requirements of detectors for the upward and downward rate of change of the food odor concentration (Tichy and Hellwig, 2018). If the rate of concentration change is truly a fundamental aspect of insect orientation in an odorant plume, information about the concentration rate should be robust across a range of different flow velocities.

Any study attempting to evaluate the individual effects of the instantaneous concentration, its rate of change and the flow velocity of the odorant-carrying air steam must satisfy two special requirements. First, it must utilize techniques and procedures to regulate, control and monitor all three stimulation variables simultaneously. Second, it must ensure that data analysis recognizes potential confusion when unscrambling the effect of interrelated variables. The present study incorporates both these requirements. The first is met by a dilution flow olfactometer that enables producing olfactory stimuli of precise air pressure, flow velocity, as well as concentration and its rate of change. The second is met by utilizing software that relates the responses of the ORNs to different combinations of the three variables and then estimates how much each variable contributes to the response.

The above considerations yield two readily testable predictions. Both predictions are critical in evaluating the function of the ON and OFF ORNs as "concentration rate detectors." Each involves two exclusive statements.

The first prediction is that variation in the level of the volume flow rate has no effect on ORN responses to slow and continuous concentration changes. Thus, the ORNs would be able to detect changes in the odorant concentration (the ratio between molecule number and air volume) regardless of the volume size, the absolute number of molecules involved in the concentration change, the rate of arrival at the antenna or the rate of air flow. Alternatively, the response to equal rates of concentration change would increase with increasing flow rate level due to the increasing absolute number of odorant molecules arriving at the sensillum.

The second prediction is that the level of the volume flow rate does not affect the increased gain for the rate of concentration change with increasing duration of the oscillation period. Alternatively, gain control varies with the flow-rate level. Then the concentration rate no longer needs to be considered as a gain control signal.

MATERIALS AND METHODS

Preparation and Recording

Adult male cockroach (*Periplaneta americana*) were anesthetized with CO_2, placed on their dorsal surface in a closely fitted holder and fixed with strips of Parafilm wrapped around the holder. One antenna was kept in a forward position by cementing it onto a ledge that extended from the holder. Action potentials were recorded extracellularly between two electrolytically sharpened tungsten wires. The reference electrode was placed lengthwise in the tip of the antenna and the recording electrode was inserted into the base of the sensillum. Impulses were amplified and band filtered (0.1–3 kHz), passed through a 1401plus A-D converter (Cambridge Electronic Design) and fed into a PC. The digitized impulses, the voltage output of the electronic flow meters and the PID signal were displayed on-line on a monitor, stored on a hard disk and analyzed off-line using Spike2 software.

Odorant Stimulation

The odor of lemon oil is known to activate antennal ORNs and antennal lobe neurons (Sass, 1978; Selzer, 1981, 1984; Boeckh et al., 1990; Zeiner and Tichy, 2000). It contains a number of odor compounds of different chemical classes (Günther, 1968; Shaw, 1979). Based on its reproducibility, synthetic lemon oil (Roth, D $\sim$ 0.85, Art. 5213.1) rather than natural fruits were used as a standardized fruit odorant stimulus.

Stimulation was provided using a dilution flow olfactometer (Prah et al., 1995; Burgstaller and Tichy, 2011, 2012). Pre-cleaned and pre-dried compressed air from a laboratory line was passed through an adsorption drier (DPS 1-8A; Filtrations-Separations-Technik, Essen, Germany). The stream was then divided into two equal-sized streams *A* and *B*. Their flow rates were regulated by manual needle valves in series with calibrated flow meters of the Rotameter type. Stream *A* was bubbled through small holes in polyethylene tubing anchored at the bottom of a 25-l tank containing 100 ml of the undiluted liquid odor of lemon oil. Stream *B* was led through an empty tank of the same design and remained clean. After emerging from the tanks, the air streams passed through electrical proportional valves (Kolvenbach KG, KWS 3/4) and electronic flow meters (AWM 3000, Honeywell). The sinusoidal concentration changes were produced by shifting the phase of the valves' control voltages (D-A converter, 1401plus, Cambridge Electronic Design) by 180°. Thus, the total volume flow rate of both air streams was held constant as the underlying odor/clean-air ratio was varied in a sinusoidal manner. This ratio was regulated by the output sequencer function of the data acquisition software [Spike2, v.3.18; Cambridge Electronic Design (CED), Cambridge, United Kingdom], using a self-written sequencer script. A feedback linearization, which integrated the voltages used to control the proportional valve with those received from the flow meters, counteracted any deviations of the flow rate set by the output sequencer. For stimulation, the mixed air stream emerged from a 7-mm-diameter nozzle at a distance of 10 mm from the recording site. The air around the antenna was continually removed by a suction tube at a speed of 2 m/s.

The digitized output voltage of the electronic flow meters, calibrated by the manufacturer for flow rate, was used to monitor the flow profiles of the two individual air streams and of the mixed air stream representing the odor delivery during stimulation. **Figure 1** illustrates an example for a 120-s oscillation period performed at five different volume flow velocities between 0.49 and 1.64 m/s. The flow-rate ratios of the oscillating odor-saturated air stream (**Figure 1A**) to the oscillating clean air stream (**Figure 1B**) determined the oscillating concentration changes, indicated as percentage of the saturated air stream in the mixed air stream (**Figure 1C**). The velocity of the odor stimulus was varied by regulating the flow rates of the input air streams *A* and *B* with the manual needle valves. Modifying the flow rates changed the oscillation amplitudes. In order to set the velocity of the mixed air stream to the required values without changing the amplitude of the concentration oscillations, the flow rates of the two air streams were adjusted via the proportional valves. Thus, the oscillations of the odor-saturated air stream (*A*) were confined to the lower half of the flow rates and, with each step-wise decrease in velocity, the amplitude of the flow rate decreased (**Figure 1A**). The oscillations of the clean air stream (*B*) initially occurred in the high range of flow rates, and then stepped downward to the lower flow rates, thereby spanning smaller amplitude flow rates (**Figure 1B**). The resulting amplitude of the concentration oscillation was 50% (**Figure 1C**). Plots of the summed flow-rate profiles of both air streams served to verify that the total output flow rate of the mixed air stream is constant at each velocity (**Figure 1D**). Nonetheless, the total flow rate indicated low-amplitude, slow fluctuations which appeared to be in phase with the flow-rate oscillations of the two air streams. Average values for these changes in the total flow rate attained a maximum of 0.7 l/h. The direction of change in the ORNs' activity and the fluctuations in the total air flow rate were not correlated. No faster fluctuations or random distribution of fluctuations in the flow rate were apparent. The fluctuations might be due to the inherent flow characteristics of the valves, taking into account the effects of piping. The total air flow rate (**Figure 1D**) that passes the cross-section area (diameter 7 mm) of the output nozzle per second specifies the velocity of the stimulating air stream (**Figure 1E**). Mean velocity values were calculated for periods indicated by dotted lines, which span two oscillation periods (**Figure 1E**); the standard deviations are low ($\pm$0.02 m/s).

A photoionization detector (200A miniPID, Aurora Scientific) was used to verify that mixing of the slowly oscillating, changing flow rates of the two air streams actually produces slowly oscillating concentration changes at the different air velocities (**Figure 1F**). Flow meters controlled the timing and amplitude of the concentration oscillations within the delivery tubes. At the same time, the PID needle was positioned between the output nozzle and the antenna. The PID signal is specified as being proportional to the concentration of the compound entering the flow-through detection cell. This signal is reproducible for a given compound and pressure. As the PID output voltage was not calibrated with a reference gas, the absolute odorant concentration was not measured. The PID output voltages were normalized such that the maximum value obtained in an experiment was arbitrarily set to the value "1." The time course

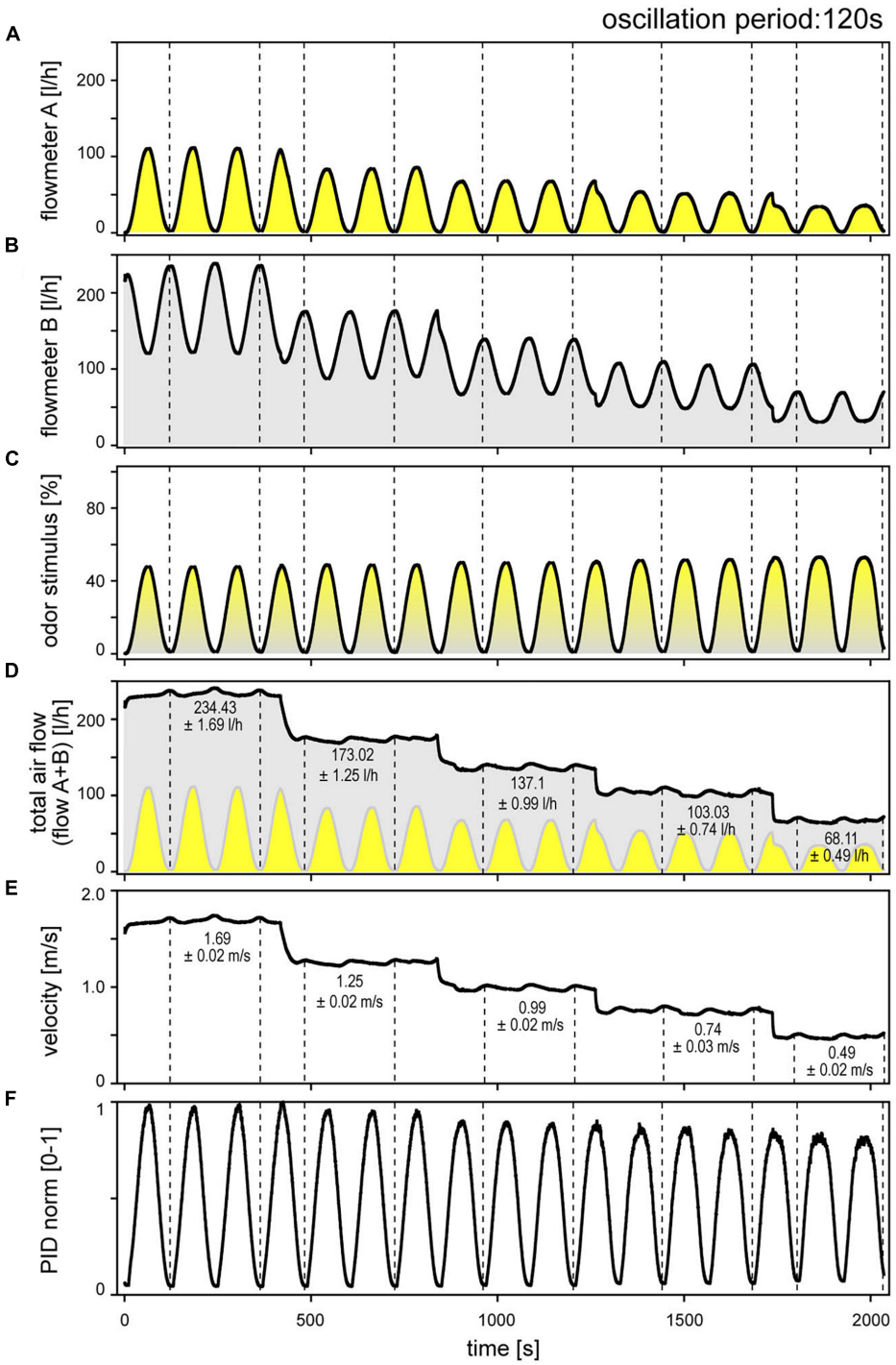

FIGURE 1 | Sinusoidal concentration changes at constant period of 120 s, delivered at five different, stepwise reduced air flow velocities. **(A)** Flowmeter *A* signals the time course of the odor-saturated air stream controlled by proportional valve *A*. **(B)** Flowmeter *B* signals the time course of the clean air stream controlled by proportional valve *B*. The control voltages of both valves were 180° phase-shifted. In order to maintain constant amplitude of the sinusoidal concentration changes when the flow velocity was decreased, the flow rates of both air streams were reduced accordingly. **(C)** Time course of sinusoidal concentration changes determined by the mixing ratio of odor-saturated air in clean air and expressed as percentage of saturated air. **(D)** Time course of summed flow rates of the odor-saturated air stream *A* (yellow oscillations) and the clean air stream *B* (gray oscillations, inverse to yellow oscillations); averaged values were determined for the periods indicated by dotted lines. **(E)** Time course of the flow velocity of the mixed air stream, calculated from the total flow rate of the two air streams in panel **(D)**. Periodic low-amplitude fluctuations in air flow velocity reflect fluctuations in the total air flow rate; they had no effect on ORN responses. Averaged values were determined for the periods indicated by dotted lines. **(F)** Normalized time course of the sinusoidal PID signal corresponds with the flowmeter signal in panel **(C)**; note slow decrease in amplitude with decreasing flow velocity.

of the oscillating PID signal with maxima and minima values (**Figure 1F**) matches with those of the concentration oscillations obtained by the electronic flow meters (**Figure 1C**). However, the amplitude of the PID signal slightly decreased with decreasing air flow velocity. The same decrease is not shown by the flow meter signal. A specific feature of the concentration measurement was the positive pressure from the nozzle and the negative pressure at the sample pump. This pressure difference depends on the volume flow velocity. No systematic attempt was made to determine whether the divergence between the oscillating PID signal and the oscillating the flow-meter signal affects the oscillating activity of the ON and OFF ORNs. However, the gain for the rate of concentration during oscillating changes appears to decrease slightly with decreasing air flow velocity, as revealed by plotting impulse frequency of the ON and OFF ORNs as function of both the rate of change and velocity. As the decrease in air velocity is correlated with the decrease in the PID signal, one may argue that the effects assigned to the decrease in the flow velocity would indeed be due to the decrease in the amplitude of the concentration oscillations. Since a possible effect becomes apparent only at a low velocity of 0.45 m/s (**Figure 1D**) and a slow rate of change of 3.5%/s (**Figure 1E**), no systematic attempt was made to determine the extent to which the divergence between the PID signal and the flow-meter signal affects gain control of the ORNs. If it does, the effects were not obvious.

Recordings

Electrodes were electrolytically sharpened tungsten wires. The reference electrode was placed in the tip of the antenna; the recording electrode was inserted into the base of the sensillum. All recordings were taken from *swC* sensilla, which are single-walled basiconic sensilla (Schaller, 1978; Altner et al., 1983; Hinterwirth et al., 2004; Tichy et al., 2005). Impulses were amplified and filtered (0.3–1 kHz), passed through a 1401plus A-D converter (Cambridge Electronic Design, United Kingdom) and fed into a PC. The digitized action potentials and the voltage output of the electronic flow meters were displayed on-line on a monitor, stored on a hard disk and analyzed off-line using the Spike2 software. Spike waveform parameters were extracted and sampled to form templates. Detected spikes were offered to the template matching system in order to create or modify the templates. Each spike was compared against the templates, and each time a template was confirmed it was added to the template by overdrawing (**Figures 3G,H**). Adding a spike to a template may change template configuration. The template boundaries displayed homogeneity of classification without a gradual change from one class to the other.

RESULTS

Identification

The ON and OFF ORNs share a specific single-walled sensillum type which arises as a hair-like structure from a ring-shaped socket (**Figure 2**). Characteristic features are longitudinal grooves in the surface of the basal part of the shaft and a slender tapering tip. Neuroanatomical and electrophysiological studies show that

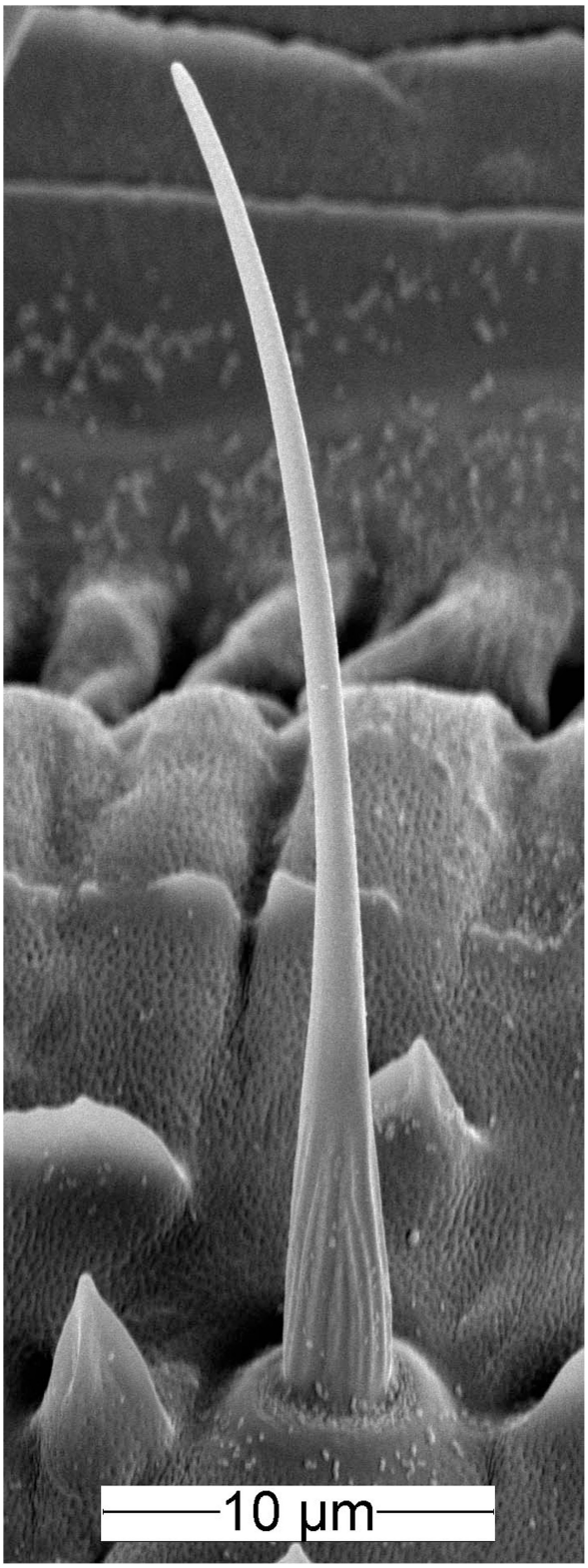

FIGURE 2 | Scanning electron micrograph of the olfactory sensillum on the cockroach antenna containing the ON and OFF ORNs. The sensillum has a slender, hair-like form with a slightly curved tip. The basal part of the shaft wall is grooved, the distal part is smooth and perforated by pores.

these sensilla are located on the distal and proximal margins of each of the 120–180 antennal segments. They make up about 6% of the olfactory sensilla in the male cockroach (Schaller, 1978; Burgstaller and Tichy, 2012; Tichy and Hellwig, 2018). Inserting the tip of a needle electrode into the sensillum base enables recording the action potentials of both ORN types at the same time. The OFF ORN typically displayed larger impulse amplitudes than the ON ORN. The clear differences in size and form of the impulses facilitated final identification of the different OFF ORNs by their antagonistic responses to slowly oscillating changes in odor concentration. A typical example is illustrated in **Figure 3**. **Figure 3A** shows the time course of the odorant concentration oscillating at a period of 60 s, and **Figure 3B** the corresponding rate at which concentration oscillates. **Figure 3C** indicates the time course of the miniPID-signal and **Figure 3D** the flow rates of both the odor-saturated and the clean air stream. Increasing the concentration of the odorant of lemon oil raises the impulse frequency in the ON ORN (**Figure 3E**) and lowers it in the OFF ORN (**Figure 3F**). Correspondingly contrary effects are elicited by decreasing the odorant concentration. As indicated by the time-histograms in **Figures 3G,H**, the ON-ORN's impulse frequency peaks just before the maximum instantaneous concentration, and that of the OFF-ORN just before the concentration minimum. The rate of concentration change, which is ahead of the oscillating instantaneous concentration, clearly also determines the activity of both ORNs.

Gain of Response for the Rate of Concentration Change

Of the 40 pairs of ON and OFF ORNs on which oscillating concentration changes were tested, only six pairs qualified for this study: those whose firing rates continued undiminished for the duration of the experiment. In most recordings, the amplitudes of the action potentials tended to decrease with time. The cause of this diminution is unclear. The shape of the electrode, its depth and position relative to the two ORNs surely differed to some extent with every insertion.

Series of constant-amplitude oscillating concentration changes were tested with periods of 6, 60, and 120 s (**Figure 4**). The rate of change averaged 30%/s during the 6-s period, 3.5%/s during the 60-s period and 2%/s during the 120-s period. To estimate the dependence of the ORNs on the instantaneous concentration and the rate of concentration change, impulse frequency was plotted as a function of both parameters (**Figure 5**). The impulse frequency curves approached closed figures resembling Lissajous figures, which are formed when two parameters oscillate with the same frequency and are plotted one as a function of the other. These shapes depend on the ratio of the frequencies of the two oscillations, the ratio of their amplitudes and their phase differences.

Multiple regressions ($F = y_0 + a\ \mathrm{d}C/\mathrm{d}t + b\ C$; where F is the impulse frequency and y_0 the intercept of the regression plane, with the F axis reflecting the height of the regression plane) were calculated to determine the gain of responses for the rate of concentration change (a slope) and the instantaneous concentration (b slope). The sign of the regression slopes is positive for the ON ORN (**Figures 5A–D**) and negative for the OFF ORN (**Figures 5E–H**), i.e., an increase in both the instantaneous concentration and its rate of change raises the impulse frequency in ON ORN and lowers it in the OFF ORN. Accordingly, during oscillating concentration change, the ON ORN's impulse frequency is high when the instantaneous concentration is high and even higher the faster the concentration rises through the higher values (**Figures 5A–D**). Conversely, the OFF ORN's impulse frequency is low when the instantaneous concentration is low and even lower the faster the concentration falls through the lower values (**Figures 5E–H**). Furthermore, slope steepness varies with the duration of the oscillation period. In both ORNs, sign ignored, the gain for the rate of change tends to be lower during short oscillation periods and higher during long periods. In the examples shown in **Figure 5**, the ON-ORN's gain for the rate of concentration change was 0.01 imp/s per %/s at a period of 6 s, 0.36 imp/s per %/s at 60 s, and 0.80 imp/s per %/s at 120 s. In the OFF ORN, the gain for the rate of concentration change was –0.04 imp/s per %/s at 6 s, –0.36 imp/s per %/s at 60 s and –0.85 imp/s per %/s at 120 s.

To confirm that the periods and amplitudes of the concentration oscillation correspond to the settings, the time course of the odorant stimulus was measured with a miniature photoionization detector (miniPID). As illustrated in **Figure 3**, the time course of the normalized PID signal was synchronous to the flowmeter signal, confirming that the dilution flow olfactometer precisely controlled the odorant stimulus. The relationship between the ORNs' responses, the instantaneous PID signal and its rate of change revealed the same double dependence as obtained with the flowmeter signal (**Figures 5D,H**). In view of this good correspondence, graphs of PID signals used for estimating stimulus-response relationships are not shown.

Gain of Response at Different Air Flow Velocities (Volume Flow Rates)

Figure 3 illustrates the activity of an ORN pair during two subsequent 60-s oscillation periods tested at different constant air flow velocities (1 and 1.25 m/s). At both velocities, the oscillating frequency curves were smooth, their phase advance on the oscillating concentration curve was present, and the signal-to-noise ratio was high. The question was whether the air velocity affects the response magnitude of both ORNs and gain control. Air flow velocity was controlled by the volume of air per unit time flowing out of the nozzle of the odorant delivery system at a distance of 10 mm from the recording site. Since the effects of flow velocity on ORN responses are comparable only for equal concentration changes, the obvious procedure was to record the responses to constant period oscillations for every volume flow rate level. On each ORN, five different flow rate levels were tested between 0.49 to 1.69 m/s.

For each oscillation period, impulse frequency of the six ON and OFF ORNs was plotted as a function of both the level of flow rate and the rate of concentration change. **Figure 6** is an example of a simultaneously recorded pair of ORNs. The oscillating impulse frequencies form elliptic Lissajous curves as illustrated in **Figure 5**. Multiple linear regressions were used to

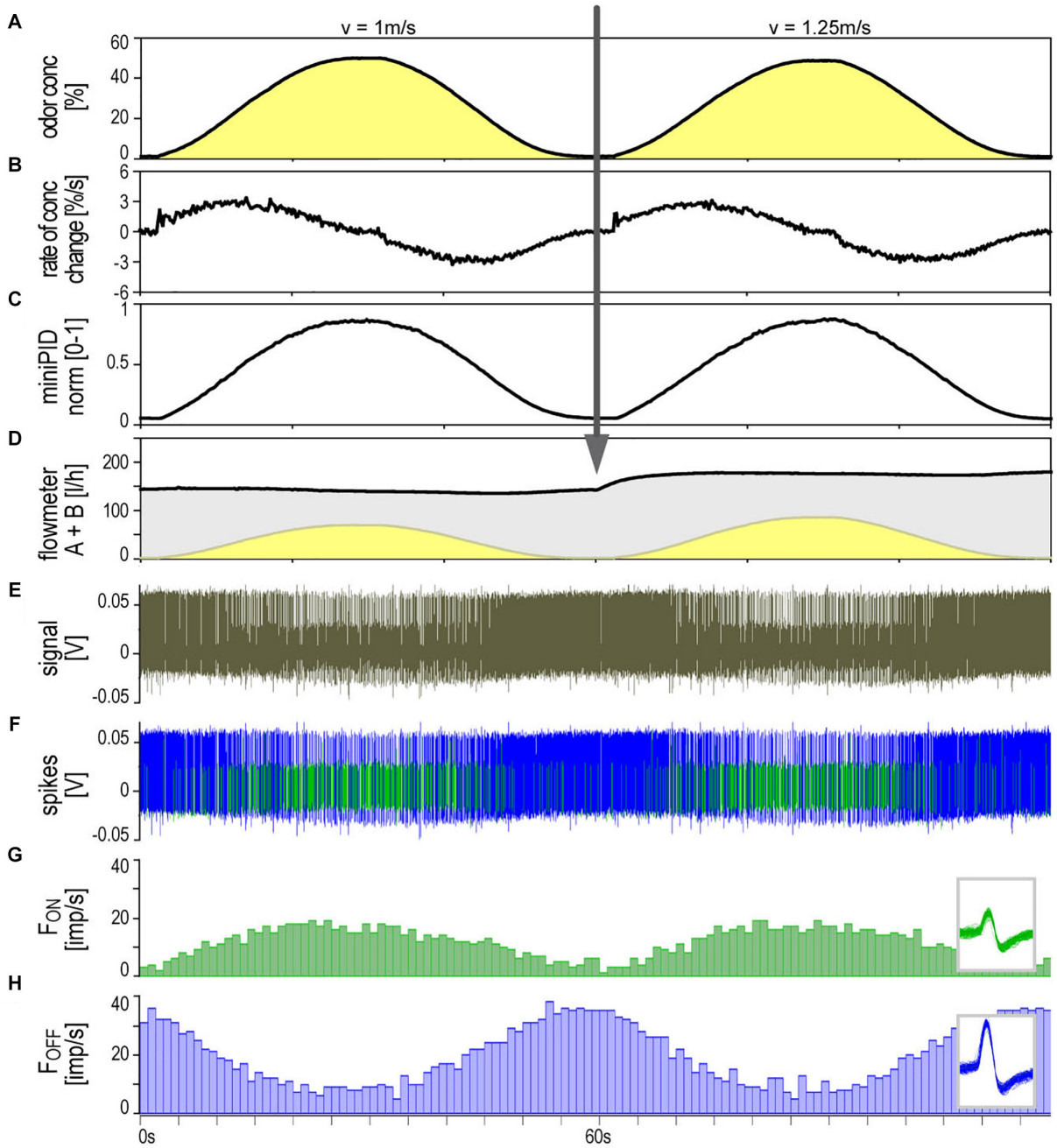

FIGURE 3 | Simultaneously recorded single sensillum responses of a pair of ON and OFF ORNs. Stimulation consisted of slow and continuous upward and downward changes of the concentration of lemon oil odorant delivered at two different air flow velocities. Arrow indicates change in air flow velocity from 1 to 1.25 m/s. **(A)** Time course of instantaneous odorant concentration. Duration of oscillation periods: 60 s. **(B)** Time course of the rate of concentration change. The maxima and minima of the oscillating rate of concentration change are in advance of the maxima and minima of the oscillating instantaneous odorant concentration (vertical dotted line). The noisy signal results from the slow rate of concentration change in a narrow range of ±3.5%/s. **(C)** Time course of odorant concentration measured with a photoionization detector (miniPID). The signal values were normalized to the maximum value obtained in each experiment and set to 1. The concentration maxima and minima indicated by the oscillating flowmeter *A* signal **(A)** correspond with the concentration maxima and minima of the PID signal. **(D)** Time course of the summed flow rates of the odor-saturated air stream measured with flowmeter *A* (yellow oscillations) and the clean air stream measured with flowmeter *B* (gray oscillations, inverse to yellow oscillations); the summed flow rates of both air streams were used to calculate the air flow velocity of the olfactory stimulus. **(E)** Extracellularly recorded activity of the ORNs. Both types discharge continuously during the concentration cycles. The OFF ORN typically generates greater impulse amplitudes than the ON ORN. **(F)** Off-line sorted action potentials of the ORNs obtained by spike detecting and template matching techniques using Spike2 software (Cambridge Electronic Design, United Kingdom). Green impulses originate from the ON ORN, blue impulses from the OFF ORN. **(G,H)** Instantaneous impulse frequency of the ON and OFF ORNs, respectively; bin width, 0.2 s. *Insets* action potentials classified by matching the shape of each action potential against shape templates. Template windows show template boundaries of spike waveforms from the two ORNs. *F* impulse frequency, *v* velocity.

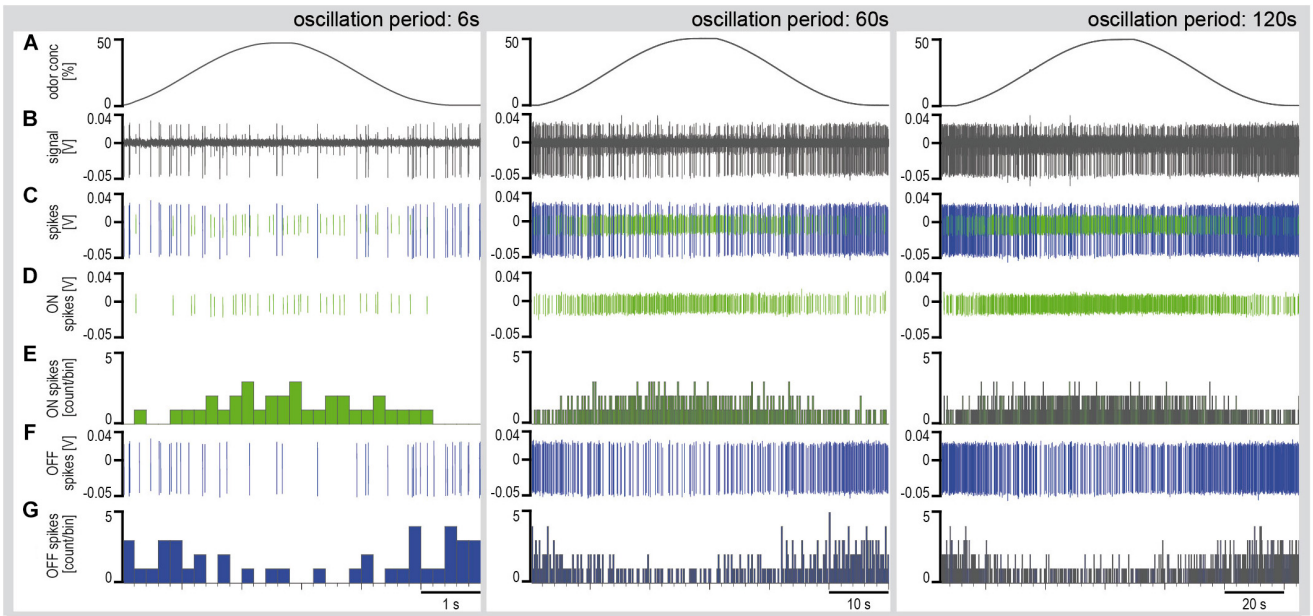

FIGURE 4 | Simultaneously recorded single sensillum responses of a pair of ON and OFF ORNs to oscillating concentration changes of the lemon oil odorant with periods of 6, 60, and 120 s. Air flow velocity: 1.69 m/s. **(A)** Time course of instantaneous odorant concentration. **(B)** Electrical activity of the ON and OFF ORNs. Both types discharge continuously during the concentration cycles. The large impulse amplitudes are from the OFF ORN. **(C)** Off-line sorted action potentials of the ORNs obtained by spike detecting and template matching techniques using Spike2 software (Cambridge Electronic Design, United Kingdom). Green impulses are from the ON ORN, blue impulses from the OFF ORN. **(D)** Discriminated impulses of the ON ORN. **(E)** Instantaneous impulse frequency of the ON ORNs; bin width, 0.2 s. **(F)** Discriminated impulses of the OFF ORN. **(G)** Instantaneous impulse frequency of the OFF ORNs; bin width, 0.2 s. *F* impulse frequency, *V* voltage.

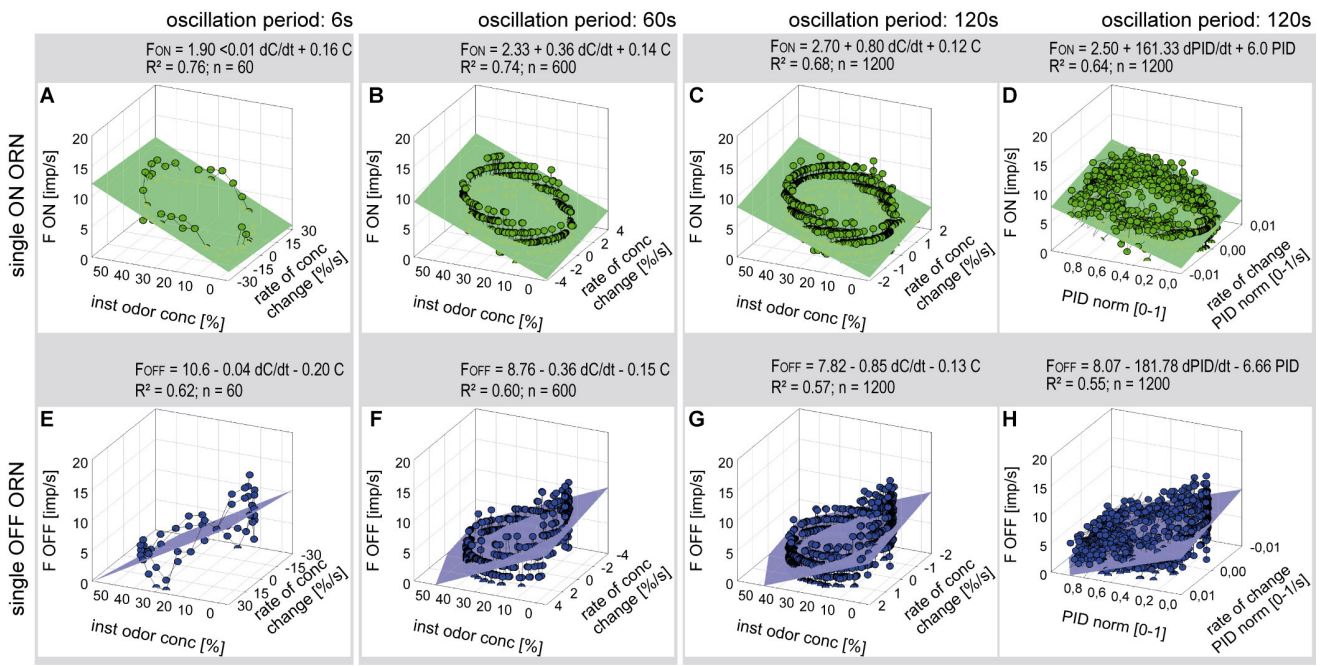

FIGURE 5 | Responses of a single ON ORN **(A–D)** and a single OFF ORN **(E–H)** during oscillating concentration changes plotted as a function of the instantaneous concentration and the rate of concentration change. Instantaneous concentration and its rate of change were measured in panels **(A–C, E–G)** with the flowmeter *A*, in panels **(D,H)** with the miniPID. Duration of oscillation period: 6 s in panels **(A,E);** 60 s in panels **(B,F);** 120 s in panels **(C,D,G,H).** Multiple regressions utilizing 3-dimensional planes $F = y_0 + a\ dC/dtC + b\ C$; where *F* is the impulse frequency, y_0 the height of the regression plane) were calculated to determine the gain of response for the rate of concentration change (*a* slope) and the instantaneous concentration (*b* slope). Note that the sign of the concentration axis in panels **(A–D)** is oriented in different direction than in panels **(E–H).** R^2 coefficient of determination, *n* number of points used to calculate regression plane.

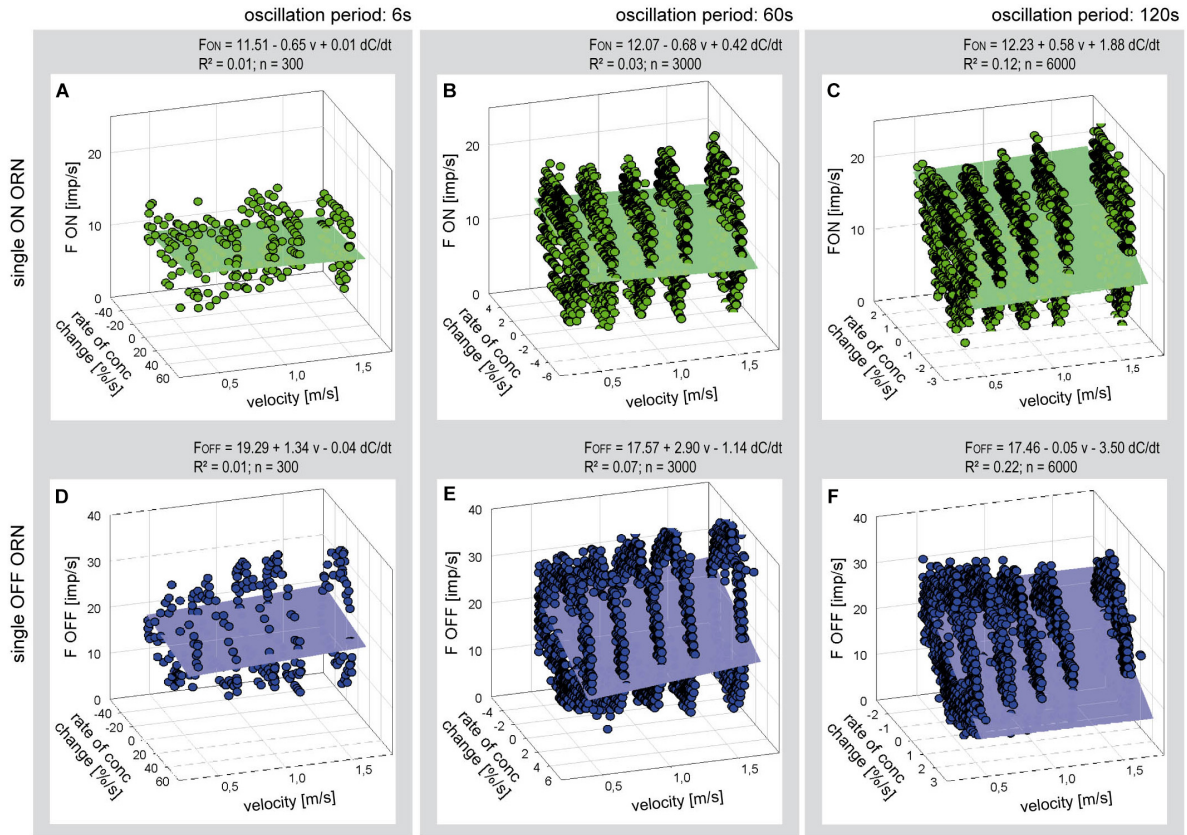

FIGURE 6 | Responses of a single ON ORN **(A–C)** and a single OFF ORN **(D–F)** during three different periods of oscillating concentration changes plotted as a function of the rate of concentration change and air flow velocity. Duration of oscillation period: 6 s in panels **(A,D)**; 60 s in panels **(B,E)**; and 120 s in panels **(C,F).** Multiple regressions utilizing 3-dimensional planes ($F = y_0 + a\,v + b\,dC/dt$; where F is the impulse frequency, y_0 the height of the regression plane) were calculated to determine the effect of velocity (*a* slope) on the responses to the rate of concentration (*b* slope) during oscillating changes. Note that the sign of the rate of concentration axis in panels **(A–C)** is oriented in different direction than in panels **(D,E)**. R^2 coefficient of determination; *n* number of points used to calculate regression plane, *v* velocity.

estimate the dependence of the oscillating impulse frequencies on the flow rate level (*a* slope) and the rate of concentration (*b* slope) for each oscillation period. The horizontal orientation of the axis representing the effect of flow velocity as well as the very low values of the coefficient of determination ($R^2 < 0.2, n = 6.000$) indicate that the regression planes failed to describe in both ORN types a dependence of the responses to the rate of concentration change on the air flow velocity.

The poor coefficient of determination values may partly reflect the fact that the impulse frequency values of both ORNs cover a large part on the frequency scale. This is because the ORNs simultaneously depend on the instantaneous concentration and its rate of change. The effect of the instantaneous concentration will be reduced by plotting the gain values for the rate of concentration change rather than the oscillating impulse frequency as a function of both the air flow velocity and the oscillation period. This expectation is largely confirmed in **Figure 7**. The variations in the gain values appear to depend on the duration of the oscillation period: with increasing duration the deviations of the gain values from the regression plane increase. The regression slopes indicate a gain increase of the ON ORN by 0.15 (imp/s)/(dC/dt) for each 1 m/s increase in air velocity (**Figure 7A**); the corresponding values for the OFF ORN are an increase by –0.46 (imp/s)/(dC/dt) per 1 m/s (**Figure 7B**). (The negative values for gain reflect the downward direction of the concentration change yielding a rise in OFF-ORN impulse frequency). To increase the gain of the ON ORN by 1 (imp/s)/(dC/dt), the flow velocity must be increased by 6.6 m/s, and by 2.2 m/s for the OFF ORN. However, the moderate values of R^2 (0.33 and 0.53 for the ON and OFF ORN, respectively) indicate that not more than 50% of the variance in the OFF-ORN's gain can be explained by the flow velocity. The remaining 50% may be attributed to an inherent variability. Note that the variation of gain is highest for the 120-s oscillation period (**Figure 7**). At this long period, concentration changes at a mean rate of as low as 2%/s need 60 s to get from 0 to 50%, and 60 s to go back from 50 to 0%. Minute concentration fluctuations may produce low-frequency fluctuations in both ORNs. Nonetheless, as the gain for the rate of change increases with increasing duration of the oscillation period and increasing flow velocity, the sensitivity for the rate of change is not diminished but instead improved at slow changes and fast velocities.

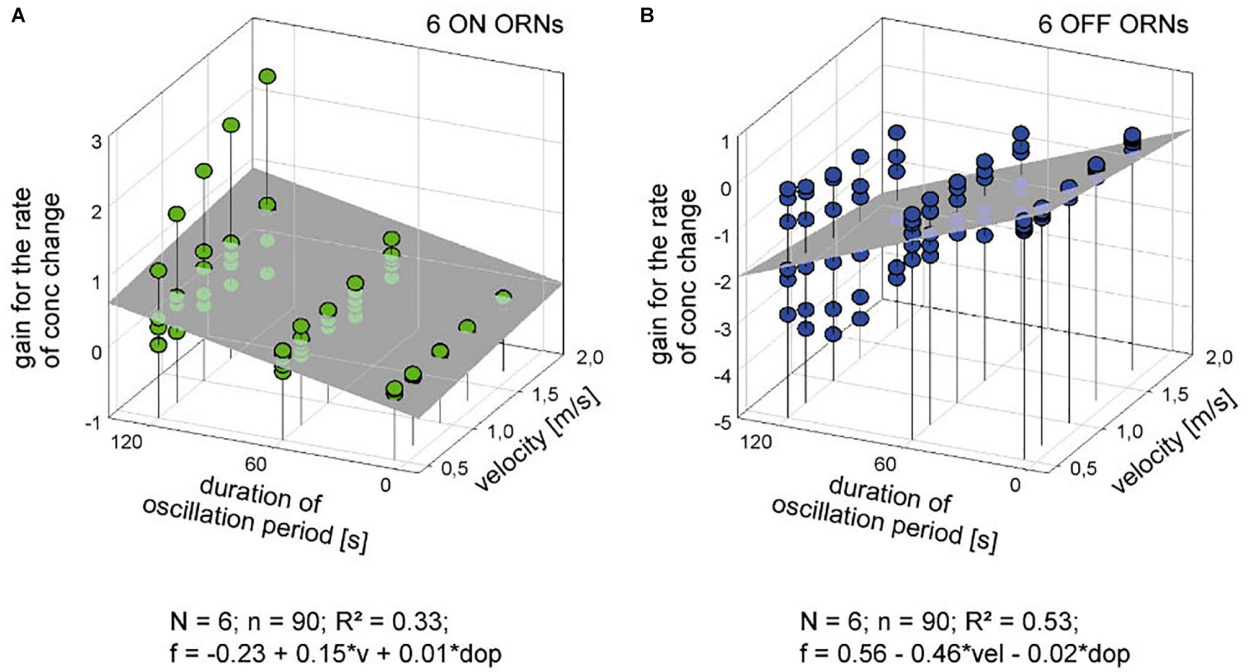

FIGURE 7 | Gain for the rate of concentration change of six pairs of ON **(A)** and OFF ORNs **(B)** plotted as a function of the oscillation period and the volume flow velocity. Multiple regressions utilizing 3-dimensional planes ($f = y_0 + a\ v + b\ dop$; where f is the gain of responses for the rate of concentration change, and y_0 the height of the regression plane) were calculated to determine the effect of velocity (*a* slope) on the gain of responses for concentration oscillations with different periods (*b* slope). R^2 coefficient of determination; *N* number of ORNs; *n* number of points used to calculate regression plane; *dop* duration of period; *v* velocity.

DISCUSSION

Insect olfaction is usually assumed to reflect the perception of the odorant by ORNs, but it is largely dependent on the air flow across the antenna. This dependency is described in various olfactory orientation experiments (Atema, 1996; Vickers, 2000; Weissburg, 2000; Webster and Weissburg, 2001; Keller and Weissburg, 2004; Willis and Avondet, 2005; Willis et al., 2008; Page et al., 2011; Reidenbach and Koehl, 2011). The data on odorant plume structure has led to testable predictions on orientation strategies. These predictions focus on the intermittent mode of the chemical signal as well as the spatial and temporal concentration patterns that is critical for mediating upwind flight and casting behavior in several species of moths (Vickers, 2006). The onset slopes of odorant pulses, indicating a concentration increase at a particular rate, were only rarely considered as a factor in determining orientation behavior. Importantly, the pattern of the pulse onset slopes and pulse amplitudes form a spatial gradient. These point toward the plume source better than other dynamic parameters (Moore and Atema, 1991; Zettler and Atema, 1999). Lobsters use the temporal and spatial distribution of odorant signals to locate the sources (Moore and Atema, 1991). Cockroaches, however, have lifestyles and feeding ecologies quite different from those of lobsters. Nonetheless, as ground dwellers they will also use temporal and spatial pulse parameters during orientation along an odorant plume. Unfortunately, we lack detailed knowledge about the sensory mechanism underlying plume tracking to initially large odorant sources and their less disrupted plumes. Rapid and accurate orientation movements require unambiguously detecting the concentration and its rate of change at various air flow velocities. The greater the velocity, the greater is the flow rate which is defined as the amount of air volume flowing across an area per unit of time. An increase in the flow rate of a dispersing air volume at constant concentration does not lead to any change in the number of molecules per unit volume (viz. the ratio between molecule number and air volume), but does increase the absolute number of molecules delivered per unit time. ORNs acting as "pulse slope detectors" must assess the rate of concentration change of the odorant-loaded air, independently of the absolute number of molecules involved in the change, the odorant-loaded air volume or its flow rate.

In the context of the present study, the two predictions pointed out in the Introduction did hold to a remarkable degree. In regard to the first prediction, the response of the ON and OFF ORNs to oscillating concentration changes with a period of 120 s and a mean rate of 2%/s increases slightly by increasing the air flow velocity from 0.49 to 1.69 m/s. At a mean rate of 3.5%/s and a 60 s oscillation period, however, the flow velocity has no effect on ORN responses. Right down to these slow rates, the response of the ORNs is modulated by changes in the air stream concentration independently of the absolute number of molecules, the air volume involved in the concentration change, the rate of arrival of the odorant molecules at the antenna or the rate of air flow. The second prediction also holds in the above results. That is, the gain for the rate of concentration change is invariant to the flow-rate level. When the odorant concentration

oscillates slowly with long periods, the cue would simply be that the ORN discharge rates begin to change at all. Because of the high gain at slow change rates, cockroaches will receive creeping changes in concentration, even if they persist in one direction. The mechanism underlying ORN gain control and the robustness of gain control against changes in odorant flow rates in the air stream is unclear.

The ability of the ON and OFF ORNs to correctly identify slow rates of concentration change despite variations in the volume flow rate agrees with the flow-rate invariant responses to concentration pulses in *Drosophila* ORNs (Zhou and Wilson, 2012). Nonetheless, there are differences in the stimulation technique, the method of evaluating the responses and probably in the physiological properties of the ORNs. In the experiments on *Drosophila*, the change in the air velocity was provided by varying the air volume delivered during the 5-s pulse. To compensate for the changing molecule arrival rate, the odorant concentration was adjusted to the flow rate. Keeping pulse concentration but varying the volume flow rate led to constant ORN responses. This makes the ORNs "concentration detectors." The authors did not evaluate the possible effect of the rate of concentration change at the pulse onset slope. Visually, the miniPID signal indicates that a concentration pulse of 50% attained within the first 100 ms of the transient concentration increase a rate of 300%/s (Figure 4 in Zhou and Wilson, 2012). Potentially, such high rates are at the upper limit of sensitivity and therefore variations in the air flow rate ranging between 1.4 and 6.6 m/s did not influence the ORNs responses.

In attempting to assign the ORNs to flux detectors or concentration detectors, the latter is preferable due to their insensitivity to air velocity (Kaissling, 1998). This mechanism was initially applied to CO_2 receptor neurons, whereas the typical odorant receptors were regarded as flux detectors. Interestingly, the two mechanisms may not be exclusive but instead complement each other in transduction (Rospars et al., 2000; Baker et al., 2012). Note that the odorant detection models are based on rapid odorant uptake, rapid ORN activation and rapid odorant deactivation. Further experiments with slow and continuous concentration changes on different insects should reveal whether the increased sensitivity according to gain control is a widespread coding strategy of encountering fluctuating concentration changes in the olfactory environment. Much work lies still ahead to refine our understanding of how ORNs satisfy the ability to discriminate differences in the rate of concentration changes despite flow velocity-dependent variations in the number of molecules.

DATA AVAILABILITY

The raw data supporting the conclusions of this manuscript will be made available by the authors, without undue reservation, to any qualified researcher.

ETHICS STATEMENT

All the experiments described in the manuscript were performed with laboratory-reared insects. No special permit was required. After experiments, cockroaches were quickly killed by freezing. All institutional and national guidelines for the care and use of laboratory animals were followed.

AUTHOR CONTRIBUTIONS

MH and HT conceived and designed the research, interpreted the results of experiments, and wrote and edited the manuscript. MH and AM performed the experiments and analyzed the data. MH prepared the figures. HT approved the final version of the manuscript.

FUNDING

Open access funding was provided by the Austrian Science Fund (FWF). This work was supported by a grant from the Austrian Science Fund (Project P30594-B17).

ACKNOWLEDGMENTS

We wish to thank Thomas Hummel for his generous and essential support of our research endeavors.

REFERENCES

Altner, H., Loftus, R., Schaller-Selzer, L., and Tichy, H. (1983). Modality-specificity in insect sensilla and multimodal input from body appendages. *Fort. Zool.* 28, 17–31.

Atema, J. (1996). Eddy chemotaxis and odor landscapes: exploration of nature with animal sensors. *Biol. Bull.* 191, 129–138. doi: 10.2307/1543074

Baker, T. C., Domingue, M. J., and Myrick, A. J. (2012). Working range of stimulus flux transduction determines dendrite size and relative number of pheromone component receptor neurons in moths. *Chem. Senses* 37, 299–313. doi: 10.1093/chemse/bjr122

Boeckh, J., Distler, P., Ernst, K. D., Hösel, M., and Malun, D. (1990). "Olfactory bulb and antennal lobe," in *Proceedings of the Chemosensory Information Processing. NATO ASI Series*, (Heidelberg: Springer).

Burgstaller, M., and Tichy, H. (2011). Functional asymmetries in cockroach ON and OFF olfactory receptor neurons. *J. Neurophysiol.* 105, 834–845. doi: 10.1152/jn.00785.2010

Burgstaller, M., and Tichy, H. (2012). Adaptation as a mechanism for gain control in cockroach ON and OFF olfactory receptor neurons. *Eur. J. Neurosci.* 35, 519–525. doi: 10.1111/j.1460-9568.2012.07989.x

Günther, H. (1968). Untersuchungen an Citronenölen mit Hilfe der Gaschromatographie und der Infrarotsprektroskopie. *Dtsch. Lebensm. Rdsch.* 64, 104–111.

Hinterwirth, A., Zeiner, R., and Tichy, H. (2004). Olfactory receptor cells on the cockroach antennae: responses to the directions and rate of change in food odour concentration. *Eur. J. Neurosci.* 19, 3389–3392. doi: 10.1111/j.0953-816x.2004.03386.x

Kaissling, K. E. (1998). Flux detectors versus concentration detectors: two types of chemoreceptors. *Chem. Senses* 23, 99–111. doi: 10.1093/chemse/23.1.99

Keller, T. A., and Weissburg, M. J. (2004). Effects of odor flux and pulse rate on chemosensory tracking in turbulent odor plumes by the blue crab. Callinectes sapidus. *Biol. Bull.* 207, 44–55. doi: 10.2307/1543627

Moore, P. A., and Atema, J. (1991). Spatial information in the three-dimensional fine structure of an aquatic odor plume. *Biol. Bull.* 181, 404–418. doi: 10.2307/1542361

Page, J. L., Dickman, B. D., Webster, D. R., and Weissburg, M. J. (2011). Getting ahead: context-dependent responses to odorant filaments drive along-stream progress during odor tracking in blue crabs. *J. Exp. Biol.* 214, 1498–1512. doi: 10.1242/jeb.049312

Prah, J. D., Sears, S. B., and Walker, J. C. (1995). "Modern approaches to air dilution olfactometry," in *Handbook of Olfaction and Gustation*, ed. R.-L. Doty (New York, NY: Dekker), 227–255.

Reidenbach, M. A., and Koehl, M. A. R. (2011). The spatial and temporal patterns of odors sampled by lobsters and crabs in a turbulent plume. *J. Exp. Biology.* 214, 3138–3153. doi: 10.1242/jeb.057547

Rospars, J.-P., Křivan, V., and Lánský, P. (2000). Perireceptor and receptor events in olfaction. Comparison of concentration and flux detectors: a modeling study. *Chem. Senses* 25, 293–311.. doi: 10.1093/chemse/25.3.293

Sass, H. (1978). Olfactory receptors on the antenna of *Periplaneta*. Response constellations that encode food odours. *J. Comp. Physiol.* 128, 227–233. doi: 10.1038/srep27495

Schaller, D. (1978). Antennal sensory system of *Periplaneta americana* L. *Cell. Tissue Res.* 191, 121–139.

Selzer, R. (1981). The processing of a complex food odour by antennal olfactory receptors of *Periplaneta americana*. *J. Comp. Physiol.* 144, 509–519. doi: 10.1007/bf01326836

Selzer, R. (1984). On the specificities of antennal olfactory receptor cells of *Periplaneta americana*. *Chem. Senses* 8, 375–395. doi: 10.3389/fncir.2017.00032

Shaw, P. E. (1979). Review of quantitative analysis of citrus essential oils. *J. Agric. Food Chem.* 27, 246–257. doi: 10.1021/jf60222a032

Tichy, H., and Hellwig, M. (2018). Independent processing of increments and decrements in odorant concentration by ON and OFF olfactory receptor neurons. *J. Comp. Physiol.* 204, 873–891. doi: 10.1007/s00359-018-1289-6

Tichy, H., Hinterwirth, A., and Gingl, E. (2005). Olfactory receptors on the cockroach antenna signal odour ON and odour OFF by excitation. *Eur. J. Neurosci.* 22, 3147–3160. doi: 10.1111/j.1460-9568.2005.04501.x

Vickers, N. J. (2000). Mechanisms of animal navigation in odor plumes. *Biol. Bull.* 2000, 203–212. doi: 10.2307/1542524

Vickers, N. J. (2006). Winging it: moth flight behavior and responses of olfactory neurons are shaped by pheromone plume dynamics. *Chem. Senses* 31, 155–166. doi: 10.1093/chemse/bjj011

Webster, D. R., and Weissburg, M. J. (2001). Chemosensory guidance cues in a turbulent chemical odor plume. *Limnol. Oceanogr.* 46, 1034–1047. doi: 10.4319/lo.2001.46.5.1034

Weissburg, M. J. (2000). The fluid dynamical context of chemosensory behavior. *Biol. Bull.* 198, 188–200.

Willis, M. A., and Avondet, J. L. (2005). Odor-modulated orientation in walking male cockroaches *Periplaneta americana*, and the effects of odor plumes of different structure. *J. Exp. Biol.* 208, 721–735. doi: 10.1242/jeb.01418

Willis, M. A., Avondet, J. L., and Finnell, A. S. (2008). Effects of altering flow and odor information on plume tracking behavior in walking cockroaches, *Periplaneta americana* (L.). *J. Exp. Biol.* 211, 2317–2326. doi: 10.1242/jeb.016006

Zeiner, R., and Tichy, H. (2000). Integration of temperature and olfactory information in cockroach antennal lobe glomeruli. *J. Comp. Physiol.* 186, 717–727. doi: 10.1007/s003590000125

Zettler, E., and Atema, J. (1999). Chemoreceptor cells as concentration slope detectors: preliminary evidence from the lobster nose. *Biol. Bull.* 198, 252–253. doi: 10.2307/1542633

Zhou, Y., and Wilson, R. I. (2012). Transduction in drosophila olfactory receptor neurons is invariant to air speed. *J. Neurophysiol.* 108, 2051–2059. doi: 10.1152/jn.01146.2011

Conflict of Interest Statement: The authors declare that the research was conducted in the absence of any commercial or financial relationships that could be construed as a potential conflict of interest.

frontiers in Physiology

ORIGINAL RESEARCH
published: 22 August 2019
doi: 10.3389/fphys.2019.01052

Sensilla-Specific Expression of Odorant Receptors in the Desert Locust *Schistocerca gregaria*

*Xingcong Jiang†, Heinz Breer and Pablo Pregitzer**

Institute of Physiology, University of Hohenheim, Stuttgart, Germany

The desert locust *Schistocerca gregaria* recognizes multiple chemical cues, which are received by olfactory sensory neurons housed in morphologically identifiable sensilla. The different sensillum types contain olfactory sensory neurons with different physiological specificities, i.e., they respond to different categories of chemical signals. The molecular basis for the sensilla-specific responsiveness of these cells is unknown, but probably based on the endogenous receptor repertoire. To explore this issue, attempts were made to elucidate whether distinct odorant receptors (ORs) may be expressed in a sensilla-specific manner. Analyzing more than 80 OR types concerning for a sensilla-specific expression revealed that the vast majority was found to be expressed in sensilla basiconica; whereas only three OR types were expressed in sensilla trichodea. Within a sensillum unit, even in the multicellular assembly of sensilla basiconica, many of the OR types were expressed in only a single cell, however, a few OR types were found to be expressed in a consortium of cells typically arranged in a cluster of 2–4 cells. The notion that the OR-specific cell clusters are successively formed in the course of development was confirmed by comparing the expression patterns in different nymph stages. The results of this study uncover some novel and unique features of locust olfactory system, which will contribute to unravel the complexity of locust olfaction.

Keywords: olfaction, insect, desert locust, antenna, odorant receptors, sensilla

OPEN ACCESS

Edited by:
Sylvia Anton,
Institut National de la Recherche Agronomique (INRA), France

Reviewed by:
Nicolas Montagné,
Sorbonne Universités, France
Shannon Bryn Olsson,
National Centre for Biological Sciences, India

****Correspondence:***
Pablo Pregitzer
p_pregitzer@uni-hohenheim.de

†Present address:
Xingcong Jiang,
Department of Evolutionary Neuroethology, Max Planck Institute for Chemical Ecology, Jena, Germany

Specialty section:
This article was submitted to Invertebrate Physiology, a section of the journal Frontiers in Physiology

Received: *23 May 2019*
Accepted: *02 August 2019*
Published: *22 August 2019*

Citation:
Jiang X, Breer H and Pregitzer P (2019) Sensilla-Specific Expression of Odorant Receptors in the Desert Locust Schistocerca gregaria. Front. Physiol. 10:1052. doi: 10.3389/fphys.2019.01052

INTRODUCTION

Locusts, like the desert locust *Schistocerca gregaria*, are characterized by a remarkable phase polyphenism and can switch between a solitarious and a gregarious phase (Van Huis et al., 2007; Pener and Simpson, 2009). In the gregarious phase, migrating locust swarms can cause severe agricultural and economic damages in the habituated areas like Africa and Asia (Roffey and Popov, 1968; Skaf et al., 2006; Simpson and Sword, 2008; Pener and Simpson, 2009). The molecular mechanisms underlying the phase transition are under rigorous investigation but still remain poorly understood (Kang et al., 2004; Guo et al., 2011; Rogers et al., 2014; Wang et al., 2014; Yang et al., 2014). Besides tactile and visual stimuli, the sense of smell plays an important role in the life cycle and phase change of locusts (Ould Ely et al., 2006; Cullen et al., 2010; Maeno et al., 2011; Wang et al., 2015, 2019; Pregitzer et al., 2017). Locusts are in fact able to recognize a variety of chemical compounds, including green leaf volatiles and chemical cues for aggregation and oviposition (Torto et al., 1994; Rai et al., 1997; Ochieng' and Hansson, 1999). The primary organ for sensing such

chemical compounds is a pair of antennae, covered by hair-like appendage structures called sensilla. The antennal sensilla have been classified based on morphological criteria as basiconic, trichoid, coeloconic, and chaetic sensilla (Stocker, 1994; Ochieng et al., 1998). Encoding the identities of chemical compounds relies on a variety of olfactory receptors including odorant receptors (ORs) which are localized on the chemosensory membrane of olfactory sensory neurons (OSNs) housed within each sensillum. For the antennae of *S. gregaria* it was recently demonstrated that only the OSNs in s. basiconica and s. trichodea express specific odorant receptors and the olfactory receptor co-receptor (Orco) (Yang et al., 2012; Pregitzer et al., 2017). In fact, a large set of OR genes was found for the migratory locust *Locusta migratoria* (Wang et al., 2014) and for *S. gregaria* as many as 119 OR types were identified through an antennal transcriptomic survey (Pregitzer et al., 2017). So far, there is little information concerning the expression of distinct OR types in either s. basiconica or s. trichodea. This issue is of particular interest in view of the unequal distribution of both sensillum types on the antennae of *Schistocerca gregaria*, which according to the studies of Ochieng et al. (1998) comprises more than 1000 sensilla basiconica each with 20–50 OSNs, compared to about 200 sensilla trichodea each with 1–3 OSNs.

Interestingly, a high number of OSNs as in the locust sensilla basiconica is rarely seen in other insect model species, like flies and noctuid moths, where most of the olfactory responsive sensilla comprise only 2–4 OSNs, similar to s. trichoidea in *S. gregaria* (Sanes and Hildebrand, 1976; Venkatesh and Singh, 1984). For these species, characteristic stereotypical patterns of OR expression have been described, indicating that cells expressing a distinct receptor type are stereotypically arranged with cells, which express a matching receptor type (Hallem et al., 2004; Krieger et al., 2009). It is currently unknown whether similar principles may also be effective for the expression of OR types in the sensilla of *S. gregaria*. Moreover, in view of the multicellular assembly in s. basiconica of *S. gregaria* it is interesting to know, whether a specific OR type is confined to a single cell, analogous to other insect species, or is concomitantly expressed in more than one cell. In the present study we set out to explore the sensilla-specific expression patterns of OR types. Moreover, attempts were made to evaluate whether in the multicellular assembly of s. basiconica, one distinct OR type may be expressed in multiple cells.

MATERIALS AND METHODS

Animals and Tissues Treatment

Adult and nymph stages of *Schistocerca gregaria* were purchased from local suppliers. Antennae were dissected using autoclaved surgical scissors. For RNA extraction, the organs were immediately frozen in liquid nitrogen and stored at −70°C.

Synthesis of Riboprobes for *in situ* Hybridization

Riboprobe generation was performed as described earlier (Pregitzer et al., 2017). OR sequences cloned into pGEM-T vector (Invitrogen) were used for *in vitro* transcription. The linearized pGEM-T vectors containing desert locust OR sequence fragments were utilized to synthesize antisense riboprobes labeled with either digoxigenin (DIG) or biotin (BIO) using the T7/SP6 RNA transcription system (Roche, Germany).

In situ Hybridization

Antennae of male and female adult *Schistocerca gregaria* locusts were crosscut into two halves, embedded in Tissue-Tek O.C.T. Compound (Sakura Finetek, Alphen aan den Rijn, Netherlands) and used to make 12 μm thick longitudinal sections with a Leica CM3050 S cryostat (Leica Microsystems, Bensheim, Germany) at −21°C. Sections were thaw mounted on Super Frost Plus slides (Menzel, Braunschweig, Germany) and stored at −70°C until use. Sections were taken out from the freezer and immediately transferred into fixation solution (4% paraformaldehyde in 0.1 M $NaHCO_3$, pH 9.5) for 22 min at 4°C. Next, sections were washed in 1×PBS (0.85% NaCl, 1.4 mM KH_2PO_4, 8 mM Na_2HPO_4, pH 7.1) for 1 min, incubated in 0.2 M HCl for 10 min and washed twice in 1×PBS for 2 min each. Then sections were incubated for 10 min in acetylation solution (0.25% acetic anhydride freshly added in 0.1 M triethanolamine) followed by three wash steps in 1×PBS (each wash step lasted 3 min). Sections were incubated in pre-hybridization solution [5×SSC (0.75 M NaCl, 0.075 M sodium citrate, pH 7.0) and 50% formamid] for 15 min at 4°C. Sections were hybridized with digoxigenin- and biotin-labeled probes simultaneously. However, for two-color FISH, 100 μl hybridization solution (50% formamide, 2×SSC, 10% dextran sulfate, 0.2 mg/ml yeast t-RNA, 0.2 mg/ml herring sperm DNA) supplemented with labeled antisense RNA was placed per slide onto the tissue sections. After placing a coverslip, slides were incubated in a humid box (50% formamide) at 60°C overnight. Visualization of labeled probes was performed as described previously (Krieger et al., 2002). In short, digoxigenin-labeled probes were visualized by the anti-digoxigenin alkaline phosphatase-conjugated antibody in combination with the HNPP fluorescent detection set (Roche Diagnostics). Incubation with the anti-digoxigenin alkaline phosphatase-conjugated antibody as well as incubation with the HNPP/Fast Red substrate was conducted overnight at 4°C. For visualization of biotin-labeled probes, the TSA fluorescein system kit (PerkinElmer, Waltham, MA, United States) was used. Incubation of sections with biotin-binding streptavidin conjugated to horse radish peroxidase and incubation with fluoresce in conjugated tyramides were conducted overnight at 4°C.

Analysis of Antennal Sections by Confocal Microscopy

Antennae used for fluorescence *in situ* hybridization were analyzed on a Zeiss LSM 510 meta laser scanning microscope (Zeiss, Oberkochen, Germany). Confocal image stacks of the red and green fluorescence channels as well as the transmitted-light channel were taken. Image stacks were utilized to generate

pictures showing projections or selected optical planes, with the fluorescence and transmitted light channels overlaid or shown separately.

For the analyses in adults between 2 and 4 slides for each OR were analyzed. Each slide harbored 10–20 sections from the antennae of 2–5 animals. An individual antennal section comprised - dependent on the quality of the section - between 3 and 15 antennal segments. Each antennal segment contains multiple basiconic OSN clusters depending on the part of the segment that was sliced; the number ranges from about ten up to several dozen clusters (Yang et al., 2012).

The studies on developmental changes in OSN organization are based on 2 to 4 slides for adults and 5th instar nymphs; for 1st instar nymphs 3 (OR67 and OR8) or 4 slides (OR17, OR29, OR35, and OR110) were analyzed. Slides were examined in two-color FISH experiments following a stringent experimental procedure until clear and convincing fluorescent signals emerged. Observed labeling patterns were documented in LSM images taken from the most convincing antennal areas.

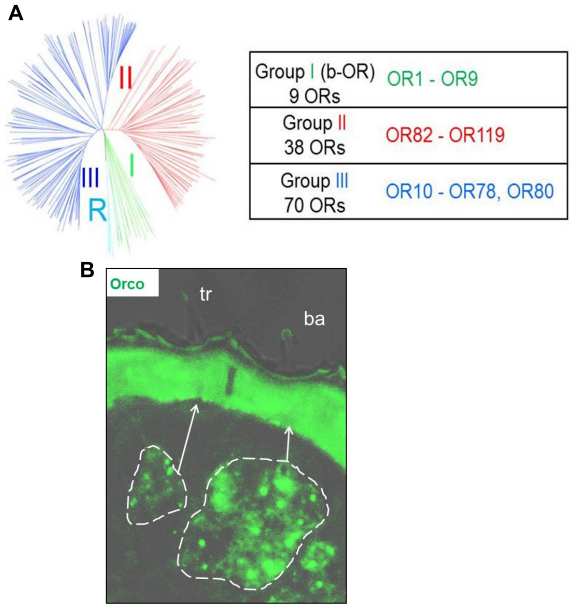

FIGURE 1 | (A) The schematic phylogenetic tree of locust OR sequences is adapted from Pregitzer et al., 2017. *Schistocerca* ORs are grouped within 3 distinct monophyletic lineages. Group **I** was previously named b-ORs, due to its close proximity to the basal Orco root group, marked by a R. A monophyletic group diverging from an inner-node in the phylogenetic tree, supported by a bootstrap value of 85, was classified as group II. The remaining branches, which diverge from another node with a bootstrap value of 59, were assigned as the group III. OR types from each of the three groups are listed in the table. **(B)** Visualization of olfactory sensory neurons in sensilla basiconica (ba) and sensilla trichodea (tr) in tissue sections from locust antennae using Orco as a marker. The cluster of OSNs is delineated by white dish lines indicating a small group of Orco positive cells in sensilla trichodea and a large cluster of Orco positive cells in sensilla basiconica.

RESULTS

Sensilla-Specific Expression of Putative Odorant Receptors

The endogenous OR repertoire is supposed to determine the chemosensory profile of individual sensilla types. For comprehensive analyses of a sensilla-specific expression of the various OR types, we simplified the previously generated phylogenetic tree of locust ORs (Pregitzer et al., 2017) into three groups, namely I, II, and III (**Figure 1A**). Tissue sections from antennae of adult locusts were analyzed by two color fluorescence *in situ* hybridization (FISH) experiments. Riboprobes labeled by Biotin for the olfactory receptor co-receptor (Orco), a marker for insect OSNs, were employed to visualize the ensemble of all sensory neurons in s. basiconica or s. trichodea, an example is depicted in **Figure 1B** indicating a large cluster of Orco-positive below a s. basiconica and a small cluster of Orco-positive cells below a s. trichodea. In addition, riboprobes labeled by Digoxigenin (DIG) were used to visualize cells expressing individual OR types. Subsequently, we set out to evaluate almost all OR types (33 ORs) from group II (38 ORs); the results of these experiments are presented in **Figure 2** and **Supplementary Figure S1**. In our analyses, the green labeling of giant OSN clusters, which are indicative of s. basiconica, could be reproducibly visualized, thus allowing to unequivocally determine the sensillum type. We found that most of the examined OR types from group II (31 out of 33) were found to be expressed in s. basiconica. In most of the examined antennal tissue sections only a single labeled cell was observed within the large cell cluster of s. basiconica (**Figures 2A,B**), however, in a few cases we detected more than one labeled cell in the cell cluster of s. basiconica (**Figures 2C,D**). This phenomenon was studied in greater detail (see further below). Two receptor types from group II, OR102 and OR111, were found to be expressed in cells housed in trichoid sensilla (**Figures 3A,C**). Trichoid sensilla comprise a very small set of cells, which make it distinguishable from s. basiconica (**Figures 3B,D**); for both OR types only a single stained cell was visualized within s. trichodea. This finding, together with the previously identified OR3 from group I, implies that s. trichodea seem to comprise a very limited number of OR types. In *Drosophila melanogaster* and many moth species cells of the trichoid sensilla are characterized by the "sensory neuron membrane protein 1" (SNMP1), a marker of pheromone responsive neurons (Benton et al., 2007; Forstner et al., 2008; Gomez-Diaz et al., 2016; Pregitzer et al., 2017). To evaluate whether the group II receptors OR102 and OR111 may be co-expressed with SNMP1 we performed FISH experiments utilizing riboprobe for each receptor type and a specific riboprobe for SNMP1 labeled by Biotin. As shown in **Figures 3E,F** the labeling clearly overlapped indicating that the two receptors OR102 and OR111 are in fact co-expressed with SNMP1.

Subsequently, the question in which sensillum type the receptors from group III may be expressed was approached by two-color FISH experiments as described above. Since group III comprises a large set of OR members, we analyzed as

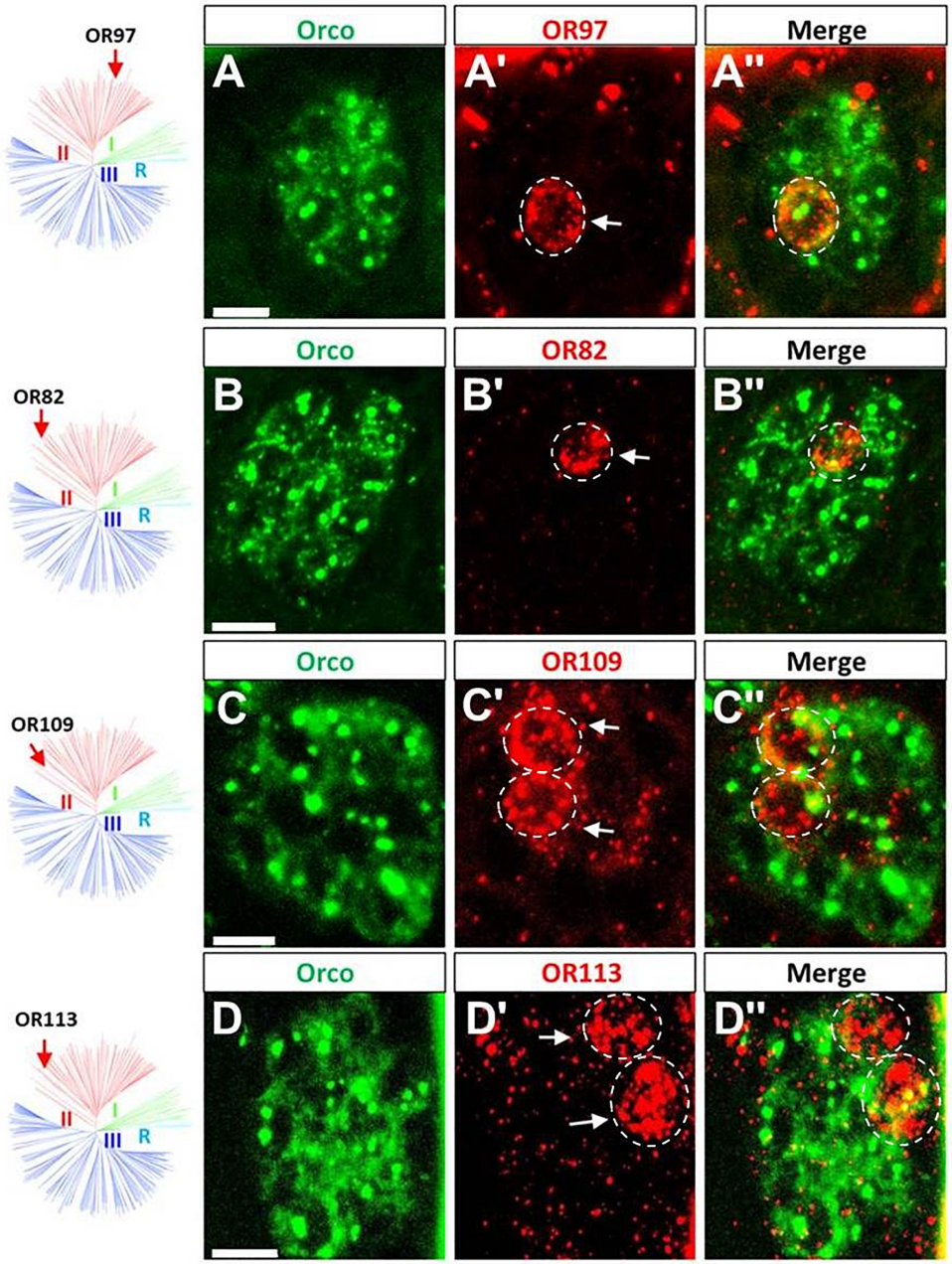

FIGURE 2 | The majority of group II ORs are specifically expressed in sensilla basiconica. **(A–D")** The Orco- and distinct OR-expressing cells were visualized by means of two-color FISH using specific antisense riboprobes labeled in Bio (green fluorescence) and DIG (red fluorescence), respectively. The four ORs (OR82, OR97, OR109, and OR113) are shown as representatives of group II ORs that are specifically expressed in sensilla basiconica. The white dash circle highlights the cell that concomitantly expresses a defined OR type and Orco. More examples are shown in the supporting data. Distinct OR cells are indicated by white arrows. Scale bars, 10 μm.

much as 42 receptor types from this group. The localization of some ORs from group III and Orco are depicted in **Figure 4** and **Supplementary Figure S2**; the results indicate that all the examined receptor types from this group were selectively expressed in s. basiconica. Interestingly, also for some of the receptor types from group III more than one labeled cell was observed in the large cell cluster of s. basiconica (**Figures 4A,D**). For none of the OR types from group III we observe any labeling of cells in s. trichodea. Together, the results of the present and previous studies concerning the sensilla specific expression of OR types from different phylogenetic groups are summarized in **Table 1**. Out of the total number of 83 examined ORs from the three groups, 80 OR types could be clearly assigned to s.

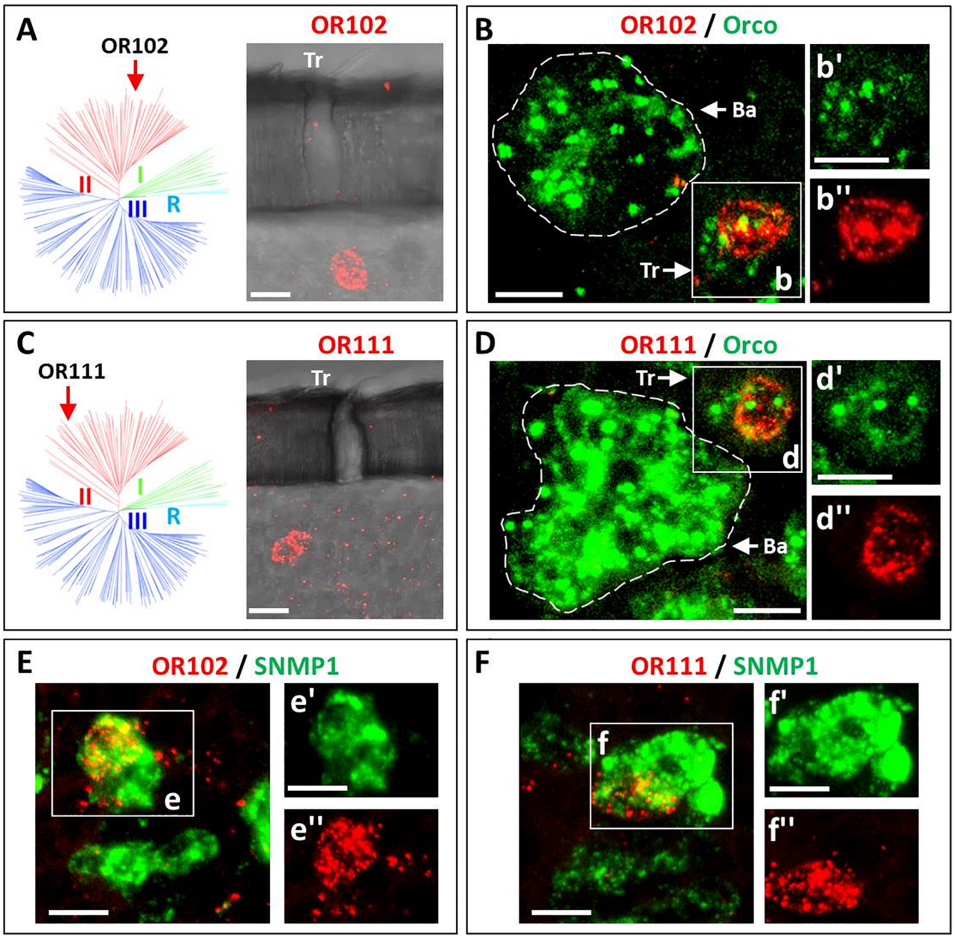

FIGURE 3 | Two ORs from group II are specifically expressed in sensilla trichodea. Cells expressing distinct OR types as well as Orco or SNMP1 were visualized by means of two-color FISH using specific antisense riboprobes labeled in either DIG (OR, red fluorescence) or Bio (Orco and SNMP1, green fluorescence). **(A–D)** The expression of OR102 and OR111 in cells housed in sensilla trichodea is visualized. As indicated in A (OR102) and in C (OR111) labeled cells are located under trichoid (Tr) sensillar hairs. In panel **B,D** co-localization of the two trichoid OR types with Orco are depicted. Discernable basiconic sensilla (Ba) and trichoid sensilla (Tr) cell clusters are indicated by white dash circles and white boxes **(B,D)**, respectively. The insets panel **B'–D"** depict the separate fluorescence channels of panels **B,D**. The white dash circle highlights the cell that concomitantly expresses the defined OR type and Orco. **(E,F)** The co-expression of OR102 and OR111 with SNMP1 is documented. In the insects panels **E'–F"** the separate fluorescence channels of the white boxed areas in panels **E,F** are depicted. The double labeled areas are indicated by white dash circles. Scale bars, 10 μm.

basiconica while only three OR types (OR3, OR102, and OR111) to s. trichodea.

Arrangement of Cells Expressing Distinct Receptor Types in Sensilla Trichodea

Extending the analysis of expression profiles for various OR types may allow evaluating a possibly stereotypical organization of cells expressing certain OR pairs in the cell assembly of an individual sensillum. First, we explored s. trichodea, which have a relatively simple cellular architecture (1–3 OSNs) with a very limited number of receptor types. We pinpointed the relative localization of the three identified OR types focusing on either the expression of two identified receptors types or the expression of all three identified types in a given sensillum. To address this issue we performed two-color FISH experiments with combinations of individual riboprobes for OR3, OR102, and OR111, which are either DIG- or Biotin-labeled; the emerged results are depicted in **Figure 5**. We have found that in s. trichodea each of the three receptors was strictly expressed in only one single cell; no indication for any over representation was observed (**Figure 3**). Using riboprobes for only two receptor types, we obtained a labeling of cells located side by side (**Figures 5A–C"**), confirming the genuine existence of such hypothesized OR combinations. Moreover, using riboprobes for all three receptor types, in rare cases we faithfully visualized a cluster of three labeled cells that are located adjacently; indicative for an expression all three OR types in a given sensillum (**Figures 5D–D"**). Such co-existence of the three receptor types within a single trichoid sensillum was additionally confirmed by conducting single color FISH experiment using DIG-labeled riboprobes for all these three receptors (**Supplementary Figure S3**). Based on these

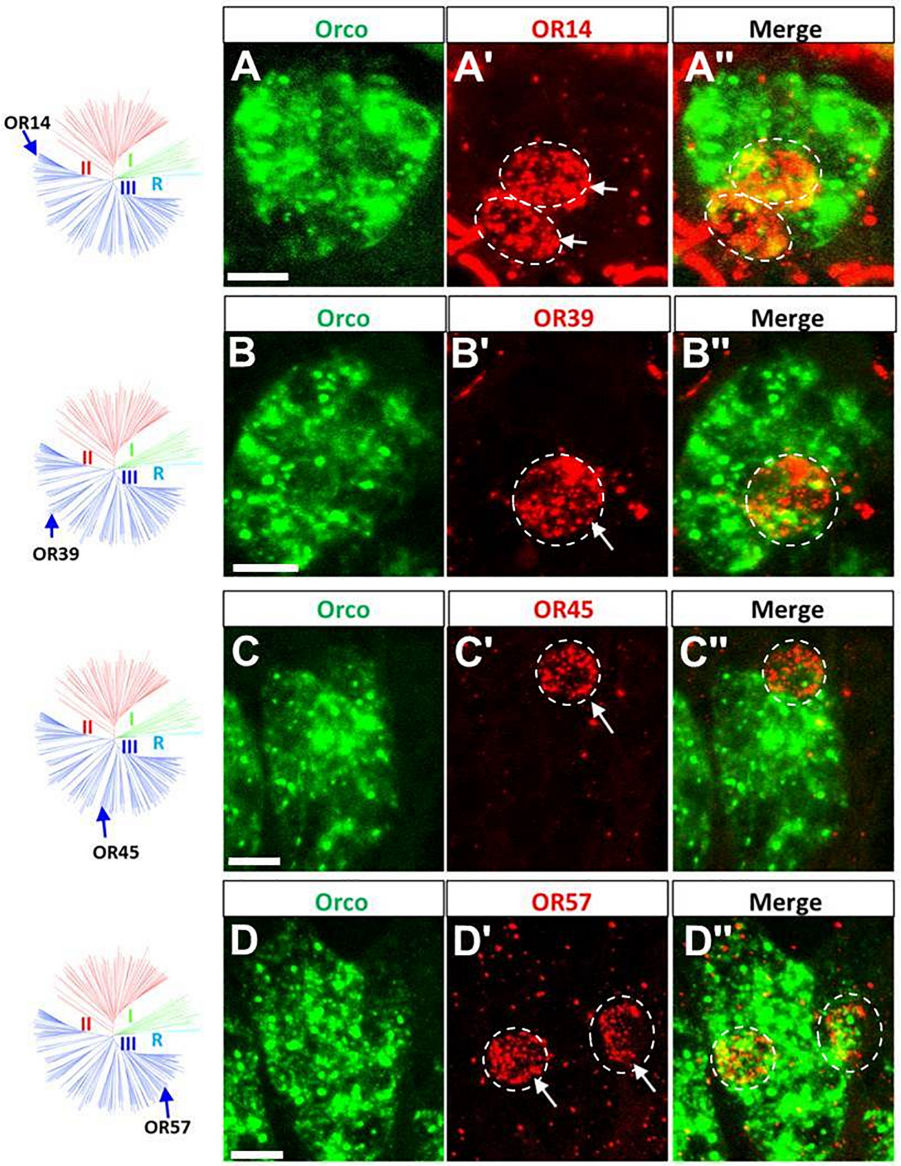

FIGURE 4 | ORs from group III are specifically expressed in sensilla basiconica. The schematic locust OR phylogenetic tree is adapted from Pregitzer et al., 2017 in which R group means Orco rooting group, group I corresponds to the previously classified "b-OR group" and group II and group III are divided based on the branches segregation. The four distinct groups are differentially colored. **(A–D")** Cells expressing Orco- and distinct OR types were visualized by means of two-color FISH using specific antisense riboprobes labeled in Bio (green fluorescence) and DIG (red fluorescence), respectively. Four OR types (OR14, OR39, OR45, and OR57) are shown as representatives of group III (blue branches) that are specifically expressed in sensilla basiconica. More examples are shown in the supporting data. Distinct OR-positive cells are indicated by white arrows. The white dash circle highlights the cell that concomitantly expresses the defined OR type and Orco. Scale bars, 10 μm.

observations it is conceivable that the cell assembly in s. trichodea adopt multiple combinations of receptor types, in which the three OR types (OR3, OR102, and OR111) readily participate in forming a variety of functional combinations.

In Sensilla Basiconica Certain OR Types Are Expressed in Multiple Cells

In the multicellular assembly of s. basiconica certain OR types were found to be expressed in more than one cell (see **Figures 2**, **3**). To address this issue of "over representation" for certain OR types in more detail, we have quantified six representative OR types from group I to III, namely OR8, OR17, OR29, OR35, OR67, and OR110. Firstly, we assessed their expression profile by performing comprehensive two-color FISH analyses using differentially labeled riboprobes targeting the selected OR types and Orco, respectively. As a result, for the multicellular expression of a given receptor type in s. basiconica as much as four labeling patterns emerged (**Figure 6**):

TABLE 1 | Summary of the sensilla specific expression for 83 receptor types.

	Sensilla basiconica	Sensilla trichodea
Group 1 (9 ORs) 8 ORs examined	OR2 OR4 OR5 OR6 OR7 OR8 OR9	OR3
Group II (38 ORs) 33 ORs examined	OR82 OR83 OR84 OR85 OR86 OR87 OR88 OR89 OR90 OR91 OR92 OR93 OR94 OR95 OR96 OR97 OR98 OR99 OR100 OR101 OR103 OR105 OR106 OR108 OR109 OR110 OR112 OR113 OR114 OR116 OR118	OR102 OR111
Group III (70 ORs) 42 ORs examined	OR11 OR13 OR14 OR15 OR16 OR17 OR22 OR23 OR38 OR25 OR26 OR27 OR28 OR29 OR30 OR31 OR32 OR33 OR34 OR35 OR37 OR39 OR40 OR41 OR43 OR45 OR47 OR49 OR51 OR52 OR53 OR54 OR57 OR61 OR62 OR66 OR67 OR68 OR70 OR71 OR76 OR80	

The specific expression of ORs in sensilla basiconica or in sensilla trichodea was determined by the two-color FISH experiments. Among the 83 analyzed OR types, only 3 ORs namely OR3, OR102 and OR111 were found to be selectively expressed in sensilla trichodea, while all other OR types were expressed in sensilla basiconica.

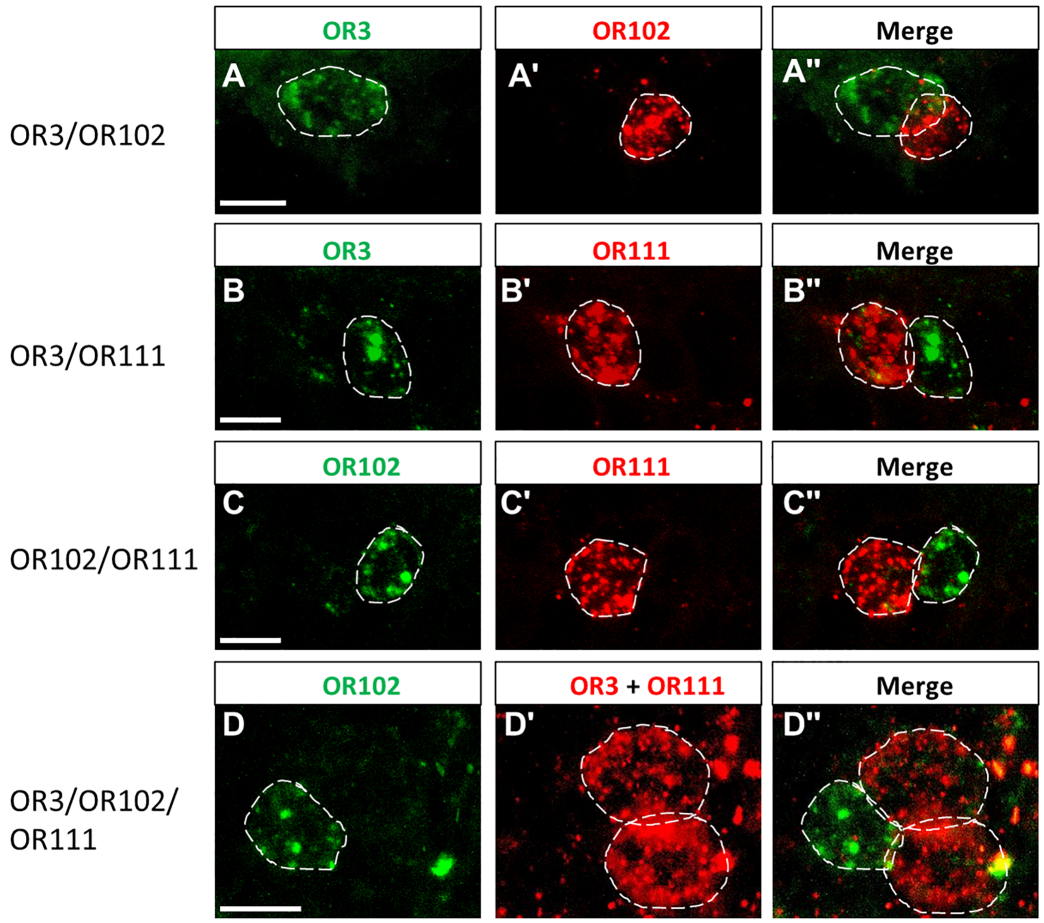

FIGURE 5 | Cells expressing distinct OR types are adjacently located in the trichoid sensilla. **(A–D")** The relative position of cells in the trichoid sensilla which express distinct OR types was visualized by means of two-color FISH using specific antisense riboprobes labeled in DIG (red fluorescence) or Bio (green fluorescence). White dash circles outline the position of cells expressing a distinct OR type. Note in panel **D** two red-labeled cells were visualized due to the usage DIG-labeled riboprobes for both OR3 and OR111. Scale bar, 10 μm.

receptors could be expressed in 2 cells (OR29, OR35), 3 cells (OR17) or even 4 cells (OR67). Upon a closer inspection, we found that in most cases cells expressing the same OR type were adjacently distributed, forming a cluster of cells. Scrutinizing antennal sections, we have observed a variety of clusters comprising 2 cells, 3 cells and even more than 3 cells (**Figure 6**).

The question arises whether the number and spatial arrangement of cells expressing a distinct receptor type is established from the very beginning or whether those cells expressing the same receptor type emerge gradually in the course of development. Desert locusts undergo a hemimetabolous life cycle and grow continuously by successive molts. In a next step, we analyzed the topographic expression of these receptors in the

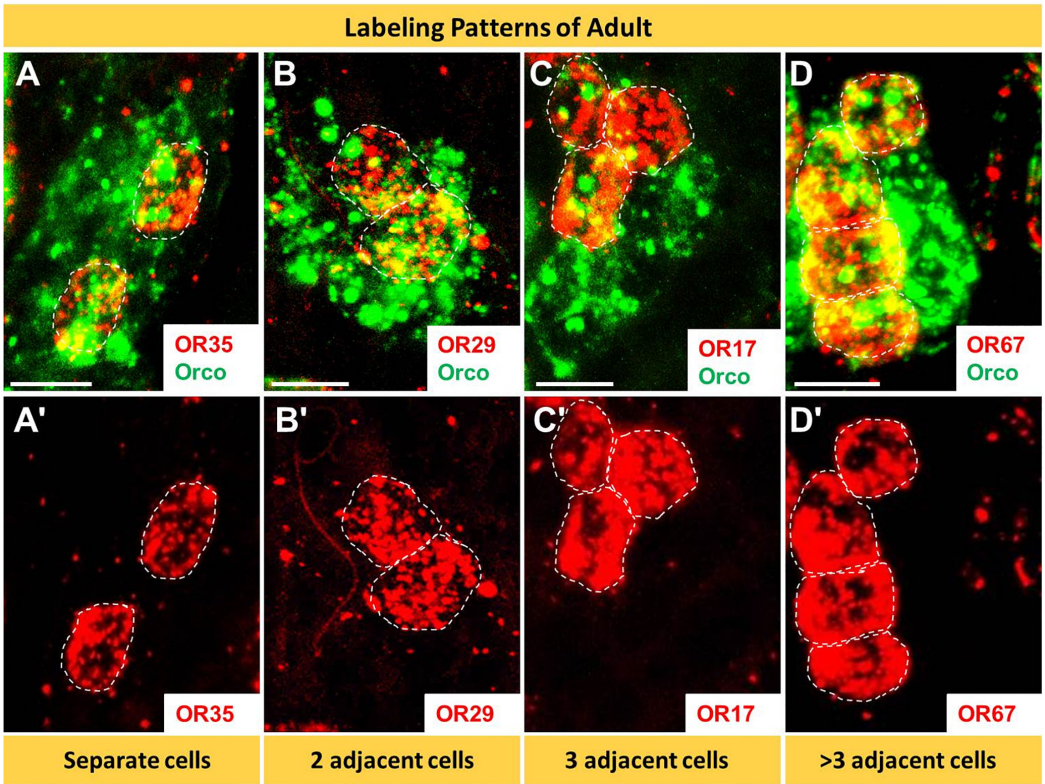

FIGURE 6 | In basiconic sensilla distinct OR types are expressed in several cells. The cells expressing distinct OR types and Orco were visualized by means of two-color FISH using specific antisense riboprobes. **(A–D')** The analyses of 10 μm optical stacks revealed four different patterns of OR expression; ranged from solitary cells to multicellular clusters. White dash circles outline cell expressing the distinct OR type. Scale bars, 10 μm.

antennae of 5th instar nymphs, the final nymph stage, when the overall body and antennal size is close to the adult stage. At this nymph stage, we found the four types of expression pattern, which closely resembled that of adults (**Figure 7**). Subsequently, we assessed antennae from 1st instar nymphs, which significantly differ in size from 5th instar nymphs. The results of the FISH assays are documented in **Figure 8** indicating that at this stage in the multicellular assembly of s. basiconica only single cells or maximal 2 cell clusters (in the case of OR67 and OR35) exist, whereas there was no indication for 3 or more cell clusters. The results concerning the dynamics of OR cell populations are summarized in **Figure 9**, which suggests that a representation of distinct OR types by several cells in individual basiconic sensilla gradually occurs in the course of locust development.

DISCUSSION

The results of the present study may contribute toward an understanding of the observation that morphologically identifiable sensilla on the antennae of the desert locust *Schistocerca gregaria* comprise OSNs, which respond to different categories of chemical signals (Ochieng' and Hansson, 1999). In order to elucidate decisive molecular elements, which may underlay the sensilla-specific responsiveness of these cells, a large repertoire of odorant receptor types was assessed concerning the sensilla-specific expression patterns. Probing more than 80 OR types revealed that the vast majority of OR types were selectively expressed in sensilla basiconica, whereas only three OR types were identified in sensilla trichodea (**Figures 2–4** and **Table 1**). The large difference correlates to some extent with the much higher number of s. basiconica on the antennal surface (more than 1000) as well as the higher number of OSNs (20–50) per sensillum basiconicum (Ochieng et al., 1998).

The finding that in the antennae of *S. gregaria* apparently only very few OR types are expressed in s. trichodea is interesting in view of the recent observation that in *Locusta migratoria* up to 16 different trichoid neuron types were identified based on different odorant response spectra (Cui et al., 2011). This discrepancy could either be due to species-specific expansion of trichoid receptors, the effect of different auxiliary proteins in the sensilla, like odorant binding proteins or biotransformation enzymes, but possibly also due to additional OR types still to be discovered in *S. gregaria*. In this context it is worthwhile to point out that in a few cases each of the three neurons in a trichoid sensillum expressed one of the trichoid-specific receptors, OR3, OR102, and OR111, whereas in most cases two of the three receptors were found to be expressed in a trichoid sensillum (**Figure 4**). This

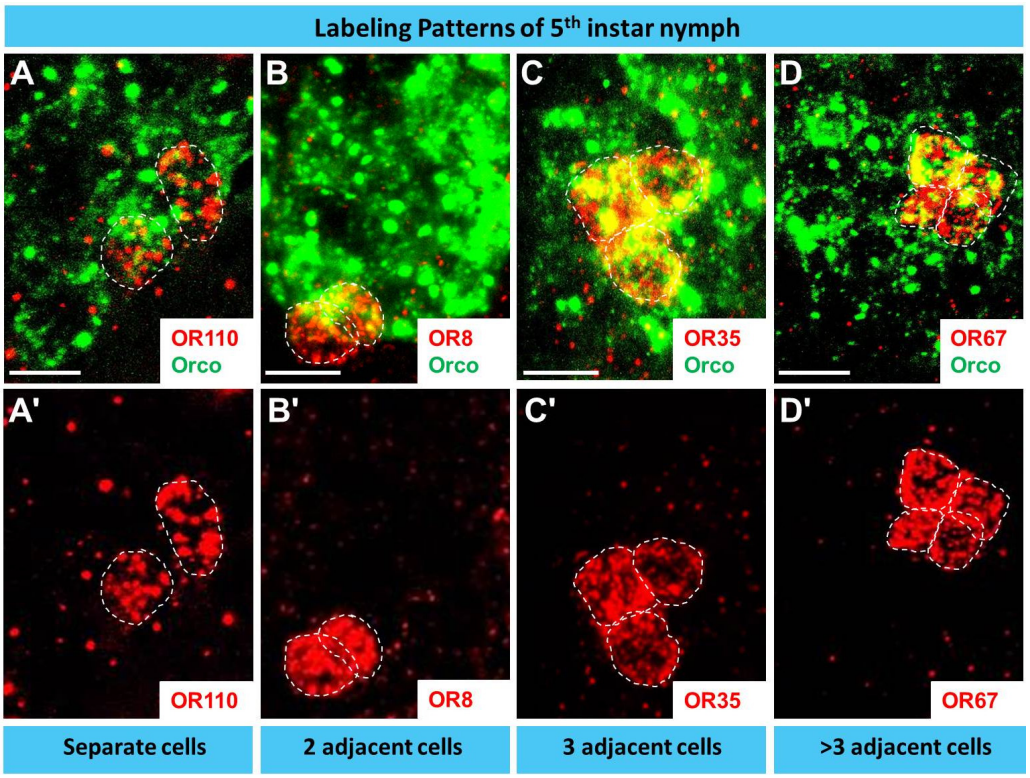

FIGURE 7 | During late development (5th instar nymph) distinct OR types are expressed in multiple cells basiconic sensilla. In **A–D'** cells expressing a distinct OR type and Orco were visualized by means of two-color FISH using specific antisense riboprobes. The analyses of 10 μm optical stacks from sections of 5th instar nymph antennae revealed four different patterns of OR expression, similar to adults. White dash circles outline distinct OR cells. Scale bar, 10 μm.

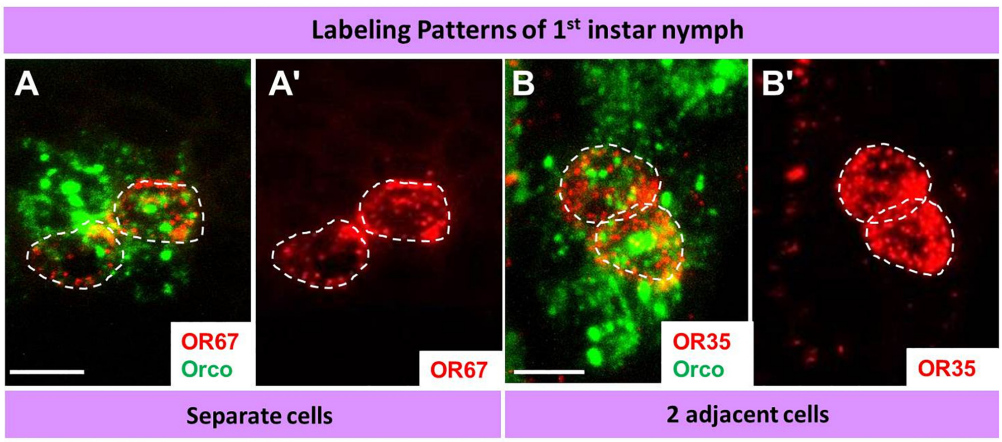

FIGURE 8 | During early development (1st instar nymph) a distinct OR type is only expressed in relatively few cells in basiconic sensilla. In **A–B'** cells expressing distinct OR types and Orco were visualized by means of two-color FISH using specific antisense riboprobes. The analyses of 10 μm optical stacks from sections of 1st instar nymph antennae revealed only two patterns OR expression: solitary cells or cell pairs. White dash circles outline distinct OR cells. Scale bars, 10 μm.

observation could either be due to the fact that a considerable proportion of trichoid sensilla comprise only two chemosensory cells (Ochieng et al., 1998; Cui et al., 2011) or that additional relevant receptor types exist; nevertheless, the current results would argue against the existence of a large number of additional trichoid-specific OR types in *S. gregaria*. Based on the currently available data it remains elusive whether in s. trichodea from *S. gregaria,* which house 1–3 OSNs (Ochieng et al., 1998), the cells stereotypically express one of the three specific OR types or whether distinct combinations of OR types are expressed in

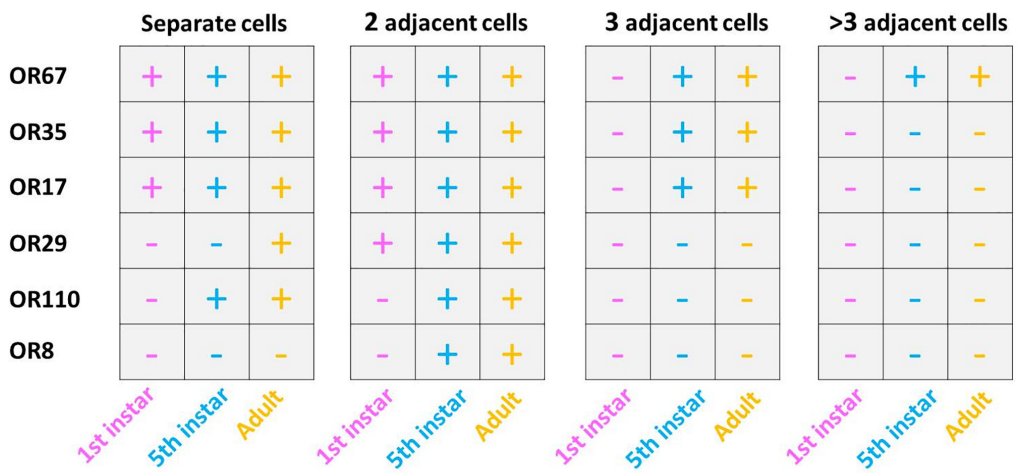

FIGURE 9 | Developmental dependent expression patterns of SgreOR's in basiconic sensilla OSNs. Expression patterns in three developmental stages of six analyzed ORs. Observed cells and labeling patterns are indicated by a "**+**," whereas the absence of such is indicated by "**–**." The results for this figure are based upon three independent FISH experiments.

different types of trichoid sensilla. In this context, it is interesting to note that in flies and moths a stereotypic expression pattern of OR types in defined sensilla has been observed, i.e., a given OR type was only expressed in a distinct type of sensillum and always distinct matching OR types were expressed in the two cells of the sensillum (Hallem et al., 2004; Krieger et al., 2009).

The approaches to explore the principles of OR expression in the multicellular assembly of s. basiconica with 20–50 sensory neurons (Ochieng et al., 1998), revealed that also in this case most of the OR types seem to be expressed in one or few of the multiple cells. However, it is interesting to note that certain OR types were found to be expressed in up to four adjacent cells (**Figures 6- 9** and **Supplementary Figure S4**). The reason and functional implication for this surprising observation is unclear. The finding that the expression of certain OR types in several cells was not observed in early stage does imply that it emerges gradually in the course of development. Such a developmental process would be in line with the hemimetabolous life cycle of *S. gregaria,* i.e., while with each molt the body size and number of antennal segments increases, probably also the number of cells in each segment rises (Ochieng et al., 1998). Whether cells determined to express a distinct receptor type proliferate during this early phase of development or whether the appropriate OR types are expressed in newborn cells is currently unclear. Moreover, it might be possible that distinct sensory cues encountered during early life induce the "over-representation" of certain OR types in multicellular assembly of s. basiconica. Though effects of external sensory cues and the developmental of sensory neurons remain elusive, it is interesting to note that exposure to certain olfactory cues can alter the volume of glomeruli (Devaud et al., 2003; Arenas et al., 2012) or the activity of higher-order sensory neurons (Sachse et al., 2007).

Extensive research over the last decades have uncovered several characteristic features of the locust olfactory system, which significantly deviate from the generally assumed design for insect olfactory systems, mainly based on studies on moths and flies. An obvious difference can be ascribed to the antennal lobe, the first-order olfactory center of the insect brain; in contrast to most insect species, the antennal lobe of locusts display a microglomerular organization with more than a thousand very small glomeruli per lobe (Ernst et al., 1977; Ignell et al., 2001). The processing of olfactory information in this unique neuronal network has been an intense area of research for many years (Anton and Hansson, 1996; Laurent, 2002). However, very little is known how the sensory information from the antennae is conveyed into the neuronal network of the lobe. This aspect is of particular interest in view of the relatively small repertoire of OR types, i.e., the number of OR-specific OSN populations are much smaller than the number of glomeruli. Although deviations from the 1 OR - 1 glomerulus rule has been observed in some other species, in locust the discrepancy is particular striking. This raises fundamental questions concerning the wiring pattern of an OR-specific OSN population.

It is conceivable that there are subpopulations of OR-specific OSNs, e.g., due to the position in the antennae, each subpopulation projecting to its microglomeruli; alternatively, the whole population of OR-specific OSNs could project to multiple microglomeruli. In this context, it is interesting to note, that in locusts the axon from an individual OSN branches and in this way can target several different glomerular structures in the antennal lobe (Hansson et al., 1996). Interestingly, using a transgenic approach such an axonal projection pattern was also visualized for OSNs in the vomeronasal system of rodents, which project their axons to six to ten glomeruli in the accessory olfactory bulb (Del Punta et al., 2002). The knowledge about the genes encoding ORs and their sensilla-specific expression may allow to employ similar approaches in locusts to label OR-specific OSNs in the

antennae and visualize the targeting pattern of their axons in the antennal lobe.

DATA AVAILABILITY

All datasets generated for this study are included in the manuscript and or **Supplementary Files**.

AUTHOR CONTRIBUTIONS

XJ, HB, and PP: current study conception and results interpretation. XJ and PP: experiment conduction, data acquisition, and preliminary manuscript composition. PP and HB: refinement and approval of final manuscript.

FUNDING

XJ was funded by a grant from China Scholarship Council (CSC) with the grant number 201406350032.

ACKNOWLEDGMENTS

We thank Heidrun Froß for her excellent technical assistance.

SUPPLEMENTARY MATERIAL

The Supplementary Material for this article can be found online at: https://www.frontiersin.org/articles/10.3389/fphys.2019.01052/full#supplementary-material

REFERENCES

Anton, S., and Hansson, B. S. (1996). Antennal lobe interneurons in the desert locust *Schistocerca gregaria* (Forskal): processing of aggregation pheromones in adult males and females. *J. Com. Neurol.* 370, 85–96. doi: 10.1002/(SICI)1096-9861(19960617)370:1<85::AID-CNE8>3.0.CO;2-H

Arenas, A., Giurfa, M., Sandoz, J. C., Hourcade, B., Devaud, J. M., and Farina, W. M. (2012). Early olfactory experience induces structural changes in the primary olfactory center of an insect brain. *Eur. J. Neurosci.* 35, 682–690. doi: 10.1111/j.1460-9568.2012.07999.x

Benton, R., Vannice, K. S., and Vosshall, L. B. (2007). An essential role for a CD36-related receptor in pheromone detection in *Drosophila*. *Nature* 450, 289–293. doi: 10.1038/nature06328

Cui, X., Wu, C., and Zhang, L. (2011). Electrophysiological response patterns of 16 olfactory neurons from the trichoid sensilla to odorant from fecal volatiles in the locust, *Locusta migratoria manilensis*. *Arch. Insect Biochem. Physiol.* 77, 45–57. doi: 10.1002/arch.20420

Cullen, D. A., Sword, G. A., Dodgson, T., and Simpson, S. J. (2010). Behavioural phase change in the Australian plague locust, *Chortoicetes terminifera*, is triggered by tactile stimulation of the antennae. *J. Insect. Physiol.* 56, 937–942. doi: 10.1016/j.jinsphys.2010.04.023

Del Punta, K., Puche, A., Adams, N. C., Rodriguez, I., and Mombaerts, P. (2002). A divergent pattern of sensory axonal projections is rendered convergent by second-order neurons in the accessory olfactory bulb. *Neuron* 35, 1057–1066. doi: 10.1016/S0896-6273(02)00904-2

Devaud, J. M., Acebes, A., Ramaswami, M., and Ferrús, A. (2003). Structural and functional changes in the olfactory pathway of adult *Drosophila* take place at a critical age. *J. Neurobiol.* 56, 13–23. doi: 10.1002/neu.10215

Ernst, K. D., Boeckh, J., and Boeckh, V. (1977). A neuroanatomical study on the organization of the central antennal pathways in insects. *Cell Tissue Res.* 176, 285–306. doi: 10.1007/BF00217877

Forstner, M., Gohl, T., Gondesen, I., Raming, K., Breer, H., and Krieger, J. (2008). Differential expression of SNMP-1 and SNMP-2 proteins in pheromone-sensitive hairs of moths. *Chem. Senses* 33, 291–299. doi: 10.1093/chemse/bjm087

Gomez-Diaz, C., Bargeton, B., Abuin, L., Bukar, N., Reina, J. H., Bartoi, T., et al. (2016). A CD36 ectodomain mediates insect pheromone detection via a putative tunnelling mechanism. *Nat. Commun.* 7:11866. doi: 10.1038/ncomms11866

Guo, W., Wang, X., Ma, Z., Xue, L., Han, J., Yu, D., et al. (2011). CSP and takeout genes modulate the switch between attraction and repulsion during behavioral phase change in the migratory locust. *PLoS Genet.* 7:e1001291. doi: 10.1371/journal.pgen.1001291

Hallem, E. A., Ho, M. G., and Carlson, J. R. (2004). The molecular basis of odor coding in the *Drosophila* antenna. *Cell* 117, 965–979. doi: 10.1016/j.cell.2004.05.012

Hansson, B. S., Ochieng', S. A., Grosmaitre, X., Anton, S., and Njagi, P. G. N. (1996). Physiological responses and central nervous projections of antennal olfactory receptor neurons in the adult desert locust, *Schistocerca gregaria* (Orthoptera: Acrididae). *J. Comp. Physiol. A* 179, 157–167. doi: 10.1007/BF00222783

Ignell, R., Anton, S., and Hansson, B. S. (2001). The Antennal lobe of orthoptera – anatomy and evolution. *Brain. Behav. Evol.* 57, 1–17. doi: 10.1159/000047222

Kang, L., Chen, X., Zhou, Y., Liu, B., Zheng, W., Li, R., et al. (2004). The analysis of large-scale gene expression correlated to the phase changes of the migratory locust. *Proc. Natl. Acad. Sci. U.S.A.* 101, 17611–17615. doi: 10.1073/pnas.0407753101

Krieger, J., Gondesen, I., Forstner, M., Gohl, T., Dewer, Y., and Breer, H. (2009). HR11 and HR13 receptor-expressing neurons are housed together in pheromone-responsive sensilla trichodea of male *Heliothis virescens*. *Chem. Senses* 34, 469–477. doi: 10.1093/chemse/bjp012

Krieger, J., Raming, K., Dewer, Y. M. E., Bette, S., Conzelmann, S., and Breer, H. (2002). A divergent gene family encoding candidate olfactory receptors of the moth *Heliothis virescens*. *Eur. J. Neurosci.* 16, 619–628. doi: 10.1046/j.1460-9568.2002.02109.x

Laurent, G. (2002). Olfactory network dynamics and the coding of multidimensional signals. *Nat. Rev. Neurosci.* 3, 884–895. doi: 10.1038/nrn964

Maeno, K., Tanaka, S., and Harano, K. (2011). Tactile stimuli perceived by the antennae cause the isolated females to produce gregarious offspring in the desert locust, *Schistocerca gregaria*. *J. Insect Physiol.* 57, 74–82. doi: 10.1016/j.jinsphys.2010.09.009

Ochieng, S. A., Hallberg, E., and Hansson, B. S. (1998). Fine structure and distribution of antennal sensilla of the desert locust, *Schistocerca gregaria* (*Orthoptera: Acrididae*). *Cell Tissue Res.* 291, 525–536. doi: 10.1007/s004410051022

Ochieng', S. A., and Hansson, B. S. (1999). Responses of olfactory receptor neurones to behaviourally important odours in gregarious and solitarious desert locust, *Schistocerca gregaria*. *Physiol. Entomol.* 24, 28–36. doi: 10.1046/j.1365-3032.1999.00107.x

Ould Ely, S., Mahamat, H., Njagi, P. G. N., Omer Bashir, M., El-Tom El-Amin, S., and Hassanali, A. (2006). Mate location mechanism and phase-related mate preferences in solitarius desert locust, *Schistocerca gregaria*. *J. Chem. Ecol.* 32, 1057–1069. doi: 10.1007/s10886-006-9045-9048

Pener, M. P., and Simpson, S. J. (2009). Locust phase polyphenism: an update. *Adv. Insect Physiol.* 36, 1–272. doi: 10.1016/S0065-2806(08)36001-9

Pregitzer, P., Jiang, X., Grosse-Wilde, E., Breer, H., Krieger, J., and Fleischer, J. (2017). In search for pheromone receptors: certain members of the odorant receptor family in the desert locust *Schistocerca gregaria* (*orthoptera: Acrididae*) are co-expressed with SNMP1. *Int. J. Biol. Sci.* 13, 911–922. doi: 10.7150/ijbs.18402

Rai, M. M., Hassanali, A., Saini, R. K., Odongo, H., and Kahoro, H. (1997). Identification of components of the oviposition aggregation pheromone of the gregarious desert locust, *Schistocerca Gregaria* (Forskal). *J. Insect Physiol.* 43, 83–87. doi: 10.1016/S0022-1910(96)00051-50

Roffey, J., and Popov, G. (1968). Environmental and behavioural processes in a desert locust outbreak. *Nature* 219, 446–450. doi: 10.1038/219446a0

Rogers, S. M., Cullen, D. A., Anstey, M. L., Burrows, M., Despland, E., Dodgson, T., et al. (2014). Rapid behavioural gregarization in the desert locust, *Schistocerca gregaria* entails synchronous changes in both activity and attraction to conspecifics. *J. Insect Physiol.* 65, 9–26. doi: 10.1016/j.jinsphys.2014.04.004

Sachse, S., Rueckert, E., Keller, A., Okada, R., Tanaka, N. K., Ito, K., et al. (2007). Activity-dependent plasticity in an olfactory circuit. *Neuron.* 56, 838–850. doi: 10.1016/j.neuron.2007.10.035

Sanes, J. R., and Hildebrand, J. G. (1976). Structure and development of antennae in a moth, *Manduca sexta*. *Dev. Biol.* 51, 282–299. doi: 10.1016/0012-1606(76)90144-5

Simpson, S. J., and Sword, G. A. (2008). Locusts. *Curr. Biol.* 18, R364–R366. doi: 10.1016/j.cub.2008.02.029

Skaf, R., Scorer, R. S., Popov, G. B., Roffey, J., and Hewitt, J. (2006). The desert locust: an international challenge. *Philos. Trans. R. Soc. B Biol. Sci.* 328, 525–538. doi: 10.1098/rstb.1990.0125

Stocker, R. F. (1994). The organization of the chemosensory system in *Drosophila melanogaster*: a rewiew. *Cell Tissue Res.* 275, 3–26. doi: 10.1007/BF00305372

Torto, B., Obeng-Ofori, D., Njagi, P. G. N., Hassanali, A., and Amiani, H. (1994). Aggregation pheromone system of adult gregarious desert locust *Schistocerca gregaria* (forskal). *J. Chem. Ecol.* 20, 1749–1762. doi: 10.1007/BF02059896

Van Huis, A., Cressman, K., and Magor, J. I. (2007). Preventing desert locust plagues: optimizing management interventions. *Entomol. Exp. Appl.* 122, 191–214. doi: 10.1111/j.1570-7458.2006.00517.x

Venkatesh, S., and Singh, R. (1984). Sensilla on the third antennal segment of *Drosophila melanogaster* meigen (*Diptera: Drosophilidae*). *Int. J. Insect Morphol. Embryol.* 13, 51–63. doi: 10.1016/0020-7322(84)90032-90031

Wang, P., Yin, X., and Zhang, L. (2019). Plant approach-avoidance response in locusts driven by plant volatile sensing at different ranges. *J. Chem. Ecol.* 45, 410–419. doi: 10.1007/s10886-019-01053-9

Wang, X., Fang, X., Yang, P., Jiang, X., Jiang, F., Zhao, D., et al. (2014). The locust genome provides insight into swarm formation and long-distance flight. *Nat. Commun.* 5:2957. doi: 10.1038/ncomms3957

Wang, Z., Yang, P., Chen, D., Jiang, F., Li, Y., Wang, X., et al. (2015). Identification and functional analysis of olfactory receptor family reveal unusual characteristics of the olfactory system in the migratory locust. *Cell. Mol. Life Sci.* 72, 4429–4443. doi: 10.1007/s00018-015-2009-2009

Yang, M., Wei, Y., Jiang, F., Wang, Y., Guo, X., He, J., et al. (2014). MicroRNA-133 inhibits behavioral aggregation by controlling dopamine synthesis in locusts. *PLoS Genet.* 10:e1004206. doi: 10.1371/journal.pgen.1004206

Yang, Y., Krieger, J., Zhang, L., and Breer, H. (2012). the olfactory co-receptor orco from the migratory locust (*Locusta migratoria*) and the desert locust (*schistocerca gregaria*): identification and expression pattern. *Int. J. Biol. Sci.* 8, 159–170. doi: 10.7150/ijbs.8.159

Conflict of Interest Statement: The authors declare that the research was conducted in the absence of any commercial or financial relationships that could be construed as a potential conflict of interest.

frontiers in Physiology

ORIGINAL RESEARCH
published: 26 September 2019
doi: 10.3389/fphys.2019.01223

Identification and Expression Analyses of Olfactory Gene Families in the Rice Grasshopper, *Oxya chinensis*, From Antennal Transcriptomes

Yang Cui†, Cong Kang†, Zhongzhen Wu and Jintian Lin**

Guang Zhou City Key Laboratory of Subtropical Fruit Tree Outbreak Control, Zhongkai University of Agriculture and Engineering, Guangzhou, China

The rice grasshopper *Oxya chinensis* is an important agricultural pest of rice and other gramineous plants. Chemosensory genes are crucial factors in direct interactions with odorants in the olfactory process. Here we identified genes encoding 18 odorant-binding proteins (OBPs), 13 chemosensory proteins (CSPs), 94 olfactory receptors (ORs), 12 ionotropic receptors (IRs), and two sensory neuron membrane proteins (SNMPs) from *O. chinensis* using an transcriptomic approach. Semi-quantitative RT-PCR assays revealed that six OBP-encoding genes (*OchiOBP4*, *5*, *8*, *9*, *10*, and *14*), one CSP gene (*OchiOBP10*) and two IR genes (*OchiIR28* and *29*) were exclusively expressed in antennae, suggesting their roles in olfaction. Real-time quantitative PCR analyses revealed that genes expressed exclusively or predominantly in antennae also displayed significant differences in expression levels between males and females. Among the differentially expressed genes, 17 OR-encoding genes, one CSP- and one SNMP-gene showed female-biased expression, suggesting that they may be involved in some female-specific behaviors such as seeking oviposition site; whereas the three remaining OR-encoding genes showed male-biased expression, indicating their possible roles in sensing female sex pheromones. Our results laid a solid foundation for future studies to reveal olfactory mechanisms as well as designing strategies for controlling this rice pest.

Keywords: antennal transcriptome, olfactory gene, identification, expression analysis, *Oxya chinensis*

OPEN ACCESS

Edited by:
Sylvia Anton,
Institut National de la Recherche Agronomique (INRA), France

Reviewed by:
Pablo Pregitzer,
University of Hohenheim, Germany
Dan-Dan Zhang,
Lund University, Sweden

****Correspondence:***
Zhongzhen Wu
zhongzhen_wu@163.com
Jintian Lin
linjtian@163.com

† These authors have contributed equally to this work

Specialty section:
This article was submitted to Invertebrate Physiology, a section of the journal Frontiers in Physiology

Received: *27 July 2019*
Accepted: *09 September 2019*
Published: *26 September 2019*

Citation:
Cui Y, Kang C, Wu Z and Lin J (2019) Identification and Expression Analyses of Olfactory Gene Families in the Rice Grasshopper, Oxya chinensis, From Antennal Transcriptomes. Front. Physiol. 10:1223. doi: 10.3389/fphys.2019.01223

INTRODUCTION

Olfaction plays an important role in regulating various physiological behaviors, such as foraging, mating, oviposition and avoiding predators (Leal, 2013). The process of olfactory perception is mediated by a series of peripheral olfactory proteins involving odorant-binding proteins (OBPs), chemosensory proteins (CSPs), sensory neuron membrane proteins (SNMPs), olfactory receptors (ORs), gustatory receptors (GRs), and ionotropic receptors (IRs) (Clyne et al., 1999, 2000; Vosshall et al., 1999; Galindo and Smith, 2001; Benton et al., 2007, 2009; Vieira and Rozas, 2011). OBPs and CSPs are suggested to be involve in binding and trafficking of hydrophobic odorant molecules across the sensillum lymph surrounding the olfactory sensory neurons (OSNs) on the sensilla of antennae and

other chemosensory organs (Vogt et al., 1985; Sandler et al., 2000; Xu et al., 2005; Gomez-Diaz et al., 2013). ORs and GRs are the principle receptor proteins responsible for the detection of odorants and tastants, whereas IRs are involved in the detection of chemosensory, thermo- and hygro-sensory stimuli (Ai et al., 2010, 2013; Grosjean et al., 2011; Silbering et al., 2011; Kain et al., 2013; Su and Carlson, 2013; Koh et al., 2014; Chen et al., 2015; Stewart et al., 2015; Gorter et al., 2016; Hussain et al., 2016; Knecht et al., 2016, 2017; Ni et al., 2016). SNMPs play important roles in pheromone detection, which are expressed on the dendritic membranes of pheromone sensitive neurons (Rogers et al., 1997, 2001; Li et al., 2014; Jiang et al., 2016).

Gene families involved in olfactory perception have been extensively reported in many species in Lepidoptera, Coleoptera, Diptera, Hemiptera, and Hymenoptera during recent decades (Grosse-Wilde et al., 2011; Andersson et al., 2013, 2014; Brand et al., 2015; Paula et al., 2016). However, in the Orthoptera order, ORs have been identified from only three species: the genome of *Locusta migratoria* (142 ORs) (Wang et al., 2015), the antennal transcriptome of *Schistocerca gregaria* (119 ORs) (Pregitzer et al., 2017), and *Oedaleus asiaticus* (60 ORs) (Zhou et al., 2019). Members of the IR families have been identified in *L. migratoria* (32 IRs) (Wang et al., 2015) and *O. asiaticus* (6 IRs) (Zhou et al., 2019), the OBP families in *S. gregaria* (14 OBPs) (Jiang et al., 2017), *Oedaleus infernalis* (18 OBPs) (Zhang et al., 2018) and *O. asiaticus* (15 OBPs) (Zhou et al., 2019), the CSP families in *L. migratoria* (58 CSPs) and *S. gregaria* (42 CSPs) (Martin-Blazquez et al., 2017), and SNMP families in *S. gregaria* (2 SNMPs) (Jiang et al., 2016) and *O. asiaticus* (3 SNMPs) (Zhou et al., 2019). Consequently, additional Orthoptera species need to be investigated to reach a better understanding on olfactory receptive mechanisms for insect olfactory system.

Oxya chinensis is an oligophagous grasshopper pest and primarily feeds on graminaceous grasses. Electroantennogram (EAG) and behavioral bioassay have showed that *O. chinensis* adults have significantly higher olfactory sensitivity to geraniol compared to other host volatiles (Lu et al., 2008). Identification of target genes that are involved in olfactory perception may lead to environmentally-friendly approaches for controlling this pest (Venthur and Zhou, 2018). The objectives of this study were to generate antennal transcriptomes to identify major olfactory-related gene families (OBPs, CSPs, ORs, IRs, and SNMPs) from *O. chinensis*, examine expression profiles of the genes in various tissues to identify the antenna-specific genes, and compare their sex-specific expression patterns to identify female- and male-specific olfactory-related genes.

MATERIALS AND METHODS

Insects, Tissue Collections, and RNA Extraction

The colony of *O. chinensis* used in this study was derived from insects originally collected from rice fields in the environs of Leizhou, Guangdong, China (110°05′E, 20°34′N). The colony was maintained in the laboratory on bristle grass in climate-controlled chamber under 30°C ± 1°C with 60% relative humidity and a photoperiod of 16 h light versus 8 h.

For transcriptomic analyses, 100 pairs of antennae were dissected separately from *O. chinensis* adult females and males. For semi-quantitative RT-PCR analysis, antennae, maxillary palps, foreleg tarsus, wings, and genitals were separately collected from adults (male: female = 1:1, n = 25 each). Two replicates were included for each tissue. For RT-qPCR analyses, 50 pairs of antennae were obtained from both females and males, separately along with other body parts including 20 pairs of maxillary palps, 20 pairs of foreleg tarsus, 20 pairs of wings, and 10 genitals from both males and females. Three replicates were included for each tissue sample. Tissues were homogenized to powder immediately in liquid nitrogen and stored at −80°C for further analyses.

Total RNA was extracted using Trizol reagent (Invitrogen, Carlsbad, CA, United States) and treated with RNase-free DNase I (Takara, Dalian, China) to remove potential genomic DNA contamination. RNA concentration, quality and quantity were analyzed on a NanoDrop ND-2000 Spectrophotometer (Nanodrop Technologies, United States) and a Qubit®2.0 Fluorometer (Invitrogen, Life Technologies, United States). RNA integrity was assessed with an Agilent 2100 Bioanalyzer (Agilent Technologies, United States).

cDNA Library Construction, Illumina Sequencing and *de novo* Assembly

Transcriptomes were generated through a commercial contract with Novogene Bioinformatics Technology, Co., Ltd. (Beijing, China). Libraries for sequencing were generated from 1.5 μg purified RNA per sample using a TruSeq RNA Sample Preparation Kit v2 (Illumina, San Diego, CA, United States) according to Illumina instructions and sequenced on an Illumina HiSeq 2500 platform (San Diego, CA, United States). Approximately 150 bp paired-end reads were generated.

Raw reads were firstly processed through in-house perl scripts. High-quality clean reads were obtained by removing reads containing adapter and unknown (poly-N) and low-quality reads. Clean reads were combined from both female and male antennae and were assembled into unigenes using Trinity (Version: r2013-11-10) with min_kmer_cov set to 2 under default settings (Grabherr et al., 2011). The clean reads from the *O. chinensis* female antennae and male antennae were deposited in the NCBI Sequence Read Archive (Female antennae: SAMN11484273; Male antennae: SAMN11484274).

Functional Annotation

Unigenes were searched against databases including NCBI non-redundant protein (nr), NCBI non-redundant nucleotide (nt), Swiss-Prot[1], the Kyoto Encyclopedia of Genes and Genomes (KEGG)[2], using BLASTx with a cut-of E-value of 10^{-5}. Gene orthology (GO) and cluster of orthologous groups of

[1]http://www.ebi.ac.uk/uniprot

[2]http://www.genome.jp/kegg/

proteins (COG)[3] using Blast2GO program (Conesa et al., 2005; Gotz et al., 2008).

Gene Identification

To identify genes coding for OBPs, CSPs, ORs, IRs, and SNMPs, known protein sequences (OBPs, CSPs, ORs, IRs, and SNMPs) from other Orthopteran species were selected as queries to search the *O. chinensis* antennal transcriptomes. *L. migratoria*, *S. gregaria*, *O. asiaticus*, *O. infernalis*, and *Ceracris kiangsu* were used for OBPs; *L. migratoria*, *S. gregaria*, and *O. asiaticus* for CSPs; *L. migratoria*, *S. gregaria*, and *O. asiaticus* for ORs; *L. migratoria* and *O. asiaticus* for IRs; *S. gregaria* and *O. asiaticus* for SNMPs (**Supplementary Table S1**). tBLASTn was used to search and identify candidate chemosensory genes against the *O. chinensis* antennal transcriptomes, with a cut-of E-value of 10^{-5}. Putative *O. chinensis* chemosensory genes were in turn used as queries to identify additional genes (tBLASTx and BLASTp). Repetitions were completed until no new candidates were identified. Candidate unigenes from the initial search were further manually examined using BLASTx against Genbank. Open reading frames (ORFs) were predicted with the ORF Finder in NCBI[4]. Amino acid sequences were aligned with MAFFT (version 7.308) (E-INS-I parameter set) (Katoh and Standley, 2013) and visualized with Geneious (version 9.1.3) (Kearse et al., 2012). Transmembrane domains, signal peptides, conserved cysteine locations in candidates were analyzed using the InterProScan tool plug-in in Geneious (Version: 9.1.3.) (Quevillon et al., 2005). Candidate genes coding for OBPs, CSPs, ORs, IRs, and SNMPs were listed in **Supplementary Table S2**, together with genetic characteristics, best matches in NCBI-nr database, protein domains and estimated expression levels.

Phylogenetic Analyses

Multiple amino acid sequence alignments were made with MAFFT (E-INS-I parameter) (Katoh and Standley, 2013). Phylogenetic trees were constructed using maximum likelihood analyses as implemented in FastTree2 [Jones-Taylor-Thornton (JTT) amino acid substitution model, 1,000 bootstrap replications] (Price et al., 2009, 2010). Dendrograms were created and colored in FigTree[5]. Sequences used for phylogenetic analysis are listed in **Supplementary Table S3**.

Analyses of Expression Levels and Differentially Expressed Genes

Gene expression levels were estimated using RSEM (Version: 1.2.15) (Li and Dewey, 2011) for each sample. The clean reads were mapped back to the assembled transcriptome. The read counts normalized using the Trimmed Mean of *M*-value normalization method (Robinson and Oshlack, 2010) for each mapped gene was used to calculate gene expression levels following the FPKM (fragments per kilobase per million read) method (Cock et al., 2010; Trapnell et al., 2010), and were used to identify differentially expressed genes between females and males using DEGseq edgeR package (Version: 3.4.2) (Robinson et al., 2010). Criteria for estimating significantly differentially expressed genes were set as q-value < 0.005 and the absolute value of log2 Fold Change > 1.

Semi-Quantitative RT-PCR and Real-Time Quantitative PCR

Semi-quantitative RT-PCR was carried out to compare expression levels of genes coding for OBPs, CSPs, and IRs in various tissues including antennae, maxillary palps, foreleg tarsus, wings and genitals. cDNA template was synthesized from total RNA using a PrimeScript RT reagent Kit (Takara, China). Two housekeeping genes, β-actin (*Ochi*β*-actin*) and ribosomal protein 49 (*Ochirp49*) were used as controls. PCR reactions were conducted in a thermal cycler from Bio-Rad (CA, United States). PCR conditions were as follows: 95°C for 2 min, followed by 35 cycles of 95°C for 30 s, 56°C for 30 s, 72°C for 1 min, and a final extension for 10 min at 72°C. PCR products were separated on 1.5% agarose gels. Individual PCR reactions were repeated twice with independently isolated RNA samples.

Expression profiles of the antenna-predominant candidate genes for OBPs, CSPs, and IRs as well as all ORs and SNMPs were analyzed on a LightCycler 480 system (Roche Applied Science). RT-qPCR cycling parameters were set at 95°C for 5 min, followed by 45 cycles of 95°C for 10 s, and 60°C for 20 s. A melting curve analysis was then performed at 95°C for 20 s, 60°C for 30 s, and 95°C for 30 s in order to determine the specificity of primers. Negative controls without cDNA template (nuclease-free water) were included for each reaction. Three independent biological replications were performed with each biological replication measured in three technique replications. The results were analyzed using the LightCycler 480 Gene Scanning Software. Relative quantification was calculated following the $2^{-\Delta\Delta CT}$ method (Livak and Schmittgen, 2001), and normalized against the two reference genes (*Ochi*β*-actin* and *Ochirp49*). Gene-specific primers were designed using Primer3[6] and listed in **Supplementary Table S4**.

Statistical Analysis

RT-qPCR data were analyzed and plotted using Prism 6.0 (GraphPad Software, CA, United States). The comparative analyses of each target gene among various tissues were determined using a one-way nested analysis of variance (ANOVA) followed by Duncan's new multiple range test ($\alpha = 0.05$) using SPSS 22.0 (SPSS Inc., Chicago, IL, United States). Values are presented as mean ± SE.

RESULTS

Illumina Sequencing and *de novo* Assembly

A total of 53.4 and 44.8 million raw reads were obtained from male and female antennae cDNA libraries of *O. chinensis*,

[3]http://clovr.org/docs/clusters-of-orthologous-groups-cogs/

[4]https://www.ncbi.nlm.nih.gov/orffinder/

[5]http://tree.bio.ed.ac.uk/software/figtree

[6]http://primer3.ut.ee/

respectively. After removing adaptor sequences, low quality reads and contaminant sequences, 52.2 and 44.7 million of clean reads were generated. The reads were assembled into 120,803 unigenes with a mean length of 1,213 bp, and an N50 of 2,458 bp. The number of unigenes longer than 500 bp was 33,079, which accounted for 35.21% of all unigenes (**Supplementary Table S5**).

Functional Annotation

There were 26,923 (45.5%), 15,092 (25.5%), 20,546 (34.7%), 5,662 (9.57%), 10,911 (18.4%), and 20,542 (34.7%) unigenes that had homologous sequences in NCBI-nr, NCBI-nt, Swiss-Prot, GO, COG, and KEGG databases, respectively. Based on the homologous sequences, a total of 29,067 (49.1%) unigenes were annotated and the remaining unigenes were unmappable at present (**Supplementary Figure S1A**). GO analyses categorized annotated genes into three functional categories, including "biological process," "cellular component," and "molecular function" (**Supplementary Figure S1B**). In "biological process," major subcategories included "cellular," "metabolic" and "single-organism." In "cellular component," the subcategories "cell" and "cell part" and "membrane" were major subcategories. In "molecular function," the subcategories "binding" and "catalytic activity" contained the largest numbers of unigenes.

Candidate Genes Coding for Odorant Binding Proteins

Eighteen OBP unigenes were identified from the *O. chinensis* antennal transcriptomes (**Supplementary Table S2: Sheet 1**). All identified unigenes except *OchiOBP18* had a full-length ORF with sizes ranged from 128 to 266 amino acid residues. Except three OBP genes (*OchiOBP12*, *14*, and *17*), all predicted proteins had a predicted signal peptide. Sequence identities of

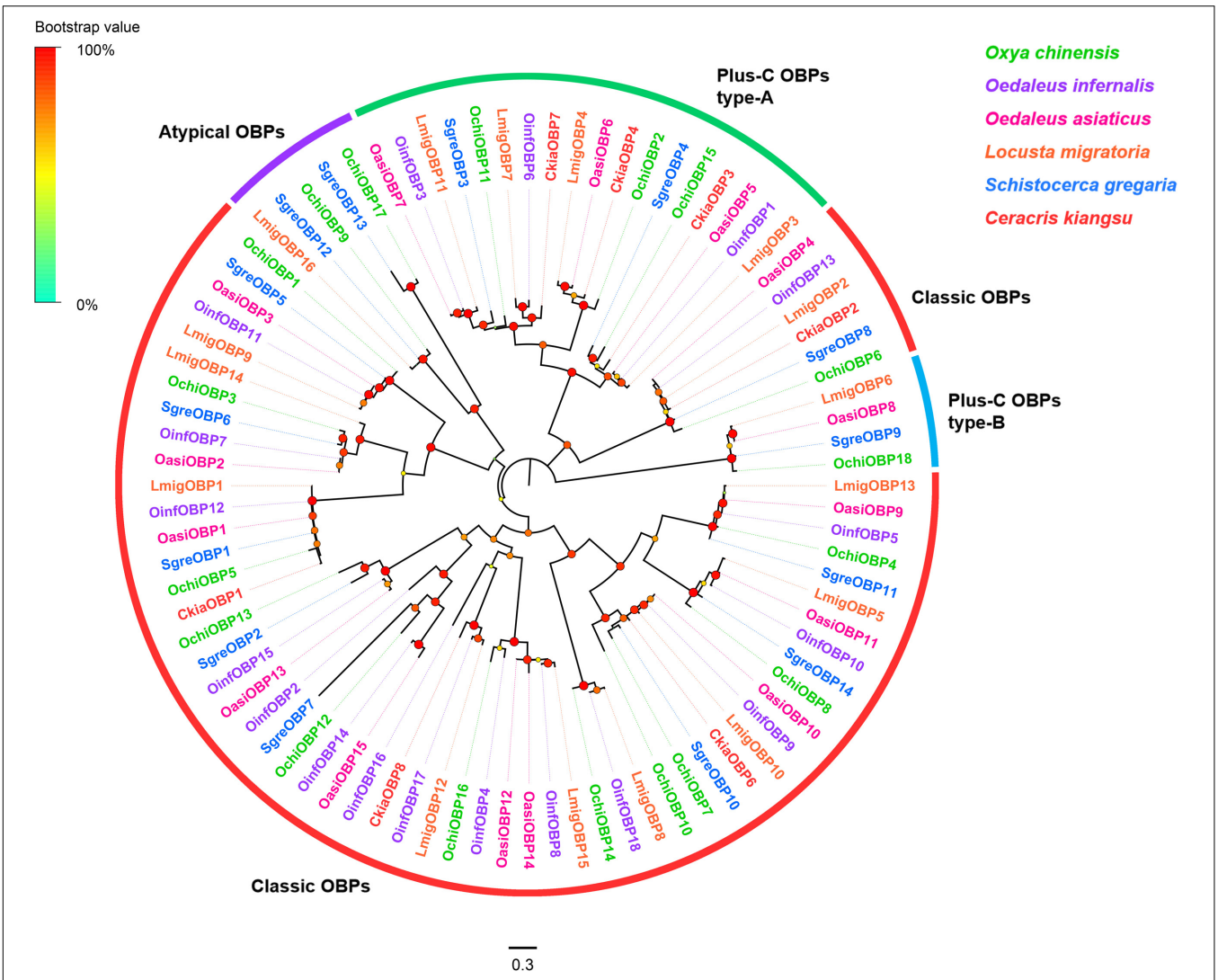

FIGURE 1 | Phylogenetic tree of putative odorant-binding proteins (OBPs). Branch support (circles at the branch nodes) was estimated using an approximate likelihood ratio test based on the scale indicated on the top left. Bars indicate branch lengths in proportion to amino acid substitutions per site. Classic OBPs are in red; plus-C OBPs type-A in green; plus-C OBPs type-B in blue; and atypical OBPs in purple.

predicted OBPs with those from other Orthopteran insects in the NCBI-nr database ranged from 45.9 to 88.6%, with an average of 73.8%. Consistent with previous Orthopteran OBP classification by Jiang et al. (2017), twelve OBPs (*OchiOBP1*, *3-8*, *10*, *12-14*, *16*) were classic OBPs, with the typical six conserved C-residues (**Supplementary Figure S2**). Two (*OchiOBP9* and *17*) were atypical OBPs, with extraordinary long stretches between conserved C1 and C2 (**Supplementary Figure S3**). Four OBPs were plus-C OBPs, which were further divided into plus-C OBP type-A (*OchiOBP2*, *11*, and *15*) (with the extra C-residue both in C4-C5 and C5-C6) (**Supplementary Figure S4**) and plus-C OBP type-B (*OchiOBP18*) (with the extra C-residue in front of C1 and behind C6) (**Supplementary Figure S5**). Phylogenetic analyses of OBPs from *O. chinensis* and other five locust species (*O. infernalis*, *O. asiaticus*, *L. migratoria*, *S. gregaria*, and *C. kiangsu*) showed that all the locust OBPs formed distinct clades based on the number and position of cysteine residues, and segregated into the classic OBP, atypical OBP, and plus-C OBP sub-families as well as other locust OBPs (**Figure 1**).

Candidate Genes Coding for Chemosensory Proteins

Thirteen unigenes encoding CSPs were identified from the *O. chinensis* antennal transcriptomes (**Supplementary Table S2: Sheet 2**). All but two (*OchiCSP11* and *13*) had full-length ORFs encoding 120–297 amino acid residues. All predicted

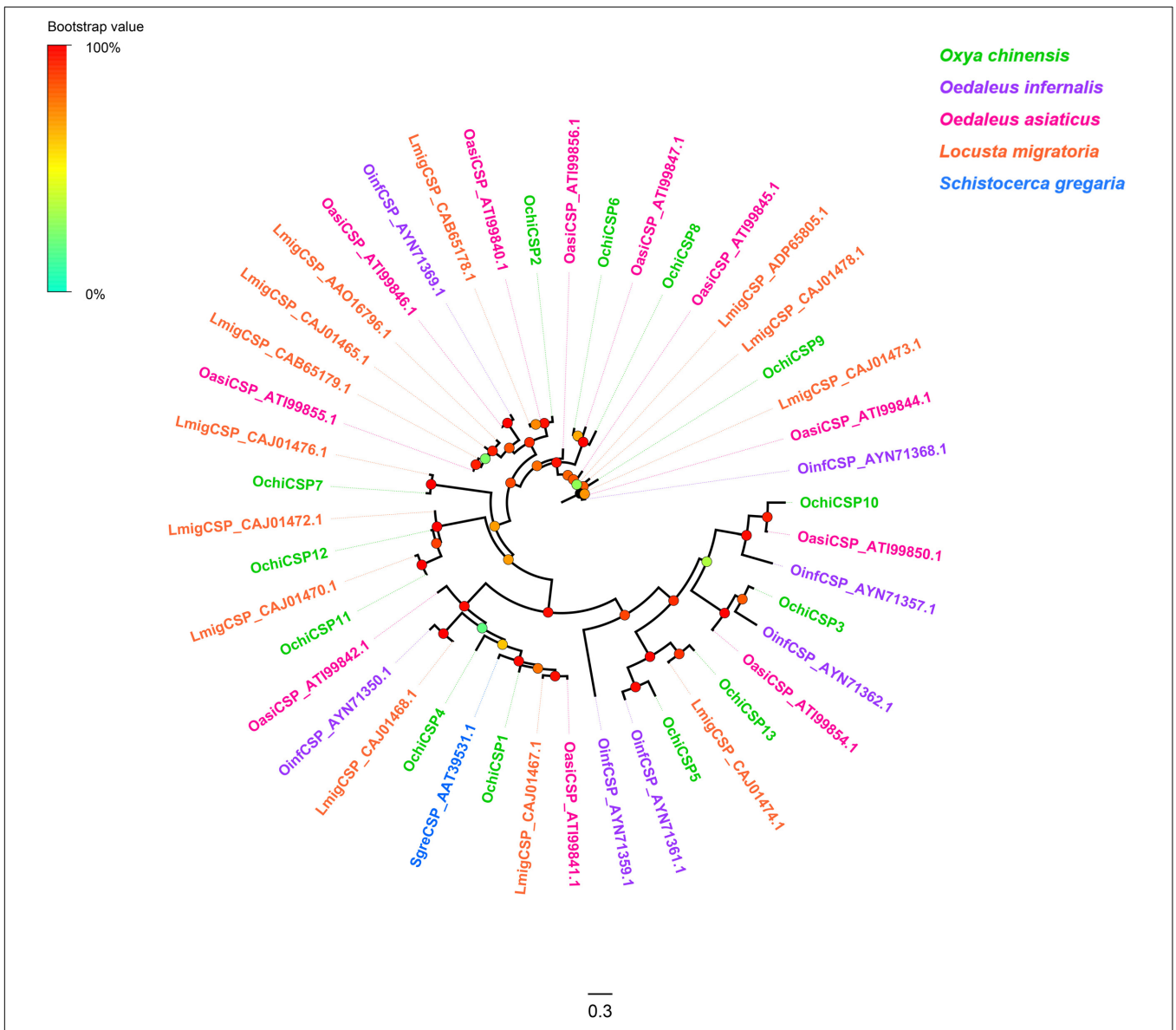

FIGURE 2 | Phylogenetic tree of putative chemosensory proteins (CSPs). Branch support (circles at the branch nodes) was estimated using an approximate likelihood ratio test based on the scale indicated at the top left. Bars indicate branch lengths in proportion to amino acid substitutions per site.

OchiCSPs contained four highly conserved four-cysteine profiles (**Supplementary Figure S6**). Except *OchiCSP1*, all predicted proteins possessed a signal peptide. A phylogenetic tree was built using all predicted OchiCSPs together with those from other locust species. Most OchiCSPs had orthologs with CSPs from other locust species, and no *O. chinensis*-specific CSP lineage was evident (**Figure 2**).

Candidate Genes Coding for Odorant Receptors

Ninety-four OR-encoding unigenes were identified, including one Orco (*OchiOR1*) and 93 conventional OR genes (*OchiOR2-94*), which were classified to the 7-transmembrane receptor superfamily (**Supplementary Table S2: Sheet 1**). Among these OR unigenes, 54 had full-length ORFs encoding proteins with 367 to 487 amino acid residues. The highly conserved co-receptor *OchiOR1* shared 94.25% identity to a co-receptor from *L. migratoria* (ALD51504.1), while other OchiORs shared 33.56 to 91.13% identity with average 68.7% with the respective *L. migratoria* ORs. A phylogenetic tree was generated using our identified ORs along with a data set containing representative ORs from *L. migratoria* and *S. gregaria* (**Figure 3**). The locust ORs formed three distinct clades, with the *O. chinensis* OR co-receptor (*OchiOR1*) formed a clade with the protein Orco from two other related species. The vast majority of OchiORs were clustered with orthologs from other locust species. Only a few species-specific clades and sister pairs were observed. Three OchiORs (*OchiOR27*, *53* and *56*) were segregated into unique clades, while *OchiOR36*/*60* and *OchiOR28*/*76* formed the sister pairs.

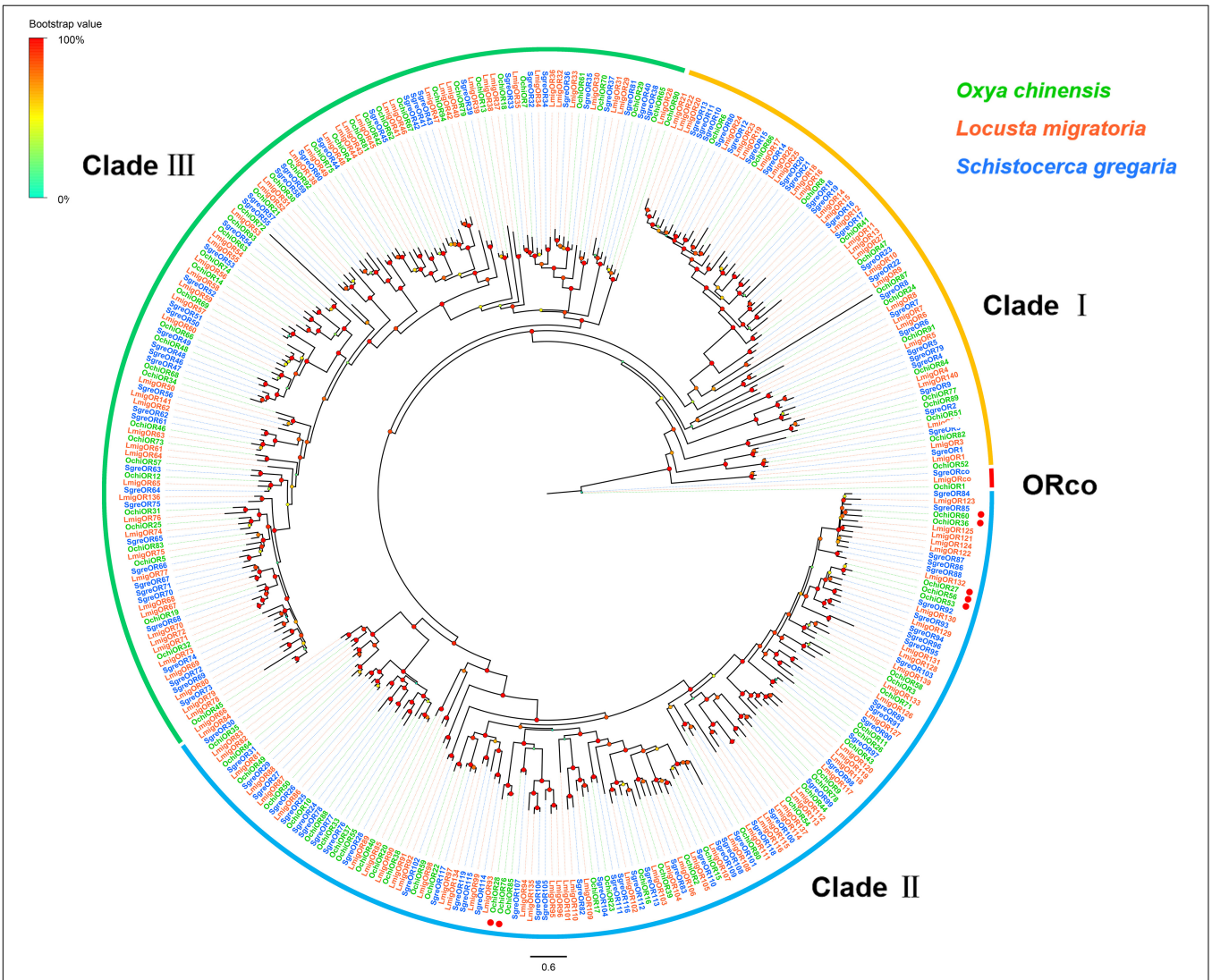

FIGURE 3 | Phylogenetic tree of putative odorant receptors (ORs). The distance tree was rooted by the conservative ORco gene orthologs (red). The species-specific clades and sister pairs are labeled with red dots. Branch support (circles at the branch nodes) was estimated using an approximate likelihood ratio test based on the scale indicated at the top left. Bars indicate branch lengths in proportion to amino acid substitutions per site. The clade I is in orange; clade II in green; and clade III in blue.

Candidate Genes Coding for Ionotropic Receptors (iGluRs/IRs)

Twelve putative iGluR/IR unigenes were identified, which were predicted to encode ligand-binding domain (S1 and S2) with three transmembrane domains (M1, M2, and M3) or portions of domains (**Supplementary Table S2: Sheet 2**). Of these iGluR/IR unigenes, eight had complete ORFs encoding at least 535 amino acid residues. Distinct clades were observed in a phylogenetic tree generated with our identified sequences and paralogs from other species including *Drosophila melanogaster* and *L. migratoria* (**Figure 4**). All identified iGluRs/IRs from *O. chinensis* were assigned to two phylogenetic groups, including N-Methyl-D-aspartic acid (NMDA) iGluRs (*OchiGluR8*, *9*, and *12*) and antennal IRs (*OchiIR25a*, *8a*, *76b*, *22*, *6*, *17*, *20*, *28*, and *29*). No candidates were assigned to non-NMDA iGluRs and divergent IRs (**Figure 4**). A set of "antennal IR" conserved among other species were absent from *O. chinensis* and *L. migratoria*, and only three "IR co-receptor" orthologs (*OchiIR25a*, *8a*, and *76b*) were clustered with *D. melanogaster* orthologs.

Candidate Genes Coding for Sensory Neuron Membrane Proteins

Two SNMP unigenes were identified, which matched the CD36 family. The genes contained complete ORFs that encoded proteins with two transmembrane domains (**Supplementary Table S2: Sheet 3**). Phylogenetic analyses revealed that all SNMPs were classified into two distinct subgroups, SNMP1 and SNMP2 (**Figure 5**). In the SNMP1 clade, *OchiSNMP1* and *OchiSNMP2* were clustered into two subclades along with those from other locust species.

Transcript Abundance Based on FPKM

In this study, genes with FPKM values ≥1,000 were defined as highly expressed genes, those with values 300–1,000 were defined as moderately expressed genes, and those with values ≤300 were defined as weakly expressed genes. Based on these criteria, *OchiOBP1-5* and *OchiCSP1-4* were highly expressed in antennae (**Supplementary Table S2: Sheets 1,2**);

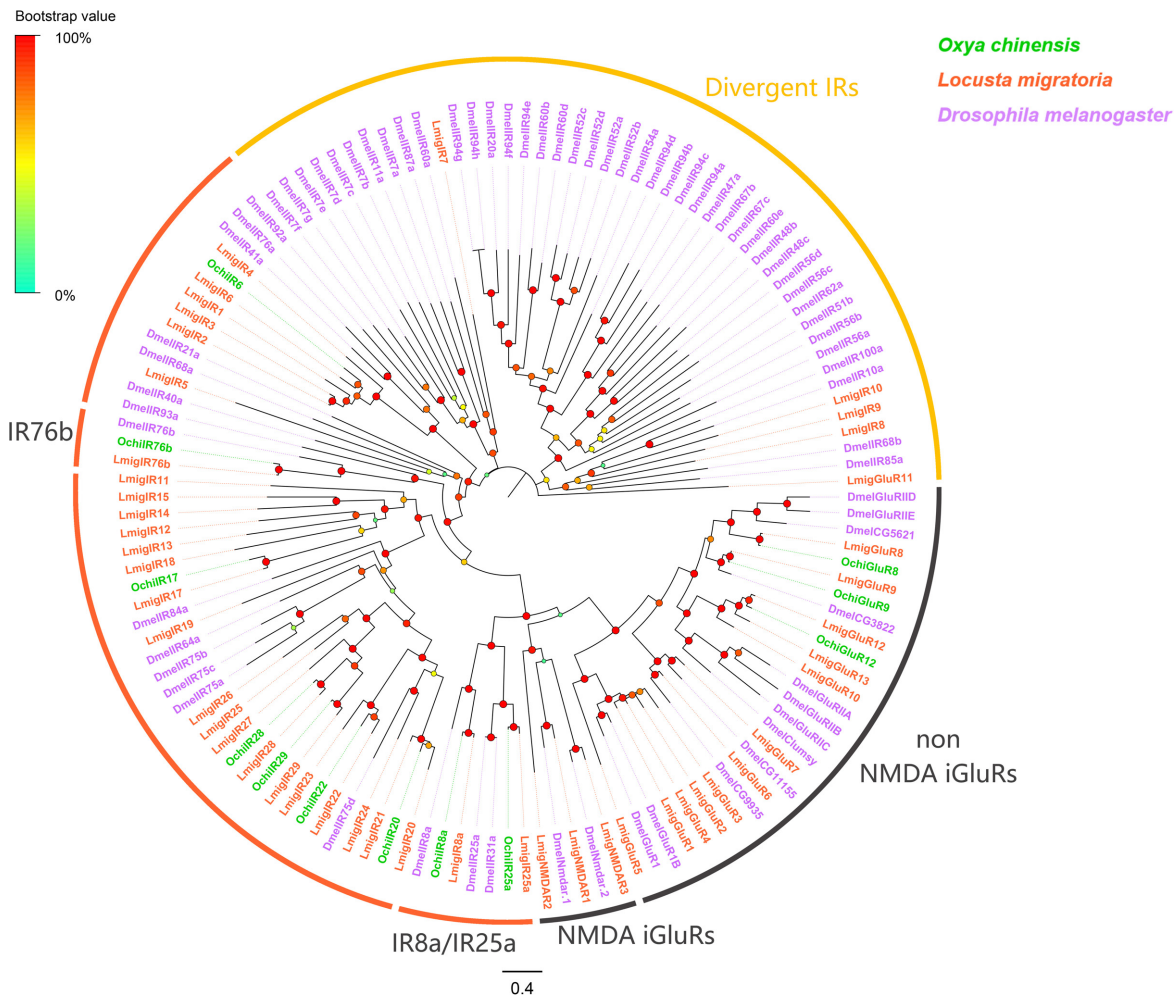

FIGURE 4 | Phylogenetic tree of putative ionotropic receptors (IRs). Branch support (circles at the branch nodes) was estimated using an approximate likelihood ratio test based on the scale indicated at the top left. Bars indicate branch lengths in proportion to amino acid substitutions per site.

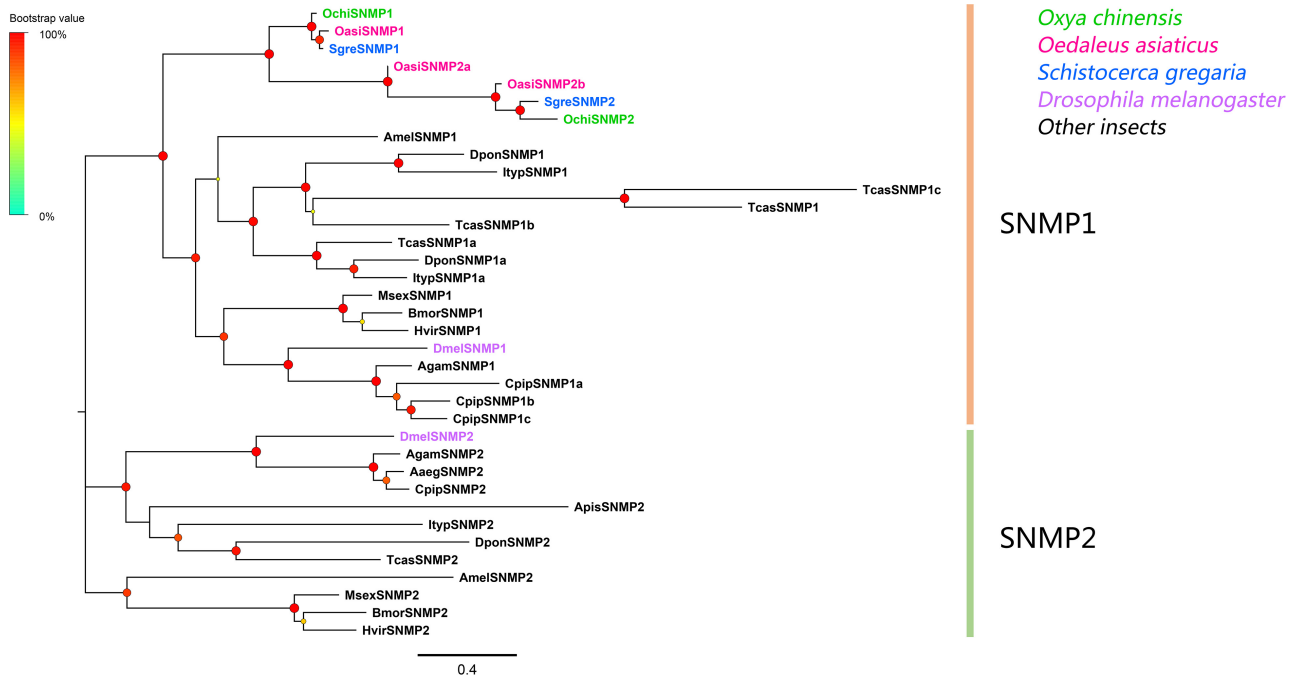

FIGURE 5 | Phylogenetic tree of putative sensory neuron membrane proteins (SNMPs). Branch support (circles at the branch nodes) was estimated using an approximate likelihood ratio test based on the scale indicated at the top left. Bars indicate branch lengths in proportion to amino acid substitutions per site.

OchiOR1 (Orco) was moderately expressed (Male FPKM: 318.52, Female FPKM: 391.73); other conventional ORs (*OchiOR2-94*), all iGluRs/IRs, and the two SNMPs were weakly expressed (RPKM $\leq$ 30) (**Supplementary Table S2: Sheet 3**). DEG analyses showed that *OchiCSP10* and *OchiOR2*, *6*, *8*, *9*, *11*, *15*, *33*, *38*, *39*, *41*, *43*, *44*, *48*, *50*, *53*, *56*, and *62* were female-predominant, whereas *OchiCSP9*, *OchiOR34*, *46* and *86*, and *OchiGluR8* and *12* were male-biased (**Supplementary Table S2: Sheets 1–5**).

Tissue- and Sex-Specific Expression

Based on semi-quantitative RT-PCR analyses, *OchiOBP4*, *5*, *8*, *9*, *10*, and *14* were almost exclusively expressed in antennae, while *OchiOBP3* and *17* were abundant in antennae and maxillary palps (**Figure 6A**). The remaining OBP-encoding genes were abundant in multiple body parts. For CSP-encoding genes, *OchiCSP10* was exclusively expressed in antennae, while other *OchiCSPs* were present multiple body parts (**Figure 6B**). For iGluR/IR-encoding genes, *OchiIR28* and *29* were expressed predominately in antennae (**Figure 6C**).

All antenna-predominant genes were further analyzed using RT-qPCR (**Figure 7**). *OchiOR2*, *6*, *8*, *9*, *11*, *15*, *33*, *38*, *39*, *41*, *43*, *44*, *48*, *50*, *53*, *56*, and *62* were significantly expressed at high levels in female antennae and *OchiOR34*, *46* and *86* were significantly expressed at higher levels in male antennae. The remaining OR-encoding unigenes were equally expressed in the antennae of both males and females (**Figure 7A**). For CSP-encoding genes, *OchiCSP10* was expressed at significantly higher levels in female antennae. Additionally, the SNMP-encoding gene *OchiSNMP1* were significantly upregulated in female antennae (**Figure 7B**). Other OBP- and IR-encoding genes were expressed largely equally in both males and females (**Figure 7B**).

DISCUSSION

Identification and characterization of chemosensory genes are important steps toward understanding the evolution and primary functions of the insect olfactory system. In this study, we identified a set of candidate chemosensory genes from *O. chinensis* via analyzing antennal transcriptomes. Genetic and phylogenetic analyses of candidate chemosensory genes in *O. chinensis* was carried out to examine the similarities and differences of molecular components in chemosensory pathways. We further analyzed the expression profiles of chemosensory genes to identify olfaction-specific genes for future functional studies.

Odorant-binding proteins play vital roles in carrying odorants through the hemolymph to OR neurons, and transducing the resultant signals to downstream effectors in the olfactory system (Hallem et al., 2006). The number of OBPs identified in our antennal transcriptome was comparable to its related Locust species, namely 18 from *O. infernalis*, 16 from *L. migratoria*, 15 from *O. asiaticus*, and 14 from *S. gregaria*) (Ban et al., 2003; Xu et al., 2009;

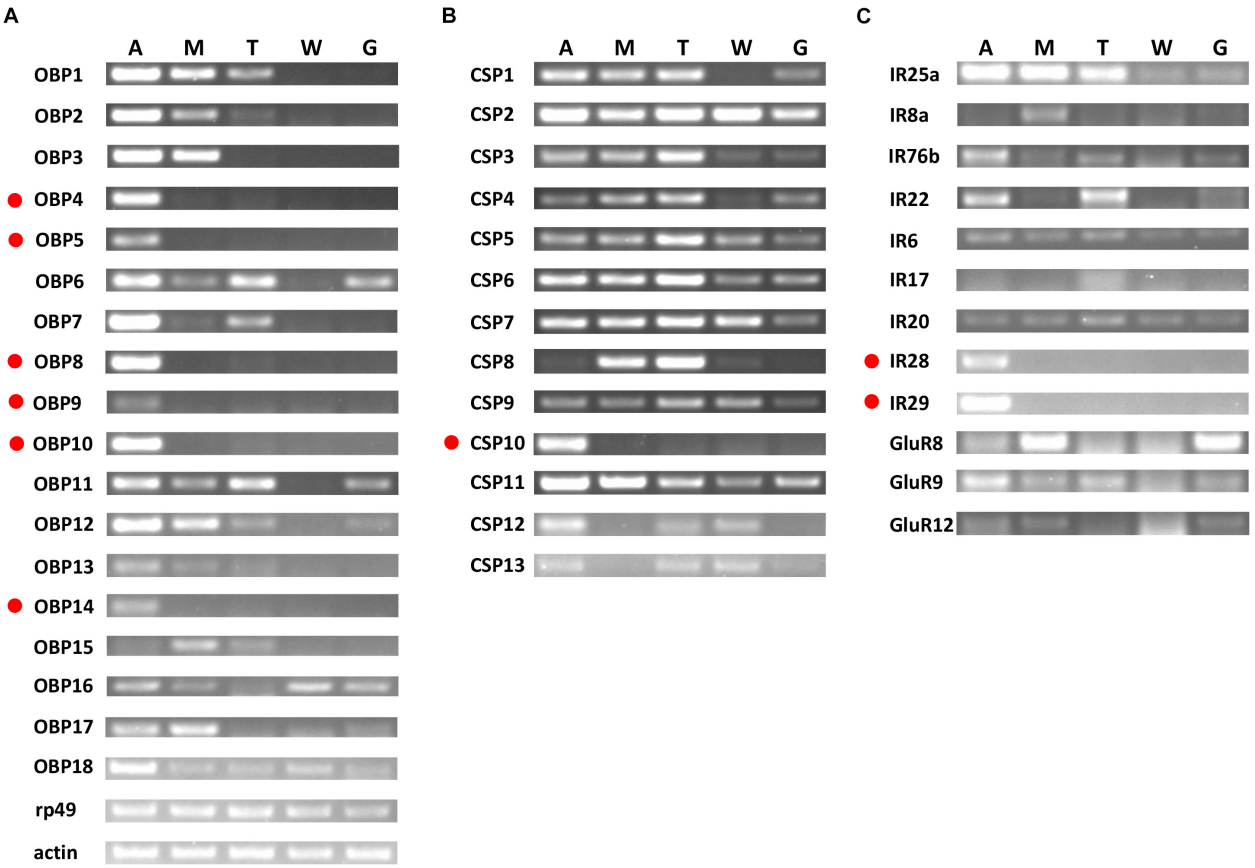

FIGURE 6 | Tissue-specific expression of *OchiOBP*s, *OchiCSP*s, and *OchilR*s. **(A)** OBPs. **(B)** CSPs. **(C)** IRs. Genes exclusively or predominantly expressed in antennae are labeled in red dots. The β-actin (*Ochiβ-actin*) and ribosomal protein 49 (*Ochirp49*) were used as internal references to test the integrity of each cDNA template. An, antennae; M, maxillary palps; T, foreleg tarsus; W, wings; G, genitals.

Yu et al., 2009; Zhang et al., 2015, 2018; Jiang et al., 2017). This may reflect physiological and evolutionary consistency between *O. chinensis* and other Locust species. OBPs from *O. chinensis* can be classified into four types: classic, atypical, plus-C (type-A and B), as well as Locust-specific OBPs (Jiang et al., 2017). Expression analysis revealed that five classic OBP (*OchiOBP4*, *5*, *8*, *10*, and *14*) and one atypical OBP (*OchiOBP9*) were expressed exclusively in antennae, suggesting that these genes are likely to have a role in antennal chemical-recognition processes. CSPs and OBPs can act as carriers for odorant molecules (Liu et al., 2012; Yi et al., 2013; Zhang T. et al., 2013; Zhang et al., 2014). However, in our RT-PCR analysis, only *OchiCSP10* showed significantly antennae-biased expression, suggesting that this CSP could be involved in olfactory function.

Olfactory receptors, which connect binding proteins and OSNs to transduce olfactory signals, are the best known group of insect chemoreceptors. Like other locust species, *O. chinensis* possesses an expanded OR family (94) compared with Dipterans, Lepidopterans, and Hemipterans (Vieira and Rozas, 2011). A large number of OR-encoding genes may be associated with its ability for diverse host-odor perception to feed on a wider range of host plants. Great variation in the number of OR genes was found in different Locust species. Specifically, 94 OR genes were identified in *O. chinensis*, less than 120 from *S. gregaria* (Pregitzer et al., 2017), and 141 from *L. migratoria* (Wang et al., 2015), but significantly more than 60 from *O. asiaticus* (Zhou et al., 2019). The variation in gene numbers may reflect that *O. chinensis* inhabits a different ecological niche than other locust species. Generally, sexually dimorphic expression of ORs in antennae indicates possible pheromone receptors contributing sexual behaviors. Typically, Lepidopteran sex pheromones are released via females to attract males. Several moth sex pheromone for ORs have been functionally characterized, and most of them are expressed at higher levels in the male antennae (Krieger et al., 2004; Wanner et al., 2010; Zhang and Löfstedt, 2013). ORs expressed predominantly in female antennae are predicted to function in the detection of egg-laying-related odorant (Pelletier et al., 2010) or male released pheromones (or signals) (Anderson et al., 2009); ORs expressed evenly in the male and female antennae are predicted to function in general odorant perception (Yan et al., 2015). Therefore, we hypothesize that some or all of female-predominant

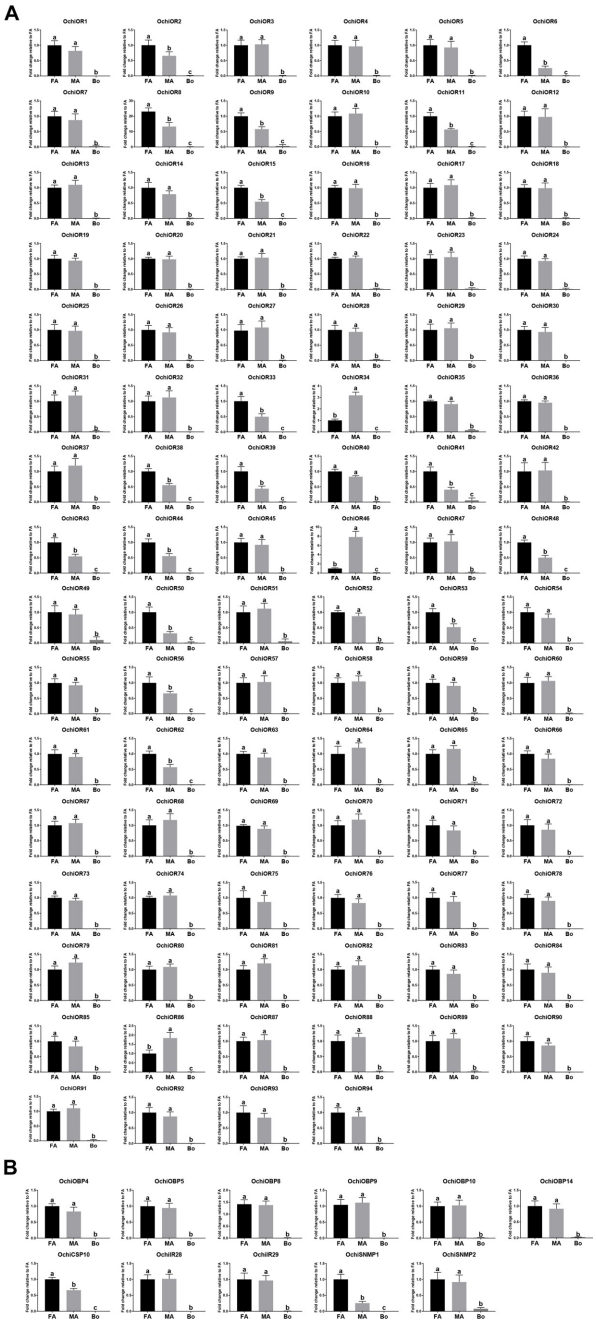

FIGURE 7 | Relative expression levels of the olfactory-related genes in the female antennae, male antennae, and other body parts from *Oxya chinensis*. **(A)** ORs. **(B)** SNMPs and the antenna-predominant candidates (OBPs, CSPs, and IRs). FA, female antennae; MA, male antennae; Bo, other body parts. The expression levels were estimated using the $2^{-\Delta\Delta CT}$ method. Bars represent standard error of three independent biological replicates with three technical duplicates for each replicate. Different small letters indicate statistically significant difference between tissues ($p < 0.05$, ANOVA, HSD).

OchiORs, including *OchiOR2*, *6*, *8*, *9*, *11*, *15*, *33*, *38*, *39*, *41*, *43*, *44*, *48*, *50*, *53*, *56*, and *62*), are likely involved in female specific behaviors such as finding plant hosts for oviposition. Male-predominant ORs (*OchiOR34*, *46*, and *86*) may be associated with detecting female sex pheromones. The remaining ORs with roughly equal expression levels in female and male antennae might be dedicated to general odorant detection.

Ionotropic receptors are conserved proteins and play key roles in the synaptic ligand-gated ion channels involved in olfaction, gustation, thermosensation and hygrosensation (Min et al., 2013; Zhang Y.V. et al., 2013; Koh et al., 2014; Chen et al., 2015; Stewart et al., 2015; Croset et al., 2016; Gorter et al., 2016; Hussain et al., 2016; Knecht et al., 2016, 2017; Ni et al., 2016; Prieto-Godino et al., 2016; Ganguly et al., 2017; Tauber et al., 2017). We identified nine antennal IR genes (*OchiIR25a*, *8a*, *76b*, *22*, *6*, *17*, *20*, *28*, and *29*) and three iGluRs (*OchiGluR8*, *9*, and *12*) from *O. chinensis*. In general, most antennal IRs were conserved across orders Diptera, Lepidoptera and Coleoptera, but only three IR co-receptor orthologs (*OchiIR25a*, *8a*, and *76b*) were found in *O. chinensis*, and there were no antennal IRs orthologs with *D. melanogaster* (Benton et al., 2009). In *D. melanogaster*, antennal IRs function as chemoreceptors (Benton et al., 2009) and are expressed in the peripheral olfactory neurons associated with the detection of amines, acids, general odors and sex pheromones (Ai et al., 2010; Silbering et al., 2011; Kain et al., 2013; Koh et al., 2014; Hussain et al., 2016). Notably, we found that two antennal IR genes (*OchiIR28* and *29*) were exclusively expressed in antennae, suggesting they potentially involved in odorant reception.

We also identified two SNMP unigenes. SNMPs are conserved throughout holometabolous insects and the SNMP1 subfamily are usually expressed in pheromone-sensitive OSNs, and mediate responses to lipid pheromones (Jin et al., 2008; Nichols and Vogt, 2008; Vogt et al., 2009; Gomez-Diaz et al., 2016). All SNMPs from locust species were clustered into the SNMP1 subclade. Both SNMPs were predominantly expressed in antennae in *O. chinensis*, supporting that these two SNMPs may perform functions in pheromone perception. Interestingly, *OchiSNMP1* was predominantly expressed in female antennae (**Figure 7B**), suggesting that *OchiSNMP1* may participate in sex pheromone reception.

DATA AVAILABILITY STATEMENT

The datasets generated for this study can be found in the clean reads from the *O. chinensis* female antennae and male antennae were deposited in the NCBI Sequence Read Archive (Female antennae: SAMN11484273; Male antennae: SAMN11484274).

AUTHOR CONTRIBUTIONS

YC and CK performed the experiments. ZW analyzed the data. ZW and JL wrote and revised the manuscript.

FUNDING

This work was supported by the Guang Zhou City Key Laboratory of Subtropical Fruit Tree Outbreak Control (Grant No. 201805010008) and the Serious Pest and Disease Mechanism and Sustainable Control Innovation Team of Guangdong Province (Grant No. 2017KCXTD018).

ACKNOWLEDGMENTS

We thank Dr. Mingshun Chen (Kansas State University, United States) for comments and editorial assistance on the manuscript.

SUPPLEMENTARY MATERIAL

The Supplementary Material for this article can be found online at: https://www.frontiersin.org/articles/10.3389/fphys.2019.01223/full#supplementary-material

FIGURE S1 | Transcriptome overview of *O. chinensis* antennae. **(A)** Unigenes annotated through different databases. **(B)** Gene ontology (GO) classification of the *O. chinensis* unigenes.

FIGURE S2 | The amino acid alignment of the predicted classic OBPs.

FIGURE S3 | The amino acid alignment of the predicted atypical OBPs.

FIGURE S4 | The amino acid alignment of the predicted plus-C OBPs type-A.

FIGURE S5 | The amino alignment of the predicted plus-C OBPs type-B.

FIGURE S6 | The amino alignment of the predicted CSPs.

TABLE S1 | List of OBPs, CSPs, ORs, IRs, and SNMPs in Orthopteran species.

TABLE S2 | A list of the identified OBPs, CSPs, ORs, IRs and SNMPs in *O. chinensis*, and detailed genetic characteristics, best matches in NCBI-nr database, protein domains and estimated expression levels found in each petal module.

TABLE S3 | The amino acid sequences used for phylogenetic analyses.

TABLE S4 | Gene-specific primers used for semi-quantitative RT-PCR and RT-qPCR.

TABLE S5 | Overview of the sequencing and assembly process.

REFERENCES

Ai, M., Blais, S., Park, J. Y., Min, S., Neubert, T. A., and Suh, G. S. (2013). Ionotropic glutamate receptors IR64a and IR8a form a functional odorant receptor complex in vivo in Drosophila. *J. Neurosci.* 33, 10741–10749. doi: 10.1523/JNEUROSCI.5419-12.2013

Ai, M., Min, S., Grosjean, Y., Leblanc, C., Bell, R., Benton, R., et al. (2010). Acid sensing by the Drosophila olfactory system. *Nature* 468, 691–695. doi: 10.1038/nature09537

Anderson, A. R., Wanner, K. W., Trowell, S. C., Warr, C. G., Jaquin-Joly, E., Zagatti, P., et al. (2009). Molecular basis of female-specific odorant responses in Bombyx mori. *Insect Biochem. Mol. Biol.* 39, 189–197. doi: 10.1016/j.ibmb.2008.11.002

Andersson, M. N., Grosse-Wilde, E., Keeling, C. I., Bengtsson, J. M., Yuen, M. M., Li, M., et al. (2013). Antennal transcriptome analysis of the chemosensory gene families in the tree killing bark beetles, *Ips typographus* and *Dendroctonus ponderosae* (Coleoptera: Curculionidae: Scolytinae). *BMC Genomics* 14:198. doi: 10.1186/1471-2164-14-198

Andersson, M. N., Videvall, E., Walden, K. K., Harris, M. O., Robertson, H. M., and Löfstedt, C. (2014). Sex- and tissue-specific profiles of chemosensory gene expression in a herbivorous gall-inducing fly (Diptera: Cecidomyiidae). *BMC Genomics* 15:501. doi: 10.1186/1471-2164-15-501

Ban, L., Scaloni, A., D'Ambrosio, C., Zhang, L., Yahn, Y., and Pelosi, P. (2003). Biochemical characterization and bacterial expression of an odorant-binding protein from *Locusta migratoria*. *Cell Mol. Life Sci.* 60, 390–400. doi: 10.1007/s000180300032

Benton, R., Vannice, K. S., Gomez-Diaz, C., and Vosshall, L. B. (2009). Variant ionotropic glutamate receptors as chemosensory receptors in Drosophila. *Cell* 136, 149–162. doi: 10.1016/j.cell.2008.12.001

Benton, R., Vannice, K. S., and Vosshall, L. B. (2007). An essential role for a CD36-related receptor in pheromone detection in Drosophila. *Nature* 450, 289–293. doi: 10.1038/nature06328

Brand, P., Ramírez, S. R., Leese, F., Quezada-Euan, J. J., Tollrian, R., and Eltz, T. (2015). Rapid evolution of chemosensory receptor genes in a pair of sibling species of orchid bees (Apidae: Euglossini). *BMC Evol. Biol.* 15:176. doi: 10.1186/s12862-015-0451-9

Chen, C., Buhl, E., Xu, M., Croset, V., Rees, J. S., Lilley, K. S., et al. (2015). Drosophila ionotropic receptor 25a mediates circadian clock resetting by temperature. *Nature* 527, 516–520. doi: 10.1038/nature16148

Clyne, P. J., Warr, C. G., and Carlson, J. R. (2000). Candidate taste receptors in Drosophila. *Science* 287, 1830–1834. doi: 10.1126/science.287.5459.1830

Clyne, P. J., Warr, C. G., Freeman, M. R., Lessing, D., Kim, J., and Carlson, J. R. (1999). A novel family of divergent seven-transmembrane proteins: candidate odorant receptors in Drosophila. *Neuron* 22, 327–338. doi: 10.1016/s0896-6273(00)81093-4

Cock, P. J., Fields, C. J., Goto, N., Heuer, M. L., and Rice, P. M. (2010). The sanger FASTQ file format for sequences with quality scores, and the Solexa/Illumina FASTQ variants. *Nucleic Acids Res.* 38, 1767–1771. doi: 10.1093/nar/gkp1137

Conesa, A., Gotz, S., Garcia-Gomez, J. M., Terol, J., Talon, M., and Robles, M. (2005). Blast2GO: a universal tool for annotation, visualization and analysis in functional genomics research. *Bioinformatics* 21, 3674–3676. doi: 10.1093/bioinformatics/bti610

Croset, V., Schleyer, M., Arguello, J. R., Gerber, B., and Benton, R. (2016). A molecular and neuronal basis for amino acid sensing in the Drosophila larva. *Sci. Rep.* 6:34871. doi: 10.1038/srep34871

Galindo, K., and Smith, D. P. (2001). A large family of divergent Drosophila odorant-binding proteins expressed in gustatory and olfactory sensilla. *Genetics* 159, 1059–1072.

Ganguly, A., Pang, L., Duong, V. K., Lee, A., Schoniger, H., Varady, E., et al. (2017). A molecular and cellular context-dependent role for Ir76b in detection of amino acid taste. *Cell Rep.* 18, 737–750. doi: 10.1016/j.celrep.2016.12.071

Gomez-Diaz, C., Bargeton, B., Abuin, L., Bukar, N., Reina, J. H., Bartoi, T., et al. (2016). A CD36 ectodomain mediates insect pheromone detection via a putative tunnelling mechanism. *Nat. Commun.* 7:11866. doi: 10.1038/ncomms11866

Gomez-Diaz, C., Reina, J. H., Cambillau, C., and Benton, R. (2013). Ligands for pheromone-sensing neurons are not conformationally activated odorant binding proteins. *PLoS Biol.* 11:e1001546. doi: 10.1371/journal.pbio.1001546

Gorter, J. A., Jagadeesh, S., Gahr, C., Boonekamp, J. J., Levine, J. D., and Billeter, J. C. (2016). The nutritional and hedonic value of food modulate sexual receptivity in *Drosophila melanogaster* females. *Sci. Rep.* 6:19441. doi: 10.1038/srep19441

Gotz, S., Garcia-Gomez, J. M., Terol, J., Williams, T. D., Nagaraj, S. H., Nueda, M. J., et al. (2008). High-throughput functional annotation and data mining with the Blast2GO suite. *Nucleic Acids Res.* 36, 3420–3435. doi: 10.1093/nar/gkn176

Grabherr, M. G., Haas, B. J., Yassour, M., Levin, J. Z., Thompson, D. A., Amit, I., et al. (2011). Full-length transcriptome assembly from RNA-Seq data without a reference genome. *Nat. Biotechnol.* 29, 644–652. doi: 10.1038/nbt.1883

Grosjean, Y., Rytz, R., Farine, J. P., Abuin, L., Cortot, J., Jefferis, G. S., et al. (2011). An olfactory receptor for food-derived odours promotes male courtship in Drosophila. *Nature* 478, 236–240. doi: 10.1038/nature10428

Grosse-Wilde, E., Kuebler, L. S., Bucks, S., Vogel, H., Wicher, D., and Hansson, B. S. (2011). Antennal transcriptome of *Manduca sexta*. *Proc. Natl. Acad. Sci. U.S.A.* 108, 7449–7454. doi: 10.1073/pnas.1017963108

Hallem, E. A., Dahanukar, A., and Carlson, J. R. (2006). Insect odor and taste receptors. *Annu. Rev. Entomol.* 51, 113–135. doi: 10.1146/annurev.ento.51.051705.113646

Hussain, A., Zhang, M., Ucpunar, H. K., Svensson, T., Quillery, E., Gompel, N., et al. (2016). Ionotropic chemosensory receptors mediate the taste and smell of polyamines. *PLoS Biol.* 14:e1002454. doi: 10.1371/journal.pbio.1002454

Jiang, X., Krieger, J., Breer, H., and Pregitzer, P. (2017). Distinct subfamilies of odorant binding proteins in locust (Orthoptera, Acrididae): molecular evolution, structural variation, and sensilla-specific expression. *Front. Physiol.* 8:734. doi: 10.3389/fphys.2017.00734

Jiang, X., Pregitzer, P., Grosse-Wilde, E., Breer, H., and Krieger, J. (2016). Identification and characterization of two "Sensory Neuron Membrane Proteins" (SNMPs) of the desert locust, *Schistocerca gregaria* (Orthoptera: Acrididae). *J. Insect Sci.* 16:33. doi: 10.1093/jisesa/iew015

Jin, X., Ha, T. S., and Smith, D. P. (2008). SNMP is a signaling component required for pheromone sensitivity in Drosophila. *Proc. Natl. Acad. Sci. U.S.A.* 105, 10996–11001. doi: 10.1073/pnas.0803309105

Kain, P., Boyle, S. M., Tharadra, S. K., Guda, T., Christine, P., Dahanukar, A., et al. (2013). Odour receptors and neurons for DEET and new insect repellents. *Nature* 502, 507–512. doi: 10.1038/nature12594

Katoh, K., and Standley, D. M. (2013). MAFFT multiple sequence alignment software version 7: improvements in performance and usability. *Mol. Biol. Evol.* 30, 772–780. doi: 10.1093/molbev/mst010

Kearse, M., Moir, R., Wilson, A., Stones-Havas, S., Cheung, M., Sturrock, S., et al. (2012). Geneious basic: an integrated and extendable desktop software platform for the organization and analysis of sequence data. *Bioinformatics* 28, 1647–1649. doi: 10.1093/bioinformatics/bts199

Knecht, Z. A., Silbering, A. F., Cruz, J., Yang, L., Croset, V., Benton, R., et al. (2017). Ionotropic receptor-dependent moist and dry cells control hygrosensation in Drosophila. *eLife* 6:e26654. doi: 10.7554/eLife.26654

Knecht, Z. A., Silbering, A. F., Ni, L., Klein, M., Budelli, G., Bell, R., et al. (2016). Distinct combinations of variant ionotropic glutamate receptors mediate thermosensation and hygrosensation in Drosophila. *eLife* 5:e17879. doi: 10.7554/eLife.17879

Koh, T. W., He, Z., Gorur-Shandilya, S., Menuz, K., Larter, N. K., Stewart, S., et al. (2014). The Drosophila IR20a clade of ionotropic receptors are candidate taste and pheromone receptors. *Neuron* 83, 850–865. doi: 10.1016/j.neuron.2014.07.012

Krieger, J., Grosse-Wilde, E., Gohl, T., Dewer, Y. M., Raming, K., and Breer, H. (2004). Genes encoding candidate pheromone receptors in a moth (*Heliothis virescens*). *Proc. Natl. Acad. Sci. U.S.A.* 101, 11845–11850. doi: 10.1073/pnas.0403052101

Leal, W. S. (2013). Odorant reception in insects: roles of receptors, binding proteins, and degrading enzymes. *Annu. Rev. Entomol.* 58, 373–391. doi: 10.1146/annurev-ento-120811-153635

Li, B., and Dewey, C. N. (2011). RSEM: accurate transcript quantification from RNA-Seq data with or without a reference genome. *BMC Bioinformatics* 12:323. doi: 10.1186/1471-2105-12-323

Li, Z., Ni, J. D., Huang, J., and Montell, C. (2014). Requirement for Drosophila SNMP1 for rapid activation and termination of pheromone-induced activity. *PLoS Genet.* 10:e1004600. doi: 10.1371/journal.pgen.1004600

Liu, R., He, X., Lehane, S., Lehane, M., Hertz-Fowler, C., Berriman, M., et al. (2012). Expression of chemosensory proteins in the tsetse fly *Glossina morsitans morsitans* is related to female host-seeking behaviour. *Insect Mol. Biol.* 21, 41–48. doi: 10.1111/j.1365-2583.2011.01114.x

Livak, K. J., and Schmittgen, T. D. (2001). Analysis of relative gene expression data using real-time quantitative PCR and the 2-DELTADELTACT method. *Methods* 25, 402–408. doi: 10.1006/meth.2001.1262

Lu, F. P., Zhao, D. X., and Wang, A. P. (2008). Electroantennogram and behavioral responses of *Oxya chinensis* (Orthoptera: Acrididae) to plant volatiles. *Chin. J. Trop. Crops* 29, 225–230.

Martin-Blazquez, R., Chen, B., Kang, L., and Bakkali, M. (2017). Evolution, expression and association of the chemosensory protein genes with the outbreak phase of the two main pest locusts. *Sci. Rep.* 7:6653. doi: 10.1038/s41598-017-07068-0

Min, S., Ai, M., Shin, S. A., and Suh, G. S. (2013). Dedicated olfactory neurons mediating attraction behavior to ammonia and amines in Drosophila. *Proc. Natl. Acad. Sci. U.S.A.* 110, E1321–E1329. doi: 10.1073/pnas.1215680110

Ni, L., Klein, M., Svec, K. V., Budelli, G., Chang, E. C., Ferrer, A. J., et al. (2016). The ionotropic receptors IR21a and IR25a mediate cool sensing in Drosophila. *eLife* 5:e13254. doi: 10.7554/eLife.13254

Nichols, Z., and Vogt, R. G. (2008). The SNMP/CD36 gene family in Diptera, Hymenoptera and Coleoptera: *Drosophila melanogaster*, *D-pseudoobscura*, *Anopheles gambiae*, *Aedes aegypti*, *Apis mellifera*, and *Tribolium castaneum*. *Insect Biochem. Mol. Biol.* 38, 398–415. doi: 10.1016/j.ibmb.2007.11.003

Paula, D. P., Togawa, R. C., Costa, M. M., Grynberg, P., Martins, N. F., and Andow, D. A. (2016). Identification and expression profile of odorant-binding proteins in *Halyomorpha halys* (Hemiptera: Pentatomidae). *Insect Mol. Biol.* 25, 580–594. doi: 10.1111/imb.12243

Pelletier, J., Hughes, D. T., Luetje, C. W., and Leal, W. S. (2010). An odorant receptor from the southern house mosquito *Culex pipiens quinquefasciatus* sensitive to oviposition attractants. *PLoS One* 5:e10090. doi: 10.1371/journal.pone.0010090

Pregitzer, P., Jiang, X., Grosse-Wilde, E., Breer, H., Krieger, J., and Fleischer, J. (2017). In search for pheromone receptors: certain members of the odorant receptor family in the desert locust *Schistocerca gregaria* (Orthoptera: Acrididae) Are Co-expressed with SNMP1. *Int. J. Biol. Sci.* 13, 911–922. doi: 10.7150/ijbs.18402

Price, M. N., Dehal, P. S., and Arkin, A. P. (2009). FastTree: computing large minimum evolution trees with profiles instead of a distance matrix. *Mol. Biol. Evol.* 26, 1641–1650. doi: 10.1093/molbev/msp077

Price, M. N., Dehal, P. S., and Arkin, A. P. (2010). FastTree 2–approximately maximum-likelihood trees for large alignments. *PLoS One* 5:e9490. doi: 10.1371/journal.pone.0009490

Prieto-Godino, L. L., Rytz, R., Bargeton, B., Abuin, L., Arguello, J. R., Peraro, M. D., et al. (2016). Olfactory receptor pseudo-pseudogenes. *Nature* 539, 93–97. doi: 10.1038/nature19824

Quevillon, E., Silventoinen, V., Pillai, S., Harte, N., Mulder, N., Apweiler, R., et al. (2005). InterProScan: protein domains identifier. *Nucleic Acids Res.* 33, W116–W120.

Robinson, M. D., McCarthy, D. J., and Smyth, G. K. (2010). edgeR: a Bioconductor package for differential expression analysis of digital gene expression data. *Bioinformatics* 26, 139–140. doi: 10.1093/bioinformatics/btp616

Robinson, M. D., and Oshlack, A. (2010). A scaling normalization method for differential expression analysis of RNA-seq data. *Genome Biol.* 11:R25. doi: 10.1186/gb-2010-11-3-r25

Rogers, M. E., Krieger, J., and Vogt, R. G. (2001). Antennal SNMPs (Sensory Neuron Membrane Proteins) of lepidoptera define a unique family of invertebrate CD36-like proteins. *J. Neurobiol.* 49, 47–61. doi: 10.1002/neu.1065

Rogers, M. E., Sun, M., Lerner, M. R., and Vogt, R. G. (1997). Snmp-1, a novel membrane protein of olfactory neurons of the silk moth *Antheraea polyphemus* with homology to the CD36 family of membrane proteins. *J. Biol. Chem.* 272, 14792–14799. doi: 10.1074/jbc.272.23.14792

Sandler, B. H., Nikonova, L., Leal, W. S., and Clardy, J. (2000). Sexual attraction in the silkworm moth: structure of the pheromone-binding-protein-bombykol complex. *Chem. Biol.* 7, 143–151. doi: 10.1016/S1074-5521(00)00078-8

Silbering, A. F., Rytz, R., Grosjean, Y., Abuin, L., Ramdya, P., Jefferis, G. S., et al. (2011). Complementary function and integrated wiring of the evolutionarily distinct drosophila olfactory subsystems. *J. Neurosci.* 31, 13357–13375. doi: 10.1523/JNEUROSCI.2360-11.2011

Stewart, S., Koh, T. W., Ghosh, A. C., and Carlson, J. R. (2015). Candidate ionotropic taste receptors in the Drosophila larva. *Proc. Natl. Acad. Sci. U.S.A.* 112, 4195–4201. doi: 10.1073/pnas.1503292112

Su, C., and Carlson, J. R. (2013). Neuroscience. Circuit logic of avoidance and attraction. *Science* 340, 1295–1297. doi: 10.1126/science.1240139

Tauber, J. M., Brown, E. B., Li, Y., Yurgel, M. E., Masek, P., and Keene, A. C. (2017). A subset of sweet-sensing neurons identified by IR56d are necessary and sufficient for fatty acid taste. *PLoS Genet.* 13:e1007059. doi: 10.1371/journal.pgen.1007059

Trapnell, C., Williams, B. A., Pertea, G., Mortazavi, A., Kwan, G., van Baren, M. J., et al. (2010). Transcript assembly and quantification by RNA-Seq reveals unannotated transcripts and isoform switching during cell differentiation. *Nat. Biotechnol.* 28, 511–515. doi: 10.1038/nbt.1621

Venthur, H., and Zhou, J. J. (2018). Odorant receptors and odorant-binding proteins as insect pest control targets: a comparative analysis. *Front. Physiol.* 9:1163. doi: 10.3389/fphys.2018.01163

Vieira, F. G., and Rozas, J. (2011). Comparative genomics of the odorant-binding and chemosensory protein gene families across the arthropoda: origin and evolutionary history of the chemosensory system. *Genome Biol. Evol.* 3, 476–490. doi: 10.1093/gbe/evr033

Vogt, R. G., Miller, N. E., Litvack, R., Fandino, R. A., Sparks, J., Staples, J., et al. (2009). The insect SNMP gene family. *Insect Biochem. Mol. Biol.* 39, 448–456. doi: 10.1016/j.ibmb.2009.03.007

Vogt, R. G., Riddiford, L. M., and Prestwich, G. D. (1985). Kinetic properties of a sex pheromone-degrading enzyme: the sensillar esterase of *Antheraea polyphemus*. *Proc. Natl. Acad. Sci. U.S.A.* 82, 8827–8831. doi: 10.1073/pnas.82.24.8827

Vosshall, L. B., Amrein, H., Morozov, P. S., Rzhetsky, A., and Axel, R. (1999). A spatial map of olfactory receptor expression in the Drosophila antenna. *Cell* 96, 725–736. doi: 10.1016/s0092-8674(00)80582-6

Wang, Z., Yang, P., Chen, D., Jiang, F., Li, Y., Wang, X., et al. (2015). Identification and functional analysis of olfactory receptor family reveal unusual characteristics of the olfactory system in the migratory locust. *Cell Mol. Life Sci.* 72, 4429–4443. doi: 10.1007/s00018-015-2009-9

Wanner, K. W., Nichols, A. S., Allen, J. E., Bunger, P. L., Garczynski, S. F. Jr., Linn, C. E., et al. (2010). Sex pheromone receptor specificity in the european corn borer moth, *Ostrinia nubilalis*. *PLoS One* 5:e8685. doi: 10.1371/journal.pone.0008685

Xu, P., Atkinson, R., Jones, D. N., and Smith, D. P. (2005). *Drosophila* OBP LUSH is required for activity of pheromone-sensitive neurons. *Neuron* 45, 193–200. doi: 10.1016/j.neuron.2004.12.031

Xu, Y. L., He, P., Zhang, L., Fang, S. Q., Dong, S. L., Zhang, Y. J., et al. (2009). Large-scale identification of odorant-binding proteins and chemosensory proteins from expressed sequence tags in insects. *BMC Genomics* 10:632. doi: 10.1186/1471-2164-10-632

Yan, S. W., Zhang, J., Liu, Y., Li, G. Q., and Wang, G. R. (2015). An olfactory receptor from *Apolygus lucorum* (Meyer-Dur) mainly tuned to volatiles from flowering host plants. *J. Insect Physiol.* 79, 36–41. doi: 10.1016/j.jinsphys.2015.06.002

Yi, X., Zhao, H., Dong, X., Wang, P., Hu, M., and Zhong, G. (2013). BdorCSP2 is important for antifeed and oviposition-deterring activities induced by Rhodojaponin-III against *Bactrocera dorsalis*. *PLoS One* 8:e77295. doi: 10.1371/journal.pone.0077295

Yu, F., Zhang, S., Zhang, L., and Pelosi, P. (2009). Intriguing similarities between two novel odorant-binding proteins of locusts. *Biochem. Biophys. Res. Commun.* 385, 369–374. doi: 10.1016/j.bbrc.2009.05.074

Zhang, D. D., and Löfstedt, C. (2013). Functional evolution of a multigene family: orthologous and paralogous pheromone receptor genes in the turnip moth, *Agrotis segetum*. *PLoS One* 8:e77345. doi: 10.1371/journal.pone.0077345

Zhang, S., Pang, B., and Zhang, L. (2015). Novel odorant-binding proteins and their expression patterns in grasshopper, *Oedaleus asiaticus*. *Biochem. Biophys. Res. Commun.* 460, 274–280. doi: 10.1016/j.bbrc.2015.03.024

Zhang, T., Wang, W., Zhang, Z., Zhang, Y., and Guo, Y. (2013). Functional characteristics of a novel chemosensory protein in the cotton bollworm *Helicoverpa armigera* (Hubner). *J. Integr. Agric.* 12, 853–861. doi: 10.1016/s2095-3119(13)60304-4

Zhang, Y., Tan, Y., Zhou, X. R., and Pang, B. P. (2018). A whole-body transcriptome analysis and expression profiling of odorant binding protein genes in *Oedaleus infernalis*. *Comp. Biochem. Physiol. Part D Genomics Proteomics* 28, 134–141. doi: 10.1016/j.cbd.2018.08.003

Zhang, Y. N., Ye, Z. F., Yang, K., and Dong, S. L. (2014). Antenna-predominant and male-biased CSP19 of *Sesamia inferens* is able to bind the female sex pheromones and host plant volatiles. *Gene* 536, 279–286. doi: 10.1016/j.gene.2013.12.011

Zhang, Y. V., Ni, J., and Montell, C. (2013). The molecular basis for attractive salt-taste coding in Drosophila. *Science* 340, 1334–1338. doi: 10.1126/science.1234133

Zhou, Y. T., Li, L., Zhou, X. R., Tan, Y., and Pang, B. P. (2019). Identification and expression profiling of candidate chemosensory membrane proteins in the band-winged grasshopper, *Oedaleus asiaticus*. *Comp. Biochem. Physiol. Part D Genomics Proteomics* 30, 33–44. doi: 10.1016/j.cbd.2019.02.002

Conflict of Interest: The authors declare that the research was conducted in the absence of any commercial or financial relationships that could be construed as a potential conflict of interest.

frontiers in Physiology

ORIGINAL RESEARCH
published: 22 October 2019
doi: 10.3389/fphys.2019.01280

Duality of 5-HT Effects on Crayfish Motoneurons

*Julien Bacqué-Cazenave[1], Pascal Fossat[1†], Fadi A. Issa[2], Donald H. Edwards[2], Jean Paul Delbecque[1] and Daniel Cattaert[1]**

[1]University of Bordeaux, CNRS, Institut de Neurosciences Cognitives et Intégratives d'Aquitaine (INCIA) UMR5287, Bordeaux, France, [2]Neuroscience Institute, College of Arts and Sciences, Georgia State University, Atlanta, GA, United States

Serotonin (5-HT) is a major neuromodulator acting on the nervous system. Its various effects have been studied in vertebrates, as well as in arthropods, from the cellular and subcellular compartments up to the behavioral level, which includes the control of mood, aggression, locomotion, and anxiety. The diversity of responses of neurons to 5-HT has been related to its mode of application, the diversity of 5-HT-receptors, and the animals' social status history. In the locomotor network of socially isolated crayfish, the duality of 5-HT-evoked responses (excitatory/inhibitory) on motoneurons (MNs), sensorimotor pathways, and their consequences on motor network activity has largely been studied. The aim of the present report is to examine if this duality of exogenous 5-HT-evoked responses in the crayfish locomotor network can be reproduced by direct activation of 5-HT neurons in the case of socially isolated animals. Our previous studies have focused on the mechanisms supporting these opposite effects on MNs, pointing out spatial segregation of 5-HT receptors responsible either for positive or negative responses. Here, we report new findings indicating that excitatory and inhibitory effects can be achieved simultaneously in different leg MNs by the activation of a single 5-HT cell in the first abdominal ganglion.

Keywords: serotonin, motoneuron, excitatory and inhibitory balance, crayfish (*Procambarus clarkii*), locomotor network, sensori-motor interactions, serotoninergic neuron

OPEN ACCESS

Edited by:
Sylvia Anton,
Institut National de la Recherche Agronomique (INRA), France

Reviewed by:
Ansgar Buschges,
University of Cologne, Germany
Wolfgang Stein,
Illinois State University, United States

***Correspondence:**
Daniel Cattaert
daniel.cattaert@u-bordeaux.fr

†Present address:
Pascal Fossat,
UMR5297 Institut Interdisciplinaire des Neurosciences (IINS), Bordeaux, France

Specialty section:
This article was submitted to Invertebrate Physiology, a section of the journal Frontiers in Physiology

Received: *31 May 2019*
Accepted: *24 September 2019*
Published: *22 October 2019*

Citation:
Bacqué-Cazenave J, Fossat P, Issa FA, Edwards DH, Delbecque JP and Cattaert D (2019) Duality of 5-HT Effects on Crayfish Motoneurons. Front. Physiol. 10:1280. doi: 10.3389/fphys.2019.01280

INTRODUCTION

The neuromodulator serotonin (5-HT) has widespread effects in the physiology of animals and humans, particularly controlling changes in behavior and motor activity in rat (Cazalets et al., 1992), insects (Buhl et al., 2008), and crustacean stomatogastric ganglion (Zhang and Harris-Warrick, 1994). In crustaceans, serotonin is particularly known to trigger dominant-like posture (Livingstone et al., 1980; Kravitz, 1988), to influence aggressiveness and the decision to retreat (Huber et al., 1997a,b; Huber and Delago, 1998; Bacqué-Cazenave et al., 2018), to modulate social status (Huber et al., 1997b, 2001), and to control escape behavior (Teshiba et al., 2001), as well as anxiety-like behavior (Fossat et al., 2014, 2015; Bacqué-Cazenave et al., 2017). Some transient effects of 5-HT, as observed during anxiety-like behavior, appear to involve brain circuits because 5-HT levels are increased in brain tissues but not in ventral nerve cord (Fossat et al., 2014), while other more durable effects of 5-HT involve changes in the ventral nerve cord (Yeh et al., 1996; Cattaert et al., 2010).

In the ventral nerve cord of crayfish, the walking leg postural network consists of sensory-motor circuits controlling leg joints, and is well studied for the second joint responsible for upward and downward leg movements (El Manira et al., 1991; Le Bon-Jego and Cattaert, 2002). At this joint, a proprioceptor, the coxo-basal chordotonal organ (CBCO), mediates a resistance reflex *via* monosynaptic connections (El Manira et al., 1991) and polysynaptic pathways (Le Bon-Jego et al., 2004), and so plays an important role in the control of leg's posture. *In vitro,* the application of 5-HT on the walking leg postural network evokes several cooperative effects involving changes in membrane potential, input resistance (R_{in}), and time constants of motoneurons (MNs), and in the level of activation of polysynaptic excitatory pathways of the resistance reflex (Le Bon-Jego et al., 2004). However, the amplitude of these effects is very variable among the MN pools in a single experiment (Le Bon-Jego et al., 2004). Moreover, the social status of the animal determines the sign of the response to 5-HT, being excitatory in dominant and inhibitory in subordinate animals (Cattaert et al., 2010). In a first attempt to decipher the origin of excitatory and inhibitory responses evoked by 5-HT, we previously used local micro-application of 5-HT on the walking leg postural network and showed that two types of responses could be evoked in the same depressor MN depending on the location of the puff electrode on the neuron (Bacqué-Cazenave et al., 2013). When 5-HT was applied close to the initial segment of MNs, the response of Dep MNs was inhibitory (opening of a presumed K^+ channel, leading to hyperpolarization of the membrane and drop in input resistance), while a more central application in the neuropile resulted in an excitatory response that involved closing of a presumed K^+ channel resulting in membrane depolarization and increase of input resistance.

However, very little is known about the natural source of 5-HT that could induce such modulatory effects. In the present report, we have studied the effect of one source of 5-HT [a pair of 5-HT cells in the first abdominal (A1) ganglia] on the walking leg postural network of crayfish. Indeed 5-HT immunocytochemical studies have demonstrated the presence of pairs of large, anteriorly projecting 5-HT cells in the fifth thoracic (T5) and first abdominal ganglia (A1) (Beltz and Kravitz, 1983, 1987; Beltz, 1999). It is therefore possible that the response to 5-HT reflects the sensitivity of the walking leg postural network to 5-HT released by these cells. However, it is not known if these 5-HT cells project onto the postural circuit, or whether the activation of the 5-HT cells could elicit the several cooperative effects observed with 5-HT application (Le Bon-Jego et al., 2004) and whether these effects would be excitatory or inhibitory.

In the present study, we addressed these questions using an *in vitro* preparation of the crayfish fifth walking leg postural network (El Manira et al., 1991) that permitted intracellular recordings to be made of both leg depressor motoneurons from the fifth thoracic ganglion (T5) and the left 5-HT cell from the first abdominal ganglion (A1). In order to eliminate the variations of responses to 5-HT due to social status, experiments were performed on socially isolated crayfish (Yeh et al., 1996). Our results show that (1) the activation of a single 5-HT cell can induce mixed excitatory and inhibitory effects on walking leg MNs; (2) these effects induce functional changes in the walking leg postural network by modifying the amplitude of the response of MNs to mechanosensory inputs; (3) the induced effects are multiple and cooperative, and they involve modifications of the intrinsic properties (input resistance, membrane potential) of Dep MNs; and (4) the effects on intrinsic properties of Dep MNs are direct, while the effects on sensory-motor response involve polysynaptic pathways.

MATERIALS AND METHODS

Experimental Animals

Experiments were performed on male adult crayfish (*Procambarus clarkii*) weighing 25–30 g. The animals were collected locally and maintained while individually isolated during 3 weeks before experiments. They were kept at 18–20°C on a 12:12 h light:dark cycle, and fed once a week with shrimp pellets and carrots.

In vitro Preparation

An *in vitro* preparation of the thoracic nervous system with motor nerves innervating the coxa-basis joint and the coxo-basipodite chordotonal organ (CBCO) of the fifth leg (**Figure 1A**) was used (Sillar and Skorupski, 1986; El Manira et al., 1991). Prior to dissection, each animal was chilled in iced-water for 30 min. Then it was decapitated and the thorax and abdomen were pinned dorsal side-up. A section of the ventral nerve cord containing the last three thoracic (*T3–T5)* and the first (*A1*) and second (*A2*) abdominal ganglia was dissected out with all the motor nerves of the two proximal segments of the left fifth leg: promotor (Pro), remotor (Rem), anterior levator (Lev), and depressor (Dep) (**Figure 1B**). The oxo-basipodite chordotonal organ (CBCO), which monitors the movements of the second joint (coxo-basipodite – **Figure 1A**), was also dissected out and kept intact. The distal end of its elastic strand was attached to an electromagnetic puller VT101 (Ling Dynamic Systems, Meudon-la-Forêt, France) controlled by a home-made function generator that allowed the application of sinewave movements to the CBCO strand (**Figure 1B**) to mimic upward (during stretch) and downward (during release) movements of the leg.

The preparation was pinned dorsal side up on a Sylgard-lined Petri dish (Dow Corning Corp., Wiesbaden, Germany). The nervous system was continuously superfused with oxygenated control saline composed of (in mM) 195 NaCl, 5 KCl, 13 $CaCl_2$, 2 $MgCl_2$, and 3 HEPES (Sigma Chemical, St Louis, MO) with a pH of 7.65. In some experiments, a high-divalent cation solution containing (in mM) 34 $CaCl_2$ and 6.4 $MgCl_2$, with the sodium concentration reduced accordingly to preserve the osmolarity of the solution, was used to raise the spiking threshold of the interneurons. The fourth and fifth thoracic ganglia and the first abdominal ganglion were desheathed to improve the superfusion of the central neurons and to allow for intracellular recordings from depressor MNs (**Figure 1B**, red inset) and ipsilateral 5-HT cell (**Figure 1B**, blue inset). For sensory-motor networks to be in a quiet state (no rhythmic activity), preparations were left resting for 1 h before starting experiments.

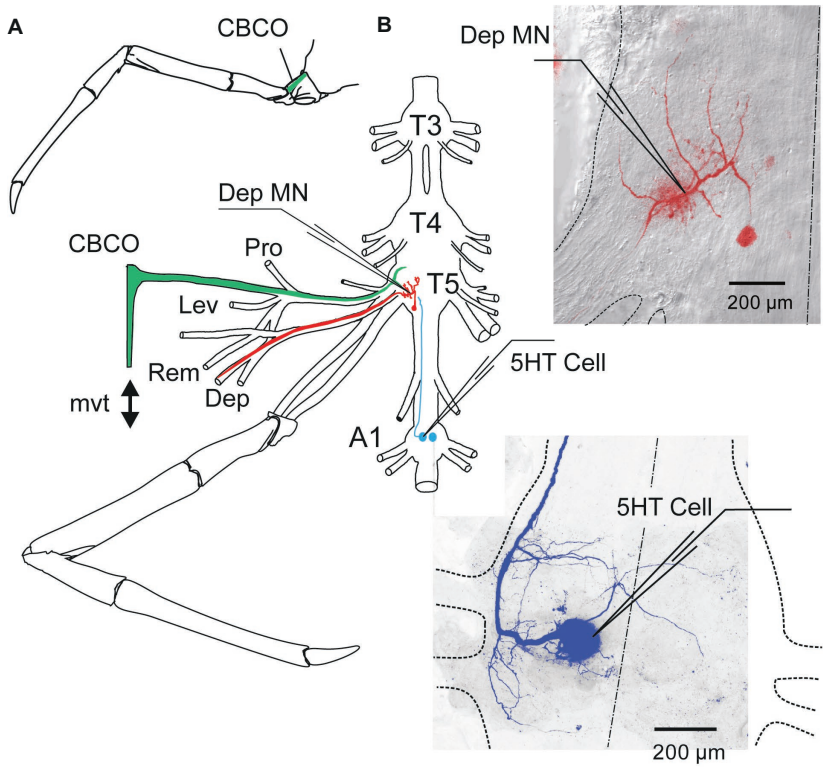

FIGURE 1 | *In vitro* preparation of crayfish walking leg postural system of fifth thoracic leg and first abdominal 5-HT cell. **(A)** Location of the coxo-basipodite chordotonal organ (CBCO) in the fifth walking leg. **(B)** The *in vitro* preparation of the crayfish thoracic locomotor system consists of thoracic ganglia 3–5 (*T3*, *T4*, *T5*) and the first abdominal ganglion (*A1*) dissected out together with motor nerves of the proximal muscles (promotor, *Pro n*; remotor, *Rem n*; levator, *Lev n*; depressor, *Dep n*) and the *CBCO*, a proprioceptor that encodes the vertical movements of the leg. A mechanical puller allowed us to mimic the vertical movements (*mvt*) of the leg by stretching and releasing the CBCO strand. The central nervous system was isolated from the CBCO by a Vaseline wall in order to superfuse only the ganglia with low calcium ringer. Intracellular recordings from depressor motoneurons (Dep MN) were performed within the neuropile of the fifth thoracic ganglion and from the left 5-HT cell of the first abdominal ganglion with glass microelectrodes. Right panels: disposition of the microelectrodes used for intracellular recording from Dep MN (in the main neurite) and 5-HT cell (in the cell body), respectively.

Sensory-Motor Circuit Studied

The depressor motoneurons (MNs) receive sensory input from the CBCO. This organ consists of an elastic strand of connective tissue that is attached proximally to the dorsal edge of the coxopodite and distally to the base of an apodeme at the proximal-dorsal edge of the basipodite (**Figure 1A**). Embedded within this strand are about 40 sensory neurons that project to the ipsilateral neuropil and make mono- and polysynaptic connections with the depressor MNs (El Manira et al., 1991; Le Bon-Jego and Cattaert, 2002). Half of the CBCO sensory neurons are activated when the CBCO strand is stretched, while the other half are activated when the band is released (El Manira et al., 1991). Thus, this proprioceptive organ monitors movements of the limb in the vertical plane. In the *in vitro* preparation, a pin holds the proximal end of the CBCO while a mechanical puller imposes movements to its distal end (**Figure 1B**).

The responses of depressor MNs to releasing movements of the elastic strand of the CBCO (that would therefore be involved in resistance reflex) were recorded intracellularly with a microelectrode generally for one MN and extracellularly for the others *via* a wire electrode on the corresponding motor nerve. To ensure that the CBCO was not damaged during the dissection, we recorded from the CBCO nerve and only used preparations with robust sensory neuron activity in response to imposed movements of the CBCO strand. In order not to damage the CBCO during the experiment, stretch movements were applied starting from the most released position of the CBCO strand, and the total amplitude of the movement was one-third of the released CBCO strand length (1–1.8 mm). The imposed CBCO movement was monitored on an oscilloscope (voltage trace) and stored on computer.

Recordings and Electrical Stimulation

Extracellular recordings from the motor nerves innervating the depressor and levator muscles and from the sensory nerve of the CBCO were made using stainless steel pin electrodes contacting the nerves and insulated with Vaseline. The differential extracellular signals were amplified 2,000–10,000 times and filtered (high-pass 30 Hz, low-pass 3 KHz, 50-Hz notch filter) using Grass Instruments AC amplifiers (model P511J). The bath solution was grounded using a small silver plate that was chlorided using chlorine bleach. Stimulation of nerves was done with a programmable pulse generator (Master-8,

A.M.P.I.) and a stimulus isolation unit (A.M.P.I.). Intracellular recordings from depressor MNs (Dep MNs, **Figure 1B**) and 5-HT cell (5-HT Cell, **Figure 1B**) were performed with glass micropipettes (Clark Electromedical Instruments, Reading, UK) filled with 3 M KCl (resistance 10–20 MΩ). The intracellular electrodes were connected to an Axoclamp 2B amplifier (Axon Instruments Inc., Foster City, CA) used in current-clamp mode. Since long recording with such electrodes could lead to changes in neuron properties (Hooper et al., 2015), we verified that no modifications in Dep MN properties occurred over time in the absence of 5-HT cell stimulation. Moreover, intracellular recordings in the same cell were maintained during less than 1 h. In addition, 5-HT cell effects on MN were observed at the beginning of stimulation. In crustacea, the somata of MNs lie outside of the neuropile (the region in which neurons form their synaptic contacts; see **Figure 1B**) and are linked to the arbor of the neuron by a thin passive neurite, and so contribute marginally in the electrical activity of the neuron. For these reasons, intracellular recordings were made from the main neurite where excitatory post-synaptic potentials (EPSPs) could be recorded (see **Figure 1B**, top right). To measure input resistance, 10 short (generally 500 ms) negative current pulses (−1 nA) were injected in the recording cell. The balance of electrode was verified and rectified if necessary. Then, the traces were averaged and the difference of membrane potential before and during pulses (at the steady state) was measured.

Depressor MNs were identified following the procedure used in Hill and Cattaert (Hill and Cattaert, 2008). Briefly, electrical stimulation of the Dep nerve would produce a spike in the Dep MN whose activity is being recorded intracellularly, and injection of current pulses in the Dep MN would produce spikes recorded in the Dep nerve. The resting membrane potential of MNs was usually in the range of −80 to −65 mV. Stability of resting membrane potential during the experiment was used as a criterion for evaluation of cell health during recordings. In crustacean MNs, soma and neurites do not actively convey spikes. Therefore, spike amplitude was generally small (<20 mV) at the recording site.

Anatomical and Immunohistochemical Techniques

In the first experiments, 5-HT-cells were injected with 5% dextran tetramethylrhodamine (3,000 molecular weight, Molecular Probes) in 0.2 M potassium acetate, with the electrode shank filled with 2 M potassium acetate. Neurons were injected for 1 h using square-wave pulses (500 ms duration at 1 Hz). Good results were obtained by injecting +10 nA for 5% dextran tetramethylrhodamine. However, in most experiments, neurobiotin was used instead of dextran rhodamine because it is a smaller molecule that allows injection of a larger current in the 5-HT cell without blocking the electrode. In this case, neurobiotin was revealed with an ABC kit (Avidin: Biotinylated enzyme Complex from Vector laboratories) coupled to a fluorescent dye (Cy5) (see **Figure 2C**).

Ganglia were fixed overnight at 4°C in 4% paraformaldehyde in a 0.2 M phosphate buffer solution (pH 7.4) and rinsed for 4 h six times in 50 ml of 0.2 M phosphate buffer solution. Preparations were then incubated for 36 h at 4°C in a $^{1}/_{2500}$ dilution of anti-serotonin antibody (Sigma-Aldrich.) generated in rabbits against a formaldehyde cross-linked serotonin-bovine serum albumin (BSA) conjugate. Following primary antibody treatment, tissues were rinsed 4 h in phosphate buffer solution with 0.5% triton X-100 and then post-incubated for 36 h at 4°C with a secondary antibody which was goat anti-rabbit IgG labeled with fluorescein isothiocyanate (FITC) diluted 1:40. Tissues were finally rinsed in 0.2 M phosphate buffer for 6 h. Ganglia were then dehydrated in series of ethanol solutions of ascending strength (50, 70, 90%, 10 min each; 95, 100%, 2 times, 10 min each), cleared in methyl salicylate (Sigma-Aldrich), and mounted in Eukitt (O.Kindler, Germany).

The ganglia were then imaged using a confocal microscope (BX51 Olympus Fluoview 500) and the resulting digital images were analyzed using Fluoview software (Olympus).

Data Acquisition and Analysis

Data were digitized and stored onto a computer hard disk through an appropriate interface (Power1401) and software (Spike2) from Cambridge Electronic Design Ltd. (Cambridge, UK).

Data were analyzed using the Spike2 analysis software. Spikes recorded from the CBCO nerve were identified according to their waveform based on a template matching protocol (wavemark). Templates were built automatically and corresponded to the mean duration of sensory spikes (about 1.5 ms in duration). The sampling rate for CBCO nerve recording was set to 15 kHz, which resulted in templates containing 20–22 points. The procedure used two criteria to identify a spike: (1) more than 90% of the points should be in the confidence limits of the template and (2) the maximum amplitude change for a match was less than 5%. This procedure was applied off-line. After the completion of this protocol, each identified CBCO unit (spike shape) was assigned an arbitrary number. Subsequently, a spike triggered average was performed for each CBCO unit, allowing us to observe in a given MN the occurrence of any postsynaptic events related to this unit.

Identification of 5-HT Neurons

In this study, A1 5-HTcells on the same side as recorded Dep MNs (i.e., left side) were intracellularly stimulated. The 5-HT cells were intracellularly recorded from their cell body on the ventral side of the nerve cord (the nerve cord was turned ventral side up between T5 and A1). The 5-HT cells were identified from their morphology, the location of their cell body in the anterior medial region of A1, and their electrophysiological properties (their resting membrane potential was in the range −35 to −45 mV, their discharge frequency was about 3–5 Hz – **Figure 2A**). Their discharge frequency reached 15–25 Hz during injection of depolarizing current pulses (40 pulses, 7 s duration, 0.1 Hz – **Figure 2B**). Injection of continuous current was used in some experiments (see **Figure 3B**). However, in most experiments, it was very difficult to get continuous firing rate of 20 Hz, and therefore, current pulses were used.

Before starting the recording, the 5-HT cell was prevented from firing by injection of hyperpolarizing current for 10 min.

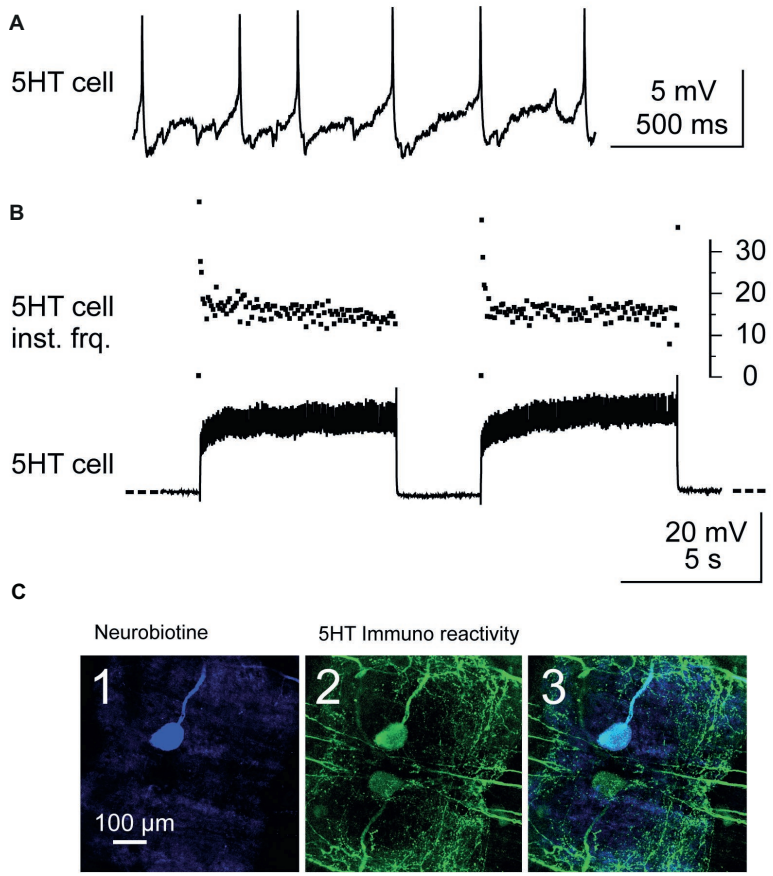

FIGURE 2 | Identification and stimulation of 5-HT cells. **(A)** Intracellular recording from a A1 5-HT cell. **(B)** Stimulation of a 5-HT cell by injection of depolarizing current pulses into the cell body (lower trace). Note the fast adaptation of the instantaneous discharge frequency (*5-HT cell inst. Frq.*) at the beginning of each current pulse (upper trace): the two first spikes may fire at up to 40 Hz and after the following two spikes, the discharge frequency decreases and stabilizes around 17 Hz. **(C)** Immunostaining against 5-HT was performed after each experiment in order to confirm that the stimulated neuron was the 5-HT cell. The stimulated neuron was injected with neurobiotin and revealed with Cy5 (ABC kit) and observed in confocal microscopy. The cell body of this neuron appears in blue when illuminated in dark red light **(C1)**. At the same location, a cell body is immunoreactive to 5-HT (green, **C2**). A superimposition of the two images confirms that the injected neuron is a 5-HT cell **(C3)**.

After the experiment, the recorded 5-HT cell was injected with neurobiotin (**Figure 2C**) (see methods) using depolarizing current pulses, and after fixing the preparation, immunohistochemistry against 5-HT was used (see below) to assess that the recorded neuron was a 5-HT cell (**Figure 2C3**). Injection of pulses of depolarizing current was controlled with a programmable pulse generator (Master-8, A.M.P.I.) connected to the current generator of the axoclamp2B. On the 36 experiments performed in this study to stimulate the left 5-HT cell, immunostaining confirmed only 16 neurons as 5-HT cells. Data on 5-HT cells presented in this paper are from these 16 experiments.

Statistical Analyses

Statistical analyses were done with the Prism program v7 (GraphPad Software, San Diego, CA). A normal distribution was verified (D'agostino and Pearson normality test), and the results were expressed as the means ± SEM. To assess the significance of 5-HT cell activation effects on each of the parameters (V_m, R_{in}, sensorimotor response amplitude) over all experiments, mean values were calculated for each MN before and after 5-HT cell activation. Then a paired *t*-test was used to assess significant difference between the averaged responses recorded before and after 5-HT cell stimulation for each MN. Previously, we demonstrated that 5-HT had direct significant excitatory or inhibitory effect on Dep MNs (Bacqué-Cazenave et al., 2013), and since excitatory and inhibitory effects observed after 5-HT cell stimulation were analyzed separately, we used one-tailed paired *t*-test. For statistical analyses, *n* represents the number of MN recording for each parameter tested and *N* the number of experiments (animals) from which the values were extracted. In some cases, we recorded two different depressor MNs from the same animal. The effects of 5-HT cell on MN response to CBCO-imposed movements were assessed by measuring the amplitude of the response to each movement cycle. Twenty cycles were measured in control and during 5-HTcell activation. The effects of 5-HT cell on EPSP recording from

MNs were assessed by measuring and averaging EPSP amplitude at peak and 15 ms after peak in the late part of the decay phase.

RESULTS

The unilateral projections of the A1 5-HT neurons into the fifth thoracic ganglion (Beltz and Kravitz, 1983; Spitzer et al., 2005) and the putative anatomical connectivity between them and the depressor neurons (Bacqué-Cazenave et al., 2013) suggested that the 5-HT neurons were likely to modulate the activity of the depressor neurons. To address this hypothesis, we stimulated the left 5-HT cell of the first abdominal ganglion, while extracellularly recording the activity of the motor nerves and intracellularly recording from depressor MNs from the fifth left thoracic ganglion.

Diversity of Effects of 5-HT-Cell Activity on Leg Motoneurons' Activity

Because our previous studies showed that local micro-applications of 5-HT could modulate the activity of MNs either excitatory or inhibitory depending on the location, we first tested if 5-HT cell stimulation could produce these two effects on the spontaneous activity of leg MNs. Stimulating the first abdominal 5-HT cell generally resulted in a global activity change of the fifth thoracic ganglion walking leg postural network (**Figure 3**) i.e., the motor activity recorded from each of the proximal leg motor nerves, promotor (Pro), remotor (Rem), anterior levator (Lev), and depressor (Dep) presented a global change of their firing frequency (from 7.15 ± 1.76 Hz in control condition to 6.86 ± 1.78 Hz after 5-HT cell activation; paired *t*-test, $p = 0.20$, $N = 7$). However, when we analyzed the discharge of each motor unit, we observed that some MNs increased their firing frequency, while other MNs were inhibited. **Figure 3A** presents such an experiment, in which the intracellularly recorded depressor MN (*MN Dep1*) is depolarized, while the extracellular recording of another MN in the depressor nerve (*Dep n unit2*) shows a decrease of its firing frequency. The other motor nerves of the fifth left leg also display a variety of responses. For example, in the anterior levator nerve (*Lev n*), unit 1 shows an increased mean discharge, while unit 2 does not display a significant change of the mean discharge in response to 5-HT cell stimulation. In the remotor motor nerve, unit 1 presents a visible activation by 5-HT cell stimulation. In this experiment, the effect of 5-HT cell increased the activity of 25% of the identified MNs in the two proximal motor nerves, decreased the activity of 37.5% of these MNs, and left 37.5% of MNs unchanged (**Figure 3B**). It is important to note that in the seven experiments in which the effect of 5-HT cell activation on motor unit activity was analyzed, we always found excitatory and inhibitory effects. Over the 27 motor units identified in these seven experiments, 10 MNs displayed an excitatory response, 12 MNs presented an inhibitory response, and five MNs did not change their activity (see **Figure 7A**). Note that most MNs were silent in such experiments, and therefore their response to 5-HT was not visible if no intracellular recording was performed. In this experiment as in others, the level of activity of the walking leg postural network was very low (below 5 Hz for all motor units), which explains why the changes in frequency were also small (below 0.5 Hz, **Figure 3C**).

Since the present work aimed at analyzing excitatory and inhibitory effects induced in intracellularly recorded Dep MNs by 5-HT cell stimulation, they are presented thereafter separately (see **Figures 4, 5**, respectively).

Excitatory Effects of 5-HT Cell Activity on Depressor Motoneurons

Membrane Potential Depolarization

Injection of depolarizing current into the left A1 5-HT cell induced a depolarization in 10 of the 16 intracellularly recorded Dep MNs (**Figure 4A**). A representative recording of such a response is shown in **Figure 4A1**. The Dep MN response started a few seconds after the beginning of 5-HT cell stimulation, and reached a maximum depolarization of 7.8 mV after 5 min of stimulation (**Figure 4A1**, ellipse). After the end of 5-HT cell stimulation, the membrane potential of the Dep MN came back close to its control value within a few mins (**Figure 4A1**). The changes in membrane potential induced in these 10 intracellularly recorded Dep MNs after 5 min 5-HT cell stimulation are presented in **Figure 4A2**. The control membrane potential was averaged over 1 min before the 5-HT cell was stimulated (green part of recordings in **Figure 4A2**, and green dots in **Figure 4A2**). The maximum of the depolarizing response was measured 5 min after the beginning of 5-HT cell stimulation and averaged over 2 min (see ellipses in **Figure 4A1**, and blue dots in **Figure 4A2**). The excitatory effects of the 5-HT cell stimulation are significant on the membrane potential of recorded MNs (**Figure 4A2**; paired *t*-test, $p < 0.01$, $n = 10$).

Input Resistance Increase

Before the left A1 5-HT cell activation and 15–20 min after, the input resistance (R_{in}) of the intracellularly recorded Dep MN was measured (**Figure 4A3**). In the six MNs in which R_{in} was measured during the depolarizing effect of 5-HT cell stimulation, an increase of R_{in} was observed, indicating that these depolarizations were excitatory (paired *t*-test, $p = 0.08$, $n = 6$).

Functional Consequence on Postural Control

The application of sinusoidal movements to the CBCO strand elicited alternately depolarizing and hyperpolarizing responses in depressor MNs (El Manira et al., 1991; Le Ray et al., 1997a,b). Release of the CBCO, which mimicked the upward movement of the leg, depolarized the depressor MNs in seven quiescent (i.e., non-rhythmically active) preparations (**Figure 4B1**, upward arrow; El Manira et al., 1991; Le Ray et al., 1997b). Conversely, stretch of the CBCO, which mimicked leg downward movement, hyperpolarized the depressor MNs, presumably by exciting inhibitory pathways (**Figure 4B1**, downward arrow; Le Bon-Jego and Cattaert, 2002).

In six experiments, in which the intracellular stimulation of the ipsilateral 5-HT-cell induced an excitatory effect on the

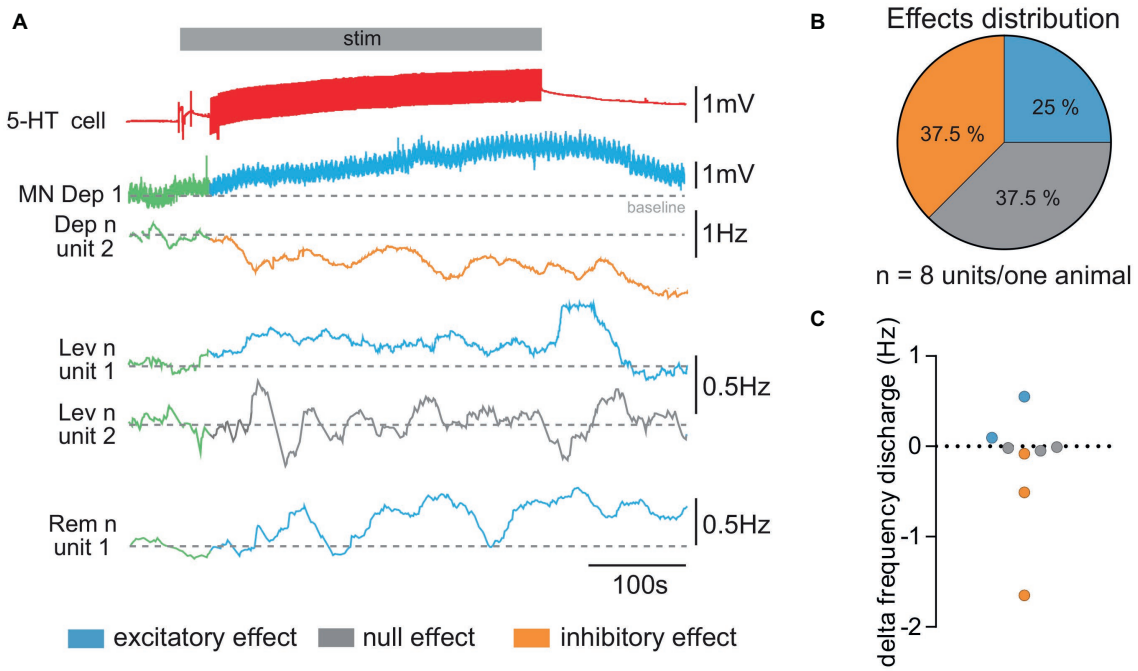

FIGURE 3 | Diversity of responses from walking leg MNs of the fifth left thoracic ganglion to stimulation of the ipsi 5-HT cell. **(A)** Diversity of responses obtained in a single experiment. The 5-HT cell stimulation (*stim* in gray horizontal bar) elicits a depolarizing response in the intracellularly recorded depressor MN (*MN Dep1*). Simultaneously, the activity of several other MNs (mean firing frequency, 100 s) was extracted from extracellular recording of the Dep, Lev, and Rem motor nerves to illustrate the diversity of responses elicited by 5-HT cell stimulation: the activity of unit 2 (*Dep n unit2*) decreases (orange trace); the anterior levator nerve (*Lev n*) unit 1 presents an increased discharge (blue trace), while unit 2 does not display any change in response (gray trace) to 5-HT cell stimulation. One unit of the remotor nerve presents an increased activity (blue traces). Note that in order to analyze changes in the sensory motor response, CBCO movements were continuously applied. This resulted in "wavelets" in the intracellular recording of the Dep1 MN. **(B)** From the same experiment, the distribution of excitatory, inhibitory, and no effects was calculated from the changes in mean firing frequency measured for each recorded motor unit. **(C)** Variety of the changes in firing frequency induced by activation of the 5-HT cell (5-HT response amplitude) in motor units recorded in Pro, Rem, Lev, and Dep motor nerves from the same experiment. Discharge frequency was calculated over 200 s before activation of 5-HT cell (control, in green, in **A**) and after the end of the stimulation (decrease in orange, increase in blue, and no effect in gray in **A**).

intracellularly recorded Dep MN, we also analyzed the response of this Dep MN to release movements of the CBCO. In these six Dep MNs, we observed an increase of the amplitude of the response to CBCO release. A representative example of a response induced in a Dep MN by 5-HT cell stimulation is given in **Figure 4B1**. In this experiment, the amplitude of the response of the Dep MN to CBCO movements (**Figure 4B2**) increased from 1.03 ± 0.07 mV in control conditions (green trace, double arrow) to 1.66 ± 0.96 mV after 5 min of 5-HT cell stimulation (blue trace, double arrow). When we compared the amplitude of the Dep MN responses in the six experiments, we observed a significant increase (paired *t*-test, $p < 0.05$, $n = 6$) in Dep MN response to CBCO when 5-HT cells were stimulated (**Figure 4B3**).

Coxo-Basal Chordotonal Organ -Induced Unitary EPSPs in Depressor Motoneurons

The unitary EPSPs evoked by CBCO sensory afferents were analyzed in experiments in which A1 5-HT cell stimulation induced a change of the amplitude of the response to CBCO movements. For example, in the experiment shown in **Figure 4B1**, the intracellularly recorded Dep MN received unitary EPSPs triggered by five different CBCO sensory units (**Figure 4C1**). Each unitary EPSP is shown before A1 5-HT cell stimulation (control – green trace) and after 5 min of 5-HT-cell stimulation. With each unitary EPSP, the shape of the corresponding CBCO afferent spike is presented, together with an identifying number. All the sensory units involved in the Dep MN response fired during release movement of the CBCO strand (i.e., upward movement of the leg in intact animals) and because they evoked an EPSP in a Dep MN, they were therefore involved in resistance reflex. The most remarkable result of this analysis was that the amplitude of unitary EPSPs was only slightly affected if at all after 5-HT-cell stimulation. For one unit, the peak amplitude of the unitary EPSP (**Figure 4C1**, black arrowhead) was slightly increased (unit 1). One out of the five unitary EPSP was unchanged (unit 2). The three other unitary EPSPs were even reduced (units 3, 4, and 5 – see black arrow heads). This result was very surprising because in the presence of 5-HT, the input resistance of this recorded Dep MN was increased by 32%, leading us to expect a proportional increase in the amplitude of individual EPSPs. Indeed, as was shown for 5-HT application in Cattaert et al. (2010), the increase of the amplitude of the MN response to CBCO movements was mainly associated

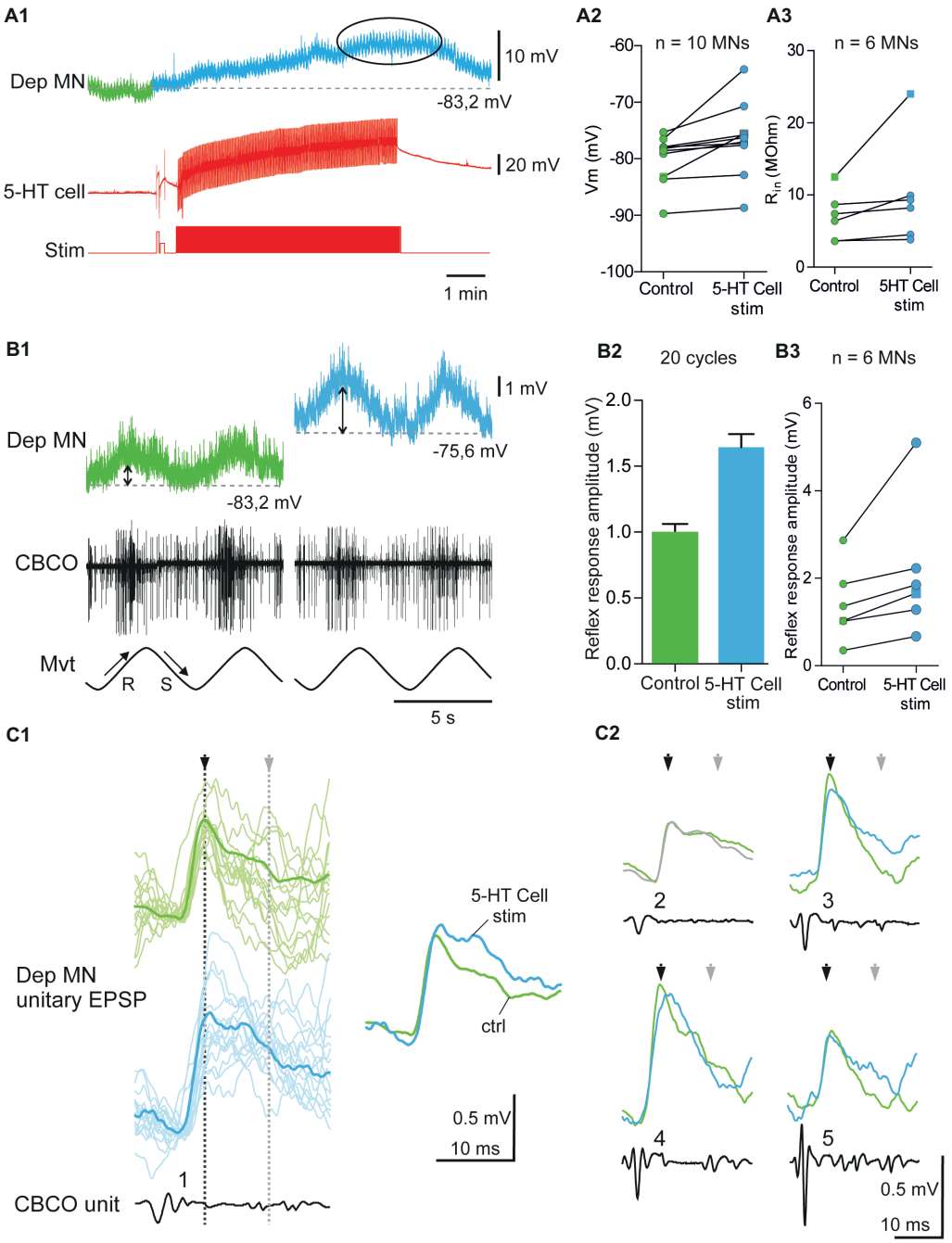

FIGURE 4 | Excitatory effects induced by 5-HT cell activation on Dep MNs. **(A1)** Depolarizing response of an intracellularly recorded Dep MN to the ipsilaterally projecting A1 5-HT cell intracellular stimulation. **(A2)** Excitatory effect of 5-HT cell activation on 10 Dep MNs. Square symbol represents trace used in **A1**. **(A3)** Increased input resistance (R_{in}) from six MNs when 5-HT cells are stimulated. Membrane potential of these MNs increases also. Square symbol represents trace used in **A1**. **(B1)** Increase of the amplitude of the sensory-motor response of an intracellularly recorded Dep MN during 5-HT cell activation. In this experiment (same as panel **A1**), sinewave movements (*Mvt*) were continuously applied to the CBCO strand and evoked sensory discharges recorded from the CBCO sensory nerve (*CBCO*). Before 5-HT cell stimulation (left column), the Dep MN depolarized during CBCO release movements (corresponding the leg levation in intact animal) and repolarized during CBCO stretch. After 5 min of 5-HT cell stimulation (right), the Dep MN potential depolarized from –83.2 to –75.6 mV and the amplitude of the sensory-motor response increased. **(B2)** In this experiment, the 5-HT cell stimulation significantly increased the amplitude of the Dep MN sensory-motor response from 0.99 ± 0.06 mV (averaged from 20 cycles) in control condition to 1.64 ± 0.099 mV (averaged from 20 cycles) after 5-HT cell stimulation. **(B3)** Increase of sensory-motor response recorded from six MNs, after the 5-HT cell stimulation. **(C1)** Examples of unitary EPSPs' shape changes induced in Dep MN that showed a depolarizing response to 5-HT cell activation. In control condition and after 5-HT cell stimulation, superimposed examples (raw data, light traces) and corresponding average EPSP traces (dark traces) are presented. **(C2)**: Mean EPSP amplitudes measured at peak (black arrows) and 15 ms after peak in the late part of the decay phase (gray arrows). These unitary EPSPs are recorded in the same Dep MN.

with late part of EPSP increase and suggests that the effect is indirect and mediated by polysynaptic sensory-motor pathways (polysynaptic component of unitary EPSPs – see also overdraws in **Figure 4C1**, showing more polysynaptic events in blue traces). Such a marked increase in the late part of EPSP was also observed in the experiment reported in **Figure 4C1** (gray arrowhead). Indeed four units presented a marked increase in the time constant of the repolarizing phase of the EPSP (units 1, 3, 4, and 5). Previously, we demonstrated that such a prolonged EPSP depolarization was responsible for the increase in the amplitude of MN response to CBCO movements in preparations exposed to applied 5-HT due to increased summation of EPSPs (Le Bon-Jego et al., 2004).

Inhibitory Effects of 5-HT Cell Activity on Depressor Motoneurons

Membrane Potential Hyperpolarization

Injection of depolarizing current into the left A1 5-HT cell induced a hyperpolarization in five of the 16 intracellularly recorded Dep MNs (**Figure 5A**). A representative recording of such a response is shown in **Figure 5A1**. The Dep MN response started a few seconds after the beginning of 5-HT cell stimulation, and reached a maximum hyperpolarization of −7.4 mV after 5 min of stimulation (**Figure 5A1**, ellipse). The results of five hyperpolarizing responses are presented in **Figure 5A2**. The control membrane potential was averaged over 1 min before the 5-HT cell was stimulated (see green part of recordings in **Figure 5A1**, and green dots in **Figure 5A2**). The maximum of the hyperpolarizing response was measured 5 min after the beginning of 5-HT cell stimulation and averaged over 2 min (see ellipses in **Figure 5A1**, and orange dots in **Figure 5A2**). A slight hyperpolarization was observed (**Figure 5A2**, paired *t*-test, $p = 0.06$, $n = 5$) in all five MNs.

Input Resistance Decrease

Before the left A1 5-HT cell activation and 15–20 min after, the input resistance (R_{in}) of the intracellularly recorded Dep MN was measured (**Figure 5A3**). In the four MNs in which R_{in} was measured during the hyperpolarizing effect of 5-HT cell stimulation, a significant decrease of R_{in}, was observed (paired *t*-test, $p < 0.05$, $n = 4$).

Functional Consequence on Postural Control

In three experiments, in which the intracellular stimulation of the ipsilateral 5-HT cell induced an inhibitory effect on the intracellularly recorded Dep MN, we also analyzed the response of this Dep MN to release movements of the CBCO. In these three Dep MNs, we observed a decrease of the amplitude of the response to CBCO release. A representative example of a hyperpolarizing response induced in a Dep MN by 5-HT cell stimulation is given in **Figure 5B1**. In this experiment, the amplitude of the response to CBCO movements measured in the Dep MN (**Figure 5B2**) decreased from 0.077 ± 0.011 mV in control condition (green trace) to 0.045 ± 0.009 mV after 5 min of 5-HT cell stimulation (orange trace). This effect was consistent in the three Dep MNs that were recorded in three different preparations (**Figure 5B3**, paired *t*-test, $p = 0.06$, $n = 3$).

In the experiments, in which 5-HT cell stimulation induced a decrease of the amplitude of the MN response to CBCO movements, the analysis of unitary EPSPs showed that very few changes occurred in EPSP shapes (**Figure 5C1**). The only noticeable modification was a decrease in the late decay phase (**Figure 5C1**, gray arrow). In this figure, the unitary EPSPs identified in two Dep MNs are presented (**Figures 5C2,C3**). In these two experiments, the faster decay time induced after 5-HT cell stimulation was likely due to inhibition of the polysynaptic pathways (as indicated by the more regular exponential decay of the EPSPs in **Figure 5C**, orange traces – see also overdraws in **Figure 5C1**, showing fewer polysynaptic events in orange traces). Concomitantly, in these experiments, the stimulation of the 5-HT cells also induced a drop in input resistance of the Dep MNs (**Figure 5B3**). This result is in accordance with the fact that the decay time constant was faster in some EPSPs (for example, units 1, 3, and 5 in **Figure 5C1**).

The Effect of 5-HT Cell Stimulation on the Depressor Motoneurons Is Direct

We wanted to determine if a part of the effect of A1 5-HT cell stimulation onto depressor MNs could be direct. To test for this possibility, we used high-divalent cation solution (2.5 × Ca^{2+}, 2.5 × Mg^{2+}) was used to raise the threshold for triggering a spike, and thereby minimizing the polysynaptic pathways. The efficacy of this procedure was assessed by the fact that sensory-motor pathways from CBCO units to Dep MNs were drastically eliminated (**Figure 6A**). In this example, in control condition (**Figure 6A,** left), the CBCO unit (black trace) triggered an EPSP with very few polysynaptic events (green traces). The perfusion of 10 μM 5-HT in the bathing medium (**Figure 6A**, middle) recruited these polysynaptic pathways. However, high-divalent cation solution prevented this recruitment (**Figure 6A**, right).

In the presence of high-divalent cation solution (perfusion restricted onto the two last thoracic ganglia), the activation of the A1 5-HT-cell could still induce changes in membrane potential of the intracellularly recorded Dep MN, either depolarizing (**Figure 6B**), or hyperpolarizing (**Figure 6C**), suggesting that the effects of ipsilateral A1 5-HT cell involved monosynaptic connections from 5-HT cell onto Dep MNs. Note that the Dep MN presented in **Figure 6C** kept a rhythmic activity in the presence of high-divalent cations solution. Plateaus (>20 mV) were produced all along the recording (visible oscillations represent mainly the plateaus). Despite this exceptional activity, 5-HT cell was nevertheless capable of hyperpolarizing Dep membrane potential.

Monotonal Distribution of Effects of 5-HT Cell Activity on Depressor Motoneurons

Because local micro-ejection of 5-HT produced inhibitory or excitatory effects depending on the site of ejection (respectively on the initial segment or in the center of the neuropile)

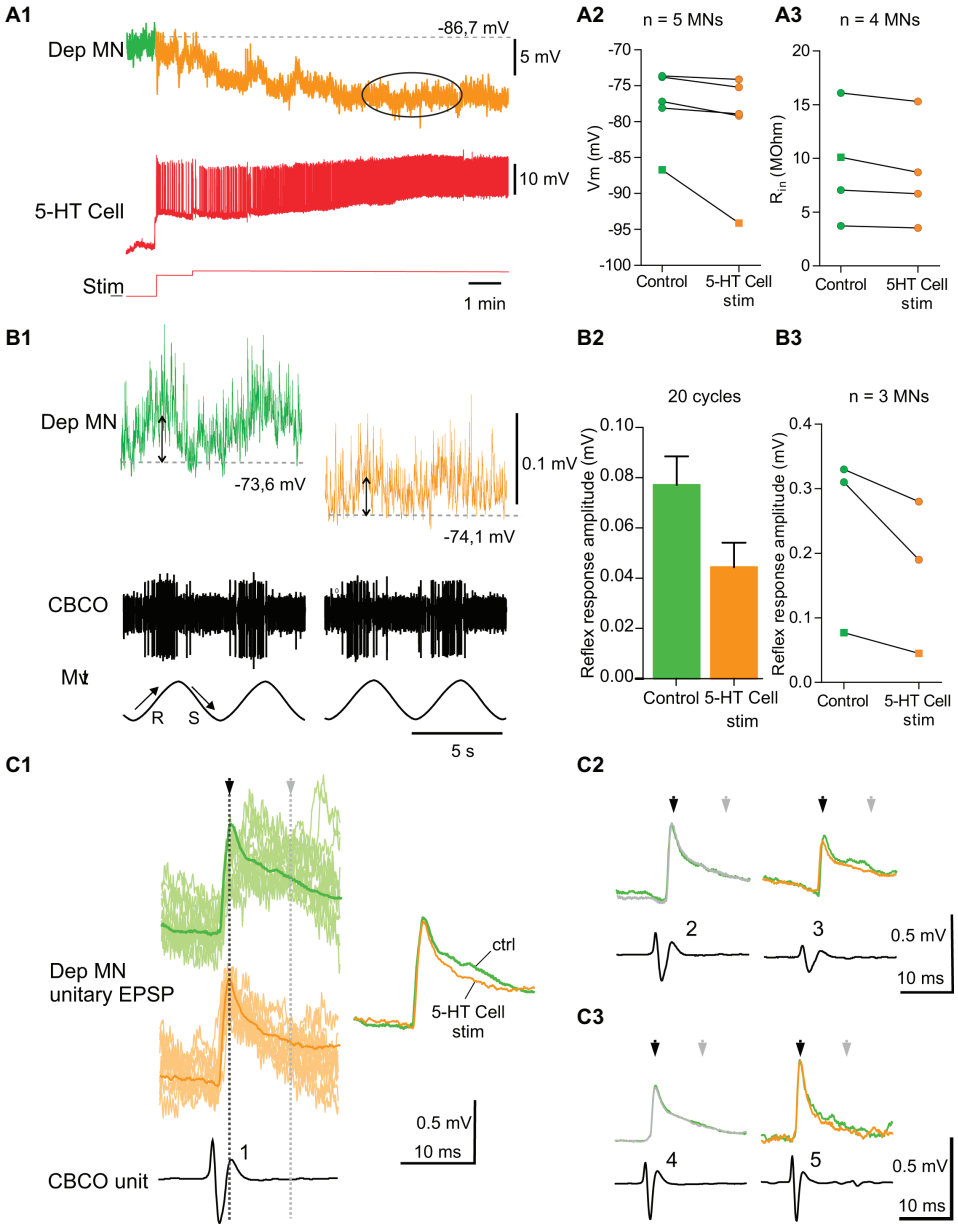

FIGURE 5 | Inhibitory effects induced by 5-HT cell activation on Dep MNs. **(A1)** hyperpolarizing response of an intracellularly recorded Dep MN to the ipsilateral A1 5-HT cell intracellular stimulation. **(A2)** Inhibitory effect of 5-HT cell activation on 5 Dep MNs. Square symbol represents trace used in **A1**. **(A3)** Decrease of input resistant (R_{in}) from four MNs when 5-HT cell are stimulated. Membrane potential of these MNs decreases also. Square symbol represents trace used in **A1**. **(B1)** Decrease of the amplitude of the sensory-motor response of an intracellularly recorded Dep MN during 5-HT cell activation (same dispositions as in **Figure 4**). **(B2)** In this experiment, reflex response amplitude decreases from 0.077 ± 0.011 mV (averaged from 20 cycles) to 0.045 ± 0.009 mV (averaged from 20 cycles). **(B3)** Decrease of sensory-motor response recorded from three MNs, after the 5-HT cell stimulation. Square symbol represents trace used in **A1**. **(C1)** Examples of change of unitary EPSPs' shape induced in Dep MN that showed a hyperpolarizing response to 5-HT cell activation. In control condition and after 5-HT cell stimulation, superimposed raw data (light traces) and corresponding average EPSP traces (dark traces) are presented. **(C2,C3)** Mean EPSP amplitudes measured at peak (black arrows) and 15 ms after peak in the late part of the decay phase (gray arrows). **C2** and **C3** represent two different experiments.

(Bacqué-Cazenave et al., 2013), one of the aims of this study was to test if 5-HT cell stimulation could also evoke excitatory and inhibitory effects in Dep MNs. The data presented above indicate that this is the case. It seems therefore likely that abdominal 5-HT cells participate in both types of modulation of Dep MN activity.

However, this result raised the question of the significance of these opposed effects. Indeed, this result may be surprising because all animals included in the present study were isolated animals, and we would have expected mostly excitatory effects. It could be that two types of responses correspond to two types of MN pools – one involved in subordinate animal responses

and the other involved in dominant animal responses as shown by Cattaert et al. (2010). To test if the two types of responses correspond to two types of MN pools, we analyzed the distribution of the effects induced by 5-HT cell stimulation on Dep MNs.

The distribution of the changes in frequency observed in the various MNs (n = 27) recorded in motor nerves over all experiments (N = 7) was fitted with a Gaussian distribution curve (**Figure 7A**), indicating that both excitatory and inhibitory responses could obey a single distributing law. Indeed the change in frequency of Dep MN ranged from −2.69 to +5.52 Hz, but no clear separation between two groups was revealed.

A similar conclusion was drawn from the effects on membrane potential (**Figure 7B**), R_{in} (**Figure 7C**) and sensory-motor response change (**Figure 7D**). There is a clear correlation between the change in R_{in} and the amplitude of the depolarization suggesting that intrinsic and network effects are parallel consequences of 5-HT cell stimulations (**Figure 7E**).

Note that the overall response on the leg postural network is excitatory because the number of measurements in favor of excitatory effects is larger and their values are also larger than for inhibitory effects. Although the various effects on discharge frequency, membrane potential, and input resistance were variable among the MN population (excitatory, inhibitory, and no change), it is interesting to note that functionally, the amplitude of the response to CBCO movement increases from 1.04 ± 0.29 mV in control to 1.68 ± 0.49 mV after 5-HT cell stimulation (paired t-test, $p < 0.05$, n = 9, N = 7).

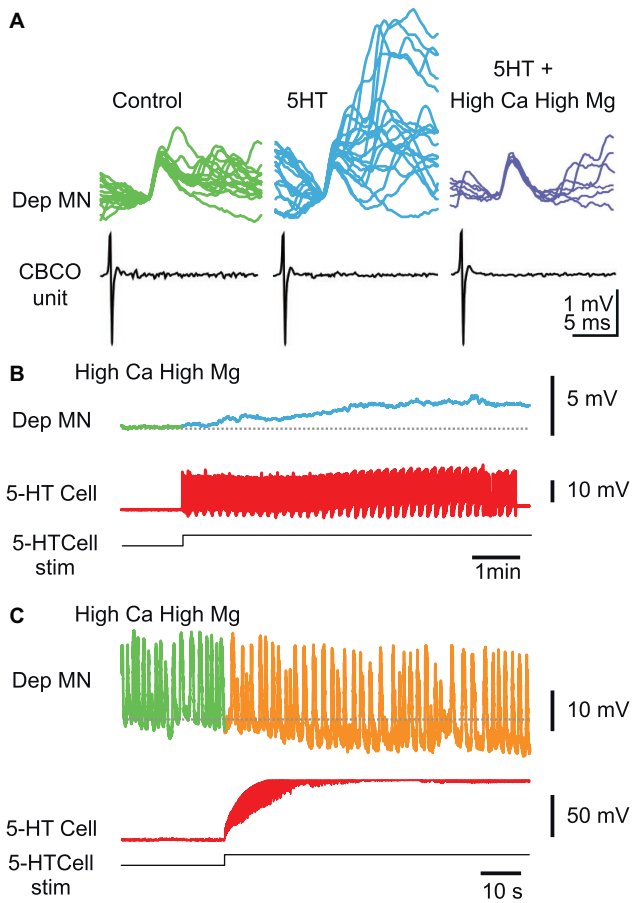

FIGURE 6 | Effect of 5-HT cell stimulation on Dep MNs persists in high-divalent cation solution. **(A)** High-divalent cation solution raises the threshold for spikes. The effect of high-divalent cation solution was tested on unitary EPSPs recorded from a Dep MN. In control situation, the CBCO unit (black trace) evoked an EPSP in the intracellularly recorded Dep MN (green trace) in which very few polysynaptic events occurred. After 10 min of perfusion of 5-HT (10 μM) in the bathing medium, the polysynaptic pathways were activated (see the numerous and variable events present in the decay phase of the monosynaptic EPSP). If the 5-HT was applied while the preparation was perfused with high-divalent cation solution, no polysynaptic event occurred (dark blue traces). **(B)** Persistence of a depolarizing response induced by 5-HT cell stimulation in high-divalent cation solution. **(C)** Persistence of a hyperpolarizing response induced by 5-HT cell stimulation in high-divalent cation solution. Note that this Dep MN was producing pacemaker properties, the frequency of which decreased during 5-HT cell stimulation.

5-HT Cell Stimulation Enhances the Response to 5-HT Motoneurons to Abdominal Sensory Cues

We have shown that left 5-HT cells from the first abdominal ganglion modulate the activity of MNs from ipsilateral fifth ganglion and their responses to proprioceptive inputs from the same leg joint. Here we address the question of the effect of the same 5-HT cell onto sensory inputs from other parts of the body. More specifically, we measured the response of the depressor nerve units to stimulation of the N2 sensory nerve of the first abdominal ganglion (that contains the axons of fringe hair afferents), with and without activation of the left 5-HT neuron (**Figure 8**, N = 5). As a control, we measured the response of the depressor nerve to ipsilateral N2 sensory stimulation while the 5-HT neuron was kept silent by injecting negative DC current in the cell soma (**Figures 8B,C**). We repeated the test as the 5-HT neuron was driven at a rate of ~10 Hz by injecting positive current. We found that the response of the depressor nerve to N2 sensory stimulation was enhanced when the 5-HT neuron was active (**Figures 8D,F**) as compared to when it was silent (**Figure 8B**). Conversely, 5-HT neuron stimulation did not change the response of the depressor nerve to stimulation of the contralateral N2 sensory stimulation (**Figures 8C,E,G**). The lack of inhibitory effect of 5-HT cell stimulation on Dep MNs' activity in these experiments may be surprising. This is likely due to the absence of spontaneous activity of Dep MNs, which probably resulted from the long-lasting period (>1.5 h) of the preparation before starting recordings. This result generalizes the modulatory role of A1 5-HT neurons onto fifth leg postural network, and confirms that this modulatory effect is limited to the ipsilateral side.

DISCUSSION

In a previous paper (Bacqué-Cazenave et al., 2013), it was shown that 5-HT could elicit excitatory or inhibitory effects, depending on where it was locally applied. When micro-ejections were

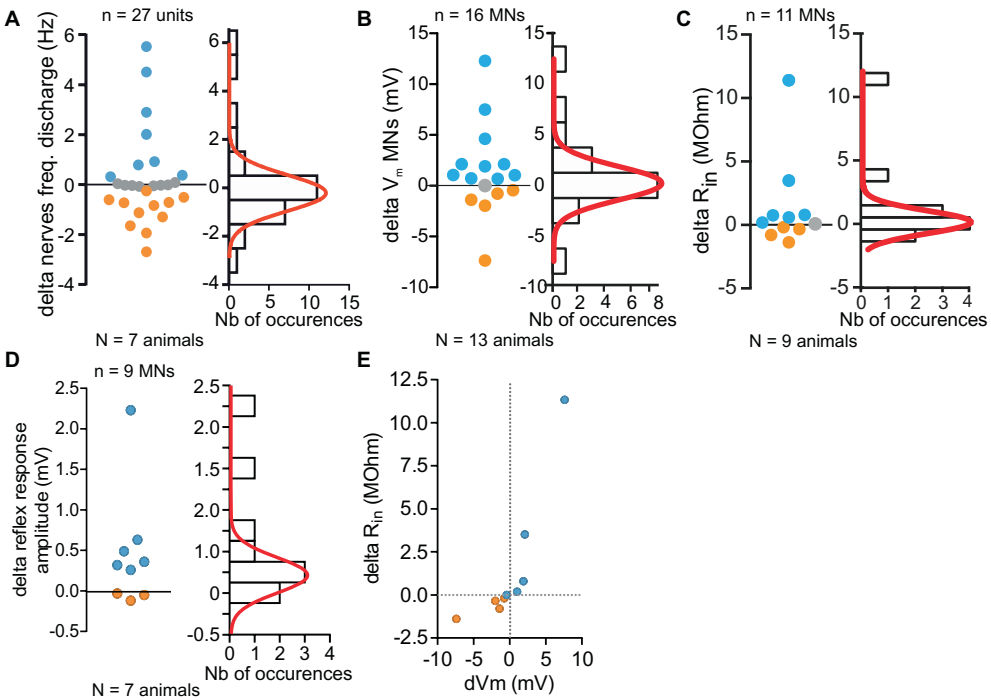

FIGURE 7 | Monotonal distribution of effects of 5-HT cell activity on Depressor MNs. **(A–D)** Variety of responses magnitude (firing frequency, **A**; V_m, **B**; R_{in}, **C**; reflex response, **D**) measured in *in vitro* preparations (left panel). Distribution of all changes and their distribution histogram fitted with a Gaussian curve (right panel). **(E)** Correlation between the changes of input resistance (R_{in}) and membrane potential changes of eight MNs. Orange and blue dots represent respectively inhibitory and excitatory effects induced by stimulation of 5-HT cell. All depolarizing changes of Dep MNs were associated with an increase of R_{in}. Hyperpolarizing changes were associated with a R_{in} decrease.

performed close to the initial segment where 5-HT immunoreactive fiber form boutons onto MN axon, the induced effect was inhibitory, while when 5-HT was micro-ejected in the center of the neuropile where no direct contact between 5-HT immunoreactive fibers and MN dendrite exist, an excitatory effect was observed. Here, in postural networks of isolated animals, we show that (1) the activation of a single 5-HT cell can induce mixed excitatory and inhibitory effects on walking leg MNs; (2) these effects induce functional changes in the walking leg postural network by modifying the amplitude of the response of MNs to mechanosensory inputs; (3) the induced effects are multiple and cooperative, and they involve modifications of the intrinsic properties (input resistance, membrane potential) of Dep MNs – as shown in Le Bon-Jego et al. (2004) when 5-HT was bath applied; and (4) the effects on intrinsic properties of Dep MNs are direct, while the effects on sensory-motor responses also involve polysynaptic pathways.

5-HT Cell Stimulation Has a Variety of Effects on the Leg Postural Network

Excitatory responses induced in Dep MNs by A1 5-HT cell stimulation consist of: (1) a tonic depolarization directly linked to the increase of input resistance and (2) an increase of the amplitude of MN response to CBCO movements linked to the prolonged repolarizing phase of EPSPs (likely due to recruitment of polysynaptic sensory-motor pathways). All these features were observed after bath application of 5-HT (10 μM) in some communal animals (Le Bon-Jego et al., 2004) and in dominant animals (Cattaert et al., 2010) or by local pressure micro-ejection in the central part of the neuropile in isolated animals (Bacqué-Cazenave et al., 2013) By contrast, inhibitory responses induced in Dep MNs by A1 5-HT cell stimulation consist of: (1) a tonic hyperpolarization associated with a decrease of input resistance and (2) a decrease of the amplitude of MN response to CBCO movements linked to a faster repolarizing phase of EPSPs (likely due to the failure to recruit polysynaptic sensory-motor pathways). All these features were observed after bath application of 5-HT (10 μM) in some communal animals (Le Bon-Jego et al., 2004) and in subordinate animals (Cattaert et al., 2010) or by local pressure micro-ejection close to the initial segment of Dep MNs in isolated animals (Bacqué-Cazenave et al., 2013). These results indicate that the activity of a single A1 5-HT cell is capable of inducing each of these cooperative effects (either excitatory or inhibitory) on the leg postural circuit.

Using local micro-application of 5-HT into the fifth thoracic ganglion that contains the postural network, it was shown that these two opposed responses to 5-HT involve different regions of MN architecture. While inhibitory effects from 5-HTcells may involve classic synaptic contacts close to the initial segment of Dep MNs, more central excitatory effects

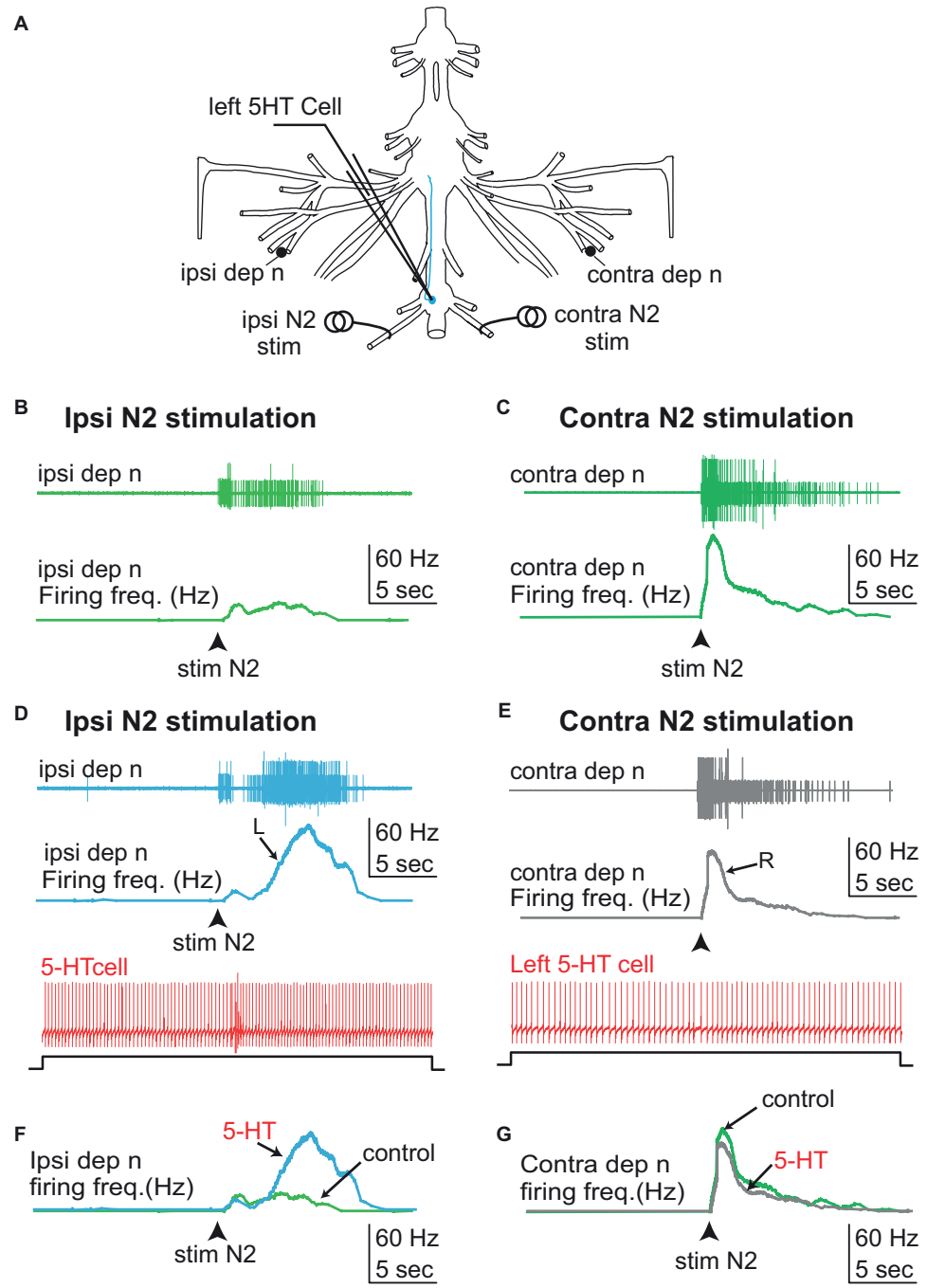

FIGURE 8 | Effect of 5-HT cell stimulation on the response pattern of the depressor nerve to N2 sensory stimulation. **(A)** Experimental disposition. **(B)** Stimulation of the left (ipsilateral) N2 sensory nerve while keeping the left 5-HT cell silent activates the left depressor nerve (light green). **(C)** Similarly, stimulation of the right (controlateral) sensory nerve while keeping the left 5-HT cell silent activates the right depressor nerve (dark green). **(D)** Driving the left 5-HT cell by current injection enhances the response of the left (ipsilateral) depressor nerve (blue trace) to stimulation of the left (ipsilateral) N2 sensory nerve. **(E)** By contrast, the same activation of the left 5-HT cell during right (contralateral) N2 sensory nerve stimulation does not enhance the response of the right (contralateral) depressor nerve (gray trace). **(F,G)** Comparison of the frequency response of the ipsi/contra depressor nerves to left N2 sensory nerve stimulation in the absence and presence of 5-HT cell stimulation. Whereas a noticeable increase of the response is observed on side ipsilateral to 5-HT cell stimulation **(F)**, no effect is observed in the contralateral side **(G)**. R, right; L, left.

on the dendritic arbor are most likely due to paracrine mechanisms (Bacqué-Cazenave et al., 2013). The present results indicate that a single 5-HT cell can trigger both types of 5-HT release: inhibitory synaptic action onto the initial segment and excitatory paracrine mechanisms on dendritic arbor. This finding raises several questions: (1) Why do some MNs respond

to 5-HT cell stimulation with a paracrine excitatory effect while other MNs respond with a synaptic inhibitory effect? (2) How does the motor network process or condition these opposed responses? (3) Are these opposed effects related to the heterogeneity of MNs in a given pool? and (4) What could be the functional schema in which 5-HT cells control network activity?

5-HT Cell Induces Both Synaptic and Paracrine Mechanisms

Our results indicate that excitatory and inhibitory effects observed in MNs after 5-HT cell stimulation are in conformity with the effects of local micro-application of 5-HT on dendritic arbor and initial segment, respectively (Bacqué-Cazenave et al., 2013). Moreover, those effects persist in high-divalent cation Ringer, indicating a direct effect of 5-HT cells' axonal branches on the two types of receptor sites onto MNs.

5-HT action is likely not due to a spillover of neurotransmitter from a synaptic site because this would have induced inhibition before paracrine activation of excitatory sites could occur, which was not observed. Moreover, in such a scenario, it is likely that the inhibitory effect would have blocked any subsequent excitatory response due to mutual interactions between the two molecular pathways as was shown in the lateral giant synapse of crayfish (Lee et al., 2008). In addition, we do not know how much time it would take for the 5-HT spillover to reach the dendritic paracrine receptors. In their report, Lee et al. (2008) observe the reversal of the response from inhibitory to excitatory during the wash, after at least 15 min for short applications of high concentration (50–1,000 μM) of 5-HT.

This consideration implies that some parts of the axonal arbor release 5-HT in a paracrine way to activate 5-HT receptors on MN dendrites to elicit an excitatory response, while other parts of the axonal arbor of the same 5-HT cell are involved in synapses at the initial segment of MNs triggering inhibitory responses (see Figure 10 in Bacqué-Cazenave et al., 2013).

Excitatory vs. Inhibitory Effects of 5-HT Cell Stimulation Onto Motoneurons

5-HT cell stimulation induces excitatory response in some MNs and inhibitory responses in other MNs, and these responses are not segregated into two separated pools but rather obey a single Gaussian-like distribution (**Figure 7**). This finding could indicate that the two types of effects occur simultaneously in different mixtures for the different MNs. However, this situation, in which both excitatory and inhibitory pathways are activated, seems unlikely because these two pathways are competitive and eventually one would overcome the other (Lee et al., 2008).

Another interpretation may be suggested in which the MNs "decide" the type of response they will make to 5-HT cell stimulation. When the stimulation was made several times, the same MN would respond in the same way each time, and this response would always be either excitatory or inhibitory but not mixed. So we may conclude that, by an unknown mechanism, each MN will be controlled either by paracrine excitatory process or by synaptic inhibitory synapse. In addition, the intensity of the response is also specific for each MN, being large, small, or absent. Altogether, those settings allow a Gaussian-like distribution of responses from negative to positive. This distribution is reminiscent of a homeostatic mechanism that would set 5-HT receptors (internalization, phosphorylation, etc.) of each MN depending on its activity in order to adjust its response to 5-HT.

Network Effect on 5-HT Neuromodulation of Motoneuron Activity

In the present report, we showed that MN responses to 5-HT cell stimulation persisted in high-divalent cation solution. This condition eliminates polysynaptic pathways by raising spike threshold. However, in the physiological situation, the activation of a MN pool would result in the inhibition of the antagonistic MN pool (Pearlstein et al., 1998). Thereby, secondary inhibitions can be observed.

Functional Consequences of Mixed Excitatory/Inhibitory Effects Induced by 5-HT Cell Activity

The above discussion pointed out a possible homeostatic mechanism allowing 5-HT cells to adapt their level of control on MNs depending on each MN's activity. Active MNs will tend to express 5-HT receptors leading to inhibition, whereas resting MNs will favor 5-HT receptors leading to excitation. If this mechanism exists, its time course must be slow, based on the level of 5-HT and on the activity of MNs. We propose a mechanism similar to the one described during social status formation concerning future subordinate crayfish (Yeh et al., 1996).

During social status formation in isolated animals, 5-HT application elicits an excitatory effect on lateral giant fiber and on its mechanosensory synaptic inputs. This effect is gradually decreased and replaced by an inhibitory effect in the animal that loses fights and becomes submissive (Yeh et al., 1997). In the present report, 3 weeks of social isolation prior to experiments erased the animals' previous social status. The observed diversity of 5-HT effects was therefore not related to their social status. Moreover, excitatory and inhibitory effects were observed in the same preparation. Nevertheless, it is possible to invoke similar mechanisms controlling the effects of 5-HT onto MNs and depending on their level of activity and depending on the level of 5-HT rather than on social status.

CONCLUDING REMARKS

Since the firing rate of a first abdominal 5-HT cell seems to control each ipsilateral fifth leg MN either with excitatory or inhibitory effects that obey a single Gaussian distribution, we assume that the present results point to a homeostatic

mechanism relying on each MN's activity. In addition, since the firing of the 5-HT cell is driven notably by mechanosensory inputs occurring during tail-flip (Issa et al., 2012), it may represent the result of integration of various cues about behavioral environment that precisely tunes 5-HT excitatory and inhibitory effects on each MN to produce a double time-scale control of their individual activities: (1) rapid modulation of each MN activity is controlled by the firing rate of 5-HT cells but (2) the sign and magnitude of these rapid effects would be tuned in a much slower way.

DATA AVAILABILITY STATEMENT

The datasets generated for this study are available on request to the corresponding author.

AUTHOR CONTRIBUTIONS

JB-C made the experiments, data analysis, writing, and editing the manuscript. PF and JD helped in writing and editing the manuscript. FI made the experiments, data analysis, writing, and editing the manuscript. DE contributed in designing Experiments, writing, and editing the manuscript. DC helped in designing experiments and made the experiments, data analysis, writing, and editing the manuscript.

FUNDING

This work was supported by University of Bordeaux, the CNRS, and National Science Foundation Research Grants 0135162 and 0641326 to DE.

REFERENCES

Bacqué-Cazenave, J., Cattaert, D., Delbecque, J. P., and Fossat, P. (2017). Social harassment induces anxiety-like behaviour in crayfish. *Sci. Rep.* 7:39935. doi: 10.1038/srep39935

Bacqué-Cazenave, J., Cattaert, D., Delbecque, J. P., and Fossat, P. (2018). Alteration of size perception: serotonin has opposite effects on the aggressiveness of crayfish confronting either a smaller or a larger rival. *J. Exp. Biol.* 221. doi: 10.1242/jeb.177840

Bacqué-Cazenave, J., Issa, F. A., Edwards, D. H., and Cattaert, D. (2013). Spatial segregation of excitatory and inhibitory effects of 5-HT on crayfish motoneurons. *J. Neurophysiol.* 109, 2793–2802. doi: 10.1152/jn.01063.2012

Beltz, B. S. (1999). Distribution and functional anatomy of amine-containing neurons in decapod crustaceans. *Microsc. Res. Tech.* 44, 105–120. doi: 10.1002/(SICI)1097-0029(19990115/01)44:2/3<105::AID-JEMT5>3.0.CO;2-K

Beltz, B. S., and Kravitz, E. A. (1983). Mapping of serotonin-like immunoreactivity in the lobster nervous system. *J. Neurosci.* 3, 585–602. doi: 10.1523/JNEUROSCI.03-03-00585.1983

Beltz, B. S., and Kravitz, E. A. (1987). Physiological identification, morphological analysis, and development of identified serotonin-proctolin containing neurons in the lobster ventral nerve cord. *J. Neurosci.* 7, 533–546. doi: 10.1523/JNEUROSCI.07-02-00533.1987

Buhl, E., Schildberger, K., and Stevenson, P. A. (2008). A muscarinic cholinergic mechanism underlies activation of the central pattern generator for locust flight. *J. Exp. Biol.* 211, 2346–2357. doi: 10.1242/jeb.017384

Cattaert, D., Delbecque, J. P., Edwards, D. H., and Issa, F. A. (2010). Social interactions determine postural network sensitivity to 5-HT. *J. Neurosci.* 30, 5603–5616. doi: 10.1523/JNEUROSCI.0367-10.2010

Cazalets, J. R., Sqalli-Houssaini, Y., and Clarac, F. (1992). Activation of the central pattern generators for locomotion by serotonin and excitatory amino acids in neonatal rat. *J. Physiol.* 455, 187–204. doi: 10.1113/jphysiol.1992.sp019296

El Manira, A., Cattaert, D., and Clarac, F. (1991). Monosynaptic connections mediate resistance reflex in crayfish (*Procambarus clarkii*) walking legs. *J. Comp. Physiol. A* 168:337.

Fossat, P., Bacqué-Cazenave, J., De Deurwaerdere, P., Cattaert, D., and Delbecque, J. P. (2015). Serotonin, but not dopamine, controls the stress response and anxiety-like behavior in the crayfish *Procambarus clarkii*. *J. Exp. Biol.* 218, 2745–2752. doi: 10.1242/jeb.120550

Fossat, P., Bacqué-Cazenave, J., De Deurwaerdere, P., Delbecque, J. P., and Cattaert, D. (2014). Comparative behavior. Anxiety-like behavior in crayfish is controlled by serotonin. *Science* 344, 1293–1297. doi: 10.1126/science.1248811

Hill, A. A., and Cattaert, D. (2008). Recruitment in a heterogeneous population of motor neurons that innervates the depressor muscle of the crayfish walking leg muscle. *J. Exp. Biol.* 211, 613–629. doi: 10.1242/jeb.006270

Hooper, S. L., Thuma, J. B., Guschlbauer, C., Schmidt, J., and Buschges, A. (2015). Cell dialysis by sharp electrodes can cause nonphysiological changes in neuron properties. *J. Neurophysiol.* 114, 1255–1271. doi: 10.1152/jn.01010.2014

Huber, R., and Delago, A. (1998). Serotonin alters decisions to withdraw in fighting crayfish, *Astacus astacus*: the motivational concept revisited. *J. Comp. Physiol. A.* 182, 573–583. doi: 10.1007/s003590050204

Huber, R., Orzeszyna, M., Pokorny, N., and Kravitz, E. A. (1997a). Biogenic amines and aggression: experimental approaches in crustaceans. *Brain Behav. Evol.* 50(Suppl. 1), 60–68.

Huber, R., Panksepp, J. B., Yue, Z., Delago, A., and Moore, P. (2001). Dynamic interactions of behavior and amine neurochemistry in acquisition and maintenance of social rank in crayfish. *Brain Behav. Evol.* 57, 271–282. doi: 10.1159/000047245

Huber, R., Smith, K., Delago, A., Isaksson, K., and Kravitz, E. A. (1997b). Serotonin and aggressive motivation in crustaceans: altering the decision to retreat. *Proc. Natl. Acad. Sci. USA* 94, 5939–5942.

Issa, F. A., Drummond, J., Cattaert, D., and Edwards, D. H. (2012). Neural circuit reconfiguration by social status. *J. Neurosci.* 32, 5638–5645. doi: 10.1523/JNEUROSCI.5668-11.2012

Kravitz, E. A. (1988). Hormonal control of behavior: amines and the biasing of behavioral output in lobsters. *Science* 241, 1775–1781. doi: 10.1126/science.2902685

Le Bon-Jego, M., and Cattaert, D. (2002). Inhibitory component of the resistance reflex in the locomotor network of the crayfish. *J. Neurophysiol.* 88, 2575–2588. doi: 10.1152/jn.00178.2002

Le Bon-Jego, M., Cattaert, D., and Pearlstein, E. (2004). Serotonin enhances the resistance reflex of the locomotor network of the crayfish through multiple modulatory effects that act cooperatively. *J. Neurosci.* 24, 398–411. doi: 10.1523/JNEUROSCI.4032-03.2004

Le Ray, D., Clarac, F., and Cattaert, D. (1997a). Functional analysis of the sensory motor pathway of resistance reflex in crayfish. I. Multisensory coding and motor neuron monosynaptic responses. *J. Neurophysiol.* 78, 3133–3143.

Le Ray, D., Clarac, F., and Cattaert, D. (1997b). Functional analysis of the sensory motor pathway of resistance reflex in crayfish. II. Integration of sensory inputs in motor neurons. *J. Neurophysiol.* 78, 3144–3153.

Lee, S. H., Taylor, K., and Krasne, F. B. (2008). Reciprocal stimulation of decay between serotonergic facilitation and depression of synaptic transmission. *J. Neurophysiol.* 100, 1113–1126. doi: 10.1152/jn.90267.2008

Livingstone, M. S., Harris-Warrick, R. M., and Kravitz, E. A. (1980). Serotonin and octopamine produce opposite postures in lobsters. *Science* 208, 76–79. doi: 10.1126/science.208.4439.76

Pearlstein, E., Watson, A. H., Bevengut, M., and Cattaert, D. (1998). Inhibitory connections between antagonistic motor neurones of the crayfish walking legs. *J. Comp. Neurol.* 399, 241–254. doi: 10.1002/(SICI)1096-9861(19980921)399:2<241::AID-CNE7>3.0.CO;2-0

Sillar, K. T., and Skorupski, P. (1986). Central input to primary afferent neurons in crayfish, *Pacifastacus leniusculus*, is correlated with rhythmic motor

output of thoracic ganglia. *J. Neurophysiol.* 55, 678–688. doi: 10.1152/jn.1986.55.4.678

Spitzer, N., Antonsen, B. L., and Edwards, D. H. (2005). Immunocytochemical mapping and quantification of expression of a putative type 1 serotonin receptor in the crayfish nervous system. *J. Comp. Neurol.* 484, 261–282. doi: 10.1002/cne.20456

Teshiba, T., Shamsian, A., Yashar, B., Yeh, S. R., Edwards, D. H., and Krasne, F. B. (2001). Dual and opposing modulatory effects of serotonin on crayfish lateral giant escape command neurons. *J. Neurosci.* 21, 4523–4529. doi: 10.1523/JNEUROSCI.21-12-04523.2001

Yeh, S. R., Fricke, R. A., and Edwards, D. H. (1996). The effect of social experience on serotonergic modulation of the escape circuit of crayfish. *Science* 271, 366–369. doi: 10.1126/science.271.5247.366

Yeh, S. R., Musolf, B. E., and Edwards, D. H. (1997). Neuronal adaptations to changes in the social dominance status of crayfish. *J. Neurosci.* 17, 697–708. doi: 10.1523/JNEUROSCI.17-02-00697.1997

Zhang, B., and Harris-Warrick, R. M. (1994). Multiple receptors mediate the modulatory effects of serotonergic neurons in a small neural network. *J. Exp. Biol.* 190, 55–77.

Conflict of Interest: The authors declare that the research was conducted in the absence of any commercial or financial relationships that could be construed as a potential conflict of interest.

frontiers in Physiology

ORIGINAL RESEARCH
published: 26 November 2019
doi: 10.3389/fphys.2019.01423

Responsiveness to Sugar Solutions in the Moth *Agrotis ipsilon*: Parameters Affecting Proboscis Extension

*Camille Hostachy, Philippe Couzi, Melissa Hanafi-Portier†, Guillaume Portemer, Alexandre Halleguen, Meena Murmu, Nina Deisig† and Matthieu Dacher**

Sorbonne Université, Université Paris Est Créteil, INRA, CNRS, IRD – Institute for Ecology and Environmental Sciences of Paris (iEES Paris), Paris, France

Adult moths need energy and nutrients for reproducing and obtain them mainly by consuming flower nectar (a solution of sugars and other compounds). Gustatory perception gives them information on the plants they feed on. Feeding and food perception are integrated in the proboscis extension response, which occurs when their antennae touch a sugar solution. We took advantage of this reflex to explore moth sugar responsiveness depending on different parameters (i.e., sex, age, satiety, site of presentation, and composition of the solution). We observed that starvation but not age induced higher response rates to sucrose. Presentation of sucrose solutions in a randomized order confirmed that repeated sugar stimulations did not affect the response rate; however, animals were sometimes sensitized to water, indicating sucrose presentation might induce non-associative plasticity. Leg stimulation was much less efficient than antennal stimulation to elicit a response. Quinine prevented and terminated sucrose-elicited proboscis extension. Males but not females responded slightly more to sucrose than to fructose. Animals of either sex rarely reacted to glucose, but curiously, mixtures in which half sucrose or fructose were replaced by glucose elicited the same response rate than sucrose or fructose alone. Fructose synergized the response when mixed with sucrose in male but not female moths. This is consistent with the fact that nectars consumed by moths in nature are mixtures of these three sugars, which suggests an adaptation to nectar perception.

Keywords: moth, sugar responsiveness, dose-response curves, nectar, sugar, quinine, gustatory perception, proboscis extension response

OPEN ACCESS

Edited by:
Sylvia Anton,
Institut National de la Recherche Agronomique (INRA), France

Reviewed by:
Romina B. Barrozo,
National Council for Scientific and Technical Research (CONICET), Argentina
Liang Sun,
Chinese Academy of Agricultural Sciences, China

****Correspondence:***
Matthieu Dacher
matthieu.dacher@upmc.fr

†Present address:
Melissa Hanafi-Portier, MNHN – Departement Systematique et Evolution, ISYEB, Paris, France; Laboratoire Environnement Profond, Unite d'Etude des Ecosystèmes Profonds, Centre Ifremer de Bretagne, IFREMER – Ressources Physiques et Écosystemes de fond de Mer, Plouzane, France
Nina Deisig, Computational Systems Neuroscience, Institute of Zoology, University of Cologne, Cologne, Germany

Specialty section:
This article was submitted to Invertebrate Physiology, a section of the journal Frontiers in Physiology

Received: *20 June 2019*
Accepted: *04 November 2019*
Published: *26 November 2019*

Citation:
Hostachy C, Couzi P, Hanafi-Portier M, Portemer G, Halleguen A, Murmu M, Deisig N and Dacher M (2019) Responsiveness to Sugar Solutions in the Moth Agrotis ipsilon: Parameters Affecting Proboscis Extension. Front. Physiol. 10:1423. doi: 10.3389/fphys.2019.01423

INTRODUCTION

Moth reproduction and its regulation by sex pheromone have been largely studied to find ways to control their populations, as their larvae are important crop pests (Cook et al., 2007; Naranjo et al., 2015; Evenden, 2016). While less exploited for managing these pests, adult moths feeding behaviors and gustatory perception are also important for their reproduction; they need energy and nutrients to produce an abundant and healthy offspring (Hill, 1989; Hill and Pierce, 1989; Boggs and Ross, 1993; Wheeler, 1996; Boggs, 1997a,b;

O'brien et al., 2000, 2004; Fischer et al., 2004; Jervis et al., 2005; Geister et al., 2008; Marchioro and Foerster, 2013; Levin et al., 2017a,b). Their food consists largely in sugars from flower nectars, which contains mainly fructose, glucose, and sucrose as well as a few amino acids and, sometimes, repellent substances (Baker and Baker, 1973; Baker, 1977; Lüttge, 1977; Gottsberger et al., 1984; Adler, 2000; O'brien et al., 2000, 2004; Pacini et al., 2003; De La Barrera and Nobel, 2004; Adler et al., 2006; Heil, 2011; Nepi et al., 2012; Atwater, 2013; Roy et al., 2017). Thus, gustatory perception is important for moths to assess food quality and discriminate what is edible from what is toxic (Glendinning, 2002; Adler and Irwin, 2005; Tiedeken et al., 2014).

When their legs, antennae, or proboscis contact a sugar solution of sufficient concentration, moths extend their proboscis and use it to imbibe the solution. This proboscis extension response (PER) first reflects the integration of gustatory perception and motivation for sugar and then allows feeding. Sucrose-elicited PER has been described and involved in associative learning in restrained insects including moths (Hartlieb, 1996; Fan et al., 1997; Hartlieb et al., 1999a,b; Fan and Hansson, 2001; Skiri et al., 2005; Jorgensen et al., 2007), butterflies (Kroutov et al., 1999), bees (Menzel, 1999, 2012; Page and Erber, 2002; Sandoz, 2011; Giurfa and Sandoz, 2012; Giurfa, 2015) and flies (Fresquet, 1999; Chabaud et al., 2006); similar feeding-related responses exist in ants (Guerrieri and d'Ettorre, 2010; Perez et al., 2013), crickets (Matsumoto et al., 2015), and bugs (Vinauger et al., 2013; Labrousse et al., 2017). PER has been used by Scheiner and her colleagues to assess responsiveness to sucrose in bees and flies (Scheiner et al., 2004a,b, 2013; Mujagic et al., 2010). These authors demonstrated that sucrose responsiveness is correlated to important parameters of honey bee biology such as division of labor, and foraging decisions are modulated by sugar gustatory perception (see for instance Nachev et al., 2013). Sugar-induced PER has been used in various moth species (Hill and Pierce, 1989; Winkler et al., 2005; Jørgensen et al., 2007; Zhang et al., 2010; Minoli et al., 2012) using different sucrose concentrations and animals in different physiological conditions; however, the impact of the physiological state on sugar responsiveness is hardly known in these insects.

Thus, we aimed for the first time at specifically looking at sugar responsiveness in relation to different physiological parameters (i.e., sex, age, and level of satiety) in the moth species *Agrotis ipsilon*. Testing systematically different concentrations and kinds of sugars composing nectar (i.e., sucrose, fructose, and glucose) further allowed us to find the optimal parameters for releasing the PER. Our work was inspired by extensive work on sucrose responsiveness in bees and flies (Scheiner et al., 2004a, 2013). We tested if sucrose responsiveness can also be induced using other sensory pathways beyond perception by the antennae (i.e., legs) and modulated by other gustatory stimuli (quinine). We also uncovered a non-associative plasticity, sensitization for water.

Abbreviations: PER, Proboscis extension response.

MATERIALS AND METHODS

Animals

This study was performed on adult *A. ipsilon* (Lepidoptera, Noctuidae), which is a native species of France. Animals were reared in our laboratory in INRA, Versailles, France. Males and females were separated at the pupal stage and kept in different climatic chambers (22°C, 60–70% relative humidity) under an inverted photoperiod (16 h of light, starting at 18 h). Newly emerged adults (i.e., animals having just completed the imaginal molt) were collected every day (so that their post-emergence age is known) and grouped by 10 in breeding boxes (20 × 11.5 × 5 cm) with *ad libitum* access to either sucrose solution (fed animals) or tap water (starved animals). The sucrose solution was 12% weight/weight (13.6% weight/volume). We did not use more than 5-day starvation delays as the moths start to be weak or even die after starving for 6 days. Moths provided with sucrose gain weight, whereas moths provided only with water lose weights (unpublished observation), and we often observed that they readily drink the 12% solution in their breeding boxes but hardly react to water. Thus, it is reasonable to assume the feeding statuses of water- and sucrose-fed moths are not the same.

Experiments were conducted under dim red light and started at the middle of the scotophase, when moths are the most active (highest responsiveness of males to the sex pheromone, sex pheromone release by females), under a temperature of 22–24°C and 65% relative humidity. Unless otherwise mentioned, experiments were performed on day 5 post-emergence. Five-day-old *A. ipsilon* are standardly studied because males of this age are sexually mature and respond to the female sex pheromone (Gemeno and Haynes, 2000). In the morning of the experiments, animals were fixed in plastic tubes made from 1 ml pipette cones cut to fit a moth, so that only the head (with antennae and proboscis) protruded. Their position was further assured by inserting a small ball of absorbing paper or cotton behind them in the tube and fixing the top of their body to the tube using adhesive tape. Legs were blocked by the tape or inside the tube, unless otherwise mentioned (section "Proboscis Extension Response Induced by Leg Stimulation" reports the effect of leg stimulation). Once restrained, animals were left to acclimatize in the experimental room until the beginning of the experiment (in the afternoon).

Sugar Responsiveness Assay and Solutions Used

We adapted Scheiner's protocol for honey bees and flies (Scheiner et al., 2004a,b, 2013) to moths. Assessing sugar sensitivity consisted in presenting solutions of increasing sugar concentration; a 10-min interval between each presentation was used, except in section "Sensitization and Presentation Timing," where a 1-min interval was also used. A solution presentation consisted in touching both antennae of the animal with a wooden toothpick imbibed with the sugar solution during 1–4 s; a response was recorded if the animal released a PER, i.e., extended its proboscis beyond its position at the

onset of the stimulation (the initial position varies from one animal to the other, but the occurrence of the proboscis extension can be observed unambiguously). Animals were not fed, and great care was taken to avoid touching the proboscis with the toothpick by coming from behind the head, while the proboscis extends in front of it. We defined PER rate as the proportion of animals releasing a PER upon presentation of a sugar solution on the antennae.

The solution concentrations were 0 (i.e., deionized water), 0.1, 0.3, 1, 3, 10, and 30% (weight/weight in deionized water, e.g., 30% is 3 g of sucrose in 7 ml of deionized water). These sugar concentrations correspond to 0.1, 0.4, 1.1, 4.3, 11.1, and 42.9% weight/volume, respectively. A second presentation of the 0% solution was made afterwise to monitor the occurrence of sensitization, i.e., the fact animals might start to respond to weak stimuli such as 0% solution just because they are excited by previous sugar presentations. Sensitization is discussed in section "Sensitization and Presentation Timing." This set of concentrations is inspired of previous studies in bees and flies (Scheiner et al., 2004a, 2013) and corresponds to a logarithmic increase in the stimulus intensity (i.e., around −1, −0.5, 0, 0.5, 1, 1.5), consistently with Weber's law in sensory physiology (Waddington and Gottlieb, 1990; Akre and Johnsen, 2014; Shafir and Yehonatan, 2014). In our experiments, the sugar used was usually sucrose, but fructose, glucose, and various mixtures of these sugars were also tested (see section "Response to Various Sugars and Sugar Mixtures"). We focused on these three sugars (obtained from Sigma) as they are the main constituents of flower nectar, the main food of adult moths: typically 10–15% of the fresh mass for each sugar, possibly up to 30% for sucrose (Lüttge, 1977; Gottsberger et al., 1984; Pacini et al., 2003; De La Barrera and Nobel, 2004; Roy et al., 2017). In some experiment (section "The Effect of Quinine on Sucrose Responsiveness"), animals were also presented with 100 mM quinine (Sigma).

To rule out the possibility of having animals responding to water rather than sugar, animals responding to the initial water presentation were not kept in the analysis. However, removing these animals hardly modified the results. Supplementary data report figures including all the animals and the corresponding analysis (**Supplementary Figures S1–S6, Supplementary Tables S13–S24**).

Experiments

Age, Sex, and Feeding Status

First, we investigated the effect of age and feeding status. Sucrose responsiveness was measured for various sucrose concentrations in five groups of males: 3-day-old moths either (1) with *ad libitum* access to sucrose solution (fed) or (2) starved (*ad libitum* access to water only), and 5-day-old moths either (3) fed, (4) starved for 3 days, or (5) starved for 5 days. Five-day-old moths starved for 3 days received sucrose from 0 to 2 days post-emergence and then only water for the following 3 days. Using this group was an attempt to discriminate between age of the animals and starvation duration, as when comparing 3-day-old and 5-day-old unfed moths, we simultaneously compare age (3-day-old or 5-day-old) and starvation duration (3 days or 5 days), so that the two factors are confused.

To assess the effect of sex, this experiment was replicated with females using the same age/starvation treatments, plus a group of 5-day-old male moths starved for 5 days for comparison purposes. Experiments reported elsewhere (Hostachy et al., submitted) indicated that sucrose responsiveness of males is not affected by the presence of sex pheromone, which allows to test them in parallel with females.

Sensitization and Inter-trial Interval

In a sucrose responsiveness assay, it is important to know whether responses (or lack thereof) to repeated presentations of sucrose of varying concentrations are independent from each other: having already been stimulated by a sucrose solution could affect responsiveness to the next simulations. This could be explained by sensitization (or habituation if we observed a decrease) and/or a time-dependent modification of motivation. To quantify this phenomenon, we performed the sucrose responsiveness assay in two groups of 5-day-old female moths: one group was presented with the sucrose solutions in the same order as previously (ascending concentrations), whereas for the other group, the six sucrose solutions were presented in a randomly determined order for each animals (keeping water as first and last stimulation). If sensitization or motivation variations alter sugar responsiveness when the solutions are presented in ascending order, then sugar responsiveness will be different in the random order group. Within each group, a sub-group was unfed for 5 days, whereas the other sub-group was fed; this was done to evaluate whether the occurrence of sensitization or motivation variations differed between fed and unfed animals.

To further explore the occurrence of sensitization and determine the importance of the inter-presentation interval, we used two inter-trial intervals: either 10 min (as previously) or 1 min. Indeed, a potential sensitization should occur more easily with a shorter inter-trial interval, as this is a form of short-term plasticity. In some animals, we also interleaved water presentations between sucrose presentations, as this was initially done in some experiments with bees to try and prevent sensitization (see for instance, Scheiner et al., 2003). For these groups, the interval between two sucrose presentations was either 2 or 20 min, with a water presentation interleaved at 1 or 10 min, respectively.

Effect of the Stimulation Site

While proboscis extension is classically elicited by antennal stimulation in bees and moths, it can also be triggered by leg stimulation (which is standard for fruit flies). Thus, we performed again the sucrose sensitivity protocol using two groups of animals, stimulating either the antennae (as previously, reference group) or the tibia and tarsi of the front legs. Leg-stimulated animals were restrained slightly differently: one of their front leg was fixed, so that it stayed outside of the tube. During leg stimulations, great care was taken to avoid touching the

antennae. After testing all sucrose concentrations using the legs, the leg-stimulated animals were then assessed a second time using the antennae (i.e., the whole protocol was completed using the legs, then performed again using the antennae).

The proboscis also bears gustatory sensilla, so that stimulating it should elicit a PER. However, in moths, it is quite inconvenient to reach when it is coiled in its rest position; furthermore, it is impossible to prevent the animals to imbibe some of the solution in this case. Thus, evaluating sucrose responsiveness by direct proboscis stimulation is not feasible with this protocol.

Effects of a Bitter Compound: Quinine

As in nature moths consume sugar solutions found in flowers, they can be exposed to alkaloids that might have a deterrent effect. To assess whether alkaloids such as quinine affect PER and sucrose responsiveness, we performed again the sucrose responsiveness protocol on 5-day-old males. Animals releasing a PER had their proboscis immediately touched either with water (control group) or with 100 mM quinine, and we recorded whether the PER would continue after this proboscis stimulation. To complement these observations, we also measured responsiveness to sucrose and sucrose plus 100 mM quinine in 5-day-old males.

Effects of Other Sugars: Fructose, Glucose, and Sugar Mixtures

Sucrose is the reference sugar used in PER experiments in various insects. However, it is well known that nectar can also include fructose and glucose in various proportions. Thus, we measured responsiveness for fructose and glucose besides sucrose, as well as mixtures between these three molecules. For mixtures, the same concentrations were used with sugars in equal amounts (i.e., a 3% sucrose/fructose solution contains 1.5% sucrose, 1.5% fructose, weight/weight; or 2.15% of each sugar, weight/volume). Experiments were done with 5-day-old males unfed for 5 days.

In another experiment, the sugar responsiveness assay was performed in females with glucose, fructose, and sucrose, as well as sucrose/fructose and sucrose/fructose/glucose mixtures. All animals were 5-day-old females unfed for 5 days, and a group of 5-day-old males unfed for 5 days and tested with sucrose was also used for comparison purpose.

Data Analysis

Data were analyzed using R 3.4.0 (R Core Team, 2017) and RStudio 1.1.423, taking an α risk of 0.050. PER rates were computed for each experimental group and are reported in the figures, with the sample sizes reported in parenthesis in the legends. Thus, a dose-response curve was obtained for each experimental group.

For each sugar concentration in a dose-response curve, PER rates were compared between experimental groups using χ^2 test or bilateral Fisher's exact test when χ^2's assumption (Cochran's rule) was not met. When more than two groups were compared and a significant p was obtained, we performed pairwise comparisons using the same tests and adjusted p for repeated testing using Holm's method (Holm, 1979); however, it sometimes happened adjusted p could not determine the source of the difference detected in the global test.

In a few cases, response variations within a group were compared using McNemar's test, using Holm's method to adjust p when needed. Logistic regression (binomial generalized linear model) was also used in section "Sensitization and Presentation Timing" to assess whether PER rates to the final water presentation were affected by the sugar concentration presented 10 min before or by the number of PER previously released (preliminary stepwise analysis indicating the interaction term was not significant, so that it was dropped). To avoid tedious lists of p in the results, most of them are only presented in tables in supplementary data (**Supplementary Tables S1–S12**, one table for each figure or figure panel).

RESULTS

The Effect of Age, Starvation Duration, and Sex on Sucrose Responsiveness

We first explored the experimental parameters required for optimally assessing sucrose responsiveness by comparing age and starvation duration. For male moths (**Figure 1A** and **Supplementary Figure S1A**), significant differences were observed for all sucrose solutions of 1% and higher (χ^2 or Fisher's exact test, $p \leq 0.004$): overall, fed animals were less responsive than unfed ones, irrespective of their age, while 5-day-old moths unfed for 5 days were consistently among the highest PER rates (details of the pairwise comparisons are in **Supplementary Table S1**).

For females (**Figure 1B** and **Supplementary Figure S1B**), results were analyzed in two steps: first, 5-day-old males and females unfed for 5 days were compared, and second, all female groups were compared. For the lowest concentrations (0.1 and 0.3%), the PER rates of females were slightly lower than males' (χ^2 or Fisher's exact test, $p \leq 0.022$), suggesting females are slightly less responsive than males for the lowest concentrations. However, the same pattern as for males was observed for the PER rates across treatments, i.e., 5-day-old females unfed for 5 days were consistently among the highest PER rates for 0.3, 1, 3, and 30% concentrations (details of the pairwise comparisons are in **Supplementary Table S2**).

Sensitization and Presentation Timing

When the independence of the stimulations and the occurrence of sensitization was assessed (**Figure 2A** and **Supplementary Figure S2A**), there was a global significant difference between the four groups for 1, 3, and 10% sucrose concentrations (χ^2 or Fisher's exact test, $p \leq 0.001$), replicating the previous finding that fed animals have a lower sucrose responsiveness; by contrast, presenting the solutions in random order or in ascending order did not have any effect (**Supplementary Table S3** reports detailed analysis). As a result, sensitization (or even habituation) or variations of motivations during the assay are unlikely to

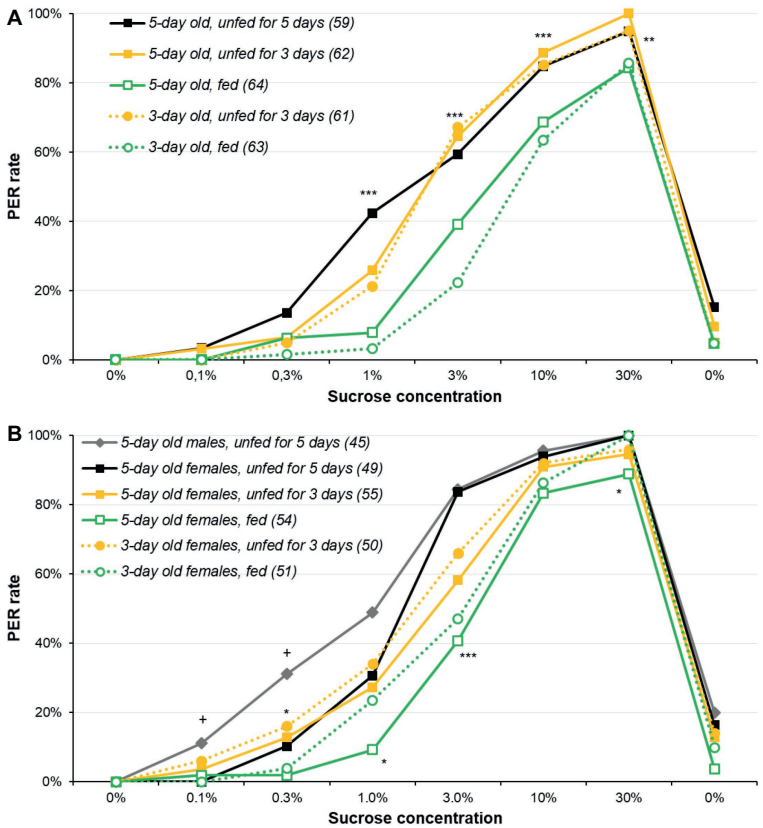

FIGURE 1 | Effect of age and starvation duration on sucrose responsiveness in *Agrotis ipsilon*. The plots present dose-response curves for various sucrose concentrations (*x*-axis); the *y*-axis reports the PER rate, i.e., the proportion of insects extending their proboscis when their antennae were briefly touched with a drop of sucrose solution. Each sucrose solution presentation was separated by 10 min. In the legend, numbers in parenthesis correspond to the sample sizes. In part **(A)**, experiments were done with males; in part **(B)**, experiments were done with females and a group of males for comparison purpose. Stars denote significant differences between male or female groups in χ^2 or Fisher's exact tests (*$p < 0.050$; **$p < 0.010$; ***$p < 0.001$); in part **(B)**, crosses denote significant differences between 5-day old males and females unfed for 5 days in χ^2 of Fisher's exact test ($^+p \leq 0.050$). Details of the analyses are reported in **Supplementary Table S1** for part **(A)** and **Supplementary Table S2** for part **(B)**.

be an important determinant of the PER rate in the sugar responsiveness assay.

However, even if sensitization does not alter sucrose responsiveness, it could explain the PER rate observed during the final water presentation. To test this, we used the data from the unfed random group and computed a logistic regression to test the effect of two factors on water responsiveness: the total number of responses before the final water test (ranging from 0 to 6, i.e., the number of responses to the 6 sugar concentrations) and the concentration of the sugar solutions used before water (which can be any of the 6 concentrations in this random order group). Both factors were significant (logistic regression $p \leq 0.046$). This indicates that animals responding to most sucrose concentrations tend to respond to the final water, even though they did not respond to the initial water presentation. Moreover, a higher concentration just before the final water presentation (typically, the 3, 10, or 30% solutions) also contributes to this sensitization to water.

Figure 2B and **Supplementary Figure S2B** report sucrose responsiveness with various inter-trial intervals and with or without interleaved water. Our hypothesis was that sensitization would occur in the 1-min group without interleaved water and be lower in the 10-min group with interleaved water, but this was not the case: the four groups were similarly responsive (χ^2 or Fisher's exact test, $p \geq 0.064$; details of the analysis are in **Supplementary Table S4**). Moreover, responses to the interleaved water presentation were low and did not differ significantly across groups (data not shown; Fisher's exact test, $p \geq 0.386$).

Proboscis Extension Response Induced by Leg Stimulation

Results on the effect of leg stimulation are presented in **Figure 3** and **Supplementary Figure S3** and details of the statistics in **Supplementary Table S5**. Leg stimulation was much less efficient to elicit PER, as it only did so to a meaningful level for the highest concentrations; in all cases, leg-elicited-PER rate was significantly smaller from antennal-elicited-PER rate (χ^2 or Fisher's exact test, $p \leq 0.005$). A second series of tests was made to compare the leg group to the reference group when

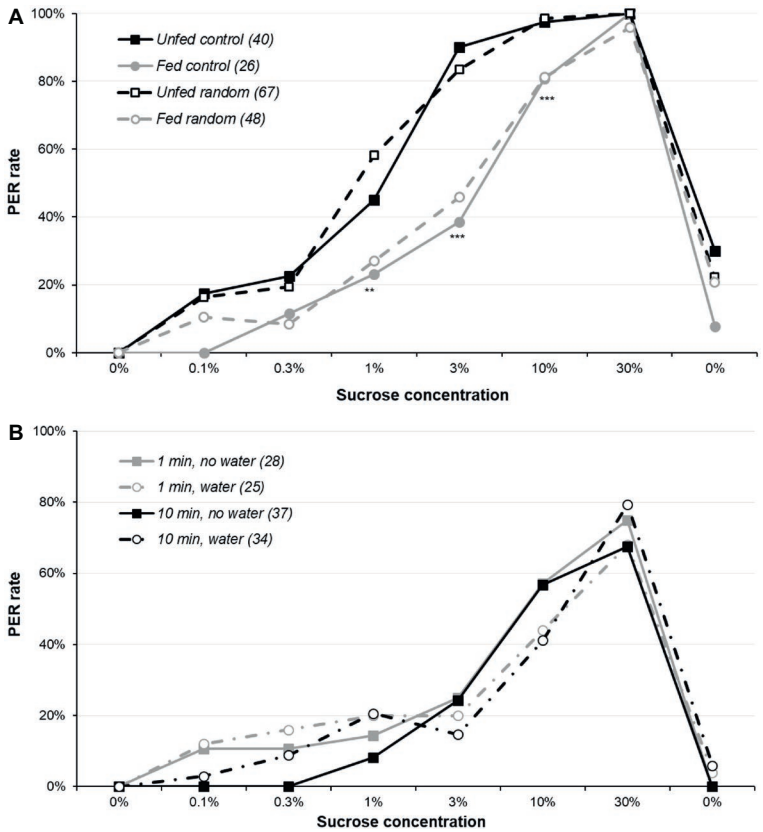

FIGURE 2 | Sensitization and sucrose responsiveness. Part **(A)** reports sucrose responsiveness in four groups of 5-day-old females: the first two were presented sucrose concentrations in ascending order (as previously), whereas for the other two, the six sucrose solutions were presented in an order randomly determined for each animal. Within each treatment, one of the two groups had been unfed for 5 days, whereas the other was fed. Part **(B)** plots the sucrose responsiveness in four groups of unfed 5-day-old males: two groups with an inter-trial interval of 10 min (as previously) and two groups with an inter-trial interval of 1 min. For each interval, one of the two groups had a water presentation every other trials, so that for these groups, the interval between two sucrose presentations was either 2 or 20 min, with a water presentation interleaved at 1 or 10 min. Some animals in the two no-water groups were not presented the final water solution. Other details are as in **Figure 1**. Details of the analyses are reported in **Supplementary Table S3** for part **(A)** and **Supplementary Table S4** for part **(B)**.

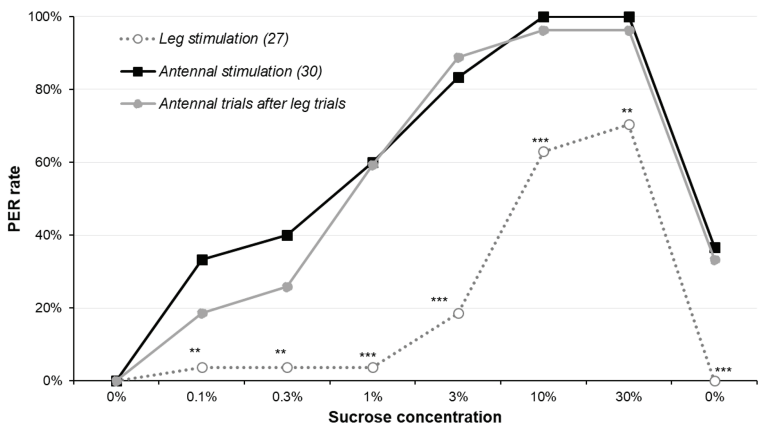

FIGURE 3 | Comparison of antennal stimulation and leg stimulation. The sucrose sensitivity experiment was conducted by stimulating either the antennae (as previously) or the legs of 5-day-old males starved for 5 days. Animal stimulated on the legs for the complete set of sucrose solutions underwent the protocol a second time with the antennae (i.e., the whole set of sucrose solutions was presented twice, one on the legs and the other on the antennae). Stars denote significant difference between the leg stimulated group and the antennal stimulated group run in parallel (χ^2 or Fisher's exact test; $^{**}p < 0.010$; $^{***}p < 0.001$). Details of the analyses are reported in **Supplementary Table S5**. Other details are as in **Figure 1**.

the leg group was retested on the antennae: this time, there was no difference between the two groups (χ^2 or Fisher's exact test, $p \geq 0.205$). This means that the leg-stimulated group had the same sucrose responsiveness as the control when tested on the antennae. This confirms that the lower PER rate is only due to the different types of stimulation.

The Effect of Quinine on Sucrose Responsiveness

The effects of quinine stimulation are reported in **Figure 4A** and **Supplementary Figure S4A** and the detailed analysis in **Supplementary Table S6**. Before contacting the proboscis with water or quinine, the sucrose responsiveness did not significantly differ between the water- and the quinine-stimulated group (χ^2 or Fisher's exact test, $p \geq 0.123$), confirming the two groups were identical at this step. Touching the proboscis with water did not affect the PER, as no animal retracted its proboscis; by contrast, most animals which proboscis touched quinine interrupted the PER and retracted the proboscis, almost significantly for sucrose concentrations 1 and 3% (McNemar's test, $p \leq 0.071$), and significantly for concentrations 10 and 30% (McNemar's test, $p \leq 0.005$); no difference was observed for other concentrations, but the PER rates were low for them anyway. We also compared the proportions of animals retracting the proboscis among those initially responding, and the results were the same (data not shown). Interestingly, the fact that the PER rates remain the same as in the control group in ulterior sucrose solution presentations means that even though quinine elicited proboscis retraction, it does not modulate sucrose responsiveness (at least after 10 min). Moreover, when quinine was added to sucrose (**Figure 4B**, **Supplementary Figure S4B**, **Supplementary Table S7**), it strongly inhibited PER (χ^2 or Fisher's exact test; $p \leq 0.024$).

Response to Various Sugars and Sugar Mixtures

In a first experiment, animals were presented with either sucrose, fructose, or a mixture of these sugars (**Figure 5A**

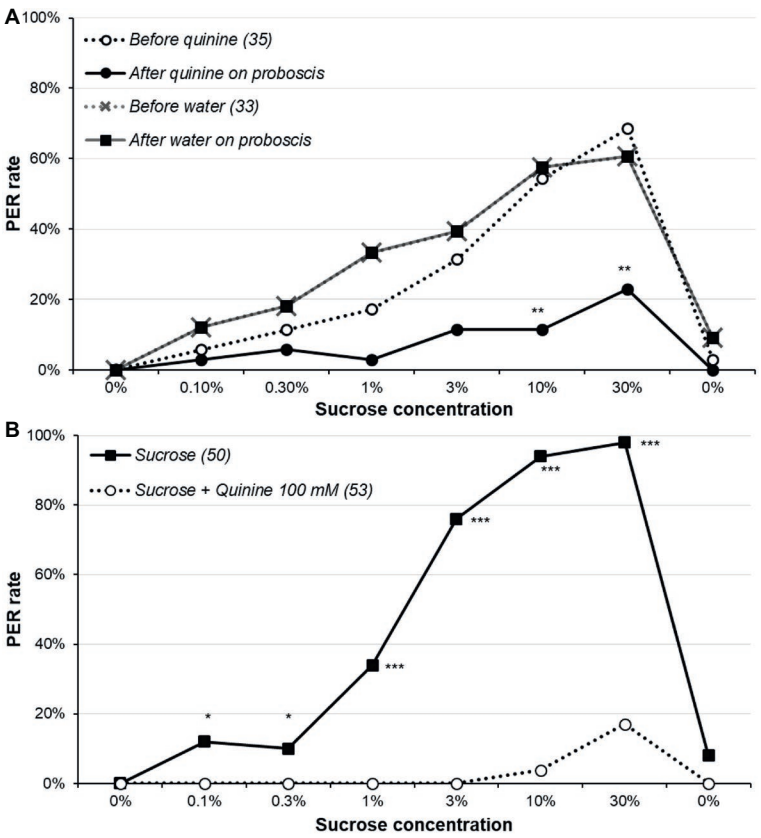

FIGURE 4 | Effect of quinine on sucrose responsiveness. In part **(A)**, animals were presented the series of sucrose solutions (dotted lines), and if they released a PER, they immediately received either 100 mM quinine or water on the extended proboscis; the continuous lines indicate the proportion of animals still releasing a PER after receiving one of these solution. Notice that as touching the proboscis with water had no effect, the two lines (before and after water) are superimposed. Stars denote a significant difference between the PER rate before and after touching the proboscis with quinine, i.e., a significant rate of proboscis retraction (McNemar's test $^{**}p < 0.010$); detailed analysis is in **Supplementary Table S6**. In part **(B)**, animals were presented the series of sucrose solutions either alone as previously or combined with 100 mM quinine. Stars denote a significant difference between the PER rate of the two groups (χ^2; $^{*}p < 0.050$, $^{***}p < 0.001$); detailed analysis is in **Supplementary Table S7**. All animals were 5-day-old males starved for 5 days; other details are as in **Figure 1**.

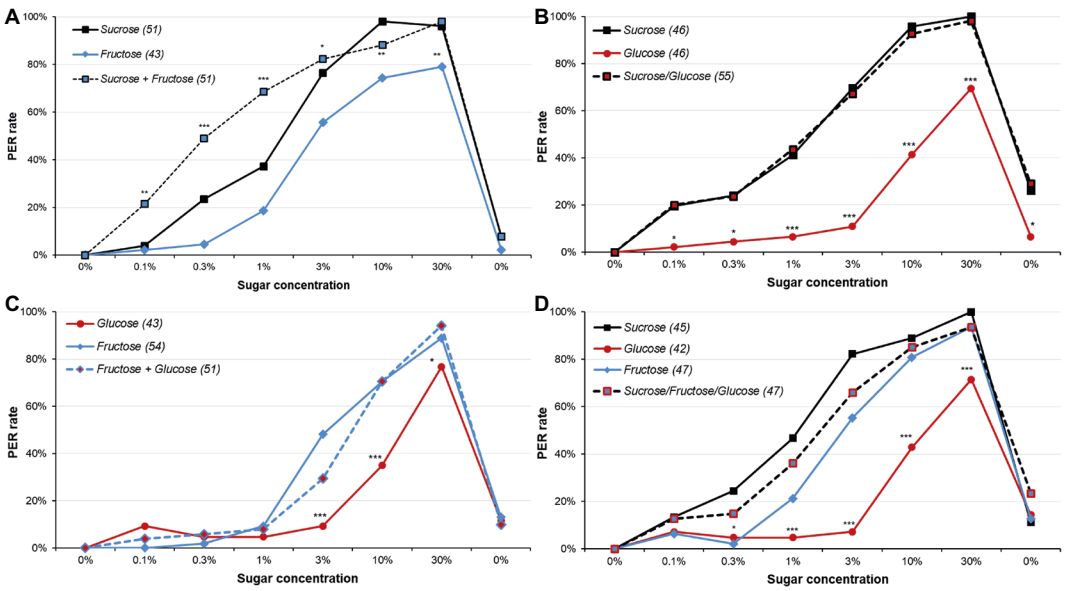

FIGURE 5 | Responsiveness to various sugars and sugar mixtures in male moths. These plots display dose-response curves for various sugars and sugar mixtures. Part **(A)** presents PER rates for fructose, sucrose, and their mixture; part **(B)** for glucose, sucrose, and their mixtures; part **(C)** for glucose, fructose, and their mixture; and part **(D)** for glucose, fructose, sucrose, and their mixtures. All mixtures involved even amount of sugars. All animals were 5-day-old male moths starved for 5 days. Other details as in **Figure 1**. Detailed analysis is reported in **Supplementary Tables S8–S11**.

and **Supplementary Figure S5A, Supplementary Table S8**). Although fructose elicited high PER rates, overall they were significantly lower than for sucrose (χ^2 or Fisher's exact test; adjusted $p = 0.068$ for 3%, $p \leq 0.046$ for 0.3, 1, 10, and 30%). Interestingly, mixtures of fructose and sucrose elicited the same level of PER rate as sucrose alone (χ^2 or Fisher's exact test; adjusted $p \geq 0.217$ for 3, 10, or 30%), or even higher responses for lower concentrations (χ^2 or Fisher's exact test; adjusted $p \leq 0.030$ for 0.1, 0.3, or 1%). Thus, while fructose tended to elicit less responses than sucrose, replacing half the sucrose by fructose in a mixture actually improved the PER rate, indicating a synergistic effect.

In a second experiment, we compared animals' responses to sucrose, glucose, and their mixture (**Figure 5B** and **Supplementary Figure S5B, Supplementary Table S9**). Glucose elicited PER much less often than the two other solutions (χ^2 or Fisher's exact test, adjusted $p \leq 0.020$) and induced less sensitization for the final water presentation (χ^2, adjusted $p \leq 0.022$). Yet, replacing half the sucrose by glucose did not modify the PER rate relatively to the sucrose group (χ^2 or Fisher's exact test, adjusted $p \geq 0.686$); thus, in spite the mixture only includes half sucrose found in the sucrose solution (e.g., the 3% mixture only includes 1.5% sucrose), and so should elicit much lower PER rates, the response is unchanged. This leads to the intriguing conclusion that while glucose did not elicit much response, replacing half of the sucrose by glucose in a solution did not decrease the response, although there was not the synergy observed for sucrose and fructose.

When the responses to fructose, glucose, and their mixture were compared (**Figure 5C** and **Supplementary Figure S5C, Supplementary Table S10**), results were similar: glucose elicited less response than fructose or fructose/glucose mixtures for 3 and 10% (χ^2, adjusted $p \leq 0.031$); for 30% sugar solution, the global test was significant (χ^2, $p = 0.038$), but pairwise comparisons were not. Fructose and fructose/glucose mixtures elicited similar PER rates, except for the 3% concentrations, where the mixture was slightly inferior (χ^2, adjusted $p = 0.049$). To sum up, while animals had lower PER rates for glucose than for fructose, replacing half of the fructose by glucose impaired only slight response. This is comparable to what was seen with sucrose/glucose mixtures.

Finally, we compared PER rates to sucrose, glucose, fructose, and a sucrose/glucose/fructose mixture (**Figure 5D** and **Supplementary Figure S5D, Supplementary Table S11**). We replicated the observation that fructose was slightly but significantly less responded to than sucrose (χ^2 or Fisher's exact test, adjusted $p \leq 0.040$ for 0.3, 1 and 3%), and that glucose was much less responded to than fructose or sucrose for 1, 3, 10, and 30% (χ^2 or Fisher's exact test: adjusted $p = 0.068$ for 1% for glucose vs. fructose, adjusted $p \leq 0.046$ for other comparisons). Moreover, glucose also elicited less PER than the mixture for 1, 3, 10, and 30% (χ^2 or Fisher's exact test, adjusted $p \leq 0.045$), whereas sucrose or fructose did not differ from it (χ^2 or Fisher's exact test, adjusted $p \geq 0.151$). Therefore, neither synergy nor inhibition was observed in this case.

When females were tested for sugar mixtures (**Figure 6** and **Supplementary Figure S6, Supplementary Table S12**), contrasting for what was seen in **Figure 1B**, males and females tested for sucrose did not differ for low concentration of sucrose (χ^2, $p \geq 0.763$) and males were only slightly higher than females for 10 and 30% sucrose, but without reaching significance (Fisher's exact test, $p = 0.060$ in both cases). While there was no difference between the female groups for 0.1 or 0.3% sugar

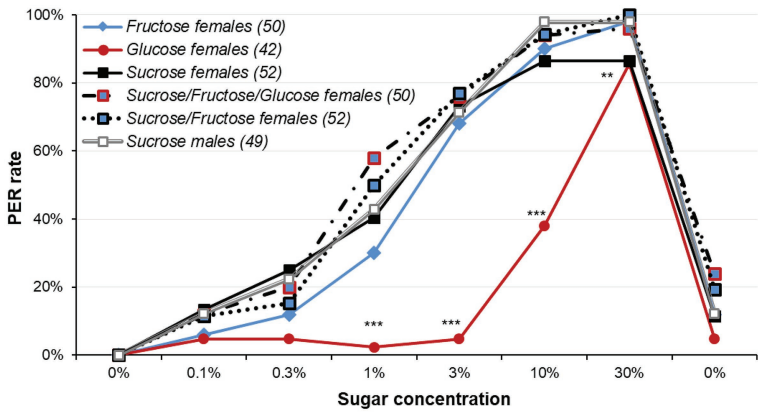

FIGURE 6 | Responsiveness to various sugars and sugar mixtures in female moths. This plot reports dose-response curves for various sugar and sugar mixtures in 5-day old female moths starved for 5 days; a group of 5-day old males starved for 5 days was also used for comparison purpose. Sucrose, fructose, and glucose were used, as well as sucrose/fructose/glucose and sucrose/fructose mixtures. Stars denote significant differences between female groups (χ^2 or Fisher's exact test; $^{**}p < 0.010$; $^{***}p < 0.001$). Other details as in **Figure 1**. Detailed analysis is reported in **Supplementary Table S12**.

concentrations (χ^2 or Fisher's exact test, $p \geq 0.080$ in both cases), there were significant differences for 1, 3, and 10% sugar concentrations (χ^2 or Fisher's exact test, $p \leq 0.004$ in all cases). This difference was mainly due to much lower PER rates to glucose solution (χ^2 or Fisher's exact test, adjusted $p \leq 0.042$ in all cases). The other groups did not differ (χ^2 or Fisher's exact test, adjusted $p \geq 0.113$), except Fructose and Sucrose/Fructose/Glucose mixture for 1% (χ^2, $p = 0.029$).

DISCUSSION

The Sugar Responsiveness Assay: Impact of Various Parameters

This study assessed sucrose responsiveness in relation to different physiological states in the moth *A. ipsilon*. Sucrose responsiveness has been extensively studied in the honey bee (Scheiner et al., 2004a, 2013) and in some moths (Winkler et al., 2005; Zhang et al., 2010; Minoli et al., 2012). We used a broad range of concentrations, consistent with what was used in bees (Scheiner et al., 2004a, 2013) and flies (Scheiner et al., 2004b), and including concentrations found in nectar (10–30% for sucrose: Lüttge, 1977; Gottsberger et al., 1984; Pacini et al., 2003; De La Barrera and Nobel, 2004; Roy et al., 2017).

Our exploration of the parameters associated to sucrose responsiveness has led to various conclusions. Overall, sucrose responsiveness depends upon starvation duration (i.e., motivation for food) and possibly sex but not age; as a result, in most experiments, we used 5-day-old moths starved for 5 days as the standard condition. The inter-trial interval or the interleaving of water are not crucial parameters in the sucrose responsiveness assay, as the response of the animals is not influenced by the previous trials; yet, we could observe some sensitization to water, a new form of behavioral plasticity in *A. ipsilon* (see also Minoli et al., 2012 for a study of sensitization in a related species). Finally, while moths can detect sucrose through their legs, this pathway is less prone to elicit a PER, either because it does not respond to sucrose very well or because it is less well coupled with the PER motor pathways.

Beyond physiological parameters, the composition of the solution is also essential to observe the PER. In the presence of quinine, moths do not release PER. Thus, quinine is more aversive than sucrose is appetitive, i.e., its ability to elicit a withdrawal of the proboscis is stronger than sucrose's ability to elicit its extension. A simple overshadowing of sucrose is unlikely, as it would not explain PER termination in **Figure 4A**. Concerning the sugars found in nectars, sucrose elicited more responses than fructose, and responses to glucose were much lower than either of them. However, replacing half of the sucrose or half of the fructose by glucose did not lower the PER rate, and mixing sucrose and fructose increased it, suggesting a synergy; interestingly, glucose did not support a synergistic effect in sucrose/fructose/glucose mixture. The results with females are quite different from those observed in males: sucrose and fructose are responded to at the same level, and mixing them (with or without glucose) had no effect. The common point is that glucose alone does not elicit much response while being able to replace the other sugars in mixture.

While simple, the sugar responsiveness assay offers many experimental opportunities. First and foremost, the words "sugar responsiveness" cover various underlying processes, which is why they were preferred to "sugar sensitivity." The dose-response curves used here simultaneously assess three functions: perception (the ability to detect sugar), motivation for sugar (the ability of sugar perception to trigger a PER), and motor response (i.e., if a PER is triggered, the ability to produce it). Detecting sugar and releasing a PER are well-defined phenomena. By contrast, while motivation is associated to them (e.g., **Figures 1** and **2** link hunger to PER rate), its definition is blurrier as it encompasses various situations: not only hunger (i.e., physiological need for food induced by starvation) but also the lack of satiety (i.e., animals' desire to eat). While certainly correlated, these

two situations are not necessarily the same; it would be possible to dissociate them by feeding animals with sweeteners, which induce satiety (i.e., they are palatable) but are physiologically non-nutritive (Schiff et al., 1989; Pszczolkowski and Brown, 2003; Dus et al., 2011; Camacho et al., 2017; Choi et al., 2017; Fisher et al., 2017; Takada et al., 2017; Mustard et al., 2018). The sucrose responsiveness assay would allow to test whether such a dissociation occurs in moth. Similarly, fed animals might have lower response not because they are hungry, but rather because they are habituated to sucrose; to test this hypothesis, animals could be reared (as adult or even as larvae) with fructose rather than sucrose, so that they would not be starved, but still naïve for sucrose. Another possibility offered by the sugar responsiveness assay is to assess lateralization of the response by presenting sugar on a single antennae rather than both; studying lateralization in invertebrate is an emerging field (Jozet-Alves et al., 2012; Baracchi et al., 2018; Niven and Frasnelli, 2018), which complements the classical studies of its role in primate higher cognitive abilities (Prieur et al., 2019). In moths, a study in *Spodoptera littoralis* reported sensitization elicited by pre-exposure to sucrose is a lateralized process (Minoli et al., 2012). All these possible experiments highlight the interest of the sucrose responsiveness assay to investigate precise questions on gustatory responses in moths. Understanding the functioning of sugar-elicited PER could help discriminating between perception, motivation, and PER release mechanisms.

Sensitization is a form of non-associative learning that would make an animal respond to a stimulus (here, the sucrose solution or water) just because it has been excited by a previous presentation of the same or another stimulus (Thompson and Spencer, 1966; Groves and Thompson, 1970; Hammer et al., 1994; Anderson et al., 2007; Anton et al., 2011; Minoli et al., 2012; Blumstein, 2016). Here, we carefully monitored this possibility by using a 10-min interval between each sugar presentation to avoid sensitization, which was hardly considered before in moth sucrose responsiveness. We found sensitization does not affect sucrose responsiveness, although it increases water responsiveness. Interestingly, it was shown in bees and flies that while a forward pairing (presentation of odor, then sugar) promotes associative learning, a backward pairing (sugar than odor) prevents it. This effect seems to be mediated by a desensitization of the PER occurring upon odor presentation at a specific 15-s delay (Dacher and Smith, 2008). Whether this type of desensitization also occurs in moths remains to be determined.

Biological Meaning of Sucrose Responsiveness: Sugar Mixture, Foraging, and Nectar Composition

It is well established in bees that associations between odors and PER/sugar made in restrained conditions can be transferred to free-flying foraging, and vice versa (Gerber et al., 1996; Sandoz et al., 2000; Chaffiol et al., 2005; Gil and De Marco, 2005). Therefore, it is sensible to assume such transfers are possible between the two situations for moths too. Under this hypothesis, sucrose responsiveness is likely to play an important role in modulating foraging behaviors in these insects, as in bees; indeed, it is well established that bees foraging for nectar are less responsive to sucrose than bees foraging for pollen (Scheiner et al., 2004a). As a result, only the most concentrated nectar sources are exploited by bee nectar foragers. Such a phenomenon could also exist in most foraging moths, which land on flowers (i.e., settling moths but not hovering moths: Oliveira et al., 2004; Makholela and Manning, 2006; Okamoto et al., 2008; Atwater, 2013): it is likely the first appendage assessing sugar concentration in nectar are the legs (or possibly the proboscis) rather than the antennae (see also experiments by Zhang et al., 2010). Thus, only highly concentrated nectar would elicit a PER in moth (**Figure 3**), just like nectar-foraging bees. To explore this hypothesis, the foraging behavior of male and female moths drinking nectar at flowers should be analyzed either in artificial flowers in wind tunnel or in a natural setting. Very little information is available on this topic.

While moths respond quite well to sucrose and fructose, they hardly react to glucose. This is consistent to what was observed in a related species, *Spodoptera littoralis*, during electrophysiological recordings of taste sensilla (Popescu et al., 2013). In spite it is hardly responded to, glucose can replace fructose or sucrose in mixtures without significantly decreasing the PER rate. As nectars are mixtures of sugars rather than single compounded, this result suggests an adaptation to nectar perception. We can make the hypothesis that moths or other animals feeding on only one type of plant (i.e., strictly monophagous) should have a sugar responsiveness specifically tuned to the specific sugar ratio found in this plant's nectar, illustrating plant-pollinator coevolution (e.g., Perret et al., 2001; Nicolson and Fleming, 2003; Lotz and Schondube, 2006). This would have important consequences for the management of pests and pollinators. This hypothesis is also consistent with the fact that learning performance depends on sugar identity in bees (Simcock et al., 2018; Chapuy et al., 2019). By contrast, polyphagous moths such as *A. ipsilon* feed on various types of flowers, possibly with differing nectars (Wynne et al., 1991; Zhu et al., 1993). Nectars can be classified in various broad categories (Percival, 1961), and usually glucose is neither the dominant sugar nor the only one. Thus, it makes sense moths detect it less well. Honey bees are much better at detecting it (Simcock et al., 2018), but it is one of the main constituent of their honey. It would be interesting to compare sucrose responsiveness of other nectar foragers, particularly pollinators.

Honey bees and *Agrotis ipsilon* are sympatric, and both are described as polyphagous (i.e., they are not specialized in a narrow range of plant species but rather forage nectar on various flowers; Wynne et al., 1991; Zhu et al., 1993); thus, they potentially forage on the same plants. However, previous results (Scheiner et al., 2004a, 2013) indicate bees are much more sensitive to low sucrose concentrations than moths and so are likely to explore a wider range of flowers, including those which have nectar less concentrated. A full exploration of the ecological and evolutionary implications of this preliminary observation is beyond the scope of this article, but it certainly deserves to be studied; indeed, nectar foraging insects are often pollinators, and it is relevant to know which plants will or will not be visited by a given insect in a context of pollination

crisis (Senapathi et al., 2015). The sucrose responsiveness assay will be useful to do so.

We found little differences between males and females, and they were not consistently observed. It would be interesting to compare sugar responsiveness in animals before and after reproduction; for males, that would mean before flying toward a female and mating, and for females, before releasing pheromone, mating and laying eggs. It is not unlikely the needs of moths change according to their reproductive status. In particular, females might need amino acids, while eggs are storing reserves (Watt et al., 1974; Heil, 2011; Hendriksma et al., 2014; Simcock et al., 2014; Levin et al., 2017a,b), so that PER rates would be affected by their presence in the tested solutions (but see O'brien et al., 2000; Marchioro and Foerster, 2013 for contradictory results); Zhang et al. (2010) reported neuronal responses and PER to amino acids. Similarly, males might need sodium and potassium for spermatophore formation (Arms et al., 1974; Adler and Pearson, 1982; Boggs and Jackson, 1991; Smedley and Eisner, 1995, 1996; Beck et al., 1999; Boggs and Dau, 2004; Watanabe and Kamikubo, 2005; Molleman, 2010), so that the presence of salt in the solution might affect the PER rate. The sugar responsiveness assay can easily be modified to test the effect of salt or amino acid on males and females of different reproductive status.

Presenting quinine on the proboscis interrupts the PER, and it inhibits response to sugar. This contrasts to the behavior of bees (which readily drink bitter solutions when they are restrained but not when they are free flying, Ayestaran et al., 2010; De Brito Sanchez et al., 2015; Guiraud et al., 2018) and flies (which accepts bitter compounds after starvation, Ledue et al., 2016). It is established that some plants produce bitter compounds in nectar (Adler, 2000; Adler et al., 2006; Heil, 2011; Roy et al., 2017), possibly to deter predatory insects. It can be expected that *A. ipsilon* would not forage on these plants, but this remains to be verified; this would be consistent with the idea that this moth is a generalist forager, because specialists tend to adapt to deterrent nectar compounds (Berenbaum et al., 1989; Glendinning, 2002; Cornell and Hawkins, 2003; Adler et al., 2006; Reisenman and Riffell, 2015). This also opens the possibility to use the sugar responsiveness assay to evaluate moths' reaction to aversive compounds such as deterrent products released in nectar, or possibly xenobiotics. Beside, some results indicate appetitive and deterrent stimuli are processed in parallel at the antenna level (Kvello et al., 2010); this raises the question of the neurophysiological convergence of these pathways, which must occur at some point as quinine prevents sucrose-induced PER. Interestingly, pre-exposing *S. littoralis* to quinine or sucrose 24 h before sucrose presentation potentiates rather than inhibits the response to 1% sucrose (Minoli et al., 2012). This suggests that previous gustatory experiments are not neutral for sucrose responsiveness.

Neurophysiological Substrates

Gustatory receptors and the downward neurophysiological pathways have been reported on antennae, proboscis, and legs (Jørgensen et al., 2006, 2007; Calas et al., 2009; Kvello et al., 2010; Zhang et al., 2010; Popescu et al., 2013; Agnihotri et al., 2016; Seada et al., 2018); these neurophysiological results are consistent with our behavioral observations, as they indicated that sugar-induced neuronal responses are lower in the legs than in the proboscis, and glucose alone elicits less responses than sucrose or fructose. Quinine was also well detected but not by the neurons responding to sucrose (Jørgensen et al., 2007). This suggests its effect result from a central integration, rather than an interaction at the level of gustatory receptors; this is different in fruit flies, where bitter compounds can interact at the level of the receptor (Meunier et al., 2003; Jeong et al., 2013; French et al., 2015a,b). Popescu et al. (2013) observed sex-dependent responses, suggesting the differences we observed in **Figure 1B** (but not in **Figure 6**) are supported by differing response levels.

To fully understand how sugars are perceived and responded to by *A. ipsilon* and other moths, it will be necessary to describe the full neuronal pathway of information from antennal gustatory receptors to PER release. At the level of antennae, characterization of the receptors has already been started in moths and involves description of the antennal gustatory sensilla that house gustatory neurons as well as molecular description of the receptors and their interactions with sugars (Balkenius and Kelber, 2006; Popescu et al., 2013; Seada, 2015; Agnihotri et al., 2016; Seada et al., 2018); it would be particularly interesting to describe interactions in mixtures of sugars, quinine, and/or amino acid, specially to find out whether synergy or masking occurs, as for odors (Rospars, 2013); a tempting hypothesis is that glucose would act as a modulator of sugar receptor, explaining it elicits little response while favoring response to other sugars. In turn, gustatory information projects to the central nervous system, particularly the suboesophageal ganglion (Jørgensen et al., 2006; Kvello et al., 2006, 2010; Popescu et al., 2013). How motivation-linked information (hunger and/or other factors) is then integrated with gustatory input to elicit (or not) a PER remains to be determined. While electrophysiological and molecular tools will be needed to reach this goal, the sucrose responsiveness assay provides a solid framework to guide such research.

As previously discussed, stimulating legs with sucrose is much less prone to elicit a PER than stimulating antennae. Assuming motivation to release a PER and the corresponding motor control are central processes, a simple explanation is that legs bear less sugar receptors than antennae and/or that they bear different receptors (i.e., less sensitive to sucrose in the legs). Alternatively, gustatory pathways from the legs could be somehow less connected to the release of PER than those from antennae. Once again, electrophysiology (recording of gustatory sensilla from legs and antennae) will be helpful to distinguish between these two hypotheses, by determining whether gustatory responses of legs and antennae are comparable (Calas et al., 2009; Zhang et al., 2010).

Finally, understanding the central integration of sucrose input that leads to PER will be the ultimate goal. A way to approach this objective will be to understand which neurotransmitter systems are involved. Promising candidates are biogenic amines such as octopamine and dopamine, as they have well-known roles on sucrose sensitivity in other insects (Pankiw and Page, 2003; Schwaerzel et al., 2003; Unoki et al., 2005, 2006;

Scheiner et al., 2006, 2014; Mizunami et al., 2009; Matsumoto et al., 2015). Interestingly, biogenic amines also modulate sex-pheromone-elicited behaviors in male moths (Linn and Roelofs, 1986; Linn et al., 1992; Pophof, 2000; Flecke and Stengl, 2009; Jarriault et al., 2009; Duportets et al., 2010; Abrieux et al., 2014; Hillier and Kavanagh, 2015), while sex pheromones do not affect sucrose responsiveness (Hostachy et al., submitted). If these neurotransmitters modulated sucrose responsiveness, this would imply that they do so through ways different from pheromone-responsiveness modulation.

DATA AVAILABILITY STATEMENT

All datasets generated for this study are included in the article/ **Supplementary Material**.

AUTHOR CONTRIBUTIONS

CH, ND, and MD designed the experiments. CH and MD prepared the figures and analyzed the data. MD wrote the first draft of the manuscript. All authors performed the experiments and contributed to manuscript revision, read and approved the submitted version.

FUNDING

This work was supported by Agence Nationale de la Recherche (project PheroMod, ANR grant number ANR-14-CE18-0003) and Sorbonne Université (project emergence HAPA, grant number SU-16-R-EMR-18-HAPA).

ACKNOWLEDGMENTS

We thank our colleagues Lucie Conchou and Camille Meslin for their comments on this article and technicians from iEES-Paris for rearing the animals used in the experiments.

SUPPLEMENTARY MATERIAL

The Supplementary Material for this article can be found online at: https://www.frontiersin.org/articles/10.3389/fphys.2019.01423/full#supplementary-material

REFERENCES

Abrieux, A., Duportets, L., Debernard, S., Gadenne, C., and Anton, S. (2014). The GPCR membrane receptor, DopEcR, mediates the actions of both dopamine and ecdysone to control sex pheromone perception in an insect. *Front. Behav. Neurosci.* 8:312. doi: 10.3389/fnbeh.2014.00312

Adler, L. S. (2000). The ecological significance of toxic nectar. *Oikos* 91, 409–420. doi: 10.1034/j.1600-0706.2000.910301.x

Adler, L. S., and Irwin, R. E. (2005). Ecological costs and benefits of defenses in nectar. *Ecology* 86, 2968–2978. doi: 10.1890/05-0118

Adler, P. H., and Pearson, D. L. (1982). Why do male butterflies visit mud puddles? *Can. J. Zool.* 60, 322–325. doi: 10.1139/z82-043

Adler, L. S., Wink, M., Distl, M., and Lentz, A. J. (2006). Leaf herbivory and nutrients increase nectar alkaloids. *Ecol. Lett.* 9, 960–967. doi: 10.1111/j.1461-0248.2006.00944.x

Agnihotri, A. R., Roy, A. A., and Joshi, R. S. (2016). Gustatory receptors in Lepidoptera: chemosensation and beyond. *Insect Mol. Biol.* 25, 519–529. doi: 10.1111/imb.12246

Akre, K. L., and Johnsen, S. (2014). Psychophysics and the evolution of behavior. *Trends Ecol. Evol.* 29, 291–300. doi: 10.1016/j.tree.2014.03.007

Anderson, P., Hansson, B. S., Nilsson, U., Han, Q., Sjoholm, M., Skals, N., et al. (2007). Increased behavioral and neuronal sensitivity to sex pheromone after brief odor experience in a moth. *Chem. Senses* 32, 483–491. doi: 10.1093/chemse/bjm017

Anton, S., Evengaard, K., Barrozo, R. B., Anderson, P., and Skals, N. (2011). Brief predator sound exposure elicits behavioral and neuronal long-term sensitization in the olfactory system of an insect. *PNAS* 108, 3401–3405. doi: 10.1073/pnas.1008840108

Arms, K., Feeny, P., and Lederhouse, R. C. (1974). Sodium: stimulus for puddling behavior by tiger swallowtail butterflies, *Papilio glaucus*. *Science* 185, 372–374. doi: 10.1126/science.185.4148.372

Atwater, M. (2013). Diversity and nectar hosts of flower-settling moths within a Florida sandhill ecosystem. *J. Nat. Hist.* 47, 2719–2734. doi: 10.1080/00222933.2013.791944

Ayestaran, A., Giurfa, M., and De Brito Sanchez, M. G. (2010). Toxic but drank: gustatory aversive compounds induce post-ingestional malaise in harnessed honeybees. *PLoS One* 5:e15000. doi: 10.1371/journal.pone.0015000

Baker, H. G. (1977). Non-sugar chemical constituents of nectar. *Apidologie* 8, 349–356. doi: 10.1051/apido:19770405

Baker, H. G., and Baker, I. (1973). Amino-acids in nectar and their evolutionary significance. *Nature* 241, 543–545. doi: 10.1038/241543b0

Balkenius, A., and Kelber, A. (2006). Colour preferences influences odour learning in the hawkmoth, *Macroglossum stellatarum*. *Naturwissenschaften* 93, 255–258. doi: 10.1007/s00114-006-0099-9

Baracchi, D., Rigosi, E., De Brito Sanchez, G., and Giurfa, M. (2018). Lateralization of sucrose responsiveness and non-associative learning in honeybees. *Front. Psychol.* 9:425. doi: 10.3389/fpsyg.2018.00425

Beck, J., Mühlenberg, E., and Fiedler, K. (1999). Mud-puddling behavior in tropical butterflies: in search of proteins or minerals? *Oecologia* 119, 140–148. doi: 10.1007/s004420050770

Berenbaum, M. R., Zangerl, A. R., and Lee, K. (1989). Chemical barriers to adaptation by a specialist herbivore. *Oecologia* 80, 501–506. doi: 10.1007/BF00380073

Blumstein, D. T. (2016). Habituation and sensitization: new thoughts about old ideas. *Anim. Behav.* 120, 255–262. doi: 10.1016/j.anbehav.2016.05.012

Boggs, C. L. (1997a). Dynamics of reproductive allocation from juvenile and adult feeding: radiotracer studies. *Ecology* 78, 192–202.

Boggs, C. L. (1997b). Reproductive allocation from reserves and income in butterfly species with differing adult diets. *Ecology* 78, 181–191.

Boggs, C. L., and Dau, B. (2004). Resource specialization in puddling Lepidoptera. *Environ. Entomol.* 33, 1020–1024. doi: 10.1603/0046-225X-33.4.1020

Boggs, C. L., and Jackson, L. A. (1991). Mud puddling by butterflies is not a simple matter. *Ecol. Entomol.* 16, 123–127. doi: 10.1111/j.1365-2311.1991.tb00199.x

Boggs, C. L., and Ross, C. L. (1993). The effect of adult food limitation on life history traits in *Speyeria mormonia* (Lepidoptera: Nymphalidae). *Ecology* 74, 433–441. doi: 10.2307/1939305

Calas, D., Marion-Poll, F., and Steinbauer, M. J. (2009). Tarsal taste sensilla of the autumn gum moth, *Mnesampela privata*: morphology and electrophysiological activity. *Entomol. Exp. Appl.* 133, 186–192. doi: 10.1111/j.1570-7458.2009.00921.x

Camacho, M., Oliva, M., and Serbus, L. R. (2017). Dietary saccharides and sweet tastants have differential effects on colonization of *Drosophila* oocytes by *Wolbachia* endosymbionts. *Biol. Open* 6, 1074–1083. doi: 10.1242/bio.023895

Chabaud, M., Devaud, J., Pham-Delègue, M., Preat, T., and Kaiser, L. (2006). Olfactory conditioning of proboscis activity in *Drosophila melanogaster*. *J. Comp. Physiol. A* 192, 1335–1348. doi: 10.1007/s00359-006-0160-3

Chaffiol, A., Laloi, D., and Pham-Delegue, M. H. (2005). Prior classical olfactory conditioning improves odour-cued flight orientation of honey bees in a wind tunnel. *J. Exp. Biol.* 208, 3731–3737. doi: 10.1242/jeb.01796

Chapuy, C., Ribbens, L., Renou, M., Dacher, M., and Armengaud, C. (2019). Thymol affects congruency between olfactory and gustatory stimuli in bees. *Sci. Rep.* 9:7752. doi: 10.1038/s41598-019-43614-8

Choi, M.-Y., Tang, S. B., Ahn, S.-J., Amarasekare, K. G., Shearer, P., and Lee, J. C. (2017). Effect of non-nutritive sugars to decrease the survivorship of spotted wing *Drosophila*, *Drosophila suzukii*. *J. Insect Physiol.* 99, 86–94. doi: 10.1016/j.jinsphys.2017.04.001

Cook, S. M., Khan, Z. R., and Pickett, J. A. (2007). The use of push-pull strategies in integrated pest management. *Annu. Rev. Entomol.* 52, 375–400. doi: 10.1146/annurev.ento.52.110405.091407

Cornell, H. V., and Hawkins, B. A. (2003). Herbivore responses to plant secondary compounds: a test of phytochemical coevolution theory. *Am. Nat.* 161, 507–522. doi: 10.1086/368346

Dacher, M., and Smith, B. H. (2008). Olfactory interference during inhibitory backward pairing in honey bees. *PLoS One* 3:e3513. doi: 10.1371/journal.pone.0003513

De Brito Sanchez, M. G., Serre, M., Avarguès-Weber, A., Dyer, A. G., and Giurfa, M. (2015). Learning context modulates aversive taste strength in honey bees. *J. Exp. Biol.* 218, 949–959. doi: 10.1242/jeb.117333

De La Barrera, E., and Nobel, P. S. (2004). Nectar: properties, floral aspects, and speculations on origin. *Trends Plant Sci.* 9, 65–69. doi: 10.1016/j.tplants.2003.12.003

Duportets, L., Barrozo, R. B., Bozzolan, F., Gaertner, C., Anton, S., Gadenne, C., et al. (2010). Cloning of an octopamine/tyramine receptor and plasticity of its expression as a function of adult sexual maturation in the male moth *Agrotis ipsilon*. *Insect Mol. Biol.* 19, 489–499. doi: 10.1111/j.1365-2583.2010.01009.x

Dus, M., Min, S., Keene, A. C., Lee, G. Y., and Suh, G. S. (2011). Taste-independent detection of the caloric content of sugar in *Drosophila*. *Proc. Natl. Acad. Sci. USA* 108, 11644–11649. doi: 10.1073/pnas.1017096108

Evenden, M. L. (2016). "Mating disruption of moth pests in integrated pest management: a mechanistic approach" in *Pheromone communication in moths: Evolution, behavior and application*. eds. J. D. Allison and R. T. Carde (Oakland, CA: University of California Press), 365–393.

Fan, R. J., Anderson, P., and Hansson, B. (1997). Behavioural analysis of olfactory conditioning in the moth *Spodoptera littoralis* (Boisd.) (Lepidoptera: Noctuidae). *J. Exp. Biol.* 200, 2969–2976.

Fan, R. J., and Hansson, B. S. (2001). Olfactory discrimination conditioning in the moth *Spodoptera littoralis*. *Physiol. Behav.* 72, 159–165. doi: 10.1016/S0031-9384(00)00394-2

Fischer, K., O'brien, D. M., and Boggs, C. L. (2004). Allocation of larval and adult resources to reproduction in a fruit-feeding butterfly. *Funct. Ecol.* 18, 656–663. doi: 10.1111/j.0269-8463.2004.00892.x

Fisher, M. L., Fowler, F. E., Denning, S. S., and Watson, D. W. (2017). Survival of the house fly (Diptera: Muscidae) on Truvia and other sweeteners. *J. Med. Entomol.* 54, 999–1005. doi: 10.1093/jme/tjw241

Flecke, C., and Stengl, M. (2009). Octopamine and tyramine modulate pheromone-sensitive olfactory sensilla of the hawkmoth *Manduca sexta* in a time-dependent manner. *J. Comp. Physiol. A* 195, 529–545. doi: 10.1007/s00359-009-0429-4

French, A., Agha, M. A., Mitra, A., Yanagawa, A., Sellier, M. J., and Marion-Poll, F. (2015a). *Drosophila* bitter taste(s). *Front. Integr. Neurosci.* 9:58. doi: 10.3389/fnint.2015.00058

French, A. S., Sellier, M.-J., Ali Agha, M., Guigue, A., Chabaud, M.-A., Reeb, P. D., et al. (2015b). Dual mechanism for bitter avoidance in *Drosophila*. *J. Neurosci.* 35, 3990–4004. doi: 10.1523/jneurosci.1312-14.2015

Fresquet, N. (1999). Effects of aging on the acquisition and extinction of excitatory conditioning in *Drosophila melanogaster*. *Physiol. Behav.* 67, 205–211. doi: 10.1016/S0031-9384(99)00058-X

Geister, T. L., Lorenz, M. W., Hoffmann, K. H., and Fischer, K. (2008). Adult nutrition and butterfly fitness: effects of diet quality on reproductive output, egg composition, and egg hatching success. *Front. Zool.* 5:10. doi: 10.1186/1742-9994-5-10

Gemeno, C., and Haynes, K. F. (2000). Periodical and age-related variation in chemical communication system of black cutworm moth, *Agrotis ipsilon*. *J. Chem. Ecol.* 26, 329–342. doi: 10.1023/A:1005468203045

Gerber, B., Geberzahn, N., Hellstern, F., Klein, J., Kowalsky, O., Wüstenberg, D., et al. (1996). Honeybees transfer olfactory memories established during flower visits to a proboscis extension paradigm in the laboratory. *Anim. Behav.* 52, 1079–1085. doi: 10.1006/anbe.1996.0255

Gil, M., and De Marco, R. J. (2005). Olfactory learning by means of trophallaxis in *Apis mellifera*. *J. Exp. Biol.* 208, 671–680. doi: 10.1242/jeb.01474

Giurfa, M. (2015). Learning and cognition in insects. *Wiley Interdiscip. Rev. Cogn. Sci.* 6, 383–395. doi: 10.1002/wcs.1348

Giurfa, M., and Sandoz, J. C. (2012). Invertebrate learning and memory: fifty years of olfactory conditioning of the proboscis extension response in honeybees. *Learn. Mem.* 19, 54–66. doi: 10.1101/lm.024711.111

Glendinning, J. I. (2002). How do herbivorous insects cope with noxious secondary plant compounds in their diet? *Entomol. Exp. App.* 104, 15–25. doi: 10.1046/j.1570-7458.2002.00986.x

Gottsberger, G., Schrauwen, J., and Linskens, H. F. (1984). Amino acids and sugars in nectar, and their putative evolutionary significance. *Plant Syst. Evol.* 145, 55–77. doi: 10.1007/BF00984031

Groves, P. M., and Thompson, R. F. (1970). Habituation: a dual-process theory. *Psychol. Rev.* 77, 419–450. doi: 10.1037/h0029810

Guerrieri, F. J., and D'ettorre, P. (2010). Associative learning in ants: conditioning of the maxilla-labium extension response in *Camponotus aethiops*. *J. Insect Physiol.* 56, 88–92. doi: 10.1016/j.jinsphys.2009.09.007

Guiraud, M., Hotier, L., Giurfa, M., and De Brito Sanchez, M. G. (2018). Aversive gustatory learning and perception in honey bees. *Sci. Rep.* 8:1343. doi: 10.1038/s41598-018-19715-1

Hammer, M., Braun, G., and Mauelshagen, J. (1994). Food-induced arousal and nonassociative learning in honeybees: dependence of sensitization on the application site and duration of food stimulation. *Behav. Neural Biol.* 62, 210–223. doi: 10.1016/S0163-1047(05)80019-6

Hartlieb, E. (1996). Olfactory conditioning in the moth *Heliothis virescens*. *Naturwissenschaften* 83, 87–88.

Hartlieb, E., Anderson, P., and Hansson, B. S. (1999a). Appetitive learning of odours with different behavioural meaning in moths. *Physiol. Behav.* 67, 671–677.

Hartlieb, E., Hansson, B. S., and Anderson, P. (1999b). Sex or food? Appetitive learning of sex odors in a male moth. *Naturwissenschaften* 86, 396–399.

Heil, M. (2011). Nectar: generation, regulation and ecological functions. *Trends Plant Sci.* 16, 191–200. doi: 10.1016/j.tplants.2011.01.003

Hendriksma, H. P., Oxman, K. L., and Shafir, S. (2014). Amino acid and carbohydrate tradeoffs by honey bee nectar foragers and their implications for plant–pollinator interactions. *J. Insect Physiol.* 69, 56–64. doi: 10.1016/j.jinsphys.2014.05.025

Hill, C. J. (1989). The effect of adult diet on the biology of butterflies. 2. The common crow butterfly, *Euploea core corinna*. *Oecologia* 81, 258–266. doi: 10.1007/BF00379813

Hill, C. J., and Pierce, N. E. (1989). The effect of adult diet on the biology of butterflies. 1. The common imperial blue, *Jalmenus evagoras*. *Oecologia* 81, 249–257. doi: 10.1007/BF00379812

Hillier, N. K., and Kavanagh, R. M. B. (2015). Differential octopaminergic modulation of olfactory receptor neuron responses to sex pheromones in *Heliothis virescens*. *PLoS One* 10:e0143179. doi: 10.1371/journal.pone.0143179

Holm, S. (1979). A simple sequentially rejective multiple test procedure. *Scand. J. Stat.* 6, 65–70.

Jarriault, D., Barrozo, R. B., Pinto, C. J. D., Greiner, B., Dufour, M. C., Masante-Roca, I., et al. (2009). Age-dependent plasticity of sex pheromone response in the moth, *Agrotis ipsilon*: combined effects of octopamine and juvenile hormone. *Horm. Behav.* 56, 185–191. doi: 10.1016/j.yhbeh.2009.04.005

Jeong, Y. T., Shim, J., Oh, S. R., Yoon, H. I., Kim, C. H., Moon, S. J., et al. (2013). An odorant-binding protein required for suppression of sweet taste by bitter chemicals. *Neuron* 79, 725–737. doi: 10.1016/j.neuron.2013.06.025

Jervis, M. A., Boggs, C. L., and Ferns, P. N. (2005). Egg maturation strategy and its associated trade-offs: a synthesis focusing on Lepidoptera. *Ecol. Entomol.* 30, 359–375. doi: 10.1111/j.0307-6946.2005.00712.x

Jørgensen, K., Almaas, T. J., Marion-Poll, F., and Mustaparta, H. (2007). Electrophysiological characterization of responses from gustatory receptor neurons of sensilla chaetica in the moth *Heliothis virescens*. *Chem. Senses* 32, 863–879. doi: 10.1093/chemse/bjm057

Jørgensen, K., Kvello, P., Almaas, T. J., and Mustaparta, H. (2006). Two closely located areas in the suboesophageal ganglion and the tritocerebrum receive projections of gustatory receptor neurons located on the antennae and the proboscis in the moth *Heliothis virescens*. *J. Comp. Neurol.* 496, 121–134. doi: 10.1002/cne.20908

Jorgensen, K., Stranden, M., Sandoz, J.-C., Menzel, R., and Mustaparta, H. (2007). Effects of two bitter substances on olfactory conditioning in the moth *Heliothis virescens*. *J. Exp. Biol.* 210, 2563–2573. doi: 10.1242/jeb.004283

Jozet-Alves, C., Viblanc, V. A., Romagny, S., Dacher, M., Healy, S. D., and Dickel, L. (2012). Visual lateralization is task and age dependent in cuttlefish, *Sepia officinalis*. *Anim. Behav.* 83, 1313–1318. doi: 10.1016/j.anbehav.2012.02.023

Kroutov, V., Mayer, M. S., and Emmel, T. C. (1999). Olfactory conditioning of the butterfly *Agraulis vanillae* (L.) (Lepidoptera, Nymphalidae) to floral but not host-plant odors. *J. Insect Behav.* 12, 833–843. doi: 10.1023/A:1020961211750

Kvello, P., Almaas, T. J., and Mustaparta, H. (2006). A confined taste area in a lepidopteran brain. *Arthr. Struc. Dev.* 35, 35–45. doi: 10.1016/j.asd.2005.10.003

Kvello, P., Jørgensen, K., and Mustaparta, H. (2010). Central gustatory neurons integrate taste quality information from four appendages in the moth *Heliothis virescens*. *J. Neurophysiol.* 103, 2965–2981. doi: 10.1152/jn.00985.2009

Labrousse, C., Lazzari, C. R., and Fresquet, N. (2017). Developmental study of the proboscis extension response to heat in *Rhodnius prolixus* along the life cycle. *J. Insect Physiol.* 98, 55–58. doi: 10.1016/j.jinsphys.2016.11.010

Ledue, E. E., Mann, K., Koch, E., Chu, B., Dakin, R., and Gordon, M. D. (2016). Starvation-induced depotentiation of bitter taste in *Drosophila*. *Curr. Biol.* 26, 2854–2861. doi: 10.1016/j.cub.2016.08.028

Levin, E., Mccue, M. D., and Davidowitz, G. (2017a). More than just sugar: allocation of nectar amino acids and fatty acids in a Lepidopteran. *Proc. R. Soc. B* 284:20162126. doi: 10.1098/rspb.2016.2126

Levin, E., Mccue, M. D., and Davidowitz, G. (2017b). Sex differences in the utilization of essential and non-essential amino acids in Lepidoptera. *J. Exp. Biol.* 220, 2743–2747. doi: 10.1242/jeb.154757

Linn, C. E., Campbell, M. G., and Roelofs, W. L. (1992). Photoperiod cues and the modulatory action of octopamine and 5-hydroxytryptamine on locomotor and pheromone response in male gypsy moths, *Lymantria dispar*. *Arch. Insect Biochem. Physiol.* 20, 265–284. doi: 10.1002/arch.940200404

Linn, C. E., and Roelofs, W. L. (1986). Modulatory effects of octopamine and serotonin on male sensitivity and periodicity of response to sex pheromone in the cabbage looper moth, *Trichoplusia ni*. *Arch. Insect Biochem. Physiol.* 3, 161–171. doi: 10.1002/arch.940030206

Lotz, C. N., and Schondube, J. E. (2006). Sugar preferences in nectar- and fruit-eating birds: behavioral patterns and physiological causes. *Biotropica* 38, 3–15. doi: 10.1111/j.1744-7429.2006.00104.x

Lüttge, U. (1977). Nectar composition and membrane transport of sugars and amino acids: a review on the present state of nectar research. *Apidologie* 8, 305–319. doi: 10.1051/apido:19770402

Makholela, T., and Manning, J. C. (2006). First report of moth pollination in *Struthiola ciliata* (Thymelaeaceae) in southern Africa. *South African J. Bot.* 72, 597–603. doi: 10.1016/j.sajb.2006.04.007

Marchioro, C. A., and Foerster, L. A. (2013). Effects of adult-derived carbohydrates and amino acids on the reproduction of *Plutella xylostella*. *Physiol. Entomol.* 38, 13–19. doi: 10.1111/phen.12000

Matsumoto, Y., Matsumoto, C.-S., Wakuda, R., Ichihara, S., and Mizunami, M. (2015). Roles of octopamine and dopamine in appetitive and aversive memory acquisition studied in olfactory conditioning of maxillary palpi extension response in crickets. *Front. Behav. Neurosci.* 9:230. doi: 10.3389/fnbeh.2015.00230

Menzel, R. (1999). Memory dynamics in the honeybee. *J. Comp. Physiol. A* 185, 323–340.

Menzel, R. (2012). The honeybee as a model for understanding the basis of cognition. *Nat. Rev. Neurosci.* 13, 758–768. doi: 10.1038/nrn3357

Meunier, N., Marion-Poll, F., Rospars, J.-P., and Tanimura, T. (2003). Peripheral coding of bitter taste in *Drosophila*. *J. Neurobiol.* 56, 139–152. doi: 10.1002/neu.10235

Minoli, S., Kauer, I., Colson, V., Party, V., Renou, M., Anderson, P., et al. (2012). Brief exposure to sensory cues elicits stimulus-nonspecific general sensitization in an insect. *PLoS One* 7:e34141. doi: 10.1371/journal.pone.0034141

Mizunami, M., Unoki, S., Mori, Y., Hirashima, D., Hatano, A., and Matsumoto, Y. (2009). Roles of octopaminergic and dopaminergic neurons in appetitive and aversive memory recall in an insect. *BMC Biol.* 7, 1–16. doi: 10.1186/1741-7007-7-46

Molleman, F. (2010). Puddling: from natural history to understanding how it affects fitness. *Entomol. Exp. Appl.* 134, 107–113. doi: 10.1111/j.1570-7458.2009.00938.x

Mujagic, S., Sarkander, J., Erber, B., and Erber, J. (2010). Sucrose acceptance and different forms of associative learning of the honey bee (*Apis mellifera* L.) in the field and laboratory. *Front. Behav. Neurosci.* 4:46. doi: 10.3389/fnbeh.2010.00046

Mustard, J. A., Alvarez, V., Barocio, S., Mathews, J., Stoker, A., and Malik, K. (2018). Nutritional value and taste play different roles in learning and memory in the honey bee (*Apis mellifera*). *J. Insect Physiol.* 107, 250–256. doi: 10.1016/j.jinsphys.2018.04.014

Nachev, V., Thomson, J. D., and Winter, Y. (2013). The psychophysics of sugar concentration discrimination and contrast evaluation in bumblebees. *Anim. Cogn.* 16, 417–427. doi: 10.1007/s10071-012-0582-y

Naranjo, S. E., Ellsworth, P. C., and Frisvold, G. B. (2015). Economic value of biological control in integrated pest management of managed plant systems. *Annu. Rev. Entomol.* 60, 621–645. doi: 10.1146/annurev-ento-010814-021005

Nepi, M., Soligo, C., Nocentini, D., Abate, M., Guarnieri, M., Cai, G., et al. (2012). Amino acids and protein profile in floral nectar: much more than a simple reward. *Flora* 207, 475–481. doi: 10.1016/j.flora.2012.06.002

Nicolson, S. W., and Fleming, P. A. (2003). Nectar as food for birds: the physiological consequences of drinking dilute sugar solutions. *Plant Syst. Evol.* 238, 139–153. doi: 10.1007/s00606-003-0276-7

Niven, J. E., and Frasnelli, E. (2018). Insights into the evolution of lateralization from the insects. *Prog. Brain Res.* 238, 3–31. doi: 10.1016/bs.pbr.2018.06.001

O'brien, D. M., Boggs, C. L., and Fogel, M. L. (2004). Making eggs from nectar: the role of life history and dietary carbon turnover in butterfly reproductive resource allocation. *Oikos* 105, 279–291. doi: 10.1111/j.0030-1299.2004.13012.x

O'brien, D. M., Schrag, D. P., and Del Rio, C. M. (2000). Allocation to reproduction in a hawkmoth: a quantitative analysis using stable carbon isotopes. *Ecology* 81, 2822–2831. doi: 10.1890/0012-9658(2000)081[2822:ATRIAH]2.0.CO;2

Okamoto, T., Kawakita, A., and Kato, M. (2008). Floral adaptations to nocturnal moth pollination in Diplomorpha (Thymelaeaceae). *Plant Species Biol.* 23, 192–201. doi: 10.1111/j.1442-1984.2008.00222.x

Oliveira, P. E., Gibbs, P. E., and Barbosa, A. A. (2004). Moth pollination of woody species in the Cerrados of Central Brazil: a case of so much owed to so few? *Plant Syst. Evol.* 245, 41–54. doi: 10.1007/s00606-003-0120-0

Pacini, E., Nepi, M., and Vesprini, L. J. (2003). Nectar biodiversity: a short review. *Plant Syst. Evol.* 238, 7–21. doi: 10.1007/s00606-002-0277-y

Page, R. E. Jr., and Erber, J. (2002). Levels of behavioral organization and the evolution of division of labor. *Naturwissenschaften* 89, 91–106. doi: 10.1007/s00114-002-0299-x

Pankiw, T., and Page, R. E. (2003). Effect of pheromones, hormones, and handling on sucrose response thresholds of honey bees (*Apis mellifera* L.). *J. Comp. Physiol. A* 189, 675–684. doi: 10.1007/s00359-003-0442-y

Percival, M. S. (1961). Types of nectar in angiosperms. *New Phytol.* 60, 235–281. doi: 10.1111/j.1469-8137.1961.tb06255.x

Perez, M., Rolland, U., Giurfa, M., and D'ettorre, P. (2013). Sucrose responsiveness, learning success, and task specialization in ants. *Learn. Mem.* 20, 417–420. doi: 10.1101/lm.031427.113

Perret, M., Chautems, A., Spichiger, R., Peixoto, M., and Savolainen, V. (2001). Nectar sugar composition in relation to pollination syndromes in Sinningieae (Gesneriaceae). *Ann. Bot.* 87, 267–273. doi: 10.1006/anbo.2000.1331

Popescu, A., Couton, L., Almaas, T.-J., Rospars, J.-P., Wright, G., Marion-Poll, F., et al. (2013). Function and central projections of gustatory receptor neurons on the antenna of the noctuid moth *Spodoptera littoralis*. *J. Comp. Physiol. A* 199, 403–416. doi: 10.1007/s00359-013-0803-0

Pophof, B. (2000). Octopamine modulates the sensitivity of silkmoth pheromone receptor neurons. *J. Comp. Physiol. A* 186, 307–313. doi: 10.1007/s003590050431

Prieur, J., Lemasson, A., Barbu, S., and Blois-Heulin, C. (2019). History, development and current advances concerning the evolutionary roots of human right-handedness and language: brain lateralisation and manual laterality in non-human primates. *Ethology* 125, 1–28. doi: 10.1111/eth.12827

Pszczolkowski, M. A., and Brown, J. J. (2003). Effect of sugars and non-nutritive sugar substitutes on consumption of apple leaves by codling moth neonates. *Phytoparasitica* 31, 283–291. doi: 10.1007/BF02980837

R Core Team (2017). *R: A language and environment for statistical computing*. Vienna, Austria: R Foundation for Statistical Computing. Available at: https://www.R-project.org/ (Accessed November 13, 2019).

Reisenman, C. E., and Riffell, J. A. (2015). The neural bases of host plant selection in a neuroecology framework. *Front. Invert. Physiol.* 6:229. doi: 10.3389/fphys.2015.00229

Rospars, J.-P. (2013). Interactions of odorants with olfactory receptors and other preprocessing mechanisms: how complex and difficult to predict? *Chem. Senses* 38, 283–287. doi: 10.1093/chemse/bjt004

Roy, R., Schmitt, A. J., Thomas, J. B., and Carter, C. J. (2017). Nectar biology: from molecules to ecosystems. *Plant Sci.* 262, 148–164. doi: 10.1016/j.plantsci.2017.04.012

Sandoz, J. C. (2011). Behavioral and neurophysiological study of olfactory perception and learning in honeybees. *Front. Syst. Neurosci.* 5:98. doi: 10.3389/fnsys.2011.00098

Sandoz, J. C., Laloi, D., Odoux, J. F., and Pham-Delegue, M. H. (2000). Olfactory information transfer in the honeybee: compared efficiency of classical conditioning and early exposure. *Anim. Behav.* 59, 1025–1034. doi: 10.1006/anbe.2000.1395

Scheiner, R., Abramson, C., Brodschneider, R., Crailsheim, K., Farina, W., Fuchs, S., et al. (2013). Standard methods for behavioural studies of *Apis mellifera*. *J. Apic. Res.* 52, 1–58. doi: 10.3896/IBRA.1.52.4.04

Scheiner, R., Barnert, M., and Erber, J. (2003). Variation in water and sucrose responsiveness during the foraging season affects proboscis extension learning in honeybees. *Apidologie* 34, 67–72. doi: 10.1051/apido:2002050

Scheiner, R., Baumann, A., and Blenau, W. (2006). Aminergic control and modulation of honeybee behaviour. *Curr. Neuropharmacol.* 4, 259–276. doi: 10.2174/157015906778520791

Scheiner, R., Page, R. E., and Erber, J. (2004a). Sucrose responsiveness and behavioral plasticity in honey bees (*Apis mellifera*). *Apidologie* 35, 133–142. doi: 10.3896/IBRA.1.52.4.04

Scheiner, R., Sokolowski, M. B., and Erber, J. (2004b). Activity of cGMP-dependent protein kinase (PKG) affects sucrose responsiveness and habituation in *Drosophila melanogaster*. *Learn. Mem.* 11, 303–311. doi: 10.1101/lm.71604

Scheiner, R., Steinbach, A., Claßen, G., Strudthoff, N., and Scholz, H. (2014). Octopamine indirectly affects proboscis extension response habituation in *Drosophila melanogaster* by controlling sucrose responsiveness. *J. Insect Physiol.* 69, 107–117. doi: 10.1016/j.jinsphys.2014.03.011

Schiff, N. M., Waldbauer, G. P., and Friedman, S. (1989). Dietary self-selection by *Heliothis zea* larvae: roles of metabolic feedback and chemosensory stimuli. *Ent. Exp. Appl.* 52, 261–270. doi: 10.1111/j.1570-7458.1989.tb01276.x

Schwaerzel, M., Monastirioti, M., Scholz, H., Friggi-Grelin, F., Birman, S., and Heisenberg, M. (2003). Dopamine and octopamine differentiate between aversive and appetitive olfactory memories in *Drosophila*. *J. Neurosci.* 23, 10495–10502. doi: 10.1523/JNEUROSCI.23-33-10495.2003

Seada, M. A. (2015). Antennal morphology and sensillum distribution of female cotton leaf worm *Spodoptera littoralis* (Lepidoptera: Noctuidae). *J. Basic Appl. Zool.* 68, 10–18. doi: 10.1016/j.jobaz.2015.01.005

Seada, M. A., Ignell, R., Al Assiuty, A. N., and Anderson, P. (2018). Functional characterization of the gustatory sensilla of tarsi of the female polyphagous moth *Spodoptera littoralis*. *Front. Physiol.* 9:1606. doi: 10.3389/fphys.2018.01606

Senapathi, D., Biesmeijer, J. C., Breeze, T. D., Kleijn, D., Potts, S. G., and Carvalheiro, L. G. (2015). Pollinator conservation — the difference between managing for pollination services and preserving pollinator diversity. *Curr. Opin. Insect Sci.* 12, 93–101. doi: 10.1016/j.cois.2015.11.002

Shafir, S., and Yehonatan, L. (2014). Comparative evaluations of reward dimensions in honey bees: evidence from two-alternative forced choice proboscis-extension conditioning. *Anim. Cogn.* 17, 633–644. doi: 10.1007/s10071-013-0694-z

Simcock, N. K., Gray, H., Bouchebti, S., and Wright, G. A. (2018). Appetitive olfactory learning and memory in the honeybee depend on sugar reward identity. *J. Insect Physiol.* 106, 71–77. doi: 10.1016/j.jinsphys.2017.08.009

Simcock, N. K., Gray, H. E., and Wright, G. A. (2014). Single amino acids in sucrose rewards modulate feeding and associative learning in the honeybee. *J. Insect Physiol.* 69, 41–48. doi: 10.1016/j.jinsphys.2014.05.004

Skiri, H. T., Stranden, M., Sandoz, J. C., Menzel, R., and Mustaparta, H. (2005). Associative learning of plant odorants activating the same or different receptor neurones in the moth *Heliothis virescens*. *J. Exp. Biol.* 208, 787–796. doi: 10.1242/jeb.01431

Smedley, S. R., and Eisner, T. (1995). Sodium uptake by puddling in a moth. *Science* 270, 1816–1818. doi: 10.1126/science.270.5243.1816

Smedley, S. R., and Eisner, T. (1996). Sodium: a male moth's gift to its offspring. *Proc. Natl. Acad. Sci. USA* 93, 809–813.

Takada, T., Sato, R., and Kikuta, S. (2017). A mannitol/sorbitol receptor stimulates dietary intake in *Tribolium castaneum*. *PLoS One* 12:e0186420. doi: 10.1371/journal.pone.0186420

Thompson, R. F., and Spencer, W. A. (1966). Habituation: a model phenomenon for the study of neuronal substrates of behavior. *Psychol. Rev.* 73, 16–43. doi: 10.1037/h0022681

Tiedeken, E. J., Stout, J. C., Stevenson, P. C., and Wright, G. A. (2014). Bumblebees are not deterred by ecologically relevant concentrations of nectar toxins. *J. Exp. Biol.* 217, 1620–1625. doi: 10.1242/jeb.097543

Unoki, S., Matsumoto, Y., and Mizunami, M. (2005). Participation of octopaminergic reward system and dopaminergic punishment system in insect olfactory learning revealed by pharmacological study. *Eur. J. Neurosci.* 22, 1409–1416. doi: 10.1111/j.1460-9568.2005.04318.x

Unoki, S., Matsumoto, Y., and Mizunami, M. (2006). Roles of octopaminergic and dopaminergic neurons in mediating reward and punishment signals in insect visual learning. *Eur. J. Neurosci.* 24, 2031–2038. doi: 10.1111/j.1460-9568.2006.05099.x

Vinauger, C., Lallement, H., and Lazzari, C. R. (2013). Learning and memory in *Rhodnius prolixus*: habituation and aversive operant conditioning of the proboscis extension response. *J. Exp. Biol.* 216, 892–900. doi: 10.1242/jeb.079491

Waddington, K., and Gottlieb, N. (1990). Actual vs perceived profitability: a study of floral choice of honey bees. *J. Insect Behav.* 3, 429–441. doi: 10.1007/BF01052010

Watanabe, M., and Kamikubo, M. (2005). Effects of saline intake on spermatophore and sperm ejaculation in the male swallowtail butterfly *Papilio xuthus* (Lepidoptera: Papilionidae). *Entomol. Sci.* 8, 161–166. doi: 10.1111/j.1479-8298.2005.00114.x

Watt, W. B., Hoch, P. C., and Mills, S. G. (1974). Nectar resource use by *Colias* butterflies. *Oecologia* 14, 353–374. doi: 10.1007/BF00384578

Wheeler, D. (1996). The role of nourishment in oogenesis. *Annu. Rev. Entomol.* 41, 407–431. doi: 10.1146/annurev.en.41.010196.002203

Winkler, K., Wäckers, F. L., Stingli, A., and Van Lenteren, J. C. (2005). *Plutella xylostella* (diamondback moth) and its parasitoid *Diadegma semiclausum* show different gustatory and longevity responses to a range of nectar and honeydew sugars. *Entomol. Exp. Appl.* 115, 187–192. doi: 10.1111/j.1570-7458.2005.00254.x

Wynne, J. W., Armon, J. K., Gerhardt, K. O., and Krause, G. F. (1991). Plant species identified as food sources for adult black cutworm (Lepidoptera: Noctuidae) in northwestern Missouri. *J. Kansas Entomol. Soc.* 64, 381–387.

Zhang, Y. F., Van Loon, J. J., and Wang, C. Z. (2010). Tarsal taste neuron activity and proboscis extension reflex in response to sugars and amino acids in *Helicoverpa armigera* (Hubner). *J. Exp. Biol.* 213, 2889–2895. doi: 10.1242/jeb.042705

Zhu, Y., Keaster, A. J., and Gerhardt, K. O. (1993). Field observations on attractiveness of selected blooming plants to noctuid moths and electroantennogram responses of black cutworm (Lepidoptera: Noctuidae) moths to flower volatiles. *Environ. Entomol.* 22, 162–166. doi: 10.1093/ee/22.1.162

Conflict of Interest: The authors declare that the research was conducted in the absence of any commercial or financial relationships that could be construed as a potential conflict of interest.

frontiers in Physiology

ORIGINAL RESEARCH
published: 27 November 2019
doi: 10.3389/fphys.2019.01444

Non-synaptic Plasticity in Leech Touch Cells

Sonja Meiser[1], Go Ashida[1,2] and Jutta Kretzberg[1,2]*

[1] Computational Neuroscience, Department of Neuroscience, Faculty VI, Carl von Ossietzky University of Oldenburg, Oldenburg, Germany, [2] Cluster of Excellence Hearing4all, Department of Neuroscience, Faculty VI, Carl von Ossietzky University of Oldenburg, Oldenburg, Germany

The role of Na^+/K^+-pumps in activity-dependent synaptic plasticity has been described in both vertebrates and invertebrates. Here, we provide evidence that the Na^+/K^+-pump is also involved in activity-dependent non-synaptic cellular plasticity in leech sensory neurons. We show that the resting membrane potential (RMP) of T cells hyperpolarizes in response to repeated somatic current injection, while at the same time their spike count (SC) and the input resistance (IR) increase. Our Hodgkin–Huxley-type neuron model, adjusted to physiological T cell properties, suggests that repetitive action potential discharges lead to increased Na^+/K^+-pump activity, which then hyperpolarizes the RMP. In consequence, a slow, non-inactivating current decreases, which is presumably mediated by voltage-dependent, low-threshold potassium channels. Closing of these putative M-type channels due to hyperpolarization of the resting potential increases the IR of the cell, leading to a larger number of spikes. By this mechanism, the response behavior switches from rapidly to slowly adapting spiking. These changes in spiking behavior also effect other T cells on the same side of the ganglion, which are connected via a combination of electrical and chemical synapses. An increased SC in the presynaptic T cell results in larger postsynaptic responses (PRs) in the other T cells. However, when the number of elicited presynaptic spikes is kept constant, the PR does not change. These results suggest that T cells change their responses in an activity-dependent manner through non-synaptic rather than synaptic plasticity. These changes might act as a gain-control mechanism. Depending on the previous activity, this gain could scale the relative impacts of synaptic inputs from other mechanoreceptors, versus the spike responses to tactile skin stimulation. This multi-tasking ability, and its flexible adaptation to previous activity, might make the T cell a key player in a preparatory network, enabling the leech to perform fast behavioral reactions to skin stimulation.

Keywords: invertebrate, mechanoreceptor, sodium–potassium pump, Hodgkin–Huxley neuron model, M-type K^+ current, spike count, resting potential, input resistance

OPEN ACCESS

Edited by:
Sylvia Anton, Institut National de la Recherche Agronomique (INRA), France

Reviewed by:
Brian Burrell, University of South Dakota, United States
Daniel A. Wagenaar, California Institute of Technology, United States

****Correspondence:***
Sonja Meiser
sonja.meiser@uni-oldenburg.de

Specialty section:
This article was submitted to Invertebrate Physiology, a section of the journal Frontiers in Physiology

Received: *31 May 2019*
Accepted: *08 November 2019*
Published: *27 November 2019*

Citation:
Meiser S, Ashida G and Kretzberg J (2019) Non-synaptic Plasticity in Leech Touch Cells. Front. Physiol. 10:1444. doi: 10.3389/fphys.2019.01444

INTRODUCTION

Understanding the mechanisms of how sensory information elicits behavioral reactions is a major goal in neuroscience. The experimentally easily amenable nervous system of the medicinal leech makes this animal a useful model organism to investigate the neuronal basis of sensory processing (Kristan et al., 2005; Wagenaar, 2015). Touching a leech's skin triggers a behavioral response with

a surprisingly high accuracy – the local bend (Kristan et al., 1982). The animal can distinguish between two touch locations just as precisely as the human fingertip (Johnson, 2001; Baca et al., 2005; Thomson and Kristan, 2006; Pirschel and Kretzberg, 2016). The leech central nervous system (CNS) contains a highly repetitive ventral nerve cord with one ganglion per segment. Each ganglion contains an ensemble of around 400 mostly paired neurons serving as the basis of diverse sensory-input motor-output networks (Kristan et al., 2005). The sensory input layer consists of three different types of leech mechanosensory cells [touch (T), pressure (P), and nociceptive (N) cells], which share several fundamental properties with the human tactile receptors (Baca et al., 2005; Smith and Lewin, 2009; Pirschel and Kretzberg, 2016). Early studies focused mostly on P cells, because stimulation of a single P cell is sufficient to elicit muscle movements for several behavioral responses, like swimming or local bending (Kristan, 1982; Kristan et al., 1982). Since T and N cells showed only minor contributions to these movements, they were not further investigated. However, Pirschel and Kretzberg (2016) suggested that T cells might play a substantial role in the local bend response, making in-depth investigations on these sensory neurons necessary.

The current study focuses on these T cells, which are low threshold, rapidly adapting sensory neurons. They primarily encode the temporal qualities, especially velocity, of applied mechanosensory stimuli during the onset and offset phases of the stimulation (Nicholls and Baylor, 1968b; Carlton and McVean, 1995). There are three bilateral pairs of T cells in one ganglion which form both electrical and chemical synaptic connections with each other (Nicholls and Baylor, 1968b; Baylor and Nicholls, 1969b; Li and Burrell, 2008). Moreover T cells receive polysynaptic input from the other mechanoreceptor type (P cells) and nociceptors (N cells), leading to a combination of excitatory and inhibitory potentials (Burgin and Szczupak, 2003). Several long-range dendritic processes of T cells run through the ipsilateral nerve roots in the body wall to branch extensively in the base of the layer of epithelial cells and end at a few micrometers from the skin surface (Blackshaw, 1981). The rapidly adapting human Meissner corpuscles show similar response properties, elicited by encapsulated unmyelinated nerve endings with stretch-sensitive ion channels in the tip. Potentially, the nerve endings of T cells may also contain these mechanosensitive channels, which may change opening probability after repeated stimulation, like in human hair cells during stimulation with a high sound pressure level (Hakizimana et al., 2012). Because the entire extent of arborization of one T cell spans three segmental ganglia, each cell responds to touch of the skin at its own and the adjacent anterior and posterior segments (Yau, 1976). The receptive fields of each T cell cover either the dorsal, lateral, or ventral skin area on one side (Nicholls and Baylor, 1968b). Like other invertebrate neurons, T cells are unipolar, meaning that dendrites and axon are not clearly separated, but form a continuum of processes (Rolls and Jegla, 2015). Moreover, like several invertebrate neurons (Calabrese, 1980; Meyrand et al., 1992), leech T cells were found to have at least two distinct spike-initiation zones. A peripheral spike initiation zone near the skin conveys information about touch stimuli, and a central one close to the soma processes synaptic inputs within the ganglion (Burgin and Szczupak, 2003; Kretzberg et al., 2007).

High frequency spiking in touch mechanoreceptors triggered by somatic electrical stimulation or peripheral skin stimulation (Baylor and Nicholls, 1969a) induces a long-term afterhyperpolarization (AHP), arising from the activation of the Na^+/K^+-pump (also called the Na^+/K^+-ATPase) and a Ca^{2+}-dependent K^+ current (Nicholls and Baylor, 1968a; Baylor and Nicholls, 1969a; Jansen and Nicholls, 1973; Scuri et al., 2002, 2007). Previous studies pointed out that modulation of the Na^+/K^+-pump activity is involved in activity-dependent synaptic plasticity between two ipsilateral T neurons (Catarsi and Brunelli, 1991; Catarsi et al., 1993; Scuri et al., 2002, 2007; Lombardo et al., 2004). Additionally, high-frequency stimulation of a T cell elicits long-term depression in the activated pathway and potentiation in the non-activated T cell synapses (Burrell and Sahley, 2004). Furthermore, low-frequency stimulation of T cells can depress synapses through an endocannabinoid-dependent mechanism, which has also been observed in the mammalian spinal cord (Li and Burrell, 2009, 2010).

Here, we show that T cell activity is also influenced by non-synaptic plasticity. Based on our electrophysiological experiments and modeling approaches, we demonstrate that repeated somatic T cell stimulation enhances Na^+/K^+-pump activity, which gradually hyperpolarizes the resting membrane potential (RMP). In consequence, a slow, non-inactivating (putative M-type K^+) current decreases, resulting in a higher input resistance (IR) and a larger number of tonic spikes. Furthermore, our T cell double recordings show that the Na^+/K^+-pump is also involved in activity-dependent non-synaptic cellular plasticity among leech sensory neurons. Our recording results indicate that the increase in presynaptic spike count (SC) due to non-synaptic plasticity also affects the PR in another ipsilateral T cell. However, this effect is not specific to stimulus history, indicating non-synaptic rather than synaptic plasticity.

MATERIALS AND METHODS

Animals and Preparation

The experiments were performed on adult hermaphrodite medicinal leeches (*Hirudo verbana*) obtained from the Biebertaler Leech Breeding Farm (Biebertal, HE, Germany). According to German regulations, no approval of an ethics committee was required for the work on these invertebrates. The animals were kept at room temperature in tanks with ocean sea-salt diluted with purified water (1:1000). All experiments were performed at room temperature. The leeches were anesthetized with ice-cold saline (mM: 115 NaCl, 4 KCl, 1.8 $CaCl_2$, 10 Glucose, 4.6 Tris–maleate, 5.4 Tris base and buffered at pH 7.4 with NaOH, modified after Muller and Scott, 1981) before and during dissection. We used isolated ganglia, dissected from segments 9–13 and pinned them, ventral side up, to a plastic petri dish, coated with the silicone elastomer *Sylgard* (Dow Corning Corporation, Midland, MI, United States) (**Figure 1A**).

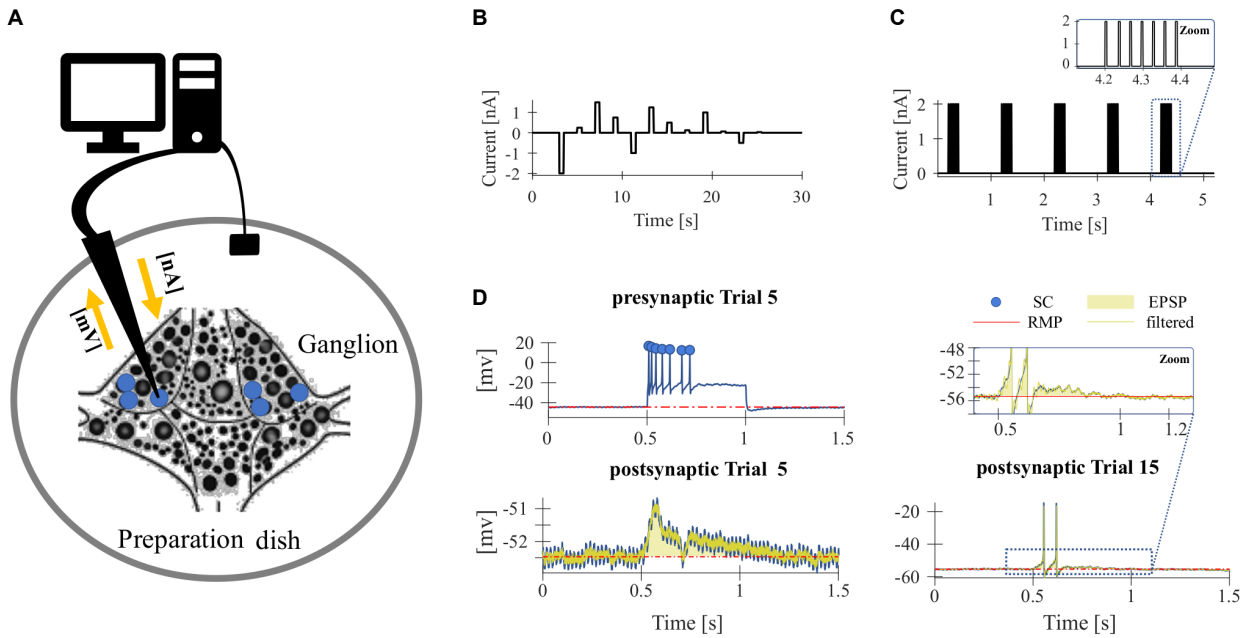

FIGURE 1 | Experimental design. **(A)** Sketch of the isolated ganglia preparation and the principle of the current-clamp recording. The membrane potential of one of the T cells (blue) was recorded with an intracellular electrode (black arrow). **(B,C)** Stimulus protocol for repeated electrical soma stimulation. Each experiment consisted of 15–20 identical trial repetitions. **(B)** For the experiments presented in **Figures 2**, **4A,B**, 12 electrical pulses of different current amplitudes were injected into the T cell soma. **(C)** For studying synaptic interaction of T cells (**Figures 4C–F**), five pulse packages were injected into the soma if one T cell. Each package contained a fixed number (1–7) of pulses that elicits the same number of single action potentials. The zoom inset shows a package with 7 pulses. **(D)** The neuronal responses were quantified by the following features: (presynaptic) spike count (SC, blue dots indicate counted spikes): total number of spikes elicited by the neuron and recorded in the soma between the stimulus onset (0.5 s) and offset (1 s); resting membrane potential (RMP, red): averaged membrane potential in the 2.5 s prior to the first current pulse; postsynaptic response (PR): averaged difference between the filtered recorded membrane potential and the RMP calculated from the start to 200 ms after the end of the presynaptic current stimulus (yellow transparent area). Synaptic potentials sometimes triggered spikes in the postsynaptic cell (see Trial 15 for an example), but not in all (see Trial 5 for an example). The calculation of PR included spikes if they were elicited.

Electrophysiological Technique

The experimental rig consisted of two mechanical micromanipulators type MX-1 (TR 1, Narishige, Tokyo, Japan) and two amplifiers (SEC-05X, NPI Electronic, Tamm, Germany) (Kretzberg et al., 2016). Neuronal responses were recorded (sample rate 100 kHz) and analyzed using custom-written MATLAB software (MATLAB 9.1-9.5, MathWorks, Natick, MA, United States). We performed intracellular single and double recordings from mechanosensory touch cells, while injecting current into one T cell soma. For these current clamp recordings, the cell soma was impaled with borosilicate microelectrodes (TW100F-4, World Precision Instruments Inc., Sarasota, FL, United States) pulled with the micropipette puller P97 Flaming Brown (Sutter Instruments Company, Novato, CA, United States). The glass electrodes were filled with 3 M potassium acetate and had resistances of 15–30 MΩ. The neurons were identified by the size and the location of their cell bodies with a binocular microscope (Olympus szx7, Olympus, Tokyo, Japan) as well as by their firing pattern (Nicholls and Baylor, 1968b).

Experimental Design

To investigate the effect of repeated mechanoreceptor stimulation on the physiological properties of T cells and their synaptic partners we used somatic current injection. Intracellular single recordings of T cells in isolated ganglia were performed by stimulating the neuron in each trial with a series of 12 current pulses in a pseudo-randomized order (**Figure 1B**). The amplitude of the pulses varied between −2 and +1.5 nA. The duration of each pulse was 500 ms and the inter-pulse-interval was 2.5 s long. The inter-trial-interval was 5 s long. Each experiment consisted of 15–20 identical trial repetitions. While injecting current into the T cell soma with the intracellular electrode, we recorded the membrane potential of the stimulated T cell with the same electrode.

To analyze the synaptic connections between T cells, we performed ipsilateral double recordings and recorded from two of the three T cells in all combinations. While injecting current into one T cell soma (presynaptic) with one electrode, we recorded the membrane potential of the unstimulated T cell (postsynaptic) with a second electrode. In addition to the protocol shown in **Figure 1B**, a pulse-package protocol (**Figure 1C**) was applied. One pulse-package comprised a fixed number (1–7) of short current pulses (2 nA, 5 ms), which were injected into the T cell soma to trigger one action potential each. In consequence, the pulse-package protocol elicited the same number and timing of presynaptic action potentials in each trial. Each trial consisted of five pulse packages and each

sub-experiment was composed of 25 trial repetitions. The pause between the single pulses in a package was 30 ms and the starting times of the packages were always separated by 1 s (independent of the number of pulses in the package).

In total, we analyzed 20 single and 23 double recordings (9 with 500 ms current pulse injections, 14 with single current pulse injections) of T cells. During the recordings, the electrode properties usually changed slightly, leading to an average increase in electrode resistance by +7 MΩ, and an average electrode offset drift by −4 mV. Five additional single recordings were excluded from the analysis, because the electrode resistance changed by more then10 MΩ due to clogging, or because the electrode offset drifted by more than −6.25 mV.

Data Analysis

The neuronal responses of the stimulated T cells and their synaptic partner neurons were quantified by the following response features (**Figure 1D**): SC, RMP, cell IR, and postsynaptic response (PR).

- **SC** [spike number] was defined as the total number of spikes elicited by the neuron and recorded in the soma during the 500 ms between the stimulus onset and offset. Spike detection was accomplished using custom-developed MATLAB software. Spikes were defined by the following parameters: minimum threshold [mV], minimum duration [ms], and minimum spike amplitude [mV]. A spike was detected when the membrane potential depolarized by the minimum spike threshold and the relative spike height, from rest to peak, was at least as high as the minimum spike amplitude. Additionally, a peak was only accepted as an action potential if the detected peak at half of the prominence had the required minimum duration.
- **RMP** [mV] of each trial (U_{rest}) was computed as the averaged membrane potential in the 2.5 s before the first current pulse starts.
- **IR** [MΩ] was calculated based on the average membrane potential (U_{stim}) in response to a 500 ms long hyperpolarizing current pulse of $I = -1$ nA to avoid the influence of active processes. It was calculated with Ohm's law: R [MΩ] = (U_{stim} [mV] − U_{rest} [mV])/I [nA].
- **PR** [mV] was calculated as average difference between the recorded membrane potential and the RMP of the postsynaptic (unstimulated) cell. The potential difference was averaged in the period from the start to 200 ms after the end of the presynaptic current stimulus, no matter if spikes were elicited postsynaptically or not. To reduce the noise caused by electric hum superimposed to the recorded postsynaptic signal, we used a notch filter which removed at least half the power of the frequency components in the range of 47–53 Hz.

In the results section, response changes (ΔSC, ΔRMP, ΔIR, ΔPR) caused by repeated stimulation are displayed as differences in the measured response features (SC, RMP, IR, PR) between the N_{th} and the first trial repetition. The observed distributions of these response feature changes are reported as median, and first (Q1) and third (Q3) quartiles in the figures. To show the increase (ΔSC, ΔIR, ΔPR) or decrease (ΔRMP) over trial repetitions, linear fits were calculated for each cell individually. The obtained slopes were tested to differ significantly from 0 (t-test, $\alpha = 0.05$). In **Figures 2**, **4**, the average of the linear fits for all cells indicates if the response features increased or decreased with trial repetitions.

Biological Neuron Model

We built a computational model of the leech T cell to investigate the physiological bases of the experimentally observed adaptive changes caused by repeated electrical stimulation. We used a single-compartment Hodgkin–Huxley-type neuron model modified with an additional Na^+/K^+-pump and a M-type slow potassium current (**Table 1**). We did not aim to create a more complex multi-compartment model, because we focus on the activity of T cells induced by somatic current injection and because the information on ion channel distribution over the T cell membrane is fundamentally lacking. This and other limitations of our modeling approach are addressed in section "Discussion."

Model Structure

Based on previous experimental recordings of leech neurons, we assumed a fast (transient) sodium channel with four activation and one inactivation gate, while the delayed rectifier potassium channel has two activation gates (Johansen, 1991). These channels are responsible for spike generation in response to positive current injections. The activity of the Na^+/K^+-pump was assumed to depend on the intracellular concentration of Na^+ ions. Increase of intracellular Na^+ due to repetitive spikes leads to the activation of the pump, which exchanges three intracellular Na^+ ions with two extracellular K^+ ions, resulting in the net negative current that hyperpolarizes the membrane potential (Forrest, 2014). The M-type K^+ conductance, whose kinetics are much slower than the spike-generating conductances, cause the cessation of spiking during current injection in a voltage dependent manner (Yamada et al., 1998; Benda and Herz, 2003). In order to focus on the fundamental biophysical mechanisms of spike-rate adaptation caused by repetitive current injections, we used this minimalistic description of ion channels and pumps, although the leech T cell may express a number of other ionic conductances (see section "Discussion").

Model Fitting

Since the operating voltage range of leech T cells is considerably more depolarized than those of neurons in most other animals, we needed to adjust the model functions (**Table 1**) and parameters (**Table 2**) to reproduce known T cell response characteristics (shown in sections "Results" and "Repeated Somatic Current Injection Induces Non-synaptic Plasticity"). Starting from previous measurements in leeches (reviewed, e.g., in Johansen, 1991), the ion channel kinetics were determined to fit our T cell data, including the RMP, spike threshold, single spike duration, and SCs. By using the standard membrane capacitance density of 1.0 μF/cm^2, the effective size of the membrane and the leak conductance were determined. The membrane area we adopted is larger than what is expected solely from the size of the soma of a T cell, because the additional contribution of the dendritic processes near the cell body was considered.

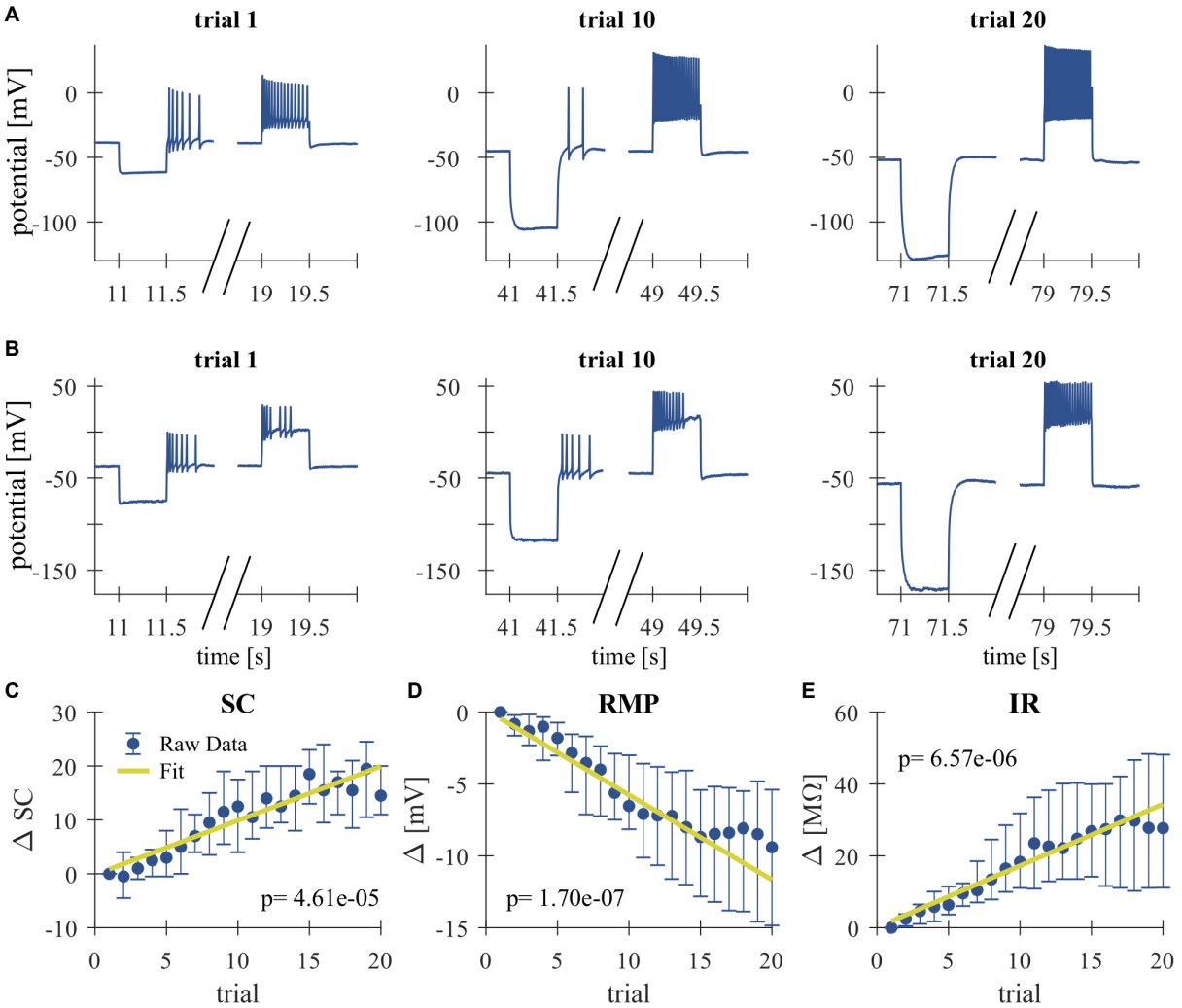

FIGURE 2 | Repeated somatic current injection effects physiological properties of T cells. **(A,B)** Representative responses of intracellularly recorded T cells to a 500 ms long somatic current pulse injection of –1 nA (seconds 11–11.5, 41–41.5, and 71–71.5), which was used for the calculation of the IR and often elicited rebound spikes, and +1 nA (seconds 19–19.5, 49–49.5, and 79–79.5) in Trial 1, 10, 20. **(A)** Example of a slowly adapting initial response, **(B)** Example of a rapidly adapting initial response. **(C–E)** Dependencies of changes in response parameters on trial repetitions shown as median and quartiles of all T cells (N = 20). Linear fits were calculated for each cell individually and the obtained slopes were tested to differ significantly from 0 (t-test, α = 0.05, p-values given in the panels). The yellow line indicates the average of the fits for all cells. **(C)** Spike count (SC) difference from first trial (absolute number). **(D)** Resting membrane potential (RMP) difference from first trial (mV). **(E)** Input resistance difference from first trial (MΩ).

There is no empirical data available for the ionic concentration in T cells at rest and at spiking. Therefore, we formulated the Na^+/K^+-pump model depending only on the change of Na^+ concentration (denoted as c_{Na}) from rest. In our simulations c_{Na} was assumed to be in a similar order as in Retzius cells (Deitmer and Schlue, 1983), namely a few tens of mM. Time-dependent changes of the intracellular Na^+ concentration is caused by the Na^+ currents through Na^+ channels and Na^+/K^+-pumps. In order to separately simulate the contribution of Na^+ channels and Na^+/K^+-pumps in c_{Na}, we adopted two conversion factors (κ_{chan} and κ_{pump} in **Table 2**). Theoretically, this conversion factor is the reciprocal of the product between the Faraday constant and the effective volume relevant to the diffusion of Na^+ ions (Barreto and Cressman, 2011). However, it is not simple to estimate these factors in a T cell, because of its complex neuronal morphology. If the diffusion of Na^+ ions, which affects the activity of Na^+/K^+-pump, is not uniform but restricted to the vicinity of the membrane, the effective volume becomes smaller, leading to a larger value of the conversion factor. Therefore, we varied κ_{chan} and κ_{pump} in the range between 0 and $1.20 \cdot 10^{-6}$ mM/pA · ms, and selected values that led to a stable decrease of membrane potential with repeated stimulations.

TABLE 1 | T cell model equations.

Variable	Equation
Membrane potential V	$c_m \frac{dV}{dt} = I_{\mathrm{Na}} + I_K + I_M + I_L + I_{\mathrm{pump}} + I_{\mathrm{inj}}$
Fast (transient) Na^+ current I_{Na}	$I_{\mathrm{Na}} = g_{\mathrm{Na}} \cdot m^4 \cdot h \cdot (E_{\mathrm{Na}} - V)$
Delayed rectifier K^+ current I_K	$I_K = g_K \cdot n^2 \cdot (E_K - V)$
M-type K^+ current I_M	$I_M = g_M \cdot z^2 \cdot (E_K - V)$
Leak current I_L	$I_L = g_L \cdot (E_L - V)$
Kinetic equations for channel variables ($x = m$, h, n, or z)	$\frac{dx(t)}{dt} = \frac{x_\infty(V) - x}{\tau_x(V)}$
Steady state function for Na^+ activation	$m_\infty(V) = \frac{1}{1 + \exp(-(V+20)/8)}$
Time constant for Na^+ activation (in ms)	$\tau_m(V) = 0.75 \cdot \left(\frac{2}{\exp(-(V+20)/16) + \exp((V+20)/16)} + 0.1 \right)$
Steady state function for fast Na^+ inactivation	$h_\infty(V) = \frac{1}{1 + \exp(+(V+36)/5)}$
Time constant for fast Na^+ inactivation (in ms)	$\tau_h(V) = 7.5 \cdot \left(\frac{2}{\exp(-(V+36)/10) + \exp((V+36)/10)} + 0.1 \right)$
Steady state function for delayed rectifier K^+ activation	$n_\infty(V) = \frac{1}{1 + \exp(-(V+20)/8)}$
Time constant for delayed rectifier K^+ activation (in ms)	$\tau_n(V) = 4.0 \cdot \left(\frac{2}{\exp(-(V+20)/16) + \exp((V+20)/16)} + 0.1 \right)$
Steady state function for M-type K^+ activation	$z_\infty(V) = \frac{1}{1 + \exp(-(V+35)/3)}$
Time constant for M-type K^+ activation (in ms)	$\tau_z(V) = 450 \cdot \left(\frac{2}{\exp(-(V+35)/6) + \exp((V+35)/6)} + 1.0 \right)$
Na^+/K^+-pump current I_{pump}	$I_{\mathrm{pump}} = -I_{\max} \cdot p(c_{\mathrm{Na}})$
Na^+/K^+-pump activation function $p(c_{Na})$	$p(c_{\mathrm{Na}}) = \left(\frac{1}{1 + \exp(-(c_{\mathrm{Na}} - 18)/18)} \right)^3$
Intracellular Na^+ concentration c_{Na} (measured from rest)	$\frac{dc_{\mathrm{Na}}}{dt} = \kappa_{\mathrm{chan}} \cdot I_{\mathrm{Na}} + 3\kappa_{\mathrm{pump}} \cdot I_{\mathrm{pump}}$

The factor 3 for the intracellular Na^+ concentration change originates from the fact that three Na^+ ions are exchanged with two K^+ ions. The membrane potential V is in mV and the intracellular Na^+ concentration c_{Na} is in mM. I_{inj} denotes injected current.

Comparison of Model Conditions

In order to investigate the effects of the Na^+/K^+-pump and putative M-type K^+ (K_M) conductance on the long-term change of repetitive spiking, we compared the following four conditions in the T cell model: (1) the "default model" introduced above with the functions and parameters fitted to our T cell data; (2) the "fixed pump" model in which the Na^+/K^+-pump current is fixed to the value at the initial steady-state obtained without any current injection; (3) the "fully fixed K_M" model in which the M-type K conductance is fixed to the value at the initial steady-state obtained without any current injection; and (4) the "partially fixed K_M" model in which the M-type K conductance is not allowed to change only during the +1 nA current stimulation in each trial. However, the K_M conductance may change normally as in the default model when there is no input, or during injected current of any other size than +1 nA (see **Figure 1B** for the stimulus protocol of each trial). The comparison of the default model and the partially fixed K_M model is expected to reveal how the dynamic property of the M-type K conductance may play a role during the specific current stimulation of +1 nA (500-ms long per trial).

TABLE 2 | T cell model parameters.

Parameter	Value
Membrane surface area S_m	15,000 μm^2
Membrane capacitance density C_m	1.0 $\mu F/cm^2$
Membrane capacitance $c_m = C_m S_m$	150 pF
Fast (transient) Na^+ conductance density G_{Na}	160 mS/cm^2
Delayed rectifier K^+ conductance density G_K	8.0 mS/cm^2
M-type K^+ conductance density G_M	4.0 mS/cm^2
Leak conductance density G_L	0.1 mS/cm^2
Fast (transient) Na^+ conductance $g_{Na} = G_{Na} S_m$	24 μS
Delayed rectifier K^+ conductance $g_K = G_K S_m$	1.2 μS
M-type K^+ conductance $g_M = G_M S_m$	0.6 μS
Leak conductance $g_L = G_L S_m$	0.015 μS
Na^+ reversal potential E_{Na}	+30 mV
K^+reversal potential E_K	−50 mV
Leak reversal potential E_L	−15 mV
Maximum pump current $I_{\max}$	800 pA
Conversion factor from Na^+ channel current into Na^+ concentration κ_{chan}	$0.60 \cdot 10^{-6}$ mM/pA · ms
Conversion factor from Na^+/K^+-pump current into Na^+ concentration κ_{pump}	$0.12 \cdot 10^{-6}$ mM/pA · ms

Parameters were fitted to reproduce the experimentally measured T cell spike shape and to produce spike counts, resting potentials and input resistances in the interquartile range of the experimental observations of the 1st and 20th trial.

RESULTS

Repeated Somatic Current Injection Induces Non-synaptic Plasticity

High-frequency spike discharge leads to an intracellular accumulation of Na^+ ions which activate Na^+/K^+-pumps and thereby provide a mechanism for intrinsic, activity-dependent regulation of excitability (Gulledge et al., 2013;

Duménieu et al., 2015). We investigated the effect of high frequency spiking due to repeated stimulation with series of current pulse injections (500 ms duration, separated by 2500 ms break) into the T cell soma (**Figure 1**). Responses were analyzed for changes in the physiological properties SC, RMP, and cell IR. As can be seen in the representative intracellular response traces (**Figures 2A,B**), repeated current injection caused an increase in SC and in IR, while the RMP hyperpolarized.

These tendencies were seen in all recordings, even though the initial responses of individual T cells varied considerably in their SCs and the duration of their spiking activity (compare **Figures 2A,B** for examples of a slowly and a rapidly adapting initial response, see **Figures 3H–J** for the interquartile ranges of SC, RMP, and IR). The activity-dependent changes were found to be highly significant ($p < 0.001$) for all three physiological properties by testing if the slopes of linear regressions of individual cell responses differed from 0 (**Figures 2C–E**). This approach is not meant to imply that the relationships are linear, but only that SC and IR increased, and RMP hyperpolarized consistently in all 20 cells.

While **Figure 2** shows the changes caused by repeated current injection, **Figures 3H–J** indicate the interquartile ranges of the observed measurements of SC, RMP, and IR. For an input current of 1 nA, the SC gradually increased from a median value of 14.5 in trial 1 to 36 in trial 20. Meanwhile the median RMP gradually hyperpolarized from −37.5 to −48.8 mV and the median T cell IR increased from 27.8 to 62.7 MΩ. The absolute changes of the physiological properties to a current injection of 1 nA, calculated as median and quartiles over cells, are shown in **Table 3** (data for current injection of 0.5, 0.75, 1.25, and 1.5 nA are not shown, but followed the same trend).

Summarizing, the RMP of T cells hyperpolarizes in response to repeated somatic current injection, while the SC increases. Usually, one would expect that the probability for action potential generation is decreased at hyperpolarized RMP (Hodgkin and Katz, 1949). However, the repetitive electrical stimulation also led to a substantial increase in cell IR, which cannot be explained by electrode clogging (see section "Experimental Design"). To investigate the reason of the experimentally observed increase in SC, we developed a Hodgkin–Huxley type neuron model, modified with an additional Na^+/K^+-pump and a M-type slow potassium current (**Table 1**).

Sodium Pump and Slow Potassium Current Can Induce Non-synaptic Plasticity

A large number of previous studies already investigated how different forms of AHPs are affected by voltage- or calcium-dependent ionic conductances (reviewed in Vogalis et al., 2003; Larsson, 2013). The time scales of intracellular calcium buffering (Yamada et al., 1998; Goldman et al., 2001) and the activation/inactivation of calcium dependent potassium currents (Vogalis et al., 2003), however, is on the order of 0.1–1 s, which is several orders of magnitude faster than the activity-dependent long-term decrease of the membrane potential we focus on (which is on the order of a few tens of seconds; **Figure 2A**). In this slow potential change, the activity of the Na^+/K^+-pump is likely to be relevant (Barreto and Cressman, 2011; Forrest, 2014). Hence, we investigated the involvement of the Na^+/K^+-pump on the changes in the physiological properties of T cells, namely the hyperpolarization of the RMP accompanied by the increase of SC and IR. To address this question, we constructed a minimalistic Hodgkin–Huxley-type neuron model of a T cell incorporating the fast Na^+, delayed rectifier K^+, leak, and slow M-type K^+ conductances as well as the Na^+/K^+-pump. Blue curves in **Figure 3** show the responses of the default T cell model. To simulate the spiking responses of the T cell, we used the same protocol as for our experimental recordings with somatic current injections (**Figure 1B**). Parameters of the model were adjusted so that the simulated spike shape matched the time course of the original spike and the adaptive changes of the main features SC, RMP and IR stayed largely within the interquartile ranges of the original data (blue curves in **Figures 3H–J**). The increase of the pump current (**Figure 3A**, blue) was responsible for the decrease of the RMP from about −39 to −48 mV (**Figure 3I**, blue), because in each pump cycle three intracellular sodium ions were exchanged with two extracellular potassium ions, leading to a net negative current. The SC of the standard model increased over trials (**Figure 3H**), because of the voltage-dependent deactivation of the M-type K^+ current (**Figures 3B,C**), which in early trials activates during the current injection and hinders the repetitive spiking. Additionally, the decrease of the M-type K^+ conductance across trials also let to a decrease of the simulated IR from about 31–60 MΩ (**Figure 3J**), which resembled the empirical observations (**Figures 2D,E**), and also had a positive effect on SC.

In order to further investigate the roles of the Na^+/K^+-pump and the putative M-type K^+ conductance, we fixed these current and examined the resulting changes of the model neuron responses from the default condition (see section "Comparison of Model Conditions" for more detail of the conditions compared). When the pump current was fixed to the initial steady-state value, the stimulus-induced hyperpolarization as well as the increase of SC and IR vanished (**Figure 3E**; compare the green and blue curves in **Figures 3H–J**). This suggests that the experimentally observed stable hyperpolarization of the RMP is mainly due to the increase of Na^+/K^+-pump current and that this hyperpolarization is the basis for all observed changes. When the M-type K^+ conductance was fixed to the initial steady-state, while the pump was allowed to change, the IR did not change, indicating that the observed increase in IR can be attributed to the changes in the slow K^+ current. In this model version, the SC decreased across trials (**Figure 3F** and black curves in **Figures 3H,J**), showing the intuitively expected effects of slow hyperpolarization (**Figure 3I**, black). This SC decrease was diminished when the M-type K^+ conductance was kept unchanged only during the +1 nA stimulation (**Figure 3G**), while it could change in an activity-dependent way at all other times. In this model, the closing of the modeled M-type K^+ channel still led to an increased IR (**Figure 3J**, red) and counteracted the reduced excitability due to hyperpolarization (compare black and red curves in **Figure 3H**). We also note, however, that the dynamic property of the M-type K^+ current, which activates on the time

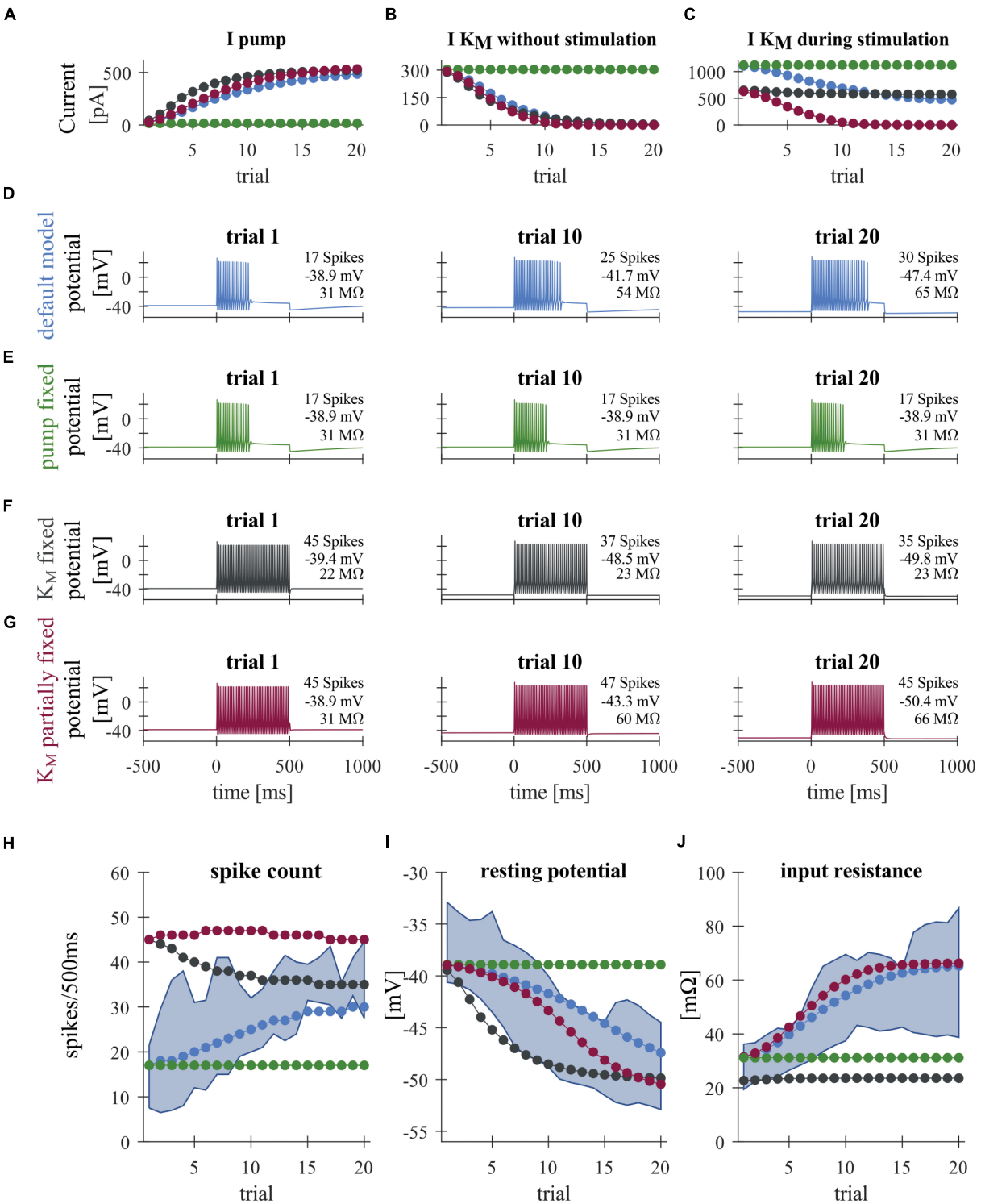

FIGURE 3 | Modeling T cell spike responses. **(A)** Average Na^+/K^+-pump current during +1 nA stimulation. **(B)** Average M-type K^+ current at 0–500 ms before the +1 nA stimulation. **(C)** Average M-type K^+ current during +1 nA stimulation. The K_M current is generally larger during stimulation **(C)** than without stimulation **(B)**, because of the increased average driving voltage (E_K–V) associated with spiking. **(D–G)** Responses of different T cell models to a current injection of +1 nA in Trials 1, 10 and 20. See **Figure 1B** for the stimulus protocol used. **(D)** Default model. **(E)** "Fixed pump model," in which the Na^+/K^+-pump current I_{pump} is fixed to the initial steady-state value. **(F)** "Fully fixed K_M model," in which the dynamics of the M-type K^+ conductance was fixed to the initial steady-state value. **(G)** "Partially fixed K_M model," in which the dynamics of the M-type K^+ conductance was fixed only during +1 nA current injection. **(H–J)** Simulated changes of the spike count **(H)**, resting potential **(I)**, and input resistance **(J)** across trials, plotted with the corresponding interquartile ranges observed experimentally (blue shading). Colors in panels **(A–C)** and **(H–J)** indicate the different model conditions: (blue) default model; (green) "fixed pump model"; (black) fully fixed K_M model; and (red) "partly fixed K_M model."

TABLE 3 | Absolute values for non-synaptic plasticity effects in T cells.

	Trial 1			Trial 20		
Property	**Q1**	**Median**	**Q3**	**Q1**	**Median**	**Q3**
SC [spikes/0.5 s]	7.5	14.5	24	27.5	36	42
RMP [mV]	−32.9	−37.5	−40.6	−44.5	−48.8	−52.9
Resistance [MΩ]	19.4	27.8	38.7	46.4	62.7	74.1

Responses to 500 ms current injection of 1 nA were obtained in 20 cells.

scale of a few 100 ms, turned out to be critical for determining the duration of repetitive spiking (compare **Figures 3D,G**). Despite the realistic increase in IR, the number of spikes in the model version with partially fixed M-type K^+ current were very large (**Figure 3H**, red), because spiking activity did not cease before the end of the stimulus (**Figure 3G**). These results suggest that the experimentally observed repetitive spiking behavior (and its cessation) of leech T cells is associated with a K_M-like slow conductance, which affects the SCs more dynamically than the static increase of IR. In sum, our modeling results suggest that the inactivation of the slow K^+ current plays a role in increasing the SC in an activity-dependent manner (**Figure 3H**). This inactivation is induced by the RMP hyperpolarization caused by the increased activity of Na^+/K^+-pumps (**Figure 3I**).

Non-synaptic Plasticity Effects Postsynaptic Responses of Other T Cells

We investigated the signal transmission between two ipsilateral T cells. Our goal was to see how the activity changes that were induced by non-synaptic plasticity in an electrically stimulated T cell (presynaptic) affected the responses in a non-stimulated T cell (postsynaptic). We analyzed how the PR, consisting of postsynaptic potentials and potentially elicited spikes, changed over repeated stimulation of the presynaptic cell (**Figure 4**). As expected, the presynaptic SC increased with repeated current stimulation from a median of 6 spikes (Q1: 4.25/Q3: 20) in trial 1 to 20 spikes (Q1: 17.75/Q3: 21) in trial 15. Postsynaptically, we observed a tendency of increased PR size, but overall the slopes of the linear regressions of PR increases were not significantly different from 0 ($p > 0.05$, cf. **Figure 4B**), because the PR increased only in 9 out of 11 cells over trials. However, the median of the averaged PR increased from 0.77 mV (Q1: 0.30/Q3: 1.23) in trial 1 to 0.96 mV (Q1: 0.44/Q3: 1.67) in trial 15.

To clarify if the increase in PR observed in most of the T cell pairs was caused solely by the increase of presynaptic SC that reflects the non-synaptic plasticity in the presynaptic (stimulated) T cell, or rather the synaptic plasticity also played a role, we elicited in the presynaptic cell a fixed number of single action potentials (**Figure 4C**) and repeated the protocol over several trials. The PR size was found to depend highly significantly ($p < 0.001$) on the presynaptic SC (**Figure 4D**), because the linear regression yielded clearly positive slopes for all the cell pairs examined. The averaged PR increased from a median value of 0.34 mV in response to one spike (Q_1: 0.31/Q_3: 0.37) to 1.02 mV (Q_1: 0.99/Q_3: 1.10) in response to seven spikes. However, the PR size did not change significantly with stimulation repetitions in six out of seven conditions with fixed SC (**Figures 4E,F**), demonstrating that synaptic plasticity did not alter the PRs.

Summarizing, the increase in SC caused by non-synaptic plasticity in the repeatedly stimulated presynaptic cell in most T cell pairs was reflected by an increase in PR size in the postsynaptic cell. However, no indication for synaptic plasticity was found, because PR size stayed stable over trials, when the presynaptic SC did not change.

DISCUSSION

Many studies have reported the involvement of the Na^+/K^+-pump in activity-dependent synaptic plasticity in both vertebrates (Wyse et al., 2004) and invertebrates (Pinsker and Kandel, 1969; Scuri et al., 2007). Based on electrophysiological and modeling results, the present study showed that the Na^+/K^+-pump might also be involved in activity-dependent non-synaptic plasticity in leech sensory neurons. Repeated somatic T cell stimulation enhances Na^+/K^+-pump activity which gradually hyperpolarizes the RMP while the SC and IR increase (**Figures 2**, **3**). Furthermore, we showed that this non-synaptic plasticity, rather than synaptic plasticity, leads to increased PRs in a second T cell on the same side of a segmental ganglion (**Figure 4**).

Biophysical Mechanisms Underlying Activity-Dependent Non-synaptic Plasticity

Our experimental and modeling results indicate that T cells modify their responses depending on their previous activity. Repeated somatic T cell stimulation enhances Na^+/K^+-pump activity which gradually hyperpolarizes the RMP. This might result in the suppression of a slow K^+ current, which leads to a higher IR and an increased SC. This putative K_M-current is involved in producing burst-patterns in many neuronal systems by raising the threshold for firing an action potential (Benda and Herz, 2003). Some of the K_M-channels are open at rest and they are even more likely to be open during depolarization, causing spike responses to stop before the end of the stimulation. But when the cell hyperpolarizes, this slow K^+ channel closes and the neuron fires in a more tonic manner. Especially in early trials, many of the recorded T cells showed cessation of spikes well before the end of the current pulse period. While the experimentally observed increase in IR could be one of the causes for the increase in SC, it did not lead to the cessation before the end of the stimulus. The changes in repetitive spiking behavior could be explained by the dynamical changes of the putative K_M current. Further experimental and modeling studies, e.g., on the effects of varied intervals between stimulus applications, are needed to understand the biophysical mechanisms of non-synaptic plasticity in more detail.

Leech sensory cells express several different ion channels (Johansen, 1991; Kleinhaus and Angstadt, 1995; Gerard et al., 2012), most of which we did not include in our model for the sake of simplicity. Sodium-dependent K^+ channels as they were found in leech pressure cells (Klees et al., 2005), for example,

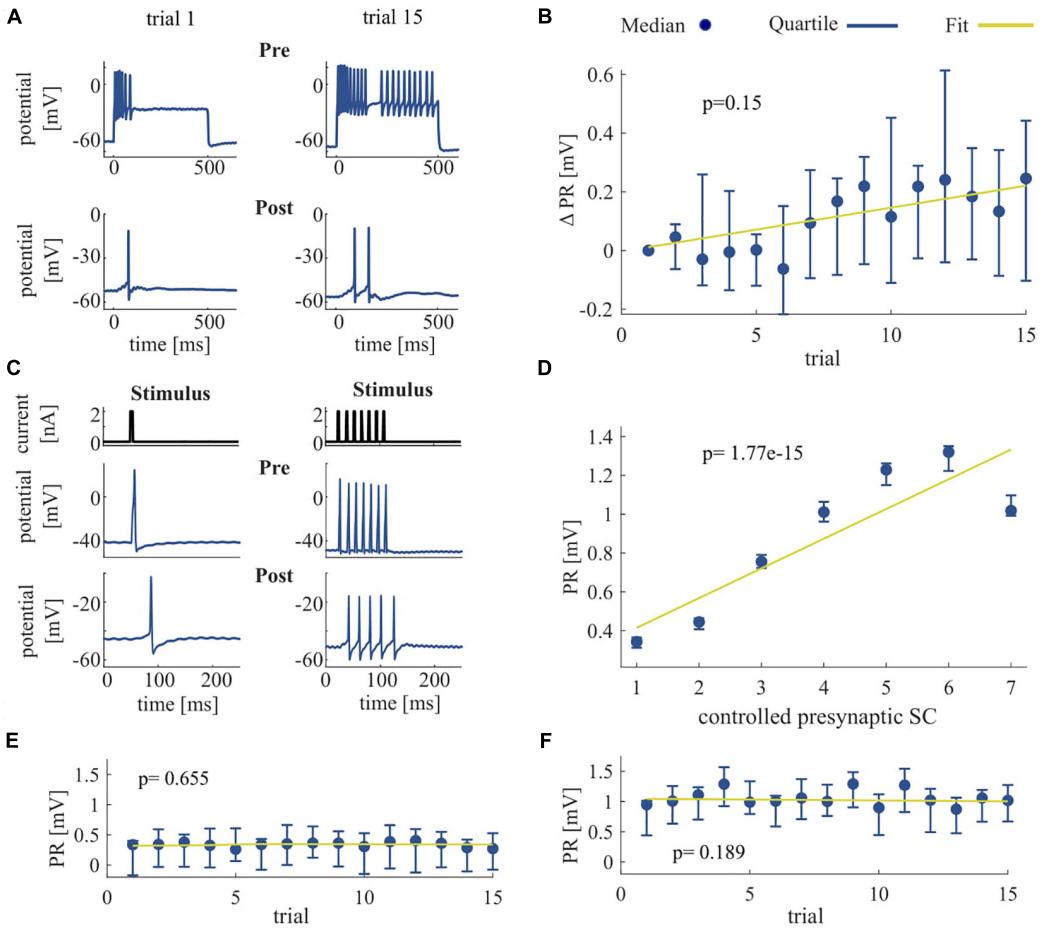

FIGURE 4 | Effect of repeated somatic current stimulation on the communication between two ipsilateral T cells. **(A)** Representative responses of an intracellularly recorded T cell pair to a 500 ms long somatic current injection of 1 nA in two different trial repetitions. **(B)** PR difference from first trial [mV] as median and quartiles of all T cells (N = 11) vs. trials. **(C)** Representative responses of an intracellularly recorded T cell pair to one and seven short current pulses. **(D)** Dependency of PR as median and quartiles of all T cells (N = 14) on controlled presynaptic SC. **(E,F)** Dependency of PR as median and quartiles of all T cells (N = 14) for one **(E)** and for seven **(F)** presynaptic spikes vs. trials. The slope of the PR vs. trial was not significant for six out of seven conditions (1 pulse, p = 0.655; 2 pulses, p = 0.032; 3 pulses, p = 0.092; 4 pulses, p = 0.051; 5 pulses, p = 0.772; 6 pulses, p = 0.512; 7 pulses, p = 0.190). Linear fits were calculated for each cell individually and the obtained slopes were tested to differ significantly from 0 (t-test, α = 0.05). Yellow line indicates the average of the fits for all cells.

might also affect T cell spiking in an activity dependent manner. Additionally, we assumed that the kinetics of the slow K^+ channels were only voltage dependent. However, the activity of M-type K^+ channels was reported to be affected also by the intracellular concentration of ATP (Simmons and Schneider, 1998). Since ATP is consumed through Na^+/K^+-pump cycles, this additional mechanism could further modulate the spike rate adaptation.

One important discrepancy between our model and the experimentally measured neuronal response was the difference in spike amplitudes. This difference might imply that the spike initiation site of the real T cell, responding to somatic stimulation, is not located exactly in the cell body. The recorded somatic spikes may only reflect the propagated action potentials that are generated elsewhere. Non-uniform distribution of ion channels in the T cell was found in previous studies: for example, T cells do have calcium-dependent K^+ channels (Kleinhaus and Angstadt, 1995) while their cell bodies largely lack voltage-dependent calcium channels (Valkanov and Boev, 1988; Johansen, 1991). To replicate the observed membrane potential changes, we had to adopt different factors (κ_{chan} and κ_{pump} in **Table 2**) that convert Na^+ channel currents and Na^+/K^+-pump currents into the intracellular Na^+ concentration; the difference between the two conversion factors possibly implies that these current sources may exist in different locations. In addition, recorded spike heights did not decrease over trials (**Figure 2A**), making contrast to the naive expectation that the increased intracellular Na^+ concentration should lead to the decrease of the sodium reversal potential. Overall, these observations support the hypothesis that somatic spikes of the T cell may actually be generated not directly within the cell body but somewhere nearby in the cell processes.

In order to experimentally confirm the role of Na^+/K^+-pumps and M-type K^+ channels in the change of IR and the spike rate

adaptation of T cells, their pharmacological blockade would be necessary. Such an experiment might not be straightforward, because, in leech neurons, conventional blockers do not always suppress ionic currents as expected (Johansen and Kleinhaus, 1986). Furthermore, leech neurons are packed in segmental ganglia, where the extracellular space is limited. To better simulate the effect of limited resources, a model would need to consider both intracellular and extracellular ionic concentrations (Hübel and Dahlem, 2014). To theoretically investigate the possible roles of spatially distributed ion channels and pumps in neuronal information processing, multicompartment models would be required (Cataldo et al., 2005; Kretzberg et al., 2007). In the present study, however, we did not aim to create a multicompartment model for several reasons. First, the main focus of our modeling was to investigate the activity-dependent long-term activity change of T cells induced by repetitive somatic current injection. Second there is almost no information available on the spatial distribution of ion channel over the T cell membrane that can be used for creating a multicompartment model. Third, we have no data recorded from the dendritic processes of T cells, which are essential for testing the simulated initiation and conduction of peripherally induced spikes.

T Cell Function and Interaction in the Network

Leeches respond to identical stimulation with multiple distinct reactions, which inspired the discussion of behavioral choice in the leech (Kristan et al., 2005; Baljon and Wagenaar, 2015). These behavioral alternatives are triggered by different patterns in neuronal activity. Due to the small number of neurons, multifunctional cells play a particular role in shaping these patterns (Kristan et al., 2005; Briggman and Kristan, 2006; Frady et al., 2016). We assume that T cells are such multifunctional players in a network that controls the response to a light touch on the leech's skin. The activated segment produces shortening on the stimulated and lengthening on the opposite side of the body wall (Kristan, 1982; Kristan et al., 1982). This local bend response is one of the fastest behaviors of the leech, with muscle movements starting only 200 ms after stimulus onset (Kristan et al., 2005). T cells respond very fast to tactile stimulation and give input to several local bend interneurons before P cell neuron spikes arrive at the central ganglion (Kretzberg et al., 2016). However, T cells are not capable of eliciting a behavior on their own (Kristan, 1982; Fathiazar et al., 2018). We assume that they activate with their very fast responses a modulatory network that regulates the gain of behaviors. Frady et al. (2016) have identified such a "preparatory network" of neurons that starts to react with a very short latency prior to the production of multiple behaviors, including local bending and whole-body shortening. After repeated stimulation causing non-synaptic plasticity, the enhanced activity might enable the T cells to transfer the animal into a state that prepares the muscles for a rapid start of a behavioral response by shifting the threshold for firing action potentials.

T cells form synaptic connections with each other that have both an electrical and a chemical component (Nicholls and Baylor, 1968b; Li and Burrell, 2008). Electrical synapses have shorter latencies compared to chemical synapses (Nicholls and Purves, 1970), and such fast-acting synaptic inputs could facilitate rapid transmission of sensory information to the preparatory network. Our experiments revealed that the increase in SC by non-synaptic plasticity also increases the PR in other T cells, which may include postsynaptic spiking. These postsynaptic changes appear to be a mere reflection of the activity-dependent changes in the presynaptic T cell. This finding might be an alternative interpretation to the conclusion of previous studies that the Na^+/K^+-pump is involved in activity-dependent synaptic plasticity between two ipsilateral T neurons (Catarsi and Brunelli, 1991; Catarsi et al., 1993; Scuri et al., 2002, 2007; Lombardo et al., 2004). Additionally, T cells have a strong synaptic connection to the S cell, a prominent element of the preparatory network (Burrell and Sahley, 2004). Each ganglion contains a single unpaired S cell, which forms strong electrical connections to the S cells in adjacent ganglia (Sahley et al., 1994). This network is reminiscent of a fast-conducting system (Mistick, 1978), but its causal role in any behavior is unclear (Sahley et al., 1994). To determine more neurons and their interactions involved in this preparatory network, VSD imaging with a double-sided-microscope would be an appropriate method (Tomina and Wagenaar, 2018). It would allow us to directly analyze functional relationships between neurons located on opposite surfaces and detect both action potentials and sub-threshold excitatory and inhibitory synaptic potentials (Miller et al., 2012).

In many vertebrate neurons, spikes are generated in the axon hillock, the part of the cell body that connects to the axon (Clarac and Cattaert, 1999). However, many invertebrate neurons are unipolar, meaning that dendrites and the axon are not clearly separated, but form a continuum of processes (Rolls and Jegla, 2015). Leech T cells send several long-range touch-sensitive dendritic processes to their receptive fields in the skin several millimeters away (Nicholls and Baylor, 1968b). Additionally, they arborize centrally to also reach the skin via both adjacent ganglia, leading to an even more extended receptive field (Yau, 1976). When the skin is touched lightly, T cells respond to the rate of skin indentation generating transient, rapidly adapting responses at stimulus onset and offset (Carlton and McVean, 1995; Kretzberg et al., 2016; Pirschel and Kretzberg, 2016; Pirschel et al., 2018). The action potentials are generated in the periphery and propagate through the ipsilateral nerve roots toward the soma. Moreover, spikes induced by central synaptic input can also travel in the opposite direction toward the periphery (Yau, 1976). Burgin and Szczupak (2003) and Kretzberg et al. (2007) suggested that leech T neurons may have at least two spike initiation zones with the different computational tasks of encoding touch stimuli in the periphery and processing synaptic inputs in the central ganglion. A similar anatomy was found in the LG motor neuron of the stomatogastric nervous system of the crab. It has a large soma with a nearby spike initiation zone and projects via dendritic processes to the periphery, where it also can initiate spikes up to 2 cm away from the soma (Meyrand et al., 1992).

In addition to the mutual T cell connections, the central part of the T cells receives polysynaptic inputs from the

other mechanoreceptors, the P and N cells. The postsynaptic potentials induced by these mechanoreceptor inputs can be excitatory, inhibitory, or a combination of both, indicating two interneuron pathways between the other mechanoreceptors and the T cells (Burgin and Szczupak, 2003). Hence, Na^+/K^+-pump activation in the context of non-synaptic plasticity probably shifts the membrane potential relative to the reversal potentials of these synapses, which could lead to an increase of the excitatory and a decrease of the inhibitory components of these postsynaptic potentials. In consequence, two complementary mechanisms following repeated T cell stimulation could increase the probability for centrally elicited spike reactions to synaptic inputs from the other mechanoreceptors: The hyperpolarization could increase excitatory postsynaptic potential size and at the same time deactivate a slow K^+-current, leading to an increase in SC. Therefore, the activity-dependent non-synaptic plasticity we described in this study could act like a gain mechanism. It could serve the purpose of tuning the T cells – and maybe in consequence also postsynaptic cells in the preparatory network – in an activity-dependent way to the combination of two computational tasks. Depending on the previous activity, T cells could react more or less to the inputs from the other mechanorecepors, and combine these synaptic responses with the spikes that encode light skin stimulation, which are elicited by T cell processes in the periphery.

Outlook

The local bend, one of the fastest movements in the leech, is initiated by sensory stimulation of the body wall. The morphology and response properties of the mechanosensory touch (T) cells suggest that T cells have at least two spike initiation zones, one in the periphery and one in the central ganglion. While spikes generated in the periphery should faithfully represent mechanical skin stimulation, the central part of the T cell should integrate and react to synaptic inputs from all three mechanoreceptor types. The activity-dependent non-synaptic plasticity introduced in this study could serve as a mechanism to tune the interaction of both spike initiation zones and their computational tasks. To test this hypothesis, further experiments are necessary to study to which extend repeated skin stimulation also triggers non-synaptic plasticity and how both spike initiation zones interact in these situations. If our hypothesis is correct, this multi-tasking ability and its activity-dependent tuning could make the T cell a key player in a fast-conducting preparatory network that regulates the gain of behaviors. The leech nervous system allows to study such network effects by further voltage-sensitive dye imaging of the ganglion during repeated skin stimulation and/or current injection to the T cell soma (Kretzberg et al., 2016; Fathiazar et al., 2018). Hence, despite the small number of neurons, the leech tactile system might be suitable for studies on general mechanisms underlying the flexibility of neural activity and behavior. As mechanoreceptors of leeches and humans share several fundamental properties (Baca et al., 2005; Pirschel and Kretzberg, 2016), our results might inspire studies in the field of prosthetics and artificial skins (Kim et al., 2014).

DATA AVAILABILITY STATEMENT

The datasets generated for this study are available on request to the corresponding author.

AUTHOR CONTRIBUTIONS

JK and SM planned the study and designed the figures. SM performed the experiments, analyzed the data, and drafted the text. GA did the neuron modeling. All authors contributed to writing the manuscript and interpreting the results.

FUNDING

This work was supported by the Deutsche Forschungsgemeinschaft (DFG, German Research Foundation) under Germany's Excellence Strategy EXC 2177/1 (Project ID 390895286).

ACKNOWLEDGMENTS

We thank Birte Groos for fitting the properties of the single T cell spike within the neuron model and all members of the computational neuroscience division for critically reading the manuscript. We also thank Christiane Thiel, Karin Dedek, and Gerrit Hilgen for commenting the manuscript and Tina Gothner for literally fruitful discussions.

REFERENCES

Baca, S. M., Thomson, E. E., and Kristan, W. B. (2005). Location and intensity discrimination in the leech local bend response quantified using optic flow and principal components analysis. *J. Neurophysiol.* 93, 3560–3572. doi: 10.1152/jn.01263.2004

Baljon, P. L., and Wagenaar, D. A. (2015). Responses to conflicting stimuli in a simple stimulus-response pathway. *J. Neurosci.* 35, 2398–2406. doi: 10.1523/jneurosci.3823-14.2015

Barreto, E., and Cressman, J. R. (2011). Ion concentration dynamics as a mechanism for neuronal bursting. *J. Biol. Phys.* 37, 361–373. doi: 10.1007/s10867-010-9212-9216

Baylor, D. A., and Nicholls, J. G. (1969a). After−effects of nerve impulses on signalling in the central nervous system of the leech. *J. Physiol.* 203, 571–589. doi: 10.1113/jphysiol.1969.sp008880

Baylor, D. A., and Nicholls, J. G. (1969b). Chemical and electrical synaptic connexions between cutaneous mechnoreceptor neurones in the central nervous system of the leech. *J. Physiol.* 203, 591–609. doi: 10.1113/jphysiol.1969.sp008881

Benda, J., and Herz, A. V. M. (2003). A universal model for spike-frequency adaptation. *Neural. Comput.* 15, 2523–2564. doi: 10.1162/089976603322385063

Blackshaw, S. E. (1981). Morphology and distribution of touch cell terminals in the skin of the leech. *J. Physiol.* 320, 219–228. doi: 10.1113/jphysiol.1981.sp013945

Briggman, K. L., and Kristan, W. B. Jr. (2006). Imaging dedicated and multifunctional neural circuits generating distinct behaviors.

J. Neurosci. 26, 10925–10933. doi: 10.1523/jneurosci.3265-06.2006

Burgin, A. M., and Szczupak, L. (2003). Network interactions among sensory neurons in the leech. *J. Comp. Physiol. A* 189, 59–67. doi: 10.1007/s00359-002-0377-378

Burrell, B. D., and Sahley, C. L. (2004). Multiple forms of long-term potentiation and long-term depression converge on a single interneuron in the leech CNS. *J. Neurosci.* 24, 4011–4019. doi: 10.1523/JNEUROSCI.0178-04.2004

Calabrese, R. L. (1980). Control of multiple impulse-initiation sites in a leech interneuron. *J. Neurophysiol.* 44, 878–896. doi: 10.1152/jn.1980.44.5.878

Carlton, T., and McVean, A. (1995). The role of touch, pressure and nociceptive mechanoreceptors of the leech in unrestrained behaviour. *J. Comp. Physiol. A* 177, 781–791. doi: 10.1007/BF00187637

Cataldo, E., Brunelli, M., Byrne, J. H., Av-Ron, E., Cai, Y., and Baxter, D. A. (2005). Computational model of touch sensory cells (T cells) of the leech: role of the afterhyperpolarization (AHP) in activity-dependent conduction failure. *J. Comput. Neurosci.* 18, 5–24. doi: 10.1007/s10827-005-5477-5473

Catarsi, S., and Brunelli, M. (1991). Serotonin depresses the after-hyperpolarization through the inhibition of the Na+/K+ electrogenic pump in T sensory neurones of the leech. *J. Exp. Biol.* 155, 261–273.

Catarsi, S., Scuri, R., and Brunelli, M. (1993). Cyclic AMP mediates inhibition of the Na+-K+ electrogenic pump by serotonin in tactile sensory neurones of the leech. *J. Physiol.* 462, 229–242. doi: 10.1113/jphysiol.1993.sp019552

Clarac, F., and Cattaert, D. (1999). Functional multimodality of axonal tree in invertebrate neurons. *J. Physiol.* 93, 319–327. doi: 10.1016/S0928-4257(00)80060-80061

Deitmer, J. W., and Schlue, W. R. (1983). Intracellular Na+ and Ca2+ in leech Retzius neurones during inhibition of the Na+-K+ pump. *Pflügers Arch. Eur. J. Physiol.* 397, 195–201. doi: 10.1007/BF00584357

Duménieu, M., Fourcaud-Trocmé, N., Garcia, S., and Kuczewski, N. (2015). Afterhyperpolarization (AHP) regulates the frequency and timing of action potentials in the mitral cells of the olfactory bulb: role of olfactory experience. *Physiol. Rep.* 3:e12344. doi: 10.14814/phy2.12344

Fathiazar, E., Hilgen, G., and Kretzberg, J. (2018). Higher network activity induced by tactile compared to electrical stimulation of leech mechanoreceptors. *Front. Physiol.* 9:173. doi: 10.3389/fphys.2018.00173

Forrest, M. D. (2014). The sodium-potassium pump is an information processing element in brain computation. *Front. Physiol.* 5:472. doi: 10.3389/fphys.2014.00472

Frady, E. P., Kapoor, A., Horvitz, E., and Kristan, W. B. Jr. (2016). Scalable semisupervised functional neurocartography reveals canonical neurons in behavioral networks. *Neural. Comput.* 218, 1453–1497. doi: 10.1162/NECO_a_00852

Gerard, E., Hochstrate, P., Dierkes, P.-W., and Coulon, P. (2012). Functional properties and cell type specific distribution of I(h) channels in leech neurons. *J. Exp. Biol.* 215, 227–238. doi: 10.1242/jeb.062836

Goldman, M. S., Golowasch, J., Marder, E., and Abbott, L. F. (2001). Global structure, robustness, and modulation of neuronal models. *J. Neurosci.* 21, 5229–5238. doi: 10.1523/JNEUROSCI.21-14-05229.2001

Gulledge, A. T., Dasari, S., Onoue, K., Stephens, E. K., Hasse, J. M., and Avesar, D. (2013). A sodium-pump-mediated afterhyperpolarization in pyramidal neurons. *J. Neurosci.* 33, 13025–13041. doi: 10.1523/JNEUROSCI.0220-13.2013

Hakizimana, P., Brownell, W. E., Jacob, S., and Fridberger, A. (2012). Sound-induced length changes in outer hair cell stereocilia. *Nat. Commun.* 3:1094. doi: 10.1038/ncomms2100

Hodgkin, A. L., and Katz, B. (1949). The effect of sodium ions on the electrical activity of the giant axon of the squid. *J. Physiol.* 108, 37–77. doi: 10.1113/jphysiol.1949.sp004310

Hübel, N., and Dahlem, M. A. (2014). Dynamics from seconds to hours in Hodgkin-Huxley model with time-dependent ion concentrations and buffer reservoirs. *PLoS Comput. Biol.* 4:e1003941. doi: 10.1371/journal.pcbi.1003941

Jansen, J. K. S., and Nicholls, J. G. (1973). Conductance changes, an electrogenic pump and the hyperpolarization of leech neurones following impulses. *J. Physiol.* 229, 635–655. doi: 10.1113/jphysiol.1973.sp010158

Johansen, J. (1991). Ion conductances in identified leech neurons. *Comp. Biochem. Physiol. Part A Physiol.* 100, 33–40. doi: 10.1016/0300-9629(91)90180-K

Johansen, J., and Kleinhaus, A. (1986). Differential sensitivity of tetrodotoxin of nociceptive neurons in 4 species of leeches. *J. Neurosci.* 6, 3499–3504. doi: 10.1523/jneurosci.06-12-03499.1986

Johnson, K. O. (2001). The roles and functions of cutaneous mechanoreceptors. *Curr. Opin. Neurobiol.* 11, 455–461. doi: 10.1016/S0959-4388(00)00234-238

Kim, J., Lee, M., Shim, H. J., Ghaffari, R., Cho, H. R., Son, D., et al. (2014). Stretchable silicon nanoribbon electronics for skin prosthesis. *Nat. Commun.* 5:5747. doi: 10.1038/ncomms6747

Klees, G., Hochstrate, P., and Dierkes, P. W. (2005). Sodium-dependent potassium channels in leech P neurons. *J. Membr. Biol.* 208, 27–38. doi: 10.1007/s00232-005-0816-x

Kleinhaus, A. L., and Angstadt, J. D. (1995). Diversity and modulation of ionic conductances in leech neurons. *J. Neurobiol.* 27, 419–433. doi: 10.1002/neu.480270313

Kretzberg, J., Kretschmer, F., and Marin-Burgin, A. (2007). Effects of multiple spike-initiation zones in touch sensory cells of the leech. *Neurocomputing* 70, 1645–1651. doi: 10.1016/j.neucom.2006.10.048

Kretzberg, J., Pirschel, F., Fathiazar, E., and Hilgen, G. (2016). Encoding of tactile stimuli by mechanoreceptors and interneurons of the medicinal leech. *Front. Physiol.* 7:506. doi: 10.3389/fphys.2016.00506

Kristan, W. B., Calabrese, R. L., and Friesen, W. O. (2005). Neuronal control of leech behavior. *Prog. Neurobiol.* 76, 279–327. doi: 10.1016/j.pneurobio.2005.09.004

Kristan, W. B., McGirr, S. J., and Simpson, G. V. (1982). Behavioural and mechanosensory neurone responses to skin stimulation in leeches. *J. Exp. Biol.* 96, 143–160.

Kristan, W. B. J. (1982). Sensory and motor neurones responsible for the local bending response in leeches. *J. Exp. Biol.* 96, 161–180.

Larsson, H. P. (2013). What determines the kinetics of the slow afterhyperpolarization (sAHP) in neurons? *Biophys. J.* 104, 281–283. doi: 10.1016/j.bpj.2012.11.3832

Li, Q., and Burrell, B. D. (2008). CNQX and AMPA inhibit electrical synaptic transmission: a potential interaction between electrical and glutamatergic synapses. *Brain Res.* 1228, 43–57. doi: 10.1016/j.brainres.2008.06.035

Li, Q., and Burrell, B. D. (2009). Two forms of long-term depression in a polysynaptic pathway in the leech CNS: one NMDA receptor-dependent and the other cannabinoid-dependent. *J. Comp. Physiol. A* 195, 831–841. doi: 10.1007/s00359-009-0462-463

Li, Q., and Burrell, B. D. (2010). Properties of cannabinoid-dependent long-term depression in the leech. *J. Comp. Physiol. A* 196, 841–851. doi: 10.1007/s00359-010-0566-569

Lombardo, P., Scuri, R., Cataldo, E., Calvani, M., Nicolai, R., Mosconi, L., et al. (2004). Acetyl-L-carnitine induces a sustained potentiation of the afterhyperpolarization. *Neuroscience* 128, 293–303. doi: 10.1016/j.neuroscience.2004.06.028

Meyrand, P., Weimann, J., and Marder, E. (1992). Multiple axonal spike initiation zones in a motor neuron: serotonin activation. *J. Neurosci.* 12, 2803–2812. doi: 10.1523/JNEUROSCI.12-07-02803.1992

Miller, E. W., Lin, J. Y., Frady, E. P., Steinbach, P. A., Kristan, W. B., and Tsien, R. Y. (2012). Optically monitoring voltage in neurons by photo-induced electron transfer through molecular wires. *Proc. Natl. Acad. Sci. U.S.A.* 109, 2114–2119. doi: 10.1073/pnas.1120694109

Mistick, D. C. (1978). Neurones in the leech that facilitate an avoidance behaviour following nearfield water disturbances. *J. Exp. Biol.* 75, 1–23.

Muller, K. J., and Scott, S. A. (1981). Transmission at a 'direct' electrical connexion mediated by an interneurone in the leech. *J. Physiol.* 311, 565–583. doi: 10.1113/jphysiol.1981.sp013605

Nicholls, J. G., and Baylor, D. A. (1968a). Long-lasting hyperpolarization after activity of neurons in leech central nervous system. *Science* 162, 279–281. doi: 10.1126/science.162.3850.279-a

Nicholls, J. G., and Baylor, D. A. (1968b). Specific modalities and receptive fields of sensory neurons in CNS of the leech. *J. Neurophysiol.* 31, 740–756. doi: 10.1152/jn.1968.31.5.740

Nicholls, J. G., and Purves, D. (1970). Monosynaptic chemical and electrical connexions between sensory and motor cells in the central nervous system of the leech. *J. Physiol.* 209, 647–667. doi: 10.1113/jphysiol.1970.sp009184

Pinsker, H., and Kandel, E. R. (1969). Synaptic activation of an electrogenic sodium pump. *Science* 163, 931–935. doi: 10.1126/science.163.3870.931

Pirschel, F., Hilgen, G., and Kretzberg, J. (2018). Effects of touch location and intensity on interneurons of the leech local bend network. *Sci. Rep.* 8, 1–11. doi: 10.1038/s41598-018-21272-21276

Pirschel, F., and Kretzberg, J. (2016). Multiplexed population coding of stimulus properties by leech mechanosensory cells. *J. Neurosci.* 36, 3636–3647. doi: 10.1523/JNEUROSCI.1753-15.2016

Rolls, M. M., and Jegla, T. J. (2015). Neuronal polarity: an evolutionary perspective. *J. Exp. Biol.* 218, 572–580. doi: 10.1242/jeb.112359

Sahley, C. L., Modney, B. K., Boulis, N. M., and Muller, K. J. (1994). The S cell: an interneuron essential for sensitization and full dishabituation of leech shortening. *J. Neurosci.* 14, 6715–6721. doi: 10.1523/jneurosci.14-11-06715.1994

Scuri, R., Lombardo, P., Cataldo, E., Ristori, C., and Brunelli, M. (2007). Inhibition of Na+/K+ATPase potentiates synaptic transmission in tactile sensory neurons of the leech. *Eur. J. Neurosci.* 25, 159–167. doi: 10.1111/j.1460-9568.2006.05257.x

Scuri, R., Mozzachiodi, R., and Brunelli, M. (2002). Activity-dependent increase of the AHP amplitude in T sensory neurons of the leech. *J. Neurophysiol.* 88, 2490–2500. doi: 10.1152/jn.01027.2001

Simmons, M. A., and Schneider, C. R. (1998). Regulation of M-Type potassium current by intracellular nucleotide phosphates. *J. Neurosci.* 18, 6254–6260.

Smith, E. S. J., and Lewin, G. R. (2009). Nociceptors: a phylogenetic view. *J. Comp. Physiol. A. Neuroethol. Sens. Neural. Behav. Physiol.* 195, 1089–1106. doi: 10.1007/s00359-009-0482-z

Thomson, E. E., and Kristan, W. B. (2006). Encoding and decoding touch location in the leech CNS. *J. Neurosci.* 26, 8009–8016. doi: 10.1523/JNEUROSCI.5472-05.2006

Tomina, Y., and Wagenaar, D. A. (2018). Dual-sided voltage-sensitive dye imaging of leech ganglia. *Bio protocol* 8:e2751. doi: 10.21769/BioProtoc.2751

Valkanov, M., and Boev, K. (1988). Ionic currents in the somatic membrane of identified T-mechanosensory neurons isolated from segmental ganglia of the medicinal leech. *Gen. Physiol. Biophys.* 7, 643–649.

Vogalis, F., Storm, J. F., and Lancaster, B. (2003). SK channels and the varieties of slow after-hyperpolarizations in neurons. *Eur. J. Neurosci.* 18, 3155–3166. doi: 10.1111/j.1460-9568.2003.03040.x

Wagenaar, D. A. (2015). A classic model animal in the 21st century: recent lessons from the leech nervous system. *J. Exp. Biol.* 218, 3353–3359. doi: 10.1242/jeb.113860

Wyse, A. T., Bavaresco, C. S., Reis, E. A., Zugno, A. I., Tagliari, B., Calcagnotto, T., et al. (2004). Training in inhibitory avoidance causes a reduction of Na+,K+-ATPase activity in rat hippocampus. *Physiol. Behav.* 80, 475–479. doi: 10.1016/J.PHYSBEH.2003.10.002

Yamada, W., Koch, C., and Adams, P. (1998). "Multiple channels and calcium dynamics," in *Methods in Neuronal Modeling: From Ions to Networks*, 2nd Edn, eds C. Koch, and I. Segev, (Cambridge, MA: MIT Press).

Yau, K. W. (1976). Receptive fields, geometry and conduction block of sensory neurones in the central nervous system of the leech. *J. Physiol.* 263, 513–538. doi: 10.1113/jphysiol.1976.sp011643

Conflict of Interest: The authors declare that the research was conducted in the absence of any commercial or financial relationships that could be construed as a potential conflict of interest.

frontiers in Physiology

REVIEW
published: 27 November 2019
doi: 10.3389/fphys.2019.01428

Odor Stimuli: Not Just Chemical Identity

Mario Pannunzi and Thomas Nowotny*

University of Sussex, Brighton, United Kingdom

In most sensory modalities the underlying physical phenomena are well understood, and stimulus properties can be precisely controlled. In olfaction, the situation is different. The presence of specific chemical compounds in the air (or water) is the root cause for perceived odors, but it remains unknown what organizing principles, equivalent to wavelength for light, determine the dimensions of odor space. Equally important, but less in the spotlight, odor stimuli are also complex with respect to their physical properties, including concentration and time-varying spatio-temporal distribution. We still lack a complete understanding or control over these properties, in either experiments or theory. In this review, we will concentrate on two important aspects of the physical properties of odor stimuli beyond the chemical identity of the odorants: (1) The amplitude of odor stimuli and their temporal dynamics. (2) The spatio-temporal structure of odor plumes in a natural environment. Concerning these issues, we ask the following questions: (1) Given any particular experimental protocol for odor stimulation, do we have a realistic estimate of the odorant concentration in the air, and at the olfactory receptor neurons? Can we control, or at least know, the dynamics of odorant concentration at olfactory receptor neurons? (2) What do we know of the spatio-temporal structure of odor stimuli in a natural environment both from a theoretical and experimental perspective? And how does this change if we consider mixtures of odorants? For both topics, we will briefly summarize the underlying principles of physics and review the experimental and theoretical Neuroscience literature, focusing on the aspects that are relevant to animals' physiology and behavior. We hope that by bringing the physical principles behind odor plume landscapes to the fore we can contribute to promoting a new generation of experiments and models.

Keywords: olfaction, odor stimuli, physics, chemistry, insect navigation, fluidodynamic

OPEN ACCESS

Edited by:
Philippe Lucas,
Institut National de la Recherche Agronomique (INRA), France

Reviewed by:
Hong Lei,
Arizona State University, United States
Shannon Bryn Olsson,
National Centre for Biological Sciences, India

****Correspondence:***
Mario Pannunzi
mario.pannunzi@gmail.com

Specialty section:
This article was submitted to Invertebrate Physiology, a section of the journal Frontiers in Physiology

Received: *19 August 2019*
Accepted: *04 November 2019*
Published: *27 November 2019*

Citation:
Pannunzi M and Nowotny T (2019) Odor Stimuli: Not Just Chemical Identity. Front. Physiol. 10:1428. doi: 10.3389/fphys.2019.01428

INTRODUCTION

Olfaction, the Complex Sense

Animals use their olfactory system in almost every aspect of their life (e.g., to locate food, hosts, oviposition sites, and sexual mates, or to avoid predators). In order to properly investigate animals' olfactory systems and their odor dependent behaviors we need to adequately define and characterize the sensory input received from the environment. For example, in the auditory system, a full understanding of the Doppler effect is needed to design experiments that meaningfully test echolocation by bats (Webster and Weissburg, 2001).

In color vision, the wavelength of light is the fundamental organizing property relating to color, and responses of cones in the retina, and subsequent color perception, can be well characterized as a function of the wavelength and intensity of light. In contrast, there is no single organizing principle for the space of all possible (volatile) compounds (Turin, 2002; Zhou et al., 2018) and the structure and dimensionality of odor space is an open problem[1], to the extent that one may even wonder whether, in spite of the common element of involving the detection of chemicals, we can speak of a single sensory modality or not[2]. Furthermore, natural odors are often defined by numerous chemical compounds (odorants) (Raguso, 2008), present at a given concentration ratio, which compounds the difficulty of the problem. However, these aspects of odor space have been addressed before (for a review see, e.g., Sell, 2006; Auffarth, 2013) and we will not focus on them here.

Besides having the organizing principle of wavelength for light stimuli, we are also able to tightly control light stimuli in experiments with respect to wavelength, intensity and arrival time at sensory cells, allowing to build up deeper insights about visual perception (Hecht, 1942; Tinsley et al., 2016). Unfortunately, the same cannot be said about odor stimuli and in this review we will focus on two important aspects of the problem of *stimulus control*:

First, each odorant has different attributes in terms of its volatility (Cometto-Muñiz et al., 2003), how it distributes in the environment, adheres to surfaces, or dissolves in liquids or a carrier gas and, these attributes can change depending on environmental conditions such as temperature, pressure, humidity or even simply the characteristics of a container. When mixtures of odorants need to be considered, the complexity of the problem increases, both for the interaction between chemical components in the environment and for their interactions with receptors (see for example, Rospars et al., 2008; Wilson, 2013; Szyszka and Stierle, 2014). There are potentially serious consequences of not considering these properties. For instance, we might incorrectly assume that we can generate identical square inputs (or step stimuli) with different odorants, while in reality the concentration time course for each odorant is different because of its physical properties (Su et al., 2011; Martelli et al., 2013). Then, we likely would wrongly attribute observed properties of the response (e.g., latency) to the transduction process while it actually was a property of the odorant. These issues become even more problematic where neural responses are not simply proportional to the instantaneous concentration, but also strongly depend on its rate of change (Kim et al., 2011, 2015; Nagel and Wilson, 2011; Wilson, 2013).

Second, odorants are part of an environment that, most of the time, is turbulent and they form highly complex odor plumes (Murlis et al., 2000). Indeed, the spatio-temporal structure of odor plumes depends on both the physical properties of the airflow and on the odorants (Moore and Crimaldi, 2004). The properties of the flow determine the characteristics of the turbulence, while the properties of the odorants determine the interaction between diffusive and advective motion. The distribution of odorant concentration in space, with its valleys, crests, and plateaus, is commonly described as "odor-landscape" (Atema, 1996; Moore and Crimaldi, 2004; Celani et al., 2014). The matter, though incredible complex, does not lack beauty revealed through technologies that allow for ever better visualizations (see Van Dyke, 1982; Samimy et al., 2004).

A good knowledge of it is also indispensable to understand the plume exploration of insects (Murlis et al., 1992, 2000; Justus et al., 2002; Vickers, 2006). Only if we know what information (e.g., concentration, intermittency, variance of the concentration) is available to the insect at any given location in the plume, we might identify the potential mechanisms driving plume navigation. For instance, the details of surge and cast behaviors will depend on the statistics of odor filaments and suggested mechanisms for odor source separation (Baker et al., 1998; Sehdev and Szyszka, 2019) and can only be understood based on how correlations between odor plumes change depending on the separation between odor sources (Erskine, 2018).

The review was originally motivated by our work on formulating mathematical models of odorant receptors and the function of the early olfactory system in insects (Nowotny et al., 2013; Chan et al., 2018). Accordingly, we mainly focus on properties and situations that are relevant to insects and odor stimuli in air. We aim to raise awareness about the most urgent deficiencies in our knowledge and promote new thinking about how to design future models and experiments.

The organization of the review reflects the increasing difficulties of the discussed aspects of odor stimuli. In the first section, we will describe the difficulties in achieving a realistic estimate of odorant concentration and its time course "inside the lab." In the second section, we will discuss the spatio-temporal structure of odorant plumes "outside the lab" up to the point of describing simple situations where mixtures of odorants are present. Each section will start with a summary of the related physical principles, followed by the review of the relevant Neuroscience literature. We will end with a brief general discussion.

THE AMPLITUDE AND DYNAMICS OF ODOR STIMULI IN THE LAB

> "A philosopher once said, 'It is necessary for the very existence of science that the same conditions always produce the same results'. Well, they do not."
>
> **R. P. Feynman**, *Lectures on Physics*, 1963

The Physics of Dilution

R. Feynman was alluding to the lack of determinism of individual experiments in quantum physics, while reminding his audience of the need for reproducibility in science: Empirical experiments rest on the ability to characterize and generate controlled conditions in which to investigate a system of interest. In olfaction research, this translates to

[1]The debate about the dimensionality of olfaction: Bushdid et al., 2014; Gerkin and Castro, 2015; Meister, 2015).

[2]The proposal of separating olfaction in multiple senses is not so absurd: magnetoception is distinguished from vision, and hygroreception is already separated from olfaction.

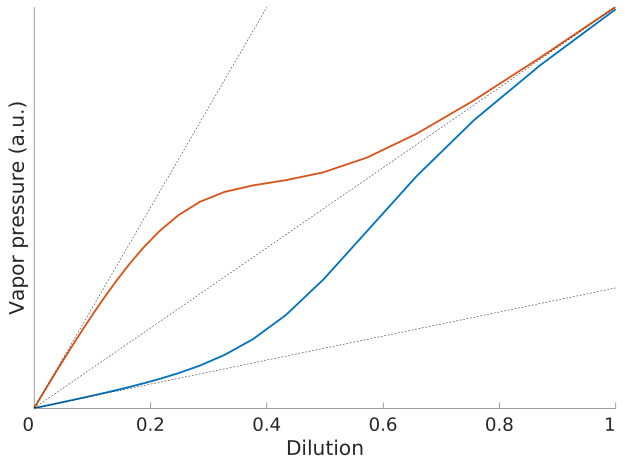

FIGURE 1 | Illustration of Henry's and Raoult's laws. Both $k_H > p^*$ (red line) and $k_H < p^*$ (blue line) can be observed for different substances.

characterizing and generating defined odor stimuli. In essence, an olfactory stimulus is the presence of odorant molecules in the ambient medium (air, water) and is characterized by the identity and concentration of odor molecules at any given spatial location over time. The identity of odorants is easy to control in a laboratory setting (see, however, Andersson et al., 2012), but controlling the concentration is a much harder problem.

One common method for generating a controlled odor stimulus is the following: For each odorant, a preset amount of the pure odorant is placed into a container, usually a pipette. Odor stimuli are then delivered by injecting a preset fraction of the odor-laden air from the pipette into a stream of clean air for a preset stimulus duration. To use an odorant at a given concentration in air, experimenters dilute the odorant in a non-volatile solvent, i.e., paraffin oil (sometimes this solution is then applied to a piece of filter paper ∼1 cm^2). The odorant will evaporate and fill the headspace of the pipette. While the variable of interest clearly is the concentration in air[3], we only know the dilution of the original solution and it would therefore be useful to know the relationship between the dilution of the odorant in the solvent and the resulting odorant concentration in the air. When a compound (the solute) is dissolved in a liquid (solvent), a part of the compound evaporates. The amount of compound that evaporates depends on several factors, including the identity of the solute (odorant we are interested in) and the solvent, temperature, pressure, and the ratio between solvent and solute. Moreover, in the case of Pasteur pipettes and filter paper, even the interaction with the filter paper, the glass of the pipette and the air (in particular its humidity) affect the amount of evaporated compound.

Without going into the details of the mechanisms governing gases dissolved in liquids here, we will focus only on the phenomenology of how the odorant concentration in the headspace of a solution relates to the dilution of the odorant in the solution. This relationship is generally described in terms of three regimes (see **Figure 1**): Henry's regime (very low amounts of odorant), the intermediate regime and Raoult's regime (very large amounts of odorant) (Gaskell, 2003). The odorant concentration/dilution relationship is monotonic in the three regimes, but it is linear only in Henry's and Raoult's regimes and the respective proportionality factors are different, Henry's constant k_H for Henry's regime and the vapor pressure of the pure odorant, p^*, for Raoult's regime (see **Box 1** and **Figure 1**).

The vapor pressure p^* is a single value for each substance and is reported widely in chemistry databases[4]. However, the

[3]If we are interested in the receptor response, the variable of interest if the concentration, but of course, if we consider the system as a whole – odor-source plus animal – the variable of interest could also be the dilution.

[4]See for example https://pubchem.ncbi.nlm.nih.gov or http://www.chemspider.com/.

BOX 1 | Volatility, dilution, and concentration.

Volatility

Volatility, in chemistry, is the tendency of a substance to vaporize. The volatility of a substance depends on many factors, e.g., temperature, pressure, other substances within the same solution, etc. Volatility itself lacks unique quantitative descriptors, but "vapor pressure" and "normal boiling point" are commonly used as proxies for volatility:

If we put a liquid in a closed container, and wait long enough to obtain a (thermodynamic) equilibrium, then a part of the liquid will have evaporated. The resulting pressure in the closed container is the **vapor pressure** of this substance at the current temperature. Being another gas present, the substance partial pressure will coincide with its vapor pressure. If we add energy to the system – for example by increasing the temperature – the vapor pressure will increase (in a non-linear fashion following the Clausius-Clapeyron equation).

A volatile substance has a very high vapor pressure at "room temperature" (around 20°C). The temperature at which the vapor pressure of a substance is equal to the ambient atmospheric pressure is defined as its "**normal boiling point**." Vapor pressure and "boiling point" are not independent, but roughly inversely related. Volatility correlates with a number of chemical properties, e.g., lipophilicity or hydrophobicity, i.e., a substance's tendency to interact via van de Waals forces. Ultimately, at a microscopic level, the mechanisms that determine volatility are molecular mass and the quantum mechanical interactions between molecules.

Henry's law and Raoult's law

Henry's law and Raoult's law are empirical relationships between the dilution of a volatile in solution and the partial pressure p of the volatile in the head space above the solution. Using mole fractions, x, as the expression of dilution, Henry's law can be written as: $p = x\,k_H$, where k_H is Henry's constant. This can be compared with Raoult's law: $p = x\,p^*$, where p^* is the vapor pressure of the pure volatile. More precisely, both laws are limit laws: Henry's law is valid for extremely diluted solutions, while Raoult's law applies at the opposite end of highly concentrated solutions. In mathematical terms:

$$\text{Henry's law:} \lim_{x \to 0} p/x = k_H$$

$$\text{Raoult's law:} \lim_{x \to 1} p/x = p^*$$

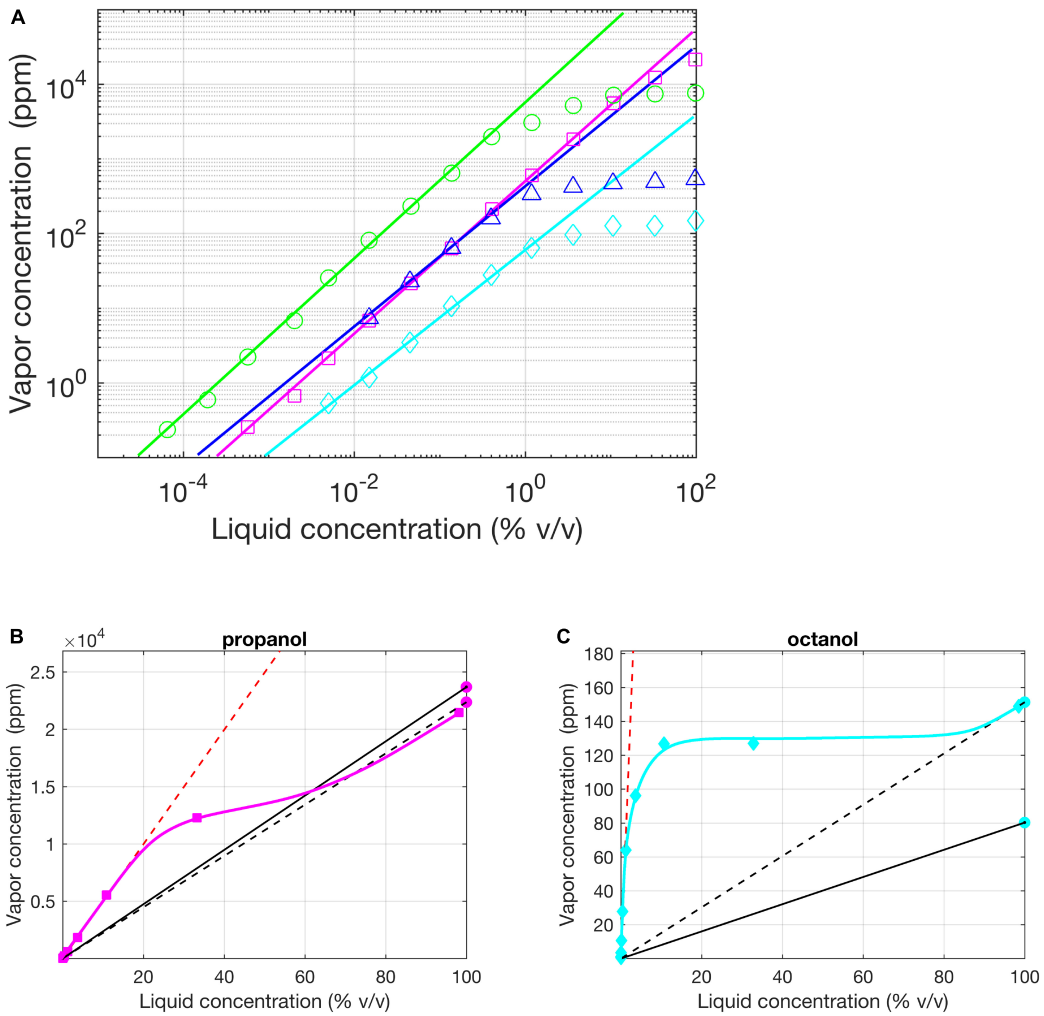

FIGURE 2 | Regimes of Henry and Raoult, experimental evidence. **(A)** Vapor (p.p.m. by volume) vs. liquid (% v/v) concentration for homologous alcohols in logarithmic coordinates (1-Butanol – red circles, 1-Propanol in H_2O – green squares, 1-Hexanol – blue triangles, 1-Octanol – cyan diamonds). Except for Propanol, the solvent was mineral oil. The solid lines indicate a fit of Henry's law to the lowest concentration values (all slope 1 in the log-log plot, indicating linear fits). **(B,C)** Same as **(A)** in a plot with linear axes for propanol in H_2O and 1-Octanol in oil. The two black lines (dashed and solid) are the fits for Raoult's law using the average values of vapor pressure reported by the UCSD (California) lab and UCL (London) lab, respectively. Red dashed line is the linear fit of the Henry's Law done with the data of Cometto-Muñiz et al. (2003) (approximating β equal 1). Modified from Cometto-Muñiz et al. (2003).

values of the vapor pressure reported by different laboratories can actually be quite disparate (see **Figure 2**). Cometto-Muñiz et al. (2003) compared the reported values of vapor pressure for 36 chemicals by a group of authors working at the University of California and a group of authors working at the University College of London; for 16 chemicals, differences between values were larger than 25%. In the same study, the authors pointed out the limit case of the *octanal* vapor pressure whose reported value in text-books spans from 0.0053 mmHg to 2.14 mmHg (Cometto-Muñiz et al., 2003).

Henry's constant depends on both the solvent and the solute and it is therefore generally more difficult to find. A valuable exception is the study of Cometto-Muñiz et al. (2003) in which the authors measured and reported k_H for several odors dissolved in mineral oil, the most commonly used solvent in olfaction research. Moreover, Cometto-Muñiz et al. also reported the extent of Henry's regime for each odorant (see some examples in **Figure 2**).

When delivering odors using liquid solutions it is necessary to establish whether Raoult's or Henry's law apply or whether the dilution falls into the transition region. Frequently, all three situations apply to different parts of the same experiment if dilutions are varied (see Table 1 in Cometto-Muñiz et al., 2003). The difference between k_H and p^* and, consequently, of the odorant concentrations estimated based on assuming either regime, can be very high (see **Table 1** for a few relevant examples). Therefore, identifying the correct regime is very important.

The investigation of the role of odorants in mixtures is a typical example where careful consideration of the relationship concentration/dilution is crucial. In this case, one would want

TABLE 1 | Example values for vapor pressure and Henry's constant in mineral oil extracted from Cometto-Muñiz et al. (2003).

	p*[mm Hg]	k_H
Ethyl acetate	94	87434
Methyl acetate	235	148568
Geraniol	0.03	1
1-hexanol	0.92	429
1-octanol	0.2	60
Butyric acid	0.43	189
Pentanoic acid	0.2	50
Hexanoic acid	0.043	6.51

to create mixtures with well-controlled concentration ratios, e.g., a mixture that contains the exact same number of molecules of each type. To do this, one needs to establish which regimes apply (it could well be different regimes for each of the odorants involved) and what the values of k_H or p^* are for each of the involved odorants. We will revisit the question of controlling concentration by dilution later on when discussing concrete examples from olfaction research in insects.

The Physics of Adsorption and Desorption of Gases on Solids

When passing through an olfactory stimulation device, volatiles will interact with the surface of the device's air ducts. Some of the odorant (adsorbate) will adhere to the surface (adsorbent) and then detach from it again under physical (i.e., van der Waals force) or chemical forces (Rabe et al., 2011). This is the phenomenon of adsorption/desorption of a gas to a solid (Shirtcliffe, 2008; Foo and Hameed, 2010). Many different models have been formulated to describe the mechanism and the dynamics of adsorption; their detailed description is beyond the scope of this review, but, thanks to a renewed interest in adsorption for environmental reasons, it can easily be found elsewhere (e.g., Foo and Hameed, 2010). In essence, the models pursue the description, at thermodynamic equilibrium, of the amount of adsorbate as a function of the relevant parameters of the system, including the partial pressure of the adsorbate, the temperature and surface area, and, of course, the chemical properties of adsorbent and adsorbate. The most common models of adsorption adopt the hypothesis of constant temperature, so-called isotherm adsorption models, and interpret the process of adsorption as minimizing the surface free energy of the combined solid/gas system. The simplest of these models (valid at very low partial pressure of the adsorbate) predicts that the fraction of adsorbed adsorbate X is a linear function of its partial pressure p, $X = H_k\ p$. The proportionality factor is called Henry's adsorption constant H_k, named for the similarity to Henry's law discussed above. The Langmuir model (Langmuir, 1932), was the first attempt of a semi-analytical model, and allowed to derive a rational function $X = H_k p/(1 + H_k p)$. For low partial pressure this law is reduced to the linear model. Some of the assumptions of this model are perfectly realized in real-life scenarios, except for the simplifying assumption used that adsorbates would form only a single layer on the surface of the solid. More recent models attempt to deal with this complexity, but they do not yet succeed in providing a complete description of the phenomenon (Foo and Hameed, 2010). For the purposes of this review, all models indicate a monotonic relationship between the partial pressure of the adsorbate and the amount of adsorbate on the surface that additionally depends on the chemical properties of the adsorbate and adsorbent. In olfaction experiments, when volatiles pass through an olfactory stimulation device, the models hence predict a dependence of the concentration flow on an odorant's partial pressure and its chemical identity, the former in turn being a function of odorant dilution with the two linear regimes (Henry's and Raoult's regime) as discussed above[5].

Application to Insect Olfaction Research

We will now proceed to review the relevance of the physics of odor delivery for designing and interpreting experiments. We will illustrate the key issues on a few typical research questions pertinent to olfaction research, for example the *relevance of different odorants* for any given insect.

Concentration of Odor Stimuli

To assess the *relevance of different odorants* for insects it is sensible to compare the physiological and behavioral responses to odorants of interest. To enable meaningful comparisons, the odor stimuli need to be of "comparable strength." However, "comparable strength" can have different meanings depending on the objective of the study. For example, if one is interested in the ecological relevance of some specific compounds for an insect, one should determine the typical concentration of the compounds in natural settings and analyze the insects' behavior with those concentration values. On the other hand, if one is interested in the general response of receptor neurons to different chemical compounds, then the choice for a fair comparison is typically to generate stimuli that deliver the same number of molecules within the same timespan to the antenna of the insect. However, as we discussed above, this quantity is not under the experimenter's direct control. In order to achieve the right concentration at the antenna, experimenters need to reverse-engineer the correct dilution using the limit laws discussed above (see section The Physics of Dilution), and, potentially, considering differences in adsorption along the odorants' path through the olfactometer (see section The Physics of Adsorption and Desorption of Gases on Solids). While this can be an arduous process, in particular if essential information about Henry's constant and the properties of adsorption for any given stimulation device are missing, we believe that it is important, because the observed relevance of an odorant will depend substantially on getting the stimulus right.

Resource constraints often mean that only a single concentration per odorant can be sampled, which makes correct stimulus design even more important. The incredible effort of DoOR, for example, where the responses of *Drosophila*

[5]Note that some materials also adsorb odorants on very long time scales and lead to long term contamination, which can be an issue in olfaction research but we will not consider it here.

olfactory receptor neurons (ORNs) to a large number of odorants are collected and normalized in order to have a "single consensus response matrix," has so far only been possible for a single concentration for each odorant (Galizia et al., 2010; Münch and Galizia, 2016). Similarly, the analysis of more than 100 odorants on 31 ORNs of Hallem and Carlson (2006) was only possible for one concentration of each odorant. Given these constraints, it would be valuable if a common process could be used to determine the correct dilutions for odorant stimulation that maximize the accuracy of comparing results. Rescaling after the fact (Galizia et al., 2010; Münch and Galizia, 2016) is a good first step but the many non-linearities in both, the physics of dilution/concentration and the early olfactory system may limit the validity of this approach.

Ideally, one would want to map the entire response profile of the insect olfactory system across different odors and different concentrations, as, for instance, pioneered in the work of Sachse et al. (1999), in which the authors performed the first systematic calcium imaging in the antennal lobe (the second phase of olfactory integration in insects) of bees with stimuli from the alcohol series (pentanol, hexanol, and so on to decanol). This allowed the systematic comparison of responses along the dimension of carbon chain length and across three different dilutions (1–10–100%). Vapor pressure decreases monotonically with carbon chain length, so that proportionately different odor concentrations would have reached the antenna of the bees for the 100% non-diluted odorants, for which Raoult's regime applies. To account for this, we can try to compensate by dividing observed responses by the vapor pressure (assuming sufficiently linear properties of the olfactory response). For higher dilutions of 10 and 1%, however, Raoult's regime is unlikely to apply (see, e.g., 1-butanol, 1-hexanol, and 1-octanol in **Figure 2**) and neither is Henry's regime, which starts somewhere beyond 1% dilution. In essence, there is no straightforward way to compensate for the unknown non-linear relationship between dilution and concentration and the interpretation of results is very difficult.

Another pertinent example where the relative concentrations of odorants are very important is the *investigation of odor mixtures*, both in the pheromone sub-system and the general olfactory system. In the pheromone sub-system, it is well-documented that females of related, but sexually incompatible, moth species may use the same substances in their pheromone blends but in different concentration ratios (see, e.g., Christensen et al., 1989; Baker, 2008) and references therein). In order to find a compatible female, male moths need to recognize the blend when encountered in the air during upwind flight (Zavada et al., 2011). Arguably, the quantity relevant to this situation is the concentration ratio as generated in the glands of the female moth, which presumably is conserved in the environment. When generating diluted versions of the blend in the lab, dilutions of the individual pheromone components would need to be adjusted so that the resulting blend in the headspace has the correct concentration ratio: Different components need to be diluted differently if their regimes and proportionality constants (k_H and p^*) differ (see **Table 1**).

These considerations also become important when considering overshadowing (e.g., Schubert et al., 2015). Overshadowing is a phenomenon where bees conditioned by pairing a mixture AB with sugar water later respond more to odor A than to odor B when the odors are presented alone. Odor A appears to overshadow odor B in the perception of the mixture. To make a fair comparison between the two odorants in the mixture, we should use dilutions for odorants A and B that are inversely proportional to their vapor pressures, if Raoult's regime applies, e.g., a dilution ratio of octanal and 2-non-anone of 0.52. However, Raoult's regime is not very wide (see **Figure 2**) so that when using dilutions of 10% or more, octanal and 2-nonanone dissolved in mineral oil are already in Henry's regime (Cometto-Muñiz et al., 2003) and their dilution ratio should be 0.62, a small but potentially significant difference. For other odorants and solvents, the difference could be much larger, depending on the values of k_H and p^*. Making the right adjustments is, however, only possible when these values are known, which is often not the case.

A possible approach to generate suitable odorant concentrations in air, albeit tedious and laborious, is to choose dilutions of odorants for experimental stimuli using the following procedure: (1) Measure the odorant concentration in the air at the antenna with a high resolution detector (see below) for different values of dilution, (2) Determine which regime the odorant solution is in for the dilution values that are relevant to the problem at hand, (3) If one of the linear regimes applies, extract the value of the relevant proportionality factor (the vapor pressure or Henry's constant), and (4) Use the odorants at a dilution that is inversely proportional to this relevant factor. Unfortunately, depending on the experimental conditions, this procedure may or may not be sufficient. One of the complications is the detector. Nowadays, the fastest detectors are those using photoionization technology, PIDs (photoionization detectors). In these detectors, a UV light source ionizes airborne molecules and the charge produced by ions is measured by the instrument. The PID measures concentrations down to low concentrations (∼few parts per billion) and a relatively high sampling rate of hundreds of Hertz (for an extensive analysis of detectors see e.g., Riffell et al., 2008). However, PIDs, like other analytical chemistry tools, e.g., gas chromatographs, do not report absolute values of concentration, but have to be calibrated to obtain this information. For PID calibration, some studies have used the *known* concentration of an odorant as a reference (e.g., Kim et al., 2011, 2015) which shifts back the problem to an initial calibration of this concentration. Alternatively, PIDs were calibrated assuming to know the concentration based on a theoretical approach, using Raoult's and Henry's law for odorants diluted in a solvent (Olsson et al., 2011); or for pure odorants, simply Raoult's law (e.g., van Breugel and Dickinson, 2014); of course, this approach can be affected by the problems related to the inconsistency of vapor pressure (see above and **Figure 2**). In a recent attempt (Gorur-Shandilya et al., 2019) proposed to calibrate PIDs based on the measurement of known masses of chemicals (similar to gas chromatograph calibration).

Until now, we have neglected another very important variable: time. We have analyzed the system in terms of a thermodynamic equilibrium, neglecting the dynamics of the processes involved. This pertains to the thermodynamic processes of evaporation

as well as the dynamics of removing odor laden air from the stimulation device in order to expose the animals to it. We will discuss the latter aspect in the next section, but conclude this one with an issue related to the processes of evaporation. A clear demonstration of the risks of repeatedly using a finite amount of odorant that depletes with time is shown in Andersson et al. (2012). The authors showed that the depletion of commonly used odorants depends strongly on the volatility of the odorants. The depletion experiment they used was designed to replicate the typical day (8 h) of neurophysiological experiments in olfaction research: Each odorant was emitted every 10 min for 50 times (or until its concentration was below response threshold). They found that each individual compound has a characteristic time-scale of odorant depletion and that for many of the tested compounds the odorant concentration depletes more rapidly than naively expected, e.g., to almost zero in only two puffs. This issue can, for example, be relevant when characterizing response specificity and sensitivity of ORNs. When correcting for depletion effects (Andersson et al., 2012) found, contrary to earlier reports of comparable responses to all three odorants (Stensmyr et al., 2003; Hallem and Carlson, 2006; Pelz et al., 2006), that the ab3A receptor in *Drosophila* is highly specific to ethyl hexanoate, and orders of magnitude less to methyl hexanoate and ethyl butyrate. To avoid the issue of depletion few adjustments should be and nowadays are applied: (1) Taking the odorant-saturated headspace of a sufficiently large reservoir of pure odorant, (2) Using a much larger headspace volume than the stimulus-volume in order to avoid measurable dilution of the odorant with air when replacing the removed odorant volume, and (3) Using a device (e.g., Mass Flow Controllers) to regulate the air flow removing the odor from the headspace in order to regulate the odorant concentration. The superior stability of repeated odor stimuli obtained with these adjustments can be seen in Gorur-Shandilya et al. (2019).

Temporal Structure of Stimuli in the Lab

Temporal patterns of neural activity in the antennal lobe are hypothesized to play an important role in olfactory coding (e.g., Laurent and Davidowitz, 1994; Brown et al., 2005; Mazor and Laurent, 2005; Wilson et al., 2017). These temporal patterns originate from at least two separate sources. They reflect the temporal pattern of the odor stimuli arriving at the antenna, and they emerge from the internal network dynamics in the recurrent antennal lobe network. To achieve an accurate description of the temporal aspects of neural responses, it is therefore essential that we have a precise control over, or at least a measurement of, the temporal properties of olfactory stimuli.

One of the most common stimuli in psychophysics is the step function: A stimulus, for example a flash of light or a sound is emitted for a duration of interest, with a constant amplitude. The advantages of using such simple stimuli in a reductionist approach are clear, in spite of their hidden complexity: the instantaneous step from 0 to x implies the use of all frequencies. Visual and auditory step stimuli have been studied for a long time and we know their properties very well, but what happens when considering rectangular steps for odor stimuli?

Many studies have analyzed insects' neural responses to chemical compounds, using an approximation of step stimuli in conjunction with electrophysiological recordings or calcium imaging (e.g., de Bruyne et al., 1999; Hallem and Carlson, 2006; Galizia et al., 2010; Münch and Galizia, 2016). In these experiments, odor stimulation pipettes are prepared with a diluted odorant. A stimulus is then generated by passing an air puff through the pipette to transport the volatile molecules to the olfactory receptors. Once the valve controlling the odorant pathway is open, the volatiles start to flow and eventually reach the olfactory sensilla on the antennae. At least two processes separate the odorant in the pipette from arriving at the receptors: passing through the stimulation device and bridging the gap from the exit of the stimulation device to the antennae, through the open air. These processes cannot be characterized as simple fixed-time delays for odorant arrival; their durations depend on many factors, for example the chemical structure of the solvent, the dilution, the storage conditions, the puff interval and puff number (Andersson et al., 2012), the airflow, the tube diameter, the distance of the insect from the tube exit, the distance from the pipette to the exit of the stimulation device, and the lateral distance from tube axis may all affect the temporal integrity of the stimulus (Vetter et al., 2006).

Evidence for the relevance of the odorant pathway through the stimulation device was presented in Nagel and Wilson (2011) and carefully analyzed in Martelli et al. (2013) and Su et al. (2011). These two studies demonstrated that the resulting stimulus dynamics can depend on odorant identity, but typically not on the odorant concentration. Furthermore, they demonstrated how the stimulus dynamics for almost 30 odorants (chosen for their ecological relevance for flies; Hallem and Carlson, 2006) can be described with an onset and an offset timescale and that these timescales are correlated with the vapor pressure of the odorants (Martelli et al., 2013). It is striking that even for this comparatively small sample of chemical compounds the variability of timescales is enormous, spanning 2 orders of magnitude from 30 ms to 1 s. This highlights the fallacy of the abstraction of a step stimulus for odor stimuli. An extensive analysis of the mechanisms behind these processes is still missing, but the large and strongly disparate deviations from an instantaneous step are likely due to the different adsorption/desorption dynamics inside the stimulation device experienced by different compounds and at different partial pressures (as previously noted by Martelli et al., 2013). However, it is important to note that it is unlikely that the relevant quantity is the vapor pressure. If adsorption/desorption is to blame, the relevant property is probably Henry's adsorption constant H_k (see section The Physics of Adsorption and Desorption of Gases on Solids), which offers a potential explanation why time-scales at times appear to scale non-linearly with the vapor pressure (Martelli et al., 2013).

It is worth noting at this point that the dynamical nature of stimulus arrival at the antennae is not only highly relevant when analyzing neuronal and behavioral response times. It also can change the response amplitude because the responses of ORNs, and subsequently of the projection and local neurons in the antennal lobe, are not simply proportional to the total

amount of volatiles bound, but also strongly depend on the rate of change of bound volatiles (Kim et al., 2011, 2015; Nagel and Wilson, 2011; Wilson, 2013). Therefore, not only is it problematic that we lack clear information on the concentration of the stimuli, but it is equally, if not more, damaging that we often do not know the rate of rise and decay. A direct comparison between neurophysiological or behavioral responses for stimuli with different rise and decay time constants, without proper rescaling, risks misinterpretation of the data and proper rescaling can only be achieved when measuring the vapor concentration time series at the antenna (e.g., Kim et al., 2011; Nagel and Wilson, 2011; Martelli et al., 2013). Further investigation of these issues may well impact on our interpretation of the existing data as, for instance, collected in DoOR (Galizia et al., 2010; Münch and Galizia, 2016) or as reported in experiments looking at the roles of odorants in mixtures (Su et al., 2011; Schubert et al., 2015; Chan et al., 2018).

The ultimate goal of olfaction research in neuroethology is to understand animals' senses as they are relevant to their behavior in a natural environment. In order to do so, researchers attempt to recreate realistic stimuli in the lab under controlled conditions. But what is a realistic "spatio-temporal structure" of an odor plume? In the next section, we will review results of experiments and theory on the distribution of odorants in natural environments outside the lab.

THE SPATIO-TEMPORAL STRUCTURE OF ODOR STIMULI IN A NATURAL ENVIRONMENT

> "There is a physical problem that is common to many fields, that is very old, and that has not been solved. It is not the problem of finding new fundamental particles, but something left over from a long time ago – over a hundred years. Nobody in physics has really been able to analyze it mathematically satisfactorily in spite of its importance to the sister sciences. It is the analysis of circulating or turbulent fluids."
>
> **Richard P. Feynman**, *Lectures on Physics*, 1963

The Physics of Odor Plumes

As described in the quote of R. Feynman, the physics of plumes is extremely complex and, even though incredible advances have been made over the past 50 years, we still cannot claim to have a complete description of the phenomenon. Consequently, we will not be able to treat this problem in its full difficulty but we will try to summarize the aspects of plume structure that are most relevant for olfaction.

Generally, the physics of fluids is described by non-linear partial differential equations, the Navier-Stokes equations. In the context of odor plumes, scientists commonly assume incompressible fluids, and so can use the simplified incompressible Navier-Stokes equations. However, even the simplified equations are analytically intractable for most real life problems (Shraiman and Siggia, 2000; Falkovich et al., 2001) and research relies on numerical simulations and empirical measurements in the field.

We will refer to theoretical works to describe the most relevant physical properties that can affect the odor landscape, but discussing them would go beyond the aim of this review (for excellent reviews of the theoretical literature (see e.g., Shraiman and Siggia, 2000; Falkovich et al., 2001). The first and most important distinction in the dynamics of flows is between laminar and turbulent flows. Turbulent flows are characterized by chaotic fluctuations of flow speed and pressure. Eddies and vortices are the typical pictorial representations of turbulent flows; laminar flows, on the contrary, reflect reversible behavior stemming from simpler parallel movements. The transition from turbulent to laminar regime is determined by the balance between viscous and inertial forces. High viscosity drives the flow toward a laminar condition and high inertial forces toward turbulence. The Reynolds number (Re) is essentially the ratio between these two kinds of forces, and hence describes this balance, even though without a clear cutoff value for the transition between turbulent and laminar regimes (see **Box 2**). The factors determining Re are the viscosity of the fluid (higher viscosity, less turbulence), the density of the fluid (higher density, higher turbulence), and the speed of the flow (higher speed, higher turbulence). The last discriminative factor is the *characteristic spatial scale* of the system: If we want to determine the turbulence of a fluid flow in a pipe, the characteristic length is the pipe diameter; while if we are interested in the air flow around an insect, the characteristic length can be estimated as the diameter of the insect. While Re is commonly calculated on average values of flow speed, we have to keep in mind that the flow speed can vary throughout the analyzed system. In particular, the speed of fluid layers close to a solid surface depends on the height: It is approximately zero in the layer in contact with the solid surface – as adhesion induces a no-slip condition – and then increases logarithmically with height until reaching the average wind speed. The region close to the surface is called a boundary layer and when the surface is the Earth's ground, it is the atmospheric boundary layer (see **Box 2**).

So far we have essentially described the flow of a single fluid. In the context of olfaction we need to analyze a more complex situation of a fluid (the odor) immersed in another fluid (the background atmosphere/ambient air). The spatio-temporal distribution of "odor fluid flow" is determined by the fluid dynamics of the ambient atmosphere (with Navier-Stoke equation see **Box 2**) and the motion of the odorant within it (Shraiman and Siggia, 2000; Falkovich et al., 2001). The equation that governs the dynamics of the odorant concentration inside the air (or water) flow is the advection-diffusion equation. The name is self-descriptive and refers to the two physical processes underlying it: advection – bulk motion – and diffusion – Brownian motion. The balance between these two processes is described by the Péclet number (Pe) (see **Box 2**), which is the ratio between the rate of advection and the rate of diffusion.

In summary, odor sources, including organic (animals, plants, or their decay products), geological (Volcanoes) and man-made sources, emit odorants in the air where they travel driven by advection, and molecular diffusion on the

BOX 2 | Fluid dynamics.

Fluid dynamics distinguishes two regimes: Turbulent flow, when pressure and flow velocity behave chaotically and laminar flow, when the fluid flows in parallel surfaces. Laminar flows are characterized by high viscosity and/or low kinetic energy. Transitions from laminar to turbulent flow can, for instance, be observed in the smoke of a flame, at few centimeters distance from the flame.

A complete analytical description of turbulence is still beyond our grasp and is included on the list of unsolved problems in physics. Physicists and engineers analyze most real-life turbulent flows through numerical analysis with computational fluid dynamics models.

The **Navier-Stokes equation** describes the motion of fluids under diffusing viscous forces.

The **Reynolds number (Re)** is defined as the ratio between inertial and viscous forces experienced by a solid body moving in a fluid (e.g., a fly in air), or, equivalently, as caused by a fluid flowing around a stationary solid body (e.g., air around a tree trunk). $Re = U/\nu/L$, where U is the advective speed, ν is the kinematic viscosity and L is the characteristic length.

The Reynolds number is used as a rough guide for the expected nature of the flow. A flow is laminar for low values of Re, and it is turbulent for high Re. For the flow in a pipe, low Re values are commonly below 10^3, but there is no precise number that marks the transition. **During turbulent flow, the fluid's fluctuations in speed and direction, are high and around the same order of magnitude of the average wind speed**. It can be instructive to see the Re value for a typical situation, e.g., a windtunnel with a diameter of 40 cm and wind speed around 0.5 m/s. The other relevant quantities are the dynamic viscosity of air (∼18.5 μPa·s) and the density of air at 20°C (∼1.2 Kg/m^3). In this situation Re ∼ 10,000, the threshold value Re* is around 3000.

Advection-diffusion equation describes how a physical scalar quantity, such as mass or heat, varies in time in a fluid flow. For example, in our case, odorant concentration, c, varies for the variation of the flux **j** of the odorant and depending to an external source (or sink) R:

$$\frac{\partial c}{\partial t} = -\nabla \cdot j + R$$

The flux results from the sum of a diffusive and an advective term. The "diffusive flux" due to random Brownian motion of molecules is typically approximated to the gradient of the local concentration: $j_{diff} = -D\nabla c$ where D is the molecular diffusivity that depends on several parameters, among them the temperature, the pressure, the molecular mass of both air and odorant diffused. The advective flux is due to a net bulk motion driven by the wind with speed $\boldsymbol{v}$: $j_{adv} = vc$

Péclet number (Pe) indicates the separation between flows that are dominantly diffusive from advective ones for a scalar variable governed by the convection-diffusion equation.

Re = $U/(D/L)$, where U is the advective speed, D/L is the diffusion rate, D is the molecular diffusivity and L is the characteristic length.

For Pe smaller than one, diffusion dominates otherwise advection dominates. For example, for pheromones, that are small volatile compounds, whose the diffusion coefficients are of the order of 10^{-6}m^2/s their Peclét number exceed unity by several orders of magnitude (Cardé and Willis, 2008) in typical conditions – wind speed around 1 m/s and **L** of ten or more meters.

The **Schmidt number** is the ratio between Péclet number and Reynolds number, that is the ratio between viscosity and the product of the density of the fluid and the diffusivity of the odorant in the air.

Batchelor scale indicates the smallest length scale at which fluctuations in scalar concentration take place before molecular diffusion dominates the dynamics $\lambda_B = \sqrt[4]{D^2\nu/\varepsilon}$, where D is the molecular diffusivity, ν is the kinematic viscosity, and ε is the mean viscous dissipation rate.

The layer of fluid close to the surface, where viscosity is strong, is called **boundary layer**. When the surface is the Earth's ground, the air layer is the **atmospheric boundary layer**. The flow speed in this layer depends on the height: It is approximately zero at few millimeters from the ground for the viscosity determine a **no-slip condition** there and then it increases logarithmically with the height until reaching the average wind speed.

background of the airflow, which can be turbulent or laminar in nature. The interaction of these transport processes generates the odor-landscape, that is the distribution of the odorant concentration in the air (Atema, 1996; Moore and Crimaldi, 2004; Celani et al., 2014).

Main Features of Odor Landscapes

The main feature that characterize an odor landscape in diffusive and laminar conditions (**Figures 3A,B**) is the (smooth) odorant concentration. It is therefore not surprising that concentration gradients are used for chemotaxis by very small insects at low Reynolds and low Peclét numbers. In the more complex turbulent regimes (**Figures 3C,D**), the most salient feature of the odor landscape is probably its patchiness: with the exception of habitats with low Reynolds number and where diffusion can be stronger than advection, odor concentration lacks a continuous, let alone smooth, spatio-temporal distribution (see **Figure 3**). It therefore proved useful to describe it in terms of *filaments* (or odor-strands), i.e., pockets of non-zero concentration of odorant, or in the temporal domain in terms of *whiffs* – time intervals with non-zero odor concentration – and the complementary concept of *blanks* – time intervals with zero odor concentration. In addition the odor landscape is typically described in terms of variables such as the average concentration $\overline{C}$ and the (temporal) fluctuations of the concentration[6] $\sigma_C/\overline{C}$, where σ_C is the standard deviation (over time) of the concentration. These and other variables were analyzed with respect to whiffs and blanks, defining "conditional measures" as the mentioned measures restricted to within whiffs. For example, the conditional average concentration is the average concentration during whiffs. The discontinuous nature of whiffs and blanks is typically called *intermittency*. There are different definitions in use. Here we use the definition of intermittency (or intermittency factor) x as the fraction of whiff time, i.e., high intermittency means many whiffs or long whiffs.

Because the viscosity and density of air does not change dramatically, the main factors related to the nature of odor plumes in (turbulent) natural air flows are the average wind speed and its fluctuations, the physical space, e.g., open field vs. forest, and the height above ground, both of the odor source and of the animal smelling it. An additional factor is the time of day, which determines the buoyancy in the atmospheric boundary layer and hence the balance between turbulence caused by buoyancy vs. turbulence due to wind shear.

[6]Sometimes also referred to as "fluctuation intensity" or "relative fluctuations of concentration."

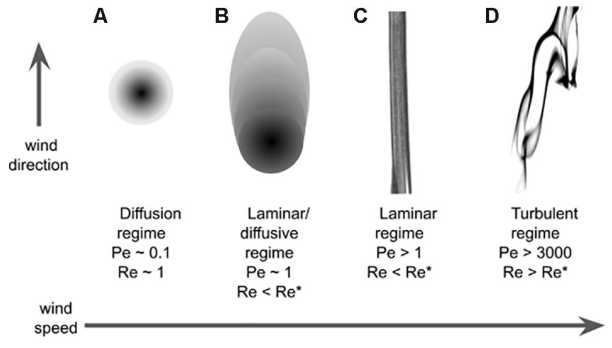

FIGURE 3 | Plume structure. Regimes that are qualitatively different for increasing value of wind speed. The regimes are identified for different values of Péclet and Reynolds numbers: **(A)** Diffusive regime, **(B)** laminar/diffusive regime, **(C)** laminar regime, and **(D)** turbulent regime (see text). In this pictorial representation the Schmidt number (Pe/Re) is around 0.1.

With respect to the advection/diffusion balance, the most important factors are the nature of the odorant, in terms of its diffusivity (reflected in the Péclet number, see **Box 2**), whether it is a simple compound or a complex mixture, or something in between, such as pheromones.

For both, the nature of the flow and of the odorant transport in the flow, scale and distance matter. The observed characteristics of the plume change with the distance from the source, either down-wind, or cross-wind, and with the size of the source and receiver.

Results on Plume Structure

> "Any experiment is reproducible until another laboratory tries to repeat it."
>
> **Kohn's Second Law**

In the following sections we will review work on aspects of plume structure, focusing on those aspects that are most relevant to animals: average concentration, concentration fluctuation, intermittency and whiff and blank durations. Ideally, we want to give enough information for an experimenter to reproduce, using an odorant stimulator, what could pass as natural stimuli. When investigating aspects of plume structure in the field, scientists typically place an odor source at a defined height and measure the odorant concentration time series at defined locations downwind/crosswind, using a detection device, for example a PID.

Average concentration

Mylne and Mason (1991) used propylene as a tracer gas to measure the concentration averaged over time, in neutral buoyancy conditions, at large distances of tens to hundreds of meters, with source (1 cm diameter) and detector 2 m above the ground and in an open field, flat and smooth for several km in all directions (Mylne and Mason, 1991). They found that, as one might expect, the average concentration decreases with the downwind distance from the source. This was also seen in other studies (e.g., Voskamp et al., 1998; Murlis et al., 2000) and for smaller distances from the source (from a few meters to 30 m), and in wind tunnels (Fackrell and Robins, 1982a,b; Justus et al., 2002; Vergara et al., 2013). Commonly used Gaussian plume models predict that the average concentration on the midline of the plume decays with a power law, with data fits indicating powers between -1.5 and -2 (Cramer et al., 1958; Fares et al., 1980).

The shape of the *probability distribution* of concentration on the centerline has been argued to (Hanna, 1984; Lewellen and Sykes, 1986; Mylne and Mason, 1991) vary as a function of downwind distance as well (75–75 0 m, see Figures 11 and 13 in Mylne and Mason, 1991; **Figure 4C**).

However, *for very small distances* (a few meters from the source), *only* the probability distribution of concentration on the centerline of a turbulent jet appears to depend on the downwind distance (and other experimental parameters), but the average concentration *does not* (Duplat et al., 2010).

Concentration fluctuation and intermittency

The fluctuations of concentration $\sigma_C/\overline{C}$ (*both conditional and not*) decrease with downwind distance, steeper close to the source and more gradually at large distances. This result was consistently demonstrated, albeit with large variability of individual measurements, in a large number of experiments (e.g., Mylne and Mason, 1991; Mylne, 1992; Yee et al., 1993; Mylne et al., 1996) for long distances (>20 m), in open field conditions, during near-neutral and stable buoyancy conditions. It was also observed for shorter distances (5–20 m) with similar meteorological conditions (Davies et al., 2000) and in small wind-tunnels (3 m) (Fackrell and Robins, 1982b; Vergara et al., 2013).

In crosswind direction, at a given downwind distance, fluctuations of concentration $\sigma_C/\overline{C}$ increase with the distance from the plume centerline (Mylne and Mason, 1991; Yee et al., 1993; Justus et al., 2002) while the conditional fluctuations are approximately constant. This indicates that the changes along a horizontal cross-section of the plume are primarily caused by decreases in intermittency and, indeed, decreases in intermittency have been observed directly (Yee et al., 1993; Justus et al., 2002).

In theoretical modeling work, Celani and colleagues used a Lagrangian approach to solve the advection-diffusion equations and calculate intermittency as a function of downwind or crosswind distance[7] from the source. They obtained a formula relating fluctuations to the intermittency factor, $x : \sigma_C/\overline{C} \approx \sqrt{x^{-1} - 1}$ (Celani et al., 2014). When combined with results on the dependence of $\sigma_C/\overline{C}$ on downwind and crosswind distance, this predicts that intermittency decreases in the crosswind direction, in agreement with the experiments, but is independent of downwind distance. Celani et al. backed their results by showing that the value of $\sigma_C/\overline{C}$ is approximately constant, at long distances, for a subset of the experimental results ("Fens," Figure 10 in Mylne and Mason, 1991, see **Figure 4B**). However, the fluctuations are not constant for other data sets at shorter distances (see "Sirhowy valley," Figure 10 in Mylne and Mason, 1991,

[7]The distance from the plume centerline (which points along the wind direction).

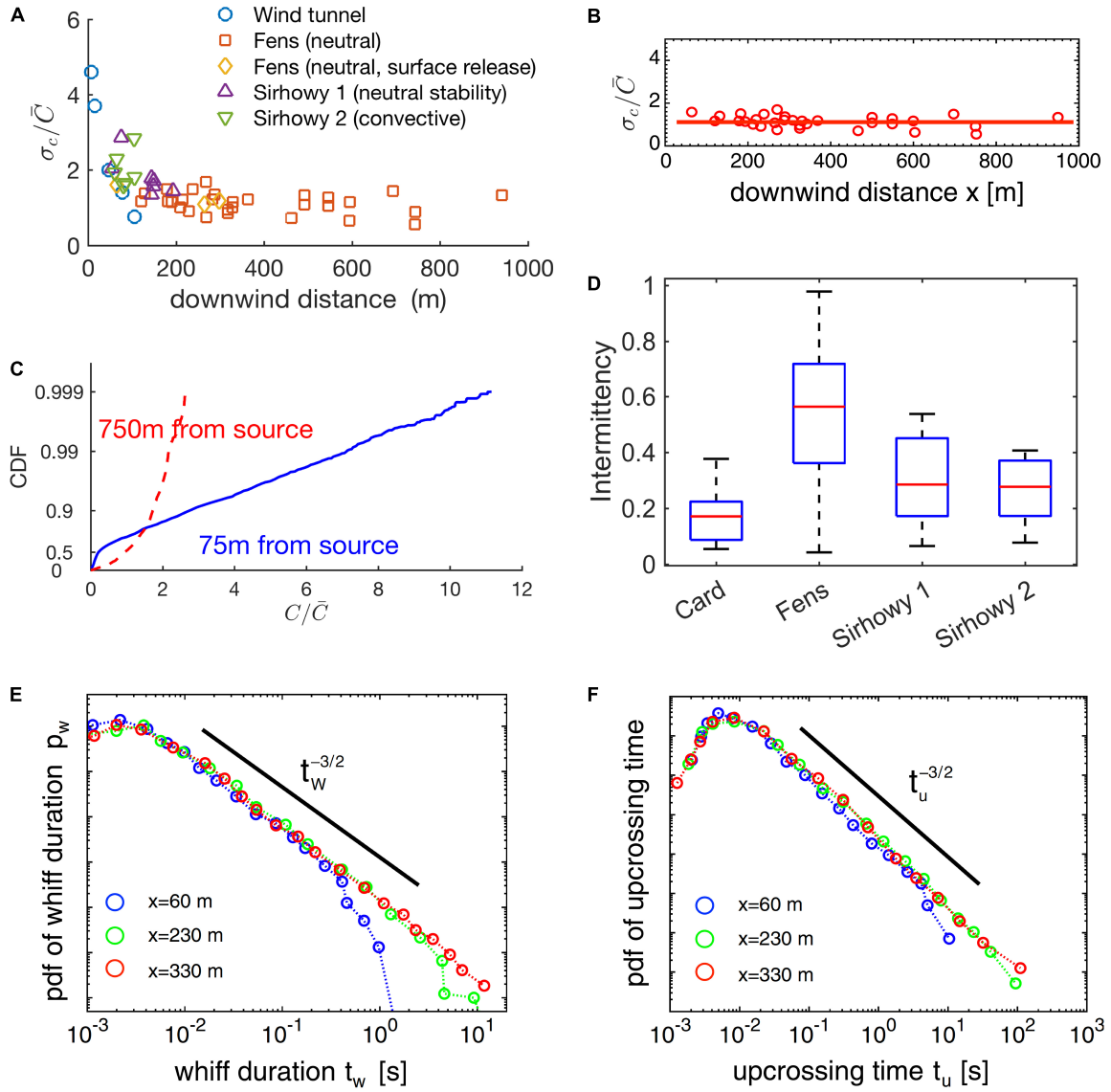

FIGURE 4 | Odor-landscape in the atmospheric boundary layer described by the statistics of its principal properties. **(A)** Fluctuation of odorant concentration $\sigma_C/\bar{C}$ for several distances from the source and for several conditions (see Mylne and Mason, 1991). **(B)** Subset ("Fens" dataset) of data reported in **(A)**. **(C)** Cumulative distribution function of the concentration for two samples at 75 and 750 m distance from the source. **(D)** Probability distribution of intermittency for several locations. The theory can partially model the experimental results reported by Yee et al. (1995). **(E,F)** Probability distribution functions for whiff durations and upcrossing durations (data from Mylne and Mason, 1991; Yee et al., 1995). **(B,C,F)** Reproduced from Celani et al. (2014), **(A,C,D)** reproduced from Mylne and Mason (1991).

Figure 5 in Fackrell and Robins, 1982a, Figure 2 in Yee et al., 1993, and Table 1 in Yee et al., 1995) as it is evident from comparing their Figure 4A vs. Figure 4B (Celani et al., 2014; or see **Figure 4A**). Moreover, for the same dataset, intermittency was empirically shown to be around 0.3 for distance around 75 m (in qualitative agreement with Celani et al. prediction), but it increased substantially for distances around 750 m (see Figures 11, 13 in Mylne and Mason, 1991; **Figure 4D**). The causes of these discrepancies remain to be determined, in particular whether they are experimental in nature or rooted in the assumptions of the theoretical work.

In the windtunnel, for much smaller distances (>30 cm), and turbulent conditions (wind speed 10 cm/s and turbulence grid in the upwind end) the intermittency factor is strongly dependent on the downwind distance (see Figure 8 of Connor et al., 2018) both for high and low turbulence conditions.

Whiff and blank durations

When looking at whiff and blank durations individually, we observe an interesting U-shaped behavior of the average duration of whiffs and upcrossing times (duration of a whiff and the subsequent blank) with downwind distance with a minimum value at around 60 m (Yee et al., 1995; Figures 5, 6). This likely

reflects that close to the source, the filaments[8] of the plume are not yet broken up as much by turbulence and hence whiffs are long. At the minimum, filaments are fully broken up by turbulence, leading to minimal whiff duration. At even larger distances, the ongoing spreading of filaments begins to dominate, which increases the whiff duration again. Interestingly, this result is independent of the concentration threshold used to define whiffs/filaments, for a reasonably wide range of concentrations (Yee et al., 1995).

For distances between 60 and 330 m we also have information about the full distribution of whiff and blank durations. Theory and experiments indicate that, in this range and for whiff/blank durations between 10^{-2} and 10^{2} s, the probability distributions are independent from the concentration threshold and the downwind distance, following a power law with exponent -3/2 (Yee et al., 1995; Celani et al., 2014). The differences in the mean values for longer distance discussed above stem from additional very rare but very long whiffs/blanks while the distribution of short whiffs remains essentially the same.

Remarkably, the maximum of the probability distribution for the whiff duration is at very short timescales, around 3 ms and remains like this for long distances (at least between 60 and 330 m; Yee et al., 1995, see **Figures 4E,F**). This indicates that even though filaments "bleed out" at longer distances, there is always a strong element of very fast fluctuations.

Unfortunately, for time intervals below 10^{-1} s, the experimental evidence is hard to interpret because: (1) While the apparatus of Yee et al. had a sample rate of up to 270 Hz, it also had a loss of 6 dB in sensitivity at the smallest measurable timescale (˜3 ms). (2) The minimal length scale of fluctuations – described by the Batchelor scale (see **Box 2**) and calculated from the value of kinematic viscosity of air and the energy dissipation rate furnished by Yee et al. (1995, **Table 2**) – is approximately 0.3 mm, which, for wind speeds around 1 m/s implies possible fluctuations on timescales as low as 0.3 ms (Yee et al., 1995).

Up to 1995, there was neither a mathematical model for the probability distribution of whiffs and blanks, nor for the amplitude of concentration (today there is the above mentioned work of Celani et al., 2014). Therefore, Yee et al. (1995) decided to simply fit the experimental distributions with a number of standard two-parameters probability distribution functions (e.g., the lognormal distribution, the gamma distribution, the conjugate beta distribution, the K-distribution, the Weibull distribution, and the Gumbel distribution). From a qualitative analysis of quantile-quantile plots, the authors observed that the best fit for the whiff durations was achieved with a lognormal distribution. This implies that the processes behind filament durations and arrival times are not memoryless[9], for otherwise their distribution should follow an exponential distribution (see e.g., Gallager, 1996). The relationship between duration/arrival time and the amplitude of the whiffs is still unknown.

[8]A filament is understood in this context as a contiguous area with non-zero odorant concentration.

[9]The exponential distribution uniquely has the property of being memoryless: if the upcrossing times were exponentially distributed, a fly that met a whiff 1 s ago, would have the same expectation to find another whiff in the near future as a fly that met a whiff 1 ms ago.

Recently, it has been shown that the frequency of bouts (significant changes in the odorant signal) can be used to determine, in a wind tunnel, the distance of the detector from the source (Schmuker et al., 2016).

Environmental features shaping plume structure

Aside from the down- and crosswind distance discussed so far, other factors such as wind speed, source position, source size and environmental conditions also have been investigated.

As explained above, *wind speed* is directly related to the degree of air turbulence as reflected by the Reynolds number (Re and the average wind speed are linearly related). Empirical evidence showed that faster wind (higher turbulence) yields thinner plume filaments (Yee et al., 1993) and a higher frequency of whiffs (Fackrell and Robins, 1982a).

The *source position* influences the temporal characteristics of plumes: A source located in a higher position will be affected by stronger advective flows than sources located closer to the ground, where "no-slip" boundary conditions constrain the flow to zero advection (see Connor et al., 2018; and **Box 2**).

The *source size* also has a significant influence on the plume structure. For small distances (within wind tunnel spatial scale, i.e., a few meters), experimental and theoretical results showed that for increasing source size, fluctuations decrease and intermittency increases [e.g., Figures 3, 4 from Fackrell and Robins, 1982b and Equation (9) of Celani et al., 2014]; theoretical analysis from Riffell et al. (2008) predicts that the source size affects the frequency of the eddies emitted. In principle, source size could even influence the plume statistics at long distances, but theoretical work of Celani et al. (2014) predicts that it does not affect any macroscopic measurements (average concentration in a whiff, intermittency, distribution of whiff duration, etc.).

Environmental conditions (via buoyancy), as mentioned before, affect the plume structure, in terms of average concentration, intensity and intermittency, but the experimental results are mixed. In Mylne (1992), the authors showed no difference for the intensity between the stable and near-neutral buoyancy case, while (Mole and Jones, 1994) showed that intensity is higher for stable than for unstable conditions: Stable conditions lead to higher average concentration and standard deviation than unstable conditions, but when normalized to the wind speed the differences are not significant (Mole and Jones, 1994).

Habitat

Contrary to flat environments like meadows or deserts, forests and other more structured environments are spatially complex and the boundary layer assumptions are not valid for them (see e.g., Aylor et al., 1976; Riffell et al., 2008); for example, large eddies are not present due to the canopy and the tree trunks, while vertical variations of the habitat are more relevant (Rauner, 1976; Hutchison and Baldocchi, 1989). Air movements due to advection are very small and therefore odor plumes are trapped into the canopy (Thistle et al., 2004). Of course, in this habitat, odorant propagation is much more difficult and even before reaching 100 m distance to the source, concentration values are typically already below 0.1% of the original values (Thistle et al.,

2004). Moreover, the odor background in these environments generates even more difficulties to detect an odor of interest and how insects can cope with them is an active research area (Gorur-Shandilya et al., 2017; Erskine, 2018; Sehdev and Szyszka, 2019).

Mixtures of Odorants

> "Experimental science hardly ever affords us more than approximations to the truth; and whenever many agents are concerned we are in great danger of being mistaken."
>
> **H. Davy, 1778–1829**

Mixtures of odorants have at least two levels of complexity that together generate the "olfactory cocktail party" problem (Rokni et al., 2014):

1. Odor responses are generally broad and overlapping: Individual chemical compounds with a defined meaning are rare exceptions and for them, early sensory areas work through dedicated paths called "labeled lines." For instance, in *Drosophila* there is a single dedicated glomerulus for CO_2 (Suh et al., 2004) (but see the recent results in van Breugel et al., 2018, and one for geosmin; Stensmyr et al., 2012). Apart from these exceptions, each odorant activates a broad profile of olfactory receptor types and each receptor type is activated by a broad profile of odorants.
2. Natural odors are mixtures of many odorants: plants and animals do generally not exude single odorants (with the exception of some pheromones) but multiple odorants at the same time. For example, floral scents can comprise more than 100 relevant odorants (Riffell, 2012; Beyaert and Hilker, 2014). It is the joint effect of these odorants that elicits the behavioral response and there is a large amount of evidence that the information about the identity or the state of the source is contained in the ratio of the odorants in the mixture (see e.g., Visser and Avé, 1978; Christensen et al., 1989; Dorn et al., 2003; Bruce et al., 2005; Baker, 2008; Najar-Rodriguez et al., 2010, and the references therein).

Mixture processing has been the subject of numerous studies in ants, bees, flies and many other insect models and while an extensive review of mixture processing in insects would go beyond the scope of this review, the major issues analyzed in the last 20 years in this field are:

1. *Olfactory coding (*Galizia et al., 1999; Carlsson et al., 2002; Dobritsa et al., 2003; Guerrieri et al., 2005; Wright et al., 2005; Deisig et al., 2006; Ito et al., 2009; Olsen et al., 2010; Andersson, 2012; Lei et al., 2013; Martin et al., 2013*)*,
2. Difference between food related receptors and pheromone receptors (van der Goes van Naters and Carlson, 2007; Wee et al., 2016),
3. *Odorant valence* (e.g., Voskamp et al., 1999; Riffell et al., 2009a; Leonard et al., 2011; Najar-Rodriguez et al., 2011; Andersson, 2012; Thoma et al., 2014; Badel et al., 2016; van Breugel et al., 2018; de Vreese and Martinez-Ortiz, 2018; Mohamed et al., 2019),
4. *The representation of the time course* (Broome et al., 2006; Su et al., 2011; Stierle et al., 2013; Martelli and Fiala, 2019),
5. *The comparative analysis between species* (Andersson et al., 2011; Clifford and Riffell, 2013),
6. *Complex overlapping plumes* (Broome et al., 2006; Myrick et al., 2009; Su et al., 2012),
7. *Learning* (Perez et al., 2015; Schubert et al., 2015),
8. *Specific effects, for example the non-synaptic interaction between ORNs* (Su et al., 2012; Zhang et al., 2019).

Here, we will focus on odor source separation and in this section, we will review experimental and theoretical results for the two most elementary situations: when two odorants are emitted from two separate sources and when they are emitted from the same, single source. Of course, this is just one of the possible starting points before approaching more complex situations with multiple odorants and multiple sources (see for example, on this same issue; Conchou et al., 2019). It is important to note that the technical difficulty of measuring two odorants simultaneously and in the same location is still a big obstacle to making further progress in this field. We will see below that several clever strategies have been developed to overcome this difficulty, for example adopting the insects' antennae to detect the odorants (Loudon, 2003; Myrick and Baker, 2011).

Two sources, two odorants

When two odorants are emitted from two sources, they start off separated, but after a while and downwind from the sources, they mix due to diffusion and turbulent motion. In mathematical terms, the correlation of the time courses of the odorants' concentrations increases with the downwind distance from the sources. Increasing the distance between the sources, this correlation decreases. Therefore, close to the sources, the odorants can be perceived as having been emitted from separated sources, but far downwind from the sources they cannot. If the distance between sources is higher, it is easier to discriminate whether they are separated or not.

A recent theoretical study (Kree et al., 2013) demonstrated that the correlation between concentrations emitted from two sources decreases exponentially for increasing inter-source distance and increases exponentially with the distance to the sources.

Davies et al. presented the first evidence of this phenomenon for large distances (source separation around 0–40 m, downwind distance 5–20 m, in near-neutral conditions, wind speed around 2 m/s). Interestingly, they adopted and modified two different detectors to obtain co-localized synchronous odorant measurements (Davies et al., 2000).

The recent work of the group of Schäfer analyzed the effect in a windtunnel on a smaller spatial scale (source separation around 0–50 cm, downwind distance 40 cm, air speed around 552 cf/m[10]). With Aurora Scientific they developed the first "dual-energy photoionization detector" and recorded the evolution of odorant concentration emitted from two sources, either mixed together or separated (Erskine, 2018; Erskine et al., 2019). The analysis of temporal correlation of the odor signal showed that "source separation" can be accurately predicted. Similar results were obtained with an odorant detector formed from four moth

[10]CFM is short for cubic feet per minute (cu ft/min). It is a measurement of the velocity at which air flows into or out of a space.

antennae (Myrick et al., 2009). In a wind tunnel of 1.5 m length, the detector was able to discriminate between plumes emitted from a single source from those coming from two closely spaced sources (2–10 cm separation). These are encouraging results that bring our technology a step closer to the performance of insects' olfactory system: 20 years ago, Baker et al. tested moths with a mixture of a binary pheromone blend and an interspecific compound (a pheromone antagonist; Fadamiro and Baker, 1997) and observed that they are able to discriminate between a single source emitting the mixture and two sources emitting the same odorants even when separated by only 1 mm (Baker et al., 1998). Interestingly, this experiment appears to have never been repeated.

One source, two odors

When two odorants are emitted from a single source, each with a given, constant concentration, the ratio of their concentrations is informative of the source identity (as noted above), but very far from the source, due to diffusion and turbulent motion, the two odorants are spread out, their concentration ratio changes and the information about the identity can get lost. The most pertinent question in this scenario is to what extent do odorants initially travel together in the same filaments maintaining the same ratio of concentrations? And if they do so, for how long? And are the mixing effects due to diffusion and advection in a turbulent flow synchronous or do they take place at different timescales and hence take effect at different distances from the source?

The answers to these questions will depend on the physical properties of the flow, on the chemical properties of the odorants and on the differences between them (for an excellent review on this issue see Conchou et al., 2019).

For example, compounds with lower adsorbing properties would travel over longer distances (and faster) than the other compounds (see Beyaert and Hilker, 2014, and references therein). This effect can have a potential function as the ratio of the two components can inform the insect of the distance from the source. For example, Xiao et al. (2012) showed that two long-chain of hydrocarbons help orientate the yellow peach moth Conogethes punctiferalis (Crambidae) to a source, but only at close range (less than 3 m).

It is generally believed that the diffusive properties of odorants are not relevant for this particular issue (Celani et al., 2014; Cardé, 2016) because for most relevant odorants (e.g., pheromones) the Peclét number is much bigger than one, so that advection dominates over diffusion and the diffusivity of common odorants is quite similar and spans a range of only one order of magnitude. For example, the diffusion coefficient for ethanol is around 10^{-5} m^2/s and that for hexadecanol (as many moth pheromones) is around 10^{-6} m^2/s (Loudon, 2003); within a pheromone blend, the difference in diffusion coefficients is even less (Cardé, 2016).

Some indirect evidence supporting this hypothesis is presented in Duplat et al. (2010) who compared temperature and concentration profiles in plumes released in a sustained turbulent medium at several distances downstream from the source. They considered temperature and odorant concentration interchangeably as they are obeying the same type of advection-diffusion equations. In particular, they showed how the profiles of the relevant scalars (temperature or odorant concentration) change for three conditions with very different values of the Schmidt number (the ratio between Péclet number and Reynolds number, see **Box 2**). They analyzed temperature in air Sc = 0.7, temperature in water at Sc = 7, and the concentration of disodium fluorescein in water at Sc = 2000. In spite of the large differences in Schmidt number, the differences in the profiles for these three cases (diffusivity spans four orders of magnitude) are quite subtle.

Application to Insect Olfaction Research

Navigating Odor Plumes

> "Information is where you find it"
> Dusenbery, 1996

The goal of insects navigating an odor-landscape is to approach or escape the odorant source. To this aim, insects must be able to "read" the plume in which they are immersed. In a previous section, we saw how the statistical properties of plumes vary depending on the source position, sensor position, temperature, wind speed, etc. Which of these pieces of information about the plume structure could potentially help insects? And which ones do they actually use? Do insects analyze and extract information from the complex structure of odor plumes as recently suggested in Boie et al. (2018) or do they use only relatively simple cues, like the presence or absence of an odorant at any given time (Pang and Farrell, 2006)? In this final section, we would like to show the relevance of these questions for the study of insect navigation. To this aim, we will use only a few illustrative examples from the literature. For an extensive review of odor-guided insect navigation (see e.g., Murlis et al., 1992; Belanger and Arbas, 1998; Vickers, 2000; Moore and Crimaldi, 2004; Gaudry et al., 2012; Cardé, 2016; Webster and Cardé, 2017; Baker et al., 2018).

We saw that both downwind and crosswind distance from the source affect intermittency, average concentration, and frequency of bouts (see e.g., Mylne and Mason, 1991; Yee et al., 1993; Schmuker et al., 2016). However, we also saw that their isolated local values (of intermittency and average concentration) prevent to unambiguously determine the distance to the source. For example, for distances over 60 m the excursion times have very similar probability distributions (known up to 300 m), with relevant differences only for very long excursion times (>1 s, see **Figures 4E,F**). Therefore, to know the distance from their objective, insects must integrate information across space and/or time. In a recent experiment, Pang et al. (2018) demonstrated the effect of memory on olfactory guided orientation decisions of flies and mosquitoes in a laminar flow within a windtunnel. Another example is the dependence of turbulence in the atmospheric boundary layer on the time of day: during the sunset there are less advection movements, and as a consequence plumes intermingle less (Mylne and Mason, 1991; Yee et al., 1993; Mole and Jones, 1994). If insects wanted to use measures of turbulence for orientation, they would need to adjust this information for the time of day. It has even been suggested that this effect influenced, via evolutionary

selection, the circadian rhythm of the moth *manduca sexta* that exhibits nocturnal foraging (Riffell et al., 2009b), presumably in order to take advantage of the more stable conditions during the night.

There are several strategies that motile organisms developed to locate an odorant source (Belanger and Arbas, 1998; Vickers, 2000; Moore and Crimaldi, 2004; Gaudry et al., 2012). A first classification of potential strategies can be performed based on the level of turbulence of the flow that the animals encounter.

For example, at low Péclet number and low Reynolds number, diffusion processes dominate the flow dynamics (see **Figures 3A,B**) and animals follow the gradient of odor concentration (chemotaxis). This strategy can range from simple biased random walks of bacteria (Weissburg, 2000) to more sophisticated active sampling behaviors observed in *Drosophila* larvae (Gomez-Marin et al., 2011). We saw that close to the surface, the no-slip boundary condition generates a layer of low speed (Connor et al., 2018) and it is well-established that *Drosophila* larvae use resulting odor gradients (Louis et al., 2008). It has also been suggested that walking insects could take advantage of the diffusive distribution of odorants (Baker et al., 2018). However, the odor landscape is patchy even for animals relatively close to the surface, like ants (few mm high), and already at small distances (>30 cm) from the source (Figure 8 in Connor et al., 2018). This is also reflected in the trajectories of desert ants which frequently change between upwind and crosswind directions, presumably because they constantly get into and out of the plume (Buehlmann et al., 2014, 2015).

For increasing advective wind, the odor-landscape becomes turbulent (high Reynolds number, high Péclet number) (see **Figures 3C,D**). In these conditions the patchiness of plumes prevents insects from using any gradient based information (Wright, 1958; Gifford, 1959; Aylor et al., 1976; Elkinton et al., 1984) and insects have to smell and navigate based on the pattern of discontinuous stimulation. Indeed, the behavioral relevance of stimulus intermittency has been repeatedly shown (Kennedy et al., 1981; Willis and Baker, 1984; Baker et al., 1985; Bjostad, 1987; Kaissling, 1997) together with empirical demonstrations of the correlation between AL intermittent responses and insect (in moth) navigation behavior (e.g., Lei et al., 2009; Huston et al., 2015). To react to plume intermittency, insects have to be fast: Indeed, for more than 20 years we have known that insects can extract information at small time scales (below 1 s; Mafra-Neto and Cardé, 1994; Vickers and Baker, 1994; Baker et al., 1998), and it is now becoming clear that even fluctuations of around 10 ms can be detected (Bhandawat et al., 2010; Szyszka et al., 2012, 2014). In a turbulent plume, insects go into and out of a plume frequently, so that in addition to locating the source, just (re-)locating the plume becomes challenging. Typically, their behavior can be described as alternating upwind surges when in a whiff and (approximately) crosswind casting during blanks (David et al., 1983; Kuenen and Cardé, 1994; Buehlmann et al., 2014; van Breugel et al., 2014). In the presence of wind, the plumes tend to be elongated along the wind direction. It can then appear intuitive to think of crosswind casting as a good approach to re-locating the plume once it has been lost. However, over the years different "optimal" models have been proposed to capture the dynamics of this behavior (Dusenbery, 1989). Unfortunately, we are still missing a complete representation of what different insects actually do when losing the plume.

Scaled-Down Odor Plumes in the Lab

Odor plumes are too complex to be used in their full details when investigating animal physiology and behavior and hence need to be simplified. Odor steps are the most radical simplification, are very easy to generate and analyze, and are, therefore, the most common inputs used in insect neurophysiology until today – with some exceptions starting 10 years ago (see e.g., Geffen et al., 2009). However, constant odor steps do not occur in natural plumes, whose most important characteristic is intermittency. In a recent study Jacob et al. (2017), recorded activity in the early olfactory sensory areas (olfactory receptors and antennal lobe) in a controlled environment using olfactory stimuli imitating the distribution of whiffs and blanks of natural plumes (a similar example is Huston et al., 2015), but simplifying the concentration to a constant value. The goals of this seminal work reflect the same thinking underlying this review: the complexity of olfactory stimuli has to be faced altogether because a reductionist approach might lead to misunderstanding the olfactory system. The introduction of correct whiff and blank statistics is a great first step and there are several further improvements that can be made: (1) Removing the approximation of a single value for the concentration, for the obvious reason that otherwise ORNs or antennal lobe neurons cannot exhibit realistic responses; (2) Implementing simulated stimulation for crosswind distances different from zero, (3) Measuring the plume-structure for very small time-scales; as discussed earlier, the distributions are not known for the time-scales below tens of milliseconds. (4) Measuring the whiff and blank distributions perceived by a moving insect: Whiff and blank distributions are extracted from a stationary point, subject to the passing of the plume, but insects usually navigate actively into plumes with a speed that is comparable with the wind speed. It is reasonable to expect different distributions of whiffs and blanks for this situation. To solve the first and second issues, no further data are needed, one can implement the results from existing experimental studies (Mylne and Mason, 1991; Yee et al., 1995) but for the other two issues, further experiments are needed.

CONCLUSION AND FUTURE DIRECTIONS

> "To advance further, we must continue our trend of placing the animal firmly in its fluid mechanical environment and probing more finely the properties of fluid flow and signal structure that have significant impacts on locomotory performance".
>
> **M. J. Weissburg, Biol. Bull. 2000**

> "[…] while the insect's powers of olfaction are remarkable they are not miraculous".
>
> **H. Wright, 1958**

We have summarized some knowledge on the nature of odor stimuli touching on two specific aspects: (1) The concentration

of odorants emanating from liquid dilutions and the temporal structure of odor stimuli produced by olfactory stimulators in the lab. (2) The structure of odor plumes in natural environments.

With respect to the odor concentration produced by using defined dilutions of odorants in a solvent, it is important to reiterate that the concentration in the air within the headspace of the liquid solution, be it on a filter paper or in a larger reservoir, is not a linear function of the dilution. As we have discussed and as is well-known there are linear regimes for the two extremes of very high dilution (very small amounts of odorants, Henry's law) and for very low dilution (almost pure odorant, Raoult's law). What may be less appreciated are the regimes where these laws apply. In a sense, both regimes are very small if looked at on a linear scale (see e.g., **Figure 2**): Henry's law typically applies from dilutions of 10^{-2} onward, while Raoult's law might apply for 90% or more odorant in the solution. However, given the typical goal of olfaction research to investigate realistic, diluted concentrations all the way down to the detection threshold, Henry's law typically applies and future research should make appropriate use of Henry's constant, not the vapor pressure. In order to do so, we need to extend the data on Henry's constant which is currently only available for a few odorant-solvent pairs. Independently, it will always remain important to ascertain using direct measurements, e.g., with a PID device, that the stimuli we think we have generated by diluting odorant solutions, are indeed what we expect them to be.

With respect to the temporal structure of odorant stimuli from odor stimulation devices, we discussed recent results showing that the odor onset of an odor stimulus depends on the identity of the odorant. Combined with other results that indicate that olfactory systems are sensitive to the derivative of the odorant concentration as well as the odorant concentration itself, the difference in odor onset slope could have measurable effects on the response and this could lead to confusing results. As with the odorant concentration, it should also become standard to ascertain the stimulus time course for any given experiment. Research in insect physiology is clearly moving toward more articulate stimuli – more odorants, more complex time courses. Moreover, nowadays it is clear that a purely reductionist approach is insufficient to gain a full understanding of the neuroscience of insects – from molecules, to neurons and synapses, and to behavior. Future experiments may eventually all have to consider the entire environment-perception-action loop (Wallach et al., 2016), including, for instance, how wing movements might implement strategies for active sensing of odor plumes (Koehl, 2006; Li et al., 2018). However, it is an immediate objective for the community to define protocols for more viable and precise spatio-temporal stimulus generation in the lab (e.g., Gorur-Shandilya et al., 2019).

For the structure of natural odor plumes we surprisingly found that many of the most salient experimental results date back to the last century, only augmented by occasional more recent studies. Even in the quite simplified overview that we were able to include here it becomes clear that ultimately we still do not fully understand the nature of odor plumes. A prime example is the measurement of intermittency, probably one of the most important plume descriptors, where theoretical results are in stark disagreement with the experimental evidence. Solving this issue is a well defined goal that should urgently be addressed by Neuroscientists and Physicists alike.

There is increasing evidence and acceptance that relevant temporal and spatial scales can be quite small, matching the recent discoveries of "fast olfaction" (see section Application to Insect Olfaction Research). When investigating insect behavior in natural plumes, in particular navigation, it will be important to better understand and experimentally characterize the particular plume conditions that insects face in any particular experiment. To this aim, a big technological effort is needed to measure odor mixtures at a high spatio-temporal resolution (Davies et al., 2000; Myrick et al., 2009). This could then feed into lab experiments for which advanced stimulation devices for arbitrary time series are under development (Kim et al., 2011, 2015; Jacob et al., 2017; Gorur-Shandilya et al., 2019).

Generally we desperately need more data and it will be essential to update the decades old data on natural odor plumes in order to make further progress in our understanding of insects' behaviors in natural environments.

AUTHOR CONTRIBUTIONS

MP and TN contributed to research and analysis of literature and writing the manuscript.

FUNDING

The research in this manuscript has received funding from the Human Frontiers Science Program, Grant RGP0053/2015 (odor objects project) and the European Union's Horizon 2020 Research and Innovation Program under Grant Agreement No. 785907 (HBP SGA2).

ACKNOWLEDGMENTS

We are really grateful to M. Stopfer, A. Barron, and C. Martelli for helpful comments that greatly improved the manuscript.

REFERENCES

Andersson, M. N. (2012). Mechanisms of odor coding in coniferous bark beetles: from neuron to behavior and application. *Psyche* 2012, 1–14. doi: 10.1155/2012/149572

Andersson, M. N., Binyameen, M., Sadek, M. M., and Schlyter, F. (2011). Attraction modulated by spacing of pheromone components and anti-attractants in a bark beetle and a moth. *J. Chem. Ecol.* 37, 899–911. doi: 10.1007/s10886-011-9995-9993

Andersson, M. N., Schlyter, F., Hill, S. R., and Dekker, T. (2012). What reaches the antenna? how to calibrate odor flux and ligand-receptor affinities. *Chem. Senses* 37, 403–420. doi: 10.1093/chemse/bjs009

Atema, J. (1996). Eddy chemotaxis and odor landscapes: exploration of nature with animal sensors. *Biol. Bull.* 191, 129–138. doi: 10.2307/1543074

Auffarth, B. (2013). Understanding smell–the olfactory stimulus problem. *Neurosci. Biobehav. Rev.* 37, 1667–1679. doi: 10.1016/j.neubiorev.2013.06.009

Aylor, D. E., Parlange, J.-Y., and Granett, J. (1976). Turbulent dispersion of disparlure in the forest and male gypsy moth 1 response. *Environ. Entomol.* 5, 1026–1032. doi: 10.1093/ee/5.5.1026

Badel, L., Ohta, K., Tsuchimoto, Y., and Kazama, H. (2016). Decoding of context-dependent olfactory behavior in drosophila. *Neuron* 91, 155–167. doi: 10.1016/j.neuron.2016.05.022

Baker, K. L., Dickinson, M., Findley, T. M., Gire, D. H., Louis, M., Suver, M. P., et al. (2018). Algorithms for olfactory search across species. *J. Neurosci.* 38, 9383–9389. doi: 10.1523/JNEUROSCI.1668-18.2018

Baker, T. C. (2008).Balanced olfactory antagonism as a concept for understanding evolutionary shifts in moth sex pheromone blends. *J. Chem. Ecol.* 34, 971–981. doi: 10.1007/s10886-008-9468-9465

Baker, T. C., Fadamiro, H. Y., and Cosse, A. A. (1998). Moth uses fine tuning for odour resolution. *Nature* 393, 530–530. doi: 10.1038/31131

Baker, T. C., Willis, M. A., Haynes, K. F., and Phelan, P. L. (1985). A pulsed cloud of sex pheromone elicits upwind flight in male moths. *Physiol. Entomol.* 10, 257–265. doi: 10.1111/j.1365-3032.1985.tb00045.x

Belanger, J. H., and Arbas, E. A. (1998). Behavioral strategies underlying pheromone-modulated flight in moths: lessons from simulation studies. *J. Comp. Physiol. A* 183, 345–360. doi: 10.1007/s003590050261

Beyaert, I., and Hilker, M. (2014). Plant odour plumes as mediators of plant-insect interactions. *Biol. Rev. Camb. Philos. Soc.* 89, 68–81. doi: 10.1111/brv.12043

Bhandawat, V., Maimon, G., Dickinson, M. H., and Wilson, R. I. (2010). Olfactory modulation of flight in Drosophila is sensitive, selective and rapid. *J. Exp. Biol.* 213, 3625–3635. doi: 10.1242/jeb.040402

Bjostad, L. B. (1987). "Mechanisms in insect olfaction," in *The Quarterly Review of Biology*, eds T. L. Payne, M. C. Birch, and C. E. J. Kennedy, (Oxford): Lady Margaret Hall), 220–220.

Boie, S. D., Connor, E. G., McHugh, M., Nagel, K. I., Ermentrout, G. B., Crimaldi, J. P., et al. (2018). Information-theoretic analysis of realistic odor plumes: what cues are useful for determining location? *PLoS Comput. Biol.* 14:e1006275. doi: 10.1371/journal.pcbi.1006275

Broome, B. M., Jayaraman, V., and Laurent, G. (2006). Encoding and decoding of overlapping odor sequences. *Neuron* 51, 467–482. doi: 10.1016/j.neuron.2006.07.018

Brown, S. L., Joseph, J., and Stopfer, M. (2005). Encoding a temporally structured stimulus with a temporally structured neural representation. *Nat. Neurosci.* 8, 1568–1576. doi: 10.1038/nn1559

Bruce, T. J. A., Wadhams, L. J., and Woodcock, C. M. (2005). Insect host location: a volatile situation. *Trends Plant Sci.* 10, 269–274. doi: 10.1016/j.tplants.2005.04.003

Buehlmann, C., Graham, P., Hansson, B. S., and Knaden, M. (2014). Desert ants locate food by combining high sensitivity to food odors with extensive crosswind runs. *Curr. Biol.* 24, 960–964. doi: 10.1016/j.cub.2014.02.056

Buehlmann, C., Graham, P., Hansson, B. S., and Knaden, M. (2015). Desert ants use olfactory scenes for navigation. *Anim. Behav.* 106, 99–105. doi: 10.1016/j.anbehav.2015.04.029

Bushdid, C., Magnasco, M. O., Vosshall, L. B., and Keller, A. (2014). Humans can discriminate more than 1 trillion olfactory stimuli. *Science* 343, 1370–1372. doi: 10.1126/science.1249168

Cardé, R. T. (2016). "Moth navigation along pheromone plumes," in *Pheromone Communication in Moths*, eds J. D. Allison, and R. T. Carde, (Berkeley, CA: University of California Press), 173–190. doi: 10.1525/9780520964433-012

Cardé, R. T., and Willis, M. A. (2008). Navigational strategies used by insects to find distant, wind-borne sources of odor. *J. Chem. Ecol.* 34, 854–866. doi: 10.1007/s10886-008-9484-9485

Carlsson, M. A., Galizia, C. G., and Hansson, B. S. (2002). Spatial representation of odours in the antennal lobe of the moth *Spodoptera littoralis* (Lepidoptera: Noctuidae). *Chem. Senses* 27, 231–244. doi: 10.1093/chemse/27.3.231

Celani, A., Villermaux, E., and Vergassola, M. (2014). Odor landscapes in turbulent environments. *Phys. Rev. X* 4:041015. doi: 10.1103/physrevx.4.041015

Chan, H. K., Hersperger, F., Marachlian, E., Smith, B. H., Locatelli, F., Szyszka, P., et al. (2018). Odorant mixtures elicit less variable and faster responses than pure odorants. *PLoS Comput. Biol.* 14:e1006536. doi: 10.1371/journal.pcbi.1006536

Christensen, T. A., Mustaparta, H., and Hilderbrand, J. G. (1989). Discrimination of sex pheromone blends in the olfactory system of the moth. *Chem. Senses* 14, 463–477. doi: 10.1093/chemse/14.3.463

Clifford, M. R., and Riffell, J. A. (2013). Mixture and odorant processing in the olfactory systems of insects: a comparative perspective. *J. Comp. Physiol. A Neuroethol. Sens. Neural Behav. Physiol.* 199, 911–928. doi: 10.1007/s00359-013-0818-6

Cometto-Muñiz, J. E., Cain, W. S., and Abraham, M. H. (2003). Quantification of chemical vapors in chemosensory research. *Chem. Senses* 28, 467–477. doi: 10.1093/chemse/28.6.467

Conchou, L., Lucas, P., Meslin, C., Proffit, M., Staudt, M., and Renou, M. (2019). Insect odorscapes: from plant volatiles to natural olfactory scenes. *Front. Physiol.* 10:972. doi: 10.3389/fphys.2019.00972

Connor, E. G., McHugh, M. K., and Crimaldi, J. P. (2018). Quantification of airborne odor plumes using planar laser-induced fluorescence. *Exp. Fluids* 59:137. doi: 10.1007/s00348-018-2591

Cramer, I.-I. E., Record, F. A., and Vaughan, H. C. (1958). *The Study of the Diffusion of Gases or Aerosols in the Lower Atmosphere. Department of Meteorology*. Cambridge, MA: MIT.

David, C. T., Kennedy, J. S., and Ludlow, A. R. (1983). Finding of a sex pheromone source by gypsy moths released in the field. *Nature* 303, 804–806. doi: 10.1038/303804a0

Davies, B. M., Jones, C. D., Manning, A. J., and Thomson, D. J. (2000). Some field experiments on the interaction of plumes from two sources. *Q. J. R. Meteorol. Soc.* 126, 1343–1366. doi: 10.1256/smsqj.56507

de Bruyne, M., Clyne, P. J., and Carlson, J. R. (1999). Odor coding in a model olfactory organ: the Drosophila maxillary palp. *J. Neurosci.* 19, 4520–4532. doi: 10.1523/jneurosci.19-11-04520.1999

de Vreese, C., and Martinez-Ortiz, C. (2018). "Message from the eScience 2018 program committee chairs for the focused session on advances in escience for the humanities and social sciences," in *Proceedings of the 2018 IEEE 14th International Conference on e-Science (e-Science)*, Amsterdam.

Deisig, N., Giurfa, M., Lachnit, H., and Sandoz, J.-C. (2006). Neural representation of olfactory mixtures in the honeybee antennal lobe. *Eur. J. Neurosci.* 24, 1161–1174. doi: 10.1111/j.1460-9568.2006.04959.x

Dobritsa, A. A., van der Goes van Naters, W., Warr, C. G., Alexander Steinbrecht, R., and Carlson, J. R. (2003). Integrating the molecular and cellular basis of odor coding in the drosophila antenna. *Neuron* 37, 827–841. doi: 10.1016/s0896-6273(03)00094-91

Dorn, S., Natale, D., Mattiacci, L., Hern, A., Pasqualini, E., and Dorn, S. (2003). Response of female cydia molesta (Lepidoptera: Tortricidae) to plant derived volatiles. *Bull. Entomol. Res.* 93, 335–342. doi: 10.1079/ber2003250

Duplat, J., Innocenti, C., and Villermaux, E. (2010). A nonsequential turbulent mixing process. *Phys. Fluids* 22:035104. doi: 10.1063/1.3319821

Dusenbery, D. B. (1989). Optimal search direction for an animal flying or swimming in a wind or current. *J. Chem. Ecol.* 15, 2511–2519. doi: 10.1007/BF01014727

Dusenbery, D. B. (1996). Information is where you find it. *Biol. Bull.* 191.1, 124–128.

Elkinton, J. S., Cardé, R. T., and Mason, C. J. (1984). Evaluation of time-average dispersion models for estimating pheromone concentration in a deciduous forest. *J. Chem. Ecol.* 10, 1081–1108. doi: 10.1007/bf00987515

Erskine, A. (2018). *Perception and Representation of Temporally Patterned Odour Stimuli in the Mammalian Olfactory Bulb*. London: UCL.

Erskine, A., Bus, T., Herb, J. T., and Schaefer, A. T. (2019). AutonoMouse: high throughput operant conditioning reveals progressive impairment with graded olfactory bulb lesions. *PLoS One* 14:e0211571. doi: 10.1371/journal.pone.0211571

Fackrell, J. E., and Robins, A. G. (1982a). Concentration fluctuations and fluxes in plumes from point sources in a turbulent boundary layer. *J. Fluid Mech.* 117, 1–26. doi: 10.1017/s0022112082001499

Fackrell, J. E., and Robins, A. G. (1982b). The effects of source size on concentration fluctuations in plumes. *Boundary Layer Meteorol.* 22, 335–350. doi: 10.1007/bf00120014

Fadamiro, H., and Baker, T. (1997). Helicoverpa zea males (Lepidoptera: Noctuidae) respond to the intermittent fine structure of their sex pheromone

plume and an antagonist in a flight tunnel. *Physiol. Entomol.* 22, 316–324. doi: 10.1046/j.1365-3032.1997.d01-1.x

Falkovich, G., Gawedzki, K., and Vergassola, M. (2001). Particles and fields in fluid turbulence. *Rev. Mod. Phys.* 73, 913–975. doi: 10.1103/revmodphys.73.913

Fares, Y., Sharpe, P. J., and Magnuson, C. E. (1980). Pheromone dispersion in forests. *J. Theor. Biol.* 84, 335–359. doi: 10.1016/s0022-5193(80)80010-5

Foo, K. Y., and Hameed, B. H. (2010). Insights into the modeling of adsorption isotherm systems. *Chem. Eng. J.* 156, 2–10. doi: 10.1016/j.cej.2009.09.013

Galizia, C. G., Giovanni Galizia, C., Sachse, S., Rappert, A., and Menzel, R. (1999). The glomerular code for odor representation is species specific in the honeybee Apis mellifera. *Nat. Neurosci.* 2, 473–478. doi: 10.1038/8144

Galizia, C. G., Münch, D., Strauch, M., Nissler, A., and Ma, S. (2010). Integrating heterogeneous odor response data into a common response model: a DoOR to the complete olfactome. *Chem. Senses* 35, 551–563. doi: 10.1093/chemse/bjq042

Gallager, R. G. (1996). *Discrete Stochastic Processes*. Boston, MA: Springer.

Gaskell, D. R. (2003). *Introduction to the Thermodynamics of Materials*, 5th Edn, Boca Raton, FL: CRC Press.

Gaudry, Q., Nagel, K. I., and Wilson, R. I. (2012). Smelling on the fly: sensory cues and strategies for olfactory navigation in Drosophila. *Curr. Opin. Neurobiol.* 22, 216–222. doi: 10.1016/j.conb.2011.12.010

Geffen, M. N., Broome, B. M., Laurent, G., and Meister, M. (2009). Neural encoding of rapidly fluctuating odors. *Neuron* 61, 570–586. doi: 10.1016/j.neuron.2009.01.021

Gerkin, R. C., and Castro, J. B. (2015). The number of olfactory stimuli that humans can discriminate is still unknown. *Elife* 4:e08127. doi: 10.7554/eLife.08127

Gifford, F. (1959). Statistical properties of a fluctuating plume dispersion model. *Adv. Geophys.* 6, 117–137. doi: 10.1016/s0065-2687

Gomez-Marin, A., Stephens, G. J., and Louis, M. (2011). Active sampling and decision making in Drosophila chemotaxis. *Nat. Commun.* 2:441. doi: 10.1038/ncomms1455

Gorur-Shandilya, S., Demir, M., Long, J., Clark, D. A., and Emonet, T. (2017). Olfactory receptor neurons use gain control and complementary kinetics to encode intermittent odorant stimuli. *eLife* 6:e27670. doi: 10.7554/eLife.27670

Gorur-Shandilya, S., Martelli, C., Demir, M., and Emonet, T. (2019). Controlling and measuring dynamic odorant stimuli in the laboratory. *bioRxiv* [Preprint]. doi: 10.1101/733055

Guerrieri, F., Schubert, M., Sandoz, J.-C., and Giurfa, M. (2005). Perceptual and neural olfactory similarity in honeybees. *PLoS Biol.* 3:e60. doi: 10.1371/journal.pbio.0030060

Hallem, E. A., and Carlson, J. R. (2006). Coding of odors by a receptor repertoire. *Cell* 125, 143–160. doi: 10.1016/j.cell.2006.01.050

Hanna, S. R. (1984). Concentration fluctuations in a smoke plume. *Atmos. Environ.* 18, 1091–1106. doi: 10.1016/0004-6981(84)90141-90140

Hecht, S. (1942). Energy, quanta, and vision. *J. Gen. Physiol.* 25, 819–840. doi: 10.1085/jgp.25.6.819

Huston, S. J., Stopfer, M., Cassenaer, S., Aldworth, Z. N., and Laurent, G. (2015). Neural Encoding of odors during active sampling and in turbulent plumes. *Neuron* 88, 403–418. doi: 10.1016/j.neuron.2015.09.007

Hutchison, B. A., and Baldocchi, D. D. (1989). "Forest meteorology," in *Analysis of Biogeochemical Cycling Processes in Walker Branch Watershed* (New York, NY: Springer), 21–95.

Ito, I., Bazhenov, M., Ong, R. C.-Y., Raman, B., and Stopfer, M. (2009). Frequency transitions in odor-evoked neural oscillations. *Neuron* 64, 692–706. doi: 10.1016/j.neuron.2009.10.004

Jacob, V., Monsempès, C., Rospars, J.-P., Masson, J.-B., and Lucas, P. (2017). Olfactory coding in the turbulent realm. *PLoS Comput. Biol.* 13:e1005870. doi: 10.1371/journal.pcbi.1005870

Justus, K. A., Murlis, J., Jones, C., and Cardé, R. T. (2002). *Environmental Fluid Mechanics*. Dordrecht: Kluwer Academic Publishers.

Kaissling, K.-E. (1997). Pheromone-controlled anemotaxis in moths. *Orientat. Commun. Arthropods* 84, 343–374. doi: 10.1007/978-3-0348-8878-3-12

Kennedy, J. S., Ludlow, A. R., and Sanders, C. J. (1981). Guidance of flying male moths by wind-borne sex pheromone. *Physiol. Entomol.* 6, 395–412. doi: 10.1111/j.1365-3032.1981.tb00655.x

Kim, A. J., Lazar, A. A., and Slutskiy, Y. B. (2011). System identification of Drosophila olfactory sensory neurons. *J. Comput. Neurosci.* 30, 143–161. doi: 10.1007/s10827-010-0265-0

Kim, A. J., Lazar, A. A., and Slutskiy, Y. B. (2015). Projection neurons in Drosophila antennal lobes signal the acceleration of odor concentrations. *eLife* 4:e06651. doi: 10.7554/eLife.06651

Koehl, M. A. R. (2006). The fluid mechanics of arthropod sniffing in turbulent odor plumes. *Chem. Senses* 31, 93–105. doi: 10.1093/chemse/bjj009

Kree, M., Duplat, J., and Villermaux, E. (2013). The mixing of distant sources. *Phys. Fluids* 25:091103. doi: 10.1063/1.4820015

Kuenen, L. P. S., and Cardé, R. T. (1994). Strategies for recontacting a lost pheromone plume: casting and upwind flight in the male gypsy moth. *Physiol. Entomol.* 19, 15–29. doi: 10.1111/j.1365-3032.1994.xtb01069.x

Langmuir, I. (1932). Vapor pressures, evaporation, condensation and adsorption. *J. Am. Chem. Soc.* 54, 2798–2832. doi: 10.1021/ja01346a022

Laurent, G., and Davidowitz, H. (1994). Encoding of olfactory information with oscillating neural assemblies. *Science* 265, 1872–1875. doi: 10.1126/science.265.5180.1872

Lei, H., Chiu, H.-Y., and Hildebrand, J. G. (2013). Responses of protocerebral neurons in Manduca sexta to sex-pheromone mixtures. *J. Comp. Physiol. A Neuroethol. Sens. Neural Behav. Physiol.* 199, 997–1014. doi: 10.1007/s00359-013-0844-4

Lei, H., Riffell, J. A., Gage, S. L., and Hildebrand, J. G. (2009). Contrast enhancement of stimulus intermittency in a primary olfactory network and its behavioral significance. *J. Biol.* 8:21. doi: 10.1186/jbiol120

Leonard, A. S., Dornhaus, A., and Papaj, D. R. (2011). Flowers help bees cope with uncertainty: signal detection and the function of floral complexity. *J. Exp. Biol.* 214, 113–121. doi: 10.1242/jeb.047407

Lewellen, W. S., and Sykes, R. I. (1986). Analysis of concentration fluctuations from lidar observations of atmospheric plumes. *J. Clim. Appl. Meteorol.* 25, 1145–1154. doi: 10.1175/1520-0450(1986)025<1145:aocffl>2.0.co;2

Li, C., Dong, H., and Zhao, K. (2018). A balance between aerodynamic and olfactory performance during flight in Drosophila. *Nat. Commun.* 9:3215. doi: 10.1038/s41467-018-05708-1

Loudon, C. (2003). "The biomechanical design of an insect antenna as an odor capture device," in *Insect Pheromone Biochemistry and Molecular Biology* (London: Academic Press), 609–630. doi: 10.1016/b978-012107151-6/50023-2

Louis, M., Piccinotti, S., and Vosshall, L. B. (2008). High-resolution measurement of odor-driven behavior in Drosophila larvae. *J. Vis. Exp.* 3:638. doi: 10.3791/638

Mafra-Neto, A., and Cardé, R. T. (1994). Fine-scale structure of pheromone plumes modulates upwind orientation of flying moths. *Nature* 369, 142–144. doi: 10.1038/369142a0

Martelli, C., Carlson, J. R., and Emonet, T. (2013). Intensity invariant dynamics and odor-specific latencies in olfactory receptor neuron response. *J. Neurosci.* 33, 6285–6297. doi: 10.1523/JNEUROSCI.0426-12.2013

Martelli, C., and Fiala, A. (2019). Slow presynaptic mechanisms that mediate adaptation in the olfactory pathway of. Drosophila. *eLife* 8:e43735. doi: 10.7554/eLife.43735

Martin, J. P., Lei, H., Riffell, J. A., and Hildebrand, J. G. (2013). Synchronous firing of antennal-lobe projection neurons encodes the behaviorally effective ratio of sex-pheromone components in male Manduca sexta. *J. Comp. Physiol. A Neuroethol. Sens. Neural Behav. Physiol.* 199, 963–979. doi: 10.1007/s00359-013-0849-z

Mazor, O., and Laurent, G. (2005). Transient dynamics versus fixed points in odor representations by locust antennal lobe projection neurons. *Neuron* 48, 661–673. doi: 10.1016/j.neuron.2005.09.032

Meister, M. (2015). On the dimensionality of odor space. *Elife* 4:e07865. doi: 10.7554/eLife.07865

Mohamed, A. A. M., Retzke, T., Das Chakraborty, S., Fabian, B., Hansson, B. S., Knaden, M., et al. (2019). Odor mixtures of opposing valence unveil inter-glomerular crosstalk in the Drosophila antennal lobe. *Nat. Commun.* 10:1201. doi: 10.1038/s41467-019-09069-1

Mole, N., and Jones, C. D. (1994). Concentration fluctuation data from dispersion experiments carried out in stable and unstable conditions. *Boundary Layer Meteorol.* 67, 41–74. doi: 10.1007/bf00705507

Moore, P., and Crimaldi, J. (2004). Odor landscapes and animal behavior: tracking odor plumes in different physical worlds. *J. Mar. Syst.* 49, 55–64. doi: 10.1016/j.jmarsys.2003.05.005

Münch, D., and Galizia, C. G. (2016). DoOR 2.0–comprehensive mapping of drosophila melanogaster odorant responses. *Sci. Rep.* 6:21841. doi: 10.1038/srep21841

Murlis, J., Elkinton, J. S., and Cardé, R. T. (1992). Odor plumes and how insects use them. *Ann. Rev. Entomol.* 37, 505–532. doi: 10.1146/annurev.en.37.010192.002445

Murlis, J., Willis, M. A., and Carde, R. T. (2000). Spatial and temporal structures of pheromone plumes in fields and forests. *Physiol. Entomol.* 25, 211–222. doi: 10.1046/j.1365-3032.2000.00176.x

Mylne, K. R. (1992). Concentration fluctuation measurements in a plume dispersing in a stable surface layer. *Boundary Layer Meteorol.* 60, 15–48. doi: 10.1007/bf00122060

Mylne, K. R., Davidson, M. J., and Thomson, D. J. (1996). Concentration fluctuation measurements in tracer plumes using high and low frequency response detectors. *Boundary Layer Meteorol.* 79, 225–242. doi: 10.1007/bf00119439

Mylne, K. R., and Mason, P. J. (1991). Concentration fluctuation measurements in a dispersing plume at a range of up to 1000 m. *Q. J. R. Meteorol. Soc.* 117, 177–206. doi: 10.1002/qj.49711749709

Myrick, A. J., and Baker, T. C. (2011). Locating a compact odor source using a four-channel insect electroantennogram sensor. *Bioinspir. Biomim.* 6:016002. doi: 10.1088/1748-3182/6/1/016002

Myrick, A. J., Park, K. C., Hetling, J. R., and Baker, T. C. (2009). Detection and discrimination of mixed odor strands in overlapping plumes using an insect-antenna-based chemosensor system. *J. Chem. Ecol.* 35, 118–130. doi: 10.1007/s10886-008-9582-4

Nagel, K. I., and Wilson, R. I. (2011). Biophysical mechanisms underlying olfactory receptor neuron dynamics. *Nat. Neurosci.* 14, 208–216. doi: 10.1038/nn.2725

Najar-Rodriguez, A. J., Galizia, C. G., Stierle, J., and Dorn, S. (2010). Behavioral and neurophysiological responses of an insect to changing ratios of constituents in host plant-derived volatile mixtures. *J. Exp. Biol.* 213, 3388–3397. doi: 10.1242/jeb.046284

Najar-Rodriguez, A. J., Galizia, C. G., Stierle, J., and Dorn, S. (2011). Behavioural and neurophysiological responses of an insect to changing ratios of constituents in host plant-derived volatile mixtures. *J. Exp. Biol.* 214, 162–162. doi: 10.1242/jeb.054262

Nowotny, T., Stierle, J. S., Galizia, C. G., and Szyszka, P. (2013). Data-driven honeybee antennal lobe model suggests how stimulus-onset asynchrony can aid odour segregation. *Brain Res.* 1536, 119–134. doi: 10.1016/j.brainres.2013.05.038

Olsen, S. R., Bhandawat, V., and Wilson, R. I. (2010). Divisive normalization in olfactory population codes. *Neuron* 66, 287–299. doi: 10.1016/j.neuron.2010.04.009

Olsson, S. B., Kuebler, L. S., Veit, D., Steck, K., Schmidt, A., Knaden, M., et al. (2011). A novel multicomponent stimulus device for use in olfactory experiments. *J. Neurosci. Methods* 195, 1–9. doi: 10.1016/j.jneumeth.2010.09.020

Pang, R., van Breugel, F., Dickinson, M., Riffell, J. A., and Fairhall, A. (2018). History dependence in insect flight decisions during odor tracking. *PLoS Comput. Biol.* 14:e1005969. doi: 10.1371/journal.pcbi.1005969

Pang, S., and Farrell, J. A. (2006). Chemical plume source localization. *IEEE Trans. Syst. Man Cybern. B Cybern.* 36, 1068–1080. doi: 10.1109/tsmcb.2006.874689

Pelz, D., Roeske, T., Syed, Z., de Bruyne, M., and Galizia, C. G. (2006). The molecular receptive range of an olfactory receptor in vivo (Drosophila melanogaster Or22a). *J. Neurobiol.* 66, 1544–1563. doi: 10.1002/neu.20333

Perez, M., Giurfa, M., and d'Ettorre, P. (2015). The scent of mixtures: rules of odour processing in ants. *Sci. Rep.* 5:8659. doi: 10.1038/srep08659

Rabe, M., Verdes, D., and Seeger, S. (2011). Understanding protein adsorption phenomena at solid surfaces. *Adv. Colloid Inter. Sci.* 162, 87–106. doi: 10.1016/j.cis.2010.12.007

Raguso, R. A. (2008). Wake up and smell the roses: the ecology and evolution of floral scent. *Ann. Rev. Ecol. Evol. Syst.* 39, 549–569. doi: 10.1146/annurev.ecolsys.38.091206.095601

Rauner, J. L. (1976). "Deciduous forests," in *Vegation and the Atmosphere, Case Studies*, Vol. II ed. J. L. Monteith (London: Academic Press), 241–264.

Riffell, J. A. (2012). Olfactory ecology and the processing of complex mixtures. *Curr. Opin. Neurobiol.* 22, 236–242. doi: 10.1016/j.conb.2012.02.013

Riffell, J. A., Abrell, L., and Hildebrand, J. G. (2008). Physical processes and real-time chemical measurement of the insect olfactory environment. *J. Chem. Ecol.* 34, 837–853. doi: 10.1007/s10886-008-9490-7

Riffell, J. A., Lei, H., Christensen, T. A., and Hildebrand, J. G. (2009a). Characterization and coding of behaviorally significant odor mixtures. *Curr. Biol.* 19, 335–340. doi: 10.1016/j.cub.2009.01.041

Riffell, J. A., Lei, H., and Hildebrand, J. G. (2009b). Neural correlates of behavior in the moth Manduca sexta in response to complex odors. *Proc. Natl. Acad. Sci. U.S.A.* 106, 19219–19226. doi: 10.1073/pnas.0910592106

Rokni, D., Hemmelder, V., Kapoor, V., and Murthy, V. N. (2014). An olfactory cocktail party: figure-ground segregation of odorants in rodents. *Nat. Neurosci.* 17, 1225–1232. doi: 10.1038/nn.3775

Rospars, J.-P., Rospars, J., Lansky, P., Chaput, M., and Duchamp-Viret, P. (2008). Competitive and noncompetitive odorant interactions in the early neural coding of odorant mixtures. *J. Neurosci.* 28, 2659–2666. doi: 10.1523/jneurosci.4670-07.2008

Sachse, S., Rappert, A., and Galizia, C. G. (1999). The spatial representation of chemical structures in the antennal lobe of honeybees: steps towards the olfactory code. *Eur. J. Neurosci.* 11, 3970–3982. doi: 10.1046/j.1460-9568.1999.00826.x

Samimy, M., Breuer, K. S., Leal, L. G., and Steen, P. H. (2004). *A Gallery of Fluid Motion*. Cambridge: Cambridge University Press.

Schmuker, M., Bahr, V., and Huerta, R. (2016). Exploiting plume structure to decode gas source distance using metal-oxide gas sensors. *Sens. Actuators B Chem.* 235, 636–646. doi: 10.1016/j.snb.2016.05.098

Schubert, M., Sandoz, J.-C., Galizia, G., and Giurfa, M. (2015). Odourant dominance in olfactory mixture processing: what makes a strong odourant? *Proc. Biol. Sci.* 7:282. doi: 10.1098/rspb.2014.2562

Sehdev, A., and Szyszka, P. (2019). Segregation of unknown odors from mixtures based on stimulus onset asynchrony in honey bees. *Front. Behav. Neurosci.* 13:155. doi: 10.3389/fnbeh.2019.00155

Sell, C. S. (2006). On the unpredictability of odor. *Angew. Chem. Int. Ed. Engl.* 45, 6254–6261. doi: 10.1002/anie.200600782

Shirtcliffe, N. (2008). Surface chemistry of solid and liquid interfaces. *Erbil. Chem. Phys. Chem.* 9, 646–647. doi: 10.1002/cphc.200700726

Shraiman, B. I., and Siggia, E. D. (2000). Scalar turbulence. *Nature* 405, 639–646.

Stensmyr, M. C., Dweck, H. K. M., Farhan, A., Ibba, I., Strutz, A., Mukunda, L., et al. (2012). A conserved dedicated olfactory circuit for detecting harmful microbes in Drosophila. *Cell* 151, 1345–1357. doi: 10.1016/j.cell.2012.09.046

Stensmyr, M. C., Giordano, E., Balloi, A., Angioy, A.-M., and Hansson, B. S. (2003). Novel natural ligands for Drosophila olfactory receptor neurones. *J. Exp. Biol.* 206, 715–724. doi: 10.1242/jeb.00143

Stierle, J. S., Galizia, C. G., and Szyszka, P. (2013). Millisecond stimulus onset-asynchrony enhances information about components in an odor mixture. *J. Neurosci.* 33, 6060–6069. doi: 10.1523/jneurosci.5838-12.2013

Su, C.-Y., Menuz, K., Reisert, J., and Carlson, J. R. (2012). Non-synaptic inhibition between grouped neurons in an olfactory circuit. *Nature* 492, 66–71. doi: 10.1038/nature11712

Su, C.-Y., Su, C., Martelli, C., Emonet, T., and Carlson, J. R. (2011). Temporal coding of odor mixtures in an olfactory receptor neuron. *Proc. Natl. Acad. Sci. U.S.A.* 108, 5075–5080. doi: 10.1073/pnas.1100369108

Suh, G. S. B., Wong, A. M., Hergarden, A. C., Wang, J. W., Simon, A. F., Benzer, S., et al. (2004). A single population of olfactory sensory neurons mediates an innate avoidance behaviour in Drosophila. *Nature* 431, 854–859. doi: 10.1038/nature02980

Szyszka, P., Gerkin, R. C., Galizia, C. G., and Smith, B. H. (2014). High-speed odor transduction and pulse tracking by insect olfactory receptor neurons. *Proc. Natl. Acad. Sci. U.S.A.* 111, 16925–16930. doi: 10.1073/pnas.1412051111

Szyszka, P., and Stierle, J. S. (2014). Mixture processing and odor-object segregation in insects. *Prog. Brain Res.* 208, 63–85. doi: 10.1016/B978-0-444-63350-7.00003-6

Szyszka, P., Stierle, J. S., Biergans, S., and Giovanni Galizia, C. (2012). The speed of smell: odor-object segregation within milliseconds. *PLoS One* 7:e36096. doi: 10.1371/journal.pone.0036096

Thistle, H. W., Peterson, H., Allwine, G., Lamb, B., Strand, T., Holsten, E. H., et al. (2004). Surrogate pheromone plumes in three forest trunk spaces: composite statistics and case studies. *Forest Sci.* 50, 610–625.

Thoma, M., Hansson, B. S., and Knaden, M. (2014). Compound valence is conserved in binary odor mixtures in Drosophila melanogaster. *J. Exp. Biol.* 217, 3645–3655. doi: 10.1242/jeb.106591

Tinsley, J. N., Molodtsov, M. I., Prevedel, R., Wartmann, D., Espigulé-Pons, J., Lauwers, M., et al. (2016). Direct detection of a single photon by humans. *Nat. Commun.* 7:12172. doi: 10.1038/ncomms12172

Turin, L. (2002). A method for the calculation of odor character from molecular structure. *J. Theor. Biol.* 216, 367–385. doi: 10.1006/jtbi.2001.2504

van Breugel, F., and Dickinson, M. H. (2014). Plume-tracking behavior of flying Drosophila emerges from a set of distinct sensory-motor reflexes. *Curr. Biol.* 24, 274–286. doi: 10.1016/j.cub.2013.12.023

van Breugel, F., Huda, A., and Dickinson, M. H. (2018). Distinct activity-gated pathways mediate attraction and aversion to CO2 in Drosophila. *Nature* 564, 420–424. doi: 10.1038/s41586-018-0732

van Breugel, F., Morgansen, K., and Dickinson, M. H. (2014). Monocular distance estimation from optic flow during active landing maneuvers. *Bioinspir. Biomim.* 9:025002. doi: 10.1088/1748-3182/9/2/025002

van der Goes van Naters, W., and Carlson, J. R. (2007). Receptors and neurons for fly odors in drosophila. *Curr. Biol.* 17, 606–612. doi: 10.1016/j.cub.2007.02.043

Van Dyke, M. (1982). *An Album of Fluid Motion*. Stanford, CA: Parabolic Agency.

Vergara, A., Fonollosa, J., Mahiques, J., Trincavelli, M., Rulkov, N., and Huerta, R. (2013). On the performance of gas sensor arrays in open sampling systems using inhibitory support vector machines. *Sens. Actuators B Chem.* 185, 462–477. doi: 10.1016/j.snb.2013.05.027

Vetter, R. S., Sage, A. E., Justus, K. A., Cardé, R. T., and Galizia, C. G. (2006). Temporal integrity of an airborne odor stimulus is greatly affected by physical aspects of the odor delivery system. *Chem. Senses* 31, 359–369. doi: 10.1093/chemse/bjj040

Vickers, N. J. (2000). Mechanisms of animal navigation in odor plumes. *Biol. Bull.* 198, 203–212. doi: 10.2307/1542524

Vickers, N. J. (2006). Winging it: moth flight behavior and responses of olfactory neurons are shaped by pheromone plume dynamics. *Chem. Senses* 31, 155–166. doi: 10.1093/chemse/bjj011

Vickers, N. J., and Baker, T. C. (1994). Reiterative responses to single strands of odor promote sustained upwind flight and odor source location by moths. *Proc. Natl. Acad. Sci. U.S.A.* 91, 5756–5760. doi: 10.1073/pnas.91.13.5756

Visser, J. H., and Avé, D. A. (1978). General green leaf volatiles in the olfactory orientation of the colorado beetle, leptinotarsa decemlineata. *Entomol. Exp. Appl.* 24, 738–749. doi: 10.1111/j.1570-7458.1978.tb02838.x

Voskamp, K., den Otter, C. J., and Noorman, N. (1998). Electroantennogram responses of tsetse flies (Glossina pallidipes) to host odours in an open field and riverine woodland. *Physiol. Entomol.* 23, 176–183. doi: 10.1046/j.1365-3032.1998.232070.x

Voskamp, K. E., Everaarts, E., and Den Otter, C. J. (1999). Olfactory responses to attractants and repellents in tsetse. *Med. Vet. Entomol.* 13, 386–392. doi: 10.1046/j.1365-2915.1999.00187.x

Wallach, A., Marom, S., and Ahissar, E. (2016). "Closing dewey's circuit," in *Closed Loop Neuroscience* (London: Elsevier Science), 93–100. doi: 10.1016/b978-0-12-802452-2.00007-x

Webster, B., and Cardé, R. T. (2017). Use of habitat odour by host-seeking insects. *Biol. Rev. Camb. Philos. Soc.* 92, 1241–1249. doi: 10.1111/brv.12281

Webster, D. R., and Weissburg, M. J. (2001). Chemosensory guidance cues in a turbulent chemical odor plume. *Limnol. Oceanogr.* 46, 1034–1047. doi: 10.4319/lo.2001.46.5.1034

Wee, S. L., Oh, H. W., and Park, K. C. (2016). Antennal sensillum morphology and electrophysiological responses of olfactory receptor neurons in trichoid sensilla of the diamondback moth (Lepidoptera: Plutellidae). *Fla. Entomol.* 99, 146–158. doi: 10.1653/024.099.sp118

Weissburg, M. J. (2000). The fluid dynamical context of chemosensory behavior. *Biol. Bull.* 198, 188–202. doi: 10.2307/1542523

Willis, M. A., and Baker, T. C. (1984). Effects of intermittent and continuous pheromone stimulation on the flight behaviour of the oriental fruit moth, *Grapholita molesta*. *Physiol. Entomol.* 9, 341–358. doi: 10.1111/j.1365-3032.1984.tb00715.x

Wilson, C. D., Serrano, G. O., Koulakov, A. A., and Rinberg, D. (2017). A primacy code for odor identity. *Nat. Commun.* 8:1477. doi: 10.1038/s41467-017-01432-4

Wilson, R. I. (2013). Early olfactory processing in Drosophila: mechanisms and principles. *Annu. Rev. Neurosci.* 36, 217–241. doi: 10.1146/annurev-neuro-062111-150533

Wright, G. A., Lutmerding, A., Dudareva, N., and Smith, B. H. (2005). Intensity and the ratios of compounds in the scent of snapdragon flowers affect scent discrimination by honeybees (Apis mellifera). *J. Comp. Physiol. A* 191, 105–114. doi: 10.1007/s00359-004-0576-576

Wright, R. H. (1958). The olfactory guidance of flying insects. *Can. Entomol.* 90, 81–89. doi: 10.4039/ent9081-2

Xiao, W., Matsuyama, S., Ando, T., Millar, J. G., and Honda, H. (2012). Unsaturated cuticular hydrocarbons synergize responses to sex attractant pheromone in the yellow peach moth, conogethes punctiferalis. *J. Chem. Ecol.* 38, 1143–1150. doi: 10.1007/s10886-012-0176-179

Yee, E., Chan, R., Kosteniuk, P. R., Chandler, G. M., Biltoft, C. A., and Bowers, J. F. (1995). Measurements of level-crossing statistics of concentration fluctuations in plumes dispersing in the atmospheric surface layer. *Boundary Layer Meteorol.* 73, 53–90. doi: 10.1007/bf00708930

Yee, E., Kosteniuk, P. R., Chandler, G. M., Biltoft, C. A., and Bowers, J. F. (1993). Statistical characteristics of concentration fluctuations in dispersing plumes in the atmospheric surface layer. *Boundary Layer Meteorol.* 65, 69–109. doi: 10.1007/bf00708819

Zavada, A., Buckley, C. L., Martinez, D., Rospars, J.-P., and Nowotny, T. (2011). Competition-based model of pheromone component ratio detection in the moth. *PLoS One* 6:e16308. doi: 10.1371/journal.pone.0016308

Zhang, Y., Tsang, T. K., Bushong, E. A., Chu, L.-A., Chiang, A.-S., Ellisman, M. H., et al. (2019). Asymmetric ephaptic inhibition between compartmentalized olfactory receptor neurons. *Nat. Commun.* 10:1560. doi: 10.1101/427252

Zhou, Y., Smith, B. H., and Sharpee, T. O. (2018). Hyperbolic geometry of the olfactory space. *Sci. Adv.* 4:eaaq1458. doi: 10.1126/sciadv.aaq1458

Conflict of Interest: The authors declare that the research was conducted in the absence of any commercial or financial relationships that could be construed as a potential conflict of interest.

frontiers in Physiology

BRIEF RESEARCH REPORT
published: 20 December 2019
doi: 10.3389/fphys.2019.01518

Exposure to Conspecific and Heterospecific Sex-Pheromones Modulates Gustatory Habituation in the Moth *Agrotis ipsilon*

Camille Hostachy, Philippe Couzi, Guillaume Portemer, Melissa Hanafi-Portier†, Meena Murmu†, Nina Deisig† and Matthieu Dacher*

CNRS, INRA, IRD, Institute for Ecology and Environmental Sciences of Paris, Sorbonne Universite, Universite Paris Est Creteil, Paris, France

In several insects, sex-pheromones are essential for reproduction and reproductive isolation. Pheromones generally elicit stereotyped behaviors. In moths, these are attraction to conspecific sex-pheromone sources and deterrence for heterospecific sex-pheromone. Contrasting with these innate behaviors, some results in social insects point toward effects of non-sex-pheromones on perception and learning. We report the effects of sex-pheromone pre-exposure on gustatory perception and habituation (a non-associative learning) in male *Agrotis ipsilon* moths, a non-social insect. We also studied the effect of Z5-decenyl acetate (Z5), a compound of the sex-pheromone of the related species *Agrotis segetum*. We hypothesized that conspecific sex-pheromone and Z5 would have opposite effects. Pre-exposure to either the conspecific sex-pheromone or Z5 lasted 15 min and was done either immediately or 24 h before the experiments, using their solvent alone (hexane) as control. In a sucrose responsiveness assay, pre-exposure to the conspecific sex-pheromone had no effect on the dose-response curve at either delays. By contrast, Z5 slightly improved sucrose responsiveness 15 min but not 24 h after pre-exposure. Interestingly, the conspecific sex-pheromone and Z5 had time-dependent effects on gustatory habituation: pre-exposing the moths with Z5 hindered learning after immediate but not 24-h pre-exposure, whereas pre-exposure to the conspecific sex-pheromone hindered learning at 24-h but not immediate pre-exposure. They did not have opposite effects. This is the first time a sex-pheromone is reported to affect learning in a non-social insect. The difference in modulation between conspecific sex-pheromone and Z5 suggests that con- and hetero-specific sex-pheromones act on plasticity through different cerebral pathways.

Keywords: insect, moth, gustatory perception, sugar responsiveness, non-associative learning, habituation, proboscis extension response, pheromone

OPEN ACCESS

Edited by:
Sylvia Anton,
Institut National de la Recherche Agronomique (INRA), France

Reviewed by:
Fernando J. Guerrieri,
Université de Tours, France
Paul G. Becher,
Swedish University of Agricultural Sciences, Sweden

***Correspondence:**
Matthieu Dacher
matthieu.dacher@upmc.fr

†Present address:
Melissa Hanafi-Portier,
MNHN, Institut de Systématique, Évolution, Biodiversité, Paris, France;
Laboratoire Environnement Profond, IFREMER, Plouzane, France
Meena Murmu,
CEA, Institut des Sciences du Vivant Frédéric Joliot, Université Paris-Saclay, Paris, France
Nina Deisig,
Institut für Zoologie, University of Cologne, Köln, Germany

Specialty section:
This article was submitted to Invertebrate Physiology, a section of the journal Frontiers in Physiology

Received: *11 July 2019*
Accepted: *03 December 2019*
Published: *20 December 2019*

Citation:
Hostachy C, Couzi P, Portemer G, Hanafi-Portier M, Murmu M, Deisig N and Dacher M (2019) Exposure to Conspecific and Heterospecific Sex-Pheromones Modulates Gustatory Habituation in the Moth Agrotis ipsilon. Front. Physiol. 10:1518. doi: 10.3389/fphys.2019.01518

INTRODUCTION

Males of many moths species display a stereotyped, very specific, and innate attraction response to the sex-pheromone released by conspecific females (Allison and Cardé, 2016a). They are also able to detect and avoid heterospecific sex-pheromones from related sympatric species, which favors reproductive isolation (Renou et al., 1996; Allison and Cardé, 2016b). These attraction/deterrence responses are crucial for moth reproduction. As these insects are exquisitely sensitive to their sex-pheromone, they have been studied a lot as models of odor specialist. Moreover, as many moth species are crop pests, behavioral manipulation by use of pheromones is an important tool for managing their populations (Cook et al., 2007; Witzgall et al., 2010; Cork, 2016; Evenden, 2016). Therefore, studying their responses to pheromones has also important applications. These features make moths important models to study how pheromone can trigger stereotyped behaviors.

While pheromones are classically described as elicitor of stereotyped behaviors, in bees and mammals non-sex-pheromones can modulate plasticity (Coureaud et al., 2006; Vergoz et al., 2007; Bredy and Barad, 2009; Jouhanneau et al., 2016). In particular, reports in bees point toward effects on gustatory learning and perception (Pankiw and Page, 2003; Urlacher et al., 2010; Baracchi et al., 2017). Many examples in moths show interactions between reproduction and gustatory perception and learning (Awmack and Leather, 2002; Geister et al., 2008; Shikano and Isman, 2009; Molleman, 2010; Minoli et al., 2012; Briscoe et al., 2013; Petit et al., 2015). Therefore, it is reasonable to hypothesize that sex-pheromones could also interact with the perception and learning of gustatory information in these insects.

Observing proboscis extension response (PER) is a convenient experimental procedure to investigate gustatory functions: when the insect antennae contact a sugar solution of sufficient concentration, a moth extends its proboscis (i.e., releases a PER). Thus, this reflex allows to assess sucrose-linked behaviors in restrained moths, which is relevant as sugars are their main food in nature (under the form of nectar). Using standardized dose-response curves, PER assays have been used to assess sucrose responsiveness in moths (Hostachy et al., 2019), as well as in bees (Scheiner et al., 2004a) and flies (Scheiner et al., 2004b). PER can also be used to train and study animals in a non-associative learning called gustatory habituation. In habituation, an animal decreases and stops its response to a stimulus, if this stimulus is ongoing or repeated and the animal does not undergo any consequence when stimulated; using a dishabituation test then confirms this response inhibition cannot be explained by fatigue or sensory adaptation (Rankin et al., 2009; Blumstein, 2016). Such dishabituation test consists in presenting of a more intense (or different) stimulus, and to observe whether the response to the original stimulus has been restored. It is easy to habituate the PER upon repeated presentations of a low-concentration sucrose solution on the antennae without feeding the animals: in that case, antennal stimulations cease eliciting the PER. Beyond moths, this protocol has been applied in bees and flies (Duerr and Quinn, 1982; Braun and Bicker, 1992; Dacher and Gauthier, 2008). Habituation can be modulated by non-sex-pheromones in bees (Baracchi et al., 2017). It is established that PER-based learning are relevant to natural conditions (Gerber et al., 1996; Sandoz et al., 2000; Chaffiol et al., 2005; Gil and De Marco, 2005; Riffell et al., 2013). Habituation leads to ignore irrelevant stimuli, which allows a reallocation of resources (Mennemeier et al., 1994; Dukas, 2002, 2004; Ramaswami, 2014; Turatto and Pascucci, 2016).

In this article, we took advantage of the PER to explore the links between reproduction and gustation in moths by assessing whether their sex-pheromone can modulate sucrose responsiveness and gustatory habituation. Male *Agrotis ipsilon* moths were thus pre-exposed to either their conspecific sex-pheromone or a heterospecific sex-pheromone compound of a related sympatric species (*Agrotis segetum*), which they can perceive and avoid (Renou et al., 1996). We then assessed whether this pre-exposure affects sucrose responsiveness or gustatory habituation either immediately or 24 h after exposition, as previous results suggest sex-pheromone elicits long-term effects (increase of the response to the sex-pheromone itself, Anderson et al., 2003, 2007). These pheromones were chosen with the idea that *A. ipsilon* sex-pheromone would be "positive" whereas *A. segetum* compound would be "negative" (as defined by Baracchi et al., 2017) as they are respectively attractive and deterrent for *A. ipsilon* males. Thus, we made the hypothesis that they would have opposite effects.

MATERIALS AND METHODS

Animals

Male *Agrotis ipsilon* (Lepidoptera, Noctuidae) were reared in our breeding facilities in Versailles, France. Adults were kept in climatic chambers (22°C, 60–70% relative humidity) and under an inverted light-dark cycle (16 h of light, starting at 18 h) as they are nocturnal insects. They were used 5 days after emergence and were provided with water *ad libitum* instead of the sucrose solution normally offered as a food source. This 5-day starvation duration optimizes the responses to sucrose without making the animals weak (Hostachy et al., 2019). Moreover, at this age, they have reached the peak of their sensitivity to the sex-pheromone. Males and females were separated at the pupal stage, so that animals were naive for the sex-pheromone before pre-exposure.

Experiments were performed between 13 and 17 h (activity peak of the animals) under dim red light. Before 10 h, animals were restrained in small tubes (made with cut 1 ml pipette cones) and their position was secured with adhesive tape and a small ball of absorbing paper behind them, so that only their heads (including antennae and proboscis) protruded from the tube.

Pheromone Pre-exposure

A behaviorally active blend consisting of Z7-dodecenyl-acetate, Z9-tetradecenyl-acetate, and Z11-hexadecenyl-acetate in a 4:1:4

Abbreviations: PER, Proboscis extension response; Z5, Z5-decenyl acetate.

ratio was used as conspecific sex-pheromone (Picimbon et al., 1997). The precise ratio of each blend was checked by gas chromatography. We also used Z5-decenyl acetate (Z5), one of the main compounds of the sex-pheromone of *Agrotis segetum*. Both the conspecific sex-pheromone and heterospecific Z5 were diluted in hexane (10 ng/µl). Pheromonal compounds were purchased from Pherobank[1] (Wijk bij Duurstede, Netherlands).

Pre-exposure was performed by positioning the moth during 15 min in a glass vial (2.5 cm diameter, 6 cm length) containing a small filter paper with 10 ng of conspecific sex-pheromone or Z5. This 15-min pre-exposure was performed either immediately or 24 h before performing sucrose responsiveness or gustatory habituation protocols. Moths were already restrained for the 15-min pre-exposure. The filter paper was prepared before by depositing 1 µl of conspecific sex-pheromone or Z5 in solution in hexane, waiting for hexane to vaporize, and then putting the paper into the vial. Control animals followed the same procedure except that the filter paper had 1 µl hexane without conspecific sex-pheromone or Z5.

Sucrose Responsiveness

The standardized sucrose responsiveness assay was described for moths by Hostachy et al. (2019), adapting Scheiner's protocol previously developed for bees and flies (Scheiner et al., 2004a,b). This assay consisted in presenting to each moth a succession of sucrose solutions of logarithmically increasing concentrations (0, 0.1, 0.3, 1, 3, 10, 30% and again 0%, weight/weight). Each presentation (every 10 min) consisted in touching both antennae during 1–4 s with a toothpick imbibed with one of the sucrose solution, and to record whether a PER was elicited; animals were not fed. A dose-response curve was then obtained, displaying for each sucrose concentration the PER rate (i.e., the percentage of moth exhibiting a PER in response to the antennal stimulation with the sucrose solution). Animals spontaneously responding to the initial water presentation were not kept in the analysis (although keeping them would not change the conclusions, data not shown). In these experimental conditions, the sugar presentations can be considered as independent of each other. Indeed, it was previously observed that presenting the solutions in a random order did not change the PER rates (Hostachy et al., 2019).

Gustatory Habituation

The habituation protocol consisted in presenting a 3% (weight/weight) sucrose solution for 1–4 s every 10 s on both antennae without feeding the animal. The habituation criterion was defined as failing to release a PER to four consecutive presentations. Moths reaching this criterion were then submitted to a dishabituation test, consisting in presenting a 66% (weight/weight) sucrose solution and then the initial 3% solution. This restored the PER in most of these animals, which were then considered habituated. Resuming the response indicates fatigue or sensory adaptation cannot explain their reaching the habituation criterion (Rankin et al., 2009). Animals not responding to the first 3% presentation or not dishabituating were removed from the analysis. However, the proportions of such animals were compared across the treatments. Otherwise, animals reaching 30 sucrose presentations without habituating were considered as non-habituated. Sucrose concentrations and inter-trial interval were established after preliminary experiments and allows to clearly and reliably notice the occurrence of habituation while keeping the protocol practicable. While more moths can be habituated by going beyond 30 trials (i.e., 5 min per animal), this also increases the duration of the experiment without making the analysis more sensitive.

Data Analysis

Statistics were performed with R 3.6, using an α risk of 5%. In sucrose responsiveness experiments, χ^2 was used to compare PER rates of different groups for each sugar concentration. Fisher's exact test was used when χ^2's assumption were not respected (i.e., when Cochran's criterion was not met). Subsequent pairwise comparisons were made when the global test was significant using the same test (χ^2 or Fisher's exact test) and adjusting p for multiple comparisons with Holm's method.

For habituation experiments, survival analyses were made using Cox regression (a survival analysis) to compare the probability of habituating between Z5- or conspecific sex-pheromone-treated animals and the control group (hexane-treated animals). Validity of the proportional hazard hypothesis in the Cox regression was confirmed by the Schoenfeld test (data not shown). Cox regression is particularly appropriate to analyze such data, as it can take into account the fact not all animals reach the habituation criterion. To compare the proportions of animals not responding to the first presentation of the 3% sucrose solution among all the animals initially tested, we used χ^2 or Fisher's exact test. Similarly, these tests were used to compare across the treatments the proportion of animals failing to dishabituate among those reaching the habituation criterion.

RESULTS

Sucrose Responsiveness After Sex Pheromone Pre-exposure

Moths were pre-exposed for 15 min to either conspecific sex-pheromone, Z5 or hexane immediately before having their sucrose responsiveness assessed (**Figure 1A**). Animals exposed to Z5 had significantly higher response rates than those exposed to sex-pheromone or hexane for 3% sucrose concentrations (χ^2, adjusted $p \leq 0.037$), whereas these two groups did not differ (χ^2, adjusted $p = 0.451$). Similarly, Z5- and pheromone-exposed animals differed for 1% sucrose concentrations (χ^2, adjusted $p = 0.001$), although neither of them differed from hexane-exposed animals (χ^2, adjusted $p = 0.094$ for both comparisons). This suggest a short-term Z5 pre-exposure somewhat increases sucrose responsiveness.

The same experiment was performed with a 24 h delay between pre-exposure and the assay (**Figure 1B**). Response

[1]http://www.pherobank.com

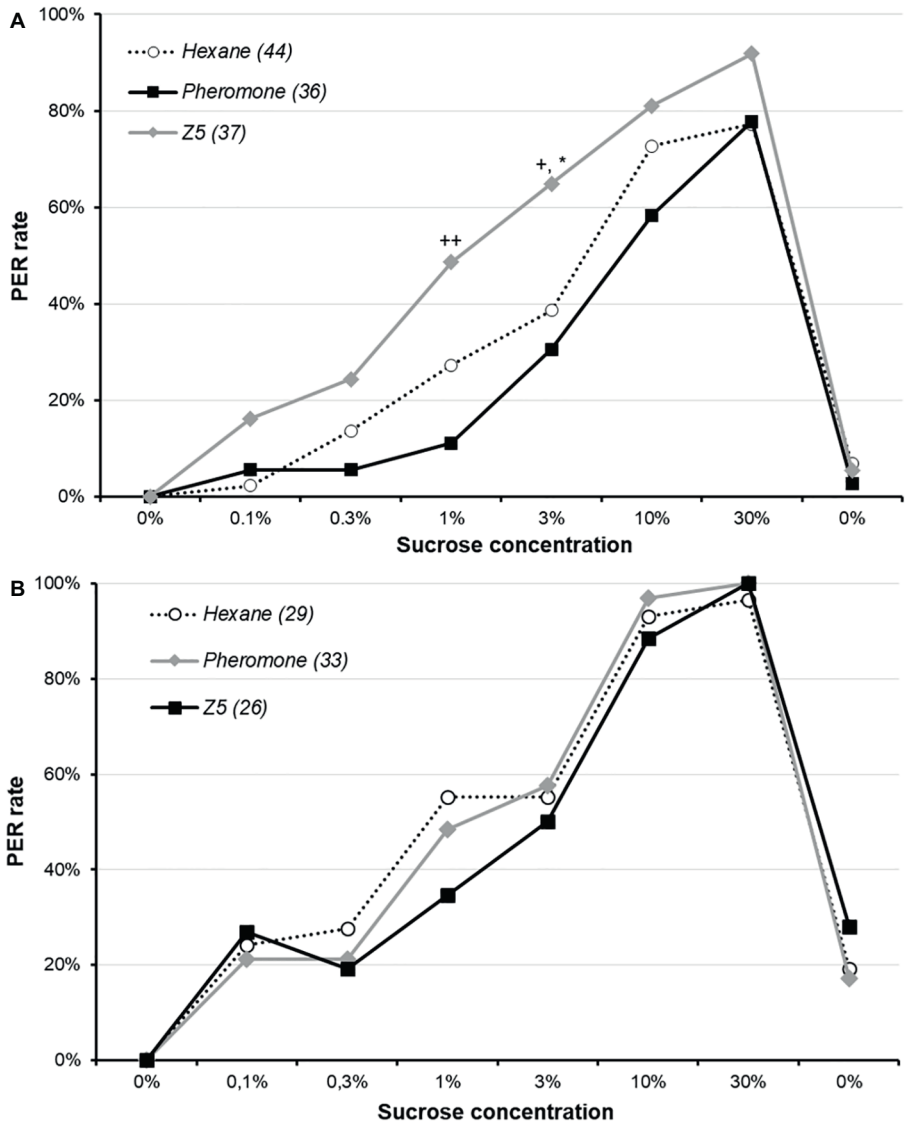

FIGURE 1 | Effect of sex-pheromone on sucrose responsiveness in male *Agrotis ipsilon*. The x-axis reports the successive sucrose solutions, and the y-axis the PER rate (i.e., percentage of animals responding by a PER). Each curve corresponds to a treatment (i.e., pre-exposure to hexane, pheromone or Z5), and values in parenthesis are the sample sizes. In part **A**, animals were exposed to either hexane, conspecific sex-pheromone or Z5 during 15 min before undertaking the sucrose responsiveness assay. In part **B**, the pre-exposure was done for 15 min 24 h before the sucrose responsiveness assay. Stars denote a significant difference between Z5 and hexane (*χ^2, adjusted $p < 0.050$), and crosses between Z5 and conspecific sex-pheromone (χ^2; +: adjusted $p < 0.050$; ++: adjusted $p < 0.050$).

rates of three treatments did not significantly differ for any sucrose concentration (χ^2 or Fisher's exact test: $p \geq 0.301$). This indicates a long-term exposure to Z5 or conspecific sex-pheromone does not affect sucrose responsiveness.

Gustatory Habituation After Sex-Pheromone Pre-exposure

The gustatory habituation protocol was performed immediately after a 15 min pre-exposure of conspecific sex-pheromone, Z5 or hexane performed as previously (**Figure 2A**). There was no difference between the three groups for the initial PER rate to the 3% sucrose solution used in the protocol (χ^2, $p = 0.165$). This was unexpected, as we previously observed Z5 enhance the PER rate for this concentration. Animals not responding to this initial stimulation were discarded. Among animals reaching the habituation criterion at the end of the protocol, some were not able to dishabituate upon presentation of a 66% sucrose solution followed by a 3% sucrose solution, and were not used in the analysis. The proportion was the same across the three groups (χ^2, $p = 0.060$). Moths pre-exposed to their sex-pheromone did not differ from the control

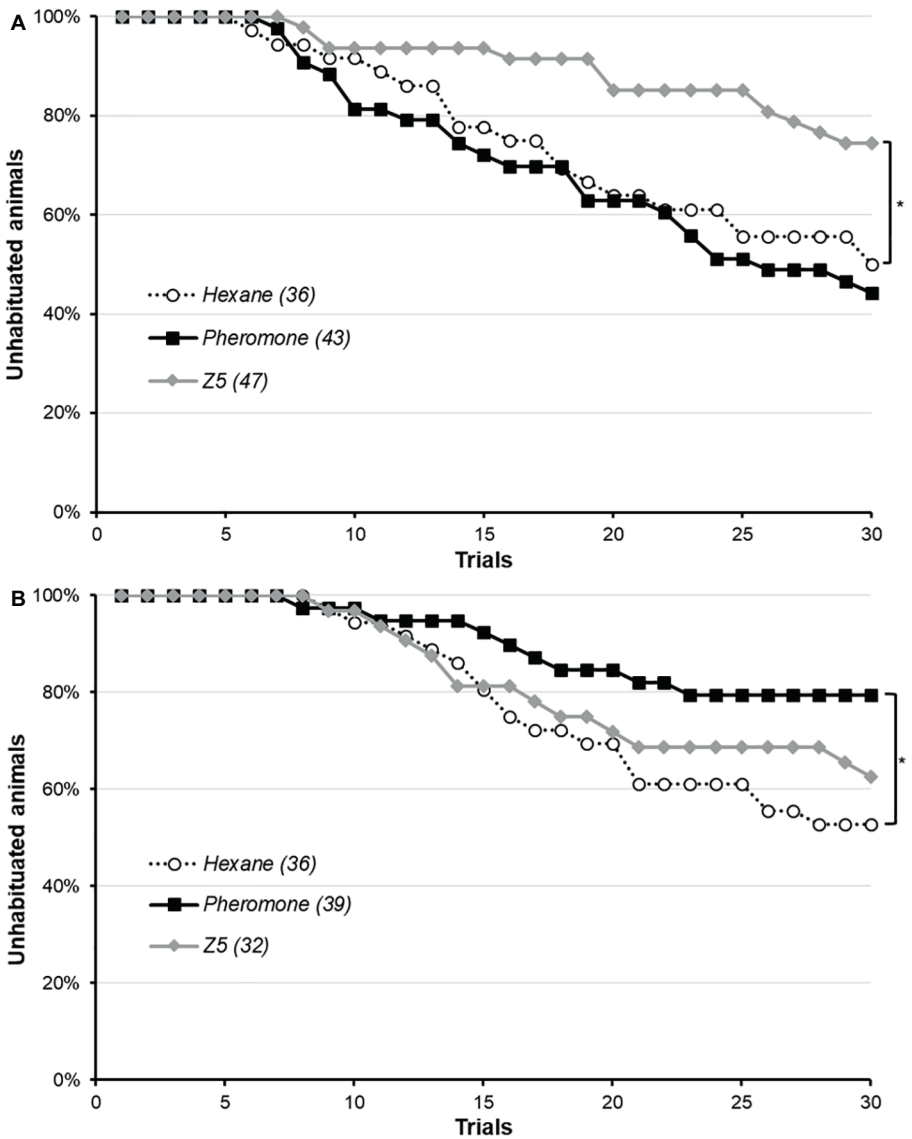

FIGURE 2 | Effect of conspecific sex-pheromone and Z5 on gustatory habituation in male *Agrotis ipsilon*. The x-axis shows the trials in the habituation protocol, and the y-axis the proportion of unhabituated moths, which starts at 100% and then decrease as more and more moths reach the habituation criterion. Each curve corresponds to a treatment (i.e., pre-exposure to hexane, conspecific sex-pheromone or Z5), and values in parenthesis are the sample sizes. In part **A**, the pre-exposure was done immediately before the habituation protocol and in part **B**, it was done 24 h before the habituation protocol. Significant difference with the control hexane group are denoted by a star (*: Cox regression, $p < 0.050$).

(Cox regression, $p = 0.578$), whereas pre-exposure to Z5 significantly hindered habituation (Cox regression, $p = 0.018$) as less animals had reached the habituation criterion at the end of the protocol. Interestingly, the opposite effect was observed for a pre-exposure 24 h before the protocol (**Figure 2B**): conspecific sex-pheromone significantly reduced habituation, whereas Z5 was not significantly different from the control (Cox regression: sex-pheromone, $p = 0.021$; Z5, $p = 0.460$). In this experiment, as expected the PER rate was the same in the three groups for the initial 3% sucrose solution (χ^2, $p = 0.152$), but the dishabituation rate was not the same (Fisher's exact test, $p = 0.037$): indeed, hexane- and sex-pheromone exposed animals always dishabituated, but not all Z5-exposed. Animals failing to dishabituate were not included in **Figure 2B**, nor in the analysis, and were a minority (for hexane, 17 were habituated and 19 not habituated, for a total of 36 moths and none failed to dishabituate; for conspecific sex-pheromone, 8 were habituated 31 not habituated, for a total of 39 moths and none failed to dishabituate; for Z5, 16 moths reached the habituation criterion but 4 of them did not dishabituate and were excluded, leaving 12 habituated moths and 20 not habituated for a total of 32 moths).

DISCUSSION

Responsiveness to sucrose was not modulated by a pre-exposition to conspecific sex-pheromone in male *A. ipsilon* moths. By contrast, the major pheromone component of a sympatric species (Z5) increased sucrose responsiveness but only at the short-term exposure. Furthermore, habituation, a form of non-associative learning was hindered by both pheromones, but at different delays: immediately but not 24 h after exposure for Z5, and 24 h but not immediately after exposure for the conspecific sex-pheromone.

Experiments in bees and ants have shown that pheromone exposure modulates sucrose responsiveness and performance during learning, including gustatory habituation (Pankiw and Page, 2003; Vergoz et al., 2007; Urlacher et al., 2010; Minoli et al., 2012; Baracchi et al., 2017; Rossi et al., 2018). Overall, pre-exposure to pheromone sensitizes or desensitize insects (according to the "positive" or "negative" value of the pheromone, Baracchi et al., 2017), thereby affecting their sucrose responsiveness. In our experiments, exposition to the conspecific sex-pheromone did not affect sucrose responsiveness. Thus, an effect on habituation through a modulation of sucrose responsiveness is excluded. By contrast, the fact that Z5 increases sucrose responsiveness is consistent with its impairing habituation to sucrose (even though it did not initially decrease the PER rate in this experiment). A striking difference is the temporal difference of conspecific sex-pheromone and Z5: the later acts immediately but not after 1 day (except for a small effect on dishabituation rate), whereas sex-pheromone needs 1 day to have an effect and only affects habituation. This indicates that they act through different pathways.

The neurophysiological mechanisms underlying these effects of conspecific sex-pheromone and Z5 remain an open question. Such mechanisms could involve biogenic amines. Indeed, these neurotransmitters modulate responsiveness to sucrose and learning (Scheiner et al., 2006, 2014), and biogenic amines are involved in sex-pheromone's actions (Duportets et al., 2010; Abrieux et al., 2014). A possible mechanism for pheromone effects would be that they could have a positive or negative valence for the animal: perceiving them as reward (conspecific sex-pheromone) or punishment (heterospecific sex-pheromone such as Z5) could explain their effect on learning (Coureaud et al., 2006; Vergoz et al., 2007; Jouhanneau et al., 2016; Baracchi et al., 2017). However, this is not what we observed; both conspecific sex-pheromone and Z5 had the same deterring effect on habituation rather than opposite ones.

Pheromonal modulation of gustatory habituation is an interaction between reproductive and feeding functions. Impairing gustatory habituation could mean moths are less prone to ignore food. In that frame, Z5 would do more than just prevent mating with incompatible females and would inform on the presence of competitors for food. In turn, habituation would be hindered (and sucrose sensitivity improved) upon detecting them, in order to promote eating in the context of competition for food. By contrast, this would not make sense anymore 24 h after. Similarly, conspecific sex-pheromone would indicate the presence of mates in the environment. While habituation should be maintained immediately after perceiving the pheromone, in the absence of mating 24 h after exposure food should not be ignored so as to gather resources to continue mate-searching. This is consistent with the observation that sucrose can sensitize the response to sex-pheromone (Minoli et al., 2012).

These hypotheses are arguably bold, but are testable as they make specific and strong predictions: presenting conspecific sex-pheromone both 24 h and immediately before mating would improve habituation, as the male would focus on mating rather than feeding.

To further investigate the functional relationships between feeding and reproduction, it would be interesting to assess the amount of sucrose consumed by *A. ipsilon* males having differing experiences with conspecific females (e.g., exposure, mating) and/or sex-pheromones (Sokolowski and Abramson, 2010). The same experiments could also be done with exposure to females of *A. segetum* and Z5. An interesting feature of males in some Lepidoptera species is puddling, i.e., drinking brackish water to get sodium needed for gamete formation (Smedley and Eisner, 1996; Boggs and Dau, 2004; Watanabe and Kamikubo, 2005; Molleman, 2010). Owing to our observations, it would also be relevant to assess whether puddling is modulated by exposure to sex-pheromones.

DATA AVAILABILITY STATEMENT

All datasets generated for this study are included in the article.

AUTHOR CONTRIBUTIONS

CH, ND, and MD designed the experiments. CH, PC, GP, MH-P, and MM performed the experiments. CH and MD prepared the figures and analyzed the data. MD wrote the first draft of the manuscript, and all authors contributed to manuscript revision, read and approved the submitted version.

FUNDING

This work was supported by Agence Nationale de la Recherche (project PheroMod, ANR grant number ANR-14-CE18-0003) and Sorbonne Université (project emergence HAPA, grant number SU-16-R-EMR-18-HAPA).

ACKNOWLEDGMENTS

We thank Thomas Chertemps for his comments on this article and technicians from iEES Paris for rearing the animals used in the experiments.

REFERENCES

Abrieux, A., Duportets, L., Debernard, S., Gadenne, C., and Anton, S. (2014). The GPCR membrane receptor, DopEcR, mediates the actions of both dopamine and ecdysone to control sex pheromone perception in an insect. *Front. Behav. Neurosci.* 8:312. doi: 10.3389/fnbeh.2014.00312

Allison, J. D., and Cardé, R. T. (Eds.) (2016a). *Pheromone communication in moths: Evolution, behavior and application.* Oakland, CA: University of California Press.

Allison, J. D., and Cardé, R. T. (2016b). "Pheromones: reproductive isolation and evolution in moths" in *Pheromone communication in moths.* eds. J. D. Allison and R. T. Cardé (Oakland, California: University of California Press), 11–23.

Anderson, P., Hansson, B. S., Nilsson, U., Han, Q., Sjoholm, M., Skals, N., et al. (2007). Increased behavioral and neuronal sensitivity to sex pheromone after brief odor experience in a moth. *Chem. Senses* 32, 483–491. doi: 10.1093/chemse/bjm017

Anderson, P., Sadek, M. M., and Hansson, B. S. (2003). Pre-exposure modulates attraction to sex pheromone in a moth. *Chem. Senses* 28, 285–291. doi: 10.1093/chemse/28.4.285

Awmack, C. S., and Leather, S. R. (2002). Host plant quality and fecundity in herbivorous insects. *Annu. Rev. Entomol.* 47, 817–844. doi: 10.1146/annurev.ento.47.091201.145300

Baracchi, D., Devaud, J. M., D'ettorre, P., and Giurfa, M. (2017). Pheromones modulate reward responsiveness and non-associative learning in honey bees. *Sci. Rep.* 7:9875. doi: 10.1038/s41598-017-10113-7

Blumstein, D. T. (2016). Habituation and sensitization: new thoughts about old ideas. *Anim. Behav.* 120, 255–262. doi: 10.1016/j.anbehav.2016.05.012

Boggs, C. L., and Dau, B. (2004). Resource specialization in Puddling Lepidoptera. *Environ. Entomol.* 33, 1020–1024. doi: 10.1603/0046-225X-33.4.1020

Braun, G., and Bicker, G. (1992). Habituation of an appetitive reflex in the honeybee. *J. Neurophysiol.* 67, 588–598.

Bredy, T. W., and Barad, M. (2009). Social modulation of associative fear learning by pheromone communication. *Learn. Mem.* 16, 12–18. doi: 10.1101/lm.1226009

Briscoe, A. D., Macias-Muñoz, A., Kozak, K. M., Walters, J. R., Yuan, F., Jamie, G. A., et al. (2013). Female behaviour drives expression and evolution of gustatory receptors in butterflies. *PLoS Genet.* 9:e1003620. doi: 10.1371/journal.pgen.1003620

Chaffiol, A., Laloi, D., and Pham-Delegue, M. H. (2005). Prior classical olfactory conditioning improves odour-cued flight orientation of honey bees in a wind tunnel. *J. Exp. Biol.* 208, 3731–3737. doi: 10.1242/jeb.01796

Cook, S. M., Khan, Z. R., and Pickett, J. A. (2007). The use of push-pull strategies in integrated pest management. *Annu. Rev. Entomol.* 52, 375–400. doi: 10.1146/annurev.ento.52.110405.091407

Cork, A. (2016). "Pheromones as management tools: mass trapping and lure-and-kill" in *Pheromone communication in moths: Evolution, behavior and application*. eds. J. D. Allison and R. T. Carde (Oakland, CA: University of California Press), 349–363.

Coureaud, G., Moncomble, A.-S., Montigny, D., Dewas, M., Perrier, G., and Schaal, B. (2006). A pheromone that rapidly promotes learning in the newborn. *Curr. Biol.* 16, 1956–1961. doi: 10.1016/j.cub.2006.08.030

Dacher, M., and Gauthier, M. (2008). Involvement of NO-synthase and nicotinic receptors in learning in the honey bee. *Physiol. Behav.* 95, 200–207. doi: 10.1016/j.physbeh.2008.05.019

Duerr, J. S., and Quinn, W. G. (1982). Three Drosophila mutations that block associative learning also affect habituation and sensitization. *Proc. Natl. Acad. Sci. USA* 79, 3646–3650.

Dukas, R. (2002). Behavioural and ecological consequences of limited attention. *Phil. Trand. R. Soc. Lond. B.* 357, 1539–1547. doi: 10.1098/rstb.2002.1063

Dukas, R. (2004). Causes and consequences of limited attention. *Brain Behav. Evol.* 63, 197–210. doi: 10.1159/000076781

Duportets, L., Barrozo, R. B., Bozzolan, F., Gaertner, C., Anton, S., Gadenne, C., et al. (2010). Cloning of an octopamine/tyramine receptor and plasticity of its expression as a function of adult sexual maturation in the male moth *Agrotis ipsilon*. *Insect Mol. Biol.* 19, 489–499. doi: 10.1111/j.1365-2583.2010.01009.x

Evenden, M. L. (2016). "Mating disruption of moth pests in integrated pest management: a mechanistic approach" in *Pheromone communication in moths: Evolution, behavior and application*. eds. J. D. Allison and R. T. Carde (Oakland, CA: University of California Press), 365–393.

Geister, T. L., Lorenz, M. W., Hoffmann, K. H., and Fischer, K. (2008). Adult nutrition and butterfly fitness: effects of diet quality on reproductive output, egg composition, and egg hatching success. *Front. Zool.* 5:10. doi: 10.1186/1742-9994-5-10

Gerber, B., Geberzahn, N., Hellstern, F., Klein, J., Kowalsky, O., Wüstenberg, D., et al. (1996). Honeybees transfer olfactory memories established during flower visits to a proboscis extension paradigm in the laboratory. *Anim. Behav.* 52, 1079–1085.

Gil, M., and De Marco, R. J. (2005). Olfactory learning by means of trophallaxis in *Apis mellifera*. *J. Exp. Biol.* 208, 671–680. doi: 10.1242/jeb.01474

Hostachy, C., Couzi, P., Hanafi-Portier, M., Portemer, G., Halleguen, A., Murmu, M., et al. (2019). Responsiveness to sugar solutions in the moth Agrotis ipsilon: parameters affecting proboscis extension. *Front. Physiol.* 10:1423. doi: 10.3389/fphys.2019.01423

Jouhanneau, M., Schaal, B., and Coureaud, G. (2016). Mammary pheromone-induced odour learning influences sucking behaviour and milk intake in the newborn rabbit. *Anim. Behav.* 111, 1–11. doi: 10.1016/j.anbehav.2015.10.003

Mennemeier, M. S., Chatterjee, A., Watson, R. T., Wertman, E., Carter, L. P., and Heilman, K. M. (1994). Contributions of the parietal and frontal lobes to sustained attention and habituation. *Neuropsychologia* 32, 703–716.

Minoli, S., Kauer, I., Colson, V., Party, V., Renou, M., Anderson, P., et al. (2012). Brief exposure to sensory cues elicits stimulus-nonspecific general sensitization in an insect. *PLoS One* 7:e34141. doi: 10.1371/journal.pone.0034141

Molleman, F. (2010). Puddling: from natural history to understanding how it affects fitness. *Entomol. Exp. Appl.* 134, 107–113. doi: 10.1111/j.1570-7458.2009.00938.x

Pankiw, T., and Page, R. E. (2003). Effect of pheromones, hormones, and handling on sucrose response thresholds of honey bees (*Apis mellifera* L.). *J. Comp. Physiol. A* 189, 675–684. doi: 10.1007/s00359-003-0442-y

Petit, C., Le Ru, B., Dupas, S., Frérot, B., Ahuya, P., Kaiser-Arnauld, L., et al. (2015). Influence of dietary experience on the induction of preference of adult moths and larvae for a new olfactory cue. *PLoS One* 10:e0136169. doi: 10.1371/journal.pone.0136169

Picimbon, J. F., Gadenne, C., Becard, J. M., Clement, J. L., and Sreng, L. (1997). Sex pheromone of the French black cutworm moth, *Agrotis ipsilon* (Lepidoptera: Noctuidae): identification and regulation of a multicomponent blend. *J. Chem. Ecol.* 23, 211–230.

Ramaswami, M. (2014). Network plasticity in adaptive filtering and behavioral habituation. *Neuron* 82, 1216–1229. doi: 10.1016/j.neuron.2014.04.035

Rankin, C. H., Abrams, T., Barry, R. J., Bhatnagar, S., Clayton, D. F., Colombo, J., et al. (2009). Habituation revisited: an updated and revised description of the behavioral characteristics of habituation. *Neurobiol. Learn. Mem.* 92, 135–138. doi: 10.1016/j.nlm.2008.09.012

Renou, M., Gadenne, C., and Tauban, D. (1996). Electrophysiological investigations of pheromone-sensitive sensilla in the hybrids between two moth species. *J. Insect Physiol.* 42, 267–277.

Riffell, J. A., Lei, H., Abrell, L., and Hildebrand, J. G. (2013). Neural basis of a pollinator's buffet: olfactory specialization and learning in *Manduca sexta*. *Science* 339, 200–204. doi: 10.1126/science.1225483

Rossi, N., D'ettorre, P., and Giurfa, M. (2018). Pheromones modulate responsiveness to a noxious stimulus in honey bees. *J. Exp. Biol.* 221:jeb172270. doi: 10.1242/jeb.172270

Sandoz, J. C., Laloi, D., Odoux, J. F., and Pham-Delegue, M. H. (2000). Olfactory information transfer in the honeybee: compared efficiency of classical conditioning and early exposure. *Anim. Behav.* 59, 1025–1034. doi: 10.1006/anbe.2000.1395

Scheiner, R., Baumann, A., and Blenau, W. (2006). Aminergic control and modulation of honeybee behaviour. *Curr. Neuropharmacol.* 4, 259–276. doi: 10.2174/157015906778520791

Scheiner, R., Page, R. E., and Erber, J. (2004a). Sucrose responsiveness and behavioral plasticity in honey bees (*Apis mellifera*). *Apidologie* 35, 133–142. doi: 10.1051/apido:2004001

Scheiner, R., Sokolowski, M. B., and Erber, J. (2004b). Activity of cGMP-dependent protein kinase (PKG) affects sucrose responsiveness and habituation in *Drosophila melanogaster*. *Learn. Mem.* 11, 303–311. doi: 10.1101/lm.71604

Scheiner, R., Steinbach, A., Claßen, G., Strudthoff, N., and Scholz, H. (2014). Octopamine indirectly affects proboscis extension response habituation in *Drosophila melanogaster* by controlling sucrose responsiveness. *J. Insect Physiol.* 69, 107–117. doi: 10.1016/j.jinsphys.2014.03.011

Shikano, I., and Isman, M. B. (2009). A sensitive period for larval gustatory learning influences subsequent oviposition choice by the cabbage looper moth. *Anim. Behav.* 77, 247–251. doi: 10.1016/j.anbehav.2008.08.033

Smedley, S. R., and Eisner, T. (1996). Sodium: a male moth's gift to its offspring. *Proc. Natl. Acad. Sci. USA* 93, 809–813.

Sokolowski, M. B. C., and Abramson, C. I. (2010). From foraging to operant conditioning: a new computer-controlled skinner box to study free-flying nectar gathering behavior in bees. *J. Neurosci. Meth.* 188, 235–242. doi: 10.1016/j.jneumeth.2010.02.013

Turatto, M., and Pascucci, D. (2016). Short-term and long-term plasticity in the visual-attention system: evidence from habituation of attentional capture. *Neurobiol. Learn. Mem.* 130, 159–169. doi: 10.1016/j.nlm.2016.02.010

Urlacher, E., Francés, B., Giurfa, M., and Devaud, J.-M. (2010). An alarm pheromone modulates appetitive olfactory learning in the honeybee (*Apis mellifera*). *Front. Behav. Neurosci.* 4:157. doi: 10.3389/fnbeh.2010.00157

Vergoz, V., Schreurs, H. A., and Mercer, A. R. (2007). Queen pheromone blocks aversive learning in young worker bees. *Science* 317, 384–386. doi: 10.1126/science.1142448

Watanabe, M., and Kamikubo, M. (2005). Effects of saline intake on spermatophore and sperm ejaculation in the male swallowtail butterfly *Papilio xuthus* (Lepidoptera: Papilionidae). *Entomol. Sci.* 8, 161–166. doi: 10.1111/j.1479-8298.2005.00114.x

Witzgall, P., Kirsch, P., and Cork, A. (2010). Sex pheromones and their impact on pest management. *J. Chem. Ecol.* 36, 80–100. doi: 10.1007/s10886-009-9737-y

Conflict of Interest: The authors declare that the research was conducted in the absence of any commercial or financial relationships that could be construed as a potential conflict of interest.

frontiers in Physiology

REVIEW
published: 08 January 2020
doi: 10.3389/fphys.2019.01540

DN1p or the "Fluffy" Cerberus of Clock Outputs

Angélique Lamaze and Ralf Stanewsky*

Institut für Neuro und Verhaltensbiologie, Westfälische Wilhelms University, Münster, Germany

Drosophila melanogaster is a powerful genetic model to study the circadian clock. Recently, three drosophilists received the Nobel Prize for their intensive past and current work on the molecular clockwork (Nobel Prize 2017). The *Drosophila* brain clock is composed of about 150 clock neurons distributed along the lateral and dorsal regions of the protocerebrum. These clock neurons control the timing of locomotor behaviors. In standard light–dark (LD) conditions (12–12 h and constant 25°C), flies present a bi-modal locomotor activity pattern controlled by the clock. Flies increase their movement just before the light-transitions, and these behaviors are therefore defined as anticipatory. Two neuronal oscillators control the morning and evening anticipation. Knowing that the molecular clock cycles in phase in all clock neurons in the brain in LD, how can we explain the presence of two behavioral activity peaks separated by 12 h? According to one model, the molecular clock cycles in phase in all clock neurons, but the neuronal activity cycles with a distinct phase in the morning and evening oscillators. An alternative model takes the environmental condition into consideration. One group of clock neurons, the dorso-posterior clock neurons DN1p, drive two peaks of locomotor activity in LD even though their neuronal activity cycles with the same phase (late night/early morning). Interestingly, the locomotor outputs they control differ in their sensitivity to light and temperature. Hence, they must drive outputs to different neuropil regions in the brain, which also receive different inputs. Since 2010 and the presentation of the first specific DN1p manipulations, many studies have been performed to understand the role of this group of neurons in controlling locomotor behaviors. Hence, we review what we know about this heterogeneous group of clock neurons and discuss the second model to explain how clock neurons that oscillate with the same phase can drive behaviors at different times of the day.

Keywords: *Drosophila melanogaster*, circadian clock, DN1p, locomotor activity, temperature response

OPEN ACCESS

Edited by:
Sylvia Anton,
Institut National de la Recherche Agronomique (INRA), France

Reviewed by:
Kenji Tomioka,
Okayama University, Japan
Frank Klaus Schubert,
University of Wuerzburg, Germany

****Correspondence:***
Angélique Lamaze
alamaze@uni-muenster.de;
angie0203@hotmail.com

Specialty section:
This article was submitted to Invertebrate Physiology, a section of the journal Frontiers in Physiology

Received: *19 September 2019*
Accepted: *05 December 2019*
Published: *08 January 2020*

Citation:
Lamaze A and Stanewsky R (2020) DN1p or the "Fluffy" Cerberus of Clock Outputs. Front. Physiol. 10:1540. doi: 10.3389/fphys.2019.01540

INTRODUCTION

The fundamental function of the circadian clock is to synchronize the organism with its ecological niche. The circadian period is genetically determined (Konopka and Benzer, 1971) and therefore, does not depend on the environment, like the ambient temperature for example. However, 24 h oscillations of environmental parameters, such as daily light and temperature cycles (TC), synchronize the clock. Also, clock-controlled behavior is phased (time of occurrence within the 24 h period) based on the current environmental status. An individual's locomotor activity pattern therefore depends on complex neuronal networks, integrating both environmental inputs and genetically encoded endogenous time information. *Drosophila melanogaster* is a reference model to study the circadian clock not only for its tremendous genetic advantages (Nobel prizes 2017), but it is also easy to tightly control the environment when it comes to study its locomotor behavior. When

isolated in a small glass tube, the "dew lover" *Drosophila* displays a highly plastic locomotor behavior that changes with light and temperature. In standard light–dark 12–12 h (LD) cycles and constant mild temperature (22–25°C), male flies present two peaks of locomotor activity. In the late night, flies start to wake up in a synchronous manner and increase their locomotor activity. The light transition induces a startle response, after which the activity decays and male flies start their siesta. Then, in the late afternoon, they again increase their locomotion in a synchronous manner "anticipating" the lights-off transition. Because these activities occur several hours before the light-transitions, they have been defined as anticipatory. However, at cooler temperatures (18°C), the morning anticipation is strongly dampened or delayed, while the evening one is advanced compared to 25°C. Inversely, at warmer temperatures (29°C), the amplitude of the morning anticipation increases and advances while the evening anticipation delays (Majercak et al., 1999).

In constant light and temperature (LL), fruit flies are arrhythmic. This is due to the constitutive degradation of the clock protein TIMELESS (TIM), mediated by the circadian photoreceptor *cryptochrome* (*cry*) (Stanewsky et al., 1998). However, flies can entrain to TC in LL (LLTC 25–16°C) (Glaser and Stanewsky, 2005; Yoshii et al., 2005). Nonetheless, the behavior observed when only light alternates is different from the one observed in LLTC, which is again different from the one observed in the same TC but in constant darkness (DD) (Gentile et al., 2013). In LLTC, we observe a unique anticipatory activity peak at the end of the thermophase, while in DDTC this peak shifts toward the beginning of the thermophase.

The *Drosophila* brain clock is composed of about 150 clock neurons (**Figure 1A**). In 2004, two labs showed that if a functional clock is restricted to a group of CRY^+ lateral neurons (LN) expressing the neuropeptide pigment dispersing factor (PDF), this is sufficient to drive the morning anticipation, which therefore was named lateral neurons-morning oscillator (LN-MO). In contrast, a clock restricted to LN expressing CRY but not PDF is sufficient to drive the evening anticipation (**Figure 1B**), and therefore was defined as lateral neurons-evening oscillator (LN-EO) (Grima et al., 2004; Stoleru et al., 2004).

In 2010, Zhang Y. et al. (2010) showed that a clock in a group of about 12 clock neurons located in the dorsal part of the protocerebrum, the DN1p, is sufficient to drive both morning and evening anticipation, albeit under distinct light and temperature conditions (**Figure 1C**). It was the first time that a group of clock neurons was found capable of controlling locomotor activity twice a day. By definition, a circadian output is a behavior that occurs every 24 h. Therefore, how do clock neurons with a 24-h molecular clock cycling in phase, control locomotor activity twice a day? Contrary to the EO and the MO whose neuronal activities cycle at different phase (Liang et al., 2016), the neuronal activity cycles in phase within the DN1p group (Flourakis et al., 2015; Liang et al., 2016). However, there is heterogeneity within this group. Half of them express *cry* (Benito et al., 2008), not all of them are glutamatergic (Hamasaka et al., 2007; Chatterjee et al., 2018) and a certain proportion of them express the neuropeptide DH31 (Kunst et al., 2014) or allatostatin-C (Diaz et al., 2019). It is still unclear which subgroup of DN1p controls the morning activity and which one controls the evening one, although the glutamatergic and CRY^+ DN1p seem to have a predominant role in regulating morning activity (Chatterjee et al., 2018).

To understand how DN1p clock neurons contribute to the complex circadian regulation of locomotor behavior, we review what is known about this intriguing cluster of neurons and will try to emphasize how their comprehension can help us to understand how neurons integrate and relay multiple inputs.

DN1p: A NON-AUTONOMOUS "CIRCADIAN" OSCILLATOR

By definition, circadian clocks tick autonomously. In the absence of environmental input (DD 25°C), organisms maintain their rhythm of about 24 h, they free run. In the *Drosophila* brain, clock proteins maintain their rhythms for days in most of the clock neurons including the DN1p, while most of the peripheral clocks stop their oscillations after a few days in constant condition (Veleri et al., 2003). However, in the absence of PDF or in the absence of PDF cells, the DN1p loose their oscillations in DD very quickly (Veleri et al., 2003; Klarsfeld et al., 2004; Yoshii et al., 2009), suggesting a dependency of these neurons on the LN-MO. Indeed, when the pace of the molecular clock is genetically modified in the LN-MO, clock proteins and *tim* mRNA oscillate in the DN1p following the pace of the LN-MO (Stoleru et al., 2005; Chatterjee et al., 2018). How do PDF neurons dictate the rhythm to the DN1p? When PDF links to its receptor (PDFR, a G protein-coupled receptor), this leads to an increase of cAMP (Shafer et al., 2008), which activates protein kinase A (PKA). Interestingly, Seluzicki et al. (2014) have observed that a rescue of PER oscillations specifically in the LN-MO is sufficient to drive TIM oscillations in DN1p. They suggested that PDF regulates TIM levels via a PKA signaling pathway (Seluzicki et al., 2014). However, we do not know whether TIM is directly phosphorylated and stabilized by PKA in a PDF-dependent manner. Nonetheless, this hypothesis provides a nice model of the DN1p pace-regulation by the LN-MO (**Figure 2**). Furthermore, in the absence of both CRY and PDF, PER expression in the DN1p becomes arrhythmic even in LD (Cusumano et al., 2009), reinforcing this dependency toward the LN-MO.

Hence, although they express the molecular circadian machinery, the DN1p miss an unknown element providing autonomy, potentially a factor that regulates TIM oscillations in a CRY and PDF independent manner. Like peripheral clocks, the DN1p are not autonomous and only maintain their rhythm in DD thanks to the PDF^+ pacemaker neurons.

THE ROLE OF DN1p IN REGULATING LOCOMOTOR BEHAVIOR IN CONSTANT DARKNESS

A rhythmic circadian output is defined by its period and the phase of its peak and trough. The period of a circadian output is genetically determined. However, the phase is determined by

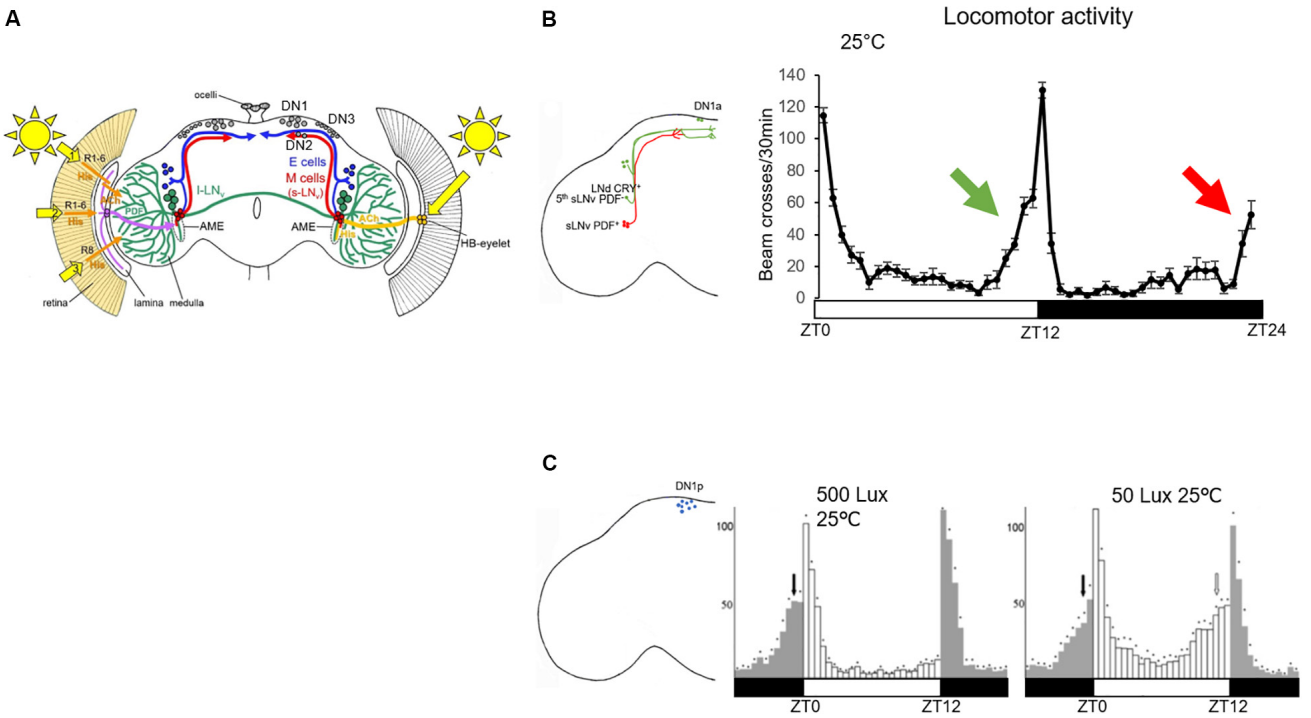

FIGURE 1 | Role of clock neurons in controlling the locomotor behavior in standard LD conditions. **(A)** Clock neurons in the *Drosophila* brain. Figure taken from Helfrich-Förster (2019). Numbers 1–3 indicate the three putative opsin-based light input pathways to the clock neurons in addition to the HB-eyelet input (Helfrich-Förster, 2019). The l-LNv are represented in green, the LN-EO (E cells) in blue and the LN-MO (M cells) in red. The dorsal neurons (DN1–DN3) are colored in gray. Their projection pattern is not shown. The axonal projections of the lateral neurons are located in the dorso-posterior area of the brain (except for the lLNv, which project to the ipsi- and contralateral medulla). Most of the clock neuron dendritic projections are in the accessory medulla (AME) (Li et al., 2018). **(B)** Left: schematic representation of the LN-MO and LN-EO only, with their output projections. Right: locomotor activity trace of a group of 31 control flies (iso31) in standard LD and constant 25°C. The green arrow indicates the control of the evening anticipation by the EO (green cells in the brain) and the red arrow the morning anticipation by the MO (red cells in the brain). **(C)** Left: schematic representation of DN1p cell bodies in the brain; right: locomotor activity traces of per^{0},*w;Clk4.1M-Gal4/UAS-per16* (functional clock only in the DN1p) taken from Zhang Y. et al. (2010) in two different light conditions. White bars represents 12 h of light, dark bars 12 h of darkness.

the interaction of the animal with its environment. In DD and constant temperature, the main peak of locomotor activity occurs in the subjective evening. The rhythm of this activity pattern is driven by the PDF^{+} neurons (Grima et al., 2004; Stoleru et al., 2004; **Figure 3A**). Interestingly, when a functional clock is restricted to these neurons, the flies remain rhythmic but their peak of activity shifts toward the subjective morning (Grima et al., 2004). Recently, Chatterjee et al. (2018) were able to change the phase of the DD locomotor activity without affecting the period by genetically modulating the speed of the DN1p clock: phase advanced when the clock was sped up and delayed when the pace was slowed down. While the PDF neurons determine the pace, the DN1p determine the phase. Therefore, we can propose that in the absence of light and temperature oscillations, the endogenous period of the locomotor rhythm is provided by the PDF^{+} neurons and the phase by the non-autonomous DN1p oscillator (**Figure 3A**). Hence, it seems logical to propose that the DN1p are downstream of the PDF neurons.

The DD locomotor rhythm of *pdf* mutant flies, or flies lacking its receptor (*pdfr*$^{-}$), is strongly dampened (Renn et al., 1999; Hyun et al., 2005). Interestingly, the rhythm strength can partially be restored when PDF reception is rescued only in DN1p neurons (Zhang L. et al., 2010). Nonetheless, flies are still rhythmic in DD when DN1p output is inhibited using the expression of tetanus toxin (Guo et al., 2016). Even more surprisingly, *gl60j* mutants that lack DN1p neurons are still rhythmic in DD (Helfrich-Förster et al., 2001; Klarsfeld et al., 2004), hence questioning a direct influence of the DN1p on DD rhythmicity.

Looking for downstream neurons important for DD rhythmicity, Cavanaugh et al. (2014) screened for neuronal drivers that lead to arrhythmic locomotor behavior when activated using the thermoreceptor dTrpA1. They identified 10 driver lines with the commonality of showing expression in neuroendocrine cells in the pars intercerebralis (PI), the fly functional homolog of the mammalian hypothalamus. They focused on a line (*kurs58*-Gal4) that is expressed in 16–18 cells in the PI. After a transcriptomic analysis of individual *kurs58* PI cells, they found that some of these neuroendocrine cells express the neuropeptide DH44 (six cells). DH44 is a diuretic hormone, the *Drosophila* homolog of the stress hormone corticotrophin releasing factor (CRF) (Cabrero et al., 2002) and downregulation of DH44 expression using a pan neuronal

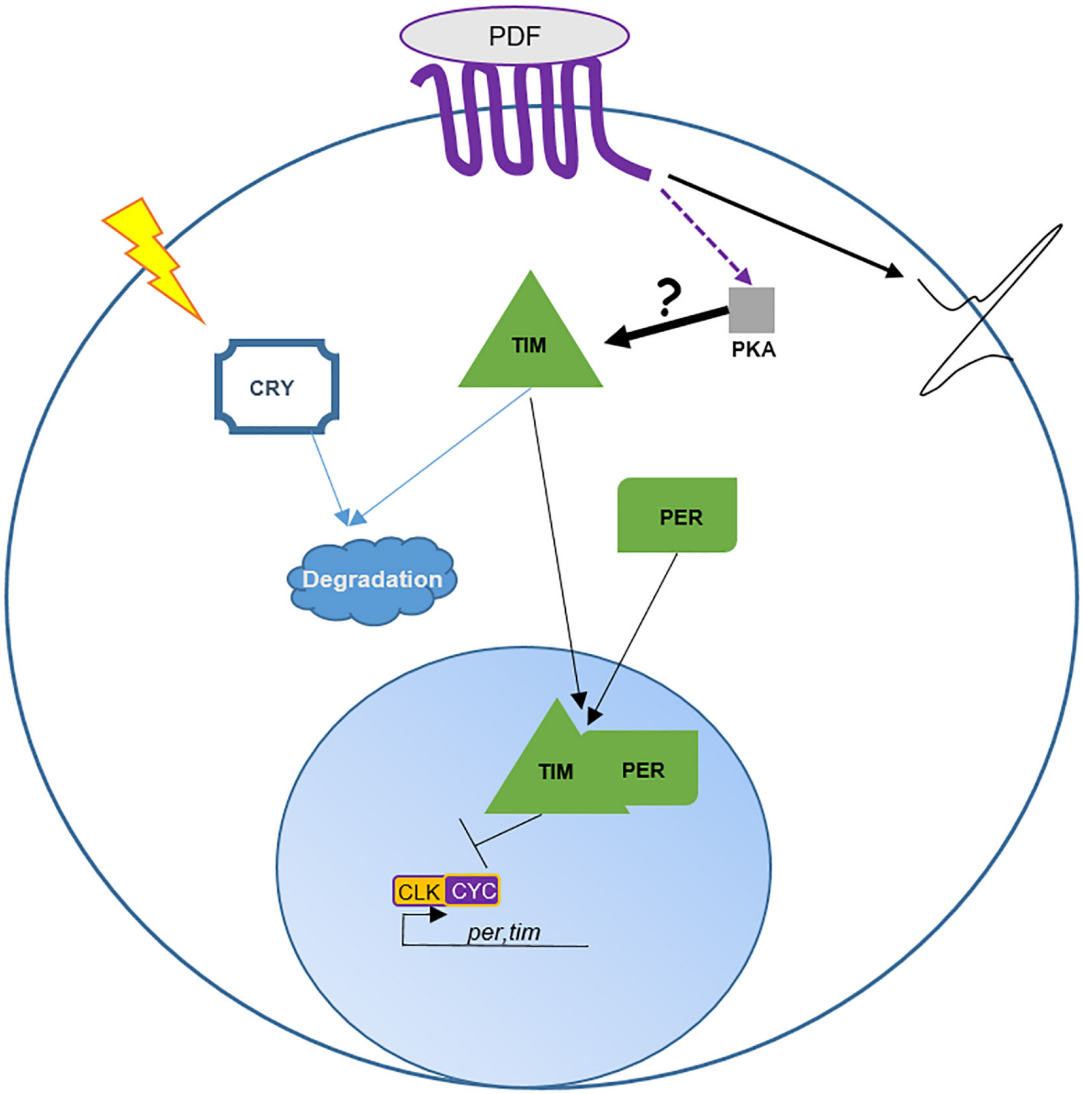

FIGURE 2 | Role of PDF in DN1p entrainment and neuronal activity. This cartoon is based on Seluzicki et al. (2014). The transcription factors CLOCK (CLK) and CYCLE (CYC) form a heterodimer promoting the expression of *period* (*per*) and *timeless* (*tim*). PER and TIM proteins undergo various post-transcriptional and post-translational modifications delaying their nuclear translocation and inhibition of their own expression by binding to CLK/CYC (Tataroglu and Emery, 2015). *Pdfr* encodes for a seven transmembrane GPCR protein (Hyun et al., 2005). Activation of PDFR leads to an increase of cAMP in the cytoplasm. cAMP interacts with and activates PKA activity. Directly or indirectly PKA stabilizes TIM in the cytoplasm. In about half of the DN1p TIM is degraded by light via CRY. Interestingly, Seluzicki et al. (2014) observed that PDF promotes DN1p neuronal activity independently of PKA. Hence, the authors suggest that PDF cells entrain the DN1p molecular clock via the control of TIM by PKA and promote DN1p neuronal activity in a PKA-independent manner.

driver strongly decreased rhythmic behavior (Cavanaugh et al., 2014). However, using the same pan neuronal driver and RNAi line, another group was not able to replicate this result (Cavey et al., 2016). Also, specific activation of DH44 neurons with dTrpA1 using the dh44^{VT}-gal4 line does not increase the proportion of arrhythmic flies (see Table 1 in Cavanaugh et al., 2014), raising doubts about the real implication of these neurons in regulating DD rhythms. Nonetheless, they do seem to respond to rhythmic input, since their neuronal activity oscillates in DD (Cavey et al., 2016). Interestingly, *kurs58*-Gal4 is also expressed in sifamide-expressing PI (SIFa) neurons, which are not overlapping with the DH44^{+} cells (Cavanaugh et al., 2014). The authors observed a decrease of DD rhythmicity in flies deprived of the SIFa neurons (SIFa > reaper) (Cavanaugh et al., 2014) consistent with the observation that pan-neuronal downregulation of SIFa expression strongly decreases rhythmicity in DD (Cavey et al., 2016). Finally, Cavanaugh et al. (2014) found a physical interaction between the DN1p and both the DH44^{+} and the SIFa^{+} PI cells. Since kurs58-Gal4 is expressed in 16–18 PI cells including the six DH44^{+} and four SIFa neurons, we cannot conclude with certainty the influence of the DH44 neurons on locomotor rhythmicity in

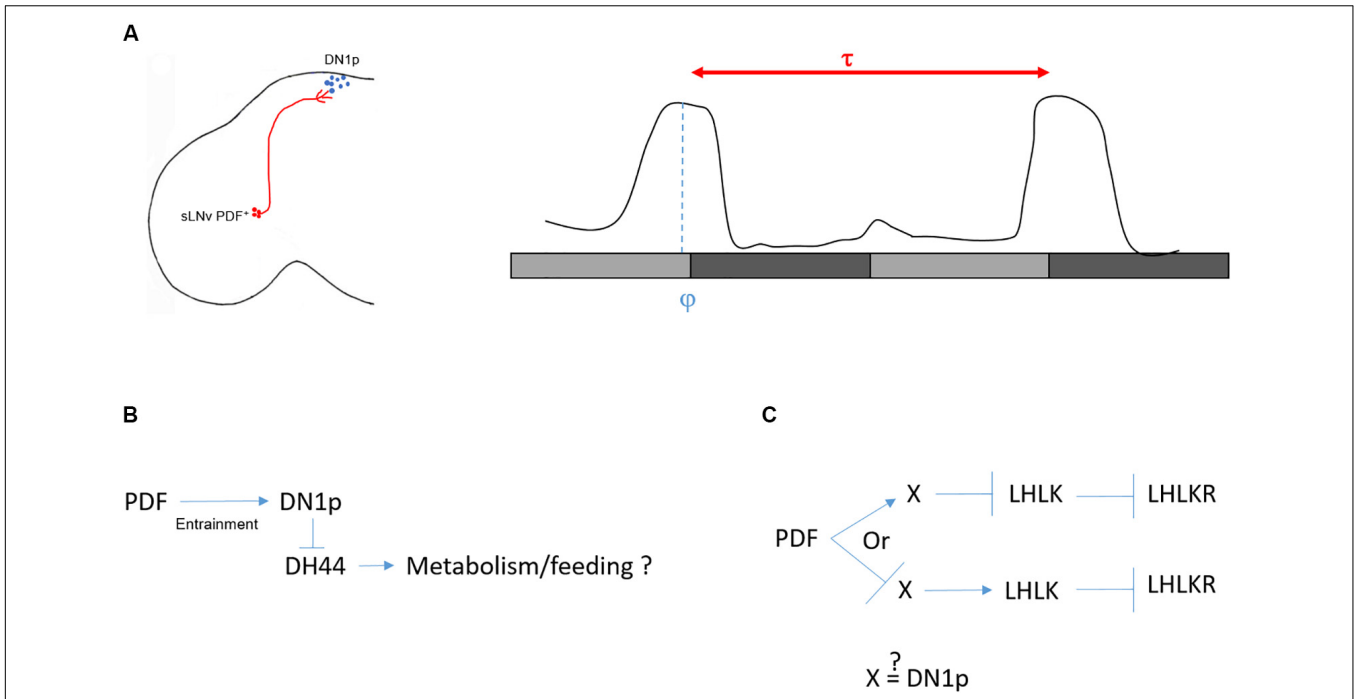

FIGURE 3 | Control of locomotor activity in DD. **(A)** Left: sketch of sLNv and DN1p in the *Drosophila* brain. Right: a typical locomotor behavior in DD. Light gray bars represent the subjective day, dark gray bars represent the subjective night. Flies free run with an activity peak at the end of the subjective day. The period (τ) is defined as the distance between two peaks. τ is controlled by the sLNv (red), while the phase (φ) (when the peak of locomotor activity happens within τ) is controlled by the DN1p (blue). **(B)** Several arguments speak against a role of DH44 in controlling locomotor rhythms in DD (see text). However, the DH44 neurons appear to be rhythmic with a phase opposite to the DN1p (Cavey et al., 2016), and they modulate feeding behavior (Dus et al., 2015). From this, we can postulate that clock neurons influence feeding behavior via rhythmic inhibitory action on the DH44 neurons. **(C)** In the second model (Cavey et al., 2016), the LHLK neurons are indirectly inhibited by PDF. Hence, either PDF activates an unknown intermediate (X) which in return inhibits the LHLK neurons, or PDF inhibits X which activates LHLK neurons. Since activation of LHLK downstream neurons, LHLKR, changes the phase of the locomotor activity without changing the period of inactivity (Cavey et al., 2016), it is possible that the intermediate are the DN1p neurons.

DD. It would be interesting to further test the potential role of the SIFa neurons.

Later, the same group proposed a potential circuit downstream of the DH44 neurons responsible for DD rhythmicity (King et al., 2017). Flies express two receptors for DH44, DH44R1 and DH44R2 (Hector et al., 2009). While DH44R1 neurons are found in the central nervous system (Dus et al., 2015; King et al., 2017), DH44R2 expressing cells were found in the gut, potentially within the enteroendocrine cells (Dus et al., 2015). King et al. (2017) proposed that a group of DH44R1 neurons localized in the subesophageal zone (SEZ) and expressing the neuropeptide *hugin* are the downstream target of the DH44 neurons for regulating DD rhythms. However, neither the null mutant for *dh44r1* nor the expression of the *dh44r1* RNAi in hugin$^+$ neurons lead to arrhythmicity in DD (see Supplementary Table 1 of King et al., 2017). Nonetheless, the authors observed arrhythmic locomotor activity in DD when hugin$^+$ neurons, along with many others using the *R21A07* driver line, are activated (King et al., 2017). DH44 neurons project dendritic arborization to the dorsal region of the SEZ, their cell bodies are highly positive for the pre-synaptic marker syt-GFP, and they send axonal projections to the gut (Dus et al., 2015). No projections have been observed in the thoracic ganglion, where motor neurons receive inputs from the brain. This projection pattern, along with the absence of arrhythmic behavior in *dh44r1* mutants, is therefore not compatible with a role for DH44 neurons in regulating locomotor activity rhythms (**Figure 3B**).

Another study used a genetic approach to find the circuit downstream of the clock responsible for rhythmic behavior in DD (Cavey et al., 2016). They screened for peptidergic function via expressing RNAis pan-neuronally. From this screen, they found that downregulation of leukokinin (LK) leads to a high percentage of arrhythmic flies (65.4%). LK is expressed in only four non-clock neurons in the adult brain: two in the lateral horn (LHLK neurons) and two in the SEZ. Because of their location and their projections to the dorsal region of the brain, they focused on the LHLK neurons and measured their activity in constant conditions using GCaMP6. Activity of these neurons peaks at the end of the subjective day and reaches a minimum at the end of the subjective night. Interestingly, the LHLK neurons are indirectly inhibited by PDF, suggesting that PDFR$^+$ neurons modulate the activity of these neurons (Cavey et al., 2016). However, we do not know whether the DN1p are directly connected with the LHLK neurons (**Figure 3C**). Finally, the authors confirmed the rhythmic activity of this circuit by recording the neuronal activity from neurons that express the

leukokinin receptor and project to the proximal region of the LHLK neurons (LHLKR neurons). Interestingly, activation of LHLKR neurons using the R65C07 driver line, for 1 day in DD, changes the phase of locomotor activity. When these neurons are active, flies are constantly active during the subjective day but decrease their activity during the entire subjective night instead of showing a wild-type peak of activity at the end of the subjective day (Cavey et al., 2016). Hence, although the pattern of activity is different from controls and the phase is not restricted to the subjective evening, they are still rhythmic, suggesting that the LHLK circuit is downstream of the DN1p to phase locomotor behavior in DD. However, it is important to consider that the R65C07 driver is expressed in many other cells in the brain, and hence the behavior observed may not be driven by the LHLKR neurons.

In summary, in DD and constant temperature, the LN-MO relays the rhythmicity, while the DN1p shape and phase the locomotor activity toward the subjective evening (**Figure 3A**) but the downstream circuits remain ambiguous. How can we explain the specific implication of these two groups of neurons in the control of the locomotor rhythms in DD? There are non-clock cells that express PDFR (Im and Taghert, 2010), such as Ring neurons (R neurons) in the ellipsoid body (EB), a structure that belongs to the central complex, the integration center for locomotion (Young and Armstrong, 2010). Hence, the activity of some of these R neurons could be directly influenced by diffusible PDF and therefore their rhythm could be under direct control of the PDF neurons (Liang et al., 2019). While the sLNv pacemaker would control the pace of these R neurons via PDF, the DN1p could phase the same or other neurons that would belong to the central complex. Although the DN1p do not physically interact with R neurons in the EB, indirect connections exist (Guo et al., 2018; Lamaze et al., 2018a) (see final chapter: "Role of DN1p in Temperature-Dependent Sleep Regulation").

THE ROLE OF DN1p IN REGULATING LOCOMOTOR ACTIVITY IN LIGHT–DARK CYCLES AND CONSTANT MILD TEMPERATURES

Interestingly, light intensity and temperature modulate the evening output of the DN1p (**Figure 1C**) (Zhang Y. et al., 2010). At 25°C the DN1p-driven evening anticipation is only visible at low light intensity (≤50 Lux). However, when the temperature drops to 20°C we can observe this output also under higher light intensities (Zhang Y. et al., 2010). How does the environment influence these DN1p outputs?

While a clock in the PDF cells is not necessary for morning anticipation (Stoleru et al., 2004; Zhang Y. et al., 2010), PDF neuropeptide or the presence of the PDF cells are (Renn et al., 1999). Interestingly, rescuing *pdfr* only in the DN1p restores morning anticipation (Zhang L. et al., 2010). Clock proteins in the DN1p cycle with high amplitude in LD, even in the absence of either *Pdf* or *cry* (Cusumano et al., 2009). However, the fact that *Pdf* mutant flies do not show a morning anticipation suggests that the neuronal activity of the DN1p, and therefore their output, depends on the neuropeptide PDF. Indeed, a shot of PDF excites the DN1p in a PKA independent manner (Seluzicki et al., 2014). This suggests that in addition of maintaining a robust molecular rhythm, PDF promotes the morning anticipation output via modulating DN1p neuronal activity (**Figure 2**). The rhythmic neuronal activity of DN1p depends on the sodium leak channel *narrow abdomen* (*na*) (Nash et al., 2002; Flourakis et al., 2015). Remarkably, na^{har} mutants lose their morning anticipation and also, the startle response to light-on (Nash et al., 2002; Zhang L. et al., 2010). Both behaviors are restored when *na* expression is rescued in the DN1p (Zhang L. et al., 2010). In gl^{60j} mutants, which lack all retinal photoreceptors and the DN1p, both morning anticipation and startle response are absent as well (Helfrich-Förster et al., 2001). This suggests that DN1p are necessary for the morning peak, but they need PDF at the end of the night to induce the increase of locomotion around dawn.

The second DN1p output regulates the evening anticipation. However, this output is highly sensitive to the surrounding environment, as for example, higher light intensities inhibit it (see above and **Figure 1C**). Interestingly, the evening peak does become visible at higher light intensity in the absence of PDF or when its expression is reduced by half (pdf^0/+) (Chatterjee et al., 2018). Furthermore, the PDF level is influenced by light intensity, as its expression increases with light (Chatterjee et al., 2018). From a yeast one-hybrid screen for transcriptional regulators of *Pdf* the nuclear receptor *Hr38* was found as a potential candidate (Mezan et al., 2016). Knock down of *Hr38* in PDF neurons leads to a decrease of PDF levels (Mezan et al., 2016) and consequently, the DN1p evening output becomes visible under high light condition (Chatterjee et al., 2018).

Intriguingly, this opposite effect of the PDF on DN1p outputs is comparable to the temperature effect on the morning and evening peaks (Majercak et al., 1999). Historically, the first *pdfr* mutant described was named *han*, which means "cold" in Korean (Hyun et al., 2005). However, apart from this interesting coincidence, it is not known if PDF levels vary with temperature.

The DN1p show heterogeneity in their response to PDF. Some respond positively to PDF neuron activation, others are inhibited (Chatterjee et al., 2018). This could explain the antagonistic effect of PDF on DN1p outputs. The morning DN1p would be activated by PDF, while the evening DN1p would be inhibited (Chatterjee et al., 2018). How this antagonistic response is regulated is not known.

One possibility is that PDF reception differs between morning and evening DN1p. The *Pdfr* locus encodes four isoforms with different coding exons, notably, isoforms C and D have an extra C-terminal coding exon in the intracellular part of the receptor (FlyBase), suggesting distinctive functions downstream of PDF reception. The *Pdfr* mutant allele han^{5304} causes a deletion of all seven transmembrane domains (Hyun et al., 2005). Hence, it is unlikely that the mutated protein will localize at the cell surface. han^{5304} mutants show a behavioral phenotype equivalent to *Pdf* null flies: absence of morning anticipation, an advance of the evening peak in LD and arrhythmic behavior in DD. However, the mutant allele han^{3369}, which leads to a partial deletion of the C terminal domain potentially affecting the C and D isoforms only, maintains its morning anticipation, while causing arrhythmicity

in DD (Hyun et al., 2005; Im and Taghert, 2010). This suggests that PDF may differentially affect neurons depending on the specific *Pdfr* isoforms they express. However, the CRY^+ $vGlut^+$ DN1p are sufficient to drive morning anticipation in standard LD (Chatterjee et al., 2018) and PDFR-MYC, a construct faithfully reporting PDFR expression, is exclusively expressed in the CRY^+ DN1p (Im and Taghert, 2010). Therefore, we propose that PDF promotes the activity of the CRY^+ morning DN1p neurons, which in turn inhibit the activity of the evening DN1p.

ROLE OF DN1p IN TEMPERATURE ENTRAINMENT

The brain clock can be entrained by light and temperature (Wheeler et al., 1993). While about half of the clock neurons in the brain expresses *cry* and therefore can be entrained by light in the absence of a functional visual system (Emery et al., 2000), they cannot be entrained by temperature in the absence of the periphery, and more specifically, the chordotonal organs and aristae (Sehadova et al., 2009; Yadlapalli et al., 2018). In *nocte* mutants, the chordotonal organs are structurally defective, and flies do not properly entrain to TC, while synchronization to light is normal (Glaser and Stanewsky, 2005; Sehadova et al., 2009; Chen et al., 2018). Wild-type flies can be entrained to TC even with a small temperature variation of only 2°C (Chen et al., 2015; Yoshii et al., 2005). The *Drosophila* ionotropic receptor IR25a is specifically required for synchronization to such low-amplitude TC (2°C) in LL or DD (Chen et al., 2015). Since IR25a mutants do not affect high-amplitude temperature entrainment, we can therefore propose that synchronization to low- and high-amplitude TC uses different molecular and potentially neuronal thermo-circuits. Interestingly, TIM oscillations respond differently to the absence of this ionotropic receptor depending on the light condition. In low amplitude LLTC, TIM peaks between ZT16 and ZT18 in all wild-type clock neurons analyzed in this study. In *IR25a* mutants, however, TIM is constantly low in the DN1p and DN2 and its oscillations are strongly disturbed in the PDF neurons, but are not, or only weakly affected in the LNd and DN3 (Chen et al., 2015), suggesting an IR25a independent mechanism for their entrainment to low amplitude TC in LL. In the same low amplitude TC during DD, TIM peaks at different phases in the clock neurons: At ZT16 in the LN, at ZT10 in the DN2, and between ZT10 and ZT16 in the DN1p and DN3. In *IR25a* mutants, TIM is at constitutively low levels in the LN, but oscillations remain unchanged in the DN2, DN3 and in the DN1p, although the amplitude is dampened and the peak narrowed. The DDTC situation is difficult to interpret because one could think that if clock neurons become insensitive to temperature entrainment they should maintain their oscillations and free run. Hence, we do not understand why TIM levels are low and flat in the LNd and sLNv. Nonetheless, in low-amplitude LLTC, the effect of *IR25a* on TIM expression in the DN1p and DN2 is very clear. Furthermore, when DN1p or DN2 neuronal activity is inhibited using tetanus toxin, flies fail to synchronize to a low amplitude TC in LL (Chen et al., 2015), also supporting a role for the DN1p (and DN2) in these conditions.

In the wild, the daily variation of temperature follows the sun. Hence, to test whether we can distinguish a light oscillator from a temperature one, like in plants (Michael et al., 2003), we need to uncouple light and TC. Using an environmental uncoupling protocol, where LD and TC were offset by 6 h, TIM expression in the lateral neurons followed the LD regime, while the dorsal neurons were preferentially entrained by temperature (Miyasako et al., 2007). Later, applying a protocol with exactly opposite LD and TC, only the CRY^- DN1p, DN2, and DN3 followed the TC (Yoshii et al., 2010). Using a different sensory conflict protocol and PER immunostaining (which is less sensitive to light inputs), Harper et al. (2016) observed that only the DN2 and DN3 follow the TC. However, in the absence of *cry*, PER oscillations in all clock neurons analyzed followed the TC, contrary to what was observed during opposite LD and TC, where the LN-MO maintained its phase in accordance with the LD cycle (Yoshii et al., 2010). Nonetheless, it is striking to observe that in cry^0 flies, PER oscillates with the highest amplitude in DN1p and DN2, whether light and temperature oscillations are in phase or not (Harper et al., 2016).

The TRPA channel *pyrexia* (*pyx*) is specifically required for synchronization to cold TC (20–16°C) (Wolfgang et al., 2013). While *IR25a* is expressed in the chordotonal neurons (Chen et al., 2015), *pyx* is expressed in the cap cells of the chordotonal organs as well as in the peripheral nervous system (PNS) (Wolfgang et al., 2013; Roessingh et al., 2019). pyx^3 mutants do not properly synchronize to cold TC in DD and free run instead (Roessingh et al., 2019). Interestingly, while PER oscillations in the sLNv of pyx^3 mutants seem to free run during the shifted TC, they are dampened in the DN1p.

Although *pyx* and IR25a are both expressed in chordotonal organs, they play a role in specific TC conditions, and differently affect temperature synchronization of various clock neurons. Chordotonal organs are present all over the *Drosophila* body. However, it is unclear how the temperature information is transferred from the chordotonal organs to the clock neurons. The light conditions are also an important factor because the DN1p are differentially affected by the absence of IR25a in presence or absence of light.

In summary, the DN1p are sensitive to temperature entrainment when they do not receive oscillating light inputs. Their molecular synchronization is strongly affected when chordotonal function or structure are disturbed (Chen et al., 2015, 2018; Roessingh et al., 2019). In low amplitude TC, their neuronal activity is required for behavioral entrainment. However, about half of them express *cry* and in a temperature-light conflict paradigm, they are synchronized with the light (Harper et al., 2016).

ROLE OF THE DN1p IN TEMPERATURE-DEPENDENT SLEEP REGULATION

Sleep is a fundamental physiological process regulated by both homeostatic and circadian mechanisms. Sleep need accumulates

during wakefulness and is released during sleep. In DD, the clock phases sleep (Shaw et al., 2000). However, a nocturnal mouse can switch to diurnality when its environment changes (food access and temperature) suggesting that the environment, independent of its entrainment function, can phase sleep (van der Vinne et al., 2014).

All animals with a complex central nervous system sleep, though the sleep pattern differs between species (Cirelli and Tononi, 2008). *D. melanogaster* is considered crepuscular for chrono biologists but diurnal for sleep biologists. In standard LD conditions, flies are mostly active around light transitions, explaining the crepuscular classification. In between, they show sleep-like behaviors, and because night sleep lasts longer than day sleep (also called siesta), they have been classified as diurnal. It is today clear that day and night sleep are differently regulated in flies (Ishimoto et al., 2012) and of different quality (Van Alphen et al., 2013). Consequently, siesta and night sleep might use different neuronal circuits.

In standard LD conditions, mutants for the peptide DH31 sleep slightly more than controls (Kunst et al., 2014). Especially during the morning anticipation period at the end of the night, flies are sleepier in the absence of DH31 (Kunst et al., 2014). Interestingly, some of the DN1p express this neuropeptide, and their activation delays day sleep onset and decreases sleep at the second half of the night (Kunst et al., 2014). This suggests that the $DH31^{+}$ DN1p play a role in wakefulness around the light-on transition. Since this behavioral phenotype was obtained using ectopic DN1p activation, the question is if, and under which conditions, these clock neurons promote arousal in the morning?

An increase of temperature above 30°C phase-shifts the siesta, and both its onset and offset are delayed. These high temperatures also advance the offset of night sleep (Lamaze et al., 2017; **Figures 4A,B**). The delay of the siesta offset and the advance of the night sleep offset mirror the evening and morning anticipatory activity behaviors at warm temperature (≥27°C) (Majercak et al., 1999; **Figure 4C**). Interestingly, the delay of the siesta onset is also clock-dependent (Lamaze et al., 2018a). Hence, both the onset and the offset of the siesta phase-shift in a clock dependent manner (**Figure 4B**). Interestingly, inhibition of the DN1p neuronal activity at warm temperature (≥30°C), using *shibire^{ts}* (*shi^{ts}*) (Dubnau et al., 2001), inhibits the delay of the siesta onset but not its offset (Lamaze et al., 2017; **Figure 6A**). This suggests that the DN1p promote morning arousal at warm temperature but their neuronal activity at the end of the day is not responsible for the phase delay of the siesta offset. Consistent with this, several groups have shown that the neuronal activity of the DN1p cycles along the day with a peak in the early morning (Flourakis et al., 2015; Liang et al., 2016) and a trough in the afternoon. Furthermore, stopping the clock in the DN1p via expressing a dominant negative form of *cyc* (Tanoue et al., 2004) does not affect the normal activity and sleep pattern at 22°C (**Figure 5A**), but their behavior becomes aberrant at 31°C (**Figure 5B**). Notably, during the day, the siesta is not restricted to a defined time of day. Interestingly, the night sleep is completely reversed compared to controls and the flies sleep when they should be awake and vice versa (**Figure 5B**). Therefore, the DN1p are essential for phasing behavior at temperatures ≥30°C, but at mild temperature, they do not play a fundamental role in controlling the locomotor pattern.

In contrast, Guo et al. (2016) have proposed that the DN1p promote sleep at mild temperatures, suggesting to have identified the first sleep-promoting clock neurons in *Drosophila*. They notably proposed that the DN1p promote sleep in the late day via inhibiting the LN-EO through a glutamatergic pathway (Guo et al., 2016). However, the LN-EO is sufficient to promote the increase of locomotion in the early evening before the light-off transition (Grima et al., 2004). Furthermore, live calcium imaging revealed that in standard LD the neuronal activity of the LNd oscillates in antiphase with the DN1p (Liang et al., 2016). Therefore, it is difficult to comprehend the relevance of an inhibitory action from DN1p sleep-promoting neurons on the LN-EO at a time when the DN1p are less active than the LN-EO. However, the locomotor behavior pattern changes with temperature, notably, at warm temperature (≥29°C) the evening anticipation is delayed compared to standard mild temperature (Majercak et al., 1999). Can the sleep-promoting DN1p inhibit the LNd in this condition and therefore delay the late-day wakefulness? This seems unlikely since the inhibition of the DN1p at ≥30°C does not inhibit the delay of the siesta offset (Lamaze et al., 2017; **Figure 6A**), suggesting that they are already inhibited at this time of day and temperature level. Finally, cooler temperatures (<20°C) advance the evening activity (Majercak et al., 1999), and the DN1p evening locomotor output is also promoted at cooler temperature (20°C) (Zhang Y. et al., 2010). Interestingly, Yadlapalli et al. (2018) have observed that cooling in the afternoon activated DN1p neuronal activity, suggesting again that the DN1p are pro-arousal. It would be interesting to test the role of a potential cooperation between LN-EO and DN1p to control the phase of the evening peak at cooler temperatures.

The thermoreceptor dTrpA1 phases the siesta and the morning anticipation at warm temperatures (>29°C) (Roessingh et al., 2015; Lamaze et al., 2017). Two groups of dTrpA1-expressing neurons, the *ppk* and the *dTrpA1[SH]* neurons, project to the dorso-posterior area of the brain where the DN1p, the LN-EO, and also the sLNv (LN-MO) project (**Figure 6C**). Downregulation of dTrpA1 expression in either the *ppk* neurons or the dTrpA1[SH] neurons, strongly dampened the phase shift of the siesta (both onset and offset) and the phase advance of the morning anticipation normally observed at warm temperature (≥30°C) (Lamaze et al., 2017). Since an inhibition of DN1p neuronal activity does not affect the delay of the siesta offset, we can propose that the dTrpA1-expressing neurons projecting to the dorso-posterior area of the brain, phase the siesta offset and onset in response to warm temperatures by directly interacting with the LN-EO and the DN1p, respectively.

The DN1p are a heterogeneous group, both transcriptomically and anatomically. Two sub-populations can be distinguished:

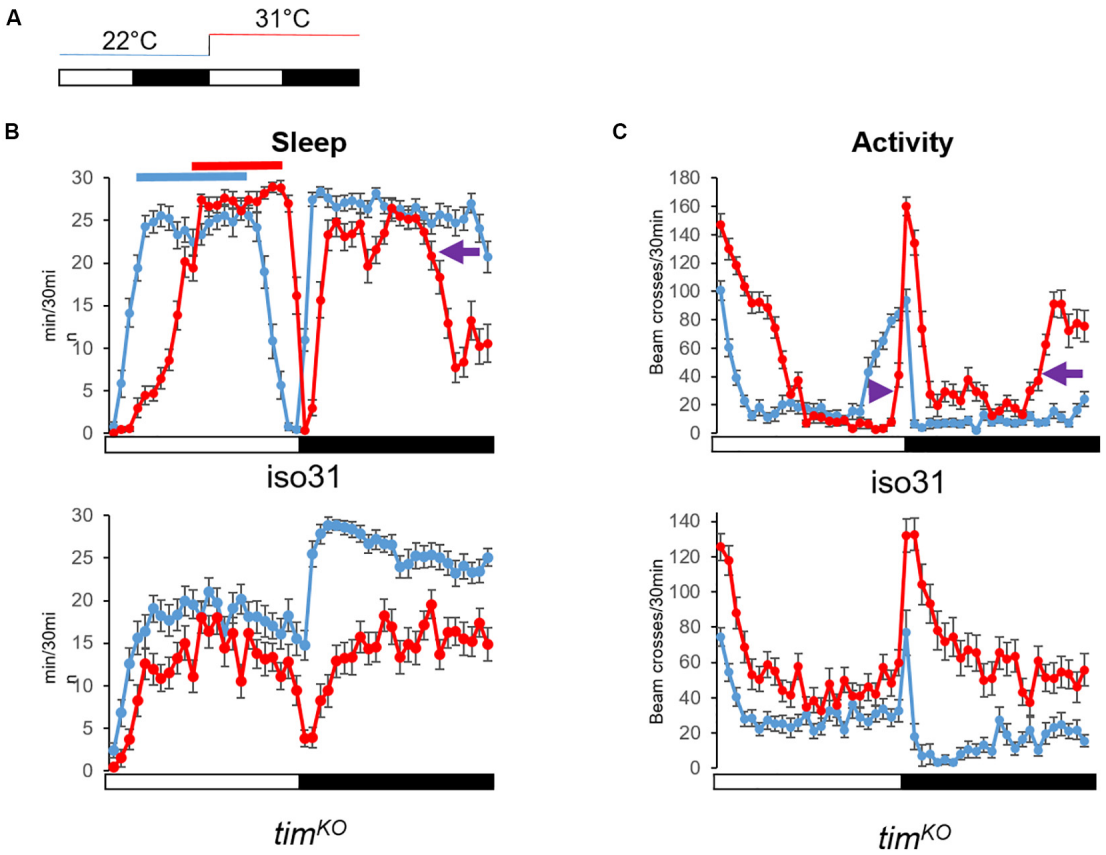

FIGURE 4 | Warm temperature differentially affects day and night sleep. **(A)** Temperature protocol: White bar 12 h of light, dark bar 12 h of darkness. Flies were kept at 22°C the first day (blue line). The next day, temperature increased at light-on to 31°C for 24 h (red line). **(B)** Average sleep trace of control flies (iso31, *N* = 31) and clock mutant males [tim^{KO} (Lamaze et al., 2017), *N* = 32] (bottom graph). Sleep was measured as the sum of 5 min of inactivity per half hour. At warm temperature, wild-type flies delay their siesta. Both onset and offset are delayed (the red line shifts to the right compared to the blue line). At night and 31°C, flies sleep less. Notably, sleep offset is advanced compared to 22°C (purple arrow). On the other hand, the siesta of clock mutant flies is less affected, i.e., we do not observe a robust phase shift. Night sleep however is strongly dampened at 31°C. **(C)** Average locomotor activity of the same flies as in Graph **(B)**. The activity is measured as the sum of beam-crossings per half hour. We can observe the delay of the evening anticipation in iso31 flies (purple arrowhead), which corresponds to the delay of sleep offset. And while the morning anticipation is barely visible at 22°C (but clearer when looking at the sleep profile), at 31°C we can observe a clear advanced morning anticipation (purple arrow). Although clock mutant flies increase their locomotion in response to warm (startle response to light-on switches from 80 beam crosses/30 min at 22°C to 130 at 31°C), they do not present a phase shift of the trough of activity as observed in wild-type flies. At night, clock mutants maintain a high level of activity. Hence, we can see that the delay of the siesta at warm temperatures is clock dependent and independent of the acute response to temperature increase. Error bars represent standard error of the mean.

one projecting anteriorly and terminating in the central domain of the small unit of the anterior optic tubercle (sAOTUc), and which are therefore called aDN1p (**Figure 6C**). The other group projects ventrally and posteriorly, and is therefore called vDN1p (Lamaze et al., 2018a). Guo et al. (2017) have described a driver line (JRC_SS00781 or Spl-DN1p) that restricts the number of sleep-promoting DN1p and their neurons belong exclusively to the vDN1p group (Lamaze et al., 2018a and Supplementary Figure 1 of Guo et al., 2017). Surprisingly, using an independent combination of driver lines to activate CRY^- DN1p, which do not project to the AOTU, the same lab found no sleep promotion (Guo et al., 2018), questioning the identity of the sleep promoting neurons.

The AOTU is a neuropil receiving visual input from specific neurons in the medulla (Omoto et al., 2017; Timaeus et al., 2017). At 31°C, activation of tubulo-bulbar neurons ($TuBu_c$) that project dendrites to the sAOTUc inhibits the delay of the siesta onset but not the delay of the siesta offset, suggesting a sleep-promoting function. Importantly, DN1p inhibition at warm temperature (≥30°C) in the morning promotes activity of $TuBu_c$ neurons, while activation of the DN1p in the warm afternoon inhibits the TuBu neuronal activity (Lamaze et al., 2018a). This suggests that the aDN1p promote arousal in the morning via the inhibition of their direct downstream target, the $TuBu_c$ neurons. The TuBu neurons project to a microglomeruli structure called the lateral triangle (or bulb), where they interact with R neurons, which in turn project axons forming rings in the EB (Omoto et al., 2017; Timaeus et al., 2017). The sleep-promoting $TuBu_c$ neurons interact with a subset of R2 neurons in the superior region of the

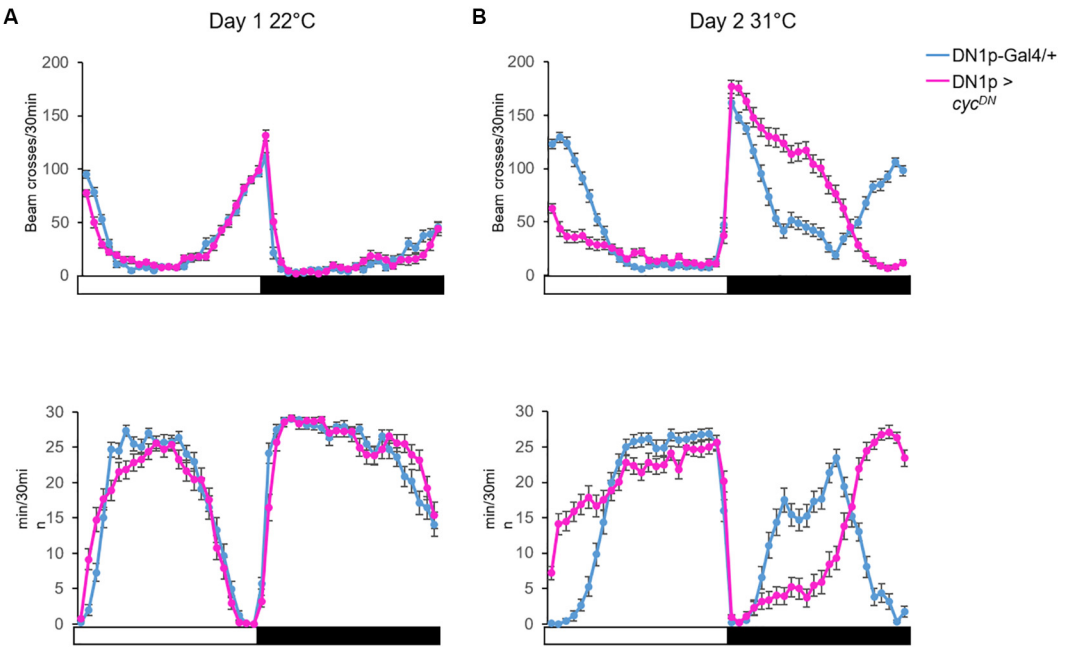

FIGURE 5 | The DN1p clock is necessary to adapt locomotor behavior during warm temperatures. **(A)** Top: the locomotor activity monitored at 22°C on day 1; Bottom: the sleep trace in the same condition from the same flies. **(B)** Activity (Top) and sleep (Bottom) pattern of the same flies monitored the next day at 31°C. We compared the locomotor activity profile between control flies (*Clk4.1M*-Gal4/+) and flies with no functional clock in the DN1p (*Clk4.1M* > cyc^{DN})(Tanoue et al., 2004). *N* (*Clk4.1M*-Gal4/+) = 51; *N* (*Clk4.1M* > cyc^{DN}) = 48; error bars represent standard error of the mean.

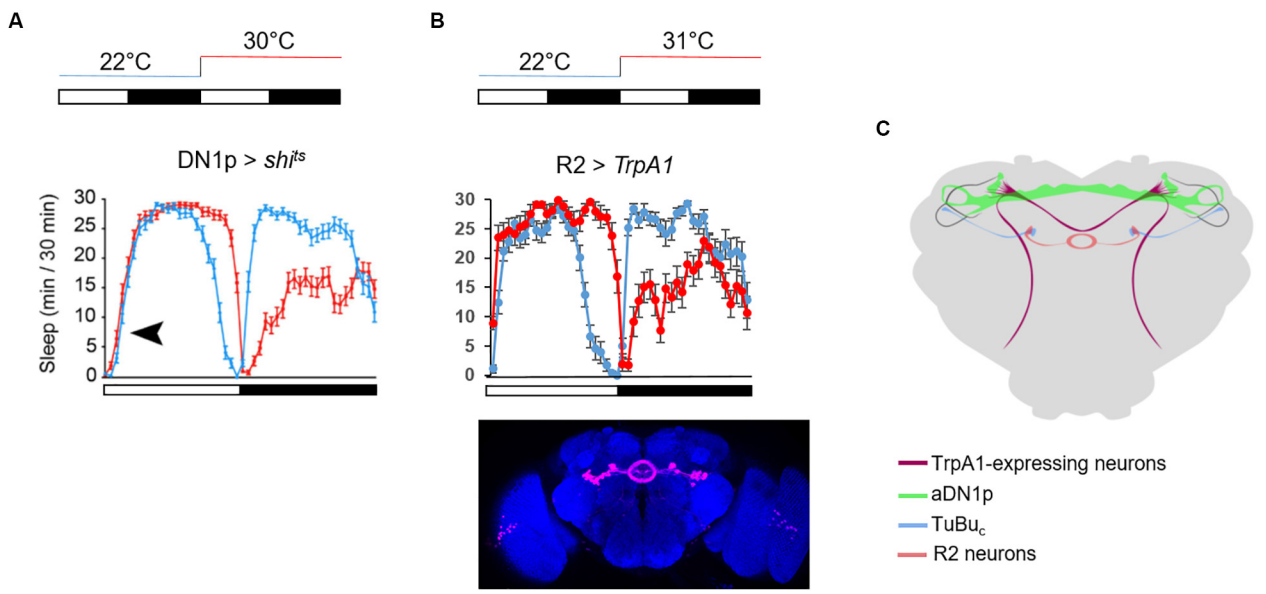

FIGURE 6 | Timing the siesta onset during warm temperatures. **(A)** Average sleep trace of male flies expressing shi^{ts} in the DN1p. The temperature protocol is sketched above the graph. The sleep trace was copied from Lamaze et al. (2017) the black arrowhead indicates the absence of delay of the siesta onset at 30°C. **(B)** Average sleep trace of male flies expressing *TrpA1* in R2 neurons, using the same driver as in Lamaze et al. (2018a) (*R20D01*-Gal4). The brain picture of the expression pattern of R20D01 is a Z stack from the Janelia FlyLight database. TrpA1 is inactive at 22°C but active at 31°C. Note the remarkable symmetry between flies with inactivated DN1p and activated R2 neurons. *N* (*R2* > *TrpA1*) = 20. **(C)** Sketch of the neuronal circuit involved in timing the siesta based from Lamaze et al. (2017, 2018a,b). The dorsal-projecting TrpA1$^+$ neurons play an essential role in phasing the siesta with warm temperatures (Lamaze et al., 2017). They physically interact with DN1p clock neurons (Lamaze et al., 2017). The aDN1p directly inhibit a subset of $TuBu_c$ neurons in the central domain of sAOTU (Lamaze et al., 2018a). These $TuBu_c$ neurons promote sleep when activated at warm temperature. They interact in the superior region of the bulb with a subset of R2 neurons (Lamaze et al., 2018a).

bulb (Lamaze et al., 2018a; **Figure 6C**). Importantly, activation of these neurons at 31°C inhibits the delay of the siesta onset (**Figure 6B**), suggesting that $TuBu_c$ neurons activate R2 neurons to promote sleep in the morning. Recently, Liang et al. (2019) measured rhythmic neuronal activity in different groups of R neurons including R2 (also called R4m). The EB is a neuropil structure integrating visual inputs and plays an important role in navigation (Sun et al., 2017). Hence, in order to fall asleep during daytime, this structure needs to decrease its sensitivity to visual inputs in order to increase the threshold of response. We can therefore propose that a subset of $TuBu_c$ neurons that receive time information input from the DN1p promote sleep by decreasing the sensitivity of the EB to visual input via the activation of a subset of R2 neurons. During the night, flies do not receive any light input and activation of these R neurons does not inhibit the sleep loss induced by temperature (**Figure 6B**). *D. melanogaste*r is crepuscular. Hence, they are more active at dawn, especially at warm temperature. A subset of DN1p promote arousal during that time, according to the ambient temperature level.

CONCLUSION AND FUTURE DIRECTIONS

The brain clock controls sleep/wake rhythms. In *D. melanogaster*, only 150 neurons express clock genes and yet, we do not know how their time information is integrated by the central nervous system. The DN1p are a very peculiar group. First, their development correlates with the development of the visual system. *glass* encodes a transcription factor required for photoreceptor development (Moses et al., 1989). gl^{60j} mutants have a profound defect of the visual system development and in addition, the DN1p fail to differentiate. This suggests a developmental and/or functional relationship between these clock neurons and the visual system (Helfrich-Förster et al., 2001; Klarsfeld et al., 2004). Second, although they express clock genes, the DN1p are not autonomous, and their DD rhythm entirely depends on the sLNv pacemaker neurons and the neuropeptide PDF (Klarsfeld et al., 2004). Finally, although the cells within this group are synchronized to the same phase (molecular clock but also presumably neuronal activity), the DN1p can drive both morning and evening activity under specific environmental conditions (Zhang Y. et al., 2010). This suggests a further separation within this group of at least two clusters.

The DN1p's evening activity is inhibited by strong light ($\geq$500 Lux) and is only visible at 25°C under low light condition ($\leq$50 Lux). Interestingly, in DD the main peak of locomotor activity happens during the subjective evening. This phase is under the control of the DN1p (Chatterjee et al., 2018), suggesting that the DN1p that drive the evening activity under LD low light condition are the same as the ones phasing the locomotor activity in DD. Can we define the two clusters of DN1p more precisely? CRY is required to phase the onset of the siesta at warm temperatures (Lamaze et al., 2017) and the CRY^- DN1p do not project to the AOTU (Chatterjee et al., 2018; Guo et al., 2018). Hence, we can propose that the aDN1p, which promote wakefulness in the warm dawn, are CRY^+. Furthermore, a clock in the $vGlut^+$ DN1p is sufficient to drive the morning anticipation (Chatterjee et al., 2018), suggesting that the aDN1p are CRY^+ and $vGlut^+$. However, two of the CRY^+ neurons are $vGlut^-$ (Chatterjee et al., 2018), indicating that the DN1p-driven evening activity is under the control of a mix of CRY^+ and CRY^- $vGlut^-$ neurons.

The distinction of DN1p clusters is less clear when we focus on the projection to the PI. The DN1p physically interact with different neuroendocrine cells in the PI. Since the DH44 neurons do not send axonal projections to the thoracic ganglion, or to the central complex, and because downregulation of its receptor DH44R1 does not lead to arrhythmicity (King et al., 2017), it seems unlikely that these neuropeptidergic neurons influence locomotor rhythms in DD. However, this circuit could play a role in feeding rhythm and/or rhythmic metabolic processes (Dus et al., 2015; **Figure 3B**). The DH44 neurons are not the only neuroendocrine cells interacting with the DN1p (Barber et al., 2016; Cavey et al., 2016), and the DN1p are not the only clock neurons projecting to this region (Schubert et al., 2018). Hence, it would be of high interest to investigate the role of the clock neurons in the control of the PI-corpora cardiaca/corpora allata activity. This circuit is considered to be the functional homolog of the vertebrate hypothalamus–hypophysis circuit (Buch and Pankratz, 2009).

The central complex in *Drosophila* could be compared to the processor of a computer. It is the part of the brain where the computation happens in order to drive the appropriate behavior in response to the various inputs the brain receives. The central complex is composed of several neuropil structures, including the fan shaped body and the EB. A direct connection between the DN1p and neurons of the central complex is not known. However, the DN1p interact with cells that do connect to neurons projecting to the central complex. The aDN1p interact with a subset of $TuBu_c$ neurons which in return contact a subset of R2 neurons in the superior part of the bulb. The symmetry of the behavior between flies with silenced DN1p and activated R2 neurons is striking (Lamaze et al., 2017; **Figure 6B**). Recently, Liang et al. (2019) have measured the neuronal activity of different groups of R neurons along 24 h during LD and the first day of DD. Interestingly, the group of R neurons that show the most homogeneous rhythmic activity are the R5 [confusingly called R2 in this study (Liang et al., 2019)]. We do not know however, whether activation or inhibition of R5 neurons affect the locomotor activity in DD, notably whether their inhibition would change the phase of the locomotor behavior in DD. Nonetheless, it is interesting to note that many neuronal groups in the brain display rhythmic activity (Barber et al., 2016; Cavey et al., 2016; Liang et al., 2019), and most of them do not interact directly with clock neurons. Actually, apart from the $TuBu_c$ neurons (Lamaze et al., 2018a) and the PI neurons (Cavanaugh et al., 2014; Barber et al., 2016) which interact

with the DN1p, none of the other groups directly interact with the DN1p. However, it is most likely that rhythmic signals end up in the central complex to control locomotor patterns. Interestingly, PDFR is expressed in different R neurons, including R2 and internal rings (Im and Taghert, 2010; Liang et al., 2019). Hence, it is totally conceivable that PDF neurons control the DD rhythm via secreted PDF action on the central complex, while the DN1p control the phase of the locomotor activity pattern via their indirect interaction with the EB.

To conclude, although the DN1p cannot be considered as a circadian oscillator, they play an essential role in phasing clock-controlled behaviors. Since the phase of a circadian behavior is the result of an integration of the environmental status with the time of day, this group of clock neurons seems to function at the crossroad between environmental input, in particular temperature, and the internal clock.

AUTHOR CONTRIBUTIONS

AL wrote the manuscript and RS commented on it.

FUNDING

AL received funding from a *WiRe* (Women in Research, WWU) fellowship. AL and RS are supported by the DFG grant STA421/71.

ACKNOWLEDGMENTS

We thank Clara Lorber for helping with behavior experiments. We also thank Cédric Lamaze for the cartoon representing the downstream neuronal network of the aDN1p.

REFERENCES

Barber, A. F., Erion, R., Holmes, T. C., and Sehgal, A. (2016). Circadian and feeding cues integrate to drive rhythms of physiology in *Drosophila* insulin-producing cells. *Genes Dev.* 30, 2596–2606. doi: 10.1101/gad.288258.116

Benito, J., Houl, J. H., Roman, G. W., and Hardin, P. E. (2008). Hardin. the blue-light photoreceptor cryptochrome is expressed in a subset of circadian oscillator neurons in the *Drosophila* CNS. *J. Biol. Rhythms* 23, 296–307. doi: 10.1177/0748730408318588

Buch, S., and Pankratz, M. (2009). Making metabolic decisions in *Drosophila*. *Fly* 3, 74–77. doi: 10.4161/fly.3.1.7795

Cabrero, P., Radford, J. C., Broderick, K. E., Costes, L., Veenstra, J. A., and Spana, E. P. (2002). The Dh gene of *Drosophila melanogaster* encodes a diuretic peptide that acts through cyclic AMP. *J. Exp. Biol.* 205, 3799–3807.

Cavanaugh, D. J., Geratowski, J. D., Wooltorton, J. R., Spaethling, J. M., Hector, C. E., and Zheng, X. (2014). Identification of a circadian output circuit for rest: activity rhythms in *Drosophila*. *Cell* 157, 689–701. doi: 10.1016/j.cell.2014.02.024

Cavey, M., Collins, B., Bertet, C., and Blau, J. (2016). Circadian rhythms in neuronal activity propagate through output circuits. *Nat. Neurosci.* 19, 587–595. doi: 10.1038/nn.4263

Chatterjee, A., Lamaze, A., De, J., Mena, W., Chélot, E., and Martin, B. (2018). Reconfiguration of a multi-oscillator network by light in the *Drosophila* circadian clock. *Curr. Biol.* 28, 2007–2017.e4. doi: 10.1016/j.cub.2018.04.064

Chen, C., Buhl, E., Xu, M., Croset, V., Rees, J. S., and Lilley, K. S. (2015). *Drosophila* ionotropic receptor 25a mediates circadian clock resetting by temperature. *Nature* 527, 516–520. doi: 10.1038/nature16148

Chen, C., Xu, M., Anantaprakorn, Y., Rosing, M., and Stanewsky, R. (2018). Nocte is required for integrating light and temperature inputs in circadian clock neurons of *Drosophila*. *Curr. Biol.* 28, 1595–1605. doi: 10.1016/j.cub.2018.04.001

Cirelli, C., and Tononi, G. (2008). Is sleep essential? *PLoS Biol.* 6:e216. doi: 10.1371/journal.pbio.0060216

Cusumano, P., Klarsfeld, A., Chélot, E., Picot, M., Richier, B., and Rouyer, F. (2009). modulated visual inputs and cryptochrome define diurnal behavior in *Drosophila*. *Nat. Neurosci.* 12, 1431–1437. doi: 10.1038/nn.2429

Diaz, M. M., Schlichting, M., Abruzzi, K. C., Long, X., and Rosbash, M. (2019). Allatostatin-C/AstC-R2 is a novel pathway to modulate the circadian activity pattern in *Drosophila*. *Curr. Biol.* 29, 13–22. doi: 10.1016/j.cub.2018.11.005

Dubnau, J., Grady, L., Kitamoto, T., and Tully, T. (2001). Disruption of neurotransmission in *Drosophila* mushroom body blocks retrieval but not acquisition of memory. *Nature* 411, 476–480. doi: 10.1038/35078077

Dus, M., Lai, J. S.-Y., Gunapala, K. M., Min, S., Tayler, T. D., and Hergarden, A. C. (2015). Nutrient sensor in the brain directs the action of the brain-gut axis in *Drosophila*. *Neuron* 87, 139–151. doi: 10.1016/j.neuron.2015.05.032

Emery, P., Stanewsky, R., Helfrich-Förster, C., Emery-Le, M., Hall, J. C., and Rosbash, M. (2000). *Drosophila* CRY is a deep brain circadian photoreceptor. *Neuron* 26, 493–504. doi: 10.1016/s0896-6273(00)81181-2

Flourakis, M., Kula-Eversole, E., Hutchison, A. L., Han, T. H., Aranda, K., and Moose, D. L. (2015). A conserved bicycle model for circadian clock control of membrane excitability. *Cell* 162, 836–848. doi: 10.1016/j.cell.2015.07.036

Gentile, C., Sehadova, H., Simoni, A., Chen, C., and Stanewsky, R. (2013). Cryptochrome antagonizes synchronization of *Drosophila's* circadian clock to temperature cycles. *Curr. Biol.* 23, 185–195. doi: 10.1016/j.cub.2012.12.023

Glaser, F. T., and Stanewsky, R. (2005). Temperature synchronization of the *Drosophila* circadian clock. *Curr. Biol.* 15, 1352–1363. doi: 10.1016/j.cub.2005.06.056

Grima, B., Chélot, E., Xia, R., and Rouyer, F. (2004). Morning and evening peaks of activity rely on different clock neurons of the *Drosophila* brain. *Nature* 431, 869–873. doi: 10.1038/nature02935

Guo, F., Chen, X., and Rosbash, M. (2017). Temporal calcium profiling of specific circadian neurons in freely moving flies. *Proc. Natl. Acad. Sci. U.S.A.* 114, E8780–E8787. doi: 10.1073/pnas.1706608114

Guo, F., Holla, M., Díaz, M. M., and Rosbash, M. (2018). A circadian output circuit controls sleep-wake arousal in *Drosophila*. *Neuron* 100, 624–635. doi: 10.1016/j.neuron.2018.09.002

Guo, F., Yu, J., Jung, H. J., Abruzzi, K. C., Luo, W., Griffith, L. C., et al. (2016). Circadian neuron feedback controls the *Drosophila* sleep–activity profile. *Nature* 536, 292–297. doi: 10.1038/nature19097

Hamasaka, Y., Rieger, D., Parmentier, M. L., Grau, Y., Helfrich-Förster, C., and Nässel, D. R. (2007). Glutamate and its metabotropic receptor in *Drosophila* clock neuron circuits. *J. Comp. Neurol.* 505, 32–45.

Harper, R. E., Dayan, P., Albert, J. T., and Stanewsky, R. (2016). Sensory conflict disrupts activity of the *Drosophila* circadian network. *Cell Rep.* 17, 1711–1718. doi: 10.1016/j.celrep.2016.10.029

Hector, C. E., Bretz, C. A., Zhao, Y., and Johnson, E. C. (2009). Functional differences between two CRF-related diuretic hormone receptors in *Drosophila*. *J. Exp. Biol.* 212, 3142–3147. doi: 10.1242/jeb.033175

Helfrich-Förster, C. (2019). Light input pathways to the circadian clock of insects with an emphasis on the fruit fly *Drosophila* melanogaster. *J. Comp. Physiol. A Neuroethol. Sens. Neural. Behav. Physiol.* doi: 10.1007/s00359-019-01379-5 [Epub ahead of print], .

Helfrich-Förster, C., Winter, C., Hofbauer, A., Hall, J. C., and Stanewsky, R. (2001). The circadian clock of fruit flies is blind after elimination of all known photoreceptors. *Neuron* 30, 249–261. doi: 10.1016/s0896-6273(01)00277-x

Hyun, S., Lee, Y., Hong, S.-T., Bang, S., Paik, D., Kang, J., et al. (2005). *Drosophila* GPCR Han is a receptor for the circadian clock neuropeptide PDF. *Neuron* 48, 267–278. doi: 10.1016/j.neuron.2005.08.025

Im, S. H., and Taghert, P. H. (2010). PDF receptor expression reveals direct interactions between circadian oscillators in *Drosophila*. *J. Comp. Neurol.* 518, 1925–1945. doi: 10.1002/cne.22311

Ishimoto, H., Lark, A. R., and Kitamoto, T. (2012). Factors that differentially affect daytime and nighttime sleep in *Drosophila melanogaster*. *Front. Neurol.* 3:24. doi: 10.3389/fneur.2012.00024

King, A. N., Barber, A. F., Smith, A. E., Dreyer, A. P., Sitaraman, D., and Nitabach, M. N. (2017). A peptidergic circuit links the circadian clock to locomotor activity. *Curr. Biol.* 27, 1915–1927.e5. doi: 10.1016/j.cub.2017.05.089

Klarsfeld, A., Malpel, S., Michard-Vanhée, C., Picot, M., Chélot, E., and Rouyer, F. (2004). Novel features of cryptochrome-mediated photoreception in the brain circadian clock of *Drosophila*. *J. Neurosci.* 24, 1468–1477. doi: 10.1523/jneurosci.3661-03.2004

Konopka, R. J., and Benzer, S. (1971). Clock mutants of *Drosophila melanogaster*. *Proc. Natl. Acad. Sci. U.S.A.* 68, 2112–2116. doi: 10.1073/pnas.68.9.2112

Kunst, M., Hughes, M. E., Raccuglia, D., Felix, M., Li, M., Barnett, G., et al. (2014). Calcitonin gene-related peptide neurons mediate sleep-specific circadian output in *Drosophila*. *Curr. Biol.* 24, 2652–2664. doi: 10.1016/j.cub.2014.09.077

Lamaze, A., Krätschmer, P., Chen, K.-F., Lowe, S., and Jepson, J. E. (2018a). A Wake-Promoting circadian output circuit in *Drosophila*. *Curr. Biol.* 28, 3098–3105.e3. doi: 10.1016/j.cub.2018.07.024

Lamaze, A., Kratschmer, P., and Jepson, J. E. (2018b). A sleep-regulatory circuit integrating circadian, homeostatic and environmental information in *Drosophila*. *bioRxiv* [preprint]. doi: 10.1101/250829

Lamaze, A., Öztürk-Çolak, A., Fischer, R., Peschel, N., Koh, K., and Jepson, J. E. (2017). Regulation of sleep plasticity by a thermo-sensitive circuit in *Drosophila*. *Sci. Rep.* 7:40304. doi: 10.1038/srep40304

Li, M.-T., Cao, L.-H., Xiao, N., Tang, M., Deng, B., Yang, T., et al. (2018). Hub-organized parallel circuits of central circadian pacemaker neurons for visual photoentrainment in *Drosophila*. *Nat. Commun.* 9:4247. doi: 10.1038/s41467-018-06506-5

Liang, X., Ho, M. C., Zhang, Y., Li, Y., Wu, M. N., Holy, T. E., et al. (2019). Morning and evening circadian pacemakers independently drive premotor centers via a specific dopamine relay. *Neuron* 102, 843–857.e4. doi: 10.1016/j.neuron.2019.03.028

Liang, X., Holy, T. E., and Taghert, P. H. (2016). Synchronous *Drosophila* circadian pacemakers display nonsynchronous Ca2+ rhythms *in vivo*. *Science* 351, 976–981. doi: 10.1126/science.aad3997

Majercak, J., Sidote, D., Hardin, P. E., and Edery, I. (1999). How a circadian clock adapts to seasonal decreases in temperature and day length. *Neuron* 24, 219–230. doi: 10.1016/s0896-6273(00)80834-x

Mezan, S., Feuz, J. D., Deplancke, B., and Kadener, S. (2016). PDF signaling is an integral part of the *Drosophila* circadian molecular oscillator. *Cell Rep.* 17, 708–719. doi: 10.1016/j.celrep.2016.09.048

Michael, T. P., Salomé, P. A., and McClung, C. R. (2003). Two arabidopsis circadian oscillators can be distinguished by differential temperature sensitivity. *Proc. Natl. Acad. Sci. U.S.A.* 100, 6878–6883. doi: 10.1073/pnas.1131995100

Miyasako, Y., Umezaki, Y., and Tomioka, K. (2007). Separate sets of cerebral clock neurons are responsible for light and temperature entrainment of *Drosophila* circadian locomotor rhythms. *J. Biol. Rhythms* 22, 115–126. doi: 10.1177/0748730407299344

Moses, K., Ellis, M. C., and Rubin, G. M. (1989). The glass gene encodes a zinc-finger protein required by *Drosophila* photoreceptor cells. *Nature* 340, 531–536. doi: 10.1038/340531a0

Nash, H. A., Scott, R. L., Lear, B. C., and Allada, R. (2002). An unusual cation channel mediates photic control of locomotion in *Drosophila*. *Curr. Biol.* 12, 2152–2158. doi: 10.1016/s0960-9822(02)01358-1

Omoto, J. J., Keleş, M. F., Nguyen, B.-C. M., Bolanos, C., Lovick, J. K., Frye, M. A., et al. (2017). Visual input to the *Drosophila* central complex by developmentally and functionally distinct neuronal populations. *Curr. Biol.* 27, 1098–1110. doi: 10.1016/j.cub.2017.02.063

Renn, S. C., Park, J. H., Rosbash, M., Hall, J. C., and Taghert, P. H. (1999). A pdf neuropeptide gene mutation and ablation of PDF neurons each cause severe abnormalities of behavioral circadian rhythms in *Drosophila*. *Cell* 99, 791–802. doi: 10.1016/s0092-8674(00)81676-1

Roessingh, S., Rosing, M., Marunova, M., Ogueta, M., George, R., Lamaze, A., et al. (2019). Temperature synchronization of the *Drosophila* circadian clock protein PERIOD is controlled by the TRPA channel PYREXIA. *Commun. Biol.* 2:246. doi: 10.1038/s42003-019-0497-0

Roessingh, S., Wolfgang, W., and Stanewsky, R. (2015). Loss of *Drosophila melanogaster* TRPA1 function affects "siesta" behavior but not synchronization to temperature cycles. *J. Biol. Rhythms* 30, 492–505. doi: 10.1177/0748730415605633

Schubert, F. K., Hagedorn, N., Yoshii, T., Helfrich-Förster, C., and Rieger, D. (2018). Neuroanatomical details of the lateral neurons of *Drosophila melanogaster* support their functional role in the circadian system. *J. Comp. Neurol.* 526, 1209–1231. doi: 10.1002/cne.24406

Sehadova, H., Glaser, F. T., Gentile, C., Simoni, A., Giesecke, A., Albert, J. T., et al. (2009). Temperature entrainment of *Drosophila's* circadian clock involves the gene nocte and signaling from peripheral sensory tissues to the brain. *Neuron* 64, 251–266. doi: 10.1016/j.neuron.2009.08.026

Seluzicki, A., Flourakis, M., Kula-Eversole, E., Zhang, L., Kilman, V., and Allada, R. (2014). Dual PDF signaling pathways reset clocks via TIMELESS and acutely excite target neurons to control circadian behavior. *PLoS Biol.* 12:e1001810. doi: 10.1371/journal.pbio.1001810

Shafer, O. T., Kim, D. J., Dunbar-Yaffe, R., Nikolaev, V. O., Lohse, M. J., and Taghert, P. H. (2008). Widespread receptivity to neuropeptide PDF throughout the neuronal circadian clock network of *Drosophila* revealed by real-time cyclic AMP imaging. *Neuron* 58, 223–237. doi: 10.1016/j.neuron.2008.02.018

Shaw, P. J., Cirelli, C., Greenspan, R. J., and Tononi, G. (2000). Correlates of sleep and waking in *Drosophila melanogaster*. *Science* 287, 1834–1837. doi: 10.1126/science.287.5459.1834

Stanewsky, R., Kaneko, M., Emery, P., Beretta, B., Wager-Smith, K., Kay, S. A., et al. (1998). The cryb mutation identifies cryptochrome as a circadian photoreceptor in *Drosophila*. *Cell* 95, 681–692. doi: 10.1016/s0092-8674(00)81638-4

Stoleru, D., Peng, Y., Agosto, J., and Rosbash, M. (2004). Coupled oscillators control morning and evening locomotor behaviour of *Drosophila*. *Nature* 431, 862–868. doi: 10.1038/nature02926

Stoleru, D., Peng, Y., Nawathean, P., and Rosbash, M. (2005). A resetting signal between *Drosophila* pacemakers synchronizes morning and evening activity. *Nature* 438, 238–242. doi: 10.1038/nature04192

Sun, Y., Nern, A., Franconville, R., Dana, H., Schreiter, E. R., and Looger, L. L. (2017). Neural signatures of dynamic stimulus selection in *Drosophila*. *Nat. Neurosci.* 20, 1104–1113. doi: 10.1038/nn.4581

Tanoue, S., Krishnan, P., Krishnan, B., Dryer, S. E., and Hardin, P. E. (2004). Circadian clocks in antennal neurons are necessary and sufficient for olfaction rhythms in *Drosophila*. *Curr. Biol.* 14, 638–649. doi: 10.1016/j.cub.2004.04.009

Tataroglu, O., and Emery, P. (2015). The molecular ticks of the *Drosophila* circadian clock. *Curr. Opin. Insect Sci.* 7, 51–57. doi: 10.1016/j.cois.2015.01.002

Timaeus, L., Geid, L., and Hummel, T. (2017). A topographic visual pathway into the central brain of *Drosophila*. *bioRxiv* [preprint]. doi: 10.1101/183707

Van Alphen, B., Yap, M. H., Kirszenblat, L., Kottler, B., and van Swinderen, B. (2013). A dynamic deep sleep stage in *Drosophila*. *J. Neurosci.* 33, 6917–6927. doi: 10.1523/JNEUROSCI.0061-13.2013

van der Vinne, V., Riede, S. J., Gorter, J. A., Eijer, W. G., Sellix, M. T., and Menaker, M. (2014). Cold and hunger induce diurnality in a nocturnal mammal. *Proc. Natl. Acad. Sci. U.S.A.* 111, 15256–15260. doi: 10.1073/pnas.1413135111

Veleri, S., Brandes, C., Helfrich-Förster, C., Hall, J. C., and Stanewsky, R. (2003). A self-sustaining, light-entrainable circadian oscillator in the *Drosophila* brain. *Curr. Biol.* 13, 1758–1767. doi: 10.1016/j.cub.2003.09.030

Wheeler, D. A., Hamblen-Coyle, M. J., Dushay, M. S., and Hall, J. C. (1993). Behavior in light-dark cycles of *Drosophila* mutants that are arrhythmic, blind, or both. *J. Biol. Rhythms* 8, 67–94. doi: 10.1177/074873049300800106

Wolfgang, W., Simoni, A., Gentile, C., and Stanewsky, R. (2013). The Pyrexia transient receptor potential channel mediates circadian clock synchronization to low temperature cycles in *Drosophila melanogaster*. *Proc. Biol. Sci.* 280:20130959. doi: 10.1098/rspb.2013.0959

Yadlapalli, S., Jiang, C., Bahle, A., Reddy, P., Meyhofer, E., and Shafer, O. T. (2018). Circadian clock neurons constantly monitor environmental temperature to set sleep timing. *Nature* 555, 98–102. doi: 10.1038/nature25740

Yoshii, T., Hermann, C., and Helfrich-Förster, C. (2010). Cryptochrome-positive and-negative clock neurons in *Drosophila* entrain differentially to light and temperature. *J. Biol. Rhythms* 25, 387–398. doi: 10.1177/0748730410381962

Yoshii, T., Heshiki, Y., Ibuki-Ishibashi, T., Matsumoto, A., Tanimura, T., and Tomioka, K. (2005). Temperature cycles drive *Drosophila* circadian oscillation in constant light that otherwise induces behavioural arrhythmicity. *Eur. J. Neurosci.* 22, 1176–1184. doi: 10.1111/j.1460-9568.2005.04295.x

Yoshii, T., Wülbeck, C., Sehadova, H., Veleri, S., Bichler, D., Stanewsky, R., et al. (2009). The neuropeptide pigment-dispersing factor adjusts period and phase of *Drosophila's* clock. *J. Neurosci.* 29, 2597–2610. doi: 10.1523/JNEUROSCI.5439-08.2009

Young, J., and Armstrong, J. (2010). Structure of the adult central complex in *Drosophila*: organization of distinct neuronal subsets. *J. Comp. Neurol.* 518, 1500–1524. doi: 10.1002/cne.22284

Zhang, L., Chung, B. Y., Lear, B. C., Kilman, V. L., Liu, Y., and Mahesh, G. (2010). DN1p circadian neurons coordinate acute light and PDF inputs to produce robust daily behavior in *Drosophila*. *Curr. Biol.* 20, 591–599. doi: 10.1016/j.cub.2010.02.056

Zhang, Y., Liu, Y., Bilodeau-Wentworth, D., Hardin, P. E., and Emery, P. (2010). Light and temperature control the contribution of specific DN1 neurons to *Drosophila* circadian behavior. *Curr. Biol.* 20, 600–605. doi: 10.1016/j.cub.2010.02.044

Conflict of Interest: The authors declare that the research was conducted in the absence of any commercial or financial relationships that could be construed as a potential conflict of interest.

frontiers in Physiology

ORIGINAL RESEARCH
published: 08 January 2020
doi: 10.3389/fphys.2019.01539

Cockroaches Show Individuality in Learning and Memory During Classical and Operant Conditioning

Cansu Arican, Janice Bulk, Nina Deisig and Martin Paul Nawrot**

Department of Computational Systems Neuroscience, Institute of Zoology, University of Cologne, Cologne, Germany

Animal personality and individuality are intensively researched in vertebrates and both concepts are increasingly applied to behavioral science in insects. However, only few studies have looked into individuality with respect to performance in learning and memory tasks. In vertebrates, individual learning capabilities vary considerably with respect to learning speed and learning rate. Likewise, honeybees express individual learning abilities in a wide range of classical conditioning protocols. Here, we study individuality in the learning and memory performance of cockroaches, both in classical and operant conditioning tasks. We implemented a novel classical (olfactory) conditioning paradigm where the conditioned response is established in the maxilla-labia response (MLR). Operant spatial learning was investigated in a forced two-choice task using a T-maze. Our results confirm individual learning abilities in classical conditioning of cockroaches that was reported for honeybees and vertebrates but contrast long-standing reports on stochastic learning behavior in fruit flies. In our experiments, most learners expressed a correct behavior after only a single learning trial showing a consistent high performance during training and test. We can further show that individual learning differences in insects are not limited to classical conditioning but equally appear in operant conditioning of the cockroach.

Keywords: classical conditioning, operant conditioning, insect cognition, learning and memory, cockroach, insect behavior, personality

OPEN ACCESS

Edited by:
Sylvia Anton,
Institut National de la Recherche Agronomique (INRA), France

Reviewed by:
Aurore Avargues-Weber,
UMR5169 Centre de Recherches sur la Cognition Animale (CRCA), France
Fernando Locatelli,
CONICET Institute of Physiology, Molecular Biology and Neurosciences (IFIBYNE), Argentina

****Correspondence:***
Nina Deisig
ndeisig@uni-koeln.de
Martin Paul Nawrot
martin.nawrot@uni-koeln.de

Specialty section:
This article was submitted to Invertebrate Physiology, a section of the journal Frontiers in Physiology

Received: *16 July 2019*
Accepted: *05 December 2019*
Published: *08 January 2020*

Citation:
Arican C, Bulk J, Deisig N and Nawrot MP (2020) Cockroaches Show Individuality in Learning and Memory During Classical and Operant Conditioning. Front. Physiol. 10:1539. doi: 10.3389/fphys.2019.01539

INTRODUCTION

A behavioral syndrome defines a consistent behavior of an individual that is correlated across time and contexts. Animal personality (Gosling and Vazire, 2002) is expressed in long-term differences among individuals across a variety of behavioral traits such as boldness-shyness, exploration-avoidance, activity level, sociability, or aggression (Sih et al., 2004a,b; Dingemanse and Wolf, 2010). While consistent behavioral traits have been heavily studied in vertebrates, literature on individuality and personality in invertebrates is still scarce (for review, see Kralj-Fišer and Schuett, 2014). The small amount of available data on invertebrate personality may be partly due to the traditional belief that invertebrates express stereotyped stimulus-response behaviors with little individual differences (e.g., Brembs, 2013). Invertebrate studies have primarily been conducted in the context of collective behavior in social contexts and mostly investigated how individual personalities influence the colony behavior (e.g., in cockroaches: Planas-Sitjà et al., 2018; Planas-Sitjà and Deneubourg, 2018, ants: Pinter-Wollman, 2012, spiders: Grinsted et al., 2013; Wright et al., 2014, pea aphids: Schuett et al., 2011; and crickets: Rose et al., 2017).

At the level of animal cognition, inter-individual performance differences may reflect variation in cognitive ability independent of animal personality. However, individual cognitive styles may also inflict personality (Carere and Locurto, 2011). Individuality has been intensively studied in learning and memory. Learning and memorizing the relevance of environmental cues is of major importance for the survival of virtually all animals. Individuals of a species can vary substantially in their learning performances as has been shown for both vertebrates (e.g., Gosling, 2001; Gallistel et al., 2004; Groothuis and Carere, 2005; Kolata et al., 2005; Schuett and Dall, 2009; Kotrschal and Taborsky, 2010; David et al., 2011) and invertebrates (for review, see Dukas, 2008).

In insects, studies have focused on bumblebees and honeybees. Bumblebees have been studied in a variety of tasks (Chittka et al., 2003). For example, individual bumblebees that learn only a single flower parameter (odor or color) were more efficient in several ways than those that had learned two: they made fewer errors, had shorter flower handling times, corrected errors faster, and transitions between flowers were initially more rapid (Chittka and Thomson, 1997). It has further been shown that individual bumblebees consistently differ in their ability to learn to discriminate stimuli from the visual and olfactory modality (Muller and Chittka, 2012). A systematic analysis of classical conditioning experiments in the honeybee found that the group-average learning behavior did not adequately represent the behavior of individual animals. This result was consistent across a large number of datasets including olfactory and tactile conditioning collected from more than 3,000 honeybees obtained during absolute and differential classical conditioning (Pamir et al., 2011, 2014). Gradually increasing learning curves reflected an artifact of group averaging and the behavioral performance of individuals was characterized by an abrupt and often step-like increase in the level of response (Pamir et al., 2011), a result that directly matches observation in vertebrates (Gallistel et al., 2004) but contradicts earlier findings in the fruit fly (*Drosophila melanogaster*) in which the group-average behavior has been described to represent the probabilistic expression of behavior in individuals (Quinn et al., 1974).

In the present work, we asked whether cockroaches show individuality in their learning performances, both in classical and operant conditioning tasks. Behavioral learning studies that used olfactory and visual cues demonstrated that cockroaches can be assayed for classical conditioning tasks while animals are immobilized (Watanabe et al., 2003; Kwon et al., 2004; Lent and Kwon, 2004; Watanabe and Mizunami, 2006) or able to move freely (Watanabe et al., 2003; Sato et al., 2006; Hosono et al., 2016). In some experiments, after classical olfactory conditioning, memory tests were performed in an open arena where cockroaches could freely choose to approach different odors (Watanabe et al., 2003; Sato et al., 2006). Open arenas and T-mazes have been used successfully for operant conditioning in cockroaches. Balderrama (1980) demonstrated for the first time that cockroaches could be trained to associate different odors with either sugar or salt solution in an open arena. Mizunami et al. (1998) studied place memory using a spatial heat maze with and without visual cues. More recent studies by Mizunami and colleagues (Sakura and Mizunami, 2001; Sakura et al., 2002) confirmed and extended operant conditioning of cockroaches in the open arena. Barraco et al. (1981) successfully trained cockroaches in a spatial discrimination task using an electric shock to punish either a left or right turn in a T-maze. Employing stimuli of different modalities, we show in the present study that cockroaches demonstrate individuality in their ability to learn and memorize stimuli employing both classical and operant conditioning tasks.

MATERIALS AND METHODS

Insects

All experiments were conducted with adult male *Periplaneta americana*. Animals were kept under a reverse light-dark cycle (12 h : 12 h) at 26°C in laboratory colonies at our rearing facilities at the University of Cologne. Cockroaches were allowed to drink water and fed on oat *ad libitum*. However, water was removed 4 days before training to increase motivation. All experiments were conducted in the active phase (scotophase) of the animals.

Experimental Setups

For classical conditioning, cockroaches were harnessed in custom-made fixation cylinders (**Figure 1A**) after anaesthetization at 4°C. After fixation, only the animals' head protruded allowing free movement of the antennae and mouthparts. After habituation in the experimental room for 16 h, cockroaches were placed in front of a 10 ml plastic syringe mounted in a holder and an exhaust system behind removing odor-loaded air (**Figure 1A**). Stimuli were diluted in mineral oil (Acros Organics™, Geel, Belgium) and odor concentrations were adjusted to match the vapor pressure of the odor with the lowest value (trans-cinnamaldehyde). Dilutions were as follows (in % v/v): isoamyl acetate (99+ %, pure, Acros Organics™, Geel, Belgium): 26.27%, butyric acid (> 99%, Aldrich, Darmstadt, Germany): 2.56%, trans-cinnamaldehyde (≥ 98%, Merck, Darmstadt, Germany) undiluted. Ten microliters of each odor were given on a piece of filter paper inserted in a 10 ml plastic syringe for olfactory stimulation. A filter paper without any odor nor the solvent was used as control stimulus testing for mechanical stimulation (Air). Isoamyl acetate and butyric acid were used as conditioned stimuli (CS+ or CS−), while trans-cinnamaldehyde served as control odor without any assigned contingency (reward or punishment). Odors were chosen based on choice behavior of cockroaches in preliminary tests in a T-maze, in which no preference was found between isoamyl acetate and butyric acid.

For operant conditioning, a custom-made flexible maze was used. Walls made from polyvinyl chloride allowed easy cleaning with alcohol between single trials. The maze was positioned on a ground plate and different tunnel pieces were combined to form a T-Maze (**Figure 1B**). Shutters allowed closing the start and target boxes (20 cm × 28 cm × 4 cm). All experiments with the T-maze were conducted under red light (**Figure 1B**).

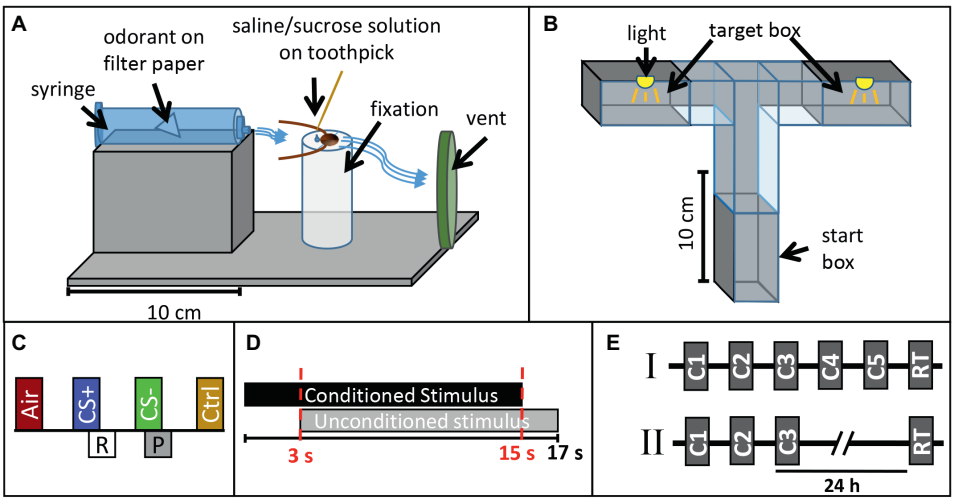

FIGURE 1 | Experimental design. Sketch of **(A)** the classical conditioning setup and **(B)** the operant conditioning setup. **(C)** Presentation of one training block in the classical conditioning paradigm. Each block contains an air puff (Air), the rewarded odor CS+ paired with sugar solution (R), the punished odor CS− paired with saline solution (P), and the control odor (Ctrl, cinnamaldehyde). **(D)** Time sequence of the conditioned stimulus (CS, odor) and unconditioned stimulus (US, sucrose or saline solution) in a single training trial during classical conditioning. **(E)** Operant conditioning protocols (I) with five consecutive training trials (C1–C5) and a retention test (RT) after 35 min and (II) with three consecutive training trials (C1–C3) and a retention test after 24 h.

Training and Test Procedures

First, we established a novel classical conditioning paradigm in the harnessed cockroach, training the animals to exhibit a specific movement of the maxilla-labia (mouthparts) as conditioned response behavior. We termed this response the maxilla-labia response (MLR). When touching the antennae and mouthparts with sucrose solution, cockroaches start to quickly move and extend their maxillae and labium, the most central mouthparts, to reach for and suck the solution. When saline solution is presented, animals touch and taste the solution without ingesting and show clear avoidance behavior (retraction of the mouthparts). In each single trial, the occurrence or non-occurrence of the MLR was recorded as a binary response (0/1). Only if the MLR was observed within the first 3 s of odor presentation (before US-onset, see **Figure 1C** and description below), it was counted as conditioned response. This novel paradigm for classical conditioning of the cockroach is similar to the proboscis extension response paradigm used in classical conditioning of honeybees, first established by Takeda (1961) and later standardized by Bitterman et al. (1983).

For classical conditioning, each block of training consisted of (1) one stimulation with a simple filter paper without an odorant to test for a mechanical response to the air puff (Air), (2) one CS+ presentation (reinforced conditioned stimulus) paired with 20% sucrose solution as positive reinforcer (unconditioned stimulus, US), (3) one CS− presentation (punished stimulus) paired with 20% saline solution as negative reinforcer, as well as (4) one stimulation with a control odor (cinnamaldehyde, Ctrl), which was not paired with a US (**Figure 1C**). In each CS+ or CS− presentation, the respective odor (CS) was presented for 15 s. Three seconds after odor onset, the US was delivered by touching the maxillary palps with sucrose or saline solution and animals were allowed to drink the respective solutions for 14 s (**Figure 1D**). In the case of the negative reinforcer, most animals did not drink the saline solution voluntarily but were "forced" to taste the salt in all trials by touching their mouthparts with the toothpick. We performed all experiments in two independent groups for which the identities of the CS+ odor and the CS− were reversed. For retention tests, the same pattern of odor presentation as in conditioning trials was used except that no US was presented.

Three differential classical conditioning experiments were conducted. In each block of training trials, the two control stimuli (air, cinnamaldehyde) were separated from the two CSs with an interstimulus interval (ISI) of 45 s, whereas the ISI between CS+ and CS− was 32 s. The first experiment was designed to investigate differential learning with an acquisition phase that consisted of five blocks of trials (each block contained one presentation of air, the CS+, the CS−, and a control stimulation, respectively) with an inter-block interval of 10 min. A retention test was conducted after 10 min. The second and third experiments were designed to investigate memory retention after differential learning at two different time intervals (1 h and 24 h). Due to the length of the experiment, only three training blocks with an inter-block interval of 10 min were used for these two experiments.

For operant conditioning, each cockroach was allowed to acclimate in the start box for 15 min before training. At the beginning of a training trial, the shutter was opened and the cockroaches were allowed to walk freely and enter the target boxes. When entering one of the target boxes for the first time, the shutter was closed and the animal was subjected to a 5 min light exposure (punishing stimulus, US). Whenever an animal entered the same target box again in a subsequent

trial, it was again subjected to the light punishment. All animals which did not start moving within the first 3 min in two consecutive attempts were excluded from the experiment.

Two different operant conditioning paradigms were used. In the first one, animals were trained in five trials with an inter-trial interval (ITI) of 35 min and memory retention was tested after 35 min. In the second, animals were trained in three trials with an ITI of 35 min and a retention test was performed 24 h later (**Figure 1E**).

Statistics

The results were analyzed with Matlab R2019a (The MathWorks, Natick, Massachusetts, USA) and IBM SPSS Statistics Version 25.0 (IBM Corp., Armonk, New York, USA) and visualized with Matlab R2019a and Photoshop (Adobe Inc., San José, California, USA).

We analyzed spontaneous responses to different odors in two groups of animals. We pooled the behavioral response to odor presentations in the first training trial and before US presentation across all individuals that had been treated in parallel and under identical experimental conditions. Chi-squared tests were used to compare responses to different odors. Additionally, we calculated the Phi coefficient to analyze the correlation between odor responses across individuals.

For the statistical analysis of the classical conditioning experiments we applied three different statistical tests. First, one-way ANOVA was used to test the evolution of responses along training trails. Second, a two-way repeated measure ANOVA was used to compare the reinforcement type (CS+ and CS−) and the reinforcement type × trial interaction. Although ANOVA is usually not allowed in case of dichotomous data such as the MLR, Monte Carlo studies have shown that ANOVA can be used under certain conditions (Lunney, 1970), which all are met by the experiments reported here. Third, χ^2 tests were used for (1) comparison of responses to the CS+ and CS− in a given trial, (2) comparison of spontaneous responses and retention tests, (3) comparison of the last training trial and retention tests, and (4) comparison between different retention tests.

For further analysis of classical conditioning experiments, we pooled all animals with the same conditioning pattern regardless of the odor that was used as CS+ or CS−. To analyze the response to CS+, we excluded all animals showing spontaneous responses to the CS+ in the first trial. For analyzing responses to the CS−, we excluded all animals that did not respond to it in the first trial. This is a common procedure to exclude spontaneously responding animals and to visualize the learning curve (Pamir et al., 2011; Giurfa and Sandoz, 2012).

For all operant conditioning paradigms, decisions in the forced two-choice tasks were analyzed with a binomial test, since chance level of choosing one of two directions randomly was $p = 0.5$.

Analysis of Individuality

To analyze individuality of learning behavior, we followed the analyses in Pamir et al. (2011, 2014). For the analyses in the classical conditioning paradigm, we only considered animals that did not show a correct response to either the CS+ or the CS− in the very first trial and before the US was presented. Two subgroups were formed for training trials and test trial following the definition in Pamir et al. (2011). For any given trial, the first subgroup included animals that expressed the correct behavior in the present trial and in the previous trial (previous correct behavior, pC). The second subgroup included animals showing the correct behavior in the present trial but did not show it in the previous trial (previous incorrect behavior, pI). The same subgroup definitions were used for the retention test with regard to a correct or incorrect response during the final training trial. We compared the two subgroups in each trial and in the retention test with a χ^2 test at a significance level at $\alpha = 0.05$. The two subgroups are represented with upward and downward pointing triangles, respectively. Filled (open) symbols indicate that significance could (not) be established.

Following the analyses in Pamir et al. (2014), we formed separate subgroups of animals that showed a correct behavior for the first time in the second (or third) trial and tracked the subgroup behaviors across subsequent conditioning trials and the memory test. This allows to assess the robustness of the expression of a correct behavior across trials and the transfer of the behavioral expression during training to the short-term and long-term memory test situation.

Finally, in order to analyze the initiation of correct behavior, we computed for each trial the fraction of animals that responded correctly for the first time in this trial as well as the fraction of animals that never behaved correctly (non-learners, Pamir et al., 2014).

RESULTS

Spontaneous Response Toward Different Odors

We first analyzed the spontaneous and naive responses to each odor (isoamyl acetate, butyric acid, and cinnamaldehyde) during the very first conditioning trial before the reinforcing stimulus (US) was presented. **Figure 2** shows the group averaged responses to all three odors. In all experiments, approx. 60% of the animals showed a spontaneous MLR in presence of isoamyl acetate, which was significantly higher than for butyric acid and cinnamaldehyde for all experiments (χ^2: $p < 0.001$). The number of spontaneous responses to butyric acid and cinnamaldehyde was only significantly different in the first experiment (χ^2: $p = 0.01$) in which animals responded more often spontaneously to butyric acid. Isoamyl acetate is the main component of the banana blend and thus strongly associated with food and attractive for cockroaches (Lauprasert et al., 2006). This is most likely the reason for very high spontaneous response rates to isoamyl acetate. In addition, we found a significant positive correlation between responses to isoamyl acetate and butyric acid in both experiments [**Figure 2**: (1) $\Phi = 0.0258$, $p = 0.016$; (2) $\Phi = 0.143$, $p = 0.017$]. However, there was no significant correlation for other odor pairings, which might be due to the generally low spontaneous response rates to cinnamaldehyde and butyric acid.

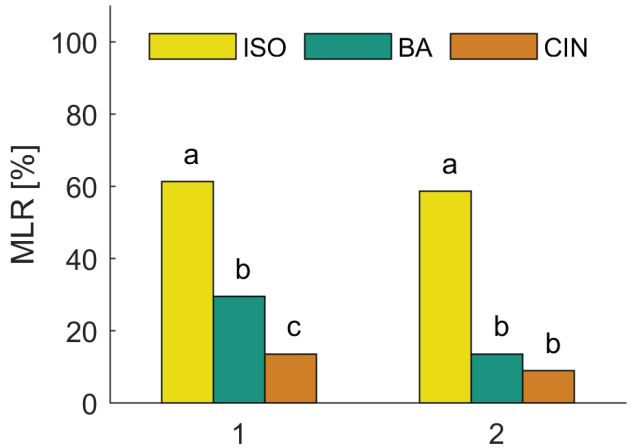

FIGURE 2 | Spontaneous responses to isoamyl acetate (ISO), butyric acid (BA), and cinnamaldehyde (CIN). Analysis of the MLR in the first trial of two classical conditioning experiments shows that ISO elicits significantly more spontaneous responses than BA and CIN (χ^2: $p < 0.001$). The spontaneous response to BA is only significantly higher compared to CIN in the first experiment (χ^2: $p = 0.01$).

A Novel Paradigm for Classical Olfactory Conditioning

We established a novel paradigm for classical conditioning in harnessed cockroaches (**Figure 1A**). The occurrence or absence of the maxilla-labia response (MLR, see section "Materials and Methods") was recorded as the conditioned response (CR) behavior. In this study, we used different protocols for differential olfactory conditioning (**Figures 1C,D**) to investigate the expression of the CR during learning and memory retention at two different time-points.

In a first protocol, we tested whether cockroaches are able to associate an odor with a reward or punishment during five consecutive training trials (inter-trial interval 10 min) followed by a retention test (after 10 min). We trained two groups of animals for which the odors isoamyl acetate and butyric acid were presented as CS+ and CS− with reversed contingencies (**Figures 3A,B**, respectively). The two odors did not elicit the same level of spontaneous responses (cf. section "Spontaneous Response Toward Different Odors"). Due to the high initial spontaneous response to isoamyl acetate, the average level of MLR was consistently high and did not significantly increase across the five trials when isoamyl acetate was used as CS+ (**Figure 3A**). However, responses to the punished odor (CS−, butyric acid) decreased significantly (one-way ANOVA: $F_{4,\ 260} = 4.23$; $p < 0.002$).

When butyric acid was used as CS+, responses showed a tendency to increase over the five training trials. In this case, responses to isoamyl acetate as CS− slightly decreased; however, this effect was not significant over the five trials. Animals still showed approximately 30% responses to the CS− in the fifth trial.

Responses to the control odor cinnamaldehyde only decreased significantly when isoamyl acetate was the CS+ (one-way ANOVA: $F_{4,\ 260} = 3.11$; $p = 0.016$), but did not change when butyric acid was used as CS+.

Overall, responses to the CS+ and CS− differed significantly when isoamyl acetate was rewarded (two-way repeated measures ANOVA: $F_{4,\ 49} = 3.095$; $p = 0.02$). When butyric acid was rewarded, CS+ and CS− did not differ significantly over trials (**Figure 3B**).

For further analyses, we pooled all animals according to CS+ and CS− and excluded those that did not behave correctly in the first trial, respectively. In both cases, correct behavior increased significantly across training trials [one-way ANOVA: **Figure 3C** (CS+): $F_{4,\ 230} = 8.808$; $p < 0.001$; **Figure 3D** (CS−): $F_{4,\ 190} = 15.544$; $p < 0.001$]. However, neither the behavior to CS− in **Figure 3C**, the CS+ in **Figure 3D**, nor the behavior to the control odor changed significantly over trials. Moreover, the interaction between trial and treatment was significant for CS+ (two-way repeated measures ANOVA: $F_{4,\ 43} = 12.156$, $p < 0.001$) and CS− (two-way repeated measures ANOVA: $F_{4,\ 35} = 17.591$, $p < 0.001$) and in both cases the behavior in retention tests were significantly different from each other (**Figures 3C,D**).

In addition, we excluded animals that did not behave correctly specifically either to the CS+, the CS- or the control. Accordingly, we could see that the effect of increasing correct behavior over trials was not only due to the exclusion of spontaneous responding or not responding animals (see **Supplementary Figure S1**).

Expression of Short-Term and Long-Term Memory After Classical Conditioning

To test memory retention after differential classical conditioning at a short- and long-term range we conducted a new experiment. A group of cockroaches were differentially trained during three consecutive trials. The group was then split in half and retention tests were performed either 1 h after the last training trial or 24 h after. In **Figure 4**, we show the training trials as unseparated groups, but the statistical analysis that include the training trials was conducted with splitted groups, which are shown in **Supplementary Figure S2**. The experiment was repeated with reversed contingencies of the odors. Responses to mechanical air stimulation (filter paper alone) did not vary and always stayed below 1.5%.

Overall, responses to the CS+ were significantly different from the CS− across three training trials in both groups (two-way repeated measures ANOVA: **Figure 4A**: $F_{2,\ 183} = 9.266$, $p < 0.001$; **Figure 4B**: $F_{2,\ 91} = 13.016$; $p < 0.001$). Responses to the CS− decreased significantly in both experiments (one-way ANOVA: **Figure 4A**: $F_{2,\ 552} = 7.181$; $p < 0.001$; **Figure 4B**: $F_{2,\ 276} = 3.291$; $p = 0.002$) while responses to the CS+ did not increase significantly. Responses to the control odor cinnamaldehyde decreased significantly only when butyric acid was used as CS+ (one-way ANOVA: $F_{2,\ 276} = 3.291$; $p = 0.039$).

During the 1 h test animals that received isoamyl acetate as CS+ maintained the elevated response level as group averaged performance, thus the retention test after 1 h was not significantly different to the response level in the last training trial (**Figure 4A**, χ^2: $p = 0.143$). Interestingly, the response level to isoamyl acetate was significantly higher in the 24 h retention test compared to the 1 h retention test (χ^2: $p < 0.001$), as well as in comparison

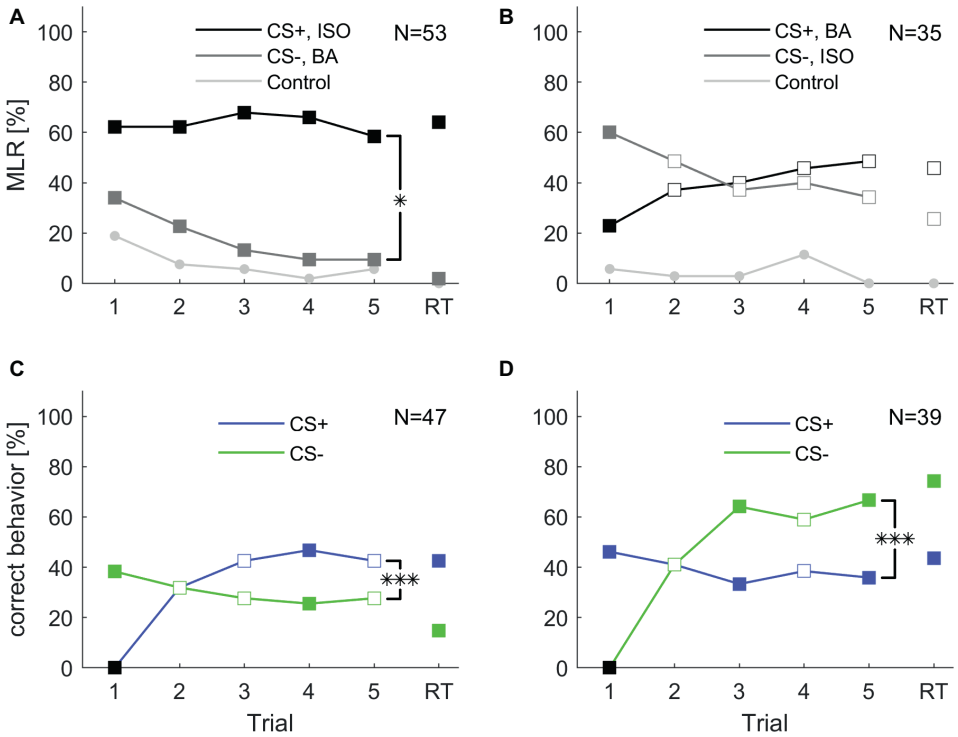

FIGURE 3 | Classical olfactory conditioning over five trials with a memory retention test after 10 min. Filled squares indicate trials in which a significant difference was found between CS+ and CS– (χ^2 test). Asterisks indicate that responses changed for the conditioned stimuli (CS+ and CS–) over trials (two-way ANOVA, repeated measures: treatment × trial interaction *: $p < 0.05$; ***: $p < 0.001$). **(A)** When isoamyl acetate (ISO) was the rewarded odor (CS+, black), the average group response did not increase during training. Responses to the punished odor BA (CS–, dark gray) decreased significantly over trials (one-way ANOVA: $p = 0.002$) and odor × trial interaction was significant (two-way repeated measures ANOVA: $p = 0.02$). **(B)** When BA was rewarded (CS+, black), responses increased considerably, however not significantly (one-way ANOVA: $p = 0.208$). Responses to ISO decreased, but again, not significantly (one-way ANOVA: $p = 0.189$). The odor × trial interaction was not significant (two-way repeated measures ANOVA: $p = 0.113$). **(C)** When excluding all spontaneous responding animals to the rewarded odor, response to CS+ increased significantly (one-way ANOVA: $p < 0.001$). Responses to the CS– decreased over trials, but not significantly (one-way ANOVA: $p = 0.686$). The treatment × trial interaction was significant (two-way repeated measures ANOVA: $p < 0.001$). **(D)** When excluding all not spontaneous responding animals to the punished odor the number of animals that behaved correctly to CS– over trials increased significantly (one-way ANOVA: $p < 0.001$), while response to CS+ did not change significantly over trials (one-way ANOVA: $p = 0.814$). The treatment × trial interaction was significant (two-way repeated measures ANOVA: $p < 0.001$). Black squares in **(C,D)** indicate the exclusion of animals that did not behave correctly in the first trial.

to the response level at the end of training (χ^2: $p < 0.001$) (**Supplementary Table S1**). When butyric acid was the rewarded odor (**Figure 6B**), response levels to the CS+ in both memory tests (after 1 and 24 h) were not different from each other (χ^2: $p = 0.475$), nor from the response level at the end of training (χ^2: 1 h: $p = 0.826$; 24 h: $p = 0.149$). The response level to the CS– resumed the initial high spontaneous response levels to isoamyl acetate during 1 and 24 h retention. All results are summarized in **Supplementary Table S2**.

For the next step of analysis, animals that did not behave correctly in the first trial were excluded and for both CS+ and CS– the percentage of correct behaving animals increased (**Figures 4C,D**, one-way ANOVA: CS+: $F_{2,\,537} = 33.537$; $p < 0.001$; CS–: $F_{2,\,306} = 43.027$; $p < 0.001$). The only other significant effect was the decrease of correct behavior to the CS– when all correct responding animals were excluded (one-way ANOVA: $F_{2,\,537} = 3.569$; $p = 0.029$). Moreover, the interaction between trial and treatment was significant in both cases (two-way repeated measures ANOVA: **Figure 4C**: $F_{2,\,178} = 46.719$; $p < 0.001$; **Figure 4D**: $F_{2,\,101} = 39.158$; $p < 0.001$).

When excluding all spontaneously responding animals, performance in the retention test stayed at the same level as at the end of training. However, the increase of the CS+ retention test after 24 h was significant (χ^2: $p < 0.001$). After exclusion of the nonspontaneous responders, performance in all retention tests stayed similar compared to the third trial of training. However, the percentage of correct behaving animals to the CS– decreased after 1 h (χ^2: $p < 0.001$) and 24 h (χ^2: $p < 0.001$).

Individual Learning Performance During Classical Conditioning

To test whether differences in learning performance exist among individual animals, we followed the analyses suggested in Pamir et al. (2011, 2014). Each of the two groups trained in the five trial classical conditioning experiment (**Figures 3C,D**) were divided into two subgroups (cf. section "Materials and Methods"): (1) individuals that behaved correctly in two consecutive trials (previous correct behavior, pC) and (2) individuals that did not behave correctly in the previous trial but started behaving

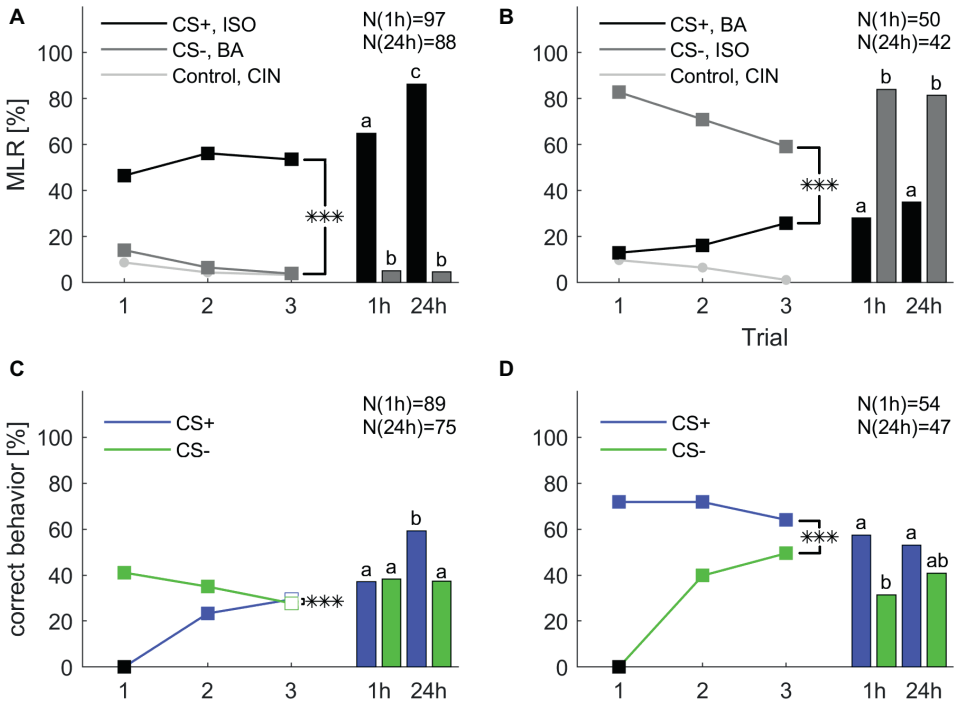

FIGURE 4 | Classical olfactory conditioning over three trials with memory retention tests after 1 and 24 h. Filled squares indicate trials in which a significant difference was found between CS+ and CS− (χ^2 test). Asterisks indicate a significant treatment × trial interaction (***: $p < 0.001$). Letters above the bars indicate significant differences between retention tests (χ^2). **(A)** When isoamyl acetate (ISO) was rewarded (CS+, black) and butyric acid (BA) punished (CS−, dark gray), responses significantly decreased for the CS− (one-way ANOVA: $p < 0.001$), but did not change for the CS+ (one-way ANOVA: $p = 0.155$). Overall, the odor × trial interaction was significant (two-way repeated measures ANOVA: $p < 0.001$). **(B)** When butyric acid was rewarded (CS+, black) and isoamyl acetate was punished (CS−, dark gray), responses to the CS+ increased, however, not significantly (one-way ANOVA: $p = 0.06$), but decreased significantly for the CS− (one-way ANOVA: $p = 0.002$). The odor × trial interaction was again significant (two-way repeated measures ANOVA: $p < 0.001$). **(C)** When excluding all spontaneous responding animals to the rewarded odor the response to CS+ increased significantly (one-way ANOVA: $p < 0.001$). The response to CS− decreased significantly over trials (one-way ANOVA: $p = 0.029$). The treatment × trial interaction was significant (two-way repeated measures ANOVA: $p < 0.001$). **(D)** When excluding all not spontaneous responding animals to the punished odor the number of animals that behaved correctly to CS− over trials increased significantly (one-way ANOVA: $p < 0.001$). The response to CS+ did not change significantly over trials (one-way ANOVA: $p = 0.38$). The treatment × trial interaction was significant (two-way repeated measures ANOVA: $p < 0.001$). Black square in **(C,D)** indicate the exclusion of animals that did not behave correctly in the first trial.

correctly in the present trial (previous incorrect behavior, pI). Previous correct behaving animals always showed a higher level of correct behavior than the average correct behavior across all animals (**Figure 5**, red upward triangles), while the previous incorrect behaving individuals always showed lower correct behavior (**Figure 5**, red downward triangles).

Next, we analyzed the across-trial behavior of those animals that showed their first correct behavior already in the second trial (i.e., after only a single pairing of CS and US) and find that this subgroup showed consistently high rates of correct responses across all trials and during retention with retention scores above 90%, both for CS+ and CS− (dark gray curves in **Figures 5A,C**). Individuals that started to respond correctly in the third trial (after two pairings of CS and US, light gray curves in **Figures 5A,C**) showed lower correct response levels than those animals that had started in the first trial but, still, these were comparably high considering the fact that the average response levels (blue and green curve in **Figures 5A,C**, respectively) included also the high performance group (dark gray curves). This indicates that fast learners are also good learners and parallels previous findings in the honeybee (Pamir et al., 2014).

In the histograms of **Figures 5B,D**, we counted for each trial separately how many animals responded correctly for the first time in that trial. From all animals that showed learning, most of them showed the correct response after a single conditioning trial. The second largest group behaved correctly for the first time after two conditioning trials. However, a substantial portion of animals never behaved correctly (black bars in **Figures 5B,D**) and this group is larger for a correct behavior toward the CS+.

Individuality in Operant Learning

We then tested learning, memory retention, and individual differences in an operant conditioning task. Cockroaches were trained to avoid a punishment and were tested for their memory for up to 24 h. For this, we designed a forced two-choice paradigm where an individual cockroach is placed in a T-maze during repeated training trials (**Figure 1B**, cf. Materials and Methods). In each trial, the cockroach was allowed to choose one of the arms and entered a target box. In the first trial and irrespective of the animal's choice, it experienced an aversive bright light stimulus. Whenever the animal chose the same side in subsequent trials, the same aversive stimulus was elicited.

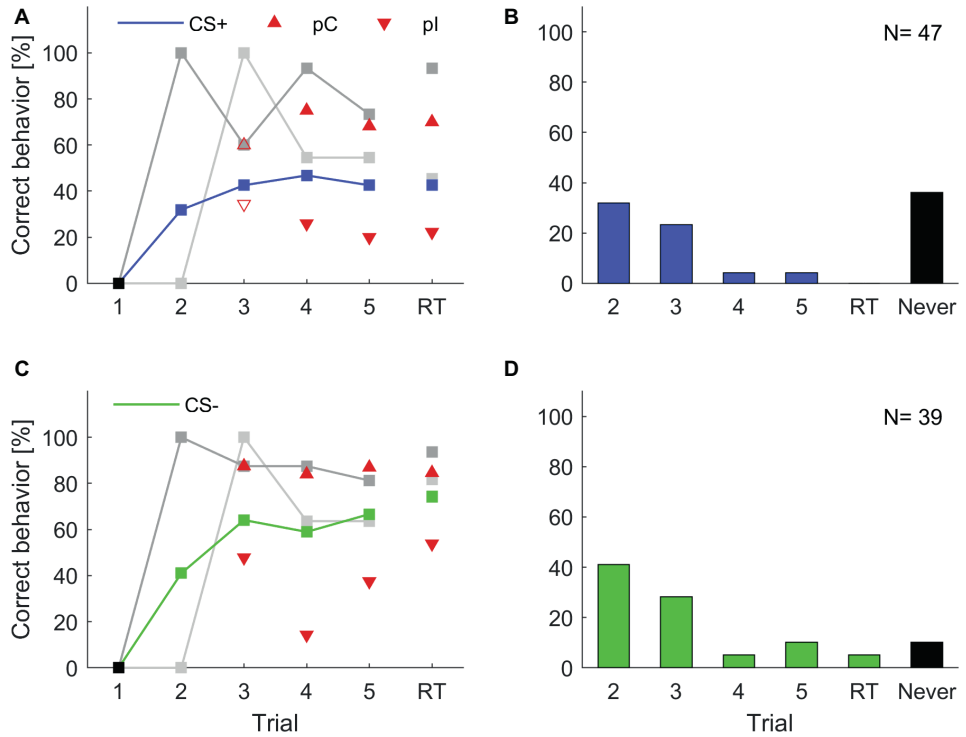

FIGURE 5 | Individual learning abilities in classical olfactory conditioning. Data for isoamyl acetate as CS+ and butyric acid as CS+ were pooled, likewise data for isoamyl acetate as CS– and butyric acid as CS– were pooled. Correct learning is represented by **(A)** increasing responses to the rewarded odor in the case of CS+ and **(C)** increasing response-suppression to the punished odor in the case of CS–. **(A,C)** Upward pointing triangles depict animals, which correctly behaved in the respective trial and already showed a correct behavior in the previous trial (pC). Triangles pointing downward depict animals that correctly behaved in the respective trial but did not do so in the previous trial (pI). Filled triangles indicate a significant difference of subgroups in the respective trials, empty triangles represent subgroups that were not significantly different (χ^2; $\alpha = 0.05$). Animals behaving correctly in trial two, i.e., after a single training trial (dark gray; CS+: $N = 15$; CS–: $N = 16$) showed consistently high probabilities of correct responses in subsequent trials (cf. Pamir et al., 2014). Similarly, high response scores were observed for animals responding correctly for the first time in trial three (light gray; CS+: $N = 11$; CS–: $N = 11$). Black squares indicate the exclusion of animals that did not behave correctly in the first trial. **(B,D)** Proportion of animals behaving correctly for the first time in the indicated trial. A high percentage of animals expressed a correct behavior already after a single training trial. A substantial proportion of animals never behaved correctly (black bars).

Learning was thus expressed in avoiding the side (left or right) that resulted in the punishment with the bright light stimulus.

In a first experiment, animals were trained for five consecutive trials and short-term memory retention was tested 35 min after the last trial. In a second experiment, animals were trained for three trials and a long-term retention test was performed 24 h later (**Figure 1E**). Animals in the first group significantly learned to avoid the punished side from the third trial onward (binomial tests: $p < 0.01$). Animals showed correct memory for the punished side in the retention test 35 min after (**Figure 6A**). Cockroaches in the second group did not significantly show learning after two training trials. However, memory for the correct side was expressed in the 24 h retention test (binomial test: $p = 0.014$, **Figure 6B**).

To study individual differences in these operant learning and memory tasks, animals were again attributed to two subgroups. In the short-term memory experiment, animals in the subgroup showing the correct behavior in two consecutive trials (pC) always performed better than the group average while animals in the subgroup pI consistently showed fewer correct choices in the present trial. Behavioral choices of previous correct deciding animals (pC) and previous incorrect deciding animals (pI) significantly differed in the third and fourth trials during training (χ^2: $p < 0.05$). This difference was not significant in the fifth learning trial, nor in the retention test after 35 min (χ^2: trial 3: $p = 0.161$; trial 4: $p = 0.186$, **Figure 6A**).

In the long-term memory experiment, the two subgroups (pC and pI) again differed significantly after two training trials. During the 24 h retention test, the subgroup of animals that had shown a correct decision in the last training trial significantly outperformed those animals that had made an incorrect decision in the last training trial (**Figure 6B**: χ^2: $p < 0.05$).

DISCUSSION

In the present work, we show that the adult American cockroach, *Periplaneta americana*, can solve classical olfactory and operant spatial conditioning tasks. In both cases, animals could learn to establish a conditioned response to the rewarded stimulus (CS+), and to diminish their responses to the punished odor (CS–) despite the fact that, in the classical conditioning task, the two odors were not equally important to the animals (high spontaneous

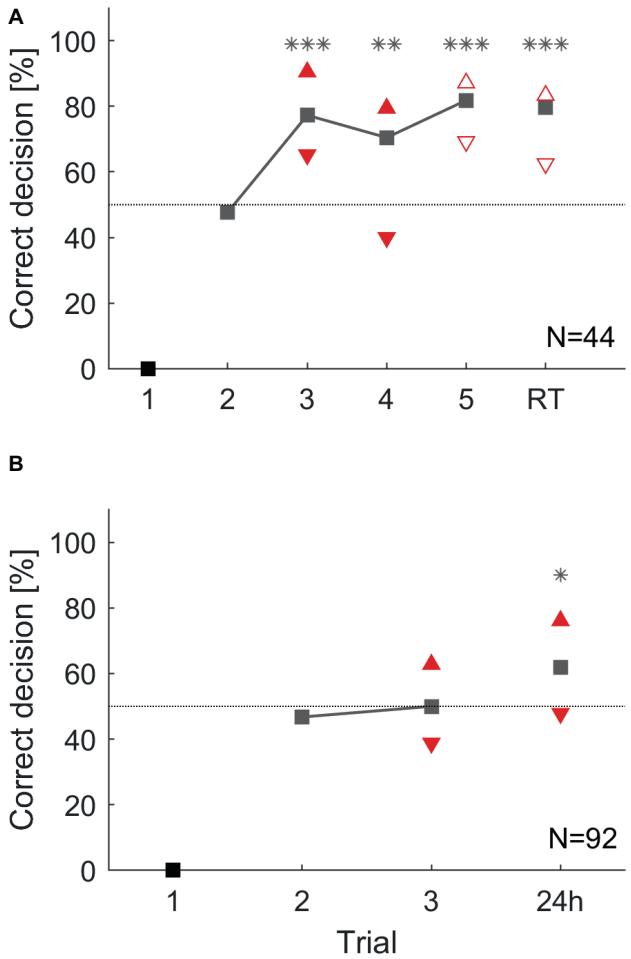

FIGURE 6 | Overall group performance and individual choices during an operant conditioning task in a T-maze **(A)** over five consecutive trials and a 35 min retention test (RT). From the third trial on cockroaches chose significantly more often the correct direction (**: $p < 0.01$; ***: $p < 0.001$). **(B)** Operant conditioning over three trials and a retention test after 24 h. However, this time cockroaches did not learn during training but chose significantly more the correct direction in the 24 h retention test (*: $p < 0.05$). Triangles that point upward depict animals that chose the correct direction in two consecutive trials (pC). Triangles that show downward depict animals that chose the correct direction in the present trial but did not choose it in the previous trial (pI). Filled triangles differ significantly from each other within a trial and empty ones do not (χ^2; $\alpha = 0.05$).

responses to isoamyl acetate). Overall, training resulted in the successful expression of short-term memory and long-term memory (after 24 h) in both conditioning tasks. We further show that cockroaches express individuality in their learning and memory performance in classical and operant conditioning.

Classical Olfactory Conditioning in the Cockroach

For the present study, we established a novel classical conditioning paradigm in harnessed cockroaches that allows to observe the expression (or non-expression) of a discrete conditioned response behavior, the **m**axilla-**l**abia **r**esponse (MLR) during learning and memory retention. The development of this paradigm was inspired by the highly successful proboscis extension reflex (PER) paradigm in the honeybee (e.g., Kuwabara, 1957; Takeda, 1961; Bitterman et al., 1983; Giurfa and Sandoz, 2012; Menzel, 2012) in which the extension (or non-extension) of the proboscis is observed as a discrete conditioned response behavior.

A number of previous studies have investigated classical conditioning in the cockroach using training and test conditions that differ fundamentally from our MLR paradigm. In studies by Watanabe et al. (2003), Sato et al. (2006), and Liu and Sakuma (2013), in the German cockroach, unrestrained cockroaches were placed in a cylindrical chamber during repeated conditioning trials with one odor paired with sucrose reward (CS+) and a second odor paired with salt punishment (CS−). Sato et al. (2006) could prove that beyond simple olfactory discrimination learning, cockroaches exhibited excellent learning performance in an occasion setting paradigm in which a visual context defines the contingency between olfactory CSs (conditioning stimuli) and gustatory USs (unconditioned stimuli). Watanabe et al. (2003) extended their classical conditioning protocol in unrestrained cockroaches to harnessed cockroaches that were subsequently tested under freely moving conditions in a test arena where they could choose between the two previously conditioned odors. This paradigm, however, did not establish a clear conditioned response observable during training and thus expression of a conditioned response behavior is only accessible during memory retention and under conditions different from training. Classical conditioning leads to an increase in response of salivary neurons to an odor associated with sucrose reward in the cockroach (Watanabe and Mizunami, 2006). After differential conditioning, one odor paired with sucrose and another odor without reward, the sucrose-associated odor induced an increase in the level of salivation, but the odor presented alone did not, proving classical conditioning of salivation in cockroaches (Watanabe and Mizunami, 2007). Classical conditioning of salivation has first been shown a century ago by Pavlov in his famous dog experiments (Pavlov, 1927). Restrained cockroaches were further used to study spatial (e.g., Kwon et al., 2004) or visual-olfactory associative learning and memory (e.g., Lent and Kwon, 2004; Pintér et al., 2005; Lent et al., 2007) by quantifying the antennal projection response (APR) of animals that were tethered in the middle of an arena (Pomaville and Lent, 2018). The APR is based on the observation that antennal motor actions can be elicited by different modalities, including olfactory, tactile, and visual stimuli (e.g., Menzel et al., 1994; Erber et al., 1997). Conditioning the APR consists in quantifying directed antennal movements toward the direction of a rewarded visual stimulus and was inspired by operant conditioning of bees to extend their antennae toward a target in order to receive a reward (e.g., Menzel et al., 1994; Kisch and Erber, 1999). The advantage of training immobilized insects provides a powerful technique for studying the neuronal basis (by, e.g., employing neurophysiological and pharmacological techniques) of learning and memory in a simpler nervous system compared to vertebrates.

Initial Response Behavior During Classical Conditioning

Stimuli used for studying olfactory learning and memory in insects mostly employ odors that are relevant in the natural context, such as communication signals (i.e., pheromones) or food-related odors. Isoamyl acetate constitutes the most salient compound of the banana blend and is perceived as the smell of banana (Schubert et al., 2014). This odor is clearly food related and thus highly attractive for cockroaches (Lauprasert et al., 2006). This likely explains why, in our olfactory conditioning experiments, we observed a high level of initial responses to isoamyl acetate in the first trial (**Figure 2**). Consequently, it was difficult to observe learning (i.e., increasing conditioned response levels) when this odor was paired with a sucrose reward (CS+) since response levels were consistently high (> ~60%) from the first trial on and throughout training (**Figure 3A**). In the 24 h retention test, however, the MLR to isoamyl acetate was significantly increased compared to the response in the last training trial (**Figure 4A**), indicating that a long-term memory had been established. When isoamyl acetate was paired with salt punishment (CS−), animals learned to suppress their responses during training (**Figure 4B**). Initial responses to butyric acid were significantly lower (~ 30%) at the beginning of training in all cases (**Figure 2**). When associated to sugar, responses increased but never exceeded 50% even after five training trials. Spontaneous responses to butyric acid were completely abolished during training and memory retention when paired with punishment (**Figure 3B**). Concluding, the two odors employed in our study were not equally attractive to the animals.

Operant Spatial Conditioning in Cockroaches

A frequently used setup for operant conditioning is a Y- or T-maze, which is extensively used to study operant learning and decision-making in rodents. T- or Y-maze (dual choice) experiments in invertebrates have been used broadly to study visual or olfactory absolute and differential learning in free-flying bees (e.g., for review: Srinivasan et al., 1998; Giurfa et al., 1999, 2001; Avarguès-Weber et al., 2011; Nouvian and Galizia, 2019), in ants (e.g., Dupuy et al., 2006; Camlitepe and Aksoy, 2010), and in wasps (Hoedjes et al., 2012). In cockroaches, operant learning has repeatedly been studied in open arenas (e.g., Balderrama, 1980; Sakura and Mizunami, 2001; Sakura et al., 2002). The first work on operant conditioning in cockroaches was carried out by Balderrama (1980) who trained free-moving cockroaches individually in a simple training chamber to associate two artificial odors to sucrose and salt solutions, respectively, and testing discriminatory learning performance by measuring the odor preference before and after training. Spontaneous preference for one of the odors before training could be modified already with one trial and retention lasted up to 7 days. To date, there are only two studies that have challenged cockroaches in T-maze tasks, the first testing the influence of feces pheromones on directional orientation (Bell et al., 1973), while the second investigated effects of protein synthesis inhibiting drugs on learning and retention by training animals to avoid shock on one of the sides (Barraco et al., 1981). Our reason to perform an operant learning paradigm in the T-maze was to establish a forced binary choice that can be analyzed during acquisition and memory retention in a defined trial design. Electric shock as used for a punishing stimulus in the previous study by Barraco et al. (1981) seems a rather unnatural aversive stimulus that is unlikely to appear in nature. We decided to use bright light as negative reinforcer since cockroaches naturally avoid bright light and seek shelter in darkness (Turner, 1912).

Cockroaches started to avoid the side that was punished after a few trials. However, training results were variable across the two experiments. Previous studies concluded that cockroaches show unpredicted searching behavior (Balderrama, 1980). Similarly, we could observe different traits in behavior, which might partly underlie the variance in choice behavior. For example, some cockroaches show a high explorative behavior, possibly in search for an exit from the maze, and these did not seem to care much about the reinforcing stimulus while others stayed almost immobile throughout a trial and moved little. The punishing effect of light is limited because it has no harming consequence for the animal. They may thus habituate to the aversive light stimulus. The T-maze experiments in Barraco et al. (1981) using electric shock as negative reinforcer resulted in surprisingly high correct choice rates. However, a strong light seems to be repellent for most cockroaches since they normally try to hide in a dark place when, e.g., the light in a room is switched on. In future experiments, we want to explore whether a paradigm for appetitive operant conditioning can lead to higher levels of correct choice performance in cockroaches.

Individual Behavioral Expression of Learning and Memory

Our approach to study individuality in learning performance during classical conditioning was inspired by two previous studies by Pamir et al. (2011, 2014) that investigated a large number of datasets on classical appetitive conditioning in the honeybee. In these studies the authors were able to extract from an immense amount of data that honeybees express individual learning behavior and that a group of animals can be separated into at least two subgroups, learners and non-learners. Both studies by Pamir and colleagues have investigated behavioral learning and memory expression only toward the CS+. We have extended their analysis including behavioral learning and memory expression toward the CS− (**Figures 5C,D**).

After exclusion of individuals that did not respond correctly in the first trial, as for the honeybee (Pamir et al., 2014), a large fraction of animals (>35%) never showed the correct behavior to the CS+ odor in any of the learning trials or the retention test (**Figures 5B,D**). These animals may be considered non-learners. When taking into account only those animals that expressed the correct conditioned behavior at least once during the training session, we find that those animals expressed this behavior for the first time after average 1.7 conditioning trials toward the CS+ and after average 1.8 conditioning trials toward the CS−. Indeed, the largest fraction (50%) of responding animals showed a correct conditioned response behavior for the first time already after a single

conditioning trial (single-trial learning), both toward the CS+ and the CS−. In effect, 86.6% of learners showed a first correct behavior to the CS+ or CS− already after the first or second conditioning trial, indicating rapid learning after a single or two trials. These numbers match closely those obtained in the honeybee where typically ~50% of individuals in a group of honeybees showed a conditioned response after a single training trial (Pamir et al., 2014). Moreover, the correct expression of learned behavior in fast learners is remarkably stable as can be seen when following the across-trial CR behavior of the subgroup of cockroaches that showed a correct behavior after a single conditioning trial (dark gray curve in **Figures 5A,C**). When looking at short-term memory retention in those animals (**Figures 5A,C**), 93.3 and 93.8% expressed the correct behavior during the test for CS+ and CS−, respectively. Conversely, of the fraction of animals that showed the correct behavior during short-term memory retention for CS+ and CS−, 95 and 82.8%, respectively, were fast learning individuals expressing the correct behavior after a single or two training trials. Similarly, Pamir et al. (2014) reported that honeybees that responded earlier showed a higher long-term memory retention than those responding later. Taken together, our results indicate that (1) individual cockroaches are able to learn efficiently during only one or two conditioning trials, and (2) fast learners are also good learners that robustly express the correct behavior throughout the training session and achieve very high retention scores.

Thus, in line with the results on honeybees reported by Pamir et al. (2011, 2014), we conclude from our results that the gradually increasing group-average learning curve does not adequately represent the behavior of individual animals. Rather, it confounds three attributes of individual learning: the ability or inability to learn a given task (learners vs. non-learners), the fast acquisition of a correct conditioned response behavior in learners, and a high robustness of the conditioned response expression during consecutive training and memory retention trials. Moreover, we could establish the same general result in an operant learning task in the cockroach. The latter result is in line with a study in bumblebees (Muller and Chittka, 2012) observing that some individuals were consistently better than others in associating different cues with reward or punishment in an operant learning task.

Interestingly, these congruent results in the honeybee and cockroach, two evolutionary far separated species, are in contrast to the long-standing notion on learning abilities in fruit flies. An early report on olfactory learning in *Drosophila melanogaster* by Quinn et al. (1974) using a meanwhile well-established and heavily used group assay for classical olfactory conditioning of flies concluded that the expression of behavior in the individual was probabilistic such that a group of flies can be treated as homogeneous with respect to the ability to acquire a correct CR behavior. This notion has been challenged by a more recent study (Chabaud et al., 2010), but awaits further conclusive investigation. We hypothesize that fruit flies exhibit individual learning performance that is very similar to those observed in the honeybee and established for the cockroach in this study.

Possible Causes for the Individual Expression of Learned Behavior

What could be the underlying causes for the observed individuality in behavioral learning performance? At the neuronal circuit level, learning-induced plasticity has been observed at different sites within the system. Two studies in honeybees found correlations between the behavioral performance in individuals and the expression of plasticity in the nervous system. Rath et al. (2011) performed calcium-imaging in the projection neurons of the antennal lobe. For their analysis, they formed two subgroups of learners and non-learners based on their conditioned response behavior and reported that, as a result of classical olfactory conditioning, odor response patterns in the projection neuron population became more distinct in learners but not in non-learners. Haenicke et al. (2018) performed Ca-imaging from the projection neuron boutons in the mushroom body calyx of the honeybee and found that the level of neuronal plasticity correlates significantly with the level of behavioral plasticity across individual animals in classical olfactory conditioning. Mushroom body output neurons have been shown to convey the valence of odors following classical conditioning in bees (Strube-Bloss et al., 2011, 2016) and flies (e.g., Aso et al., 2014; Hige et al., 2015). In bees, the level of observed plasticity in these neurons after classical conditioning again correlates with the behavioral performance during the retention test (Strube-Bloss, d'Albis, Menzel & Nawrot, unpublished data). Thus, individuality in the conditioned response performance during memory retention has been linked to the underlying plasticity in the neural circuitry.

In bees, a significant correlation between their sensitivity to sucrose concentration and learning performance during an olfactory task has been reported (Scheiner et al., 2004). Pamir et al. (2014) re-analyzed data from Scheiner et al. (2001) showing that sucrose responsiveness, interpreted as a proxy to the state of satiety, correlates with learning performance, both in olfactory and tactile classical conditioning.

In addition, a number of studies have linked variations in learning abilities with genetic variation across individuals. In the honeybee, for example, animals that performed well in olfactory/mechanosensory conditioning also performed well in visual learning (Brandes and Menzel, 1990). On the other hand, good and poor learners from strains selected for olfactory conditioning differed significantly in their visual learning values. Thus, genetic differences exist between different strains and such genetic variation can account for differences in learning in individuals (e.g., Brandes et al., 1988; Brandes and Menzel, 1990). Another study on honeybees considering individual differences in a latent inhibition learning task (learning that some stimuli are *not* signals of important events) also proved a genetic predisposition for learning this task (Chandra et al., 2000). Furthermore, a very recent study on honeybees showed that genetic determinism underlies the trade-off between appetitive and aversive learning (Junca et al., 2019). In a different study, fruit flies were trained to associate a chemical cue (quinine) with a particular substrate. It showed that individuals still avoided this substrate several hours after

the cue had been removed, were expected to contribute more alleles to the next generation. From about generation 15 onward the experimental populations showed marked ability to avoid oviposition substrates that several hours earlier had contained the chemical cue (for review, see: Mery and Kawecki, 2002; Dukas, 2008). Indeed, genetic variation might underlie individuality in behavior in general and in learning behavior specifically. However, to our knowledge, genetic variation has not been studied in cockroaches in relation to behavioral traits. Unfortunately, maturation and reproduction cycles in cockroaches are rather long.

Outlook

In the present study, we investigated individual learning performance and learning speed in single learning tasks (classical olfactory conditioning or operant place learning). In future studies, we will extend our analyses of individuality in two directions. First, we will investigate whether the behavioral performance of individuals is consistent across different learning paradigms, i.e., whether good and fast learners in one classical conditioning paradigm will also perform above average in different classical or operant conditioning tasks. To our knowledge, there is only one invertebrate study where something comparable was published with honeybees (Tait et al., 2019). Second, we are interested in consistency across days or weeks investigating whether a high/low performance of one individual is equally high/low during a repetition of the same or similar task at a later point in time.

DATA AVAILABILITY STATEMENT

The datasets generated for this study are available on request to the corresponding authors.

AUTHOR CONTRIBUTIONS

CA, JB, and ND conducted the experiments. CA, ND, and MN designed the experiments and the experimental setups and wrote the manuscript.

FUNDING

CA received a PhD scholarship from the Research Training Group *Neural Circuit Analysis on the Cellular and Subcellular Level* funded through the German Research Foundation (DFG-GRK 1960, grant no. 233886668 to MN). Additional funding was received from the German Research Foundation within the Research Unit *Structure, Plasticity, and Behavioral Function of the Drosophila Mushroom Body* (DFG-FOR 2705, grant no. 403329959 to MN).

ACKNOWLEDGMENTS

We thank Sandra Mastani for contributions in an early stage of this project. We thank Peter Kloppenburg for discussion, sharing cockroach facilities, and use of animals. We thank the team of our mechanical workshop headed by Leo Lesson, which designed and manufactured the odor stimulation devices and the flexible cockroach maze kit.

SUPPLEMENTARY MATERIAL

The Supplementary Material for this article can be found online at: https://www.frontiersin.org/articles/10.3389/fphys.2019.01539/full#supplementary-material

REFERENCES

Aso, Y., Sitaraman, D., Ichinose, T., Kaun, K. R., Vogt, K., Belliart-Guérin, G., et al. (2014). Mushroom body output neurons encode valence and guide memory-based action selection in drosophila. *elife* 3, 1–42. doi: 10.7554/eLife.04580

Avarguès-Weber, A., Deisig, N., and Giurfa, M. (2011). Visual cognition in social insects. *Annu. Rev. Entomol.* 56, 423–443. doi: 10.1146/annurev-ento-120709-144855

Balderrama, N. (1980). One trial learning in the American cockroach, *Periplaneta americana*. *J. Insect Physiol.* 26, 499–504. doi: 10.1016/0022-1910(80)90123-7

Barraco, D. A., Lovell, K. L., and Eisenstein, E. M. (1981). Effects of cycloheximide and puromycin on learning and retention in the cockroach, *P. americana*. *Pharmacol. Biochem. Behav.* 15, 489–494. doi: 10.1016/0091-3057(81)90282-3

Bell, W. J., Burk, T., and Salds, G. R. (1973). Cockroach aggregation pheromone: directional orientation. *Behav. Biol.* 279, 251–255.

Bitterman, M. E., Menzel, R., Fietz, A., and Schäfer, S. (1983). Classical conditioning of proboscis extension in honeybees (*Apis mellifera*). *J. Comp. Psychol.* 97, 107–119. doi: 10.1037/0735-7036.97.2.107

Brandes, C., Frisch, B., and Menzel, R. (1988). Time-course of memory formation differs in honey bee lines selected for good and poor learning. *Anim. Behav.* 36, 981–985. doi: 10.1016/S0003-3472(88)80056-3

Brandes, C., and Menzel, R. (1990). Common mechanisms in proboscis extension conditioning and visual learning revealed by genetic selection in honeybees (*Apis mellifera* capensis). *J. Comp. Physiol. A* 166, 545–552. doi: 10.1007/BF00192025

Brembs, B. (2013). Invertebrate behavior—actions or responses? *Front. Neurosci.* 7, 1–2. doi: 10.3389/fnins.2013.00221

Camlitepe, Y., and Aksoy, V. (2010). First evidence of fine colour discrimination ability in ants (Hymenoptera, Formicidae). *J. Exp. Biol.* 213, 72–77. doi: 10.1242/jeb.037853

Carere, C., and Locurto, C. (2011). Interaction between animal personality and animal cognition. *Curr. Zool.* 57, 491–498. doi: 10.1093/czoolo/57.4.491

Chabaud, M.-A., Preat, T., and Kaiser, L. (2010). Behavioral characterization of individual olfactory memory retrieval in *Drosophila melanogaster*. *Front. Behav. Neurosci.* 4, 1–11. doi: 10.3389/fnbeh.2010.00192

Chandra, S. B. C., Hosler, J. S., and Smith, B. H. (2000). Heritable variation for latent inhibition and its correlation with reversal learning in honeybees (*Apis mellifera*). *J. Comp. Psychol.* 114, 86–97. doi: 10.1037/0735-7036.114.1.86

Chittka, L., Dyer, A. G., Bock, F., and Dornhaus, A. (2003). Bees trade off foraging speed for accuracy. *Nature* 424:388. doi: 10.1038/424388a

Chittka, L., and Thomson, J. D. (1997). Sensori-motor learning and its relevance for task specialization in bumble bees. *Behav. Ecol. Sociobiol.* 41, 385–398. doi: 10.1007/s002650050400

David, M., Auclair, Y., and Cézilly, F. (2011). Personality predicts social dominance in female zebra finches, *Taeniopygia guttata*, in a feeding context. *Anim. Behav.* 81, 219–224. doi: 10.1016/j.anbehav.2010.10.008

Dingemanse, N. J., and Wolf, M. (2010). Recent models for adaptive personality differences: a review. *Philos. Trans. R. Soc. Lond. B Biol. Sci.* 365, 3947–3958. doi: 10.1098/rstb.2010.0221

Dukas, R. (2008). Evolutionary biology of insect learning. *Annu. Rev. Entomol.* 53, 145–160. doi: 10.1146/annurev.ento.53.103106.093343

Dupuy, F., Sandoz, J.-C., Giurfa, M., and Josens, R. (2006). Individual olfactory learning in *Camponotus* ants. *Anim. Behav.* 72, 1081–1091. doi: 10.1016/j.anbehav.2006.03.011

Erber, J., Pribbenow, B., Grandy, K., and Kierzek, S. (1997). Tactile motor learning in the antennal system of the honeybee (*Apis mellifera* L.). *J. Comp. Physiol. A* 181, 355–365. doi: 10.1007/s003590050121

Gallistel, C. R., Fairhurst, S., and Balsam, P. (2004). The learning curve: implications of a quantitative analysis. *Proc. Natl. Acad. Sci. USA* 101, 13124–13131. doi: 10.1073/pnas.0404965101

Giurfa, M., Hammer, M., Stach, S., Stollhoff, N., Müller-Deisig, N., and Mizyrycki, C. (1999). Pattern learning by honeybees: conditioning procedure and recognition strategy. *Anim. Behav.* 57, 315–324. doi: 10.1006/anbe.1998.0957

Giurfa, M., and Sandoz, J.-C. (2012). Invertebrate learning and memory: fifty years of olfactory conditioning of the proboscis extension response in honeybees. *Learn. Mem.* 19, 54–66. doi: 10.1101/lm.024711.111

Giurfa, M., Zhang, S., Jenett, A., Menzel, R., and Srinivasan, M. V. (2001). The concepts of 'sameness' and 'difference' in an insect. *Nature* 410, 930–933. doi: 10.1038/35073582

Gosling, S. D. (2001). From mice to men: what can we learn about personality from animal research? *Psychol. Bull.* 127, 45–86. doi: 10.1037/0033-2909.127.1.45

Gosling, S. D., and Vazire, S. (2002). Are we barking up the right tree? Evaluating a comparative approach to personality. *J. Res. Pers.* 36, 607–614. doi: 10.1016/S0092-6566(02)00511-1

Grinsted, L., Pruitt, J. N., Settepani, V., and Bilde, T. (2013). Individual personalities shape task differentiation in a social spider. *Proc. R. Soc. B Biol. Sci.* 280:20131407. doi: 10.1098/rspb.2013.1407

Groothuis, T. G. G., and Carere, C. (2005). Avian personalities: characterization and epigenesis. *Neurosci. Biobehav. Rev.* 29, 137–150. doi: 10.1016/j.neubiorev.2004.06.010

Haenicke, J., Yamagata, N., Zwaka, H., Nawrot, M., and Menzel, R. (2018). Neural correlates of odor learning in the presynaptic microglomerular circuitry in the honeybee mushroom body calyx. *eNeuro* 5:ENEURO.0128-18.2018. doi: 10.1523/ENEURO.0128-18.2018

Hige, T., Aso, Y., Rubin, G. M., and Turner, G. C. (2015). Plasticity-driven individualization of olfactory coding in mushroom body output neurons. *Nature* 526, 258–262. doi: 10.1038/nature15396

Hoedjes, K. M., Steidle, J. L. M., Werren, J. H., Vet, L. E. M., and Smid, H. M. (2012). High-throughput olfactory conditioning and memory retention test show variation in Nasonia parasitic wasps. *Genes Brain Behav.* 11, 879–887. doi: 10.1111/j.1601-183X.2012.00823.x

Hosono, S., Matsumoto, Y., and Mizunami, M. (2016). Interaction of inhibitory and facilitatory effects of conditioning trials on long-term memory formation. *Learn. Mem.* 23, 669–678. doi: 10.1101/lm.043513.116

Junca, P., Garnery, L., and Sandoz, J.-C. (2019). Genotypic trade-off between appetitive and aversive capacities in honeybees. *Sci. Rep.* 9, 1–14. doi: 10.1038/s41598-019-46482-4

Kisch, J., and Erber, J. (1999). Operant conditioning of antennal movements in the honey bee. *Behav. Brain Res.* 99, 93–102. doi: 10.1016/S0166-4328(98)00076-X

Kolata, S., Light, K., Townsend, D. A., Hale, G., Grossman, H. C., and Matzel, L. D. (2005). Variations in working memory capacity predict individual differences in general learning abilities among genetically diverse mice. *Neurobiol. Learn. Mem.* 84, 241–246. doi: 10.1016/j.nlm.2005.07.006

Kotrschal, A., and Taborsky, B. (2010). Environmental change enhances cognitive abilities in fish. *PLoS Biol.* 8:e1000351. doi: 10.1371/journal.pbio.1000351

Kralj-Fišer, S., and Schuett, W. (2014). Studying personality variation in invertebrates: why bother? *Anim. Behav.* 91, 41–52. doi: 10.1016/j.anbehav.2014.02.016

Kuwabara, M. (1957). Bildung des bedingten Reflexes von Pavlovs Typus bei der Honigbiene, Apis mellifica. *J. Fat. Sci. Hokkaido Univ.* 13, 458–464.

Kwon, H.-W., Lent, D. D., and Strausfeld, N. J. (2004). Spatial learning in the restrained American cockroach *Periplaneta americana*. *J. Exp. Biol.* 207, 377–383. doi: 10.1242/jeb.00737

Lauprasert, P., Laupraset, P., Sitthicharoenchai, D., Thirakhupt, K., and Pradatsudarasar, A.-O. (2006). Food preference and feeding behavior of the German cockroach, *Blattella germanica* (Linnaeus). *J. Sci. Res. Chula Univ.* 31, 121–126. Available at: http://www.thaiscience.info/journals/Article/CJSR/10324268.pdf

Lent, D. D., and Kwon, H.-W. (2004). Antennal movements reveal associative learning in the American cockroach *Periplaneta americana*. *J. Exp. Biol.* 207, 369–375. doi: 10.1242/jeb.00736

Lent, D. D., Pintér, M., and Strausfeld, N. J. (2007). Learning with half a brain. *Dev. Neurobiol.* 67, 740–751. doi: 10.1002/dneu.20374

Liu, J.-L., and Sakuma, M. (2013). Olfactory conditioning with single chemicals in the German cockroach, *Blattella germanica* (Dictyoptera: Blattellidae). *Appl. Entomol. Zool.* 48, 387–396. doi: 10.1007/s13355-013-0199-x

Lunney, G. H. (1970). Using analysis of variance with a dichotomous dependent variable: an empirical study. *J. Educ. Meas.* 7, 263–269. doi: 10.1111/j.1745-3984.1970.tb00727.x

Menzel, R. (2012). The honeybee as a model for understanding the basis of cognition. *Nat. Rev. Neurosci.* 13, 758–768. doi: 10.1038/nrn3357

Menzel, R., Durst, C., Erber, J., Eichmüller, S., Hammer, M., Hildebrandt, H., et al. (1994). The mushroom bodies in the honeybee: from molecules to behaviour. *Fortschr. Zool.* 39, 81–102.

Mery, F., and Kawecki, T. J. (2002). Experimental evolution of learning ability in fruit flies. *Proc. Natl. Acad. Sci. USA* 99, 14274–14279. doi: 10.1073/pnas.222371199

Mizunami, M., Weibrecht, J. M., and Strausfeld, N. J. (1998). Mushroom bodies of the cockroach: their participation in place memory. *J. Comp. Neurol.* 402, 520–537. doi: 10.1002/(SICI)1096-9861(19981228)402:4<520::AID-CNE6>3.0.CO;2-K

Muller, H., and Chittka, L. (2012). Consistent interindividual differences in discrimination performance by bumblebees in colour, shape and odour learning tasks (Hymenoptera: *Bombus terrestris*). *Entomol. Gener.* 34, 1–6. doi: 10.1127/entom.gen/34/2012/1

Nouvian, M., and Galizia, C. G. (2019). Aversive training of honey bees in an automated Y-maze. *Front. Physiol.* 10, 1–17. doi: 10.3389/fphys.2019.00678

Pamir, E., Chakroborty, N. K., Stollhoff, N., Gehring, K. B., Antemann, V., Morgenstern, L., et al. (2011). Average group behavior does not represent individual behavior in classical conditioning of the honeybee. *Learn. Mem.* 18, 733–741. doi: 10.1101/lm.2232711

Pamir, E., Szyszka, P., Scheiner, R., and Nawrot, M. P. (2014). Rapid learning dynamics in individual honeybees during classical conditioning. *Front. Behav. Neurosci.* 8:313. doi: 10.3389/fnbeh.2014.00313

Pavlov, I. P. (1927). *Conditioned reflexes. An investigation of the physiological activity of the cerebral cortex*. Oxford, England: Oxford University Press.

Pintér, M., Lent, D. D., and Strausfeld, N. J. (2005). Memory consolidation and gene expression in *Periplaneta americana*. *Learn. Mem.* 12, 30–38. doi: 10.1101/lm.87905

Pinter-Wollman, N. (2012). Personality in social insects: how does worker personality determine colony personality? *Curr. Zool.* 58, 580–588. doi: 10.1093/czoolo/58.4.580

Planas-Sitjà, I., and Deneubourg, J.-L. (2018). The role of personality variation, plasticity and social facilitation in cockroach aggregation. *Biol. Open* 7:bio036582. doi: 10.1242/bio.036582

Planas-Sitjà, I., Nicolis, S. C., Sempo, G., and Deneubourg, J.-L. (2018). The interplay between personalities and social interactions affects the cohesion of the group and the speed of aggregation. *PLoS One* 13:e0201053. doi: 10.1371/journal.pone.0201053

Pomaville, M. B., and Lent, D. D. (2018). Multiple representations of space by the cockroach, *Periplaneta americana*. *Front. Psychol.* 9, 1–15. doi: 10.3389/fpsyg.2018.01312

Quinn, W. G., Harris, W. A., and Benzer, S. (1974). Conditioned behavior in *Drosophila melanogaster* (learnin/memory/odor discrimination/color vision). *Proc. Natl. Acad. Sci. USA* 71, 708–712.

Rath, L., Giovanni Galizia, C., and Szyszka, P. (2011). Multiple memory traces after associative learning in the honey bee antennal lobe. *Eur. J. Neurosci.* 34, 352–360. doi: 10.1111/j.1460-9568.2011.07753.x

Rose, J., Cullen, D. A., Simpson, S. J., and Stevenson, P. A. (2017). Born to win or bred to lose: aggressive and submissive behavioural profiles in crickets. *Anim. Behav.* 123, 441–450. doi: 10.1016/j.anbehav.2016.11.021

Sakura, M., and Mizunami, M. (2001). Olfactory learning and memory in the cockroach *Periplaneta americana*. *Zool. Sci.* 18, 21–28. doi: 10.2108/zsj.18.21

Sakura, M., Okada, R., and Mizunami, M. (2002). Olfactory discrimination of structurally similar alcohols by cockroaches. *J. Comp. Physiol. A Neuroethol. Sens. Neural Behav. Physiol.* 188, 787–797. doi: 10.1007/s00359-002-0366-y

Sato, C., Matsumoto, Y., Sakura, M., and Mizunami, M. (2006). Contextual olfactory learning in cockroaches. *Neuroreport* 17, 553–557. doi: 10.1097/01.wnr.0000209002.17610.79

Scheiner, R., Page, R. E., and Erber, J. (2001). The effects of genotype, foraging role, and sucrose responsiveness on the tactile learning performance of honey bees (*Apis mellifera* L.). *Neurobiol. Learn. Mem.* 76, 138–150. doi: 10.1006/nlme.2000.3996

Scheiner, R., Page, R. E., and Erber, J. (2004). Sucrose responsiveness and behavioral plasticity in honey bees (*Apis mellifera*). *Apidologie* 35, 133–142. doi: 10.1051/apido:2004001

Schubert, M., Hansson, B. S., and Sachse, S. (2014). The banana code—natural blend processing in the olfactory circuitry of *Drosophila melanogaster*. *Front. Physiol.* 5, 1–13. doi: 10.3389/fphys.2014.00059

Schuett, W., and Dall, S. R. X. (2009). Sex differences, social context and personality in zebra finches, *Taeniopygia guttata*. *Anim. Behav.* 77, 1041–1050. doi: 10.1016/j.anbehav.2008.12.024

Schuett, W., Dall, S. R. X., Baeumer, J., Kloesener, M. H., Nakagawa, S., Beinlich, F., et al. (2011). Personality variation in a clonal insect: the pea aphid, *Acyrthosiphon pisum*. *Dev. Psychobiol.* 53, 631–640. doi: 10.1002/dev.20538

Sih, A., Bell, A., and Johnson, J. C. (2004a). Behavioral syndromes: an ecological and evolutionary overview. *Trends Ecol. Evol.* 19, 372–378. doi: 10.1016/j.tree.2004.04.009

Sih, A., Bell, A. M., Johnson, J. C., and Ziemba, R. E. (2004b). Behavioral syndromes: an integrative overview. *Q. Rev. Biol.* 79, 241–277. doi: 10.1086/422893

Srinivasan, M., Zhang, S., and Lehrer, M. (1998). Honeybee navigation: odometry with monocular input. *Anim. Behav.* 56, 1245–1259. doi: 10.1006/anbe.1998.0897

Strube-Bloss, M. F., Nawrot, M. P., and Menzel, R. (2011). Mushroom body output neurons encode odor-reward associations. *J. Neurosci.* 31, 3129–3140. doi: 10.1523/JNEUROSCI.2583-10.2011

Strube-Bloss, M. F., Nawrot, M. P., and Menzel, R. (2016). Neural correlates of side-specific odour memory in mushroom body output neurons. *Proc. R. Soc. B Biol. Sci.* 283:20161270. doi: 10.1098/rspb.2016.1270

Tait, C., Mattise-Lorenzen, A., Lark, A., and Naug, D. (2019). Interindividual variation in learning ability in honeybees. *Behav. Process.* 167:103918. doi: 10.1016/j.beproc.2019.103918

Takeda, K. (1961). Classical conditioned response in the honey bee. *J. Insect Physiol.* 6, 168–179. doi: 10.1016/0022-1910(61)90060-9

Turner, C. H. (1912). An experimental investigation of an apparent reversal of the responses to light of the roach (Periplaneta Orientalis L.). 23, 371–386.

Watanabe, H., Kobayashi, Y., Sakura, M., Matsumoto, Y., and Mizunami, M. (2003). Classical olfactory conditioning in the cockroach *Periplaneta americana*. *Zool. Sci.* 20, 1447–1454. doi: 10.2108/zsj.20.1447

Watanabe, H., and Mizunami, M. (2006). Classical conditioning of activities of salivary neurones in the cockroach. *J. Exp. Biol.* 209, 766–779. doi: 10.1242/jeb.02049

Watanabe, H., and Mizunami, M. (2007). Pavlov's cockroach: classical conditioning of salivation in an insect. *PLoS One* 2:e529. doi: 10.1371/journal.pone.0000529

Wright, C. M., Holbrook, C. T., and Pruitt, J. N. (2014). Animal personality aligns task specialization and task proficiency in a spider society. *Proc. Natl. Acad. Sci. USA* 111, 9533–9537. doi: 10.1073/pnas.1400850111

Conflict of Interest: The authors declare that the research was conducted in the absence of any commercial or financial relationships that could be construed as a potential conflict of interest.

frontiers in Physiology

ORIGINAL RESEARCH
published: 11 February 2020
doi: 10.3389/fphys.2020.00095

Bogong Moths Are Well Camouflaged by Effectively Decolourized Wing Scales

Doekele G. Stavenga[1†], Jesse R. A. Wallace[2] and Eric J. Warrant[2,3†]*

[1] Surfaces and Thin Films, Zernike Institute for Advanced Materials, University of Groningen, Groningen, Netherlands, [2] Research School of Biology, Australian National University, Canberra, ACT, Australia, [3] Lund Vision Group, Department of Biology, Lund University, Lund, Sweden

Moth wings are densely covered by wing scales that are assumed to specifically function to camouflage nocturnally active species during day time. Generally, moth wing scales are built according to the basic lepidopteran Bauplan, where the upper lamina consists of an array of parallel ridges and the lower lamina is a thin plane. The lower lamina hence acts as a thin film reflector having distinct reflectance spectra that can make the owner colorful and thus conspicuous for predators. Most moth species therefore load the scales' upper lamina with variable amounts of melanin so that dull, brownish color patterns result. We investigated whether scale pigmentation in this manner indeed provides moths with camouflage by comparing the reflectance spectra of the wings and scales of the Australian Bogong moth (*Agrotis infusa*) with those of objects in their natural environment. The similarity of the spectra underscores the effective camouflaging strategies of this moth species.

Keywords: *Agrotis infusa*, coloration, wing patterning, melanin, reflectance spectra, scale anatomy

OPEN ACCESS

Edited by:
Sylvia Anton,
Institut National de la Recherche Agronomique, France

Reviewed by:
Justin Marshall,
The University of Queensland, Australia
Ian Z. W. Chan,
National University of Singapore, Singapore

***Correspondence:**
Eric J. Warrant
Eric.Warrant@cob.lu.se

†ORCID:
Doekele G. Stavenga
orcid.org/0000-0002-2518-6177
Eric J. Warrant
orcid.org/0000-0001-7480-7016

Specialty section:
This article was submitted to Invertebrate Physiology, a section of the journal Frontiers in Physiology

Received: *06 October 2019*
Accepted: *27 January 2020*
Published: *11 February 2020*

Citation:
Stavenga DG, Wallace JRA and Warrant EJ (2020) Bogong Moths Are Well Camouflaged by Effectively Decolourized Wing Scales. Front. Physiol. 11:95. doi: 10.3389/fphys.2020.00095

INTRODUCTION

Bogong moths (*Agrotis infusa*) are night-flying moths, well-known for their highly directional, biannual long-distance seasonal migrations to and from the Australian Alps (Common, 1954; Warrant et al., 2016), a feat which requires the Earth's magnetic field and visual landmarks as navigational cues (Dreyer et al., 2018). The adults aestivate over the summer in cool alpine caves in the mountains of southeast Australia, including the Brindabella Ranges of the Australian Capital Territory, the Snowy Mountains of New South Wales and the Bogong High Plains in Victoria. Following this period of aestivation, the same individuals that arrived in the mountains months earlier leave the caves and return to their breeding grounds (a journey of up to 1000 km) to mate, lay their eggs and die. The Bogong moth is culturally important for the Aboriginal people, who used the moths as a significant source of protein and fat during their annual summer gatherings in alpine areas (Flood, 1980, 1996).

The moths' name, bogong, is derived from the Aboriginal word bugung, meaning "brown moth" (from the extinct Dhudhuroa language of northeast Victoria), which aptly describes their coloration. The moth's brown colors presumably serve background matching (Stevens and Merilaita, 2009), i.e., to make the moths inconspicuous to other predators during the day, both during their migration across the plains and following arrival in the mountains (when they can be preyed upon by the Mountain pygmy possum (Gibson et al., 2018) and various species of birds, among other predators). The classical example of camouflage is the peppered moth (*Biston betularia*), which developed a darker wing scale color as trees became covered in industrial soot and via the forces of natural selection induced by

predatory birds (Majerus et al., 2000; Cook et al., 2012). Light-colored moths, resting in the daytime on dark-brown trees, are easily recognizable prey, so that dark-brown colored moths have a higher chance of survival.

The color of lepidopteran insects (moths and butterflies) is determined by the lattice of scales that cover the wings like shingles on a roof (Nijhout, 1991; Kinoshita, 2008). The chitinous wing scales are organized into two laminae, i.e., a thin, more or less flat lower lamina, and a highly structured upper lamina which consists of rows of parallel ridges with interlinking cross-ribs that leave more or less open windows. The upper lamina is connected to the lower lamina by trabeculae, pillar-like elements serving as mechanical struts and spacers (Ghiradella, 1991, 1998, 2010).

Commonly, the color of the individual scales has a pigmentary (or chemical) origin. If the scale contains a considerable amount of pigment, incident light reflected and scattered by the scale structures is then selectively filtered, dependent on the pigment's absorption spectrum, so that a distinct pigmentary color remains. Various pigment classes are expressed in lepidopteran wing scales. Pterins are the pigments generally encountered in pierid butterflies (Descimon, 1975; Wijnen et al., 2007), kynurenine and its derivatives, the ommochromes, are generally identified in nymphalids (Nijhout, 1997; Wilts et al., 2017), and the papilionids are colored by papiliochrome pigments (Umebachi, 1985; Nijhout, 2010; Nishikawa et al., 2013; Wilts et al., 2014). Some papilionids, as well as the Geometrinae and other moths, use blue-green bile pigments, neopterobilins (Choussy et al., 1973; Barbier, 1986). Within the Geometrinae a novel green pigment type, geoverdin, has also been reported (Cook et al., 1994). But undoubtedly the commonest pigment found in the Lepidoptera, and certainly in moths, is melanin, a broadband-absorbing pigment responsible for most brown and black colors.

A wing scale's color can also have a structural (or physical) basis. Regularly arranged, nanosized scale structures cause wavelength-dependent light interferences, as for instance is the case in intense blue *Morpho* butterflies, where the building blocks of the scale ridges, the lamellae, form a stack that functions as an optical multilayer (Vukusic and Sambles, 2003; Giraldo et al., 2016). The lower lamina can also create a structural color, because its thickness is of the order of 100–200 nm. It hence acts as an optical thin film, causing a distinct reflectance in a restricted wavelength range, critically depending on the precise thickness of the thin film and angle of illumination or view. The lower lamina can thus determine the scale color in the specific case that the scale is unpigmented (Stavenga et al., 2014). The highly convoluted upper lamina commonly acts as a broad-band light diffuser that spreads light in a wide spatial angle, resulting in less angle dependence of the iridescent colors (e.g., Stavenga et al., 2014).

The anatomical organization and pigmentation of the scales and wing colors resulting from the lattice of scales have been investigated in only a few moth species, and mostly in those featuring conspicuous colors, as in the extremely colorful day-flying swallowtail moths *Urania fulgens* and *Urania leilus* (Onslow, 1923; Süffert, 1924; Lippert and Gentil, 1959). A particularly exuberantly colored species is the sunset moth *Chrysiridia ripheus* (Uraniinae), which applies advanced multilayer optics in sometimes strongly curved scales, resulting in distinct color mixing and polarization effects (Yoshioka and Kinoshita, 2007; Yoshioka et al., 2008). The scales of the basal moth *Micropterix aureatella*, which like the diurnally active uraniines is a day-flying moth, have a fused upper and lower lamina. The thickness of the resulting single thin film varies slightly, thus causing metallic gold, bronze and purple colors (Kilchoer et al., 2018). The similarly day-active palm borer moth *Paysandisia archon* has brownish forewings with prominently orange colored hindwings due to a cover of ommochrome-pigmented scales (Stavenga et al., 2018). The nocturnal moth *Eudocima materna* (Noctuidae) has similarly ommochrome-pigmented hindwings with sparkling effects caused by patches with mirror scales (which have a thin film reflector in their lower lamina; Kelley et al., 2019). However, moths are generally dull colored, due to high concentrations of melanin in their scales, presumably for suppressing possible structural coloration. Here we focus on the Bogong moth, to investigate how dull-brown moths organize their appearance by variously expressing melanin in their wing scales.

MATERIALS AND METHODS

Specimens

Bogong moths used in this study were bred in Lund from adults captured in Australia. We furthermore collected pieces of granite from a Bogong moth aestivation cave (South Rams Head, Kosciuszko National Park, elevation 1860 m), as well as a variety of bark samples taken from: Coastal tea-tree (*Leptospermum laevigatum*), River bottlebrush (*Callistemon sieberi*), Crimson bottlebrush (*Callistemon citrinus*), River oak (*Casuarina cunninghamiana*), Brittle gum (*Eucalyptus mannifera*), Argyle apple (*Eucalyptus cinerea*), Silver-leaved ironbark (*Eucalyptus melanophloia*), Mountain gum (*Eucalyptus cypellocarpa*), Scribbly gum (*Eucalyptus rossii*), Snow gum (*Eucalyptus pauciflora*), Weeping snow gum (*Eucalyptus lacrimans*), Narrow-leaved Sally (*Eucalyptus moorei*), Parramatta red gum (*Eucalyptus parramettensis*), and *Eucalyptus* sp. aff. *notabilus*. These tree species were chosen because they are likely to be encountered along the migratory route as well as upon arrival in sub-alpine areas where moths feed for some weeks before ascending to their aestivation caves at higher elevation (**Supplementary Figure S1** and **Table 1**). We have not given attention to sexual differences, as there is no marked sexual dimorphism. We have to note that the moths do come in many shades of brown; particularly males can (although not always) be much lighter in color than females.

Scanning Electron Microscopy

Wing pieces and isolated scales were prepared for scanning electron microscopy by sputter-coating with gold (Cressington 108 auto, 45 s, 20 mA). The preparations were viewed using a scanning electron microscope (SEM; Hitachi SU3500) at 5 kV.

TABLE 1 | The distributions of Australian trees species used for bark spectra measurements (**Supplementary Figure S1**) and their likelihood of being encountered by migrating Bogong moths.

Species	Likely resting spot?	Notes[1]
Eucalyptus sp. aff. *notabilus*	No	Distribution is predominantly east of the Great Dividing Range
Leptospermum laevigatum	No	Distribution confined to coastal habitats. Bogong moths may be found here, but it is not where most are coming from
Eucalyptus moorei	No	Distribution is predominantly east of the Great Dividing Range
Eucalyptus parramattensis	No	Relatively localized around the Sydney region
Eucalyptus mannifera	**Yes**	Widespread and abundant in south-eastern NSW
Callistemon sieberi	**Yes**	Widespread and abundant in eastern NSW
Callistemon citrinus	No	Distribution mostly east of Great Dividing Range
Casuarina cunninghamiana	**Yes**	Widespread and abundant across eastern NSW and QLD
Eucalyptus cinerea	**Yes**	Locally abundant just north of the NSW Snowy Mountains; also occurs in VIC
Eucalyptus melanophloia	No	Distributed across northern NSW as well as QLD
Eucalyptus cypellocarpa	No	Occurs in wet forest in sheltered valleys, eastern slopes of the Great Dividing Range
Eucalyptus rossii	**Yes**	Widespread and abundant in eastern NSW, although these would not provide adequate hiding places for Bogong moths due to their light color; another moth, *Ogmograptis scribula*, in contrast, highly favors them
Eucalyptus pauciflora	**Yes**	Widespread and dominant across eastern NSW, and throughout VIC and TAS (occurs in alpine areas); Bogong moths have been observed feeding on them
Eucalyptus lacrimans	**Yes**	Subalpine species, restricted to the Adaminaby region of the NSW Snowy Mountains

[1] *NSW, New South Wales; VIC, Victoria; QLD, Queensland; TAS, Tasmania.*

Spectrophotometry

Reflectance spectra of different areas of the Bogong moth wings, as well as of the granite and bark samples, were measured with a bifurcated reflection probe (Avantes FCR 7-UV-200), using an AvaSpec 2048-CCD detector array spectrometer (Avantes, Apeldoorn, Netherlands). The light source was a deuterium-halogen lamp (AvaLight-D(H)-S), and the reference was a white diffuse reflectance tile (Avantes WS-2). Reflectance spectra of isolated scales, attached to a glass micropipette using Bison glass kit (hardening under UV light), were measured with a microspectrophotometer (MSP). The MSP was a Leitz Ortholux microscope (Leitz, Wetzlar, Germany) with an Olympus 20× objective, NA 0.46 (Olympus, Tokyo, Japan). A xenon arc lamp was used as a light source. The area measured with the MSP was a square with edge length 5–10 μm, determined by a square diaphragm in the microscope's image plane, which was in turn imaged at the entrance of an optical fiber connected to the detector array spectrometer; the white diffuse reflectance tile was also here used as a reference. Due to the glass optics in the microscope, the MSP spectra were limited to wavelengths >350 nm. Absorbance spectra of isolated scales were also measured with the MSP, while the scales were immersed in immersion oil ($n = 1.515$) in order to reduce scattering.

Imaging Scatterometry of Single Wing Scales

For investigating the spatial reflection characteristics of the scales, we performed imaging scatterometry (Stavenga et al., 2009; Wilts et al., 2009). A scale attached to a glass micropipette was positioned at the first focal point of the ellipsoidal mirror of the imaging scatterometer. The scatterograms were obtained by focusing a white light beam with a narrow aperture (<5°) at a small circular area (diameter 13 μm), and the spatial distribution of the far-field scattered light was then monitored. The exposure times of the scatterograms were appropriately adjusted so as to obtain an image of maximal contrast.

Modeling the Reflectance Spectra of Thin Films

The reflectance spectra of chitinous optical thin films in air were calculated for normally incident light using an expression derived from the classical Airy formula (Stavenga, 2014).

RESULTS

Wing Colors and Reflectance Spectra

Bogong moths have brown bodies and wings. The dorsal forewings are dark-brown with black patches, which cover (when resting) the more or less uniformly light brown dorsal hindwings and the intermediate brownish thorax and abdomen (**Figure 1A**). The ventral wing edges are light brown. As an example of the differences in saturation, **Figure 1B** shows reflectance spectra of local areas of the dorsal fore- and hindwing. In both cases, the reflectance increases monotonically with increasing wavelength, which is characteristic of a melanin-pigmented tissue (**Figure 1B**).

Scale Structures

The wings have a cover of numerous scales, and thus the wing coloration will be determined by how the scales reflect incident light. The primary determinant of the scale reflectance is melanin pigment, as suggested by **Figure 1B**. Yet, a crucial contributing factor can be the scales' fine-structure, which was investigated by performing scanning electron microscopy. The size of the wing scales appears to be rather variable, but the structure adheres to

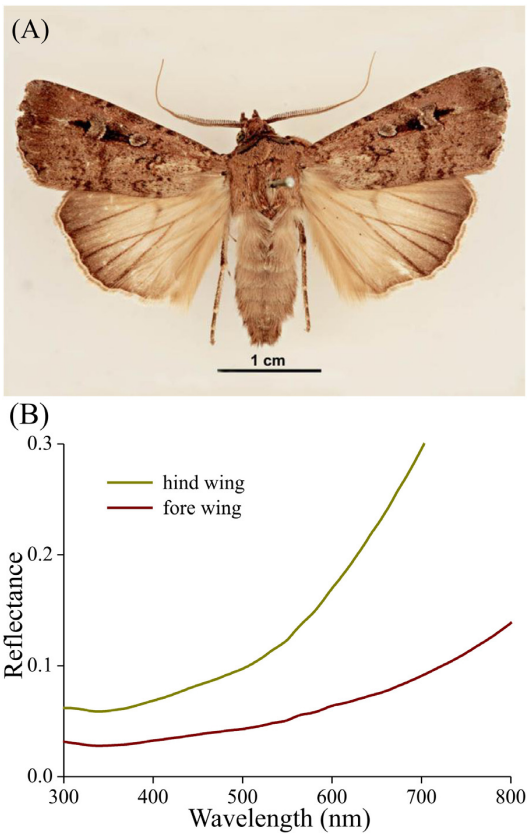

FIGURE 1 | Bogong moth coloration. **(A)** A pinned specimen with exposed fore and hind wings (from http://www.padil.gov.au/pests-and-diseases/pest/main/136308/5837#; source Lucinda Gibson and Ken Walker, Museum Victoria, Australia). Image available for free use under a Creative Commons Attribution 3.0 Australia License, CC BY 3.0 AU. **(B)** Reflectance spectra of the upper sides of the hind and fore wing measured with a bifurcated reflection probe.

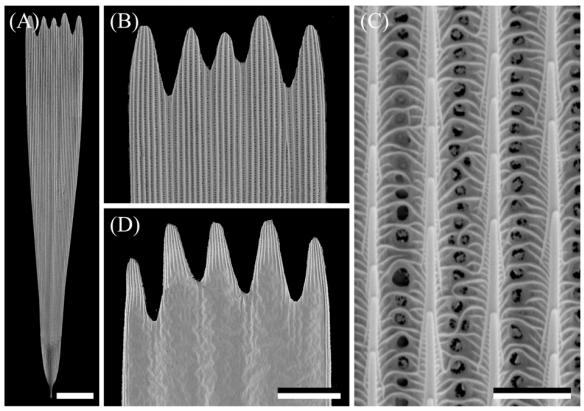

FIGURE 2 | Scanning electron micrographs of a forewing scale. **(A)** An isolated scale with dented tip area and on the other end the root. **(B)** Magnified view of the abwing (upper) side of the tip area of **(A)**. **(C)** The scale ridges, consisting of slightly overlapping lamellae and connected by cross-ribs, which leave minor open windows. **(D)** The adwing (under) side of a tip area. Scale bars: **(A)** 50 μm, **(B,D)** 25 μm, **(C)** 2.5 μm.

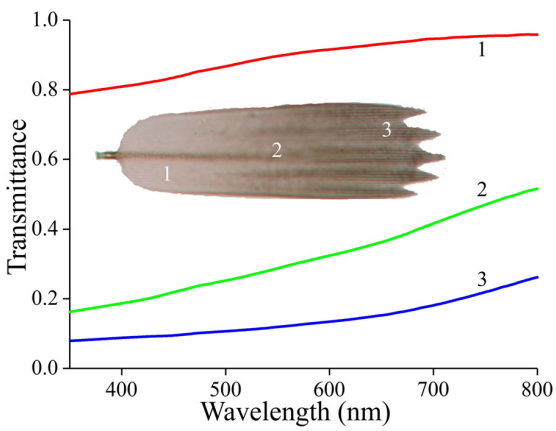

FIGURE 3 | Transmittance spectra of an isolated forewing scale immersed in immersion oil, in the root (1), middle (2), and tip (3) area, measured with a microspectrophotometer.

the classical format. The upper side is an array of ridges that are connected by cross-ribs, which leave minor open windows (**Figures 2A–C**), and the underside features a more or less flat, slightly wrinkled plane (**Figure 2D**).

The ridges of lepidopteran wing scales consist of overlapping lamellae, but the overlap of the ridge lamellae in Bogong moth scales is very minor, so that a possible structural coloration of the scales' upper lamina can be neglected. As is universally the case in lepidopteran scales, the lower lamina will act as a thin film reflector, and thus some structural coloration contributions can be expected.

Scale Pigmentation, Reflection, and Scattering

To first check whether the scales contain a melanin-like pigment, we performed transmission-microspectrophotometry on single scales immersed in oil (**Figure 3**). At all scale locations, the transmittance increased monotonically with increasing wavelength, which is indeed the hallmark of melanin. The transmittance strongly varied along the length of the scale, however. Near the root, the transmittance was high, i.e., at this location the scale is almost transparent (**Figure 3**, #1), but near the tip the transmittance was hardly more than ∼10% across the whole visible wavelength range (**Figure 3**, #3).

How this steep gradient in melanin pigmentation might affect scale coloration was then investigated by epi-illumination microscopy. This revealed that the coloration of the lattice of scales on the forewing is far from uniform (**Figure 4A**). When observing isolated, single scales, the diverse coloration was particularly apparent, as shown in the example of **Figures 4B-D**. The under (or adwing) side features a diverse color pattern, from blue near the root to purplish in the center and tip area, which indicates that the lower lamina of the scales, acting as a thin film reflector, has a variable thickness (**Figure 4B**). The upper, abwing side is blue-greenish at the root but reddish-brown at the tip (**Figure 4C**). In transmitted light, the scale

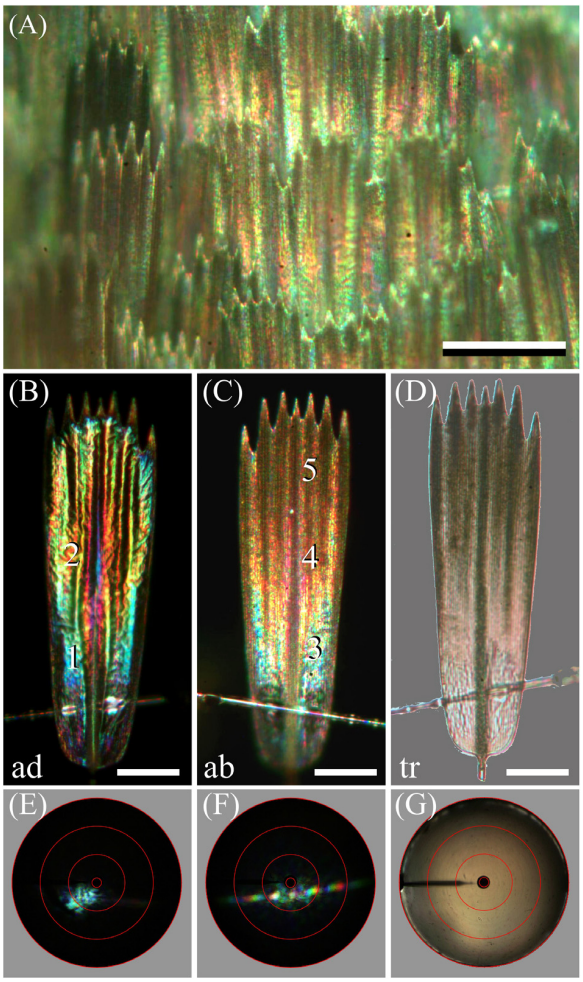

FIGURE 4 | Spectral and spatial characteristics of Bogong moth scales. **(A)** Epi-illumination micrograph of the scale pattern, locally in the forewing. **(B)** Epi-illumination of the adwing side of an isolated forewing scale glued to a glass micropipette. **(C)** Same as **(B)** except for the abwing side. **(D)** Same as **(B)** but with transmitted light. **(E)** Scatterogram of area 1 of **(B)** with narrow-aperture illumination. **(F)** Scatterogram of area 4 of **(C)** with narrow-aperture illumination. **(G)** Scatterogram of area 4 of **(C)** with wide-aperture illumination. Scale bars: **(A)** 100 μm, **(B–D)** 50 μm. The red circles in **(E–G)** indicate reflection angles of 5°, 30°, 60°, and 90°. For reflectance spectra measured at locations numbered 1–5, see **Figure 5**.

showed a dull, brown color, as expected from the scale's melanin pigmentation (**Figure 4D**).

The color differences in the reflection patterns obtained from both scale sides is readily explained from the gradient in pigmentation. The adwing bottom area, near the root (**Figure 4B**), has a similar blue-green color as the abwing bottom area (**Figure 4C**), although the color of the latter is slightly more diffuse. The explanation is similar to that of the coloration of a transparent, unpigmented scale (Stavenga et al., 2014). When incident light enters an unpigmented scale from above, from the abwing side, a major fraction of it will pass the upper lamina and reach the lower lamina, where it will be partly reflected, depending on the thin film's reflectance spectrum. A major fraction of this reflected light will then pass again to the upper lamina, and thus, in the absence of a pigment filter, the color of the reflected light will be equal to the color of the adwing reflected light.

However, the middle and tip areas of the upper lamina do contain a major amount of melanin pigment – these areas will then act as a gradual spectrally long-pass brown filter. Consequently, incident light that enters the pigmented scale areas from the abwing side will suffer from the pigment filter before it reaches the lower lamina. There it is subsequently reflected, and the resulting light flux will have to pass again through the pigment filter on its way back before it leaves the scale at the abwing side. An increasingly brown color thus results, proportionally with the pigment density (**Figures 4C,D**).

We further investigated the structural coloration by applying imaging scatterometry, using a narrow aperture illumination beam. The scatterogram of a blue area on the adwing side featured a local blue spot, meaning a strongly directional, spatially restricted reflection, confirming the action of a specular thin film reflector (**Figure 4E**). On the other, abwing side, of the scale, the scatterogram showed a striking diffraction pattern (**Figure 4F**). This can be immediately understood, because the upper lamina of the scales consists of an array of parallel ridges, which acts as a diffraction grating. We finally applied a wide-angled illumination beam to the abwing scale side (central area #4 of **Figure 4C**), which yielded the scatterogram of **Figure 4G**. Clearly, the cumulative diffraction patterns created by the large-aperture illumination then superimpose, resulting in a diffuse scatterogram. The overall brown color demonstrates that the backscattered light is effectively filtered by the considerable amount of melanin pigment.

To further ascertain that the lower lamina acts as a thin film, we used a microspectrophotometer to measure reflectance spectra from the lower lamina in locations #1 and 2 of **Figure 4B** (**Figures 5A,B**, solid curves). Except for a background offset, the spectra closely resemble the reflectance spectra of thin films with thickness 230 and 290 nm, respectively (**Figures 5A,B**, dotted curves). The reflectance offset can be easily understood, because a major fraction of the applied light is transmitted by the thin film and subsequently will be partly backscattered by the upper lamina. A large fraction of that light flux will be subsequently transmitted by the lower lamina and thus contribute to the reflected light. Painstaking transmission electron microscopy will be necessary to confirm the derived thicknesses of the scale's lower lamina.

The reflectance spectra measured from the abwing scale side are rather different (**Figure 5C**). In the spectrum of the blue-green colored root area (**Figure 4C**, #3), the contribution of the underlying thin film can be recognized, but the reflectance spectra of the more distal areas (**Figure 4C**, #4, 5) are dominated by melanin filtering (**Figure 5C**).

In the scale lattice on the wing, the scales strongly overlap, so that only the most distal part is exposed. Therefore, the reflectance spectra of intact wings (**Figure 1B**) will have the monotonically rising form characteristic of melanin-pigmented tissue (as seen in **Figure 5C**, #5). In conclusion, because the tip area is fully exposed in intact moths, the thin film reflections that

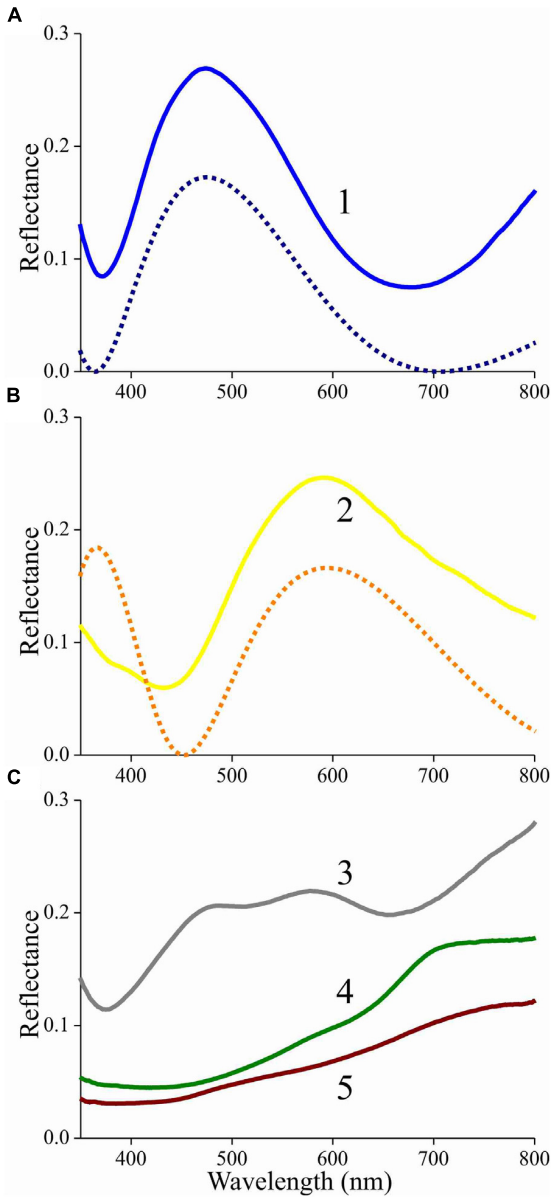

FIGURE 5 | Reflectance spectra of an isolated scale measured with a microspectrophotometer. **(A)** Solid curve: reflectance spectrum of area 1 of **Figure 4B** (adwing); dashed curve: modeled reflectance spectrum for a chitinous thin film in air with thickness 230 nm. **(B)** Solid curve: reflectance spectrum of area 2 of **Figure 4B** (adwing); dashed curve: modeled reflectance spectrum for a chitinous thin film in air with thickness 290 nm. **(C)** Reflectance spectra of areas 3–5 of **Figure 4C** (abwing).

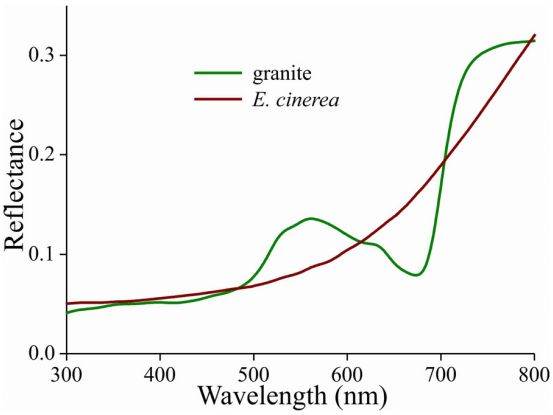

FIGURE 6 | Reflectance spectra of a piece of cave granite and a piece of bark from the Argyle apple tree (*Eucalyptus cinerea*).

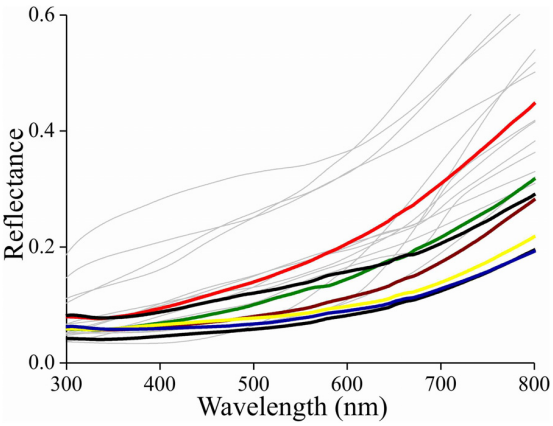

FIGURE 7 | Reflectance spectra of the bark of the trees listed in **Table 1** as likely resting spots (thin lines) and reflectance spectra of various places on the forewings of a few Bogong moths (bold lines).

are intrinsic to the lower lamina are effectively removed in that area by a high concentration of melanin pigment.

Reflectance Spectra of Granite and Bark

Due to the melanin pigmentation and its effective blocking of the thin film reflections, the coloration of Bogong moths is not particularly striking, especially on their dorsal forewings. An obvious reason for the dull colors is to achieve suitable background matching when the moth is resting with the forewings covering the body. To underscore this view, we assembled a variety of objects – granite from their aestivation caves and the bark of several trees that are potential resting places for the moths (**Table 1**) – and measured their reflectance spectra (**Figures 6**, **7** and **Supplementary Figure S1**). The reflectance spectrum of the granite has a slight hump in the green part of the spectrum, presumably due to a thin algal coating arising from the moist conditions of the cave, while bark samples from the species of trees tested have a clear brown color. The greenish surface of the cave granite is clearly less well matched to the Bogong moth's wing color than the trees' bark, although some degree of camouflage will be nonetheless provided (**Figures 6**, **8a,b**). The reflectance spectra of the bark of trees that are likely resting places vary considerably, but the reflectance spectra of the forewings of the rather dark female Bogong moths we were using vary in the same range (**Figure 7**). Less darkly-colored specimens will still be able to achieve background matching on trees having higher spectral reflectance. Whether Bogong moths

FIGURE 8 | Bogong moth camouflage on bark of the Argyle apple (*Eucalyptus cinerea*) **(a)**, and on a small piece of granite **(b)** taken from the wall of an aestivation cave at South Ramshead in the Kosciuszko National Park, New South Wales (elevation 1860 m). **(c)** Bogong moths aestivating in the same cave from which the granite sample was taken in **(b)**. Inset: close-up. (Photographs taken by EJW on December 23rd 2010).

actively select resting places that precisely match the reflectance of the background (as has been noted in other moths, e.g., Sargent, 1966), will be the theme of a future study.

DISCUSSION

The gradient of melanin expressed in the wing scales of the Bogong moth is very sensible, because the high melanin concentration in the distal, exposed part of the scales filters the reflections of the scales' lower lamina, so that only the long-wavelength part of the lower lamina's reflectance spectrum contributes to the total wing reflectance. Several butterfly species do use the lower lamina's thin film properties to create a distinct scale color, for instance the strikingly iridescent wing scales of the Mother-of-pearl, *Salamis parhassus* (Onslow, 1923) and the pigmentless blue scales of nymphalines (Stavenga et al., 2014). In most butterflies, however, the wing colors are due to pigments, which are expressed in the upper lamina and absorb selectively in a restricted wavelength range, thus resulting in a scale reflectance spectrum in the complementary wavelength range. Remarkably, the reflectance spectra of lower and upper lamina are often tuned, so that their summed reflections create bright scale colors (Stavenga et al., 2015; Wilts et al., 2015). On the other hand, most butterflies also have black scales, frequently marking the wing margin, which is caused by very dense melanin pigmentation that fully suppresses the lamina reflections (e.g., Stavenga et al., 2014).

Butterflies are admired for their striking, colorful appearances, but interestingly, many butterfly species have ventral wings that are darkly colored, for example the nymphaline Peacock butterfly *Aglais io* and the Admiral *Vanessa atalanta* (e.g., Stavenga et al., 2014). When at rest, their wings are closed and then they are camouflaged owing to their inconspicuous ventral coloration. The iconic *Morpho* butterflies have dorsal wings that have a bright-blue structural color, but their ventral wings are only mildly colored by pigmented scales and patterned by modest eyespots. As for *Vanessa*, the ventral wings of *Morpho* will provide camouflage when these butterflies are not on the wing. Other remarkable cases of background matching are offered by some lycaenids: the scales at the ventral wing sides of the Green Hairstreak, *Callophrys rubi*, have highly sophisticated gyroid cuticular structures that create a green reflectance matching that of leaves (Michielsen et al., 2010), and the variable thin films of the ventral scales of the Angled Sunbeam, *Curetis acuta*, act as silvery reflectors that radiate the green colors of the leaves on which the butterflies have landed (Wilts et al., 2013).

In the Bogong moth's wings, a dense melanin filter blocks the lower lamina reflections and thus prevents the danger of conspicuousness. The correspondence of the moth's coloration with that of the objects in its habitat underscores the hypothesis that the dull colors of this moth (and others) function for camouflage through background matching (Thayer, 1909; Cott, 1940). The measured reflectance spectra from the bark samples are well matched to the spectra measured from the moth's wings (**Figures 7**, **8**), thus suggesting that visual camouflage from diurnal predators has been a major selective pressure during the evolution of Bogong moth coloration, and most likely that of many other species of nocturnal moths that need to find concealing shelter during daytime hours (e.g., Thayer, 1909; Cott, 1940; Sargent, 1966). Indeed, many species of moths are even capable of optimizing their orientations and locations on tree bark to maximize this camouflage (Sargent, 1966; Endler, 1984; Kang et al., 2012).

Interestingly, the melanin pigment is deposited preferentially in the tip of the wing scale, suggesting that this is an optimization of production costs. A study on the brown colored-satyrine butterfly *Pararge aegeria* concluded that melanization of the wing scales is indeed costly (Talloen et al., 2004). The wing scales of moths have a high melanin content, the cost of which is necessary to block the thin film reflections of the lower lamina and to obtain a camouflaging brown color. How the pigmentation is locally controlled is an emerging question that is not only intriguing but at the same time complex, since melanin synthesis is co-regulated with scale structure as was revealed in another satyrine, *Bicyclus anynana* (Matsuoka and Monteiro, 2018).

The melanization of the Bogong moths' wing scales is not uniform in a single scale (**Figure 3**), but it is also rather variable among the different scales of the wings' cover (**Figure 1A**).

This serves to give resting moths a mottled appearance, which may add to matching the background of similarly inhomogeneously colored tree bark (Endler, 1984; Kang et al., 2012). Furthermore, the moth's contours, together with the more or less striped wing patterning, may endow the moths with a potentially disruptive coloration, thus further enforcing camouflage (e.g., Schaefer and Stobbe, 2006; Stevens and Merilaita, 2009). The dark spots on the forewings may act as distractive markings or for surface disruption (Stevens and Merilaita,2009; Cuthill, 2019).

The scales are very densely packed and overlap each other multifold. The dense scale cover may, however, not primarily function for (in)visibility, as it has additional functions. For instance, by providing thermal insulation, the moths can migrate over long distances during cold nights and withstand up to 4 months of dormancy in their high-altitude aestivation caves where nighttime temperatures, even in summer, can fall to several degrees Celsius below zero. The wing scales of moths can also have an acoustical function, by absorbing sound frequencies corresponding to the calls of echo-locating bats, thus reducing echo power (Zeng et al., 2011). Furthermore, scale attachment in sockets on the wings is sufficiently loose that the scales are shed when their owner becomes caught in a spider web, hence allowing the moth to escape (Eisner, 2003).

Whereas the Bogong moths are well matched to a bark background, the color of the granite rock in their caves deviates by not providing as good a match. However, the moths tile tightly (with up to 17,000 individuals per square meter; Common, 1954), thus fully carpeting the cave walls so well and so extensively that the granite cave wall is only seen at the periphery of these moth carpets (**Figure 8c**). In other words, although the reflectance spectra of granite and moths may somewhat differ, within the interior of such a carpet, the moths are camouflaged against themselves.

DATA AVAILABILITY STATEMENT

All datasets generated for this study are included in the article/**Supplementary Material**.

AUTHOR CONTRIBUTIONS

DS and EW conceived the project. DS, EW, and JW collected the data. DS wrote the first version of the manuscript. All authors edited the draft until the final version was complete.

FUNDING

This study was financially supported by the Air Force Office of Scientific Research/European Office of Aerospace Research and Development AFOSR/EOARD (Grant No. FA9550-15-1-0068 to DS and Grant No. FA9550-14-1-0242 to EW). EW and JW are grateful for funding from the European Research Council (Grant No. 741298), the Swedish Research Council (Grant No. 2016-04014), and the Royal Physiographic Society of Lund. JW is thankful for the support of an Australian Government Research Training Program (RTP) Scholarship.

ACKNOWLEDGMENTS

EW holds Scientific Permits for collection and experimental manipulations of Bogong moths in several alpine national parks and nature reserves (NSW: Permit SL100806; Vic: Permit 10008966). We thank Drs. Ken Green, Ola Gustafsson, and Hein Leertouwer for essential collaboration and Dr. Bodo Wilts for valuable comments an the manuscript. We are grateful for the constructive comments of the two reviewers.

SUPPLEMENTARY MATERIAL

The Supplementary Material for this article can be found online at: https://www.frontiersin.org/articles/10.3389/fphys.2020.00095/full#supplementary-material

FIGURE S1 | Reflectance spectra of aestivation cave wall granite and tree bark measured with a bifurcated reflection probe. When the bark color was rather uniform, only one spectrum is shown. Several spectra are included when the surface coloration was varied.

REFERENCES

Barbier, M. (1986). Butterfly and moth neopterobilins: sarpedobilin as a natural metachromatic pigment. *Comp. Biochem. Physiol.* 84B, 619–621. doi: 10.1016/0305-0491(86)90131-8

Choussy, M., Barbier, M., Rüdiger, W., and Klose, W. (1973). Preliminary report on the neopterobilins, blue-green pigments from Lepidoptera. *Comp. Biochem. Physiol.* 44B, 47–52. doi: 10.1016/0305-0491(73)90340-4

Common, I. A. (1954). A study of the ecology of the adult Bogong moth *Agrotis infusa* (Boisd.) (Lepidoptera: Noctuidae), with special reference to its behaviour during migration and aestivation. *Aust. J. Zool.* 2, 223–263.

Cook, L. M., Grant, B. S., Saccheri, I. J., and Mallet, J. (2012). Selective bird predation on the peppered moth: the last experiment of Michael Majerus. *Biol. Lett.* 8, 609–612. doi: 10.1098/rsbl.2011.1136

Cook, M. A., Harwood, L. M., Scoble, M. J., and McGavin, G. C. (1994). The chemistry and systematic importance of the green wing pigment in emerald moths (Lepidopera: Geometridae, Geometrinae). *Biochem. Syst. Ecol.* 22, 43–51. doi: 10.1016/0305-1978(94)90113-9

Cott, H. B. (1940). *Adaptive Coloration in Animals*. London: Meuthuen.

Cuthill, I. C. (2019). Camouflage. *J. Zool.* 308, 75–92.

Descimon, H. (1975). "Biology of pigmentation in Pieridae butterflies," in *Chemistry and Biology of Pteridines*, ed. W. Pfleiderer, (Berlin: De Gruyter), 805–840. doi: 10.1515/9783110838053-065

Dreyer, D., Frost, B. J., Mouritsen, H., Green, K. P., Whitehouse, M., Heinze, S., et al. (2018). The Earth's magnetic field and visual landmarks steer migratory flight behavior in the nocturnal Australian Bogong moth. *Curr. Biol.* 28, 2160–2166. doi: 10.1016/j.cub.2018.05.030

Eisner, T. (2003). *For Love of Insects*. Cambridge MA: Harvard University Press.

Endler, J. A. (1984). Progressive background matching in moths, and a quantitative measure of crypsis. *Biol. J. Linn. Soc.* 22, 187–231. doi: 10.1111/j.1095-8312.1984.tb01677.x

Flood, J. M. (1980). *The Moth Hunters*. Canberra: Australian Institute of Aboriginal Studies.

Flood, J. M. (1996). *Moth Hunters of the Australian Capital Territory*. Lewisham, NSW: Clarendon.

Ghiradella, H. (1991). Light and color on the wing: structural colors in butterflies and moths. *Appl. Optics* 30, 3492–3500. doi: 10.1364/AO.30.003492

Ghiradella, H. (1998). "Hairs, bristles, and scales," in *Microscopic Anatomy of Invertebrates, Vol 11A: Insecta*, ed. M. Locke, (New York, NY: Wiley-Liss), 257–287.

Ghiradella, H. (2010). Insect cuticular surface modifications: scales and other structural formations. *Adv. Insect. Physiol.* 38, 135–180. doi: 10.1016/s0065-2806(10)38006-4

Gibson, R. K., Broome, L., and Hutchison, M. F. (2018). Susceptibility to climate change via effects on food resources: the feeding ecology of the endangered mountain pygmy-possum (*Burramys parvus*). *Wildlife Res.* 45, 539–550.

Giraldo, M. A., Yoshioka, S., Liu, C., and Stavenga, D. G. (2016). Coloration mechanisms and phylogeny of *Morpho* butterflies. *J. Exp. Biol.* 219, 3936–3944. doi: 10.1242/jeb.148726

Kang, C. K., Moon, J. Y., Lee, S. I., and Jablonski, P. G. (2012). Camouflage through an active choice of resting spot and body orientation in moths. *J. Evol. Biol.* 25, 1695–1702. doi: 10.1111/j.1420-9101.2012.02557.x

Kelley, J. L., Tatarnic, N. J., Schröder-Turk, G. E., Endler, J. A., and Wilts, B. D. (2019). A dynamic optical signal in a nocturnal moth. *Curr. Biol.* 29, 2919–2925. doi: 10.1016/j.cub.2019.07.005

Kilchoer, C., Steiner, U., and Wilts, B. D. (2018). Thin-film structural coloration from simple fused scales in moths. *J. R. Soc. Interf. Focus* 9:20180044. doi: 10.1098/rsfs.2018.0044

Kinoshita, S. (2008). *Structural Colors in the Realm of Nature*. Singapore: World Scientific.

Lippert, W., and Gentil, K. (1959). Über lamellare Feinstrukturen bei den Schillerschuppen der Schmetterlinge vom Urania- und Morpho-Typ. *Zool. Morph. Oekol. Tiere* 48, 115–122. doi: 10.1007/bf00407836

Majerus, M., Brunton, C., and Stalker, J. (2000). A bird's eye view of the peppered moth. *J. Evol. Biol.* 13, 155–159. doi: 10.1046/j.1420-9101.2000.00170.x

Matsuoka, Y., and Monteiro, A. (2018). Melanin pathway genes regulate color and morphology of butterfly wing scales. *Cell Rep.* 24, 56–65. doi: 10.1016/j.celrep.2018.05.092

Michielsen, K., DeRaedt, H., and Stavenga, D. G. (2010). Reflectivity of the gyroid biophotonic crystals in the ventral wing scales of the Green Hairstreak butterfly. *Callophrys rubi. J. R. Soc. Interf.* 7, 765–771. doi: 10.1098/rsif.2009.0352

Nijhout, H. F. (1991). *The Development and Evolution of Butterfly Wing Patterns*. Washington, DC: Smithsonian Institution Press.

Nijhout, H. F. (1997). Ommochrome pigmentation of the *linea* and *rosa* seasonal forms of *Precis coenia* (Lepidoptera: Nymphalidae). *Arch. Insect. Biochem. Physiol.* 36, 215–222.

Nijhout, H. F. (2010). Molecular and physiological basis of colour pattern formation. *Adv. Insect. Physiol.* 38, 219–265. doi: 10.1016/s0065-2806(10)38002-7

Nishikawa, H., Iga, M., Yamaguchi, J., Saito, K., Kataoka, H., Suzuki, Y., et al. (2013). Molecular basis of wing coloration in a Batesian mimic butterfly. *Papilio polytes. Sci. Rep.* 3:3184. doi: 10.1038/srep03184

Onslow, H. (1923). On a periodic structure in many insect scales, and the cause of their iridescent colours. *Philos. Trans. R. Soc. Lond. B* 211, 1–74. doi: 10.1098/rstb.1923.0001

Sargent, T. D. (1966). Background selections of geometrid and noctuid moths. *Science* 154, 1674–1675. doi: 10.1126/science.154.3757.1674

Schaefer, H. M., and Stobbe, N. (2006). Disruptive coloration provides camouflage independent of background matching. *Proc. R. Soc. B* 273, 2427–2432. doi: 10.1098/rspb.2006.3615

Stavenga, D. G. (2014). Thin film and multilayer optics cause structural colors of many insects and birds. *Mat. Today Proc.* 1S, 109–121. doi: 10.1016/j.matpr.2014.09.007

Stavenga, D. G., Leertouwer, H. L., Meglič, A., Drašlar, K., Wehling, M. F., Pirih, P., et al. (2018). Classical lepidopteran wing scale colouration in the giant butterfly-moth *Paysandisia archon*. *PeerJ* 6:e4590. doi: 10.7717/peerj.4590

Stavenga, D. G., Leertouwer, H. L., Pirih, P., and Wehling, M. F. (2009). Imaging scatterometry of butterfly wing scales. *Opt. Express* 17, 193–202.

Stavenga, D. G., Leertouwer, H. L., and Wilts, B. D. (2014). Coloration principles of nymphaline butterflies - thin films, melanin, ommochromes and wing scale stacking. *J. Exp. Biol.* 217, 2171–2180. doi: 10.1242/jeb.098673

Stavenga, D. G., Matsushita, A., and Arikawa, K. (2015). Combined pigmentary and structural effects tune wing scale coloration to color vision in the swallowtail butterfly *Papilio xuthus*. *Zool Lett.* 1:14. doi: 10.1186/s40851-015-0015-2

Stevens, M., and Merilaita, S. (2009). Animal camouflage: current issues and new perspectives. *Philos. Trans. R. Soc.* 364, 423–427. doi: 10.1098/rstb.2008.0217

Süffert, F. (1924). Morphologie und Optik der Schmetterlingsschuppen, insbesondere die Schillerfarben der Schmetterlinge. *Z. Morphol. Oekol. Tiere.* 1, 171–308. doi: 10.1007/bf00403572

Talloen, W., Dyck, H. V., and Lens, L. (2004). The cost of melanization: butterfly wing coloration under environmental stress. *Evolution* 58, 360–366. doi: 10.1111/j.0014-3820.2004.tb01651.x

Thayer, G. H. (1909). *Concealing-Coloration in the Animal Kingdom*. New York, NY: Macmillan.

Umebachi, Y. (1985). Papiliochrome, a new pigment group of butterfly. *Zool. Sci.* 2, 163–174.

Vukusic, P., and Sambles, J. R. (2003). Photonic structures in biology. *Nature* 424, 852–855. doi: 10.1038/nature01941

Warrant, E. J., Frost, B. J., Green, K. P., Mouritsen, H., Dreyer, D., Adden, A., et al. (2016). The Australian Bogong moth *Agrotis infusa*: a long-distance nocturnal navigator. *Front. Behav. Neurosci.* 10:77. doi: 10.3389/fnbeh.2016.00077

Wijnen, B., Leertouwer, H. L., and Stavenga, D. G. (2007). Colors and pterin pigmentation of pierid butterfly wings. *J. Insect Physiol.* 53, 1206–1217. doi: 10.1016/j.jinsphys.2007.06.016

Wilts, B. D., IJbema, N., and Stavenga, D. G. (2014). Pigmentary and photonic coloration mechanisms reveal taxonomic relationships of the Cattlehearts (Lepidoptera: Papilionidae: Parides). *BMC Evol. Biol.* 14:160. doi: 10.1186/s12862-014-0160-9

Wilts, B. D., Leertouwer, H. L., and Stavenga, D. G. (2009). Imaging scatterometry and microspectrophotometry of lycaenid butterfly wing scales with perforated multilayers. *J. R. Soc. Interf.* 6, S185–S192. doi: 10.1098/rsif.2008.0299.focus

Wilts, B. D., Matsushita, A., Arikawa, K., and Stavenga, D. G. (2015). Spectrally tuned structural and pigmentary coloration of birdwing butterfly wing scales. *J. R. Soc. Interf.* 12:20150717. doi: 10.1098/rsif.2015.0717

Wilts, B. D., Pirih, P., Arikawa, K., and Stavenga, D. G. (2013). Shiny wing scales cause spec(tac)ular camouflage of the angled sunbeam butterfly. *Curetis acuta*. *Biol. J. Linn. Soc.* 109, 279–289. doi: 10.1111/bij.12070

Wilts, B. D., Vey, A. J., Briscoe, A. D., and Stavenga, D. G. (2017). Longwing (*Heliconius*) butterflies combine a restricted set of pigmentary and structural coloration mechanisms. *BMC Evol. Biol.* 17:226. doi: 10.1186/s12862-017-1073-1

Yoshioka, S., and Kinoshita, S. (2007). Polarization-sensitive color mixing in the wing of the Madagascan sunset moth. *Opt. Express* 15, 2691–2701.

Yoshioka, S., Nakano, T., Nozue, Y., and Kinoshita, S. (2008). Coloration using higher order optical interference in the wing pattern of the Madagascan sunset moth. *J. R. Soc. Interf.* 5, 457–464. doi: 10.1098/rsif.2007.1268

Zeng, J., Xiang, N., Jiang, L., Jones, G., Zheng, Y., Liu, B., et al. (2011). Moth wing scales slightly increase the absorbance of bat echolocation calls. *PLoS One* 6:e27190. doi: 10.1371/journal.pone.0027190

Conflict of Interest: The authors declare that the research was conducted in the absence of any commercial or financial relationships that could be construed as a potential conflict of interest.

frontiers in Physiology

ORIGINAL RESEARCH
published: 11 February 2020
doi: 10.3389/fphys.2020.00053

Stochastic and Arbitrarily Generated Input Patterns to the Mushroom Bodies Can Serve as Conditioned Stimuli in *Drosophila*

Carmina Carelia Warth Pérez Arias, Patrizia Frosch, André Fiala and Thomas D. Riemensperger*†*

Department of Molecular Neurobiology of Behavior, Johann-Friedrich-Blumenbach-Institute of Zoology and Anthropology, University of Göttingen, Göttingen, Germany

OPEN ACCESS

Edited by:
Sylvia Anton, Institut National de la Recherche Agronomique (INRA), France

Reviewed by:
Emmanuel Perisse, Université de Montpellier, France
Angelique Christine Paulk, Massachusetts General Hospital, Harvard Medical School, United States

***Correspondence:**
André Fiala
afiala@gwdg.de
Thomas D. Riemensperger
triemens@uni-koeln.de

†Present address:
Thomas D. Riemensperger, Institute for Zoology, University of Cologne, Cologne, Germany

Specialty section:
This article was submitted to Invertebrate Physiology, a section of the journal Frontiers in Physiology

Received: *30 September 2019*
Accepted: *21 January 2020*
Published: *11 February 2020*

Citation:
Warth Pérez Arias CC, Frosch P, Fiala A and Riemensperger TD (2020) Stochastic and Arbitrarily Generated Input Patterns to the Mushroom Bodies Can Serve as Conditioned Stimuli in Drosophila. Front. Physiol. 11:53. doi: 10.3389/fphys.2020.00053

Single neurons in the brains of insects often have individual genetic identities and can be unambiguously identified between animals. The overall neuronal connectivity is also genetically determined and hard-wired to a large degree. Experience-dependent structural and functional plasticity is believed to be superimposed onto this more-or-less fixed connectome. However, in *Drosophila melanogaster*, it has been shown that the connectivity between the olfactory projection neurons (OPNs) and Kenyon cells, the intrinsic neurons of the mushroom body, is highly stochastic and idiosyncratic between individuals. Ensembles of distinctly and sparsely activated Kenyon cells represent information about the identity of the olfactory input, and behavioral relevance can be assigned to this representation in the course of associative olfactory learning. Previously, we showed that in the absence of any direct sensory input, artificially and stochastically activated groups of Kenyon cells could be trained to encode aversive cues when their activation coincided with aversive stimuli. Here, we have tested the hypothesis that the mushroom body can learn any stochastic neuronal input pattern as behaviorally relevant, independent of its exact origin. We show that fruit flies can learn thermogenetically generated, stochastic activity patterns of OPNs as conditioned stimuli, irrespective of glomerular identity, the innate valence that the projection neurons carry, or inter-hemispheric symmetry.

Keywords: *Drosophila melanogaster*, olfactory projection neurons, mushroom body, antennal lobe, learning and memory, thermogenetics, olfaction

INTRODUCTION

Drosophila melanogaster is a model organism, widely used in studies of the neuronal basis of behavior. This is not only because of the wealth of elaborate genetic tools available to allow specific neurons can be genetically targeted and manipulated (Venken et al., 2011), but also to the highly individually stereotypic and genetically determined connectivity between neurons that facilitate the analytical dissection of neuronal circuits (Meinertzhagen and Lee, 2012). The stereotypic connectivity in *Drosophila* contrasts with that in the vertebrate brain, where neurons usually cannot be identified at the level of individual cells and compared across animals. One well-studied example of highly stereotypic connectivity

is the olfactory system of the fruit fly (Grabe and Sachse, 2018). Olfactory sensory neurons express olfactory receptors that have evolved to detect behaviorally relevant odorants. Sensory neurons that express the same receptors project into the same glomeruli in the antennal lobes that also have stereotypic anatomical locations at the inter-individual and inter-hemispheric levels (Couto et al., 2005; Fishilevich and Vosshall, 2005). As a result, stereotypic chemotopic maps of odor representations can be detected across individuals (Rodrigues and Buchner, 1984; Fiala et al., 2002). Olfactory projection neurons (OPNs), the second-order olfactory neurons of the insect brain receive input from the glomeruli of the antennal lobes and target the lateral horn and the calyx of the mushroom body (schematically depicted in **Figure 1A**). Their individual identities and anatomical projections to the target brain regions are also relatively constant across individuals (Marin et al., 2002; Wong et al., 2002; Tanaka et al., 2004; Jeanne et al., 2018). Even at the level of gene expression, individual OPN types can be unambiguously distinguished, highlighting their genetic individualities (Li et al., 2017). This connectivity also leads to chemotopic maps in those higher-order brain regions targeted by OPNs (Fiala et al., 2002; Jefferis et al., 2007). This deterministic, hard-wired connectivity, together with specific sensory receptors, has led to the idea of multiple neuronal "labeled lines," wherein each olfactory input stimulates a route of connections that ultimately evoke an appropriate behavioral response, such as the avoidance of harmful substances (Suh et al., 2007; Stensmyr et al., 2012), egg-laying on odorous substrates (Dweck et al., 2015), or pheromone-induced courtship behavior (van der Goes van Naters and Carlson, 2007; Datta et al., 2008).

However, at least one exception from the rule of genetically determined, hard-wired connectivity exists in the *Drosophila* brain olfactory system. The ∼2000 intrinsic neurons of the mushroom body (Kenyon cells) per hemisphere (Aso et al., 2009) receive stochastic input from ∼150 OPNs, and the dendrites of each Kenyon cell receive input from several OPNs (Caron et al., 2013). Substantial evidence has accumulated showing that the process of associative olfactory learning is localized to the mushroom bodies (Heisenberg et al., 1985; de Belle and Heisenberg, 1994; Connolly et al., 1996; Zars et al., 2000; Dubnau et al., 2001; McGuire et al., 2001; Qin et al., 2012). In particular, to the lobes as the main output structures (Aso et al., 2014a). During the learning regime, an odor is presented as a conditioned stimulus in temporal coincidence with a rewarding or punishing unconditioned stimulus, such as sugar or an electric shock (Tempel et al., 1983; Tully and Quinn, 1985). Each odor evokes the activity of a distinct, sparsely distributed ensemble of Kenyon cells (Honegger et al., 2011). The axons of the Kenyon cells are compartmentalized such that distinct populations of dopaminergic neurons, which signal rewarding or punishing unconditioned stimuli, innervate distinct partitions (Aso et al., 2014b). It has long been accepted that the coincidental release of dopamine onto Kenyon cell axons and the odor-evoked calcium influx therein causes presynaptic modification of transmitter release onto a small number of mushroom body output neurons that instruct the behavior of the animal (Heisenberg, 2003; Aso et al., 2014a) and that are, again, highly anatomically stereotypic at the inter-hemispheric and inter-individual levels (Aso et al., 2014b).

To summarize, data collected to date suggest that the large number of Kenyon cells organized in parallel are not identifiable at the individual-neuron level, and show random connectivity with OPNs (Caron et al., 2013). In addition, distinct stimuli evoke non-stereotypic, idiosyncratic activity patterns across Kenyon cells (Murthy et al., 2008; Gruntman and Turner, 2013). It has been proposed that the stochastic nature of OPN-to-Kenyon cell connectivity and the resulting stochastic response patterns of Kenyon cells could reflect the evolutionary unpredictability of stimuli to be learned. In this sense, the stimulus-activated ensembles of Kenyon cells do not encode odors, visual images, or tastes. Rather, they encode arbitrary patterns to which value(s) can be assigned through learning, and which can ultimately instruct behavior. They are arbitrary in the sense that no genetically determined pattern of Kenyon cell activity or circuit diagram carries any behaviorally relevant information about the odor or any other stimulus. In a previous study, we showed that artificially and stochastically activated groups of Kenyon cells, in coincidence with a punishing electric shock, can be learned as aversive cue without direct sensory input (Vasmer et al., 2014). By modifying their behavior, trained animals avoided reactivation of those Kenyon cell ensembles whose activities were associated with the punishment. This finding suggests that the overall Kenyon cell array can learn any neuronal input pattern to be avoided, independent of the nature of the actual sensory stimulus and inter-hemispheric symmetry. Here, we tested this hypothesis. Our results indicate that fruit flies can indeed learn to avoid stochastic, thermogenetically generated OPN activity patterns as conditioned stimuli.

MATERIALS AND METHODS

Drosophila Strains

Fly stocks were raised on standard cornmeal-agar medium at 18°C, 60% relative humidity, and under a 12 h light–dark cycle. Flies were generated as described by Vasmer et al. (2014). A Hsp70-FLP insertion on the X-chromosome (provided by G. Struhl) was combined with the GH146-Gal4 (Stocker et al., 1997) insertion on the second chromosome to generate a strain homozygous for both P-element inserts. These flies were crossed with a strain carrying the UAS-FRT-CD2(Stop)-FRT-mCherry-dTRPA1 (Vasmer et al., 2014; Pooryasin and Fiala, 2015) construct with the insertion balanced over CyO. Female F1 offspring younger than 2 days were anesthetized using CO_2 and transferred to a fresh food vial. Unless otherwise indicated, flies were incubated at 30°C for 4 h to induce FLP-mediated expression. **Figure 1B** illustrates how this causes stochastic heat-shock-induced expression of mCherry-dTRPA1 in neurons determined by the Gal4 line.

Behavioral Analysis

Flies were trained as described by Vasmer et al. (2014), schematically illustrated in **Figure 1C**. Female flies aged 4–6 days

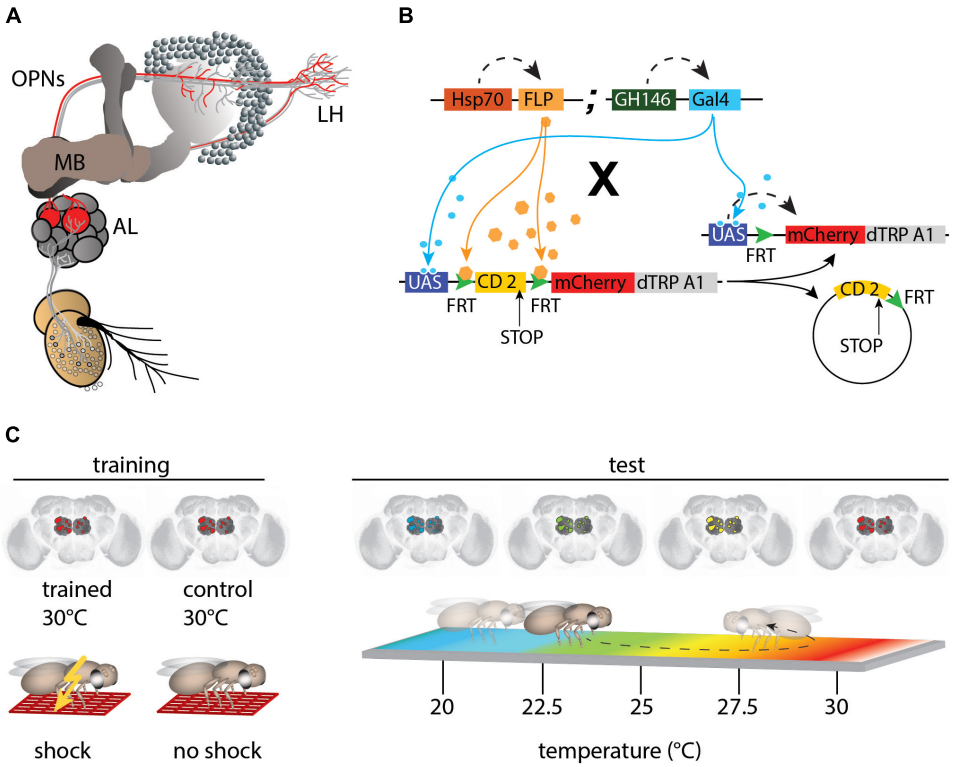

FIGURE 1 | mCherry-dTRPA1 expression in random subsets of olfactory projection neurons (OPNs). **(A)** Illustration of the olfactory pathway in *Drosophila*. Odors are detected by olfactory receptor neurons (ORNs) that project to the antennal lobes (AL). Olfactory information is conveyed by OPNs from the AL to the calyx of the mushroom bodies (MBs) and the lateral horns (LH). **(B)** Random expression of mCherry-dTRPA1: Flies carrying GH146-Gal4 and a flippase under Hsp-70 control were crossed with flies that carried a UAS-coupled FRT-flanked CD2 (stop) cassette followed by the mCherry-dTRPA1 DNA construct. Heat shock-mediated activation of the flippase causes a random excision of the FRT-cassette and transcription of mCherry-dTRPA1. **(C)** Schematic depiction of the training protocol and behavioral read-out. The OPNs were thermogenetically activated for 2 min. One group of flies was simultaneously exposed to electric shocks ("Training") while a second group of flies was treated similarly but did not receive electric shocks and served as controls. Subsequently, the flies were individually transferred to a temperature gradient arena ("Test") where they could freely distribute according to their temperature preference. Through movements along the temperature gradient, the flies triggered or avoided thermogenetic depolarization of the OPNs expressing mCherry-dTRPA1.

old were transferred into pre-warmed (30°C) tubes covered on the inside with an electrifiable copper grid. Training was performed in an illuminated incubator at 30°C and at an air humidity of ∼60%. Animals were kept in these tubes for 2 min, during which time 24 90 V DC electric shocks of 1.25 s each in duration were applied, separated by 3.75 s breaks, for a total shock interval of 5 s. Control animals were treated in a similar manner; that is, they were exposed to a temperature of 30°C in the same tubes but did not receive the electric shocks. Subsequently, the flies were transferred to a heat-gradient chamber (schematically depicted in **Figure 1C**, right) that consisted of an aluminum block with eight walking tracks (275 mm length × 5 mm width × 4 mm height) covered with a Plexiglas lid. The entire apparatus was kept in an incubator under a constant white light, and at a temperature of 16°C and ∼65% humidity, producing a linear and stable temperature gradient over the length of the arena ranging from 18 to 35°C. Individual flies were transferred without anesthesia into the walking tracks through small holes in the lid and were permitted to move freely for 20 min. Locomotion was monitored from above using a high-definition video camera (Panasonic HC-V500). Flies were tracked using the Noldus Ethovision XT 8.5 software (Wageningen) to generate data used in the analysis. The temperature preference of each fly over the observation period of 20 min was determined in 5 min time bins as the time spent above or below 24°C. The flies were anesthetized immediately after the behavioral experiments and their brains were dissected. Localization of mCherry-dTRPA1 expression was determined using immunohistochemistry.

Immunohistochemistry

Brains were dissected in ice-cold Ringer's solution containing 5 mM Hepes (pH 7.3), 130 mM NaCl, 5 mM KCl, 2 mM $MgCl_2$, 2 mM $CaCl_2$, and 36 mM sucrose (Estes et al., 1996) and fixed for 2 h on ice in 4% paraformaldehyde dissolved in phosphate-buffered saline (PBS). Subsequently, brains were washed three times for 20 min each in PBS containing 0.6% Triton X-100 (PBST), then incubated in PBST containing 2% bovine serum albumin (block solution) for 2 h. Afterward, the brains were incubated overnight at 4°C in block solution containing mouse anti-nc82 antibody against Bruchpilot (provided by Erich Buchner) (Wagh et al., 2006) diluted 1:10. Brains were again washed three times for 20 min

each in PBST and incubated for at least 4 h with goat anti-mouse 1:300 conjugated with Alexa Fluor 488-conjugated goat anti-mouse (Invitrogen). Brains were washed three times in PBST for 20 min each, washed in PBS overnight at 4°C, and embedded in Vectashield (Vector Laboratories). Images were acquired using a confocal laser scan microscope (Leica SP8) equipped with hybrid detectors and analyzed using *ImageJ*. The antennal lobe glomeruli were determined using anti-bruchpilot (anti-*Brp*) immunoreactivity and mCherry-dTRPA1 expression was characterized. The antennal lobes of both hemispheres were examined when possible.

Statistical Analysis

The symmetry index was defined as the ratio between symmetrically innervated glomeruli by OPNs expressing dTRPA1-mCherry and the total number of innervated glomeruli by mCherry-dTRPA1 expressing OPNs. All statistical tests were conducted using *GraphPad Prism7* and *OriginPro* software. A Kolmogorov–Smirnov test was used to test for a normal distribution of data. Normally distributed data were analyzed using one-way ANOVA followed by Bonferroni *post hoc* tests for multiple pairwise comparisons. Non-normally distributed data were analyzed using the Kruskal–Wallis test followed by Dunn's *post hoc* tests for multiple pairwise comparisons. For correlation analyses, Spearman correlations were calculated. For testing for randomness of dTRPA1-mCherry expression in glomeruli a Runs test (Wald–Wolfowitz test) was conducted for all flies and for each glomerulus and each brain hemisphere independently.

RESULTS

Expression of mCherry-Tagged dTRPA1 in Stochastic Ensembles of OPNs

To obtain expression of mCherry-dTRPA1 in stochastic subsets of OPNs (**Figure 1B**), flies carrying the DNA construct of a mCherry-tagged thermo-inducible cation-channel dTRPA1 (Vasmer et al., 2014; Pooryasin and Fiala, 2015) were crossed with flies carrying a flippase under control of the heat shock promoter Hsp-70 (Basler and Struhl, 1994) together with the GH146-Gal4 driver line (Stocker et al., 1997; **Figure 1B**). The groups of neurons that express dTRPA1 can be artificially depolarized by raising the temperature above ∼25°C (Hamada et al., 2008; Tang et al., 2013; Vasmer et al., 2014; Pooryasin and Fiala, 2015). dTRPA1 induces a relatively sharp increase in excitation in neurons expressing it, with a peak at ∼32°C (Hamada et al., 2008; Tang et al., 2013). The flippase-mediated mCherry-dTRPA1 expression is induced by heat shock within the first 2 days after hatching. To test whether the animals can associate the activity of stochastic sets of OPNs with a punishing electric shock, OPNs expressing mCherry-dTRPA1 were thermogenetically activated at 30°C and this activation was temporally paired with 2 min of electric shocks of 90 V. The shocks were 1.25 s in duration and separated by 3.75 s intervals, as described (Vasmer et al., 2014). Control animals of the same genotype were treated in the same manner but did not receive the electric shocks (**Figure 1C**). In a typical aversive olfactory conditioning procedure, the animals learn to avoid the odor that has been temporally paired with the punishment (Tully and Quinn, 1985). In our experiment, the stochastically distributed activity of OPNs did not reflect any real odor representation that could be tested for. To bypass any olfactory input also in the memory test phase, directly after the training procedure the animals were individually transferred to a test chamber in which they could walk freely along a temperature gradient ranging from 18 to 35°C (**Figure 1C** right). The movement of each animal was monitored and temperature preference during the first 5 min was used as the memory readout. The mCherry-dTRPA1 channel starts opening at ∼25°C (Vasmer et al., 2014); that is, within the preferred temperature range of naïve fruit flies (Sayeed and Benzer, 1996; Hamada et al., 2008). Therefore, the relative amount of time the animals spent >24°C, i.e., at a temperature that is still within the range of their innate temperature preference but just below the onset of dTRPA1-mediated excitation, after training was used to determine whether the animals approached or avoided re-activation of the population of OPNs expressing mCherry-dTRPA1.

Thermogenetic Induction of Associative Learning

First, the effect of heat shock duration during development on the number of mCherry-dTRPA1 expressing OPNs was examined: The longer and more often the heat shock was, the more neurons should express mCherry-dTRPA1. This was the case as an increase in heat exposure time after hatching gradually increased the number of mCherry-dTRPA1 expressing OPNs, as determined by quantifying mCherry-labeled somata (**Figures 2A,B** and **Table 1**). We then asked whether flies can associate activation of OPNs with a punishment, and whether this association depends on the number of activated OPNs. Therefore, four groups of flies were tested, namely, flies that did not receive any heat-induction of mCherry-dTRPA1 expression during development and thus only expressed the DNA construct in small populations of random subsets of OPNs, and flies that received a 20 min, 1 h, or 4 h heat induction of mCherry-dTRPA1 in OPNs. All groups were subjected to electric shocks simultaneous to the thermogenetic induction of neuronal activity. These groups were compared with control flies that did not receive electric shocks and with "naïve" flies that were not exposed to either increased temperature or electric shocks. Flies without heat-induction expressed mCherry-dTRPA1 in only 15.17 ± 0.64 (mean ± SEM; **Figure 2B**). OPNs and did not show any significant changes in temperature preference compared with control or naïve flies (**Figure 2C** and **Table 2**). Similarly, we did not find a change in the preferred temperature of trained flies that received a 20 min or 1 h induction of expression (**Figures 2D,E** and **Table 2**). However, flies expressing mCherry-dTRPA1 in random subsets of 31.1 ± 1.72 (mean ± SEM; **Figure 2F**) OPNs after a 4 h induction of expression during development showed a significant shift toward lower temperatures when treated with

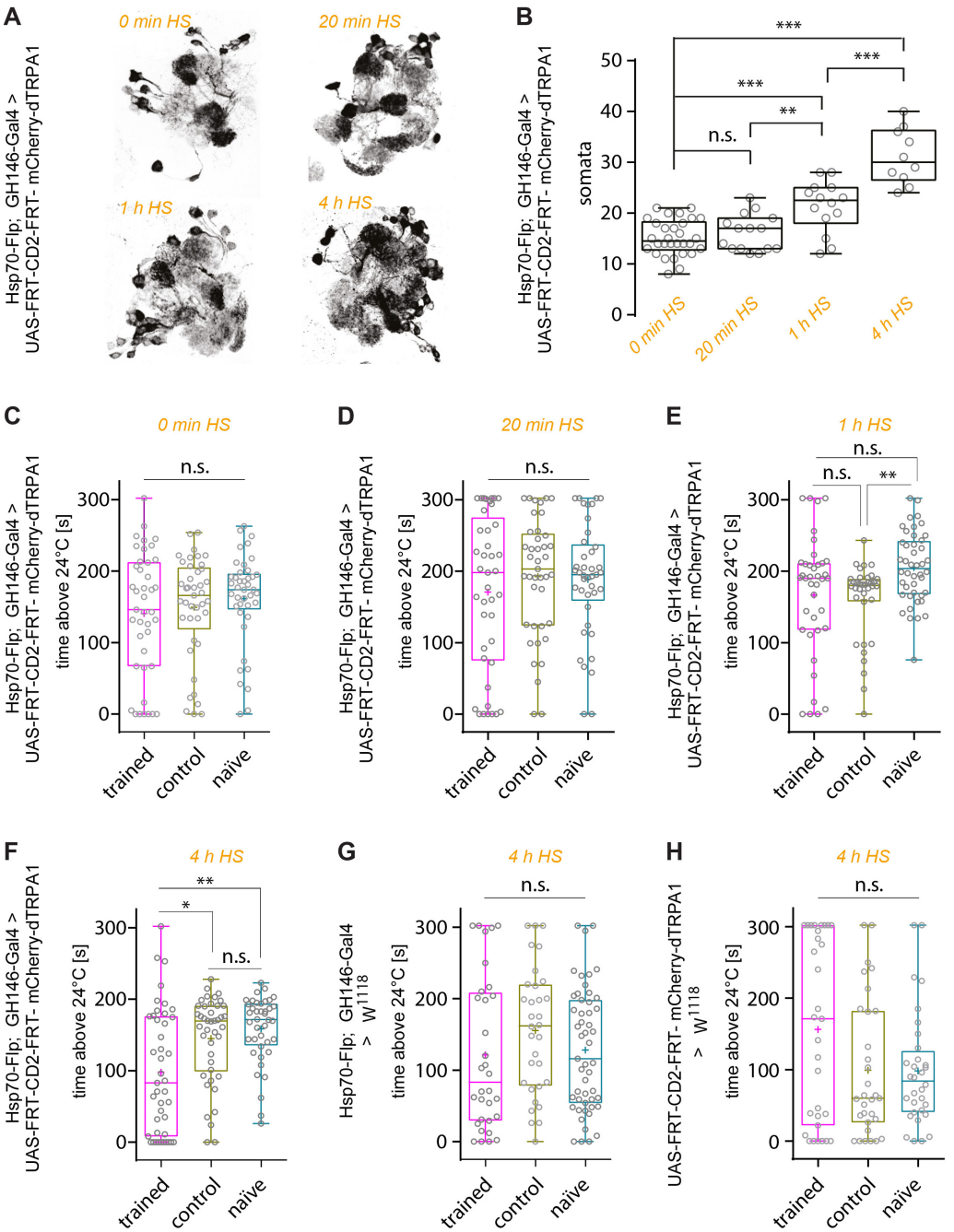

FIGURE 2 | Thermogenetic induction of associative learning. **(A)** Expression of mCherry-dTRPA1 in random ensembles of OPNs in the AL resulting from a 0 min, 20 min, 1 h, and 4 h heat exposure during development. **(B)** Prolonged exposure to heat during development causes mCherry-dTRPA1 expression in an increased number of OPNs expressing mCherry-dTRPA1. **(C–H)** Average time the flies spent >24°C in four different groups of animals expressing mCherry-dTRPA1 in random ensembles of OPNs. Flies that were treated at 30°C with electric shocks ("shock") were compared to flies that were treated similarly but did not receive electric shocks ("control") and to "naïve" flies that did not receive any pre-treatment. The four groups differed in the duration of the heat shock-mediated induction of gene expression and the average number of OPNs expressing mCherry-dTRPA1. No significant differences between the three groups were observed in flies that did not receive any heat shock **(C)** or a 20 min exposure **(D)**. In animals that received a 1 h induction, only naïve individuals showed significantly higher activity than control animals. However, the test group did not differ significantly from control animals. Animals that received a 4 h induction **(F)** of gene expression showed a significant reduction in the mean time spent >24°C during the trial compared to both control and "naïve" flies. Genetic control strains that carried the UAS construct only **(G)** or the flippase and the Gal4 constructs **(H)** did not show differences between the three groups. n.s., $p > 0.05$; *$p < 0.05$; **$p < 0.01$; ***$p < 0.001$. Box plots indicate medians, interquartile ranges, and minimum and maximum values; means are indicated by crosses.

TABLE 1 | Prolonged exposure to heat during development causes mCherry-dTRPA1 expression in an increased number of OPNs expressing mCherry-dTRPA1.

	Heat shock duration	Somata/ hemisphere	*SD*	*n*	Bonferroni corr. one-way ANOVA	Somata/difference between hemispheres	*SD*	Bonferroni corr. one-way ANOVA
Hsp70-Flp; 146-Gal4 >	0 min	15.17	2.749	15		3.267	2.987	$p > 0.05$
USA-FRT-CD2-FRT-	20 min	16.38	3.303	8	vs. 0 min, $p > 0.05$	2.857	1.864	$p > 0.05$
mCherry-dTRPA1	1 h	21.29	4.05	7	vs. 0 min, $p = 0.0027$	5.429	3.309	$p > 0.05$
	4 h	31.1	4.436	5	vs. 0 min, $p < 0.0001$ vs. 20 min, $p < 0.0001$ vs. 1 h, $p = 0.0002$	5.4	4.159	$p > 0.05$

TABLE 2 | Prolonged induction of mCherry-dTRPA1 expression in OPNs significantly reduces the mean time flies > 24°C during the test situation compared to both control and "naïve" flies.

	Heat shock duration	Exp. group	*n*	Mean time [s] >24°C	Lower 95% CI of mean	Upper 95% CI of mean	Kruskal–Wallis test with Dunn's multiple comparsion			Figures
Hsp70-Flp; GH146-Gal4 >	0 min	Trained	40	144.3	116.8	171.7	vs. control	$p > 0.999$	n.s.	**2C**
UAS-FRT-CD2-FRT-		Control	40	153.3	131.3	175.2	vs. naive	$p > 0.999$	n.s.	
mCherry-dTRPA1		Naive	40	165.6	146.3	184.8	vs. trained	$p = 0.8064$	n.s.	
	20 min	Trained	41	170.8	136.1	205.4	vs. control	$p > 0.999$	n.s.	**2D**
		Control	41	192.4	166.0	218.8	vs. naive	$p > 0.999$	n.s.	
		Naive	41	188.7	163.6	213.7	vs. trained	$p > 0.999$	n.s.	
	1 h	Trained	39	166.7	139.3	194.2	vs. control	$p = 0.5091$	n.s.	**2E**
		Control	36	159.8	141.4	178.2	vs. naive	$p = 0.0021$	**	
		Naive	44	205.2	190.2	220.1	vs. trained	$p = 0.1296$	n.s.	
	4 h	Trained	43	97.86	71.12	124.6	vs. control	$p = 0.0189$	*	**2F**
		Control	42	144.9	126.0	163.7	vs. naive	$p > 0.999$	n.s.	
		Naive	40	158.7	143.6	173.7	vs. trained	$p = 0.001$	**	
Hsp70-Flp; GH146-Gal4	4 h	Trained	31	156.3	109.7	203.0	vs. control	$p = 0.3283$	n.s.	**2G**
		Control	31	98.94	63.72	134.1	vs. naive	$p = 0.7226$	n.s.	
		Naive	32	98.03	69.29	126.8	vs. trained	$p > 0.999$	n.s.	
UAS-FRT-CD2-FRT-	4 h	Trained	32	121.3	82.95	159.6	vs. control	$p = 0.3072$	n.s.	**2H**
mCherry-dTRPA1		Control	32	155.3	123.5	187.1	vs. naive	$p = 0.6088$	n.s.	
		Naive	52	128.2	104.3	152.0	vs. trained	$p > 0.999$	n.s.	

*n.s., $p > 0.05$; *$p < 0.05$; **$p < 0.01$; ***$p < 0.001$.*

punitive electric shocks simultaneously with OPN activation (**Figure 2F** and **Table 2**). Genetic controls, i.e., the heterozygous UAS > CD2 > mCherry-dTRPA1 strain and the heterozygous Hsp-70-FLP; GH146-Gal4 strain, that received the same duration of heat shock during development and training did not show any difference in temperature preference after training compared with control and naïve animals (**Figures 2G,H** and **Table 2**). This finding indicates that the animals actively prevented reactivation of the OPNs if the activity of a sufficient number of OPNs was paired with a punishment, i.e., through associative learning. However, this learned avoidance was restricted to the first 5 min within the observation time period. At later time points the temperature avoidance was not different between test and control groups (**Supplementary Figure 1**).

No Correlation Between Activated Number of OPNs and Memory Expression

The identity of OPNs expressing mCherry-dTRPA1 was largely stochastic and differed between the two brain hemispheres. A Runs test for each glomerulus and for each brain hemisphere independently confirmed that for most glomeruli included in the expression pattern of GH146-Gal4 mCherry-dTRPA1 expression occurred stochastically, with the exception of VL2a on theleft hemisphere and VA1ml on both hemispheres. In these two cases expression occurred more often than predicted for complete randomness (**Table 3**). The glomeruli innervated by the OPNs could be identified. We utilized this knowledge to test whether the identity of OPNs and their odor-specific input to the mushroom body has relevance to efficient learning. For example, a more symmetric, and therefore more unambiguous, mushroom body input could potentially be learned more efficiently; the actual number of active OPNs, and therefore the "intensity" of mushroom body input, or the innate behavioral valence of the odor signaled via the activity of distinct OPNs could potentially affect aversive associative learning. Alternatively, the function of the mushroom body might not depend on the actual source of the input. In this case, learning would not be expected to be influenced by the parameters indicated above. To distinguish among these alternatives, the thermogenetic learning experiment

TABLE 3 | Stochastic expression of heat shock induced mCherry-dTRPA1 expression in GH146-Gal4 targeted olfactory projection neurons confirmed by a Runs test for individual glomeruli on each brain hemisphere.

Glomerulus		Left		Right	Glomerulus		Left		Right
VM1	h:0	$p = 0.8929$	h:0	$p = 0.8605$	VM5d	h:0	$p = 0.7057$	h:0	$p = 1$
VM6	h:0	$p = 1$	h:0	$p = 1$	VM5v	h:0	$p = 1$	h:0	$p = 0.6976$
VP2	h:0	$p = 1$	h:0	$p = 1$	VM2	h:0	$p = 0.3264$	h:0	$p = 0.4987$
VP1	h:0	$p = 1$	h:0	$p = 1$	VA2	h:0	$p = 0.1127$	h:0	$p = 0.4064$
VP3	h:0	$p = 1$	h:0	$p = 1$	VA7m	h:0	$p = 0.3306$	h:0	$p = 0.2725$
V	h:0	$p = 1$	h:0	$p = 1$	VA3	h:0	$p = 0.6191$	h:0	$p = 0.5301$
VL1	h:0	$p = 0.5090$	h:0	$p = 0.5090$	VA7l	h:0	$p = 0.6308$	h:0	$p = 1$
VL2p	h:0	$p = 0.2527$	h:0	$p = 0.9194$	VA5	h:0	$p = 0.6526$	h:0	$p = 1$
DP1l	h:0	$p = 1$	h:0	$p = 1$	**VA1ml	h:1	$p = 0.0400$	h:1	$p = 0.0095$
DP1m	h:0	$p = 1$	h:0	$p = 1$	VA1d	h:0	$p = 0.6138$	h:0	$p = 0.7571$
DC4	h:0	$p = 1$	h:0	$p = 1$	DA3	h:0	$p = 0.6808$	h:0	$p = 0.6808$
DM1	h:0	$p = 0.8641$	h:0	$p = 0.3690$	DA4m	h:0	$p = 1$	h:0	$p = 1$
DM4	h:0	$p = 0.0618$	h:0	$p = 0.6013$	DA4l	h:0	$p = 1$	h:0	$p = 0.8928$
VC3m	h:0	$p = 1$	h:0	$p = 0.7057$	VA6	h:0	$p = 0.3732$	h:0	$p = 0.5525$
VC1	h:0	$p = 0.6036$	h:0	$p = 0.7994$	DA2	h:0	$p = 0.4988$	h:0	$p = 0.1956$
VC3l	h:0	$p = 1$	h:0	$p = 1$	DM6	h:0	$p = 0.7047$	h:0	$p = 0.8929$
VM4	h:0	$p = 0.1653$	h:0	$p = 1$	DM5	h:0	$p = 0.0930$	h:0	$p = 0.1800$
* VL2a	h:1	$p = 0.0197$	h:0	$p = 1$	VC2	h:0	$p = 0.9349$	h:0	$p = 0.5642$
DL2v	h:0	$p = 0.7057$	h: 0	$p = 1$	VA4	h:0	$p = 1$	h:0	$p = 0.2251$
DL2d	h:0	$p = 0.3111$	h:0	$p = 1$	DA1	h:0	$p = 0.2725$	h:0	$p = 1$
DL1	h:0	$p = 0.5301$	h:0	$p = 0.105$	DC3	h:0	$p = 0.3111$	h:0	$p = 1$
DL5	h:0	$p = 0.7756$	h:0	$p = 0.5124$	DL3	h:0	$p = 0.4064$	h:0	$p = 0.0991$
DM3	h:0	$p = 0.5383$	h:0	$p = 0.5176$	DL4	h:0	$p = 0.9225$	h:0	$p = 0.4973$
“"1"",	h:0	$p = 1$	h:0	$p = 0.7057$	D	h:0	$p = 0.1786$	h:0	$p = 0.7800$
DM2	h:0	$p = 0.6330$	h:0	$p = 1$	DC1	h:0	$p = 0.3336$	h:0	$p = 0.9347$
VM7	h:0	$p = 1$	h:0	$p = 0.9349$	DC2	h:0	$p = 0.9225$	h:0	$p = 1$
VM3	h:0	$p = 0.8721$	h:0	$p = 0.9614$	(**Figure 4D**) Runs test on contingency of expression pattern with $h = 0$ indicating that the expression values of glomerulus are in random order at the default 5% significance level.				

*n.s., $p > 0.05$; *$p < 0.05$.*

was repeated using 4 h of heat shock during development. Subsequently, the brains of the tested flies were removed from the head capsule, subjected to immunohistochemical staining, and the glomeruli that harbored OPNs expressing mCherry-dTRPA1 were identified. **Figure 3** exemplifies how immunostaining against the active zone protein Bruchpilot (Wagh et al., 2006) was used to identify all glomeruli in comparison with stochastic mCherry fluorescence. It should be noted that some glomeruli were innervated by mCherry-dTRPA1-expressing OPNs symmetrically between the brain hemispheres, which were sometimes visible only in different confocal planes (e.g., glomerulus VC2 in **Figure 3**). A total of 71 flies were analyzed, 26 of which were subjected to the associated training procedure and 45 to control conditions, without electric shocks (**Figure 4A**). Trained animals spent significantly less time at temperatures >24°C (**Figure 4B**). Moreover, this effect was accompanied by an overall reduction in the speed of locomotion (**Figure 4C**). However, no correlation between the actual number of glomeruli innervated by the mCherry-dTRPA1-expressing OPNs and temperature preference or locomotion speed was detected in trained or control animals (**Figures 4D,E**). These data suggest that flies can associate this neuronal signal with an unconditioned stimulus provided that a threshold number of OPNs is reached (**Figure 2F**); learning efficiency as measured by memory expression was not dependent on the actual number of activated OPNs. However, thermogenetic activation of all neurons covered by the GH146-Gal4 line simultaneously with electric shocks did not lead to associative learning (**Supplementary Figure 2**), indicating that there is also an upper limit of how many OPNs can be activated to serve as neuronal correlate of a conditioned stimulus. Alternatively, the fact that the inhibitory anterior paired lateral (APL) neuron, which innervates calyx and lobes of the ipsilateral mushroom body, is included in the expression pattern of GH146-Gal4 (Wilson and Laurent, 2005) might prevent successful associative conditioning in this case. In fact, it has been reported that in aversive associative learning the APL neuron becomes inhibited (Zhou et al., 2019), which is precluded in our case by the thermogenetic activation. However, in those experiments that involved a heat-induced stochastic expression of mCherrydTRPA1- only 2 out of 71 tested flies showed unilateral expression in the APL neuron (**Figure 4A**).

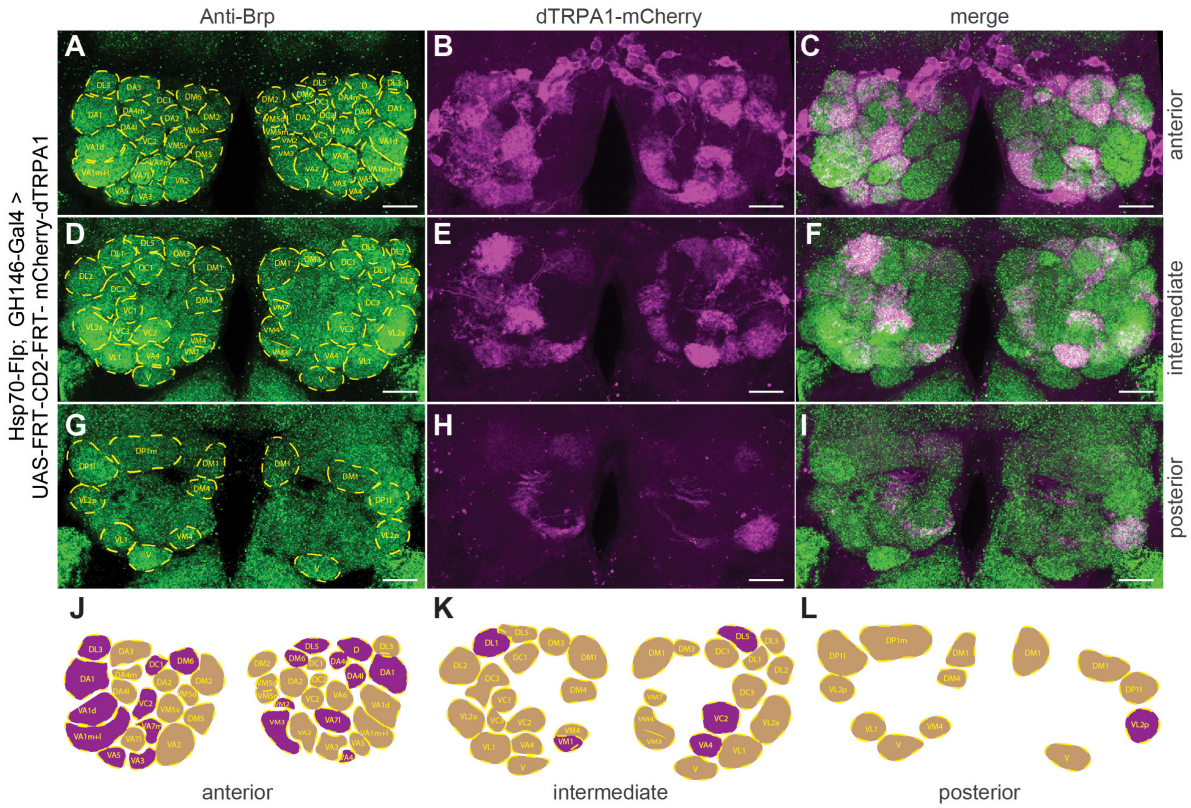

FIGURE 3 | Stochastic OPN expression pattern of mCherry-dTRPA1 in the antennal lobes of one exemplary fly. **(A)** Immunostaining against the pre-synaptic protein Brp (green, left, lower panel) for identification of glomeruli. **(B,E,H)** mCherry-dTRPA1 expression in OPNs in anterior **(A)**, intermediate **(D)**, and posterior **(G)** optical sections across the antennal lobes and the according merged images **(C,F,I)**. Scale bar: 10 μm. **(J–L)** Schematic illustration of olfactory glomeruli expressing mCherry-dTRPA1 (magenta) and remaining glomeruli (beige).

No Correlation Between the Valence Signaled by OPNs and Aversive Associative Learning

Odors can influence diverse behaviors such as feeding or oviposition and can therefore act as attractive or aversive cues. Highly stereotyped connectivity from the olfactory sensory neurons to the OPNs and similar stereotyped olfactory receptor expression has enabled researchers to correlate the activity of distinct neurons with attractive or aversive valence (Semmelhack and Wang, 2009; Knaden et al., 2012), and induce either attraction or aversion via artificial activation of distinct neurons (Bellmann et al., 2010). Knaden et al. (2012) found that the activity of OPNs is more distinctly indicative for the valence of the odor-evoked behavior compared with sensory neuron activity. The OPNs innervating glomeruli DM2, DM4, DM5 responded predominantly to attractive odorants, whereas those innervating glomeruli D, DL1, and DL5 responded to aversive odorants (Knaden et al., 2012). We asked whether aversive associative learning is affected in either direction if OPNs that are activated primarily by attractive or repulsive odorants express mCherry-dTRPA1 within the overall stochastic expression pattern. Glomeruli expressing mCherry-dTRPA1 in the 71 analyzed flies were determined (**Figures 4A**, **5A**). None of the flies showed expression in the OPNs innervating DL2. However, the remaining valence-indicative glomeruli were included in the stochastic expression patterns. No correlation was observed between the number of attraction-mediating or repulsion-mediating glomeruli in either brain hemisphere and the duration of time that the trained animals spent >24°C (**Figures 5B,C**). There was also no correlation between the number of attractive or aversive glomeruli and the locomotion velocity of movement after training (**Figures 5D,E**). Thus, our analysis did not reveal any potential influence of the valence the OPNs signal and the efficiency of aversive associative learning or memory expression. This finding is perhaps not entirely surprising considering how learned information can override naïve information, e.g., through appetitive conditioning using innately aversive odorants.

No Correlation Between Inter-Hemispheric Symmetry of OPN Activity and Aversive Associative Learning

Our data did not indicate that the particular individuality of the OPNs that provide input to the mushroom body skews the efficiency of associative learning in either direction. Rather,

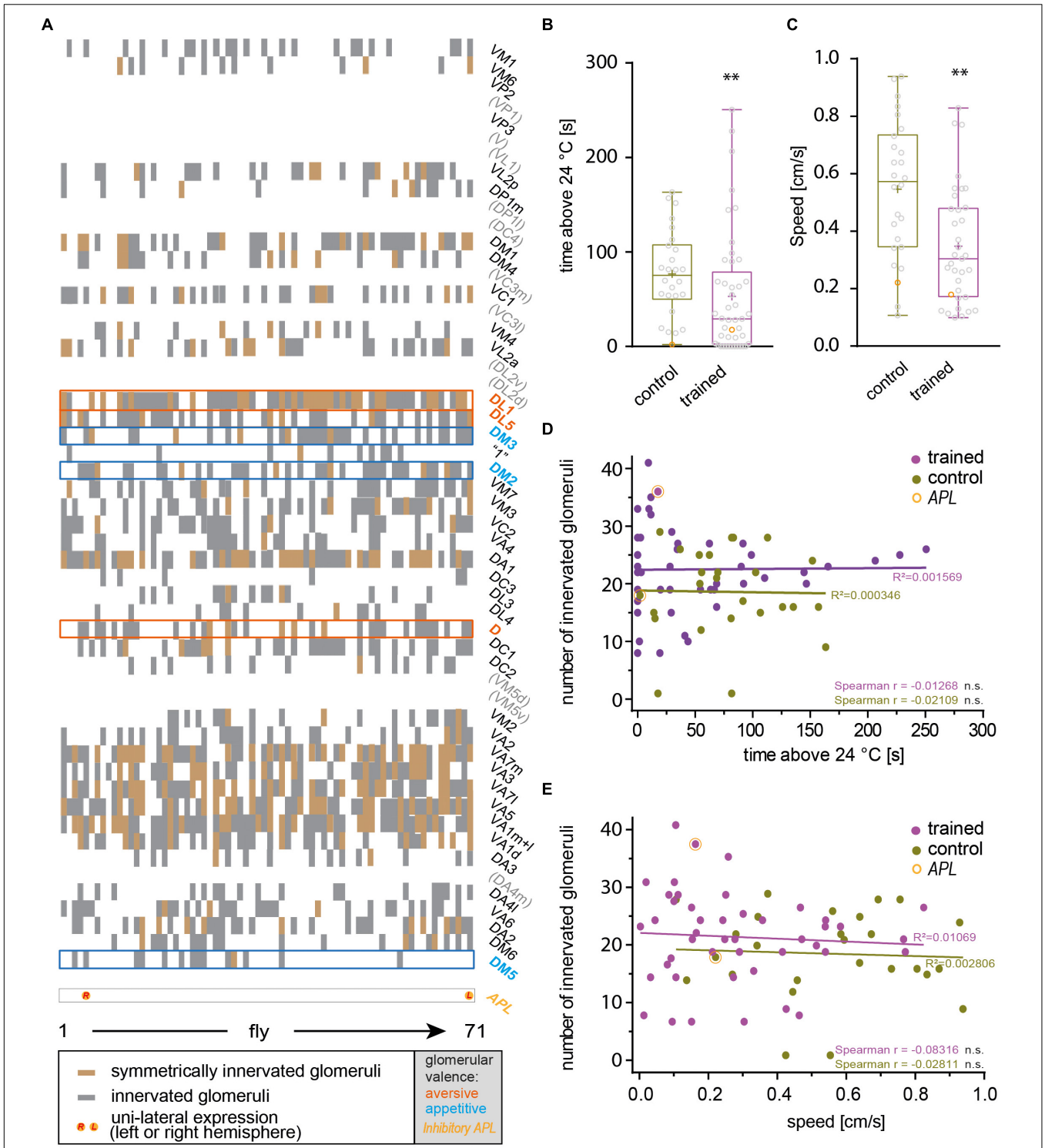

FIGURE 4 | The total number of artificially activated glomeruli does not correlate with learned avoidance. **(A)** Glomeruli innervated by mCherry-dTRPA1-expressing OPNs were determined in 71 individual flies that received a 4 h induction of gene expression during development. In each fly a stochastic population of OPNs showed expression, either symmetrically between the two brain hemispheres or only on one hemisphere. Glomeruli that have been reported to mediate olfactory aversion or attraction are indicated in magenta or cyan, respectively. Twenty-six animals were trained by pairing thermogenetic activation with electric shocks, 45 animals served as controls and did not receive electric shocks. Flies showed a reduction in the time spent >24°C **(B)** and in locomotion speed **(C)** when data from all animals, irrespective of the valence the glomeruli innervated by mCherry-dTRPA1-expressing OPNs mediate, were taken into account. **(D,E)** The total number of innervated glomeruli did not correlate significantly (Spearman *R*: n.s.) with the locomotion speed or the time spent >24°C. Lines indicate calculated linear correlations with coefficients (R^2) indicated (see **Table 4** for details). n.s., $p > 0.05$; $^{**}p < 0.01$.

TABLE 4 | Correlations between innervation characteristics, and time spent > 24°C and speed in control and trained animals.

Correlation	Exp. group	R^2	Spearman *r*	*p*-value		Figures
Number of innervated glomeruli vs. time > 24°C (s)	Trained	0.0001569	−0.01268	0.9341	n.s.	**4D**
	Control	0.000346	−0.02109	0.9186	n.s.	
Number of innervated glomeruli vs. speed (cm/s)	Trained	0.01069	−0.08316	0.5940	n.s.	**4E**
	Control	0.002806	−0.02811	0.8916	n.s.	
Number of innervated app. glomeruli vs. time > 24°C (s)	Trained	0.002525	−0.05034	0.7397	n.s.	**5B**
	Control	0.1036	0.3127	0.0814	n.s.	
Number of innervated avers. glomeruli vs. time > 24°C (s)	Trained	$3.631 * e^{-005}$	−0.1277	0.3975	n.s.	**5C**
	Control	0.003145	0.06007	0.7440	n.s.	
Number of innervated app. glomeruli vs. speed (cm/s)	Trained	0.0002323	0.02763	0.8554	n.s.	**5D**
	Control	0.046	0.2016	0.2686	n.s.	
Number of innervated avers. glomeruli vs. speed (cm/s)	Trained	0.01958	−0.0819	0.5885	n.s.	**5E**
	Control	0.006542	−0.07814	0.6708	n.s.	
Symmetry vs. time > 24°C (cm/s)	Trained	0.002375	−0.02268	0.8824	n.s.	**6A**
	Control	0.02534	0.1566	0.4450	n.s.	
Symmetry vs. speed (cm/s)	Trained	0.00363	0.1006	0.5107	n.s.	**6B**
	Control	0.01826	0.1528	0.4562	n.s.	

it appeared that the mushroom body did not take the actual identity of OPN input into account. If so, the efficiency of associative learning should also be independent of whether OPNs are symmetrically activated between brain hemispheres or not. To test this hypothesis, we calculated a symmetry index (see the section "Materials and Methods") that quantified the degree of inter-hemispheric symmetry between identified glomeruli innervated by mCherry-dTRPA1-expressing OPNs. Indeed, no correlation between the symmetry index and the time the flies spent >24°C or their locomotion speed was detected in either trained animals or controls (**Figures 6A,B**). This result suggests that learned avoidance behavior is independent of the degree of inter-hemispheric symmetry of glomerular activity.

DISCUSSION

The neuronal circuits that control an animal's behavior are often highly stereotyped between individuals. Evolution has optimized these circuits to fulfil the requirements imposed by the ecology and life history of the species. For example, *Drosophila* has evolved mechanisms to detect the nutritious, fermenting fruits of particular plants and to be attracted to them. Similarly, mechanisms have evolved to avoid harmful substances. Thus, stereotyped gene expression and neuronal circuit wiring reflect innate ecological and behavioral programs. This is also reflected in stereotyped chemotopic maps, observable in the antennal lobes (Fiala et al., 2002; Wang et al., 2003), that result from fixed olfactory-receptor expression and hard-wired neuronal connectivity (Vosshall et al., 2000; Couto et al., 2005; Fishilevich and Vosshall, 2005). Such hard-wired and stereotyped connectivity is also found at higher-order brain regions, such as in the projection areas of OPNs in the lateral horn (Marin et al., 2002; Wong et al., 2002; Tanaka et al., 2004) or intrinsic lateral horn neurons (Strutz et al., 2014; Jeanne et al., 2018; Frechter et al., 2019). The innate behavioral valence of odorants is more reliably and distinctly represented by the combinatorial activity pattern of second-order OPNs compared with first-order olfactory sensory neurons (Knaden et al., 2012). This is in line with the stronger categorization of combinatorial odor representations in OPNs compared with those in sensory neurons (Niewalda et al., 2011). Interestingly, representation of the innate valence of an odor is segregated in different partitions of the lateral horn (Strutz et al., 2014; Seki et al., 2017), indicating that this hard-wired connectivity extends beyond the sensory periphery to the behavior-instructing neuropils.

By contrast, learning is a mechanism that allows organisms to deal with environmental unpredictability. As a human commensal (Keller, 2007), fruit flies have to adapt to environments that differ from their ancestral African habitat (Mansourian et al., 2018). Therefore, the ability to learn appears essential for their survival. The well-documented random, variable, non-stereotyped connectivity between OPNs and Kenyon cells at the calyx of the mushroom body (Murthy et al., 2008; Caron et al., 2013) is thought to reflect this environmental unpredictability (e.g., Luo et al., 2010), despite some degree of spatially determined projections of OPN axons in the calyx (Lin et al., 2007; Christiansen et al., 2011). Key factors that distinguish the mushroom bodies from other neuropils, like the lateral horn, include a relatively high number of uniform intrinsic neurons (Kenyon cells) that lack apparent individual genetic identities, and the highly selective responsiveness of a very few of those Kenyon cells (∼5%) out of a large number (∼2000) (Honegger et al., 2011; Gruntman and Turner, 2013) (sparse code). The principle of randomly generated, sparsely distributed neuronal activity as a favorable memory store was formally described in 1988 (Kanerva, 1988), and in a diversity of neuronal circuits this principle has been found to be implemented, including the cerebellum, the piriform cortex, and the mushroom body (Babadi and Sompolinsky, 2014; Litwin-Kumar et al., 2017). This suggests that the exact identity of the neurons that

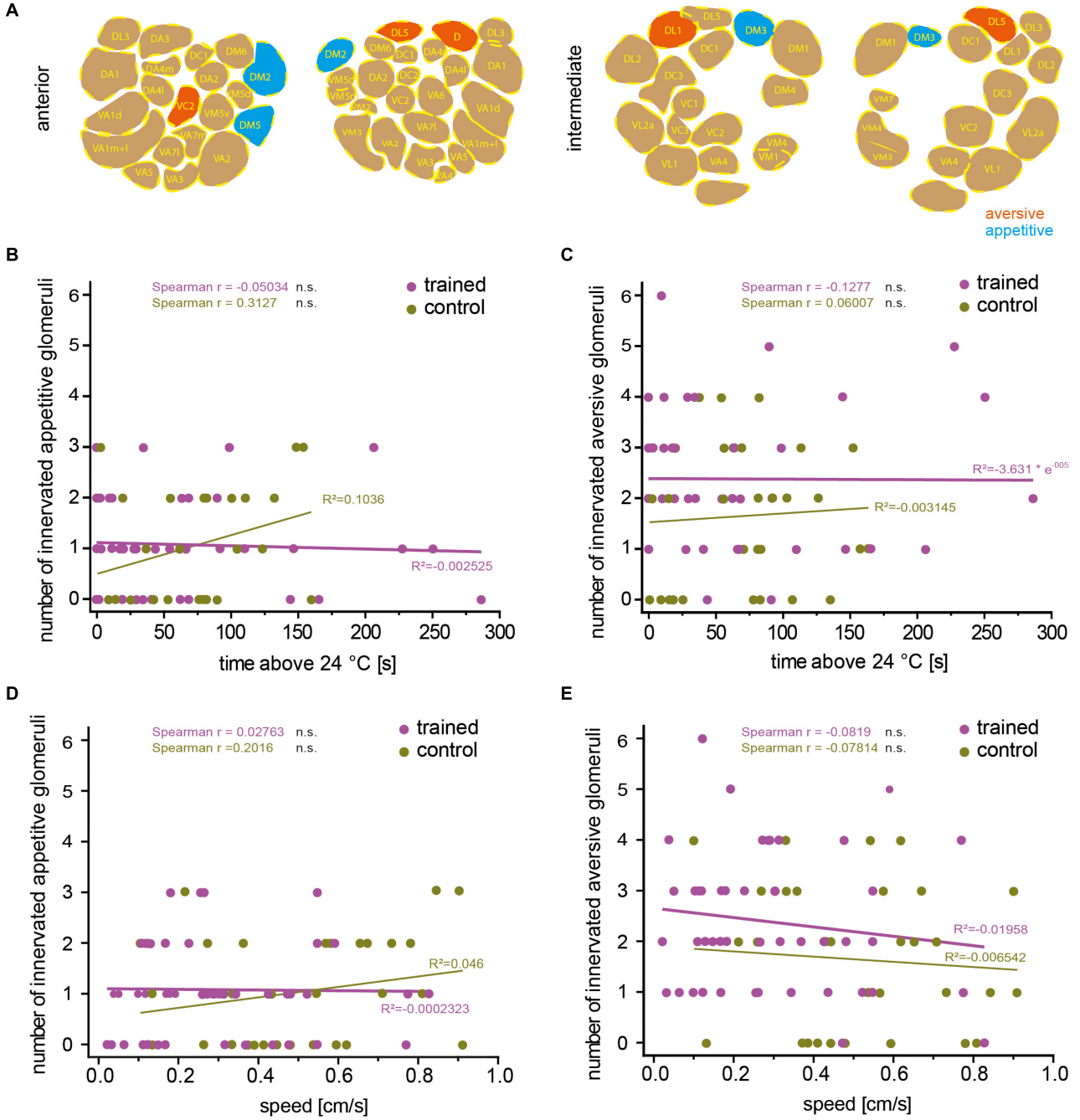

FIGURE 5 | The number of attraction- or aversion-mediating glomeruli does not correlate with learned avoidance. **(A)** Example of one brain showing stochastic mCherry-dTRPA1 expression in attraction (green) or aversion-mediating (magenta) glomeruli in a symmetric or non-symmetric manner. The number of "appetitive" **(B)** or "aversive" **(C)** glomeruli did not correlate significantly (Spearman *R*: n.s.) with the time the trained animals spent >24°C, and **(D,E)** did not correlate significantly (Spearman *R*: n.s.) with the animals' locomotion speed. Lines are calculated linear correlations with coefficients (R^2) indicated (see **Table 4** for details).

encode a learned stimulus is irrelevant for the functionality of the circuit. Indeed, arbitrarily activated, stochastic patterns of piriform cortex cells can be learned by mice as being either aversive or attractive (Choi et al., 2011). Similarly, *Drosophila* can learn to behaviorally avoid activation of a stochastic, arbitrary pattern of Kenyon cell activity that has been temporally paired with a punishing electric shock (Vasmer et al., 2014). However, this suggests that the exact circuit input itself is not a deterministic factor for the Kenyon cells to be used as a learnable pattern. Rather, Kenyon cells can use any input pattern as template to be associated with a rewarding or punishing stimulus. This does not necessarily implicate that the sensory input of the

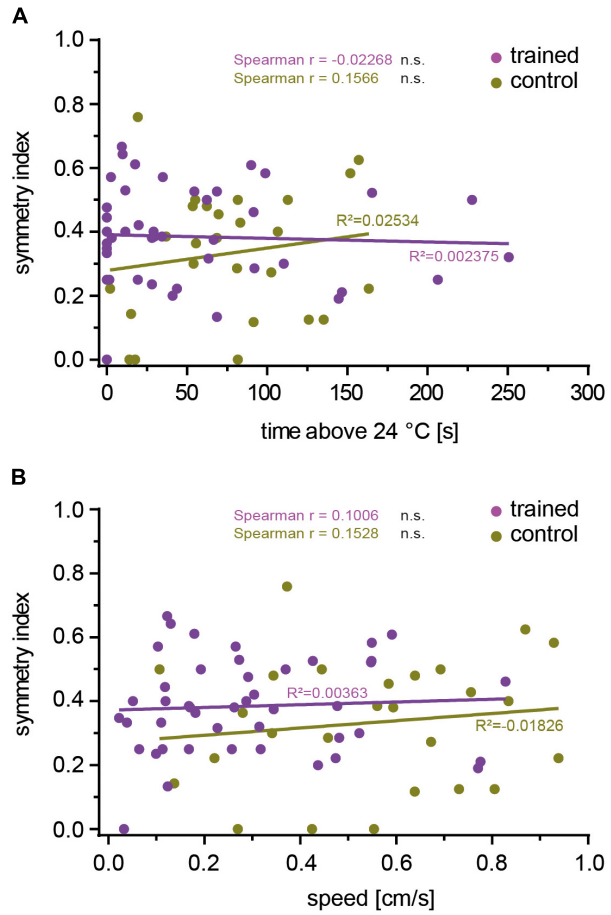

FIGURE 6 | The inter-hemispheric symmetry between glomeruli innervated by mCherry-dTRPA1 does not affect learning. The degree of symmetry, as determined by a symmetry index (see the section "Materials and Methods"), was not significantly (Spearman *R*: n.s.) correlated with the time the flies spent >24°C after learning **(A)** or locomotion speed **(B)**, either after associative training or under control conditions (see **Table 4** for details).

insect mushroom body is anatomically or functionally chaotic. In fact, input into the calyces of mushroom bodies are often highly structured and segregated according to the sensory modality they convey. However, the mushroom body can learn any input pattern, irrespective of the exact identity of the OPNs, the exact odor and the odor valence it signals, or the symmetry between the two hemispheres. The data presented here are consistent with this idea.

The animals' learning-dependent avoidance to reactivate OPNs was observed only within the first 5 min of the test situation, and not at later time points. This time-dependent decrease in learned avoidance might perhaps be due to an intrinsic adaptation of OPNs to continuous excitation (Cafaro, 2016; discussion in: Martelli and Fiala, 2019). This is in contrast to the slowly developing occurrence of learned avoidance thermogenetically induced in Kenyon cells (Vasmer et al., 2014), pointing toward different physiological properties of these cells. It must also be noted that when the animals move along the test arena to temperatures >25°C, excitation of OPNs expressing mCherry-dTRPA1 is likely to increase in dependence of the ambient temperature. However, this potential change in excitation does probably not resemble changes in real odor concentration, because the identity of excited OPNs is determined by the expression of mCherry-*d*TRPA1. These potential variations in excitation do likely not result in different combinatorial activities of OPNs or a recruitment of active glomeruli, as it is the case for increasing odor concentrations (Wang et al., 2003). It might be interesting to see in the future whether the principle of using stochastic input patterns into the mushroom body to override innate behavioral tendencies through learning is also true for appetitive conditioning using sugar reward as unconditioned stimulus.

It should be noted that most of the animals tested in this study showed expression of the thermogenetic actuator mCherry-dTRPA1 in both aversive and attractive glomeruli. The net effect of the combined activity of both remains unclear. Moreover, the probability of achieving expression in a large proportion of symmetric glomeruli between the hemispheres is low, leaving open the possibility that an exact symmetric activation between the hemispheres might have a more profound effect on learnability. However, we can conclude that the animals have the ability to learn stochastic and arbitrarily activated ensembles of OPN activity and to subsequently avoid their re-activation. When a real odor stimulus is learned, the innate valence represented by the combinatorial OPN pattern and signaled to the lateral horn (Strutz et al., 2014) has to be integrated with the learned information to induce an appropriate behavior. This cross-talk between the mushroom body and the lateral horn has been characterized (Dolan et al., 2018).

In other insects with more elaborate mushroom bodies and often much more complex behavior, such as eusocial hymenoptera (e.g., honey bees or ants), butterflies, or cockroaches, large parts of the mushroom body calyces receive not only olfactory, but also massive multimodal, visual, and mechanosensory input (Mobbs, 1982; Gronenberg and Hölldobler, 1999; Strausfeld and Li, 1999; Gronenberg, 2001; Ehmer and Gronenberg, 2002; Strausfeld, 2002; Paulk and Gronenberg, 2008; Kinoshita et al., 2015). Anatomically, the different sensory input fibers targeting the calyces are not randomly organized, but show a high degree of orderly structure. The less-complex mushroom body of *Drosophila* is dominated by olfactory input; however, afferent sensory fibers providing information about temperature (Frank et al., 2015) or visual input (Vogt et al., 2016; Yagi et al., 2016) also exist. It might be interesting to investigate in the future whether also for the representation of sensory modalities other than olfactory ones and also in insects with more complex mushroom bodies the diverse "input patterns" are integrated by Kenyon cells in a stochastic manner or, alternatively, whether in these cases exact topographical representations (e.g., retinotopic activity patterns) or stereotypic labeled lines are of importance for the behavioral functions of mushroom bodies, such as associative learning.

DATA AVAILABILITY STATEMENT

The raw data supporting the conclusions of this article will be made available by the authors, without undue reservation, to any qualified researcher.

AUTHOR CONTRIBUTIONS

AF conceived the project and wrote the manuscript. AF and TR supervised the work. TR, CW, and PF performed the experiments and analyzed the data.

FUNDING

This work was supported by the German Research Foundation through the Collaborative Research Center SFB 889/B4 "Mechanisms of Sensory Processing" to AF and the Research Unit for 2705 "Dissection of a Brain Circuit: Structure, Plasticity and Behavioral Function of the *Drosophila* Mushroom Body" to AF. We acknowledge the support by the Open Access Publication Funds of the University of Göttingen.

ACKNOWLEDGMENTS

We are grateful to Tobias Mühmer and Jan Hoffman for constructing the technical devices used in this study. We would like to thank Sandor Kovacs for help on statistical analysis and Annekathrin Widmann for helpful discussions on the manuscript.

SUPPLEMENTARY MATERIAL

The Supplementary Material for this article can be found online at: https://www.frontiersin.org/articles/10.3389/fphys.2020.00053/full#supplementary-material

REFERENCES

Aso, Y., Grübel, K., Busch, S., Friedrich, A. B., Siwanowicz, I., and Tanimoto, H. (2009). The mushroom body of adult *Drosophila* characterized by GAL4 drivers. *J. Neurogenet.* 23, 156–172. doi: 10.1080/01677060802471718

Aso, Y., Hattori, D., Yu, Y., Johnston, R. M., Iyer, N. A., Ngo, T. T., et al. (2014a). The neuronal architecture of the mushroom body provides a logic for associative learning. *eLife* 3:e04577. doi: 10.7554/eLife.04577

Aso, Y., Sitaraman, D., Ichinose, T., Kaun, K. R., Vogt, K., Belliart-Guérin, G., et al. (2014b). Mushroom body output neurons encode valence and guide memory-based action selection in *Drosophila*. *eLife* 3:e04580. doi: 10.7554/eLife.04580

Babadi, B., and Sompolinsky, H. (2014). Sparseness and expansion in sensory representations. *Neuron* 83, 1213–1226. doi: 10.1016/j.neuron.2014.07.035

Basler, K., and Struhl, G. (1994). Compartment boundaries and the control of *Drosophila* limb pattern by hedgehog protein. *Nature* 368, 208–214. doi: 10.1038/368208a0

Bellmann, D., Richardt, A., Freyberger, R., Nuwal, N., Schwärzel, M., Fiala, A., et al. (2010). Optogenetically induced olfactory stimulation in *Drosophila* larvae reveals the neuronal basis of odor-aversion behavior. *Front. Behav. Neurosci.* 4:27. doi: 10.3389/fnbeh.2010.00027

Cafaro, J. (2016). Multiple sites of adaptation lead to contrast encoding in the *Drosophila* olfactory system. *Physiol. Rep.* 4:e12762. doi: 10.14814/phy2.12762

Caron, S. J., Ruta, V., Abbott, L. F., and Axel, R. (2013). Random convergence of olfactory inputs in the *Drosophila* mushroom body. *Nature* 497, 113–117. doi: 10.1038/nature12063

Choi, G. B., Stettler, D. D., Kallman, B. R., Bhaskar, S. T., Fleischmann, A., and Axel, R. (2011). Driving opposing behaviors with ensembles of piriform neurons. *Cell* 146, 1004–1015. doi: 10.1016/j.cell.2011.07.041

Christiansen, F., Zube, C., Andlauer, T. F., Wichmann, C., Fouquet, W., Owald, D., et al. (2011). Presynapses in Kenyon cell dendrites in the mushroom body calyx of Drosophila. *J. Neurosci.* 31, 9696–9707. doi: 10.1523/JNEUROSCI.6542-10.2011

Connolly, J. B., Roberts, I. J., Armstrong, J. D., Kaiser, K., Forte, M., Tully, T., et al. (1996). Associative learning disrupted by impaired Gs signaling in *Drosophila* mushroom bodies. *Science* 274, 2104–2107. doi: 10.1126/science.274.5295.2104

Couto, A., Alenius, M., and Dickson, B. J. (2005). Molecular, anatomical, and functional organization of the *Drosophila* olfactory system. *Curr. Biol.* 15, 1535–1547. doi: 10.1016/j.cub.2005.07.034

Datta, S. R., Vasconcelos, M. L., Ruta, V., Luo, S., Wong, A., Demir, E., et al. (2008). The *Drosophila* pheromone cVA activates a sexually dimorphic neural circuit. *Nature* 452, 473–477. doi: 10.1038/nature06808

de Belle, J. S., and Heisenberg, M. (1994). Associative odor learning in *Drosophila* abolished by chemical ablation of mushroom bodies. *Science* 263, 692–695. doi: 10.1126/science.8303280

Dolan, M. J., Belliart-Guérin, G., Bates, A. S., Frechter, S., Lampin-Saint-Amaux, A., Aso, Y., et al. (2018). Communication from learned to innate olfactory processing centers is required for memory retrieval in *Drosophila*. *Neuron* 100, 651–668. doi: 10.1016/j.neuron.2018.08.037

Dubnau, J., Grady, L., Kitamoto, T., and Tully, T. (2001). Disruption of neurotransmission in *Drosophila* mushroom body blocks retrieval but not acquisition of memory. *Nature* 411, 476–480. doi: 10.1038/35078077

Dweck, H. K., Ebrahim, S. A., Kromann, S., Bown, D., Hillbur, Y., Sachse, S., et al. (2015). Olfactory preference for egg laying on citrus substrates in *Drosophila*. *Curr. Biol.* 23, 2472–2480. doi: 10.1016/j.cub.2013.10.047

Ehmer, B., and Gronenberg, W. (2002). Segregation of visual input to the mushroom bodies in the honeybee (Apis mellifera). *J. Comp. Neurol.* 451, 362–373. doi: 10.1002/cne.10355

Estes, P. S., Roos, J., van der Bliek, A., Kelly, R. B., Krishnan, K. S., and Ramaswami, M. (1996). Traffic of dynamin within individual *Drosophila* synaptic boutons relative to compartment-specific markers. *J. Neurosci.* 16, 5443–5456. doi: 10.1523/JNEUROSCI.16-17-05443.1996

Fiala, A., Spall, T., Diegelmann, S., Eisermann, B., Sachse, S., Devaud, J. M., et al. (2002). Genetically expressed cameleon in *Drosophila melanogaster* is used to visualize olfactory information in projection neurons. *Curr. Biol.* 12, 1877–1884. doi: 10.1016/S0960-9822(02)01239-3

Fishilevich, E., and Vosshall, L. B. (2005). Genetic and functional subdivision of the *Drosophila* antennal lobe. *Curr. Biol.* 15, 1548–1553. doi: 10.1016/j.cub.2005.07.066

Frank, D. D., Jouandet, G. C., Kearney, P. J., Macpherson, L. J., and Gallio, M. (2015). Temperature representation in the *Drosophila* brain. *Nature* 519, 358–361. doi: 10.1038/nature14284

Frechter, S., Bates, A. S., Tootoonian, S., Dolan, M. J., Manton, J., Jamasb, A. R., et al. (2019). Functional and anatomical specificity in a higher olfactory centre. *eLife* 8:e44590. doi: 10.7554/eLife.44590

Grabe, V., and Sachse, S. (2018). Fundamental principles of the olfactory code. *Biosystems* 164, 94–101. doi: 10.1016/j.biosystems.2017.10.010

Gronenberg, W. (2001). Subdivisions of hymenopteran mushroom body calyces by their afferent supply. *J. Comp. Neurol.* 435, 474–489. doi: 10.1002/cne.1045

Gronenberg, W., and Hölldobler, B. (1999). Morphologic representation of visual and antennal information in the ant brain. *J. Comp. Neurol.* 412, 229–240. doi: 10.1002/(sici)1096-9861(19990920)412:2<229::aid-cne4>3.0.co;2-e

Gruntman, E., and Turner, G. C. (2013). Integration of the olfactory code across dendritic claws of single mushroom body neurons. *Nat. Neurosci.* 16, 1821–1829. doi: 10.1038/nn.3547

Hamada, F. N., Rosenzweig, M., Kang, K., Pulver, S. R., Ghezzi, A., Jegla, T. J., et al. (2008). An internal thermal sensor controlling temperature preference in *Drosophila*. *Nature* 454, 217–220. doi: 10.1038/nature07001

Heisenberg, M. (2003). Mushroom body memoir: from maps to models. *Nat. Rev. Neurosci.* 4, 266–275. doi: 10.1038/nrn1074

Heisenberg, M., Borst, A., Wagner, S., and Byers, D. (1985). *Drosophila* mushroom body mutants are deficient in olfactory learning. *J. Neurogenet.* 2, 1–30. doi: 10.3109/01677068509100140

Honegger, K. S., Campbell, R. A., and Turner, G. C. (2011). Cellular-resolution population imaging reveals robust sparse coding in the *Drosophila* mushroom body. *J. Neurosci.* 31, 11772–11785. doi: 10.1523/JNEUROSCI.1099-11.2011

Jeanne, J. M., Fişek, M., and Wilson, R. I. (2018). The organization of projections from olfactory glomeruli onto higher-order neurons. *Neuron* 98, 1198–1213.e8. doi: 10.1016/j.neuron.2018.05.011

Jefferis, G. S., Potter, C. J., Chan, A. M., Marin, E. C., Rohlfing, T., Maurer, C. R. Jr., et al. (2007). Comprehensive maps of Drosophila higher olfactory centers: spatially segregated fruit and pheromone representation. *Cell* 128, 1187–1203. doi: 10.1016/j.cell.2007.01.040

Kanerva, P. (1988). *Sparse Distributed Memory*. Cambridge, MA: The MIT Press.

Keller, A. (2007). *Drosophila melanogaster's* history as a human commensal. *Curr. Biol.* 17, 77–81. doi: 10.1016/j.cub.2006.12.031

Kinoshita, M., Shimohigasshi, M., Tominaga, Y., Arikawa, K., and Homberg, U. (2015). Topographically distinct visual and olfactory inputs to the mushroom body in the Swallowtail butterfly, *Papilio xuthus*. *J. Comp. Neurol.* 521, 162–182. doi: 10.1002/cne.23674

Knaden, M., Strutz, A., Ahsan, J., Sachse, S., and Hansson, B. S. (2012). Spatial representation of odorant valence in an insect brain. *Cell Rep.* 1, 392–399. doi: 10.1016/j.celrep.2012.03.002

Li, H., Horns, F., Wu, B., Xie, Q., Li, J., Li, T., et al. (2017). Classifying *Drosophila* olfactory projection neuron subtypes by single-cell RNA sequencing. *Cell* 171, 1206–1220. doi: 10.1016/j.cell.2017.10.019

Lin, H. H., Lai, J. S., Chin, A. L., Chen, Y. C., and Chiang, A. S. (2007). A map of olfactory representation in the *Drosophila* mushroom body. *Cell* 128, 1205–1217. doi: 10.1016/j.cell.2007.03.006

Litwin-Kumar, A., Harris, K. D., Axel, R., Sompolinsky, H., and Abbott, L. F. (2017). Optimal degrees of synaptic connectivity. *Neuron* 93, 1153–1164. doi: 10.1016/j.neuron.2017.01.030

Luo, S. X., Axel, R., and Abbott, L. F. (2010). Generating sparse and selective third-order responses in the olfactory system of the fly. *Proc. Natl. Acad. Sci. U.S.A.* 107, 10713–10718. doi: 10.1073/pnas.1005635107

Mansourian, S., Enjin, A., Jirle, E. V., Ramesh, V., Rehermann, G., Becher, P. G., et al. (2018). Wild African *Drosophila melanogaster* are seasonal specialists on marula fruit. *Curr. Biol.* 28, 3960–3968. doi: 10.1016/j.cub.2018.10.033

Marin, E. C., Jefferis, G. S., Komiyama, T., Zhu, H., and Luo, L. (2002). Representation of the glomerular olfactory map in the *Drosophila* brain. *Cell* 109, 243–255. doi: 10.1016/s0092-8674(02)00700-6

Martelli, C., and Fiala, A. (2019). Slow presynaptic mechanisms that mediate adaptation in the olfactory pathway of *Drosophila*. *eLife* 8:e43735. doi: 10.7554/eLife.43735

McGuire, S. E., Le, P. T., and Davis, R. L. (2001). The role of *Drosophila* mushroom body signaling in olfactory memory. *Science* 293, 1330–1333. doi: 10.1126/science.1062622

Meinertzhagen, I. A., and Lee, C.-H. (2012). The genetic analysis of functional connectomics in *Drosophila*. *Adv. Genet.* 80, 99–151. doi: 10.1016/B978-0-12-404742-6.00003-X

Mobbs, P. G. (1982). The brain of the honeybee *Apis mellifera*. I. The connections and spatial organization of the mushroom bodies. *Phil. Trans. B* 298, 309–354. doi: 10.1098/rstb.1982.0086

Murthy, M., Fiete, I., and Laurent, G. (2008). Testing odor response stereotypy in the *Drosophila* mushroom body. *Neuron* 59, 1009–1023. doi: 10.1016/j.neuron.2008.07.040

Niewalda, T., Völler, T., Eschbach, C., Ehmer, J., Chou, W. C., Timme, M., et al. (2011). A combined perceptual, physico-chemical, and imaging approach to 'odour-distances' suggests a categorizing function of the *Drosophila* antennal lobe. *PLoS One* 6:e24300. doi: 10.1371/journal.pone.0024300

Paulk, A. C., and Gronenberg, W. (2008). Higher order visual input to the mushroom bodies in the bee, Bombus impatiens. *Arthropod. Struct. Dev.* 37, 443–458. doi: 10.1016/j.asd.2008.03.002

Pooryasin, A., and Fiala, A. (2015). Identified serotonin-releasing neurons induce behavioral quiescence and suppress mating in *Drosophila*. *J. Neurosci.* 35, 12792–12812. doi: 10.1523/JNEUROSCI.1638-15.2015

Qin, H., Cressy, M., Li, W., Coravos, J. S., Izzi, S. A., and Dubnau, J. (2012). Gamma neurons mediate dopaminergic input during aversive olfactory memory formation in *Drosophila*. *Curr. Biol.* 22, 608–614. doi: 10.1016/j.cub.2012.02.014

Rodrigues, V., and Buchner, E. (1984). [3H]2-deoxyglucose mapping of odor-induced neuronal activity in the antennal lobes of *Drosophila melanogaster*. *Brain Res.* 324, 374–378. doi: 10.1016/0006-8993(84)90053-2

Sayeed, O., and Benzer, S. (1996). Behavioral genetics of thermosensation and hygrosensation in *Drosophila*. *Proc. Natl. Acad. Sci. U.S.A.* 93, 6079–6084. doi: 10.1073/pnas.93.12.6079

Seki, Y., Dweck, H. K. M., Rybak, J., Wicher, D., Sachse, S., and Hansson, B. S. (2017). Olfactory coding from the periphery to higher brain centers in the *Drosophila* brain. *BMC Biol.* 15:56. doi: 10.1186/s12915-017-0389-z

Semmelhack, J. L., and Wang, J. W. (2009). Select *Drosophila* glomeruli mediate innate olfactory attraction and aversion. *Nature* 459, 218–223. doi: 10.1038/nature07983

Stensmyr, M. C., Dweck, H. K. M., Farhan, A., Ibba, I., Strutz, A., Mukunda, L., et al. (2012). A conserved dedicated olfactory circuit for detecting harmful microbes in *Drosophila*. *Cell* 151, 1345–1357. doi: 10.1016/j.cell.2012.09.046

Stocker, R. F., Heimbeck, G., Gendre, N., and de Belle, J. S. (1997). Neuroblast ablation in *Drosophila* P[GAL4] lines reveals origins of olfactory interneurons. *J. Neurobiol.* 32, 443–456.

Strausfeld, N. J. (2002). Organization of the honey bee mushroom body: representation of the calyx within the vertical and gamma lobes. *J. Comp. Neurol.* 450, 4–33. doi: 10.1002/cne.10285

Strausfeld, N. J., and Li, Y. (1999). Organization of olfactory and multimodal afferent neurons supplying the calyx and pedunculus of the cockroach mushroom bodies. *J. Comp. Neurol.* 409, 603–625.

Strutz, A., Soelter, J., Baschwitz, A., Farhan, A., Grabe, V., Rybak, J., et al. (2014). Decoding odor quality and intensity in the *Drosophila* brain. *eLife* 3:e04147. doi: 10.7554/eLife.04147

Suh, G. S., Ben-Tabou de Leon, S., Tanimoto, H., Fiala, A., Benzer, S., and Anderson, D. J. (2007). Light activation of an innate olfactory avoidance response in *Drosophila*. *Curr. Biol.* 17, 905–908. doi: 10.1016/j.cub.2007.04.046

Tanaka, N. K., Awasaki, T., Shimada, T., and Ito, K. (2004). Integration of chemosensory pathways in the *Drosophila* second-order olfactory centers. *Curr. Biol.* 14, 449–457. doi: 10.1016/j.cub.2004.03.006

Tang, X., Platt, M. D., Lagnese, C. M., Leslie, J. R., and Hamada, F. N. (2013). Temperature integration at the AC thermosensory neurons in *Drosophila*. *J. Neurosci.* 33, 894–901. doi: 10.1523/JNEUROSCI.1894-12.2013

Tempel, B. L., Bonini, N., Dawson, D. R., and Quinn, W. G. (1983). Reward learning in normal and mutant *Drosophila*. *Proc. Natl. Acad. Sci. U.S.A.* 80, 1482–1486. doi: 10.1073/pnas.80.5.1482

Tully, T., and Quinn, W. G. (1985). Classical conditioning and retention in normal and mutant *Drosophila melanogaster*. *J. Comp. Physiol. A.* 157, 263–277. doi: 10.1007/BF01350033

van der Goes van Naters, W., and Carlson, J. R. (2007). Receptors and neurons for fly odors in *Drosophila*. *Curr. Biol.* 17, 606–612. doi: 10.1016/j.cub.2007.02.043

Vasmer, D., Pooryasin, A., Riemensperger, T., and Fiala, A. (2014). Induction of aversive learning through thermogenetic activation of Kenyon cell ensembles in *Drosophila*. *Front. Behav. Neurosci.* 8:174. doi: 10.3389/fnbeh.2014.00174

Venken, K. J., Simpson, J. H., and Bellen, H. J. (2011). Genetic manipulation of genes and cells in the nervous system of the fruit fly. *Neuron* 72, 202–230. doi: 10.1016/j.neuron.2011.09.021

Vogt, K., Aso, Y., Hige, T., Knapek, S., Ichinose, T., Friedrich, A. B., et al. (2016). Direct neural pathways convey distinct visual information to *Drosophila* mushroom bodies. *eLife* 5:e14009. doi: 10.7554/eLife.14009

Vosshall, L. B., Wong, A. M., and Axel, R. (2000). An olfactory sensory map in the fly brain. *Cell.* 102, 147–159. doi: 10.1016/s0092-8674(00)00021-0

Wagh, D. A., Rasse, T. M., Asan, E., Hofbauer, A., Schwenkert, I., Dürrbeck, H., et al. (2006). Bruchpilot, a protein with homology to ELKS/CAST, is required for structural integrity and function of synaptic active zones in *Drosophila*. *Neuron* 49, 833–844. doi: 10.1016/j.neuron.2006.02.008

Wang, J. W., Wong, A. M., Flores, J., Vosshall, L. B., and Axel, R. (2003). Two-photon calcium imaging reveals an odor-evoked map of activity in the fly brain. *Cell* 112, 271–282. doi: 10.1016/S0092-8674(03)00004-7

Wilson, R. I., and Laurent, G. (2005). Role of GABAergic inhibition in shaping odor-evoked spatiotemporal patterns in the Drosophila antennal lobe. *J Neurosci.* 25, 9069–9079. doi: 10.1523/jneurosci.2070-05.2005

Wong, A. M., Wang, J. W., and Axel, R. (2002). Spatial representation of the glomerular map in the *Drosophila* protocerebrum. *Cell* 109, 229–241. doi: 10.1016/s0092-8674(02)00707-9

Yagi, R., Mabuchi, Y., Mizunami, M., and Tanaka, N. K. (2016). Convergence of multimodal sensory pathways to the mushroom body calyx in Drosophila melanogaster. *Sci. Rep.* 6:29481. doi: 10.1038/srep29481

Zars, T., Fischer, M., Schulz, R., and Heisenberg, M. (2000). Localization of a short-term memory in *Drosophila*. *Science* 288, 672–675. doi: 10.1126/science.288.5466.672

Zhou, M., Chen, N., Tian, J., Zeng, J., Zhang, Y., Zhang, X., et al. (2019). Suppression of GABAergic neurons through D2-like receptor secures efficient conditioning in Drosophila aversive olfactory learning. *Proc Natl Acad Sci U.S.A.* 116, 5118–5125. doi: 10.1073/pnas.1812342116

Conflict of Interest: The authors declare that the research was conducted in the absence of any commercial or financial relationships that could be construed as a potential conflict of interest.

frontiers in Physiology

REVIEW
published: 21 February 2020
doi: 10.3389/fphys.2020.00135

On the Role of the Head Ganglia in Posture and Walking in Insects

*Stav Emanuel[1], Maayan Kaiser[1], Hans-Joachim Pflueger[2] and Frederic Libersat[1]**

[1] Department of Life Sciences and Zlotowski Center for Neuroscience, Ben-Gurion University of the Negev, Beersheba, Israel, [2] Fachbereich Biologie Chemie Pharmazie, Institut für Biologie, Neurobiologie, Freie Universität Berlin, Berlin, Germany

In insects, locomotion is the result of rhythm generating thoracic circuits and their modulation by sensory reflexes and by inputs from the two head ganglia, the cerebral and the gnathal ganglia (GNG), which act as higher order neuronal centers playing different functions in the initiation, goal-direction, and maintenance of movement. Current knowledge on the various roles of major neuropiles of the cerebral ganglia (CRG), such as mushroom bodies (MB) and the central complex (CX), in particular, are discussed as well as the role of the GNG. Thoracic and head ganglia circuitries are connected by ascending and descending neurons. While less is known about the ascending neurons, recent studies in large insects and *Drosophila* have begun to unravel the identity of descending neurons and their appropriate roles in posture and locomotion. Descending inputs from the head ganglia are most important in initiating and modulating thoracic central pattern generating circuitries to achieve goal directed locomotion. In addition, the review will also deal with some known monoaminergic descending neurons which affect the motor circuits involved in posture and locomotion. In conclusion, we will present a few issues that have, until today, been little explored. For example, how and which descending neurons are selected to engage a specific motor behavior and how feedback from thoracic circuitry modulate the head ganglia circuitries. The review will discuss results from large insects, mainly locusts, crickets, and stick insects but will mostly focus on cockroaches and the fruit fly, *Drosophila*.

Keywords: walking, insect, cerebral ganglia, gnathal ganglia, motor control, central complex, posture, neuroethology

OPEN ACCESS

Edited by:
Sylvia Anton,
Institut National de la Recherche Agronomique, France

Reviewed by:
Ansgar Buschges,
University of Cologne, Germany
Karen J. Thompson,
Agnes Scott College, United States

***Correspondence:**
Frederic Libersat
libersat@bgu.ac.il

Specialty section:
This article was submitted to Invertebrate Physiology, a section of the journal Frontiers in Physiology

Received: *18 September 2019*
Accepted: *07 February 2020*
Published: *21 February 2020*

Citation:
Emanuel S, Kaiser M, Pflueger H-J and Libersat F (2020) On the Role of the Head Ganglia in Posture and Walking in Insects. Front. Physiol. 11:135. doi: 10.3389/fphys.2020.00135

INTRODUCTION

Most of us have heard of the expression "running around like a headless chicken." Of course, headless chicken cannot walk or run in a coordinated manner and what is true about chickens is also true for insects. The neuronal control of rhythmic behaviors is regulated by two main functional circuitries that are similar in architecture in invertebrate and vertebrate systems. Such rhythmic behaviors have been examined in various groups of invertebrate phyla ranging from worms to

Abbreviations: CirC (connects the cerebral ganglia and the gnathal ganglia), circumesophageal connectives; CPGs, central pattern generators; CRG (formerly "supraesophageal ganglion" or brain), cerebral ganglia; CX, central complex; dFB, dorsal fan-shaped body; DINs, descending interneurons; EB (or central body lower: CBL), ellipsoid body; FB (or central body upper: CBU), fan-shaped body; GNG (formerly "subesophageal ganglion"), gnathal ganglia; LAL, lateral accessory lobe; MB, mushroom bodies; neck connectives, connects the gnathal ganglia (GNG) and the first (pro)thoracic ganglion; NO, paired noduli; PB, protocerebral bridge.

mollusk to arthropods. A common feature in the organization of the neuronal circuit underlying such rhythmic behaviors is a task distribution along the animal's nervous system axis. First, movements in a given appendage must be organized in a spatiotemporal pattern and be coordinated with other appendages (**Figure 1**). This function is generated by local networks generally referred to as CPGs. Such CPGs include motor and inter-neuronal constituents and are strongly modulated by peripheral sensory elements as well (Marder and Bucher, 2001; Marder et al., 2005; Selverston, 2010). Rhythmicity in these local networks is rarely expressed spontaneously (Knop et al., 2001) and often requires an appropriate mechanical or pharmacological stimulus (Arshavsky et al., 1997; Marder and Bucher, 2001; Knebel et al., 2019). In the absence of any sensory input, CPGs are able to generate a rhythm which pre-structures the rhythmicity but not the coordination pattern of the natural behavior (Knebel et al., 2017; review: Bidaye et al., 2017). However, if this rhythm exhibits similar phase relations as the natural behavior it has been called a fictive behavior (for example, fictive walking or stepping; Ryckebusch and Laurent, 1993). Typically, such functional unit namely the CPGs of a given locomotory behavior reside in the "lower" portion of the central nervous system: the ventral nerve cord. The second functional unit is that involved in initiation, modulation, maintenance, and termination of the rhythmic motor pattern generated in the nerve cord. These two functional units interact with feedforward and feedback interactions. While considerable knowledge has been gathered regarding the single neuron and circuit architecture of CPGs and the interactions between sensory and central components of such circuits including an arsenal of reflexes confined to the thoracic ganglia (Burrows, 1996), less is known regarding the role of head ganglia in the control of such circuitries.

As far as head ganglia are concerned, a difference exists between hemimetabolous (stick insects, locusts, cockroaches) and holometabolous insects (fruit flies). In hemimetabolous insects, the GNG (formerly known as the "subesophageal ganglion"), ventral to the gut, is well separated by CirC from the CRG (formerly known as "supraesophageal ganglion" or brain). In holometabolous insects, the GNG are more or less fused with the CRG to form one cerebral mass with the gut running through an opening in between (the GNG are only indicated by being located ventral to the gut in this otherwise uniform cerebral structure) and no CirC are visible from outside. To understand the interactions between the thoracic circuits and those in the head ganglia, various rhythmic behaviors have extensively studied. While several rhythmic behaviors in insects can be executed without the head ganglia meaning both the cerebral and GNG, for example, flight (Wilson, 1961; Gal and Libersat, 2006) righting (Gal and Libersat, 2006), and grooming with the metathoracic legs (Eaton and Farley, 1969; Reingold and Camhi, 1977; Berkowitz and Laurent, 1996), others such as walking will be poorly or not performed in the absence of the head ganglia. The role of the head ganglia in the orchestration of walking has been addressed in several reviews (Heinrich, 2002; Borgmann and Bueschges, 2015; Bidaye et al., 2017) and there is task specificity between CRG and GNG. That being noted, there has been considerable progress unraveling the action of the descending control from the CRG of insects taking advantage of neurogenetic tools in *Drosophila* and a combination of behavioral analysis and electrophysiology in large insects. A review covering at any depth all circuit organization that generates behaviors as diverse as those mentioned above would be unmanageable. Hence, in this review, we will limit our focus on the role of the head ganglia in posture and walking in insects. Until quite recently the bulk of work on this topic has been done on large hemimetabolous insects such as locusts, stick insects, crickets, and cockroaches. But today, the fruit fly, *Drosophila*, has also become a major model for investigating the neuronal basis of walking from circuits to behavior. In the fly, one can use mutations of discrete areas of the central nervous system as genetic tools to identify specific neurons and networks and manipulate or monitor their activity. But with this mind, one should not forget that *Drosophila* stands on the shoulders of giants. Among those giants, we will focus our review on cockroaches which have been extensively studied with regard to walking (Ritzmann and Zill, 2017). Moreover, as most studies have been carried out on the adult stage of large insects, we limit our comparative and complementary survey on walking in the adult *Drosophila*. Insects belong to the subphylum *Hexapoda*, characterized by three pairs of legs. Most insects use, at some speed, the alternating tripod ground locomotion in which three legs are on the ground when the other three are off the ground. Adjacent legs from the same segment are in antiphase while legs from two consecutive segments on opposite side of the body move nearly synchronously (**Figure 1**). Other coordination patterns do occur speed-dependently as well (Wosnitza et al., 2013).

THE CEREBRAL GANGLIA (CRG)

The CRG (formerly brain or supraesophageal ganglion) and GNG (formerly subesophageal ganglion), which are connected to each other by the CirC in large insects, are considered as "higher order" neuronal centers which modulate different aspects of locomotion (**Figure 2**). The picture that emerges from early and recent research is that the CRG are primarily but not exclusively involved in initiation, regulation, and probably termination of walking. The GNG, in contrast, are predominantly involved in coordination as we shall discuss later.

Insects with the CirC cut exhibit long bouts of unoriented walking activity (Roeder, 1937; Bässler and Wegner, 1983; Kien, 1983; Ridgel and Ritzmann, 2005) suggesting that the CRG is a source of inhibitory influence on thoracic walking centers. CRG removal in stick insect (*Carausius morosus*) or cockroaches (*Periplaneta americana*) has little effect on tripod-gait coordination in walking, though it mildly increases the variability in inter-leg phase relationship (**Figure 2**). The latter suggests that the "fine tuning" of the inter-leg coordination might be controlled by the CRG which integrates visual, olfactory, and tactile-antennal information (Graham, 1979; Gal and Libersat, 2006). In contrast, lesions of the neck connectives, those between the GNG and the first (pro)thoracic ganglion, dramatically decrease spontaneous and evoked walking in

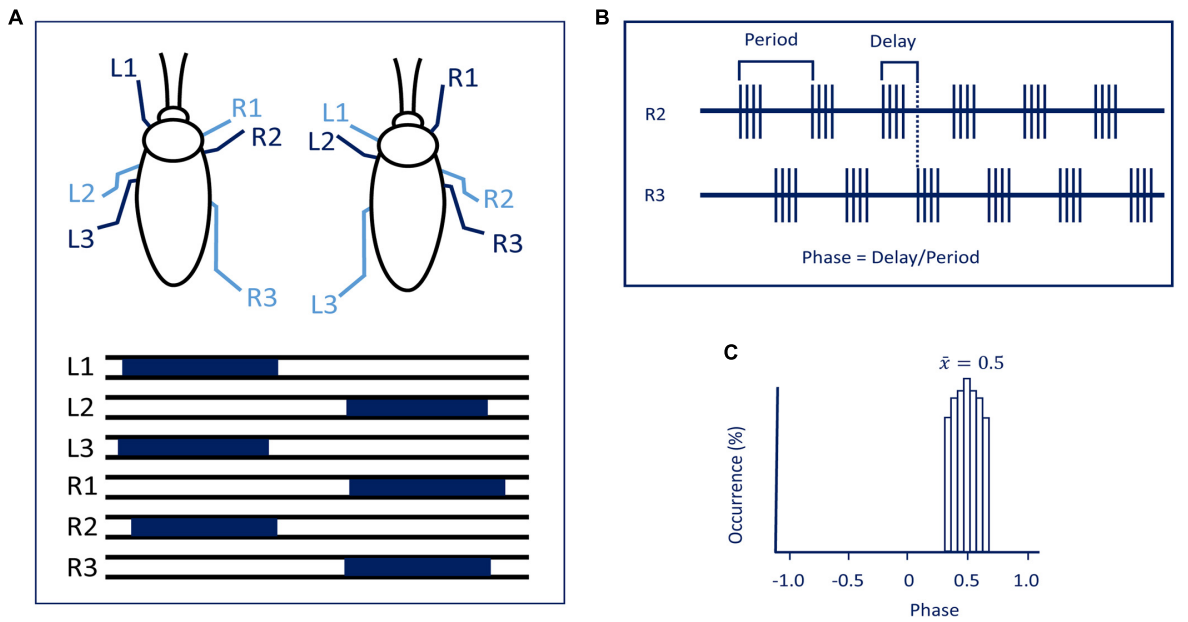

FIGURE 1 | (A) The tripod gait predominantly used by cockroaches. Blue bars represent swing phases of the left (L) and right (R) front (1), middle (2), and hind legs (3) (modified with permission from Ayali et al., 2015). **(B)** To evaluate synchronization and coordination, activity (EMG) is recorded from the same muscle in two different legs. Period and time delay are measured cycle by cycle. **(C)** Relative occurrence of phases of R2 in the cycle of R3 is represented as a histogram. In the present case, the median phase is 0.5 showing that this pair of legs are active in anti-phase.

locusts (Kien, 1983). Gal and Libersat (2006) demonstrated the inhibitory neural influences on walking behavior by examining cockroaches following removal of the CRG. Using more discrete lesions of the CRG in praying mantis, Roeder (1937) was able to identify that the locomotor inhibiting center lies in the dorsal region of the protocerebral ganglion and suggested it is the MB. It is a few decades later that Huber (1960) showed that stimulation of the MB usually inhibited walking in crickets whereas stimulation of another CRG structure, the CX, initiated walking. In support of this, Martin et al. (1998) showed that MB suppress locomotor activity in *Drosophila melanogaster*. Electrophysiological recordings from cockroach MB neurons in freely moving cockroaches revealed several classes of neurons associated with movements (Mizunami et al., 1998a,b,c). Moreover, motor behavioral measurements over period of weeks of MB defective flies showed that MB suppress activity (Helfrich-Förster et al., 2002). In cockroaches, procaine (a reversible voltage dependent sodium channels blocker) injection to the MB increases spontaneous walking (Kaiser and Libersat, 2015). In *Drosophila*, the MB are also required for daily rhythmic locomotor activity (Mabuchi et al., 2016) and enhance motor activity in the beginning of light-evoked walking (Serway et al., 2009). Hence, all aforementioned experimental evidence suggests that the MB have a regulatory role for walking related locomotion. When looking for a CRG structure that is permissive on walking, the CX was shown to be critical in the selection of motor actions. The CX exhibits an elaborate CRG center in its layered architecture. The CX is defined as a group of four midline neuropils: the PB, the FB or (central body upper: CBU), the EB (or central body lower: CBL), the NO, and LAL (**Figure 3**). Research across many species has shown that the CX contains the circuitry for elementary navigational decisions (for a recent review: Honkanen et al., 2019). Its function as a multi-sensory processing hub has been reviewed elsewhere (Pfeiffer and Homberg, 2014; Homberg, 2015). While numerous investigations have shown that the CX is involved in sensory integration and pre-motor processing, others have uncovered its role in the initiation and ongoing regulation of locomotion. We will first discuss the role of the CX in the initiation and regulation of walking and posture.

The Central Complex (CX) and the Initiation and Maintenance of Walking

Kaiser and Libersat (2015) showed that injection of procaine to the CX results in a decrease in spontaneous walking. *Drosophila* CX mutants, with altered internal CX neuropils (the PB, the FB, and the EB), show a decrease in walking activity. Walking speed and step length as a function of the stepping period are both reduced (Strauss and Heisenberg, 1993). While locomotor activity in these mutants is clustered in bouts that are initiated at a normal frequency, their duration is reduced and the interval between bouts is increased (Martin et al., 1999). However, these studies did not find deficits in the initiation of the locomotor activity. But in other studies, some of the strains of *Drosophila* CX mutants are less likely to initiate walking (Heisenberg, 1994; Strauss, 2002). To further investigate the possible role of the CX in walking, Bender et al. (2010) achieved chronic tetrode recordings from the CX of tethered but otherwise intact cockroaches performing

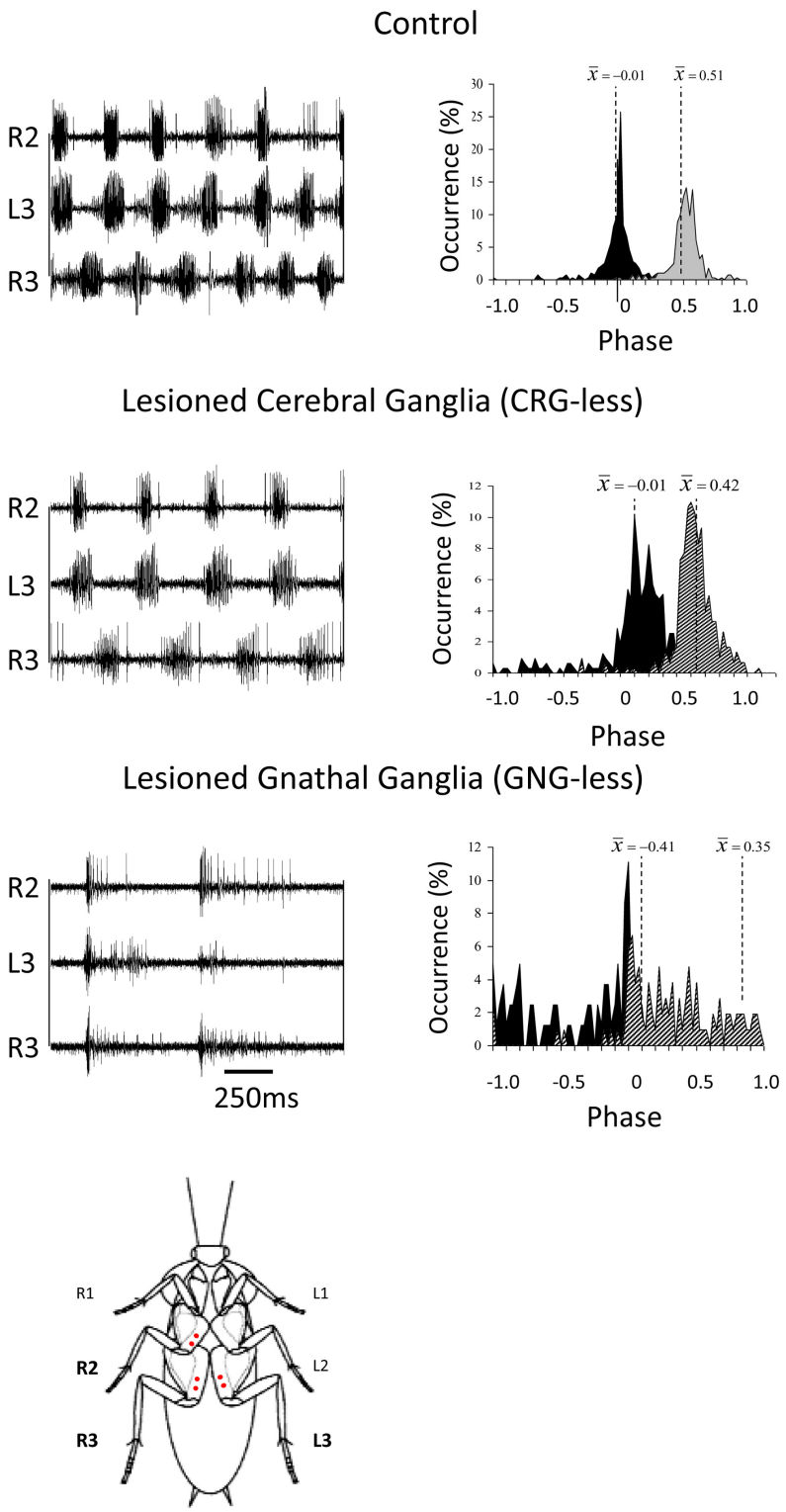

FIGURE 2 | Coordination in cockroaches with head ganglia lesions. Left panels: EMG traces from the coxal depressor muscles, demonstrating the coordination between the right mesothoracic leg (R2) and the right and left metathoracic legs (R3 and L3) in control, CRG-less, and GNG-less cockroaches. Spontaneously initiated locomotion of control and brainless cockroaches is characterized by the tripod-gait coordination. GNG-less cockroaches fail to show spontaneous tripod-gait coordinated locomotion. Right panels: Relative occurrence of phases of R2 and R3 in the cycle of L3. The median phases are also indicated. Note the lack of tripod-gait coordination in GNG-less cockroaches (adapted with permission from Gal and Libersat, 2006). A cockroach is also shown ventral side up with red dots indicating the location of the insertion of the EMG electrodes.

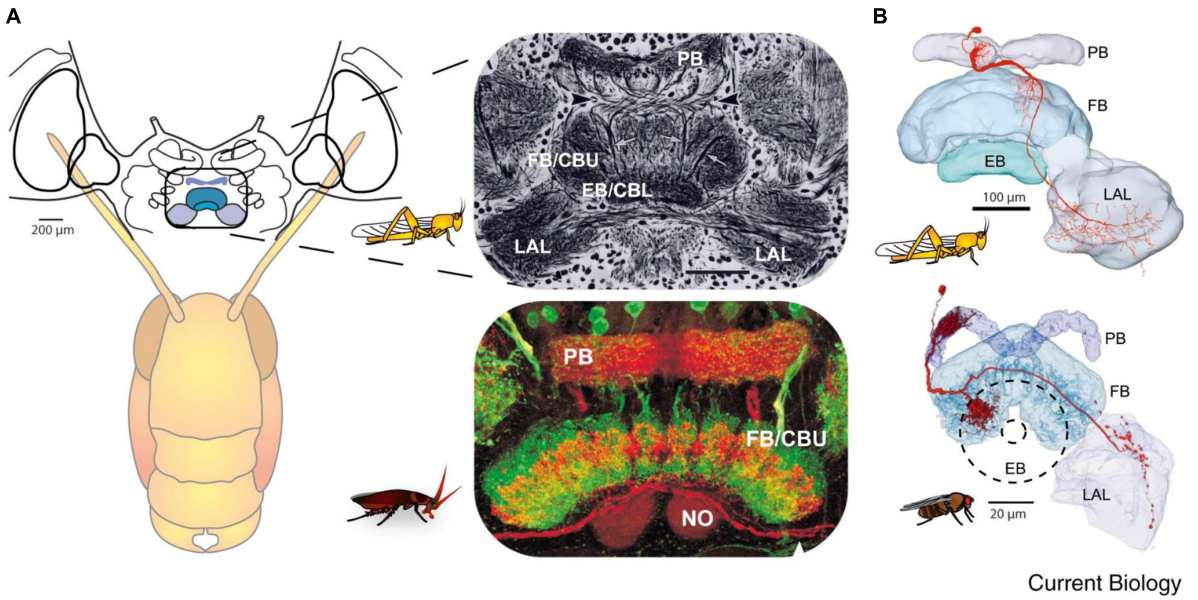

FIGURE 3 | Similarity of the anatomy of the central complex across species. **(A)** Overview of the central complex and support structures: The protocerebral bridge (PB), fan-shaped body (FB) or central body upper (CBU), ellipsoid body (EB) or central body lower (CBL), noduli (NO), and lateral accessory lobe (LAL) in the locust and cockroach. **(B)** Same like in **A** for locust and fly (reprinted with permission from Turner-Evans and Jayaraman, 2016; with permission of Copyright Clearance center, license number 4597641450839 and courtesy of Vivek Jayaraman).

stationary walking or walking on a slippery surface. The recorded neural activity was correlated with stepping rate. Moreover, electrical stimulation of the CX could initiate or regulate walking (Bender et al., 2010). Recent advances in understanding the mechanisms by which the initiation and maintenance of walking in cockroaches come from an unexpected source of natural history: the zombification of cockroaches by a parasitoid wasp (**Figure 4**). The American cockroach (*P. americana*) can fall victim to the parasitoid Jewel Wasp (*Ampulex compressa*), which uses them as live and immobile food supply for its larva. This wasp stings directly inside the cerebral and GNG in the head capsule to immobilize its cockroach prey. The venom injected in the head ganglia induces a dramatic change in the cockroach's ability to show spontaneous walking and to escape from tactile or wind stimuli. While unresponsive, the wasp cuts off both antennae to feed on the cockroach hemolymph from the broken ends. The wasp then grasps one of the antennal stumps and, walking backward, leads its prey to a pre-selected burrow to be later consumed by a single wasp larva. The highest concentration of venom was localized in and around the CX (Haspel et al., 2003).

Using affinity chromatography and Label Free Quantitative Mass Spectrometry (LFQMS), Kaiser et al. (2019) found that the venom binds to synaptic proteins and that numerous proteins are differentially expressed in the CX of stung cockroaches. Many of differentially expressed proteins are involved in signal transduction pathways, such as the Rho GTPase pathway, which is implicated in synaptic plasticity. This suggests that the Jewel Wasp exerts control over cockroach behavior through a molecular cross-talk between venom components and primarily neuronal molecular targets in the host CRG, leading to broad-based alteration of synaptic efficacy in the CX. Such a decrease in synaptic drive to the CX would result in a decrease in descending activity and a reduction in excitatory drive from the CRG to the thoracic motor circuitries. This may account for the observed motor impairments induced by the venom. In support of this, removing the input from the CRG (or "brain") or after a wasp sting, the activity of thoracic octopaminergic neurons is altered (decreases) in stung and "brainless" animals (Rosenberg et al., 2006). The alteration in the activity of octopamine neurons may be part of the mechanism by which the wasp induces a change in the behavioral state of its prey.

Distinct peptidergic pathways in the CX have specific roles in the fine tuning of locomotor activity of *Drosophila.* Two different neuropeptides in *Drosophila's* CX, Drosophila tachykinin (DTK) and short neuropeptide F (sNPF), are shown to modulate locomotor activity (Kahsai et al., 2010). DTK is expressed in two specific populations of neurons innervating the FB and in other CX neurons. RNA interference (RNAi) directed to this peptide caused increasing avoidance behavior and increased number of activity–rest bouts. sNPF is expressed in CX neurons and inhibits the overall motor activity level, as reduced sNPF levels by RNAi in those neurons increased distance traveled and mean walking speed (Kahsai et al., 2010).

Walking behavior is strongly related to rest-activity cycle (sleep cycle) of the animal. Therefore, walking behavior must be under the control of a sleep control system. In *Drosophila*, a circuitry for inducing sleep is well established and involves CX neuropils (Donlea et al., 2011, 2014; Liu et al., 2016; Pimentel et al., 2016). It was recently shown by Donlea et al. (2018) that

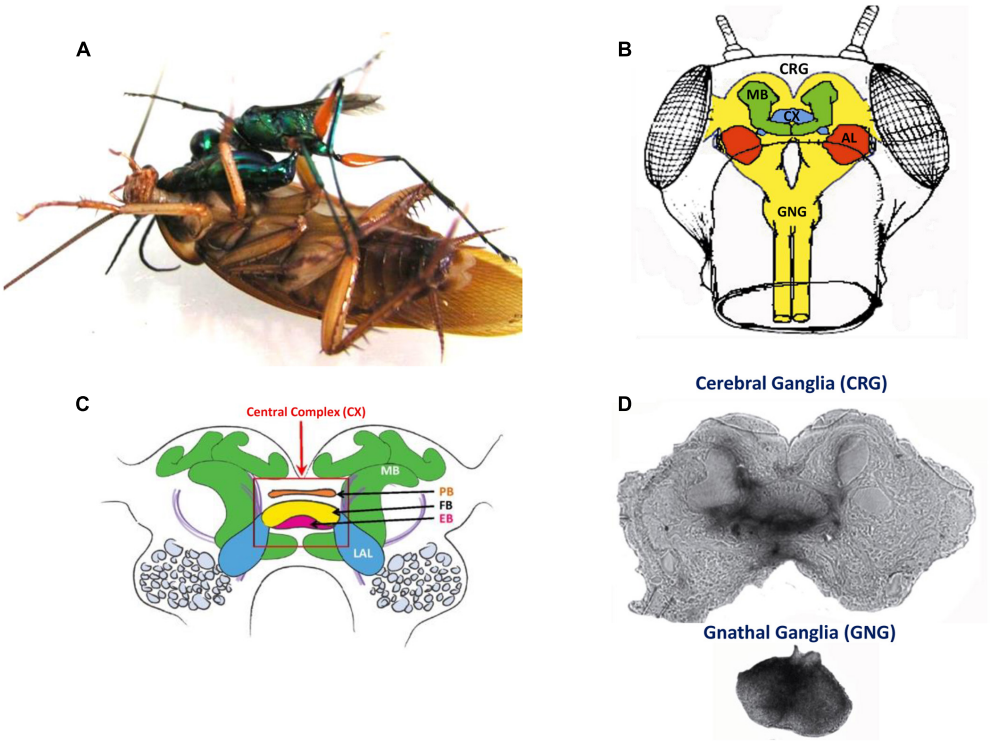

FIGURE 4 | (A) An adult wasp stings a cockroach into the head to manipulate the cockroach behavior. **(B)** Drawing of a frontal view of the cockroach head ganglia (CRG: cerebral ganglia, CX: central complex, AL: antennal lobes, MB: mushroom bodies; GNG: gnathal ganglia). **(C)** Diagram of the cockroach CRG. Central complex is within red rectangle. PB: protocerebral bridge, FB: fan-shaped body, EB: ellipsoid body, LAL: lateral accessory lobes, MB: mushroom bodies (reproduced with permission from Ritzmann et al., 2012; courtesy of Josh Martin and Roy Ritzmann; License: CC BY 4) **(D)** Autoradiographs of the cerebral ganglia and the gnathal ganglia of a cockroach stung by a radio-labeled wasp. Black staining indicates the presence of venom (adapted with permission from Haspel et al., 2003).

dFB neurons induce sleep by inhibitory transmitters including neuropeptide allatostatin-A (AstA). Among the targets of AstA is a group of interneurons in the EB of the CX that they named "helicon cells." These neurons are inhibited by sleep-promoting AstA, excited by visual input, and are permissive for locomotion. Therefore, one way of inducing a rest period is by inhibition of walking-permissive circuits in the *Drosophila* CRG. Another way to modulate walking behavior is in the activity of CRG circuits that promote wakefulness. In *Drosophila*, two dopaminergic neurons signal to the dFB and their activity reduces sleep and promotes arousal (Liu et al., 2012).

The Central Complex (CX) and Navigation in Walking

After a mid-line section and removal of one side of the CRG, a mantis makes small circular walking toward the intact side. These circular movements are due in part to the unequal right–left body tonus (Roeder, 1937). Research across many species has shown that the CX contains the circuitry that process sensory information to perform proper navigation (Honkanen et al., 2019).

Analysis of recording of the CX in freely moving cockroaches leads to the grouping of movement-predictive cells for slow or fast forward walking, left or right turns, or combinations of forward and turning speeds (Martin et al., 2015). Moreover, they showed that the CX via its descending output neurons may modulate leg reflexes in the thorax to facilitate turning. The role of certain sub-regions of the CX is uncovered by cockroaches with lesions to the PB and EB that exhibit turning deficits (Harley and Ritzmann, 2010). Moreover, stimulation through recording wires inserted in the CX produced consistent trajectories of forward walking or turning in these animals (Guo and Ritzmann, 2013). They concluded that asymmetrical activity in the CX precedes and influences cockroach turning behavior. More recently, Varga and Ritzmann (2016) uncovered head-direction cells in the CX of the cockroach. Such cells encode the animal's heading relative to a landmark's position in several ways. Some cells are tuned to a particular direction apparently rely on internal cues while others rely on external sensory cues (Varga and Ritzmann, 2016).

It was recently shown that *Drosophila* follow straight courses relative to landmarks (Green et al., 2018). Wolff et al. (2015) had recently mapped the structure of the PB of the *Drosophila* CX and identified several classes of neurons. A class of columnar neurons of the PB which sends dendrites to a specific area of the EB encodes the fly's azimuth relative to its environment. These neurons (termed EB-PB-gall or E-PG neurons) were shown to be tracking the fly's angular movements (heading) even in darkness (Seelig and Jayaraman, 2015; Green et al., 2017; Turner-Evans et al., 2017). Inhibiting synaptic transmission in

E-PG neurons destabilized these neurons phase activity and reduced the distance and speed of walking (Green et al., 2018). These findings, however, do not fully account for the body angle tracking necessary for directional navigation over distances.

The Central Complex (CX) and Posture

First, it should be noted that posture is also handled at the single ganglion level by feedback from sense organs, primarily campaniform sensilla embedded in the cuticle of the legs (Zill et al., 2004). But reflexes handled at the local level of thoracic ganglia can be modulated by the CX. Hence, electrical stimulation of the CX in a restrained animal while recording from the slow depressor motoneuron (Ds) impacts on the femoral chordotonal organ to Ds reflex pathway (Martin et al., 2015). In praying mantis, removal of the CRG results in great decrease of tonus on both sides of the body (Roeder, 1937). Likewise, normal posture is altered in headless cockroaches (Ridgel and Ritzmann, 2005). But immediately after lesion of the neck connectives, cockroaches first show a hyper-extended posture, which is decreased thereafter over a few days. In contrast, the posture of cockroaches with lesions of the CirC appears similar to intact cockroaches. Yet, when challenged with the more difficult task of climbing, cockroaches with their CirC cut show a postural deficit (Ritzmann and Quinn, 2004) which affects their ability to climb up on smooth inclines. When confronted with a substantial incline, these cockroaches fail systematically to manage this obstacle. The ongoing activity of the coxal slow motoneuron ongoing activity, known to be involved in posture, is reduced after injection of procaine into the cockroach's CX (Emanuel and Libersat, 2017). Moreover, the regular tonic firing of the slow motoneuron is greatly reduced in cockroaches stung by the jewel wasp (Emanuel and Libersat, 2017). Hence, postural tonus might be mediated by the head ganglia pre-motor circuits since injection of procaine to the CX decreases coxal slow motoneuron activity in a similar manner to the wasp venom injection in the CX (**Figure 5**).

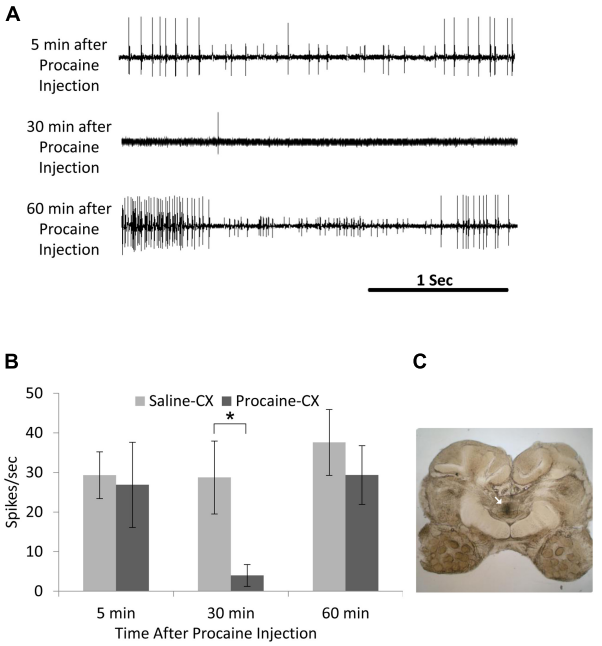

FIGURE 5 | Activity in coxal slow motoneuron recorded as EMG spikes from the coxal depressor muscle after procaine injection to the central complex (CX). **(A)** Representative EMG recordings traces of coxal slow motoneuron ongoing activity 5 min after (upper trace; before procaine effect), 30 min after (middle trace; peak procaine effect), and 30 min after (lower trace; recovery from procaine effect) procaine injection to the CX. **(B)** Comparison of EMG spikes (spikes/sec) following saline (control; $n = 6$) and procaine ($n = 6$) injection to the CX. A significant decrease ($P < 0.05$; t-test) was found 30 min after procaine injection as compared to 30 min after saline injection. Each bar represents the averaged spikes/second ± SEM; significance is indicated with asterisk. **(C)** A representative image for postmortem verification of injection site. Arrow indicates the injection site in the fan-shaped body of the CX (adapted with permission from Emanuel and Libersat, 2017).

The Central Complex (CX) Connectivity to Descending Interneurons (DINs)

Neuroanatomy of the DINs

The sensory information processed in the CX must be transferred to DINs projecting to the ventral nerve cord. There are approximately 200 pairs of neurons in the CRG that have axons that descend to and beyond the thoracic ganglia in cockroaches (Okada et al., 2003) and crickets (Staudacher, 1998). In addition, there are another 100 neurons that connect the CRG only with the GNG in locusts (Heinrich, 2002). In cockroaches, the dendrites of such DINs are distributed in most CRG areas, including the MB and the CX (Okada et al., 2003), two structures that have been implicated with walking. In crickets, none of the DINs identified so far extend collaterals into the CX and the MB. This difference could be due to incomplete staining of the small dendritic branches of DINs in crickets. Neurons leaving the CX project to a region of the CX termed the LAL, and several neurons that ultimately descend to the thoracic ganglia also pass through this region. Although the anatomical studies in cricket (Staudacher, 1998) and cockroach (Okada et al., 2003) have identified how DINs are organized, the lack of genetic tools in these insects currently limits a systematic investigation of their roles in motor control. A comparison of a recent study on *Drosophila* DINs shows a high degree of conservation in the number and organization of DINs in both hemimatebolous and holometabolous insects (Hsu and Bhandawat, 2016; Namiki et al., 2018). There are 350 pairs of DINs in the fly head ganglia of which roughly 180 pairs are located in GNG (Namiki et al., 2018). These numbers compare well with those reported in crickets and cockroaches and the spatial distribution of DINs in the CRG in clusters is also similar in all three species (Hsu and Bhandawat, 2016). Likewise, the number of DINs in *Drosophila* GNG is 121 pairs and comparable to the roughly 150 pairs reported in locusts (Knebel et al., 2019). Interestingly, DINs of cockroaches and flies receive input from regions of the CRG that are innervated by outputs from MB and CX (Hsu and Bhandawat, 2016). In *Drosophila*, none of the DINs originate in the CX or MB (Namiki et al., 2018). Equally importantly, none of DINs innervate the CX or MB, implying that these neuropils do not directly affect motor output. Roughly 65% of the

DINs send an axon in neck connective ipsilateral to their soma (Namiki et al., 2018).

DINs and Walking

In an attempt to record and identify DINs, Böhm and Schildberger (1992) found neurons that changed their levels of activity when the animal was walking. The activity of two DINs was directly correlated with walking activity and seemed to control walking parameters. Activation of one DIN caused the resting animal to begin walking, and interrupting the discharge of this DIN brought the walking animal to a halt. While investigating DINs associated with phonotaxis in crickets, Zorović and Hedwig (2013) recorded intracellularly at least four DINs while the animals were standing or walking on an open-loop trackball system. They found that activity of all four DINs was correlated to forward walking. Furthermore, injection of depolarizing current elicited walking and/or steering in three of four neurons. Some neurons showed arborizations in the LALs supporting the hypothesis that this region bridges between the CX and the DINs. Activation of different DINs in *Drosophila* induces running or freezing in a state-dependent manner (Zacarias et al., 2018). Some DINs when stimulated induce backward walking in *Drosophila*. The DIN which earned the name of moonwalker descending neuron (MDN) is required for flies to walk backward and is sufficient to trigger backward walking under conditions in which flies would otherwise walk forward (Bidaye et al., 2014). Optogenetic activation of 26 DINs drove locomotion behaviors such as slow locomotion, fast locomotion, and global increase in locomotor activity (Cande et al., 2018). These activated behaviors were often dependent on the behavior of the fly immediately before descending neuron activation, indicating a context dependent role for these descending neurons.

THE GNATHAL GANGLIA (GNG)

In contrast to headless insects, animals in which the CRG have been removed (or the CirC severed) engage longer bouts of spontaneous walking than intact animals. There are about 90 DINs with a cell body in the GNG most of which have a contralateral axon (Kien et al., 1990; Gal and Libersat, 2006). Such a number might be an underestimate as a recent study labeled roughly 150 descending GNG neurons (Knebel et al., 2019). In *Drosophila*, the GNG DINs group provides the major pathway to the leg motor neuropiles in the ventral nerve cord (Namiki et al., 2018). Locust GNG DINs show an elevated activity during and after the preparatory phase of walking (Kien, 1990a). These neurons typically fire throughout the walking bout, as temporally structured patterns that are not directly correlated with the stepping cycles (Kien, 1990b). Performing a mid-sagittal section through the GNG removes the effect of GNG DINs on thoracic CPGs while leaving the connectivity between the CRG and thoracic ganglia (the "through running axons" of CRG DINs, B-DINs) (Gal and Libersat, 2006). The direct descending pathway from the CRG to the thorax (the "through running axons") is mostly unaffected by this midline cut since this pathway runs through the margins of the GNG (Altman and Kien, 1987). Such operated animals show very little, if any spontaneous walking. But if challenged to "walk" on water, their leg movements are mostly uncoordinated (Gal and Libersat, 2006). This is in sharp contrast to the walking pattern of cockroaches after removal of the CRG which show normal coordination both on land and water. This strongly suggests that the GNG is involved in leg coordination.

MONOAMINERGIC DESCENDING INTERNEURONS (DINS) AND DESCENDING CONTROL OF WALKING

Multiple neurotransmitters have been found to be manufactured by the DINs. These include acetylcholine, GABA, glutamate, serotonin, dopamine, and octopamine (Hsu and Bhandawat, 2016). Hsu and Bhandawat (2016) also found that acetylcholine and GABA, the major excitatory and inhibitory neurotransmitter, respectively, are produced equally and represent roughly 75% of the DINs population (Hsu and Bhandawat, 2016). The monoamines serotonin, dopamine, and octopamine are known to modulate well-defined behaviors. The idea of chemical coding of specific behaviors was born out of experiments showing that local application of certain monoamines in the central nervous system can reproducibly evoke a single coherent behavior (Libersat and Pflueger, 2004). This idea was coined as the orchestration hypothesis by Graham Hoyle when he and his colleagues revealed that injection of octopamine in the locust thoracic ganglia released flight-like behavior (Sombati and Hoyle, 1984). This observation was later confirmed in *Drosophila* where application of these compounds induces a set of complex behavioral responses in the decapitated flies including the stimulation of grooming and locomotion (Yellman et al., 1997). In fact, octopamine injected into the neuropiles of locust thoracic ganglia primes the motor system to flight in contrast to other modulators such as pilocarpine or tyramine that act concentration dependently and can release either fictive stepping/walking or fictive flight or both simultaneously (Rillich et al., 2013). One population of octopaminergic DINs, with unpaired median morphology, originates in the GNG of locusts (Bräunig and Burrows, 2004). Recently, a cluster of DINs of the deutocerebrum containing tyramine/octopamine has been identified in cockroaches, stick insects, and locust (Kononenko et al., 2019). In locusts, these DINs synthesize octopamine from tyramine only after the insect experiences stimuli associated with stress and, thus, these DINS could convey information about the "stress status" to thoracic circuits. It would be interesting to identify such octopaminergic DINs in *Drosophila* head ganglia and manipulate their activity in the intact adult to observe their impact on walking.

Taking advantage of the neurogenetics tools available with *Drosophila* model system, Tschida and Bhandawat (2015) found two dopaminergic DINs in *Drosophila* GNG and tested whether their activity promotes walking. This investigation was motivated by previous studies in reduced preparations which showed that application of dopamine receptor agonists elicits fictive motor rhythms. The authors found that dopaminergic DINs

activity correlated with certain leg movements and walking speed. But increasing dopaminergic DINs activity failed to impact on walking (Tschida and Bhandawat, 2015).

CONCLUSION AND FUTURE PROSPECTS

While numerous investigations have shown that the CRG, and in particular the CX is involved in sensory integration and processing, for example, of polarized light, others have uncovered its role in the initiation and ongoing regulation of locomotion. First, the CX appears to be involved in the arousal state of insects in preparation for the initiation of walking. Further experimental evidence indicates its role in the initiation and maintenance of walking. Asymmetrical recruitment of the CX also reveals its involvement in turning and negotiating obstacle during ongoing walking. How is the CX premotor command transferred to DINs is not known but some experimental evidence points to a region of the CX called "the LAL" (Namiki and Kanzaki, 2016). The GNG, also part of the head ganglia, and origin of many DINs appear to be involved in maintenance and inter-leg coordination of walking. Numerous DINs organized as clusters project downstream to motor centers in the nerve cord. How these neurons are involved in the initiation and regulation of coordination for steering is still unknown. Likewise, the connectivity between the CX and the DINs needs attention. Therefore, the studies compiled and reviewed here raise a number of questions where insects may still have to offer interesting insights in the neural basis of locomotion.

For instance, all moving animals require that stimuli generated by self-motion be discarded and information on self-generated movements have to be integrated into feedback systems. Therefore, circuits of corollary discharge or efference copies are most likely a component of all sensory-to-motor systems in insect and vertebrate respectively (Poulet and Hedwig, 2006; Combes et al., 2008). In contrast to most vertebrates, most insects do not possess eyes that can be moved separately from the head and, thus, for gaze stabilization the whole head has to be moved, mainly by the neck muscles which means one degree of freedom less. However, many insects and cockroaches in particular, possess long movable antennae which act as active sensors for olfactory and tactile ("haptic") stimuli. They are moved by muscles inserting at the base of the antenna. How neck and antennal muscles are activated during walking is, to our knowledge, less studied.

The nature of the feedforward and feedback loops between the cerebral and the GNG and how these are involved in the control of walking is largely unexplored. A further unresolved issue in insects is the nature of the thoracic ascending input to the head ganglia and what is its role in fine tuning walking initiation, regulation, and coordination. Bidaye et al. (2014) addressed this issue by studying descending control of backward walking in flies. Briefly, they identified a descending neuron that initiate backward walking (MDN) and an ascending neuron (MAN: moonwalker ascending neuron that appears to inhibit forward and facilitate backward walking. Finally, there must be location in the CRG where the sensory information from the head sensors (goal direction) and legs sensors (proprioception) converge for appropriate initiation and coordination of walking.

The expression of multiple neuropeptides and neurotransmitters in *Drosophila* and other insect CX must be associated with different functional roles. As several neuropeptides are expressed in the circuitry of the CX, some may be modulators of locomotor behavior. The CX complex is rich in neuroactive substances. Among the biogenic amines and neuropeptides substances in neurons or innervating neurons of the CX are octopamine, serotonin, dopamine and allatotropin, leucokinin, myoinihibitory peptide, RFamides, Tachykinin-like peptide, and more (Pfeiffer and Homberg, 2014). Moreover, mapping metabotropic, G-protein-coupled receptors (GPCRs) of several neurotransmitters and neuromodulators to neurons of the CX show that chemical signaling and signal modulation are diverse and highly complex in the different compartments and circuits of the *Drosophila* CX (Kahsai et al., 2012). Only a few studies have addressed the role of these substances in locomotion. When the roles of two different neuropeptides (tachykinin and sNPF) in of Drosophila locomotor behavior, Kahsai et al. (2010) found that each is involved in different aspects of locomotion, orientation during locomotion, and locomotor activity levels, respectively. The initiation and maintenance of walking is context dependent and must be regulated by the internal state of the insect which depends on the metabolic and/or hormonal states and neuromodulatory systems. Such internal state must have an impact on the selection of a subpopulation of descending neurons dedicated to specific motor behavior such as, to name a few, walking, flight, grooming, righting.

Although the evolution of the brain in vertebrate and invertebrate phyla may follow a different "bauplan," such difference does not imply that vertebrate and invertebrate motor systems are functionally different. Both systems control an articulated skeletal system using muscles which are in turn controlled by motor neurons. Notably, Strausfeld and Hirth (2013) draw functional similarities between the insect CX and the vertebrate basal ganglia as well as the insect GNG with the brain stem of the vertebrate brain. Future studies on different insects, combining electrophysiological, molecular, and behavioral studies with, for example, CRISPR-based genetics strategies might lead to answer these questions and further our understanding of the role of the head ganglia in walking and behavioral spontaneity. With this knowledge and by comparing the organization of locomotor system in invertebrates with that of vertebrates, we should uncover how such systems solve similar problems.

AUTHOR CONTRIBUTIONS

All authors contributed equally to the writing of this review.

FUNDING

H-JP and FL were supported by DFG grant Pf128/32-1.

REFERENCES

Altman, J., and Kien, J. (1987). "Functional organization of the subesophageal ganglion in arthropods," in *Arthropod Brain: Its Evolution, Development, Structure and Function*, ed. A. P. Gupta, (New York, NY: John Wiley & Sons), 265–301.

Arshavsky, Y. I., Deliagina, T. G., and Orlovsky, G. N. (1997). Pattern generation. *Curr. Opin. Neurobiol.* 7, 781–789.

Ayali, A., Borgmann, A., Bueschges, A., Couzin-Fuchs, E., Daun-Gruhn, S., and Holmes, P. (2015). The comparative investigation of the stick insect and cockroach models in the study of insect locomotion. *Curr. Opin. Insect Sci.* 12, 1–10.

Bässler, U., and Wegner, U. (1983). Motor output of the denervated thoracic ventral nerve cord in the stick insect *Carausius morosus*. *J. Exp. Biol.* 105, 127–145.

Bender, J. A., Pollack, A. J., and Ritzmann, R. E. (2010). Neural activity in the central complex of the insect brain is linked to locomotor changes. *Curr. Biol.* 20, 921–926. doi: 10.1016/j.cub.2010.03.054

Berkowitz, A., and Laurent, G. (1996). Central generation of grooming motor patterns and interlimb coordination in locusts. *J. Neurosci.* 16, 8079–8091.

Bidaye, S. S., Bockemühl, T., and Büschges, A. (2017). Six-legged walking in insects: how CPGs, peripheral feedback, and descending signals generate coordinated and adaptive motor rhythms. *J. Neurophysiol.* 119, 459–475. doi: 10.1152/jn.00658.2017

Bidaye, S. S., Machacek, C., Wu, Y., and Dickson, B. J. (2014). Neuronal control of *Drosophila* walking direction. *Science* 344, 97–101.

Böhm, H., and Schildberger, K. (1992). Brain neurones involved in the control of walking in the cricket *Gryllus bimaculatus*. *J. Exp. Biol.* 166, 113–130.

Borgmann, A., and Bueschges, A. (2015). Insect motor control: methodological advances, descending control and inter-leg coordination on the move. *Curr. Opin. Neurobiol.* 33, 8–15. doi: 10.1016/j.conb.2014.12.010

Bräunig, P., and Burrows, M. (2004). Projection patterns of posterior dorsal unpaired median neurons of the locust subesophageal ganglion. *J. Comp. Neurol.* 478, 164–175.

Burrows, M. (1996). *The Neurobiology of an Insect Brain*. Oxford: Oxford University Press.

Cande, J., Namiki, S., Qiu, J., Korff, W., Card, G. M., Shaevitz, J. W., et al. (2018). Optogenetic dissection of descending behavioral control in *Drosophila*. *Elife* 7:e34275.

Combes, D., Le Ray, D., Lambert, F. M., Simmers, J., and Straka, H. (2008). An intrinsic feed-forward mechanism for vertebrate gaze stabilization. *Curr. Biol.* 18, R241–R243.

Donlea, J. M., Pimentel, D., and Miesenböck, G. (2014). Neuronal machinery of sleep homeostasis in *Drosophila*. *Neuron* 81, 860–872. doi: 10.1016/j.neuron.2013.12.013

Donlea, J. M., Pimentel, D., Talbot, C. B., Kempf, A., Omoto, J. J., Hartenstein, V., et al. (2018). Recurrent circuitry for balancing sleep need and sleep. *Neuron* 97, 378–389.e4. doi: 10.1016/j.neuron.2017.12.016

Donlea, J. M., Thimgan, M. S., Suzuki, Y., Gottschalk, L., and Shaw, P. J. (2011). Inducing sleep by remote control facilitates memory consolidation in *Drosophila*. *Science* 332, 1571–1576. doi: 10.1126/science.1202249

Eaton, R. C., and Farley, R. D. (1969). The neural control of cercal grooming behaviour in the cockroach, *Periplaneta americana*. *J. Insect Physiol.* 15, 1047–1065.

Emanuel, S., and Libersat, F. (2017). Do quiescence and wasp venom-induced lethargy share common neuronal mechanisms in cockroaches? *PloS One* 12:e0168032. doi: 10.1371/journal.pone.0168032

Gal, R., and Libersat, F. (2006). New vistas on the initiation and maintenance of insect motor behaviors revealed by specific lesions of the head ganglia. *J. Comp. Physiol. A Neuroethol. Sens. Neural Behav. Physiol.* 192, 1003–1020.

Graham, D. (1979). Effects of circum-oesophageal lesion on the behaviour of the stick insect *Carausius morosus*. *Biol. Cybern.* 32, 139–145.

Green, J., Adachi, A., Shah, K. K., Hirokawa, J. D., Magani, P. S., and Maimon, G. (2017). A neural circuit architecture for angular integration in *Drosophila*. *Nature* 546, 101–106. doi: 10.1038/nature22343

Green, J., Vijayan, V., Pires, P. M., Adachi, A., and Maimon, G. (2018). Walking *Drosophila* aim to maintain a neural heading estimate at an internal goal angle. *Biorxiv* [Preprint]. doi: 10.1101/315796

Guo, P., and Ritzmann, R. E. (2013). Neural activity in the central complex of the cockroach brain is linked to turning behaviors. *J. Exp. Biol.* 216, 992–1002. doi: 10.1242/jeb.080473

Harley, C., and Ritzmann, R. (2010). Electrolytic lesions within central complex neuropils of the cockroach brain affect negotiation of barriers. *J. Exp. Biol.* 213, 2851–2864. doi: 10.1242/jeb.042499

Haspel, G., Rosenberg, L. A., and Libersat, F. (2003). Direct injection of venom by a predatory wasp into cockroach brain. *J. Neurobiol.* 56, 287–292.

Heinrich, R. (2002). Impact of descending brain neurons on the control of stridulation, walking, and flight in orthoptera. *Microsc. Res. Tech.* 56, 292–301.

Heisenberg, M. (1994). Central brain function in insects: genetic studies on the mushroom bodies and central complex in *Drosophila*. *Fortschr. Zool.* 39, 61–79.

Helfrich-Förster, C., Wulf, J., and de Belle, J. S. (2002). Mushroom body influence on locomotor activity and circadian rhythms in *Drosophila melanogaster*. *J. Neurogenet.* 16, 73–109.

Homberg, U. (2015). Sky compass orientation in desert locusts—evidence from field and laboratory studies. *Front. Behav. Neurosci.* 9:346. doi: 10.3389/fnbeh.2015.00346

Honkanen, A., Adden, A., da Silva Freitas, J., and Heinze, S. (2019). The insect central complex and the neural basis of navigational strategies. *J. Exp. Biol.* 222(Pt Suppl. 1):jeb188854. doi: 10.1242/jeb.188854

Hsu, C. T., and Bhandawat, V. (2016). Organization of descending neurons in *Drosophila melanogaster*. *Sci. Rep.* 6:20259. doi: 10.1038/srep20259

Huber, F. (1960). Untersuchungen über die Funktion des Zentralnervensystems und insbesondere des Gehirnes bei der Fortbewegung und der Lauterzeugung der Grillen. *Z. Vergl. Physiol.* 44, 60–132.

Kahsai, L., Carlsson, M. A., Winther, ÅM., and Nässel, D. R. (2012). Distribution of metabotropic receptors of serotonin, dopamine, GABA, glutamate, and short neuropeptide F in the central complex of *Drosophila*. *Neuroscience* 208, 11–26. doi: 10.1016/j.neuroscience.2012.02.007

Kahsai, L., Martin, J.-R., and Winther, ÅM. (2010). Neuropeptides in the *Drosophila* central complex in modulation of locomotor behavior. *J. Exp. Biol.* 213, 2256–2265.

Kaiser, M., Arvidson, R., Zarivach, R., Adams, M. E., and Libersat, F. (2019). Molecular cross-talk in a unique parasitoid manipulation strategy. *Insect Biochem. Mol. Biol.* 106, 64–78.

Kaiser, M., and Libersat, F. (2015). The role of the cerebral ganglia in the venom-induced behavioral manipulation of cockroaches stung by the parasitoid jewel wasp. *J. Exp. Biol.* 218, 1022–1027.

Kien, J. (1983). The initiation and maintenance of walking in the locust: an alternative to the command concept. *Proc. R. Soc. Lond. B Biol. Sci.* 219, 137–174.

Kien, J. (1990a). Neuronal activity during spontaneous walking– I. Starting and stopping. *Comp. Biochem. Physiol. A Comp. Physiol.* 95, 607–621.

Kien, J. (1990b). Neuronal activity during spontaneous walking– II. Correlation with stepping. *Comp. Biochem. Physiol. A Comp. Physiol.* 95, 623–638.

Kien, J., Fletcher, W., Altman, J., Ramirez, J.-M., and Roth, U. (1990). Organisation of intersegmental interneurons in the suboesophageal ganglion of *Schistocerca gregaria* (Forksal) and *Locusta migratoria* migratorioides (Reiche & Fairmaire) (Acrididae, Orthoptera). *Int. J. Insect Morphol. Embryol.* 19, 35–60.

Knebel, D., Ayali, A., Pflueger, H.-J., and Rillich, J. (2017). Rigidity and flexibility: the central basis of inter-leg coordination in the locust. *Front. Neural Circuits* 10:112. doi: 10.3389/fncir.2016.00112

Knebel, D., Rillich, J., Nadler, L., Pflueger, H.-J., and Ayali, A. (2019). The functional connectivity between the locust leg pattern generators and the subesophageal ganglion higher motor center. *Neurosci. Lett.* 692, 77–82.

Knop, G., Denzer, L., and Büschges, A. (2001). A central pattern-generating network contributes to "Reflex-Reversal"–like leg motoneuron activity in the locust. *J. Neurophysiol.* 86, 3065–3068.

Kononenko, N. L., Hartfil, S., Willer, J., Ferch, J., Wolfenberg, H., and Pflueger, H. J. (2019). A population of descending tyraminergic/octopaminergic projection neurons of the insect deutocerebrum. *J. Comp. Neurol.* 527, 1027–1038. doi: 10.1002/cne.24583

Libersat, F., and Pflueger, H.-J. (2004). Monoamines and the orchestration of behavior. *Bioscience* 54, 17–25.

Liu, Q., Liu, S., Kodama, L., Driscoll, M. R., and Wu, M. N. (2012). Two dopaminergic neurons signal to the dorsal fan-shaped body to promote

wakefulness in *Drosophila*. *Curr. Biol.* 22, 2114–2123. doi: 10.1016/j.cub.2012.09.008

Liu, S., Liu, Q., Tabuchi, M., and Wu, M. N. (2016). Sleep drive is encoded by neural plastic changes in a dedicated circuit. *Cell* 165, 1347–1360. doi: 10.1016/j.cell.2016.04.013

Mabuchi, I., Shimada, N., Sato, S., Ienaga, K., and Sakai, T. (2016). Mushroom body signaling is required for locomotor activity rhythms in *Drosophila*. *Neurosci. Res.* 111, 25–33.

Marder, E., and Bucher, D. (2001). Central pattern generators and the control of rhythmic movements. *Curr. Biol.* 11, R986–R996.

Marder, E., Bucher, D., Schulz, D. J., and Taylor, A. L. (2005). Invertebrate central pattern generation moves along. *Curr. Biol.* 15, R685–R699.

Martin, J. P., Guo, P., Mu, L., Harley, C. M., and Ritzmann, R. E. (2015). Central-complex control of movement in the freely walking cockroach. *Curr. Biol.* 25, 2795–2803.

Martin, J.-R., Ernst, R., and Heisenberg, M. (1998). Mushroom bodies suppress locomotor activity in *Drosophila melanogaster*. *Learn. Mem.* 5, 179–191.

Martin, J.-R., Raabe, T., and Heisenberg, M. (1999). Central complex substructures are required for the maintenance of locomotor activity in *Drosophila melanogaster*. *J. Comp. Physiol. A* 185, 277–288.

Mizunami, M., Iwasaki, M., Okada, R., and Nishikawa, M. (1998a). Topography of four classes of Kenyon cells in the mushroom bodies of the cockroach. *J. Comp. Neurol.* 399, 162–175.

Mizunami, M., Iwasaki, M., Okada, R., and Nishikawa, M. (1998b). Topography of modular subunits in the mushroom bodies of the cockroach. *J. Comp. Neurol.* 399, 153–161.

Mizunami, M., Okada, R., Li, Y., and Strausfeld, N. J. (1998c). Mushroom bodies of the cockroach: activity and identities of neurons recorded in freely moving animals. *J. Comp. Neurol.* 402, 501–519.

Namiki, S., Dickinson, M. H., Wong, A. M., Korff, W., and Card, G. M. (2018). The functional organization of descending sensory-motor pathways in *Drosophila*. *Elife* 7:e34272. doi: 10.7554/eLife.34272

Namiki, S., and Kanzaki, R. (2016). Comparative neuroanatomy of the lateral accessory lobe in the insect brain. *Front. Physiol.* 7:244. doi: 10.3389/fphys.2016.00244

Okada, R., Sakura, M., and Mizunami, M. (2003). Distribution of dendrites of descending neurons and its implications for the basic organization of the cockroach brain. *J. Comp. Neurol.* 458, 158–174.

Pfeiffer, K., and Homberg, U. (2014). Organization and functional roles of the central complex in the insect brain. *Annu. Rev. Entomol.* 59, 165–184.

Pimentel, D., Donlea, J. M., Talbot, C. B., Song, S. M., Thurston, A. J., and Miesenböck, G. (2016). Operation of a homeostatic sleep switch. *Nature* 536, 333–337. doi: 10.1038/nature19055

Poulet, J. F., and Hedwig, B. (2006). The cellular basis of a corollary discharge. *Science* 311, 518–522.

Reingold, S. C., and Camhi, J. M. (1977). A quantitative analysis of rhythmic leg movements during three different behaviors in the cockroach, *Periplaneta americana*. *J. Insect Physiol.* 23, 1407–1420.

Ridgel, A. L., and Ritzmann, R. E. (2005). Effects of neck and circumoesophageal connective lesions on posture and locomotion in the cockroach. *J. Comp. Physiol. A Neuroethol. Sens. Neural Behav. Physiol.* 191, 559–573.

Rillich, J., Stevenson, P. A., and Pflueger, H. J. (2013). Flight and walking in locusts–cholinergic co-activation, temporal coupling and its modulation by biogenic amines. *PloS One* 8:e62899. doi: 10.1371/journal.pone.0062899

Ritzmann, R. E., Harley, C. M., Daltorio, K. A., Tietz, B. R., Pollack, A. J., Bender, J. A., et al. (2012). Deciding which way to go: how do insects alter movements to negotiate barriers? *Front. Neurosci.* 6:97. doi: 10.3389/fnins.2012.00097

Ritzmann, R. E., and Quinn, R. D. (2004). "Locomotion in complex terrain," in *Walking: Biological and Technological Aspects. International Centre for Mechanical Sciences (Courses and Lectures)*, eds F. Pfeiffer, and T. Zielinska, (Vienna: Springer).

Ritzmann, R. E., and Zill, S. N. (2017). "Control of locomotion in hexapods," in *The Oxford Handbook of Invertebrate Neurobiology*, ed. J. H. Byrne, (Oxford: Oxford University Press), 1–28.

Roeder, K. D. (1937). The control of tonus and locomotor activity in the praying mantis (*Mantis religiosa* L.). *J. Exp. Zool.* 76, 353–374.

Rosenberg, L., Pflueger, H., Wegener, G., and Libersat, F. (2006). Wasp venom injected into the prey's brain modulates thoracic identified monoaminergic neurons. *J. Neurobiol.* 66, 155–168.

Ryckebusch, S., and Laurent, G. (1993). Rhythmic patterns evoked in locust leg motor neurons by the muscarinic agonist pilocarpine. *J. Neurophysiol.* 69, 1583–1595.

Seelig, J. D., and Jayaraman, V. (2015). Neural dynamics for landmark orientation and angular path integration. *Nature* 521, 186–191. doi: 10.1038/nature14446

Selverston, A. I. (2010). Invertebrate central pattern generator circuits. *Philos. Trans. R. Soc. B Biol. Sci.* 365, 2329–2345.

Serway, C. N., Kaufman, R. R., Serway, C. N., Kaufman, R. R., Strauss, R., and de Belle, J. S. (2009). Mushroom bodies enhance initial motor activity in *Drosophila*. *J. Neurogenet.* 23, 173–184. doi: 10.1080/01677060802572895

Sombati, S., and Hoyle, G. (1984). Generation of specific behaviors in a locust by local release into neuropil of the natural neuromodulator octopamine. *J. Neurobiol.* 15, 481–506.

Staudacher, E. (1998). Distribution and morphology of descending brain neurons in the cricket *Gryllus bimaculatus*. *Cell Tissue Res.* 294, 187–202.

Strausfeld, N. J., and Hirth, F. (2013). Deep homology of arthropod central complex and vertebrate basal ganglia. *Science* 340, 157–161. doi: 10.1126/science.1231828

Strauss, R. (2002). The central complex and the genetic dissection of locomotor behaviour. *Curr. Opin. Neurobiol.* 12, 633–638.

Strauss, R., and Heisenberg, M. (1993). A higher control center of locomotor behavior in the *Drosophila* brain. *J. Neurosci.* 13, 1852–1861.

Tschida, K., and Bhandawat, V. (2015). Activity in descending dopaminergic neurons represents but is not required for leg movements in the fruit fly *Drosophila*. *Physiol. Rep.* 3:e12322. doi: 10.14814/phy2.12322

Turner-Evans, D., Wegener, S., Rouault, H., Franconville, R., Wolff, T., Seelig, J. D., et al. (2017). Angular velocity integration in a fly heading circuit. *Elife* 6:e23496. doi: 10.7554/eLife.23496

Turner-Evans, D. B., and Jayaraman, V. (2016). The insect central complex. *Curr. Biol.* 26, R453–R457. doi: 10.1016/j.cub.2016.04.006

Varga, A. G., and Ritzmann, R. E. (2016). Cellular basis of head direction and contextual cues in the insect brain. *Curr. Biol.* 26, 1816–1828. doi: 10.1016/j.cub.2016.05.037

Wilson, D. M. (1961). The central nervous control of flight in a locust. *J. Exp. Biol.* 38, 471–490.

Wolff, T., Iyer, N. A., and Rubin, G. M. (2015). Neuroarchitecture and neuroanatomy of the *Drosophila* central complex: a GAL4—based dissection of protocerebral bridge neurons and circuits. *J. Comp. Neurol.* 523, 997–1037.

Wosnitza, A., Bockemühl, T., Dübbert, M., Scholz, H., and Büschges, A. (2013). Inter-leg coordination in the control of walking speed in *Drosophila*. *J. Exp. Biol.* 216, 480–491. doi: 10.1242/jeb.078139

Yellman, C., Tao, H., He, B., and Hirsh, J. (1997). Conserved and sexually dimorphic behavioral responses to biogenic amines in decapitated *Drosophila*. *Proc. Natl. Acad. Sci. U.S.A.* 94, 4131–4136.

Zacarias, R., Namiki, S., Card, G. M., Vasconcelos, M. L., and Moita, M. A. (2018). Speed dependent descending control of freezing behavior in *Drosophila melanogaster*. *Nat. Commun.* 9:3697. doi: 10.1038/s41467-018-05875-1

Zill, S., Schmitz, J., and Büschges, A. (2004). Load sensing and control of posture and locomotion. *Arthropod Struct. Dev.* 33, 273–286.

Zorović, M., and Hedwig, B. (2013). Descending brain neurons in the cricket *Gryllus bimaculatus* (de Geer): auditory responses and impact on walking. *J. Comp. Physiol. A Neuroethol. Sens. Neural Behav. Physiol.* 199, 25–34.

Conflict of Interest: The authors declare that the research was conducted in the absence of any commercial or financial relationships that could be construed as a potential conflict of interest.

frontiers in Physiology

ORIGINAL RESEARCH
published: 13 March 2020
doi: 10.3389/fphys.2020.00176

Identification of a General Odorant Receptor for Repellents in the Asian Corn Borer *Ostrinia furnacalis*

Jie Yu[1], Bin Yang[1], Yajun Chang[1,2], Yu Zhang[1,3] and Guirong Wang[1,4]**

[1] State Key Laboratory for Biology of Plant Diseases and Insect Pests, Institute of Plant Protection, Chinese Academy of Agricultural Sciences, Beijing, China, [2] College of Plant Protection, Henan Agricultural University, Zhengzhou, China, [3] Research Center for Grassland Entomology, Inner Mongolia Agricultural University, Hohhot, China, [4] Lingnan Guangdong Laboratory of Modern Agriculture, Genome Analysis Laboratory of the Ministry of Agriculture, Agricultural Genomics Institute at Shenzhen, Chinese Academy of Agricultural Sciences, Shenzhen, China

Attractants and repellents are considered to be an environment-friendly approach for pest management. Odorant receptors (ORs), which are located on the dendritic membranes of olfactory sensory neurons in insects, are essential genes for recognizing attractants and repellents. In the Asian corn borer, *Ostrinia furnacalis*, ORs that respond to sex pheromones have been characterized, but general ORs for plant odorants, especially for repellents, have not been identified. Nonanal is a plant volatile of maize that could result in avoidance of the oviposition process for female adults in *O. furnacalis.* In this study, we identified a female-biased OR that responds to nonanal using a *Xenopus* oocyte expression system. In addition, we found that OfurOR27 was also sensitive to two other compounds, octanal and 1-octanol. Behavioral analysis showed that octanal and 1-octanol also caused female avoidance of oviposition. Our results indicated that *OfurOR27* is an OR that is sensitive to repellents. Moreover, the two newly identified repellents may help to develop a chemical ecology approach for pest control in *O. furnacalis*.

Keywords: odorant receptor, heterologous expression system, host plant volatile, repellent, nonanal

OPEN ACCESS

Edited by:
Philippe Lucas, Institut National de la Recherche Agronomique, France

Reviewed by:
Ya-Nan Zhang, Huaibei Normal University, China
Hao Guo, Chinese Academy of Sciences, China

****Correspondence:***
Bin Yang
byang@ippcaas.cn
Guirong Wang
wangguirong@caas.cn

Specialty section:
This article was submitted to Invertebrate Physiology, a section of the journal Frontiers in Physiology

Received: *26 November 2019*
Accepted: *17 February 2020*
Published: *13 March 2020*

Citation:
Yu J, Yang B, Chang Y, Zhang Y and Wang G (2020) Identification of a General Odorant Receptor for Repellents in the Asian Corn Borer Ostrinia furnacalis. Front. Physiol. 11:176. doi: 10.3389/fphys.2020.00176

INTRODUCTION

Chemical ecology is now established as an approach for pest management. Pheromones have been identified in many insects and are great attractants to interfere with mating behaviors by trapping large numbers of male adults (Witzgall et al., 2010). However, pheromones only attract males, which is a major limitation, because females lay eggs and the mating rate might not be affected if the males can mate many times, as in some species. In this case, plant volatiles are considered to have great application prospects since they were effective for trapping both males and females (Gregg et al., 2010). Some plant volatiles have been identified as involved in oviposition, although the perception mechanism for those plant volatiles was still unknown (Mitchell et al., 1990; Koul et al., 2013). Studies on this topic should help to develop chemical ecology methods for pest management.

Insects have evolved a complex olfactory system to detect various odorants to search for mating partners, locate host plants, identify oviposition sites, and evade toxicants and predators (Bruce et al., 2005; Bruyne and Baker, 2008; Pelletier et al., 2015; Gadenne et al., 2016). Antennae of insects are the main organs for chemoreception and function directly in the process of sensing

environmental information. On the antennae, a variety of sensilla are distributed, which usually contain two or more olfactory sensory neurons (OSNs) inside. Odorant receptors (ORs) are expressed on the dendritic membrane of OSNs for reception of the odorants. The external liposoluble odorant molecules penetrate the pores on the sensilla, go into the lymph, are recognized by odorant-binding proteins (OBPs), and delivered to the ORs. The ORs specifically receive the chemicals, transmitting an electrical signal to the brain, and thereby resulting in corresponding behaviors of insects (Clyne et al., 1999; Hallem et al., 2004; Zwiebel and Takken, 2004; Leal, 2013).

Odorant receptors have always been the core of olfactory research because they are essential in the odor recognition process. The first insect OR was identified in *Drosophila melanogaster* (Clyne et al., 1999; Gao and Chess, 1999). Compared with vertebrate ORs, which are G-protein-coupled receptors, insect ORs have the opposite membrane topology, with their N-terminus inside and their C-terminus outside the cell (Benton et al., 2006; Fleischer et al., 2018). The ORs identified in insects can be divided into two types: the first is the non-conventional OR, the olfactory receptor coreceptor (Orco), which is highly conserved and widely expressed among different insects; the second is the conventional OR, which varies widely among various species (Mombaerts, 1999; Benton et al., 2006). It has been widely accepted that insect ORs transduce chemical signals by forming heteromeric complexes with *Orco* (Sato et al., 2008; Grosse-Wilde et al., 2011).

The number of putative insect ORs identified has increased with the progress in sequencing technology and bioinformatics tools, but still varies considerably among insect species. For example, 66 ORs in *Bombyx mori* (Tanaka et al., 2009) and 65 ORs in *Helicoverpa armigera* (Zhang et al., 2015) were identified based on genome and antennal transcriptomic analysis. Moreover, 170 ORs have been found from the genome of *Apis mellifera* (Robertson and Wanner, 2006). The differences in the number of ORs in different insects is assumed to be driven by certain physiological and ecological demands (Fleischer et al., 2018).

As insect ORs continue to be identified, researchers have begun to study the function of ORs at the molecular and cellular levels. Many ORs in several species have been functionally analyzed by heterologous expression systems *in vitro* or *in vivo*, such as *Xenopus* oocyte expression system or the "empty neuron system" in *Drosophila* (Nakagawa et al., 2005; Wanner et al., 2010; Montagné et al., 2012; Liu et al., 2013; Cao et al., 2016; Gonzalez et al., 2016). Using these systems, functional analyses have been carried out for pheromone receptors and other general ORs in several species, including *B. mori* (Sakurai et al., 2004, 2011; Liu et al., 2017), *D. melanogaster* (Hallem et al., 2004, 2006; Kreher et al., 2005), *Spodoptera littoralis* (Fouchier et al., 2017), *H. armigera* (Liu et al., 2013; Cao et al., 2016; Chang et al., 2016; Di et al., 2017), and *H. assulta* (Chang et al., 2016; Cui et al., 2018).

The Asian corn borer, *Ostrinia furnacalis* (Lepidoptera: Crambidae), feeds on various plants including the economic crop maize, causing serious damage and resulting in about 10–30% yield loss of maize in China (Nafus and Schreiner, 1991; Wang et al., 2000). The whole repertoire of the chemosensory genes expressed in the antennae have been identified in *O. furnacalis*, including 54 ORs, 24 OBPs, 19 chemosensory proteins (CSPs), 21 IRs (ionotropic receptors), 5 GRs (gustatory receptors), 2 sensory neuron membrane proteins (SNMPs), and 26 odorant degrading enzymes (ODEs) (Yang et al., 2015). Among them, ORs have been identified as essential for pheromone sensing (Yang et al., 2016). In addition, all the pheromone receptors have been functionally analyzed for understanding the details of pheromone perception in this species (Liu et al., 2018). General ORs should be considered equally important to the pheromone receptors; however, none of them have been studied in *O. furnacalis*.

Nonanal is a plant volatile of maize, which causes a significant electrophysiological response of gas chromatography–electroantennographic detection (GC-EAD) in females of *O. furnacalis* (Zhang et al., 2018). Behavior studies have confirmed that nonanal at a certain concentration has a repellent effect on the oviposition process for female adults in this species. In this study, we identified a female-biased expressed OR that responds to the repellent nonanal using a *Xenopus* oocyte expression system. In addition, we found that OfurOR27 was also sensitive to two other compounds, octanal and 1-octanol, which were confirmed to be repellents in a subsequent behavioral assay. Our results provide two additional repellents for the Asian corn borer by a reverse chemical ecological method and may help to develop new approaches for controlling this pest.

MATERIALS AND METHODS

Insect Rearing

Ostrinia furnacalis colonies were maintained at laboratory conditions in the Chinese Academy of Agricultural Sciences, Beijing, China. Insects were reared on an artificial diet at 28°C and kept at 15:9 (L/D) and 80% relative humidity. Male and female adults were fed with 10% sugar solution. Tissues including antennae, proboscis, thorax, legs, and sex glands were dissected from 3-day-old adults, immediately placed in liquid nitrogen, and then stored at −80°C until use.

Plant Volatile Organic Compounds

A total of 95 odorants from Sigma-Aldrich were used for this experiment (**Supplementary Table S1**) and were divided into eight groups: pheromone components, green leaf volatiles, terpenoids, aromatics, aldehydes, ketones, alcohols, and esters. All compounds were dissolved in dimethyl sulfoxide (DMSO) at a concentration of 1 M as a stock solution. Before the experiment, the stock solution was diluted to working concentration in 1 × Ringer's buffer, and 1 × Ringer's buffer containing 0.1% DMSO was used as a negative control.

RNA Extraction and cDNA Synthesis

Total RNA from 50 male or female adults was isolated using TRIzol reagent (Invitrogen, Carlsbad, CA, United States) following the manufacturer's instructions. The RNA was dissolved in RNase-free water, and the integrity was assessed by gel electrophoresis. The concentration and purity of RNA were determined on a NanoDrop ND-2000 spectrophotometer

(NanoDrop products, Wilmington, DE, United States). The first-strand complementary DNA (cDNA) was synthesized using the RevertAid First Strand cDNA Synthesis Kit (Fermentas, Vilnius, Lithuania) according to the manufacturer's instructions.

Gene Cloning and Expression Vector Construction of *OfurOR27*

The full-length open reading frame (ORF) encoding *OfurOR27* (Acc. No. LC002721) was obtained from antennal transcriptome and was 1,206 bp in length, encoding for 402 amino acids (Yang et al., 2015). The sequence of *OfurOR27* was cloned using the cDNA isolated from antennae, with primers designed by Primer 5.0 (PREMIER Biosoft International, Palo Alto, CA, United States) (**Table 1**). PrimeSTAR HS DNA polymerase (2 × premix) was used for the PCR reactions (TaKaRa, Dalian, China). A final volume of 50 μl PCR reaction included 25 μl 2 × primerSTAR HS, 2 μl sense and antisense primers (10 mM), 2 μl cDNA, and 19 μl double-distilled H_2O. The PCR reactions were carried out under the following conditions: incubated at 98°C for 3 min; run with 35 cycles of 98°C for 10 s, 55°C for 15 s, 72°C for 1 min 30 s; and incubated at 72°C for 10 min before being held at 4°C. The amplified PCR products were analyzed on a 1.0% agarose gel and inserted into the cloning vector pEASY-Blunt (TransGene Biotech, Beijing, China) and further sequenced to confirm the sequence. The full-length gene sequence of *OfurOR27* was then ligated into a pT7Ts expression vector using a pair of newly designed primers with *Apa*I and *Xho*I restriction sites (**Table 1**). The pT7Ts expression vector of *OfurOrco* (*OfurOR2*) was stored at −80°C (Yang et al., 2015). The accession number in DDBJ is LC002697.

Functional Analysis of OfurOR27 Using a *Xenopus* Oocyte Ectopic Expression System

The expression vector was linearized by restriction enzyme *Sma*I and subsequently used for cRNA synthesis with an mMESSAGE mMACHINE T7 kit (Ambion, Austin, TX, United States). Mature healthy *Xenopus* oocytes (stages V–VII) were incubated with 2 mg/ml collagenase I at pH 7.6 in wash buffer consisting of 96 mM NaCl, 2 mM KCl, 5 mM $MgCl_2$, and 5 mM HEPES (pH 7.6) at room temperature for about 1 h until almost all of them were separated (Liu et al., 2013). After being cultured overnight in an incubator at 18°C, the 1:1 mixture of *OfurOR27* and *OfurOrco* cRNA (27.6 ng each) was microinjected into the oocytes. After an incubation for 2–4 days at 18°C in incubation medium (1 × Ringer's buffer, 5% dialyzed horse serum, 50 mg/ml tetracycline, 100 mg/ml streptomycin, and 550 mg/ml sodium pyruvate), oocytes were connected to a two-electrode voltage clamp, and then, the currents were recorded. Currents induced by odorants were recorded using an OC-725C oocyte clamp (Warner Instruments, Hamden, CT, United States) at a holding potential of −80 mV. Oocytes were exposed to 10^{-4} concentrations of different compounds in a random order for 15 s each, and the interval between exposures allowed the current to return to baseline. Data acquisition and analysis were carried out with Digidata 1440A and Pclamp 10.0 software (Axon Instruments Inc., Union City, CA, United States). At the same time, dose-response data were analyzed using GraphPad Prism 7 (GraphPad Software, San Diego, CA, United States). Statistical comparison of responses to different odors of *OfurOR27* was assessed using GraphPad Prism 7, followed by least-significant difference (LSD) tests.

TABLE 1 | Primers used in this study.

Primers	Sequences 5′–3′	Purpose
OfurOR27-F	ATGTCCGACATAACGCTTTC	Gene cloning
OfurOR27-R	TTATTTGTCGTTGTACATAGTGTAA	
OfurOrco-F	ATGATGACCAAAGTGAAAGCTCAG	
OfurOrco-R	CTACTTCAGTTGTACCAAAACCATGA	
OfurOR27F-RT	CGCTAGCAACTATGGAACAGAC	qPCR
OfurOR27R-RT	GGTTCCAGCAAGACAATGGTG	
OfurActinF-RT	CCGTCCTCCTGACCGAGGCTC	
OfurActinR-RT	GGTGTGGGAGACACCATCTCCG	
OfurOR27F-P	TCAGGGCCCGCCACCATGTCCGACATAACGCTTTC	cRNA synthesizing
OfurOR27R-P	TCACTCGAGTTATTTGTCGTTGTACATAGTGTAA	
OfurOrcoF-P	TCAACTAGTGCCACCATGATGACCAAGTGAAAGCTCAG	
OfurOrcoR-P	TCAGCGGCCGCCTACTTCAGTTGTACCAAAACCATGA	

Tissue-Specific Expression of *OfurOR27*

To reveal the expression level of *OfurOR27* in different tissues of adults, quantitative polymerase chain reaction (qPCR) was performed using cDNA obtained from antennae (A), proboscis (P), thorax (T), legs (L), and sex glands (SG). *OfurActin* was chosen as the reference gene. The primers are listed in **Table 1**. GoTaq qPCR Master Mix (Promega, Madison, WI, United States) was used for qPCR, and the reactions were carried out on an Applied Biosystems 7500 Fast Real-Time PCR System (ABI, Carlsbad, CA, United States). The reactions (20 μl) consisted of 10 μl 2 × GoTaq qPCR Master Mix, 1 μl gene primer (10 mM), 1 μl cDNA, and 8 μl RNase-free water. The conditions were 95°C for 2 min; 40 cycles of 95°C for 15 s; and 60°C for 50 s. Each qPCR reaction was performed in triplicate with three separate biological samples to check for reproducibility. The specificity of the primers was measured using a melting curve, and the amplification efficiency was calculated using a standard curve method. *OfurOR27* relative expression levels were analyzed using the relative $2^{-\Delta CT}$ quantitation method, where $\Delta C_T = C_T$ (*OfurOR27*) – C_T (*OfurActin*). Statistical comparison of expression of *OfurOR27* was assessed using one-way nested analysis of variance (ANOVA), followed by LSD tests.

Bioassay of Oviposition in Gravid Female Adults

Behavior analysis for oviposition was carried on for nonanal and other identified candidate odorants. A net cage (25 × 25 × 25 cm) was used with two pieces of plastic wrap (15 × 15 cm) hanging on opposite sides that contained odorants and solvent, respectively.

Each odorant was diluted into 100 ng/μl with paraffin oil as the solvent. Fifty gravid females were put into the cage, and after 24 h, eggs laid on the two pieces of plastic wrap were collected and counted under a stereomicroscope (Huang et al., 2009). Three repeats were done for each odorant. The preference of oviposition was calculated as: preference (%) = eggs (odorant)/[eggs (odorants) + eggs (control)], following the methods described in Huang et al. (2009).

Single-Sensillum Recording (SSR)

Sensilla trichoidea from 2-day-old female adults were used for the recordings. Individuals were fixed in a 1 ml plastic pipette tip and the settings for recording were the same as discribed in Liu et al. (2018). Tungsten wires were used as electrodes, one was inserted into the sensillun (recording electrode) and another was inserted into the opposite eye (reference electrode). The single-sensillum recording (SSR) system was set up with a air pulse controller CS55 and a data acquisition controller IDAC-4 made by Syntech (Kirchzarten, Germany). Recording was performed under a LEICA Z16 APO microscope at 920 × magnification. AutoSpike software (V3.9, Syntech) was used to analyze the data. Odorants at the concentration of 1 μg/μl were used for the recording.

Phylogenetic Analysis of *OfurOR27*

For the phylogenetic analysis of genes homologous to *OfurOR27*, OR gene repertoires from 14 species in six orders were collected including *O. furnacalis* (Yang et al., 2015), *H. armigera* (Liu et al., 2012; Zhang et al., 2015), *H. assulta* (Zhang et al., 2015), *B. mori* (Wanner et al., 2007), *Chilo suppressalis* (Cao et al., 2014), *Mythimna separata* (Du et al., 2018), *Cydia pomonella* (Walker et al., 2016), *Plutella xylostella* (Yang et al., 2017), *Manduca sexta* (Koenig et al., 2015), *Apis florea* (Karpe et al., 2016), *Locusta migratoria* (Wang et al., 2015), *D. melanogaster* (Clyne et al., 1999; Vosshall et al., 1999; Zwiebel and Takken, 2004), *Apolygus lucorum* (An et al., 2016), and *Acyrthosiphon pisivorum* (Smadja et al., 2009). These species belong to the orders Lepidoptera, Hymenoptera, Orthoptera, Diptera, Hemiptera, and Homoptera. The amino acid sequences were aligned using MAFFT v7.130 (Katoh and Toh, 2010). The phylogenetic tree was constructed and analyzed by the maximum likelihood method using bootstrap replicates with 1,000 × resampling in RAxML version 8 with the Jones–Taylor–Thornton amino acid substitution model (JTT) (Stamatakis, 2014). The transmembrane domains of these genes were predicted using TMHMM version 2.0[1].

RESULTS

OfurOR27 Responds to Nonanal, 1-Octanol, and Octanal

In total, 95 compounds were used to identify candidate ligands of OfurOR27 with a two-electrode voltage clamp. OfurOR27 was identified as responding to nonanal but responded to eight chemical substances in total: 1-octanol, 1-heptanol, octanal, nonyl acetate, heptanal, hexanal, nonanal, and decanal (**Table 2**). Among them, OfurOR27 was most sensitive to nonanal, with responses of about 328.3 ± 41.91 nA. Moreover, OfurOR27 was also sensitive to 1-octanol and octanal, with responses of 260 ± 36.51 nA and 225 ± 43.8 nA, respectively ($p < 0.01$, one-way ANOVA followed LSD test, $n = 6$) (**Figure 1**). The dose–response study confirmed the sensitivity of OfurOR27 to nonanal, 1-octanol, and octanal, with the EC50 value of 3.673×10^{-7} M, 1.406×10^{-5} M, and 1.184×10^{-6} M, respectively (**Figure 1D**). Response values to 1-heptanol, nonyl acetate, heptanal, hexanal, and decanal were not as high, at only ∼100 nA (**Figures 1A–C**).

TABLE 2 | Ligands identified for OfurOR27/Orco.

Name	CAS. No.	Chemical formula	Structural formula
1-Octanol	111-87-5	$C_8H_{18}O$	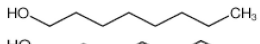
1-Heptanol	111-70-6	$C_7H_{16}O$	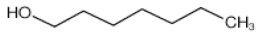
Octanal	124-13-0	$C_8H_{16}O$	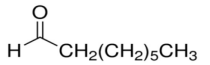
Nonyl acetate	143-13-5	$C_{11}H_{22}O_2$	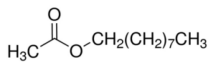
Heptanal	111-71-7	$C_7H_{14}O$	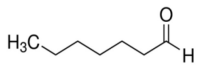
Hexanal	66-25-1	$C_6H_{12}O$	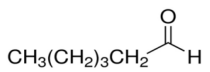
Nonanal	124-19-6	$C_9H_{18}O$	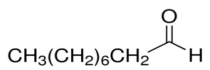
Decanal	112-31-2	$C_{10}H_{20}O$	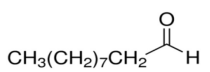

CAS. No., Chemical abstracts Service number.

Tissue Expression Profiles of OfurOR27

The tissue-specific expression analysis indicated that *OfurOR27* was predominantly expressed in the antennae of adults, with relative expression levels of more than 0.1, compared to those in proboscis, thorax, legs, and sex glands, with the relative expression levels of 0.00291, 0.00192, 0.00223, and 0.00255, respectively (**Figure 2**). Moreover, *OfurOR27* showed female-biased expression in the antennae, which was consistent with a previous study (Yang et al., 2015).

Nonanal, 1-Octanol, and Octanal Are Repellents for *O. furnacalis*

Ostrinia furnacalis females laid fewer eggs on the plastic containing nonanal. This result was consistent with a previous study (Zhang et al., 2018). In addition, we identified that 1-octanol and octanal also had a repellent effect causing females to avoid laying eggs while these odorants were present. The preference rates of nonanal, 1-octanol, and octanal were 39.7, 17.3, and 38.8%, respectively (**Figure 3**). Among them, 1-octanol displayed a better effect as a repellent to oviposition for *O. furnacalis* females.

[1]http://www.cbs.dtu.dk/services/TMHMM/

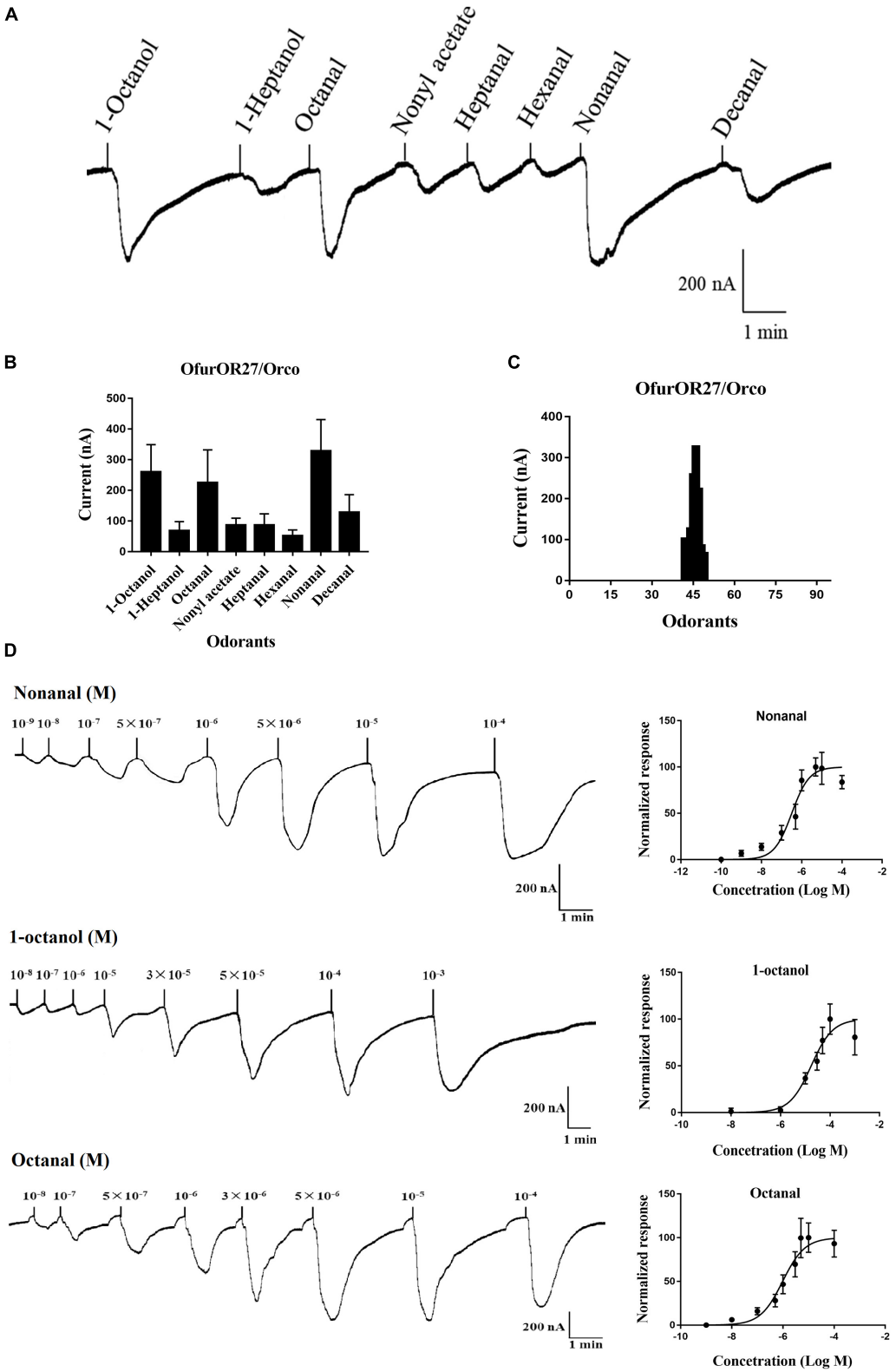

FIGURE 1 | Functional analysis of OfurOR27 using a *Xenopus* oocyte expression system. **(A)** Responses of OfurOR27/Orco to eight identified odorants (10^{-4} M). **(B)** Response profile of OfurOR27/Orco. Error bars indicate standard error of the mean [$p < 0.001$, ANOVA, least-significant difference (LSD), $n = 6$]. **(C)** Tuning curve for the OfurOR27/Orco to an odorant panel comprising 95 odorants, arranged along the *x*-axis according to the strength of the response they elicit. The odorants that elicited the strongest responses were placed near the center of the distribution, while those that elicited the weakest responses were placed near the edges. **(D)** Dose–response curve for OfurOR27/Orco in responding to nonanal, 1-octanol, and octanal. Error bars indicate SEM ($n = 6$).

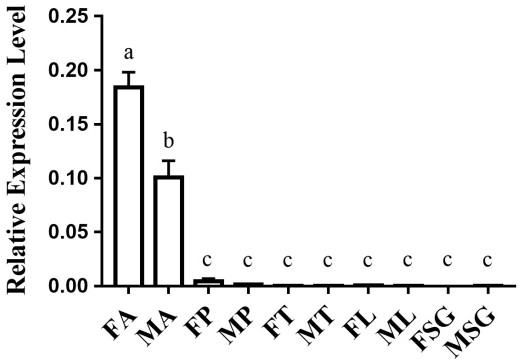

FIGURE 2 | Tissue-specific expression of *OfurOR27* in *O. furnacalis*. FA, female antennae; MA, male antennae; FP, female proboscis; MP, male proboscis; FT, female thorax; MT, male thorax; FL, female legs; ML, male legs; FSG, female sex glands; MSG, male sex glands. Error bars represent the standard error; those labeled with different letters are significantly different [$p < 0.05$, ANOVA, least-significant difference (LSD)].

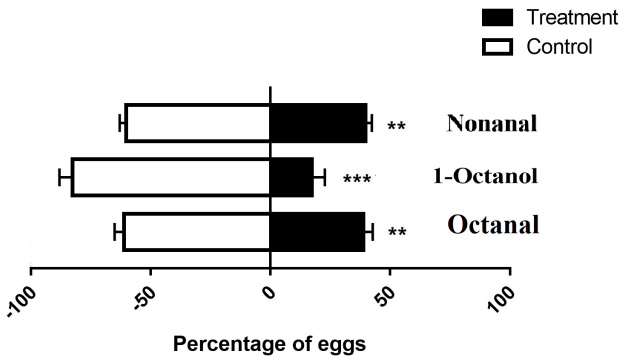

FIGURE 3 | Oviposition assay using three repellents for gravid females in *O. furnacalis*. The black bars indicate the preference of oviposition for each test chemical. The asterisks indicate a significant difference (**$p < 0.01$; ***$p < 0.001$).

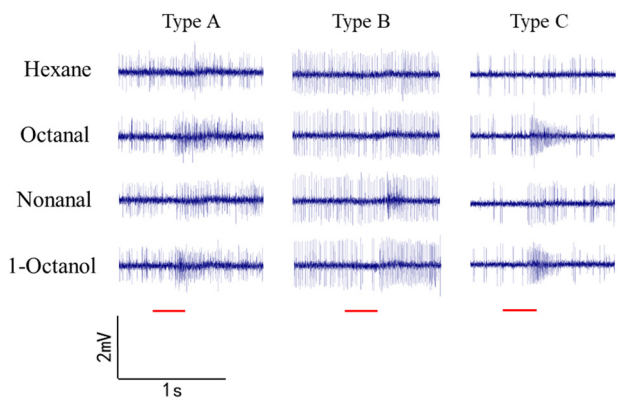

FIGURE 4 | Single sensillum recordings of *s. trichoidea* from female adults in *O. furnacalis*. Three different types (Type A–C) of *s. trichoidea* characterized by the response to nonanal, 1-octanol and octanal. The stimulus was applied for 300 ms which was represented with a red line under the trace.

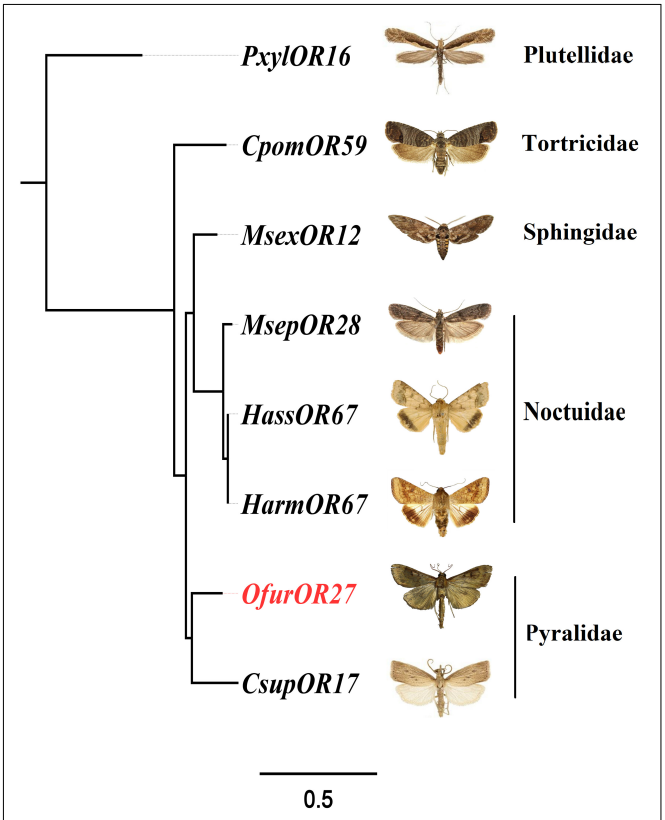

FIGURE 5 | Phylogenetic analysis for *OfurOR27* and its homologous genes. Odorant receptors including *PxylOR16*, *MsexOR12*, *MsepOR28*, *HassOR67*, *HarmOR67*, *CsupOR17*, and *CpomOR59* (**Supplementary Dataset S1**) were downloaded from the National Center for Biotechnology Information. All sequences were aligned using MAFFT software. The phylogenetic analysis was conducted by RAxML version 8. The final tree was visualized by FigTree version 1.4.0 software (http://tree.bio.ed.ac.uk/software/figtree/).

Single-Sensillum Recording for Nonanal, 1-Octanol, and Octanal

Sensilla trichoidea were used for SSR in *O. furnacalis*. Most of the recorded sensilla did not respond to nonanal, 1-octanol, or octanal. Three types of sensilla responded to the odorants (**Figure 6**). Type A is a short sensilla trichoidea mainly distributed on the side of the female antennae, while types B and C are long sensilla trichoidea at the center of the female antennae. Type C responded to nonanal, 1-octanol, and octanal. Type A responded to 1-octanol and octanal. Type B seemed to only respond to nonanal, but we only recorded it once, possibly due to interference by insect movement.

Phylogenetic Analysis of Homologous Genes of *OfurOR27*

To identify homologous genes of *OfurOR27*, phylogenetic analysis was carried out with 1,075 ORs from 14 species. Seven ORs clustered into the same clade with *OfurOR27*, including *PxylOR16*, *MsexOR12*, *MsepOR28*, *HassOR67*, *HarmOR67*, *CsupOR17*, and *CpomOR59* from five families in Lepidoptera (**Figure 4**). Homologous genes were only found in lepidoptera

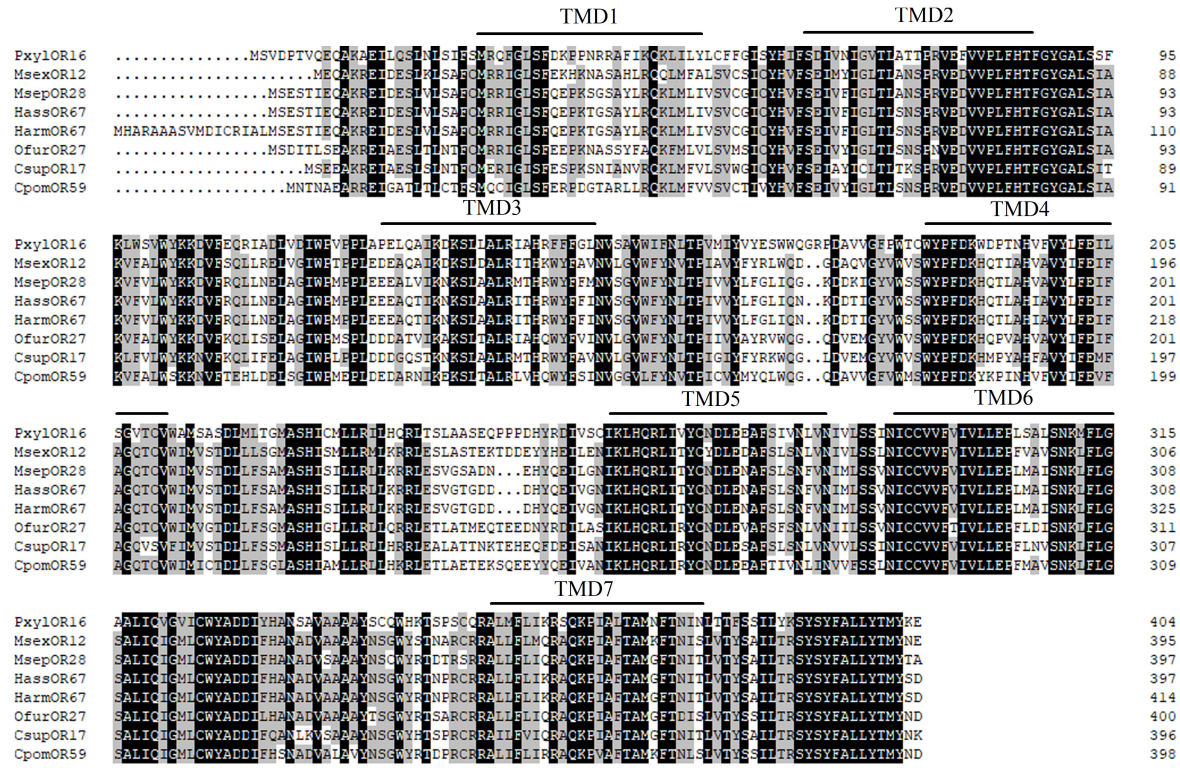

FIGURE 6 | Alignment of the amino acid sequences of *OfurOR27* and its homologous genes. The transmembrane domains of genes were predicted using TMHMM version 2.0 (http://www.cbs.dtu.dk/services/TMHMM/), and sequences were aligned using DNAMAN version 8 software (Lynnon LLC, San Ramon, CA, United States). Amino acids identical in all sequences were marked with black shading. Numbers to the left refer to the position of the last residue in a line in each odorant receptor (OR) sequence. The horizontal lines indicated the position of predicted transmembrane domains.

insects, but no homologous genes were found in *B. mori*. We speculated that degradation may have occurred in *B. mori*. All the homologous genes were aligned with *OfurOR27*. The correlation prediction software was used to predict the number of transmembrane structures of seven ORs, and the results showed that they all have seven transmembrane domains and the N-terminus was located within the cell membrane (**Figure 5**). Sequence alignment of *OfurOR27* with its seven orthologous genes showed that they shared 77.56% amino acid identity. Moreover, *PxylOR16*, *MsexOR12*, *MsepOR28*, *HassOR67*, *HarmOR67*, *CsupOR17*, and *CpomOR59* were aligned with *OfurOR27* and found to have 56.67, 73.81, 69.29, 70, 70, 72.62, and 69.52% identity, respectively.

DISCUSSION

Use of chemical pesticides is still the primary approach for controlling pests. Integrated pest management (IPM) has been strongly advocated in modern agriculture. The new approach of pest management using chemical ecology is an important part of IPM. Attractants such as pheromones have been applied controlling various pests due to a high degree of commercialization. For repellents, only a few compounds have been made as commercial products. The most famous odorant is *N,N*-diethyl-m-toluamide (DEET), which was an effective broad-spectrum mosquito repellent (Bressac and Chevrier, 1998). However, most of these repellents were identified for controlling pests of human health concern such as mosquitos and cockroaches (Li and Boyaro, 2002). For agricultural pests, the "pull and push" strategy was favored. In this strategy, researchers combined attractants and repellents together to control pests (Miller and Cowles, 1990). Recently, herbivore-induced plant volatiles were identified to mediate tritrophic interactions (Turlings and Erb, 2018). This research opened a new approach for pest management through chemical ecology.

Olfaction allows insects to distinguish chemical signals to complete a series of behaviors, such as locating food, sexual partners, and oviposition sites. To successfully perform these behaviors, the sensitive olfactory system of insects must respond to chemical stimuli at the appropriate time (Gadenne et al., 2016). Previous studies have shown that some general ORs may be involved in the common behaviors in both males and females (Zhang et al., 2013), whereas other ORs with biased expression in females or males may be involved in sex-specific behaviors (Anderson et al., 2009; Liu et al., 2014; Yan et al., 2015). Plant volatiles such as linalool, benzoic acid, and 2-phenylethanol have been used as oviposition clues for some female moths (Røstelien et al., 2005; Anderson et al., 2009). Some ORs are functionally characterized as receptors to these key compounds

(Anderson et al., 2009; Jordan et al., 2009). OR4 from domestic mosquitoes selectively responds to the released odor of humans and functions directly in host identification and blood sucking (McBride et al., 2014). *AlucOR46* might be related to locate the host plants of *Apolygus lucorum* (Zhang et al., 2016). However, many other ORs are still orphans, and we lack overall awareness of how insects detect plant volatiles.

In this study, we identified an OR with female-biased expression that responds to the repellent nonanal using a *Xenopus* oocyte expression system. In addition, we found that OfurOR27 was also sensitive to two other compounds, octanal and 1-octanol, which were confirmed to be repellents by a subsequent behavioral assay. Single-sensillum recordings were conducted for nonanal, octanal, and 1-octanol, and indicated that *OfurOR27* may be expressed on the sensilla trichoidea. Octanal is a plant green leaf compound, which was confirmed to significantly repel mosquitoes (Logan et al., 2010). Moreover, 1-octanol, an aroma component of tea, may not be a repellent for pest, but it is an attractant for natural enemies *Sphaerophoria menthastri* and *Chrysopa pallens* in tea gardens (Han and Zhou, 2004). Phylogenetic analysis showed that some pest species have genes homologous to *OfurOR27*, which might indicate that they have similar functions and that all three repellents might be applied in other species.

Above all, our results indicated that OfurOR27 is one of the corresponding ORs for nonanal, octanal, and 1-octanol, which all negatively affect *O. furnacalis*. A further study should be carried out to identify other ORs that respond to the three repellents to clarify the molecular mechanism of chemosensation for each odorant. Using reverse chemical ecology, we determined that OfurOR27 is a common receptor for repellents and found two additional repellents for *O. furnacalis*, which may contribute to developing environment-friendly approaches to control this maize pest.

DATA AVAILABILITY STATEMENT

The data relating to OfurOR27 (LC002721) may be accessed from the DDBJ website: http://getentry.ddbj.nig.ac.jp/getentry/na/LC002721/?format=flatfile&filetype=html&trace=true&show_suppressed=false&limit=10.

AUTHOR CONTRIBUTIONS

GW and BY designed the experiments. JY, YC, and YZ carried out the experiments. JY and BY analyzed the experimental results. JY and BY wrote the manuscript.

FUNDING

This work was supported by the National Natural Science Foundation of China (31701859, 31725023, and 31621064).

ACKNOWLEDGMENTS

We thank Song Cao, Yipeng Liu, and Nana Ma (Institute of Plant Protection, Chinese Academy of Agricultural Sciences) for help with molecular biology experiments. We thank Ms. Qiuyan Wang (Institute of Plant Protection, Chinese Academy of Agricultural Sciences) for rearing insects.

SUPPLEMENTARY MATERIAL

The Supplementary Material for this article can be found online at: https://www.frontiersin.org/articles/10.3389/fphys.2020.00176/full#supplementary-material

REFERENCES

An, X. K., Sun, L., Liu, H. W., Liu, D. F., Ding, Y. X., Li, L. M., et al. (2016). Identification and expression analysis of an olfactory receptor gene family in green plant bug Apolygus lucorum (Meyer-Dür). *Sci. Rep.* 6:37870. doi: 10.1038/srep37870

Anderson, A. R., Wanner, K. W., Trowell, S. C., Warr, C. G., Jaquin-Joly, E., Zagatti, P., et al. (2009). Molecular basis of female-specific odorant responses in Bombyx mori. *Insect. Biochem. Mol. Biol.* 39, 189–197. doi: 10.1016/j.ibmb.2008.11.002

Benton, R., Sachse, S., Michnick, S. W., and Vosshall, L. B. (2006). Atypical membrane topology and heteromeric function of Drosophila odorant receptors in vivo. *PLoS Biol.* 4:e20. doi: 10.1371/journal.pbio.0040020

Bressac, C., and Chevrier, C. (1998). Offspring and sex ratio are independent of sperm management in Eupelmus orientalis females. *J. Insect Physiol.* 44, 351–359. doi: 10.1016/s0022-1910(97)00119-4

Bruce, T. J., Wadhams, L. J., and Woodcock, C. M. (2005). Insect host location: a volatile situation. *Trends Plant Sci.* 10, 269–274. doi: 10.1016/j.tplants.2005.04.003

Bruyne, M. D., and Baker, T. C. (2008). Odor detection in insects: volatile codes. *J. Chem. Ecol.* 34, 882–897. doi: 10.1007/s10886-008-9485-4

Cao, D., Liu, Y., Wei, J., Liao, X., Walker, W. B., Li, J., et al. (2014). Identification of Candidate Olfactory Genes in Chilo suppressalis by Antennal Transcriptome Analysis. *Int. J. Biol. Sci.* 10, 846–860. doi: 10.7150/ijbs.9297

Cao, S., Liu, Y., Guo, M., and Wang, G. (2016). A conserved odorant receptor tuned to floral volatiles in three heliothinae species. *PLoS One* 11:e0155029. doi: 10.1371/journal.pone.0155029

Chang, H., Guo, M., Wang, B., Liu, Y., Dong, S., and Wang, G. (2016). Sensillar expression and responses of olfactory receptors reveal different peripheral coding in two Helicoverpa species using the same pheromone components. *Sci. Rep.* 6:18742. doi: 10.1038/srep18742

Clyne, P. J., Warr, C. G., Freeman, M. R., Lessing, D., Kim, J., and Carlson, J. R. (1999). A novel family of divergent seven-transmembrane proteins: candidate odorant receptors in Drosophila. *Neuron* 22, 327–338. doi: 10.1016/s0896-6273(00)81093-4

Cui, W. C., Wang, B., Guo, M. B., Liu, Y., Jacquin-Joly, E., Yan, S. C., et al. (2018). A receptor-neuron correlate for the detection of attractive plant volatiles in Helicoverpa assulta (Lepidoptera: Noctuidae). *Insect Biochem. Mol. Biol.* 97, 31–39. doi: 10.1016/j.ibmb.2018.04.006

Di, C., Ning, C., Huang, L. Q., and Wang, C. Z. (2017). Design of larval chemical attractants based on odorant response spectra of odorant receptors in the cotton bollworm. *Insect Biochem. Mol. Biol.* 84, 48–62. doi: 10.1016/j.ibmb.2017.03.007

Du, L., Zhao, X., Liang, X., Gao, X., Liu, Y., and Wang, G. (2018). Identification of candidate chemosensory genes in Mythimna separata by transcriptomic analysis. *BMC Genom.* 19:518. doi: 10.1186/s12864-018-4898-0

Fleischer, J., Pregitzer, P., Breer, H., and Krieger, J. (2018). Access to the odor world: olfactory receptors and their role for signal transduction in insects. *Cell. Mole. Life Sci.* 75, 485–508. doi: 10.1007/s00018-017-2627-5

Fouchier, A. D., Walker, W. B., Montagné, N., Steiner, C., Binyameen, M., Schlyter, F., et al. (2017). Functional evolution of Lepidoptera olfactory receptors revealed by deorphanization of a moth repertoire. *Nat. Commun.* 8, 15709. doi: 10.1038/ncomms15709

Gadenne, C., Barrozo, R. B., and Anton, S. (2016). Plasticity in Insect Olfaction: To Smell or Not to Smell? *Annu. Rev. Entomol.* 61, 317–333. doi: 10.1146/annurev-ento-010715-023523

Gao, Q., and Chess, A. (1999). Identification of candidate Drosophila olfactory receptors from genomic DNA sequence. *Genomics* 60, 31–39. doi: 10.1006/geno.1999.5894

Gonzalez, F., Witzgall, P., and Walker Iii, W. B. (2016). Protocol for heterologous expression of insect odourant receptors in Drosophila. *Front. Ecol. Evol.* 4:24. doi: 10.3389/fevo.2016.00024

Gregg, P. C., Del Socorro, A. P., and Henderson, G. S. (2010). Development of a synthetic plant volatile−based attracticide for female noctuid moths. II. Bioassays of synthetic plant volatiles as attractants for the adults of the cotton bollworm, Helicoverpa armigera (Hübner)(*Lepidoptera*: *Noctuidae*). *Austr. J. Entomol.* 49, 21–30. doi: 10.1111/j.1440-6055.2009.00734.x

Grosse-Wilde, E., Kuebler, L. S., Bucks, S., Vogel, H., Wicher, D., and Hansson, B. S. (2011). Antennal transcriptome of Manduca sexta. *Proc. Nat. Acad. Sci.* 108, 7449–7454. doi: 10.1073/pnas.1017963108

Hallem, E. A., Dahanukar, A., and Carlson, J. R. (2006). Insect odor and taste receptors. *Annu. Rev. Entomol.* 51, 113–135. doi: 10.1146/annurev.ento.51.051705.113646

Hallem, E. A., Ho, M. G., and Carlson, J. R. (2004). The molecular basis of odor coding in the Drosophila antenna. *Cell* 117, 965–979. doi: 10.1016/j.cell.2004.05.012

Han, B., and Zhou, C. (2004). The attraction of major volatiles from tea leaves and Camellia to the *Sphaerophoria menthastri* and *Chrysopa pallens*. *Chin. J. Appl. Ecol.* 4, 623–626.

Huang, C. H., Yan, F. M., Byers, J. A., Wang, R. J., and Xu, C. R. (2009). Volatiles induced by the larvae of the Asian corn borer (*Ostrinia furnacalis*) in maize plants affect behavior of conspecific larvae and female adults. *Insect Sci.* 16, 311–320. doi: 10.1111/j.1744-7917.2009.01257.x

Jordan, M. D., Anderson, A., Begum, D., Carraher, C., Authier, A., Marshall, S. D., et al. (2009). Odorant receptors from the light brown apple moth (Epiphyas postvittana) recognize important volatile compounds produced by plants. *Chem. Sen.* 34, 383–394. doi: 10.1093/chemse/bjp010

Karpe, S. D., Jain, R., Brockmann, A., and Sowdhamini, R. (2016). Identification of complete repertoire of *Apis florea* odorant receptors reveals complex orthologous relationships with *Apis mellifera*. *Genome. Biol. Evol.* 8, 2879–2895. doi: 10.1093/gbe/evw202

Katoh, K., and Toh, H. (2010). Parallelization of the MAFFT multiple sequence alignment program. *Bioinformatics* 26, 1899–1900. doi: 10.1093/bioinformatics/btq224

Koenig, C., Hirsh, A., Bucks, S., Klinner, C., Vogel, H., Shukla, A., et al. (2015). A reference gene set for chemosensory receptor genes of Manduca sexta. *Insect Biochem. Mol. Biol.* 66, 51–63. doi: 10.1016/j.ibmb.2015.09.007

Koul, O., Singh, R., Kaur, B., and Kanda, D. (2013). Comparative study on the behavioral response and acute toxicity of some essential oil compounds and their binary mixtures to larvae of Helicoverpa armigera, Spodoptera litura and Chilo partellus. *Indust. Crops Products* 49, 428–436. doi: 10.1016/j.indcrop.2013.05.032

Kreher, S. A., Kwon, J. Y., and Carlson, J. R. (2005). The molecular basis of odor coding in the Drosophila larva. *Neuron* 46, 445–456. doi: 10.1016/j.neuron.2005.04.007

Leal, W. S. (2013). Odorant reception in insects: roles of receptors, binding proteins, and degrading enzymes. *Annu. Rev. Entomol.* 58, 373–391. doi: 10.1146/annurev-ento-120811-153635

Li, Q., and Boyaro. (2002). Past, present and future of insect repellents. *Modern Agrochem.* 5,

Liu, C., Liu, Y., Guo, M., Cao, D., Dong, S., and Wang, G. (2014). Narrow tuning of an odorant receptor to plant volatiles in Spodoptera exigua (H übner). *Insect Mole. Biol.* 23, 487–496. doi: 10.1111/imb.12096

Liu, Q., Liu, W., Zeng, B., Wang, G., Hao, D., and Huang, Y. (2017). Deletion of the *Bombyx mori* odorant receptor co-receptor (*BmOrco*) impairs olfactory sensitivity in silkworms. *Insect Biochem. Mole. Biol.* 86, 58–67. doi: 10.1016/j.ibmb.2017.05.007

Liu, W., Jiang, X. C., Cao, S., Yang, B., and Wang, G. R. (2018). Functional studies of sex pheromone receptors in asian corn borer *Ostrinia furnacalis*. *Front. Physiol.* 9:591. doi: 10.3389/fphys.2018.00591

Liu, Y., Gu, S., Zhang, Y., Guo, Y., and Wang, G. (2012). Candidate olfaction genes identified within the *Helicoverpa armigera* antennal transcriptome. *PLoS One* 7:e48260. doi: 10.1371/journal.pone.0048260

Liu, Y., Liu, C., Lin, K., and Wang, G. (2013). Functional specificity of sex pheromone receptors in the cotton bollworm *Helicoverpa armigera*. *PLoS One* 8:e62094. doi: 10.1371/journal.pone.0062094

Logan, J. G., Stanczyk, N. M., Hassanali, A., Kemei, J., Santana, A. E., Ribeiro, K. A., et al. (2010). Arm-in-cage testing of natural human-derived mosquito repellents. *Mal. J.* 9:239. doi: 10.1186/1475-2875-9-239

McBride, C. S., Baier, F., Omondi, A. B., Spitzer, S. A., Lutomiah, J., Sang, R., et al. (2014). Evolution of mosquito preference for humans linked to an odorant receptor. *Nature* 515:222. doi: 10.1038/nature13964

Miller, J. R., and Cowles, R. S. (1990). Stimulo-deterrent diversion: a concept and its possible application to onion maggot control. *J. Chem. Ecol.* 16, 3197–3212. doi: 10.1007/BF00979619

Mitchell, E. R., Tingle, P. C., and Heath, R. R. (1990). Ovipositional response of three Heliothis species (Lepidoptera: Noctuidae) to allelochemicals from cultivated and wild host plants. *J. Chem. Ecol.* 16, 1817–1827. doi: 10.1007/bf01020496

Mombaerts, P. (1999). Molecular biology of odorant receptors in vertebrates. *Annu. Rev. Neurosci.* 22, 487–509. doi: 10.1146/annurev.neuro.22.1.487

Montagné, N., Chertemps, T., Brigaud, I., François, A., François, M. C., De Fouchier, A., et al. (2012). Functional characterization of a sex pheromone receptor in the pest moth Spodoptera littoralis by heterologous expression in Drosophila. *Eur. J. Neurosci.* 36, 2588–2596. doi: 10.1111/j.1460-9568.2012.08183.x

Nafus, D. M., and Schreiner, I. H. (1991). Review of the biology and control of the Asian corn borer, *Ostrinia furnacalis* (Lep: Pyralidae). *Int. J. Pest Manag.* 37, 41–56. doi: 10.1080/09670879109371535

Nakagawa, T., Sakurai, T., Nishioka, T., and Touhara, K. (2005). Insect sex-pheromone signals mediated by specific combinations of olfactory receptors. *Science* 307, 1638–1642. doi: 10.1126/science.1106267

Pelletier, J., Xu, P., Yoon, K. S., Clark, J. M., and Leal, W. S. (2015). Odorant receptor-based discovery of natural repellents of human lice. *Insect Biochem. Mole. Biol.* 66, 103–109. doi: 10.1016/j.ibmb.2015.10.009

Robertson, H. M., and Wanner, K. W. (2006). The chemoreceptor superfamily in the honey bee, Apis mellifera: expansion of the odorant, but not gustatory, receptor family. *Genome Res.* 16, 1395–1403. doi: 10.1101/gr.5057506

Røstelien, T., Stranden, M., Borg-Karlson, A. K., and Mustaparta, H. (2005). Olfactory receptor neurons in two heliothine moth species responding selectively to aliphatic green leaf volatiles, aromatic compounds, monoterpenes and sesquiterpenes of plant origin. *Chem. Senses* 30, 443–461. doi: 10.1093/chemse/bji039

Sakurai, T., Mitsuno, H., Haupt, S. S., Uchino, K., Yokohari, F., Nishioka, T., et al. (2011). A single sex pheromone receptor determines chemical response specificity of sexual behavior in the silkmoth *Bombyx mori*. *PLoS Genetics* 7:e1002115. doi: 10.1371/journal.pgen.1002115

Sakurai, T., Nakagawa, T., Mitsuno, H., Mori, H., Endo, Y., Tanoue, S., et al. (2004). Identification and functional characterization of a sex pheromone receptor in the silkmoth *Bombyx mori*. *Proc. Nat. Acad. Sci.* 101, 16653–16658. doi: 10.1073/pnas.0407596101

Sato, K., Pellegrino, M., Nakagawa, T., Nakagawa, T., Vosshall, L. B., and Touhara, K. (2008). Insect olfactory receptors are heteromeric ligand-gated ion channels. *Nature* 452, 1002. doi: 10.1038/nature06850

Smadja, C., Shi, P., Butlin, R. K., and Robertson, H. M. (2009). Large gene family expansions and adaptive evolution for odorant and gustatory receptors in the pea aphid. Acyrthosiphon pisum. *Mol. Biol. Evol.* 26, 2073–2086. doi: 10.1093/molbev/msp116

Stamatakis, A. (2014). RAxML version 8: a tool for phylogenetic analysis and post-analysis of large phylogenies. *Bioinformatics* 30, 1312–1313. doi: 10.1093/bioinformatics/btu033

Tanaka, K., Uda, Y., Ono, Y., Nakagawa, T., Suwa, M., Yamaoka, R., et al. (2009). Highly selective tuning of a silkworm olfactory receptor to a key mulberry leaf volatile. *Curr. Biol.* 21:623. doi: 10.1016/j.cub.2011.03.046

Turlings, T. C. J., and Erb, M. (2018). Tritrophic interactions mediated by herbivore-induced plant volatiles: mechanisms, ecological relevance, and application potential. *Annu. Rev. Entomol.* 63, 433–452. doi: 10.1146/annurev-ento-020117-043507

Vosshall, L. B., Amrein, H., Morozov, P. S., Rzhetsky, A., and Axel, R. (1999). A spatial map of olfactory receptor expression in the Drosophila antenna. *Cell* 96, 725–736. doi: 10.1016/s0092-8674(00)80582-6

Walker III, W. B., Gonzalez, F., Garczynski, S. F., and Witzgall, P. (2016). The chemosensory receptors of codling moth *Cydia pomonella* – expression in larvae and adults. *Sci. Rep.* 6:23518. doi: 10.1038/srep23518

Wang, Z., Lu, X., He, K., and Zhou, D. (2000). Review of history, present situation and prospect of the Asian maize borer research in China. *Yournal of Shenyang Agricult. University* 31, 402–412.

Wang, Z., Yang, P., Chen, D., Jiang, F., Li, Y., Wang, X., et al. (2015). Identification and functional analysis of olfactory receptor family reveal unusual characteristics of the olfactory system in the migratory locust. *Cell. Mol. Life Sci.* 72, 4429–4443. doi: 10.1007/s00018-015-2009-9

Wanner, K., Anderson, A., Trowell, S., Theilmann, D., Robertson, H. M., and Newcomb, R. (2007). Female−biased expression of odourant receptor genes in the adult antennae of the silkworm. Bombyx mori. *Insect Mol Biol.* 16, 107–119. doi: 10.1111/j.1365-2583.2007.00708.x

Wanner, K. W., Nichols, A. S., Allen, J. E., Bunger, P. L., Garczynski, S. F., Linn, C. E. Jr., et al. (2010). Sex pheromone receptor specificity in the European corn borer moth. Ostrinia nubilalis. *PLoS One* 5:e8685. doi: 10.1371/journal.pone.0008685

Witzgall, P., Kirsch, P., and Cork, A. (2010). Sex Pheromones and Their Impact on Pest Management. *J. Chem. Ecol.* 36, 80–100. doi: 10.1007/s10886-009-9737-y

Yan, S. W., Zhang, J., Liu, Y., Li, G. Q., and Wang, G. R. (2015). An olfactory receptor from *Apolygus lucorum* (Meyer-Dur) mainly tuned to volatiles from flowering host plants. *J. Insect Physiol.* 79, 36–41. doi: 10.1016/j.jinsphys.2015.06.002

Yang, B., Fujii, T., Ishikawa, Y., and Matsuo, T. (2016). Targeted mutagenesis of an odorant receptor co-receptor using TALEN in Ostrinia furnacalis. *Insect Biochem. Mol. Biol.* 70, 53–59. doi: 10.1016/j.ibmb.2015.12.003

Yang, B., Ozaki, K., Ishikawa, Y., and Matsuo, T. (2015). Identification of candidate odorant receptors in asian corn borer Ostrinia furnacalis. *PLoS One* 10:e0121261. doi: 10.1371/journal.pone.0121261

Yang, S., Cao, D., Wang, G., and Liu, Y. (2017). Identification of genes involved in chemoreception in *Plutella xyllostella* by antennal transcriptome analysis. *Scienti. Rep.* 7:11941. doi: 10.1038/s41598-017-11646-7

Zhang, J., Liu, C., Yan, S., Liu, Y., Guo, M., Dong, S., et al. (2013). An odorant receptor from the common cutworm (*Spodoptera litura*) exclusively tuned to the important plant volatile cis−3−H exenyl acetate. *Insect Mole. Biol.* 22, 424–432. doi: 10.1111/imb.12033

Zhang, J., Wang, B., Dong, S., Cao, D., Dong, J., Walker, W. B., et al. (2015). Antennal transcriptome analysis and comparison of chemosensory gene families in two closely related noctuidae moths. Helicoverpa armigera and H. assulta. *PLoS One* 10:e0117054. doi: 10.1371/journal.pone.0117054

Zhang, W., Wang, W., Bai, S., Zhang, T., He, K., and Wang, Z. (2018).). Screening of host plants for spawning preference of females of Asian corn borer and electrophysiological responses to volatile chemical constituents of Valeriana. *Acta Entomol. Sin.* 61, 224–231.

Zhang, Z., Zhang, M., Yan, S., Wang, G., and Liu, Y. (2016). A female-biased odorant receptor from *Apolygus lucorum* (Meyer-Dür) tuned to some plant odors. *Int. J. Mol. Sci.* 17:1165. doi: 10.3390/ijms17081165

Zwiebel, L., and Takken, W. (2004). Olfactory regulation of mosquito–host interactions. *Insect Biochem. Mol. Biol* 34, 645–652. doi: 10.1016/j.ibmb.2004.03.017

Conflict of Interest: The authors declare that the research was conducted in the absence of any commercial or financial relationships that could be construed as a potential conflict of interest.

frontiers in Physiology

ORIGINAL RESEARCH
published: 17 March 2020
doi: 10.3389/fphys.2020.00221

The Role of Serotonin in the Influence of Intense Locomotion on the Behavior Under Uncertainty in the Mollusk *Lymnaea stagnalis*

Hitoshi Aonuma[1,2†], Maxim Mezheritskiy[3†], Boris Boldyshev[4], Yuki Totani[5], Dmitry Vorontsov[3], Igor Zakharov[3], Etsuro Ito[5] and Varvara Dyakonova[3]*

[1] Research Center of Mathematics for Social Creativity, Research Institute for Electronic Science, Hokkaido University, Hokkaido, Japan, [2] Core Research for Evolutional Science and Technology (CREST), Japan Science and Technology Agency, Saitama, Japan, [3] Koltzov Institute of Developmental Biology of the Russian Academy of Sciences (RAS), Moscow, Russia, [4] Trapeznikov Institute of Control Sciences of Russian Academy of Sciences (RAS), Moscow, Russia, [5] Department of Biology, Waseda University, Tokyo, Japan

OPEN ACCESS

Edited by:
Sylvia Anton,
Institut National de la Recherche Agronomique, France

Reviewed by:
Jean-Marc Devaud,
Université Toulouse III Paul Sabatier, France
Russell Wyeth,
St. Francis Xavier University, Canada

***Correspondence:**
Varvara Dyakonova
dyakonova.varvara@gmail.com

[†] These authors have contributed equally to this work

Specialty section:
This article was submitted to Invertebrate Physiology, a section of the journal Frontiers in Physiology

Received: 26 April 2019
Accepted: 26 February 2020
Published: 17 March 2020

Citation:
Aonuma H, Mezheritskiy M, Boldyshev B, Totani Y, Vorontsov D, Zakharov I, Ito E and Dyakonova V (2020) The Role of Serotonin in the Influence of Intense Locomotion on the Behavior Under Uncertainty in the Mollusk Lymnaea stagnalis. Front. Physiol. 11:221. doi: 10.3389/fphys.2020.00221

The role of serotonin in the immediate and delayed influence of physical exercise on brain functions has been intensively studied in mammals. Recently, immediate effects of intense locomotion on the decision-making under uncertainty were reported in the Great Pond snail, *Lymnaea stagnalis* (Korshunova et al., 2016). In this animal, serotonergic neurons control locomotion, and serotonin modulates many processes underlying behavior, including cognitive ones (memory and learning). Whether serotonin mediates the behavioral effects of intense locomotion in mollusks, as it does in vertebrates, remains unknown. Here, the delayed facilitating effects of intense locomotion on the decision-making in the novel environment are described in *Lymnaea*. Past exercise was found to alter the metabolism of serotonin, namely the content of serotonin precursor and its catabolites in the cerebral and pedal ganglia, as measured by high-performance liquid chromatography. The immediate and delayed effects of exercise on serotonin metabolism were different. Moreover, serotonin metabolism was regulated differently in different ganglia. Pharmacological manipulations of the serotonin content and receptor availability suggests that serotonin is likely to be responsible for the locomotor acceleration in the test of decision-making under uncertainty performed after exercise. However, the exercise-induced facilitation of decision-making (manifested in a reduced number of turns during the orienting behavior) cannot be attributed to the effects of serotonin.

Keywords: serotonin, decision-making, mollusks, effect of exercise on the brain, goal-directed locomotion

INTRODUCTION

The influence of physical exercise on brain function has been thoroughly investigated in various mammalian species (van Praag et al., 1999; Salmon, 2001; Cotman et al., 2007; Hillman et al., 2008; Roig et al., 2012; Laurence et al., 2015). It has been suggested that feedforward brain activation caused by intense locomotion is a widespread phenomenon throughout the animal kingdom that

may be especially beneficial for subsequent orientation and adaptation in the novel environment (Stevenson et al., 2005; Dyakonova and Krushinsky, 2008; Korshunova et al., 2016).

In mammals, physical activity affects neuromodulatory and neurotrophic systems (Heijnen et al., 2016), namely, the serotonergic and dopaminergic systems (Kondo and Shimada, 2015; Heijnen et al., 2016), endogenous opioid and cannabinoid systems (Heijnen et al., 2016), brain-derived neurotrophic factor (BDNF) (Vaynman et al., 2004), insulin-like growth factor-1 (Carro et al., 2001), and other factors and neuromodulators (Heijnen et al., 2016). The increased release of these factors activates neurogenesis in the hippocampus (van Praag et al., 1999, Lee et al., 2013). The later had been considered a key factor for improved cognitive performance after exercise. However, stimulation of neurogenesis alone was recently found to be insufficient to reproduce the behavioral effects of exercise in rodents (Choi et al., 2018). Activation of BDNF synthesis and release, known to have strong interactions with the serotonergic system (Popova et al., 2017), is required to mimic these effects (Choi et al., 2018). Strong effects of intense locomotion on subsequent behavior are reported in a distantly related group of animals, the protostomes (Hofmann and Stevenson, 2000; Dyakonova and Krushinsky, 2008; Korshunova et al., 2016), suggesting that mechanisms other than augmentation of hippocampal neurogenesis can mediate the behavioral benefits of exercise.

Previously, we reported that the behavioral effects of intense locomotion in the *Lymnaea stagnalis* snail are, in many aspects, similar to those observed in rodents and humans, with a decrease in defensive responses, an increase in general activity (D'yakonova, 2014) and a facilitation of decision-making in the novel environment (Korshunova et al., 2016). Terrestrial-like crawling in low water for 2 h prior to the test promoted the transition from slow circular locomotion to the fast goal-oriented crawl in asymmetrically lit arena (Korshunova et al., 2016). We concluded that exercise "facilitates the transition from uncertainty to decision-making in snails."

Serotonin activates many forms of behavior (Sakharov, 1990; Gillette, 2006) and participates in the regulation of cognitive functions, such as learning and memory, in mollusks (Balaban et al., 2016; Nikitin et al., 2018; Totani et al., 2019). The neurons that control locomotion in *L. stagnalis* include a large serotonergic PeA cluster of cells which release serotonin to the muscles and cilia in the sole (Syed and Winlow, 1989; Longley and Peterman, 2013). The PeA neurons have also been suggested to have a neuromodulatory and neurohormonal role in the central nervous system (Chistopol'skii and Sakharov, 2003; Dyakonova et al., 2015). Many of the above-mentioned behavioral effects of exercise are similar to the influences ascribed to the increased level of serotonin in *Lymnaea*. Therefore, we hypothesized that the increased activity of these neurons is required for intense locomotion (Dyakonova et al., 2019) and that enhanced extrasynaptic release of serotonin may underlie the behavioral changes observed after the motor load.

The aim of the present study was to elucidate possible involvement of serotonin in the regulation of behavior in the novel environment and in the effects of intense locomotion on this behavior. Specifically, we addressed the following questions: (1) whether the behavioral effects of the exercise persist for 2 h after its termination; (2) what metabolic changes in the serotonergic system accompany intense locomotion and recovery; and (3) how serotonergic ligands influence the above-described behavior of *Lymnaea* in the novel environment. The obtained data suggest that serotonin is involved in the mediation of motor arousal in the novel environment. At the same time, serotonin is not responsible for faster decision-making observed after exercise. It is likely that along with serotonin, other factors participate in the mechanism of the exercise effect on decision-making.

MATERIALS AND METHODS

Animals

The *Lymnaea stagnalis* snails were taken from a breeding colony initially obtained from the Netherlands (1992) and mixed with specimen from wild population of the Oka River, Moscow region, Russia. They were fed daily on lettuce *ad libitum* and kept in dechlorinated tap water at room temperature.

Forced Locomotion in Low Water (Experiments 1 and 2)

Enhanced motor activity was evoked (as in Korshunova et al., 2016) by putting the snails into a tank (50 × 50 cm) filled with 1–2 mm layer of water for 2 or 4 h. As was reported earlier this procedure "protected snails from drying but forced them to use intense muscular crawling to compensate for the lack of water supporting the weight of their shells" (Korshunova et al., 2016, **Figure 1A**). Control snails were kept in deep water so they could use ciliary locomotion in similar light conditions. In addition, the control group was divided into the snails taken directly from their breeding colony (Ch) and the snails that were kept for 2 h in 300 ml containers filled with the same water as in the breeding stock (Cn). The Ch group was used to control whether novelty by itself produces locomotor arousal in snails. Rest after exercise was evoked by putting snails into a cylinder filled with water up to 9 cm for 2 h after intense terrestrial motor activity in low water. The experimental and control animals were investigated in random order in a single experiment.

Test for Behavior in the Novel Environment (Experiment 1)

We used the same test and set up as in Korshunova et al. (2016). Individual snails (one or four at a time in different experiments) were placed into a rectangular arena (60 × 45 cm) on a flat dry plastic surface (**Figure 1B**). One of the shorter walls of the arena was made of transparent plastic to provide the asymmetric illumination. All other walls were covered with non-transparent black film. A 40W white light bulb placed at a distance outside the arena served as a source of light. The light intensity at the arena's center (measured 3cm above the surface with the Proskit MT-4017 luxmeter) was adjusted to 30 lux, and it was 83 and 12 lux near the light and the dark walls, respectively. No measurable

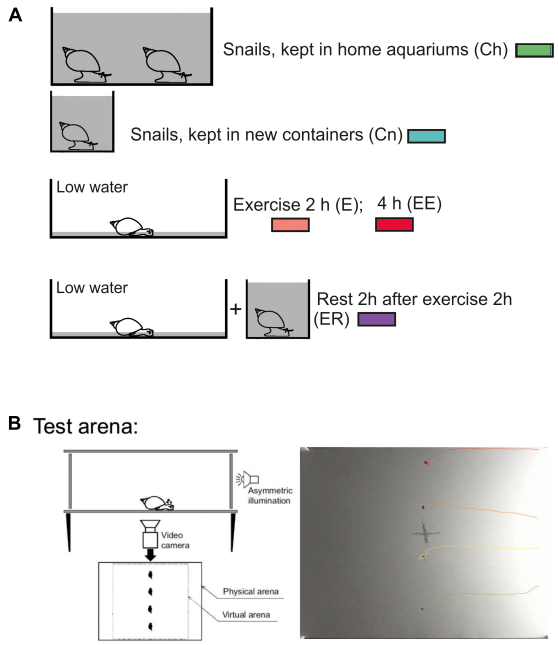

FIGURE 1 | Schematic representation of the experimental procedure. **(A)** Procedure for the investigation of the effects of enhanced motor activity (exercise, E, EE) and rest after exercise (ER), redrawn after (Korshunova et al., 2016; Dyakonova et al., 2019). In double-blind experiments, snails were divided into control and experimental groups and resided in similar light conditions before being placed in the test arena. Control snails were kept in deep water so they could use ciliary locomotion for 2 h in similar light conditions. Two control groups were used: snails taken directly from their breeding colony (Ch, marked with green color) and snails that were kept for 2 h in 300 ml containers filled with the same water as in the breeding stock (Cn, marked with blue color). The last group was used to test whether novelty by itself produces locomotor arousal in snails. The experimental and control animals were investigated in parallel in one experiment. Snails of the 'exercise' experimental group (E, marked with red color) were kept in a tank (25 × 50 cm) filled with a thin (1 mm) layer of water which protected them from drying but forced them to use crawling (intense muscular locomotion) to compensate for the lack of water supporting the weight of the shell for 2 h (E, marked with light red color) or 4 h (EE, marked with dark red color). Snails of the "rest after exercise" experimental group (ER, marked with purple color) were placed into in a cylinder filled with water up to 9 cm to be able to use ciliary locomotion for 2 h after 2 h of exercise in low water. In different experimental series, the combination of control and experimental groups could vary, for details see Methods and Results. **(B)** Behavioral paradigm for the investigation of decision-making in a novel environment. One or four snails (in different experimental series) were placed on the same central points of a square arena on a flat and dry plastic surface with one-side asymmetric illumination. All snail movements were tracked and video-recorded for 15 min in each experiment. The camera was placed under the transparent plastic bottom of the arena. For the behavioral analysis, the virtual arena border (22 cm from the central point) was defined. C, example of one record from four simultaneously tracked snails. In their behavior, the two clearly distinct phases can be seen: (1) uncertain movements, characterized by comparatively low speeds of movement, stops and repeated changes of movement direction and (2) an intense fast locomotion in a chosen direction as previously reported by Korshunova et al. (2016).

amount of light came to the arena from below. We did not attempt to avoid temperature gradient (less than 1°C, measured with a mini-infrared thermometer) caused by the light source in order to maintain natural conditions in which more lighted areas are typically warmer.

The movements of each snail were recorded at 15 frames per second for 15 min with the Microsoft LifeCam HD-3000 video camera. The recordings were video-tracked using the EthoVision XT software (Noldus, the Netherlands) and independently scored manually with RealTimer (Openscience, Russia). The camera was placed under the transparent plastic bottom of the arena. The traces left by the crawling snails were removed with a clean paper towel before each new test.

During the analysis, a centered square zone (22 × 22 cm) that limited the track and scoring analysis was defined (**Figure 1B**). This zone was used to exclude from the analysis snail's movements near the physical borders of the arena, especially near the brightly lit wall. We evaluated (i) the time to the snail's first movement, (ii) the total rotation prior to the crawling in the chosen direction, (iii) the mean velocity of locomotion (iv) the time taken to crawl to the virtual border of the arena. If the snail would not reach the virtual border, the time was given as the total time of observation, which was 15 min. Blind procedure was used for the tests performed manually (i, ii).

Measurement of 5-HT and Its Metabolites in the Pedal and Cerebral Ganglia of *Lymnaea* (Experiment 2)

5-HT and its precursor and catabolites were measured as described previously (Aonuma and Watanabe, 2012; Aonuma et al., 2016, 2017, 2018). Briefly, snails were quickly frozen using liquid N_2, and the pedal and cerebral ganglia were dissected out of the ice-cold *Lymnaea* physiological solution. Each paired ganglion was homogenized in 50 μl ice-cold 0.1M perchloric acid containing 5 ng of N-ω-methyl-5-hydroxytryptamine oxalate (NMET; Sigma-Aldrich, St. Louis, MO, United States) as an internal standard. After centrifugation of the homogenate (at 0°C, 21.500 g (15.000 rpm), for 30 min), 40 μl of supernatant was collected. Using high-performance liquid chromatography with electrochemical detection (HPLC-ECD; EICOM, Kyoto, Japan), we measured the following compounds in each of the four groups: (1) serotonin (5-HT); (2) a precursor of 5-HT (5-hydroxytryptophan, 5-HTP); and two catabolites of 5-HT, (3) N-acetylserotonin (Nac-5-HT) and (4) 5-hydroxyindole acetaldehyde (5-HIAA). The mobile phase containing 0.18M chloroacetic acid and 16 μM disodium EDTA was adjusted to pH3.6 with NaOH. Sodium-1-octanesulfonate at 1.85 mM as an ion-pair reagent and acetonitrile (CH3CN) at 8.40% (v/v) as an organic modifier were added to the mobile phase solution. The supernatants of samples were injected directly onto the HPLC column (C18 reversed-phase column, CAPCELL PAK C18MG, Shiseido, Tokyo, Japan) heated to 30°C in a column oven. A glass carbon electrode (WE-GC, EICOM Co.) was used for electrochemical detection (ECD-100, EICOM Co.). The detector potential was set at 890 mV versus an Ag/AgCl reference electrode. The chromatographs were acquired using the computer program PowerChrom (eDAQ Pty, Denistone East, NSW, Australia).

Drug Administration (Experiments 3, 4, 5)

Two different procedures of drug administration were used: (1) immersion of snails in groups of four (5-HT experiment) or individually (5-HTP experiment) into water (300 ml) taken from the breeding stock, with the drug added, for 2 h prior to the test, or (2) injection of 100 μl physiological solution (50 mM NaCl, 1.6 mM KCl, 4 mM $CaCl_2$, 8 mM $MgCl_2$, 10 mM Tris, pH7.6) containing the drug (ketanserin) 15 min prior to the test. The control snails for the experiments with 5-HTP and 5-HT were placed into the 300 ml containers filled with water taken from the breeding stock for 2 h. Snails injected with 100 μl vehicle (physiological solution) comprised the control group in the experiment with the serotonin antagonist ketanserin. The drugs were administered in the following concentrations: 5-HTP (0.1 mM), 5-HT (0.1 mM), ketanserin (0.02 and 0.1 mÌ). All drugs were obtained from Sigma Aldrich (Moscow, Russia). The test procedure was the same as in Experiment 1 (decision-making in the novel environment).

Data Analysis

The significance of the differences was tested by the non-parametric Mann–Whitney *U*-test for experiments with one control and one experimental group. The non-parametric Kruskal-Wallis test for multiple comparisons with *post hoc* comparisons was applied for three and more groups investigated in one experiment. The analysis was performed using the STATISTICA software (Statsoft). The values presented in the figures are given as the median with upper and lower quartiles.

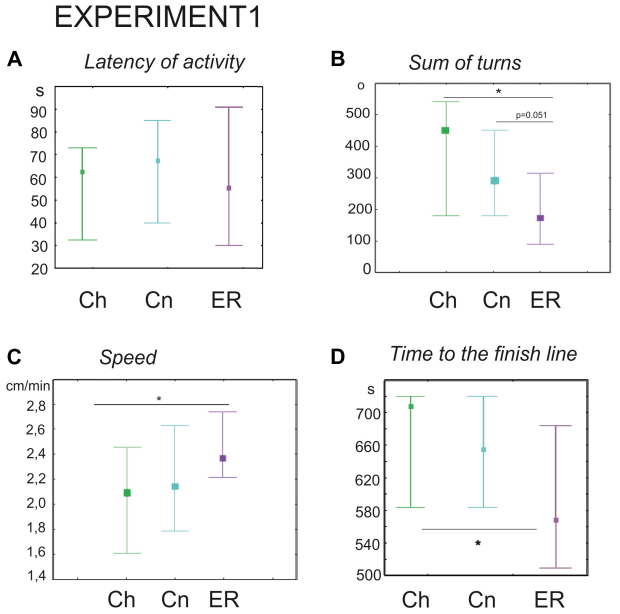

FIGURE 2 | Effects of novelty and "exercise then rest" on the behavior of snails on a dry surface. **(A)** The latency of the first movement in the new environment, in seconds. **(B)** The sum of turns prior to decision-making, in degrees. **(C)** The speed of locomotion, cm/min. **(D)** Time to the finish line (virtual arena borders), in seconds. Left to right in each diagram: green color indicates snails that were taken from the breeding stock (Ch, $n = 30$); blue color indicates snails that were kept for 2 h in a cylinder filled with water up to 9 cm (Cn, $n = 30$); purple color indicates snails that were placed for 2 h in low water to exercise and then rested for 2 h in a container filled with water up to 9 cm (ER, $n = 31$); The significance of differences was tested using the multiple comparisons Kruskal–Wallis test, followed by *post hoc* tests. All values are given as median with the lower and upper quartiles * indicates $p < 0.05$.

RESULTS

The Delayed Effects of Intense Locomotion on Decision-Making (Experiment 1)

In mammals, exercise has both immediate and long-term cognitive effects, which recruits different mechanisms (Heijnen et al., 2016). We have demonstrated earlier that 2 h of muscular crawling in *Lymnaea* results in the facilitation of decision-making and acceleration of locomotion when snails are placed in the novel environment (Korshunova et al., 2016). Here, we tested whether or not the exercise has any delayed effects following 2 h of rest.

The snails that rested in 300 ml aquatic containers filled with the water taken from the breeding stock ($n = 31$, ER) for 2 h after exercise, control snails taken directly from their breeding colony ($n = 30$, Ch) and control snails that resided in 300 ml containers for 2 h ($n = 30$, Cn) were used as three groups in this experiment. The third group (Cn, snails kept in novel containers) was used since the novelty by itself produces locomotor arousal in snails.

The latency of the first movement was no different (Kruskal–Wallis test: $H = 0.28$, $p = 0.8$), however, the ER snails made fewer turns prior to decision-making (Kruskal–Wallis test: H (2, $N = 91$) = 13.01, $p = 0.0015$; **Figures 2B**, **3A–C**, *post hoc* tests ER/Ch $p = 0.0013$; ER/Cn $p = 0.051$; Ch/Cn $p = 0.79$) and had higher speed of locomotion compared to the control group taken from the breeding stock (Kruskal–Wallis test: H (2, $N = 91$) = 7.5, $p = 0.0234$; **Figure 2C**, *post hoc* tests ER/Ch $p = 0.020$; ER/Cn $p = 0.2$; Ch/Cn $p = 0.9$). Recently, we reported that locomotor arousal developed more quickly in the ER snails than in the Cn group (Dyakonova et al., 2019). Similar trend can be seen in **Figure 3D**. However, there was no significant difference in the mean speed between the ER and the Cn group. The ER snails reached and crossed the virtual border faster than the Ch snails (Kruskal–Wallis test: H (2, $N = 91$) = 9.1, $p = 0.010$, **Figure 2D**, *post hoc* tests ER/Ch $p = 0.011$; ER/Cn p = 0.1; Ch/Cn $p = 0.9$). The ratio of light/dark choice was approximately the same in all groups ca. 75/25% (**Figures 3–C**). This ratio corresponded to the one reported earlier (Korshunova et al., 2016). No cases of intermediate choice were observed.

We performed an additional set of experiments with only one control group kept in novel conditions (Cn, $n = 65$) to validate the delayed effect of exercise (ER, $n = 62$) on the performance of turns. ER snails made significantly fewer turns (181 ± 17 versus 258 ± 22 degrees in the Cn, Mann–Whitney *U*-test, $z = 2.7$; $p = 0.0058$, not illustrated).

Therefore, exercise followed by rest decreased the display of "uncertainty" in the snail behavior in the novel environment,

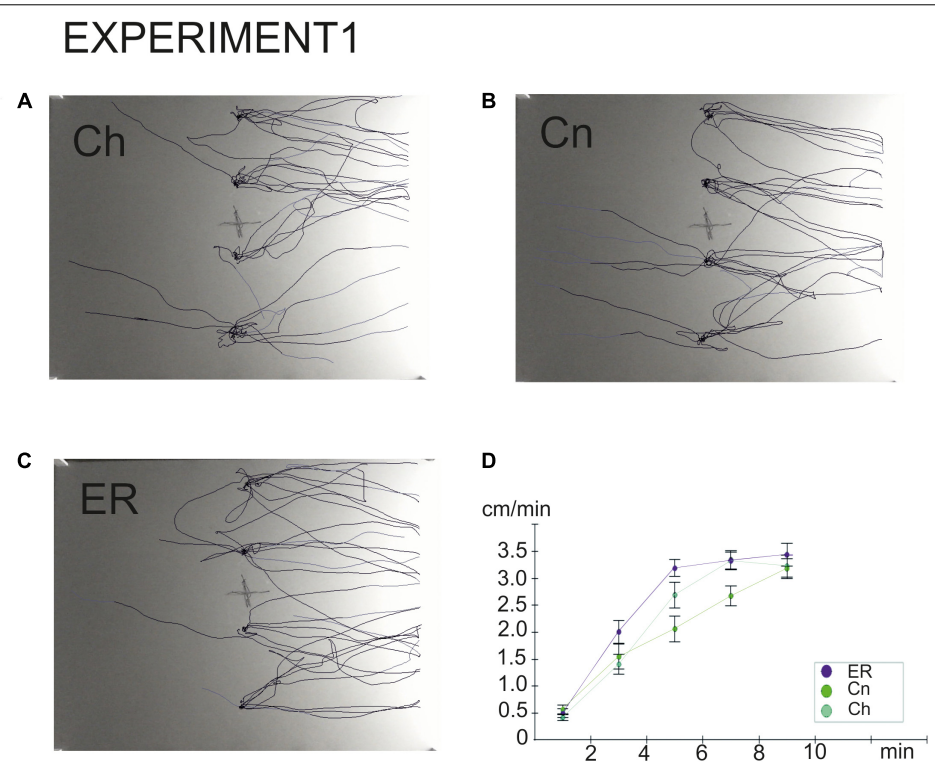

FIGURE 3 | Overlay tracks of snails the locomotor arousal in control and "exercise then rest." **(A)** Snails that were taken from the breeding colony (Ch). **(B)** Snails that were kept for 2 h in a cylinder filled with water up to 9 cm (Cn). **(C)** Snails that were placed for 2 h in low water to exercise and then rested for 2 h in a container filled with water up to 9cm (ER). Tracks presented in C show that ER snails spent less time in the central zone and made fewer turns than Ch and Cn snails although the dark/light choice was not different between Ch, Cn, and ER. In **(B)**, the effect of novelty can be seen as well, the rotational behavior is weaker in **(B)** than in **(A)**. **(D)** Locomotor arousal in the Ch, Cn, and ER groups: the mean speed of locomotion by equal time intervals (1–2 min, 2–4 min, 4–6 min, 6–8 min, 8–10 min).

promoting the switch from rotational behavior to decision-making. Preconditioning in novel containers has not induced significant behavioral effects in comparison to intact control (Cn versus Ch).

Immediate and Delayed Effects of Intense Locomotion on the Serotonin Content Within the Pedal and Cerebral Ganglia of *Lymnaea* (Experiment 2)

Four separate groups of snails were used (**Figure 1A**): (1) control snails taken from aquatic conditions (Cn); (2) snails that had been crawling (exercising) for 2 h in low water (E); (3) snails that had been "resting" in deep water for 2 h after 2 h of exercise (ER); and (4) snails that had been crawling (exercising) for 4 h in low water (EE). We measured the levels of 5-HTP, 5-HT, Nac-5-HT, and 5-HIAA in the in the pedal and cerebral ganglia. The pedal ganglia contain neurons related to locomotion, including the serotonergic PeA cluster, whose activity is influenced by intense locomotion (Korshunova et al., 2016; Dyakonova et al., 2019). The cerebral ganglia were included in the analysis for two reasons: first, to verify the hypothesis that serotonin metabolism in the functionally distinct parts of the CNS can be differently affected by the same behavioral context; second, to check whether the exercise produces any changes in the serotonin metabolism within the "cognitive" (cerebral) ganglia of the snail CNS that are believed to participate in learning, memory and decision-making.

Pedal Ganglia

The most prominent changes in the content of the substances being investigated were observed in the group that rested after exercise (ER, **Figure 4**). The concentration of the serotonin precursor 5-HTP was more than 10 times higher ($p < 0.001$) than in all other groups (Kruskal–Wallis test: H (3, $N = 46$) = 29.16, $p = 0.0001$, **Figure 4** *post hoc* tests ER/Cn $p = 0.0016$; ER/E $p = 0.002$; ER/EE $p = 0.0001$; E/Cn $p = 0.9$; EE/Cn $p = 0.79$).

Similarly, the 5-HIAA content was the highest in the ER group, with highly significant differences compared to the control and the 4 h -exercised (EE) snails (Kruskal-Wallis test: H (3, $N = 46$) = 13.08, $p = 0.0045$, **Figure 4**, the third group of bars, *post hoc* tests ER/Cn $p = 0.029$; ER/E $p = 0.49$; ER/EE $p = 0.004$; E/Cn $p = 0.9$; EE/Cn $p = 0.85$).

The Nac-5-HT content was significantly higher in the ER group compared to all other groups [Kruskal–Wallis test: H (3, $N = 45$) = 12.8, $p = 0.0051$, **Figure 4**, the last group of bars, *post hoc* tests ER/Cn $p = 0.019$; ER/E $p = 0.04$; ER/EE $p = 0.01$; E/Cn $p = 0.9$; EE/Cn $p = 0.9$].

There were no significant differences in the serotonin content [H (3, $N = 47$) = 4.07, $p = 0.25$]. In the ER group, serotonin showed the lowest concentration, but the tendency did not reach

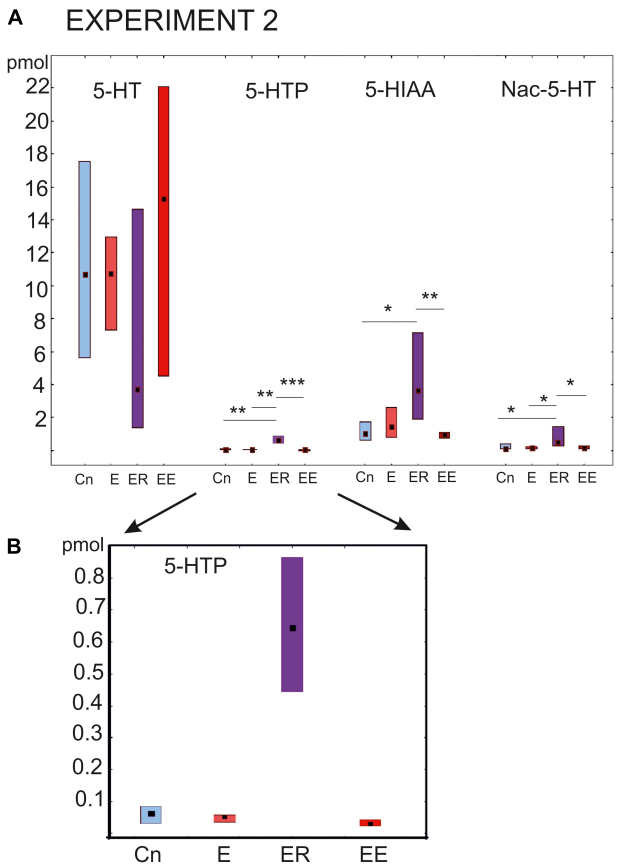

FIGURE 4 | Acute and delayed effects of intense locomotion on the content of serotonin and its catabolites within the pedal ganglia of *Lymnaea* measured with high-performance liquid chromatography with electrochemical detection (pmol). **(A)** Left to right: Serotonin (5-HT); a precursor of 5-HT (5-hydroxytryptophan, 5-HTP, see also below in a higher scale); N-acetylserotonin, Nac-5-HT; 5-hydroxyindole acetoaldehyde, 5-HIAA. **(B)** The magnified scale for 5-HTP content shown in **(A)** second to the left. Blue color indicates control snails that were kept in a new cylinder filled with water up to 9 cm for 2 h (Cn, $n = 13$); light red color indicates snails that were placed for 2 h in low water to exercise (E, $n = 11$); purple color indicates snails that were placed for 2 h in low water to exercise and then rested for 2 h in a container filled with water up to 9 cm (ER, $n = 13$); dark red color indicates snails that were placed for 4 h in low water to exercise (EE, $n = 12$). The significance of differences was tested using the multiple comparisons Kruskal-Wallis test, followed by *post hoc* tests. All values are given as median with the lower and upper quartiles *, **, *** indicate $p < 0.05$, 00.1 and 0.001, respectively.

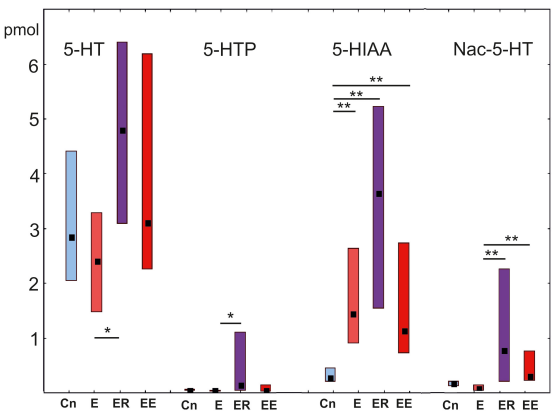

FIGURE 5 | Acute and delayed effects of intense locomotion on the content of serotonin and its catabolites within the cerebral ganglia of *Lymnaea* measured with high-performance liquid chromatography with electrochemical detection (pmol). Left to right: Serotonin (5-HT); a precursor of 5-HT (5-hydroxytryptophan, 5-HTP); N-acetylserotonin, Nac-5-HT; 5-hydroxyindole acetoaldehyde, 5-HIAA. Blue color indicates control snails that were kept in a cylinder filled with water up to 9 cm for 2 h (Cn, $n = 13$); light red color indicates snails that were placed for 2 h in low water to exercise (E, $n = 14$); purple color indicates snails that were placed for 2 h in low water to exercise and then rested for 2 h in a container filled with water up to 9 cm (ER, $n = 13$); dark red color indicates snails that were placed for 4 h in low water to exercise (EE, $n = 12$). The significance of differences was tested using the multiple comparisons Kruskal-Wallis test, followed by *post hoc* tests. Values are given as median with the lower and upper quartiles *, ** indicate $p < 0.05$ and 0.01, respectively.

the level of significance (**Figure 4**, first group of bars). Neither 2 nor 4 h of intense locomotion resulted in any significant increase in the serotonin content within the pedal ganglia, although in the group exercised for 4 h, a trend of increased serotonin was observed but only achieved a p value equal to 0.1.

Cerebral Ganglia

The 5-HT content in the cerebral ganglia changed significantly within the four groups [Kruskal–Wallis test for multiple comparisons: H (3, $N = 48$) = 7.94, $p = 0.0473$, **Figure 5**, the right group of bars]. *Post hoc* tests indicated a significant difference between the E and ER groups, $p = 0.043$).

The 5-HTP content had a similar profile of changes to that of 5-HT [Kruskal–Wallis test: H (3, $N = 48$) = 9.77. $p = 0.02$; **Figure 5**, the second group of bars]. Namely, a significant increase in the 5-HTP was found in ER group in comparison to the E group after *post hoc* tests ($z = 3.08$; $p = 0.012$).

The 5-HIAA content was significantly higher in all three experimental groups compared to the control [Kruskal–Wallis test: H (3, $N = 48$) = 24.15, $p = 0.001$, **Figure 5**, the third group of bars, E/Cn $p = 0.005$; ER/Cn $p = 0.0001$; EE/Cn $p = 0.02$].

The Nac-5-HT content was higher in the ER and EE groups compared to the E group [Kruskal–Wallis test: H (3, $N = 48$) = 22. 07, $p = 0.0001$] and as a tendency compared to the control (*post hoc* ER/Cn $p = 0.054$; EE/Cn $p = 0.058$).

The Effects of Pharmacological Manipulations With the Serotonergic System on Snail Decision-Making Under Uncertainty

The Effect of Serotonin Metabolic Precursor 5-Hydroxytryptamine (5-HTP) on Snail Behavior on the Dry Surface (Experiment 3)

5-HTP is known to increase the speed of locomotion in *Lymnaea* (Pavlova, 2001, 2019; Tsyganov et al., 2004). Here we found that

the snails immersed in 5-HTP (n = 27) demonstrated a more rapid onset of activity compared to the control group (n = 27). The delay of the first movement was significantly smaller in the experimental snails (**Figure 6A**, z = 2.05, p = 0.03, Mann–Whitney U-test). There were no differences in the rotational behavior, which is considered to be the orienting phase of the behavior under uncertainty, preceeding the decision-making process. The mean total rotation did not differ between the two groups (z = 0.4, p = 0.67, Mann–Whitney U-test, **Figure 6B**). The mean speed of locomotion was faster (z = 2.09, p = 0.03, Mann–Whitney U-test, **Figure 6C**), and the 5-HTP-treated snails reached the border of the arena significantly faster (**Figure 6D**, z = 2.47, p = 0.013, Mann–Whitney U-test). The ratio of light/dark choice was similar in both groups.

The Effect of Serotonin on Snail Behavior on the Dry Surface (Experiment 4)

The snails of the experimental group were immersed in 0.1 mM serotonin (n = 24 versus n = 30 in the control group). The delay in the first movement was significantly smaller (z = 2.54, p = 0.01, Mann–Whitney U-test, **Figure 7A**), and the increase in the rotational behavior only achieved a p value equal to 0.06 (**Figure 7B**). The mean velocity achieved a p value equal to ca. 0.055. Nevertheless, the snails pretreated with serotonin reached the border of the arena significantly faster (z = 1.96; p = 0.0049, Mann–Whitney U-test). We hypothesized that there were no statistically significant differences in the mean speed (p = 0.055), because 5-HT- treated snails tended to spend more time in the orienting phase of the behavior (performed more turns). To check this possibility we measured the mean velocity during the phase of the directional crawl (6–8 min after the start of the experiment). It was indeed significantly higher than in the control group (z = 2, p = 0.03, Mann–Whitney U-test, **Figure 7C**). This finding explains why 5-HT treated snails reached the border of the arena more quickly (**Figure 7D**). The ratio of light/dark choice was the same for both groups.

The Effect of Serotonin Receptor Antagonist Ketanserin on Snail Behavior on the Dry Surface (Experiment 5)

Experimental snails received injection of 100 µl physiological solution containing 0.02 mM (n = 9) or 0.1 mM (n = 13) ketanserin 15 min prior to the test. The control groups (n = 9 and n = 13, respectively) received 100 µl of physiological solution. Snails, injected with 0.02 mM ketanserin demonstrated the tendency for later onset of activity (93 ± 32 s versus 28 ± 12, z = 1.9, p = 0.051, Mann Whitney U test). The effect was significant in the group that received 0.1 mM ketanserin (424 ± 110 versus 78 ± 20, z = 2.1, p = 0.035, Mann–Whitney U-test, **Figure 8A**).

There were no differences in the mean total rotation between the 0.02 mM ketanserin group and the control group (z = 0.68,

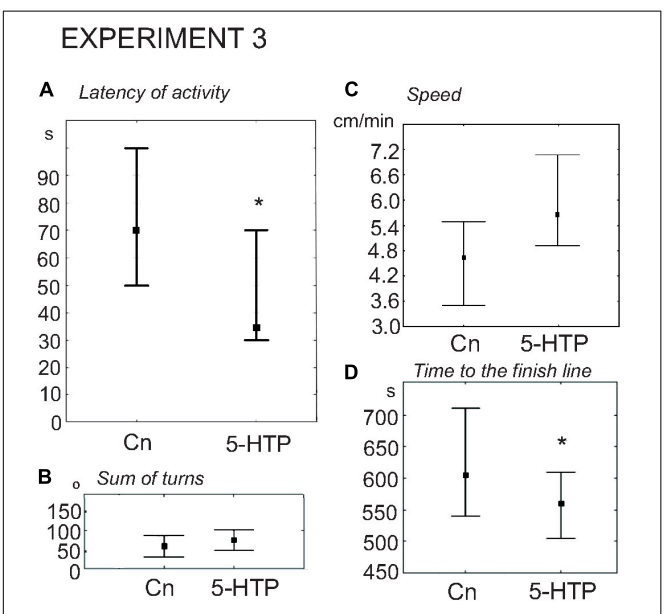

FIGURE 6 | Effects of serotonin precursor 5-HTP on the behavior of snails on a dry surface. **(A)** The latency (in seconds) of the first movement. **(B)** The sum of turns prior to decision-making, in degrees. **(C)** The mean speed of locomotion (in cm/min). **(D)** Time to the finish line (crossing of the virtual arena border) in seconds. The significance of differences was tested using the Mann–Whitney U-test. All values are given as median with the lower and upper quartiles * indicates $p < 0.05$.

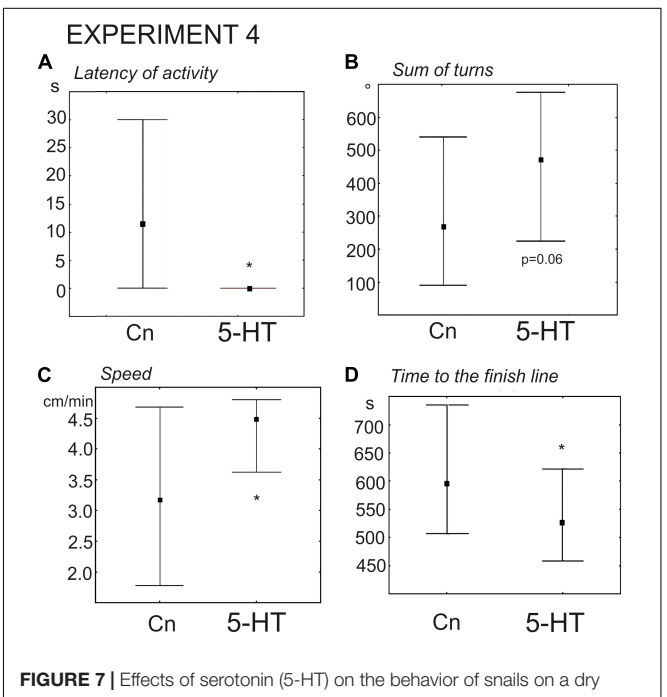

FIGURE 7 | Effects of serotonin (5-HT) on the behavior of snails on a dry surface. **(A)** The latency (in seconds) of the first movement. **(B)** Total rotation prior to decision-making, in degrees. **(C)** The mean speed of locomotion (in cm/min) measured during the phase of the directional crawl (6–8 min from the beginning of the experiment). **(D)** Time to the finish line (crossing of the virtual arena border) in seconds. The significance of differences was tested using the Mann–Whitney U-test. The significance of differences was tested using the Mann–Whitney U-test. All values are given as median with the lower and upper quartiles * indicates $p < 0.05$.

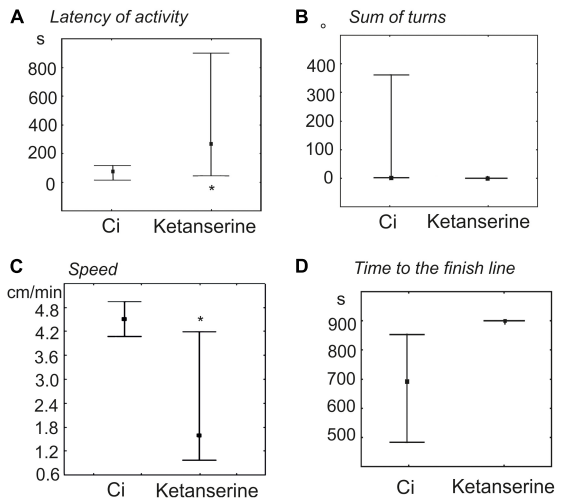

FIGURE 8 | Effects of the serotonin receptor antagonist ketanserin 0.1 mM on the behavior of snails on a dry surface. **(A)** The latency (in seconds) of the first movement. **(B)** The sum of turns prior to decision-making, in degrees. **(C)** The mean speed of locomotion (in cm/min). **(D)** Time to the finish line (crossing of the virtual arena border) in seconds. The significance of differences was tested using the Mann–Whitney *U*-test. All values are given as median with the lower and upper quartiles * indicates $p < 0.05$.

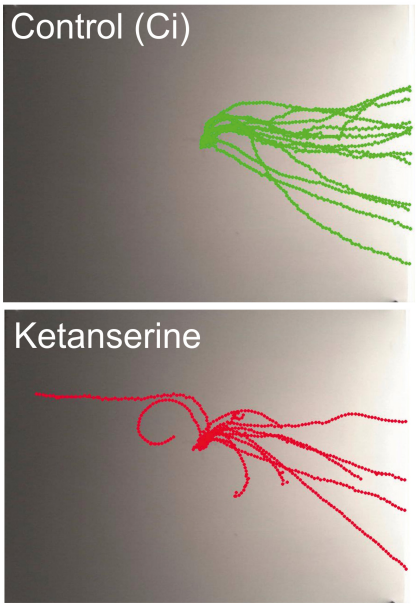

FIGURE 9 | Overlay tracks of snails from the control group injected with saline and the experimental group injected with 0.1 mM ketanserin. In the group injected with ketanserin (lower image, red tracks), the intermediate direction choices (semi-circular routes) can be seen which never occurred in any other groups. The tracks of experimental snails are also obviously shorter since the speed of locomotion was lower in ketanserin-treated animals.

p = 0.49, Mann–Whitney *U*-test). Higher concentration of ketanserin decreased total rotation (z = 1.9, p = 0.049, **Figure 8B**).

The overall speed of locomotion was significantly lower in snails treated with 0.02 and 0.1 mM ketanserin than in the control groups (z = 2.0, p = 0.045 and z = 2.2, p = 0.027, respectively, Mann–Whitney *U*-test (**Figure 8C**).

The experimental snails reached the border of the arena later, if ever. The time to the finish line was 808 ± 51 s and 837 ± 45 s in the 0.02 and 0.1 mM ketanserin in contrast to the 556 ± 32 s and 680 ± 55 s in respective controls (z = 2.85, p = 0.004 and z = 2.29, p = 0.02, **Figures 8D**, **9**).

In the snails injected with ketanserin, the choices of intermediate directions (semi-circular routes) were observed (n = 5), which never occurred in any other groups (**Figure 9**).

DISCUSSION

The role of serotonin in the immediate and delayed effects of physical exercise has been intently studied in mammals (Kondo and Shimada, 2015; Heijnen et al., 2016). The serotonergic system is linked with the activation of neurotrophic factors, increased neurogenesis, improved emotional state and memory after exercise. Interestingly, in a quite distant zoological taxon, mollusks, serotonin is involved in the control of locomotion on the one hand (Kabotyanski et al., 1990; Satterlie, 1995; Pavlova, 2001, 2019; Gillette, 2006) and modulates cognitive traits such as memory on the other (Benjamin et al., 2000; Balaban, 2002; Balaban et al., 2016; Deryabina et al., 2018; Nikitin et al., 2018; Totani et al., 2019). Recently, immediate effects of intense locomotion on decision-making under uncertainty were reported in the snail *Lymnaea stagnalis*, suggesting a possible link between motor and cognitive functions of serotonin in mollusks (D'yakonova, 2014; Korshunova et al., 2016). However, there are substantial differences between mammals and mollusks in the structure of their serotonergic systems. One of the most prominent ones is the opposite functioning of serotonin autoreceptors, which are inhibitory in mammals and excitatory in mollusks (Gillette, 2006; Dyakonova et al., 2009). Whether serotonin mediates the behavioral effects of intense locomotion in *Lymnaea* despite these differences remains to be explained.

We demonstrated that intense locomotion has delayed effects on decision-making in *Lymnaea*. Previous exercise manifests itself not only in the electrical properties of serotonergic neurons as reported earlier (Korshunova et al., 2016; Dyakonova et al., 2019) but also in the altered metabolism of serotonin. Immediate and delayed effects are directly manifested in the metabolism in the serotonergic neurons related to locomotion. Moreover, serotonin metabolism appears to be regulated differently in different ganglia of the snail. Remarkably, the most prominent changes were detected in the rest-after-exercise group. Pharmacological manipulation of serotonin content and receptor availability (**Table 1**) suggests that serotonin is likely to be responsible for the general acceleration of behavior in the conditions of uncertainty immediately after the exercise. This effect can be explained by the serotonin influence on the

motor activity (faster onset of movements and higher speed of locomotion). However, our results clearly show that the decreased number of turns during orienting behavior, caused by preceding motor activity and resulting in the facilitation of decision-making, can not be attributed to serotonin.

Intense Locomotion and/or Stress?

Shallow water is not an artificial situation for *Lymnaea* ecology as the pond snails can be observed crawling in low water in their natural habitats. Such crawling is a particular type of locomotion, a muscular one, because ciliary locomotion is not effective enough in such conditions. However, low water is not their optimal niche, and, in addition, it is also unusual for the snails kept as laboratory stock. We have discussed the possible involvement of stress in the effects of intense locomotion in our previous paper (Korshunova et al., 2016). Indeed, mild stress unavoidably accompanies intense physical load in natural and experimental conditions in animals, including mammals and humans. Some signatures of mild stress, such as cognitive arousal and resistance to threatening stimuli resemble the effects of motor load in mammals as well as in snails (Kavaliers, 1987; Heijnen et al., 2016). Numerous observations associate serotonin with stress-induced behavior in vertebrates and invertebrates (Shartau et al., 2010; Bacqué-Cazenave et al., 2017; Rillich and Stevenson, 2018). On the other hand, the behavioral and neurochemical effects differ between the exercise-induced stress and stress due to "negative life events" in mammals (Heijnen et al., 2016).

In *Lymnaea*, we found that novelty-induced stress does not explain increased locomotion (Korshunova et al., 2016 and present data with the Cn control group). We also knew (an unpublished observation) that severe acute stressors, such as nociceptive stimuli, have consequences opposite to those of intense locomotion, increasing the latency of motor activity in the arena. Recently, we finished an experiment in *Lymnaea* imitating another natural stressful situation, turbulent water (**Supplemenatry Material**). It was induced by 2 h shaking with the frequency of 200 cycles per min., which prevented snails from gliding and crawling. The effect of this treatment on subsequent behavior on the dry surface was highly significant, but it was not at all similar to the exercise effect (**Supplementary Figures S1A–E**). Intense shaking decreased the speed and increased the time to the finish line, with no changes in the performance of turns and the delay of the initial movement.

Therefore, it seems that the consequences of stress in *Lymnaea* depend on the procedure used to induce it. In these circumstances, we still do not exclude the involvement of mild stress effects in the effects of intense locomotion but, however, prefer to describe the exact behavioral treatment rather than use a vague notion of "stress".

The Delayed Effects of Intense Locomotion and the Preadaptation to Novelty Hypothesis

In mammals, including humans, physical activity has long-lasting behavioral and cognitive effects that have attracted the attention of researchers as being beneficial and even curative (Heijnen et al., 2016). The similarity of the behavioral effects of exercise in animals of various phyla prompted us to formulate a general hypothesis on the possible biological benefits of these effects. The hypothesis suggests that: (1) The immediate effects of the exercise can be beneficial for the acceleration of decision-making during fast locomotion to cope with rapid changes in the environment; (2) The delayed behavioral changes are a manifestation of the feedforward preadaptation to a less familiar environment, which animals are likely to face following a period of intense locomotion. Preadaptation means the possession of certain characteristics by an organism which make it more adaptable to a future environmental changes. The new environment means high uncertainty, low predictability of events and excess of new information. These are serious challenges for the animal, which reduce the chances of its survival, and therefore preadaptation to possibly new conditions seems biologically justified.

The known effects of exercise, such as facilitation of learning and memory for novel information (Epp et al., 2016), activation of neurogenesis (van Praag et al., 1999, Lee et al., 2013), enhancement of goal-oriented behavior and "effortfulness" (Laurence et al., 2015, Korshunova et al., 2016), decreasing the sensitivity to external disturbances and stress (Stevenson et al., 2005) and facilitation of effort-based decision-making (Bernacer et al., 2019) agree with this hypothesis. These behavioral and physiological changes may help the organism to cope with excess of novel information and stress.

To the best of our knowledge, this is the first study to demonstrate the delayed effects of intense locomotion on the behavior under uncertainty in an invertebrate, the mollusk *Lymnaea stagnalis*. The delayed effects of exercise were detected in this animal at both the behavioral and the metabolic levels. In our behavioral paradigm, the delayed effect of intense crawling was a decreased number of orienting turns in the first phase of snail behavior in the novel environment. This parameter depends on the level of uncertainty in the environment (Korshunova et al., 2016), therefore we suggest that a decreased performance of turns can be considered as a facilitation of the decision-making process. This effect had been demonstrated in our previous study as an immediate result of intense locomotion (Korshunova et al., 2016), and it can now be extended to the delayed effects of the exercise. The persistence of this effect is contrasted by the disappearance of changes in the latency and speed of locomotion in the novel environment after rest. The mean speed of locomotion of the ER snails was significantly increased compared to the intact control (Ch) group, but not compared to snails kept in novel conditions (Cn), in contrast to those that were tested immediately after exercise (Korshunova et al., 2016). Nevertheless, faster locomotor arousal was observed in ER snails (Dyakonova et al., 2019). The illustration provided here (**Figure 3D**) agrees with this earlier finding.

Intense locomotion affected the process of decision making (the total rotation and, hence, the delay of the transfer from rotational to goal-oriented behavior) but not the result, the choice between the light and dark sides of the arena. For a snail, which has a very low speed of locomotion, in the situation of limited time and high uncertainty, long exploration

TABLE 1 | The effects of behavioral and pharmacological treatments on behavior of snails in a novel environment (asymmetricaly lit dry arena).

Procedure (source)\parameter	Latency of movement	Performance of turns (orienting phase)	Locomotion speed	Time to the finish line
Exercise 2 h (Korshunova et al., 2016)	Decreased (Korshunova et al., 2016)	Decreased (Korshunova et al., 2016)	Increased (Korshunova et al., 2016)	Decreased (Korshunova et al., 2016)
Exercise 2 h and rest 2 h (Dyakonova et al., 2019; here, Experiment 1)	No change (**Figure 2A**)	Decreased (**Figures 2B,C**)	No change in the mean speed (**Figure 2C**, locomotor arousal develops faster (**Figure 3D**; see also Dyakonova et al., 2019).	No change (**Figure 2D**)
Treatment with serotonin precursor 5-HTP (here, Experiment 3)	Decreased (**Figure 6A**)	No change (**Figure 6B**)	Increased (**Figure 6C**)	Decreased (**Figure 6D**)
Treatment with serotonin (here, Experiment 4)	Decreased (**Figure 7A**)	No change (**Figure 7B**)	Increased as tendency (**Figure 7C**, $p = 0.055$)	Decreased (**Figure 7D**)
Treatment with the $5HT_2$ antagonist, ketanserine (here, Experiment 5)	Increased (**Figure 8A**)	Decreased (**Figure 8B**)	Decreased (**Figure 8C**)	Increased (**Figure 8D**)
Stress by shaking 2 h (here, **Supplementary Material**)	No change (**Supplementary Figure S1A**)	No change (**Supplementary Figure S1B**)	Decreased (**Supplementary Figure S1C**)	Increased (**Supplementary Figure S1D**)

of the environment with frequent changes of direction is hardly the best strategy. Investing time and energy into crawling in the chosen direction will make the survival more probable. Preadaptation, as we propose, increases the level of confidence in ambiguous situations (when animals need to solve problems that have no clear or defined answers) (Vorontsov and Dyakonova, 2017).

The observed behavioral effects of past exercise are in line with electrophysiological data obtained from the pedal serotonergic neurons PeA controlling locomotion in *Lymnaea* (Dyakonova et al., 2019). Rest after exercise eliminates the excitatory effect of exercise on the activity of these neurons in the CNS, but not in completely isolated neurons. In other words, serotonergic neurons remain in the internally excited state under external network inhibition in animals that rest after the terrestrial locomotion. This ambiguous state may underlay faster transition from the aquatic to terrestrial locomotion.

Differential Regulation of Serotonin Metabolism During Exercise and Rest

Exercise causes dynamic fluctuations in the content of serotonin in the mammalian brain, which may change in opposite directions in some brain regions (Heijnen et al., 2016). In *Lymnaea*, the sensitivity of serotonin metabolism to exercise is shown in our experiments performed on four groups of snails with different experience of intense locomotion: crawling for 2 or 4 h and 2 h of crawling followed by 2 h of rest. In general, the results suggest an elevation of serotonin metabolism in response to exercise. Interesting details are identified regarding site-specificity and time-course of this effect.

Thus, we demonstrated that the level of serotonin metabolites changes differently, in response to intense locomotion, in the cerebral compared to the pedal ganglia. The cerebral and pedal ganglia are functionally different. The pedal ganglia are strongly involved with the control of locomotion and respiration, while the cerebral ganglia seem to play part in the modulation of various forms of behavior, from feeding to learning. In the cerebral ganglia, the higher level of serotonin content was observed in the rest-after-exercise group (statistically significant in comparison to the exercise group and as a tendency in comparison to the control one). By contrast, in the pedal ganglia, the content of serotonin did not statistically change in the ER group (and it tended to be lower than in other groups). Therefore, serotonin metabolism seems to be differently regulated in different parts of the CNS in mollusks. Presumably, the change in distribution helps to cope with different needs for serotonin by different neuronal ensembles in various behavioral contexts.

The absence of differences in the content of serotonin in the pedal ganglia in the ER group compared to control was accompanied by a 10-fold increase in the 5-HTP concentration and a significant increase in the content of both catabolites of serotonin. It is likely that the increased catabolism of serotonin and the termination of its synthesis could be responsible for the effects of rest described above. Our data point to aromatic amino acid decarboxylase (AAD) activity as the main source of the observed changes. It is likely that transient inhibition of AAD in the rest-after-exercise group was responsible for the accumulation of 5-HTP. This possibility can be experimentally verified in the future.

Several other studies have suggested that the AAD activity is an additional source of regulation in the metabolism of monoamines. Independent regulation of 5-HT and 5-HTP content and similar accumulation of 5-HTP had been identified in the CNS of *Lymnaea* earlier, specifically, after food deprivation (Aonuma et al., 2016). Potentiation of L-DOPA effects in the presence of high dopamine concentration similarly suggests that AAD is inhibited by dopamine (Dyakonova et al., 2009).

One interesting result of our HPLC analysis was that the strongest changes in the serotonin precursor and catabolites were found in the snails that rested for 2 h after intense crawling. Therefore, rest after exercise produces highly specific effects on serotonin metabolism that are not identical to simple vanishing of exercise effects or compensatory synthesis.

Serotonin and Behavioral Changes Caused by Preceding Intense Locomotion in Lymnaea

Serotonin appears to be the strongest candidate for the evolutionary conserved neuromodulator that mediates the behavioral effects of exercise. It remained, however, unknown to what extent serotonin can mimic the behavioral effects of exercise in *Lymnaea*.

We addressed this question by testing the effects of serotonin precursor, serotonin and the serotonin receptor antagonist ketanserin on snail behavior on the dry, asymmetrically lit arena. In this behavioral test, the immediate and delayed effects of exercise were described in detail (**Table 1**). The immediate effects of exercise were characterized by the reduced latency of the first movement, the reduced number of orienting turns, faster decision-making and higher speed of locomotion (Korshunova et al., 2016). The delayed effects described here were also characterized by the reduced number of turns and faster locomotor arousal, with only weak differences in the mean speed of locomotion.

The effects of serotonergic drugs investigated here (**Table 1**) are in concordance with each other and suggests certain conclusions about the role of serotonin in the behavioral effects of intense locomotion. Serotonin and its metabolic precursor decreased the latency to start movement in a novel arena. This effect was similar to the effect of immediate exercise. 5-HTP, similarly to exercise, decreased the time of the onset of the movement and the time it took to reach the virtual border of the arena. Serotonin produced similar but weaker changes. We suggest that the difference in the effectiveness of the two drugs can be explained by different mechanisms of their action on the serotonin receptors. There is no evidence that 5-HTP has any direct effect on serotonin receptors. The serotonergic neurons first uptake it, then metabolize into the serotonin by AAD. 5-HTP acts via the enhanced release of serotonin at the conventional sites of serotonin release. In contrast, incubation in serotonin may result in less specific action on various serotonin and monoamine receptors. 5-HTP is more effective than serotonin in many other experimental models: a variety of gastropod mollusks (for review, see Sakharov, 1991); crickets (Ureshi et al., 2002; Dyakonova and Krushinsky, 2013; Rillich and Stevenson, 2018); locust (Anstey et al., 2009). Neither serotonin in any concentration nor its metabolic precursor affected the orienting phase of the behavior (the rotation prior to decision-making). The serotonin antagonist ketanserin increased the latency to start movement, reduced the number of turns, and strongly suppressed locomotion (**Table 1**).

The data suggest that serotonin can mediate locomotor arousal in the exercise effects but is not responsible for the reduction in the length of the orienting phase. Therefore, the neurochemical mechanism responsible for faster decision-making after exercise in *Lymnaea* remains to be found.

This suggestion is in line with the effects of serotonergic drugs in mollusks reported earlier. Activation of the aquatic and terrestrial locomotion in *Lymnaea stagnalis* by serotonin or 5-HTP was found in several studies (Pavlova, 2001, 2019; Tsyganov et al., 2004). Activation of searching movements by serotonin was shown in the terrestrial snails *Helix* (Roshchin and Balaban, 2012) and *Cepaea* (Dyakonova et al., 1995). In *Lymnaea stagnalis*, serotonin precursor also promoted approaching unfamiliar objects as well as orienting turns in response to tactile stimuli of tentacles (D'yakonova and Sakharov, 1995). The possible influence of intense locomotion on cognitive functions like learning, memory and predictive abilities has not yet been investigated in mollusks. Therefore, serotonin, although it does not seem to be involved in the facilitation of decision-making after the exercise, might still influence other cognitive functions.

In several models where the central and peripheral effects of serotonin were elucidated, a notable agreement between them had been found (Sakharov, 1990; Satterlie, 1995; Gillette, 2006; Roshchin and Balaban, 2012; Pavlova, 2019). These findings support the hypothesis of the integrative function of serotonin (Sakharov, 1990), which implies that, in relatively simple organisms, the effects of the neurotransmitter on various targets and receptors may serve the same integrative function. This view later received important elaborations (Gillette, 2006; Harris-Warrick and Johnson, 2010). The first approach suggests that neurotransmitter's synergistic effects can be seen within the one functional system, while the switching between the functional systems (for example between escape and feeding behavior, both of which are controlled, in mollusks, by serotonin) relies on competitive interactions between central neurons (Gillette, 2006). The second review collected and analyzed examples of neurotransmitter's antagonistic effects within the same functional group, and suggested the role for these antagonistic interactions in fine-tuning of neuromodulator's effects (Harris-Warrick and Johnson, 2010). One needs to keep these complexities in mind when we discuss the effects of neurotransmitters applied through a bath, the procedure used in our investigation.

We have discussed earlier that it is difficult to specify whether serotonin exerts its behavioral effects as a synaptic neurotransmitter, an extrasynaptic neurotransmitter, a neuromodulator, a neurohormone or a metamodulator (Dyakonova et al., 2015). We believe that this difficulty is only partially explained by the absence of empirical details. The modern classification of neuronal signal molecules is based on the outdated conception that a neurotransmitter only transmits the electrical events between the synaptically connected neurons, while the very same chemical substance, spilled over the synapse or involved in volume transmission, is called a neuromodulator. Instead, all neurochemical events, from synaptic to hormonal, can be put on a single scale, thus avoiding the redundant classification of neuroactive substances and at the same time allowing for a better explanation of empirical data.

We can conclude that the results of our behavioral, pharmacological and biochemical experiments suggest that serotonin is likely to play a role in the effects of exercise on the *Lymnaea* behavior in a novel environment. However, it appears to be responsible for the locomotor activation and the increase in the intensity of the whole behavioral program in the novel environment, having no effect on the structure of this behavior. Neuromodulators that control rotational searching behavior and are responsible for faster cessation of the orienting phase (facilitation of decision-making) after exercise remain to be found in *Lymnaea*. Therefore, the effects of exercise on the facilitation of decision-making are likely to be mediated by multitransmitter neuromodulatory control in mollusks.

DATA AVAILABILITY STATEMENT

The datasets generated for this study are available on request to the corresponding author.

ETHICS STATEMENT

This study was carried out in invertebrate animals, the pond snails Lymnaea stagnalis, in accordance the protocol has been approved by the responsible authorities of our institutions.

AUTHOR CONTRIBUTIONS

HA performed HPLC experiments and edited the manuscript. MM performed behavioral experiments (delayed effects of locomotion, 5-HT and supplementary stress experiment). BB performed behavioral experiments (5-HTP and ketanserin effects). YT performed behavioral experiments and made dissections for HPLC analysis. DV performed analysis of behavioral data using the EthoVision software. IZ participated in behavioral experiments and discussed results. EI analyzed the results and edited the manuscript. VD planned the experiments and wrote the present manuscript.

FUNDING

This work was supported by the RFBR Grants 17-29-07029 and 19-04-00628. The work of VD, MM, DV, and IZ was conducted under the IDB RAS Government basic research program 2020 and funded by the Presidium of the Russian Academy of Sciences.

SUPPLEMENTARY MATERIAL

The Supplementary Material for this article can be found online at: https://www.frontiersin.org/articles/10.3389/fphys.2020.00221/full#supplementary-material

REFERENCES

Anstey, M. L., Rogers, S. M., Ott, S. R., Burrows, M., and Simpson, S. J. (2009). Serotonin mediates behavioral gregarization underlying swarm formation in desert locusts. *Science.* 323, 627–630. doi: 10.1126/science.1165939

Aonuma, H., Kaneda, M., Hatakeyama, D., Watanabe, Y., Lukowiak, K., and Ito, E. (2016). Relationship between the grades of a learned aversive-feeding response and the dopamine contents in *Lymnaea*. *Biol. Open.* 5, 1869–1873. doi: 10.1242/bio.021634

Aonuma, H., Kaneda, M., Hatakeyama, D., Watanabe, Y., Lukowiak, K., and Ito, E. (2017). Weak involvement of octopamine in aversive taste learning in a snail. *Neurobiol. Learn. Mem.* 141, 189–198. doi: 10.1016/j.nlm.2017.04.010

Aonuma, H., Totani, Y., Sakakibara, M., Lukowiak, K., and Ito, E. (2018). Comparison of brain monoamine content in three populations of Lymnaea that correlates with taste-aversive learning ability. *Biophys. Physicobiol.* 15, 129–135. doi: 10.2142/biophysico.15.0_129

Aonuma, H., and Watanabe, T. (2012). Changes in the content of brain biogenic amine associated with early colony establishment in the Queen of the ant, Formica japonica. *PLoS One*, 7:e43377. doi: 10.1371/journal.pone.0043377

Bacqué-Cazenave, J., Cattaert, D., Delbecque, J. P., and Fossat, P. (2017). Social harassment induces anxiety-like behaviour in crayfish. *Sci Rep.* 7:39935. doi: 10.1038/srep39935

Balaban, P. M. (2002). Cellular mechanisms of behavioral plasticity in terrestrial snail. *Neurosci. Biobehav. Rev.* 26, 597–630. doi: 10.1016/s0149-7634(02)00022-2

Balaban, P. M., Vinarskaya, A. K., Zuzina, A. B., Ierusalimsky, V. N., and Malyshev, A. Y. (2016). Impairment of the serotonergic neurons underlying reinforcement elicits extinction of the repeatedly reactivated context memory-forming. *Sci. Rep.* 6:36933. doi: 10.1038/srep36933

Benjamin, P. R., Staras, K., and Kemenes, G. (2000). A systems approach to the cellular analysis of associative learning in the pond snail *Lymnaea*. *Learn. Mem.* 7, 124–131. doi: 10.1101/lm.7.3.124

Bernacer, J., Martinez-Valbuena, I., Martinez, M., Pujol, N., Luis, E. O., Ramirez-Castillo. D., et al. (2019). An amygdala-cingulate network underpins changes in effort-based decision making after a fitness program. *Neuroimage.* 203:116181. doi: 10.1016/j.neuroimage.2019.116181

Carro, E., Trejo, J. L., Busiguina, S., and Torres-Aleman, I. (2001). Circulating insulin-like growth factor 1 mediates the protective effects of physical exercise against brain insults of different etiology and anatomy. *J. Neurosci.* 21, 5678–5684.

Chistopol'skii, I. A., and Sakharov, D. A. (2003). Non-synaptic integration of the cell bodies of neurons into the central nervous system of the snail. *Neurosci. Behav. Physiol.* 33, 295–300.

Choi, S. H., Bylykbashi, E., Chatila, Z. K., Lee, S. W., Pulli, B., Clemenson, G. D., et al. (2018). Combined adult neurogenesis and BDNF mimic exercise effects on cognition in an Alzheimer's mouse model. *Science* 361. eaan8821. doi: 10.1126/science.aan8821

Cotman, C. W., Berchtold, N. C., and Christie, L. A. (2007). Exercise builds brain health: key roles of growth factor cascades and inflammation. *Trends Neurosci.* 30, 464–472.

Deryabina, I. B., Muranova, L. N., Andrianov, V. V., and Gainutdinov, K. L. (2018). Impairing of serotonin synthesis by p-chlorphenylanine prevents the forgetting of contextual memory after reminder and the protein synthesis inhibition. *Front Pharmacol.* 9:607. doi: 10.3389/fphar.2018.00607

Dyakonova, T. L., Sultanakhmetov, G. S., Mezheritskiy, M. I., Sakharov, D. A., and Dyakonova, V. E. (2019). Storage and erasure of behavioural experiences at the single neuron level. *Sci Rep.* 9:14733. doi: 10.1038/s41598-019-51331-5

D'yakonova,V. (2014). Neurotransmitter Mechanisms of Context-Dependent Behavior. *Neurosci. Behav. Physiol.* 44, 256–267.

Dyakonova, V. E., Chistopolsky, I. A., Dyakonova, T. L., Vorontsov, D. D., and Sakharov, D. A. (2009). Direct and decarboxylation-dependent effects of neurotransmitter precursors on firing of isolated monoaminergic neurons. *J. Comp. Physiol. A* 195, 515–527. doi: 10.1007/s00359-009-0428-5

Dyakonova, V. E., Elofsson, R., Carlberg, M., and Sakharov, D. A. (1995). Complex avoidance behaviour and its neurochemical regulation in the land snail *Cepaea nemoralis*. *Gen. Pharmac.* 26, 773–777.

Dyakonova, V. E., Hernadi, L., Ito, E., Dyakonova, T. L., Chistopolsky, I. A., Zakharov, I. S., et al. (2015). The activity of isolated neurons and the modulatory

state of an isolated nervous system represent a recent behavioural state. *J. Exp. Biol.* 218, 1151–1158. doi: 10.1242/jeb.111930

Dyakonova, V. E., and Krushinsky, A. L. (2008). Previous motor experience enhances courtship behavior in male cricket *Gryllus bimaculatus*. *J. Insect Behavior* 21, 172–180. doi: 10.1007/s10905-008-9117-4

Dyakonova, V. E., and Krushinsky, A. L. (2013). Serotonin precursor (5-hydroxytryptophan) causes substantial changes in the fighting behavior of male crickets, *Gryllus bimaculatus*. *J. Comp. Physiol. A.* 199, 601–609. doi: 10.1007/s00359-013-0804-z

D'yakonova, V. E., and Sakharov, D. A. (1995). Neurotransmitter basis of mollusc behavior: control of choice between the orienting and the defense response to the presentation of an unfamiliar object. *Neurosci. Behav. Physiol.* 25, 247–251

Epp, J. R., Silva, M. R., Köhler, S., Josselyn, S. A., and Frankland, P. W. (2016). Neurogenesis-mediated forgetting minimizes proactive interference. *Nat. Commun.* 26:10838. doi: 10.1038/ncomms10838

Gillette, R. (2006). Evolution and function in serotonergic systems. *Integr. Comp. Biol.* 46, 838–846. doi: 10.1093/icb/icl024

Harris-Warrick, R. M., and Johnson, B. R. (2010). Checks and balances in neuromodulation. *Front. Behav. Neurosci.* 4:47. doi: 10.3389/fnbeh.2010.00047

Heijnen, S., Hommel, B, Kibele, A., and Colzato, L. S. (2016). Neuromodulation of aerobic exercise. *A Rev. Front. Psychol.* 6:1890. doi: 10.3389/fpsyg.2015.01890

Hillman, C. H., Erickson, K. I., and Kramer, A. F. (2008). Be smart, exercise your heart: exercise effects on brain and cognition. *Nat. Rev. Neurosci.* 9, 58–65.

Hofmann, H. A., and Stevenson, P. A. (2000). Flight restores fight in crickets. *Nature* 403:613.

Kabotyanski, E. A., Milosevich, I., and Sakharov, D. A. (1990).Neuronal correlates of 5-hydroxytryptophan-induced sustained swimming in *Aplysia fasciata*. *Comp. Biochem. Physiol.* 95, 39–44.

Kavaliers, M. (1987). Evidence for opioid and non-opioid forms of stress-induced analgesia in the snail, *Cepaea nemoralis*. *Brain Res.* 410, 111–115. doi: 10.1016/S0006-8993(87)80029-X

Kondo, M., and Shimada, S. (2015). Serotonin and exercise-induced brain plasticity. *Neurotransmitter* 2:e793. doi: 10.14800/nt.793

Korshunova, T. A., Vorontsov, D. D., and Dyakonova, V. E. (2016).Previous motor activity affects transition from uncertainty to decision-making in snails. *J. Exp. Biol.* 219, 3635–3641.

Laurence,N. C., Labuschagne, L. G., Lura, B. G., and Hillman, K. L. (2015). Regular exercise enhances task-based industriousness in laboratory rats. *PLoS One.* 10:e0129831. doi: 10.1371/journal.pone.0129831

Lee, M. C., Inoue, K., Okamoto, M., Liu, Y. F., Matsui, T., Yook, J. S., et al. (2013). Voluntary resistance running induces increased hippocampal neurogenesis in rats comparable to load-free running. *Neurosci. Lett.* 537, 6–10. doi: 10.1016/j.neulet.2013.01.005

Longley, R. D., and Peterman, M. (2013). Neuronal control of pedal sole cilia in the pond snail *Lymnaea stagnalis appressa*. *J. Comp. Physiol. A* 199, 71–86. doi: 10.1007/s00359-012-0770-x

Nikitin, V. P., Solntseva, S. V., Kozyrev, S. A, Nikitin, P. V., and Shevelkin, A. V. (2018). NMDA or 5-HT receptor antagonists impair memory reconsolidation and induce various types of amnesia. *Behav. Brain Res.* 345,72–82. doi: 10.1016/j.bbr.2018.02.036

Pavlova, G. A. (2001). Effects of serotonin, dopamine and ergometrine on locomotion in the pulmonate mollusc *Helix lucorum*. *J. Exp. Biol.* 204,1625–1633.

Pavlova, G. A. (2019). The similarity of crawling mechanisms in aquatic and terrestrial gastropods. *J. Comp. Physiol. A* 205, 1–11. doi: 10.1007/s00359-018-1294-9

Popova, N. K., Ilchibaeva, T. V., and Naumenk, V. S. (2017). Neurotrophic factors (BDNF, GDNF) and the serotonergic system. *Biochemistry* 82, 449–459.

Rillich, J., and Stevenson, P. A. (2018). Serotonin mediates depression of aggression after acute and chronic social defeat stress in a model insect. *Front. Behav. Neurosci.* 12:233. doi: 10.3389/fnbeh.2018.00233

Roig, M., Skriver, K., Lundbye-Jensen, J., Kiens, B., and Nielsen, J. B. (2012). A single bout of exercise improves motor memory. *PLoS One* 7, e44594 doi: 10.1371/journal.pone.0044594

Roshchin, M., and Balaban, P. M. (2012). Neural control of olfaction and tentacle movements by serotonin and dopamine in terrestrial snail. *J. Comp. Physiol. A* 198, 145–158. doi: 10.1007/s00359-011-0695-9

Sakharov, D. A. (1990). "Integrative function of serotonin common to distantly related invertebrate animals," in *The Early Brain*, ed. M. Gustaffson, and M. Reuter (Turku: Akademi Press), 73–88.

Sakharov, D. A. (1991). "Use of transmitter precursors in gastropod neuroethology," in *Molluscan Neurobiology*, eds K. S. Kits, H. H. Boer, and J. Joosse (Amsterdam: North Holland Publishing Co.), 236–242.

Salmon, P. (2001). Effects of physical exercise on anxiety, depression, and sensitivity to stress: a unifying theory. *Clin. Psychol. Rev.* 21, 33–61.

Satterlie, R. A. (1995). Serotonergic modulation of swimming speed in the pteropod mollusc Clione limacina. II. Peripheral modulatory neurons. *J. Exp. Biol.* 198, 905–916.

Shartau, R. B., Tam, R., Patrick, S., and Goldberg, J. I. (2010). Serotonin prolongs survival of encapsulated pond snail embryos exposed to long-term anoxia. *J. Exp. Biol.* 213, 1529–1535. doi: 10.1242/jeb.040873

Stevenson, P. A., Dyakonova, V. E., Rillich, J., and Schildberger, K. (2005). Octopamine and experience-dependent modulation of aggression in crickets. *J. Neurosci.* 25, 1431–1441.

Syed, N. I., and Winlow, W. (1989). Morphology and electrophysiology of neurons innervating the ciliated locomotor epithelium in *Lymnaea stagnalis* (L.). *Comp. Biochem. Physiol.* 93A, 633–644.

Totani, Y., Aonuma, H., Oike, A., Watanabe, T., Hatakeyama, D., Sakakibara, M., et al. (2019). Monoamines, insulin and the roles they play in associative learning in pond snails. *Front. Behav. Neurosci.* 13:65.doi: 10.3389/fnbeh.2019.00065

Tsyganov, V. V., Vorontsov, D. D., and Sakharov, D. A. (2004). Phasic coordination of locomotion and respiration in a freshwater snail *Lymnaea*: transmitter-dependent modifications. *Doklady Akademii Nauk.* 395, 103–105.

Ureshi, M., Dainobu, M., and Sakai, M. (2002). Serotonin precursor (5-hydroxytryptophan) has a profound effect on the post-copulatory time-fixed sexually refractory stage in the male cricket, *Gryllus bimaculatus* DeGeer. *J. Comp. Physiol. A* 188,767–779.

van Praag, H., Christie, B. R., Sejnowski, T. J., and Gage, F. H. (1999). Running enhances neurogenesis, learning, and long-term potentiation in mice. *Proc. Natl. Acad. Sci. U.S.A.* 96, 13427–13431.

Vaynman, S., Ying, Z., and Gomez-Pinilla, F. (2004). Hippocampal BDNF mediates the efficacy of exercise on synaptic plasticity and cognition. *Eur. J. Neurosci.* 20, 2580–2590.

Vorontsov, D. D., and Dyakonova, V. E. (2017). Light-dark decision making in snails: Do preceding light conditions matter? *Commun. Integr. Biol.* 10:e1356515 doi: 10.1080/19420889.2017.1356515

Conflict of Interest: The authors declare that the research was conducted in the absence of any commercial or financial relationships that could be construed as a potential conflict of interest.

frontiers in Physiology

ORIGINAL RESEARCH
published: 07 May 2020
doi: 10.3389/fphys.2020.00418

Cloning and Expression of Cockroach α7 Nicotinic Acetylcholine Receptor Subunit

*Alison Cartereau[1], Emiliane Taillebois[1], Balaji Selvam[2], Carine Martin[1], Jérôme Graton[3], Jean-Yves Le Questel[3] and Steeve H. Thany[1]**

[1] LBLGC, UPRES EA 1207-USC INRA 1328, Université d'Orléans, Orléans, France, [2] Roger Adams Laboratory, University of Illinois at Urbana-Champaign, Urbana, IL, United States, [3] CEISAM-UMR CNRS 6230, Faculté des Sciences et des Techniques, Université de Nantes, Nantes, France

Understanding insect nicotinic acetylcholine receptor (nAChR) subtypes is of major interest because they are the main target of several insecticides. In this study, we have cloned a cockroach Pameα7 subunit that encodes a 518 amino acid protein with futures typical of nAChR subunit, and sequence homology to α7 subunit. Pameα7 is differently expressed in the cockroach nervous system, in particular in the antennal lobes, optical lobes and the mushroom bodies where specific expression was found in the non-compact Kenyon cells. In addition, we found that cockroach Pameα7 subunits expressed in *Xenopus laevis* oocytes can assemble to form homomeric receptors. Electrophysiological recordings using the two-electrode voltage clamp method demonstrated that nicotine induced an I_{max} current of −92 ± 27 nA at 1 mM. Despite that currents are low with the endogenous ligand, ACh, this study provides information on the first expression of cockroach α7 homomeric receptor.

Keywords: nicotinic receptor, insect, α7 subunit, acetylcholine, nicotine, neonicotinoid

OPEN ACCESS

Edited by:
Sylvia Anton,
Institut National de la Recherche Agronomique (INRA), France

Reviewed by:
Wolfgang Blenau,
Leipzig University, Germany
Cedric Neveu,
INRAE Val de Loire, France

****Correspondence:***
Steeve H. Thany
steeve.thany@univ-orleans.fr

Specialty section:
This article was submitted to Invertebrate Physiology, a section of the journal Frontiers in Physiology

Received: *23 August 2019*
Accepted: *07 April 2020*
Published: *07 May 2020*

Citation:
Cartereau A, Taillebois E, Selvam B, Martin C, Graton J, Le Questel J-Y and Thany SH (2020) Cloning and Expression of Cockroach α7 Nicotinic Acetylcholine Receptor Subunit. Front. Physiol. 11:418. doi: 10.3389/fphys.2020.00418

INTRODUCTION

Insect neuronal nicotinic acetylcholine receptors (nAChRs) are of particular interest because they are the main target of neonicotinoid insecticides, which are important in agriculture and veterinary medicine for controlling insect pests, and preventing transmission of insect borne diseases (Casida, 2009). In general, the pharmacological properties of insect native nAChRs are studied using electrophysiological approaches, with isolated neurons expressing nAChR subtypes (Thany et al., 2007; Barbara et al., 2008; Salgado, 2016). Cockroach neurons from thoracic ganglia and dorsal unpaired median (DUM) neurons are currently used to characterize the pharmacological properties of insect native nAChR subtypes, and the mode of action of neonicotinoid insecticides (Courjaret and Lapied, 2001; Courjaret et al., 2003; Calas-List et al., 2012; Salgado, 1998; Salgado and Saar, 2004; Thany et al., 2008). Using cockroach thoracic ganglia, two α-bungarotoxin (α-Bgt)-sensitive nAChR subtypes were characterized: nAChD and nAChN. nAChD was desensitizing, and selectively inhibited by IMI, and nAChN was non-desensitizing, and selectively inhibited by methyllicaconitine (MLA) (Salgado, 2016; Salgado and Saar, 2004). Moreover, nAChD receptors are potently inhibited by neonicotinoid insecticides whereas nAChN are activated by neonicotinoids (Salgado and Saar, 2004). α-Bgt-sensitive and -insensitive nAChR subtypes were also found in the DUM neurons. Two α-Bgt-insensitive receptors were identified as nAChR1 and nAChR2. nAChR1

was sensitive to imidacloprid, and selectively blocked by d-tubocurarine (d-TC), and nAChR2 was inhibited by mecamylamine (MEC) (Courjaret and Lapied, 2001; Courjaret et al., 2003; Thany et al., 2008; Bodereau-Dubois et al., 2012). Unfortunately, although detailed information is available concerning the pharmacological properties of cockroach native nAChR subtypes, the subunit combination of these receptors is unknown.

Genes encoding insect nAChR subunits were cloned from several insect species, including the fruit fly *Drosophila melanogaster*, the honey bee *Apis mellifera* and the mosquito *Anopheles gambiae* for which the genome is known. From comparison of the insect and vertebrate nAChR subunits it appeared that the monophyletic group including drosophila Dα5, Dα6 and Dα7, is closely related to mammalian α7 subunit (Thany et al., 2007). This group is of specific interest because mammalian α7 subunits form homomeric receptors which are currently used to study the pharmacology and functional properties of nAChR subtypes (Gill et al., 2013; Delbart et al., 2018). Binding investigations using nicotinic agonists showed that α7 nAChR mediates inward currents sensitive to nAChR antagonists such as α-Bgt or MLA when applied coincidentally with agonists, or pre-exposed to antagonists before agonist application (Cuevas et al., 2000; Virginio et al., 2002; Zhao et al., 2003). A previous study suggests that members of this group could form homomeric receptors when they are expressed in heterologous systems (Lansdell et al., 2012). Indeed, despite there having been only limited success in expressing insect nAChR subunits, a direct expression of the drosophila Dα7 subunit in *Xenopus laevis* oocytes formed a functional receptor when it was co-expressed with the chaperone resistant to inhibitors of acetylcholinesterase (RIC-3) (Lansdell et al., 2012). However, no specific α-Bgt binding was detected (Lansdell et al., 2012), suggesting that drosophila α7 receptors could be insensitive to α-Bgt. Moreover, the drosophila Dα5 subunit was able to form a homomeric α-Bgt-sensitive receptor when co-expressed with RIC-3 (Lansdell and Millar, 2004; Lansdell et al., 2012). Thus, the pharmacological properties of the α7 monophyletic group seemed to be more complex.

In the present study, we report the cloning and expression of a cockroach Pameα7 subunit in the *Xenopus laevis* oocytes. We show that Pameα7 subunit can form a functional receptor in the *Xenopus* oocytes.

MATERIALS AND METHODS

Insects

All experiments were performed with cockroach *Periplaneta americana* laboratory-reared insects.

Compounds

ACh, nicotine, MLA, MEC, d-TC and atropine were purchased from Sigma Chemical Co. (St Quentin, France). α-Bgt was purchased from Biotrend (Köln, Germany).

Bioinformatic Analysis

Sequence alignment were made with BioEdit software and deduced amino acid sequences were analyzed using the ClustalW program (Thompson et al., 1994). The location of the functional domains was determined using TMHMM 2.0 software (Moller et al., 2001). nAChR subunit sequences used for phylogenetic analysis were downloaded from GenBank database[1]. A phylogenetic tree was constructed using neighbor-joining statistical method (Saitou and Nei, 1987) with Bootstrap test at 1,000 replications and p-distance as substitution model. Branches corresponding to partitions reproduced in less than 50% bootstrap replicates were collapsed. The *D. melanogaster* GABAa subunit was used as outgroup. Analyses were conducted with the MEGA6 program (Tamura et al., 2013).

RT-PCR Amplification, Cloning and Sequencing of the Cockroach Pameα7 Subunit

Total RNA was isolated from adult brain using the RNeasy Mini Kit (Qiagen). RT-PCR and cDNA cloning was performed as follows: first-strand cDNA was product from 2 μg of total RNA, incubated at 65° for 5 min in the presence of 100 ng oligodT, 0.5 mM dNTP, 10 mM DTT, 1x RT buffer. After adding 1 μl of Superscript II RT (Invitrogen, Carlsbad, CA, United States), the reaction was proceeded at 42° for 50 min and at 70° for 10 min. The complete Pameα7 cDNA sequence was amplified using the following sense and antisense primers: AAGGATCCCCAACCATGGA GTCAACAGCAGCCTCCGA (sense) and CAAAATCTAGATTACGTCACGATGATGTG GGGCG (antisense). PCR amplification conditions were: 94°C 2 min, 30 cycles (94°C for 30 s, 65°C for 30 s, 72°C for 1 min 40 s) and 72°C for 5 min. PCR products were cloned in pGem vector (pGem T-easy vector system, Promega) and sequenced.

Semi-Quantitative PCR Amplification

For semi-quantitative PCR amplification, the following primers were used GATGGCTTCTCTTCGTCTGC (sense) and CAGCTACCGCTATCCCTGAC (antisense) for Pameα7 subunit. CTGACCCTTAAATACCCCATTG (sense) and CACAATTTCTCGTTCGGCAGTG (antisense) for actin. PCR was performed in a total volume of 25 μl containing 1 μl of RT products, 0.4 μM of each primer, 0.2 mM desoxyribonucleotide triphosphates (dNTP), 1.5 mM $MgCl_2$ and 0.125 μl of Taq polymerase (Invitrogen, Carlsbad, CA, United States). The following PCR conditions were used: 20 cycles at 95°C for 30 s, 58°C for 30 s, 72°C for 1 min and a final elongation of 72°C for 5 min. Data were analyzed using image J software. Pameα7 expression level in each sample was normalized with the corresponding actin expression (Taillebois et al., 2014).

In situ Hybridization

In situ hybridization on cryostat frontal sections was performed with digoxigenin-labeled RNA probes (Sigma-Aldrich, France) as described previously (Thany et al., 2003; Thany and Gauthier,

[1]http://www.ncbi.nlm.nih.gov/genbank/

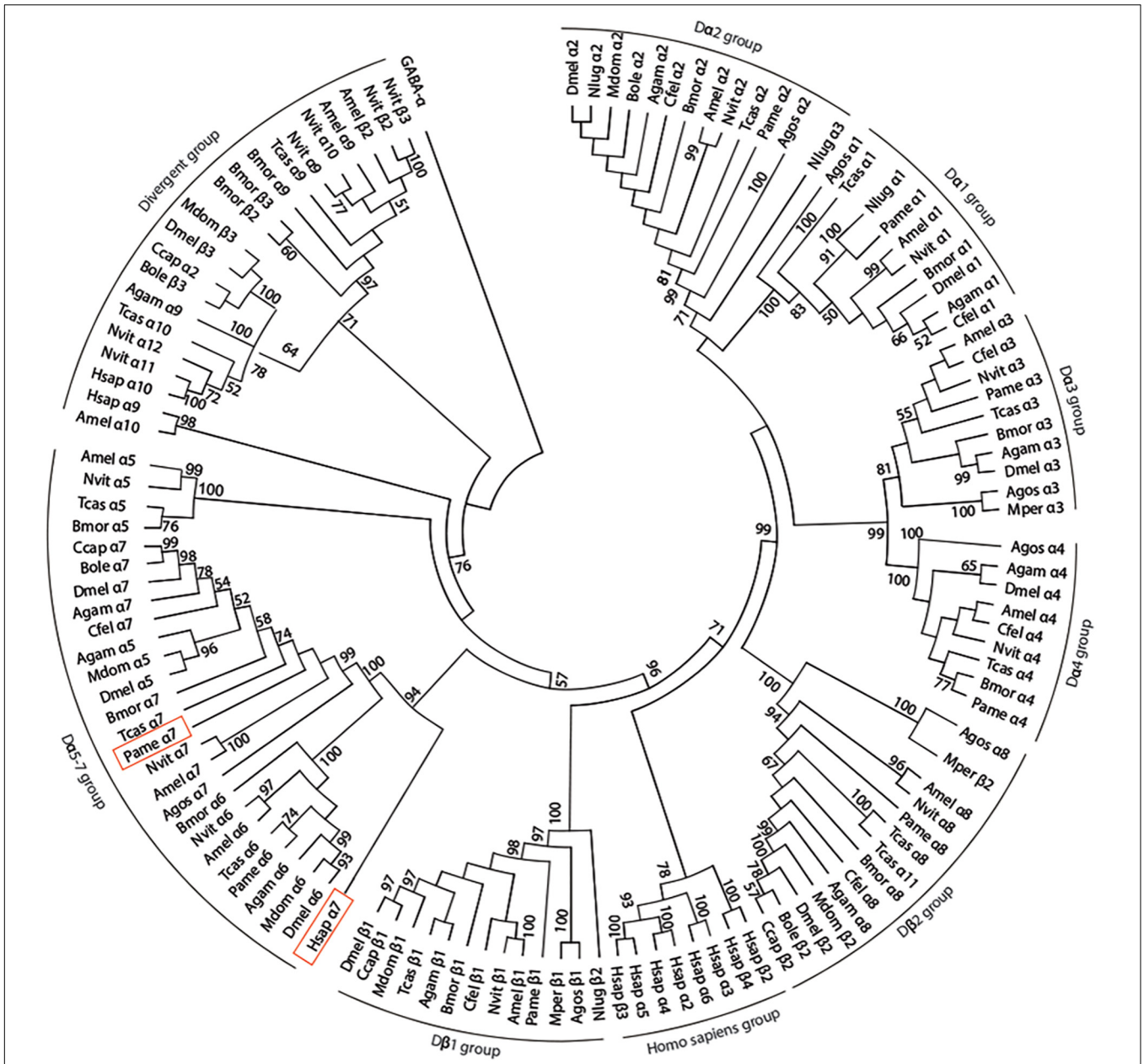

FIGURE 1 | Phylogenetic tree showing relationships of alpha 7 nAChR subunit protein sequence of the cockroach *P. americana* and its orthologs in several insect species and human. The bootstrap support value (%) based on 1,000 replicates are shown when higher than 50%. The *D. melanogaster* $GABA_A$ subunit (accession number AAA28556.1) was used as outgroup. Accession sequence identifiers are as follows: ***Anopheles gambiae***: Agamα1 (AAU12503.1), Agamα2 (AAU12504.1), Agamα3 (XP_310786.3), Agamα4 (XP_566274.3), Agamα5 (XP_314691.2), Agamα6 (XP_308042.3), Agamα7 (XP_309153.3), Agamα8 (XP_311925.3), Agamα9 (XP_310203.3), Agamβ1 (XP_309158.3); ***Aphis gossypii***: Agosα1 (AAM94383.1), Agosα2 (AAM94382.1), Agosα3 (ABR21379.1), Agosα4 (ABR21380.1), Agosα7 (AFM78640.1), Agosα8 (BBA21164.1), Agosβ1 (AAM94384.1); ***Apis mellifera***: Amelα1 (NP_001091690.1), Amelα2 (NP_001011625.1), Amelα3 (NP_001073029.1), Amelα4 (NP_001091691.1), Amelα5 (AJE70263.1), Amelα6 (NP_001073564.1), Amelα7 (AJE70265.1), Amelα8 (NP_001011575.1), Amelα9 (NP_001091694.1), Amelα10 (XP_392070.3), Amelβ1 (NP_001073028.1), Amelβ2 (NP_001091699.1); ***Bactrocera oleae***: Boleα2 (XP_014100082.1), Boleα7 (XP_014102300.1), Boleβ2 (XP_0111204502.1), Boleβ3 (XP_014090987.1); ***Bombyx mori***: Bmorα1 (ABV45511.1), Bmorα2 (ABV45512.1), Bmorα3 (ABV45513.1), Bmorα4 (ABV45514.1), Bmorα5 (ABV45516.1), Bmorα6 (NP_001091830.1), Bmorα7 (ABV45520.2), Bmorα8 (ABV45521.1), Bmorα9 (ABV45523.1), Bmorβ1 (NP_001166819.1), Bmorβ2 (NP_001103400.1), Bmorβ3 (NP_00110341.1); ***Ceratitis capitata***: Ccapα2 (XP_004536261.1), Ccapα7 (JAB87466.1), Ccapβ1 (XP_012156453.1), Ccapβ2 (XP_012162675.1); ***Drosophila melanogaster***: Dmelα1 (CAA30172.1), Dmelα2 (NP_524482.1), Dmelα3 (CAA75688.1), Dmelα4 (CAB77445.1), Dmelα5 (AAM13390.1), Dmelα6 (NP_723494.2), Dmelα7 (CAD86936.1), Dmelβ1 (P04755.1), Dmelβ2 (CAA39211.1), Dmelβ3 (NP_525098.1); ***Musca domestica***: Mdomα2 (ABD37617.1), Mdomα5 (ABY40460.1), Mdomα6 (ABJ09669.1), Mdomβ1 (XP_005180169.1), Mdomβ2 (XP_005185796.1), Mdomβ3 (ABY40465.1); ***Myzus persicae***: Mperα3 (CAB52297.1), Mperβ1 (XP_022165274.1), Mperβ2 (XP_022167599.1); ***Nasonia vitripennis***: Nvitα1 (ACY82683.1), Nvitα2 (ACY82684.1), Nvitα3 (ACY82685.1), Nvitα4 (ACY82686.1), Nvitα5 (ACY82688.1), Nvitα6 (ACY82689.1), Nvitα7 (ACY82692.1), Nvitα8 (ACY82693.1), Nvitα9 (ACY82694.1), Nvitα10 (ACY82695.1), Nvitα11 (ACY82696.1), Nvitα12 (ACY82697.1), Nvitβ1 (ACY82698.1), Nvitβ2 (ACY82699.1), Nvitβ3 (ACY82700.1);

(Continued)

FIGURE 1 | Continued
Nilaparvata lugens; Nlugα1 (AAQ75737.1), Nlugα2 (AAQ7574101), Nlugα3 (AAQ75739.1), Nlugβ2 (AAQ75742.2); ***Periplaneta americana***: Pameα1 (AKV94620.1), Pameα2 (AKV94621.1), Pameα3 (AKR16132.1), Pameα4 (AFA28129.1), Pameα6 (AKV94622.1), Pameα7 (MK790056), Pameα8 (AFA28130.1), Pameβ1 (AKV94624.1); ***Tribolium castaneum***: Tcasα1 (ABS86902.1), Tcasα2 (ABS86903.1), Tcasα3 (ABS86904.1), Tcasα4 (ABS86905.1), Tcasα5 (ABS86907.1), Tcasα6 (ABS86908.1), Tcasα7 (ABS86911.1), Tcasα8 (ABS86912.1), Tcasα9 (ABS86913.1), Tcasα10 (ABS86914.1), Tcasα11 (ABS86915.1), Tcasβ1 (ABS86916.1); ***Homo sapiens***: Hsapα2 (AAB40109.1), Hsapα3 (AAA59942.1), Hsapα4 (AAA64743.1), Hsapα5 (AAA58357.1), Hsapα6 (AAB40113.1), Hsapα7 (CAA49778.1), Hsapα9 (CAB65091.1), Hsapα10 (CAC20435.1), Hsapβ2 (CAA37320.1), Hsapβ3 (CAA47851.1), Hsapβ4 (CAA48336.1); ***Ctenocephalides felis***: Cfelα1 (ABB42999), Cfelα2 (ABB43000), Cfelα3 (ABB43001), Cfelα4 (ABB43003), Cfelα7 (ABB43004), Cfelα8 (ABB43002), Cfelβ1 (ABB43005).

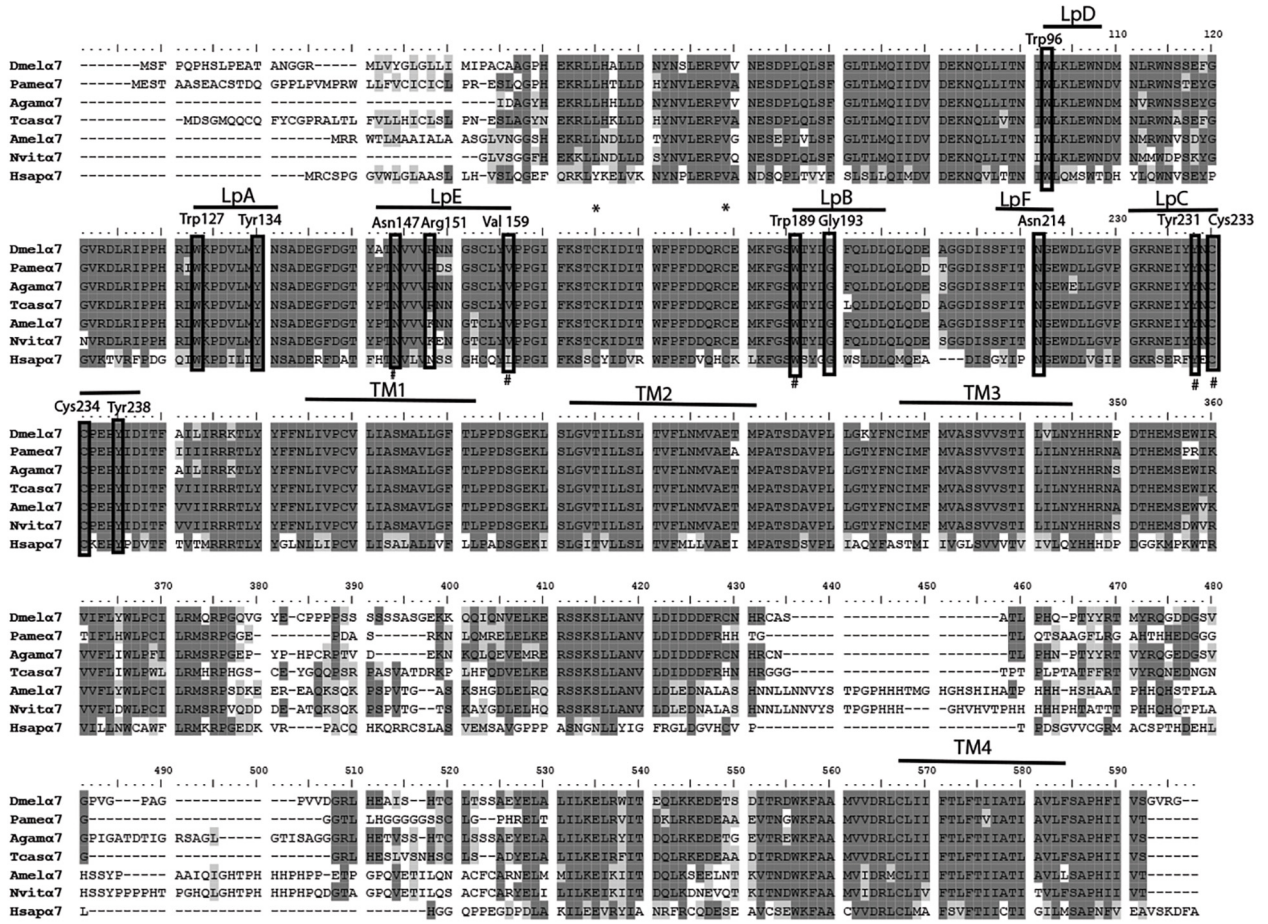

FIGURE 2 | Alignment of nAChR α7 subunit protein sequences of the cockroach *P. americana* with its orthologs in several insect species and human. The loops (LpA-F) involved in ligand binding and transmembrane motifs (TM1-4) forming the ion channel are indicated. Sites of cysteine residues involved in the Cys-loop are marked with asterisk; the vicinal cysteine residues characteristic of alpha-type and the key residues are shown in frame. Alignment was done with drosophila sequence as reference, identical residues (dark gray shading) and similar residues (light gray shading) are indicated.

2005). A cDNA fragment of 1.6 Kb corresponding to Pameα7 was cloned in pCR 4-TOPO vector (ThermoFisher Scientific, France) with HindIII and XhoI restriction enzymes. After linearization with NotI, *in vitro* transcription was performed with T7 RNA polymerase to generate antisense DIG-labeled RNA probes.

Preparation of cDNA for Expression in the Xenopus Oocytes

Cockroach Pameα7 (GenBank accession number: JX466891) subunit was cloned into XbaI/BamHI (Invitrogen, Carlsbad, CA, United States) digested pGEM-HEJUEL plasmid (Provided by Prof. Olaf Pongs, Institute for Neural Signal Transduction, Germany, to Prof Christian Legros, University of Angers, France) as previously described (Bourdin et al., 2015). pGEM contains both 5′ and 3′ UTR from the *Xenopus* beta-globin gene, allowing high expression of foreign protein in *Xenopus* oocytes.

Oocyte Injection in the Xenopus Laevis Oocytes

Xenopus laevis oocytes were obtained from the CRB xenope, University of Rennes, France. The CRB xenope is a French national platform dedicated to xenopus breeding for

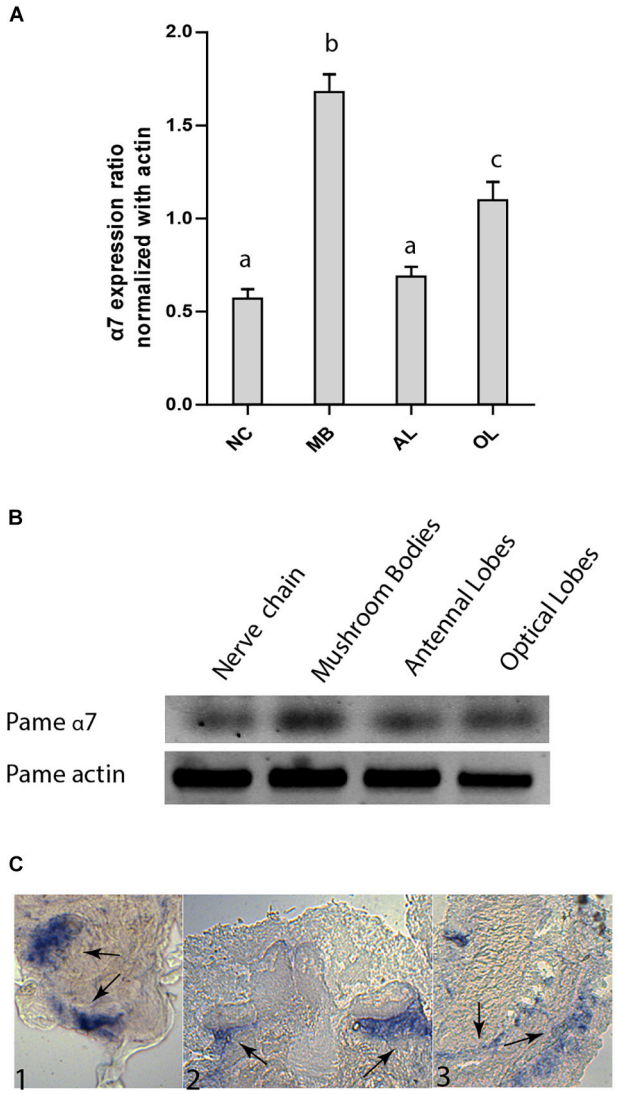

FIGURE 3 | Expression pattern of Pameα7 subunit in the cockroach nervous system. **(A)** Expression level of Pameα7 using semi-quantitative RT-PCR experiments. Data are shown as expression ratio normalized with actin. Expression pattern was determined in the nerve chain (NC), antennal lobes (AL), mushroom bodies (MB) and optical lobes (OL). Significant differences are designated by different letters. **(B)** Electrophoresis showing Pameα7 and actin (used as quantitative and positive control). Dara are the mean of four independent experiments. Significant difference was determined using one-way ANOVA and Bonferroni *post hoc* test. All statistical analyses were added in **Supplementary Figure S1C**. **(C)** *In situ* hybridization of Pameα7 mRNA on cockroach adult brain. Expression is detected in the antennal lobes (C1), the non-compact Kenyon cells of the mushroom bodies (C2) and the optic lobes (C2).

experimental research. *Xenopus laevis* oocytes were stored in a standard oocyte saline solution (SOS) of the following composition: in mM, 100 NaCl, 2 KCl, 1 MgCl2, 1.8 $CaCl_2$ and 5 HEPES, pH 7.5. Stage V and VI oocytes were harvested and defolliculated after treatment with 2 mg/ml collagenase IA (Sigma, France) in Ca^{2+}-free SOS solution, supplemented with 0.8 mg/ml trypsin inhibitor. Defolliculated oocytes were injected with 2 ng of α7 cDNA cloned in pGEM (Couturier et al., 1990; Ihara et al., 2003). Injected oocytes were maintained at 18°C in SOS solution supplemented with penicillin (100 U/ml), streptomycin (100 mg/ml), gentamycin (50 mg/ml) and sodium pyruvate (2.5 mM).

Voltage-Clamp Recordings

Currents were recorded 4 days after injection, using two microelectrodes filled with 3 M KCl. The oocyte membrane potential was held at −80 mV (Taylor-Wells et al., 2017), and perfused continuously with recording buffer at room temperature (20–22°C). To suppress potential endogenous muscarinic responses, saline solution containing 0.5 μM atropine was employed (Matsuda et al., 1998, 2000). The dose response curves were estimated by using increasing concentrations of the compounds on the same oocyte. Oocytes were challenged with a test compound at 5 min intervals to minimize receptor desensitization (Ihara et al., 2003). To assess the pharmacological profile of these receptors, experiments were conducted with different antagonists. Experimental data was digitized with a Digidata-1322A A/D converter and then analyzed with pCLAMP (Molecular Devices, Union City, CA, United States). All compound solutions were prepared using the recording buffer.

Statistical Analysis

For statistical analysis of Pameα7 expression levels, one-way ANOVA and Bonferroni *post hoc* test were employed. All currents were shown as mean ± SEM and analyzed using Prism 7 (GraphPad Software, La Jolla, CA, United States). Note that for all compounds, experiments were also performed on non-injected oocytes to avoid native responses (data not shown). Oocytes were assigned to each group without knowledge of the treatments (blinded). The dose response curves were derived from the fitted curve following the equation: $Y = I_{min} + (I_{max} - I_{min})/(1 + 10^{(log(EC50X)H)})$ where Y is the normalized response, I_{max} and I_{min} are the maximum and minimum responses, H is the Hill coefficient, EC_{50} is the concentration giving half the maximum response and X is the logarithm of the compound concentration. For the electrophysiological recordings, "n" represents the number of experiments. Thus, currents were analyzed using the Kruskal-wallis one-way ANOVA and Bonferroni *post hoc* test. $P < 0.05$ was the minimum level of significance.

RESULTS

Cloning and Expression Pattern of Cockroach α7 Subunit in the Nervous System

We have amplified by a nested PCR approach using putative cockroach *Periplaneta americana* α7 subunit sequences (JX466891 and JF731242) available in the GenBank database a full Pameα7 cDNA sequence. Two independent clones were obtained and sequenced, one encoded for a truncated form

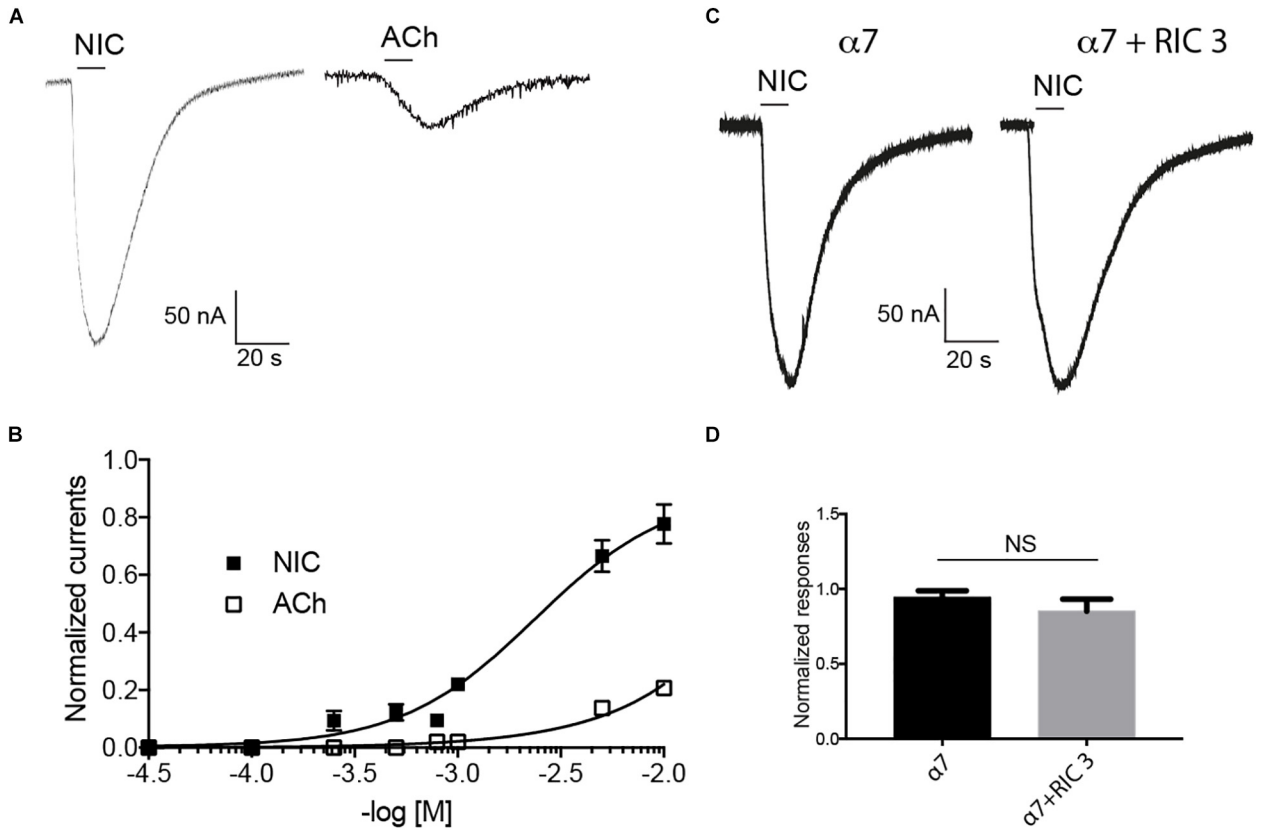

FIGURE 4 | Effect of nicotine (Nic) and acetylcholine (ACh) on cockroach α7 nAChRs expressed in *Xenopus laevis* oocytes. **(A)** Typical example of nicotine- and acetylcholine-induced currents. Currents are recorded at 10 mM nicotine or acetylcholine, respectively. **(B)** Dose-response curve are represented for nicotine and acetylcholine. Data are normalized to 10 mM nicotine and each point represents a mean ± S.E.M of *n* = 12 tested oocytes. **(C,D)** Nicotine (10 mM) evoked currents recorded after the expression of cockroach α7 subunit alone or with rat RIC-3. Each histogram represents mean ± S.E.M of *n* = 10 oocytes. NS = no significant difference using one-way ANOVA and Bonferroni *post hoc* test.

of Pameα7 (data not shown) and a complete cDNA sequence of Pameα7 subunit (GenBank accession number MK790056) with 1554 bp in length (Cartereau, 2018). This ORF encoded a protein of 518 amino acids with a predicted molecular weight of 58.02 kDa, and an estimated p*I* of 5.45. Comparison of our cloned sequence with putative cockroach α7 sequences available in the GenBank database revealed 98% sequence homology. Additional putative subunit sequences of the cockroach were identified and help us to propose a phylogenetic tree and homogenate nomenclature (**Figure 1**). Phylogenetic analysis with insect and mammalian nAChR subunits demonstrated that Pameα7 was included in the Dα5-Dα7 group which was defined as closed to the mammalian α7 subunit. The present Pameα7 subunit nomenclature takes this fact into account. We also found two distinct clusters formed by insect β subunits and a divergent cluster formed by nAChR subunits from different insect species (**Figure 1**). Moreover, amino acid sequence alignment showed that Pameα7 has features typical of the α subunit nAChR family. It contains the functional domains and key amino acids for agonist binding. The four hydrophobic putative transmembrane domains TM1-TM4, the two adjacent cysteines, and extracellular loops (LpA-F) as well as key amino acid residues (Asn147, Trp189, Tyr231,Cys233-234) (Shimomura et al., 2004; Yao et al., 2009; Wu et al., 2015) which are highly conserved between insect and human α nAChR subunits. Except for Val159 which seemed specific to insect species. In addition, the amino acid sequences between TM3 and TM4 appears highly variable (**Figure 2**). To further investigate the expression of Pameα7 in the cockroach nervous system, we compared its expression level in several nervous tissues (**Figures 3A,B**). Semi-quantitative PCR experiments highlighted a strong expression in mushroom bodies and optical lobes compared to antennal lobes and nerve chain. In the MBs, using Pameα7-specific RNA probes, we found an expression in outer Kenyon cells of the MBs, in the cells between the lamina and the lobula, and in some cells of the antennal lobes (**Figure 3C**). Substantial analyses comparing RT-PCR conditions after several PCR cycles were added in the **Supplementary Figures S1A,B** and **Supplementary Table S1**).

Expression of Pameα7 Subunit in *Xenopus laevis* Oocytes

The functional expression of the cockroach α7 homomeric receptor was first studied using direct expression of the Pameα7 subunit in *Xenopus laevis* oocytes. The functional

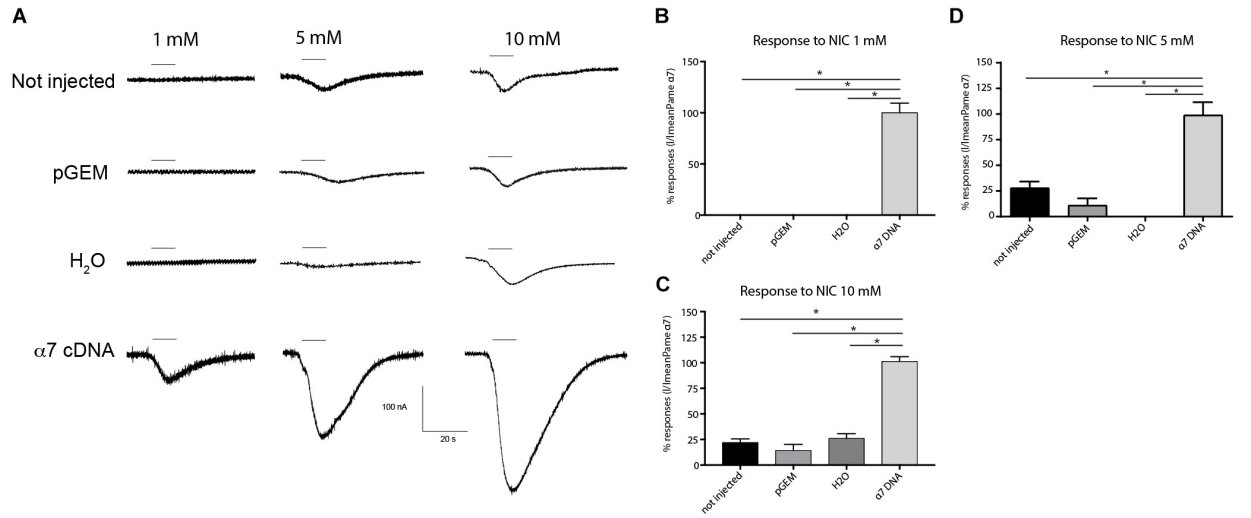

FIGURE 5 | Comparative effect of nicotine on different experimental conditions. **(A)** Typical examples of nicotine-induced currents on not injected oocytes (native oocytes), oocytes with only water, oocytes with pGem vector and oocytes with α7 cDNA. Bars indicate 10 s application of nicotine at 1, 5 or 10 mM. **(B–D)** Histograms summarize applications of nicotine at different experimental conditions. Each histogram represents $n = 12$ oocytes, $^*p < 0.05$ using One-way ANOVA and Bonferroni *post hoc* test.

expression of cockroach α7 homomeric receptor was first studied using direct expression of α7 subunit in the *Xenopus laevis* oocytes. ACh and nicotine induced inward currents but nicotine activated Pameα7 receptors in a dose-dependent manner and the maximum responses with nicotine were greater than the maximum responses evoked by ACh (**Figures 4A,B**). At 10 mM, the max currents for nicotine and ACh were −212 ± 0.13 and −56 ± 09 nA, respectively. The EC_{50} for Nicotine was 790 μM whereas for ACh, we were not able to calculate it. Co-expression of cockroach Pameα7 subunit with a rat RIC-3 did not enhance or change the response induced by nicotine (**Figures 4C,D**, $n = 18$, $p > 0.05$). We proposed that rat RIC-3 is not necessary for the functional expression of Pameα7 receptor and that Pameα7 subunit can form a functional homomeric receptor alone. Moreover, we found also that Pameα7 cDNA formed a functional receptor compared to Pameα7 cRNA (see **Supplementary Figure S1C**). Thus, we used Pameα7 cDNA, as described in previous studies (Hurst et al., 2005; Moroni et al., 2006; Alcaino et al., 2017). In addition, we decided to select as a test concentration 10 mM nicotine, in consistency with the conditions used for cockroach DUM neurons expressing nAChR subtypes (Courjaret and Lapied, 2001; Courjaret et al., 2003) and because currents induced by ACh were low to conduct a robust analysis. We then tested the effect of nicotine on oocytes containing water and pGem vector. As illustrated in **Figure 5**, despite that native currents were recorded when we used 5 or 10 mM nicotine, currents induced following 10 s application of 1 mM nicotine demonstrated that Pameα7 cDNA injection expressed a functional receptor in the oocytes. The percentage of successful expression of cockroach Pameα7 receptors that respond to nicotine applications was around 75% ($n = 120$ tested oocytes at 1 mM nicotine). The I_{max} values at 1 mM nicotine was −92 ± 27 nA. Moreover, bath application of 10 μM α-Bgt, did not block or reduce nicotine-evoked currents (**Figure 6A**, $n = 10$ cells, $p > 0.05$, one-way ANOVA and Bonferroni *post hoc* test) but MLA, a potent specific nicotinic antagonist of vertebrate neuronal α7 nAChRs (Davies et al., 1999), reduced 24% of the nicotine evoked currents (**Figure 6B**, $n = 12$, $p < 0.05$, one-way ANOVA and Bonferroni *post hoc* test). Additional data were performed to investigate if MLA reduced currents on not injected eggs. MLA has no effect on not injected oocytes (see **Supplementary Figure S1D**). In addition, no blocking or reduction of nicotine currents was found with 5 μM MEC (**Figure 6C**, $n = 8$, $p > 0.05$, one-way ANOVA and Bonferroni *post hoc* test) or 10 μM d-TC (**Figure 6D**, $n = 8$, $p > 0.05$, one-way ANOVA and Bonferroni *post hoc* test).

DISCUSSION

We have cloned using putative sequence available in the GenBank database a DNA fragment corresponding to the cockroach Pameα7. The cDNA for Pameα7 encodes a protein sequence of 518 amino acids which is closely related to the human α7 subunit. Temporal and spatial expression of Pameα7 mRNA demonstrated a specific expression in the MBs. This tissue specific expression was also found with other insects using *in situ* hybridization of transcripts from the honey bee Amelα7. Indeed, Amelα7 was also expressed in the antennal lobes and optic lobes. Expression in the MBs was found in the outer and non-compact Kenyon cells (Thany et al., 2005).

We then studied the expression of the Pameα7 subunit in the *Xenopus laevis* oocytes and found that it can form functional homomeric receptors in the *Xenopus laevis* oocytes. To date functional expressions of an insect homomeric α receptor had been demonstrated in *Xenopus laevis* oocytes with the

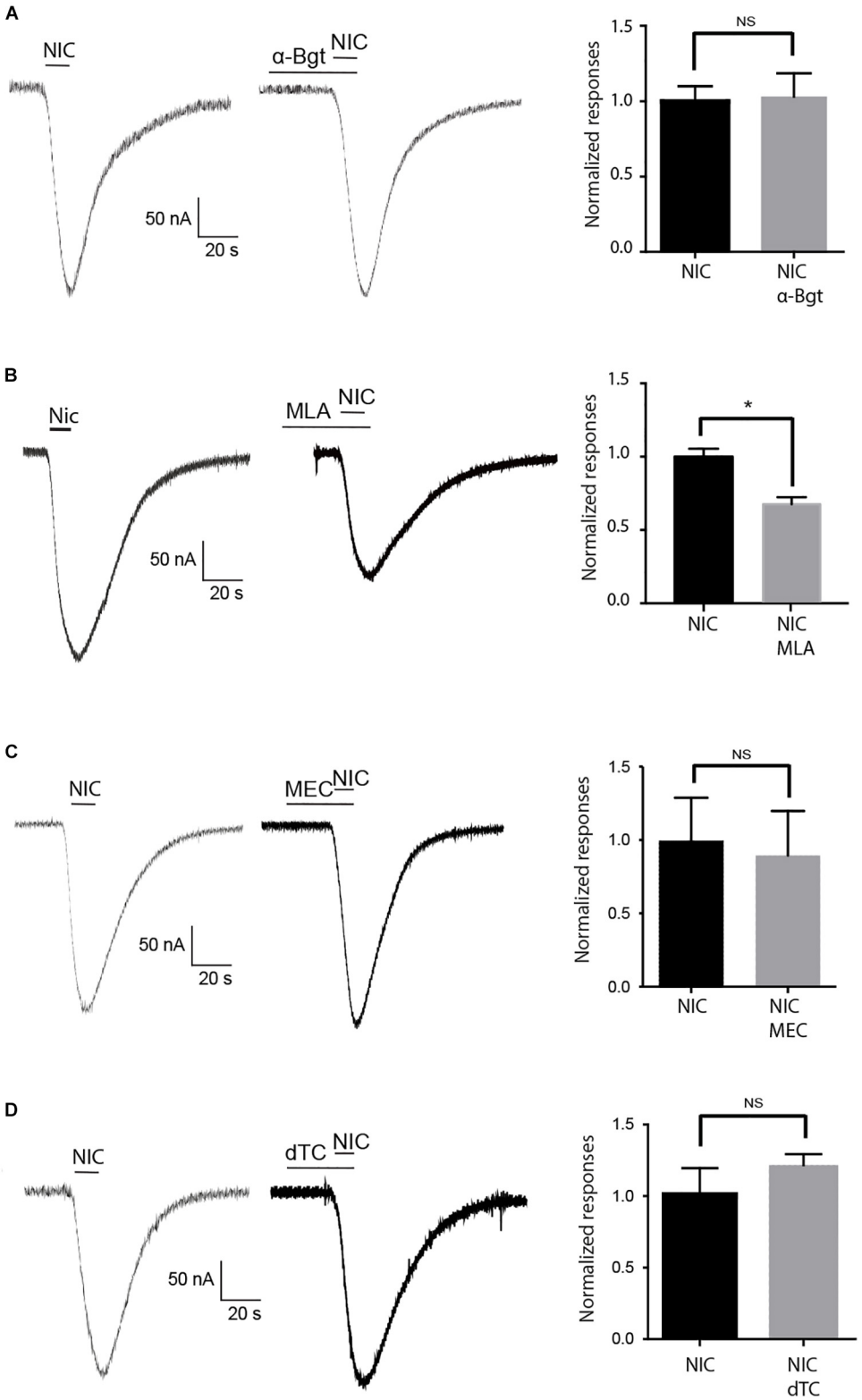

FIGURE 6 | Effect of nAChR antagonists on nicotine evoked currents. **(A)** 5 min pretreatment with 10 μM α-Bgt, **(B)** 10 μM MLA, **(C)** 5 μM mecamylamine (MEC), and **(D)** 10 μM d-TC. Bars indicate application of 10 s nicotine at 10 mM. Histograms illustrate the effect of each antagonist on nicotine-evoked currents. In each case, data are mean ± S.E.M of $n = 12$ oocytes, $^*p < 0.05$ using one-way ANOVA and Bonferroni *post hoc* test. NS = no significant.

Drosophila melanogaster Dα5 and Dα7 subunits co-expressed with the molecular chaperone CeRIC-3. Our investigations suggest that the cockroach Pameα7 receptor is insensitive to α-Bgt. This result was not surprising as there was also a lack of specific α-Bgt binding sites on drosophila S2 cells, expressing full-length Dα6 or Dα7 subunits. The only exception were the use of chimeric Dα6/5HT$_{3A}$ and Dα7/5HT$_{3A}$ receptors or recombinant Dα6 and Dα7 receptors expressed with RIC-3 (Lansdell and Millar, 2004; Lansdell et al., 2012). Moreover, cockroach *Periplaneta americana* did not express an α5 subunit compared to other insect species such as *Drosophila melanogaster*. Similar lack of α5 subunit ortholog was also shown in the pea aphid *Acyrthosiphon pisum* (Dale et al., 2010). The lack of this subunit may impact the expression and the functional properties of α7 subunit because it can form an heteromeric receptor with α7 subunit as found with *Drosophila melanogaster*.

In conclusion, in the present study, the challenge was to identify a cockroach Pameα7 subunit which was able to express functional receptor from direct expression in the *Xenopus* oocytes. But, we are aware that additional efforts are needed because we have to consider that currents are low when we use low acetylcholine and nicotine concentrations. Indeed, at low concentration, we did not find endogenous responses following application of nicotine (at 1 mM). At high nicotine (5 and 10 mM) concentrations, despite that currents are high, endogenous currents were found which lead us to be care on the results. Nevertheless, with all due caution, we consider that Pameα7 subunit can form functional homomeric receptor. Moreover, The low sensitivity could suggest that Pameα7 needs cockroach chaperone proteins like RIC-3 or NACHO (Gu et al., 2016). We have started to clone cockroach orthologs of RIC-3 and the nAChR regulator, NACHO which we hope will help increasing currents through cockroach Pameα7 receptors. Indeed, despite that the mammalian RIC-3 increases α7 activity, it is not sufficient for efficient assembly of α7 but NACHO can synergize with RIC-3 for α7-type nAChRs surface expression (Matta et al., 2017). In addition to the cloning of RIC-3 and NACHO, we aim to study the involvement of lynx proteins identified in *Locusta migratoria*, in particular lynx3 which increased epibatidine-evoked current amplitudes when it was co-expressed with both Locα1 and rat β2 or Locα4 and rat β2 in the *Xenopus* oocytes (Bao et al., 2017). All these studies will be our future goal.

DATA AVAILABILITY STATEMENT

The datasets generated for this study can be found in the GenBank accession number: JX466891.

ETHICS STATEMENT

All the experiments were performed with laboratory-reared insect. No special permit was required. All European guidelines for the care and use of laboratory animals were followed.

AUTHOR CONTRIBUTIONS

ST and J-YL designed the experiments. AC, ET, and CM performed the experiments. AC, ET, BS, JG, J-YL, and ST analyzed the data and wrote the manuscript.

FUNDING

This work was supported by grants from the Région Centre Val de Loire "SCREENROBOT project," from the Région Pays de la Loire "ECRIN project," and a Ph.D. grant for AC from the Région Centre Val de Loire.

SUPPLEMENTARY MATERIAL

The Supplementary Material for this article can be found online at: https://www.frontiersin.org/articles/10.3389/fphys.2020.00418/full#supplementary-material

REFERENCES

Alcaino, C., Musgaard, M., Minguez, T., Mazzaferro, S., Faundez, M., Iturriaga-Vasquez, P., et al. (2017). Role of the Cys loop and transmembrane domain in the allosteric modulation of alpha4beta2 nicotinic acetylcholine receptors. *J. Biol. Chem.* 292, 551–562.

Bao, H., Zhang, Y., Liu, Y., Yu, N., and Liu, Z. (2017). The functional interaction between nicotinic acetylcholine receptors and Ly-6/neurotoxin proteins in *Locusta migratoria*. *Neurochem. Int.* 108, 381–387.

Barbara, G. S., Grunewald, B., Paute, S., Gauthier, M., and Raymond-Delpech, V. (2008). Study of nicotinic acetylcholine receptors on cultured antennal lobe neurones from adult honeybee brains. *Invert Neurosci.* 8, 19–29.

Bodereau-Dubois, B., List, O., Calas-List, D., Marques, O., Communal, P. Y., Thany, S. H., et al. (2012). Transmembrane potential polarization, calcium influx, and receptor conformational state modulate the sensitivity of the imidacloprid-insensitive neuronal insect nicotinic acetylcholine receptor to neonicotinoid insecticides. *J. Pharmacol. Exp. Ther.* 341, 326–339.

Bourdin, C. M., Lebreton, J., Mathe-Allainmat, M., and Thany, S. H. (2015). Pharmacological profile of zacopride and new quaternarized fluorobenzamide analogues on mammalian alpha7 nicotinic acetylcholine receptor. *Bioorg. Med. Chem. Lett.* 15, 3184–3188.

Calas-List, D., List, O., and Thany, S. H. (2012). Nornicotine application on cockroach dorsal unpaired median neurons induces two distinct ionic currents: implications of different nicotinic acetylcholine receptors. *Neurosci. Lett.* 14, 64–68.

Cartereau, A. (2018). *Caractérisation Des Sous-Types de Récepteurs Nicotiniques Neuronaux d'Insectes et Étude de la Modulation de Leurs Profils Pharmacologiques par les Insecticides Néonicotinoïdes.* Dissertation thesis, University of Orléans, Orléans.

Casida, J. E. (2009). Pest toxicology: the primary mechanisms of pesticide action. *Chem. Res. Toxicol.* 22, 609–619.

Courjaret, R., Grolleau, F., and Lapied, B. (2003). Two distinct calcium-sensitive and -insensitive PKC up- and down-regulate an alpha-bungarotoxin-resistant nAChR1 in insect neurosecretory cells (DUM neurons). *Eur. J. Neurosci.* 17, 2023–2034.

Courjaret, R., and Lapied, B. (2001). Complex intracellular messenger pathways regulate one type of neuronal alpha-bungarotoxin-resistant nicotinic acetylcholine receptors expressed in insect neurosecretory

cells (dorsal unpaired median neurons). *Mol. Pharmacol.* 60, 80–91.

Couturier, S., Bertrand, D., Matter, J. M., Hernandez, M. C., Bertrand, S., Millar, N., et al. (1990). A neuronal nicotinic acetylcholine receptor subunit (alpha 7) is developmentally regulated and forms a homo-oligomeric channel blocked by alpha-BTX. *Neuron* 5, 847–856.

Cuevas, J., Roth, A. L., and Berg, D. K. (2000). Two distinct classes of functional 7-containing nicotinic receptor on rat superior cervical ganglion neurons. *J. Physiol.* 525(Pt 3), 735–746.

Dale, R. P., Jones, A. K., Tamborindeguy, C., Davies, T. G., Amey, J. S., Williamson, S., et al. (2010). Identification of ion channel genes in the Acyrthosiphon pisum genome. *Insect. Mol. Biol.* 19(Suppl. 2), 141–153.

Davies, A. R., Hardick, D. J., Blagbrough, I. S., Potter, B. V., Wolstenholme, A. J., and Wonnacott, S. (1999). Characterisation of the binding of [3H]methyllycaconitine: a new radioligand for labelling alpha 7-type neuronal nicotinic acetylcholine receptors. *Neuropharmacology.* 38, 679–690.

Delbart, F., Brams, M., Gruss, F., Noppen, S., Peigneur, S., Boland, S., et al. (2018). An allosteric binding site of the alpha7 nicotinic acetylcholine receptor revealed in a humanized acetylcholine-binding protein. *J. Biol. Chem.* 293, 2534–2545.

Gill, J. K., Chatzidaki, A., Ursu, D., Sher, E., and Millar, N. S. (2013). Contrasting properties of alpha7-selective orthosteric and allosteric agonists examined on native nicotinic acetylcholine receptors. *PLoS ONE* 8:e55047. doi: 10.1371/journal.pone.0055047

Gu, S., Matta, J. A., Lord, B., Harrington, A. W., Sutton, S. W., Davini, W. B., et al. (2016). Brain alpha7 nicotinic acetylcholine receptor assembly requires NACHO. *Neuron.* 89, 948–955.

Hurst, R. S., Hajos, M., Raggenbass, M., Wall, T. M., Higdon, N. R., Lawson, J. A., et al. (2005). A novel positive allosteric modulator of the alpha7 neuronal nicotinic acetylcholine receptor: in vitro and in vivo characterization. *J. Neurosci.* 25, 4396–4405.

Ihara, M., Matsuda, K., Otake, M., Kuwamura, M., Shimomura, M., Komai, K., et al. (2003). Diverse actions of neonicotinoids on chicken alpha7, alpha4beta2 and Drosophila-chicken SADbeta2 and ALSbeta2 hybrid nicotinic acetylcholine receptors expressed in *Xenopus laevis* oocytes. *Neuropharmacology* 45, 133–144.

Lansdell, S. J., Collins, T., Goodchild, J., and Millar, N. S. (2012). The *Drosophila* nicotinic acetylcholine receptor subunits Dalpha5 and Dalpha7 form functional homomeric and heteromeric ion channels. *BMC Neurosci.* 13:73. doi: 10.1186/1471-2202-13-73

Lansdell, S. J., and Millar, N. S. (2004). Molecular characterization of Dalpha6 and Dalpha7 nicotinic acetylcholine receptor subunits from *Drosophila*: formation of a high-affinity alpha-bungarotoxin binding site revealed by expression of subunit chimeras. *J. Neurochem.* 90, 479–489.

Matsuda, K., Buckingham, S. D., Freeman, J. C., Squire, M. D., Baylis, H. A., and Sattelle, D. B. (1998). Effects of the alpha subunit on imidacloprid sensitivity of recombinant nicotinic acetylcholine receptors. *Br. J. Pharmacol.* 123, 518–524.

Matsuda, K., Shimomura, M., Kondo, Y., Ihara, M., Hashigami, K., Yoshida, N., et al. (2000). Role of loop D of the alpha7 nicotinic acetylcholine receptor in its interaction with the insecticide imidacloprid and related neonicotinoids. *Br. J. Pharmacol.* 130, 981–986.

Matta, J. A., Gu, S., Davini, W. B., Lord, B., Siuda, E. R., Harrington, A. W., et al. (2017). NACHO mediates nicotinic acetylcholine receptor function throughout the brain. *Cell Rep.* 19, 688–696.

Moller, S., Croning, M. D., and Apweiler, R. (2001). Evaluation of methods for the prediction of membrane spanning regions. *Bioinformatics* 17, 646–653.

Moroni, M., Zwart, R., Sher, E., Cassels, B. K., and Bermudez, I. (2006). alpha4beta2 nicotinic receptors with high and low acetylcholine sensitivity: pharmacology, stoichiometry, and sensitivity to long-term exposure to nicotine. *Mol. Pharmacol.* 70, 755–768.

Saitou, N., and Nei, M. (1987). The neighbor-joining method: a new method for reconstructing phylogenetic trees. *Mol. Biol. Evol.* 4, 406–425.

Salgado, V. L. (1998). Studies on the mode of action of spinosad: insect symptoms and physiological correlates. *Pest Biochem. Physiol.* 60, 91–102.

Salgado, V. L. (2016). Antagonist pharmacology of desensitizing and non-desensitizing nicotinic acetylcholine receptors in cockroach neurons. *Neurotoxicology* 56, 188–195.

Salgado, V. L., and Saar, R. (2004). Desensitizing and non-desensitizing subtypes of alpha-bungarotoxin-sensitive nicotinic acetylcholine receptors in cockroach neurons. *J. Insect. Physiol.* 50, 867–879.

Shimomura, M., Yokota, M., Matsuda, K., Sattelle, D. B., and Komai, K. (2004). Roles of loop C and the loop B-C interval of the nicotinic receptor alpha subunit in its selective interactions with imidacloprid in insects. *Neurosci. Lett.* 363, 195–198.

Taillebois, E., Beloula, A., Quinchard, S., Jaubert-Possamai, S., Daguin, A., Servent, D., et al. (2014). Neonicotinoid binding, toxicity and expression of nicotinic acetylcholine receptor subunits in the aphid *Acyrthosiphon pisum*. *PLoS ONE* 9:e96669.

Tamura, K., Stecher, G., Peterson, D., Filipski, A., and Kumar, S. (2013). MEGA6: molecular evolutionary genetics analysis version 6.0. *Mol. Biol. Evol.* 30, 2725–2729.

Taylor-Wells, J., Hawkins, J., Colombo, C., Bermudez, I., and Jones, A. K. (2017). Cloning and functional expression of intracellular loop variants of the honey bee (Apis mellifera) RDL GABA receptor. *Neurotoxicology* 60, 207–213.

Thany, S. H., Courjaret, R., and Lapied, B. (2008). Effect of calcium on nicotine-induced current expressed by an atypical alpha-bungarotoxin-insensitive nAChR2. *Neurosci. Lett.* 438, 317–321.

Thany, S. H., Crozatier, M., Raymond-Delpech, V., Gauthier, M., and Lenaers, G. (2005). Apisalpha2, Apisalpha7-1 and Apisalpha7-2: three new neuronal nicotinic acetylcholine receptor alpha-subunits in the honeybee brain. *Gene* 344, 125–132.

Thany, S. H., and Gauthier, M. (2005). Nicotine injected into the antennal lobes induces a rapid modulation of sucrose threshold and improves short-term memory in the honeybee *Apis mellifera*. *Brain Res.* 1039, 216–219.

Thany, S. H., Lenaers, G., Crozatier, M., Armengaud, C., and Gauthier, M. (2003). Identification and localization of the nicotinic acetylcholine receptor alpha3 mRNA in the brain of the honeybee, *Apis mellifera*. *Insect Mol. Biol.* 12, 255–262.

Thany, S. H., Lenaers, G., Raymond-Delpech, V., Sattelle, D. B., and Lapied, B. (2007). Exploring the pharmacological properties of insect nicotinic acetylcholine receptors. *Trends Pharmacol. Sci.* 28, 14–22.

Thompson, J. D., Higgins, D. G., and Gibson, T. J. (1994). CLUSTAL W: improving the sensitivity of progressive multiple sequence alignment through sequence weighting, position-specific gap penalties and weight matrix choice. *Nucleic Acids Res.* 22, 4673–4680.

Virginio, C., Giacometti, A., Aldegheri, L., Rimland, J. M., and Terstappen, G. C. (2002). Pharmacological properties of rat alpha 7 nicotinic receptors expressed in native and recombinant cell systems. *Eur. J. Pharmacol.* 445, 153–161.

Wu, S., Zuo, K., Kang, Z., Yang, Y., Oakeshott, J. G., and Wu, Y. (2015). A point mutation in the acetylcholinesterase-1 gene is associated with chlorpyrifos resistance in the plant bug *Apolygus lucorum*. *Insect. Biochem. Mol. Biol.* 65, 75–82.

Yao, X., Song, F., Zhang, Y., Shao, Y., Li, J., and Liu, Z. (2009). Nicotinic acetylcholine receptor beta1 subunit from the brown planthopper, *Nilaparvata lugens*: a-to-I RNA editing and its possible roles in neonicotinoid sensitivity. *Insect. Biochem. Mol. Biol.* 39, 348–354.

Zhao, L., Kuo, Y. P., George, A. A., Peng, J. H., Purandare, M. S., Schroeder, K. M., et al. (2003). Functional properties of homomeric, human alpha 7-nicotinic acetylcholine receptors heterologously expressed in the SH-EP1 human epithelial cell line. *J. Pharmacol. Exp. Ther.* 305, 1132–1141.

Conflict of Interest: The authors declare that the research was conducted in the absence of any commercial or financial relationships that could be construed as a potential conflict of interest.

frontiers in Physiology

REVIEW
published: 30 November 2021
doi: 10.3389/fphys.2021.719038

Behavior Individuality: A Focus on *Drosophila melanogaster*

*Rubén Mollá-Albaladejo and Juan A. Sánchez-Alcañiz**

Instituto de Neurociencias, UMH&CSIC, San Juan de Alicante, Spain

Among individuals, behavioral differences result from the well-known interplay of nature and nurture. Minute differences in the genetic code can lead to differential gene expression and function, dramatically affecting developmental processes and adult behavior. Environmental factors, epigenetic modifications, and gene expression and function are responsible for generating stochastic behaviors. In the last decade, the advent of high-throughput sequencing has facilitated studying the genetic basis of behavior and individuality. We can now study the genomes of multiple individuals and infer which genetic variations might be responsible for the observed behavior. In addition, the development of high-throughput behavioral paradigms, where multiple isogenic animals can be analyzed in various environmental conditions, has again facilitated the study of the influence of genetic and environmental variations in animal personality. Mainly, *Drosophila melanogaster* has been the focus of a great effort to understand how inter-individual behavioral differences emerge. The possibility of using large numbers of animals, isogenic populations, and the possibility of modifying neuronal function has made it an ideal model to search for the origins of individuality. In the present review, we will focus on the recent findings that try to shed light on the emergence of individuality with a particular interest in *D. melanogaster*.

Keywords: behavior individuality, *Drosophila melanogaster*, animal personality, neurobiology, stochasticity

OPEN ACCESS

Edited by:
Philippe Lucas, Institut National de la Recherche Agronomique (INRA), France

Reviewed by:
Ralf Stanewsky, University of Münster, Germany
Marko Brankatschk, Technische Universität Dresden, Germany

****Correspondence:***
Juan A. Sánchez-Alcañiz
juan.sanchez@umh.es

Specialty section:
This article was submitted to Invertebrate Physiology, a section of the journal Frontiers in Physiology

Received: *01 June 2021*
Accepted: *11 October 2021*
Published: *30 November 2021*

Citation:
Mollá-Albaladejo R and Sánchez-Alcañiz JA (2021) Behavior Individuality: A Focus on Drosophila melanogaster. Front. Physiol. 12:719038. doi: 10.3389/fphys.2021.719038

1. INTRODUCTION

Individuality, temperament, behavioral syndromes, or animal personality are terms used to define the display of specific behavioral traits that are stable over time (Dall et al., 2004; Sih et al., 2004; Bell, 2007). At the population level, animals tend to show homogeneous behavior. However, if analyzed in more detail, it is clear that individuals within a group show behavioral patterns that differentiate them from the average. For example, in humans, food perception is highly personal, and it depends on the combination of both sociocultural experience and genetic polymorphisms that affect the function of gustatory (Kim et al., 2003) and olfactory receptors (Wysocki and Beauchamp, 1984; Kowalewski and Ray, 2020). This interindividual variation is not exclusive to humans and is generally observed in all living beings. For example, bacteria grown in the laboratory display variations in swimming behavior due to changes in gene expression, indicating that even in populations with the same genetic background and grown in similar conditions, heterogeneous behaviors can be observed (Davidson and Surette, 2008). Experiments with the clonal fish *Poecilia formosa* show that individuals grown in standardized conditions in isolation after birth display considerable differences in their behavior (Bierbach et al., 2017). Those results would suggest that stochastic developmental events lead to high variability in behavior. For example, variations in mushroom body size in *D. melanogaster*, affecting aggression, lifespan, and sleep, have been

linked with polymorphisms in more than 100 genes (Zwarts et al., 2015). It is important to remark that those variations in behavior are consistent over time. We are not referring to just an acute change in their behavioral pattern or the minor variations resulting from the "noise" in the system that might induce temporary changes in a particular behavior (Faisal et al., 2008). Other stochastic events, inherent to any biological system, such as changes in gene expression or development, will have a more profound impact on the outcome of the behavior, contributing to persistent variations in behavior and the emergence of individuality (Honegger and de Bivort, 2018).

The genetic background of the organism and the developmental history of an individual dramatically affect how the animal will express this individuality (Dall et al., 2004; Sih et al., 2004; Wolf and Weissing, 2010). Although animals of the same species share the same genome, subtle changes during development (i.e., axon guidance) can have severe effects on the final connectivity of the neurons due to stochastic events altering specific behaviors (Linneweber et al., 2020; Kiral et al., 2021). In addition, environmental factors during growth and epigenetic changes will modify gene expression. It is important to remark that although animal personality defines the animal and shows specific stability, it has certain levels of plasticity, as happens with foraging behaviors on a day-to-day basis (Anreiter and Sokolowski, 2019). Previous experiences, growth and developmental conditions, and epigenetic factors form a complex milieu where behavior and individual differences emerge.

D. melanogaster is an outstanding model to study behavior individuality for several reasons. For example, it is possible to dispose of a large number of individuals to analyze per experiment; there is an extensive collection of isogenic lines available with sequenced genomes, and we can manipulate flies at the genetic level (Casillas and Barbadilla, 2017). Moreover, with only 100,000 neurons in the central brain (Raji and Potter, 2021) and a large collection of tools to manipulate neural circuits, *D. melanogaster* is an excellent model system to understand the genetic and neural basis of behavior heterogeneity.

The present review presents the scientific advances in the study of behavior individuality in *D. melanogaster*. We will cover the knowledge gained in genetics, development, epigenetics, and the methods used to study individual behavior in flies.

2. GENETIC BASIS OF ANIMAL INDIVIDUALITY

Animal behavior and, ultimately, animal personality results from the interaction of genetic and non-genetic factors. Indeed, animals combine genetic and environmental traits to promote specific adaptation to available resources from the environment and their gene expression adapts to the circumstances (**Figure 1A**) (Honegger and de Bivort, 2018; Koyama et al., 2020). However, neither nature nor nurture in isolation can explain how and why animals behave the way they do, as each of the two components has its weight. Even more, the expression of specific genes is not constant over time but can change through the life course of the animal, causing modifications in the personality of an individual (Juneja et al., 2016; Lin et al., 2016). Hence, genes are in constant communication with non-genetic factors coupling complex and sensitive networks that will finally define the personality of an individual in response to natural pressure.

The advent of genomics during the last decades has revolutionized the field of behavioral neuroscience, providing evidence on how genes can face natural dynamic variation between individuals and affect different behavioral outputs contributing to population performance (Jin et al., 2001; Ueno and Takahashi, 2020). How, when, and where a gene or genes are expressed and modulate brain activity and processing, could explain why two individuals from the same species, similar genetic backgrounds, and raised in similar conditions behave differently. For example, in *D. melanogaster* genetic variation in olfactory receptors (*Or22a/Or22b, Or35a, and Or47a*) affect different odor guidance perceptions among individuals of the same population (Richgels and Rollmann, 2011). Also, variation in odor guidance to 2,3-butanedione showed genes associated with neural development and the later processing in the central nervous system which might be related to that behavioral variation (Brown et al., 2013). This genotypic variation is seen not only at the behavioral level but also, for example, in lifespan or morphological and anatomical traits as brain, wing, thorax, or eye size (Carreira et al., 2016; Buchberger et al., 2021).

In behavioral neuroscience (and neuroscience in general), the use of inbred lines can reduce phenotypic variability. However, even in highly controlled experimental conditions, high levels of variability can be observed both in mice and *D. melanogaster* (Honegger and de Bivort, 2018). Many animals available and short reproductive time made it possible to generate numerous collections of isogenic lines. The Drosophila Genetic Reference Panel (DGRP) are a set of fly populations derived from subsequent inbred generations producing lines with sequenced genomes and all its polymorphisms annotated (Mackay et al., 2012). As the genome of each of those fly lines is sequenced, it is possible to test the variations in behavior for each line to later search for the genetic basis responsible for such behavior. Also, studies in simple stereotyped behaviors have found complex genetic architectures involved in the final output performance of specific behaviors that differ between individuals. Thirteen genes are involved in the flight performance in *D. melanogaster* where the variation in the expression and regulation of these genes may reflect the variation in the flight performance among individuals. Among them, polymorphisms at the regulatory region of the transmembrane tyrosine kinase, Egfr, showed the largest behavioral variation affecting wing shape (Spierer et al., 2021). Other studies have used DGRP lines to search genetic variation in aggressive behavior, virgin egg retention, or immune response against pathogens (i.e., *Coxiella burnetii*) (Akhund-Zade et al., 2017; Guzman et al., 2021). Interestingly, interindividual variation can also be observed in *D. melanogaster* mating behavior. During courtship, male flies execute a series of stereotyped and progressive behaviors that culminate in mating (Hall, 1994). Even in behavior as stereotyped as courtship, which must avoid interspecies mating, studies made in natural

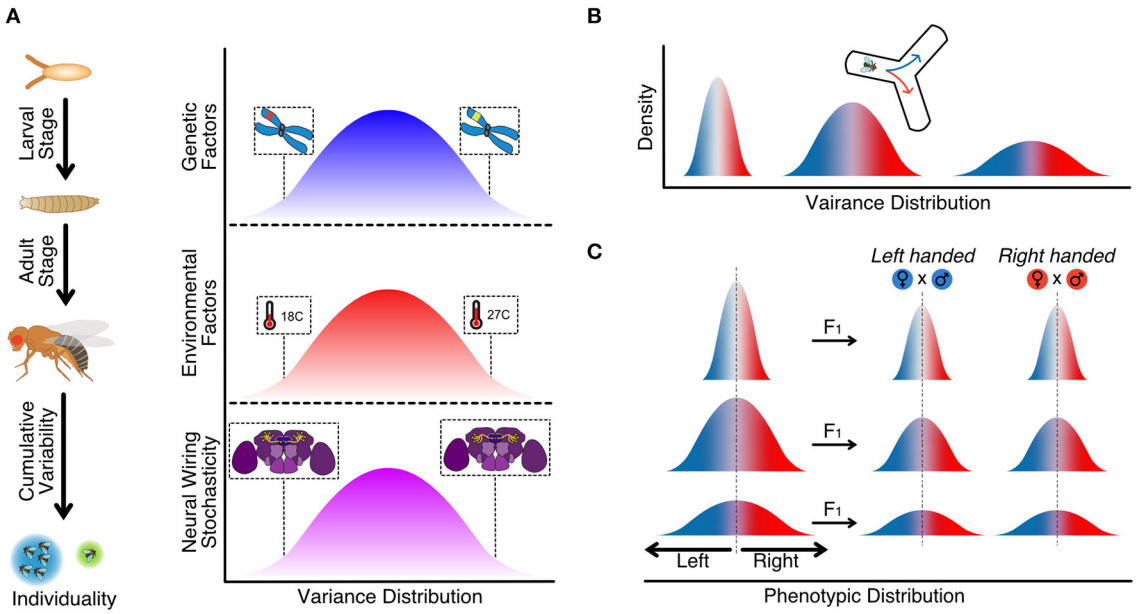

FIGURE 1 | (A) Cumulative and relative contribution of different sources of interindividual variability from early development stages to adult life experience. Individuality emerges from the combination of genetic factors, environmental factors, and stochastic factors. **(B)** Variance distribution for a given phenotypic trait evoking variability among individuals within a population (Buchanan et al., 2015). **(C)** Variance distribution of phenotypic handedness is inherited to next generations within a population (Ayroles et al., 2015).

populations have observed variability in male courtship behaviors toward mated females (Ruedi and Hughes, 2008). Genome-Wide Association Studies (GWAS) performed in the inbred collection of DGRP flies showed the influence of genetic variation in courtship variability. Particularly, the transition from copulation to no engagement was associated with SNPs in *Serrate* and *Furin-1* genes (Gaertner et al., 2015).

A key question in behavior individuality is why animals show this range of erratic behaviors. A possible explanation derives from the natural variability in the surrounding environment. A genetically uniform population might be desirable in a stable environment with no threats, as individuals diverting from the average might not be well-adapted. However, in an ever-changing environment, animals must develop strategies to survive. One option would be phenotypic plasticity, where individuals have developed the ability to change their behavior upon environmental requirements. For example, fruit flies adapt their diet to environmental temperature. *D. melanogaster* feeds primarily from yeast, but if the temperature drops below 15°C, flies change to a plant-based diet. Plants provide the flies with unsaturated fatty acids, increasing cell membrane fluidity and lifespan (Brankatschk et al., 2018). Phenotypic plasticity can also be observed in overwintering *Drosophila*, winter morphs, where flies display different phenotypic plasticity to adapt to low temperatures (Panel et al., 2020; Stockton et al., 2020).

Another possibility is to hedge their options or diversified bet-hedging. In this scenario, a single genotype produces a distribution of phenotypes, assuring that at least some individuals within the population will be well-adapted to cope with any environmental change (Honegger and de Bivort, 2018). Under those circumstances, individuals show heterogeneous natural behavior. This natural variability would be heritable, causing the behavioral individuality observed. Experiments using wild-type and inbreed lines exploring the animal idiosyncrasies have studied the mechanistic behind animal handedness or better performance using left or right hand. This behavior can be observed in *D. melanogaster* when it is forced to choose to go left or right in an arena with no other stimulus. In this paradigm, flies showed considerable variability in this particular trait, which relates to specific genotypes (Ayroles et al., 2015; Buchanan et al., 2015). The authors showed that although each population averaged a 50% chance of turning either right or left, some were more variable, with more individuals either turning left or right (**Figure 1B**). Thus, the turning bias of individual flies was not heritable but was the degree of variability of the population. Furthermore, crossing two "righty" or two "lefty" individuals did not produce hybrids all "righty" and "lefty," respectively, as the F1 progeny would show average turn vias of 50%. However, the variability of the particular line would be inherited (**Figure 1C**). A gene encoding an axon guidance molecule, *Tenascin-a*, has been proposed as a candidate involved in the observed behavior heterogeneity (refer to next section) (Ayroles et al., 2015; Buchanan et al., 2015). This distribution of phenotypes observed might be an evolutionary strategy, diversified bet-hedging, to guarantee that at least some individuals will be well-adapted when facing unpredictable environments. Bet-hedging could be the possible source of variation in the phototactic behavior of flies in two populations of flies from two different climates.

Flies from very stable tropical regions where day/light time is relatively stable would show less variability in a phototactic choice assay than the ones from a nordic region, where seasonal changes in light/dark are more dramatic. Serotonin variation among the populations could be the source of such variation as feeding flies with serotonin would decrease variability (Kain et al., 2012; Krams et al., 2021). To reinforce this idea, other studies focused on other species such as *Caenorhabditis elegans* show that in isogenic sibling individuals raised under the same conditions, serotonin might regulate behavioral variability. Complete depletion of serotonin (*tph-1*) or some of the G-protein coupled receptors (SER-1, SER-4, and SER-7) induce changes in the individual roaming behavior across development (Stern et al., 2017).

As we have seen, some of those genes affect the development of specific neural circuits. In contrast, others affect neuromodulatory networks, such as serotonin in locomotor behavior in *C. elegans*. In other cases, mutations in particular alleles affect particular gene regulatory networks, ultimately affecting neuronal function. For example, it is the case of the chaperone *heat shock protein 90* (HSP90), involved in the folding and maturation of other proteins. HSP90 mutants show high levels of interindividual morphology variation (Rutherford and Lindquist, 1998). In addition, recent studies have shown that HSP90 mutant flies display a high interindividual variation in circadian motor control (Hung et al., 2009). Daily cycles of light and darkness can entrain the circadian clock. Once established, a gene network can keep it oscillating without environmental cues (Williams and Sehgal, 2001). While wild-type flies showed low variations in their rhythmic activity, flies with decreased activity of the chaperone HSP90 showed variation between individuals, from rhythmic and arrhythmic to other complex behaviors. Those results indicated that HSP90 could be acting as a capacitor of behavior individuality, affecting the degree of variation in circadian behavioral activity (Hung et al., 2009).

All these studies support the idea that in flies from the same population, there is an accumulation of polymorphisms due to spontaneous mutations, natural pressure, or simple genomic diversification from the average of the population, conferring different behavioral personalities among them. Consistent individual differences can result from intra-genotypic variations among individuals and differences in the value of state variables such as metabolic rate, growth rate, or energetic reserves (Amat et al., 2018). Also, stochastic gene expression may underlie the phenomenon of partial penetrance of mutations and variability that may interfere in individual personality (Topalidou and Chalfie, 2011).

3. DEVELOPMENTAL AND GROWTH CONDITIONS SHAPE ANIMAL PERSONALITY

In the previous section, we have discussed the genetic basis for behavioral variability. However, we also mentioned the critical role of the developmental process and growth in individual behaviors. We refer to the variations of behavior that are non-genetic as intragenotypic variation. This variability derives from stochastic microenvironmental effects such as temperature, isolation, or food sources that force individuals to adapt phenotypically to the environment (Becher et al., 2010).

Temperature is a wide-ranging environmental factor that flies can experience and must manage to maintain their homeostasis. In *D. melanogaster*, the life cycle takes longer at low temperatures and accumulates more fat energy stores as a mechanism to cope with possible future starvation periods (Klepsatel et al., 2019, 2020). Previous studies have shown that there is gene expression variation in response to low temperatures in *D. melanogaster* due to plasticity phenomena (Fry, 2008). Whole-genome sequencing in fly populations evolved in different temperatures has revealed the role of different genes in the recombination rate divergence between populations (Winbush and Singh, 2021). The transcription factors *chimo* and *eve* show different levels of expression between flies reared at different temperatures (25 vs. 17°C). This variation modifies the arborization of sensory neurons inducing interindividual variability perceiving temperature (Alpert et al., 2020; Huang et al., 2020). Those temperature changes affect synaptic connectivity in the *D. melanogaster* visual system, as flies grown at low temperatures (19°C) have more synapse numbers than the ones grown at higher temperatures (25°C) (Kiral et al., 2021). Furthermore, phenotypic plasticity in front of temperature variation is not exclusive of drosophilids as other social insects as honey bees show different learning abilities related to labors within the colony depending on the larvae developmental temperature (Tautz et al., 2003; Jeanson, 2019). Those results indicate that temperature is a major source of phenotypic plasticity and interindividual variability within a population.

Environmental factors can dramatically influence the development of the animal and condition its growth, modifying its behavior. Flies raised in stimulating naturalistic environment vials vs. vials without any enrichment that could match natural environments showed significant differences in fitness. Enriched populations showed higher intragenotypic variability for most of the behavioral traits measured, concluding that enrichment stimuli environment is one of the central sources of variability for behavior traits crucial to surviving (Akhund-Zade et al., 2019). Also, gene expression noise varies depending on the specific gene function, suggesting that variance in gene expression noise in order to evoke phenotypic plasticity may be beneficial for survival to environmental changes (Blake et al., 2006; Newman et al., 2006; Viney and Reece, 2013).

Even in conditions where genetic background and environment are kept constant, similar individuals can develop non-heritable idiosyncratic behaviors, morphology, and gene expression profiles evoking variability that could be consistent with development and life. Stochastic development wiring or minute differences in growth conditions can contribute to the trait under study. Identical populations of pea aphids and flies grown in identical environmental conditions display heterogeneous behaviors, eliminating the role of any internal factor (Schuett et al., 2011; Kain et al., 2012; Ayroles et al., 2015). Therefore, the role of those non-heritable traits in brain development and, therefore, in individual behavior is

gaining importance in neuroscience. Studies carried on the visual orientation behavior in *D. melanogaster* showed that the Dorsal Cluster Neurons axonal projections within the medulla brain are a predictor of visual orientation, suggesting that stochastic variation in brain wiring evoke non-heritable behavioral variations (Linneweber et al., 2020). We mentioned in the previous section that different populations of flies showed variations in their handedness behavior. *Tenascin-a* encodes a cell surface protein involved in axon guidance and synaptogenesis. GWAS studies of the DGRP lines showed that this protein participates in the wiring of the neural circuits involved in locomotor behavior. Presumably, variations in the protein function might affect the synaptic connectivity of the neurons in the Central Complex of the fly brain, creating the high individual to individual variations, which ultimately will affect the apparent random choice, left or right, creating a bias in specific individuals (Ayroles et al., 2015; Buchanan et al., 2015). These studies indicate how intricate the relation between genes and environment is, showing that the genetic background of a population would determine the observed variability level, becoming heritable. However, the stochastic neuronal wiring in individuals can also be the source of particular behaviors.

These findings support the idea that stochastic variation in brain wiring and gene expression combined with different genetic traits are determinants of such behavior variability.

4. HOW EPIGENETICS INFLUENCE BEHAVIOR

Epigenetics involve any biological mechanisms that regulate the expression of genes without changing the DNA sequences, becoming the crossroad between the genetic and the environmental factors leading to a biological impact upon gene expression (Heard and Martienssen, 2014; Schuebel et al., 2016; Schiele and Domschke, 2018). Different factors influence epigenetic modifications such as diet, experience, characteristics of the ecosystem, lifestyle, and the physiological state of the individuals, impacting on disease outcome, social organization, and individual behavior, among others (Waterland and Jirtle, 2003; Cunliffe, 2016; Dawson et al., 2018; Baenas and Wagner, 2019).

Epigenetic modifications affect animals at the individual and social level, modifying the role of individuals inside specific social contexts (Anreiter et al., 2017; Sara et al., 2019). For example, honey bees display DNA methylation after intruders encounter, leading to aggressive behavior (Herb et al., 2018). Differential histone 3 (H3) acetylation (H3K27) affects morphologically and behaviorally *Camponotus floridanus* ant workers. Those modifications induce differences in foraging and scouting behaviors leading to high levels of task distribution (Simola et al., 2013, 2016; Yan et al., 2014). Epigenetic modifications also alter parasocial insects like the fruit fly behavioral, developmental, and physiological traits. For example, a low-protein diet induces H3K27 heterochromatin trimethylation shortening the lifespan of flies. In addition, acetylation of H3K27 by blocking the *Drosophila Polycomb* gene induces a dysregulation of the repression of homeotic genes (Tie et al., 2009, 2016). Furthermore, epigenetic regulation affects foraging behavior by histone methylation of the *for* (foraging) gene promoter *pr4* establishing a polymorphism between sitters and rovers behaviors in *D. melanogaster* (Anreiter et al., 2017). Other studies showed that euchromatin histone methyltransferase activity affects non-associative learning and courtship memory in *Drosophila* (Kramer et al., 2011).

5. INDIVIDUALITY IN COLLECTIVE BEHAVIOR

Animals coordinate their behavior with other individuals for benefits, including increased opportunities to mate, greater migratory and foraging efficiency, less chance of being attacked, and better energy costs (Handegard et al., 2012; Berdahl et al., 2013; Jolles et al., 2019). Several researchers have focused their research on the study of the neurogenetic bases of collective behavior in order to understand how individuals can form complex social networks among themselves, improving their survival as occurs in social animals like fishes, ducks, bees, or flies (Becher et al., 2010; Bialek et al., 2014; Ramdya et al., 2017).

Behavior individuality within a colony can emerge from self-organization and social interactions benefiting host hospitalization and decision-making processes (Jeanson, 2019). Individual roles within an animal social network can change over time as an evolutionary method to decrease disease transmission (Stroeymeyt et al., 2018). In other cases, biological roles can be persistent for each individual, such as birds taking turns as alarm-calling sentinels in the colony or the task distribution in ant colonies, respectively (Nagy et al., 2010; Yan et al., 2014; Ramdya et al., 2017; Friedman et al., 2020). Individuals in social networks experience social encounters to spread information from informed to uninformed to transmit beneficial information for survival and relevant future decision-making processes (Canright and Engø-Monsen, 2006). Different studies revealed that fruit flies coordinate their oviposition sites based on the information shared by experienced flies through social encounters. Those experiments suggest that highly clustered flies show a high potential to spread information among individuals (Pasquaretta et al., 2016). Besides, flies are aware of the number of individuals and adjust their interactive behavior to the group size (Rooke et al., 2020). Other studies have shown that collective aggregation depends on external stimuli. For example, the *Poxn* transcription factor and Orco co-receptor are involved in the chemical detection of fly cuticle hydrocarbon pheromones that may be involved in clustering mechanisms (Schneider et al., 2012b). In addition, the mechanoreceptor NompC is involved in collective behavior as *NompC* mutant flies only avoid noxious CO_2 when are clustered with wild-type flies compared with isolated *NompC* mutant ones. These results indicate that there is spread of information from wild type flies to *NompC* mutants (Ramdya et al., 2015). These studies, in addition to others, support the idea that fruit flies integrate sensory information in order to drive appropriate collective behavior and facilitate social learning and foraging decisions in larvae and adulthood to buffer

efficiently environmental stress (Tinette et al., 2004; Billen, 2006; Lihoreau et al., 2016; Dombrovski et al., 2017; Jolles et al., 2017; Jiang et al., 2020).

Despite all the benefits derived from the establishment of social networks within a group of individuals, *D. melanogaster* has a parasocial organization where collective and individual behavior remains cohesive. Each group member behaving differently could explain that the cascade of group motion likely emerges from specific individual patterns of behavior (Rosenthal et al., 2015). Nevertheless, there is no evidence that some individuals act as leaders beginning the clustering within groups of fruit flies. However, the aggregation process grows as more flies join the pioneer ones, affecting information spreading (Jiang et al., 2020).

Even if *D. melanogaster* organization does not fit in a eusocial pattern where there is specific and hierarchical task distribution, the presence of individual behavior heterogeneity may drive crucial collective behavior beneficial for both the individual and the conspecifics individuals. Thus, understanding the dynamics of collective behavior in the fruit fly may guide understanding the neurogenetic bases involved and how the behavioral patterns of animal societies arise.

6. METHODS TO STUDY BEHAVIOR INDIVIDUALITY

D. melanogaster has emerged as an excellent model to study behavior individuality for several reasons: the small size and short breeding time allow us to obtain large quantities of animals to test in small setups in short periods of time; there is a large number of inbred lines with sequenced and annotated genomes to search for the possible genetic basis of individuality, and; finally, the possibility to manipulate the genome and neurons of the flies allow us to test ultimately how the candidate genes (and neural circuits) affect the generation of behavioral variation (Venken et al., 2011). The number of behavioral paradigms developed to study *Drosophila* (and in general animal behavior) have blossomed in the last years due to an increase in computer capacity and the development of machine learning algorithms dedicated to it. In **Figure 2**, we describe some hardware (with custom associated software) used to study behavior in individual flies. For example, the classic Y-maze, where flies can choose between two paths, is scaled up to allow multiple simultaneous recordings of individual flies. With this high-throughput system, the behavior of 25,000 individuals was analyzed and permitted the study of the neural and genetic basis of handedness in flies, identifying candidate genes and neurons (Buchanan et al., 2015) (**Figure 2A**). As mentioned in previous sections, animals, and particularly *D. melanogaster* display idiosyncratic behavioral responses to odors. To study this behavior, Honegger et al. build a paradigm arena where individual flies could choose between two odors emanating from opposing ends of a corridor. By video tracking the fly behavior, it was possible to show how neuromodulation was involved in the preferential choice of individuals (**Figure 2B**) (Honegger et al., 2019). Other innate behaviors like object orientation responses can be analyzed in a high-throughput manner using multiple Buridian paradigm arenas and video tracking (**Figure 2C**). Using this set up, the authors demonstrated that stochastic developmental events were altering the Dorsal Cluster Neuron circuits of different individuals, leading to idiosyncratic behaviors in flies (Linneweber et al., 2020). Finally, it is also possible to study feeding in *D. melanogaster*. *FlyPad* is an automated high-throughput method to study fly ingestion in individual flies. This system would allow the analysis of behavior individuality in, for example, the ability of flies to choose between two types of foods (Itskov et al., 2014) (**Figure 2D**). Recently, an upgrade in *FlyPad* named *OptoPad* allows optogenetically modifying the activity of selected circuits in real-time by ectopically expressing channelrhodopsins in those neurons. With this method, it is possible to couple the feeding activity of the fly with the modification of the neural activity in a closed-loop manner (Moreira et al., 2019).

The previously described methods are focused on the analysis of individual flies. However, the social context is lost, and although flies are non-eusocial insects, flies can aggregate both *in vitro* (Jiang et al., 2020) and in the wild (Soto-Yéber et al., 2019). The formation of *Drosophila* clusters is motivated by the presence of mating partners or food, with pheromones like cis-Vaccenyl acetate (Bartelt et al., 1985) and neuromodulators like serotonin (Sun et al., 2020) playing an essential role. As shown in the previous section, individuality can affect collective behavior. For example, within a group, some individuals display "bold" or "shy" behaviors. Newer software, like *idtracker.ai*, can identify each individual unequivocally in large groups (i.e., up to 70 flies), track overtime their trajectory, and the interaction with other members of the group (Romero-Ferrero et al., 2019). Finally, it is essential to mention that all those methods require standardized procedures, which start with the breeding conditions. Different mediums to homogenize the growth of flies can decrease variability due to external conditions (Piper et al., 2014). **Table 1** contains a thorough description of many hardware and software developed in recent years that are applied or can be applied to study behavior individuality. Most of the software and hardware listed are open source and shared with any laboratory that requests its use. We indicate the species for which they were designed or most used. However, researchers can modify the published versions to adapt them to their model system of interest. We apologize in advance for the methods we forgot to mention or did not find, as many appear constantly.

After describing the behavior of interest, we need to understand such behavior's genetic and neural basis. The advancement of genomic tools like Next Generation Sequencing, QTL, and GWAS is helping to understand how genes relate to behavioral traits (Bengston et al., 2018) (Figure 1E). Furthermore, we have seen the advantage of working with already sequenced collections of isogenic lines (Mackay et al., 2012). In addition, now we can do experiments to study large natural populations of flies and sequence all individuals with excellent coverage depth at low cost.

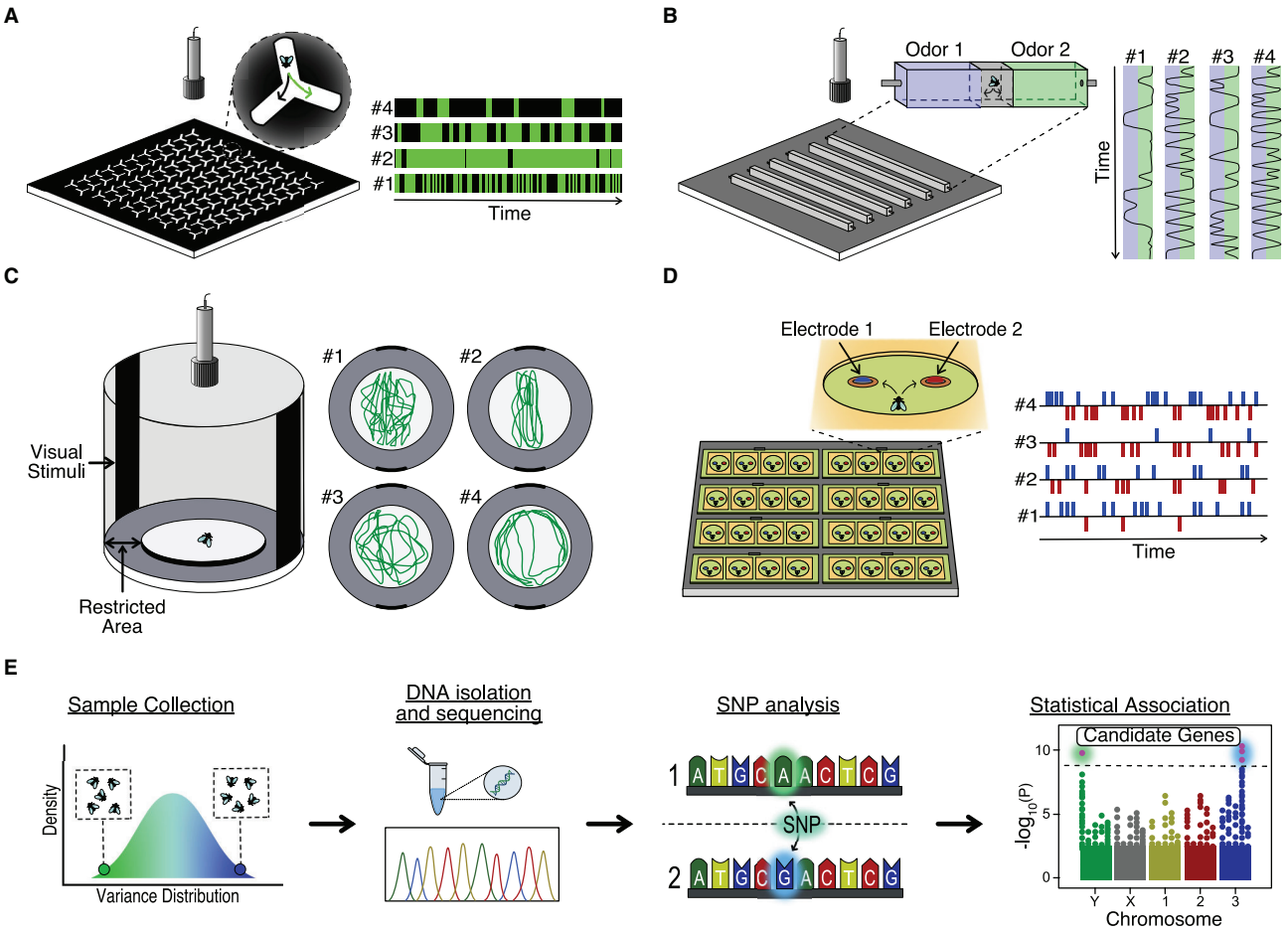

FIGURE 2 | High throughput analysis of behavior variance. **(A)** Schematic set up for study locomotor handedness variability by Y-maze (Ayroles et al., 2015; Buchanan et al., 2015). **(B)** Schematic setup for study olfactory guidance variability. Adapted from Honegger et al. (2019). **(C)** Schematic Buridian arena to study visual orientation variability (Colomb et al., 2012). **(D)** Schematic FlyPAD set-up to study feeding microstructure variability (Itskov et al., 2014). **(E)** Genome-Wide Association Studies (GWAS) workflow.

Finally, the study of the neural circuitry involved in behavior, *D. melanogaster*, is an excellent system as many different transgenic lines have been created to label, trace, and analyze complete neural circuits (Jenett et al., 2012). Similar to *C. elegans*, we aim to map all synaptic partners in the brain of *D. melanogaster* through electron microscopy (EM). Although we still need to map the whole brain, the connectome for the central brain already exists (Scheffer et al., 2020). So far, those data provide a standalone image of the *Drosophila* brain. However, it would be desirable to have a full EM reconstruction of each individual's brain analyzed, although this looks right now as an impossible effort. Even for smaller organisms, it is a daunting task, but it could be beneficial as a recent work where EM reconstruction of eight *C. elegans* brains showed variations in synaptic connectivity between them, making each brain unique (Witvliet et al., 2021). As we learn more about the circuitry involved in particular behaviors, it might be possible in the future to focus our EM reconstruction efforts on small regions of the brain known to control particular behaviors. We could then reconstruct those regions synaptically for multiple individuals, gaining excellent knowledge regarding neural circuit variability between individuals.

7. CONCLUSIONS

How do heritable (genetic) and non-heritable (stochastic events) factors interact to shape behavior? It could be possible that individuals carrying particular polymorphisms might be more susceptible to environmental changes, leading to enough variations among individuals to show specific individual persistent behaviors. It would not be easy to differentiate between the genetic and non-genetic basis of such behavior as there is a constant interplay in this particular case. To add more complexity to the problem epigenetic modifications, alter gene function. It means we cannot just focus our efforts on finding particular genetic sequences as the final goal, as we need to understand how genomes change along with the life of an individual. Finally, from a behavioral point of view, we are constantly talking about individuality. At the same time, animals modify their behaviors during their lifetime as they interact with other conspecifics. All

TABLE 1 | Overview of automated and high throughput software and hardware for animal behavior analysis.

Hardware/software	Utility	Software/ hardware	Programming language	Species*	References
AnTrax	Tracking software for color-tagged individuals of small species	Software	Matlab	*Ooceraea biroi*	Gal et al., 2020
Automated *Drosophila* Olfactory Conditioning System	Automated software and hardware system to study olfactory behavior coupled with learning and memory assessment	Software and Hardware	Arduino and Labview	*Drosophila melanogaster*	Jiang et al., 2016
BEEtag	Image tracking software to track labeled identified individual bees or anatomical markers	Software	Matlab	*Apis mellifera*	Crall et al., 2015
Buritrack	Tracking software either in the presence or in the absence of visual targets in a Buridian paradigm setup	Software and Hardware	R	Different species	Colomb et al., 2012
ClockLab	Analysis of circadian locomotor activity data collected using DAM system	Software	Matlab	*Drosophila melanogaster*	Pfeiffenberger et al., 2010
CTrax	Tracking software for automatically quantify individual and social behavior of fruit flies	Software	Matlab	*Drosophila melanogaster*	Branson et al., 2009
DAM	*Drosophila Activity Monitor* . System from Trikinetics for locomotion, sleep and circadian rhythms activity quantification	Hardware	None	*Drosophila melanogaster*	www.trikinetics.com
DART	*Drosophila Arousal Tracking*. Hardware and software that reports locomotor and positional activity data of individual flies in multiple chambers	Software and Hardware	Matlab	*Drosophila melanogaster*	Faville et al., 2015
DeepLabCut	Markerless pose estimation based on machine learning with deep neural networks that achieves excellent results with minimal training data to study behavior by tracking various body parts	Software	Python	*Mus musculus* and *Drosophila melanogaster*	Mathis et al., 2018
DeepPoseKit	Machine learning software for deep estimation of pose location to analyze specific behavior parameters	Software	Python	Different species	Graving et al., 2019
DIAS	*Dynamic Image Analysis System*. Tracking software to analyze locomotor behavior in the adult fruit fly as in other individuals	Software	Matlab	*Drosophila melanogaster*	Slawson et al., 2009
Drosophila Island	Algorithm that quantify locomotor and flight activity behavior from fruit flies on specific Island platforms	Software	Fiji and R	*Drosophila melanogaster*	Eidhof et al., 2017
Ethoscopes	Machine learning software to track and profile behavior in real time while trigger stimulus to flies in a feedback-loop mode	Software	R	*Drosophila melanogaster*	Geissmann et al., 2017
Expresso	Automated feeding hardware to measure individual meal-bouts with high temporal and volume resolution	Hardware	Matlab	*Drosophila melanogaster*	Yapici et al., 2016
FIM / FIMTrack	*FTIR-based Imaging Method*. Tracking hardware and software to study locomotion behavior based on internal reflection of infrared light (FTIR) operating at all wavelengths allowing *in vivo* detection of fluorescent proteins	Software and Hardware	C++	*Drosophila melanogaster*	Risse et al., 2013
FLIC	*Fly Liquid-Food Interaction Counter*. Automated hardware to detect and quantify physical contact with liquid food to study feeding behavior in fruit flies	Software and Hardware	Matlab	*Drosophila melanogaster*	Ro et al., 2014
Flyception	Retroreflective based tracking coupled with imaging brain activity on free walking fruit flies	Hardware	C++	*Drosophila melanogaster*	Grover et al., 2020
FlyGrAM	*Fly Group Activity Monitor*. Software for monitoring real-time group locomotion based on background subtraction	Software	Python	*Drosophila melanogaster*	Scaplen et al., 2019
FlyMAD	*Fly Mind-Altering Device*. Infrared laser targeting hardware for accurately thermogenetic silencing or activation on freely walking flies	Hardware	None	*Drosophila melanogaster*	Bath et al., 2014
FlyPAD	*Fly Proboscis and Activity Detector*. Detailed, automated and high-throughput quantification of feeding behavior based on capacitance data	Software and Hardware	Matlab	*Drosophila melanogaster*	Itskov et al., 2014

(Continued)

TABLE 1 | Continued

Hardware/software	Utility	Software/ hardware	Programming language	Species*	References
FlyPEZ	High-throughput hardware system to rapidly analyze individual fly behavior with tracking and controlled sensory or optogenetic stimulation	Hardware	Matlab	*Drosophila melanogaster*	Williamson et al., 2018
Flywalk	Automatic olfactory preference tracking hardware for screening individual flies	Hardware	Matlab	*Drosophila melanogaster*	Steck et al., 2012
Idtrackerai	Individual tracking of all trajectories from small and large collectives with high identification accuracy	Software	Python	Different species	Romero-Ferrero et al., 2019
Imaging system for zebrafish larvae behavior analyses	Three-camera imaging system hardware to image zebrafish larvae behavior in front of visual stimuli provided by specific slides in a high-throughput manner	Hardware	None	*Danio rerio*	Richendrfer and Créton, 2013
JAABA	Machine learning-based system for automatically quantify different animal behavior parameters	Software	Matlab	Different species	Kabra et al., 2013
Machine learning tracking software	Machine learning-based tracking software for individual trajectories inside a group	Software	None	Insects	Wario et al., 2017
pySOLO	Sleep and locomotor activity software analyzer of multiple isolated flies	Software	Python	*Drosophila melanogaster*	Gilestro, 2012
RFID	Radiofrequency identification based tracking hardware on individual ID infrared detection by antennas	Hardware	Matlab	Different species	Schneider et al., 2012a; Torquet et al., 2018; Reinert et al., 2019
RING	*Rapid Iterative Negative Geotaxis*. Digital photography based hardware to measure negative geotaxis in individual or collective animal groups simultaneously	Hardware	Scion Image - Pascal	*Drosophila melanogaster*	Gargano et al., 2005
The Tracked Program	Tracking of small movements at any location on a DAM set up to study sleep behavior and structure	Software	Java	*Drosophila melanogaster*	Donelson et al., 2012
WormFarm	Integrated microfluidic hardware to quantify different behaviors such as survival from images and videos	Hardware	None	*Caenorhabditis elegans*	Xian et al., 2013

**Species for which the hardware or software was initially designed. Nevertheless, most of them can be adapted to other species.*

this information indicates that the emergence of individuality or animal personality requires the study at different levels.

The latest advancements and development of high-throughput sequencing have finally opened the door to looking for the genetic basis of animal individuality and how the environment affects gene expression. We know individual animals show particular personalities, from flies to mice, monkeys to humans. However, at this very moment, we can start thinking to move from pure ethological studies to the molecular dissection of those behaviors. Neural circuitry tracing and reconstruction through electron microscopy are helping to build a map of the neural connections of the brain. So far, we do not have more than a few individuals. However, understanding and dissecting those circuits might help us finally understand how the expression of particular genes during a particular period or the subtle variations in connectivity could lead to a deeper understanding of individuality.

It is intriguing that nervous systems, like many other biological systems, are plastic within certain boundaries, so we can expect that personal individuality will be expressed deferentially over time or under certain environmental circumstances. *D. melanogaster* offers an excellent model system as we can test our hypothesis in large groups of animals in a short period of time (Buchanan et al., 2015). In addition, we can control to a large degree the genetic variation of our population by using inbred lines (Ayroles et al., 2015; Linneweber et al., 2020). The generation of the DGRP lines has helped advance this field, as controlling the genetic variation of the populations of interest can help us narrow down the candidate genetic variants, if any, or discard the genetic variation and ascribe it to stochastic developmental processes.

We have focused on the genetic and epigenetic changes that alter individual behavior. We have also studied how stochastic developmental processes alter neural connectivity leading to interindividual variation. However, another possible source of potential behavioral variability might come from the interaction of individuals with environmental microbes, from *Wolbachia* infections to changes in the gut microbiome. In this particular case, no genetic variation or neural circuit alteration would be responsible for the change in behavior. It is known that *Wolbachia* infection affects different *D. melanogaster* behaviors such as sleep (Bi et al., 2018), temperature preference (Truitt et al., 2019), or aggression (Rohrscheib et al., 2015). Alteration in the gut microbiome can affect aggression in *Drosophila* males (Jia et al., 2021) or sleep and memory (Silva et al., 2021). Those results point to the interaction of individuals with microorganisms as another potential source of interindividual behavior variability that must be taken into consideration.

Finally, from an evolutionary point of view, individuality might play an essential role in providing an adaptative advantage. For example, we have described that animals might use diversified bet-hedging as a mechanism to produce high levels of variation within a population to ensure that at least some individuals will be well-adapted when facing unpredictable environments. Although more experimental evidence accumulates to support this theory, without any doubt, we are in front of a growing field of knowledge that will evolve soon.

AUTHOR CONTRIBUTIONS

RM-A and JS-A conceived and wrote the manuscript. All authors contributed to the article and approved the submitted version.

FUNDING

This study was supported by grants from the Generalitat Valenciana, CIDEGENT program (CIDEGENT/2018/035), Spanish Ministry of Science and Innovation (PID2019-105839GA-I00) and Program Ramón y Cajal (RyC2019-026747-I).

ACKNOWLEDGMENTS

We thank the Generalitat Valenciana and Spanish Ministry of Science for financial support and José María Buil Gómez for critical discussions and comments on the manuscript.

REFERENCES

Akhund-Zade, J., Bergland, A. O., Crowe, S. O., and Unckless, R. L. (2017). The genetic basis of natural variation in Drosophila (Diptera: Drosophilidae) virgin egg retention. *J. Insect Sci.* 17. doi: 10.1093/jisesa/iew094

Akhund-Zade, J., Ho, S., O'Leary, C., and de Bivort, B. (2019). The effect of environmental enrichment on behavioral variability depends on genotype, behavior, and type of enrichment. *J. Exp. Biol.* 222. doi: 10.1242/jeb.202234

Alpert, M. H., Frank, D. D., Kaspi, E., Flourakis, M., Zaharieva, E. E., Allada, R., et al. (2020). A circuit encoding absolute cold temperature in Drosophila. *Curr. Biol.* 30, 2275.e5–2288.e5. doi: 10.1016/j.cub.2020.04.038

Amat, I., Desouhant, E., Gomes, E., Moreau, J., and Monceau, K. (2018). Insect personality: what can we learn from metamorphosis? *Curr. Opin. Insect Sci.* 27, 46–51. doi: 10.1016/j.cois.2018.02.014

Anreiter, I., Kramer, J. M., and Sokolowski, M. B. (2017). Epigenetic mechanisms modulate differences in Drosophila foraging behavior. *Proc. Natl. Acad. Sci. U.S.A.* 114, 12518–12523. doi: 10.1073/pnas.1710770114

Anreiter, I., and Sokolowski, M. B. (2019). The foraging gene and its behavioral effects: pleiotropy and plasticity. *Annu. Rev. Genet.* 53, 373–392. doi: 10.1146/annurev-genet-112618-043536

Ayroles, J. F., Buchanan, S. M., O'Leary, C., Skutt-Kakaria, K., Grenier, J. K., Clark, A. G., et al. (2015). Behavioral idiosyncrasy reveals genetic control of phenotypic variability. *Proc. Natl. Acad. Sci. U.S.A.* 112:6706. doi: 10.1073/pnas.1503830112

Baenas, N., and Wagner, A. E. (2019). *Drosophila melanogaster* as an alternative model organism in nutrigenomics. *Genes Nutr.* 14:14. doi: 10.1186/s12263-019-0641-y

Bartelt, R. J., Schaner, A. M., and Jackson, L. L. (1985). Cis-vaccenyl acetate as an aggregation pheromone inDrosophila *melanogaster*. *J. Chem. Ecol.* 11, 1747–1756. doi: 10.1007/BF01012124

Bath, D. E., Stowers, J. R., Hörmann, D., Poehlmann, A., Dickson, B. J., and Straw, A. D. (2014). FlyMAD: Rapid thermogenetic control of neuronal activity in freely walking Drosophila. *Nat. Methods* 11, 756–762. doi: 10.1038/nmeth.2973

Becher, M. A., Hildenbrandt, H., Hemelrijk, C. K., and Moritz, R. F. (2010). Brood temperature, task division and colony survival in honeybees: a model. *Ecol. Modell.* 221, 769–776. doi: 10.1016/j.ecolmodel.2009.11.016

Bell, A. M. (2007). Future directions in behavioural syndromes research. *Proc. R. Soc. B Biol. Sci.* 274, 755–761. doi: 10.1098/rspb.2006.0199

Bengston, S. E., Dahan, R. A., Donaldson, Z., Phelps, S. M., van Oers, K., Sih, A., et al. (2018). Genomic tools for behavioural ecologists to understand repeatable individual differences in behaviour. *Nat. Ecol. Evol.* 2, 944–955. doi: 10.1038/s41559-017-0411-4

Berdahl, A., Torney, C. J., Ioannou, C. C., Faria, J. J., and Couzin, I. D. (2013). Emergent sensing of complex environments by mobile animal groups. *Science* 339, 574–576. doi: 10.1126/science.1225883

Bi, J., Sehgal, A., Williams, J. A., and Wang, Y.-F. (2018). Wolbachia affects sleep behavior in *Drosophila melanogaster*. *J. Insect Physiol.* 107, 81–88. doi: 10.1016/j.jinsphys.2018.02.011

Bialek, W., Cavagna, A., Giardina, I., Mora, T., Pohl, O., Silvestri, E., et al. (2014). Social interactions dominate speed control in poising natural flocks near criticality. *Proc. Natl. Acad. Sci. U.S.A.* 111, 7212–7217. doi: 10.1073/pnas.1324045111

Bierbach, D., Laskowski, K. L., and Wolf, M. (2017). Behavioural individuality in clonal fish arises despite near-identical rearing conditions. *Nat. Commun.* 8:15361. doi: 10.1038/ncomms15361

Billen, J. (2006). Signal variety and communication in social insects. *Proc. Neth. Entomol. Soc. Meet* 17, 9–25.

Blake, W. J., Balázsi, G., Kohanski, M. A., Isaacs, F. J., Murphy, K. F., Kuang, Y., et al. (2006). Phenotypic consequences of promoter-mediated transcriptional noise. *Mol. Cell* 24, 853–865. doi: 10.1016/j.molcel.2006.11.003

Brankatschk, M., Gutmann, T., Knittelfelder, O., Palladini, A., Prince, E., Grzybek, M., et al. (2018). A temperature-dependent switch in feeding preference improves Drosophila development and survival in the cold. *Dev. Cell* 46, 781.e4–793.e4. doi: 10.1016/j.devcel.2018.05.028

Branson, K., Robie, A. A., Bender, J., Perona, P., and Dickinson, M. H. (2009). High-throughput ethomics in large groups of Drosophila. *Nat. Methods* 6, 451–457. doi: 10.1038/nmeth.1328

Brown, E. B., Layne, J. E., Zhu, C., Jegga, A. G., and Rollmann, S. M. (2013). Genome-wide association mapping of natural variation in odour-guided behaviour in Drosophila. *Genes Brain Behav.* 12, 503–515. doi: 10.1111/gbb.12048

Buchanan, S. M., Kain, J. S., and de Bivort, B. L. (2015). Neuronal control of locomotor handedness in Drosophila. *Proc. Natl. Acad. Sci. U.S.A.* 112:6700. doi: 10.1073/pnas.1500804112

Buchberger, E., Bilen, A., Ayaz, S., Salamanca, D., Matas de las Heras, C., Niksic, A., et al. (2021). Variation in pleiotropic hub gene expression is associated with interspecific differences in head shape and eye size in Drosophila. *Mol. Biol. Evol.* 38, 1924–1942. doi: 10.1093/molbev/msaa335

Canright, G. S., and Engø-Monsen, K. (2006). Spreading on networks: a topographic view. *Complexus* 3, 131–146. doi: 10.1159/000094195

Carreira, V. P., Mensch, J., Hasson, E., and Fanara, J. J. (2016). Natural genetic variation and candidate genes for morphological traits in *Drosophila melanogaster*. *PLoS ONE* 11:e0160069. doi: 10.1371/journal.pone.0160069

Casillas, S., and Barbadilla, A. (2017). Molecular population genetics. *Genetics* 205, 1003–1035. doi: 10.1534/genetics.116.196493

Colomb, J., Reiter, L., Blaszkiewicz, J., Wessnitzer, J., and Brembs, B. (2012). Open source tracking and analysis of adult Drosophila locomotion in Buridan's paradigm with and without visual targets. *PLoS ONE* 7:e42247. doi: 10.1371/journal.pone.0042247

Crall, J. D., Gravish, N., Mountcastle, A. M., and Combes, S. A. (2015). BEEtag: a low-cost, image-based tracking system for the study of animal behavior and locomotion. *PLoS ONE* 10:e0136487. doi: 10.1371/journal.pone.0136487

Cunliffe, V. T. (2016). The epigenetic impacts of social stress: how does social adversity become biologically embedded? *Epigenomics* 8, 1653–1669. doi: 10.2217/epi-2016-0075

Dall, S. R. X., Houston, A. I., and McNamara, J. M. (2004). The behavioural ecology of personality: consistent individual differences from an adaptive perspective. *Ecol. Lett*. 7, 734–739. doi: 10.1111/j.1461-0248.2004.00618.x

Davidson, C. J., and Surette, M. G. (2008). Individuality in bacteria. *Annu. Rev. Genet*. 42, 253–268. doi: 10.1146/annurev.genet.42.110807.091601

Dawson, E. H., Bailly, T. P. M., Dos Santos, J., Moreno, C., Devilliers, M., Maroni, B., et al. (2018). Social environment mediates cancer progression in Drosophila. *Nat. Commun*. 9:3574. doi: 10.1038/s41467-018-05737-w

Dombrovski, M., Poussard, L., Moalem, K., Kmecova, L., Hogan, N., Schott, E., et al. (2017). Cooperative behavior emerges among Drosophila larvae. *Curr. Biol*. 27, 2821.e2–2826.e2. doi: 10.1016/j.cub.2017.07.054

Donelson, N., Kim, E. Z., Slawson, J. B., Vecsey, C. G., Huber, R., and Griffith, L. C. (2012). High-resolution positional tracking for long-term analysis of Drosophila sleep and locomotion using the "tracker?? program. *PLoS ONE* 7:e37250. doi: 10.1371/journal.pone.0037250

Eidhof, I., Fenckova, M., Elurbe, D. M., van de Warrenburg, B., Nobau, A. C., and Schenck, A. (2017). High-throughput analysis of locomotor behavior in the Drosophila island assay. *J. Visual. Exp*. 2017, 1–11. doi: 10.3791/55892

Faisal, A. A., Selen, L. P. J., and Wolpert, D. M. (2008). Noise in the nervous system. *Nat. Rev. Neurosci*. 9, 292–303. doi: 10.1038/nrn2258

Faville, R., Kottler, B., Goodhill, G. J., Shaw, P. J., and Van Swinderen, B. (2015). How deeply does your mutant sleep? Probing arousal to better understand sleep defects in Drosophila. *Sci. Rep*. 5:8454. doi: 10.1038/srep08454

Friedman, D., Johnson, B., and Linksvayer, T. (2020). Distributed physiology and the molecular basis of social life in eusocial insects. *Hormones Behav*. 122:104757. doi: 10.1016/j.yhbeh.2020.104757

Fry, J. D. (2008). Genotype-environment interaction for total fitness in Drosophila. *J. Genet*. 87:355. doi: 10.1007/s12041-008-0058-7

Gaertner, B. E., Ruedi, E. A., McCoy, L. J., Moore, J. M., Wolfner, M. F., and Mackay, T. F. C. (2015). Heritable variation in courtship patterns in *Drosophila melanogaster*. *Genes Genomes Genet*. 5, 531–539. doi: 10.1534/g3.114.014811

Gal, A., Saragosti, J., and Kronauer, D. J. (2020). antrax, a software package for high-throughput video tracking of color-tagged insects. *eLife* 9:e58145. doi: 10.7554/eLife.58145

Gargano, J. W., Martin, I., Bhandari, P., and Grotewiel, M. S. (2005). Rapid iterative negative geotaxis (RING): a new method for assessing age-related locomotor decline in Drosophila. *Exp. Gerontol*. 40, 386–395. doi: 10.1016/j.exger.2005.02.005

Geissmann, Q., Garcia Rodriguez, L., Beckwith, E. J., French, A. S., Jamasb, A. R., and Gilestro, G. F. (2017). Ethoscopes: an open platform for high-throughput ethomics. *PLoS Biol*. 15:e2003026. doi: 10.1371/journal.pbio.2003026

Gilestro, G. F. (2012). Video tracking and analysis of sleep in *Drosophila melanogaster*. *Nat. Protoc*. 7, 995–1007. doi: 10.1038/nprot.2012.041

Graving, J. M., Chae, D., Naik, H., Li, L., Koger, B., Costelloe, B. R., et al. (2019). Deepposekit, a software toolkit for fast and robust animal pose estimation using deep learning. *eLife* 8, 1–42. doi: 10.7554/eLife.47994

Grover, D., Katsuki, T., Li, J., Dawkins, T. J., and Greenspan, R. J. (2020). Imaging brain activity during complex social behaviors in Drosophila with flyception2. *Nat. Commun*. 11:623. doi: 10.1038/s41467-020-14487-7

Guzman, R. M., Howard, Z. P., Liu, Z., Oliveira, R. D., Massa, A. T., Omsland, A., et al. (2021). Natural genetic variation in *Drosophila melanogaster* reveals genes associated with *Coxiella burnetii* infection. *Genetics* 217. doi: 10.1093/genetics/iyab005

Hall, J. C. (1994). The mating of a fly. *Science* 264, 1702–1714. doi: 10.1126/science.8209251

Handegard, N. O., Boswell, K. M., Ioannou, C. C., Leblanc, S. P., Tjøstheim, D. B., and Couzin, I. D. (2012). The dynamics of coordinated group hunting and collective information transfer among schooling prey. *Curr. Biol*. 22, 1213–1217. doi: 10.1016/j.cub.2012.04.050

Heard, E., and Martienssen, R. A. (2014). Transgenerational epigenetic inheritance: myths and mechanisms. *Cell* 157, 95–109. doi: 10.1016/j.cell.2014.02.045

Herb, B. R., Shook, M. S., Fields, C. J., and Robinson, G. E. (2018). Defense against territorial intrusion is associated with DNA methylation changes in the honey bee brain. *BMC Genomics* 19:216. doi: 10.1186/s12864-018-4594-0

Honegger, K., and de Bivort, B. (2018). Stochasticity, individuality and behavior. *Curr. Biol*. 28, R8-R12. doi: 10.1016/j.cub.2017.11.058

Honegger, K. S., Smith, M. A.-Y., Churgin, M. A., Turner, G. C., and de Bivort, B. L. (2019). Idiosyncratic neural coding and neuromodulation of olfactory individuality in Drosophila. *Proc. Natl. Acad. Sci. U.S.A*. doi: 10.1073/pnas.1901623116

Huang, W., Carbone, M. A., Lyman, R. F., Anholt, R. R. H., and Mackay, T. F. C. (2020). Genotype by environment interaction for gene expression in *Drosophila melanogaster*. *Nat. Commun*. 11:5451. doi: 10.1038/s41467-020-19131-y

Hung, H.-C., Kay, S. A., and Weber, F. (2009). Hsp90, a capacitor of behavioral variation. *J. Biol. Rhythms* 24, 183–192. doi: 10.1177/0748730409333171

Itskov, P. M., Moreira, J.-M., Vinnik, E., Lopes, G., Safarik, S., Dickinson, M. H., et al. (2014). Automated monitoring and quantitative analysis of feeding behaviour in Drosophila. *Nat. Commun*. 5:4560. doi: 10.1038/ncomms5560

Jeanson, R. (2019). Within-individual behavioural variability and division of labour in social insects. *J. Exp. Biol*. 222. doi: 10.1242/jeb.190868

Jenett, A., Rubin, G. M., Ngo, T.-T., Shepherd, D., Murphy, C., Dionne, H., et al. (2012). A gal4-driver line resource for Drosophila neurobiology. *Cell Rep*. 2, 991–1001. doi: 10.1016/j.celrep.2012.09.011

Jia, Y., Jin, S., Hu, K., Geng, L., Han, C., Kang, R., et al. (2021). Gut microbiome modulates Drosophila aggression through octopamine signaling. *Nat. Commun*. 12:2698. doi: 10.1038/s41467-021-23041-y

Jiang, H., Hanna, E., Gatto, C. L., Page, T. L., Bhuva, B., and Broadie, K. (2016). A fully automated Drosophila olfactory classical conditioning and testing system for behavioral learning and memory assessment. *J. Neurosci. Methods* 261, 62–74. doi: 10.1016/j.jneumeth.2015.11.030

Jiang, L., Cheng, Y., Gao, S., Zhong, Y., Ma, C., Wang, T., et al. (2020). Emergence of social cluster by collective pairwise encounters in *Drosophila*. *eLife* 9:e51921. doi: 10.7554/eLife.51921

Jin, W., Riley, R. M., Wolfinger, R. D., White, K. P., Passador-Gurgell, G., and Gibson, G. (2001). The contributions of sex, genotype and age to transcriptional variance in *Drosophila melanogaster*. *Nat. Genet*. 29, 389–395. doi: 10.1038/ng766

Jolles, J. W., Boogert, N. J., Sridhar, V. H., Couzin, I. D., and Manica, A. (2017). Consistent individual differences drive collective behavior and group functioning of schooling fish. *Curr. Biol*. 27, 2862.e7–2868.e7. doi: 10.1016/j.cub.2017.08.004

Jolles, J. W., King, A. J., and Killen, S. S. (2019). The role of individual heterogeneity in collective animal behaviour. *Trends Ecol. Evol*. doi: 10.1016/j.tree.2019.11.001

Juneja, P., Quinn, A., and Jiggins, F. M. (2016). Latitudinal clines in gene expression and cis-regulatory element variation in *Drosophila melanogaster*. *BMC Genomics* 17:981. doi: 10.1186/s12864-016-3333-7

Kabra, M., Robie, A. A., Rivera-Alba, M., Branson, S., and Branson, K. (2013). Jaaba: interactive machine learning for automatic annotation of animal behavior. *Nat. Methods* 10, 64–67. doi: 10.1038/nmeth.2281

Kain, J. S., Stokes, C., and de Bivort, B. L. (2012). Phototactic personality in fruit flies and its suppression by serotonin and white. *Proc. Natl. Acad. Sci. U.S.A*. 109, 19834–19839. doi: 10.1073/pnas.1211988109

Kim, U.-K., Jorgenson, E., Coon, H., Leppert, M., Risch, N., and Drayna, D. (2003). Positional cloning of the human quantitative trait locus underlying taste sensitivity to phenylthiocarbamide. *Science* 299, 1221–1225. doi: 10.1126/science.1080190

Kiral, F. R., Dutta, S. B., Linneweber, G. A., Poppa, C., von Kleist, M., Hassan, B. A., et al. (2021). Variable brain wiring through scalable and relative synapse formation in Drosophila. *bioRxiv*. doi: 10.1101/2021.05.12.443860

Klepsatel, P., Girish, T. N., and Gáliková, M. (2020). Acclimation temperature affects thermal reaction norms for energy reserves in Drosophila. *Sci. Rep*. 10:21681. doi: 10.1038/s41598-020-78726-z

Klepsatel, P., Wildridge, D., and Gáliková, M. (2019). Temperature induces changes in Drosophila energy stores. *Sci. Rep*. 9:5239. doi: 10.1038/s41598-019-41754-5

Kowalewski, J., and Ray, A. (2020). Predicting human olfactory perception from activities of odorant receptors. *iScience* 23. doi: 10.1016/j.isci.2020.101361

Koyama, T., Texada, M. J., Halberg, K. A., and Rewitz, K. (2020). Metabolism and growth adaptation to environmental conditions in Drosophila. *Cell. Mol. Life Sci*. 77, 4523–4551. doi: 10.1007/s00018-020-03547-2

Kramer, J. M., Kochinke, K., Oortveld, M. A. W., Marks, H., Kramer, D., de Jong, E. K., et al. (2011). Epigenetic regulation of learning and memory by Drosophila EHMT/G9a. *PLoS Biol*. 9:e1000569. doi: 10.1371/journal.pbio.1000569

Krams, I. A., Krama, T., Krams, R., Trakimas, G., Popovs, S., Jøers, P., et al. (2021). Serotoninergic modulation of phototactic variability underpins a bet-hedging strategy in *Drosophila melanogaster*. *Front. Behav. Neurosci*. 15:66. doi: 10.3389/fnbeh.2021.659331

Lihoreau, M., Clarke, I. M., Buhl, J., Sumpter, D. J. T., and Simpson, S. J. (2016). Collective selection of food patches in Drosophila. *J. Exp. Biol*. 219, 668–675. doi: 10.1242/jeb.127431

Lin, Y., Chen, Z. X., Oliver, B., and Harbison, S. T. (2016). Microenvironmental gene expression plasticity among individual *Drosophila melanogaster*. *Genes Genomes Genetics* 6, 4197–4210. doi: 10.1534/g3.116.035444

Linneweber, G. A., Andriatsilavo, M., Dutta, S. B., Bengochea, M., Hellbruegge, L., Liu, G., et al. (2020). A neurodevelopmental origin of behavioral individuality in the Drosophila visual system. *Science* 367, 1112–1119. doi: 10.1126/science.aaw7182

Mackay, T. F. C., Richards, S., Stone, E. A., Barbadilla, A., Ayroles, J. F., Zhu, D., et al. (2012). The *Drosophila melanogaster* genetic reference panel. *Nature* 482, 173–178. doi: 10.1038/nature10811

Mathis, A., Mamidanna, P., Cury, K. M., Abe, T., Murthy, V. N., Mathis, M. W., et al. (2018). DeepLabCut: markerless pose estimation of user-defined body parts with deep learning. *Nat. Neurosci*. 21, 1281–1289. doi: 10.1038/s41593-018-0209-y

Moreira, J.-M., Itskov, P. M., Goldschmidt, D., Baltazar, C., Steck, K., Tastekin, I., et al. (2019). optopad, a closed-loop optogenetics system to study the circuit basis of feeding behaviors. *eLife* 8:e43924. doi: 10.7554/eLife.43924

Nagy, M., Ákos, Z., Biro, D., and Vicsek, T. (2010). Hierarchical group dynamics in pigeon flocks. *Nature* 464, 890–893. doi: 10.1038/nature08891

Newman, J. R. S., Ghaemmaghami, S., Ihmels, J., Breslow, D. K., Noble, M., DeRisi, J. L., et al. (2006). Single-cell proteomic analysis of *S. cerevisiae* reveals the architecture of biological noise. *Nature* 441, 840–846. doi: 10.1038/nature04785

Panel, A. D. C., Pen, I., Pannebakker, B. A., Helsen, H. H. M., and Wertheim, B. (2020). Seasonal morphotypes of Drosophila suzukii differ in key life-history traits during and after a prolonged period of cold exposure. *Ecol. Evol*. 10, 9085–9099. doi: 10.1002/ece3.6517

Pasquaretta, C., Battesti, M., Klenschi, E., Bousquet, C. A. H., Sueur, C., and Mery, F. (2016). How social network structure affects decision-making in *Drosophila melanogaster*. *Proc. R. Soc. B Biol. Sci*. 283:20152954. doi: 10.1098/rspb.2015.2954

Pfeiffenberger, C., Lear, B. C., Keegan, K. P., and Allada, R. (2010). Processing circadian data collected from the Drosophila activity monitoring (DAM) system. *Cold Spring Harbor Protoc*. 2010:5519. doi: 10.1101/pdb.prot5519

Piper, M. D. W., Blanc, E., Leitão-Gonçalves, R., Yang, M., He, X., Linford, N. J., et al. (2014). A holidic medium for *Drosophila melanogaster*. *Nat. Methods* 11, 100–105. doi: 10.1038/nmeth.2731

Raji, J. I., and Potter, C. J. (2021). The number of neurons in Drosophila and mosquito brains. *PLoS ONE* 16:e0250381. doi: 10.1371/journal.pone.0250381

Ramdya, P., Lichocki, P., Cruchet, S., Frisch, L., Tse, W., Floreano, D., et al. (2015). Mechanosensory interactions drive collective behaviour in Drosophila. *Nature* 519, 233–236. doi: 10.1038/nature14024

Ramdya, P., Schneider, J., and Levine, J. D. (2017). The neurogenetics of group behavior in *Drosophila melanogaster*. *J. Exp. Biol*. 220, 35–41. doi: 10.1242/jeb.141457

Reinert, J. K., Schaefer, A. T., and Kuner, T. (2019). High-throughput automated olfactory phenotyping of group-housed mice. *Front. Behav. Neurosci*. 13:267. doi: 10.3389/fnbeh.2019.00267

Richendrfer, H., and Créton, R. (2013). Automated high-throughput behavioral analyses in zebrafish larvae. *J. Visual. Exp*. 7, 1–6. doi: 10.3791/50622

Richgels, P. K., and Rollmann, S. M. (2011). Genetic variation in odorant receptors contributes to variation in olfactory behavior in a natural population of *Drosophila melanogaster*. *Chem. Senses* 37, 229–240. doi: 10.1093/chemse/bjr097

Risse, B., Thomas, S., Otto, N., Löpmeier, T., Valkov, D., Jiang, X., et al. (2013). FIM, a novel FTIR-based imaging method for high throughput locomotion analysis. *PLoS ONE* 8:e53963. doi: 10.1371/journal.pone.0053963

Ro, J., Harvanek, Z. M., and Pletcher, S. D. (2014). FLIC: high-throughput, continuous analysis of feeding behaviors in Drosophila. *PLoS ONE* 9:e101107. doi: 10.1371/journal.pone.0101107

Rohrscheib, C. E., Bondy, E., Josh, P., Riegler, M., Eyles, D., van Swinderen, B., et al. (2015). Wolbachia influences the production of octopamine and affects Drosophila male aggression. *Appl. Environ. Microbiol*. 81, 4573–4580. doi: 10.1128/AEM.00573-15

Romero-Ferrero, F., Bergomi, M. G., Hinz, R. C., Heras, F. J. H., and de Polavieja, G. G. (2019). idtracker.ai: tracking all individuals in small or large collectives of unmarked animals. *Nat. Methods* 16, 179–182. doi: 10.1038/s41592-018-0295-5

Rooke, R., Rasool, A., Schneider, J., and Levine, J. D. (2020). *Drosophila melanogaster* behaviour changes in different social environments based on group size and density. *Commun. Biol*. 3:304. doi: 10.1038/s42003-020-1024-z

Rosenthal, S. B., Twomey, C. R., Hartnett, A. T., Wu, H. S., and Couzin, I. D. (2015). Revealing the hidden networks of interaction in mobile animal groups allows prediction of complex behavioral contagion. *Proc. Natl. Acad. Sci. U.S.A*. 112, 4690–4695. doi: 10.1073/pnas.1420068112

Ruedi, E. A., and Hughes, K. A. (2008). Natural genetic variation in complex mating behaviors of male *Drosophila melanogaster*. *Behav. Genet*. 38, 424–436. doi: 10.1007/s10519-008-9204-5

Rutherford, S. L., and Lindquist, S. (1998). Hsp90 as a capacitor for morphological evolution. *Nature* 396, 336–342. doi: 10.1038/24550

Sara, M., Merrill, N. G., and Kobor, M. S. (2019). Social environment and epigenetics. *Curr. Top. Behav. Neurosci*. 42, 289–320. doi: 10.1007/7854_2019_114

Scaplen, K. M., Mei, N. J., Bounds, H. A., Song, S. L., Azanchi, R., and Kaun, K. R. (2019). Automated real-time quantification of group locomotor activity in *Drosophila melanogaster*. *Sci. Rep*. 9, 1–16. doi: 10.1038/s41598-019-40952-5

Scheffer, L. K., Xu, C. S., Januszewski, M., Lu, Z., Takemura, S.-,y., Hayworth, K. J., et al. (2020). A connectome and analysis of the adult *Drosophila* central brain. *eLife* 9:e57443. doi: 10.7554/eLife.57443

Schiele, M. A., and Domschke, K. (2018). Epigenetics at the crossroads between genes, environment and resilience in anxiety disorders. *Genes Brain Behav*. 17:e12423. doi: 10.1111/gbb.12423

Schneider, C. W., Tautz, J., Grünewald, B., and Fuchs, S. (2012a). RFID tracking of sublethal effects of two neonicotinoid insecticides on the foraging behavior of *Apis mellifera*. *PLoS ONE* 7:e30023. doi: 10.1371/journal.pone.0030023

Schneider, J., Dickinson, M. H., and Levine, J. D. (2012b). Social structures depend on innate determinants and chemosensory processing in Drosophila. *Proc. Natl. Acad. Sci. U.S.A*. 109(Suppl 2), 17174–17179. doi: 10.1073/pnas.1121252109

Schuebel, K., Gitik, M., Domschke, K., and Goldman, D. (2016). Making sense of epigenetics. *Int. J. Neuropsychopharmacol*. 19:pyw058. doi: 10.1093/ijnp/pyw058

Schuett, W., Dall, S. R. X., Baeumer, J., Kloesener, M. H., Nakagawa, S., Beinlich, F., et al. (2011). Personality variation in a clonal insect: the pea aphid, acyrthosiphon pisum. *Dev. Psychobiol*. 53, 631–640. doi: 10.1002/dev.20538

Sih, A., Bell, A. M., Johnson, J. C., and Ziemba, R. E. (2004). Behavioral syndromes: an integrative overview. *Q. Rev. Biol*. 79, 241–277. doi: 10.1086/422893

Silva, V., Palacios-Munoz, A., Okray, Z., Adair, K. L., Waddell, S., Douglas, A. E., et al. (2021). The impact of the gut microbiome on memory and sleep in Drosophila. *J. Exp. Biol*. 224:jeb233619. doi: 10.1242/jeb.233619

Simola, D. F., Graham, R. J., Brady, C. M., Enzmann, B. L., Desplan, C., Ray, A., et al. (2016). Epigenetic (re)programming of caste-specific behavior in the ant camponotus floridanus. *Science* 351:6268. doi: 10.1126/science.aac6633

Simola, D. F., Wissler, L., Donahue, G., Waterhouse, R. M., Helmkampf, M., Roux, J., et al. (2013). Social insect genomes exhibit dramatic evolution in gene composition and regulation while preserving regulatory features linked to sociality. *Genome Res*. 23, 1235–1247. doi: 10.1101/gr.155408.113

Slawson, J. B., Kim, E. Z., and Griffith, L. C. (2009). High-resolution video tracking of locomotion in adult *Drosophila melanogaster*. *J. Visual. Exp*. 24, 1–3. doi: 10.3791/1096

Soto-Yéber, L., Soto-Ortiz, J., Godoy, P., and Godoy-Herrera, R. (2019). The behavior of adult Drosophila in the wild. *PLoS ONE* 13:e0209917. doi: 10.1371/journal.pone.0209917

Spierer, A. N., Mossman, J. A., Smith, S. P., Crawford, L., Ramachandran, S., and Rand, D. M. (2021). Natural variation in the regulation of neurodevelopmental

genes modifies flight performance in Drosophila. *PLoS Genet*. 17:e1008887. doi: 10.1371/journal.pgen.1008887

Steck, K., Veit, D., Grandy, R., Badia, S. B. I., Mathews, Z., Verschure, P., et al. (2012). A high-throughput behavioral paradigm for Drosophila olfaction - the Flywalk. *Sci. Rep*. 2, 1–9. doi: 10.1038/srep00361

Stern, S., Kirst, C., and Bargmann, C. I. (2017). Neuromodulatory control of long-term behavioral patterns and individuality across development. *Cell* 171, 1649.e10–1662.e10. doi: 10.1016/j.cell.2017.10.041

Stockton, D. G., Wallingford, A. K., Brind'amore, G., Diepenbrock, L., Burrack, H., Leach, H., et al. (2020). Seasonal polyphenism of spotted-wing Drosophila is affected by variation in local abiotic conditions within its invaded range, likely influencing survival and regional population dynamics. *Ecol. Evol*. 10, 7669–7685. doi: 10.1002/ece3.6491

Stroeymeyt, N., Grasse, A. V., Crespi, A., Mersch, D. P., Cremer, S., and Keller, L. (2018). Social network plasticity decreases disease transmission in a eusocial insect. *Science* 362, 941–945. doi: 10.1126/science.aat4793

Sun, Y., Qiu, R., Li, X., Cheng, Y., Gao, S., Kong, F., et al. (2020). Social attraction in Drosophila is regulated by the mushroom body and serotonergic system. *Nat. Commun*. 11:5350. doi: 10.1038/s41467-020-19102-3

Tautz, J., Maier, S., Groh, C., Rössler, W., and Brockmann, A. (2003). Behavioral performance in adult honey bees is influenced by the temperature experienced during their pupal development. *Proc. Natl. Acad. Sci. U.S.A*. 100, 7343–7347. doi: 10.1073/pnas.1232346100

Tie, F., Banerjee, R., Fu, C., Stratton, C. A., Fang, M., and Harte, P. J. (2016). Polycomb inhibits histone acetylation by CBP by binding directly to its catalytic domain. *Proc. Natl. Acad. Sci. U.S.A*. 113, E744-E753. doi: 10.1073/pnas.1515465113

Tie, F., Banerjee, R., Stratton, C. A., Prasad-Sinha, J., Stepanik, V., Zlobin, A., et al. (2009). Cbp-mediated acetylation of histone h3 lysine 27 antagonizes Drosophila polycomb silencing. *Development* 136, 3131–3141. doi: 10.1242/dev.037127

Tinette, S., Zhang, L., and Robichon, A. (2004). Cooperation between Drosophila flies in searching behavior. *Genes Brain Behav*. 3, 39–50. doi: 10.1046/j.1601-183x.2003.0046.x

Topalidou, I., and Chalfie, M. (2011). Shared gene expression in distinct neurons expressing common selector genes. *Proc. Natl. Acad. Sci. U.S.A*. 108, 19258–19263. doi: 10.1073/pnas.1111684108

Torquet, N., Marti, F., Campart, C., Tolu, S., Nguyen, C., Oberto, V., et al. (2018). Social interactions impact on the dopaminergic system and drive individuality. *Nat. Commun*. 9:3081. doi: 10.1038/s41467-018-05526-5

Truitt, A. M., Kapun, M., Kaur, R., and Miller, W. J. (2019). Wolbachia modifies thermal preference in *Drosophila melanogaster*. *Environ. Microbiol*. 21, 3259–3268. doi: 10.1111/1462-2920.14347

Ueno, T., and Takahashi, Y. (2020). Intrapopulation genetic variation in the level and rhythm of daily activity in Drosophila immigrans. *Ecol. Evol*. 10, 14388–14393. doi: 10.1002/ece3.7041

Venken, K. J. T., Simpson, J. H., and Bellen, H. J. (2011). Genetic manipulation of genes and cells in the nervous system of the fruit fly. *Neuron* 72, 202–230. doi: 10.1016/j.neuron.2011.09.021

Viney, M., and Reece, S. E. (2013). Adaptive noise. *Proc. R. Soc. B Biol. Sci*. 280:20131104. doi: 10.1098/rspb.2013.1104

Wario, F., Wild, B., Rojas, R., and Landgraf, T. (2017). Automatic detection and decoding of honey bee waggle dances. *PLoS ONE* 12:e0188626. doi: 10.1371/journal.pone.0188626

Waterland, R. A., and Jirtle, R. L. (2003). Transposable elements: targets for early nutritional effects on epigenetic gene regulation. *Mol. Cell. Biol*. 23, 5293–5300. doi: 10.1128/MCB.23.15.5293-5300.2003

Williams, J. A., and Sehgal, A. (2001). Molecular components of the circadian system in Drosophila. *Annu. Rev. Physiol*. 63, 729–755. doi: 10.1146/annurev.physiol.63.1.729

Williamson, W. R., Peek, M. Y., Breads, P., Coop, B., and Card, G. M. (2018). Tools for rapid high-resolution behavioral phenotyping of automatically isolated Drosophila. *Cell Rep*. 25, 1636.e5–1649.e5. doi: 10.1016/j.celrep.2018.10.048

Winbush, A., and Singh, N. D. (2021). Genomics of recombination rate variation in temperature-evolved *Drosophila melanogaster* Populations. *Genome Biol. Evol*. 13, 1–18. doi: 10.1093/gbe/evaa252

Witvliet, D., Mulcahy, B., Mitchell, J. K., Meirovitch, Y., Berger, D. R., Wu, Y., et al. (2021). Connectomes across development reveal principles of brain maturation. *Nature*. doi: 10.1038/s41586-021-03778-8

Wolf, M., and Weissing, F. J. (2010). An explanatory framework for adaptive personality differences. *Philos. Trans. R. Soc. B Biol. Sci*. 365, 3959–3968. doi: 10.1098/rstb.2010.0215

Wysocki, C. J., and Beauchamp, G. K. (1984). Ability to smell androstenone is genetically determined. *Proc. Natl. Acad. Sci. U.S.A*. 81, 4899–4902. doi: 10.1073/pnas.81.15.4899

Xian, B., Shen, J., Chen, W., Sun, N., Qiao, N., Jiang, D., et al. (2013). WormFarm: A quantitative control and measurement device toward automated *Caenorhabditis elegans* aging analysis. *Aging Cell* 12, 398–409. doi: 10.1111/acel.12063

Yan, H., Simola, D. F., Bonasio, R., Liebig, J., Berger, S. L., and Reinberg, D. (2014). Eusocial insects as emerging models for behavioural epigenetics. *Nat. Rev. Genet*. 15, 677–688. doi: 10.1038/nrg3787

Yapici, N., Cohn, R., Schusterreiter, C., Ruta, V., and Vosshall, L. B. (2016). A taste circuit that regulates ingestion by integrating food and hunger signals. *Cell* 165, 715–729. doi: 10.1016/j.cell.2016.02.061

Zwarts, L., Vanden Broeck, L., Cappuyns, E., Ayroles, J. F., Magwire, M. M., Vulsteke, V., et al. (2015). The genetic basis of natural variation in mushroom body size in *Drosophila melanogaster*. *Nat. Commun*. 6:10115. doi: 10.1038/ncomms10115

Conflict of Interest: The authors declare that the research was conducted in the absence of any commercial or financial relationships that could be construed as a potential conflict of interest.

Publisher's Note: All claims expressed in this article are solely those of the authors and do not necessarily represent those of their affiliated organizations, or those of the publisher, the editors and the reviewers. Any product that may be evaluated in this article, or claim that may be made by its manufacturer, is not guaranteed or endorsed by the publisher.

Advantages of publishing in Frontiers

OPEN ACCESS
Articles are free to read for greatest visibility and readership

FAST PUBLICATION
Around 90 days from submission to decision

HIGH QUALITY PEER-REVIEW
Rigorous, collaborative, and constructive peer-review

TRANSPARENT PEER-REVIEW
Editors and reviewers acknowledged by name on published articles

Frontiers
Avenue du Tribunal-Fédéral 34
1005 Lausanne | Switzerland

Visit us: www.frontiersin.org
Contact us: frontiersin.org/about/contact

REPRODUCIBILITY OF RESEARCH
Support open data and methods to enhance research reproducibility

DIGITAL PUBLISHING
Articles designed for optimal readership across devices

FOLLOW US
@frontiersin

IMPACT METRICS
Advanced article metrics track visibility across digital media

EXTENSIVE PROMOTION
Marketing and promotion of impactful research

LOOP RESEARCH NETWORK
Our network increases your article's readership